The Development of Stereoselective Photocycloadditions *via* Lewis and Brønsted Acid Catalysis

By

Evan Michael Sherbrook

A dissertation submitted in partial fulfillment of
the requirements for the degree of

Doctor of Philosophy
(Chemistry)

at the
University of Wisconsin–Madison
2019

Date of final oral examination: August 15th, 2019

The dissertation is approved by the following members of the Final Oral Committee:

Tehshik P. Yoon, Professor, Chemistry

Jennifer M. Schomaker, Professor, Chemistry

Clark R. Landis, Professor, Chemistry

Andrew J. Boydston, Associate Professor, Chemistry

The Development of Stereoselective Photocycloadditions *via* Lewis and Brønsted Acid Catalysis

Evan Michael Sherbrook

Under the supervision of Tehshik P. Yoon

At the University of Wisconsin–Madison

Stereoselective cycloadditions are highly regarded transformations for their ability to introduce both molecular complexity and asymmetry in a single step. As photocatalysis has become an increasingly valuable tool in organic synthesis, there has been significant interest in the development of enantioselective photochemical cycloaddition reactions. Despite this, there are few general approaches to the control of absolute stereochemistry of photocycloadditions. This thesis describes the use of chiral catalysts, including Lewis and Brønsted acids, to enable highly enantioselective photocycloadditions. Chiral Lewis acids were employed in conjunction with a ruthenium photocatalyst to facilitate the photoreductive ring opening of cyclopropyl ketones in a reaction with alkenes to generate enantioenriched cyclopentanes. Following this, protic acids were explored as catalysts for enabling the triplet sensitization of imidazoyl enones in [2+2] photocycloadditions with several types of olefins. Lastly, investigations of BINOL-derived phosphoramidates as chiral Brønsted acid catalysts have allowed for the stereoselective synthesis of cyclobutanes, surprisingly without the need for transition metal photocatalysts.

Acknowledgments

I would first like thank my advisor, Tehshik Yoon for being an immensely supportive and creative mentor. There has never been a single moment where I felt that Tehshik wasn't completely invested in me or my project. There were certainly moments when experiments didn't work, every hypothesis seemed to fall apart, and *I* felt unsure of what I was doing, but Tehshik always pushed me to keep thinking, to keep doing experiments, and to keep moving forward. Tehshik has always impressed upon his students that experiencing graduate school isn't just learning a lot about one specific thing (although that's a rather sizable chunk of it), it's about learning how to think like a scientist. So, if you know how to ask the right questions, really care about the answers, and are never satisfied with 'good enough', you can be any kind of scientist you want.

About six years ago, when I was visiting graduate schools, my visit to UW-Madison was magical. It felt right, so I came here without really understanding why. I've since realized the why is because there are so many enthusiastic and brilliant people here. These unique people really love what they do and are willing to spend countless hours to make sure their students are successful and love what they do too. So, I'd like to thank my committee members, Profs. Jen Schomaker, Clark Landis, and AJ Boydston for being a crucial part of this amazing place and taking the time to make me a better scientist.

None of the research that we do would be remotely possible without our incredibly devoted and patient facility managers and staff. I would like to thank Charlie Fry, Heike Hofstetter, and Martha Vestling for their devotion to tirelessly maintaining UW-Madison's world-class instrumentation facility. Thanks also to Karen Stevens for keeping the organic division running so smoothly and for the homemade snacks and yearly check-ins.

Every member of the Yoon group that I have had the pleasure of knowing has made it an incredibly positive place to work and to do research. Specifically, I would like to thank the OG members of the “broffice”, Elliot, Spencer, and Adrian for being excellent colleagues and friends, especially in my first year in the group. Thanks to Mary Beth and Kaz for your mentorship and insights on science, and your companionship in trips to the Terrace and to Paul’s for “dumps”. More recently, thanks to patriotic Puerto Ricans Jesse and BJ, for keeping me sane while writing this monstrous document. Also, thanks to Matt for bravely throwing yourself on difficult diastereomer separations and chiral phosphoramidate syntheses.

I would like to thank my parents for being immensely supportive of me during this challenging experience. Weekly phone calls, Madison staycations, trips to the Badlands, and impromptu nordic ski marathons have been an incredible respite from the day-to-day. Thank you to my sister, Alex, for your love and support, but also your vocal intolerance to bullshit, especially mine. Lastly, I want to thank Kate. I doubt I could have guessed that my life would change as much as it has in the last year, but I sincerely doubt I would have made it without you. A friendship based on a mutual love for cat cuddling and fried food is bound to last forever.

Table of Contents

List of Figures

Chapter 1

Chapter 2

Chapter 3

Chapter 4

List of Schemes

Chapter 1

Chapter 2

Chapter 3

Chapter 4

List of Tables

Chapter 1

Chapter 2

Chapter 1. Asymmetric Catalysis of Triplet-State Photoreactions

1.1: Introduction

1.1.1: Asymmetric Catalysis in Triplet-State Reactions

The chemical and biological properties of organic molecules are intrinsically tied to their stereochemistry. The ability to construct complex chiral molecules ranks among the most important challenges facing contemporary synthetic organic chemistry.[1–3] Asymmetric catalysis has become an essential technique for the enantioselective preparation of a variety of molecular scaffolds including drugs, functional organic materials, and chemical feedstocks. An important frontier for continued research in this area is the development of new, highly enantioselective catalytic strategies that are applicable to a broader range of reaction types and product structures.

Chemists have long been intrigued by the unique effects of light on organic molecules.[4] Photochemical activation frequently results in the formation of highly energetic intermediates that react in distinctive ways and provide access to structural patterns that are otherwise difficult to access. However, these highly reactive intermediates are also generally short-lived, which can hamper their interception by exogenous chiral catalysts used to modulate their reactivity. In the last century, photochemical reactions have come to represent a large and diverse class of synthetically useful transformations for which stereocontrol has remained challenging.[5–7] Robust strategies for the design of highly enantioselective catalytic photoreactions have only become available within the last decade.

The majority of these successful enantioselective transformations, however, can be classified as *secondary photoreactions*: reactions of photogenerated intermediates such as radicals or radical ions in their ground-state electronic configurations (Figure 1-1).[8–10] The reactions that are accessible using photoinduced electron transfer, or photoredox catalysis,

belong to this class, and the recent renewal of interest in these reactions[11–13] has motivated much of the development in enantioselective photocatalysis. Stereocontrol in *primary photoreactions*, in which the key bond-forming steps occur from electronically excited-state intermediates, has proven to be an even more challenging objective. In addition, while photoredox catalysis offers a convenient means to access the reactivity of open-shelled, odd-electron intermediates, there exist numerous classical non-photochemical methods for the initiation of radical reactions.[14] The chemistry of electronically excited organic molecules, on the other hand, is uniquely accessible using photochemical activation methods like energy transfer and cannot be recapitulated through alternate means.

Figure 1-1. Energy transfer and electron transfer photoactivation.

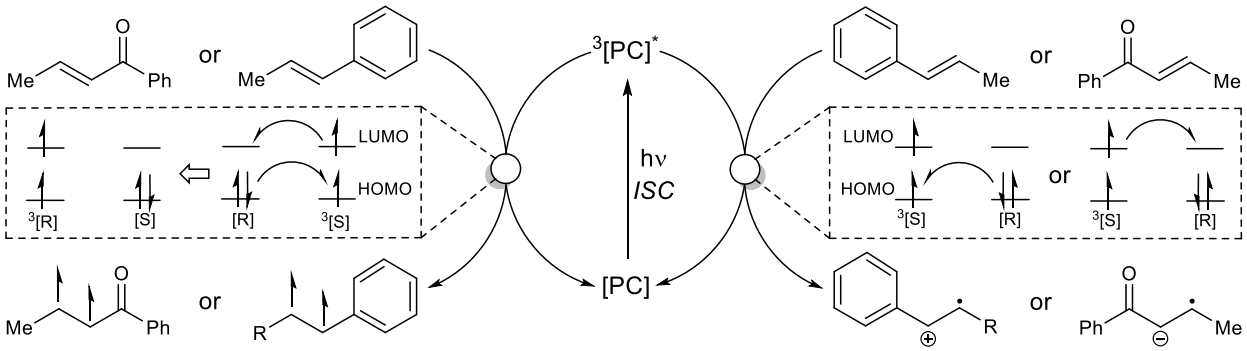

Much of the early research in enantioselective excited-state reactions involved chiral analogues of well-studied organic photosensitizers. These studies, however, generally resulted in low enantioselectivities, a feature that was attributed to weak, poorly-defined associations with the excited-state intermediates. More successful studies have shown that ground-state preassociation between the substrate and chiral catalyst prior to the excitation process can confer higher levels of selectivity in these reactions. This Chapter will focus both upon early exploratory investigations, which helped to establish an understanding of controlling excited-state reactivity, as well as more recent developments, which have made use of these insights

to develop highly enantioselective excited-state photoreactions.

1.1.2: Scope of This Overview

The broadest class of enantioselective photoreactions are those that utilize enantiopure photocatalysts to transfer stereochemical information to prochiral or racemic substrate molecules. Still others involve the use of asymmetric catalysts and racemic photocatalysts that work cooperatively. Overall, this Chapter summarizes asymmetric photochemical transformations enabled by substoichiometric small-molecule catalysts. Photoreactions involving stoichiometric and superstoichiometric chiral environments, complex supramolecular scaffolds (e.g. enzymes and zeolites), chiral auxiliaries, and circularly polarized light have not been included. For surveys of these areas, we direct the reader to several important reviews published in recent years.[5,15–17]

1.2 Early Work: Isomerizations and Rearrangments

1.2.1: Arenes

Historically, arene sensitizers were among the first classes of photocatalysts to be explored in asymmetric photochemistry. In 1965, Hammond and Cole reported the desymmetrization of racemic *trans*-*1*,2-diphenylcyclopropane (DPC) (*rac*-**1.1**) using 12 mol% of a chiral naphthalene acetamide sensitizer (**1.3**, Scheme 1-1).[18] Enriched *trans*-DPC (**1.1**) was recovered in 7% ee, along with the *meso* cyclopropane (**1.2**). While the process is a simple geometrical photoisomerization, this represents the first catalytic enantioselective excited-state photoreaction.

Scheme 1-1. The deracemization of trans-1,2-diphenylcyclopropane

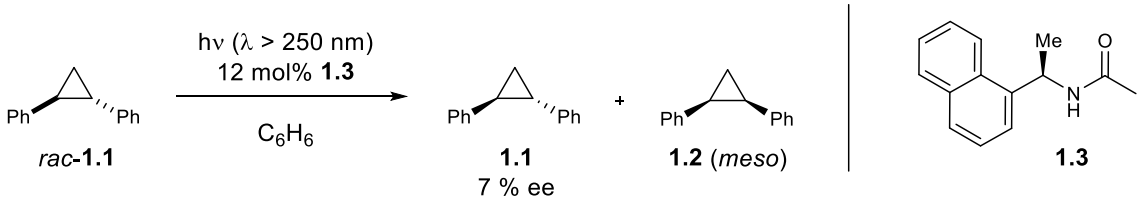

The enantioselectivity observed in this experiment is relatively low by modern standards; however, the insight that chiral sensitizers could affect the stereochemical course of a photoreaction was profound. It was originally reported that chiral induction process occurred by triplet energy transfer, but it was later determined that the reaction occurs through a singlet manifold.[19] Indeed, this latter discovery is consistent with a trend observed for chiral substituted arene photosensitizers, which often form singlet-state exciplexes with substrates.

Chiral arene photosensitizers have also been used extensively for the desymmetrization/isomerization of (Z)-cyclooctene[20–23] and in the development of the enantioselective triplex Diels–Alder reaction.[24–26] However, as these reactions occur through a singlet exciplex, they will not be discussed at length here.

1.2.2: Aryl Ketones

In contrast to arenes, aryl ketones undergo highly efficient intersystem crossing (ISC) and, therefore, are more likely to participate in triplet sensitization reactions. The first asymmetric photoreaction to occur by a triplet manifold was the familiar desymmetrization of *rac*-**1.1** using 34 mol% indanone sensitizer **1.4**, reported by Ouannès in 1980 (Figure 1-2).[27] Ouannès proposed that *trans*-DPC (ca. 53 kcal/mol) would be easily sensitized by a high triplet energy aryl ketone.[28] This experiment produced *trans*-DPC (**1.1)** in 3% ee, while other aromatic ketones **1.4** and **1.5** were reported to be less successful.[29]

Figure 1-2. Triplet sensitizers for the desymmetrization of DPC

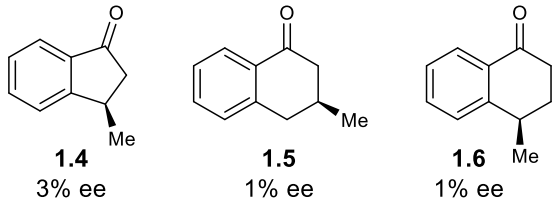

In that same year, the first asymmetric triplet-state photorearrangement was reported by Sato.[30] Oxepinone *rac*-**1.7** was sensitized using several naphthyl carbonyls including **1.10**, **1.11**, and **1.12** at a variety of catalyst loadings (0.5 to 2.0 equiv., Scheme 1-2). Sensitization of the substrate effects a 1,5-phenyl shift to **1.8**, followed by di-π-methane rearrangement to give oxabicyclo[4.1.0]heptanone (**1.9**) as the product. When the reactions were halted at 50% conversion, both the starting oxepinone (**1.7)** and the product (**1.9**) were found to be optically active. The enrichment of both the starting material and the product suggest that the stereochemistry-determining step is the initial sensitization itself.

Scheme 1-2. Rearrangement of oxapinone **1.7** *via* sensitization by naphthyl carbonyls.

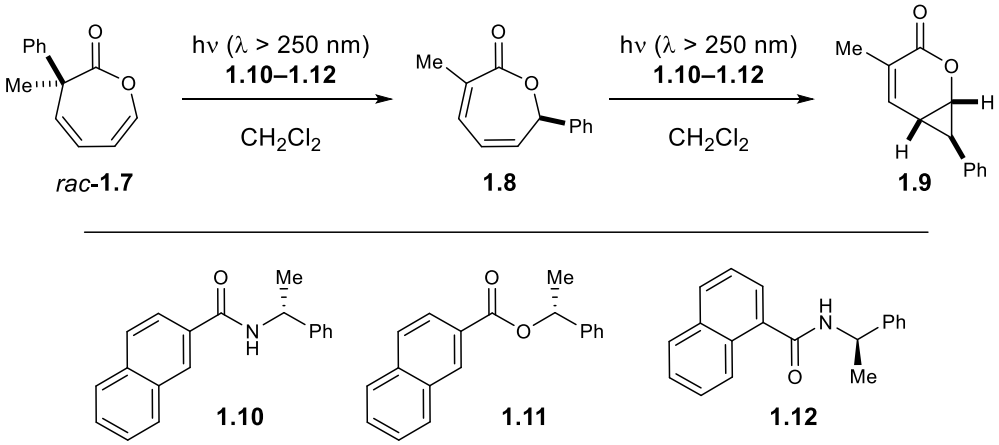

Demuth and Schaffner investigated the oxa-di-π-methane rearrangement of bicyclooctenone *rac*-**1.14** to tricyclooctenone **1.15** using 12 mol% chiral ketone **1.16** as a sensitizer (Scheme 1-3).[31] Quantitative evaluation of optical rotation data showed that the

product was formed in 4.5% ee at room temperature and 10% ee at –78 °C. Interestingly, direct irradiation of *rac*-**1.14** instead gave **1.13** *via* a 1,3 acyl shift. This divergent reactivity is an excellent demonstration of the potential utility of sensitized reactions, as access to different excited-state intermediates allows for the formation of different products.

Scheme 1-3. Reaction outcomes for ***rac*-1.14** under direct irradiation and triplet energy transfer

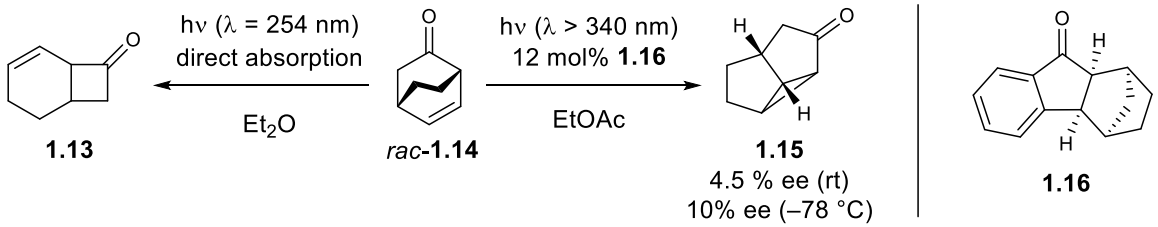

Scheme 1-4. Asymmetric photoextrusion of **1.17** to **1.1** by (–)-rotenone and (+)-testosterone

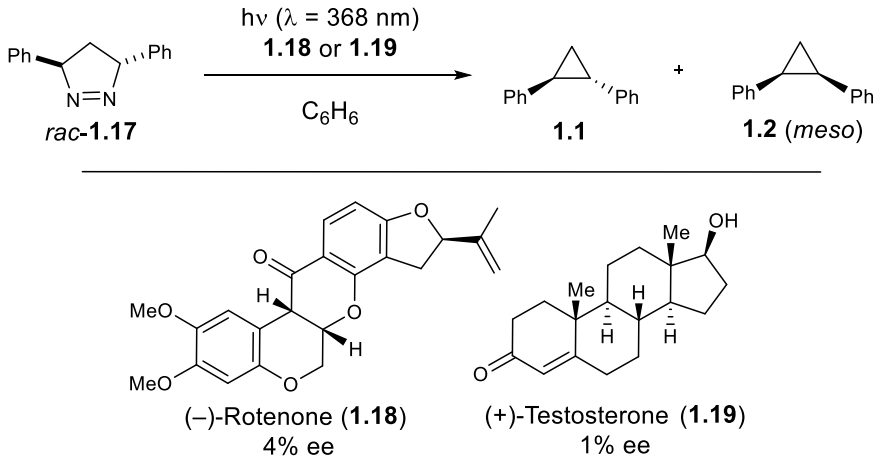

Asymmetric photoextrusion occurring from *trans*-3,5-diphenylpyrazoline (DPY) (*rac*-**1.17**) to give **1.1** and **1.2** was reported in 1981 by Rau and Horman (Scheme 1-4).[32] Chiral photosensitizers (–)-rotenone (**1.18**) and (+)-testosterone (**1.19**) gave **1.1** in 4% ee and 1% ee, respectively. While DPY can react to afford racemic **1.1** upon direct photolysis,[33] it also has a triplet energy of 55 kcal/mol.[34] Both **18** and **19**, with triplet energies of ~70 kcal/mol, are competent photosensitizers for this reaction. Irradiation was conducted above 350 nm where the absorbance of DPY is minimal, but where **18** and **19** absorb strongly, in an effort to

maximize the photosensitized process. An intramolecular variant of this was also explored in which the pyrazoline is covalently linked to the ketone, but enantioenrichment was very low.[35]

1.3 [2+2] Cycloadditions

1.3.1: H-Bond Donors

The shift away from simple arenes and aryl ketones marked a turning point in the development of enantioselective excited-state reactions. All these early catalysts lacked an important feature which was later recognized as crucial to the development of truly selective asymmetric excited state reactions: ground-state associations. Photosensitizers containing H-bond donors were the first asymmetric catalysts that began offering useful levels of selectivity, which coincided with increased interest in the application of excited-states to useful constructive reactions like [2+2] cycloadditions.

1.3.1.1: Amides

The first asymmetric [2+2] photocycloaddition *via* a triplet manifold was published by Krische,[36] who studied the reaction of quinolone **1.20** in the presence of benzophenone-modified bisamide **1.22** (Scheme 1-5) as a chiral, hydrogen-bonding host. When this mixture was irradiated at –70 °C, cyclobutane **1.21** was produced in quantitative yield and 19% ee, using 25 mol% loading of the catalyst. This approach stands out from previous efforts as the hydrogen-bonding scaffold results in a significant ground-state preassociation between the substrate and the photosensitizer. This both maximizes the probability that the reactive excited-state intermediate is generated within a well-defined chiral environment defined by the

hydrogen-bonding sensitizer, and equally importantly, extends the lifetime of the substrate–catalyst interaction. Although the enantioselectivities observed in these experiments are still only modest by modern standards, the improvement in selectivity over previous approaches shifted the focus of research in this field towards other catalysts capable of similar ground-state interactions.

Scheme 1-5. The [2+2] photocycloaddition of **1.20** using chiral H-bonding bisamide **1.22**

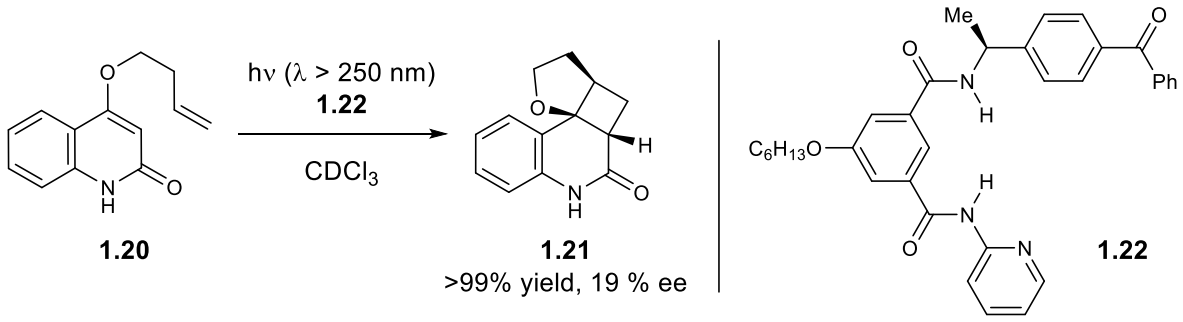

1.3.1.2: Xanthones and Thioxanthones

The first photocatalysts capable of producing truly useful enantioselectivities in triplet-state asymmetric photoreactions were developed by Bach and coworkers. In previous work, Bach had demonstrated that Kemp's triacid-derived hydrogen-bonding host structures bearing benzoxazole units (**1.23**, Figure 1-3**)** could be used as superstoichiometric chiral hosts to control a number of photocycloadditions and photocyclization reactions.[37–41]

Figure 1-3. A series of chiral H-bonding photocatalysts investigated by Bach

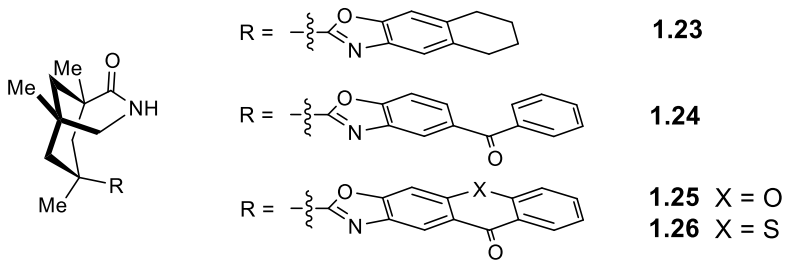

The benzoxazole moiety in this design serves as a steric shield that blocks one of the prochiral π faces of bound quinolone substrates. By the replacing benzoxazole with benzophenone (**1.24**), Bach was later able to design a *photocatalytically* active hydrogen-bonding scaffold. This compound was shown to be a moderately enantioselective photocatalyst at substoichiometric loadings for the spirocyclization reaction of α-amino alkyl radicals generated through photoinduced electron transfer.[42]

The first excited-state photoreaction using this strategy involved a structurally similar catalyst featuring a photoactive xanthone moiety (**1.25)**. This sensitizer has the benefit of both a red-shifted absorption profile (40 nm) compared to benzophenone, and a higher triplet energy (74 vs. 69 kcal/mol). Again, this catalyst was used to sensitize the intramolecular cycloaddition of quinolone **1.20** (Table 1-1). Both the regioisomers *ent*-**1.21** and **1.27** were produced in an unprecedented 91% ee (3.3:1 r.r.) with 10 mol % of **1.25** at –25 °C.[43]

Table 1-1. Intramolecular [2+2] photocycloadditions of **1.20** by H-bonding xanthone **1.25**

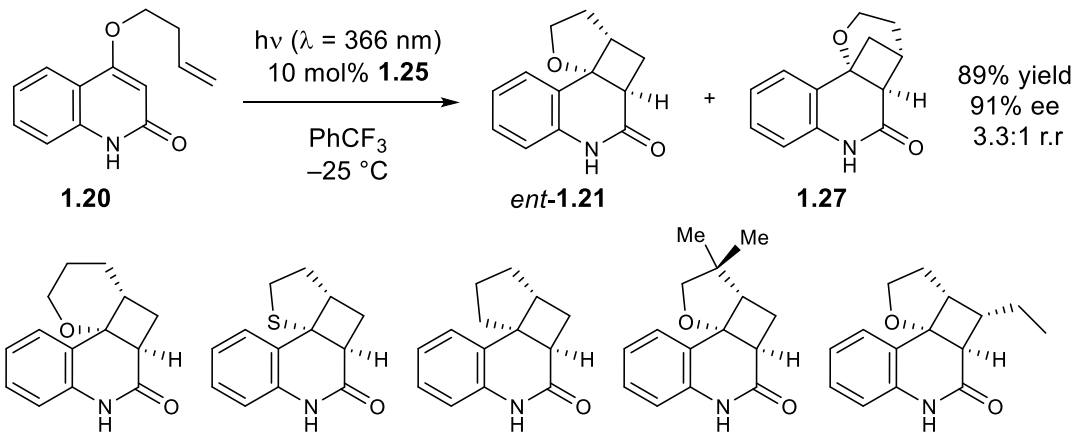

Subsequent studies of this reaction[44,45] revealed that the high enantioselectivities could be obtained for a variety of modified substrates provided that the [2+2] cycloaddition proceeds at a fast rate. Bach suggested that compounds that underwent cycloaddition more slowly (e.g., **1.28**) gave poor selectivities, as the rate of dissociation from the photocatalyst could become competitive, enabling a portion of the product to be formed in an achiral environment. Xanthone **1.25** was also used to carry out intermolecular [2+2] cycloadditions (Scheme 1-6) between pyridone **1.42** and acetylenedicarboxylates to give cyclobutene products **28a-f** with good enantioselectivities.[46] While catalyst loadings could be reduced to only 2.5–5.0 mol%, reactions must be performed at –65 °C using an unusual solvent mixture of trifluorotoluene/hexafluoro-*m*-xylene (HFX), as well as 50 equivalents of alkyene.

Scheme 1-6. Intermolecular [2+2] photocycloaddition of pyridone and acetylenedicarboxylate

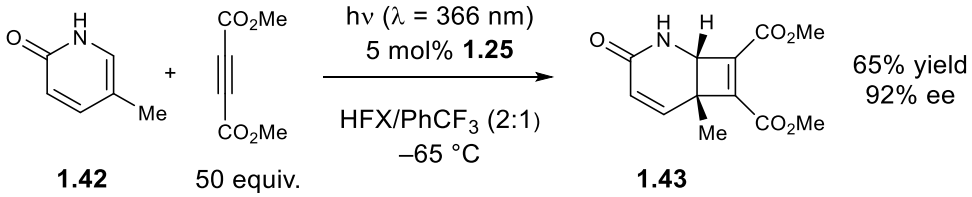

Thioxanthone catalyst **1.26** is structurally analogous to xanthone **1.25** but exhibits a longer-wavelength absorption spectrum.[47] As such, the former can mediate sensitization reactions using visible light instead of UV. Bach demonstrated that this catalyst enables several quinolones to undergo intramolecular cycloadditions with 400–700 nm light. Selectivities were found to be consistently high using only 10 mol% of the catalyst at –25 °C. For example, using **1.26**, cycloadduct **1.30** was generated in 86% yield and 91% ee, improving on the reaction outcome observed with **1 25**. Bach suggests that the longer wavelength irradiation minimizes the formation of product by direct irradiation of the quinolone, which minimizes the rate of formation of racemic cycloadduct.

This improved thioxanthone catalyst also enables the highly enantioselective intermolecular cycloaddition of quinolone **1.44** (Scheme 1-7) with ethyl vinyl ketone to give cyclobutane **14.5** as a single diastereomer in high yields and selectivities.[48] A variety of other alkenes, including benzyl acrylate, methyl vinyl ketone, and acrolein offer similarly good results, although a consistently large excess of the acceptor alkene is required.

Scheme 1-7. Intermolecular [2+2] photocycloaddition of quinolones and electron poor olefins by a chiral H-bonding thioxanthone

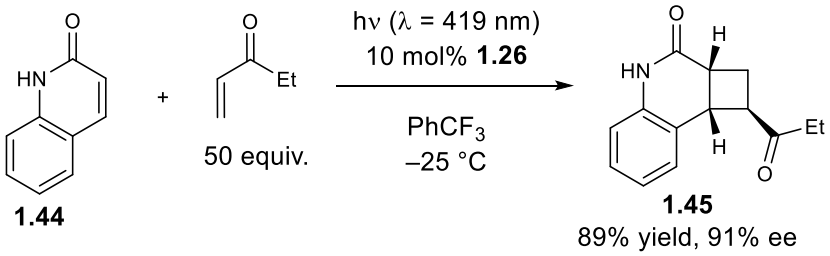

1.3.1.3: Thioureas

In 2014, concurrent with much of Bach's work on chiral xanthones and thioxanthones, Sibi and Siviguru reported an intramolecular [2+2] photocycloaddition of 4-alkenyl coumarins using chiral binaphthyl thiourea **1.48** as a photocatalyst (Scheme 1-8).[49] Irradiation of coumarin **1.46** in the presence of this thiourea catalyst using 350 nm light at –78 °C gave **1.47** in 84% yield and 74% ee in only 30 min. Structural optimizations of the catalyst led to the identification of **1.49**, which afforded quantitative yield of the product in 96% ee with only 10 mol % catalyst loading. From a design perspective, this thiourea catalyst is akin to Bach's xanthone catalysts, as it couples a hydrogen-bonding domain to a π-conjugated chromophore.

Mechanistically, however, the mode of catalysis in the Sivaguru system appears distinct. First, energy transfer was determined to be energetically infeasible, as fluorescence

spectroscopy revealed that both the lowest singlet and triplet excited states were insufficiently energetic to sensitize coumarin **1.46**. Sibi and Sivaguru instead proposed the formation of an absorption complex. UV/vis spectroscopic analysis revealed that the catalyst-substrate complex exhibited a distinct bathochromic shift compared to the catalyst or substrate species in isolation. Thus, a chiral substrate–catalyst complex was proposed to absorb long-wavelength light preferentially over the free substrate.

Scheme 1-8. Intramolecular [2+2] photocycloadditions of **1.46** by chiral naphthyl thioureas

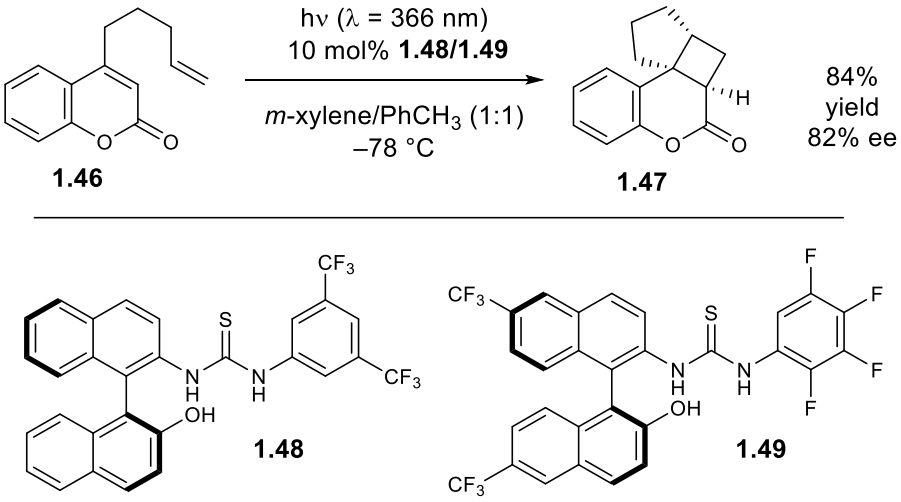

However, a nonlinear Stern-Volmer response to substrate concentration was also observed, indicative of competitive static and dynamic quenching mechanisms. Consequently, a concentration-dependent mechanism was proposed. At low substrate concentration (high concentrations of **1.49**), the higher optical density of the biaryl catalyst results in its selective photoexcitation; product formation was proposed to proceed through the formation of an exciplex. At high substrate concentration, on the other hand, the pre-associated absorption complex is selectively photoexcited, similarly leading to product. A variety of diverse chiral thiourea scaffolds were further investigated as catalysts for the same intramolecular coumarin cycloaddition.[50] Interestingly, while none of these catalysts gave enantioselectivities

comparable to **1.48** or **1.49**, the precise mechanism of photochemical activation varied as a function of catalyst structure.

1.3.2: Lewis Acids

Seminal studies on the modulation of excited states by Lewis acids were conducted by Lewis in the 1980s.[51] While the [2+2] photodimerization of coumarin can be achieved through direct excitation, this process is inefficient because the singlet excited state of coumarin relaxes rapidly to the ground state. However, it was observed that coordination of a Lewis acid to coumarin significantly increases the lifetime of the excited state. Consequently, intermolecular cycloadditions between coumarins and alkenes are considerably faster in the presence of Lewis acids such as BF_3 and $EtAlCl_2$.[52] Similar effects have also been observed in the rates of cinnamate photocycloadditions.[53]

Figure 1-4. A series of chiral oxazaborolidine-$AlBr_3$ Lewis acids

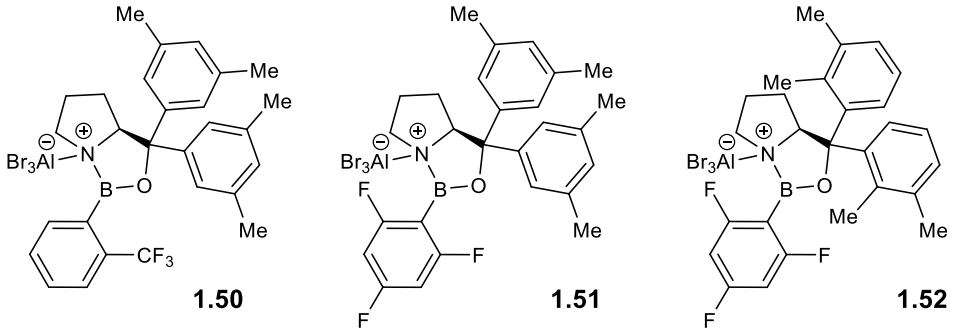

This effect was successfully exploited for asymmetric cyclobutane synthesis by Bach.[54,55] Chiral oxazaborolidine catalyst **1.50** (Figure 1-4) is an effective asymmetric catalyst for the cycloaddition of 4-alkenyl coumarin **1.46** to afford cyclobutane *ent*-**1.47** in 84% yield and 82% ee. This catalyst allows for significant alkene tether modifications, while maintaining high yields and good selectivities (Figure 1-5). Bach has proposed that, while the uncatalyzed

reaction proceeds through a singlet manifold, the catalysed reaction proceeds through a triplet-state biradical intermediate. Consistent with this hypothesis, coumarins featuring isomeric (*E*) and (*Z*) alkene-containing substituents undergo a stereoconvergent cycloaddition.

Figure 1-5. Partial scope of an intramolecular [2+2] coumarin photocycloadditions with **1.50**

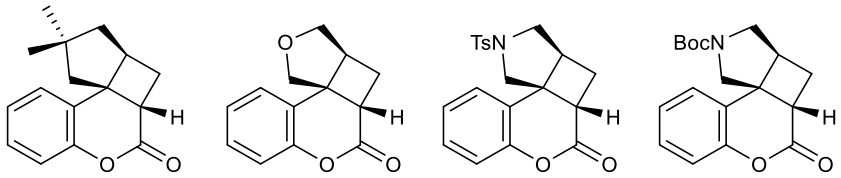

1.53 96% yield 74% ee | **1.54** 72% yield 88% ee | **1.55** 91% yield 76% ee | **1.56** 81% yield 90% ee

The UV-vis absorption spectra of this class of coumarin compounds undergoes a bathochromic shift in the presence of Lewis acids. An important feature of this successful strategy, therefore, is selective irradiation at the red-shifted tail of the coumarin absorption with a monochromatic light (λ = 366 nm), which maximizes the photoexcitation of the Lewis acid-bound substrate and minimizes direct photoexcitation of unbound coumarin.

Table 1-2. Intramolecular [2+2] photocycloaddition of pyridones

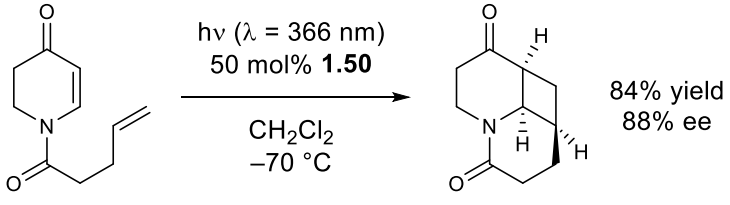

1.57 → **1.58**

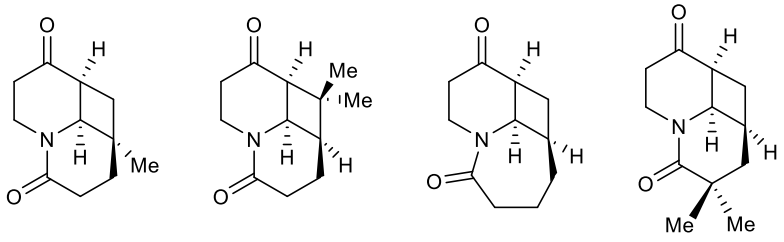

1.59 81% yield 88% ee | **1.60** 48% yield 82% ee | **1.61** 84% yield 90% ee | **1.62** 87% yield 80% ee

This Lewis acid-mediated strategy has enabled asymmetric photocycloaddition reactions to be applied to a much broader range of enone substrates.[56] Bach has developed conditions for the highly enantioselective [2+2] cycloaddition of dihydropyridone **1.57** (Table 1-12) to afford **1.58** in 84% yield and 88% ee, again using catalyst **1.50**.

The mode of catalysis for this substrate features a subtle but important mechanistic difference. Unlike coumarin photocycloadditions, there is no change in the reactive spin state of photoexcited **1.57** in the presence of a Lewis acid catalyst; both the free and Lewis-acid-bound pyridine undergo cycloaddition through the triplet state when irradiated at 366 nm. Indeed, the intrinsic rate of cycloaddition is somewhat depressed upon coordination of **1.57** to a Lewis acid. However, in addition to a significant 50 nm bathochromatic shift of the π,π* transition feature (Figure 1-6), the UV-vis spectrum of the Lewis acid-pyridone complex also exhibits an increase in molar absorptivity. Thus, the high selectivities appears largely to be a consequence of the higher extinction coefficient of the Lewis acid-bound substrate compared to the achiral free pyridone, which provides an alternative means to minimize the participation of racemic background cycloaddition.[57]

Figure 1-6. UV/Vis of **1.57** (—), **1.57**·$EtAlCl_2$(—) and **1.57**·BCl_3(—)[56]

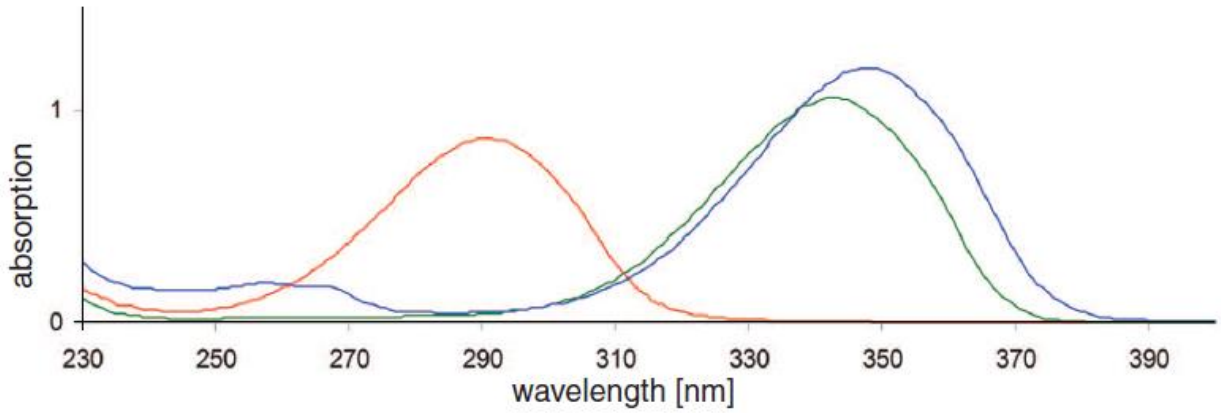

Further investigations by Bach have continued to extend the scope of this strategy towards simpler enone substrates. Catalyst **1.51** has been applied in the intramolecular photocycloaddition of β-alkoxysubstituted cycloalkenones.[58] Very recently, oxazaborolidine **1.52** was identified as an optimal catalyst for the enantioselective intermolecular cycloadditions of simple cycloalkenones such as **1.63** (Table 1-3) with an impressive variety of 1,1- and 1,2-disubstututed alkenes to give cyclobutene products **1.64–1.69**.[59]

Table 1-3. Intermolecular [2+2] photocycloadditions of cyclohexenones and alkenes.

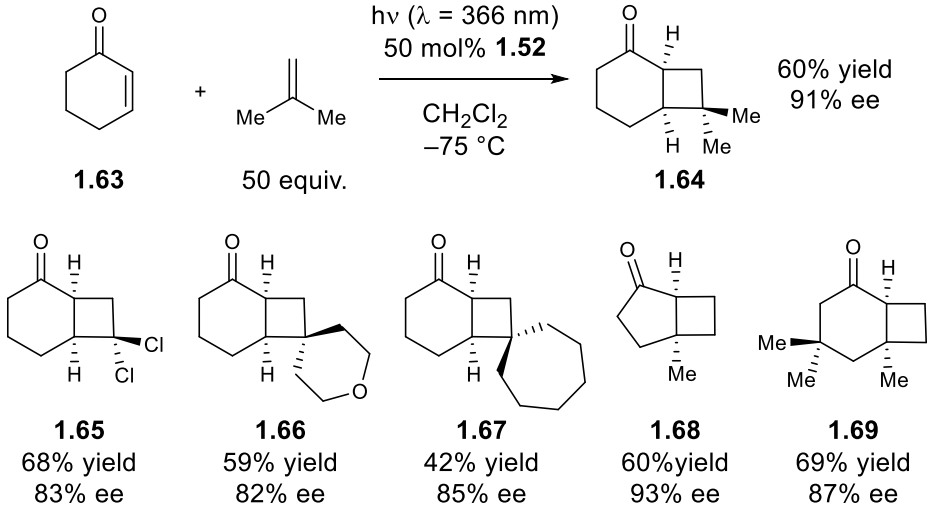

This is an important contribution because many of the classic applications of photocycloadditions to the synthesis of natural products have involved such simple cycloalkenone substrates.[60] Bach's strategy thus appears to provide a strategy to render these syntheses enantioselective. Although the alkene coupling partner must be used in significant excess, the structural variety of olefins that participate in this reaction is impressive and distinctive to this approach. Intermolecular cycloadditions between phenanthrene-9-carboxaldehydes and both 1,2-disubstituted and tetrasubstituted alkenes have also very recently been reported using this type of oxazaborolidine-$AlBr_3$ Lewis acid.[61]

Although nearly all methodologies in asymmetric triplet state photochemistry employ

chiral enantiopure photocatalysts, several dual catalyst strategies for highly enantioselective photoredox reactions have been developed.[62] The approach is appealing because it allows for independent optimization of the chiral stereocontrolling co-catalyst without altering the robust photophysical and photoelectrochemical properties of an achiral or racemic photoredox catalyst.[63] Until recently, this strategy had not been applied to transformations involving excited-state photochemistry, and our group has taken a particular interest in this approach.

Table 1-4. Intermolecular [2+2] photocycloadditions of 2'-hydroxychalcones and alkenes using chiral Lewis acid complex **1.76** (Figure 1-7)

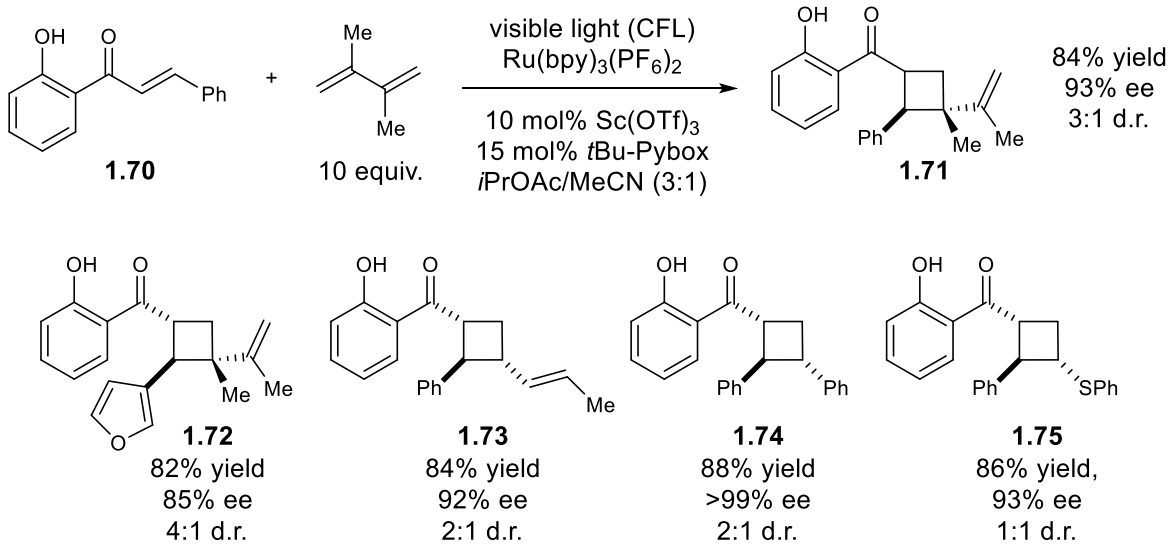

In 2016, we reported a dual catalytic approach to asymmetric intermolecular [2+2] photocycloadditions between 2'-hydroxychalcone **1.70** (Table 1-4) and 2,3-dimethylbutadiene to give **1.71** in 84% yield, 93% ee, and 3:1 d.r..[64] Furthermore, the reaction was expanded to include other dienes, as well as styrenes and vinyl sulfides,[65] to give **1.72–1.75** in excellent yields and selectivities. In this transformation, $Ru(bpy)_3(PF_6)_2$ acts as a photosensitizer and a $Sc(OTf)_3$-*t*BuPybox complex (**1.76**, Figure 1-7A) serves as the chiral controller. The distinctive mechanistic feature of this process is a Lewis acid-mediated lowering of the triplet

energy (E_T) of the substrate (Figure 1-7B. Thus, triplet energy transfer only occurs between $^3Ru(bpy)_3^{2+}$ and **1.70a**, while **1.70** alone is unreactive and racemic background reaction is minimized. To support this hypothesis, we utilized a combination of computational and spectroscopic studies to show that the E_T of **1.70** decreases from from 54 kcal/mol to 33 kcal/mol upon coordination to the Lewis acid (Figure 1-7C). Therefore, sensitization by $Ru(bpy)_3^{2+}$ (E_T = 47 kcal/mol), is only thermodynamically feasible with the Lewis acid-bound complex.

Figure 1-7. (**A**) Structure of Lewis acid-ligand complex **1.72** (**B**) Computationally and experimentally derived E_T for free and Sc-bound 2'-hydroxychalcone (**C**) Emission data for Sc-bound 2'-hydroxychalcone

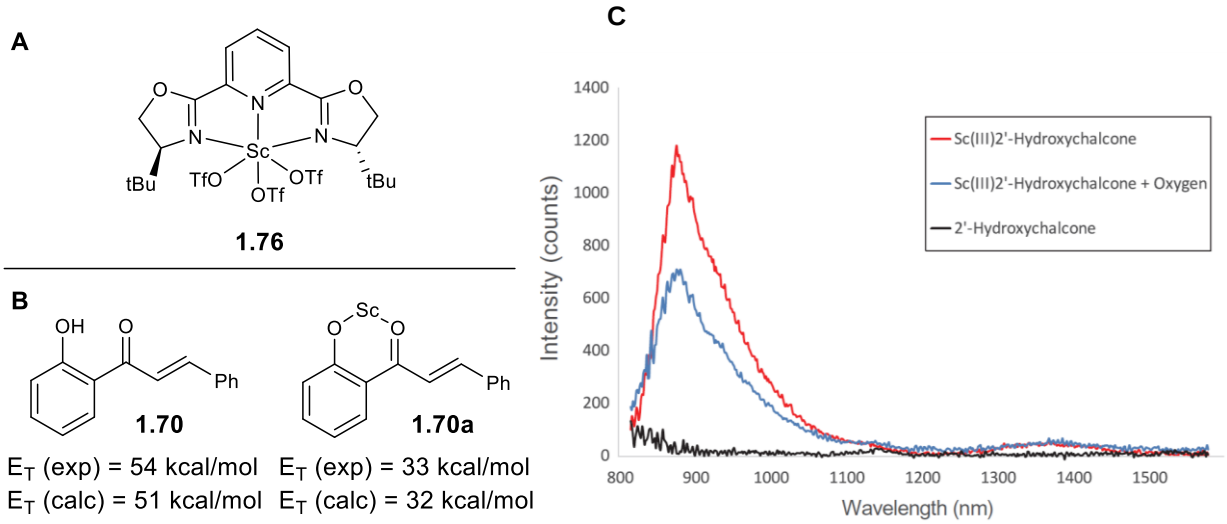

While the phenoxy ketone moiety of 2'-hydroxychalcone **1.70** proved to be an effective chelating group for mildly oxophilic Lewis acids, its removal from the cycloadducts through oxidation proved difficult. Further studies of this dual catalytic approach led to the development of an enantioselective [2+2] cycloaddition between simple cinnamate ester **1.77** and styrenes using a monodentate oxazaborolidine-$HNTf_2$ Lewis acid **1.79** (Scheme 1-9).[66] This reaction proved effective in the cyclization of several cinnamate esters and a large variety

of substituted styrenes, providing good yields, excellent enantioselectivities, and diastereoselectivities routinely greater than 6:1. Intriguingly, we found that the mechanism by which cinnamate esters are activated toward triplet energy transfer to be somewhat different than for 2'-hydroxychalcones. While the coordination of **1.79** to cinnamate esters results in a 6.9 kcal/mol reduction in E_T, other additional factors were found to have a significant influence on the energy transfer process (Figure 1-8).

Scheme 1-9. Intermolecular [2+2] photocycloadditions of cinnamate esters and styrenes using chiral Lewis acid complex **1.79**.

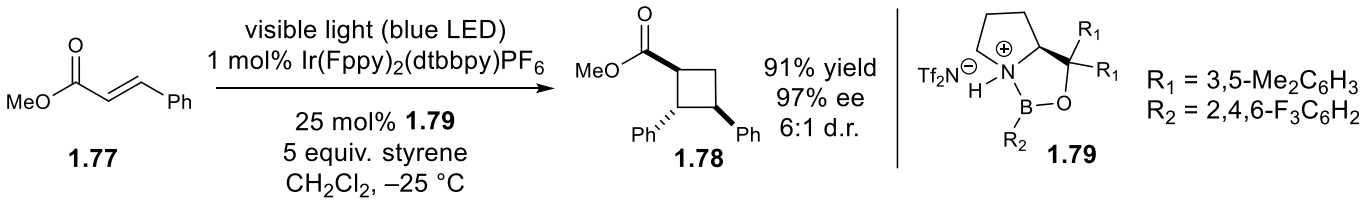

Figure 1-8. Triplet energies and frontier molecular orbital energies of **1.77**, **1.77-BF$_3$** and **1.77-1.79** adducts, and Ir(Fppy)$_2$(dtbbpy)PF$_6$.

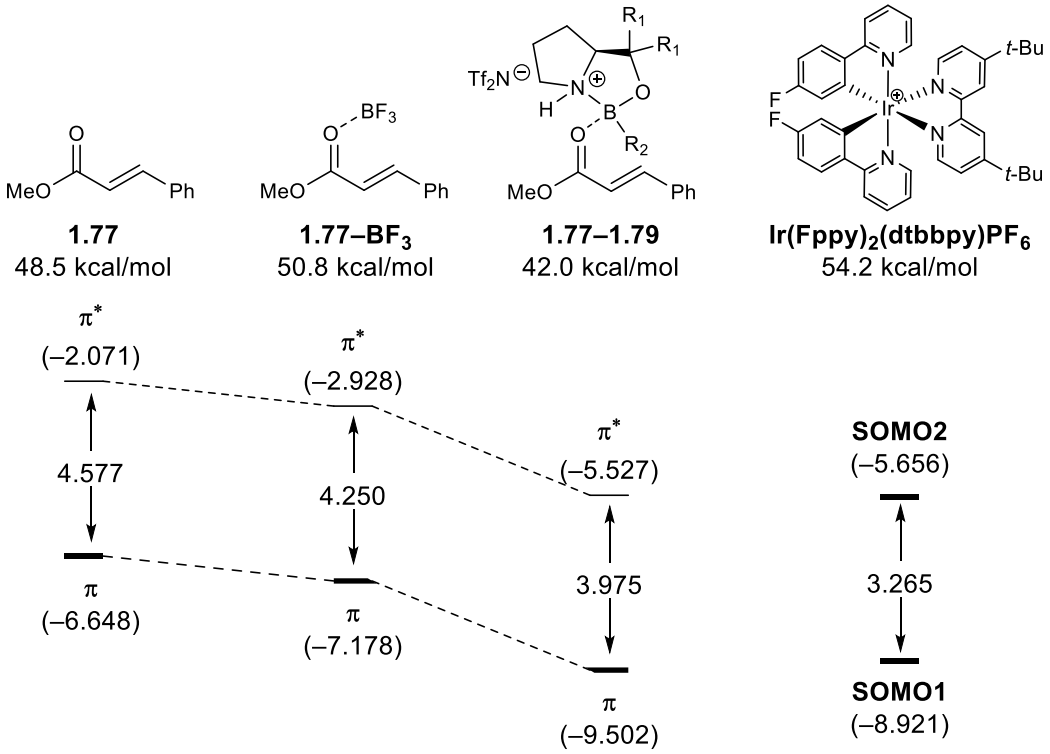

The results of additional DFT calculations examining the frontier molecular orbitals of **1.77**, Lewis acid adducts, and $Ir(Fppy)_2(dtbbpy)PF_6$ are summarized in Figure 1-6. These results show that the FMOs of **1.77** and the photocatalyst are quite mismatched, while the coordination of BF_3 reduces both the π and π* slightly. The chiral Lewis acid **1.79** further decreases these FMO energies such that are almost isoenergetic with the SOMO orbitals of the excited-state photocatalyst. This results in a significant increase in electronic coupling of the donor and acceptor and increases the rate of energy transfer.

1.3.3: Transition Metal Photocatalysts

Figure 1-9. Chiral-at-metal iridium and rhodium photocatalysts

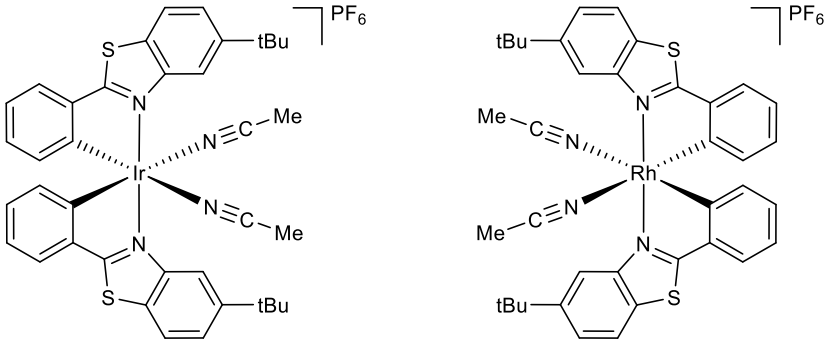

1.80 (Λ-Ir) **1.81** (Δ-Rh)

Most chiral photocatalysts investigated for organic transformations rely on the tetrahedral chirality of chiral organic sensitizers or co-catalysts. Approaches exploiting the helical chirality of octahedral transition metal complexes have recently been reported. Meggers has played a pioneering role in designing chiral-at-metal octahedral Lewis acidic catalysts capable of controlling the stereochemistry of a variety of photoredox reactions with exceptional enantiocontrol (**1.80**, Figure 1-9).[67] Recently, Meggers demonstrated that this class of catalysts can also control excited state photoreactions through the formation of direct

absorption complexes.[68] Chiral-at-rhodium complex **1.81** binds to imidazoyl enone **1.82** to form an adduct with a distinct absorption feature that is red-shifted compared to the UV-vis spectra of either the enone or rhodium catalyst on its own (Table 1-5).

Table 1-5. Intermolecular [2+2] photocycloadditions of imidazoyl, pyridyl, and pyrazoyl enones with alkenes

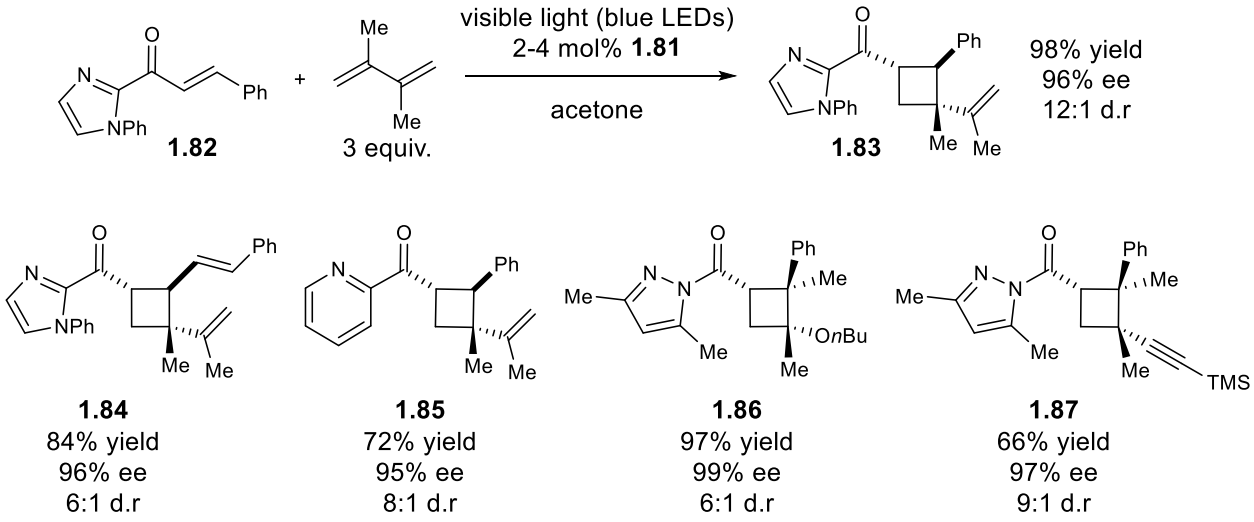

When this adduct is excited with visible light, it undergoes a facile intermolecular [2+2] photocycloaddition with electron-rich alkenes to afford a diverse array of vinylcyclobutanes **1.83**–**1.87** in excellent yield and ee using quite low catalyst loadings (2–4 mol %). Interestingly, the reaction was found to be feasible without a catalyst, albeit at a substantially slower rate. The origin of the extremely high selectivities is attributable to a nearly 170-fold increase in molar extinction coefficient for the complex as compared to the substrate, effectively outcompeting any direct background cycloaddition. More recently, Meggers has developed an asymmetric dearomatization of benzofurans *via* [2+2] photocycloadditions with styrenes, which also employs the formation of absorption complexes with helically chiral rhodium Lewis acids.[69]

Our group recently designed a chiral-at-iridium catalyst **1.88** (Scheme 1-10) that employs outer-sphere hydrogen-bonding interactions via a functionalized pyrazole ligand rather than substrate-metal interactions.[70] Using this catalyst, quinolone **1.89** undergoes highly enantioselective intramolecular [2+2] cycloaddition to afford **1.90** in 98% yield and 91% ee using visible light and only 1 mol% of catalyst at –78 °C. The mode of interaction between the quinolone substrate and the pryazole ligand is unique; the primary hydrogen-bonding interaction occurs between the Brønsted acidic N–H moiety of the pyrazole and the quinolone carbonyl, and that a weak, secondary H–bonding interaction from the quinolone N–H to the pyrazole π-surface orients the substrate relative to the chiral Ir stereocenter and facilitates rapid triplet energy transfer. Consistent with this model, coumarin and *N*-methylquinoline undergo rapid but essentially unselective cycloaddition upon sensitization with **1.88**.

Scheme 1-10. Intramolecular [2+2] photocycloadditions of quinolones with an H-bonding chiral-at-metal iridium photocatalyst

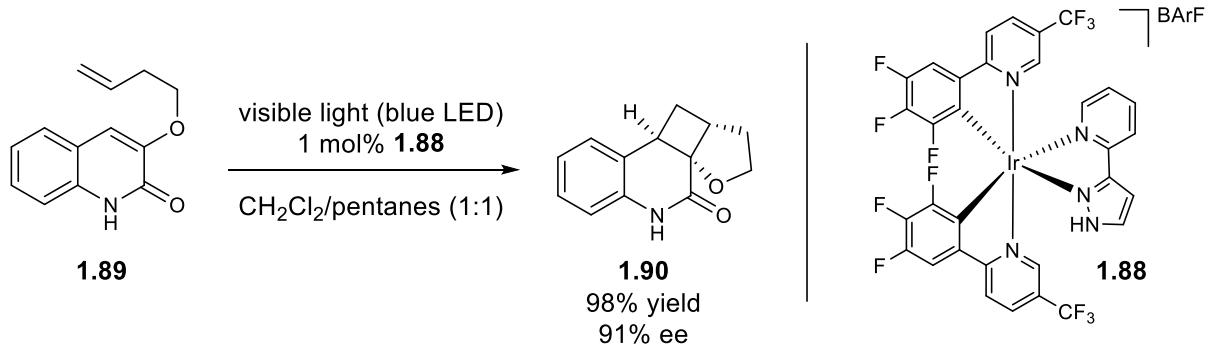

1.4 [3+2] Cycloadditions

The general approach to substrate activation by helically chiral transition metal complexes developed by Meggers has recently been applied to the [3+2] synthesis of 1-pyrrolines (Table 1-6).[71] This is a significant advance because it was the first report of a highly enantioselective catalytic triplet-state photoreaction that is not a [2+2] cycloaddition. In this transformation, pyrazoyl enone **1.91** coordinates to ent-**1.81** (Λ-Rh), which results in a bathochromic shift and increase in absorbance. Upon excitation to its triplet state, the substrate reacts with vinyl azide **1.92**, resulting in extrusion of N_2 and generation of the triplet iminyl 1,5-biradical **1.93**. This then must undergo intersystem crossing and then cyclize to generate the five-membered products **1.94**–**1.97**, which are then released by the catalyst.

Table 1-6. [3+2] Photocycloadditions of pyrazoyl enones and vinyl azides using helically chiral rhodium catalyst *ent*-**1.81**.

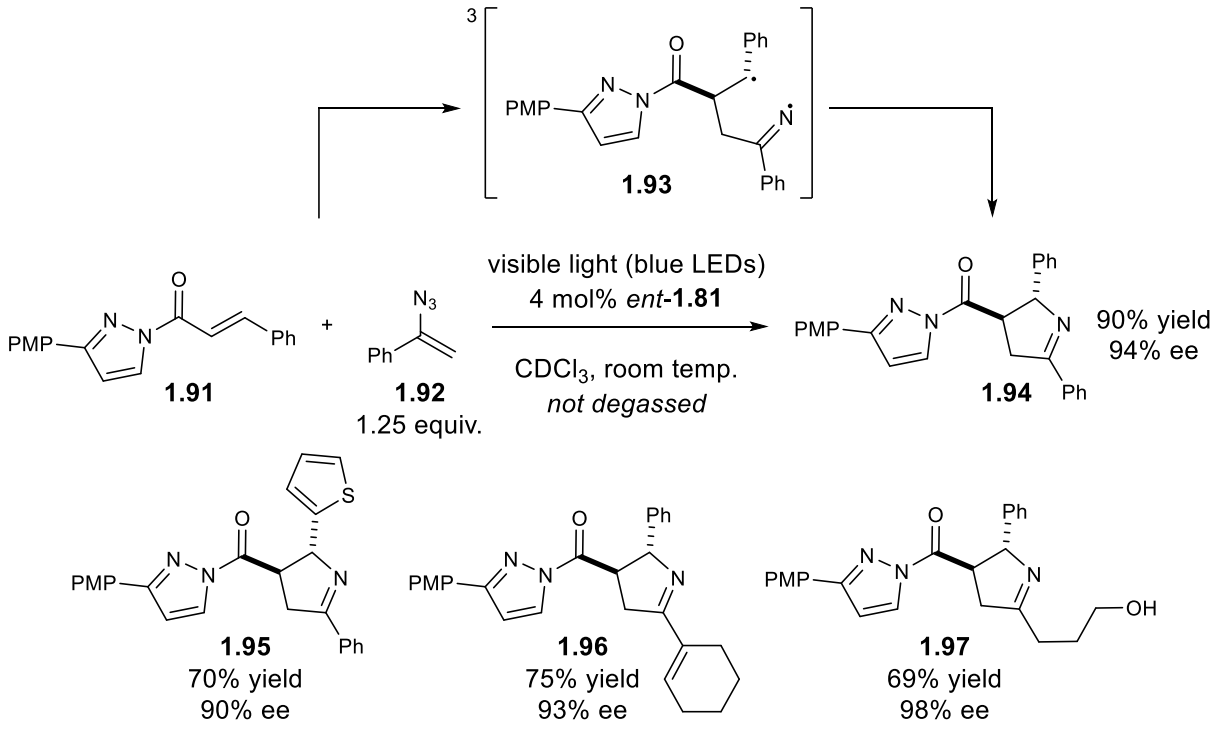

1.5 Revisiting Isomerizations and Rearrangements with Modern Catalysts

Early developments of asymmetric triplet state reactions focused on simple geometric isomerization reactions. This early groundbreaking work did not achieve selectivities competitive with modern asymmetric catalysis, and the development of highly enantioselective photochemical isomerization reactions has subsequently lagged behind photocycloaddition chemistry. In the last several decades, the importance of ground state interactions between substrates and chiral controllers in asymmetric photoreactions has been firmly established. Contemporary work has revisited this important topic and exploited these key insights.

Table 1-7. Deracemization of allene lactams using chiral thioxanthone **1.26**

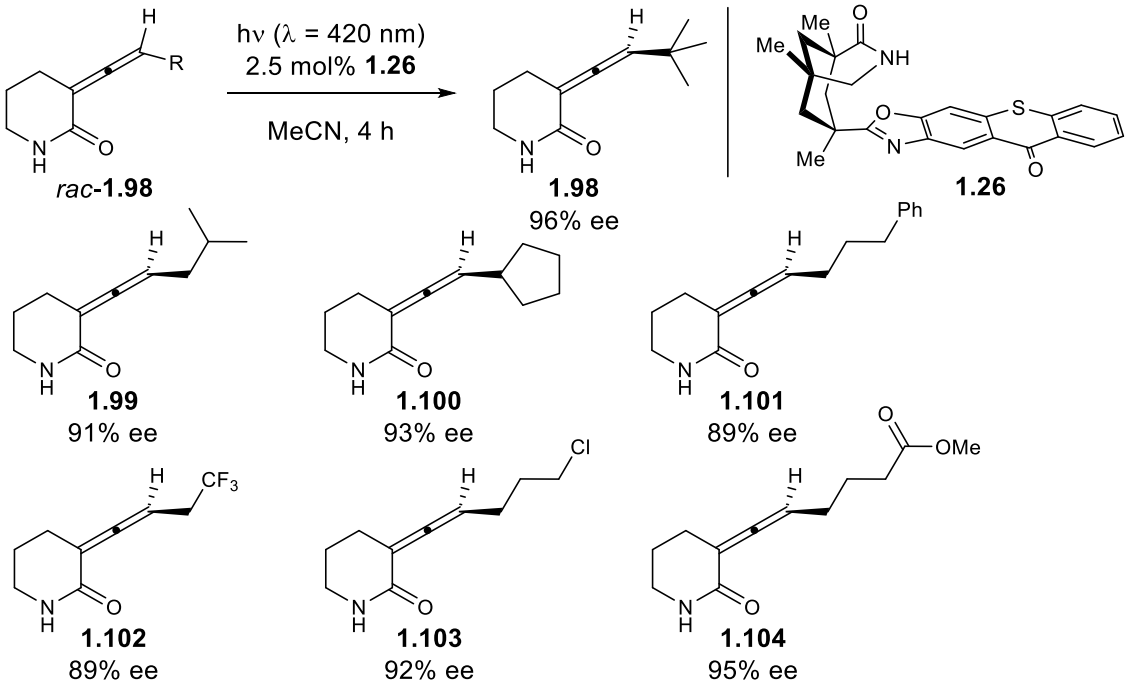

In 2018, Bach described the photosensitized deracemization of allene lactam **1.98** using his previously developed hydrogen-bond donor thioxanthone photocatalyst **1.26** (Figure 1-3, Table 1-7).[72] The deracemization gives excellent enantioselectivities of a variety of alkyl-substitued allene lactams (**1.99**–**1.101**) at room temperature. This system also tolerated a modest selection of

functional groups (**1.102**–**1.105**), though optimal enantioselectivities require cooling–40 °C. Importantly, this class of allenes is configurationally stable under irradiation by 420 nm light. Upon binding with **1.26**, however, they can undergo Dexter energy transfer from the excited state thioxanthone moiety. One diastereomeric form of the allene-thioxanthone complex is significantly disfavored due to steric interactions between the large R group of the allene and the thioxanthone. The now-facile isomerization process linearly enriches the allene until it is nearly enantiopure.

Figure 1-10. Di-π-methane rearrangement and asymmetric isomerization of **1.105** to cyclopropane **1.106** using chiral thioxanthone **1.26**

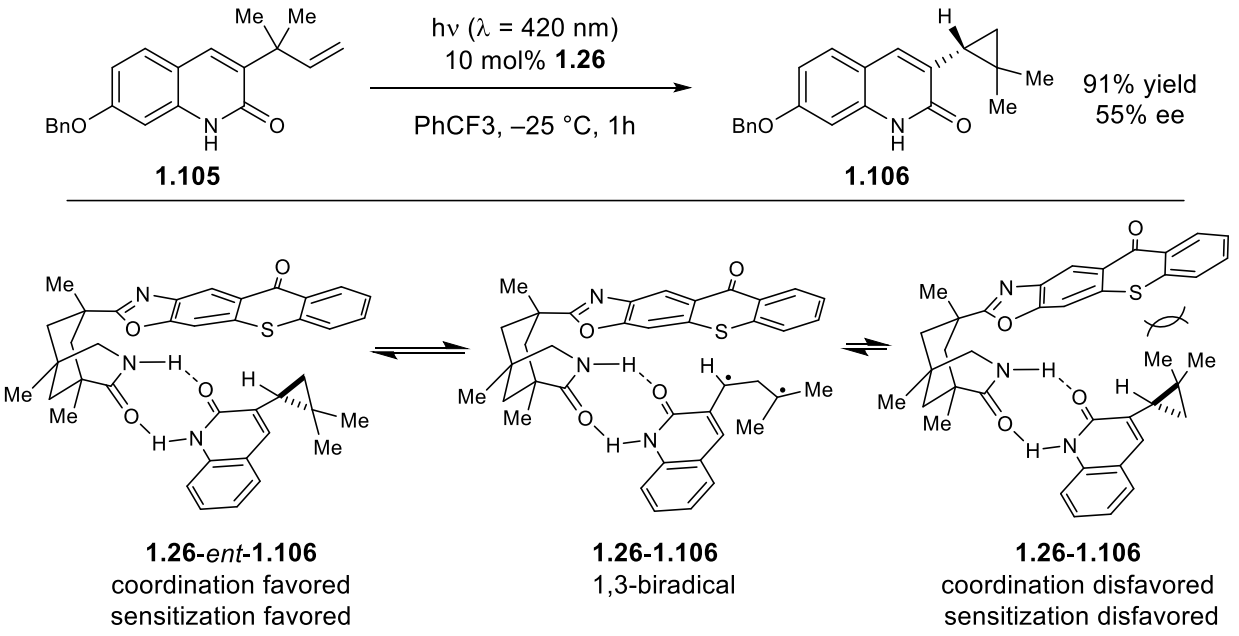

Bach has also revisited the topic of asymmetric cyclopropane isomerization, the first type of enantioselective excited-state reaction developed in 1965 by Hammond and Cole. [19] In this more recent example, the enantioselective di-π-methane rearrangement of **1.105** to cyclopropane **1.106** using **11.26 is** reported (Figure 1-10).[73] Although the overall yields for this rearrangement are high, enantioselectivities for the isomerization step do not exceed 55% ee. Nevertheless, this outcome

represents an unusually high enantioinduction compared to all previous photochemical cyclopropane isomerizations.[27]

Intriguingly, several mechanistic experiments revealed that the di-π-methane rearrangement itself is not a selective process. First, it was observed that enantioenrichement increased gradually over the course of the reaction. Second, the triplet energies of the starting material and the product were determined to be nearly identical. Lastly, the absolute configuration of the product was the opposite of what was predicted by 3D-modeling if the di-π-methane rearrangement occurred within the chiral sphere of thioxanthone **1.26**.

The proposed mechanism instead posits that *rac*-**1.106** is formed, and then subsequently becomes enriched through an asymmetric cyclopropane isomerization process. This is a result of the extremely facile coordination of *ent*-**1.106** to the thioxanthone catalyst to give **1.26**-*ent*-**1.106**, followed by homolytic cleavage of the cyclopropane. Formation of the 1,3-biradical leads to both enantiomers, but binding of **1.106** to **1.26** is disfavored. Additionally, sensitization of **1.106** by **1.26** becomes much more difficult in the adducts that do form due to a reduction in π stacking of the substrate and the thioxanthone moiety. Thus, the preferential formation of **1.106** as the major product is attributable to the unfavorable steric interations in complex **1.26-1.106**.

1.6 Summary and Looking Forward

Over the past decade, the development of multiple highly enantioselective excited-state photoreactions has demonstrated conclusively that stereocontrol in this class of transformations is indeed feasible using small-molecule chiral catalysts. A key feature common to all of these successful catalytic asymmetric photoreactions has been the use of catalysts (both sensitizers or co-catalysts) with ground-state preassociation interations between

the substrate and the chiral controller that facilitate the photoactivation step. Many of the most successful chiral catalyst structures reported to date for these applications are the same well-understood privileged catalysts that have been broadly applied to other non-photochemical transformations. Thus, the field of asymmetric photochemistry is poised for a period of significant growth as synthetic chemists learn to apply these principles asymmetric catalyst to a broader range of excited-state photoreaction types. The reactivity of these photogenerated intermediates afford structurally unique products that have previously been difficult to access in enantiomerically enriched form, and these efforts to develop stereoselective photochemistry into a robust contemporary synthetic tool is an exciting prospect for modern organic chemistry.

1.7 References and Notes

[1] Walsh, P. J.; Kozlowski, M. C. *Fundamentals of Asymmetric Catalysis*; Murdzek, J. Eds.; University Science Books: Sausalio, CA, 2009.

[2] Ojima, I. *Catalytic Asymmetric Synthesis*; Wiley: Hoboken, NJ, 2010.

[3] Gawley, R. E.; Aube, J. *Principles of Asymmetric Synthesis, 2nd Ed.*; Elsevier: Oxford, UK, 2012.

[4] Ciamician, G. The photochemistry of the future. *Science* **1912**, *36,* 385–394.

[5] Rau, H. Asymmetric Photochemistry in Solution. *Chem Rev.*, **1983**, *83*, 535–547.

[6] Inoue, Y. Asymmetric Photochemical Reactions in Solution. *Chem. Rev.*, **1992**, *92*, 741–770.

[7] Inoue, Y.; Ramamurthy, V. *Molecular and Supramolecular Photochemistry, Vol. 11: Chiral Photochemistry*; Marcel Dekker: New York, NY, 2004.

[8] Hopkinson, M. N.; Sahoo, B.; Li, J.-L.; Glorius, F. Dual Catalysis Sees the Light: Combining Photoredox with Organo-, Acid, and Transition-Metal Catalysis. *Chem. Eur. J.* **2014**, *20*, 3874–3886.

[9] Brimioulle, R.; Lenhart, D.; Maturi, M. M.; Bach, T. Enantioselective Catalysis of Photochemical Reactions. *Angew. Chem. Int. Ed.*, **2015**, *54*, 3872–3890.

[10] Meggers, E. Asymmetric Catalysis Activated by Visible Light. *Chem Commun.* **2015**, *51*, 3290–3301.

[11] Albini, A.; Fagnoni, M. *Photochemically Generated Intermediates in Synthesis*; Wiley & Sons: Hoboken, NJ, 2013.

[12] Prier, C. K.; Rankic, D. A.; MacMillan, D. W. C. Visible Light Photoredox Catalysis with Transition Metal Complexes: Applications in Organic Synthesis. *Chem. Rev.* **2013**, *113*, 5322–5363.

[13] Stephenson, C. R. J.; Yoon, T. P.; MacMillan, D. W. C. *Visible Light Photocatalysis in Organic Chemistry*; Wiley-VCH: Weinheim, Germany, 2018.

[14] Studer, A.; Curran, D. P. Catalysis of Radical Reactions: A Radical Chemistry Perspective. *Angew. Chem. Int. Ed.*, **2016**, *55*, 58–102.

[15] Svoboda, J.; König, B. Templated Photochemistry: Toward Catalysts Enhancing the Efficiency and Selectivity of Photoreactions in Homogeneous Solutions. *Chem. Rev*, **2006**, *106*, 5413–5430.

[16] Yang, C.; Inoue, Y. Supramolecular Photochirogenesis. *Chem Soc. Rev.*, **2014**, *43*, 4123–4143.

[17] Bibal, B.; Mognin, C.; Bassini, D. M. Template Effects and Supramolecular Control of Photoreactions in Solution. *Chem Soc. Rev.*, **2014**, *43*, 4179–4198.

[18] Hammond, G. S.; Cole, R. S. Asymmetric Induction During Energy Transfer. *J. Am. Chem. Soc.*, **1965**, *87*, 3256–3257.

[19] Murov, S. L.; Cole, R. S.; Hammond, G. S. Mechanisms of Photochemical Reactions in Solution LIV. A New Mechanism for Photosensitization. *J. Am. Chem. Soc.*, **1968**, *90*, 2957–2958.

[20] Inoue, Y.; Kunitomi, Y.; Takamuku, S.; Sakurai, H. Asymmetric *cis–trans* Photoisomerization of Cyclo-octene Sensitized by Chiral Aromatic Esters. *J. Chem. Soc., Chem. Commun.* **1978**, 1024–1025.

[21] Inoue, Y.; Takamuku, S.; Kunitomi, Y.; Sakurai, H. Singlet Photosensitization of Simple Alkenes. Part 1. *cis–trans*-Photoisomerization of Cyclo-octene Sensitized by Aromatic Esters. *J. Chem. Soc. Perkin Trans. 2* **1980**, 1672–1677.

[22] Inoue, Y.; Yokoyama, T.; Yamasaki, N.; Tai, A. Temperature Switching of Product Chirality upon Photosensitized Enantiodifferentiating *cis-trans* Isomerization of Cyclooctene. *J. Am. Chem. Soc.* **1989**, *111*, 6480–6482.

[23] Inoue, Y.; Matsushima, E.; Wada, T. Pressure and Temperature Control of Product Chirality in Asymmetric Photochemistry. Enantiodifferentiating Photoisomerization of Cyclooctene Sensitized by Chiral Benzenepolycarboxylates. *J. Am. Chem. Soc.* **1998**, *120*, 10687–10696.

[24] Kim, J.-I.; Schuster, G. B. Enantioselective Catalysis of the Triplex Diels–Alder Reaction: Addition of *trans*-B-Methylstyrene to 1,3-Cyclohexadiene Photosensitized with (–)-1,1'-Bis(2,4-dicyanonaphthalene). *J. Am. Chem. Soc.* **1990**, *112*, 9635–9637.

[25] Kim, J.-I.; Schuster, G. B. *J.* Enantioselective Catalysis of the Triplex Diels–Alder Reaction: A Study of Scope and Mechanism. *Am. Chem. Soc.* **1992**, *114*, 9309–9317.

[26] Hoffmann, R.; Inoue, Y. Trapped Optically Active (E)-Cycloheptene Generated by Enantiodifferentiating Z−E Photoisomerization of Cycloheptene Sensitized by Chiral Aromatic Esters. *J. Am. Chem. Soc.* **1999**, *121*, 10702–10710.

[27] Ouannès, C.; Beugelmans, R.; Rossi, G. Asymmetric Induction During Triplet Energy Transfer. *J. Am. Chem. Soc.*, **1973**, *95*, 8472–8474.

[28] Based on the triplet energy of 1-indanone (76.6 kcal/mol), which should be very similar to 3-methyl-1-indanone; Case, W. A.; Kearns, D. R. Investigation of S → T and S → S Transitions by Phosphorescence Excitation Spectroscopy VII. 1-Indanone and Other Aromatic Ketones. *J. Chem. Phys.*, **1970**, *52*, 2175–2191.

[29] Data never published/based on a private communication: note 9 in reference 21.

[30] Hoshi, N.; Furukawa, Y.; Hagiwara, H.; Uda, H.; Sato, K. *Chem. Lett.*, **1980**, *9*, 47–50.

[31] Demuth, M.; Raghavan, P. R.; Carter, C.; Nakano, K. Schaffner, K. Photochemical High-yield Preparation of Tricyclo[3.3.0.0]octan-3-ones. Potential Synthons for Polycyclopentanoid Terpenes and Prostacyclin Analogues. Preliminary Communication. *Hel. Chim. Acta*, **1980**, *63*, 2434–2439.

[32] Rau, H.; Hörman, M. Kinetic Resolution of Optically Active Molecules and Asymmetric Chemistry: Asymmetrically Sensitized Photolysis of *trans*-3,5-Diphenylpyrazoline. *J. Photochem.*, **1981**, *16*, 231–247.

[33] Schneider, M. P.; Bibi, H.; Rau, H.; Ufermann, D.; Hörman, M. Photolysis of *cis*- and *trans*-3,5-Diphenyl-1-pyrazolines: Competing Trimethylene and Cycloreversion Pathways. *J. Chem. Soc., Chem. Commun.*, **1980**, 957–958.

[34] Engel, P. S.; Steel, C. Photochemistry of Aliphatic Azo Compounds in Solution. *Acc. Chem. Res.* **1973**, *6*, 275–281.

[35] Becker, E.; Weiland, R.; Rau, H. Photochemistry of Biochromophoric Molecules with Camphor Structure I. Energy Transfer and Asymmetric Effects. *J. Photochem. Photobiol. A: Chem.*, **1988**, *41*, 311–330.

[36] Cauble, D. F.; Lynch, V.; Krische, M. J. Studies on the Enantioselective Catalysis of Photochemically Promoted Transformations: "Sensitizing Receptors" as Chiral Catalysts. *J. Org. Chem.*, **2003**, *68*, 15–21.

[37] Bach, T.; Bergmann, H.; Harms, K. Enantioselective Intramolecular [2+2]-Photocycloadditions in Solution. *Angew. Chem. Int. Ed.*, **2000**, *112*, 2391–2393.

[38] Bach, T.; Bergmann, H. Enantioselective Intermolecular [2+2]-Photocycloaddition Reactions of Alkenes and a 2-Quinolone in Solution. *J. Am. Chem. Soc.*, **2000**, *122*, 11525–11526.

[39] Bach, T.; Aechtner, T.; Neumüller, B. Intermolecular Hydrogen Binding of a Chiral Host and A Prochiral Imidazolidinone: Enantioselective Norrish–Yang Cyclization in Solution. *Chem. Commun.* **2001**, 607–608.

[40] Bach, T.; Bergmann, H.; Grosch, B.; Harms, K. Highly Enantioselective Intra- and Intermolecular [2 + 2] Photocycloaddition Reactions of 2-Quinolones Mediated by a Chiral Lactam Host: Host−Guest Interactions, Product Configuration, and the Origin of the Stereoselectivity in Solution. *J. Am. Chem. Soc.*, **2002**, *124*, 7982–7990.

[41] Grosch, B.; Orlebar, C.; Herdtweck, E.; Massa, W.; Bach, T. Highly Enantioselective Diels–Alder Reaction of a Photochemically Generated *o*-Quinodimethane with Olefins. *Angew. Chem. Int. Ed.*, **2003**, *42*, 3693–3696.

[42] Bauer, A.; Westkämper, F.; Grimme, S.; Bach, T. Catalytic Enantioselective Reactions Driven by Photoinduced Electron Transfer. *Nature*, **2005**, *436*, 1139–1140.

[43] Müller, C.; Bauer, A.; Bach, T. Light-Driven Enantioselective Organocatalysis. *Angew. Chem. Int. Ed.*, **2009**, *48*, 6640–6642.

[44] Müller, C.; Bauer, A.; Maturi, M. M.; Cuquerella, M. C.; Miranda, M. A.; Bach, T. Enantioselective Intramolecular [2 + 2]-Photocycloaddition Reactions of 4-Substituted Quinolones Catalyzed by a Chiral Sensitizer with a Hydrogen-Bonding Motif. *J. Am. Chem. Soc.*, **2011**, *133*, 16689–16697.

[45] Maturi, M. M.; Wenninger, M.; Alonso, R.; Bauer, A.; Pöthig, A.; Riedle, E.; Bach, T. *Chem. Eur. J.*, **2013**, *19*, 7461–7472.

[46] Maturi, M. M.; Bach, T. Enantioselective Catalysis of the Intermolecular [2+2] Photocycloaddition between 2-Pyridones and Acetylenedicarboxylates. *Angew. Chem. Int. Ed.* **2014**, *53*, 7661–7664.

[47] Alonso, R.; Bach, T. A Chiral Thioxanthone as an Organocatalyst for Enantioselective [2+2] Photocycloaddition Reactions Induced by Visible Light. *Angew. Chem. Int. Ed.* **2014**, *53*, 4368–4371.

[48] Tröster, A.; Alonso, R.; Bauer, A.; Bach, T. Enantioselective Intermolecular [2 + 2] Photocycloaddition Reactions of 2(1*H*)-Quinolones Induced by Visible Light Irradiation. *J. Am. Chem. Soc.*, **2016**, 138, 7808–7811.

[49] Vallavoju, N.; Selvakumar, S.; Jockusch, S.; Sibi, M. P.; Sivaguru, J. Enantioselective Organo-Photocatalysis Mediated by Atropisomeric Thiourea Derivatives. *Angew. Chem. Int. Ed.* **2014**, *53*, 5604–5608.

[50] Vallavoju, N.; Selvakumar, S.; Jockusch, S.; Prabhakaran, M. J.; Sibi, M. P.; Sivaguru, J. Evaluating Thiourea Architecture for Intramolecular [2+2] Photocycloaddition of 4-Alkenylcoumarins. *Adv. Synth. Catal.* **2014**, *356*, 2763–2768.

[51] Lewis, F.D.; Howard, D. K.; Oxman, J. D. Lewis Acid Catalysis of Coumarin Photodimerization. *J. Am. Chem. Soc.* **1983**, *105*, 3344–3345.

[52] F. D. Lewis and S. V. Barancyk, *J. Am. Chem. Soc.*, 1989, **111**, 8653.

[53] Lewis, F. D.; Quillen, S. L.; Hale, P. D.; Oxman, J. D. Lewis Acid Catalysis of Photochemical Reactions. 7. Photodimerization and Cross-Cycloaddition of Cinnamic Esters. *J. Am. Chem. Soc.* **1988**, *110*, 1261–1267.

[54] Guo, H.; Herdtweck, E.; Bach, T. Enantioselective Lewis Acid Catalysis in Intramolecular [2+2] Photocycloaddition Reactions of Coumarins. *Angew. Chem. Int. Ed.* **2010**, *49*, 7782–7785.

[55] Brimoulle, R.; Guo, H.; Bach, T. Enantioselective Intramolecular [2+2] Photocycloaddition Reactions of 4-Substituted Coumarins Catalyzed by a Chiral Lewis Acid. *Chem. Eur. J.* **2012**, *18*, 7552–7560.

[56] Brimoulle, R.; Bach, T. Enantioselective Lewis Acid Catalysis of Intramolecular Enone [2+2] Photocycloaddition Reactions. *Science* **2013**, *342*, 840–843.

[57] Brimioulle, R.; Bauer, A.; Bach, T. Enantioselective Lewis Acid Catalysis in Intramolecular [2 + 2] Photocycloaddition Reactions: A Mechanistic Comparison between Representative Coumarin and Enone Substrates. *J. Am. Chem. Soc.* **2015**, *137*, 5170–5176.

[58] Brimoulle, R.; Bach, T. [2+2] Photocycloaddition of 3-Alkenyloxy-2-cycloalkenones: Enantioselective Lewis Aicd Catalysis and Ring Expansion. *Angew. Chem. Int. Ed.* **2014**, *53*, 12921–12924.

[59] Poplata, S.; Bach, T. Enantioselective Intermolecular [2+2] Photocycloaddition Reaction of Cyclic Enones and Its Application in a Synthesis of (−)-Grandisol. *J. Am. Chem. Soc.*, **2018**, *140*, 3228–3231.

[60] Hoffman, N. Photochemical Reactions as Key Steps in Organic Synthesis. *Chem. Rev.* **2008**, *108*, 1052–1103.

[61] Stegbauer, S.; Jandl, C.; Bach, T. Enantioselective Lewis Acid Catalyzed *ortho* Photocycloaddition of Olefins to Phenanthrene-9-carboxyaldehydes. *Angew. Chem. Int. Ed.* **2018**, *57*, 14593–14596.

[62] Skubi, K.L.; Blum, T. R; Yoon, T.P. Dual Catalysis Strategies in Photochemical Synthesis. *Chem. Rev.*, **2016**, *116*, 10035–10074.

[63] Yoon, T. P. Photochemical Stereocontrol Using Tandem Photoredox–Chiral Lewis Acid Catalysis *Acc. Chem. Res.*, **2016**, *49*, 2307–2315.

[64] Blum, T.R.; Miller, Z. D.; Bates, D. M.; Guzei, I. A.; Yoon, T. P. Enantioselective Photochemistry through Lewis Acid-Catalyzed Triplet Energy Transfer. *Science* **2016**, *354*, 1391–1395.

[65] Miller, Z. D., Lee, B.J.; Yoon, T. P. Enantioselective Crossed Photocycloadditions of Styrenic Olefins by Lewis Acid Catalyzed Triplet Sensitization. *Angew. Chem. Int. Ed.* **2017**, *56*, 11891–11895.

[66] Daub, M. E.; Jung. H.; Lee, B. J.; Won, J.; Baik, M.-H.; Yoon, T. P. Enantioselective [2+2] Cycloadditions of Cinnamate Esters: Generalizing Lewis Acid Catalysis of Triplet Energy Transfer. *J. Am. Chem. Soc.* **2019**, *141*, 9543–9547.

[67] Huo, H.; Shen, X.; Wang, C.; Zhang, L.; Röse, P.; Chen. L.–A.; Harms, K.; Marsch, M.; Hilt, G.; Meggers, E. Asymmetric Photoredox Transition-Metal Catalysis Activated by Visible Light. *Nature*, **2014**, *515*, 100–103.

[68] Huang, X.; Quinn, T.R.; Harms, K.; Webster, R. D.; Zhang, L.; Wiest, O.; Meggers, E. Direct Visible-Light-Excited Asymmetric Lewis Acid Catalysis of Intermolecular [2+2] Photocycloadditions. *J. Am. Chem. Soc.* **2017**, *139*, 9120–9123.

[69] Hu, N.; Jung, H.; Zheng, Y.; Lee, J.; Zhang, L.; Ullah, Z.; Xie, X.; Harms, K.; Baik, M.-H.; Meggers, E. Catalytic Asymmetric Dearomatization by Visible-Light-Activated [2+2] Photocycloaddition. *Angew. Chem. Int. Ed.* **2018**, *57*, 6242–6246.

[70] Skubi, K. L.; Kidd, J. B.; Jung, H.; Guzei, I. A.; Baik, M.-H.; Yoon, T. P. Enantioselective Excited-State Photoreactions Controlled by a Chiral Hydrogen-Bonding Iridium Sensitizer. *J. Am. Chem. Soc.* **2017**, *139*, 17186–17192.

[71] Huang, X.; Li, X.; Xie, X. Harms, K.; Riedel, R.; Meggers, E. Catalytic Asymmetric Synthesis of a Nitrogen Hetereocycle Through Stereocontrolled Direct Photoreaction from Electronically Excited State. *Nat. Commun.* **2017**, *8*, Article 2245.

[72] Hobmeier, A.-H.; Bauer, A.; Silva, A. V.; Huber, S. M.; Bannwarth, C.; Bach, T. Catalytic Deracemization of Chiral Allenes by Sensitized Excitation with Visible Light. *Nature* **2018**, *564*, 240–243.

[73] Tröster, A.; Bauer, A.; Jandl, C.; Bach, T. Enantioselective Visible-Light Mediated Formation of 3-Cyclopropylquinolones by Triplet-Sensitized Deracemization. *Angew. Chem. Int. Ed.* **2019**, *58*, 3538–3541.

Chapter 2. Enantioselective Intermolecular [3+2] Cycloadditions *via* Lewis-Acid Catalyzed Photoinduced Electron Transfer

Portions of this work have previously been published:

Amador, A. G.; Sherbrook, E. M.; Yoon, T. P. Enantioselective Photocatalytic [3+2] Cycloadditions of Aryl Cyclopropyl Ketones. *J. Am. Chem. Soc.* **2016**, *138*, 4722–4725.

2.1: Introduction

2.1.1: Stereocontrol in [2+2] Photocycloadditions *via* a Dual Catalytic Approach

Stereoselective ring-forming reactions are highly regarded for their ability to rapidly build up molecular complexity in few chemical steps.[1–3] Cycloadditions are particularly useful in the preparation of complex, biologically-relevant molecules, in addition to serving as a compelling model reaction for the development of new conceptual approaches in asymmetric catalysis. Despite these motivations, there are few broadly applicable methods for the control of absolute stereochemistry in *photochemical* cycloadditions.[4,5] In the past decade, a short list of primarily organocatalytic[6–11] and Lewis acid[12–19] catalyzed asymmetric photocycloadditions have been developed. However, these have largely focused on [2+2] cycloadditions involving enones, and other types of photocycloadditions have remained surprisingly underrepresented, despite the prevalence of five- and six-membered rings among molecules with useful bioactive properties.

In 2014, our group reported a stereoselective intermolecular [2+2] photocycloaddition reaction between aryl and alkyl enones to efficiently and selectively generate functionalized cyclobutane products in excellent diastereomeric and enantiomeric ratios (Scheme 2-1).[20] This method relies on a dual catalytic approach that allows for largely independent optimization of photochemical and stereochemical variables, while still requiring both catalysts for the key photochemical activation to occur. The latter relies on a photoinduced single-electron transfer event, which reduces the aryl enone (**2.1**) to its corresponding radical anion (**2.3**). This key photoreduction step requires an oxophillic Lewis acid which, through coordination to the enone, alters its reduction potential to allow for the generation of the key chiral radical anion intermediate.

Scheme 2-1. Enantioselective [2+2] cycloadditions *via* dual photoredox and Lewis acid catalysis

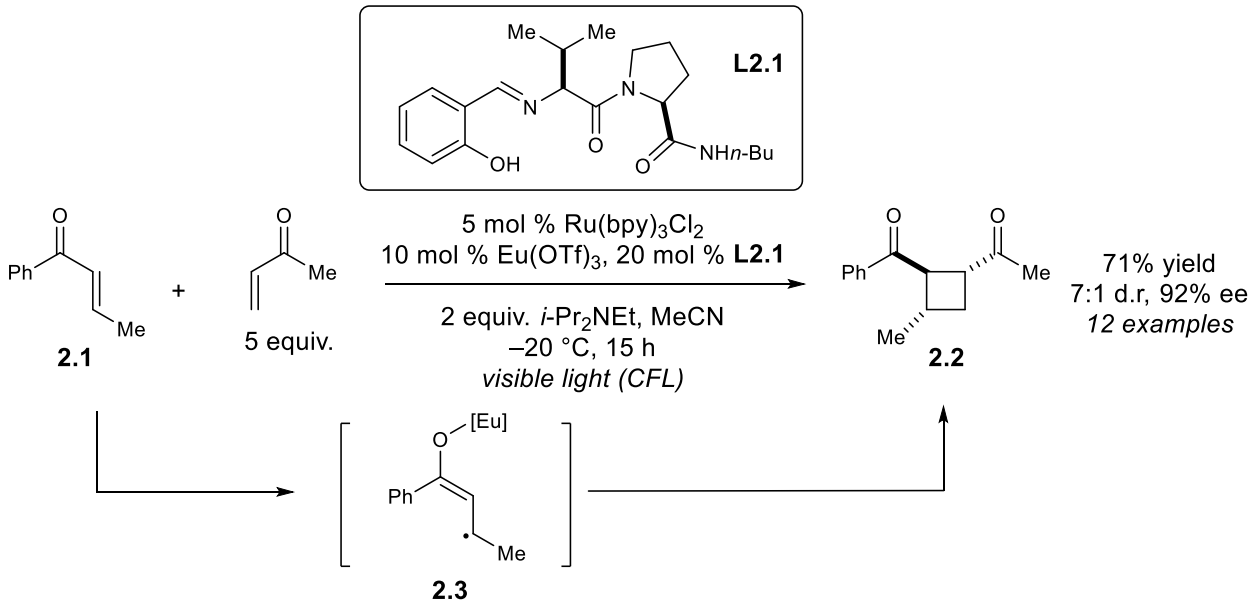

The Lewis acid and ligand combinations which facilitate this single electron transfer step are highly variable. In development of the above reaction, both parameters were extensively tuned to select for both high yields and high stereoselectivities. Within the field of asymmetric catalysis, the variety of chiral ligands that have been developed for use in conjunction with simple Lewis acids is quite extensive. Given this well-established platform, we speculated that this dual catalytic strategy might not be capable of stereocontrol only in [2+2] cycloaddition reactions but also in other reactions that have been demonstrated to be compatible with photoredox catalysis.[21–23,]

2.1.2: Development of Intra- and Intermolecular [3+2] Photocycloadditions

Our laboratory has recently demonstrated that [3+2] photocycloadditions are amenable to activation by photoredox catalysis, allowing for the preparation of cyclopentanes from olefin and cyclopropane building blocks (Scheme 2-2).[24] While cyclopropanes have been previously

employed in asymmetric [3+2] cycloaddition reactions,[25–29] virtually all of these methods require the use of highly activated "donor-acceptor" cyclopropanes. This requirement is based on the weakening of a specific C–C bond in the strained backbone of the cyclopropane ring between two polarizing functional groups, such that it can undergo a cycloaddition as a functional 1,3-dipole.

Scheme 2-2. Intramolecular [3+2] photocycloadditions of aryl cyclopropyl ketones

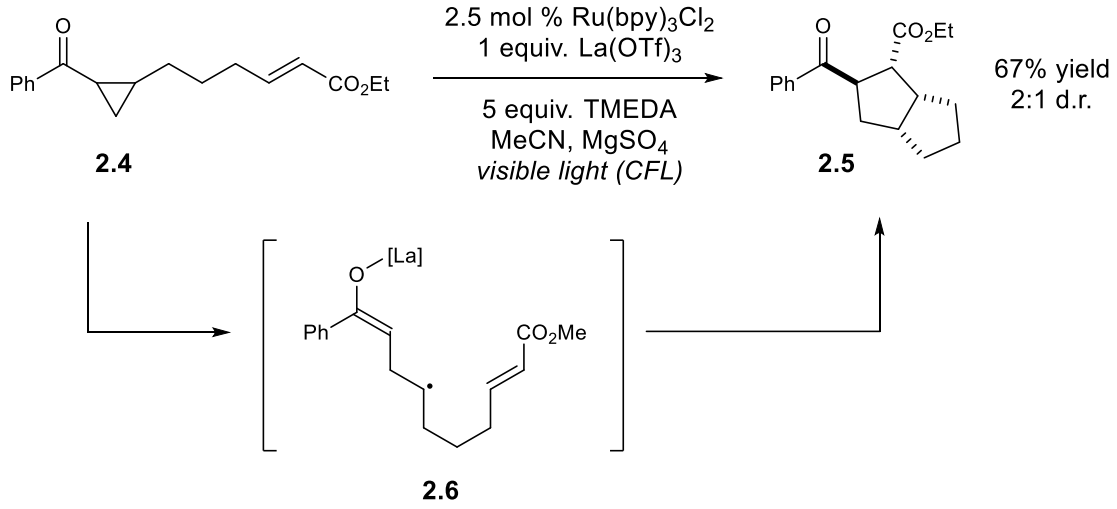

The basis of the activation of cyclopropyl ketones through photoredox catalysis does not impose this requirement. Instead, this type of activation relies on the propensity of cyclopropane-adjacent radicals to trigger a rapid ring-opening process. In the example above, the Lewis-acid catalyzed reduction of an aryl ketone (**2.4**) to the corresponding ketyl radical triggers the ring opening to generate radical intermediate **2.6**. This ring-opened radical then reacts with the tethered alkene and is re-oxidized to generate the bicyclopentane product (**2.5**).

Further investigation revealed that, with some additional optimization, this reaction could also be performed in an intermolecular fashion (Scheme 2-3).[30] Through the use of substoichiometric quantities of a different lanthanide Lewis acid, $Gd(OTf)_3$, as well as decreased quantities of tetramethylethyenediamine (TMEDA), which serves both as a reductive quencher for

$Ru(bpy)_3^{2+*}$ and as a ligand for $Gd(OTf)_3$, high-yielding and highly diastereoselective reaction conditions were identified a variety of cyclopropane and olefin reaction partners.

Scheme 2-3. Development of an intermolecular [3+2] cycloaddition

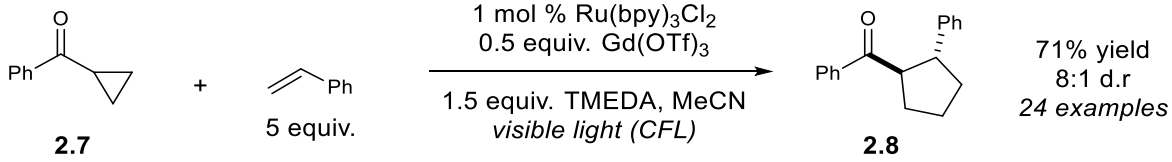

Notably, a key feature shared by the intramolecular and intermolecular [3+2] cycloadditions described above is the requirement of an oxophillic Lewis acid. In both cases, the Lewis acid is required to enable the one-electron photoreduction of the aryl ketone, which then triggers the necessary cyclopropane ring-opening step. Consequently, we were interested to see if the inclusion of a series of chiral ligands capable of binding to these Lewis acids would allow us to carry out this reaction with high enantiocontrol. Due to the involvement of both the Lewis acid and photocatalyst in the key step, we were confident that background reactivity in the absence of a chiral catalyst could be easily minimized given the judicious choice of a ligand which remains tightly bound to the chosen Lewis acid. Furthermore, we were intrigued by the potential synthetic utility of a stereoselective [3+2] cycloaddition that would not be restricted by the need for highly pre-functionalized cyclopropanes.

2.2: Results and Discussion

2.2.1: Reaction Optimization

Initial reaction development began with the investigation of several different classes of chiral ligands that are known to be effective in binding lanthanide Lewis acids (Table 2-1). The

optimal Lewis acid from the racemic intermolecular [3+2] cycloaddition, $Gd(OTf)_3$ was carried forward as the chosen catalyst. However, *i*-Pr_2NEt was chosen to serve as the reductive quencher instead of TMEDA, as the former is less coordinating and so is less likely to out-compete a chiral ligand. In the absence of ligand under these reaction conditions, 93% yield of the desired cycloadduct (**2.10**) was obtained in 5:1 d.r.. Of the classes of ligand screened (**L2.2**-**L2.5**), most had essentially no effect on the enantioselectivity of the [3+2] cycloaddition. Fortunately, we did observe small but appreciable selectivities with *i*-PrPybox (**L2.5**, 10% yield, 38% ee), although the desired product was generated in a very low yield. Further investigation of Pybox ligands (**L2.6**-**L2.8**) with variable side chains revealed improved results with *s*-BuPybox (**L2.8**, 25% yield, 59% ee), although yields remained fairly low.[31–34]

Table 2-1. Preliminary investigation of chiral ligand scaffolds

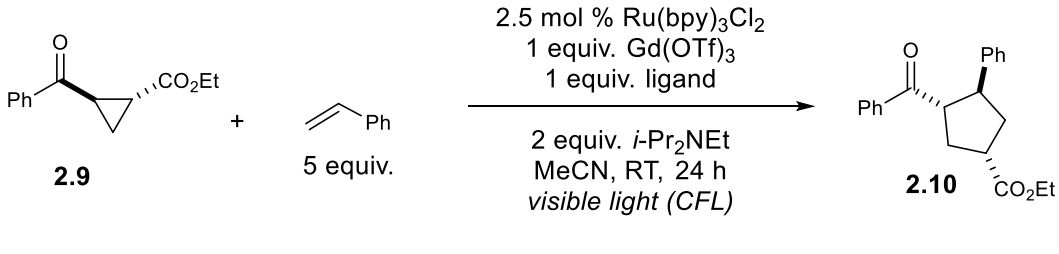

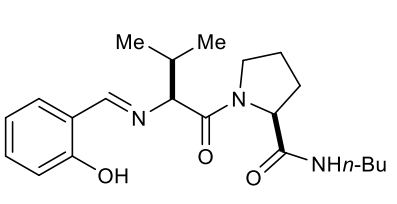

L2.2
70% yield
0 % ee

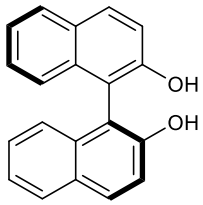

L2.3
0% yield

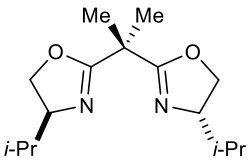

L2.4
92% yield
0 % ee

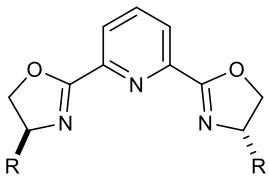

L2.5 R = *i*-Pr, 10% yield, 2.5:1 d.r., 38% ee
L2.6 R = *t*-Bu, 96% yield, 3:1 d.r., 45% ee
L2.7 R = *i*-Bu, 0% yield
L2.8 R = *s*-Bu, 25% yield, 2:1 d.r., 59% ee

Table 2-2. Final optimization studies

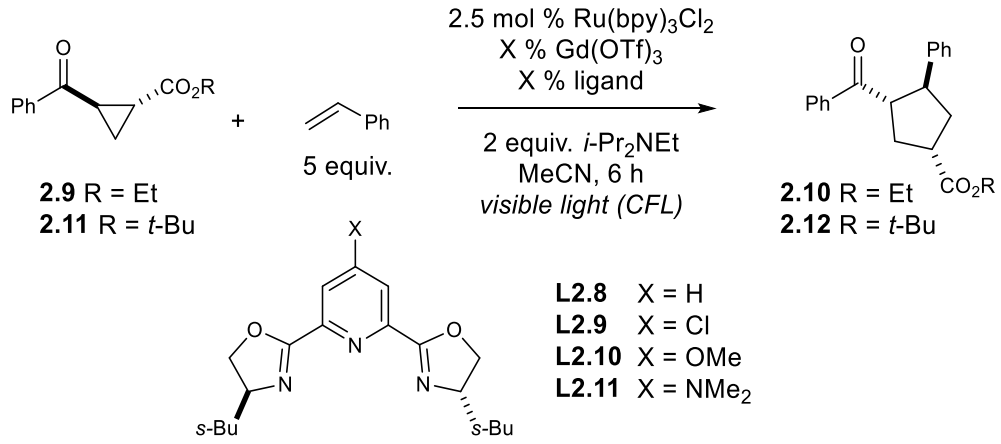

Entry	Conditions[a]	Yield[b]	d.r.; % ee
1	100% $Gd(OTf)_3$, 100% **L2.8**	25 %	2:1; 59 %
2	100% $Gd(OTf)_3$, 200% **L2.8**	36 %	3:1; 63 %
3	100% $Gd(OTf)_3$, 200% **L2.9**	0 %	--; --
4	100% $Gd(OTf)_3$, 200% **L2.10**	90 %	2:1; 64%
5	100% $Gd(OTf)_3$, 200% **L2.11**	89 %	2:1; 85%
6	10% $Gd(OTf)_3$, 20% **L2.11**	96 %	2:1; 79%
7	10% $Gd(OTf)_3$, 20% **L2.11,** 0 °C	80 %	3:1; 85%
8[c]	10% $Gd(OTf)_3$, 20% **L2.11,** 0 °C	86 %	3:1; 90%
9[c,d]	10% $Gd(OTf)_3$, 20% **L2.11,** 0 °C	95 %	3:1; 93%

[a] Reactions carried out on 0.045 mmol scale using a 23 W CFL. [b] Yields determined by ^{1}H-NMR using phenanthrene as an internal standard.[c] Using **2.11** instead of **2.9**. [d] Using 1 equiv. *i*-Pr_2NEt.

Additional experiments with **L2.8** revealed that a majority of product formation occurred within the first hour, beyond which increasing amounts of an inactive Lewis acid-base complex (composed of $Gd(OTf)_3$ and i-Pr_2NEt) were observed. Increasing the ligand-to-metal ratio to slow the formation of a deactivated complex was met with little benefit (Table 2-2, entry 2). Alternatively, we wondered if the active Gd-pybox complex could be stabilized by increasing the coordinating ability of the ligand. Gratifyingly, while a chloride-substituted Pybox ligand (**L2.9**,

entry 3) resulted in no product formation, a methoxy-substituted pybox ligand (**L2.10**, entry 4) provided **2.8** in excellent yield. Finally, dimethylamino-*sec*-butylpybox ligand **L2.11** provided excellent rates and stereoselectivities (entry 5). Furthermore, this ligand allowed for the Lewis acid loading to be decreased to 10 mol% with little effect on ee (entry 6). Lowering the temperature to 0 °C resulted in an increase in the enantioselectivity to 85% ee (entry 7). Increasing the bulk of the ester substituent provided somewhat higher ee at 0 °C (entry 8), and the occurrence of a reductive ring-opening side-product could be minimized by lowering the concentration of i-Pr_2NEt (entry 9). Under these conditions, cycloadduct **2.12** was obtained in 95% yield, 93% ee, and 3:1 d.r.

2.2.2: Substrate Scope

We next conducted an exploration of the scope of the enantioselective cycloaddition under these optimized conditions. First, we studied the effect of varying the structure of the alkene reaction partner (Table 2-3).[35] In section 2.2.3, we propose a stepwise cycloaddition initiated by radical addition of a ring-opened distonic radical anion to an alkene. Consistent with this, simple aliphatic alkenes are not reactive. However, a variety of electronically modified styrenes react smoothly and with good ee (**2.12–2.15**). Potentially reactive aryl halides are well tolerated (**2.16**), providing a handle for derivatization of the enantioenriched cycloadducts. The enantioselectivity is relatively insensitive to the position of substituents on the aryl ring (**2.17**). Internal olefins, unfortunately, were unreactive under these reaction conditions; however, 1,1-disubstituted styrenes react smoothly and provide excellent ee (**2.18–2.20**). While heterocycles containing Lewis basic heteroatoms resulted in a loss in stereoselectivity, alkenes bearing less basic heterocycles such as

carbazoles react smoothly with good ee (**2.21**). Finally, dienes are also competent reaction partners, affording vinyl cyclopentane products in good ee (**2.22**, **2.23**).

Table 2-3. Alkene substrate scope[a]

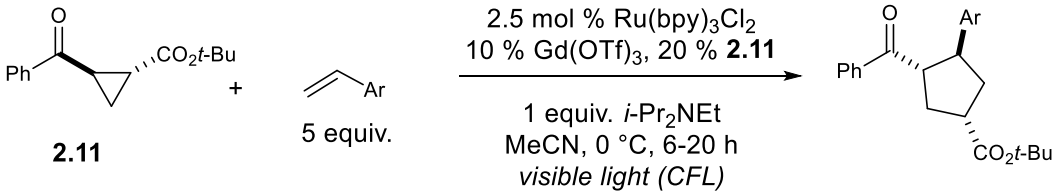

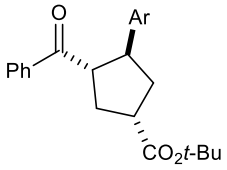

2.12 Ar = C_6H_5, 95% yield, 93% ee, 3:1 d.r.
2.13 Ar = 4-$MeOC_6H_4$, 89% yield, 91% ee, 3:1 d.r.
2.14 Ar = 4-MeC_6H_4, 90% yield, 89% ee, 3:1 d.r.
2.15 Ar = 4-$CF_3C_6H_4$, 81% yield, 89% ee, 2:1 d.r.
2.16 Ar = 4-BrC_6H_4, 86% yield, 90% ee, 2:1 d.r.
2.17 Ar = 2-MeC_6H_4, 75% yield, 87% ee, 2:1 d.r.

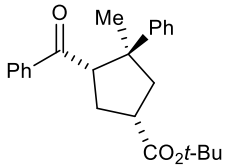

2.18
80% yield
90% ee, 3:1 d.r.

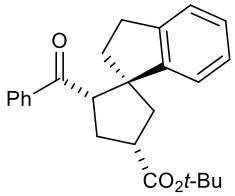

2.19
95% yield
97% ee, 3:1 d.r.

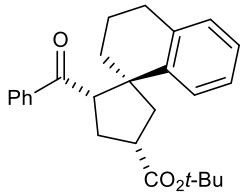

2.20
95% yield
>99% ee, 2:1 d.r.

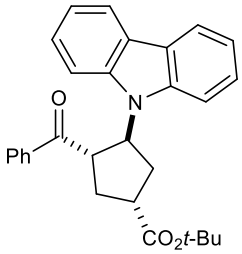

2.21
55% yield
86% ee, 2:1 d.r.

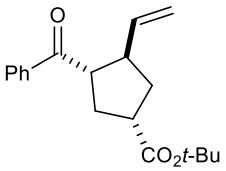

2.22
59% yield
87% ee, 3:1 d.r.

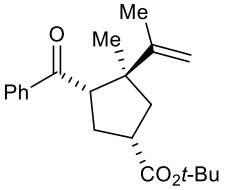

2.23
77% yield
86% ee, 3:1 d.r.

[a] Combined isolated yields of all diastereomers. Major diastereomer shown.

The scope of this reaction with respect to the cyclopropyl aryl ketone component was next explored (Table 2-4). The aryl moiety tolerates significant electronic variation: both electron-rich

and electron-deficient substituents provided the corresponding cyclopentanes in good yield and excellent ee (**2.24**–**2.27**). Heteroaryl cyclopropyl ketones are also tolerated (**2.28**), although the enantioselectivity suffers if the heterocycle is positioned to provide an alternate site for Lewis acid chelation (**2.29**). Similarly, while arenes with substituents at the 3-position have minimal impact on the selectivity of the reaction (**2.30**), those with substituents at the 2-position appear to interrupt binding of the Lewis acid (**2.31**)**.** The ester moiety can be replaced by a ketone with minimal impact on the stereoselectivity and an improvement in diastereoselectivity (**2.32**), but a methyl-substituted cyclopropane provides poor ee (**2.33**). Selectivity can be recovered using cyclopropyl ketones bearing geminal β-dialkyl substituents (**2.34**, **2.35**), although forcing conditions were required.

Table 2-4. Cyclopropane substrate scope[a]

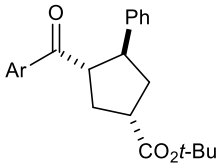

2.24 Ar = 4-$MeOC_6H_4$, 88% yield, 91% ee, 3:1 d.r.
2.25 Ar = 4-MeC_6H_4, 90% yield, 96% ee, 3:1 d.r.
2.26 Ar = 4-$CF_3C_6H_4$, 87% yield, 99% ee, 3:1 d.r.
2.27 Ar = 4-ClC_6H_4, 90% yield, 92% ee, 3:1 d.r.

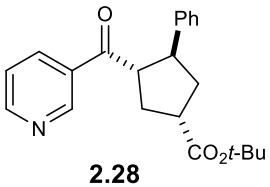

2.28
57% yield
94% ee, 2:1 d.r.

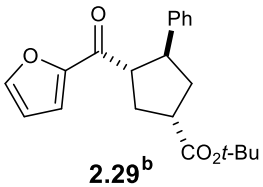

2.29[b]
80% yield
80% ee, 4:1 d.r.

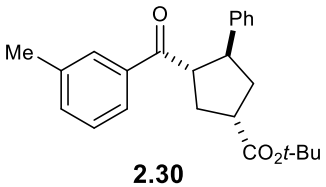

2.30
87% yield
89% ee, 3:1 d.r.

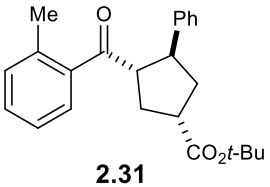

2.31
61% yield
71% ee, 2:1 d.r.

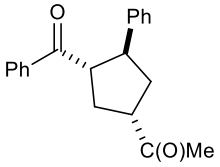

2.32
47% yield
88% ee, >20:1 d.r.

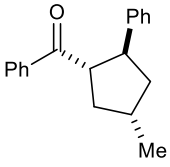

2.33[b]
57% yield
50% ee, >20:1 d.r.

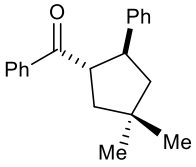

2.34[b]
85% yield
89% ee, 5:1 d.r.

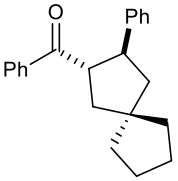

2.35[b]
88% yield
94% ee, 5:1 d.r.

[a] Conditions identical to those in Table 2-3, with a time of 6 h. Combined isolated yields of all diastereomers. Major diastereomer shown. [b] Using 20 mol% $Gd(OTf)_3$, 30 mol% **L2.11**, and 2 equiv. *i*-Pr_2NEt at –20 °C for 48 h.

2.2.3: Reaction Mechanism

The proposed reaction mechanism for this enantioselective [3+2] photocycloaddition is shown below (Scheme 2-4). Photoexcitation of $Ru(bpy)^{2+}$ is followed by reductive quenching by the electron rich amine to generate $Ru(bpy)^{+}$, a potent reductant. This selectively carries out the one electron reduction of a Gd-bound cyclopropyl ketone, [Gd]-**2.11**, to afford the corresponding ketyl radical. This species undergoes a rapid and reversible ring opening to generate a linear alkyl radical, followed by slow, stepwise addition to styrene to generate the ketyl radical [Gd]-**2.12**$^{\bullet-}$. Formation of **2.12** *via* one-electron oxidation can occur either through electron transfer with the photogenerated amine radical cation or through a chain mechanism involving an available molecule of [Gd]-**2.11.**

Scheme 2-4. Proposed reaction mechanism

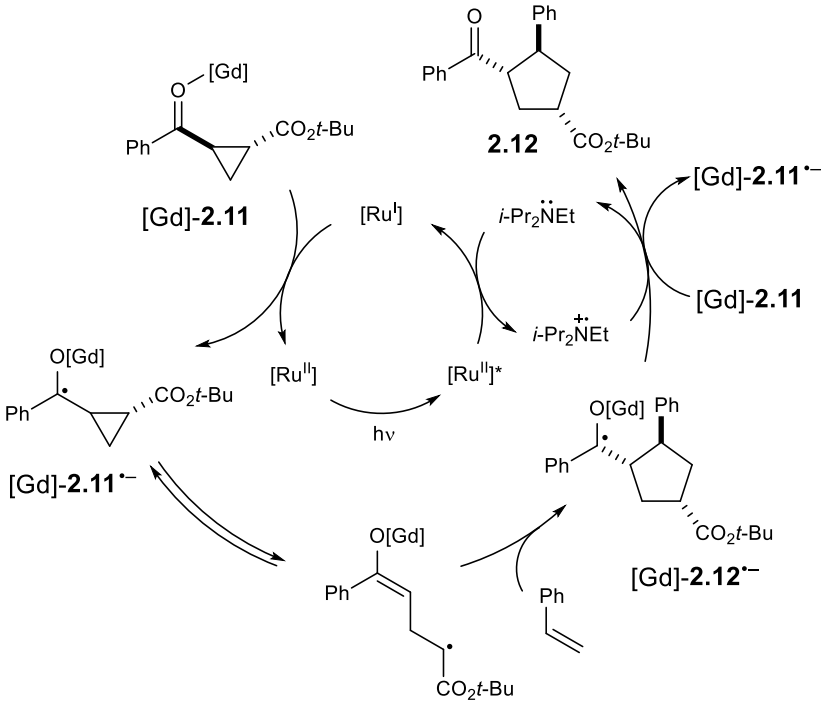

Scheme 2-5. Kinetic isotope effect study

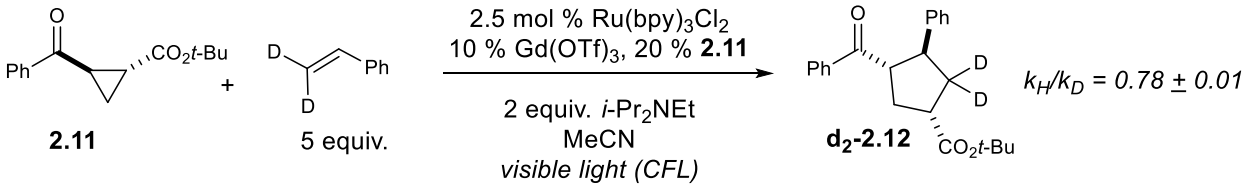

The mechanism proposed above is supported by several experiments. First, comparison of the standard reaction involving styrene to a reaction with d_2-styrene results in a secondary inverse kinetic isotope effect (k_H/k_D = 0.78), consistent with a rate-limiting step of intermolecular C–C bond formation (Scheme 2-5, also section 2.5.10.2**)**. This is further supported by extremely sluggish reactivity with olefins bearing a 1,2-disubstitution pattern.

Scheme 2-6. [3+2] cycloadditions with trisubstituted cyclopropyl ketones

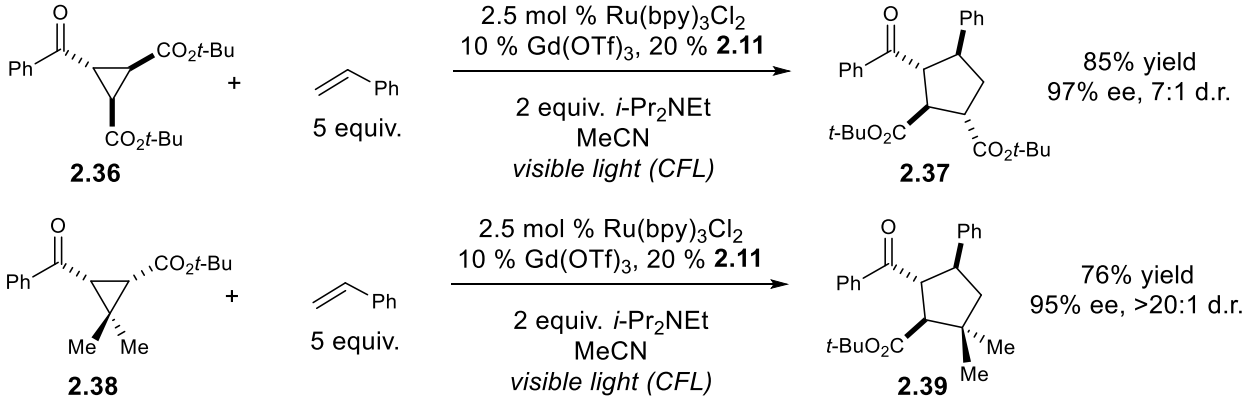

Second, the ring opening of similar cyclopropyl ketyl radicals has been reported by Tanko to be both reversible and endergonic.[36] In line with this, we observed that a reaction with *cis*-**2.11** resulted in nearly complete isomerization to *trans*-**2.11** in only 1 h, well before the reaction is complete (see supporting information, Figure 2-2). Furthermore, racemic trisubstituted cyclopropane **3.36** undergoes a stereoconvergent reaction to generate **3.37** good diastereoselectivity and excellent enantioselectivitity (Scheme 2-6). Interestingly, for **3.38**,

exquisite chemoelectivity for the formation of **3.39** is observed with none of its constitutional isomer, despite the ability for the starting cyclopropane to undergo C–C bond cleavage two possible positions. The resulting high diastereo- and enantioselectivity are then necessarily the result of a dynamic kinetic transformation.

2.2.4: Product Derivatization

Scheme 2-7. Divergent cleavage of the aryl ketone moiety *via* Baeyer–Villiger oxidation

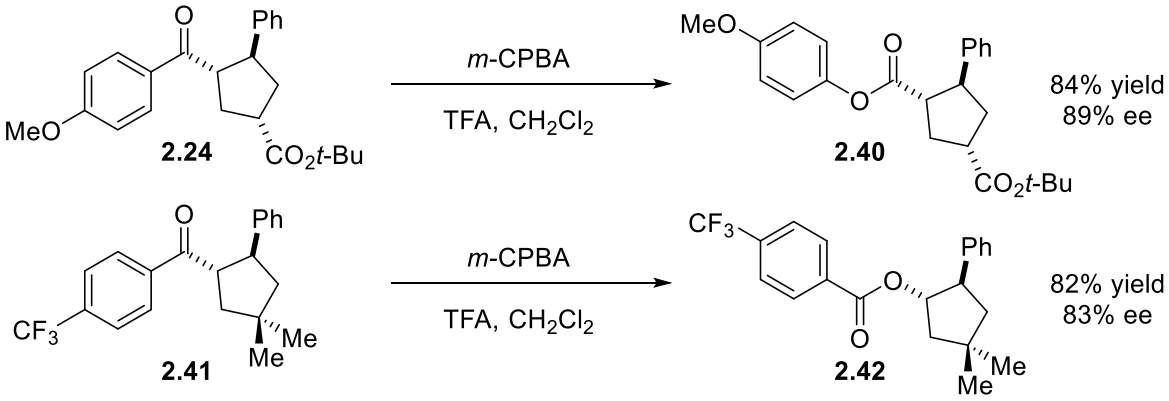

This asymmetric [3+2] photocycloaddition is a complementary approach to known enantioselective reactions of donor-acceptor cyclopropanes. Therefore, the strict requirement that an *aryl ketone* be present to enable initial one-electron reduction process appears to impose a significant limitation on scope. For this reason, we wondered if the aryl ketone could be removed through a Baeyer–Villiger cleavage reaction without impacting the any stereochemical information (Scheme 2-7). Conveniently, we found that 4-methoxyphenyl ketone **2.24** undergoes a high yielding regioselective oxidation to afford **2.40**, which is now poised for further manipulation into diverse carboxylic acid derivatives. Under these same conditions, 4-trifluoromethylphenyl ketone **2.41** undergoes a complementary oxidation to afford benzoate ester

2.42, which now permits access to enantioenriched cyclopentanols. While the specifics of the photoredox activation mechanism employed in this reaction imposes certain limitations on the cyclopropane component of this reaction, simple Baeyer–Villiger oxidation chemistry mitigates this limitation. Furthermore, reactivity with a variety of electronically diverse aryl cyclopropyl ketones in conjunction with this cleavage reaction permits access to a rather an unexpectedly diverse array of stereochemically enriched five-membered carbocycles.

2.3: Conclusion

These investigations have resulted in several distinct advancements. First, we have developed an operationally convenient and highly enantioselective method for the preparation of complex cyclopentane products. This method retains distinct advantages over existing methodologies, which typically require highly prefunctionalized donor-acceptor cyclopropanes. Furthermore, the involvement of radical intermediates allows for the use of substrates which are highly electronically varied and facilitates ring-opening through a mechanism that is not typically employed in [3+2] cycloadditions. Beyond these practical benefits, this reaction showcases that the compatibility of chiral Lewis acid catalysis and photocatalysis can be extended beyond [2+2] cycloadditions. This ongoing effort demonstrates that this dual catalytic approach is potentially a general solution to stereocontrol in reactions amenable to activation by photoredox catalysis.

2.4: Contributions

Adrian Amador was responsible for initial optimization of this reaction and was instrumental in the development of the reaction scope and mechanistic experiments.

2.5: Supporting Information

2.5.1: General Information

MeCN, THF, and CH_2Cl_2 were purified by elution through alumina as described by Grubbs.[37] $Gd(OTf)_3$, $La(OTf)_3$, and other Lewis acids were purchased from Strem, stored in a glove box, and used without further purification. Styrene, diisopropylethylamine, *N,N,N',N'*-tetramethylethylenediamine, triethylamine, tributylamine, 1,4-dimethylpiperazine, N-methylpyrrolidine, *N,N,N',N'*-tetramethylpropylenediamine, *N,N,N',N'*-tetramethylbutanediamine, ethyldicyclohexylamine, N,N-dimethylbenzylamine, *N*-methylpiperidine, 4-methylmorpholine, *N,N,N',N'*-tetramethylphenylenediamine, *N,N,N',N'*-tetramethylbenzidine, *N,N,N',N'',N''*-pentamethyldiethylenetriamine, 1,2,2,6,6-pentamethylpiperidine, 4-aminophenol, *p*-toluidine, 4-methoxy-*N*,*N*-diphenylaniline, 2,6-di-*tert*-butyl-4-methyl-phenol, 2,4,6-trimethylaniline, DABCO, 2,6-lutidine, and DBU were purchased from Sigma Aldrich and subsequently purified either by distillation or recrystallization. K_4FeCN_6 hexahydrate, cesium oxalate, and *(R,R)*-binaphthol were purchased from Sigma Aldrich and used without further purification. All glassware was oven-dried at 130 °C overnight or flame-dried immediately prior to use. Flash column chromatography was performed with Silicycle 40-63A silica (230-400 mesh). A 23W (1200 lumens) SLI Lighting Mini-Lynx compact fluorescent light bulb was used for all photochemical reactions.

^1H and ^{13}C NMR data for all previously uncharacterized compounds were obtained using a Bruker AVANCE-400 spectrometer and are referenced to TMS (0.0 ppm) and $CDCl_3$ (77.0 ppm), respectively. This instrument and supporting facilities are funded by the NSF (CHE-1048642) and the University of Wisconsin. NMR data are reported as follows: chemical shift, multiplicity (s =

singlet, d = doublet, t = triplet, q = quartet, p = pentet, sext = sextet, sept = septet, m = multiplet), coupling constant(s) in Hz, integration. NMR spectra were obtained at 298 K unless otherwise noted. IR spectral data were obtained using a Bruker Vector 22 spectrometer. Melting points were obtained using a Mel-Temp II (Laboratory Devices, Inc., USA) melting point apparatus. Mass spectrometry was performed with a Micromass LCT (electrospray ionization, time-of-flight analyzer or electron impact). These facilities are funded by the NSF (CHE-9974839, CHE-9304546) and the University of Wisconsin. Enantiomeric excesses were determined by chiral SFC of isolated material using a Waters Investigator system with Daicel CHIRALPAK® columns and Chromasolv®-grade *i*-PrOH, MeOH, and hexanes. Optical rotations were measured using a Rudolph Research Autopol III polarimeter at room temperature in CH_2Cl_2.

2.5.2: Ligand Synthesis

Synthesis of Box and PyBox ligands: Bis(oxazoline) ligands and pyridine bis(oxazoline) ligands were synthesized as described by Pires.[38] A representative procedure is shown below.

2,6-Bis(*(S)*-4-isopropyl-4,5-dihydrooxazol-2-yl)pyridine: A 250 mL round bottom flask was

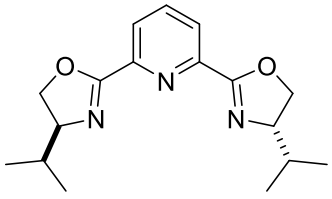

charged with pyridine-2,6-dicarbonitrile (2.1692 g, 16.8 mmol, 1 equiv.), zinc triflate (422 mg, 1.2 mmol, 0.07 equiv.) and anhydrous toluene (100 mL). A solution of *(S)*-valinol (3.47 g, 33.6 mmol, 2 equiv.) in toluene (20 mL) was added. The flask was fit with a reflux condenser and purged several times with nitrogen. The solution was heated under reflux for 48 h. After cooling, the reaction mixture was diluted with EtOAc (200 mL). The solution was then washed with saturated NaCl

(3x100 mL), saturated $NaHCO_3$ (3x100 mL), and water (100 mL). The organic layer was then dried over Na_2SO_4, filtered, and concentrated under reduced pressure to give the product as an off-white crystalline solid. The crude product was purified by recrystallization from hexanes and EtOAc to give the pure product as a white crystalline solid (4.31 g, 14.3 mmol, 85 % yield). Spectroscopic data match those reported previously in the literature.[2]

2,6-Dicarboxypyridine 1-oxide: Prepared using a procedure described by Mitsui and Parquette.[39]

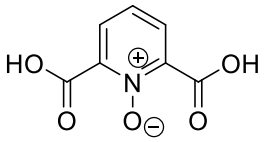

A 500 mL round-bottomed flask was charged with $Na_2WO_4 \cdot 2H_2O$ (1.91 g, 5.79 mmol), pyridine-2,6-dicarboxylic acid (30.0 g, 180 mmol), and 30 % aq. H_2O_2 (90 mL). The reaction flask was equipped with a reflux condenser and heated to 100 °C . After 2 h, an additional 210 mL of 30 % aq. H_2O_2 was added at room temperature. The reaction mixture was stirred at 100 °C for an additional 14 h, after which the reaction mixture had become homogeneous. The reaction mixture was then cooled to 0 °C, and the resulting white precipitate was separated by filtration. The filter cake was washed several times with ice-cold H_2O. The filtrate was washed with $CHCl_3$ (3x200 mL) to afford additional product. The combined solid crude product was purified by recrystallization from boiling H_2O. The isolated crystalline product was dried over P_2O_5 under reduced pressure at 80 °C for 15 h to provide 2,6-dicarboxypyridine-N-oxide as a white crystalline solid (19.1 g, 104 mmol, 58 % yield). All spectroscopic data match those reported previously in the literature. ^{1}H NMR (400 MHz, $CDCl_3$) δ 15.9 (br s, 2H), 8.23 (d, *J* = 8.0 Hz, 2H), 7.95 (t, *J* = 8.0 Hz, 1H). ^{13}C NMR (125 MHz, $CDCl_3$) δ 161.3, 139.7, 132.7, 129.4. Mp = 157–159 °C.

4-Chloropyridine-2,6-dicarbonyl dichloride: Prepared using a procedure described by Mitsui and Parquette.[39] A 250 mL flame-dried round-bottomed flask was charged with 2,6-dicarboxypyridine 1-oxide (5.30 g, 22.2 mmol) and anhydrous CH_2Cl_2 (50 mL). The reaction flask was sealed with a septum and purged several times with nitrogen. The reaction flask was then cooled to –10 °C and oxalyl chloride (25.0 mL, 291 mmol) was added slowly over 5 min. After stirring for 10 min, one drop of dry DMF was added to the suspension via syringe. The reaction mixture was allowed to warm very slowly to room temperature over a 12 h period and then stirred an additional 60 h. The excess oxalyl chloride and solvent were removed under aspirator pressure at room temperature to yield crude 4-chloropyridine-2,6-dicarbonyl dichloride as a pale yellow solid. The crude product was further purified by bulb-to-bulb distillation to afford the pure product as a white crystalline solid (4.24 g, 17.8 mmol, 80 % yield). All spectroscopic data match those reported previously in the literature. ^{1}H NMR (400 MHz, $CDCl_3$) δ 8.32 (s, 2H). ^{13}C NMR (125 MHz, $CDCl_3$) δ 168.6, 150.2, 147.9, 128.9. Mp = 96–98 °C.

4-Chloro-*N2,N6*-bis((*2S,3S*)-1-hydroxy-3-methylpentan-2-yl)pyridine-2,6-dicarboxamide: A flame-dried 250 mL round-bottomed flask was charged with *(S)*-isoleucinol (1.78 g, 15.2 mmol), NEt_3 (3.0 mL, 21 mmol), and CH_2Cl_2 (45 mL). The reaction flask was sealed with a septum, purged several times with N_2 (g), and cooled to 0 °C. A solution of 4-chloropyridine-2,6-dicarbonyl dichloride (1.8120 g, 7.5988 mmol) in CH_2Cl_2 (10 mL) was then added via syringe over 5 min. The reaction mixture was then allowed to warm to room temperature and stirred overnight. After this time the reaction mixture was washed with saturated $NaHCO_3$ (3x

30 mL) and water (30 mL). The organic layer was then dried over Na_2SO_4, filtered, and concentrated under reduced pressure to yield the crude product as an off-white solid. The crude product was carried forward without further purification or characterization (2.69 g, 6.73 mmol, 89 % crude yield). ^{1}H NMR (400 MHz, $CDCl_3$) δ 8.31 (s, 2H), 7.98 (d, *J* = 8.4 Hz, 2H), 4.00 (tt, *J* = 8.6, 4.6 Hz, 2H), 3.89 – 3.80 (m, 4H), 1.91 – 1.75 (m, 2H), 1.67 – 1.48 (m, 2H), 1.24 (tt, *J* = 14.7, 7.4 Hz, 2H), 1.02 (d, *J* = 5.2 Hz, 6H), 0.95 (t, *J* = 7.4 Hz, 6H).

(S,4S,4'S)-2,2'-(4-Chloropyridine-2,6-diyl)bis(4-((S)-sec-butyl)-4,5-dihydrooxazole): A

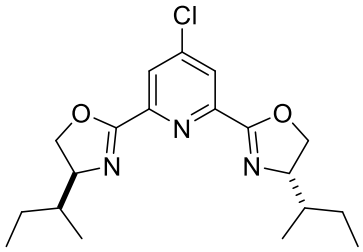

flame-dried 100 mL round-bottomed flask was charged with 4-chloro-*N2*,*N6*-bis((2*S*,3*S*)-1-hydroxy-3-methylpentan-2-yl)pyridine-2,6-dicarboxamide (2.69 g, 6.73 mmol) and CH_2Cl_2 (30 mL). The reaction vessel was sealed with a rubber septum, purged several times with N_2 (g), and cooled to –78 °C. Diethylaminosulfur trifluoride (DAST) (1.87 mL, 14.2 mmol) was then added slowly via syringe. The reaction mixture was stirred for 12 h at this temperature. After 12 h, solid K_2CO_3 (2.7 g) was added in one portion and the reaction mixture was allowed to warm to room temperature The reaction was then carefully quenched by slow addition of saturated $NaHCO_3$. The reaction mixture was diluted with additional CH_2Cl_2 (30 mL) and transferred to a separatory funnel. The organic layer was washed with H_2O and the aqueous layer was extracted with CH_2Cl_2 (3x30 mL). The combined organics were dried over Na_2SO_4, filtered, and concentrated under reduced pressure to provide the crude product as a yellow oil. The crude product was purified by column chromatography (1:3 to 1:2 EtOAc/hexanes) to provide the product as a colorless oil (1.49 g, 4.11 mmol, 61 % yield). All spectroscopic data matched those reported previously in the literature.[40] ^{1}H NMR (400 MHz, $CDCl_3$) δ 8.20 (s, 2H), 4.56-4.47 (m,

2H), 4.30-4.21 (m, 4H), 1.77-1.68 (m, 4H), 1.69-1.61 (m, 2H), 0.96 (t, *J* = 7.5 Hz, 6H), 0.88 (d, *J* = 7.0 Hz). ^{13}C NMR (125 MHz, $CDCl_3$) δ 161.3, 148.0, 145.3, 125.8, 71.5, 70.8, 39.0, 26.0, 14.5, 11.4. HRMS (ESI) calculated for $[C_{19}H_{26}ClN_3O_2]^+$ ($M+H^+$) requires *m/z* 363.1714, found 363.1711.

2,6-Bis((*S*)-4-((*S*)-sec-butyl)-4,5-dihydrooxazol-2-yl)-*N*,*N*-dimethylpyridin-4-amine (L2.11):

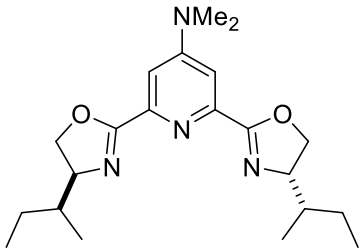

Prepared using a modified procedure provided by Tse *et al*.[41] A 100 mL round-bottomed flask was charged with **L4** (0.4601 g, 1.264 mmol), THF (15 mL), and 40 % aq. $HNMe_2$ (50 mL). The reaction mixture was then heated at 40 °C for 24 hours. The reaction mixture was then extracted with CH_2Cl_2 (3x 50 mL). The combined organics were then dried over Na_2SO_4 and concentrated under reduced pressure to provide the crude product as a yellow oil which slowly solidified. The product was purified by column chromatography (85 % hexane, 10 % NEt_3, 5 % EtOH) followed by recrystallization from EtOAc:hexane to give the product as a white crystalline solid (386.1 mg, 1.037 mmol, 82 % yield). $[\alpha]_D^{22}$ -47.6 (*c*1.76, CH_2Cl_2). ν_{max} (film) / cm^{-1} 2963, 2930, 2876, 1643, 1590, 1522, 1405, 1002, 983. ^{1}H NMR (400 MHz, $CDCl_3$) δ 7.41 (s, 2H), 4.60 – 4.33 (m, 4H), 4.34 – 4.11 (m, 4H), 3.10 (s, 6H), 1.8 – 1.7 (m, 2H), 1.67 – 1.59 (m, 2H), 1.30 – 1.19 (m, 2H), 0.95 (t, *J* = 7.4 Hz, 6H), 0.87 (d, *J* = 6.7 Hz, 6H). ^{13}C NMR (125 MHz, $CDCl_3$) δ 163.16, 154.94, 146.99, 107.97, 71.23, 70.11, 39.51, 39.09, 26.24, 14.39, 11.60. HRMS (ESI) calculated for $[C_{21}H_{32}N_4O_2]^+$ ($M+H^+$) requires *m/z* 373.2598, found 373.2598. Mp = 115.8-120.0 ^{o}C.

2.5.3: Substrate Synthesis

Trans Ethyl *2*-benzoylcyclopropanecarboxylate (**2.9**) was prepared according to a procedure described by Taylor and coworkers.[42] *Trans tert*-Butyl 2-benzoylcyclopropanecarboxylate (**2.11**) and 1-((2-benzoylcyclopropyl)ethanone were prepared according to procedures reported by Gaunt and coworkers.[43] 1-Methylene-1,2,3,4-tetrahydronaphthalene and 1-methylene-2,3-dihydro-1H-indene were prepared according to a procedure by Liwosz and Chemler.[44] 4-Trifluoromethylstyrene was prepared according to a procedure described by Warren and coworkers.[45]

***trans tert*-Butyl 2-(4-methoxybenzoyl)cyclopropanecarboxylate (2.43):** A 100 mL round-

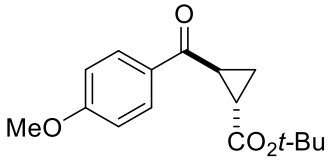

bottomed flask was charged with dry MeCN (17 mL), DABCO (0.449 g, 4.0 mmol), and 2-bromo-1-(4-methoxyphenyl)ethanone (0.916 g, 4.0 mmol). A thick white precipitate formed immediately, and the mixture was allowed to stir at room temperature under a nitrogen atmosphere for 30 min. After this time NaOH (0.241 g, 6.0 mmol) and tert-butyl acrylate (0.6 mL, 4 mmol) were added. The reaction flask was equipped with a reflux condenser and the reaction mixture brought to 80 °C until completion as indicated by TLC. The reaction was then quenched with saturated aqueous ammonium chloride and extracted three times with Et_2O. The combined organic layers were washed once with brine, dried over Na_2SO_4, and concentrated under reduced pressure to give the crude product as a dark red oil. The crude product was then purified by bulb-to-bulb distillation (190 °C, 1 Torr) to give 0.939 g (3.4 mmol, 85% yield) as a colorless oil. ν_{max} (film) / cm^{-1} 2978, 1720, 1663, 1599, 1335, 1213, 1148, 1016. ^{1}H-NMR: (400 MHz, $CDCl_3$) δ 8 (d, J = 9.5 Hz, 2H), δ 7 (d, J = 9.5 Hz, 2H), δ 3.9 (s, 3H), δ 3.1

(ddd, J = 9.3, 5.7, 3.9 Hz, 1H), δ 2.3 (ddd, J = 9.5, 6, 3.9 Hz, 1H), δ 1.57-1.48 (m, 2H), δ 1.47 (s, 9H); ^{13}C NMR (101 MHz, $CDCl_3$) δ 195.65, 171.63, 163.70, 130.56, 130.21, 113.80, 81.17, 55.50, 28.09, 25.45, 25.45, 17.53. HRMS (ESI) calculated for $[C_{16}H_{21}O_4]^+$ ($M+H^+$) requires *m/z* 277.1434, found 277.1425.

***trans* tert-Butyl 2-(4-methylbenzoyl)cyclopropanecarboxylate (2.44):** A 100 mL round-

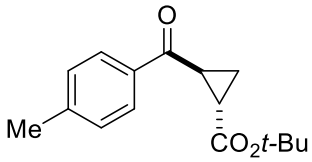

bottomed flask was charged with dry MeCN (17 mL), DABCO (0.449 g, 4.0 mmol), and 2-bromo-1-(4-methylphenyl)ethanone (0.852 g, 4.0 mmol). A thick white precipitate formed immediately, and the mixture was allowed to stir at room temperature under a nitrogen atmosphere for 30 min. After this time NaOH (0.242 g, 6.0 mmol) and tert-butyl acrylate (0.60 mL, 4.0 mmol) were added. The reaction flask was equipped with a reflux condenser and the reaction mixture brought to 80 °C until completion as indicated by TLC. The reaction was then quenched with saturated aqueous ammonium chloride and extracted three times with Et_2O. The combined organic layers were washed once with brine, dried over Na_2SO_4, and concentrated under reduced pressure to give the crude product as a dark red oil. The crude product was then purified by bulb-to-bulb distillation (180 °C, 1 Torr) to give 0.906 g (3.5 mmol, 87% yield) as a white solid. ν_{max} (film) / cm^{-1} 2978, 1722, 1669, 1607, 1368, 1335, 1150, 1014. ^{1}H NMR (400 MHz, $CDCl_3$) δ 7.92 (d, *J* = 8.2 Hz, 2H), 7.29 (d, *J* = 8.2 Hz, 2H), 3.10 (ddd, *J* = 8.6, 5.7, 3.8 Hz, 1H), 2.43 (s, 3H), 2.28 (ddd, *J* = 8.6, 5.9, 3.8 Hz, 1H), 1.58 – 1.51 (m, 2H), 1.47 (s, 9H). ^{13}C NMR (101 MHz, $CDCl_3$) δ 196.89, 171.55, 144.15, 134.69, 129.33, 128.40, 81.22, 28.11, 25.69, 25.65, 21.68, 17.69. HRMS (ESI) calculated for $[C_{16}H_{24}NO_3]^+$ ($M+NH_4^+$) requires *m/z* 278.1751, found 278.1749. Mp = 50-52 ºC.

***trans* tert-Butyl 2-(4-(trifluoromethyl)benzoyl)cyclopropanecarboxylate (2.45):** A 100 mL round-bottomed flask was charged with dry MeCN (17 mL), DABCO (0.450 g, 4.0 mmol), and 2-bromo-1-(4-trifluoromethyl)phenyl)ethanone (1.07 g, 4.0 mmol). A thick white precipitate formed immediately and the mixture was allowed to stir at room temperature under a nitrogen atmosphere for 30 min. After this time NaOH (0.243 g, 6.0 mmol) and tert-butyl acrylate (0.60 mL, 4 mmol) were added. The reaction flask was equipped with a reflux condenser and the reaction mixture brought to 80 °C until completion as indicated by TLC. The reaction was then quenched with saturated aqueous ammonium chloride and extracted three times with Et_2O. The combined organic layers were washed once with brine, dried over Na_2SO_4, and concentrated under reduced pressure to give the crude product as a dark red oil. The crude product was then purified by bulb-to-bulb distillation (200 °C, 1 Torr) to give 0.893 g (2.84 mmol, 71% yield) as a white solid. ν_{max} (film) / cm^{-1} 2978, 1724, 1680, 1322, 1157, 1133, 1068, 1012. ^1H NMR (400 MHz, $CDCl_3$) δ 8.12 (d, *J* = 8.1 Hz, 2H), 7.76 (d, *J* = 8.1 Hz, 2H), 3.10 (ddd, *J* = 8.6, 5.7, 3.8 Hz, 1H), 2.34 (ddd, *J* = 8.6, 6.1, 3.8 Hz, 1H), 1.60 (dddd, *J* = 11.8, 8.3, 6.6, 3.6 Hz, 2H), 1.48 (s, 9H). ^{13}C NMR (101 MHz, $CDCl_3$) δ 196.57, 171.07, 139.78, 134.6 (q, J = 32.7 Hz), 128.60, 125.73 (q, *J* = 3.8 Hz), 123.57 (q, *J* = 272.7 Hz), 81.57, 28.09, 26.21, 25.98, 18.24. ^{19}F NMR (377 MHz, $CDCl_3$) δ -63.14. HRMS (ESI) calculated for $[C_{16}H_{21}NO_3F_3]^+$ ($M+NH_4^+$) requires *m/z* 332.1468, found 332.1467. Mp = 74.0-75.5 ^oC.

***trans* tert-Butyl 2-(4-chlorobenzoyl)cyclopropanecarboxylate (2.46):** A 100 mL round-bottomed flask was charged with dry MeCN (17 mL), DABCO (0.448 g, 4.0 mmol), and 2-bromo-1-(4-chlorophenyl)ethanone (0.934 g, 4.0 mmol). A thick white precipitate formed immediately, and the mixture was allowed to stir at room temperature under a nitrogen atmosphere for 30 min. After this time NaOH (0.240 g, 6.0 mmol) and tert-butyl acrylate (0.6 mL, 4 mmol) were added. The reaction flask was equipped with a reflux condenser and the reaction mixture brought to 80 °C until completion as indicated by TLC. The reaction was then quenched with saturated aqueous ammonium chloride and extracted three times with Et_2O. The combined organic layers were washed once with brine, dried over Na_2SO_4, and concentrated under reduced pressure to give the crude product as a dark red oil. The crude product was then purified by bulb-to-bulb distillation (190 °C, 1 Torr) to give 0.910 g (3.2 mmol, 81% yield) as a white solid. ν_{max} (film) / cm^{-1} 2978, 1721, 1672, 1589, 1334, 1216, 1150, 1092, 1009. ^{1}H-NMR: (400 MHz, $CDCl_3$) δ 7.96 (d, J = 7.7 Hz, 2H), δ 7.47 (d, J = 7.7 Hz, 2H), δ 3.1 (ddd, J = 9.4, 5.5, 3.9 Hz, 1H), δ 2.3 (ddd, J = 8.7, 6, 3.9 Hz, 1H), δ 1.6-1.52 (m, 2H), δ 1.47 (s, 9H); ^{13}C NMR (101 MHz, $CDCl_3$) δ 196.17, 171.26, 139.80, 135.45, 129.68, 128.98, 81.43, 28.10, 25.92, 25.69, 18.01. HRMS (ESI) calculated for $[C_{15}H_{21}NO_3Cl]^+$ ($M+NH_4^+$) requires *m/z* 298.1205, found 298.1204. Mp = 62.6-63.6 °C.

***trans* tert-Butyl 2-nicotinoylcyclopropanecarboxylate (2.47):** A 100 mL round-bottomed flask was charged with dry MeCN (17 mL), DABCO (0.890 g, 8.0 mmol), and 3-(2-bromoacetyl)pyridin-1-ium bromide (1.12 g, 4.0 mmol). A thick white precipitate formed immediately, and the mixture was allowed to stir at room temperature under a

nitrogen atmosphere for 30 min. After this time NaOH (0.324 g, 8.0 mmol) and tert-butyl acrylate (0.60 mL, 4 mmol) were added. The reaction flask was equipped with a reflux condenser and the reaction mixture brought to 80 °C until completion as indicated by TLC. The reaction was then quenched with saturated aqueous ammonium chloride and extracted three times with Et_2O. The combined organic layers were washed once with brine, dried over Na_2SO_4, and concentrated under reduced pressure to give the crude product as a dark red oil. The crude product was then purified by bulb-to-bulb distillation (190 °C, 1 Torr) to give 0.584 g (2.36 mmol, 59% yield) as a white solid. ν_{max} (film) / cm^{-1} 2980, 1722, 1675, 1586, 1341, 1216, 1153, 1010. ^1H NMR (400 MHz, $CDCl_3$) δ 9.25 (d, *J* = 1.8 Hz, 6H), 8.81 (dd, *J* = 4.8, 1.6 Hz, 5H), 8.27 (dt, *J* = 8.0, 2.0 Hz, 4H), 7.45 (dd, *J* = 8.0, 4.8 Hz, 5H), 3.09 (ddd, *J* = 9.3, 5.7, 3.9 Hz, 5H), 2.35 (ddd, *J* = 8.7, 6.1, 3.8 Hz, 5H), 1.66 – 1.54 (m, 1H), 1.48 (s, 37H). ^{13}C NMR (101 MHz, $CDCl_3$) δ 196.34, 170.96, 153.70, 149.75, 135.50, 132.39, 123.62, 81.60, 28.09, 26.17, 25.93, 18.08. HRMS (ESI) calculated for $[C_{14}H_{18}NO_3]^+$ ($M+H^+$) requires *m/z* 248.1281, found 248.1274. Mp = 48.7-51.2 ^oC.

2-Bromo-1-(furan-2-yl)ethanone: A 100 mL round-bottomed flask was charged with 2-

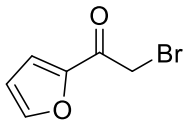

acetylfuran (2.20 g, 20.0 mmol) and anhydrous Et_2O (30 mL). The reaction vessel was sealed with a septum and purged several times with N_2 (g). The reaction vessel was cooled to 0 °C and Br_2 (1.03 mL, 20.0 mmol) was added dropwise via syringe. The reaction mixture was allowed to stir 20 min at 0 °C before slowly warming to room temperature After 12 h the reaction was quenched by addition of H_2O (20 mL). The mixture was then extracted with Et_2O (2x 20 mL) and the combined organics were dried over Na_2SO_4 and concentrated under reduced pressure. The crude product was purified by column chromatography (Et_2O/pentane) to

provide the product as a clear oil (3.44 g, 18.2 mmol, 91% yield). Spectral data were in agreement with those published previously in the literature.[46] ^{1}H NMR (300 MHz, $CDCl_3$) δ 7.65 (dd, *J* = 1.7, 0.7 Hz, 1H), 7.34 (dd, *J* = 3.6, 0.7 Hz, 1H), 6.60 (dd, *J* = 3.6, 1.7 Hz, 1H), 4.32 (s, 2H).

***trans*-tert-Butyl 2-(furan-2-carbonyl)cyclopropanecarboxylate (2.48):** A flame-dried 100 mL

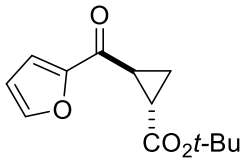

round-bottomed flask was charged with 2-bromo-1-(furan-2-yl)ethanone (3.44 g, 18.2 mmol), DABCO (2.04 g, 18.2 mmol) and anhydrous MeCN (45 mL). The reaction mixture was allowed to stir for 30 min. at room temperature under a N_2 atmosphere. After this time dry NaOH (1.13 g, 28.1 mmol) and *tert*-butyl acrylate (2.6 mL, 18.2 mmol) was added in quick succession. The reaction vessel was equipped with a reflux condenser and the reaction mixture was stirred at 85 °C for 16 h. After cooling to room temperature, the reaction was quenched by addition of saturated aq. NH_4Cl and extracted with Et_2O (3x 50 mL). The combined organic were dried over Na_2SO_4 and concentrated under reduced pressure to provide the crude product as a dark yellow oil. The crude product was purified by column chromatography (Et_2O/pentane) to provide **1j** as a white solid (3.48 g, 14.7 mmol, 81 % yield). ν_{max} (film) / cm^{-1} 2979, 1723, 1666, 1570, 1469, 1336, 1215, 1154. ^{1}H NMR (400 MHz, $CDCl_3$) δ 7.74 – 7.61 (m, 1H), 7.31 – 7.25 (m, 1H), 6.58 (dd, *J* = 3.6, 1.7 Hz, 1H), 3.01 (ddd, *J* = 9.4, 5.7, 3.9 Hz, 1H), 2.28 (ddd, *J* = 8.8, 6.0, 3.9 Hz, 1H), 1.58 – 1.49 (m, 2H), 1.47 (s, 9H). ^{13}C NMR (101 MHz, $CDCl_3$) δ 185.88, 171.25, 152.75, 146.86, 117.64, 112.44, 81.31, 28.09, 25.85, 25.45, 17.29. HRMS (ESI) calculated for [$C_{13}H_{17}O_4^+$] ($M+H^+$) requires 237.1121, found 237.1119. Mp = 68.2-70.2 °C

***trans* tert-Butyl 2-(3-methylbenzoyl)cyclopropanecarboxylate (2.49):** A 100 mL round-bottomed flask was charged with dry MeCN (17 mL), DABCO (0.449 g, 4.0 mmol), and 2-bromo-1-(3-methylphenyl)ethanone (0.852 g, 4.0 mmol). A thick white precipitate formed immediately and the mixture was allowed to stir at room temperature under a nitrogen atmosphere for 30 min. After this time NaOH (0.243 g, 6.0 mmol) and tert-butyl acrylate (0.60 mL, 4 mmol) were added. The reaction flask was equipped with a reflux condenser and the reaction mixture brought to 80 °C until completion as indicated by TLC. The reaction was then quenched with saturated aqueous ammonium chloride and extracted three times with Et_2O. The combined organic layers were washed once with brine, dried over Na_2SO_4, and concentrated under reduced pressure to give the crude product as a dark red oil. The crude product was then purified by bulb-to-bulb distillation (180 °C, 1 Torr) to give 0.923 g (3.16 mmol, 79% yield) as a colorless oil. ν_{max} (film) / cm^{-1} 2978, 1721, 1671, 1368, 1333, 1214, 1149. ^1H NMR (400 MHz, $CDCl_3$) δ 7.88 – 7.73 (m, 2H), 7.39 (m, 2H), 3.11 (ddd, *J* = 8.6, 5.7, 3.9 Hz, 1H), 2.43 (s, 2H), 2.30 (ddd, *J* = 8.6, 5.9, 3.9 Hz, 1H), 1.59 – 1.50 (m, 2H), 1.47 (s, 9H). ^{13}C NMR (101 MHz, $CDCl_3$) δ 197.49, 171.49, 138.44, 137.20, 134., 128.79, 128., 125.49, 81.23, 28., 25.87, 25., 21., 17.82. HRMS (ESI) calculated for $[C_{16}H_{24}NO_3]^+$ ($M+NH_4^+$) requires *m/z* 278.1751, found 278.1743.

***trans* tert-Butyl 2-(2-methylbenzoyl)cyclopropanecarboxylate (2.50):** A 100 mL round-bottomed flask was charged with dry MeCN (17 mL), DABCO (0.450 g, 4.0 mmol), and 2-bromo-1-(2-methylphenyl)ethanone (0.850 g, 4.0 mmol). A thick white precipitate formed immediately and the mixture was allowed to stir at room

temperature under a nitrogen atmosphere for 30 min. After this time NaOH (0.243 g, 6.0 mmol) and tert-butyl acrylate (0.60 mL, 4 mmol) were added. The reaction flask was equipped with a reflux condenser and the reaction mixture brought to 80 °C until completion as indicated by TLC. The reaction was then quenched with saturated aqueous ammonium chloride and extracted three times with Et_2O. The combined organic layers were washed once with brine, dried over Na_2SO_4, and concentrated under reduced pressure to give the crude product as a dark red oil. The crude product was then purified by bulb-to-bulb distillation (180 °C, 1 Torr) to give 0.854 g (3.28 mmol, 82% yield) as a colorless oil. ν_{max} (film) / cm^{-1} 2978, 1722, 1675, 1368, 1329, 1213, 1150, 1009. ^1H NMR (400 MHz, $CDCl_3$) δ 7.75 (dd, *J* = 7.7, 1.4 Hz, 1H), 7.39 (td, *J* = 7.5, 1.5 Hz, 1H), 7.35 – 7.18 (m, 2H), 2.90 (ddd, *J* = 8.5, 5.7, 3.8 Hz, 1H), 2.50 (s, 3H), 2.29 (ddd, *J* = 8.7, 5.9, 3.8 Hz, 1H), 1.61 – 1.49 (m, 2H), 1.47 (s, 9H). ^{13}C NMR (101 MHz, $CDCl_3$) δ 201.05, 171.23, 138.33, 137.69, 131.74, 131.49, 128.88, 125.78, 81.25, 28.95, 28.09, 26.16, 21.01, 17.92. HRMS (ESI) calculated for $[C_{16}H_{24}NO_3]^+$ ($M+NH_4^+$) requires *m/z* 278.1751, found 278.1743.

***trans* 2-Methylcyclopropyl(phenyl)methanone:** A flame-dried 100 mL flask was charged with

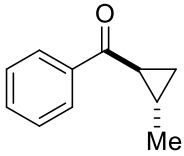

solid NaH (60% in mineral oil, 190.3 mg, 4.8 mmol) and trimethylsulfoxonium iodide (1.05 g, 4.80 mmol) and the flask was placed under a nitrogen atmosphere. DMSO (10 mL) was then added dropwise to the flask. After hydrogen evolution ceased, the reaction mixture was stirred for an additional 15 min, during which time the solution became clear. (E)-1-Phenylbut-2-en-1-one (585 mg, 4.0 mmol) was then added in one portion via syringe. The reaction mixture was allowed to stir for 24 h at room temperature. The reaction was then quenched by addition of water, and the mixture extracted three times with Et_2O. The combined organic layers

were dried over Na_2SO_4, and volatiles were removed under reduced pressure to yield the crude product as a dark residue. The crude product was purified by bulb-to-bulb distillation (170 °C, 1 Torr) to give 0.506 g (79% yield, 3.16 mmol) as a clear oil. Spectral data were in agreement with those published previously in the literature.[47] ^{1}H NMR (400 MHz, $CDCl_3$) δ 7.99 (d, *J* = 7.1 Hz, 2H), 7.56 (t, *J* = 7.3 Hz, 1H), 7.47 (t, *J* = 7.5 Hz, 2H), 2.40 (dt, *J* = 8.1, 4.3 Hz, 1H), 1.61 (dqd, *J* = 8.5, 6.1, 3.9 Hz, 1H), 1.49 (ddd, *J* = 8.4, 4.6, 3.5 Hz, 1H), 1.23 (d, *J* = 6.0 Hz, 3H), 0.90 (ddd, *J* = 7.8, 6.4, 3.4 Hz, 1H). ^{13}C NMR (101 MHz, $CDCl_3$) δ 200.15, 138.14, 132.59, 128.47, 127.97, 26.41, 21.35, 20.16, 18.33.

2,2-Dimethylcyclopropyl(phenyl)methanone: A flame-dried 100 mL flask was charged with

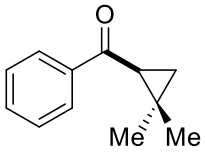

solid NaH (60% in mineral oil, 193 mg, 4.8 mmol) and trimethylsulfoxonium iodide (1.06 g, 4.8 mmol) and the flask was placed under a nitrogen atmosphere. DMSO (10 mL) was then added dropwise to the flask. After hydrogen evolution ceased, the reaction mixture was stirred for an additional 15 min, during which the solution became clear. 3-Methyl-1-phenylbut-2-en-1-one (641 mg, 4.0 mmol) was then added in one portion via syringe. The reaction mixture was allowed to stir for 24 h at room temperature. The reaction was then quenched by addition of water and the mixture extracted three times with Et_2O. The combined organic layers were dried over Na_2SO_4, and volatiles were removed under reduced pressure to yield the crude product as a dark residue. The crude product was purified by bulb-to-bulb distillation (180 °C, 1 Torr) to give 0.432 g (62% yield, 2.48 mmol) as a clear oil. Spectral data were in agreement with those published previously in the literature.[48] ^{1}H NMR (400 MHz, $CDCl_3$) δ 7.95 (d, *J* = 7.1 Hz, 2H), 7.55 (t, *J* = 7.3 Hz, 1H), 7.47 (t, *J* = 7.4 Hz, 2H), 2.48 (dd, *J* = 7.5, 5.6 Hz,

1H), 1.52 (dd, *J* = 5.6, 4.1 Hz, 1H), 1.36 (s, 2H), 1.09 (s, 2H), 0.96 (dd, *J* = 7.5, 4.1 Hz, 1H). ^{13}C NMR (101 MHz, $CDCl_3$) δ 198.60, 139.06, 132.41, 128.46, 127.99, 32.89, 27.07, 26.98, 22.00, 18.50.

2-Cyclopentylidene-1-phenylethanone (2.51): A 50 mL flame-dried round-bottomed flask was

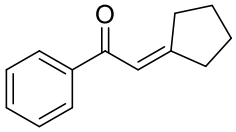

charged with NaH (60 % dispersion in mineral oil, 0.147 g, 3.74 mmol) and dry tetrahydrofuran. The flask was sealed with a rubber septum and purged 3x with N_2(g). To the mixture diethyl (2-oxo-2-phenylethyl)phosphonate (0.898 g, 3.50 mmol) was added dropwise via syringe and the reaction mixture was allowed to stir for 15 min at room temperature. Cyclopentanone (0.282 g, 3.35 mmol) was added via syringe. The reaction flask was then equipped with a reflux condenser stirred at reflux overnight. After this time the reaction mixture was filtered and carefully diluted with Et_2O followed by brine. The aqueous layer was extracted twice more with Et_2O. The combined organics were dried over Na_2SO_4 and concentrated in vacuo to give the crude product as a dark yellow oil. The product was then purified by flash column chromatography (Et_2O/pentanes) to give the final product as a pale yellow oil (0.318 g, 1.71 mmol, 51% yield). The crude product was carried forward without additional purification or characterization. ^{1}H NMR (400 MHz, $CDCl_3$) δ 7.93 (d, *J* = 6.7 Hz, 2H), 7.51 (t, *J* = 7.2 Hz, 1H), 7.44 (t, *J* = 7.0 Hz, 2H), 7.00 (p, *J* = 2.2 Hz, 1H), 2.91 (t, *J* = 6.6 Hz, 2H), 2.56 (t, *J* = 7.0 Hz, 2H), 1.80 (p, *J* = 7.5 Hz, 2H), 1.71 (p, *J* = 6.1 Hz, 2H).

Phenyl(spiro[2.4]heptan-1-yl)methanone (2.52): A flame-dried 100 mL flask was charged with 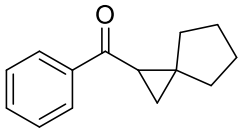 solid NaH (60% in mineral oil, 82.5 mg, 2.05 mmol) and trimethylsulfoxonium iodide (0.451 g, 2.05 mmol) and the flask was placed under a nitrogen atmosphere. DMSO (5 mL) was then added dropwise to the flask. After hydrogen evolution ceased, the reaction mixture was stirred for an additional 15 min, during which the solution became clear. 3-Methyl-1-phenylbut-2-en-1-one (0.318 g, 1.71 mmol) was then added in one portion via syringe. The reaction mixture was allowed to stir for 24 h at room temperature. The reaction was then quenched by addition of water and the mixture extracted three times with Et_2O. The combined organic layers were dried over Na_2SO_4 and volatiles were removed under reduced pressure to yield the crude product as a dark residue. The crude product was purified by flash column chromatography (Et_2O/pentanes) to give the product as a clear oil (0.216 g, 1.08 mmol, 63% yield). ν_{max} (film) / cm^{-1} 2942, 1667, 1431, 1390, 1208 ^1H NMR (400 MHz, $CDCl_3$) δ 7.96 (d, *J* = 7.1 Hz, 2H), 7.55 (t, *J* = 7.3 Hz, 1H), 7.47 (t, *J* = 7.4 Hz, 2H), 2.69 (dd, *J* = 7.6, 5.6 Hz, 1H), 2.03 – 1.35 (m, 10H). ^{13}C NMR (101 MHz, $CDCl_3$) δ 198.95, 138.98, 132.42, 128.47, 127.86, 38.64, 37.35, 32.45, 29.82, 26.09, 26.03, 21.89. HRMS (ESI) calculated for $[C_{14}H_{20}NO]^+$ ($M+NH_4^+$) requires *m/z* 218.1122, found 218.1119.

(2-(tert-Butoxy)-2-oxoethyl)dimethylsulfonium bromide: A 50 mL round-bottomed flask was 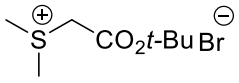 charged with *tert*-butyl bromoacetate (5.00 g, 25.7 mmol), Acetone (15 mL), and dimethylsulfide (5.1 mL, 69 mmol). The reaction vessel was sealed and placed in the refridgerator overnight, during which the product precipitated. The solid product was then filtered and washed several times with cold acetone and dried under reduced presure to give the product

as a white crystalline solid (6.62 g, 25.7 mmol, quant.). The product was used in the subsequent step without further purification or characterization.

(2-(tert-Butoxy)-2-oxoethyl)dimethylsulfonium ylide: A 25 mL round-bottomed flask was 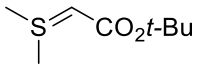 charged with (2-(tert-butoxy)-2-oxoethyl)dimethylsulfonium bromide (1.82 g, 7.10 mmol) and $CHCl_3$ (8 mL). The reaction mixture was allowed to stir for 5 min until the reaction mixture had become homogeneous. The reaction mixture was cooled to 0 °C and saturated K_2CO_3 (4.6 mL) and aq. NaOH solution (1 mL, 12 M, 7.2 mmol) were added in quick succession with vigorous stirring. The reaction mixture immediately became heterogeneous and the reaction mixture was brought to room temperature and stirred. After 15 min the reaction mixture was filtered, and the top organic layer was separated from the aqueous layer. The aqueous layer was extracted once more with $CHCl_3$. The combined organics were dried over K_2CO_3 and concentrated under reduced pressure to provide the crude product as an off-white solid in quantitative yield (1.25 g, 7.09 mmol), which was used in the subsequent step without further purification. ^{1}H NMR (400 MHz, $CDCl_3$) δ 2.84 (br s, 1H), 2.73 (s, 6H), 1.46 (s, 9H). ^{13}C NMR (101 MHz, $CDCl_3$) δ 170.63, 32.78, 30.79, 30.75, 29.27, 29.07.

Phenylglyoxal: A 500 mL round-bottomed flask was charged with selenium dioxide (18.0 g, 162.2 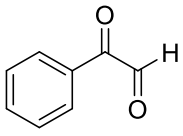 mmol), EtOH (100 mL), and H_2O (4 mL). The reaction vessel was equipped with a reflux condenser and stirred at 50 °C until the reaction mixture became homogeneous. Acetophenone (18.9 mL, 162 mmol) was then added and the reaction mixture brought to reflux for 12 h. During this time the reaction mixture turned dark red and eventually

became colorless again. The hot reaction mixture was then decanted away from precipitated selenium and filtered. The solvent was carefully removed under reduced pressure to give the crude product. Pure phenylglyoxal was obtained by distillation under reduced pressure, collecting the fractions distilling at 90-100 °C. Phenylglyoxal was obtained as a yellow oil which polymerized readily at room temperature (16.3 g, 121.7 mmol, 75% yield). The product was used in subsequent step without further characterization.

(E)-tert-Butyl 4-oxo-4-phenylbut-2-enoate: A flame-dried 25 mL round-bottomed flask was 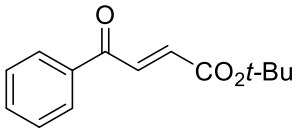 charged with phenylglyoxal (0.345 g, 2.57 mmol), *tert*-butoxycarbonylmethylenetriphenylphosphorane (0.968 g, 2.57 mmol), and CH_2Cl_2 (5 mL). The reaction mixture was stirred for 24 h at room temperature under an N_2 atmosphere. The solvent was then stripped under reduced pressure and crude product purified by column chromatography (Et_2O/pentanes) to provide the product as a colorless oil (0.457 g, 1.97 mmol, 77 % yield). Spectral data were in agreement with those reported previously in the literature.[49] ^{1}H NMR (400 MHz, $CDCl_3$) δ 7.99 (d, *J* = 7.2 Hz, 2H), 7.81 (d, *J* = 15.6 Hz, 1H), 7.62 (t, *J* = 7.4 Hz, 1H), 7.51 (t, *J* = 7.6 Hz, 2H), 6.81 (d, *J* = 15.6 Hz, 1H), 1.54 (s, 9H).

(1R,2S,3S)-tert-Butyl 3-benzoylcyclopropane-1,2-dicarboxylate (2.36): A flame-dried 25 mL 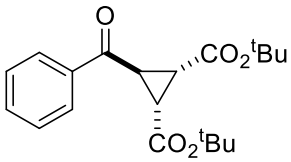 round-bottomed flask was charged with (E)-tert-butyl 4-oxo-4-phenylbut-2-enoate (0.464 g, 2.0 mmol), (2-(tert-butoxy)-2-oxoethyl)dimethylsulfonium ylide (0.514 g, 2.92 mmol), and acetone (10 mL). The reaction mixture was fit with a reflux condenser, purged several times with N_2, and stirred at reflux for 6

h. After this time the solvent was stripped under reduced pressure to give the crude product as a yellow oil. Crude product was purified by column chromatography (Et_2O/pentane) to give the pure product as a white crystalline solid (0.425 g, 1.23 mmol, 62% yield). ν_{max} (film) / cm^{-1} 2980, 1726, 1679, 1368, 1301, 1215, 1144. ^1H NMR (400 MHz, $CDCl_3$) δ 8.09 (d, *J* = 7.2 Hz, 2H), 7.61 (t, *J* = 7.4 Hz, 1H), 7.50 (t, *J* = 7.6 Hz, 2H), 3.67 (t, *J* = 5.6 Hz, 1H), 2.62 (d, *J* = 5.6 Hz, 2H), 1.48 (s, 18H). ^{13}C NMR (101 MHz, $CDCl_3$) δ 195.67 , 167.13 , 136.68 , 133.63 , 128.73 , 128.56 , 81.88 , 31.47 , 29.11 , 28.06. HRMS (ESI) calculated for $[C_{20}H_{27}O_5]^+$ {$M+H^+$) requires 347.1853, found 347.1851. Mp = 100.3-103.3 ºC.

3-Methyl-1-phenylbut-2-en-1-ol: A flame-dried 250 mL round-bottomed flask was charged with

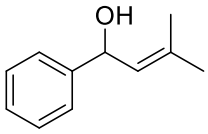

crushed magnesium turnings (0.761 g, 31.4 mmol). The flask was placed under vacuum and magnesium was flame-dried. The flask was backfilled with N_2, THF (55 mL) was added, and the flask sealed with a rubber septum. 1-Bromo-2-methyl-prop-1-ene (4.22 g, 31.2 mmol) was then added to the flask via syringe. Heat was soon evolved and the reaction mixture took on a dark brown color. After all of the magnesium turnings had been consumed (30 min), freshly distilled benzaldehyde (3.0 mL, 29 mmol) was added dropwise via syringe. Reaction was complete after 1 h and quenched by addition of saturated NH_4Cl and diluted with EtOAc. The reaction mixture was transferred to a separatory funnel and the organic layer was washed with saturated $NaHCO_3$ followed by brine. The organic layer was dried over Na_2SO_4 and concentrated under reduced pressure to give the crude product as a pale green oil. Crude product was purified by bulb-to-bulb distillation (140 °C, 15 Torr) to give the product as a colorless oil (3.86 g, 23.8 mmol, 82% yield). Spectral data matched those reported previously in the literature.[50]

^{1}H NMR (400 MHz, $CDCl_3$) δ 7.41 – 7.32 (m, 4H), 7.29 – 7.23 (m, 1H), 5.47 (d, *J* = 9.8 Hz, 1H), 5.44 – 5.39 (m, 1H), 1.81 (d, *J* = 1.1 Hz, 3H), 1.75 (d, *J* = 1.0 Hz, 3H).

3-Methyl-1-phenylbut-2-en-1-one: A 250 mL round-bottomed flask was charged with 3-methyl-

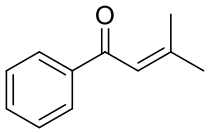

1-phenylbut-2-en-1-ol (3.86 g, 23.8 mmol), CH_2Cl_2 (150 mL), and activated MnO_2 (20.2 g, 232 mmol). The reaction was then allowed to stir at room temperature for 20 h under open air. The reaction mixture was then filtered through a pad of Celite and the filter cake was washed several times with CH_2Cl_2. The filtrate was then concentrated under reduced pressure to give the crude product as a thick oil. Spectral data matched those reported previously in the literature.[51] ^{1}H NMR (400 MHz, $CDCl_3$) δ 7.93 (d, *J* = 7.3 Hz, 2H), 7.45 (t, *J* = 7.4 Hz, 1H), 7.34 (t, *J* = 7.5 Hz, 2H), 6.75 (s, 1H), 2.21 (s, 3H), 2.02 (s, 3H).

tert-Butyl 3-benzoyl-2,2-dimethylcyclopropanecarboxylate (2.38): A flame-dried 25 mL

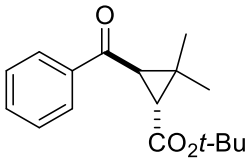

round-bottomed flask was charged with 3-methyl-1-phenylbut-2-en-1-one (0.34 g, 2.13 mmol), (2-(tert-butoxy)-2-oxoethyl)dimethylsulfonium ylide (0.564 g, 3.2 mmol), and acetone (12 mL). The reaction mixture was fit with a reflux condenser, purged several times with N_2(g), and stirred at reflux for 6 h. After this time the solvent was stripped under reduced pressure to give the crude product as a yellow oil. Crude product was purified by column chromatography (Et_2O/pentane) to give the pure product as a clear oil (0.24 g, 0.87 mmol, 41% yield). ν_{max} (film) / cm^{-1} 1978, 1720, 1670, 1364, 1150, 1010. ^{1}H NMR (400 MHz, $CDCl_3$) δ 7.88 (d, *J* = 7.1 Hz, 2H), 7.49 (t, *J* = 7.4 Hz, 1H), 7.40 (t, *J* = 7.5 Hz, 2H), 3.00 (d, *J* = 5.7 Hz, 1H), 2.44 (d, *J* = 5.7 Hz, 1H), 1.39 (m, 12H), 1.08 (s, 3H). ^{13}C NMR (101 MHz, $CDCl_3$) δ

196.27, 169.94, 138.07, 132.98, 128.59, 128.16, 80.94, 38.53, 34.26, 32.77, 28.19, 20.18. HRMS (ESI) calculated for $[C_{17}H_{26}NO_3]^+$ ($M+NH_4^+$) requires 292.1907, found 292.1905.

3-Methyl-1-(4-(trifluoromethyl)phenyl)but-2-en-1-one: Prepared as described previously by

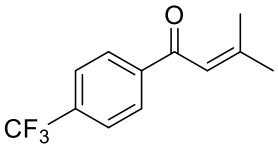

Okamoto *et al.*[52] ^{1}H NMR (400 MHz, $CDCl_3$) δ 8.02 (d, *J* = 8.1 Hz, 2H), 7.71 (d, *J* = 8.2 Hz, 2H), 6.74 (s, 1H), 2.25 (s, 3H), 2.05 (s, 3H).

(2,2-Dimethylcyclopropyl)(4-(trifluoromethyl)phenyl)methanone (2.53): A flame-dried 50

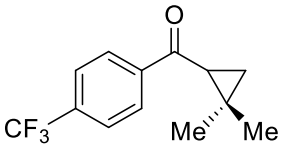

mL flask was charged with solid NaH (60% in mineral oil, 80.5 mg, 2.0 mmol) and trimethylsulfoxonium iodide (0.440 g, 2.0 mmol) and the flask was placed under a nitrogen atmosphere. DMSO (5 mL) was then added dropwise to the flask. After hydrogen evolution ceased, the reaction mixture was stirred for an additional 15 min during which the solution became clear. 3-Methyl-1-(4-(trifluoromethyl)phenyl) but-2-en-1-one (0.380 g, 1.67 mmol) was then added in one portion via syringe. The reaction mixture was allowed to stir for 24 h at room temperature. The reaction was then quenched by addition of water, and the mixture extracted three times with Et_2O. The combined organic layers were dried over Na_2SO_4 and volatiles were removed under reduced pressure to yield the crude product as a dark residue. The crude product was purified by column chromatography (3.3% Et_2O in pentane) to give the product as a colorless oil. ν_{max} (film) / cm^{-1} 2978, 1688, 1432, 1318, 1159, 1010. ^{1}H NMR (400 MHz, $CDCl_3$) δ 8.04 (d, *J* = 8.1 Hz, 2H), 7.73 (d, *J* = 8.2 Hz, 2H), 2.48 (dd, *J* = 7.4, 5.7 Hz, 1H), 1.59 – 1.55 (m, 1H), 1.38 (s, 3H), 1.10 (s, 3H), 1.03 (dd, *J* = 7.4, 4.1 Hz, 1H). ^{13}C NMR (101 MHz, $CDCl_3$) δ 197.60, 141.69, 133.76 (q, *J* = 32.6 Hz), 128.25, 125.54 (q, *J* = 3.8 Hz), 123.71 (d, *J* = 272.6 Hz),

33.18, 27.99, 27.03, 22.64, 18.42. ^{19}F NMR (377 MHz, $CDCl_3$) δ –63.02. HRMS (ESI) calculated for $[C_{13}H_{17}F_3NO]^+$ ($M+NH_4^+$) requires *m/z* 260.1257, found 260.1257.

***cis* 2-Benzoylcyclopropanecarboxylic acid:** Prepared using a modification of the procedure by

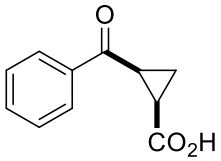

Augustine and coworkers.[53] A 50 mL flame-dried round bottom flask was charged with $AlCl_3$ (2.01 g, 15.1 mmol) and anhydrous benzene (8 mL). The flask was sealed with a rubber septum and purged several times with N_2 (g). 3-Oxabicyclo[3.1.0]-hexane-2,4-dione (0.688 g, 6.14 mmol) was dissolved in anhydrous benzene (7 mL) and slowly added to the flask containing $AlCl_3$ via syringe. The reaction mixture was allowed to stir overnight. After this time the reaction mixture was refluxed for 3 h, cooled to room temperature and quenched by pouring into a beaker containing cold dilute HCl. The heterogeneous mixture was extracted by washing with EtOAc (4x). The combined organics were dried over Na_2SO_4 and concentrated under reduced pressure to provide the crude product as a yellow solid. The crude product was purified by recrystallization from hot CH_2Cl_2 to provide the pure product as a white crystalline solid (0.716 g, 3.76 mmol, 61% yield). All spectroscopic data were in agreement with those reported previously in the literature. ^{1}H NMR (400 MHz, CD_3OD) δ 8.07 (d, *J* = 7.6 Hz, 2H), 7.61 (t, *J* = 7.4 Hz, 1H), 7.50 (t, *J* = 7.6 Hz, 2H), 2.96 (ddd, *J* = 9.5, 8.2, 7.0 Hz, 1H), 2.36 (ddd, *J* = 9.3, 8.1, 6.3 Hz, 1H), 1.75 (td, *J* = 6.6, 4.4 Hz, 1H), 1.37 (td, *J* = 8.1, 4.4 Hz, 1H).

***cis* tert-Butyl 2-benzoylcyclopropanecarboxylate (2.54):** A 100 mL round bottom flask was 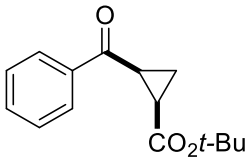

charged with cis 2-benzoylcyclopropanecarboxylic acid (0.716 g, 3.76 mmol), *t*-butanol (30 mL), Boc_2O (1.232 g, 5.65 mmol), and DMAP (3 mg, 24.6 μmol). The flask was then sealed with a rubber septum and purged with N_2(g). The reaction mixture was then stirred at 40 ^oC for 5 h. After cooling, the reaction mixture was quenched by the addition of saturated NH_4Cl solution and the mixture was extracted 3x with CH_2Cl_2. The combined organics were dried over Na_2SO_4 and concentrated under reduced pressure to provide the crude product as a yellow solid. The crude product was purified by column chromatography (25 % Et_2O/pentanes) to provide the pure product as a white solid (0.834 g, 3.39 mmol, 90% yield). ν_{max} (film) / cm^{-1} 2977, 1713, 1675, 1391, 1450, 1369, 1233, 1153. ^1H NMR (400 MHz, $CDCl_3$) δ 8.07 (d, *J* = 7.6 Hz, 2H), 7.56 (t, *J* = 7.4 Hz, 1H), 7.47 (t, *J* = 7.6 Hz, 2H), 2.78 – 2.62 (m, 1H), 2.22 (td, *J* = 8.7, 6.3 Hz, 1H), 1.92 – 1.77 (m, 1H), 1.33 – 1.23 (m, 3H), 1.18 (s, 8H). ^{13}C NMR (101 MHz, $CDCl_3$) δ 194.31, 169.20, 137.20, 133.08, 128.50, 128.42, 81.12, 27.66, 26.51, 23.88, 10.87HRMS (ESI) calculated for $[C_{15}H_{19}O_3]^+$ ($M+H^+$) requires *m/z* 247.1334, found 247.1334. Mp = 146.5-149.4 ^oC.

2.5.4: Optimization Data

Table 2-5. Pybox ligand screen

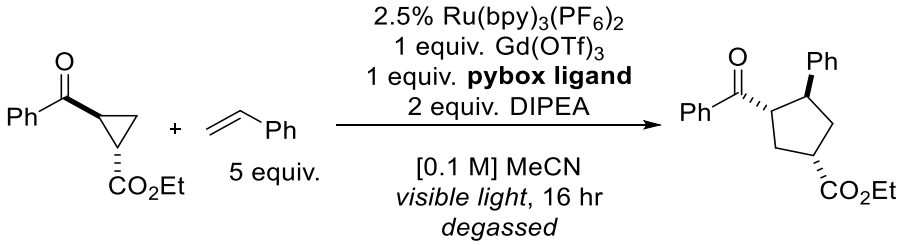

Entry	Ligand	% Yield[a] (time)	% conversion	% ee
1	*i*-Pr-pybox	10 % (16 h)	15 %	38 %
2	*t*-Bu-pybox	95 % (3 h)	100 %	40 %
3	*s*-Bu-pybox	32 % (16 h)	56 %	58 %
4	Bn-pybox	100 % (3 h)	100 %	<4 %
5	*i*-Bu-pybox	trace (16 h)	<5 %	N.D.
6	indano-pybox	6 % (16 h)	10 %	11 %
7	Ph-dbfox	85 % (16 h)	100 %	0 %

[a]Yield determined by ^{1}H-NMR using phenanthrene as an internal standard.

Table 2-6. Optimization of photocatalyst

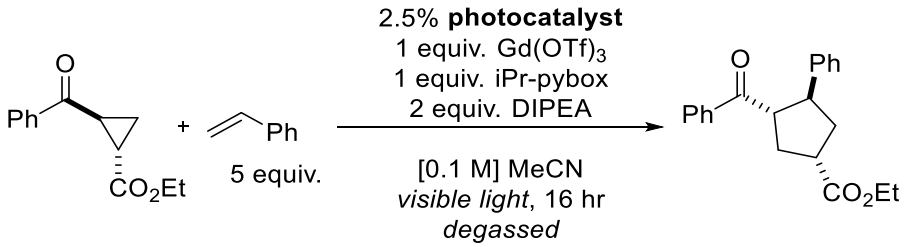

Entry	Photocatalyst	% Yield[a]	% RSM
1	$Ru(bpy)_3(PF_6)_2$	21.2 %	78 %
2	$Ru(dtbbpy)_3(PF_6)_2$	12.5 %	85 %
3	$Ir(ppy)_3$	5.4 %	93 %
4	$Ir(ppy)_2dtbbpy(PF_6)$	23.2 %	70 %

[a]Yield determined by ^{1}H-NMR using phenanthrene as an internal standard.

Table 2-7. Optimization of *s*-Bu-pybox equivalents

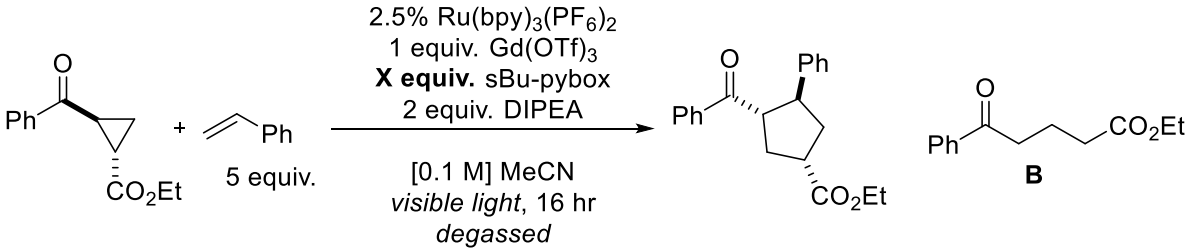

Entry	Equiv. *s*-Bu-pybox	% yield[a]	% conversion	%B	d.r.	% ee
1	1 equiv.	32 %	56 %	23 %	2.3:1	58 %
2	2 equiv.	36 %	50 %	11 %	2.5:1	60 %
3	3 equiv.	13 %	15 %	3 %	2:1	N.D.

[a]Yields determined by ^{1}H-NMR using phenanthrene as internal standard.
[b]Compound **B** is a known compound[54]

Table 2-8. Lewis acid screen with *t*-Bu-pybox

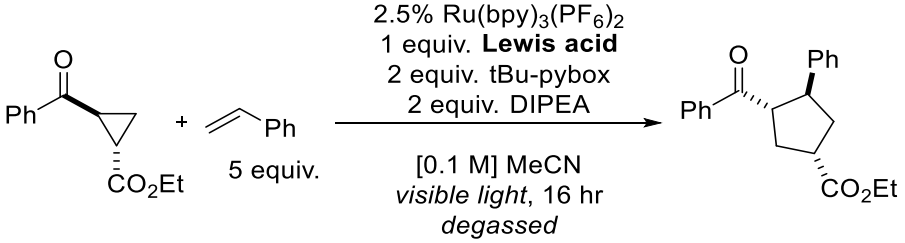

Entry	Lewis acid	% yield[a]	% RSM	% ee
1	$Gd(OTf)_3$	53 %	40 %	41 %
2	$La(OTf)_3$	5 %	94 %	---
3	$Y(OTf)_3$	27 %	71 %	38 %
4	$Fe(OTf)_2$	0 %	100 %	---
5	$Cu(OTf)_2$	0 %	100 %	---
6	$Ni(OTf)_2$	0 %	100 %	---
7	$In(OTf)_3$	trace	92 %	---
8	$Yb(OTf)_3$	11 %	71 %	---
9	$Zn(OTf)_2$	trace	>95 %	---
10	$Sc(OTf)_3$	26 %	60 %	0 %
11	$ZrCl_4$	0 %	93 %	---
12	$Mg(OTf)_2$	0 %	100 %	---
13	$Er(OTf)_3$	trace	>95 %	---
14	$Bi(OTf)_3$	0 %	100 %	---
15	$Sm(OTf)_3$	0 %	100 %	---
16	$Sn(OTf)_2$	trace	93 %	---
17	$Ce(OTf)_3$	0 %	100 %	---
18	$Mn(ClO_4)_2$	0 %	100 %	---
19	$Al(OTf)_3$	3 %	96 %	---
20	$Mg(ClO_4)_2$	0 %	100 %	---
21	$Cd(ClO_4)_2$	0 %	100 %	---

22	$Ba(ClO_4)_2$	21 %	73 %	4 %
23	$Eu(OTf)_3$	0 %	100 %	---
24	$Nd(OTf)_3$	3 %	>95 %	---
25	$Dy(OTf)_3$	10 %	89 %	0 %
26	$Pr(OTf)_3$	15 %	82 %	8 %

[a]Yield determined by ^{1}H-NMR using phenanthrene as internal standard

Table 2-9. Reductive quencher screen

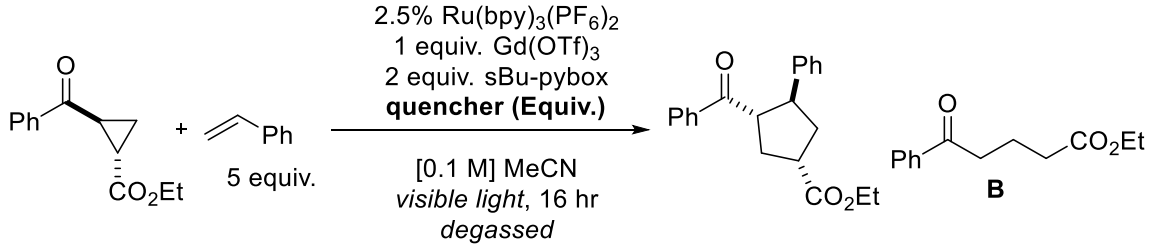

Entryy	Quencher (equiv.)	% yield[a]	% B	% RSM	% ee
1	DIPEA (1)	15 %	trace	80 %	N.D.
2	DIPEA (2)	24 %	6 %	32 %	63 %
3	DIPEA (5)	36 %	11 %	50 %	60 %
4	DIPEA (10)	trace	trace	>95 %	N.D.
5	TMEDA (1)	40 %	11.5 %	48 %	57 %
6	NEt_3 (2)	35 %	18 %	42 %	55 %
7	NBu_3 (2)	32 %	25 %	32 %	N.D.
8	1,4-dimethylpiperazine (2)	trace	trace	>95 %	N.D.
9	N-methyl-pyrrolidine (2)	37 %	25 %	26 %	N.D.
10	*N,N,N',N'*-tetramethylpropylenediamine (2)	41 %	30 %	20 %	58.5 %

11	*N,N,N',N'*-tetramethylbutanediamine (2)	17 %	13.5 %	65 %	N.D.
12	$NEtCy_2$ (2)	21 %	7 %	68 %	N.D.
13	*N*,*N*-dimethylbenzylamine (2)	20 %	13 %	68 %	N.D.
14	4-methylmorpholine (2)	trace	trace	>95 %	N.D.
15	N-methylpiperidine (2)	0 %	0 %	100 %	---
16	*N,N,N',N'*-tetramethyl-p-phenylene diamine (2)	0 %	0 %	100 %	---
17	*N,N,N',N'*- tetramethylbenzidine (2)	0 %	0 %	100 %	---
18	*N,N,N',N'',N''*-pentamethyldiethylenetramine (2)	25 %	22 %	10 %	63 %
19	1,2,2,6,6-pentamethylpiperidine (2)	26 %	4.5 %	61 %	60 %
20	4-aminophenol (2)	0 %	0 %	100 %	---
21	p-toluidine (2)	0 %	0 %	100 %	---
22	4-MeO-*N*,*N*-diphenylaniline (2)	0 %	0 %	100 %	---
23	2,6-di-tert-butyl-4-methylphenol (2)	0 %	0 %	100 %	---
24	2,4,6-trimethylaniline (2)	0 %	0 %	100 %	---
25	DABCO (2)	0 %	0 %	100 %	---
26	2,6-lutidine (2)	0 %	0 %	100 %	---
27	DBU (2)	trace	trace	50 %	N.D.
28	K_4FeCN_6 hexahydrate (2)	0 %	0 %	100 %	---
29	cesium oxalate (2)	0 %	0 %	100 %	---

[a]Yields determined by ^{1}H-NMR using phenanthrene as an internal standard

Table 2-10. Solvent optimization

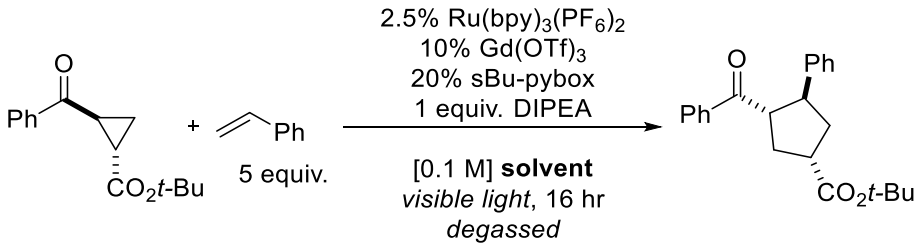

Entry	Solvent	% yield[a]	dr	% ee
1[b]	Toluene	37 %	15:1	3.5 %
2[b]	Et_2O	66 %	3.9:1	39 %
3[b]	THF	50 %	2.3:1	45 %
4[b]	CH_2Cl_2	95%	4.5:1	71 %
5	Acetone	86 %	2.6:1	84 %
6	MeCN	93 %	2.3:1	85 %
7[b]	MeCN	92 %	2.3:1	85 %
8	DMF	52 %	2.6:1	15 %

[a]Yields determined by ^{1}H-NMR spectroscopy using phenanthrene as internal standard.
[b]Reaction carried out using $Ir(ppy)_2(dtbbpy)(PF_6)$ as photocatalyst.

2.5.5: Control Experiments

Table 2-11. Control studies with *tert*-butyl 2-benzoylcyclopropanecarboxylate

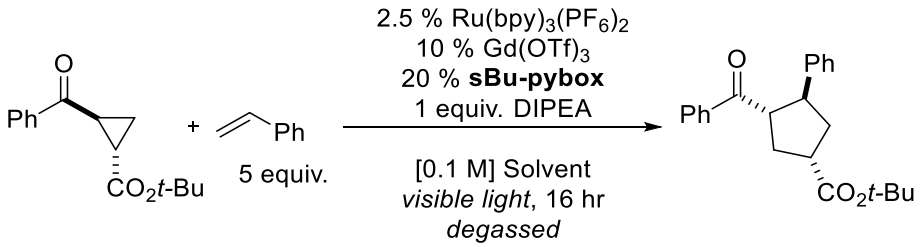

Entry	Change from std. conditions	% yield[a]	dr
1	none	95 %	3:1
2	No photocatalyst	trace	N.D.
3	No light	0 %	---
4	No $Gd(OTf)_3$	0 %	---
5	No *i*-Pr_2NEt	0%	---

[a]Yields determined by ^{1}H-NMR using phenanthrene as an internal standard

Table 2-12. Control studies with (2,2-dimethylcyclopropyl)(phenyl)methanone

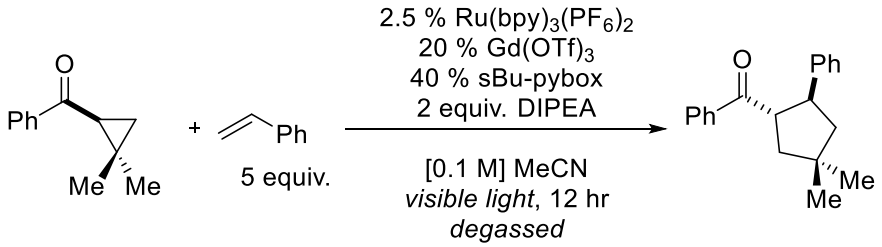

Entry	Change from std. conditions	% yield[a]	dr
1	none	55 %	5:1
2	No photocatalyst	36 %	5:1
3	No light	0 %	---
4	1 equiv. $Gd(OTf)_3$, 3 equiv. TMEDA, no ligand, no *i*-Pr_2NEt	0 %	---
5	No photocatalyst, no *i*-Pr_2NEt	0 %	---
6	No photocatalyst, blue LEDS instead of 23W fluorescent bulb	0 %	---

[a]Yields determined by ^{1}H-NMR using phenanthrene as an internal standard

Scheme 2-8. Product isomerization control

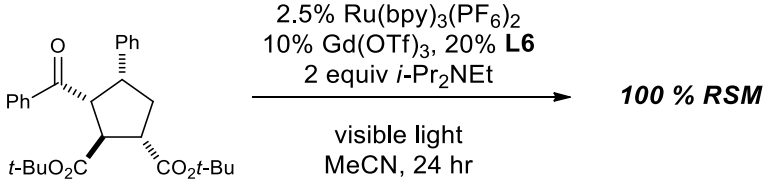

2.5.6: Asymmetric [3+2] Cycloadditions

General asymmetric procedure: An oven-dried 2 mL volumetric flask was charged with $Gd(OTf)_2$ (0.04 mmol) and 4-NMe_2-^{s}Bu-pybox (0.08 mmol). The solids were dissolved in MeCN (2 mL total volume). A separate 2 mL volumetric flask was charged with cyclopropane (0.4 mmol), alkene (2.0 mmol), $Ru(bpy)_3(PF_6)_2$ (0.01 mmol), diisopropylethylamine (0.4 mmol), and MeCN (4 mL total volume). The contents of both volumetric flasks were then transferred to a dry Schlenk tube equipped with a magnetic stir-bar. The reaction mixture was then thoroughly degassed through three freeze-pump-thaw cycles, then backfilled with N_2. The reaction flask was then transferred to a cooling bath of 0 °C in front of a 23 W (1380 lumen) compact fluorescent lamp. Upon consumption of starting material, the reaction was diluted with 1:1 Et_2O/pentanes and passed through a short plug of silica. The filtrate was concentrated and the residue purified by column chromatography. Diastereomeric ratios were determined by ^{1}H-NMR analysis of the crude reaction mixture. Only two diastereomers were observed in the crude reaction mixtures.

Ethyl 3-benzoyl-4-phenylcyclopentanecarboxylate (2.10): Prepared according to the general procedure using 24.5 mg (0.04 mmol) of $Gd(OTf)_3$, 30.1 mg (0.08 mmol) of 4-NMe_2-^{s}Bu-pybox, 87.3 mg (0.4 mmol) of *trans* ethyl 2-benzoylcyclopropanecarboxylate, 209.4 mg (2.0 mmol) of styrene, 8.7 mg (0.01 mmol) of $Ru(bpy)_3(PF_6)_2$, and 58.1 mg (0.4 mmol) of diisopropylethylamine with a total volume of 4 mL (0.1 M) in MeCN. The reaction was complete after 6 h. The crude product was purified by column chromatography (1:5, Et_2O/pentanes) to give 123.8 mg (0.384 mmol, 96 % yield) of cycloadduct as two separable diastereomers (3:1 d.r.). Major Diastereomer: 79.3% ee

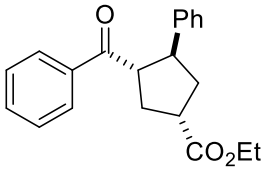

[Daicel Chiracel AD-H, 10 to 40 % iPrOH, 3 mL/min, 263 nm; t_1=4.71 min, t_2=6.04 min]. $[\alpha]_D^{22}$ 38.7 (*c*1.021, CH_2Cl_2) White solid (mp = 43.9-46.8 ºC). ν_{max} (film) / cm^{-1} 2978, 1728, 1680, 1597, 1265, 1180 ^{1}H NMR (400 MHz, $CDCl_3$) δ 7.73 (d, *J* = 7.3 Hz, 2H), 7.42 (t, *J* = 7.4 Hz, 1H), 7.29 (t, *J* = 7.7 Hz, 2H), 7.24 – 7.14 (m, 4H), 7.13 – 7.02 (m, 1H), 4.09 (q, *J* = 7.2 Hz, 2H), 3.82 (q, *J* = 8.9 Hz, 1H), 3.73 (q, *J* = 8.7 Hz, 1H), 3.11 (qd, *J* = 8.4, 6.2 Hz, 1H), 2.57 – 2.39 (m, 2H), 2.21 (dt, *J* = 13.2, 8.9 Hz, 1H), 2.10 (dt, *J* = 13.3, 8.9 Hz, 1H), 1.19 (t, *J* = 7.1 Hz, 3H). ^{13}C NMR (101 MHz, $CDCl_3$) δ 200.52, 174.95, 143.58, 136.80, 132.98, 128.57, 128.49, 128.40, 127.29, 126.49, 60.72, 54.67, 47.25, 43.43, 37.31, 35.17, 14.26. HRMS (ESI) calculated for $[C_{21}H_{23}O_3]^+$ ($M+H^+$) requires *m/z* 323.1642, found 323.1642.

tert-Butyl 3-benzoyl-4-phenylcyclopentanecarboxylate (2.12): Prepared according to the general procedure using 24.6 mg (0.04 mmol) of $Gd(OTf)_3$, 30.0 mg (0.08 mmol) of 4-NMe_2-^{s}Bu-pybox, 98.5 mg (0.4 mmol) of *trans* tert-butyl 2-benzoylcyclopropanecarboxylate, 209.5 mg (2.0 mmol) of styrene, 8.7 mg (0.01 mmol) of $Ru(bpy)_3(PF_6)_2$, and 58.2 mg (0.4 mmol) of diisopropylethylamine with a total volume of 4 mL (0.1 M) in MeCN. The reaction was complete after 6 h. The crude product was purified by column chromatography (1:9, Et_2O/pentanes) to give 133.2 mg (0.384 mmol, 95 % yield) of cycloadduct as two separable diastereomers (2.7:1 d.r.). <u>Major diastereomer:</u> 93% ee [Daicel Chiracel AD-H, 5 to 50 % iPrOH, 3 mL/min, 263 nm; t_1=6.10 min, t_2=7.08 min]. $[\alpha]_D^{22}$ 40.6 (*c*0.990, CH_2Cl_2). ν_{max} (film) / cm^{-1} 2980, 1722, 1682, 1368, 1265, 1151. ^{1}H NMR (400 MHz, $CDCl_3$) δ 7.81 (d, *J* = 7.9 Hz, 2H), 7.49 (t, *J* = 7.4 Hz, 1H), 7.37 (t, *J* = 7.7 Hz, 2H), 7.28-7.22 (m, 4H), 7.16 (dq, *J* = 9.1, 4.3 Hz, 1H), 3.94 – 3.73 (m, 2H), 3.17 – 3.00 (m, 1H), 2.58 – 2.44 (m, 2H), 2.22 (dt, *J* = 13.3, 9.0 Hz, 1H), 2.13 (dt, *J* = 13.1, 9.0 Hz, 1H), 1.46 (s, 9H). ^{13}C NMR (101 MHz, $CDCl_3$) δ 200.56, 174.21,

143.74, 136.85, 132.92, 128.52, 128.47, 128.39, 127.31, 126.42, 80.52, 54.75, 47.14, 44.46, 37.31, 35.36, 28.08. Mp = 97.1-98.5 ºC. HRMS (ESI) calculated for $[C_{23}H_{27}O_3]^+$ ($M+H^+$) requires *m/z* 351.1955, found 351.1955. Minor Diastereomer: ν_{max} (film) / cm^{-1} 2981, 1719, 1684, 1365, 1262, 1150. ^1H NMR (400 MHz, $CDCl_3$) δ 7.82 (d, *J* = 7.6 Hz, 2H), 7.49 (t, *J* = 7.4 Hz, 1H), 7.37 (t, *J* = 7.7 Hz, 2H), 7.28-7.22 (m, 4H), 7.15 (t, *J* = 6.8 Hz, 1H), 3.99 (q, *J* = 9.3 Hz, 1H), 3.68 (dt, *J* = 11.0, 8.4 Hz, 1H), 3.00 (ddd, *J* = 16.6, 9.2, 7.5 Hz, 1H), 2.62 – 2.43 (m, 2H), 2.14 (dt, *J* = 13.2, 8.9 Hz, 2H), 1.48 (s, 9H). ^{13}C NMR (101 MHz, $CDCl_3$) δ 201.32, 174.92, 142.96, 136.62, 133.04, 128.51, 128.50, 127.42, 126.53, 80.49, 53.70, 48.34, 44.20, 38.84, 34.83, 28.13. Mp = 111.5-113.0ºC. HRMS (ESI) calculated for $[C_{23}H_{30}NO_3]^+$ ($M+NH_4^+$) requires *m/z* 368.2220, found 368.2220.

***tert*-Butyl 3-benzoyl-4-(4-methoxyphenyl)cyclopentanecarboxylate (2.13):** Prepared according

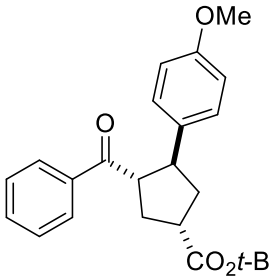

to the general procedure using 24.4 mg (0.04 mmol) of $Gd(OTf)_3$, 30.6 mg (0.08 mmol) of 4-NMe_2-^{s}Bu-pybox, 98.5 mg (0.4 mmol) of *trans* tert-butyl 2-benzoylcyclopropanecarboxylate, 241.2 mg (2.0 mmol) of 4-vinylanisole, 8.9 (0.01 mmol) mg of $Ru(bpy)_3(PF_6)_2$, 53.4 mg (0.4 mmol) of diisopropylethylamine with a total volume of 4 mL (0.1 M). The reaction was ended after 20 h. The crude product was purified by column chromatography (1:29, acetone/pentanes) to give 135 mg (0.36 mmol, 89% yield) of the cycloadduct as two separable diastereomers (2.8:1 d.r.). Major diastereomer: 90.7% ee [Daicel Chiracel AD-H, 10 to 20 % iPrOH, 3 mL/min, 240 nm; t_1=6.09 min, t_2=8.71 min]. $[\alpha]_D^{22}$ 65.9 (*c*1.080, CH_2Cl_2). White solid (mp = 95.5 – 98.5 °C). ν_{max} (film) / cm^{-1} 2975, 1721, 1679, 1612, 1513, 1448, 1366, 1246, 1149, 1035, 1012, 829, 701. ^1H NMR (400 MHz, $CDCl_3$) δ 7.81 (d, *J* = 6.9 Hz, 2H), 7.49 (t, *J* = 7.4 Hz, 1H), 7.37 (t, *J* = 7.8 Hz, 2H), 7.15 (d,

J = 8.7 Hz, 2H), 6.78 (d, *J* = 8.6 Hz, 2H), 3.82 (td, *J* = 9.5, 8.0 Hz, 1H), 3.77 – 3.71 (m, 1H), 3.75 (s, 3H), 3.07 (qd, *J* = 8.4, 5.7 Hz, 1H), 2.54 – 2.43 (m, 2H), 2.21 (ddd, *J* = 13.2, 9.8, 8.3 Hz, 1H), 2.08 (dt, *J* = 13.3, 9.1 Hz, 1H), 1.46 (s, 9H). ^{13}C NMR (101 MHz, $CDCl_3$) δ 200.72, 174.30, 158.12, 136.92, 135.69, 132.90, 128.47, 128.39, 128.23, 113.90, 80.46, 55.24, 54.88, 46.54, 44.30, 37.40, 35.27, 28.08. HRMS (ESI) calculated for $[C_{24}H_{29}O_4]^+$ ($M+H^+$) requires *m/z* 381.2060, found *m/z* 381.2053. Minor diastereomer: White solid (mp = 110.5 – 113.5 °C_. ν_{max} (film) / cm^{-1} 2975, 1723, 1680, 1514, 1448, 1367, 1249, 1220, 1152, 1036, 830, 701. ^{1}H NMR (400 MHz, $CDCl_3$) δ 7.82 (d, *J* = 7.2 Hz, 2H), 7.50 (t, *J* = 7.4 Hz, 1H), 7.37 (t, *J* = 7.7 Hz, 2H), 7.18 (d, *J* = 8.6 Hz, 2H), 6.78 (d, *J* = 8.7 Hz, 2H), 3.93 (q, *J* = 9.4 Hz, 1H), 3.74 (s, 3H), 3.69 – 3.54 (m, 1H), 2.99 (ddd, *J* = 16.6, 9.3, 7.3 Hz, 1H), 2.54 – 2.41 (m, 2H), 2.18 – 2.01 (m, 2H), 1.48 (s, 15H). ^{13}C NMR (101 MHz, $CDCl_3$) δ 201.51, 175.01, 158.20, 136.69, 134.93, 133.01, 128.49, 128.49, 128.34, 113.89, 80.46, 55.24, 53.85, 47.74, 44.11, 38.92, 34.76, 28.14. HRMS (ESI) calculated for $[C_{24}H_{32}NO_4]^+$ ($M+NH_4^+$) requires *m/z* 398.2326, found *m/z* 398.2322.

***tert*-Butyl 3-benzoyl-4-(4-methylphenyl)cyclopentanecarboxylate (2.14):** Prepared according

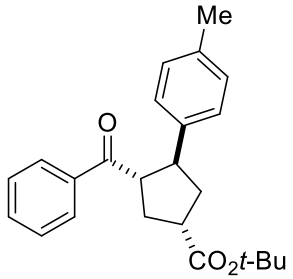

to the general procedure using 24.6 mg (0.04 mmol) of $Gd(OTf)_3$, 30.1 mg (0.08 mmol) of 4-NMe_2-^{s}Bu-pybox, 98.9 mg (0.4 mmol) of *trans* tert-butyl 2-benzoylcyclopropanecarboxylate, 242.0 mg (2.0 mmol) of 4-methylstyrene, 9.0 mg (0.01 mmol) of $Ru(bpy)_3(PF_6)_2$, 52.2 mg (0.4 mmol) of diisopropylethylamine with a total volume of 4 mL (0.1 M). The reaction was ended after 20 h. The crude product was purified by column chromatography (1:69 acetone/pentanes) to give 131 mg (0.36 mmol, 90% yield) of the cycloadduct as two separable diastereomers (2.8:1

d.r.). Major diastereomer: 88.7% ee [Daicel Chiracel AD-H, 10 to 40 % iPrOH, 3 mL/min, 241 nm; t_1=6.01 min, t_2=7.36 min]. $[\alpha]_D^{22}$ 60.7 (*c*1.060, CH_2Cl_2). White solid (mp = 84.2 – 85.9 °C). ν_{max} (film) / cm^{-1} 2976, 1723, 1681, 1515, 1448, 1367, 1249, 1150, 848, 815, 700. ^{1}H NMR (400 MHz, $CDCl_3$) δ 7.82 (d, *J* = 7.3 Hz, 2H), 7.49 (t, *J* = 7.4 Hz, 1H), 7.37 (t, *J* = 7.7 Hz, 2H), 7.13 (d, *J* = 8.0 Hz, 2H), 7.05 (d, *J* = 8.0 Hz, 2H), 3.85 (q, *J* = 9.0 Hz, 1H), 3.77 (q, *J* = 8.6 Hz, 1H), 3.08 (qd, *J* = 8.4, 6.2 Hz, 1H), 2.56 – 2.42 (m, 2H), 2.27 (s, 3H), 2.20 (dt, *J* = 13.1, 9.3 Hz, 1H), 2.10 (dt, *J* = 13.2, 8.9 Hz, 1H), 1.45 (s, 9H). ^{13}C NMR (101 MHz, $CDCl_3$) δ 200.62, 174.26, 140.70, 136.89, 135.91, 132.88, 129.19, 128.46, 128.41, 127.17, 80.47, 54.71, 46.73, 44.43, 37.38, 35.33, 28.08, 20.97. HRMS (ESI) calculated for $[C_{24}H_{29}O_3]^+$(M+H^+) requires *m/z* 365.2111, found *m/z* 365.2105. Minor diastereomer: White solid (mp = 129.1 – 131.9 °C). ν_{max} (film) / cm^{-1} 2973, 2930, 1726, 1678, 1448, 1365, 1280, 1245, 1227, 1155, 818, 699. ^{1}H NMR (400 MHz, $CDCl_3$) δ 7.83 (d, *J* = 7.4 Hz, 2H), 7.50 (t, *J* = 7.3 Hz, 1H), 7.37 (t, *J* = 7.7 Hz, 2H), 7.16 (d, *J* = 8.0 Hz, 2H), 7.05 (d, *J* = 7.9 Hz, 2H), 3.96 (q, *J* = 9.3 Hz, 1H), 3.69 – 3.60 (m, 1H), 2.99 (ddd, *J* = 16.7, 9.3, 7.5 Hz, 1H), 2.54 – 2.44 (m, 2H), 2.27 (s, 3H), 2.11 (tdd, *J* = 17.1, 9.8, 4.3 Hz, 2H), 1.48 (s, 9H). ^{13}C NMR (101 MHz, $CDCl_3$) δ 201.40, 174.96, 139.90, 136.66, 136.04, 133.00, 129.18, 128.52, 128.48, 127.28, 80.45, 53.71, 47.93, 44.19, 38.93, 34.83, 28.14, 20.98. HRMS (ESI) calculated for $[C_{24}H_{32}NO_3]^+$ (M+NH_4^+) requires *m/z* 382.2377, found *m/z* 382.2372.

***tert*-Butyl 3-benzoyl-4-(4-trifluoromethylphenyl)cyclopenanecarboxylate (2.15):** Prepared

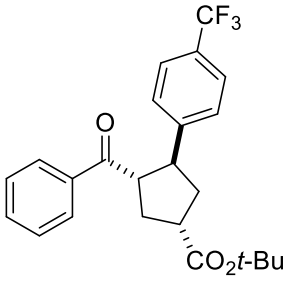

according to the general procedure using 24.2 mg (0.04 mmol) of $Gd(OTf)_3$, 28.8 mg (0.08 mmol) of 4-NMe_2-^{s}Bu-pybox, 98.0 mg (0.4 mmol) of *trans* tert-butyl 2-benzoylcyclopropanecarboxylate, 344.6 mg (2.0 mmol) of 4-trifluoromethylstyrene, 8.8 mg (0.01 mmol) of

$Ru(bpy)_3(PF_6)_2$, 52.6 mg (0.4 mmol) of diisopropylethylamine with a total volume of 4 mL (0.1 M). The reaction was ended after 20 h. The crude product was purified by column chromatography (1:49 acetone/pentanes) to give 135 mg (0.34 mmol, 81% yield) of the cycloadduct as two separable diastereomers (2.4:1 d.r.). Major diastereomer: 89.4% ee [Daicel Chiracel AD-H, 10 to 20 % iPrOH, 3 mL/min, 240 nm; t_1=3.38 min, t_2=4.67 min]. $[\alpha]_D^{22}$ 52.1 (*c*1.000, CH_2Cl_2). White solid. (mp = 106.9 – 108.4 °C). ν_{max} (film) / cm^{-1} 2978, 1724, 1682, 1619, 1449, 1368, 1326, 1258, 1156, 1124, 1069, 1017, 842, 701. ^{1}H NMR (400 MHz, $CDCl_3$) δ 7.82 (d, *J* = 7.1 Hz, 2H), 7.55 – 7.47 (m, 3H), 7.40 (t, *J* = 7.8 Hz, 2H), 7.36 (d, *J* = 8.1 Hz, 2H), 3.93 – 3.81 (m, 2H), 3.15 – 3.07 (m, 1H), 2.55 (qd, *J* = 8.2, 4.1 Hz, 2H), 2.19 (ddd, *J* = 13.1, 9.5, 8.0 Hz, 1H), 2.12 (dt, *J* = 13.5, 9.2 Hz, 1H), 1.46 (s, 9H). ^{13}C NMR (101 MHz, $CDCl_3$) δ 199.89, 173.95, 147.72, 136.59, 133.17, 128.75 (q, *J* = 32.5 Hz), 128.59, 128.35, 127.70, 125.45 (q, *J* = 3.9 Hz), 124.47 (q, *J* = 272.9 Hz), 80.73, 54.76, 46.57, 44.28, 37.02, 35.45, 28.05. **^{19}**F NMR (377 MHz, $CDCl_3$) δ -62.46. HRMS (ESI) calculated for $[C_{24}H_{26}F_3O_3]^+$($M+H^+$) requires *m/z* 419.1829, found *m/z* 419.1826. Minor diastereomer: White solid (mp = 122.8 – 125.9 °C). ν_{max} (film) / cm^{-1} 2974, 1722, 1677, 1369, 1327, 1281, 1247, 1225, 1164, 1138, 1170, 1018, 842, 699. ^{1}H NMR (400 MHz, $CDCl_3$) δ 7.84 (d, *J* = 7.1 Hz, 2H), 7.57 – 7.46 (m, 3H), 7.40 (t, *J* = 7.5 Hz, 4H), 3.98 (q, *J* = 9.4 Hz, 1H), 3.83 – 3.71 (m, 1H), 3.01 (ddd, *J* = 16.4, 9.2, 7.3 Hz, 1H), 2.60 – 2.48 (m, 2H), 2.20 – 2.06 (m, 2H), 1.49 (s, 9H). ^{13}C NMR (101 MHz, $CDCl_3$) δ 200.62, 174.73, 147.10, 136.36, 133.29, 128.80 (q, *J* = 31.1 Hz), 128.62, 128.45, 127.82, 125.44 (q, *J* = 3.7 Hz), 124.16 (q, *J* = 271.3), 80.72, 53.75, 47.67, 44.03, 38.34, 34.99, 28.11. **^{19}**F NMR (377 MHz, $CDCl_3$) δ –62.47. HRMS (ESI) calculated for $[C_{24}H_{29}F_3NO_3]^+$($M+NH_4^+$) requires *m/z* 436.2095, found *m/z* 436.2093.

***tert*-Butyl 3-benzoyl-4-(4-bromophenyl)cyclopentanecarboxylate (2.16):** Prepared according

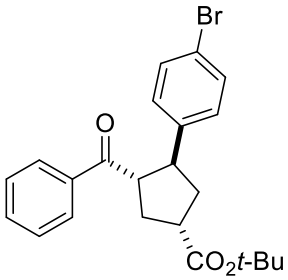

to the general procedure using 24.5 mg (0.04 mmol) of $Gd(OTf)_3$, 30.0 mg (0.08 mmol) of 4-NMe_2-^{s}Bu-pybox, 100.6 mg (0.4 mmol) of *trans* tert-butyl 2-benzoylcyclopropanecarboxylate, 367.0 mg (2.0 mmol) of 4-bromostyrene, 9.0 mg (0.01 mmol) of $Ru(bpy)_3(PF_6)_2$, 52.6 mg (0.4 mmol) of diisopropylethylamine with a total volume of 4 mL (0.1 M). The reaction was ended after 20 h. The crude product was purified by column chromatography (1:29, acetone/pentanes) to give 148 mg (0.34 mmol, 84% yield) of the cycloadduct as two separable diastereomers (2.3:1 d.r.). Major Diastereomer: 89.7% ee [Daicel Chiracel AD-H, 10 to 40 % iPrOH, 3 mL/min, 239 nm; t_1 =7.91, t_2=10.09 min]. $[\alpha]_D^{22}$ 50.8 (*c*1.020, CH_2Cl_2). White solid (mp = 103.1 – 104.4 °C). ν_{max} (film) / cm^{-1} 2976, 1722, 1681, 1490, 1448, 1366, 1257, 1150, 1074, 1010, 848, 821, 701. ^{1}H NMR (400 MHz, $CDCl_3$) δ 7.82 (d, *J* = 7.3 Hz, 2H), 7.52 (t, *J* = 7.4 Hz, 1H), 7.42 – 7.34 (m, 4H), 7.12 (d, *J* = 8.4 Hz, 2H), 3.83 – 3.74 (m, 2H), 3.08 (qd, *J* = 8.2, 5.7 Hz, 1H), 2.57 – 2.45 (m, 2H), 2.23 – 2.13 (m, 1H), 2.07 (dt, *J* = 13.4, 9.2 Hz, 1H), 1.45 (s, 9H). ^{13}C NMR (101 MHz, $CDCl_3$) δ 200.16, 174.05, 142.62, 136.69, 133.11, 131.56, 129.10, 128.57, 128.35, 120.13, 80.65, 54.77, 46.40, 44.26, 37.09, 35.41, 28.06. HRMS (ESI) calculated for $[C_{23}H_{26}BrO_3]^+$($M+H^+$) requires *m/z* 429.1060, found *m/z* 429.1074. Minor Diastereomer: White solid (mp = 129.1 – 132.8 °C). ν_{max} (film) / cm^{-1} 2975, 1722, 1680, 1490, 1448, 1367, 1284, 1246, 1220, 1152, 1074, 1011, 823, 700. ^{1}H NMR (400 MHz, $CDCl_3$) δ 7.83 (d, *J* = 7.3 Hz, 2H), 7.52 (t, *J* = 7.4 Hz, 1H), 7.44 – 7.32 (m, 4H), 7.15 (d, *J* = 8.4 Hz, 2H), 3.92 (q, *J* = 9.4 Hz, 1H), 3.65 (ddd, *J* = 11.3, 9.5, 7.6 Hz, 1H), 2.99 (ddd, *J* = 16.5, 9.3, 7.3 Hz, 1H), 2.50 (ddd, *J* = 13.3, 9.8, 6.8 Hz, 2H), 2.17 – 2.02 (m, 2H), 1.48 (s, 9H). ^{13}C NMR (101 MHz, $CDCl_3$) δ 200.92, 174.82, 141.95, 136.47, 133.23, 131.56, 129.20,

128.60, 128.46, 120.25, 80.64, 53.74, 47.56, 44.03, 38.46, 34.93, 28.12. HRMS (ESI) calculated for $[C_{23}H_{29}BrNO_3]^+$(M+NH_4^+) requires *m/z* 446.1326, found *m/z* 446.1313.

***tert*-Butyl 3-benzoyl-4-(2-methylphenyl)cyclopentanecarboxylate (2.17):** Prepared according

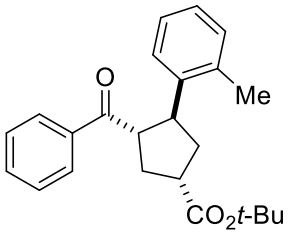

to the general procedure using 25.5 mg (0.04 mmol) of $Gd(OTf)_3$, 30.7 mg (0.08 mmol) of 4-NMe_2-^{s}Bu-pybox, 98.4 mg (0.4 mmol) of *trans* tert-butyl 2-benzoylcyclopropanecarboxylate, 236.3 mg (2.0 mmol) of 2-methylstyrene, 8.7 mg (0.01 mmol) of $Ru(bpy)_3(PF_6)_2$, 56.7 mg (0.4 mmol) of diisopropylethylamine with a total volume of 4 mL (0.1 M). The reaction was ended after 20 h. The crude product was purified by column chromatography (1:49 Et_2O/pentanes) to give 110 mg (0.30 mmol, 75% yield) of cycloadduct as two separable diastereomers (2.0:1 d.r.). Major Diastereomer: 86.8% ee [Daicel Chiracel AD-H, 10 to 20 % iPrOH, 3 mL/min, 240 nm; t_1=4.20 min, t_2=5.47 min]. $[\alpha]_D^{22}$ 47.0 (*c*1.020, CH_2Cl_2). White solid (mp = 70.7 – 74.1 °C). ν_{max} (film) / cm^{-1} 2975, 1723, 1681, 1448, 1367, 1218, 1149, 1101, 848, 753, 700. ^{1}H NMR (400 MHz, $CDCl_3$) δ 7.81 (d, *J* = 7.3 Hz, 2H), 7.49 (t, *J* = 7.4 Hz, 1H), 7.37 (t, *J* = 7.7 Hz, 2H), 7.26 (d, *J* = 7.7 Hz, 1H), 7.16 (dt, *J* = 7.9, 4.3 Hz, 2H), 7.10 – 7.01 (m, 3H), 4.08 – 3.92 (m, 3H), 3.09 (td, *J* = 8.5, 6.5 Hz, 2H), 2.59 – 2.45 (m, 3H), 2.31 (s, 3H), 2.24 (dt, *J* = 13.1, 8.8 Hz, 1H), 1.96 (dt, *J* = 13.3, 8.5 Hz, 1H), 1.46 (s, 9H). ^{13}C NMR (101 MHz, $CDCl_3$) δ 200.83, 174.40, 142.30, 136.88, 136.65, 133.05, 130.57, 128.60, 128.49, 126.38, 126.28, 125.49, 80.60, 54.16, 44.80, 43.00, 37.70, 35.29, 28.21, 20.00. HRMS (ESI) calculated for $[C_{24}H_{29}O_3]^+$(M+H^+) requires *m/z* 365.2111, found *m/z* 365.2105. Minor Diastereomer: Colorless oil. ν_{max} (film) / cm^{-1} 2976, 1723, 1680, 1448, 1367, 1290, 1216, 1151, 848, 575, 700. ^{1}H NMR (400 MHz, $CDCl_3$) δ 7.81 (d, *J* = 7.4 Hz, 2H), 7.49 (t,

J = 7.4 Hz, 1H), 7.41 – 7.31 (m, 3H), 7.23 – 7.12 (m, 1H), 7.10 – 7.01 (m, 2H), 4.09 (q, *J* = 9.0 Hz, 1H), 3.88 (dt, *J* = 11.0, 8.3 Hz, 1H), 3.01 (p, *J* = 8.9 Hz, 1H), 2.51 (dq, *J* = 13.5, 7.3 Hz, 2H), 2.28 (s, 3H), 2.23 – 2.12 (m, 1H), 2.05 – 1.91 (m, 1H), 1.48 (s, 9H). ^{13}C NMR (101 MHz, $CDCl_3$) δ 201.48, 174.93, 141.45, 136.53, 136.33, 133.01, 130.31, 128.46, 128.46, 126.42, 126.20, 125.81, 80.45, 53.47, 44.43, 43.81, 39.39, 34.61, 28.13, 19.83.HRMS (ESI) calculated for $[C_{24}H_{32}NO_3]^+$(M+NH_4^+) requires *m/z* 382.2377, found *m/z* 382.2372.

***Tert*-butyl 3-benzoyl-4-methyl-4-phenylcyclopenanecarboxylate (2.18):** Prepared according to

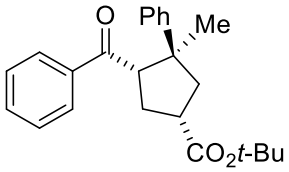

the general procedure using 24.4 mg (0.04 mmol) of $Gd(OTf)_3$, 28.7 mg (0.08 mmol) of 4-NMe_2-^{s}Bu-pybox, 98.2 mg (0.4 mmol) of *trans* tert-butyl 2-benzoylcyclopropanecarboxylate, 236.0 mg (2.0 mmol) of α-methylstyrene, 8.8 mg (0.01 mmol) of $Ru(bpy)_3(PF_6)_2$, 53.6 mg (0.4 mmol) of diisopropylethylamine with a total volume of 4 mL (0.1 M) in MeCN. The reaction was ended after 20 h. The crude product was purified by column chromatography (neat toluene to 1:9 acetone/toluene) to give 118 mg (0.32 mmol, 81% yield) of the cycloadduct as two separable diastereomers (2.9:1 d.r.). Major Diastereomer: 89.5% ee [Daicel Chiracel AD-H, 10 to 20 % iPrOH, 3 mL/min, 240 nm; t_1=4.16 min, t_2=4.78 min]. $[\alpha]_D^{22}$ 117.5 (*c*=0.930, CH_2Cl_2). White solid (mp = 74.2 – 79.5 °C). ν_{max} (film) / cm^{-1} 2977, 1675, 1597, 1447, 1367, 1285, 1253, 848, 732, 700. ^{1}H NMR (400 MHz, $CDCl_3$) δ 7.52 (d, *J* = 7.0 Hz, 2H), 7.41 (t, *J* = 7.4 Hz, 1H), 7.31 – 7.16 (m, 7H), 4.09 (dd, *J* = 9.8, 6.7 Hz, 1H), 3.08 (dt, *J* = 18.3, 9.3 Hz, 1H), 2.63 (dt, *J* = 13.3, 10.0 Hz, 1H), 2.53 (dd, *J* = 13.7, 9.2 Hz, 1H), 2.29 – 2.14 (m, 2H), 1.49 (s, 9H), 1.26 (s, 3H). ^{13}C NMR (101 MHz, $CDCl_3$) δ 201.35, 174.34, 148.87, 137.78, 132.57, 128.39, 128.38, 128.15, 126.15, 125.88, 80.38, 57.65, 49.53, 45.42, 43.63, 32.71, 28.14, 24.30.

HRMS (ESI) calculated for $[C_{24}H_{29}O_3]^+$(M+H^+) requires *m/z* 365.2112, found *m/z* 365.2115. Minor Diastereomer: Colorless oil. ν_{max} (film) / cm^{-1} 2977, 1724, 1676, 1449, 1369, 1258, 1222, 1154, 1086, 1026, 803, 700. ^{1}H NMR (400 MHz, $CDCl_3$) δ 7.49 (d, *J* = 7.1 Hz, 2H), 7.37 (t, *J* = 7.4 Hz, 1H), 7.31 (d, *J* = 8.1 Hz, 2H), 7.25 – 7.09 (m, 5H), 4.17 (t, *J* = 8.7 Hz, 1H), 3.17 (qd, *J* = 9.0, 5.6 Hz, 1H), 2.68 – 2.57 (m, 2H), 2.28 (ddd, *J* = 13.9, 8.6, 5.6 Hz, 1H), 2.17 (dd, *J* = 13.1, 8.2 Hz, 1H), 1.49 (s, 9H), 1.30 (s, 3H). ^{13}C NMR (101 MHz, $CDCl_3$) δ 201.56, 175.76, 147.07, 137.78, 132.47, 128.29, 128.23, 128.05, 126.21, 126.19, 80.42, 56.74, 50.65, 46.99, 42.29, 32.17, 28.15, 22.14. HRMS (ESI) calculated for $[C_{24}H_{32}NO_3]^+$(M+NH_4^+) requires *m/z* 382.2377, found *m/z* 382.2376.

tert-Butyl 2-benzoyl-2',3'-dihydrospiro[cyclopentane-1,1'-indene]-4-carboxylate (2.19):

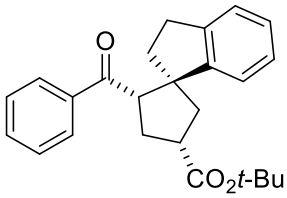

Prepared according to the general procedure using 24.3 (0.04 mmol) of $Gd(OTf)_3$, 30.3 mg (0.08 mmol) of 4-NMe_2-^{s}Bu-pybox, 100.0 mg (0.4 mmol) of *trans* tert-butyl 2-benzoylcyclopropanecarboxylate, 260.9 mg (1.5 mmol) of 1-methylene-2,3-dihydro-1H-indene, 8.3 mg (0.01 mmol) of $Ru(bpy)_3(PF_6)_2$, 57.8 mg (0.4 mmol) of diisopropylethylamine with a total volume of 4 mL (0.1 M). The reaction was ended after 20 h. The crude product was purified by column chromatography (1:49 acetone/pentanes) to give 144 mg (0.38 mmol, 95% yield) of cycloadduct as two separable diastereomers (2.7:1 d.r.). Major diastereomer: 97.2% ee [Daicel Chiracel AD-H, 5% iPrOH, 8 mL/min, 240 nm; t_1=3.57 min, t_2=5.09 min]. $[\alpha]_D^{22}$ 102.3 (*c*1.580, CH_2Cl_2). Colorless oil. ν_{max} (film) / cm^{-1} 2975, 2935, 1724, 1672, 1478, 1448, 1392, 1367, 1225, 1151, 1002, 849, 756, 732, 691. ^{1}H NMR (500 MHz, $CDCl_3$) δ 7.49 (d, *J* = 7.0 Hz, 2H), 7.40 – 7.32 (m, 2H), 7.26 (m, 3H),

7.17 (t, *J* = 7.8 Hz, 2H), 7.09 (t, *J* = 7.3 Hz, 1H), 6.93 (d, *J* = 6.9 Hz, 1H), 3.91 (dd, *J* = 10.4, 6.9 Hz, 1H), 3.06 (dt, *J* = 17.3, 8.3 Hz, 1H), 2.73 – 2.60 (m, 2H), 2.44 (dd, *J* = 13.3, 9.1 Hz, 1H), 2.38 – 2.22 (m, 4H), 1.93 – 1.83 (m, 1H), 1.48 (s, 9H). ^{13}C NMR (126 MHz, $CDCl_3$) δ 201.23, 174.36, 149.28, 143.69, 137.38, 132.57, 128.16, 128.02, 127.08, 126.62, 124.69, 122.27, 80.35, 59.06, 56.04, 44.49, 43.23, 36.75, 33.47, 30.97, 28.12. HRMS (ESI) calculated for $[C_{25}H_{29}O_3]^+$($M+H^+$) requires *m/z* 377.2111, found *m/z* 377.2107. Minor diastereomer: Colorless oil. ν_{max} (film) / cm^{-1} 2976, 2932, 1720, 1671, 1448, 1367, 1220, 1150, 908, 846, 729, 690. ^{1}H NMR (400 MHz, $CDCl_3$) δ 7.49 – 7.41 (m, 3H), 7.31 (t, *J* = 7.4 Hz, 1H), 7.26 – 7.18 (m, 1H), 7.11 (t, *J* = 7.8 Hz, 2H), 7.03 (t, *J* = 7.6 Hz, 1H), 6.84 (d, *J* = 7.5 Hz, 1H), 4.05 (t, *J* = 8.7 Hz, 1H), 3.11 (tdd, *J* = 9.9, 7.6, 6.1 Hz, 1H), 2.71 (dt, *J* = 13.6, 9.7 Hz, 1H), 2.67 – 2.57 (m, 1H), 2.54 (dd, *J* = 12.8, 9.8 Hz, 1H), 2.47 – 2.25 (m, 2H), 2.27 – 2.09 (m, 2H), 1.76 (dt, *J* = 12.4, 8.9 Hz, 1H), 1.50 (s, 9H). ^{13}C NMR (101 MHz, $CDCl_3$) δ 201.42, 175.61, 147.06, 143.90, 137.16, 132.45, 128.14, 127.82, 127.19, 126.54, 124.57, 122.60, 80.39, 60.28, 55.35, 46.18, 42.58, 34.90, 31.96, 30.78, 28.17. HRMS (ESI) calculated for $[C_{25}H_{32}NO_3]^+$($M+NH_4^+$) requires *m/z* 394.2377, found *m/z* 394.2374.

tert-Butyl 2-benzoyl-3',4'-dihydro-2'H-spiro[cyclopentane-1,1'-naphthalene]-4-carboxylate

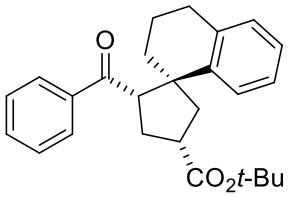

(2.20): Prepared according to the general procedure using 18.1 mg (0.03 mmol) of $Gd(OTf)_3$, 22.4 mg (0.06 mmol) of 4-NMe_2-^{s}Bu-pybox, 78.9 mg (0.3 mmol) of *trans* tert-butyl 2-benzoylcyclopropanecarboxylate, 216.3 mg (1.5 mmol) of 1-methylene-1,2,3,4-tetrahydronaphthalene, 6.4 mg (0.0075 mmol) of $Ru(bpy)_3(PF_6)_2$, 38.8 mg (0.3 mmol) of diisopropylethylamine with a total volume of 3 mL (0.1 M). The reaction was ended after 20 h. The crude product was purified by column chromatography

(1:49 acetone/pentanes) to give 95 mg (0.33 mmol, 83% yield) of the cycloadduct as two separable diastereomers (2.7:1 d.r.). Major Diastereomer: 99.5% ee [Daicel Chiracel AD-H, 5 % iPrOH, 8 mL/min, 241 nm; t_1=4.14 min, t_2=5.94 min]. $[\alpha]_D^{22}$ 169.0 (*c*0.720, CH_2Cl_2). White solid (mp = 104.0 – 106.8 °C). ν_{max} (film) / cm^{-1} 2974, 2936, 1724, 1673, 1447, 1366, 1254, 1230, 1152, 754, 720, 691. ^{1}H NMR (400 MHz, $CDCl_3$) δ 7.52 (d, *J* = 7.9 Hz, 1H), 7.44 (d, *J* = 8.4 Hz, 2H), 7.35 (t, *J* = 7.4 Hz, 1H), 7.27 (d, *J* = 6.2 Hz, 1H), 7.14 (t, *J* = 7.8 Hz, 2H), 7.10 (t, *J* = 7.7 Hz, 1H), 6.90 (d, *J* = 7.6 Hz, 1H), 4.16 (dd, *J* = 11.6, 6.4 Hz, 1H), 3.10 (dtd, *J* = 11.6, 9.3, 7.2 Hz, 1H), 2.72 (q, *J* = 11.8 Hz, 1H), 2.57 (dt, *J* = 16.5, 5.5 Hz, 1H), 2.36 (qd, *J* = 11.7, 10.4, 4.5 Hz, 2H), 2.23 (ddd, *J* = 13.5, 7.9, 5.5 Hz, 2H), 1.81 – 1.64 (m, 2H), 1.66 – 1.50 (m, 2H), 1.47 (s, 9H). ^{13}C NMR (101 MHz, $CDCl_3$) δ 201.38, 174.27, 143.94, 137.78, 137.47, 132.45, 129.28, 128.34, 128.08, 126.70, 126.46, 125.88, 80.39, 58.96, 49.24, 48.71, 43.93, 34.36, 33.26, 29.98, 28.13, 20.23. HRMS (ESI) calculated for $[C_{26}H_{31}O_3]^+$($M+H^+$) requires *m/z* 391.2273, found *m/z* 391.2263. Minor Diastereomer: Colorless oil. ν_{max} (film) / cm^{-1} 2976, 2937, 1723, 1674, 1447, 1366, 1218, 1151, 733, 691. ^{1}H NMR (400 MHz, $CDCl_3$) δ 7.67 (d, *J* = 8.0 Hz, 1H), 7.46 (d, *J* = 8.2 Hz, 2H), 7.32 (t, *J* = 7.4 Hz, 1H), 7.30 – 7.21 (m, 1H), 7.13 (t, *J* = 7.8 Hz, 2H), 7.04 (t, *J* = 7.3 Hz, 1H), 6.85 (d, *J* = 7.6 Hz, 1H), 4.32 (t, *J* = 8.3 Hz, 1H), 3.17 – 3.04 (m, 1H), 2.73 (dt, *J* = 13.7, 8.7 Hz, 1H), 2.52 (dt, *J* = 16.1, 5.0 Hz, 1H), 2.40 – 2.22 (m, 4H), 1.73 (ddd, *J* = 13.1, 9.4, 3.4 Hz, 1H), 1.67 – 1.49 (m, 3H), 1.49 (s, 9H). ^{13}C NMR (101 MHz, $CDCl_3$) δ 202.08, 175.59, 141.75, 138.18, 137.82, 132.34, 129.00, 128.31, 127.96, 127.36, 126.41, 125.88, 80.36, 58.12, 50.62, 49.53, 42.83, 32.01, 31.97, 30.32, 28.16, 20.50. HRMS (ESI) calculated for $[C_{26}H_{34}NO_3]^+$($M+NH_4^+$) requires *m/z* 408.2533, found *m/z* 408.2529.

tert-Butyl 3-benzoyl-4-(9H-carbazol-9-yl)cyclopentanecarboxylate (2.21): Prepared according

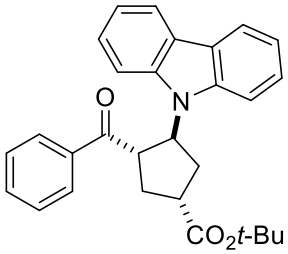

to the general procedure using 18.1 mg (0.03 mmol) of $Gd(OTf)_3$, 22.4 mg (0.06 mmol) of 4-NMe_2-^{s}Bu-pybox, 73.9 mg (0.3 mmol) of *trans* tert-butyl 2-benzoylcyclopropanecarboxylate, 289.8 mg (1.5 mmol) of 9-vinylcarbazole, 6.4 mg (0.0075 mmol) of $Ru(bpy)_3(PF_6)_2$, 38.8 mg (0.3 mmol) of diisopropylethylamine with a total volume of 3 mL (0.1 M). The reaction was ended after 20 h. The crude product was purified by column chromatography (1:29, acetone/pentanes) to give 74 mg (0.17 mmol, 57% yield) of the cycloadduct as two separable diastereomers (1.9:1 d.r.). Major diastereomer: 85.8% ee [Daicel Chiracel AD-H, 5% MeOH, 3 mL/min, 241 nm; t_1=5.76 min, t_2=9.18 min]. $[\alpha]_D^{22}$ 35.8 (*c*0.550, CH_2Cl_2). Colorless oil. ν_{max} (film) / cm^{-1}2976, 1724, 1682, 1597, 1484, 1453, 1367, 1337, 1227, 1154, 847, 750, 724, 698. ^{1}H NMR (400 MHz, $CDCl_3$) δ 8.04 (d, *J* = 7.7 Hz, 2H), 7.62 (d, *J* = 7.2 Hz, 2H), 7.57 (d, *J* = 8.3 Hz, 2H), 7.44 (t, *J* = 7.8 Hz, 2H), 7.35 (t, *J* = 7.5 Hz, 1H), 7.27 – 7.14 (m, 4H), 5.94 (q, *J* = 9.1 Hz, 1H), 4.66 (q, *J* = 9.1 Hz, 1H), 3.40 (p, *J* = 8.1 Hz, 1H), 2.85 – 2.57 (m, 3H), 2.38 (dt, *J* = 13.3, 9.1 Hz, 1H), 1.50 (s, 9H). ^{13}C NMR (101 MHz, $CDCl_3$) δ 199.53, 173.42, 139.31, 136.18, 133.14, 128.39, 128.26, 125.66, 123.41, 120.39, 119.08, 109.76, 81.12, 56.17, 49.49, 44.09, 34.36, 31.36, 28.10. HRMS (ESI) calculated for $[C_{29}H_{30}NO_3]^+$(M+H^+) requires *m/z* 440.2220, found *m/z* 440.2217. Minor diastereomer: Colorless oil. ν_{max} (film) / cm^{-1} 2977, 1722, 1681, 1597, 1484, 1453, 1367, 1337, 1221, 1151, 750, 724, 699. ^{1}H NMR (400 MHz, $CDCl_3$) δ 8.05 (d, *J* = 7.7 Hz, 2H), 7.71 (d, *J* = 7.2 Hz, 2H), 7.49 – 7.35 (m, 3H), 7.41 (s, 0H), 7.28 – 7.17 (m, 5H), 5.81 (dt, *J* = 11.0, 8.5 Hz, 1H), 4.85 – 4.74 (m, 1H), 3.09 (dt, *J* = 15.9, 7.8 Hz, 1H), 2.97 – 2.84 (m, 1H), 2.76 (ddd, *J* = 13.5, 9.9, 7.7 Hz, 1H), 2.51 (dt, *J* = 13.3, 8.1 Hz, 1H), 2.30 (dt, *J* = 14.0, 7.6 Hz, 1H), 1.52 (s, 9H). ^{13}C NMR (101 MHz, $CDCl_3$) δ 200.20, 174.24, 139.40, 135.75, 133.31, 128.49, 128.47, 125.71, 123.40, 120.34, 119.11,

109.90, 81.07, 56.75, 47.76, 42.78, 33.31, 32.53, 28.15. HRMS (ESI) calculated for $[C_{29}H_{30}NO_3]^+$(M+H^+) requires *m/z* 440.2220, found *m/z* 440.2217.

tert-Butyl 3-benzoyl-4-vinylcyclopentanecarboxylate (2.22): Prepared according to general procedure using 24.6 mg (0.04 mmol) of $Gd(OTf)_3$, 30.0 mg (0.08 mmol) of 4-NMe_2-^{s}Bu-pybox, 98.4 mg (0.4 mmol) of *trans* tert-butyl 2-benzoylcyclopropanecarboxylate, 140 μL (2.0 mmol) of butadiene (15 wt% in toluene), 8.7 mg (0.01 mmol) of $Ru(bpy)_3(PF_6)_2$, 53.5 mg (0.4 mmol) of diisopropylethylamine with a total volume of 4 mL (0.1 M) in MeCN. The reaction was complete after 6 h. The crude product was purified by column chromatography (1:9 Et_2O/pentanes) to give 70.8 mg (0.2357 mmol, 59 % yield) of cycloadduct as two separable diastereomers (3:1 dr). Major Diastereomer: 87.2% ee [Daicel Chiracel AD-H, 5 to 50 % MeOH, 3 mL/min, 240 nm; t_1=3.63 min, t_2=4.68 min]. $[\alpha]_D^{22}$ 58.1 (*c*0.410, CH_2Cl_2). Colorless oil. ν_{max} (film) / cm^{-1} 2977, 2933, 1725, 1681, 1449, 1367, 1258, 1152. ^{1}H NMR (400 MHz, $CDCl_3$) δ 7.87 (d, *J* = 7.3 Hz, 2H), 7.48 (t, *J* = 7.4 Hz, 1H), 7.39 (t, *J* = 7.6 Hz, 2H), 5.71 (ddd, *J* = 17.4, 10.2, 7.4 Hz, 1H), 4.95 (d, *J* = 17.1 Hz, 1H), 4.87 (d, *J* = 10.3 Hz, 1H), 3.49 (q, *J* = 8.3 Hz, 1H), 3.10 (p, *J* = 7.9 Hz, 1H), 2.95 – 2.73 (m, 1H), 2.28 (dt, *J* = 13.1, 8.2 Hz, 1H), 2.17 (ddd, *J* = 14.0, 8.0, 6.4 Hz, 1H), 2.07 (dt, *J* = 13.1, 9.1 Hz, 1H), 1.76 (dt, *J* = 13.1, 8.6 Hz, 1H), 1.37 (s, 9H). ^{13}C NMR (101 MHz, $CDCl_3$) δ 200.70, 174.32, 140.11, 137.02, 132.99, 128.56, 128.46, 114.72, 80.39, 52.21, 45.98, 43.86, 35.09, 34.47, 28.06. HRMS (ESI) calculated for $[C_{19}H_{25}O_3]^+$ (M+H^+) requires *m/z* 301.1804, found *m/z* 301.1803. Minor Diastereomer: Colorless oil. ν_{max} (film) / cm^{-1} 2981, 2934, 1719, 1678, 1368, 1155. ^{1}H NMR (400 MHz, $CDCl_3$) δ 7.90 (d, *J* = 7.3 Hz, 2H), 7.54 (t, *J* = 7.4 Hz, 1H), 7.44 (t, *J* = 7.6 Hz, 2H), 5.61 (dt, *J* = 16.9, 9.7

Hz, 1H), 4.81 – 4.71 (m, 2H), 3.92 (q, *J* = 9.0 Hz, 1H), 3.05 (p, *J* = 8.0 Hz, 1H), 2.83 (dt, *J* = 17.3, 8.7 Hz, 1H), 2.48 (dt, *J* = 13.2, 10.0 Hz, 1H), 2.22 (dt, *J* = 13.4, 8.0 Hz, 1H), 2.12 (dt, *J* = 13.9, 7.4 Hz, 1H), 1.99 (ddd, *J* = 13.3, 8.9, 7.4 Hz, 1H), 1.47 (s, 9H). ^{13}C NMR (101 MHz, $CDCl_3$) δ 200.46, 174.29, 138.13, 137.62, 132.81, 128.48, 128.31, 115.40, 80.30, 50.58, 47.40, 44.08, 35.63, 31.60, 28.10. HRMS (ESI) calculated for $[C_{19}H_{18}NO_3]^+$ ($M+NH_4^+$) requires *m/z* 318.2069, found 318.2067.

tert-Butyl 4-benzoyl-3-methyl-3-(prop-1-en-2-yl)cyclopentanecarboxylate (2.23): Prepared

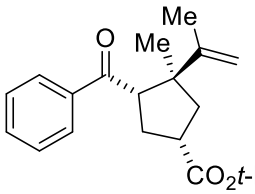

according to general procedure using 24.6 mg (0.04 mmol) of $Gd(OTf)_3$, 30.0 mg (0.08 mmol) of 4-NMe_2-^{s}Bu-pybox, 98.4 mg (0.4 mmol) of *trans* tert-butyl 2-benzoylcyclopropanecarboxylate, 166.7 mg (2.0 mmol) of 2,3-dimethyl-1,3-butadiene, 8.7 mg (0.01 mmol) of $Ru(bpy)_3(PF_6)_2$, 53.5 mg (0.4 mmol) of diisopropylethylamine with a total volume of 4 mL (0.1 M) in MeCN. The reaction was complete after 6 h. The crude product was purified by column chromatography (1:9 Et_2O/pentanes) to give 101.0 mg (0.3076 mmol, 77 % yield) of cycloadduct as two separable diastereomers (3:1 dr). Major Diastereomer: 95.6% ee [Daicel Chiracel AD-H, 5 % MeOH, 3 mL/min, 239 nm; t_1=3.44 min, t_2=5.45 min]. $[\alpha]_D^{22}$ 47.0 (*c*0.540, CH_2Cl_2). Colorless oil. ν_{max} (film) / cm^{-1} 2978, 1719, 1674, 1368, 1265, 1154. ^{1}H NMR (400 MHz, $CDCl_3$) δ 7.86 (d, *J* = 7.3 Hz, 2H), 7.53 (t, *J* = 7.4 Hz, 1H), 7.42 (t, *J* = 7.6 Hz, 2H), 4.78 (s, 1H), 4.73 (s, 1H), 3.94 (dd, *J* = 8.8, 7.2 Hz, 1H), 2.87 (p, *J* = 9.1 Hz, 1H), 2.51 (dt, *J* = 13.1, 9.4 Hz, 1H), 2.20-2.10 (m, 2H), 1.91 (dd, *J* = 13.5, 9.6 Hz, 1H), 1.85 (s, 3H), 1.48 (s, 9H), 1.02 (s, 3H). ^{13}C NMR (101 MHz, $CDCl_3$) δ 202.02, 174.40, 149.71, 138.42, 132.75, 128.39, 128.33, 110.86, 80.24, 51.67, 50.85, 43.26, 41.92, 32.48, 28.13, 23.24, 20.05.

HRMS (ESI) calculated for $[C_{21}H_{29}O_3]^+$ ($M+H^+$) requires *m/z* 329.2117, found *m/z* 329.2118. Minor Diastereomer: Colorless oil. ν_{max} (film) / cm^{-1} 2975, 1724, 1677, 1448, 1367, 1219, 1152. ^1H NMR (400 MHz, $CDCl_3$) δ 7.85 (d, *J* = 7.3 Hz, 2H), 7.60 (t, *J* = 7.4 Hz, 1H), 7.42 (t, *J* = 7.6 Hz, 2H), 4.72 (s, 1H), 4.69 (s, 1H), 4.00 (t, *J* = 8.3 Hz, 1H), 3.08 (ddd, *J* = 17.8, 9.3, 6.4 Hz, 1H), 2.48 – 2.37 (m, 1H), 2.26 – 2.17 (m, 2H), 1.84 (dd, *J* = 12.9, 8.3 Hz, 1H), 1.80 (s, 3H), 1.47 (s, 9H), 1.09 (s, 3H). ^{13}C NMR (101 MHz, v) δ 202.29, 175.59, 149.19, 138.54, 132.75, 128.41, 128.15, 111.41, 80.27, 52.04, 51.55, 43.44, 42.28, 32.44, 28.12, 21.46, 20.15. HRMS (ESI) calculated for $[C_{21}H_{32}NO_3]^+$ ($M+NH_4^+$) requires *m/z* 346.2381, found 346.2382.

tert-Butyl 3-(4-methoxybenzoyl)-4-phenylcyclopentanecarboxylate (2.24): Prepared

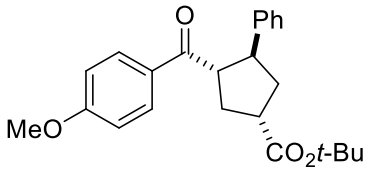

according to the general procedure using 24.6 mg (0.04 mmol) of $Gd(OTf)_3$, 30.0 mg (0.08 mmol) of 4-NMe_2-^{s}Bu-pybox, 109.9 mg (0.4 mmol) of *trans* tert-butyl 2-(4-methoxybenzoyl)cyclopropanecarboxylate, 209.6 mg (2.0 mmol) of styrene, 8.7 mg (0.01 mmol) or $Ru(bpy)_3(PF_6)_2$, and 58.2 mg (0.4 mmol) of diisopropylethylamine with a total volume of 4 mL (0.1 M). The reaction was complete after 6 h. The crude product was purified by column chromatography (1:9, Et_2O/pentanes) to give 142.2 mg (0.37 mmol, 94 % yield) of cycloadduct as two separable diastereomers (3:1 dr). Major diastereomer: 91.1% ee [Daicel Chiracel AD-H, 5 to 50 % iPrOH, 3 mL/min, 238 nm; t_1=7.65 min, t_2=8.98 min]. $[\alpha]_D^{22}$ 45.0 (*c*0.667, CH_2Cl_2). White solid (mp = 97.5-98.2 °C). ν_{max} (film) / cm^{-1} 2795, 1725, 1672, 1600, 1259, 1152. ^1H NMR (400 MHz, $CDCl_3$) δ 7.79 (d, *J* = 8.9 Hz, 2H), 7.25 (m, 5H), 7.15 (dq, *J* = 5.8, 3.0 Hz, 1H), 6.84 (d, *J* = 8.9 Hz, 2H), 3.83 (s, 3H), 3.88 – 3.72 (m, 2H), 3.08 (qd, *J* = 8.7, 6.3 Hz, 1H), 2.60 – 2.39 (m, 2H), 2.31 – 2.01 (m, 2H), 1.46 (s, 9H). ^{13}C NMR (101 MHz, $CDCl_3$) δ 199.02, 174.26, 163.36, 143.92, 130.67, 129.92, 128.50, 127.31,

126.35, 113.61, 80.45, 55.44, 54.40, 47.25, 44.49, 37.25, 35.54, 28.08. HRMS (ESI) calculated for $[C_{24}H_{29}O_4]^+$ ($M+H^+$) requires *m/z* 381.2060, found 381.2060. Minor diastereomer: White solid (mp = 86.6-89.1 ^oC). ν_{max} (film) / cm^{-1} 2792, 1726, 1671, 1606, 1301, 1150. ^1H NMR (400 MHz, $CDCl_3$) δ 7.80 (d, *J* = 8.9 Hz, 2H), 7.27-7.10 (m, 5H), 6.84 (d, *J* = 8.9 Hz, 2H), 3.98 – 3.89 (m, 1H), 3.83 (s, 3H), 3.71 – 3.60 (m, 1H), 3.05 – 2.94 (m, 1H), 2.55-2.4 (m, 2H), 2.2-2.0 (m, 2H), 1.48 (s, 9H). ^{13}C NMR (101 MHz, $CDCl_3$) δ 199.84, 175.04, 163.45, 143.11, 130.80, 129.73, 128.49, 127.43, 126.47, 113.64, 80.43, 55.45, 53.32, 48.43, 44.22, 38.86, 34.94, 28.14. HRMS (ESI) calculated for $[C_{24}H_{32}NO_4]^+$ ($M+NH_4^+$) requires *m/z* 398.2326, found 398.2325.

tert-Butyl 3-(4-methylbenzoyl)-4-phenylcyclopentanecarboxylate (2.25): Prepared according

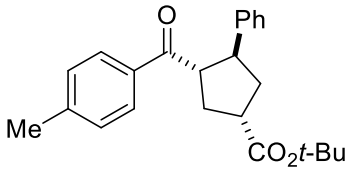

to the general procedure using 24.3 mg (0.04 mmol) of $Gd(OTf)_3$, 29.7 mg (0.08 mmol) of 4-NMe_2-^{s}Bu-pybox, 105.0 mg (0.4 mmol) of *trans* tert-butyl 2-(4-methylbenzoyl)cyclopropanecarboxylate, 208.9 mg (2.0 mmol) of styrene, 8.7 mg (0.01 mmol) of $Ru(bpy)_3(PF_6)_2$, and 52.3 mg (0.4 mmol) of diisopropylethylamine with a total volume of 4 mL (0.1 M, MeCN). The reaction was complete after 6 h. The crude product was purified by column chromatography (1:10, Et_2O/pentanes) to give 137.0 mg (0.38 mmol, 94% yield) of cycloadduct as two separable diastereomers (3:1 dr). Major diastereomer: 96.8% ee [Daicel Chiracel AD-H, 10 to 40 % iPrOH, 3 mL/min, 238 nm; t_1=5.91 min, t_2=8.09 min]. $[\alpha]_D^{22}$ 30.2 (*c*0.940, CH_2Cl_2). White solid (mp = 103-105 ^oC). ν_{max} (film) / cm^{-1} 2977, 1725, 1675, 1607, 1366, 1261, 1150. ^1H NMR (400 MHz, $CDCl_3$) δ 7.71 (d, *J* = 8.2 Hz, 2H), 7.28-7.17 (m, 5H), 7.17 (d, *J* = 8.2Hz, 2H), 4.02 – 3.69 (m, 2H), 3.16 – 3.03 (m, 1H), 2.58 – 2.42 (m, 2H), 2.36 (s, 3H), 2.26 – 2.05 (m, 2H), 1.45 (s, 9H). ^{13}C NMR (101 MHz, $CDCl_3$) δ 200.13, 174.24, 143.86, 143.73, 134.37, 129.16, 128.53, 128.50, 127.31, 126.36, 80.47, 54.58, 47.09, 44., 37.27, 35.51, 28.08,

21.60. HRMS (ESI) calculated for $[C_{24}H_{29}O_3]^+$ ($M+H^+$) requires *m/z* 365.2111, found 365.2111. Minor diastereomer: White solid (mp = 86.4-88.0 °C). ν_{max} (film) / cm^{-1} 2975, 1724, 1675, 1604, 1370, 1256, 1152. ^1H NMR (400 MHz, $CDCl_3$) δ 7.73 (d, *J* = 8.2 Hz, 2H), 7.34 – 7.15 (m, 5H), 7.17 (d, *J* = 8.2 Hz, 2H), 4.05 – 3.85 (m, 1H), 3.74 – 3.55 (m, 1H), 2.61 – 2.40 (m, 2H), 2.36 (s, 3H), 2.20 – 1.99 (m, 2H), 1.48 (s, 9H). ^{13}C NMR (101 MHz, $CDCl_3$) δ 200.93, 174.97, 143., 143.06, 134.15, 129.19, 128.63, 128.49, 127.43, 126.48, 80.45, 53.52, 48.28, 44.22, 38.84, 34.92, 28.13, 21.61. HRMS (ESI) calculated for $[C_{24}H_{32}NO_3]^+$ ($M+NH_4^+$) requires *m/z* 382.2377, found 382.2377.

tert-Butyl 3-phenyl-4-(4-(trifluoromethyl)benzoyl)cyclopentane carboxylate (2.26): Prepared

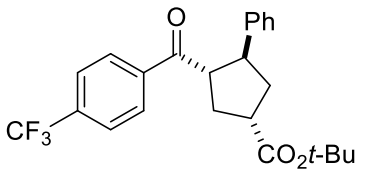

according to the general procedure using 24.3 mg (0.04 mmol) of $Gd(OTf)_3$, 29.7 mg (0.08 mmol) of 4-NMe_2-^{s}Bu-pybox, 126.1 mg (0.4 mmol) of *tert*-butyl 2-(4-(trifluoromethyl)benzoyl)cyclopropanecarboxylate, 209.2 mg (2.0 mmol) of styrene, 8.6 mg (0.01 mmol) of $Ru(bpy)_3(PF_6)_2$, and 51.3 mg (0.4 mmol) of diisopropylethylamine with a total volume of 4 mL (0.1 M, MeCN). The reaction was complete after 6 h. The crude product was purified by column chromatography (1:10, Et_2O/pentanes) to give 144.8 mg (0.35 mmol, 87 % yield) of cycloadduct as two separable diastereomers (2.8:1 dr). Major diastereomer: 89.5% ee [Daicel Chiracel OD-H, 1 to 20 % iPrOH, 3 mL/min, 263 nm; t_1=5.97 min, t_2=6.28 min]. $[\alpha]_D^{22}$ 54.6 (*c*0.780, CH_2Cl_2). White solid (mp = 83-87 °C). ν_{max} (film) / cm^{-1} 2980, 1729, 1691, 1328, 1160, 1136, 1070. ^1H NMR (400 MHz, $CDCl_3$) δ 7.86 (d, *J* = 8.2 Hz, 2H), 7.62 (d, *J* = 8.3 Hz, 2H), 7.32 – 7.10 (m, 5H), 3.84 (q, *J* = 8.9 Hz, 1H), 3.75 (q, *J* = 8.7 Hz, 1H), 3.11 (qd, *J* = 8.2, 5.6 Hz, 1H), 2.60 – 2.41 (m, 2H), 2.27 (ddd, *J* = 13.3, 9.3, 7.9 Hz, 1H), 2.15 (dt, *J* = 13.3, 9.0 Hz, 1H), 1.46 (s, 9H). ^{13}C NMR (101 MHz, $CDCl_3$) δ 199.83, 174.08, 143.34,

139.57, 134.14 (q, *J* = 32.5 Hz), 128.67, 128.65, 127.25, 126.66, 125.50 (q, *J* = 3.7 Hz), 123.6 (q, J = 271.2), 80.66 , 55.19, 47.47, 44.39, 37.43, 34.84, 28.07. ^{19}F NMR (377 MHz, $CDCl_3$) δ -63.14. HRMS (ESI) calculated for $[C_{24}H_{26}F_3O_3]^+$ ($M+H^+$) requires *m/z* 419.1829, found 419.1829. Minor diastereomer: White solid (mp = 58.9-61.7 ºC). ν_{max} (film) / cm^{-1} 2983, 1730, 1692, 1330, 1160, 1135, 1073. ^{1}H NMR (400 MHz, $CDCl_3$) δ 7.88 (d, *J* = 8.2 Hz, 2H), 7.62 (d, *J* = 8.3 Hz, 2H), 7.27 – 7.22 (m, 4H), 7.20 – 7.14 (m, 2H), 3.98 (q, *J* = 9.3 Hz, 1H), 3.62 (ddd, *J* = 11.3, 9.4, 7.6 Hz, 1H), 3.02 (ddd, *J* = 16.5, 9.2, 7.3 Hz, 1H), 2.67 – 2.33 (m, 2H), 2.33 – 2.02 (m, 2H), 1.49 (s, 9H). ^{13}C NMR (101 MHz, $CDCl_3$) δ 200.55, 174.79, 142.55, 139.32, 134.26 (q, *J* = 32.8 Hz), 128.77, 128.64, 127.35, 126.77, 125.53 (q, *J* = 3.6 Hz), 123.54 (q, *J* = 272.8 Hz), 80.64, 54.20, 48.80, 44.13, 38.86, 34.54, 28.12. ^{19}F NMR (377 MHz, $CDCl_3$) δ -63.16 . HRMS (ESI) calculated for $[C_{24}H_{29}NF_3O_3]^+$ ($M+NH_4^+$) requires *m/z* 436.2094, found 436.2094.

tert-Butyl 3-(4-chlorobenzoyl)-4-phenylcyclopentanecarboxylate (2.27): Prepared according

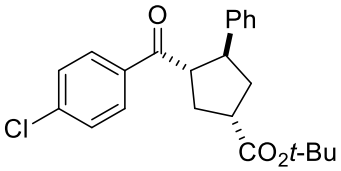

to the general procedure using 24.9 mg (0.04 mmol) of $Gd(OTf)_3$, 30.7 mg (0.08 mmol) of 4-NMe_2-^{s}Bu-pybox, 112.3 mg (0.4 mmol) of *trans* tert-butyl 2-(4-chlorobenzoyl)cyclopropanecarboxylate, 210.1 mg (2.0 mmol) of styrene, 8.7 mg (0.01 mmol) or $Ru(bpy)_3(PF_6)_2$, and 54.2 mg (0.4 mmol) of diisopropylethylamine with a total volume of 4 mL (0.1 M). The reaction was complete after 6 h. The crude product was purified by column chromatography (1:9, Et_2O/pentanes) to give 138.6 mg (0.36 mmol, 90 % yield) of cycloadduct as two separable diastereomers (4:1 dr). Major diastereomer: 92.4% ee [Daicel Chiracel AD-H, 5 to 50 % iPrOH, 3 mL/min, 263 nm; t_1=6.34 min, t_2=7.00 min]. $[\alpha]_D^{22}$ 51.0 (*c*0.980, CH_2Cl_2). White solid (mp = 109-111 ºC). ν_{max} (film) / cm^{-1} 3056, 2987, 1725, 1684, 1591, 1372, 1265, 1156. ^{1}H NMR (400 MHz, $CDCl_3$) δ 7.72 (d, *J* = 8.5 Hz, 2H), 7.33 (d, *J* = 8.5 Hz,

2H), 7.28 – 7.10 (m, 2H), 3.97 – 3.54 (m, 2H), 3.09 (qd, *J* = 8.2, 6.0 Hz, 1H), 2.49 (ddt, *J* = 21.0, 15.9, 6.9 Hz, 3H), 2.19 (ddt, *J* = 44.0, 13.3, 8.8 Hz, 2H), 1.46 (s, 8H). ^{13}C NMR (101 MHz, $CDCl_3$) δ 199.44, 174.13, 143.52, 139.36, 135.16, 129.80, 128.76, 128.60, 127.26, 126.56, 80.58, 54.80, 47.42, 44.42, 37.37, 35.08, 28.08. HRMS (ESI) calculated for $[C_{23}H_{26}ClO_3]^+$ ($M+H^+$) requires *m/z* 385.1565, found 385.1565. Minor diastereomer: White solid (mp = 82.9-88.3 ºC). ν_{max} (film) / cm^{-1} 3057, 2984, 1727, 1681, 1590, 1367, 1260, 1164. ^{1}H NMR (400 MHz, $CDCl_3$) δ 7.73 (d, *J* = 8.5 Hz, 2H), 7.33 (d, *J* = 8.5 Hz, 2H), 7.29 – 7.21 (m, 4H), 7.17 (h, *J* = 4.3 Hz, 1H), 3.92 (q, *J* = 9.3 Hz, 1H), 3.61 (ddd, *J* = 11.3, 9.4, 7.5 Hz, 1H), 3.05 – 2.95 (m, 1H), 2.58 – 2.40 (m, 2H), 2.20 – 2.06 (m, 2H), 1.48 (s, 9H). ^{13}C NMR (101 MHz, $CDCl_3$) δ 200.21, 174.87, 142.73, 139.51, 134.95, 129.90, 128.79, 128.59, 127.38, 126.68, 80.57, 53.77, 48.70, 44.16, 38.88, 34.65, 28.13. HRMS (ESI) calculated for $[C_{23}H_{29}NClO_3]^+$ ($M+NH_4^+$) requires *m/z* 402.1830, found 402.1830.

tert-Butyl 3-nicotinoyl-4-phenylcyclopentanecarboxylate (2.28): Prepared according to the general procedure using 24.3 mg (0.04 mmol) of $Gd(OTf)_3$, 30.0 mg (0.08 mmol) of 4-NMe_2-^{s}Bu-pybox, 99.2 mg (0.4 mmol) of *trans* tert-butyl 2-nicotinoylcyclopropanecarboxylate, 210.1 mg (2.0 mmol) of styrene, 8.7 mg (0.01 mmol) of $Ru(bpy)_3(PF_6)_2$, and 51.7 mg (0.4 mmol) of diisopropylethylamine with a total volume of 4 mL (0.1 M, MeCN). The reaction was complete after 8 h. The crude product was purified by column chromatography (2:1, Et_2O/pentanes) to give 80.4 mg (0.23 mmol, 57 % yield) of cycloadduct as two separable diastereomers (2:1 dr). Major diastereomer: 88.5% ee [Daicel Chiracel AD-H, 5 to 50 % iPrOH, 3 mL/min, 238 nm; t_1=6.45 min, t_2=6.92 min]. $[\alpha]_D^{22}$ 65.7 (*c*0.420, CH_2Cl_2). White solid (mp = 86.1-88.5 ºC). ν_{max} (film) / cm^{-1} 2982, 1722, 1687, 1586, 1368, 1265, 1151. ^{1}H NMR (400 MHz, $CDCl_3$) δ 8.96 (d, *J* = 1.8 Hz, 1H), 8.69 (dd, *J* = 4.8, 1.6 Hz, 1H), 8.05 (dt, *J* = 8.0, 1.9

Hz, 1H), 7.31 (dd, *J* = 8.1, 5.0 Hz, 1H), 7.30 – 7.11 (m, 5H), 3.82 (q, *J* = 9.0 Hz, 1H), 3.75 (q, *J* = 8.7 Hz, 1H), 3.11 (qd, *J* = 8.2, 5.8 Hz, 1H), 2.59 – 2.40 (m, 2H), 2.29 (dt, *J* = 13.3, 8.6 Hz, 1H), 2.23 – 2.09 (m, 1H), 1.47 (s, 9H). ^{13}C NMR (101 MHz, $CDCl_3$) δ 199.62, 174.10, 153.30, 149.83, 143.16, 135.69, 132.05, 128.68, 127.25, 126.71, 123.48, 80.66, 55.25, 47.46, 44.33, 37.45, 34.69, 28.08. HRMS (ESI) calculated for $[C_{22}H_{26}NO_3]^+$ ($M+H^+$) requires *m/z* 352.1907, found 352.1907. Minor Diastereomer: White solid (mp = 88.0-89.6 ^{o}C). ν_{max} (film) / cm^{-1} 2980, 1724, 1682, 1583, 1370, 1265, 1145. ^{1}H NMR (400 MHz, $CDCl_3$) δ 8.98 (d, *J* = 1.8 Hz, 1H), 8.69 (dd, *J* = 4.8, 1.6 Hz, 1H), 8.04 (dt, *J* = 8.0, 1.9 Hz, 1H), 7.30 (dd, *J* = 7.6, 4.8 Hz, 1H), 7.2 (s, 4H), 7.22 – 7.12 (m, 1H), 3.96 (q, *J* = 9.4 Hz, 1H), 3.61 (ddd, *J* = 11.4, 9.5, 7.5 Hz, 1H), 3.09 – 2.90 (m, 1H), 2.59 – 2.40 (m, 2H), 2.26 – 2.09 (m, 2H), 1.49 (s, 6H). ^{13}C NMR (101 MHz, $CDCl_3$) δ 200.46, 174.71, 153.39, 149.97, 142.42, 135.72, 131.82, 128.68, 127.35, 126.83, 123.43, 80.66, 54.25, 48.87, 44.16, 38.82, 34.37, 28.13. HRMS (ESI) calculated for $[C_{22}H_{26}NO_3]^+$ ($M+H^+$) requires *m/z* 352.1907, found 352.1907.

tert-Butyl 3-(furan-2-carbonyl)-4-phenylcyclopentanecarboxylate (2.29): Prepared according

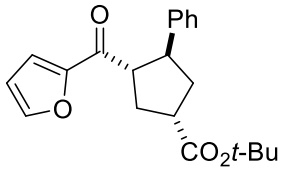

to the general procedure at –30 ^{o}C using 24.2 mg (0.04 mmol) of $Gd(OTf)_3$, 30.1 mg (0.08 mmol) of 4-NMe_2-^{s}Bu-pybox, 94.5 mg (0.4 mmol) of *trans* tert-butyl 2-(furan-2-carbonyl)cyclopropanecarboxylate, 210.0 mg (2.0 mmol) of styrene, 8.7 mg (0.01 mmol) of $Ru(bpy)_3(PF_6)_2$, and 51.4 mg (0.4 mmol) of diisopropylethylamine with a total volume of 4 mL (0.1 M, MeCN). The reaction was complete after 6 h. The crude product was purified by column chromatography (4:1, Et_2O/pentanes) to give 108.9 mg (0.320 mmol, 80 % yield) of cycloadduct as two separable diastereomers (4:1 dr). Major diastereomer: 78.8% ee [Daicel Chiracel AD-H, 10 % iPrOH, 6 mL/min, 263 nm; t_1=1.89 min, t_2=2.74 min].

$[\alpha]_D^{22}$ 49.6 (*c*1.130, CH_2Cl_2). White solid (mp = 100.2-103.6 ^oC). ν_{max} (film) / cm^{-1} 2977, 1722, 1670, 1466, 1367, 1151. ^1H NMR (400 MHz, $CDCl_3$) δ 7.51 – 7.47 (m, 1H), 7.32 – 7.19 (m, 5H), 7.20 – 7.11 (m, 1H), 6.97 (d, *J* = 3.5 Hz, 1H), 3.79 – 3.59 (m, 2H), 3.08 (qd, *J* = 8.5, 6.0 Hz, 1H), 2.50 (ddt, *J* = 15.4, 13.0, 6.8 Hz, 2H), 2.25 (dt, *J* = 13.0, 9.2 Hz, 1H), 2.11 (dt, *J* = 13.3, 9.1 Hz, 1H), 1.47 (s, 9H). ^{13}C NMR (101 MHz, $CDCl_3$) δ 189.52, 174.24, 152.74, 146.41, 143.47, 128.48, 127.30, 126.45, 117.51, 112.13, 80.52, 55.34, 47.29, 44.36, 37.33, 34.90, 28.09. HRMS (ESI) calculated for $[C_{21}H_{25}O_4]^+$ ($M+H^+$) requires 341.1747, found 341.1747. Minor Diastereomer: White solid (mp = 94.9-98 ^oC). ν_{max} (film) / cm^{-1} 2976, 1724, 1673, 1464, 1365, 1150. ^1H NMR (400 MHz, $CDCl_3$) δ 7.52 – 7.47 (m, 1H), 7.29 – 7.20 (m, 5H), 7.21 – 7.11 (m, 1H), 6.96 (d, *J* = 3.5 Hz, 1H), 6.41 (dd, *J* = 3.6, 1.7 Hz, 1H), 3.77 (q, *J* = 9.4 Hz, 1H), 3.57 (ddd, *J* = 11.4, 9.7, 7.3 Hz, 1H), 3.02 (ddd, *J* = 16.7, 9.5, 7.3 Hz, 1H), 2.55 – 2.38 (m, 2H), 2.29 – 2.03 (m, 2H), 1.48 (s, 9H). ^{13}C NMR (101 MHz, $CDCl_3$) δ 190.26, 174.92, 148.16, 146.73, 142.62, 128.48, 127.39, 126.60, 118.01, 112.11, 80.47, 54.14, 48.84, 44.10, 38.87, 34.23, 28.13. HRMS (ESI) calculated for $[C_{21}H_{25}O_4]^+$ ($M+H^+$) requires 341.1747, found 341.1748.

tert-Butyl 3-(3-methylbenzoyl)-4-phenylcyclopentanecarboxylate (2.30): Prepared according

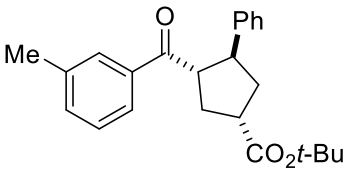

to the general procedure using 24.2 mg (0.04 mmol) of $Gd(OTf)_3$, 29.8 mg (0.08 mmol) of 4-NMe_2-^{s}Bu-pybox, 106.8 mg (0.4 mmol) of *trans* tert-butyl 2-(3-methylbenzoyl)cyclopropanecarboxylate, 208.3 mg (2.0 mmol) of styrene, 8.7 mg (0.01 mmol) of $Ru(bpy)_3(PF_6)_2$, and 51.7 mg (0.4 mmol) of diisopropylethylamine with a total volume of 4 mL (0.1 M, MeCN). The reaction was complete after 6 h. The crude product was purified by column chromatography (1:10, Et_2O/pentanes) to give 130.0 mg (0.36 mmol, 89 % yield) of cycloadduct as a white solid as two separable diastereomers (3:1 d.r.). Major

diastereomer: 89.3% ee [Daicel Chiracel AD-H, 5 to 50 % iPrOH, 3 mL/min, 238 nm; t_1=5.37 min, t_2=6.00 min]. $[\alpha]_D^{22}$ 55.2 (*c*1.000, CH_2Cl_2). White solid (mp = 87-89 ºC). ν_{max} (film) / cm^{-1} 2978, 1721, 1671, 1368, 1333, 1214, 1149. ^{1}H NMR (400 MHz, $CDCl_3$) δ 7.60 (d, *J* = 8.5 Hz, 2H), 7.30 (d, *J* = 7.4 Hz, 1H), 7.29 – 7.20 (m, 5H), 7.20 – 7.11 (m, 1H), 3.91 – 3.79 (m, 1H), 3.78 (q, *J* = 8.6 Hz, 1H), 3.09 (qd, *J* = 8.4, 6.1 Hz, 1H), 2.59 – 2.42 (m, 2H), 2.32 (s, 3H), 2.17 (ddt, *J* = 33.6, 13.2, 9.0 Hz, 2H), 1.46 (s, 9H). ^{13}C NMR (101 MHz, $CDCl_3$) δ 200.74, 174.24, 143.86, 138.22, 136.89, 133.68, 129.01, 128.51, 128.32, 127.34, 126.39, 125.58, 80.49, 54.88, 47.21, 44.50, 37.28, 35.43, 28.09, 21.31. HRMS (ESI) calculated for $[C_{24}H_{29}O_3]^+$ ($M+H^+$) requires *m/z* 365.2111, found 365.2110. Minor Diastereomer: Colorless oil. ν_{max} (film) / cm^{-1} 2986, 1932, 1720, 1677, 1367, 1265, 1151. ^{1}H NMR (400 MHz, $CDCl_3$) δ 7.65 – 7.56 (m, 2H), 7.34 – 7.20 (m, 6H), 7.20 – 7.10 (m, 1H), 3.96 (td, *J* = 9.4, 7.8 Hz, 1H), 3.65 (ddd, *J* = 11.4, 9.3, 7.4 Hz, 1H), 2.99 (ddd, *J* = 16.8, 9.4, 7.3 Hz, 1H), 2.62 – 2.41 (m, 2H), 2.32 (s, 3H), 2.22 – 2.06 (m, 2H), 1.48 (s, 9H). ^{13}C NMR (101 MHz, $CDCl_3$) δ 201.50, 174.93, 143.05, 138.25, 136.64, 133.79, 129.10, 128.50, 128.37, 127.46, 126.52, 125.72, 80.46, 53.77, 48.46, 44.27, 38.85, 34.80, 28.14, 21.30. Mp = 72.5-76 ºC. HRMS (ESI) calculated for $[C_{24}H_{32}\ NO_3]^+$ ($M+NH_4^+$) requires *m/z* 382.2377, found 382.2377.

tert-butyl 3-(2-methylbenzoyl)-4-phenylcyclopentanecarboxylate (2.31): Prepared according

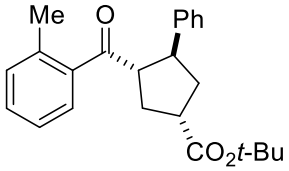

to the general procedure using 24.3 mg (0.04 mmol) of $Gd(OTf)_3$, 29.7 mg (0.08 mmol) of 4-NMe_2-^{s}Bu-pybox, 105.3 mg (0.4 mmol) of *Trans* tert-butyl 2-(2-methylbenzoyl)cyclopropanecarboxylate, 209.3 mg (2.0 mmol) of styrene, 8.7 mg (0.01 mmol) of $Ru(bpy)_3(PF_6)_2$, and 52.6 mg (0.4 mmol) of diisopropylethylamine with a total volume of 4 mL (0.1 M, MeCN). The reaction was complete after 6 hours. The crude product was

purified by column chromatography (1:20, Et_2O/pentanes) to give 88.0 mg (0.244 mmol, 61 % yield) of cycloadduct as two separable diastereomers (2:1 dr). Major diastereomer: 71.3% ee [Daicel Chiracel AD-H, 7 % iPrOH, 6 mL/min, 263 nm; t_1=2.47 min, t_2=4.65 min]. $[\alpha]_D^{22}$ 52.9 (*c*0.982, CH_2Cl_2). White solid (mp = 66-68 ºC. ν_{max} (film) / cm^{-1} 2983, 1714, 1694, 1422, 1265, 1154. ^1H NMR (400 MHz, $CDCl_3$) δ 7.33 – 7.06 (m, 9H), 3.76-3.68 (m, 2H), 3.04 (qd, *J* = 8.4, 5.7 Hz, 1H), 2.55 – 2.45 (m, 1H), 2.45 – 2.36 (m, 1H), 2.35 (s, 3H), 2.26 – 2.15 (m, 1H), 2.14 – 2.03 (m, 1H), 1.47 (s, 9H). ^{13}C NMR (101 MHz, $CDCl_3$) δ 205.05 , 174.35 , 143.62 , 138.66 , 137.73 , 131.59 , 130.81 , 128.50 , 127.84 , 127.26 , 126.42 , 125.39 , 80.49 , 58.03 , 47.57 , 44.25 , 37.39 , 34.98 , 28.10 , 20.81. HRMS (ESI) calculated for $[C_{24}H_{29}O_3]^+$ ($M+H^+$) requires *m/z* 365.2111, found 365.2111. Minor diastereomer: White solid (mp = 93-94.8 ºC. ν_{max} (film) / cm^{-1} 2975, 2931, 1724, 1684, 1455, 1367, 1249, 1151. ^1H NMR (400 MHz, $CDCl_3$) δ 7.35 – 7.20 (m, 6H), 7.19 – 7.05 (m, 3H), 3.86 (q, *J* = 9.3 Hz, 1H), 3.59 (ddd, *J* = 11.5, 9.7, 7.4 Hz, 1H), 3.00 (ddd, *J* = 16.6, 9.4, 7.2 Hz, 1H), 2.55 – 2.45 (m, 1H), 2.45 – 2.33 (m, 4H), 2.22 – 2.03 (m, 2H), 1.47 (s, 9H). ^{13}C NMR (101 MHz, $CDCl_3$) δ 205.80, 174.93, 142.71, 138.24, 137.96, 133.58, 131.64, 131.05, 128.49, 128.35, 127.34, 126.56, 125.53, 80.47, 56.70, 49.17, 44.02, 38.78, 34.48, 28.12, 21.05. HRMS (ESI) calculated for $[C_{24}H_{32}NO_3]^+$ ($M+NH_4^+$) requires *m/z* 382.2377, found 382.2375.

1-(3-Benzoyl-4-phenylcyclopentyl)ethanone (2.32): Prepared according to the general procedure

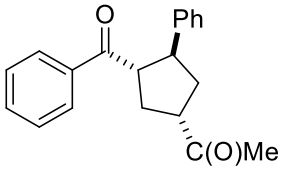

using 24.2 mg (0.04 mmol) of $Gd(OTf)_3$, 29.8 mg (0.08 mmol) of 4-NMe_2-^{s}Bu-pybox, 77.3 mg (0.4 mmol) of 1-((2-benzoylcyclopropyl)ethanone), 416.4 mg (4.0 mmol) of styrene, 8.7 mg (0.01 mmol) of $Ru(bpy)_3(PF_6)_2$, and 51.9 mg (0.4 mmol) of diisopropylethylamine with a total volume of 4 mL (0.1 M, MeCN). The reaction was complete after 6 h. The crude product was purified by column

chromatography (1:15, acetone/pentanes) to give 56.4 mg (0.19 mmol, 48 % yield) of cycloadduct as a clear oil (single diastereomer). 88.2% ee [Daicel Chiracel AD-H, 5 % iPrOH, 6 mL/min, 238 nm; t_1=3.02 min, t_2=3.78 min]. $[\alpha]_D^{22}$ 47.8 (*c*1.213, CH_2Cl_2). ν_{max} (film) / cm^{-1} 2966, 1708, 1683, 1262, 1114. ^1H NMR (400 MHz, $CDCl_3$) δ 7.72 (d, *J* = 8.6 Hz, 2H), 7.45 – 7.38 (m, 1H), 7.30 (dd, *J* = 8.4, 7.1 Hz, 2H), 7.23 – 7.04 (m, 4H), 6.97 – 6.84 (m, 1H), 3.85 (q, *J* = 8.7 Hz, 1H), 3.60 (q, *J* = 8.7 Hz, 1H), 3.19 (qd, *J* = 8.5, 5.9 Hz, 1H), 2.55 – 2.32 (m, 2H), 2.23 – 2.18 (m, 1H), 2.15 (s, 3H), 2.04 (dt, *J* = 13.3, 9.4 Hz, 1H). ^{13}C NMR (101 MHz, $CDCl_3$) δ 208.91, 200.61, 143.46, 136.73, 133.00, 128.59, 128.49, 128.40, 127.27, 126.55, 54.47, 51.45, 47.51, 36.23, 33.80, 28.41. HRMS (ESI) calculated for $[C_{20}H_{21}O_2]^+$ ($M+H^+$) requires *m/z* 293.1536, found 293.1535.

(4-Methyl-2-phenylcyclopentyl)(phenyl)methanone (2.33): Prepared according to the general procedure at -20 °C using 60.4 mg (0.1 mmol) of $Gd(OTf)_3$, 74.5 mg (0.2 mmol) of 4-NMe_2-^{s}Bu-pybox, 32.3 mg (0.2 mmol) of *trans* 2-methylcyclopropyl(phenyl)methanone, 104.2 mg (1.0 mmol) of styrene, 4.2 mg (0.005 mmol) of $Ru(bpy)_3(PF_6)_2$, and 51.7 mg (0.4 mmol) of diisopropylethylamine with a total volume of 4 mL (0.1 M, MeCN). The reaction was complete after 48 h. The crude product was purified by column chromatography (1:10, Et_2O/pentanes) to give 21.3 mg (0.08 mmol, 40 % yield) of cycloadduct as a white solid as a single diastereomer. 49.5% ee [Daicel Chiracel AD-H, 5 % iPrOH, 3 mL/min, 263 nm; t_1=3.78 min, t_2=6.26 min]. $[\alpha]_D^{22}$ 38.2 (*c*1.011, CH_2Cl_2). White solid (mp = 44.9-51 °C). ν_{max} (film) / cm^{-1} 2957, 2868, 1681, 1602, 1451, 1266, 1012. ^1H NMR (400 MHz, $CDCl_3$) δ 7.74 (d, *J* = 7.4 Hz, 2H), 7.42 (t, *J* = 7.4 Hz, 1H), 7.30 (t, *J* = 7.7 Hz, 2H), 7.24 – 7.11 (m, 4H), 7.13 – 7.00 (m, 1H), 3.90 – 3.69 (m, 2H), 2.48 – 2.22 (m, 2H), 2.02 (dt, *J* = 15.2, 7.8 Hz, 1H), 1.82 (ddd, *J* = 13.0, 8.8, 7.2 Hz, 1H), 1.55 – 1.43 (m, 1H), 1.03 (d, *J* = 6.5 Hz, 3H). ^{13}C NMR (101 MHz,

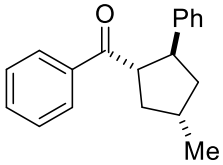

$CDCl_3$) δ 201.90, 145.50, 132.80, 128.55, 128.44, 128.41, 127.37, 127.30, 126.07, 55.96, 46.89, 42.50, 41.01, 34.44, 20.78. HRMS (ESi) calculated for $[C_{19}H_{24}O]^+$ ($M+NH_4^+$) requires *m/z* 282.1852, found 282.1853.

(4,4-Dimethyl-2-phenylcyclopentyl)(phenyl)methanone (2.34): Prepared according to the general procedure at –20 °C using 48.6 mg (0.04 mmol) of $Gd(OTf)_3$, 59.4 mg (0.08 mmol) of 4-NMe_2-^{s}Bu-pybox, 69.7 mg (0.4 mmol) of *tert*-butyl (2,2-dimethylcyclopropyl)(phenyl)methanone, 209.2 mg (2.0 mmol) of styrene, 8.6 mg (0.01 mmol) of $Ru(bpy)_3(PF_6)_2$, and 51.3 mg (0.4 mmol) of diisopropylethylamine with a total volume of 4 mL (0.1 M, MeCN). The reaction was complete after 6 h. The crude product was purified by column chromatography (1:10, Et_2O/pentanes) to give 96.8 mg (0.35 mmol, 87 % yield) of cycloadduct as two separable diastereomers (2.8:1 dr). Major diastereomer: 88.6% ee [Daicel Chiracel AD-H, 5 to 50 % iPrOH, 3 mL/min, 238 nm; t_1=5.19 min, t_2=6.70 min]. $[\alpha]_D^{22}$ 68.7 (*c*0.591, CH_2Cl_2). White solid (mp = 105.3-107.8 °C). ν_{max} (film) / cm^{-1} 2941, 2863, 1678, 1448, 1283, 1015. ^{1}H NMR (400 MHz, $CDCl_3$) δ 7.82 (d, *J* = 8.4 Hz, 2H), 7.48 (t, *J* = 7.4 Hz, 1H), 7.37 (t, *J* = 8.0 Hz, 2H), 7.29 – 7.18 (m, 4H), 7.12 (t, *J* = 7.0 Hz, 1H), 4.04 – 3.84 (m, 2H), 2.12 (dd, *J* = 13.0, 9.2 Hz, 1H), 2.04 (dd, *J* = 12.7, 6.8 Hz, 1H), 1.86 (t, *J* = 11.9 Hz, 1H), 1.73 (dd, *J* = 13.1, 7.8 Hz, 1H), 1.21 (s, 3H), 1.13 (s, 3H). ^{13}C NMR (101 MHz, $CDCl_3$) δ 201.72, 144.08, 137.00, 132.80, 128.43, 128.38, 127.39, 126.15, 54.88, 49.42, 46.79, 46.76, 39.02, 30.59, 29.55. HRMS (ESI) calculated for $[C_{20}H_{23}O]^+$ ($M+H^+$) requires *m/z* 279.1743, found 279.1743. Minor Diastereomer: White solid (mp = 71.6-73.4 °C). ν_{max} (film) / cm^{-1} 2953, 1927, 2866, 1679, 1463, 1448, 1367, 1221. ^{1}H NMR (400 MHz, $CDCl_3$) δ 7.88 (d, *J* = 8.2 Hz, 2H), 7.62 (d, *J* = 8.3 Hz, 2H), 7.33 – 7.06 (m, 5H), 3.98 (q, *J* = 9.3 Hz, 1H), 3.62 (ddd, *J* = 11.3, 9.4, 7.6 Hz, 1H), 3.02 (ddd,

J = 16.5, 9.2, 7.3 Hz, 1H), 2.63 – 2.38 (m, 2H), 2.25 – 2.00 (m, 2H), 1.49 (s, 9H). ^{13}C NMR (101 MHz, $CDCl_3$) δ 202.23, 142.11, 136.99, 132.03, 128.46, 127.96, 127.93, 127.71, 125.98, 50.97, 48.93, 48.45, 43.26, 38.47, 29.40, 28.53. HRMS (ESI) calculated for $[C_{20}H_{23}O]^+$ ($M+H^+$) requires *m/z* 279.1743, found 279.1741.

Phenyl(3-phenylspiro[4.4]nonan-2-yl)methanone (2.35): Prepared according to the general procedure at –20 ºC using 24.4 mg (0.04 mmol) of $Gd(OTf)_3$, 29.9 mg (0.08 mmol) of 4-NMe_2-^{s}Bu-pybox, 80.1 mg (0.4 mmol) of phenyl(spiro[2.4]heptan-1-yl)methanone, 209.8 mg (2.0 mmol) of styrene, 8.7 mg (0.01 mmol) of $Ru(bpy)_3(PF_6)_2$, and 51.5 mg (0.4 mmol) of diisopropylethylamine with a total volume of 4 mL (0.1 M, MeCN). The reaction was complete after 48 h. The crude product was purified by column chromatography (1:30, Et_2O/pentanes) to give 107.2 mg (0.352 mmol, 88% yield) of cycloadduct as two separable diastereomers (5.3:1 d.r.). Major Diastereomer: 94.1% ee [Daicel Chiracel AD-H, 10 to 50 % iPrOH, 3 mL/min, 263 nm; t_1=5.49 min, t_2=6.60 min]. $[\alpha]_D^{22}$ 96.7 (*c*0.999, CH_2Cl_2). Colorless oil. ν_{max} (film) / cm^{-1} 2945, 2858, 1680, 1448, 1216. ^{1}H NMR (400 MHz, $CDCl_3$) δ 7.83 (d, *J* = 7.1 Hz, 2H), 7.49 (t, *J* = 7.4 Hz, 1H), 7.38 (t, *J* = 7.6 Hz, 2H), 7.32 – 7.18 (m, 4H), 7.13 (t, *J* = 6.9 Hz, 1H), 3.97 – 3.82 (m, 2H), 2.21 (dd, *J* = 12.9, 9.6 Hz, 1H), 2.12 (dd, *J* = 12.6, 6.5 Hz, 1H), 2.02 – 1.88 (m, 1H), 1.83 (dd, *J* = 12.9, 6.9 Hz, 1H), 1.77 – 1.49 (m, 9H). ^{13}C NMR (101 MHz, $CDCl_3$) δ 201.76 , 144.22 , 136.98 , 132.77 , 128.44 , 128.42 , 128.36 , 127.38 , 126.13 , 54.64 , 50.57 , 47.52 , 46.91 , 44.98 , 40.28 , 39.78 , 24.40 , 24.34. HRMS (ESI) calculated for $[C_{22}H_{25}O]^+$ ($M+H^+$) requires *m/z* 305.1900, found 305.1899. Minor Diastereomer: Colorless oil. ν_{max} (film) / cm^{-1} 2950, 2863, 1679, 1448, 1220, 1023. ^{1}H NMR (400 MHz, $CDCl_3$) δ 7.56 (d, *J* = 7.2 Hz, 2H), 7.36 (t, *J* = 7.3 Hz, 1H), 7.29 – 7.18 (m, 2H), 6.97 (7.02 – 6.90 (m, 5H), 4.34 – 4.21

(m, 1H), 3.71 (td, *J* = 10.4, 7.6 Hz, 1H), 2.39 (dd, *J* = 13.0, 9.0 Hz, 1H), 2.16 – 1.97 (m, 2H), 1.90 – 1.47 (m, 9H). ^{13}C NMR (101 MHz, $CDCl_3$) δ 202.33, 142.17, 138.18, 132.06, 128.39, 127.97, 127.96, 127.72, 125.97, 50.89, 49.81, 48.59, 46.82, 41.52, 39.26, 38.89, 24.81, 24.66. HRMS (ESI) calculated for $[C_{22}H_{25}O]^+$ ($M+H^+$) requires *m/z* 305.1900, found 305.1900.

Di-tert-butyl 3-benzoyl-4-phenylcyclopentane-1,2-dicarboxylate (2.37): Prepared according to

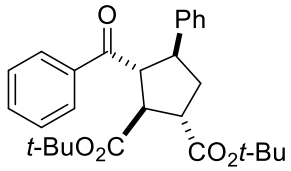

the general procedure using 24.3 mg (0.04 mmol) of $Gd(OTf)_3$, 29.9 mg (0.08 mmol) of 4-NMe_2-^{s}Bu-pybox, 138.6 mg (0.4 mmol) of (1R,2S,3s)-di-tert-butyl 3-benzoylcyclopropane-1,2-dicarboxylate, 209.6 mg (2.0 mmol) of styrene, 8.7 mg (0.01 mmol) of $Ru(bpy)_3(PF_6)_2$, and 51.2 mg (0.4 mmol) of diisopropylethylamine with a total volume of 4 mL (0.1 M, MeCN). The reaction was complete after 6 h. The crude product was purified by column chromatography (1:5, Et_2O/pentanes) to give 153.2 mg (0.340 mmol, 85 % yield) of cycloadduct as two separable diastereomers (7:1 dr) Major Diastereomer: 98.7% ee [Daicel Chiracel OD-H, 5 to 30 % iPrOH, 3 mL/min, 238 nm; t_1=4.26 min, t_2=4.67 min]. $[\alpha]_D^{22}$ 56.4 (*c*1.010, CH_2Cl_2). White solid (mp = 96-97 ^{o}C). ν_{max} (film) / cm^{-1} 2977, 1724, 1681, 1393, 1368, 1257, 1158. ^{1}H NMR (400 MHz, $CDCl_3$) δ 7.70 (d, *J* = 7.7 Hz, 2H), 7.43 (t, *J* = 7.3 Hz, 1H), 7.29 (t, *J* = 7.7 Hz, 2H), 7.24-7.2 (m, 4H), 7.14 (dq, *J* = 8.2, 5.5, 4.8 Hz, 1H), 4.17 (t, *J* = 9.5 Hz, 1H), 3.64 (dt, *J* = 25.1, 8.8 Hz, 2H), 3.36 (dq, *J* = 9.3, 5.5 Hz, 1H), 2.51 (ddd, *J* = 13.4, 8.1, 5.5 Hz, 1H), 2.27 (dt, *J* = 13.2, 9.8 Hz, 1H), 1.49 (s, 9H), 1.25 (s, 9H). ^{13}C NMR (75 MHz, $CDCl_3$) δ 200.49 , 173.03 , 172.54 , 141.91 , 137.22 , 132.93 , 128.59 , 128.40 , 128.29 , 127.20 , 126.81 , 81.21 , 80.89 , 57.00 , 53.04 , 49.76 , 47.34 , 37.16 , 28.05 , 27.78. HRMS (ESI) calculated for $[C_{28}H_{35}O_5]$ ($M+H^+$) requires 451.2479, found 451.2479. Minor Diastereomer: White solid (mp = 83.7-85.1 ^{o}C). ν_{max} (film) / cm^{-1} 2978, 2936, 1725, 1680, 1367, 1257, 1154. ^{1}H NMR (400 MHz,

$CDCl_3$) δ 7.57 (d, *J* = 7.0 Hz, 2H), 7.46 – 7.33 (m, 1H), 7.27 – 7.23 (m, 2H), 7.07 – 6.91 (m, 5H), 4.50 (dd, *J* = 10.0, 7.7 Hz, 1H), 3.93 (dd, *J* = 10.3, 7.7 Hz, 1H), 3.70 (td, *J* = 10.0, 7.3 Hz, 1H), 3.10 (td, *J* = 10.5, 7.9 Hz, 1H), 2.57 – 2.36 (m, 2H), 1.53 (s, 9H), 1.43 (s, 9H). ^{13}C NMR (101 MHz, $CDCl_3$) δ 172.61, 132.42, 128.32, 128.07, 128.05, 127.94, 126.59, 53.83, 48.52, 48.27, 36.85, 28.15, 28.08. HRMS (ESI) calculated for $[C_{28}H_{35}O_5]$ ($M+H^+$) requires 451.2479, found 451.2478.

tert-Butyl 5-benzoyl-2,2-dimethyl-4-phenylcyclopentanecarboxylate (2.39): Prepared

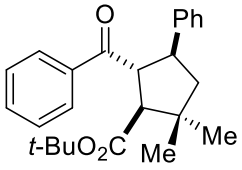

according to the general procedure at –20 °C using 48.6 mg (0.04 mmol) of $Gd(OTf)_3$, 59.4 mg (0.08 mmol) of 4-NMe_2-^{s}Bu-pybox, 109.7 mg (0.4 mmol) of tert-butyl 3-benzoyl-2,2-dimethylcyclopropanecarboxylate, 209.2 mg (2.0 mmol) of styrene, 8.6 mg (0.01 mmol) of $Ru(bpy)_3(PF_6)_2$, and 103.4 mg (0.8 mmol) of diisopropylethylamine with a total volume of 4 mL (0.1 M, MeCN). The reaction was complete after 48 h. The crude product was purified by column chromatography (1:10, Et_2O/pentanes) to give 132.5 mg (0.35 mmol, 87% yield) of cycloadduct as a single diastereomer. 96.5% ee [Daicel Chiracel OD-H, 5 to 30 % iPrOH, 3 mL/min, 238 nm; t_1=3.64 min, t_2=4.69 min]. $[\alpha]_D^{22}$ 76.4 (*c*1.110, CH_2Cl_2). White solid (mp = 134.7-138.5 °C). ν_{max} (film) / cm^{-1} 2960, 1722, 1667, 1369, 1153. ^{1}H NMR (400 MHz, $CDCl_3$) δ 7.70 (d, *J* = 7.1 Hz, 2H), 7.42 (t, *J* = 7.4 Hz, 1H), 7.28 (t, *J* = 8.1 Hz, 4H), 7.20 (t, *J* = 7.6 Hz, 2H), 7.11 (t, *J* = 7.3 Hz, 1H), 4.37 (dd, *J* = 10.2, 8.1 Hz, 1H), 3.68 (td, *J* = 10.5, 8.4 Hz, 1H), 2.86 (d, *J* = 8.1 Hz, 1H), 2.15 – 1.94 (m, 2H), 1.40 (s, 9H), 1.28 (s, 3H), 1.18 (s, 3H). ^{13}C NMR (101 MHz, $CDCl_3$) δ 201.86 , 173.23, 142.94, 137.18, 132.79, 128.47 (d, *J* = 6.8 Hz), 128.22, 127.58, 126.46, 80.96, 59.98, 57.17, 49.51, 47.24, 42.31, 30.24, 28.09, 26.41. HRMS (ESI) calculated for $[C_{25}H_{31}O_3]^+$ ($M+H^+$) requires *m/z* 379.2268, found 379.2268.

(4,4-Dimethyl-2-phenylcyclopentyl)(4-(trifluoromethyl)phenyl)methanone (2.41) : Prepared

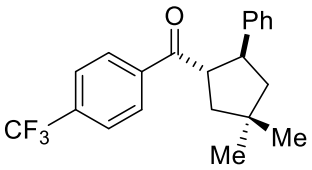

according to the general procedure at –20 °C using 24.2 mg (0.04 mmol) of $Gd(OTf)_3$, 29.8 mg (0.08 mmol) of 4-NMe_2-^{s}Bu-pybox, 96.9 mg (0.4 mmol) of (2,2-dimethylcyclopropyl)(4-(trifluoromethyl)phenyl)methanone, 209.2 mg (2.0 41mmol) of styrene, 8.7 mg (0.01 mmol) of $Ru(bpy)_3(PF_6)_2$, and 51.3 mg (0.4 mmol) of diisopropylethylamine with a total volume of 4 mL (0.1 M, MeCN). The reaction was complete after 48 h. The crude product was purified by column chromatography (1:30, Et_2O/pentanes) to give 103.9 mg (0.300 mmol, 75 % yield) of cycloadduct (>10:1 dr). Major Diastereomer: 82.9% ee [Daicel Chiracel OD-H, 5 to 50 % (1:4 iPrOH/hexane), 3 mL/min, 235 nm; t_1=2.68 min, t_2=3.66 min]. $[\alpha]_D^{22}$ 62.6 (*c*0.991, CH_2Cl_2). White solid (mp = 63.9-65.7 °C). ν_{max} (film) / cm^{-1} 2942, 2866, 1690, 1445, 1281, 1015. ^{1}H NMR (400 MHz, $CDCl_3$) δ 7.88 (d, *J* = 8.1 Hz, 2H), 7.63 (d, *J* = 8.3 Hz, 2H), 7.29 – 7.19 (m, 4H), 7.18 – 7.08 (m, 1H), 3.90 (tt, *J* = 9.8, 5.0 Hz, 2H), 2.08 (ddd, *J* = 20.9, 13.0, 8.0 Hz, 2H), 1.93 – 1.83 (m, 1H), 1.82 – 1.71 (m, 1H), 1.22 (s, 3H), 1.14 (s, 3H). ^{13}C NMR (101 MHz, $CDCl_3$) δ 200.99, 143.67, 139.72, 134.03 (q, *J* = 32.7 Hz), 128.68, 128.49, 127.32, 126.38, 125.46 (q, *J* = 3.8 Hz), 123.59 (q, *J* = 272.7 Hz), 55.35, 49.43, 47.22, 46.33, 39.12, 30.52, 29.47. ^{19}F NMR (377 MHz, $CDCl_3$) δ -63.13 . HRMS (ESI) calculated for $[C_{20}H_{23}O]^+$ ($M+H^+$) requires *m/z* 347.1617, found 347.1617.

2.5.7: Racemic [3+2] Cycloadditions

General racemic procedure: A flame-dried Schlenk tube equipped with a magnetic stir-bar was charged with $Gd(OTf)_3$ (0.2 mmol). A 2 mL volumetric flask was charged with cyclopropane (0.2 mmol), alkene (1.0 mmol), $Ru(bpy)_3(PF_6)_2$ (0.005 mmol), TMEDA (0.6 mmol) and MeCN (2 mL total volume). The contents of the volumetric flask were then transferred to the Schlenk tube. The reaction mixture was then thoroughly degassed through three freeze-pump-thaw cycles, then backfilled with N_2. The reaction flask was then placed in front of a 23 W (1380 lumen) compact fluorescent lamp and stirred at room temperature. Upon consumption of starting material, the reaction was diluted with 1:1 Et_2O/pentanes and passed through a short plug of silica. The filtrate was concentrated and the residue purified by column chromatography.

Ethyl 3-benzoyl-4-phenylcyclopentanecarboxylate (2.10): Reaction was carried out with *trans* ethyl 2-benzoylcyclopropanecarboxylate (43.6 mg, 0.200 mmol), styrene (104.3 mg, 1.001 mmol), TMEDA (69.8 mg, 0.601 mmol), $Ru(bpy)_3(PF_6)_2$ (4.3 mg, 0.005 mmol), $Gd(OTf)_3$ (120.9 mg, 0.200 mmol), and MeCN (2 mL total volume). The reaction was complete after 3 h providing ethyl 3-benzoyl-4-phenylcyclopentanecarboxylate as a white solid (60.0 mg, 0.186 mmol, 93 % yield, 4:1 dr). All spectroscopic data match those reported above.

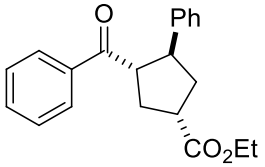

tert-Butyl 3-benzoyl-4-phenylcyclopentanecarboxylate (2.12): Reaction was carried out with *trans* tert-butyl 2-benzoylcyclopropanecarboxylate (49.3 mg, 0.200 mmol), styrene (104.3 mg, 1.001 mmol), TMEDA (69.8 mg, 0.601 mmol), $Ru(bpy)_3(PF_6)_2$ (4.3 mg, 0.005 mmol), $Gd(OTf)_3$ (120.9 mg,

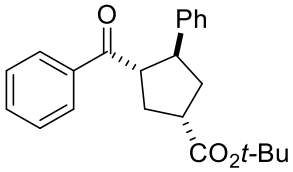

0.200 mmol), and MeCN (2 mL total volume). The reaction was complete after 3 h providing tert-butyl 3-benzoyl-4-phenylcyclopentanecarboxylate as a white solid (65.9 mg, 0.188 mmol, 94 % yield, 3:1 dr). All spectroscopic data match those reported above.

***tert*-Butyl 3-benzoyl-4-(4-methoxyphenyl)cyclopentanecarboxylate (2.13):** Reaction was carried out with *trans* tert-butyl 2-benzoylcyclopropanecarboxylate (49.6 mg, 0.201 mmol), 4-methoxystyrene (139.0 mg, 1.04 mmol), TMEDA (72.0 mg, 0.620 mmol), $Ru(bpy)_3(PF_6)_2$ (4.2 mg, 0.005 mmol), $Gd(OTf)_3$ (120.9 mg, 0.200 mmol), and MeCN (2 mL total volume). The reaction was complete after 3 h providing *tert*-butyl 3-benzoyl-4-(4-methoxyphenyl)cyclopentanecarboxylate as a white solid (65 mg, 0.170 mmol, 85 % yield, 3:1 dr). All spectroscopic data match those reported above.

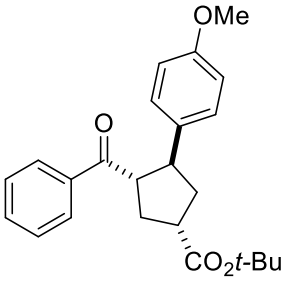

***tert*-butyl 3-benzoyl-4-(4-methylphenyl)cyclopentanecarboxylate (2.14):** Reaction was carried out with *trans* tert-butyl 2-benzoylcyclopropanecarboxylate (49.5 mg, 0.201 mmol), 4-methylstyrene (120.5 mg, 1.02 mmol), TMEDA (69.5 mg, 0.598 mmol), $Ru(bpy)_3(PF_6)_2$ (4.4 mg, 0.005 mmol), $Gd(OTf)_3$ (122.8 mg, 0.203 mmol), and MeCN (2 mL total volume). The reaction was complete after 3 h providing *tert*-butyl 3-benzoyl-4-(4-methylphenyl)cyclopentanecarboxylate as a white solid (43 mg, 0.118 mmol, 59 % yield, 1.7:1 dr). All spectroscopic data match those reported above.

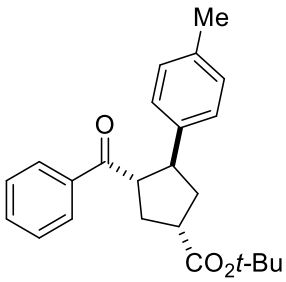

***tert*-Butyl 3-benzoyl-4-(4-trifluoromethylphenyl)cyclopentanecarboxylate (2.15):** Reaction

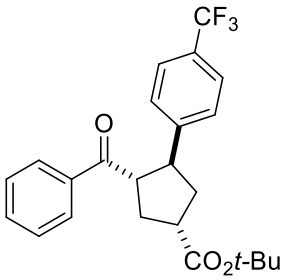

was carried out with *trans* tert-butyl 2-benzoylcyclopropanecarboxylate (50.0 mg, 0.203 mmol), 4-trifluoromethylstyrene (172.5 mg, 1.000 mmol), TMEDA (69.5 mg, 0.598 mmol), $Ru(bpy)_3(PF_6)_2$ (4.8 mg, 0.006 mmol), $Gd(OTf)_3$ (120.9 mg, 0.200 mmol), and MeCN (2 mL total volume). The reaction was complete after 3 h providing *tert*-butyl 3-benzoyl-4-(4-trifluoromethylphenyl)cyclopentanecarboxylate as a white solid (50 mg, 0.119 mmol, 59% yield, 1.3:1 dr). All spectroscopic data match those reported above.

***tert*-Butyl 3-benzoyl-4-(4-bromophenyl)cyclopentanecarboxylate (2.16):** Reaction was carried

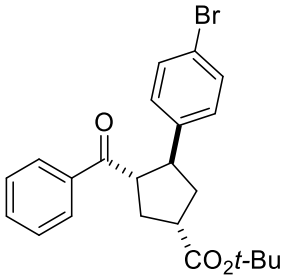

out with *trans* tert-butyl 2-benzoylcyclopropanecarboxylate (49.6 mg, 0.201 mmol), 4-bromostyrene (181.5 mg, 0.991 mmol), TMEDA (69.8 mg, 0.601 mmol), $Ru(bpy)_3(PF_6)_2$ (4.3 mg, 0.005 mmol), $Gd(OTf)_3$ (119.1 mg, 0.197 mmol), and MeCN (2 mL total volume). The reaction was complete after 3 h providing *tert*-butyl 3-benzoyl-4-(4-bromophenyl)cyclopentanecarboxylate as a white solid (51 mg, 0.118 mmol, 59% yield, 1:1 dr). All spectroscopic data match those reported above.

***tert*-Butyl 3-benzoyl-4-(2-methylphenyl)cyclopentanecarboxylate (2.17):** Reaction was carried

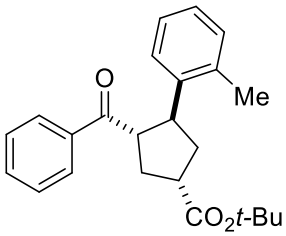

out with *trans* tert-butyl 2-benzoylcyclopropanecarboxylate (49.2 mg, 0.200 mmol), 2-methylstyrene (118.2 mg, 1.000 mmol), TMEDA (72.4 mg, 0.623 mmol), $Ru(bpy)_3(PF_6)_2$ (4.4 mg, 0.005 mmol), $Gd(OTf)_3$ (121.6 mg, 0.201 mmol), and MeCN (2 mL total volume). The reaction was complete after 3 h

providing *tert*-butyl 3-benzoyl-4-(2-methylphenyl)cyclopentanecarboxylate as a colorless oil (62 mg, 0.170 mmol, 85% yield, 1.7:1 d.r). All spectroscopic data match those reported above.

***tert*-Butyl 3-benzoyl-4-(4-methylphenyl)cyclopentanecarboxylate (2.18):** Reaction was carried out with *trans* tert-butyl 2-benzoylcyclopropanecarboxylate (50.3 mg, 0.204 mmol), α-methylstyrene (120.5 mg, 1.019 mmol), TMEDA (69.7 mg, 0.599 mmol), $Ru(bpy)_3(PF_6)_2$ (4.4 mg, 0.005 mmol), $Gd(OTf)_3$ (121.8mg, 0.202 mmol), and MeCN (2 mL total volume). The reaction was complete after 3 h providing *tert*-butyl 3-benzoyl-4-(4-methylphenyl)cyclopentanecarboxylate as a colorless oil (66 mg, 0.181 mmol, 89% yield, 2.0:1 d.r.). All spectroscopic data match those reported above.

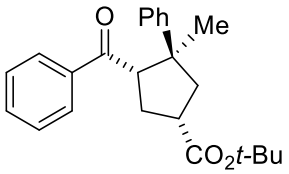

tert-Butyl 2-benzoyl-2',3'-dihydrospiro[cyclopentane-1,1'-indene]-4-carboxylate (2.19): Reaction was carried out with *trans* tert-butyl 2-benzoylcyclopropanecarboxylate (48.8 mg, 0.198 mmol), 1-methylene-2,3-dihydro-1H-indene (130.2 mg, 1.000 mmol), TMEDA (72.8 mg, 0.626 mmol), $Ru(bpy)_3(PF_6)_2$ (4.2 mg, 0.005 mmol), $Gd(OTf)_3$ (121.5 mg, 0.201 mmol), and MeCN (2 mL total volume). The reaction was complete after 24 h providing tert-butyl 2-benzoyl-2',3'-dihydrospiro[cyclopentane-1,1'-indene]-4-carboxylate as a colorless oil (58 mg, 0.154 mmol, 78% yield, 1.4:1 dr). All spectroscopic data match those reported above.

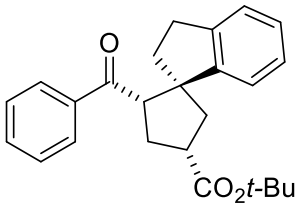

tert-Butyl 2-benzoyl-3',4'-dihydro-2'H-spiro[cyclopentane-1,1'-naphthalene]-4-carboxylate

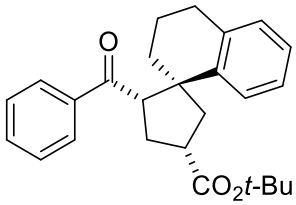

(2.20): Reaction was carried out with *trans* tert-butyl 2-benzoylcyclopropanecarboxylate (50.0 mg, 0.203 mmol), 1-methylene-1,2,3,4-tetrahydronaphthalene (145.0 mg, 1.005 mmol), TMEDA (70.9 mg, 0.610 mmol), $Ru(bpy)_3(PF_6)_2$ (4.4 mg, 0.005 mmol), $Gd(OTf)_3$ (121.1mg, 0.200 mmol), and MeCN (2 mL total volume). The reaction was complete after 6 h providing tert-butyl 2-benzoyl-3',4'-dihydro-2'H-spiro[cyclopentane-1,1'-naphthalene]-4-carboxylate as a colorless oil (69 mg, 0.177 mmol, 87% yield, 1.1:1 dr). All spectroscopic data match those reported above.

tert-Butyl 3-benzoyl-4-(9H-carbazol-9-yl)cyclopentanecarboxylate (2.21): Reaction was carried out with *trans* tert-butyl 2-benzoylcyclopropanecarboxylate (50.1 mg, 0.203 mmol), 9-vinylcarbazole (195.0 mg, 1.010 mmol), TMEDA (70.6 mg, 0.607 mmol), $Ru(bpy)_3(PF_6)_2$ (4.5 mg, 0.005 mmol), $Gd(OTf)_3$ (120.9 mg, 0.200 mmol), and MeCN (2 mL total volume). The reaction was complete after 3 h providing tert-butyl 3-benzoyl-4-(9H-carbazol-9-yl)cyclopentanecarboxylate as a white foam (68 mg, 0.155 mmol, 76% yield, 1.6:1 dr). All spectroscopic data match those reported above.

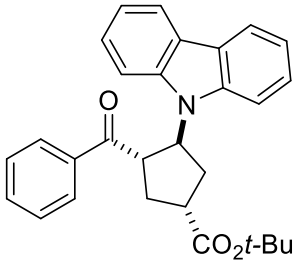

tert-Butyl 3-benzoyl-4-vinylcyclopentanecarboxylate (2.22): Reaction was carried out with *trans* tert-butyl 2-(4-methoxybenzoyl)cyclopropanecarboxylate (152.6 mg, 0.620 mmol), butadiene (1.36 mL, 3.098 mmol, 15 %wt solution in toluene), TMEDA (216.0 mg, 1.860 mmol), $Ru(bpy)_3(PF_6)_2$ (5.2 mg, 0.006 mmol), $Gd(OTf)_3$ (368.1 mg, 0.620 mmol), and MeCN (6 mL total volume). The reaction

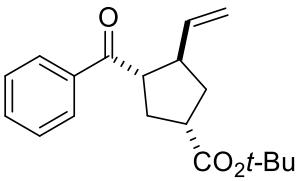

was complete after 6 h providing tert-butyl 3-benzoyl-4-vinylcyclopentanecarboxylate as a colorless oil (122.8 mg, 0.409 mmol, 66% yield,1.5:1 dr). All spectroscopic data match those reported above.

tert-Butyl 4-benzoyl-3-methyl-3-(prop-1-en-2-yl)cyclopentanecarboxylate (2.23): Reaction

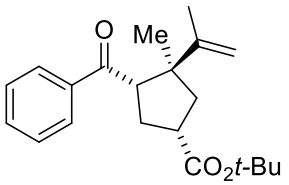

was carried out with *trans* tert-butyl 2-(4-methoxybenzoyl)cyclopropanecarboxylate (103.2 mg, 0.419 mmol), 2,3-dimethyl-1,2-butadiene (166.8 mg, 2.031 mmol), TMEDA (141.5 mg, 1.218 mmol), $Ru(bpy)_3(PF_6)_2$ (8.7 mg, 0.01 mmol), $Gd(OTf)_3$ (245.0 mg, 0.405 mmol), and MeCN (4 mL total volume). The reaction was complete after 3 h providing tert-butyl 4-benzoyl-3-methyl-3-(prop-1-en-2-yl)cyclopentanecarboxylate as a colorless oil (71.6 mg, 0.218 mmol, 52% yield, 1.44:1 dr). All spectroscopic data match those reported above.

tert-Butyl 3-(4-methoxybenzoyl)-4-phenylcyclopentanecarboxylate (2.24): Reaction was

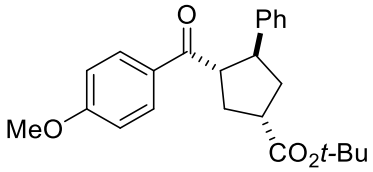

carried out with *trans* tert-butyl 2-(4-methoxybenzoyl)cyclopropanecarboxylate (55.3 mg, 0.200 mmol), styrene (104.3 mg, 1.001 mmol), TMEDA (69.8 mg, 0.601 mmol), $Ru(bpy)_3(PF_6)_2$ (4.3 mg, 0.005 mmol), $Gd(OTf)_3$ (120.9 mg, 0.200 mmol), and MeCN (2 mL total volume). The reaction was complete after 3 h providing tert-butyl 3-(4-methoxybenzoyl)-4-phenylcyclopentanecarboxylate as a white solid (61.0 mg, 0.174 mmol, 87% yield, 2.7:1 dr). All spectroscopic data match those reported above.

tert-Butyl 3-(4-methylbenzoyl)-4-phenylcyclopentanecarboxylate (2.25): Reaction was carried

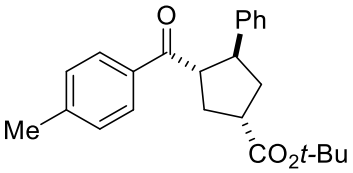

out with *trans* tert-butyl 2-(4-methylbenzoyl)cyclopropanecarboxylate (52.1 mg, 0.200 mmol), styrene (104.3 mg, 1.001 mmol), TMEDA (69.8 mg, 0.601 mmol), $Ru(bpy)_3(PF_6)_2$ (4.3 mg, 0.005 mmol), $Gd(OTf)_3$ (120.9 mg, 0.200 mmol), and MeCN (2 mL total volume). The reaction was complete after 3 h providing tert-butyl 3-(4-methylbenzoyl)-4-phenylcyclopentanecarboxylate as a white solid (63.4 mg, 0.174 mmol, 87% yield, 3:1 dr). All spectroscopic data match those reported above.

tert-Butyl 3-phenyl-4-(4-(trifluoromethyl)benzoyl)cyclopentane carboxylate (2.26): Reaction

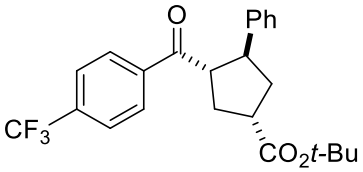

was carried out with *trans* tert-butyl 2-(4-(trifluoromethyl)benzoyl)cyclopropanecarboxylate (62.9 mg, 0.200 mmol), styrene (104.3 mg, 1.001 mmol), TMEDA (69.8 mg, 0.601 mmol), $Ru(bpy)_3(PF_6)_2$ (4.3 mg, 0.005 mmol), $Gd(OTf)_3$ (120.9 mg, 0.200 mmol), and MeCN (2 mL total volume). The reaction was complete after 3 hours providing tert-butyl 3-phenyl-4-(4-(trifluoromethyl)benzoyl)cyclopentanecarboxylate as a white solid (80.3 mg, 0.192 mmol , 96 % yield, 1.6:1 dr). All spectroscopic data match those reported above.

tert-Butyl 3-(4-chlorobenzoyl)-4-phenylcyclopentanecarboxylate (2.27): Reaction was carried

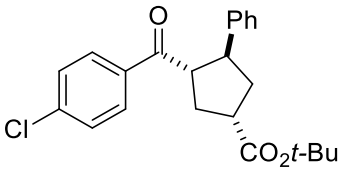

out with *trans* tert-butyl 2-(4-chlorobenzoyl)cyclopropanecarboxylate (56.1 mg, 0.200 mmol), styrene (104.3 mg, 1.001 mmol), TMEDA (69.8 mg, 0.601 mmol), $Ru(bpy)_3(PF_6)_2$ (4.3 mg, 0.005 mmol), $Gd(OTf)_3$ (120.9 mg, 0.200 mmol), and MeCN (2 mL total

volume). The reaction was complete after 3 h providing tert-butyl 3-(4-chlorobenzoyl)-4-phenylcyclopentanecarboxylate as a white solid (71.6 mg, 0.186 mmol, 93% yield, 1:1 dr). All spectroscopic data match those reported above.

tert-Butyl 3-nicotinoyl-4-phenylcyclopentanecarboxylate (2.28): Reaction was carried out with

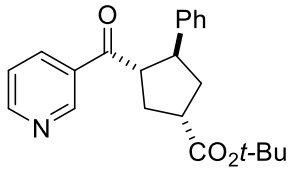

trans tert-butyl 2-nicotinoylcyclopropanecarboxylate (49.5 mg, 0.200 mmol), styrene (104.3 mg, 1.001 mmol), TMEDA (69.8 mg, 0.601 mmol), $Ru(bpy)_3(PF_6)_2$ (4.3 mg, 0.005 mmol), $Gd(OTf)_3$ (120.9 mg, 0.200 mmol), and MeCN (2 mL total volume). The reaction was complete after 3 h providing tert-butyl 3-nicotinoyl-4-phenylcyclopentanecarboxylate as a white solid (35.8 mg, 0.102 mmol, 51% yield, 1.6:1 dr). All spectroscopic data match those reported above.

tert-Butyl 3-(furan-2-carbonyl)-4-phenylcyclopentanecarboxylate (2.29): Reaction was

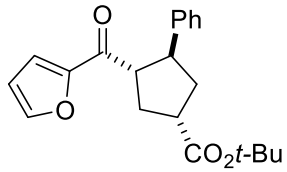

carried out with *trans* tert-butyl 2-(furan-2-carbonyl)cyclopropanecarboxylate (47.3 mg, 0.200 mmol), styrene (104.3 mg, 1.001 mmol), TMEDA (69.8 mg, 0.601 mmol), $Ru(bpy)_3(PF_6)_2$ (4.3 mg, 0.005 mmol), $Gd(OTf)_3$ (120.9 mg, 0.200 mmol), and MeCN (2 mL total volume). The reaction was complete after 3 h providing tert-butyl 3-(furan-2-carbonyl)-4-phenylcyclopentanecarboxylate as a white solid (60.6 mg, 0.178 mmol, 89% yield, 1.6:1 dr). All spectroscopic data match those reported above.

tert-Butyl 3-(3-methylbenzoyl)-4-phenylcyclopentanecarboxylate (2.30): Reaction was carried

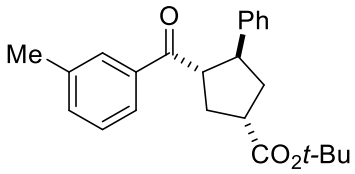

out with *trans* tert-butyl 2-(3-methylbenzoyl)cyclopropanecarboxylate (52.1 mg, 0.200 mmol), styrene (104.3 mg, 1.001 mmol), TMEDA (69.8 mg, 0.601 mmol), $Ru(bpy)_3(PF_6)_2$ (4.3 mg, 0.005 mmol), $Gd(OTf)_3$ (120.9 mg, 0.200 mmol), and MeCN (2 mL total volume). The reaction was complete after 3 h providing tert-butyl 3-(3-methylbenzoyl)-4-phenylcyclopentanecarboxylate as a white solid (59.8 mg, 0.164 mmol, 82% yield, 2.4:1 dr). All spectroscopic data match those reported above.

tert-Butyl 3-(2-methylbenzoyl)-4-phenylcyclopentanecarboxylate (2.31): Reaction was carried

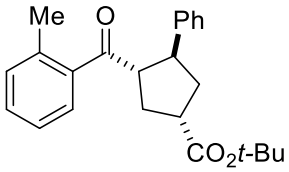

out with *trans* tert-butyl 2-(2-methylbenzoyl)cyclopropanecarboxylate (52.1 mg, 0.200 mmol), styrene (104.3 mg, 1.001 mmol), TMEDA (69.8 mg, 0.601 mmol), $Ru(bpy)_3(PF_6)_2$ (4.3 mg, 0.005 mmol), $Gd(OTf)_3$ (120.9 mg, 0.200 mmol), and MeCN (2 mL total volume). The reaction was complete after 3 h providing tert-butyl 3-(2-methylbenzoyl)-4-phenylcyclopentanecarboxylate as a white solid (37.9 mg, 0.104 mmol, 52% yield, 1.5:1 dr). All spectroscopic data match those reported above.

1-(3-Benzoyl-4-phenylcyclopentyl)ethanone (2.32): Reaction was carried out with *trans* 2-

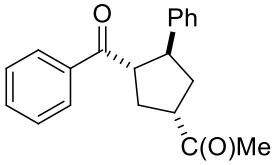

benzoylcyclopropylethanone (37.6 mg, 0.200 mmol), styrene (104.3 mg, 1.001 mmol), DIPEA (51.7 mg, 0.400 mmol), 2,6-bis(4,5-dihydrooxazol-2-yl)-N,N-dimethylpyridin-4-amine (78.1 mg, 0.300 mmol), $Ru(bpy)_3(PF_6)_2$ (4.3 mg, 0.005 mmol), $Gd(OTf)_3$ (120.9 mg, 0.200 mmol), and MeCN (2 mL total volume). The reaction was

complete after 3 h providing 1-(3-benzoyl-4-phenylcyclopentyl)ethanone as a white solid (21.1 mg, 0.072 mmol, 36% yield, 4.7:1 dr). All spectroscopic data match those reported above.

(4-Methyl-2-phenylcyclopentyl)(phenyl)methanone (2.33): Reaction was carried out with *trans* 2-methylcyclopropyl)(phenyl)methanone (32.0 mg, 0.200 mmol), styrene (104.3 mg, 1.001 mmol), TMEDA (69.8 mg, 0.601 mmol), $Ru(bpy)_3(PF_6)_2$ (4.3 mg, 0.005 mmol), $Gd(OTf)_3$ (120.9 mg, 0.200 mmol), and MeCN (2 mL total volume). The reaction was complete after 3 h providing (4-methyl-2-phenylcyclopentyl)(phenyl)methanone as a white solid (42.8 mg, 0.162 mmol, 81% yield, 11:1 dr). All spectroscopic data match those reported above.

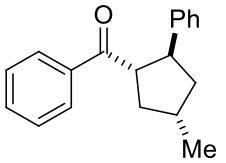

(4,4-Dimethyl-2-phenylcyclopentyl)(phenyl)methanone (2.34): Reaction was carried out with (2,2-dimethylcyclopropyl)(phenyl)methanone (34.8 mg, 0.200 mmol), styrene (104.3 mg, 1.001 mmol), TMEDA (69.8 mg, 0.601 mmol), $Ru(bpy)_3(PF_6)_2$ (4.3 mg, 0.005 mmol), $Gd(OTf)_3$ (120.9 mg, 0.200 mmol), and MeCN (2 mL total volume). The reaction was complete after 3 h providing (4,4-dimethyl-2-phenylcyclopentyl)(phenyl)methanone as a white solid (52.3 mg, 0.188 mmol, 94% yield, 1.5:1 dr). All spectroscopic data match those reported above.

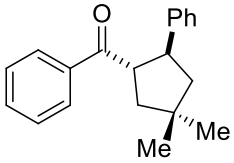

Phenyl(3-phenylspiro[4.4]nonan-2-yl)methanone (2.35): Reaction was carried out with phenyl(spiro[2.4]heptan-1-yl)methanone (40.1 mg, 0.200 mmol), styrene (104.3 mg, 1.001 mmol), TMEDA (69.8 mg, 0.601 mmol), $Ru(bpy)_3(PF_6)_2$ (4.3 mg, 0.005 mmol), $Gd(OTf)_3$ (120.9 mg, 0.200 mmol), and MeCN (2 mL total

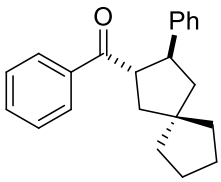

volume). The reaction was complete after 3 h providing phenyl(3-phenylspiro[4.4]nonan-2-yl)methanone as a white solid (51.1 mg, 0.168 mmol, 84 % yield, 1:1 dr). All spectroscopic data match those reported above.

Di-tert-butyl 3-benzoyl-4-phenylcyclopentane-1,2-dicarboxylate (2.37): Reaction was carried out with (1R,2S,3s)-di-tert-butyl 3-benzoylcyclopropane-1,2-dicarboxylate (69.3 mg, 0.200 mmol), styrene (104.3 mg, 1.001 mmol), TMEDA (69.8 mg, 0.601 mmol), $Ru(bpy)_3(PF_6)_2$ (4.3 mg, 0.005 mmol), $Gd(OTf)_3$ (120.9 mg, 0.200 mmol), and MeCN (2 mL total volume). The reaction was complete after 3 h providing tert-butyl 5-benzoyl-2,2-dimethyl-4-phenylcyclopentanecarboxylate as a white solid (84.7 mg, 0.188 mmol, 94% yield, 1.3:1 dr). All spectroscopic data match those reported above.

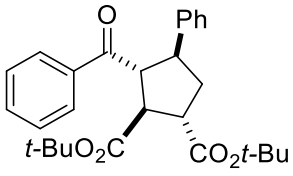

tert-Butyl 5-benzoyl-2,2-dimethyl-4-phenylcyclopentanecarboxylate (2.39): Reaction was carried out with tert-butyl 3-benzoyl-2,2-dimethylcyclopropanecarboxylate (54.9 mg, 0.200 mmol), styrene (104.3 mg, 1.001 mmol), TMEDA (69.8 mg, 0.601 mmol), $Ru(bpy)_3(PF_6)_2$ (4.3 mg, 0.005 mmol), $Gd(OTf)_3$ (120.9 mg, 0.200 mmol), and MeCN (2 mL total volume). The reaction was complete after 3 h providing tert-butyl 5-benzoyl-2,2-dimethyl-4-phenylcyclopentanecarboxylate as a white solid (74.2 mg, 0.196 mmol, 97% yield, 20:1 dr). All spectroscopic data match those reported above.

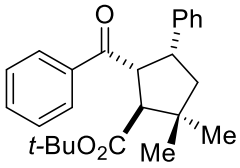

(4,4-Dimethyl-2-phenylcyclopentyl)(4-(trifluoromethyl)phenyl)methanone (2.41): Reaction 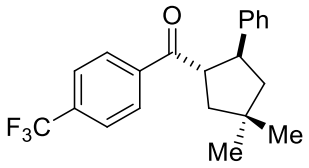 was carried out with (2,2-dimethylcyclopropyl)(4-(trifluoromethyl)phenyl)methanone (48.4 mg, 0.200 mmol), styrene (104.3 mg, 1.001 mmol), TMEDA (69.8 mg, 0.601 mmol), $Ru(bpy)_3(PF_6)_2$ (4.3 mg, 0.005 mmol), $Gd(OTf)_3$ (120.9 mg, 0.200 mmol), and MeCN (2 mL total volume). The reaction was complete after 3 h providing (4,4-dimethyl-2-phenylcyclopentyl)(4-(trifluoromethyl)phenyl)methanone as a white solid (41.6 mg, 0.120 mmol, 60% yield, 0.8:1 dr). All spectroscopic data match those reported above.

2.5.8: Bayer Villiger Product Derivitization

General procedure: A small flame-dried vial with magnetic stir bar was charged with cyclopentyl ketone (0.05 mmol), *m*-CPBA (≤77%, 26.0 mg, 0.15 mmol), and CH_2Cl_2 (1.0 mL). The vial was sealed with a rubber septum, purged three times with N_2(g) and cooled to 0 ^oC with an ice bath. Trifluoroacetic acid (9.1 μL, 0.05 mmol) was then added via syringe. The vial was then sealed with a Teflon cap, covered in aluminum foil, and stirred for 36 h at room temperature. After this time the reaction was quenched by washing with saturated aqueous Na_2SO_3. The aqueous layer was washed twice more with CH_2Cl_2. The combined organics were washed with brine, dried over Na_2SO_4, and concentrated under reduced pressure to give the crude product as a yellow oil. Products were purified by flash column chromatography (Et_2O/pentane).

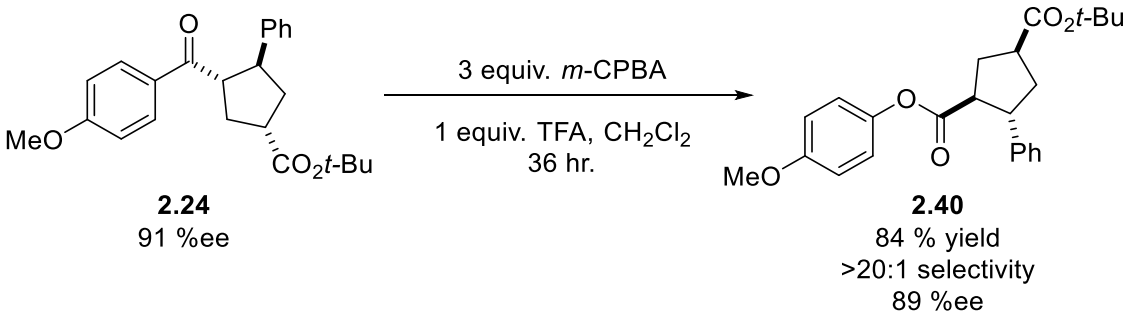

2.24
91 %ee

2.40
84 % yield
>20:1 selectivity
89 %ee

1-tert-Butyl 3-(4-methoxyphenyl) 4-phenylcyclopentane-1,3-dicarboxylate (2.40): Reaction

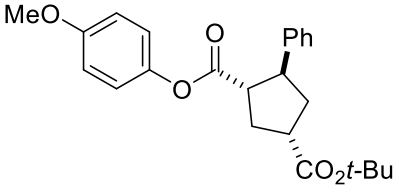

was carried out according to the general procedure with cyclopentane **19** (19.1 mg, 0.05 mmol), *m*-CPBA (28.3 mg, 0.15 mmol), CH_2Cl_2 (1.0 mL) and trifluoroacetic acid (9.1 μL, 0.05 mmol) to give rearrangement product **33** as a clear oil as the sole product. Product was purified by column chromatography (20% Et_2O/pentanes) to give the pure product (16.7 mg, 0.042 mmol, 84% yield). 88.7% ee [Daicel Chiracel AD-H, 15 % iPrOH, 3 mL/min, 263 nm; t_1=4.08 min, t_2=5.70 min]. $[\alpha]_D^{22}$ 45.1 (*c*0.901, CH_2Cl_2). ν_{max} (film) / cm^{-1} 2974, 1752, 1723, 1506, 1455, 1367, 1248, 1195, 1134, 1033. ^{1}H NMR (400 MHz, $CDCl_3$) δ 7.36 – 7.27 (m, 4H), 7.25-7.21 (m, 1H), 6.82 (m, 4H), 3.76 (s, 3H), 3.61 (q, *J* = 9.9 Hz, 1H), 3.14 – 2.97 (m, 2H), 2.61 – 2.44 (m, 2H), 2.38 (ddd, *J* = 13.1, 10.4, 8.4 Hz, 1H), 2.08 (dt, *J* = 13.4, 9.8 Hz, 1H), 1.48 (s, 9H). ^{13}C NMR (101 MHz, $CDCl_3$) δ 174.57, 173.33, 157.28, 144.27, 142.63, 128.75, 127.40, 126.92, 122.33, 114.46, 80.75, 55.70, 52.49, 48.99, 43.78, 37.63, 34.35, 28.23. HRMS (ESI) calculated for $[C_{24}H_{29}O_5]^+$ ($M+H^+$) requires *m/z* 397.2010, found 397.2010.

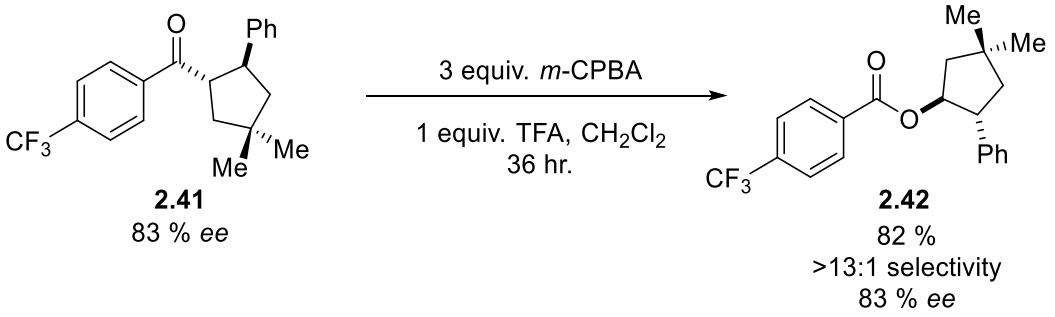

4,4-Dimethyl-2-phenylcyclopentyl 4-(trifluoromethyl)benzoate (2.42): Reaction was carried out according to the general procedure with cyclopentane **34** (50.1 mg, 0.144 mmol), *m*-CPBA (74.6 mg, 0.432 mmol), CH_2Cl_2 (2.9 mL), and trifluoroacetic acid (26.2 μL, 0.144 mmol) to give the rearranged product **35** as a clear oil. Product was purified by column chromatography (5% Et_2O/pentanes) (42.8 mg, 0.118 mmol, 82% isolated yield). 83.1% ee [Daicel Chiracel OD-H, 5 to 30 % iPrOH, 3 mL/min, 235 nm; t_1=4.71 min, t_2=6.04 min]. $[\alpha]_D^{22}$ 63.3 (*c*0.900, CH_2Cl_2). ν_{max} (film) / cm^{-1} 2956, 1723, 1412, 1325, 1275, 1131, 1067, 1018. ^{1}H NMR (400 MHz, $CDCl_3$) δ 8.11 (d, *J* = 8.1 Hz, 2H), 7.68 (d, *J* = 8.2 Hz, 2H), 7.35 – 7.25 (m, 4H), 7.24 – 7.16 (m, 1H), 5.44 (td, *J* = 8.0, 5.8 Hz, 1H), 3.57 (dt, *J* = 11.9, 7.9 Hz, 1H), 2.28 (dd, *J* = 13.8, 8.1 Hz, 1H), 2.05 (dd, *J* = 13.0, 7.9 Hz, 1H), 1.78 – 1.66 (m, 2H), 1.24 (s, 3H), 1.19 (s, 3H). ^{13}C NMR (101 MHz, $CDCl_3$) δ 164.97, 142.27, 134.30 (q, *J* = 32.7 Hz), 133.69, 129.92, 128.55, 127.20, 126.59, 125.35 (q, *J* = 3.7 Hz), 123.64 (q, *J* = 273.6 Hz), 82.63, 50.52, 47.33, 47.08, 37.07, 30.71, 30.18. ^{19}F NMR (377 MHz, $CDCl_3$) δ -63.10. HRMS (ESI) calculated for $[C_{21}H_{24}NF_3O_2]^+$ ($M+NH_4^+$) requires *m/z* 380.1832, found 380.1832.

2.5.9: NOE Assignment of Relative Stereochemistry

Figure 2-1. Observed NOe enhancements

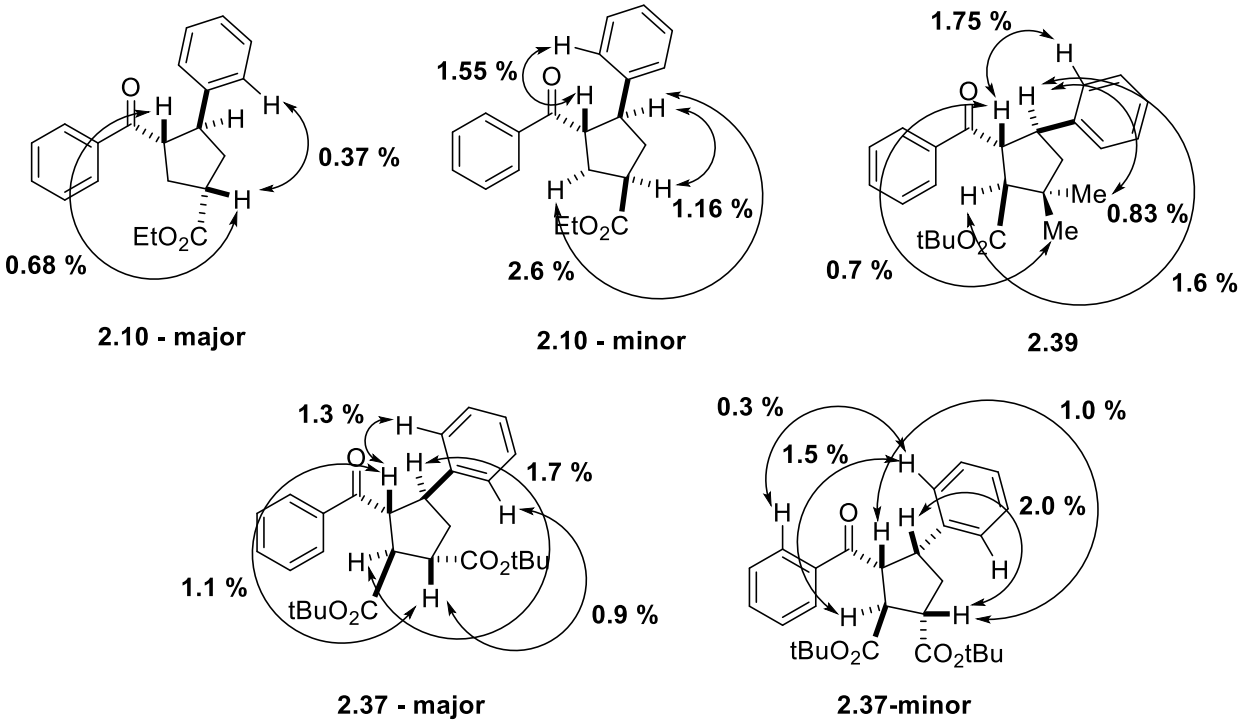

2.5.10: Mechanistic Experiments

2.5.10.1: Isomerization of cis-Cyclopropanes under Photocatalytic Conditions

Scheme 2-9. Control reaction in the absence of photocatalyst

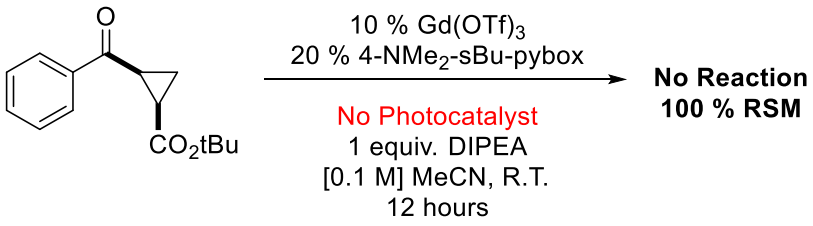

Figure 2-2. Time course of photocatalytic [3+2] cycloaddition of cis-cyclopropane with styrene

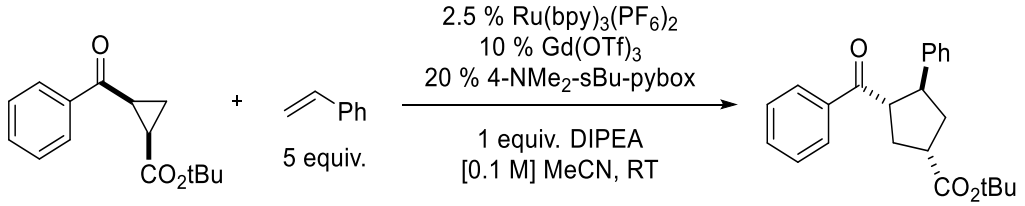

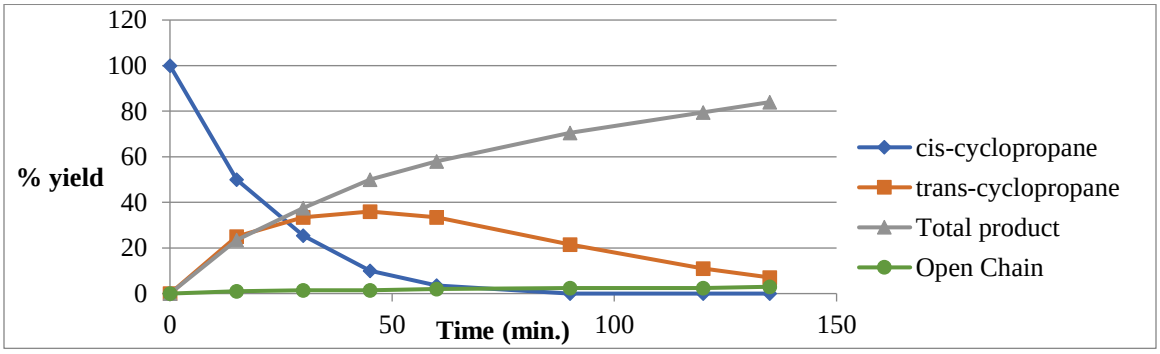

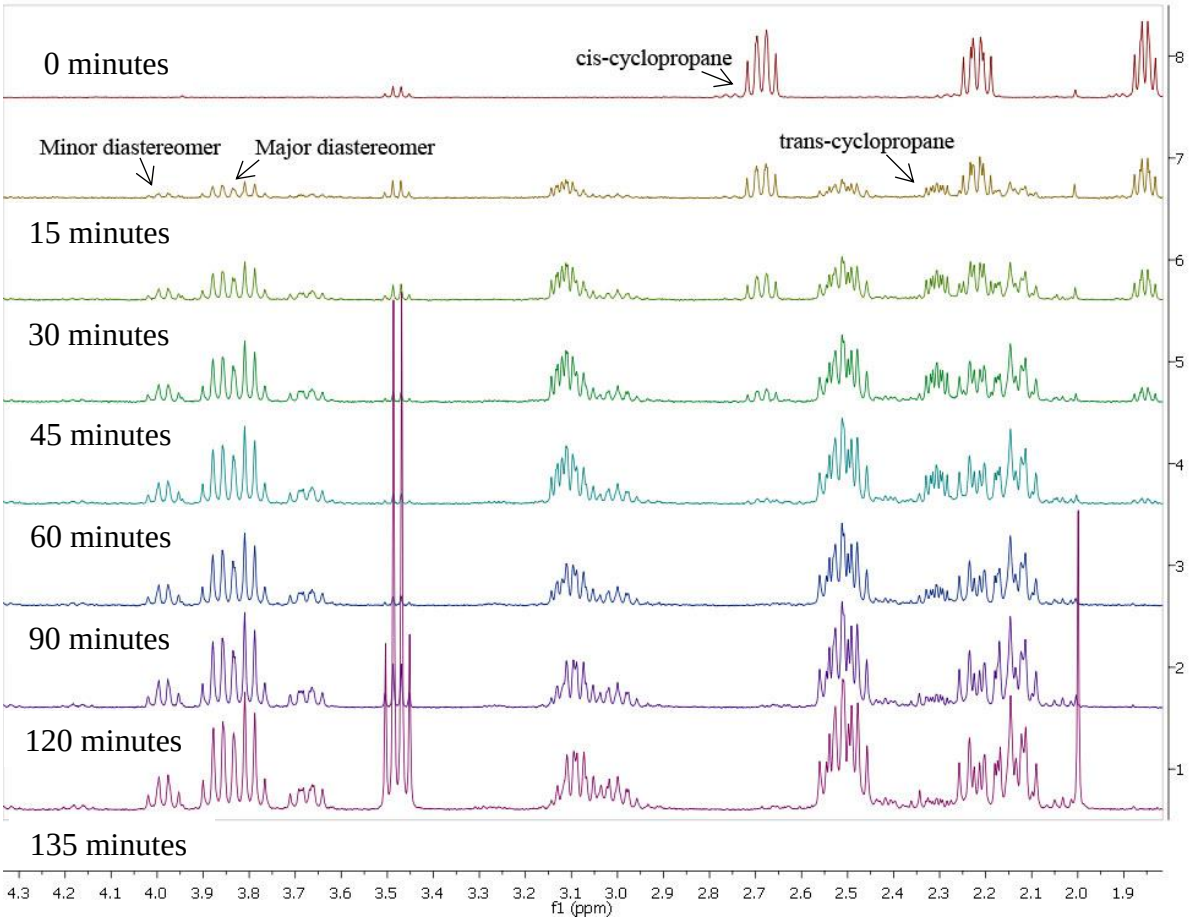

2.5.10.2: Kinetic Isotope Effect Measurements

The intermolecular kinetic isotope effect of the [3+2] photocycloaddition was determined by studying the initial rates of reactions with (a) tert-butyl 2-benzoylcyclopropanecarboxylate **2.11** and styrene and (b) tert-butyl 2-benzoylcyclopropanecarboxylate **2.11** and β,β-dideuterostyrene.

General procedure for kinetic experiments: The experiments were conducted in dry 15 mL Schlenk tubes under degassed conditions 15 cm from a 26 W fluorescent lamp. Reaction run to ~20% conversion and the data ([product] versus time) was analyzed by the initial rates method. Reported values for initial rates are the average of the experiments all conducted under identical conditions using the same stock solutions. The reported error is the standard deviation of three experiments. Representative kinetics experiments are shown in Figure 2-3 and 2-4.

Reaction procedure: For three-fold experiments a 10 mL stock solution was generated containing substrate (123.15 mg, 0.5 mmol), styrene (260.4 mg, 2.5 mmol), $Ru(bpy)_3(PF_6)_2$ (10.7 mg, 0.125 mmol), $Gd(OTf)_3$ (30.2 mg, 0.05 mmol), ligand **L2.11** (37.3 mg, 0.1 mmol), phenanthrene (internal standard), and MeCN (10 mL total volume in a volumetric flask). Stock solution (2 mL) was transferred to a flame-dried 15 mL Schlenk tube and degassed by three freeze/pump/thaw cycles under N_2 in the dark. After backfilling with N_2 the reaction was stirred at 0 ^oC while being irradiated by a 23 W lightbulb at a distance of 15 cm. For each time point, the Schlenk tube's side arm was purged several times with N_2, opened under a positive pressure of N_2, and a small aliquot was taken with a N_2 purged needles. The aliquot was diluted in 1:1 Et_2O/pentanes, flashed through a short pipette silica plug and concentrated under reduced pressure for analysis by ^{1}H-NMR spectroscopy. The yield of product was determined versus phenanthrene as the internal standard.

Figure 2-3. Kinetics experiment with proteo-styrene

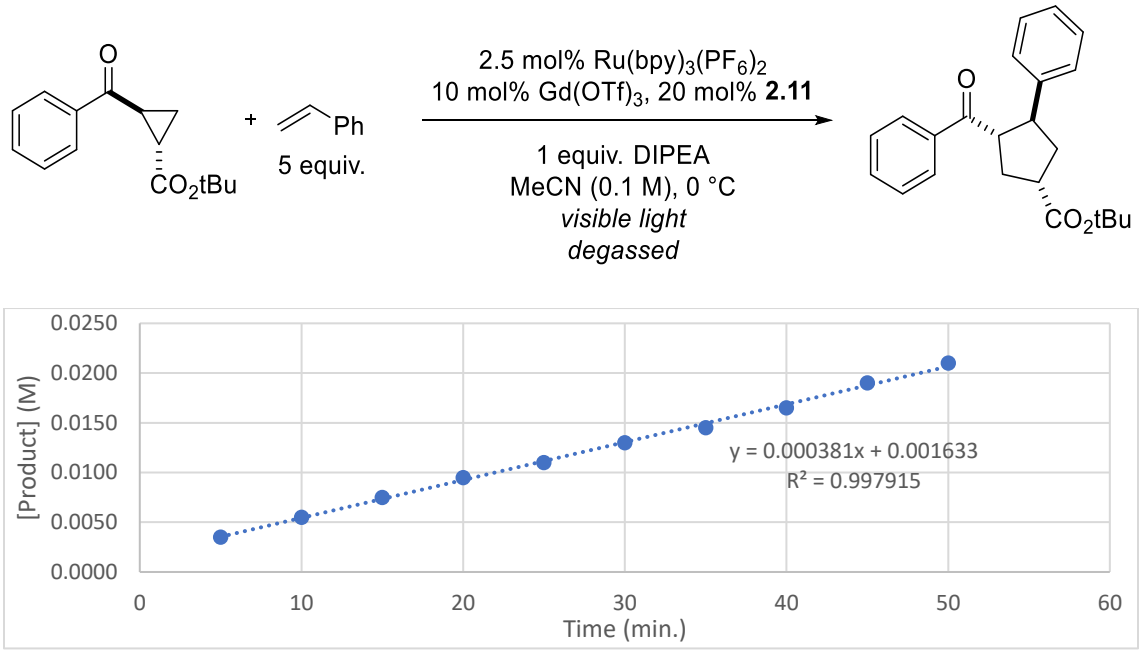

Figure 2-4. Kinetics experiment with deutero-styrene

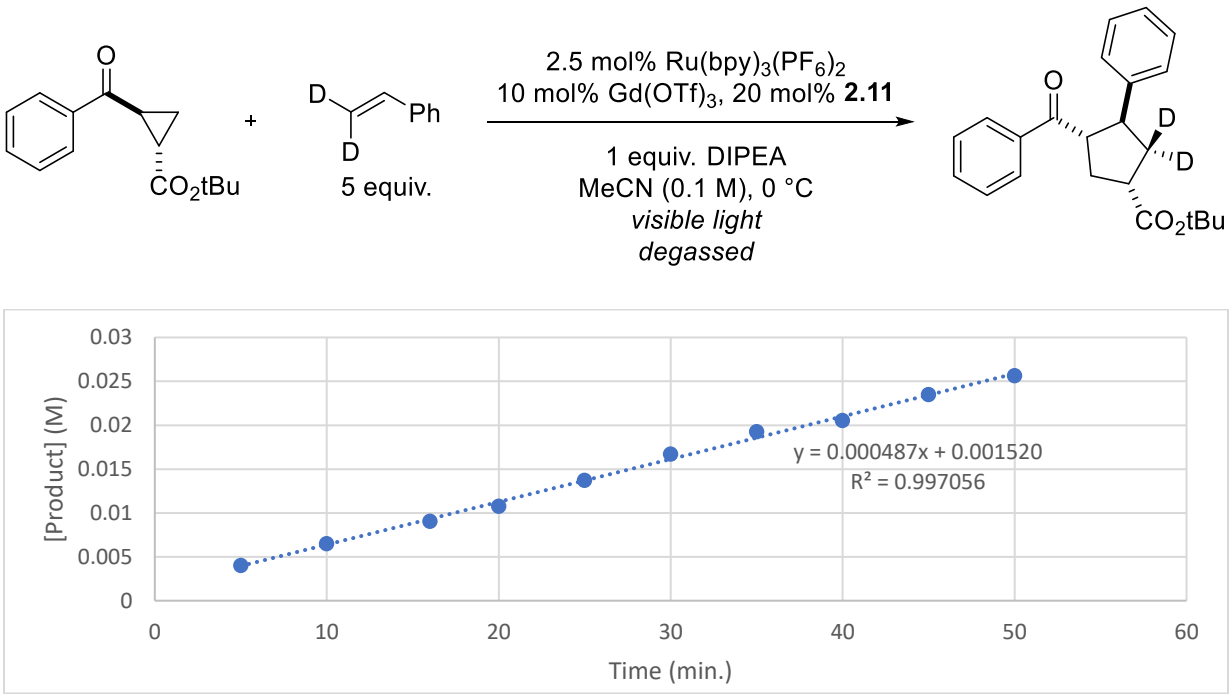

Kinetic isotope effects. Obtained values for rate constants and its use in the calculation of kinetic isotope effects are displayed below.

Figure 2-5. Computed kinetic isotope effect.

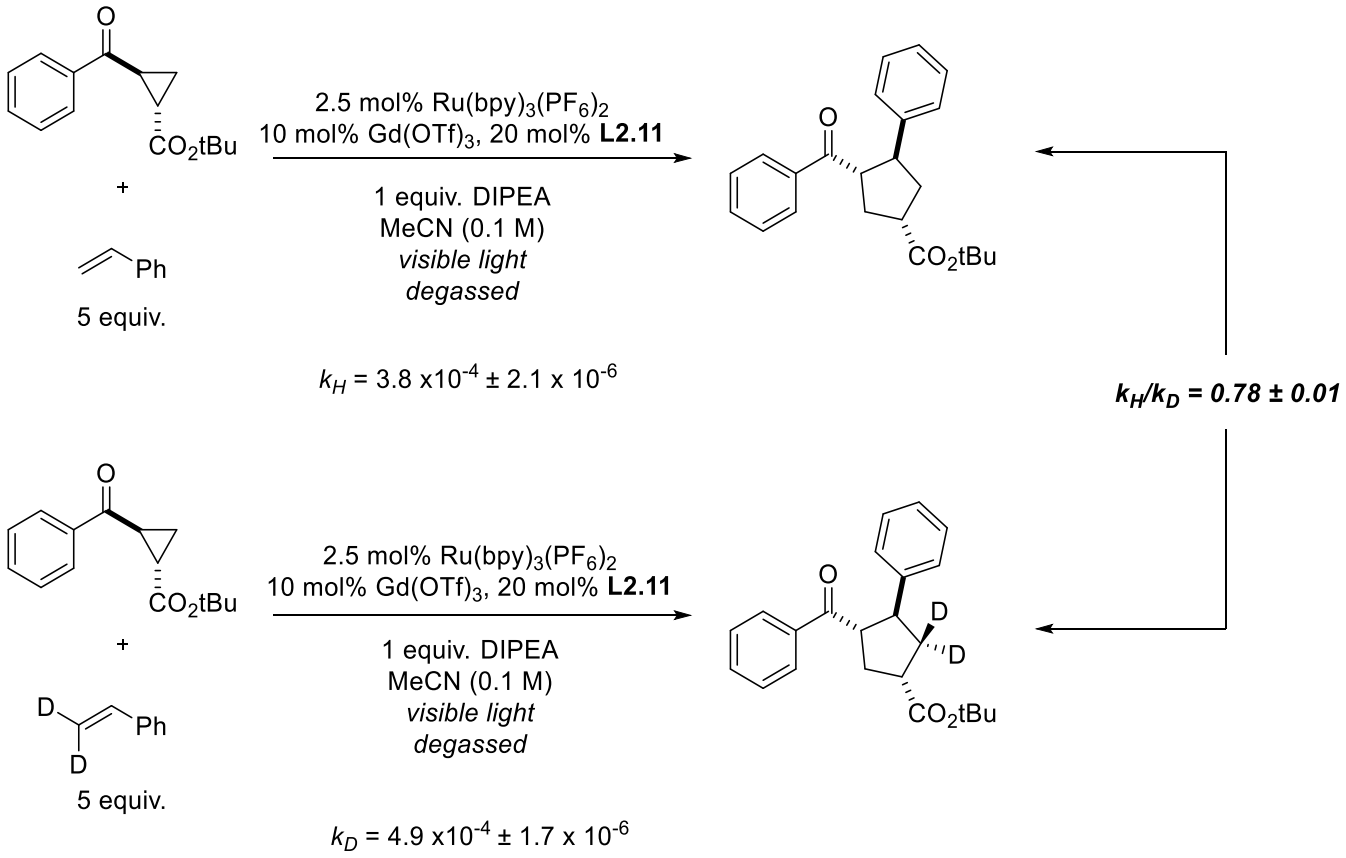

2.5.11: X-Ray Crystallographic Information

Data Collection: A colorless crystal with approximate dimensions 0.184 × 0.037 × 0.026 mm^3 was selected under oil under ambient conditions and attached to the tip of a MiTeGen MicroMount©. The crystal was mounted in a stream of cold nitrogen at 100(1) K and centered in the X-ray beam by using a video camera.

The crystal evaluation and data collection were performed on a Bruker Quazar SMART APEXII diffractometer with Mo K_α (λ = 0.71073 Å) radiation and the diffractometer to crystal distance of 4.96 cm.[55]

The initial cell constants were obtained from three series of ω scans at different starting angles. Each series consisted of 12 frames collected at intervals of 0.5º in a 6º range about ω with the exposure time of 10 seconds per frame. The reflections were successfully indexed by an automated indexing routine built in the APEXII program suite. The final cell constants were calculated from a set of 8678 strong reflections from the actual data collection.

The data were collected by using the full sphere data collection routine to survey the reciprocal space to the extent of a full sphere to a resolution of 0.70 Å. A total of 30318 data were harvested by collecting 4 sets of frames with 0.5º scans in ω and φ with exposure times of 120 sec per frame. These highly redundant datasets were corrected for Lorentz and polarization effects. The absorption correction was based on fitting a function to the empirical transmission surface as sampled by multiple equivalent measurements.[56]

Structure Solution and Refinement: The systematic absences in the diffraction data were uniquely consistent for the space group $P2_12_12_1$ that yielded chemically reasonable and computationally stable results of refinement.[57–62]

A successful solution by the direct methods provided most non-hydrogen atoms from the *E*-map. The remaining non-hydrogen atoms were located in an alternating series of least-squares cycles and difference Fourier maps. All non-hydrogen atoms were refined with anisotropic displacement coefficients. All hydrogen atoms were included in the structure factor calculation at idealized positions and were allowed to ride on the neighboring atoms with relative isotropic displacement coefficients.

The only crystal large enough for the single-crystal X-ray diffraction experiment proved to be a crystal with at least two smaller crystals attached to it in a random manner. These smaller crystals were not visible under the microscope and their presence was inferred from the diffraction pattern. The data collection was treated as if the major crystal were single.

The final least-squares refinement of 247 parameters against 4215 data resulted in residuals *R* (based on F^2 for $I \geq 2\sigma$) and *wR* (based on F^2 for all data) of 0.0365 and 0.0885, respectively.

Crystal Data for $C_{23}H_{25}BrO_3$ (*M* =429.34 g/mol): orthorhombic, space group $P2_12_12_1$ (no. 19), a = 5.633(2) Å, b = 16.777(7) Å, c = 21.917(8) Å, V = 2071.4(14) Å^3, Z = 4, T = 100.0 K, μ(MoKα) = 2.004 mm^{-1}, *Dcalc* = 1.377 g/cm^3, 30318 reflections measured ($3.058° \leq 2\Theta \leq 52.822°$), 4215 unique ($R_{int}$ = 0.0568, R_{sigma} = 0.0382) which were used in all calculations. The final R_1 was 0.0365 ($I > 2\sigma(I)$) and wR_2 was 0.0885 (all data).

Figure 2-6. A molecular drawing of **2.16** shown with 50% probability ellipsoids. All H atoms are omitted unless they are on anomeric carbon atoms.

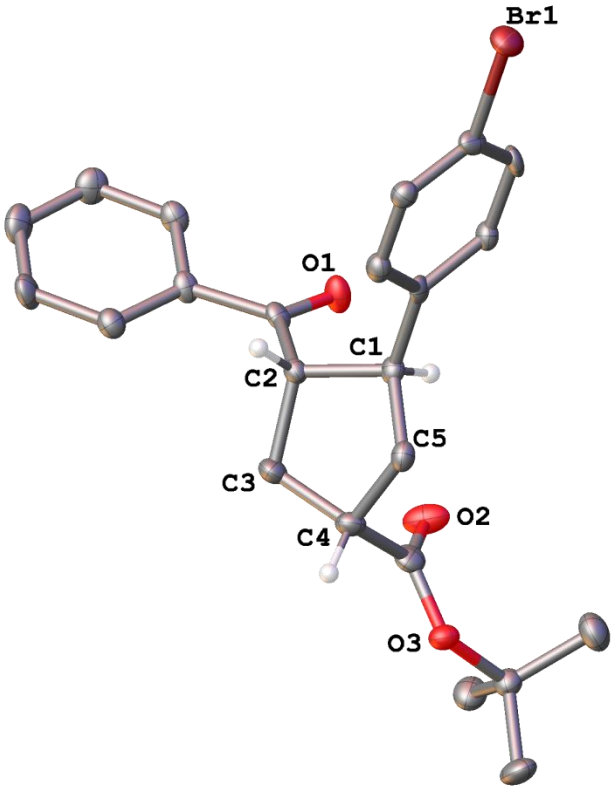

Table 2-13. Crystal data and structure refinement for **2.16**

Identification code	yoon42
Empirical formula	$C_{23}H_{25}BrO_3$
Formula weight	429.34
Temperature/K	100.0
Crystal system	orthorhombic
Space group	$P2_12_12_1$
a/Å	5.633(2)
b/Å	16.777(7)
c/Å	21.917(8)
α/°	90
β/°	90
γ/°	90
Volume/Å^3	2071.4(14)
Z	4
ρ_{calc}g/cm^3	1.377
μ/mm^{-1}	2.004
F(000)	888.0
Crystal size/mm^3	0.184 × 0.037 × 0.026
Radiation	MoKα (λ = 0.71073)
2Θ range for data collection/°	3.058 to 52.822
Index ranges	$-7 \leq h \leq 7$, $-20 \leq k \leq 20$, $-25 \leq l \leq 27$
Reflections collected	30318
Independent reflections	4215 [R_{int} = 0.0568, R_{sigma} = 0.0382]
Data/restraints/parameters	4215/0/247
Goodness-of-fit on F^2	1.068
Final R indexes [I>=2σ (I)]	R_1 = 0.0365, wR_2 = 0.0858
Final R indexes [all data]	R_1 = 0.0449, wR_2 = 0.0885
Largest diff. peak/hole / e Å^{-3}	0.51/-0.28
Flack parameter	0.002(5)

Table 2.14. Fractional Atomic Coordinates ($\times 10^4$) and Equivalent Isotropic Displacement Parameters ($Å^2 \times 10^3$) for **2.16**. U_{eq} is defined as 1/3 of of the trace of the orthogonalised U_{IJ} tensor.

Br1	9807.7(8)	1810.9(3)	3546.2(2)	28.62(14)
O1	4364(5)	5424.9(19)	4753.8(15)	25.1(7)
O2	5841(5)	5574(2)	6384.9(16)	32.8(8)
O3	8823(5)	5545.7(19)	7076.8(14)	21.2(7)
C1	8355(7)	4702(3)	5269(2)	17.0(9)
C2	8501(7)	5523(3)	4958(2)	16.1(9)
C3	9177(9)	6118(3)	5484(2)	24.6(10)
C4	9889(9)	5604(2)	6039.3(18)	21.0(9)
C5	10216(8)	4754(2)	5775.7(18)	19.7(9)
C6	8708(7)	4006(3)	4843(2)	16.3(9)
C7	6958(7)	3427(3)	4784(2)	17.8(9)
C8	7252(8)	2766(3)	4398(2)	21.5(10)
C9	9342(8)	2698(2)	4079(2)	20.7(10)
C10	11129(7)	3266(3)	4124.4(19)	18.5(9)
C11	10784(7)	3914(3)	4507(2)	20(1)
C12	6225(7)	5755(3)	4636(2)	16.7(9)
C13	6283(7)	6393(3)	4158(2)	18.2(9)
C14	8185(7)	6917(3)	4082(2)	21.2(10)
C15	8153(9)	7483(3)	3616(2)	27.1(11)
C16	6223(9)	7522(3)	3233(2)	29.9(11)
C17	4350(8)	6997(3)	3293(2)	27.3(11)
C18	4365(8)	6442(3)	3754(2)	22(1)
C19	7922(8)	5584(3)	6509(2)	23(1)
C20	7238(8)	5477(3)	7615(2)	21.6(10)
C21	5439(10)	6146(3)	7621(2)	30.7(11)
C22	6068(9)	4663(3)	7617(3)	34.4(12)
C23	8976(9)	5565(3)	8143(2)	32.1(12)

Table 2-15. Anisotropic Displacement Parameters ($Å^2 \times 10^3$) for **2.16**. The Anisotropic displacement factor exponent takes the form: $-2\pi^2[h^2a^{*2}U_{11}+2hka^*b^*U_{12}+\ldots]$.

Atom	U_{11}	U_{22}	U_{33}	U_{23}	U_{13}	U_{12}
Br1	38.9(3)	18.0(2)	28.9(2)	-5.8(2)	-0.2(2)	1.1(2)
O1	16.9(16)	23.2(17)	35.1(19)	8.4(14)	-1.1(13)	-3.2(13)
O2	21.1(17)	52(2)	25.7(19)	-10.3(17)	-1.9(14)	7.7(14)
O3	24.0(16)	22.4(17)	17.2(16)	-2.2(13)	-2.0(13)	0.9(13)
C1	17(2)	17(2)	17(2)	1.5(18)	3.5(17)	-0.3(17)
C2	17(2)	14(2)	17(2)	-0.8(18)	1.5(17)	-1.8(17)
C3	35(3)	17(2)	22(2)	-2.9(19)	-3.6(19)	-5.8(19)
C4	23(2)	21(2)	19(2)	-3.5(16)	-5(2)	-1(2)
C5	21(2)	17(2)	20(2)	4.1(16)	2(2)	0(2)
C6	20(2)	11(2)	18(2)	5.9(18)	-0.9(17)	1.4(17)
C7	17(2)	16(2)	20(2)	3.5(18)	2.2(17)	-0.7(16)
C8	23(2)	13(2)	28(3)	5(2)	-2(2)	-8.9(18)
C9	32(3)	12(2)	19(2)	-0.8(17)	-4.8(19)	4.2(18)
C10	17.8(19)	20(2)	18(2)	1.5(19)	-0.8(16)	1.1(19)
C11	18(2)	20(2)	22(2)	3.6(19)	-0.6(17)	-2.9(17)
C12	17(2)	10(2)	23(2)	-2.0(18)	1.9(17)	1.1(16)
C13	15(2)	14(2)	27(3)	2.1(19)	1.6(18)	3.2(17)
C14	21(2)	17(2)	25(2)	0(2)	0.3(17)	0.5(18)
C15	33(2)	12(2)	36(3)	5(2)	-4(2)	-2.2(18)
C16	35(3)	19(2)	36(3)	9(2)	4(2)	6(2)
C17	24(2)	25(3)	32(3)	4(2)	-2.6(19)	7.4(18)
C18	17(2)	18(2)	30(3)	1.3(19)	-0.5(17)	0.6(17)
C19	30(2)	15(2)	24(2)	-6(2)	1(2)	2.2(17)
C20	26(2)	20(2)	18(2)	-1(2)	2.8(19)	-0.5(19)
C21	42(3)	24(2)	26(2)	-3(2)	6(2)	3(2)
C22	41(3)	22(3)	41(3)	0(2)	2(2)	-6(2)
C23	38(3)	43(3)	15(2)	0(2)	-4(2)	-7(2)

Table 2-16. Bond Lengths for **2.16**

Atom	Atom	Length/Å	Atom	Atom	Length/Å
Br1	C9	1.909(4)	C7	C8	1.404(6)
O1	C12	1.213(5)	C8	C9	1.375(6)
O2	C19	1.204(6)	C9	C10	1.389(6)
O3	C19	1.346(6)	C10	C11	1.387(6)
O3	C20	1.483(5)	C12	C13	1.498(6)
C1	C2	1.539(6)	C13	C14	1.396(6)
C1	C5	1.530(6)	C13	C18	1.400(6)
C1	C6	1.509(6)	C14	C15	1.395(6)
C2	C3	1.571(6)	C15	C16	1.375(7)
C2	C12	1.515(6)	C16	C17	1.380(7)
C3	C4	1.545(6)	C17	C18	1.375(6)
C4	C5	1.549(6)	C20	C21	1.512(7)
C4	C19	1.512(6)	C20	C22	1.517(7)
C6	C7	1.390(6)	C20	C23	1.523(7)
C6	C11	1.390(6)			

Table 2-17. Bond Angles for **2.16**

Atom	Atom	Atom	Angle/°	Atom	Atom	Atom	Angle/°
C19	O3	C20	120.8(3)	C10	C11	C6	121.7(4)
C5	C1	C2	103.5(3)	O1	C12	C2	121.0(4)
C6	C1	C2	114.4(4)	O1	C12	C13	119.6(4)
C6	C1	C5	113.8(4)	C13	C12	C2	119.4(4)
C1	C2	C3	104.9(3)	C14	C13	C12	123.4(4)
C12	C2	C1	113.0(3)	C14	C13	C18	118.6(4)
C12	C2	C3	112.6(4)	C18	C13	C12	117.9(4)
C4	C3	C2	106.6(3)	C15	C14	C13	120.4(4)
C3	C4	C5	104.6(3)	C16	C15	C14	119.3(4)
C19	C4	C3	111.0(4)	C15	C16	C17	121.1(5)
C19	C4	C5	108.8(4)	C18	C17	C16	119.9(4)
C1	C5	C4	104.0(3)	C17	C18	C13	120.6(4)
C7	C6	C1	120.4(4)	O2	C19	O3	125.1(4)
C7	C6	C11	118.0(4)	O2	C19	C4	124.1(5)
C11	C6	C1	121.6(4)	O3	C19	C4	110.7(4)
C6	C7	C8	121.6(4)	O3	C20	C21	110.7(4)
C9	C8	C7	118.2(4)	O3	C20	C22	109.5(4)
C8	C9	Br1	119.6(3)	O3	C20	C23	102.1(4)
C8	C9	C10	121.8(4)	C21	C20	C22	112.1(4)
C10	C9	Br1	118.6(3)	C21	C20	C23	110.6(4)
C11	C10	C9	118.7(4)	C22	C20	C23	111.3(4)

Table 2-18. Torsion Angles for **2.16**

A	B	C	D	Angle/°	A	B	C	D	Angle/°
Br1	C9	C10	C11	179.5(3)	C6	C1	C2	C3	-156.6(4)
O1	C12	C13	C14	166.0(4)	C6	C1	C2	C12	80.4(5)
O1	C12	C13	C18	-16.6(6)	C6	C1	C5	C4	166.0(4)
C1	C2	C3	C4	11.3(5)	C6	C7	C8	C9	0.4(6)
C1	C2	C12	O1	18.0(6)	C7	C6	C11	C10	-0.3(6)
C1	C2	C12	C13	-161.0(4)	C7	C8	C9	Br1	-179.7(3)
C1	C6	C7	C8	-179.0(4)	C7	C8	C9	C10	-0.6(6)
C1	C6	C11	C10	178.7(4)	C8	C9	C10	C11	0.4(6)
C2	C1	C5	C4	41.3(4)	C9	C10	C11	C6	0.0(6)
C2	C1	C6	C7	-121.7(4)	C11	C6	C7	C8	0.1(6)
C2	C1	C6	C11	59.3(5)	C12	C2	C3	C4	134.6(4)
C2	C3	C4	C5	13.8(5)	C12	C13	C14	C15	178.2(4)
C2	C3	C4	C19	-103.3(4)	C12	C13	C18	C17	-177.9(4)
C2	C12	C13	C14	-15.0(6)	C13	C14	C15	C16	0.2(7)
C2	C12	C13	C18	162.4(4)	C14	C13	C18	C17	-0.4(7)
C3	C2	C12	O1	-100.6(5)	C14	C15	C16	C17	-1.7(7)
C3	C2	C12	C13	80.3(5)	C15	C16	C17	C18	2.2(7)
C3	C4	C5	C1	-34.0(5)	C16	C17	C18	C13	-1.1(7)
C3	C4	C19	O2	36.4(6)	C18	C13	C14	C15	0.8(7)
C3	C4	C19	O3	-146.3(4)	C19	O3	C20	C21	-55.0(5)
C5	C1	C2	C3	-32.2(4)	C19	O3	C20	C22	69.1(5)
C5	C1	C2	C12	-155.2(3)	C19	O3	C20	C23	-172.8(4)
C5	C1	C6	C7	119.6(4)	C19	C4	C5	C1	84.6(4)
C5	C1	C6	C11	-59.4(5)	C20	O3	C19	O2	0.6(7)
C5	C4	C19	O2	-78.1(5)	C20	O3	C19	C4	-176.7(3)
C5	C4	C19	O3	99.2(4)					

Table 2-19. Hydrogen Atom Coordinates ($Å \times 10^4$) and Isotropic Displacement Parameters ($Å^2 \times 10^3$) for **2.16**

Atom	x	y	z	U(eq)
H1	6756	4650	5463	20
H2	9820	5513	4653	19
H3A	10518	6462	5357	29
H3B	7807	6463	5587	29
H4	11400	5801	6224	25
H5A	11837	4684	5609	24
H5B	9930	4345	6092	24
H7	5526	3480	5009	21
H8	6039	2375	4360	26
H10	12558	3211	3898	22
H11	11996	4305	4541	24
H14	9510	6887	4349	25
H15	9451	7837	3563	33
H16	6178	7917	2922	36
H17	3054	7020	3016	33
H18	3061	6087	3798	26
H21A	6253	6656	7562	46
H21B	4608	6150	8014	46
H21C	4289	6065	7291	46
H22A	5276	4577	8009	52
H22B	7277	4250	7555	52
H22C	4896	4635	7287	52
H23A	8112	5529	8530	48
H23B	9771	6083	8116	48
H23C	10162	5138	8123	48

2.6: References and Notes

[1] Walsh, P. J.; Kozlowski, M. C. *Fundamentals of Asymmetric Catalysis*; Murdzek, J. Eds.; University Science Books: Sausalio, CA, 2009.

[2] Ojima, I. *Catalytic Asymmetric Synthesis*; Wiley: Hoboken, NJ, 2010.

[3] Gawley, R. E.; Aube, J. *Principles of Asymmetric Synthesis, 2nd Ed.*; Elsevier: Oxford, UK, 2012.

[4] Inoue, Y. Asymmetric Photochemical Reactions in Solution. *Chem. Rev.*, **1992**, *92*, 741–770.

[5] Brimioulle, R.; Lenhart, D.; Maturi, M. M.; Bach, T. Enantioselective Catalysis of Photochemical Reactions. *Angew. Chem. Int. Ed.*, **2015**, *54*, 3872–3890.

[6] Müller, C.; Bauer, A.; Bach, T. Light-Driven Enantioselective Organocatalysis. *Angew. Chem. Int. Ed.*, **2009**, *48*, 6640–6642.

[7] Müller, C.; Bauer, A.; Maturi, M. M.; Cuquerella, M. C.; Miranda, M. A.; Bach, T. Enantioselective Intramolecular [2 + 2]-Photocycloaddition Reactions of 4-Substituted Quinolones Catalyzed by a Chiral Sensitizer with a Hydrogen-Bonding Motif. *J. Am. Chem. Soc.*, **2011**, *133*, 16689–16697.

[8] Maturi, M. M.; Wenninger, M.; Alonso, R.; Bauer, A.; Pöthig, A.; Riedle, E.; Bach, T. Intramolecular [2+2] Photocycloaddition of 3- and 4-(But-3-enyl)oxyquinolones: Influence of the Alkene Substitution Pattern, Photophysical Studies, and Enantioselective Catalysis by a Chiral Sensitizer. *Chem. Eur. J.* **2013**, *19*, 7461–7472.

[9] Alonso, R.; Bach, T. A Chiral Thioxanthone as an Organocatalyst for Enantioselective [2+2] Photocycloaddition Reactions Induced by Visible Light. *Angew. Chem. Int. Ed.* **2014**, *53*, 4368–4371.

[10] Vallavoju, N.; Selvakumar, S.; Jockusch, S.; Sibi, M. P.; Sivaguru, J. Enantioselective Organo-Photocatalysis Mediated by Atropisomeric Thiourea Derivatives. *Angew. Chem. Int. Ed.* **2014**, *53*, 5604–5608.

[11] Vallavoju, N.; Selvakumar, S.; Jockusch, S.; Prabhakaran, M. J.; Sibi, M. P.; Sivaguru, J. Evaluating Thiourea Architecture for Intramolecular [2+2] Photocycloaddition of 4-Alkenylcoumarins. *Adv. Synth. Catal.* **2014**, *356*, 2763–2768.

[12] Guo, H.; Herdtweck, E.; Bach, T. Enantioselective Lewis Acid Catalysis in Intramolecular [2+2] Photocycloaddition Reactions of Coumarins. *Angew. Chem. Int. Ed.* **2010**, *49*, 7782–7785.

[13] Brimoulle, R.; Guo, H.; Bach, T. Enantioselective Intramolecular [2+2] Photocycloaddition Reactions of 4-Substituted Coumarins Catalyzed by a Chiral Lewis Acid. *Chem. Eur. J.* **2012**, *18*, 7552–7560.

[14] Brimoulle, R.; Bach, T. Enantioselective Lewis Acid Catalysis of Intramolecular Enone [2+2] Photocycloaddition Reactions. *Science* **2013**, *342*, 840–843.

[15] Brimoulle, R.; Bach, T. [2+2] Photocycloaddition of 3-Alkenyloxy-2-cycloalkenones: Enantioselective Lewis Aicd Catalysis and Ring Expansion. *Angew. Chem. Int. Ed.* **2014**, *53*, 12921–12924.

[16] Blum, T.R.; Miller, Z. D.; Bates, D. M.; Guzei, I. A.; Yoon, T. P. Enantioselective Photochemistry through Lewis Acid-Catalyzed Triplet Energy Transfer. *Science* **2016**, *354*, 1391–1395.

[17] Daub, M. E.; Jung. H.; Lee, B. J.; Won, J.; Baik, M.-H.; Yoon, T. P. Enantioselective [2+2] Cycloadditions of Cinnamate Esters: Generalizing Lewis Acid Catalysis of Triplet Energy Transfer. *J. Am. Chem. Soc.* **2019**, *141*, 9543–9547.

[18] Huang, X.; Quinn, T.R.; Harms, K.; Webster, R. D.; Zhang, L.; Wiest, O.; Meggers, E. Direct Visible-Light-Excited Asymmetric Lewis Acid Catalysis of Intermolecular [2+2] Photocycloadditions. *J. Am. Chem. Soc.* **2017**, *139*, 9120–9123.

[19] Hu, N.; Jung, H.; Zheng, Y.; Lee, J.; Zhang, L.; Ullah, Z.; Xie, X.; Harms, K.; Baik, M.-H.; Meggers, E. Catalytic Asymmetric Dearomatization by Visible-Light-Activated [2+2] Photocycloaddition. *Angew. Chem. Int. Ed.* **2018**, *57*, 6242–6246.

[20] Du, J.; Skubi, K. L.; Schulz, D. M.; Yoon, T. P. A Dual-Catalysis Approach to Enantioselective [2+2] Photocycloadditions Using Visible Light. *Science* **2014**, *344*, 392–396.

[21] Prier, C. K. Rankic, D. A.; MacMillan, D. W. C. Visible Light Photoredox Catalysis with Transition Metal Complexes: Applications in Organic Synthesis. *Chem. Rev.* **2013**, *113*, 5322–5363.

[22] Espelt, L. R.; McPherson, I. S.; Wiensch, E. M.; Yoon, T. P. Enantioselective Conjugate Additions of α-Amino Radicals via Cooperative Photoredox and Lewis Acid Catalysis. *J. Am. Chem. Soc.* **2015**, *137*, 2452–2455.

[23] Hopkinson, M. N.; Sahoo, B.; Li, J.-L.; Glorius, F. Dual Catalysis Sees the Light: Combining Photoredox with Organo-, Acid, and Transition-Metal Catalysis. *Chem. Eur. J.* **2014**, *20*, 3874–3886.

[24] Lu, Z.; Shen, M.; Yoon, T. P. [3+2] Cycloadditions of Aryl Cyclopropyl Ketones by Visible Light Photocatalysis. *J. Am. Chem. Soc.* **2011**, *133*, 1162-1164.

[25] Parsons, A. T.; Johnson, J. S. Catalytic Enantioselective Synthesis of Tetrahydrofurans: A Dynamic Kinetic Asymmetric [3 + 2] Cycloaddition of Racemic Cyclopropanes and Aldehydes. *J. Am. Chem. Soc.* **2009**, *131*, 3122–3123.

[26] Parsons, A. T.; Smith, A. G.; Neel, A. J.; Johnson, J. S. Dynamic Kinetic Asymmetric Synthesis of Substituted Pyrrolidines from Racemic Cyclopropanes and Aldimines: Reaction Development and Mechanistic Insights. *J. Am. Chem. Soc.* **2010**, *132*, 9688–9692.

[27] Trost, B. M.; Morris, P. J. Palladium-Catalyzed Diastereo- and Enantioselective Synthesis of Substituted Cyclopentanes through a Dynamic Kinetic Asymmetric Formal [3+2]-Cycloaddition of Vinyl Cyclopropanes and Alkylidene Azlactones. *Angew. Chem. Int. Ed.* **2011**, *50*, 6167–6170.

[28] Xiong, H.; Xu, H.; Liao, S.; Xie, Z.; Tang, Y. Copper-Catalyzed Highly Enantioselective Cyclopentannulation of Indoles with Donor–Acceptor Cyclopropanes. *J. Am. Chem. Soc*. **2013**, *135*, 7851–7853.

[29] Hashimoto, T.; Kawamata, Y.; Maruoka, K. An Organic Thiyl Radical Catalyst for Enantioselective Cyclization. *Nat. Chem.* **2014**, *6*, 702–705.

[30] Amador, A. G.; Sherbrook, E. M.; Lu, Z.; Yoon. T. P. A General Protocol for Radical Anion [3+2] Cycloaddition Enanabled by Tandem Lewis Acid Photoredox Catalysis. *Synthesis* **2018**, *50*, 539–547.

[31] Evans, D. A.; Wu, J. Enantioselective Rare-Earth Catalyzed Quinone Diels−Alder Reactions. *J. Am. Chem. Soc.* **2003**, *125*, 10162–10163.

[32] Evans, D. A.; Song, H.-J.; Fandrick, K. R. Enantioselective Nitrone Cycloadditions of α,β-Unsaturated 2-Acyl Imidazoles Catalyzed by Bis(oxazolinyl)pyridine−Cerium(IV) Triflate Complexes. *Org. Lett.* **2006**, *8*, 3351–3354.

[33] Suga, H.; Ishimoto, D.; Higuchi, S.; Ohtsuka, M.; Arikawa, T.; Tsuchida, T.; Kakehi, A.; Baba, T. Dipole-LUMO/Dipolarophile-HOMO Controlled Asymmetric Cycloadditions of Carbonyl Ylides Catalyzed by Chiral Lewis Acids. *Org. Lett.* **2007**, *9*, 4359–4362.

[34] Suga, H.; Higuchi, S.; Ohtsuka, M.; Ishimoto, D.; Arikawa, T.; Hashimoto, Y.; Misawa, S.; Tsuchida, T.; Kakehi, A.; Baba, T. Inverse Electron Demand Asymmetric Cycloadditions of Cyclic Carbonyl Ylides Catalyzed by Chiral Lewis Acids—Scope and Limitations of Diazo and Olefinic Substrates. *Tetrahedron* **2010**, *66*, 3070–3089.

[35] The absolute configuration of **2.16** was determined by X-ray crystallographic analysis; the configuration of other cycloadducts were assigned by analogy.

[36] Tanko, J. M.; Drumright, R. E. Radical Ion Probes. 2. Evidence for the Reversible Ring Opening of Arylcyclopropylketyl Anions. Implications for Mechanistic Studies. *J. Am. Chem. Soc.* **1992**, *114*, 1844–1854.

[37] Pangborn, A. B.; Giardello, M. A.; Grubbs, R. H.; Rosen, R. K.; Timmers, F. J. Safe and Convenient Procedure for Solvent Purification. *Organometallics*, **1996**, *15*, 1518–1520.

[38] Cornejo, A.; Fraile, J. M.; Garcia, J. I.; Gil, M. J.; Martinez-Merino, V.; Mayoral, J. A.; Pires, E.; Villalba, I. An Efficient and General One-Pot Method for the Synthesis of Chiral Bis(oxazoline) and Pyridine Bis(oxazoline) Ligands. *Synlett*, **2005**, *15*, 2321–2324.

[39] Mitsui, K.; Parquette, J. R. Convenient Multigram Synthesis of 4-Chloropyridine-2,6-dicarbonyl -Dichloride. *Synthesis*, **2009**, *5*, 713–714.

[40] Yu, X.; Yang, Y.; Wang, S.; Xu, H.; Gong, H. Nickel-Catalyzed Reductive Cross-Coupling of Unactivated Alkyl Halides. *Org. Lett.* **2011,** *13*, 2138–2141.

[41] Tse, M. K.; Bhor, S.; Klawonn, M.; Anilkumar, G.; Jiao, H.; Doebler, C.; Spannenberg, A.; Maegerlein, W.; Hugl, H.; Beller, M. Ruthenium-Catalyzed Asymmetric Epoxidation of Olefins Using H2O2, Part I: Synthesis of New Chiral N,N,N-Tridentate Pybox and Pyboxazine Ligands and Their Ruthenium Complexes. *Chem. Eur. J.* **2006**, *12*, 1855–1874.

[42] McAllister, G. D.; Oswald, M. F.; Paxton, R. J.; Raw, S. A.; Taylor, R. J. K. The Direct Preparation of Functionalised Cyclopropanes from Allylic Alcohols or α-Hydroxyketones Using Tandem Oxidation Processes. *Tetrahedron*, **2006**, *62*, 6681–6694.

[43] Papageorgiou, C.D.; Ley, S. V.; Gaunt, M. J. Organic-Catalyst-Mediated Cyclopropanation Reaction. *Angew. Chem. Int. Ed.* **2003**, *42*, 828–831.

[44] Liwosz, T. W.; Chemler, S. R. Copper-Catalyzed Oxidative Amination and Allylic Amination of Alkenes. *Chem. Eur. J.* **2013**, *19*, 12771–12777.

[45] Casalnuovo, A. L.; RajanBabu, T. V.; Ayers, T. A.; Warren. T. H. Ligand Electronic Effects in Asymmetric Catalysis: Enhanced Enantioselectivity in the Asymmetric Hydrocyanation of Vinylarenes. *J. Am. Chem. Soc.* **1994**, *116*, 9869–9882.

[46] Pirtsch, M.; Paria, S.; Matsuno, T.; Isobe, H.; Reiser, O. [Cu(dap)2Cl] As an Efficient Visible-Light-Driven Photoredox Catalyst in Carbon–Carbon Bond-Forming Reactions. *Chem. Eur. J.* **2012**, *18*, 7336–7340.

[47] Wessig, P.; Mühling, O. Photochemical Synthesis of Highly Functionalized Cyclopropyl Ketones. *Helv. Chim. Act.* **2003**. *86*, 865–893.

[48] House, H. O.; Prabhu, A. V.l.; Wilkins, J. M.; Lee, L. F. Reactions Involving Electron Transfer. 9. Reaction of Lithium Dimethylcuprate with Alkyl Aryl Ketones. *J. Org. Chem.* **1976**, *41*, 3067–3076.

[49] Chien, C.; Kawasaki, T.; Sakamoto, M.; Tamura, Y.; Kita, Y. Stereospecific Epoxidation of *cis*-2-Butene-1,4-diones to *cis*-2,3-Epoxybutane-1,4-diones with Oxodiperoxomolybdenum (VI), $MoO_5 \cdot H_2O \cdot$HMPA. *Chem. and Pharm. Bull.* **1985**, *7*, 2743–2749.

[50] Asada, M.; Obitsu, T.; Nagase, T.; Tanaka, M.; Yamaura, Y.; Takizawa, H.; Yoshikawa, K.; Sato, K.; Narita, M.; Ohuchida, S.; Nakai, H.; Toda, M. 3-(2-Aminocarbonylphenyl)propanoic Acid Analogs as Potent and Selective EP3 Receptor Antagonists. Part 1: Discovery and Exploration of the Carboxyamide Side Chain. *Bioorg. and Med. Chem.* **2010,** *18*, 80–90.

[51] Inaba, S.; Rieke, R. D. Metallic Nickel-Mediated Synthesis of Ketones by the Reaction of Benzylic, Allylic, Vinylic, and Pentafluorophenyl Halides with Acid Halides. *J. Org. Chem.* **1984**, *50*, 1373–1381.

[52] Okamoto, K.; Hayashi, T. Platinum-Catalyzed Addition of Dimethylsilylene to β-Methyl α,β-Unsaturated Ketones: γ-Silylation Forming 1-Oxa-2-silacyclohex-5-enes. *Org. Lett.* **2007**, *9*, 5067–5069.

[53] Augustine, R. L; Pinto, F. G. Further Aspects of the Assisted Thermal Decompostion of Mixed Carbonic Anhydrides. *J. Org. Chem.* **1968**, *33*, 1877–1884.

[54] Yasuda, M.; Chiba, K.; Ohigashi, N.; Katoh, Y.; Baba, A. Michael Addition of Stannyl Ketone Enolate to α,β-Unsaturated Esters Catalyzed by Tetrabutylammonium Bromide and an ab Initio Theoretical Study of the Reaction Course. *J. Am. Chem. Soc.* **2003**, *125*, 7291–7300.

[55] Bruker-AXS (2015). *APEX3.* Version 2015.9-0. Madison, Wisconsin, USA.

[56] Krause, L.; Herbst-Irmer, R.; Sheldrick, G. M.; Stalke, D. Comparison of Silver and Molybdenum Microfocus X-ray Sources for Single-Crystal Structure Determination. *J. Appl. Cryst.* **2015**, *48*, 3–10.

[57] Sheldrick, G. M. (2013b). *XPREP*. Version 2013/1. Georg-August-Universität Göttingen, Göttingen, Germany.

[58] Sheldrick, G. M. (2013a). The *SHELX* homepage, http://shelx.uni-ac.gwdg.de/SHELX/.

[59] Sheldrick, G. M. SHELXT – Integrated Space-Group and Crystal-Structure Determination. *Acta Cryst. A* **2015**, *71*, 3–8.

[60] Sheldrick, G. M. Crystal structure refinement with SHELXL. *Acta Cryst. C* **2015**, *71*, 3–8.

[61] Dolomanov, O. V.; Bourhis, L. J.; Gildea, R. J.; Howard, J. A. K.; Puschmann, H. OLEX2: A Complete Structure Solution, Refinement and Analysis Program. *J. Appl. Crystallogr.* **2009**, 42, 339–341.

[62] Guzei, I. A. (2007-2013). Programs *Gn*. University of Wisconsin-Madison, Madison, Wisconsin, USA.

Chapter 3. Brønsted Acid Catalysis of Triplet Energy Transfer in [2+2] Photocycloadditions

3.1: Introduction

3.1.1 Photochemical Synthesis with Visible Light

In the last two decades, there has been substantial renewed interest in the synthetic potential of visible light photochemistry.[1,2] This resurgence has largely focused on transformations enabled by photoredox catalysis,[3–7] in which well-studied substiochiometric organometallic chromophores[8–10] such as $Ru(bpy)_3^{2+}$ undergo photoinduced single-electron transfer events with variety of organic functional groups (see Chapter 2). In these *secondary photoprocesses*, the ability to generate and manipulate the reactivity of ground-state radical intermediates has been exceedingly varied and fruitful in its use in organic synthesis.

As a more challenging objective, *primary photoprocesses* that generate and engage excited-state intermediates in a selective manner have been comparatively underdeveloped. While the quenching of $Ru(bpy)_3^{2+}$ by organic compounds to generate their corresponding triplet states is well documented,[11] the characteristically short lifetimes of excited states has resulted in molecular activation by energy transfer being poorly represented in organic synthesis, particularly among carbon-carbon bond forming reactions.[12,13] This discrepancy has synthetic relevance. While photoredox catalysis is a convenient means of accessing open-shell odd-electron intermediates, there exist many non-photochemical methods of initiating radical reactions.[14] In contrast, the chemistry of excited-state organic molecules is uniquely available through photochemical activation. Furthermore, intermediates generated through energy transfer are not subject to the same electrochemical constraints as those generated through electron transfer. Energy transfer may facilitate the activation of substrates for which redox manipulation has proven difficult. Therefore, the development of synthetic reactions which facilitate the generation and manipulation of these intermediates has the potential to be highly enabling.

3.1.2: Lewis Acid-Catalyzed Photosensitization

The influence of Lewis acids on the reactivity of excited-state organic molecules has long been the subject of investigation. In 1910, Praetorius and Korn first observed that while dibenzylideneacetone typically "becomes resinous" (polymerizes) when subjected to irradiation by sunlight, it instead undergoes smooth head-to-tail dimerization under similar conditions in the presence of UO_2Cl_2. In 1925, Stobbe and Färber replicated this observation using $SnCl_4$. More recently, studies by Lewis and coworkers established that photoreactions of coumarins and cinnamate esters can be dramatically influenced by strong oxophilic Lewis acids, resulting in both increased reaction efficiencies and drastically altered product distributions.[15,16] These stark changes in rate and outcome exemplify why the modulation of excited-state photoreactions with simple catalysts are growing in appeal within synthetic photochemistry.

Lewis acids are also appealing because they have the potential to render photochemical reactions stereoselective. Several contemporary synthetic researchers, including Bach[17–21] and Meggers,[22,23] have developed highly enantioselective photoreactions that use Lewis acid catalysts to control the reaction dynamics of excited-state conjugated carbonyl compounds. Much of this work relies on the concept of *chromophore activation*, in which coordination of Lewis acid to a carbonyl compound results in a bathochromatic shift in its absorption spectrum, allowing for selective irradiation of the Lewis acid-bound complex.[24]

Scheme 3-1. The effect of Lewis acids on the triplet excited-state of chalcones

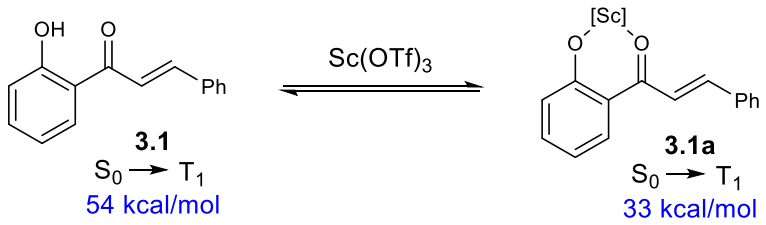

Our group has recently demonstrated that Lewis acids can also catalyze excited-state photoreactions by increasing the rate of Dexter energy transfer between an appropriate triplet sensitizer and an enone substrate (Scheme 3-1).[25,26] In this example, the effect is a result of a decrease in the energy of the triplet state of chalcone **3.1** upon binding to a chiral $Sc(OTf)_3$-pybox complex. This in turn enables efficient energy transfer from a photosensitizer, enabling a high-yielding, enantioselective intermolecular [2+2] photocycloaddition of chalcones with diene and styrene coupling partners. Recent studies of methyl cinnamate-styrene cycloadditions indicate that the lowering of the absolute energies of the frontier molecular orbitals (i.e., an increase in orbital overlap) is another role that Lewis acids may play in enone sensitization.[27] From these studies, we propose that the impact of Lewis acids on triplet sensitization reactions may therefore be quite general and applicable to the design of a range of synthetically useful excited-state photoreactions.

3.1.3: Brønsted Acid-Catalyzed Photosensitization

Consequently, we were curious if there might be a similarly general effect of protic acids on triplet sensitization processes. The impact of Brønsted acids on the structure and reactivity of organic compounds can be analogous to that of Lewis acid catalysts, but comparatively little is known about the influence of Brønsted acids on the outcome of excited-state organic photoreactions.[24,28,29] In analogy to the effect of Lewis acid catalysis, the protonation of α,β-unsaturated carbonyl compounds has been determined to produce a bathochromatic shift in their absorption spectra; Zalewski and Dale reported that the absorption of benzaldehyde, crotonaldehyde, and cyclopentenone each exhibited a significant red-shift upon addition of sulfuric acid.[30,31] Subsequently, the effect of Brønsted acids on photochemical *E*/*Z* isomerizations[32–34] and rearrangements[35] of α,β-unsaturated

carbonyls was investigated in detail. Sibi and Siviguru have recently reported an enantioselective intramolecular [2+2] cycloaddition of coumarins using chiral thioureas as hydrogen-bonding photocatalysts,[36,37] and Beeler has reported that bis(thiourea) catalysts can accelerate and alter the diastereoselecitivity of the [2+2] photodimerization of cinnamate esters.[38]

In 1971, Leermakers reported that Brønsted acids could alter the energy of a carbonyl compound's triplet excited state. The phosphorescence of benzophenone **3.2** was observed to be significantly red-shifted in strongly acidic media compared to non-polar solvents, with a concomitant 200-fold increase in its excited state lifetime (Scheme 3-2).[39] This suggested to us that Brønsted acids might catalyze triplet energy transfer processes from transition metal photosensitizers in a fashion similar to Lewis acids; however, to the best of our knowledge, these observations have never been leveraged for a synthetic purpose. This finding could significantly broaden the diversity of binding interactions and co-catalyst structures that could be exploited to modulate the reactivity of excited-state organic compounds. In this chapter, we describe the first example of an organic photoreaction enabled by Brønsted acid catalyzed triplet energy transfer. Moreover, an in-depth computational analysis of this reaction reveals the importance of acid-catalyzed optimization of the excited-state geometry for vertical Dexter energy transfer.

Scheme 3-2. The effects of Brønsted acids on the triplet excited-state of benzophenone

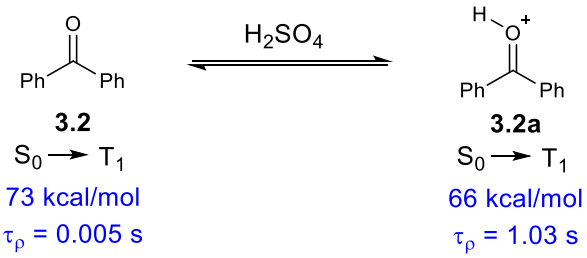

3.2 Results and Discussion

3.2.1: Reaction Design

The first objective in the development of this acid-catalyzed system was the selection of a substrate that undergoes a substantial reactivity change in an intermolecular [2+2] cycloaddition *uniquely upon inclusion of a Brønsted acid*. We proposed a general reaction design (Scheme 3-3), in which basic substrates (**3.3** or **3.6)** would be protonated by catalytic quantities of a protic acid, H–A. Subsequently, protonated intermediates (**3.4** or **3.7)** would undergo a rapid energy transfer event with an excited-state photocatalyst (PC) to give the respective triplet-state intermediates (**3.5** or **3.8)**. Lastly, these excited-state species would undergo a cycloaddition reaction with another alkene to generate product and regenerate H–A. Importantly, we sought a substrate that *does not undergo the corresponding cycloadditions in its unprotonated form.*

Scheme 3-3. Design of a Brønsted acid-catalyzed intermolecular [2+2] cycloaddition

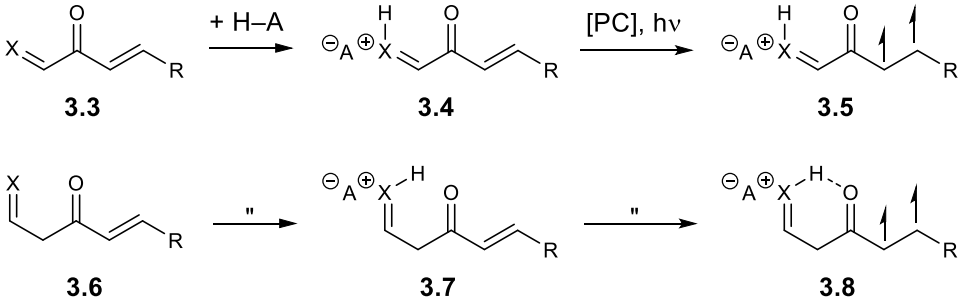

3.2.1 Preliminary Reaction Development

Several α,β-unsaturated carbonyls tethered to basic functional groups were synthesized to test this design in an intermolecular [2+2] cycloaddition with styrene, using $Ru(bpy)_3^{2+}$ as the photosensitizer (Table 3-1). Substrates were chosen on the speculation that adjacency of a basic

unit to an enone moiety would exert a significant influence on the electronic structure of the substrate's excited state. Oxazolidinone **3.9** and pyrazole **3.10** gave negligible yields under both standard and acidic reaction conditions. While oxazole **3.11** returns significant amounts of product under both conditions, the comparable yields suggest the reaction is not significantly accelerated by acid. Gratifyingly, cinnamoyl imidazole **3.12**, the most basic of the chosen substrates, was significantly activated toward the desired cycloaddition *under acidic conditions.* While **3.12** is not perfectly selective for product generation under acidic conditions alone, the significant enhancement in yield was sufficient for further exploration of this acid-catalyzed intermolecular [2+2] cycloaddition.

Table 3-1. Preliminary investigations for a Bronsted acid-catalyzed [2+2] cycloaddition

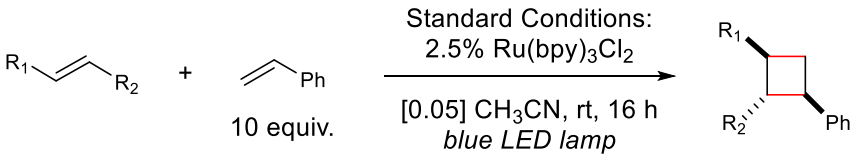

Substrate	**Structure**	**% Yield**	**% Yield** (+ 20 mol% *p*-TsOH)
3.9	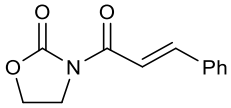	0	0
3.10	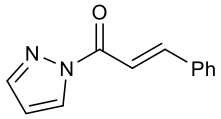	2	4
3.11	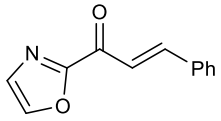	57	73
3.12	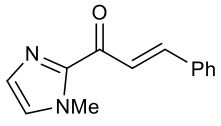	**11**	**75**

A series of additional experiments designed to establish the roles of both the Brønsted acid and the photocatalyst in the cycloaddition of **3.12** and styrene are outlined below (Table 3-2). Entry **1** is direct recapitulation of the results previously indicated for this photocycloaddition under standard conditions in the absence of acid (Table 3-1). In comparison, entries **2-5** demonstrate that a series of acids of increasing acidity gradually increase reaction yield of **3.13** from 17% (using acetic acid) up through 75% (using *p*-TsOH), in which no remaining starting material is observed. This correlation between pKa and reaction conversion supports the premise that this reaction is acid catalyzed. Furthermore, entries **6** and **7** indicate that the reaction does require a photosensitizer to proceed efficiently and that the reaction is a result of acid catalysis alone. Together these results reveal a synergistic effect arising from the combination of both a photosensitizer and a strong Brønsted acid co-catalyst in this photocycloaddition.

Table 3-2. Experimental analysis for the photosensitized [2+2] cycloaddition of 3.12 and styrene

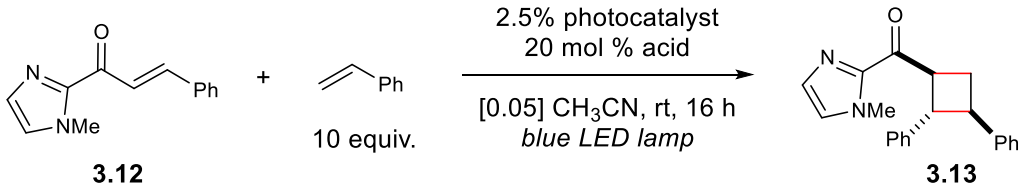

Entry	Photocatalyst	Acid (pKa)	% Yield [d.r.]
1	$Ru(bpy)_3Cl_2$	none	11 [2:1]
2	$Ru(bpy)_3Cl_2$	CH_3CO_2H (23.5)	17 [2:1]
3	$Ru(bpy)_3Cl_2$	$ClCH_2CO_2H$ (18.8)	28 [2:1]
4	$Ru(bpy)_3Cl_2$	CF_3CO_2H (12.6)	68 [2:1]
5	$Ru(bpy)_3Cl_2$	*p*-TsOH (2.6)	75 [2:1]
6	none	none	0
7	none	*p*-TsOH (2.6)	trace

3.2.3 Reaction Scope and Product Derivatization

Experiments probing the generality of this Brønsted acid-catalyzed cycloaddition are summarized below (Table 3-3). Variations of the structure of imidazoyl enone **3.12** were investigated first. A variety of electron-rich and electron-deficient aryl olefins (**3.13-3.18)** all demonstrated good reactivity. Thiophene-substituted enone **3.19** demonstrates a modest tolerance for hetereocycles, provided they are not so basic that they compete with imidazole for protonation. Consistent with having a less-conjugated π system, *C*-crotonoyl imidazoles (~58 kcal/mol) have a significantly higher triplet energy than *C*-cinnamoyl imidazoles (~48 kcal/mol), and therefore generate none of the cycloadduct **3.20**. While we observe E/Z isomerization of trisubstituted olefins **3.21** and **3.22**, indicative of their photosensitization, none of the corresponding products are observed. This suggests that although the organic triplets are being efficiently formed, the increased steric bulk of the enone is likely making decay to the ground state a competitive process.

Table 3-3. Substrate scope studies for the imidazoyl enone

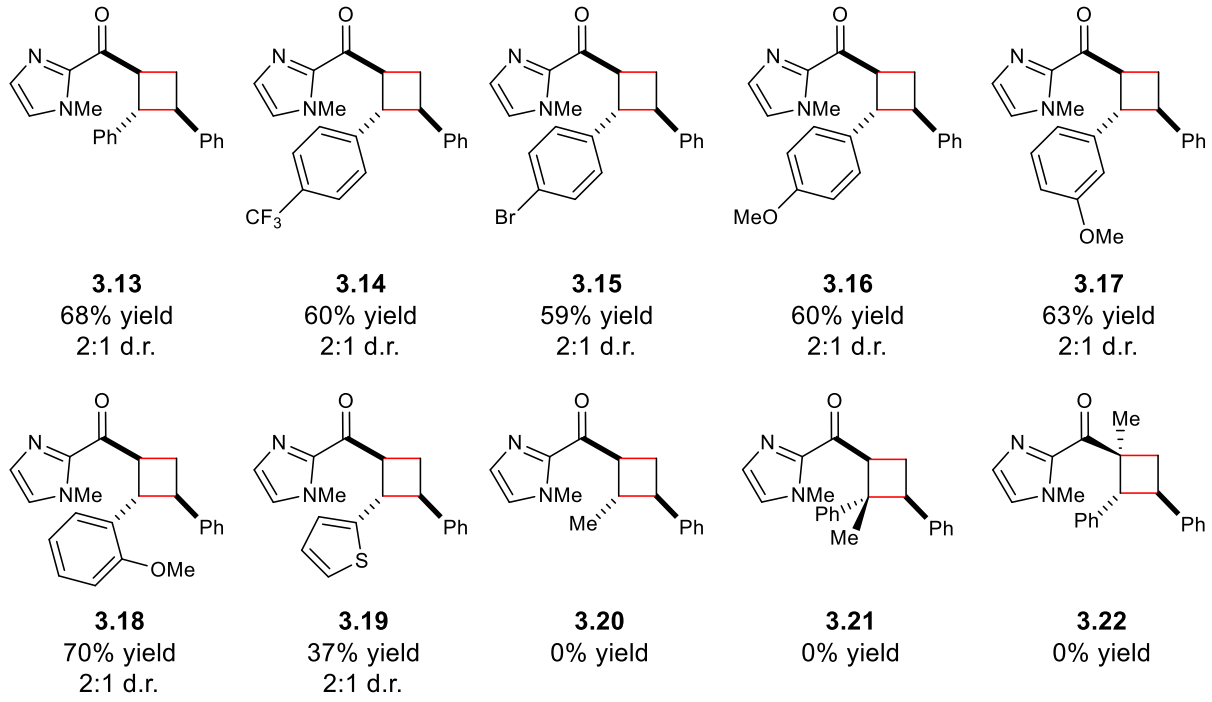

3.13	**3.14**	**3.15**	**3.16**	**3.17**
68% yield	60% yield	59% yield	60% yield	63% yield
2:1 d.r.	2:1 d.r.	2:1 d.r.	2:1 d.r.	2:1 d.r.

3.18	**3.19**	**3.20**	**3.21**	**3.22**
70% yield	37% yield	0% yield	0% yield	0% yield
2:1 d.r.	2:1 d.r.			

The alkene component in this transformation reacts from its ground state, and the scope with respect to this component is somewhat broader (Table 3-4). A range of aromatic acceptors including electron-deficient (**3.23**), electron-rich (**3.24**), sterically hindered (**3.25**), and 1,1-disubstututed styrenes (**3.26**) were all well tolerated under these conditions. Gratifyingly, this scope is not limited to styrenes: electron-rich aliphatic alkenes such as methylenecyclopentane give modest yields of an unusual spirocyclic cyclobutane (**3.27**). Both 2,3-dimethylbutadiene (**3.28**) and phenyl vinyl sulfide (**3.29**) undergo the indicated cycloaddition in high yield, further expanding the classes of cyclobutane product that are available using this method. Unfortunately, highly electron-rich olefins such as ethyl vinyl ether give none of the corresponding product (**3.30**) due to polymerization under acidic conditions. Finally, although *trans*-β-methylstyrene failed to return the desired cycloadduct (**3.31**), indene provided a reasonable yield of the cyclobutane product (**3.32**).

Table 3-4. Substrate scope studies for the alkene coupling partner

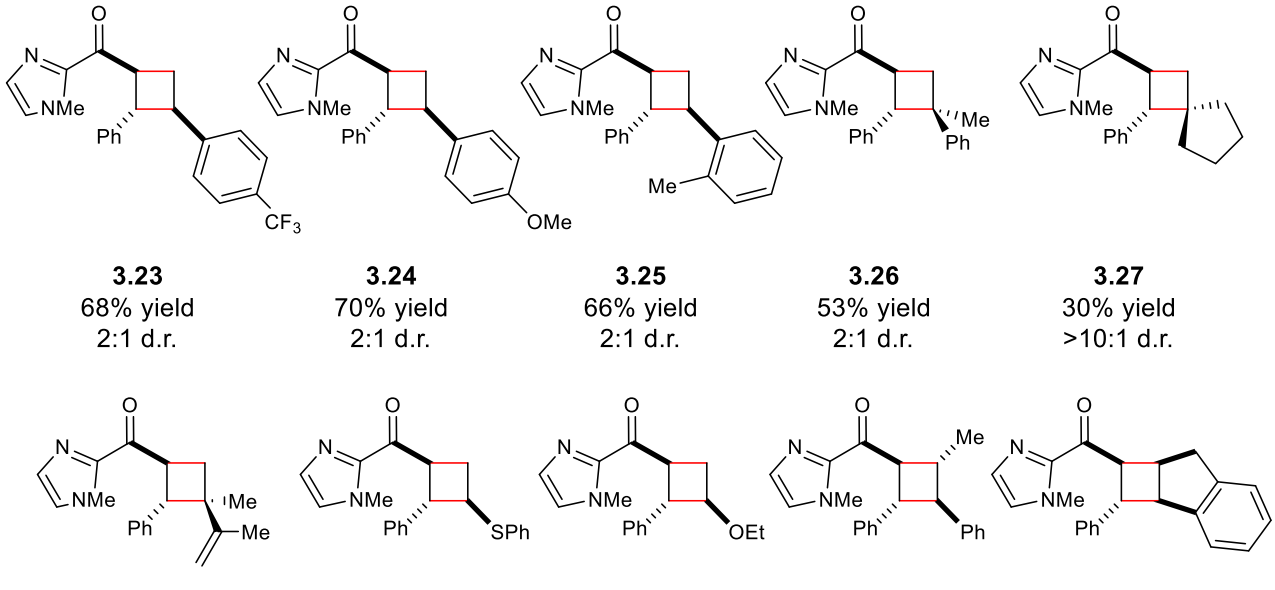

3.23	**3.24**	**3.25**	**3.26**	**3.27**
68% yield	70% yield	66% yield	53% yield	30% yield
2:1 d.r.	2:1 d.r.	2:1 d.r.	2:1 d.r.	>10:1 d.r.

3.28	**3.29**	**3.30**	**3.31**	**3.32**
66% yield	37% yield	0% yield	0% yield	62% yield
7:1 d.r.	1.5:1 d.r.			1:1 d.r.

One reason that *C*-acyl imidazoles make attractive substrates for this study is the ease with which the moieties are cleaved under fairly mild conditions.[40–42] This entails alkylation of the imidazoyl nitrogen, followed by displacement of *N*-heterocyclic carbene leaving group by a variety of nucleophiles. An operationally convenient one-pot protocol allows for rapid cleavage of the imidazoyl group to generate good yields of several cyclobutyl carboxylic esters (**3.33-3.34**) and amides (**3.35-3.36**) from several structurally varied alcohols and amines (Scheme 3-4).

Scheme 3-4. Cleavage of imidazoyl cycloadducts by acyl substitution

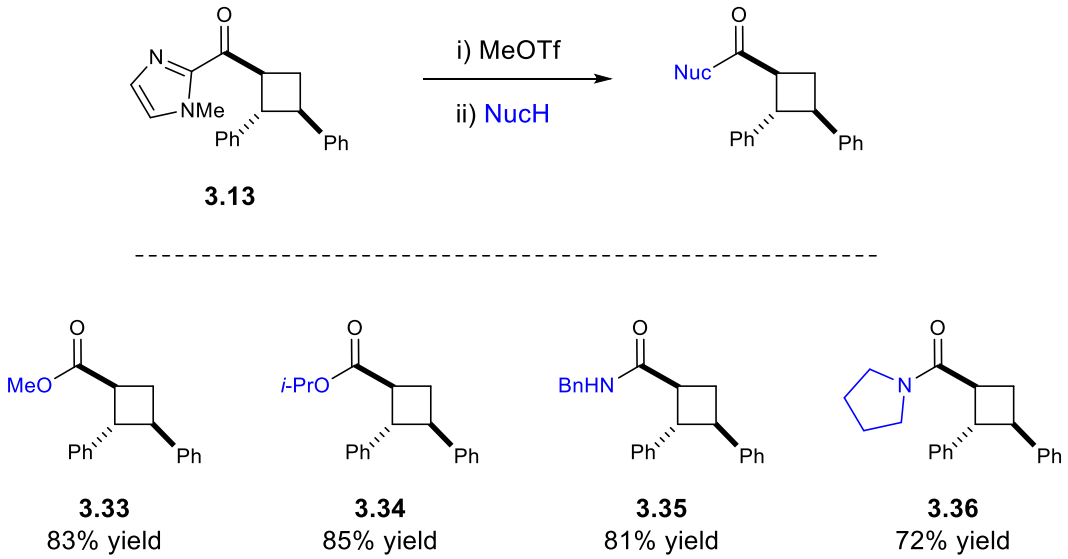

3.13

3.33 83% yield

3.34 85% yield

3.35 81% yield

3.36 72% yield

3.2.4 Experimental Evidence for Triplet Energy Transfer

To support the hypothesis that the acid co-catalyst drastically accelerates substrate photosensitization, we conducted a series of Stern–Volmer luminescence quenching experiments (Figure 3-1). First, these studies indicate that the phosphorescence of $Ru^*(bpy)_3^{2+}$ is unimpacted by the addition of *p*-TsOH. The photocatalyst it is only modestly quenched in the presence of the cinnamoyl imidazole **3.12**, which is consistent with the slow rate of background

photocycloaddition observed in the absence of acid. However, quenching is significantly increased upon the addition of *p*-TsOH together with **3.12**. An analysis of these Stern–Volmer plots indicates that the rate constant for quenching of $Ru^*(bpy)_3^{2+}$ by **3.12** increases by an order of magnitude in the presence of one equivalent of *p*-TsOH (1.2×10^6 M^{-1} sec^{-1} to 1.2×10^7 M^{-1} sec^{-1}). These data establish that the Brønsted acid co-catalyst has a significant effect on the rate of the key photocatalytic activation step.

Figure 3-1. Stern-Volmer luminescence quenching experiments

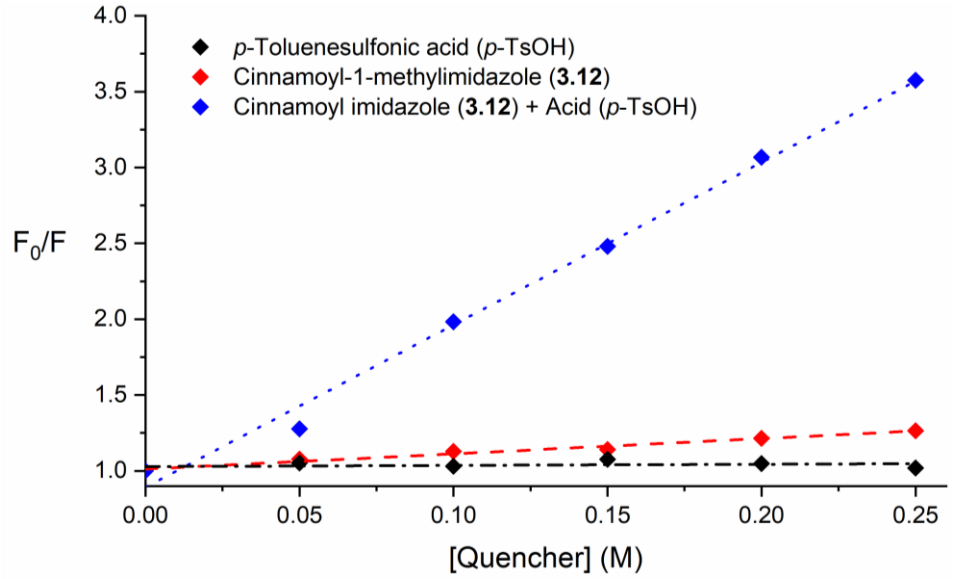

To investigate if the key photoinitiation step in this transformation involves electron-transfer (photoredox catalysis) or energy transfer (photosensitization), we next examined the influence of the Brønsted acid co-catalyst on the electrochemical properties of the substrate. The cyclic voltammogram (CV) of **3.12** exhibits an irreversible reduction feature whose half-wave potential was estimated to be –1.5 V vs. SCE (see section **3.5.7** for CV data), well outside of the range of the excited-state $[Ru^*(bpy)_3]^{2+}$ photocatalyst (–0.81 V). Addition of p-TsOH to this solution results in a significantly more complex voltammogram, with the most positive reduction wave featuring a half-wave potential of approximately –0.5 V. Thus, while these data suggest that

the background reaction in the absence of TsOH must arise from an energy transfer process (Table 3-2, Entry 1), one-electron photoreduction of protonated **3.12** cannot be entirely ruled out from these data as a pathway to product formation in the presence of the Brønsted acid co-catalyst.

We find, however, that the electron-poor, ligand-modified Ru(II) complex $Ru(deeb)_3(PF_6)_2$ successfully catalyzes the formation of **3.13** in similar yield and identical diastereoselectivity to the standard optimized conditions (Scheme 3-5). While its significantly less-reducing excited state (–0.28 V vs SCE) is insufficient for substrate reduction, even in the presence of Brønsted acid, its triplet energy (E_T = 45 kcal/mol) is quite similar to reported for $Ru(bpy)_3Cl$ (E_T = 46 kcal/mol).[8] Similarly, the well-studied organic triplet sensitizer benzil (E_T = 54 kcal/mol) is a good catalyst for the transformation and affords the same ratio of diastereomeric cycloadducts. Finally, replacing the photocatalyst with one equivalent of several one-electron chemical reductants (TDAE, $Co(Cp)_2$, SmI_2) and oxidants (CAN, $Mn(OAc)_3$, $Fe(acac)_3$) failed to produce any observable trace of [2+2] products. Collectively, these experiments generally support the hypothesis that this reaction occurs through a Brønsted acid-catalyzed triplet energy transfer process, and that an electron transfer mechanism is unlikely to be relevant to the formation of the cycloadduct.

Scheme 3-5. Successful photocycloaddition using alternative photosensitizers

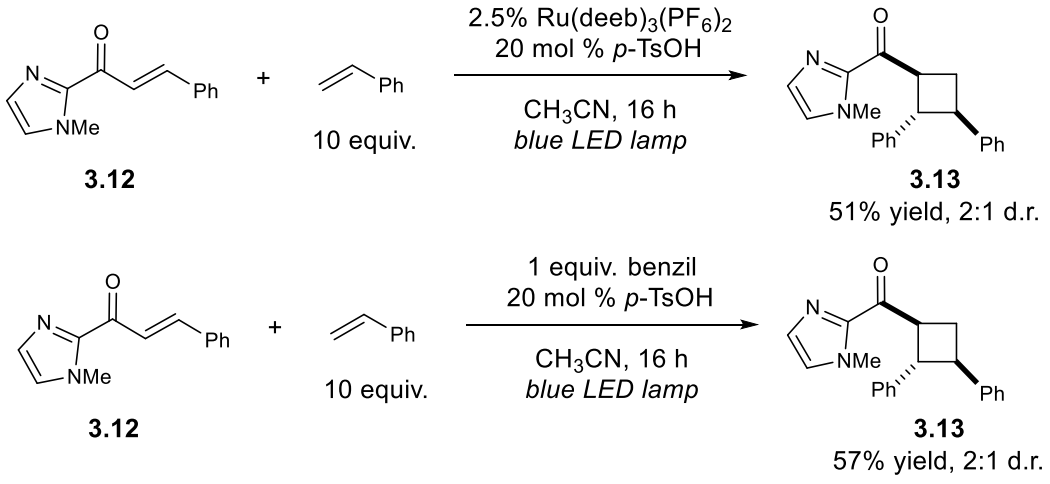

3.2.5 Effects of Brønsted Acids on the Rate Energy Transfer: Computational Analysis

Having established the plausibility of an energy transfer mechanism, we sought understand the means by which Brønsted acids accelerate the rate of this [2+2] photocycloaddition. Ultimately, we also hoped to understand if there was a general photophysical insight to be gleaned from this system. Thus, we interrogated this system using density-function theory (DFT) calculations in collaboration with the Baik group. Our previous work[25] with Lewis acids suggested that thermodynamic driving force, the difference in the triplet energies of the triplet donor and the single acceptor, can serve as a useful metric for the feasibility of an energy transfer process. We calculated the triplet energies of cinnamoyl imidazole **3.12** and its protonated form **3.12–H$^+$**. The triplet energy for **3.12** was estimated to be 48.1 kcal/mol, which decreased by 4.2 kcal/mol after protonation (Figure 3-2). Compared to our previous study using $Sc(OTf)_3$, in which Lewis acid coordination lowers the triplet energy of 2'-hydroxychalcone by ~20 kcal/mol, the effect of Brønsted acids on triplet energy is notably smaller. This result suggested that thermodynamic driving force might not be singlehandedly responsible for the facilitation of energy transfer in this example.

Figure 3-2. Triplet energies and frontier molecular orbitals (FMOs) for **3.12** and **3.12-H$^+$**

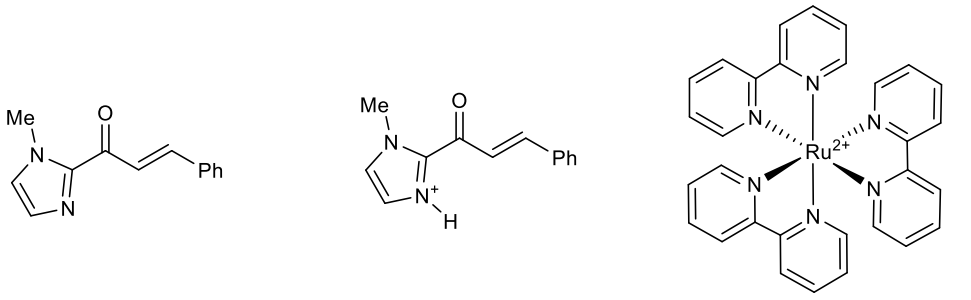

E_T (Calc) = 48.07 kcal/mol E_T (Calc) = 43.90 kcal/mol E_T (Calc) = 43.84 kcal/mol

The vertical Dexter energy transfer process can be modeled using a reaction coordinate diagram depicting the intersection of the net electronic states of each system (Figure 3-3). The black parabolic surface is the state before energy transfer, with the donor in its triplet state (^{3}D) and the acceptor in its singlet state (^{1}A). The blue parabolic surface depicts the state after energy transfer, with the spin states swapped to a singlet donor (^{1}D) and triplet acceptor (^{3}A). The transition state for the energy transfer event occurs at the intersection of these two surfaces, and the barrier for this process can be estimated using equation 1, which is derived from the Marcus equation for rate of electron transfer.

$$\Delta G^{\ddagger} = \frac{(\Delta G+\lambda)^2}{4\lambda} \qquad (1)$$

Figure 3-3. The potential energy surfaces for triplet energy transfer and calculations for reorganization energy, thermodynamic driving force and the barrier to energy transfer

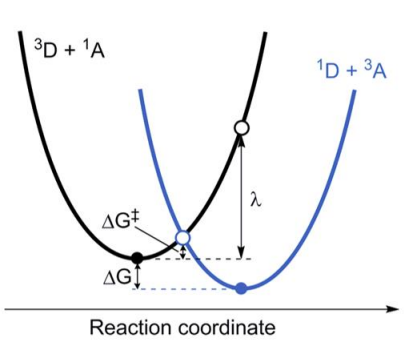

Triplet donor (D)
^{3}Ru(bpy)$_3^{2+}$
+
^{1}3.12 or ^{1}3.12-H$^+$
Triplet acceptor (A)

$\Delta G^{\ddagger} = \frac{(\Delta G + \lambda)^2}{4\lambda}$

Energy transfer

^{1}Ru(bpy)$_3^{2+}$
+
^{3}3.12 or ^{3}3.12-H$^+$

kcal/mol	λ_A	λ_D	λ_{Total}	ΔG	$\Delta G^{\ddagger}$
^{1}3.12	10.63	22.07	32.70	3.73	10.14
^{1}3.12-H$^+$	6.34	22.07	28.41	0.59	7.40

While the thermodynamic driving force (ΔG) can be assessed by calculating the triplet energy difference of triplet donor and singlet acceptor, reorganization energy (λ) is related to the structural distortion cost during the energy transfer event. The reorganization energy of the substrate (triplet acceptor) can be calculated by assessing the singlet state energy in its triplet state geometry. Using equation 1, these two parameters (ΔG and λ) can

be used to evaluate the energy transfer barrier ($\Delta G^{\ddagger}$). Notably, this straightforward approach has been previously used by others to estimate the barrier of single electron transfer steps.[43–47]

Changes in total reorganization energy (λ), thermodynamic driving force (ΔG), and the energy transfer barrier ($\Delta G^{\ddagger}$) as consequence of protonation were evaluated (Figure 3-3). First, the reorganization energies were evaluated for **3.12** and **3.12-H**$^{+}$ and determined to be 10.6 kcal/mol and 6.3 kcal/mol, respectively. Similarly, the reorganization energy of $^{3}Ru(bpy)_{3}^{2+}$ was evaluated and found to be 22.1 kcal/mol. The total reorganization cost is computed by adding the reorganization energies of substrate and photocatalyst. Second, the thermodynamic driving force was evaluated and determined to 3.7 kcal/mol for **3.12**, meaning this process is slightly thermodynamically unfavorable. However, the driving force for **3.12-H**$^{+}$ was determined to be nearly thermoneutral at 0.6 kcal/mol.

In concert, these calculations allow for the estimation of the total barrier to energy transfer ($\Delta G^{\ddagger}$). Interestingly, the Marcus energy transfer barrier is 10.1 kcal/mol for **3.12** and 7.4 kcal/mol for **3.12-H**$^{+}$, which is in good qualitative agreement with the Stern-Volmer quenching outcome that Brønsted acids substantially enhance Dexter energy transfer. These calculations further show that the effect of protonation on both λ and ΔG contribute similarly to the lowering of the energy transfer barrier. This change in ΔG lowers the barrier by 1.7 kcal/mol, whereas the reduction of λ is responsible for 1.1 kcal/mol of the overall 2.8 kcal/mol that the barrier has been lowered. The importance of the reorganization energy for electron-transfer rates within the Marcus expression is recognized.[48] However, its role within energy transfer reactions is underappreciated, particularly in combination with Brønsted acid catalysis.

Figure 3-4. The structures of ^{1}**3.12,** ^{3}**3.12**, ^{1}**3.12-H**$^{+}$, and ^{3}**3.12-H**$^{+}$

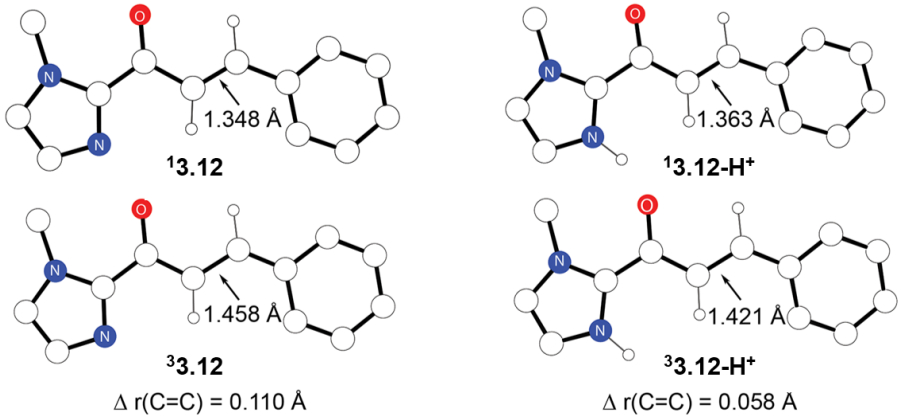

The reduction of the reorganization energy upon substrate protonation can be rationalized by examining computed geometries (Figure 3-4). Upon entering its triplet state, the C=C double bond of the substrate elongates as the π* orbital becomes occupied. Upon excitation, the C=C bond of ^{1}**3.12** lengthens by 0.110 Å from 1.348 to 1.458 Å. When protonated, the double bond becomes slightly longer to 1.363 Å in its singlet ground state. However, compared to ^{3}**3.12**, the C=C bond in ^{3}**3.12-H**$^{+}$ is nearly 0.04 Å shorter at 1.421 Å. These trends are easy to understand. By protonating the imidazole fragment, the electron-withdrawing ability of this molecular fragment is significantly increased. Partial electron-density removal from the olefinic fragment in the ground state leads to a slight weakening and lengthening of the double bond. In the triplet state, however, where the excess electron resides in a π* orbital, partial electron density removal leads to a shortening of the same bond. Overall, protonation brings the ground and excited states closer together structurally, which consequently results in a smaller reorganization energy.

Figure 3-5. Energy profile of this [2+2] photocycloaddition with and without Brønsted acid

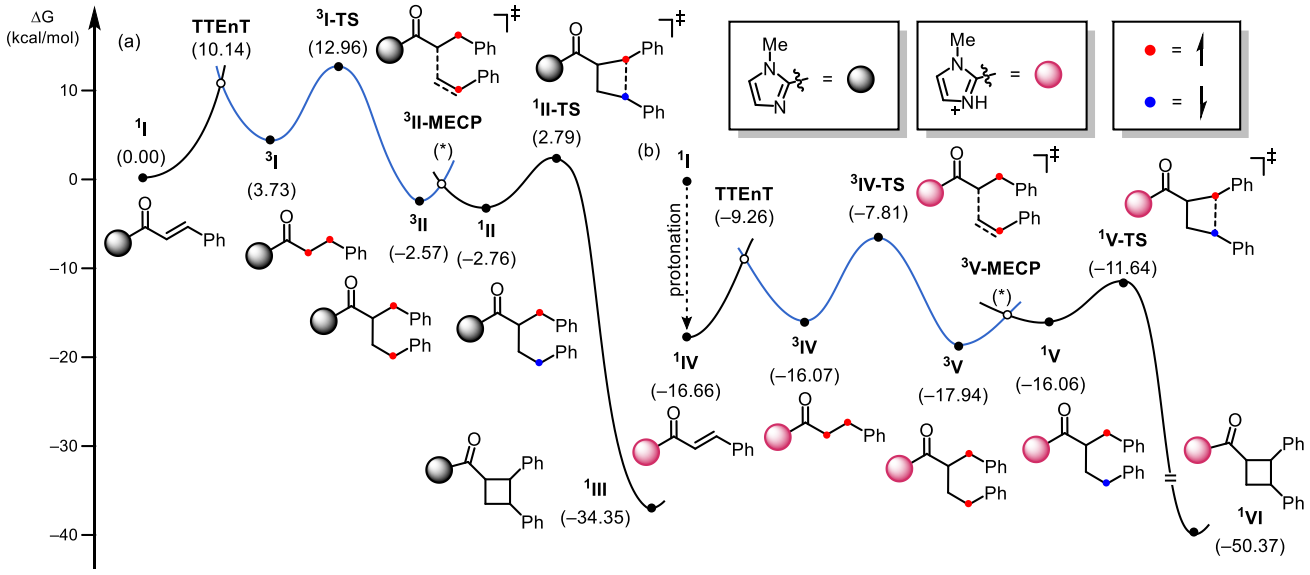

The computed energy profile for the reaction of the cinnamoyl imidazole (**I** to **III**) and that of its protonated analogues (**IV** to **VI**) are shown above (Figure 3-5). The general energy profile is based on the general mechanism of [2+2] photocycloadditions *via* triplet states.[3b,49] The base substrate(**^{1}I**) can be sensitized *via* triplet energy transfer with 10.1 kcal/mol barrier. The α-carbon of cinnamoyl imidazole undergoes C–C coupling with β-carbon of styrene with 9.2 kcal/mol barrier to afford intermediate **^{3}II**, which possesses two α spins on each benzylic position. **^{3}II** can convert to open-shell singlet species **^{1}II** by traversing the minimum energy crossing point (MECP) and this process facilitate a remaining diradical recombination easily only with 5.6 kcal/mol barrier.

The protonation of the imidazole group by *p*-TsOH is thermodynamically preferred by 16.7 kcal/mol. This protonated cinnamoyl imidazole species **^{1}IV** is much more effective in triplet energy transfer, which only has a barrier of 7.6 kcal/mol, as explained above. The subsequent processes follow the mechanism seen for the non-protonated substrate with

similar barriers. Furthermore, the rather significant impact of the Brønsted acid catalyst in this transformation is entirely a result of its ability to facilitate the energy transfer process.

3.3 Conclusion

Over the course of this study we have demonstrated that imidazole heterocycles can serve as a functional handle for the Brønsted acid-catalyzed triplet sensitization of aryl enones. In turn, these photoexcited intermediates undergo [2+2] cycloadditions with electron-rich alkenes, allowing for access to a variety of functionalized cyclobutane products. These products can also be further modified *via* their *C*-acyl imidazole functionality.

This study has revealed that Brønsted acid catalysts are capable of modifying the excited-state reactivity of organic molecules, as has previously been demonstrated with Lewis acids. While we were not surprised to find that protonation of this class of molecule facilitates energy transfer through the lowering of substrate triplet energy, we were interested to discover that this is not the only role of the Brønsted acid in the energy transfer process. Protonation also appears to decrease the reorganization energy require for photosensitization. This occurs through both the increase of the enone C-C double bond in the ground state and decrease of the enone C-C single bond in the triplet excited state. Together this decreases the amount of elongation this bond must undergo, and therefore, increases the overall feasibility of energy transfer. Effects of reorganization energy are not well appreciated in considerations of energy transfer, especially within a synthetic context, and we speculate that these new insights might be applicable to a range of interesting photoreactions involving Dexter energy transfer.

3.4 Contributions

Hoimin Jung, Dasol Cho, and Prof. Mu-Hyun Baik of the Korea Advanced Institute of Science and Technology (KAIST) carried out the computational studies (Chapter 3.2.5).

3.5 Supporting Information

3.5.1 General Information

MeCN, THF, CH_2Cl_2, and toluene were purified by elution through alumina as described by Grubbs.[50] Acetic acid, chloroacetic acid, trifluoroacetic acid, *p*-toluenesulfonic acid monohydrate, and $Ru(bpy)_3Cl_2 \cdot 6H_2O$ were purchased from Sigma Aldrich and used without further purification. All styrenes, 2,3-dimethylbutadiene, phenyl vinyl sulfide, methylenecyclopentane, and indene were purchased from Sigma Aldrich and distilled prior to use. Unless indicated below, all other compounds or solvents were purchased and used as received. Manual flash-column chromatography (FCC) was performed with Silicycle 40-63 Å (230-40 mesh) silica. Automated flash-column chromatography was performed with a Teledyne ISCO CombiFlashR_f+ Lumen system. Photochemical reactions were carried out with a 15 W EagleLight PAR38 blue LED flood light (500 lumens) unless otherwise indicated.

Diastereomer ratios for reactions were determined by ^{1}H NMR analysis of crude reaction mixtures vs. a phenanthrene internal standard. ^{1}H and ^{13}C NMR data were obtained using a Bruker Avance-500 spectrometer with DCH cryoprobe and are referenced to tetramethylsilane (0.0 ppm) and $CDCl_3$ (77.0 ppm), respectively. This instrument and supporting facilities are funded by Paul J. Bender, Margaret M. Bender, and the University of Wisconsin. ^{19}F NMR data were obtained using Bruker Avance-400 spectrometer. This instrument and supporting facilities are funded by

the NSF (CHE-1048642) and the University of Wisconsin. NMR data are reported as follows: chemical shift, multiplicity (s = singlet, d = doublet, t = triplet, q = quartet, p = pentet, sext = sextet, sept = septet, m = multiplet), coupling constant(s) in Hz, integration. NMR spectra were obtained at 298 K unless otherwise noted. FT-IR spectra were obtained using a Bruker Tensor 27 spectrometer and are reported in terms of frequency of absorption (cm^{-1}). Melting points (mp) were obtained using a Stanford Research Systems DigiMelt MPA160 melting point apparatus and are uncorrected. Mass spectrometry was performed with a Thermo Q Exactive™ Plus using ESI-TOF (electrospray ionization-time of flight). This instrument and supporting facilities are funded by the NIH (1S10 OD020022-1) and the University of Wisconsin.

3.5.2 Substrate Synthesis

***N*-Methoxy-*N*-methylcinnamide:** A flame-dried 50 mL round bottom flask (RBF) was charged

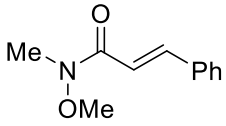

with cinnamoyl chloride (8.64 g, 52.0 mmol, 1.0 equiv.) and *N,O*-dimethylhydroxylamine hydrochloride (5.34 g, 54.7 mmol, 1.05 mmol) in dry CH_2Cl_2 (150 mL). The mixture was cooled to 0 °C and pyridine (9.20 mL, 114.4 mmol, 2.2 equiv.) added slowly. The reaction was then warmed to room temperature and stirred overnight. Then 1 M HCl was added, the organic layer separated, and the aqueous layer extracted with additional EtOAc (3x25 mL). The combined organics were washed with sat. aq. $NaHCO_3$ (25 mL) and sat. aq. NaCl (25 mL). After drying over Na_2SO_4, the crude material was concentrated. Purification by FCC (1:1 Et_2O/pentanes) gave 8.14 g (42.6 mmol, 82% yield) of a viscous oil which solidified after extended drying on high-vacuum. The compound was consistent with reported spectroscopic data.[51] ^{1}H NMR (400 MHz, $CDCl_3$) δ 7.74 (d, *J* = 15.9 Hz, 1H), 7.59–7.56 (m, 2H), 7.41–7.36 (m, 3H), 7.04 (d, *J* = 15.9 Hz, 1H), 3.77(s, 3H), 3.32 (s, 3H).

***N*-Methoxy-*N*-methylcrotonamide:** A flame-dried 250 mL RBF was charged with crotonoyl chloride (4.79 mL, 50.0 mmol, 1.0 equiv.) and *N*,*O*-dimethylhydroxylamine hydrochloride (5.15 g, 52.5 mmol, 1.05 mmol) in dry CH_2Cl_2 (100 mL). The mixture was cooled to 0 °C and pyridine (8.90 mL, 33.0 mmol, 2.2 equiv.) added slowly. The resulting slurry was warmed to room temperature and stirred overnight. Subsequently, 1 M HCl was added and the resulting biphase separated and the aqueous layer extracted with EtOAc (50 mL). The combined organics were washed with sat. aq. $NaHCO_3$ (50 mL) and sat. aq. NaCl (50 mL). After drying over Na_2SO_4, the crude material was concentrated. Purification by FCC (1:1 EtOAc/hexanes) gave 2.48 g (19.0 mmol, 38% yield) of a viscous oil. The compound was consistent with reported spectroscopic data.[51] ^{1}H NMR (400 MHz, $CDCl_3$) δ 6.98 (dq, *J* = 15.3, 6.9 Hz, 1H), 6.42 (dq, *J* = 15.3, 1.6 Hz, 1H), 3.70 (s, 3H), 3.24 (s, 3H), 1.91 (dd, *J* = 6.9, 1.6 Hz, 3H).

(*E*)-Methyl 3-phenylbut-2-enoate: A flame-dried 100 mL RBF was charged with phenylboronic acid (1.22 g, 10.0 mmol, 1.0 equiv.), Pd(OAc)2 (45.0 mg, 0.2 mmol, 0.02 equiv.), and 1,3-bis(diphenylphosphino)propane (dPPP)(123.7 mg, 0.3 mmol, 0.03 equiv.). The flask was purged with N_2 and dry acetone (30 mL) added, followed by methyl crotonate (2.1 mL, 20.0 mmol, 2.0 equiv.) and trifluoroacetic acid (0.23 mL, 3.0 mmol, 0.3 equiv.). The light orange solution was heated to reflux (70 °C). After 30 minutes, the solution had become an intense blood-red color. The reflux was continued for 20 h. Upon cooling the reaction mixture to room temperature, the solvent was removed *via* rotary evaporation. The residue was taken up in CH_2Cl_2 (30 mL), washed once with H_2O (10 mL), dried over Na_2SO_4, and concentrated. The crude orange oil was purified by FCC (gradient 1:49 to 1:24 Et_2O/pentanes) to give 850 mg (4.8 mmol,

48% yield) of a colorless oil. The compound was consistent with reported spectroscopic data.[52] ^{1}H NMR (500 MHz, $CDCl_3$) δ 7.48–7.45 (m, 2H), 7.40–7.35 (m, 3H), 6.14 (q, *J* = 1.3 Hz, 1H), 3.76 (s, 3H), 2.58 (d, *J* = 1.3 Hz, 3H).

(E)-*N*-Methyl-*N*-methoxy-3-phenylbut-2-enamide: A flame dried 25-mL RBF was charged 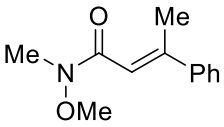

with (E)-Methyl 3-phenylbut-2-enoate (529 mg, 3.0 mmol, 1.0 equiv.), *N*,*O*-dimethylhydroxylamine hydrochloride (585 mg, 6.0 mmol, 2.0 equiv.), and dry THF (5 mL). This suspension was cooled to 0 °C and iPrMgCl (2.0 M in THF) (6 mL, 12.0 mmol, 4.0 equiv.) added over ~20 min. At this point, the reaction was stirred at 0 °C for 1 hour, then slowly quenched by sat. aq. NH_4Cl. The reaction mixture was transferred to a sep. funnel with EtOAc (80 mL) and H_2O added (10 mL). The organic layer was separated and the aqueous washed with EtOAc (2x10 mL). The combined organics were washed with sat. aq. NaCl (20 mL), dried over Na_2SO_4, and concentrated. The residue was purified by FCC (1:1 Et_2O/pentanes) to give 553 mg (2.7 mmol, 90% yield) of a viscous oil. The compound was consistent with reported spectroscopic data.[53] ^{1}H NMR (500 MHz, $CDCl_3$) δ 7.50–7.46 (m, 2H), 7.40–7.33 (m, 3H), 6.57 (s, 1H), 3.71 (s, 3H), 3.27 (s, 3H), 2.53 (d, *J* = 1.2 Hz, 3H).

2-Acetyl-1-methylimidazole: A solution of 1-methylimidazole (0.84 mL, 10.5 mmol, 1.05 equiv.) 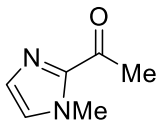

in dry THF (25 mL) was prepared in a flame-dried 100 mL RBF. After cooling to –78 °C, recently titrated nBuLi (5.5 mL, 1.91 M in hexanes, 10.5 mmol, 1.05 equiv.) was added portionwise. The reaction was allowed to warm to 0 °C for about 30 minutes before returning to –78 °C. A solution of 4-acetylmorpholine (1.15 mL, 10.0 mmol, 1.0 equiv.) in THF (25 mL) was prepared in a flame-dried 50 mL conical bottom flask and added to the solution of

deprotonated 1-methylimidazole *via* cannula. The reaction was warmed to room temperature and stirred overnight. The resulting solution was stirred vigorously and glacial acetic acid (2 mL) added dropwise. This solution was transferred to sep. funnel with EtOAc (100 mL), then washed with sat. aq. $NaHCO_3$ (30 mL) and sat. aq. NaCl (30 mL). Each wash solution was back-extracted with additional EtOAc (1x30 mL). The combined organics were dried over Na_2SO_4 and concentrated. Purification by FCC (2:3 EtOAc/pentanes) gave 700 mg (5.6 mmol, 56% yield) of a colorless oil. The compound was consistent with reported spectroscopic data.[54] ^1H NMR (400 MHz, $CDCl_3$) δ 7.14 (s, 1H), 7.03 (s, 1H), 4.00 (s, 3H), 2.66 (s, 3H).

General Method A for the Preparation of Cinnamoyl Methylimidazole Derivatives: A flame-dried RBF was charged with *N*-methylimidazole (1.05 equiv.) and dry THF, then cooled to –78 °C. Recently titrated nBuLi (in hexanes, 1.05 equiv.) was added portionwise. The reaction was warmed to 0 °C for 30 minutes, then returned to –78 °C. A solution of the Weinreb amide (1.0 equiv.) in THF was prepared in a flame-dried conical bottom flask and added to the solution of deprotonated 1-methylimidazole *via* cannula. The reaction was warmed to room temperature and stirred overnight. The resulting solution was stirred vigorously and glacial acetic acid added dropwise. This solution was transferred to sep. funnel with EtOAc and shaken with water. The organic layer was separated and the aqueous extracted with additional EtOAc (2-3x). The combined organics were then washed with sat. aq. $NaHCO_3$ and sat. aq. NaCl, dried over Na_2SO_4, and concentrated. Products were purified by FCC as indicated below.

General Method B for the Preparation of Cinnamoyl Methylimidazole Derivatives: A RBF was charged with 2-acetyl-1-methylimidazole (1.0 equiv.), EtOH, and H_2O. This solution was

sparged briefly with N_2 (~5 minutes). Freshly distilled aromatic aldehyde (1.0-1.1 equiv.) was then added to the solution, followed by a catalytic quantity of KOH. This was then stirred under N_2 for 12-16 h. The resulting mixture was diluted with CH_2Cl_2 and transferred to sep. funnel and shaken with H_2O. The organic layer was separated and the aqueous extracted with additional CH_2Cl_2 (2-3x). The combined organics were dried over Na_2SO_4 and concentrated. The products were typically quite clean by ^{1}H NMR. Purification by FCC was performed with 1:1 Et_2O/pentanes.

2-cinnamoyl-1-methyl-1*H*-imidazole (3.12): Prepared using general method A using 1-

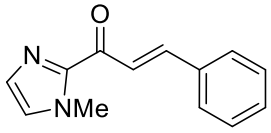

methylimidazole (0.71 mL, 8.93 mmol, 1.05 equiv.) and nBuLi (3.6 mL, 2.50 M in hexanes, 8.93 mmol, 1.05 equiv.) in THF (30 mL), and *N*-methoxy-*N*-methylcinnamide (1.62 g, 8.50 mmol, 1.0 equiv.) in THF (10 mL). Purified by flash column chromatography with 1:1 Et_2O/pentanes. Yield: 1.32 g (6.2 mmol, 73% yield) of an off-white solid. The compound was consistent with reported spectroscopic data.[55] ^{1}H NMR (400 MHz, $CDCl_3$) δ 8.08 (d, *J* = 16.0 Hz, 1H), 7.83 (d, *J* = 16.0 Hz, 1H), 7.72–7.68 (m, 2H), 7.43–7.38 (m, 3H), 7.23 (s, 1H), 7.09 (s, 1H), 4.10 (s, 3H).

2-crotonoyl-1-methyl-1*H*-imidazole: Prepared using general method A using 1-methylimidazole

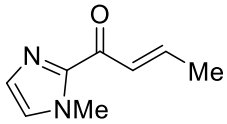

(1.51 mL, 18.9 mmol, 1.05 equiv.) and nBuLi (10.6 mL, 1.78 M in hexanes, 18.9 mmol, 1.05 equiv.) in THF (50 mL), and *N*-methoxy-*N*-methylcrotonamide (2.32 g, 18.0 mmol, 1.0 equiv.) in THF (50 mL). Purified by flash column chromatography with 1:9 EtOAc/pentanes. Yield: 1.28 g (8.5 mmol, 47% yield) of a colorless oil. The compound was consistent with reported spectroscopic data.[55] ^{1}H NMR (400 MHz, $CDCl_3$) δ

7.41 (dq, *J* = 15.6, 1.6 Hz, 1H), 6.18 (s, 1H), 7.13 (dq, *J* = 15.6, 6.9 Hz, 1H), 7.05 (s, 1H), 4.05 (s, 3H), 1.99 (dd, *J* = 6.9, 1.6 Hz, 3H).

2-(3-methylcinnamoyl)-1-methyl-1*H*-imidazole (3.37): Prepared using general method A using

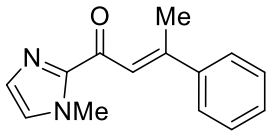

1-methylimidazole (0.18 mL, 2.2 mmol, 1.05 equiv.) and nBuLi (1.4 mL, 1.6 M in hexanes, 2.2 mmol, 1.05 equiv.) in THF (10 mL), and (*E*)-*N*-Methyl-*N*-methoxy-3-phenylbut-2-enamide (431 mg, 2.1 mmol, 1.0 equiv.) in THF (2 mL). Purified by flash column chromatography with 1:1 Et2O/pentanes. Yield: 280 mg (1.2 mmol, 59% yield) of an off-white solid (mp = 71 – 73 °C). ν_{max} (film) / cm^{-1} 2954, 1648, 1596, 1447, 1403, 1291, 1224, 1155, 1039, 947, 917, 850. ^{1}H NMR (400 MHz, $CDCl_3$) δ 7.80 (q, *J* = 1.2 Hz, 1H), 7.64–7.61 (m, 2H), 7.42–7.36 (m, 3H), 7.16 (s, 1H), 7.02(s, 1H), 4.09 (s, 3H), 2.68 (d, *J* = 1.2 Hz, 1H). ^{13}C NMR (125 MHz, $CDCl_3$) δ 182.11, 156.00, 144.98, 142.67, 129.18, 128.72, 128.44, 126.81, 126.71, 121.81, 36.50, 18.52. HRMS (ESI) calculated for $[C_{14}H_{15}N_2O]^+$ ($M+H^+$) requires *m/z* 227.1179, found 227.1175.

(*E*)-3-(4-trifluoromethylphenyl)-1-(1-methyl-1*H*-imidazol-2-yl)prop-2-en-1-one (3.38):

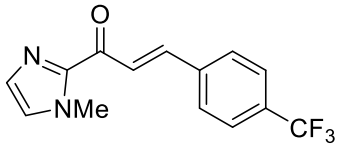

Prepared using general method B using 2-acetyl-1-methylimidazole (328.0 mg, 3.0 mmol, 1.0 equiv.), 4-trifluoromethylbenzaldehyde (0.45 mL, 3.3 mmol, 1.1 equiv.), KOH (½ pellet, ~25 mg), EtOH (12 mL), and H_2O (6 mL). Purified by flash column chromatography with 1:1 Et_2O/pentanes. Yield: 442 mg (1.59 mmol, 53% yield) of an off-white solid (mp = 85 – 88 °C). ν_{max} (film) / cm^{-1} 1663, 1610, 1403, 1320, 1280, 1163, 1108, 1067, 1015, 984, 956, 919, 831. ^{1}H NMR (400 MHz, $CDCl_3$) δ 8.14 (d, *J* = 16.0 Hz, 1H), 7.81 (d, *J* = 16.0 Hz, 1H), 7.79 (d, *J* = 8.3 Hz, 2H), 7.65 (d, *J* = 8.3 Hz, 2H), 7.24 (s, 1H), 7.11 (s, 1H), 4.11 (s, 3H). ^{13}C NMR (125 MHz, $CDCl_3$) δ 179.98, 143.85, 141.21, 138.28 (q, *J* =

1.3 Hz), 131.74 (q, *J* = 32.7 Hz), 129.58, 128.74, 127.59, 125.78 (q, *J* = 3.8 Hz), 125.08, 123.87 (q, *J* = 272.4 Hz), 36.40. ^{19}F NMR (337 MHz, $CDCl_3$) δ –62.82. HRMS (ESI) calculated for $[C_{14}H_{12}F_3N_2O]^+$ ($M+H^+$) requires *m/z* 281.0896, found 281.0890.

(*E*)-3-(4-bromophenyl)-1-(1-methyl-1*H*-imidazol-2-yl)prop-2-en-1-one: Prepared using

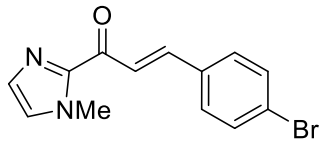

general method B using 2-acetyl-1-methylimidazole (377.9 mg, 3.0 mmol, 1.0 equiv.), 4-bromobenzaldehyde (558.0 mg, 3.0 mmol, 1.0 equiv.), KOH (1 pellet, ~50 mg), and EtOH (6 mL). Purified by flash column chromatography with 1:1 Et_2O/pentanes. Yield: 561 mg (1.92 mmol, 64% yield) of an off-white solid. The compound was consistent with reported spectroscopic data.[56] ^{1}H NMR (400 MHz, $CDCl_3$) δ 8.06 (d, *J* = 16.0 Hz, 1H), 7.74 (d, *J* = 16.0 Hz, 1H), 7.57–7.52 (m, 4H), 7.22 (s, 1H), 7.09 (s, 1H), 4.10 (s, 3H).

(*E*)-3-(4-methoxyphenyl)-1-(1-methyl-1*H*-imidazol-2-yl)prop-2-en-1-one: Prepared using

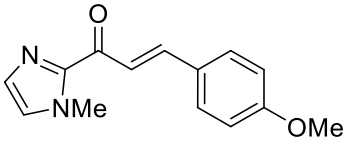

general method B using 2-acetyl-1-methylimidazole (372.7 mg, 3.0 mmol, 1.0 equiv.), 4-methoxybenzaldehyde (0.26 mL, 3.0 mmol, 1.0 equiv.), KOH (½ pellet, ~25 mg), and EtOH (6 mL). Purified by flash column chromatography with 1:1 Et_2O/pentanes. Yield: 382 mg (1.59 mmol, 53% yield) of an off-white solid. The compound was consistent with reported spectroscopic data.[56] ^{1}H NMR (400 MHz, $CDCl_3$) δ 7.96 (d, *J* = 15.9 Hz, 1H), 7.80 (d, *J* = 15.9 Hz, 1H), 7.66 (d, *J* = 8.7 Hz, 1H), 7.21 (s, 1H), 7.07 (s, 1H), 6.92 (d, *J* = 8.7 Hz, 1H), 4.10 (s, 3H), 3.85 (s, 3H).

(*E*)-3-(3-methoxyphenyl)-1-(1-methyl-1*H*-imidazol-2-yl)prop-2-en-1-one (3.39: Prepared 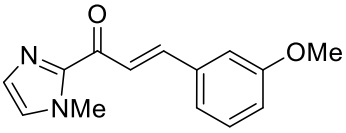

using general method B using 2-acetyl-1-methylimidazole (327.4 mg, 3.0 mmol, 1.0 equiv.), 3-methoxybenzaldehyde (0.41 mL, 3.3 mmol, 1.1 equiv.), KOH (½ pellet, ~25 mg), EtOH (12 mL), and H_2O (6 mL). Purified by flash column chromatography with 1:1 Et_2O/pentanes. Yield: 531 mg (2.19 mmol, 73% yield) of an off-white solid (mp = 91 – 94 °C). ν_{max} (film) / cm^{-1} 2957, 1658, 1601, 1464, 1400, 1287, 1249, 1156, 1081, 1020, 992, 918, 838.0. ^{1}H NMR (400 MHz, $CDCl_3$) δ 8.05 (d, *J* = 16.1 Hz, 1H), 7.80 (d, *J* = 16.1 Hz, 1H), 7.32 (t, *J* = 7.7 Hz, 1H), 7.28 (dt, *J* = 7.7, 1.5 Hz, 1H), 7.23 (s, 1H), 7.21 (t, *J* = 1.8 Hz, 1H), 7.09 (s, 1H), 6.95 (ddd, *J* = 7.8 2.4, 1.2 Hz, 1H), 4.10 (s, 1H), 3.86 (s, 1H). ^{13}C NMR (125 MHz, $CDCl_3$) δ 180.46, 159.89 144.03, 143.42, 136.27, 129.80, 129.32, 127.30, 122.90, 121.76, 116.80, 112.95, 55.40, 36.40. HRMS (ESI) calculated for $[C_{14}H_{15}N_2O_2]^+$ ($M+H^+$) requires *m/z* 243.1128, found 243.1125.

(*E*)-3-(2-methoxyphenyl)-1-(1-methyl-1*H*-imidazol-2-yl)prop-2-en-1-one (3.40): Prepared 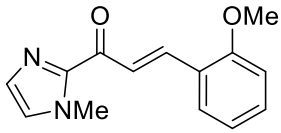

using general method B using 2-acetyl-1-methylimidazole (499.6 mg, 4.0 mmol, 1.0 equiv.), 2-methoxybenzaldehyde (0.41 mL, 4.4 mmol, 1.1 equiv.), KOH (½ pellet, ~25 mg), and EtOH (8 mL). Purified by flash column chromatography with 1:1 Et_2O/pentanes. Yield: 877 mg (3.6 mmol, 90% yield) of an off-white solid (mp = 136 – 139°C). The compound **not consistent** with reported spectroscopic data[56], and therefore is independently characterized here.[57] ν_{max} (film) / cm^{-1} 2944, 1654, 1593, 1464, 1401, 1314, 1289, 1245, 1157, 1051, 1019, 920, 810. ^{1}H NMR (400 MHz, $CDCl_3$) δ 8.24 (d, *J* = 16.2 Hz, 1H), 8.09 (d, *J* = 16.2 Hz, 1H), 7.76 (dd, *J* = 7.6, 1.6 Hz, 1H), 7.37 (ddd, *J* = 8.9, 7.6, 1.6 Hz, 1H), 7.21 (s, 1H), 7.07 (s, 1H), 6.97 (t, *J* = 7.6 Hz, 1H), 6.93 (t, *J* = 8.9 Hz, 1H), 4.10 (s, 3H), 3.91 (s, 3H). ^{13}C

NMR (125 MHz, $CDCl_3$) δ 180.91, 158.73, 144.23, 138.48, 131.77, 129.18, 128.62, 127.04, 123.95, 122.83, 120.63, 111.11, 55.56, 36.37. HRMS (ESI) calculated for $[C_{14}H_{15}N_2O_2]^+$ ($M+H^+$) requires *m/z* 243.1128, found 243.1124.

(*E*)-1-(1-methyl-1*H*-imidazol-2-yl)-3-(thiophen-2-yl)prop-2-en-1-one: Prepared using general method B using 2-acetyl-1-methylimidazole (280.0 mg, 2.25 mmol, 1.0 equiv.), 2-thiophenecarboxaldehyde (0.23 mL, 3.0 mmol, 1.0 equiv.), KOH (1 pellet, ~50 mg), and EtOH (5 mL). Purified by flash column chromatography with 1:1 Et_2O/pentanes. Yield: 250 mg (1.15 mmol, 51% yield) of an off-white solid. The compound was consistent with reported spectroscopic data.[56] ^{1}H NMR (400 MHz, $CDCl_3$) δ 7.95 (d, *J* = 15.7 Hz, 1H), 7.84 (d, *J* = 15.7 Hz, 1H), 7.42 (d, *J* = 5.0 Hz, 1H), 7.38 (d, *J* = 3.5 Hz, 1H), 7.22 (s, 1H), 7.08 (s, 1H), 7.08 (dd, *J* = 5.0, 3.5 Hz, 1H), 4.09 (s, 3H).

3.5.3 [2+2] Photocycloaddition Reactions

Small Scale Experiments for Reaction Development: An oven-dried 2 dram vial with a stir bar was charged with enone (0.10 mmol, 1.0 equiv.), *p*-toluenesulfonic acid monohydrate (0.02 mmol, 0.2 equiv.), and $Ru(bpy)_3Cl_2$•$6H_2O$ (0.0025 mmol, 0.025 equiv.). These were dissolved in dry MeCN (2 mL, 0.05 M in cinnamoyl imidazole) before addition of styrene (1.0 mmol, 10.0 equiv.). The solution was sealed with a septum and degassed by sparging the solution with N_2 for 10 minutes. The septum was covered with parafilm and the reaction mixture subjected to irradiation by a blue LED lamp for 16-24 h. The resulting mixture was then diluted with 4 mL of Et_2O and passed through a short plug of silica to remove the photocatalyst. Phenanthrene (approx. 0.1 mmol) was added to the mixture for analysis by ^{1}H NMR and the solvent removed under reduced pressure.

Isolation Scale Experiments: An oven-dried Schlenk tube with a stir bar was charged with cinnamoyl imidazole (0.40 mmol, 1 equiv.), *p*-toluenesulfonic acid monohydrate (0.08 mmol, 0.2 equiv.), and $Ru(bpy)_3Cl_2•6H_2O$ (0.01 mmol, 0.025 equiv.). These were dissolved in dry MeCN (8 mL, 0.05 M in cinnamoyl imidazole) before addition of alkene (4.0 mmol, 10 equiv.). The Schlenk tube was then sealed with a glass stopper and degassed *via* freeze-pump-thaw technique (3 x 5 minutes). Following the final thaw, the reaction mixture was subjected to irradiation by a blue LED lamp for 24 h. The resulting mixture was then diluted with 10-12 mL of Et_2O and passed through a short plug of silica to remove the photocatalyst. Phenanthrene (0.1 mmol) was added to the mixture for preliminary analysis by ^1H NMR and the solvent removed under reduced pressure. After recombining the NMR sample, the residue was purified by FCC with 1:1 Et_2O/pentanes to give a mixture of diastereomers. For most reactions, these diastereomers could be further separated through additional purification – for specifics see each reaction.

(2,3-diphenylcyclobutyl)(1-methyl-1H-imidazol-2-yl)methanone (3.13): Prepared according to

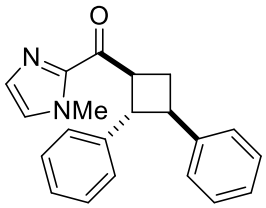

general procedure for isolation scale experiments using 84.6 mg (0.4 mmol) 2-cinnamoyl-1-methyl-1*H*-imidazole, 15.1 mg (0.08 mmol) *p*-toluenesulfonic acid monohydrate, 7.4 mg (0.01 mmol) $Ru(bpy)_3Cl_2•6H_2O$, and 0.45 mL (4.0 mmol) styrene in MeCN with a total volume of 8 mL (0.05 M). Isolation of products was performed by FCC with 1:1 Et_2O/pentanes to give 86 mg (0.27 mmol, 68% yield) of two diastereomers (1.8:1 d.r.). Separation of diastereomers for characterization purposes was achieved by automated FCC (ISCO) using a continuous gradient of 15% → 100% EtOAc in hexanes. Major Diastereomer: Viscous oil/semisolid. ν_{max} (film) / cm^{-1} 3027, 2932, 2360, 1666, 1602, 1495, 1456, 1409, 1290, 1235, 1155, 1077, 1022, 947, 913, 855, 754, 698, 662. ^1H NMR

(500 MHz, $CDCl_3$) δ 7.31–7.25 (m, 8 H), 7.23–7.16 (m, 2H), 7.15 (d, *J* = 0.8 Hz, 1H), 7.04 (s, 1H), 4.57 (td, *J* = 9.8, 8.7 Hz, 1H), 4.08 (t, *J* = 9.8 Hz, 1H), 4.03 (s, 3H), 3.63 (td, *J* = 10.1, 8.1 Hz), 2.83 (dt, *J* = 10.3, 8.5 Hz, 1H), 2.31 (q, *J* = 10.2 Hz, 1H). ^{13}C NMR (125 MHz, $CDCl_3$) δ 192.44, 143.58, 142.63, 142.52, 129.40, 128.38, 128.36, 127.25, 126.96, 126.94, 126.42 (2C), 48.56, 44.97, 43.48, z36.18, 31.92. HRMS (ESI) calculated for $[C_{21}H_{21}N_2O]^+$ ($M+H^+$) requires *m/z* 317.1648, found 317.1646. Minor Diastereomer: Viscous oil/semisolid. ν_{max} (film) / cm^{-1} 3027, 1666, 1495, 1455, 1406, 1289, 1229, 1154, 1030, 913, 838, 734, 696, 634. ^{1}H NMR (500 MHz, $CDCl_3$) δ 7.18 (d, *J* = 0.8 Hz, 1H), 7.14–7.02 (m, 8H), 6.99–6.98 (m, 3H), 5.05 (q, *J* = 9.0 Hz, 1H), 4.47 (t, *J* = 9.3 Hz, 1H), 4.04 (s, 3H), 4.03–3.96 (m, 1H), 2.78–2.74 (m, 2H). ^{13}C NMR (125 MHz, $CDCl_3$) δ 193.05, 142.57, 140.74, 139.62, 129.40, 128.23, 127.93, 127.84, 127.64, 127.34, 125.80, 125.78, 45.75, 43.74, 41.96, 36.24, 28.61. HRMS (ESI) calculated for $[C_{21}H_{21}N_2O]^+$ ($M+H^+$) - requires *m/z* 317.1648, found 317.1646.

(1-methyl-1H-imidazol-2-yl)(3-phenyl-2-(4-(trifluoromethyl)phenyl)cyclobutyl)methanone

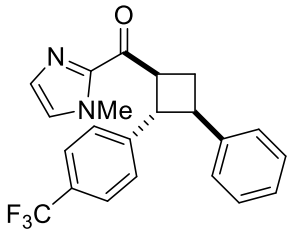

(3.14): Prepared according to general procedure for isolation scale experiments using 113.2 mg (0.4 mmol) (E)-3-(4-trifluoromethylphenyl)-1-(1-methyl-1*H*-imidazol-2-yl)prop-2-en-1-one, 13.0 mg (0.08 mmol) *p*-toluenesulfonic acid monohydrate, 7.8 mg (0.01 mmol) $Ru(bpy)_3Cl_2•6H_2O$, and 0.48 mL (4.0 mmol) styrene in MeCN with a total volume of 8 mL (0.05 M). Isolation of products was performed by FCC with 1:1 Et_2O/pentanes to give 91 mg (0.24 mmol, 60% yield) of two diastereomers (1.8:1 d.r.). Separation of diastereomers for characterization purposes was achieved by automated FCC (ISCO) using a continuous gradient of 15% → 100% EtOAc in hexanes. Major Diastereomer: Viscous oil/semisolid. ν_{max} (film) / cm^{-1} 2950, 1667, 1619, 1409, 1325, 1236, 1163,

1117, 1068, 1018, 912, 858, 775, 699, 666. ^{1}H NMR (500 MHz, $CDCl_3$) δ 7.51 (d, *J* = 8.2 Hz, 2H), 7.38 (d, *J* = 8.2 Hz, 2H), 7.34–2.29 (m, 4H), 7.23 (tt, *J* = 6.8, 1.9 Hz, 1H), 7.16 (d, *J* = 0.8 Hz, 1H), 7.07 (s, 1H), 4.57 (td, *J* = 9.8, 8.7 Hz, 1H), 4.11 (t, *J* = 9.9 Hz, 1H), 3.62 (td, 9.9, 8.5 Hz), 2.85 (dt, *J* = 10.2, 8.5 Hz, 1H), 2.37 (q, *J* = 10.3 Hz). ^{13}C NMR (125 MHz, $CDCl_3$) δ 191.94, 146.46 (q, *J* = 1.2 Hz), 142.98, 142.45, 129.54, 128.53, 127.46, 127.24, 126.91, 126.70, 125.33 (q, *J* = 3.7 Hz), 124.2 (q, *J* = 271.7 Hz), 48.38, 44.72, 43.50, 36.18, 31.84. ^{19}F NMR (377 MHz, $CDCl_3$) δ –62.39. HRMS (ESI) calculated for $[C_{22}H_{20}F_3N_2O]^+$ ($M+H^+$) requires *m/z* 385.1522, found 385.1517. Minor Diastereomer: Viscous oil/semisolid. ν_{max} (film) / cm^{-1} 2947, 1668, 1619, 1456, 1409, 1326, 1291, 1162, 1115, 1068, 1017, 913, 847, 774, 699, 668. ^{1}H NMR (500 MHz, $CDCl_3$) δ 7.30 (d, *J* = 8.1 Hz, 2H), 7.19 (d, *J* = 0.7 Hz, 1H), 7.16–7.13 (m, 2H), 7.10–7.05 (m, 6H), 5.05 (q, *J* = 9.0 Hz, 1H), 4.49 (t, *J* = 9.3 Hz, 1Hf), 4.05 (s, 3H), 4.03–3.99 (m, 1H), 2.81–2.74 (m, 2H). ^{13}C NMR (125 MHz, $CDCl_3$) δ 192.50, 143.84 (q, *J* = 1.2 Hz), 142.41, 140.15, 129.55, 128.17, 128.11, 128.09, 127.52, 126.18, 124.54 (q, *J* = 3.8 Hz), 124.25 (q, 272.0 Hz), 45.51 43.78, 41.95, 36.24, 28.53. ^{19}F NMR (377 MHz, $CDCl_3$) δ –62.37. HRMS (ESI) calculated for $[C_{22}H_{20}F_3N_2O]^+$ ($M+H^+$) requires *m/z* 385.1522, found 385.1519.

(2-(4-bromophenyl)-3-phenylcyclobutyl)(1-methyl-1H-imidazol-2-yl)methanone (3.15):

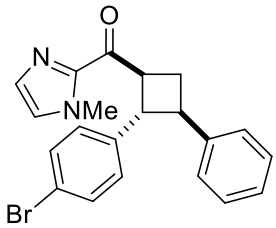

Prepared according to general procedure for isolation scale experiments using 116.4 mg (0.4 mmol) (E)-3-(4-bromophenyl)-1-(1-methyl-1*H*-imidazol-2-yl)prop-2-en-1-one, 13.9 mg (0.08 mmol) *p*-toluenesulfonic acid monohydrate, 7.3 mg (0.01 mmol) $Ru(bpy)_3Cl_2•6H_2O$, and 0.48 mL (4.0 mmol) styrene in MeCN with a total volume of 8 mL (0.05 M). Isolation of products was performed by FCC with 1:1 Et_2O/pentanes to give 93 mg (0.24 mmol, 59% yield) of two diastereomers (1.8:1 d.r.).

Separation of major diastereomer for characterization purposes was achieved by automated FCC (ISCO) using a continuous gradient of 10% → 50% EtOAc in hexanes. Major Diastereomer: Viscous oil/semisolid. ν_{max} (film) / cm^{-1} 2945, 1664, 1488, 1406, 1289, 1235, 1155, 1073, 1010, 911, 856, 824, 771, 699, 670, 622. ^{1}H NMR (500 MHz, $CDCl_3$) δ 7.38 (d, *J* = 8.4 Hz, 2H), 7.33–2.27 (m, 4H), 7.22 (tt, *J* = 7.0, 1.8 Hz, 1H), 7.16–7.14 (m, 3H), 7.05 (s, 1H), 4.52 (q, *J* = 9.5 Hz, 1H), 4.03 (s, 3H), 4.00 (t, *J* = 9.8 Hz, 1H), 3.56 (td, *J* = 10.1, 8.2 Hz, 1H), 2.81 (dt, *J* = 10.3, 8.3 Hz, 1H), 2.33 (q, *J* = 10.3 Hz, 1H). ^{13}C NMR (125 MHz, $CDCl_3$) δ 192.09, 143.15, 142.51, 141.46, 131.42, 129.48, 128.71, 128.47, 127.38, 126.88, 126.59, 120.24, 48.25, 44.85, 43.56, 36.17, 31.65. HRMS (ESI) calculated for $[C_{21}H_{20}BrN_2O]^+$ ($M+H^+$) requires *m/z* 395.0754, found 395.0753. Minor Diastereomer: Unable to separate from major diastereomer cleanly.

(2-(4-methoxyphenyl)-3-phenylcyclobutyl)(1-methyl-1H-imidazol-2-yl)methanone (3.16):

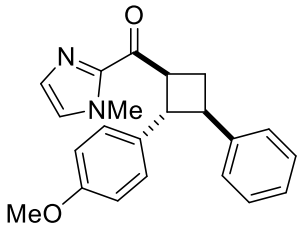

Prepared according to general procedure for isolation scale experiments using 97.6 mg (0.4 mmol) (E)-3-(4-methoxyphenyl)-1-(1-methyl-1*H*-imidazol-2-yl)prop-2-en-1-one, 15.4 mg (0.08 mmol) *p*-toluenesulfonic acid monohydrate, 7.7 mg (0.01 mmol) $Ru(bpy)_3Cl_2•6H_2O$, and 0.46 mL (4.0 mmol) styrene in MeCN with a total volume of 8 mL (0.05 M). Isolation of products was performed by FCC with 1:1 Et_2O/pentanes to give 83 mg (0.24 mmol, 60% yield) of two diastereomers (1.8:1 d.r.). Separation of diastereomers for characterization purposes was achieved by manual FCC using a gradient of 1:2 → 1:1 Et_2O/pentanes. Major Diastereomer: Viscous oil/semisolid. ν_{max} (film) / cm^{-1} 2928, 1665, 1611, 1513, 1457, 1408, 1291, 1248, 1178, 1155, 1033, 912, 858, 831, 776, 700. ^{1}H NMR (500 MHz, $CDCl_3$) δ 7.32–7.29 (m, 4H), 7.22–7.18(m, 3H), 7.15 (s, 1H), 7.04(s, 1H), 6.81 (d, *J* = 8.6 Hz, 2H), 4.52 (q, *J* = 9.5 Hz, 1H), 4.03 (s, 3H), 3.99 (t, *J* = 9.7 Hz, 1H), 3.58 (q, *J* = 9.3

Hz, 1H), 2.81 (q, *J* = 8.8 Hz, 1H), 2.30 (q, *J* = 10.2 Hz, 1H) . ^{13}C NMR (125 MHz, $CDCl_3$) δ 192.52, 158.20, 143.62, 142.69, 134.71, 129.37, 128.35, 128.00, 127.22, 126.92, 126.36, 113.75, 55.23, 48.28, 45.28, 43.79, 36.17, 31.59. HRMS (ESI) calculated for $[C_{22}H_{23}N_2O_2]^+$ ($M+H^+$) - requires *m/z* 347.1754, found 347.1753. Minor Diastereomer: Viscous oil/semisolid. ν_{max} (film) / cm^{-1} 2935, 1164, 1611, 1512, 1455, 1405, 1290, 1247, 1178, 1154, 1032, 912, 835, 775, 699. ^{1}H NMR (500 MHz, $CDCl_3$) δ 7.17 (s, 1H), 7.16–7.13 (m, 2H), 7.09–7.05 (m, 3H), 7.04 (s, 1H), 6.89 (d, *J* = 8.5 Hz, 2H), 6.59 (d, *J* = 8.5 Hz, 2H), 4.98 (q, *J* = 8.8 Hz, 1H), 4.39 (t, *J* = 9.2 Hz, 1H), 4.03(s, 3H), 3.95 (td, *J* = 8.9, 4.8 Hz, 1H), 3.67 (s, 3H), 2.78–2.69 (m, 2H). ^{13}C NMR (125 MHz, $CDCl_3$) δ 193.13, 157.66, 142.63, 140.77, 131.85, 129.39, 128.25, 127.88, 127.30, 125.77, 113.07, 55.05, 45.31, 44.28, 41.99, 36.23, 28.31. HRMS (ESI) calculated for $[C_{22}H_{23}N_2O_2]^+$ ($M+H^+$) - requires *m/z* 347.1754, found 347.1753.

(2-(3-methoxyphenyl)-3-phenylcyclobutyl)(1-methyl-1H-imidazol-2-yl)methanone (3.17):

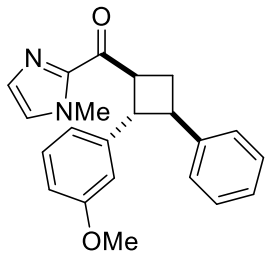

Prepared according to general procedure for isolation scale experiments using 97.9 mg (0.4 mmol) (E)-3-(3-methoxyphenyl)-1-(1-methyl-1*H*-imidazol-2-yl)prop-2-en-1-one, 15.4 mg (0.08 mmol) *p*-toluenesulfonic acid monohydrate, 7.8 mg (0.01 mmol) $Ru(bpy)_3Cl_2•6H_2O$, and 0.46 mL (4.0 mmol) styrene in MeCN with a total volume of 8 mL (0.05 M). Isolation of products was performed by FCC with 1:1 Et_2O/pentanes to give 98 mg (0.28 mmol, 71% yield) of two diastereomers (1.7:1 d.r.). Separation of major diastereomer for characterization purposes was achieved by automated FCC (ISCO) using a continuous gradient of 10% → 100% EtOAc in hexanes. Major Diastereomer: Viscous oil/semisolid. ν_{max} (film) / cm^{-1} 2927, 1666, 1601, 1491, 1456, 1409, 1289, 1158, 1045, 879, 773, 699. ^{1}H NMR (500 MHz, $CDCl_3$) δ 7.32–7.29 (m, 4H),

7.23–7.15 (m, 3H), 7.05 (s, 1H), 6.88–6.85 (m, 2H), 6.72 (dd, *J* = 8.2, 2.0 Hz, 1H), 4.56 (td, 9.6, 8.7 Hz, 1H), 4.05 (t, *J* = 9.7 Hz, 1H), 4.03 (s, 3H), 3.61 (td, *J* = 10.1, 8.2 Hz, 1H), 2.82 (dt, *J* = 10.1, 8.5 Hz, 1H), 2.32 (q, *J* = 10.1 Hz, 1H). ^{13}C NMR (125 MHz, $CDCl_3$) δ 192.39, 159.59, 144.23, 143.56, 142.64, 129.39, 129.36, 128.39, 127.27, 126.97, 126.43, 119.30, 112.61, 111.86, 55.15, 48.67, 44.88, 43.44, 36.18, 31.76. HRMS (ESI) calculated for $[C_{22}H_{23}N_2O_2]^+$ ($M+H^+$) - requires *m/z* 347.1754, found 347.1752. Minor Diastereomer: Unable to separate from major diastereomer cleanly.

(2-(2-methoxyphenyl)-3-phenylcyclobutyl)(1-methyl-1H-imidazol-2-yl)methanone (3.18):

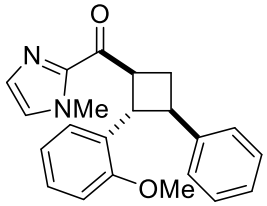

Prepared according to general procedure for isolation scale experiments using 98.0 mg (0.4 mmol) (E)-3-(2-methoxyphenyl)-1-(1-methyl-1*H*-imidazol-2-yl)prop-2-en-1-one, 15.2 mg (0.08 mmol) *p*-toluenesulfonic acid monohydrate, 7.5 mg (0.01 mmol) $Ru(bpy)_3Cl_2•6H_2O$, and 0.46 mL (4.0 mmol) styrene in MeCN with a total volume of 8 mL (0.05 M). Isolation of products was performed by FCC with 1:1 Et_2O/pentanes to give 88 mg (0.25 mmol, 63% yield) of two diastereomers (1.7:1 d.r.). Separation of diastereomers for characterization purposes was achieved by manual FCC using a gradient of 1:2 → 1:1 Et_2O/pentanes. Major Diastereomer: White solid (mp = 109–112 °C). ν_{max} (film) / cm^{-1} 2928, 1665, 1601, 1492, 1457, 1409, 1289, 1246, 1154, 1125, 1051, 1028, 911, 859, 752, 699, 663. ^{1}H NMR (500 MHz, $CDCl_3$) δ 7.40 (d, *J* = 7.5 Hz, 2H), 7.32–7.29 (m, 3H), 7.19 (t, *J* = 7.3 Hz, 1H), 7.14 (td, *J* = 7.5, 1.8 Hz, 1H), 7.11 (s, 1H), 7.04 (s, 1H), 6.89 (t, *J* = 7.5 Hz, 1H), 6.69 (d, *J* = 8.0 Hz, 1H), 4.57 (q, *J* = 9.0 Hz, 1H), 4.22 (t, *J* = 9.5 Hz, 1H), 4.09 (s, 3H), 3.74 (q, *J* = 9.4 Hz, 1H), 3.33 (s, 3H), 2.70 (dt, *J* = 10.2, 8.3 Hz, 1H), 2.38 (q, *J* = 9.9 Hz, 1H). ^{13}C NMR (125 MHz, $CDCl_3$) δ 193.07, 157.24, 144.24, 143.32, 130.66, 129.11, 128.23, 127.38, 127.19,

127.10, 126.91, 126.18, 120.31, 109.86, 54.43, 45.29, 43.74, 41.16, 36.26, 31.46. HRMS (ESI) calculated for $[C_{22}H_{23}N_2O_2]^+$ ($M+H^+$) requires *m/z* 347.1454, found 347.1454. Minor Diastereomer: Viscous oil/semisolid. ν_{max} (film) / cm^{-1} 2933, 1664, 1602, 1493, 1455, 1406, 1290, 1245, 1155, 1122, 1030, 913, 839, 752, 699, 668. ^1H NMR (500 MHz, $CDCl_3$) δ 7.20 (s, 1H), 7.17 (d, *J* = Hz, 1H), 7.12 (d, *J* = Hz, 2H), 7.08–7.05 (m, 2H), 7.05 (s, 1H), 7.00–6.95 (m, 2H), 6.69 (t, *J* = 7.5 Hz, 1H), 6.54 (d, *J* = 8.0 Hz, 1H), 5.20 (q, *J* = 9.4 Hz, 1H), 4.62 (t, *J* = 9.4 Hz, 1H), 4.01 (s, 3H), 3.99 (td, *J* = 9.4, 3.8 Hz, 1H), 3.65 (s, 3H), 2.81 (dt, 11.7, 9.0 Hz, 1H), 2.62 (ddd, *J* = 11.6, 9.5, 3.7 Hz, 1H). ^{13}C NMR (125 MHz, $CDCl_3$) δ 193.35, 156.76, 142.83, 141.71, 129.35, 128.07, 127.95, 127.65, 127.45, 127.31, 126.98, 125.59, 119.75, 109.16, 54.79, 41.90, 41.89, 41.79, 36.26, 28.93. HRMS (ESI) calculated for $[C_{22}H_{23}N_2O_2]^+$ ($M+H^+$) requires *m/z* 347.1754, found 347.1754.

(1-methyl-1H-imidazol-2-yl)(3-phenyl-2-(thiophen-2-yl)cyclobutyl)methanone (3.19):

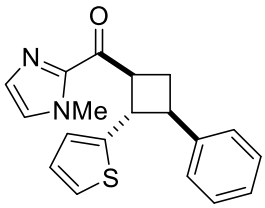

Prepared according to general procedure for isolation scale experiments using 88.5 mg (0.4 mmol) (E)-1-(1-methyl-1*H*-imidazol-2-yl)-3-(thiophen-2-yl)prop-2-en-1-one, 16.2 mg (0.08 mmol) *p*-toluenesulfonic acid monohydrate, 8.4 mg (0.01 mmol) $Ru(bpy)_3Cl_2•6H_2O$, and 0.46 mL (4.0 mmol) styrene in MeCN with a total volume of 8 mL (0.05 M). Isolation of products was performed by FCC with 1:1 Et_2O/pentanes to give 47 mg (0.15 mmol, 36% yield) of two diastereomers (1.7:1 d.r.). Separation of diastereomers for characterization purposes was achieved by automated FCC (ISCO) using a continuous gradient of 15% → 100% EtOAc in hexanes. Major Diastereomer: Viscous oil/semisolid. ν_{max} (film) / cm^{-1} 2946, 1665, 1456, 1408, 1289, 1235, 1155, 1079, 1020, 903, 855, 775, 698, 662. ^1H NMR (500 MHz, $CDCl_3$) δ 7.33–7.30 (m, 4H), 7.23–7.20 (m, 1H), 7.16 (d, *J* = 0.8 Hz, 1H), 7.12 (dd, *J* = 5.0, 1.2 Hz, 1H), 7.05 (s, 1H), 6.93 (dt, *J* = 3.4, 1.0 Hz, 1H), 6.90 (dd,

J = 5.1, 3.5 Hz, 1H), 4.53 (td, *J* = 9.6, 8.7 Hz, 1H), 4.19 (t, *J* = 9.6 Hz, 1H), 4.03(s, 3H), 3.64 (td, *J* = 10.0, 8.1 Hz, 1H), 2.83 4.53 (dt, *J* = 10.4, 8.5 Hz, 1H), 2.32 (q, *J* = 10.3 Hz, 1H). ^{13}C NMR (125 MHz, $CDCl_3$) δ 191.73, 146.55, 142.84, 142.54, 129.48, 128.39, 127.29, 126.82, 126.81, 126.57, 123.75, 123.60, 47.05, 45.35, 44.17, 36.15, 31.24. HRMS (ESI) calculated for $[C_{19}H_{19}N_2OS]^+$ ($M+H^+$) requires *m/z* 323.1213, found 323.1210. Minor Diastereomer: Viscous oil/semisolid. ν_{max} (film) / cm^{-1} 2944, 1667, 1495, 1455, 1408, 1290, 1235, 1155, 1078, 1032, 907, 849, 775, 698. ^{1}H NMR (50fz0 MHz, $CDCl_3$) δ 7.22–7.17 (m, 5H), 7.14–7.11 (m, 1H), 7.06 (s, 1H), 6.93 (dd, *J* = 5.1, 1.1 Hz, 1H), 6.71 (dd, *J* = 4.9, 3.6 Hz, 1H), 6.64 (dt, *J* = 3.5, 1.1 Hz, 1H), 4.88(q, *J* = 8.6 Hz, 1H), 4.62 (t, *J* = 8.8 Hz, 1H), 4.05 (s, 3H), 3.97 (td, *J* = 9.1, 5.1Hz, 1H), 2.86 (ddd, *J* = 11.8, 10.2, 5.0 Hz, 1H), 2.68 (dt, *J* = 12.0, 8.5 Hz, 1H). ^{13}C NMR (125 MHz, $CDCl_3$) δ 192.30, 143.45, 142.43, 140.16, 129.51, 128.17, 127.94, 127.34, 126.22, 126.19, 124.90, 123.77, 46.71, 42.47, 41.28, 36.23, 28.37. HRMS (ESI) calculated for $[C_{19}H_{19}N_2OS]^+$ ($M+H^+$) requires *m/z* 323.1213, found 323.1210.

(1-methyl-1H-imidazol-2-yl)(2-phenyl-3-(4-(trifluoromethyl)phenyl)cyclobutyl)methanone

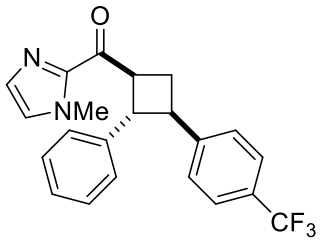

(3.23): Prepared according to general procedure for isolation scale experiments using 85.4 mg (0.4 mmol) 2-cinnamoyl-1-methyl-1*H*-imidazole, 16.2 mg (0.08 mmol) *p*-toluenesulfonic acid monohydrate, 8.0 mg (0.01 mmol) $Ru(bpy)_3Cl_2•6H_2O$, and 0.59 mL (4.0 mmol) 4-trifluoromethylstyrene in MeCN with a total volume of 8 mL (0.05 M). Isolation of products was performed by FCC with 1:1 Et_2O/pentanes to give 105 mg (0.27 mmol, 68% yield) of two diastereomers (1.7:1 d.r.). Separation of diastereomers for characterization purposes was achieved by automated FCC (ISCO) using a continuous gradient of 15% → 100% EtOAc in hexanes. Major Diastereomer: Viscous

oil/semisolid. ν_{max} (film) / cm^{-1} 2945, 1667, 1619, 1410, 1325, 1236, 1163, 1121, 1068, 1017, 912, 834, 770, 699. ^{1}H NMR (500 MHz, $CDCl_3$) δ 7.56 (d, *J* = 8.3 Hz, 2H), 7.40 (d, *J* = 8.3 Hz, 2H), 7.28–7.27 (m, 4H), 7.21–7.18 (m, 1H), 7.15 (s, 1H), 7.05 (s, 1H), 4.61 (q, *J* = 9.3 Hz, 1H), 4.07 (t, *J* = 9.9 Hz, 1H), 4.03 (s, 3H), 3.68, (q, *J* = 9.3 Hz, 1H), 2.86 (dt, *J* = 10.2, 8.4 Hz, 1H), 2.36 (q, *J* = 10.3 Hz, 1H). ^{13}C NMR (125 MHz, $CDCl_3$) δ 192.07, 147.59 (q, *J* = 1.2 Hz), 142.52, 141.94, 129.50, 128.51, 127.40, 127.25, 126.89, 126.71, 125.34 (q, *J* = 3.7 Hz), 124.29 (q, *J* = 272.2 Hz), 48.63, 44.88, 43.23, 36.18, 31.50. ^{19}F NMR (377 MHz, $CDCl_3$) δ –62.34. HRMS (ESI) calculated for $[C_{22}H_{20}F_3N_2O]^+$ ($M+H^+$) requires *m/z* 385.1522, found 385.1518. Minor Diastereomer: Viscous oil/semisolid. ν_{max} (film) / cm^{-1} 2937, 1669, 1618, 1409, 1325, 1162, 1115, 1069, 1017, 914, 837, 773, 699, 642. ^{1}H NMR (500 MHz, $CDCl_3$) δ 7.37 (d, *J* = 8.2 Hz, 2H), 7.19–7.16 (m, 3H), 7.09–7.05 (m, 3H), 7.02–6.97 (m, 3H), 5.05 (q, *J* = 8.8 Hz, 1H), 4.51 (t, *J* = 9.4 Hz, 1H), 4.07–4.02 (m, 1H), 4.04 (s, 3H), 2.82–2.73 (m, 2H). ^{13}C NMR (125 MHz, $CDCl_3$) δ 192.62, 145.08 (q, *J* = 1.3 Hz), 142.47, 139.02, 129.51, 128.46, 127.89, 127.78, 127.47, 126.14, 124.73 (q, *J* = 3.8 Hz), 124.25 (q, *J* = 272.3 Hz), 45.70, 43.50, 41.84, 36.24, 28.47. ^{19}F NMR (377 MHz, $CDCl_3$) δ –62.34. HRMS (ESI) calculated for $[C_{22}H_{20}F_3N_2O]^+$ ($M+H^+$) requires *m/z* 385.1522, found 385.1519.

(3-(4-methoxyphenyl)-2-phenylcyclobutyl)(1-methyl-1H-imidazol-2-yl)methanone (3.24):

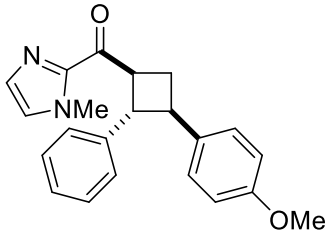

Prepared according to general procedure for isolation scale experiments using 84.5 mg (0.4 mmol) 2-cinnamoyl-1-methyl-1*H*-imidazole, 15.0 mg (0.08 mmol) *p*-toluenesulfonic acid monohydrate, 7.6 mg (0.01 mmol) $Ru(bpy)_3Cl_2•6H_2O$, and 0.53 mL (4.0 mmol) 4-methoxystyrene in MeCN with a total volume of 8 mL (0.05 M). Isolation of products was performed by FCC with 1:1

Et_2O/pentanes to give 97 mg (0.28 mmol, 70% yield) of two diastereomers (1.5:1 d.r.). Separation of major diastereomer for characterization purposes was achieved by manual FCC using a gradient of 1:2 → 1:1 Et_2O/pentanes. Major Diastereomer: White solid (mp = 83–85 °C). ν_{max} (film) / cm^{-1} 2934, 1666, 1611, 1513, 1409, 1291, 1248, 1177, 1033, 829, 699. ^1H NMR (500 MHz, $CDCl_3$) δ 7.27–7.23 (m, 6H), 7.18–7.15 (m, 1H), 7.15 (s, 1H), 7.04 (s, 1H), 6.85 (d, *J* = 8.7 Hz, 2H), 4.56 (td, *J* = 9.7, 8.6 Hz, 1H), 4.04–4.00 (m, 1H), 4.03 (s, 3H), 3.79 (s, 3H), 3.54 (td, *J* = 10.1, 8.2 Hz, 1H), 2.80 (dt, *J* = 10.2, 8.4 Hz, 1H), 2.27 (q, *J* = 10.2 Hz, 1H). ^{13}C NMR (125 MHz, $CDCl_3$) δ 192.55, 158.22, 142.67, 142.56, 135.76, 129.39, 128.33, 128.01, 127.25, 126.90, 126.37, 113.78, 55.27, 48.97, 44.72, 43.05, 36.18, 32.23. HRMS (ESI) calculated for $[C_{22}H_{23}N_2O_2]^+$ ($M+H^+$) - requires *m/z* 347.1754, found 547.1754. Minor Diastereomer: Unable to separate from major diastereomer cleanly.

(1-methyl-1H-imidazol-2-yl)(2-phenyl-3-(o-tolyl)cyclobutyl)methanone (3.25): Prepared

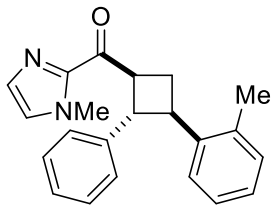

according to general procedure for isolation scale experiments using 85.0 mg (0.4 mmol) 2-cinnamoyl-1-methyl-1*H*-imidazole, 15.8 mg (0.08 mmol) *p*-toluenesulfonic acid monohydrate, 7.2 mg (0.01 mmol) $Ru(bpy)_3Cl_2•6H_2O$, and 0.52 mL (4.0 mmol) 2-methylstyrene in MeCN with a total volume of 8 mL (0.05 M). Isolation of products was performed by FCC with 1:1 Et_2O/pentanes to give 79 mg (0.24 mmol, 60% yield) of two diastereomers (1.5:1 d.r.). Separation of major diastereomer for characterization purposes was achieved by automated FCC (ISCO) using a continuous gradient of 15% → 100% EtOAc in hexanes. Major Diastereomer: White solid (mp = 94–97 °C). ν_{max} (film) / cm^{-1} 2949, 1666, 1458, 1409, 1289, 1235, 1155, 1024, 913, 856, 754, 699, 662. ^1H NMR (500 MHz, $CDCl_3$) δ 7.47 (d, *J* = 7.5 Hz, 1H), 7.30 (d, *J* = 7.5 Hz, 2H), 7.27–7.24 (m, 2H), 7.22–7.19

(m, 1H), 7.18–7.15 (m, 2H), 7.15–7.11 (m, 2H), 7.04 (s, 1H), 4.53 (q, *J* = 9.1 Hz, 1H), 4.29 (t, *J* = 9.9 Hz, 1H), 4.03 (s, 3H), 3.81 (td, *J* = 10.1, 8.1 Hz, 1H), 2.95 (dt, *J* = 10.1, 8.4 Hz, 1H), 2.22 (s, 3H), 2.11 (q, *J* = 10.1 Hz, 1H). ^{13}C NMR (125 MHz, $CDCl_3$) δ. HRMS (ESI) calculated for $[C_{22}H_{23}N_2O]^+$ ($M+H^+$) requires *m/z* 331.1805, found 331.1801. Minor Diastereomer: Unable to separate from major diastereomer cleanly.

(1-methyl-1H-imidazol-2-yl)((3-methyl-2,3-diphenylcyclobutyl)methanone (3.26): Prepared

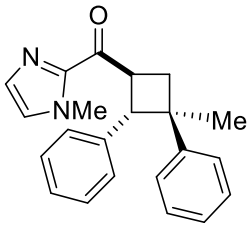

according to general procedure for isolation scale experiments using 86.0 mg (0.4 mmol) 2-cinnamoyl-1-methyl-1*H*-imidazole, 15.6 mg (0.08 mmol) *p*-toluenesulfonic acid monohydrate, 8.1 mg (0.01 mmol) $Ru(bpy)_3Cl_2•6H_2O$, and 0.52 mL (4.0 mmol) α-methylstyrene in MeCN with a total volume of 8 mL (0.05 M). Isolation of products was performed by FCC with 1:1 Et_2O/pentanes to give 70.5 mg (0.21 mmol, 53 % yield) of two diastereomers (2.1:1 d.r.). Separation of diastereomers for characterization purposes was achieved by manual FCC using a gradient of 1:3 → 1:1 Et_2O/pentanes. Major Diastereomer: Viscous oil/semisolid. ν_{max} (film) / cm^{-1} 2959, 1665, 1496, 1444, 1408, 1291, 1234, 1155, 1080, 1030, 914, 839, 767, 699, 664. ^{1}H NMR (500 MHz, $CDCl_3$) δ 7.40–7.38 (m, 2H), 7.36–7.28 (m, 6H). 7.23–7.19 (m, 1H), 7.19 (s, 1H), 7.04 (s, 1H), 4.98 (q, *J* = 9.5 Hz, 1H), 4.27(d, *J* = 10.1 Hz, 1H), 2.62 (t, *J* = 10.2 Hz), 2.45 (dd, *J* = 10.3, 9.3 Hz), 1.34 (s, 3H). ^{13}C NMR (125 MHz, $CDCl_3$) δ 192.85, 150.44, 142.80, 139.42, 129.34, 128.30, 128.22, 128.10, 127.35, 126.44, 125.79, 125.41, 50.66, 43.32, 40.40, 37.24, 36.20, 23.97. HRMS (ESI) calculated for $[C_{22}H_{23}N_2O]^+$ ($M+H^+$) - requires *m/z* 331.1805, found 331.1800. Minor Diastereomer: Viscous oil/semisolid. ν_{max} (film) / cm^{-1} 2956, 1667, 1602, 1496, 1452, 1408, 1291, 1155, 1031, 984, 915, 765, 698, 662. ^{1}H NMR (500 MHz, $CDCl_3$) δ 7.15 (d, *J* = 0.8 Hz, 1H), 7.13–7.10 (m, 2H), 7.07–7.03 (m, 6H), 7.02 (s, 1H),

6.91 (dd, *J* = 8.0, 1.7 Hz, 2H), 4.78 (q, *J* = 9.5 Hz, 1H), 4.01 (d, *J* = 10.0 Hz, 1H), 4.00 (s, 3H), 3.11 (dd, *J* = 11.6, 9.1 Hz, 1H), 2.34 (dd, *J* = 11.6, 9.7 Hz, 1H), 1.68 (s, 3H). ^{13}C NMR (125 MHz, $CDCl_3$) δ 192.94, 143.32, 142.80, 139.47, 129.37, 128.20, 127.62, 127.59, 127.28, 127.23, 126.17, 125.59, 54.02 45.88, 40.98, 36.20, 35.54, 31.41. HRMS (ESI) calculated for $[C_{22}H_{23}N_2O]^+$ ($M+H^+$) requires *m/z* 331.1805, found 331.1802.

(1-methyl-1H-imidazol-2-yl)(1-phenylspiro[3.4]octan-2-yl)methanone (3.27): Prepared

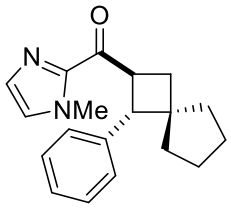

according to general procedure for isolation scale experiments using 85.4 mg (0.4 mmol) 2-cinnamoyl-1-methyl-1*H*-imidazole, 16.4 mg (0.08 mmol) *p*-toluenesulfonic acid monohydrate, 7.5 mg (0.01 mmol) $Ru(bpy)_3Cl_2•6H_2O$, and 0.42 mL (4.0 mmol) methylenecyclohexane in MeCN with a total volume of 8 mL (0.05 M). Isolation of products was performed by FCC with 1:1 Et_2O/pentanes to give 35 mg (0.12 mmol, 30% yield) of a single diastereomer (>10:1 d.r.). White solid (mp = 100–105 °C). ν_{max} (film) / cm^{-1} 2931, 1665, 1497, 1407, 1289, 1154, 1031, 915, 765, 699. ^{1}H NMR (500 MHz, $CDCl_3$) δ 7.28–7.26 (m, 4H), 7.19–7.15 (m, 1H), 7.16 (s, 1H), 7.02 (s, 1H), 4.79 (q, *J* = 9.5 Hz, 1H), 3.98 (s, 3H), 3.91 (d, *J* = 10.0 Hz, 1H), 2.21 (t, *J* = 9.6 Hz, 1H), 2.06 (t, *J* = 9.8 Hz, 1H), 1.83–1.72 (m, 2H), 1.55–1.45 (m, 4H), 1.32–1.27(m, 2H) . ^{13}C NMR (125 MHz, $CDCl_3$) δ 193.10, 142.85, 139.90, 129.24, 128.04, 127.76, 127.18, 126.15, 49.02, 48.57, 40.44, 39.70, 38.19, 36.19, 33.34. HRMS (ESI) calculated for $[C_{19}H_{23}N_2O]^+$ ($M+H^+$) requires *m/z* 295.1805, found 295.1805.

(1-methyl-1H-imidazol-2-yl)(3-methyl-2-phenyl-3-(prop-1-en-2-yl)cyclobutyl)methanone

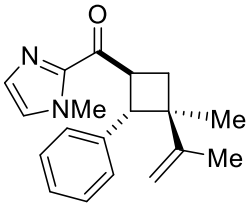

(3.28): Prepared according to general procedure for isolation scale experiments using 84.9 mg (0.4 mmol) 2-cinnamoyl-1-methyl-1*H*-imidazole, 15.1 mg (0.08 mmol) *p*-toluenesulfonic acid monohydrate, 7.4 mg (0.01 mmol) $Ru(bpy)_3Cl_2•6H_2O$, and 0.45 mL (4.0 mmol) 2,3-dimethylbutadiene in MeCN with a total volume of 8 mL (0.05 M). Isolation of products was performed by FCC with 1:1 Et_2O/pentanes to give 78 mg (0.26 mmol, 66% yield) of two diastereomers (7:1 d.r.). Separation of major diastereomer for characterization purposes was achieved by manual FCC using a gradient of 1:2 → 1:1 Et_2O/pentanes. Major Diastereomer: White solid (mp = 100–103 °C). ν_{max} (film) / cm^{-1} 2962, 1665, 1513, 1407, 1290, 1239, 1154, 1031, 915, 838, 767, 699. ^1H NMR (500 MHz, $CDCl_3$) δ 7.30–7.25 (m, 4H), 7.19–7.16 (m, 1H), 7.18 (s, 1H), 7.04 (s, 1H), 4.91 (s, 1H), 4.84 (m, 1H), 4.79 (q, *J* = 9.5 Hz, 1H), 4.13 (d, *J* = 9.9 Hz, 1H), 3.99 (s, 3H), 2.28 (t, *J* = 9.8 Hz, 1H), 2.19 (t, *J* = 9.7 Hz, 1H), 1.78 (s, 3H), 1.10 (s, 3H). ^{13}C NMR (125 MHz, $CDCl_3$) δ 193.07, 152.58, 142.78, 139.94, 129.30, 128.17, 127.97, 127.27, 126.14, 108.79, 47.67, 44.93, 39.92, 36.20, 36.11, 21.29, 18.99. HRMS (ESI) calculated for $[C_{19}H_{23}N_2O]^+$ ($M+H^+$) requires *m/z* 295.1805, found 295.1806. Minor Diastereomer: Unable to separate from major diastereomer cleanly.

(1-methyl-1H-imidazol-2-yl)(2-phenyl-3-(phenylthio)cyclobutyl)methanone (3.29): Prepared

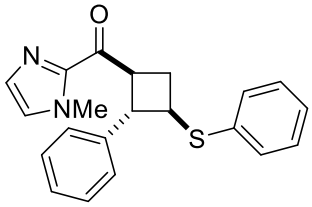

according to general procedure for isolation scale experiments using 85.1 mg (0.4 mmol) 2-cinnamoyl-1-methyl-1*H*-imidazole, 16.0 mg (0.08 mmol) *p*-toluenesulfonic acid monohydrate, 7.6 mg (0.01 mmol) $Ru(bpy)_3Cl_2•6H_2O$, and 0.52 mL (4.0 mmol) phenyl vinyl sulfide in MeCN with a total volume of 8 mL (0.05 M). Isolation of products was performed by FCC with 1:1 Et_2O/pentanes to give 110

mg (0.31 mmol, 79% yield) of two diastereomers (1.4:1 d.r.). Separation of diastereomers for characterization purposes was achieved by manual FCC using a gradient of 10% → 30% EtOAc in pentanes. Major Diastereomer: White solid (mp = 81–84 °C). ν_{max} (film) / cm^{-1} 2944, 1665, 1583, 1496, 1479, 1438, 1407, 1289, 1233, 1155, 1090, 1024, 845, 740, 699. ^{1}H NMR (500 MHz, $CDCl_3$) δ 7.34 (d, *J* = 7.6 Hz, 2H), 7.30–7.27 (m, 4H), 7.25–7.16 (m, 4H), 7.12 (s, 1H), 7.02 (s, 1H), 4.49 (q, *J* = 9.4 Hz, 1H), 3.99 (s, 3H), 3.93 (t, *J* = 9.5 Hz, 1H), 3.85 (td, *J* = 9.6, 7.5 Hz, 1H), 2.94 (dt, *J* = 10.7, 8.2 Hz, 1H), 2.20 (q, *J* = 10.0 Hz, 1H). ^{13}C NMR (125 MHz, $CDCl_3$) δ 190.73, 142.28, 141.01, 135.18, 130.84, 129.44, 128.82, 128.44, 127.31, 126.96, 126.82, 126.56, 48.39, 45.20, 44.76, 36.11, 33.99. HRMS (ESI) calculated for $[C_{21}H_{21}N_2OS]^+$ ($M+H^+$) requires *m/z* 349.1369, found 349.1369. Minor Diastereomer: White solid (mp = 105–107 °C). ν_{max} (film) / cm^{-1} 2939, 1664, 1585, 1480, 1438, 1407, 1289, 1224, 1155, 1026, 915, 837, 739, 697. ^{1}H NMR (500 MHz, $CDCl_3$) δ 7.36 (d, *J* = 7.8 Hz, 2H), 7.29 (t, *J* = 7.7 Hz, 2H), z7.22 (t, *J* = 7.3 Hz, 1H), 7.18–7.15 (m, 3H), 7.11–7.07 (m, 3H), 7.04 (s, 1H), 5.14 (q, *J* = 9.0 Hz, 1H), 4.47 (t, *J* = 8.5 Hz, 1H), 4.36 (td, *J* = 8.0, 3.3 Hz, 1H), 4.01 (s, 3H), 2.76 (dt, *J* = 11.9, 7.9 Hz, 1H), 2.47 (ddd, *J* = 12.1, 9.7, 3.0 Hz, 1H). ^{13}C NMR (125 MHz, $CDCl_3$) δ 192.29, 142.38, 138.28, 136.12, 129.53, 129.16, 128.61, 128.27, 127.93, 127.41, 126.89, 125.59, 44.41, 43.62, 43.59, 36.17, 31.85. HRMS (ESI) calculated for $[C_{21}H_{21}N_2OS]^+$ ($M+H^+$) requires *m/z* 349.1369, found 349.1369.

(1-methyl-1H-imidazol-2-yl)(2-phenyl-2,2a,7,7a-tetrahydro-1H-cyclobuta[*a*]inden-1-yl)methanone (3.32): Prepared according to general procedure for isolation scale experiments using 84.5 mg (0.4 mmol) 2-cinnamoyl-1-methyl-1*H*-imidazole, 15.8 mg (0.08 mmol) *p*-toluenesulfonic acid monohydrate, 7.6 mg (0.01 mmol) $Ru(bpy)_3Cl_2•6H_2O$, and 0.47 mL (4.0 mmol) indene in MeCN

with a total volume of 8 mL (0.05 M). Isolation of products was performed by FCC with 1:1 Et_2O/pentanes to give 82 mg (0.25 mmol, 62% yield) of two diastereomers (1.1:1 d.r.). Separation of diastereomers for characterization purposes was achieved by manual FCC using a gradient of 10% → 30% EtOAc in pentanes. Major Diastereomer: Viscous oil/semisolid. ν_{max} (film) / cm^{-1} 2923, 1663, 1407, 1291, 1154, 872, 772, 699, 662. ^{1}H NMR (500 MHz, $CDCl_3$) δ 7.32 (d, *J* = 7.6 Hz, 1H), 7.16–7.09 (m, 5H), 7.02 (s, 1H), 6.99 (d, *J* = 7.6 Hz, 2H), 6.90 (t, *J* = 7.6 Hz, 1H), 6.41 (d, *J* = 7.6 Hz, 1H), 4.55 (dd, *J* = 9.7, 7.5 Hz, 1H), 4.44 (t, *J* = 9.5 Hz, 1H), 4.10 (t, *J* = 7.7 Hz, 1H), 4.00 (s, 3H), 3.43 (d, *J* = 16.3 Hz, 1H), 3.24 (q, *J* = 7.1 Hz, 1H), 3.15 (dd, *J* = 16.5, 7.4 Hz, 1H). ^{13}C NMR (125 MHz, $CDCl_3$) δ 192.50, 144.35, 142.99, 141.57, 139.28, 129.32, 128.18, 127.68, 127.33 (2C), 126.86, 126.15, 125.67, 125.61, 49.85, 48.56, 43.35, 39.89, 38.32, 36.15. HRMS (ESI) calculated for $[C_{22}H_{21}N_2O]^+$ ($M+H^+$) requires *m/z* 329.1648, found 329.1648. Minor Diastereomer: Viscous oil/semisolid. ν_{max} (film) / cm^{-1}, 2955, 1665, 1496, 1458, 1407, 1289, 1154, 1007, 917, 866, 756, 699. ^{1}H NMR (500 MHz, $CDCl_3$) δ 7.37–7.31 (m, 4H), 7.23–7.14 (m, 6H), 7.04 (s, 1H), 4.69 (t, *J* = 9.3 Hz, 1H), 4.01 (s, 3H), 3.98 (dd, *J* = 9.0, 7.0 Hz, 1H), 3.93 (t, *J* = 7.1 Hz, 1H), 3.86–3.80 (m, 1H), 3.09 (dd, *J* = 17.5, 10.0 Hz, 1H), 2.93 (dd, *J* = 17.5, 5.0 Hz, 1H). ^{13}C NMR (125 MHz, $CDCl_3$) δ 191.63, 146.03, 145.11, 143.58, 142.62, 129.37, 128.49, 126.82, 126.76, 126.67, 126.66, 126.25, 124.98, 123.57, 50.71, 49.72, 46.24, 39.47, 36.10, 34.19. HRMS (ESI) calculated for $[C_{22}H_{21}N_2O]^+$ ($M+H^+$) requires *m/z* 329.1648, found 329.1648.

3.5.4 Derivitization of Cyclobutane Products

Large Scale Synthesis of 2: A 50 mL RBF with a stir bar was charged with 427.3 mg (2.0 mmol) 2-cinnamoyl-1-methyl-1*H*-imidazole, 79.3 mg (0.40 mmol) *p*-toluenesulfonic acid monohydrate, 37.5 mg (0.05 mmol) $Ru(bpy)_3Cl_2$•$6H_2O$, and dry MeCN (40 mL), then fitted with a septum. A

volume 2.3 mL (20.0 mmol) styrene was added and the reaction sparged with N_2 for 20 minutes. The reaction was then stirred in front of a of a blue LED lamp for 48 h. The mixture was diluted with 50 mL Et_2O, pushed through a short plug of silica, and the plug washed with 50 mL Et_2O. The resulting colorless solution was concentrated and purified by FCC with 1:1 Et_2O/pentanes to give 410 mg (1.3 mmol, 64% yield) of a viscous oil composed of two diastereomers (~2:1 d.r.).

Scheme 3-6. Procedure for the conversion of 2-acyl imidazoles to carboxylic acid derivatives

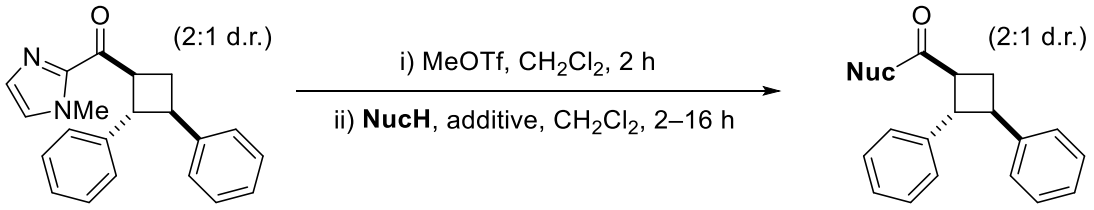

General Procedure for [2+2] Cycloadduct Derivatizations (Scheme 3-6): An oven-dried 1.5 dram vial with a small stir bar was charged with cyclobutane **2** (0.20–0.30 mmol, 1.0 equiv.) as a 2:1 mixture of diastereomers. This vial was fitted with a cap with a Teflon septum, then CH_2Cl_2 added (0.1–0.2 M in cyclobutane). This solution was stirred under a flow of N_2 for 5 minutes before freshly distilled MeOTf (1.2-1.4 equiv.) was added. The reaction mixture was sealed and stirred for 2 hours. At this point the starting material appeared entirely consumed or trace by TLC. The solvent and any remaining MeOTf were removed under vacuum and the resulting colorless solid dried under high vacuum for 30 minutes. After redissolving the salt in CH_2Cl_2 (0.1–0.2 M in cyclobutane), nucleophile (20.0–45.0 equiv.) was added. For ROH nucleophiles, 1,4-diazabicyclo[2.2.2]octane (DABCO, 0.2 equiv.) was also added. The reactions were then stirred for 2–16 h. Upon completion, the mixtures were directly concentrated and then purified by FCC.

Methyl-2,3-diphenylcyclobutane-1-carboxylate (3.33): Prepared according to general procedure for derivatizations using 95.0 mg (0.30 mmol) cyclobutane **2** (2:1 mixture of diastereomers), 40 µL (0.36 mmol) MeOTf, and 1.5 mL (0.2 M) CH_2Cl_2 for the methylation step. For the nucleophile displacement step, 0.57 mL (14.0 mmol) MeOH, 8.2 mg DABCO (0.07 mmol), and 1.5 (0.2 M) CH_2Cl_2 were used. Reaction time: 2 hours. The resulting mixture was purified by FCC with 5% Et_2O in pentanes to give 66.7 mg (0.25 mmol, 83% yield) clear oil composed of two diastereomers (2:1 d.r.). Spectroscopic data for the major diastereomer was consistent with that previously reported.[27] ^{1}H NMR (500 MHz, $CDCl_3$) δ 7.35–7.19 (m, 10H), 3.85 (t, *J* = 9.7 Hz, 1H), 3.72 (s, 3H), 3.53 (td, *J* = 10.1, 8.3 Hz, 1H) 3.20 (td, *J* = 9.7, 8.4 Hz, 1H), 2.62 (dt, *J* = 10.6, 8.3 Hz, 1H) 2.41 (q, *J* = 10.4 Hz, 1H).

Isopropyl-2,3-diphenylcyclobutane-1-carboxylate (3.34): Prepared according to general procedure for derivatization experiments using 96.5 mg (0.30 mmol) cyclobutane **2** (2:1 mixture of diastereomers), 40 µL (0.36 mmol) MeOTf, and 1.5 mL (0.2 M) CH_2Cl_2 for the methylation step. For the nucleophile displacement step, 0.91 mL (12.0 mmol) *i*PrOH, 6.2 mg DABCO (0.06 mmol), and 1.5 (0.2 M) CH_2Cl_2 were used. Reaction time: 2 hours. The resulting mixture was purified by FCC with 5% Et_2O in pentanes to give 76.7 mg (0.26 mmol, 85% yield) clear oil composed of two diastereomers (2:1 d.r.). Spectroscopic data for the major diastereomer was consistent with that previously reported.[27] ^{1}H NMR (500 MHz, $CDCl_3$) δ 7.35–7.19 (m, 10H), 5.06 (sept, *J* = 6.4 Hz, 1H), 3.84 (t, *J* = 9.9 Hz, 1H), 3.55 (td, *J* = 10.1, 8.3 Hz, 1H), 3.12 (td, *J* = 9.8, 8.4 Hz, 1H), 2.62 (dt, *J* = 10.5, 8.4 Hz, 1H), 2.38 (q, *J* = 10.4 Hz, 1H), 1.25 (d, *J* = 6.3 Hz, 3H), 1.24 (d, *J* = 6.3 Hz, 3H).

***N*-benzyl-2,3-diphenylcyclobutane-1-carboxamide (3.35):** Prepared according to general procedure for derivatizations using 61.1 mg (0.19 mmol) cyclobutane **2** (2:1 mixture of diastereomers), 30 µL (0.27 mmol) MeOTf, and 2.0 mL (0.1 M) CH_2Cl_2 for the methylation step. For the nucleophile displacement step, 0.44 mL (4.0 mmol) benzylamine and 2.0 mL (0.1 M) CH_2Cl_2 were used. Reaction time: 16 hours. The resulting mixture was purified by FCC with 1:1 Et_2O/pentanes to give 53.4 mg (0.16 mmol, 81% yield) of two diastereomers (2:1 d.r.). Separation of these diastereomers for characterization purposes was achieved by automated FCC (ISCO) using a continuous gradient of 15% → 100% EtOAc in hexanes. Major Diastereomer: White solid (mp = 144–146 °C). ν_{max} (film) / cm^{-1} 3277, 3028, 2927, 1640, 1603, 1543, 1495, 1454, 1358, 1249, 1080, 1029. ^{1}H NMR (500 MHz, $CDCl_3$) δ 7.34–7.19 (m, 15H), 5.57 (br s, 1H), 4.50–4.42 (m, 2H), 3.81(t, *J* = 9.7 Hz, 1H), 3.57 (td, *J* = 10.1, 8.3 Hz, 1H), 2.94 (td, *J* = 9.6, 8.0 Hz, 1H), 2.59–2.48 (m, 2H). ^{13}C NMR (125 MHz, $CDCl_3$) δ 172.97, 143.17, 142.09, 138.26, 128.71, 128.66, 128.40, 127.76, 127.52, 126.85 (2C), 126.83, 126.51, 51.38, 44.41, 43.61, 42.86, 28.77. HRMS (ESI) calculated for $[C_{24}H_{24}NO]^+$ ($M+H^+$) requires *m/z* 342.1852, found 342.1850. Minor Diastereomer: Colorless oil. ν_{max} (film) / cm^{-1} 3277, 3060, 3028, 1638, 1603, 1541, 1495, 1454, 1388, 1357, 1245, 1074, 1029, 1013, 910. ^{1}H NMR (500 MHz, $CDCl_3$) δ 7.32–7.27 (m, 3H), 7.21 (d, *J* = 7.0 Hz, 2H), 7.12 (t, *J* = 7.4 Hz, 2H), 7.09 –7.02 (m, 4H), 6.96 (d, *J* = 7.5 Hz, 2H), 6.85 (d, *J* = 7.0 Hz, 2H), 5.60 (br s, 1H), 4.50–4.39 (m, 2H), 4.24 (t, *J* = 9.2 Hz, 1H), 3.99 (td, *J* = 9.3, 4.0 Hz, 1H), 3.48 (q, *J* = 8.9 Hz, 1H), 2.86 (dt, *J* = 12.0, 8.8 Hz, 1H), 2.59 (ddd, *J* = 12.2, 8.7, 4.0 Hz, 1H). ^{13}C NMR (125 MHz, $CDCl_3$) δ 173.73, 140.20, 139.26, 138.25, 128.70, 128.07, 127.94, 127.91, 127.84, 127.65, 127.48, 126.32, 125.93, 48.11, 43.57, 42.85, 42.16, 26.12. HRMS (ESI) calculated for $[C_{24}H_{24}NO]^+$ ($M+H^+$) requires *m/z* 342.1852, found 342.1849.

(2,3-diphenylcyclobutyl)(pyrrolidin-1-yl)methanone (3.36): Prepared according to general procedure for derivatization experiments using 85.2 mg (0.27 mmol) cyclobutane **2** (2:1 mixture of diastereomers), 40 µL (0.36 mmol) MeOTf, and 2.0 mL (0.1 M) CH_2Cl_2 for the methylation step. For the nucleophile displacement step, 0.44 mL (5.4 mmol) pyrrolidine and 2.0 mL (0.1 M) CH_2Cl_2 were used. Reaction time: 16 hours. The resulting mixture was purified by FCC with 1:1 EtOAc/pentanes with 2% Et_3N to give 58.9 mg (0.19 mmol, 72% yield) of two diastereomers (2:1 d.r.). Separation of these diastereomers for characterization purposes was achieved by manual FCC using 1:1 EtOAc/pentanes with 2% Et_3N. Major Diastereomer: White solid (mp = 99–101 °C). ν_{max} (film) / cm^{-1} 2973, 2872, 1628, 1495, 1434, 1341, 1226, 1190, 1030, 914, 843. ^1H NMR (500 MHz, $CDCl_3$) δ 7.31–7.27 (m, 8H), 7.22–7.17 (m, 2H), 4.01 (t, *J* = 9.8 Hz, 1H), 3.59 (td, *J* = 10.1, 8.4 Hz, 1H), 3.50–3.47 (m, 2H), 3.35–3.30 (m, 1H), 3.24–3.17 (m, 2H), 2.60 (dt, *J* = 10.3, 8.3 Hz, 1H), 2.40 (q, *J* = 10.2 Hz, 1H), 1.91–1.79 (m, 4H). ^{13}C NMR (125 MHz, $CDCl_3$) δ 171.68, 143.50, 142.91, 128.44, 128.34, 126.95, 126.88, 126.50, 126.38, 49.98, 46.09, 45.81, 42.85, 42.72, 29.43, 26.06, 24.24. HRMS (ESI) calculated for $[C_{21}H_{24}NO]^+$ ($M+H^+$) requires *m/z* 306.1852, found 306.1848. Minor Diastereomer: White solid (mp = 97–99 °C). ν_{max} (film) / cm^{-1} 2928, 2872, 1629, 1496, 1432, 1342, 1227, 1192, 1031, 1009, 914. ^1H NMR (500 MHz, $CDCl_3$) δ 7.12 (t, *J* = 7.3 Hz, 2H), 7.08–7.00 (m, 4H), 6.96 (d, *J* = 7.4 Hz, 2H), 6.88 (d, *J* = 7.1 Hz, 2H), 4.32 (dd, *J* = 9.6, 8.0 Hz, 1H), 4.04 (td, *J* = 9.4, 5.3 Hz, 1H), 3.62 (q, *J* = 8.3 Hz, 1H), 3.55–3.46 (m, 2H), 3.40–3.36 (m, 1H), 3.29–3.24 (m, 1H), 2.82 (ddd, *J* = 11.8, 8.8, 7.8 Hz, 1H), 2.62 (ddd, *J* = 11.8, 9.2, 5.2 Hz, 1H), 1.93–1.79 (m, 4H). ^{13}C NMR (125 MHz, $CDCl_3$) δ 172.32, 140.79, 140.09, 128.03, 127.99, 127.82, 127.72, 125.98, 125.74, 47.33, 46.29, 42.92, 41.82, 40.98, 26.39, 26.07, 24.27. HRMS (ESI) calculated for $[C_{21}H_{24}NO]^+$ ($M+H^+$) requires *m/z* 306.1852, found 306.1849.

3.5.5 Assignment of Relative Stereochemistry by 1D-NOE

Figure 3-6. Observed nOe enhancements of diastereomers of **3.18**, **3.28** and **3.32**.

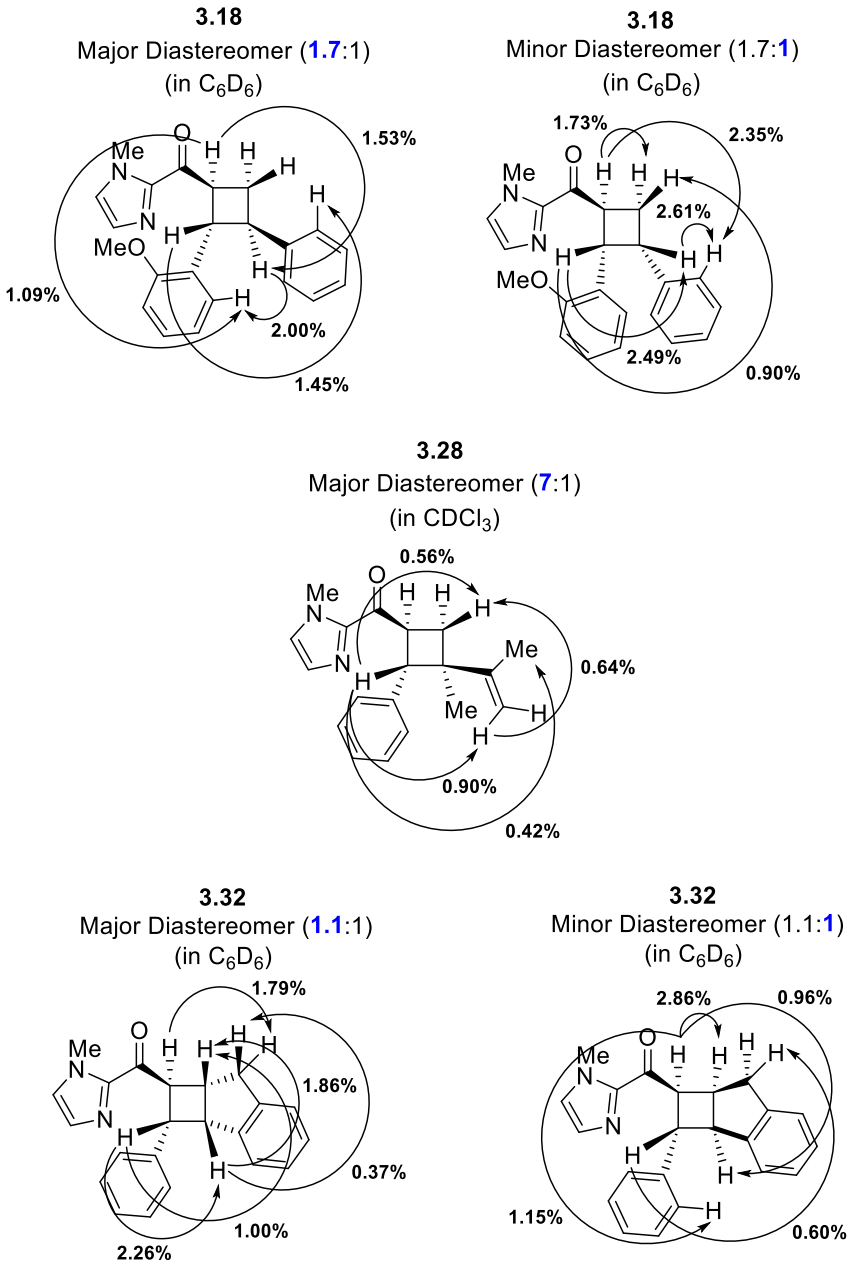

3.5.6 Photocatalyst Data

Figure 3-7. Summary of photochemical properties of $Ru(bpy)_3Cl_2$ and $Ru(4\text{-deeb})_3(PF_6)_2$

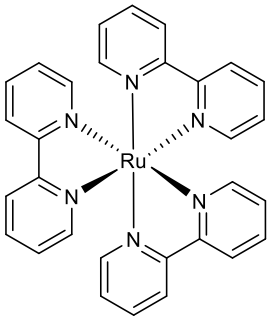

$Ru(bpy)_3Cl_2$
E_0 (2+*/3+) = –0.81
λ_{max} = 613 nm
E_T = 46.6 kcal/mol

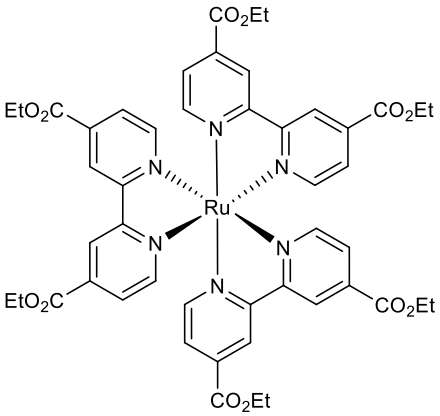

$Ru(4\text{-deeb})_3(PF_6)_2$
E_0 (2+*/3+) = –0.28
λ_{max} = 630 nm
E_T = 45.4 kcal/mol

Figure 3-8. Fluorescence Spectrum for $Ru(4\text{-deeb})_3(PF_6)_2$

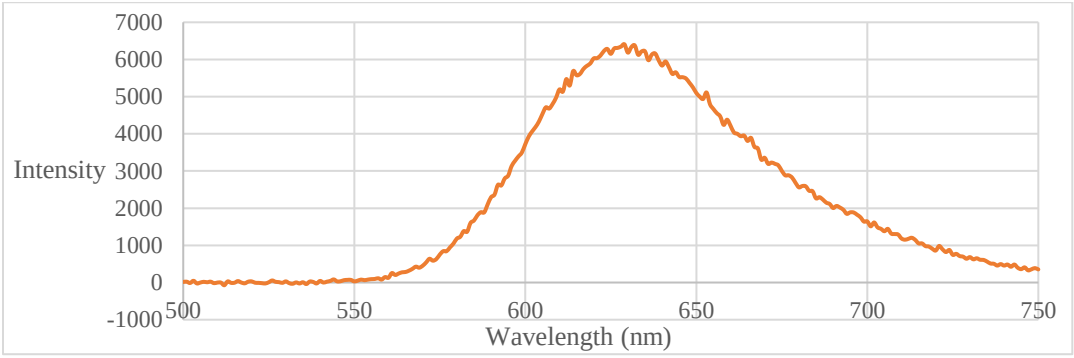

3.5.7 Electrochemical Data

Experimental Details: All cyclic voltammograms (CV) were acquired on a Pine Research Instrumentation Wavenow Potentiostat in MeCN with 0.1 M Bu_4NPF_6 and 1 mM substrate using a platinum auxiliary electrode, a glassy carbon working electrode, and a Ag/AgNO3 reference electrode. All data was referenced versus the ferrocene/ferrocenium (Fc/Fc^+) redox couple through added ferrocene. Data acquired in two passes at a scan rate of 0.05 V/s.

Figure 3-9. CV for cinnamoyl-1-methylimidazole (**3.12**):

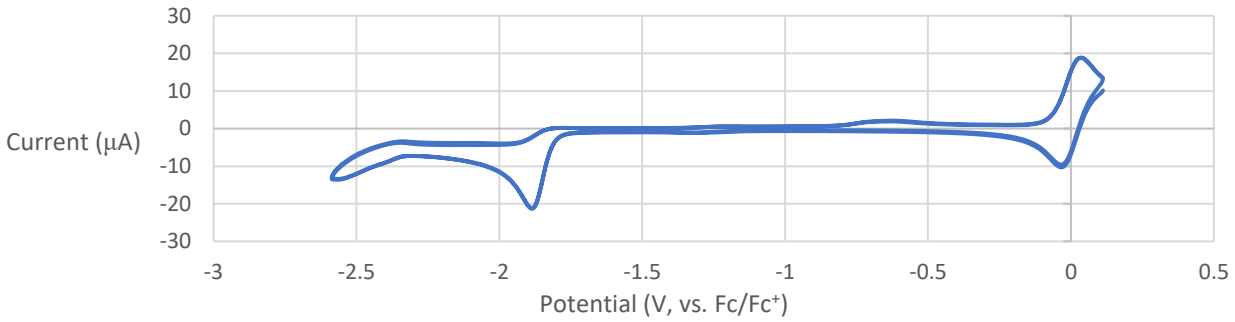

$E_{1/2}$ (vs. Fc/Fc^+) = –1.84 V, $E_{1/2}$ (vs. SCE) = –1.54 V

Figure 3-10. CV for cinnamoyl-1-methylimidazole (**3.12**) + *p*-toluenesulfonic acid monohydrate

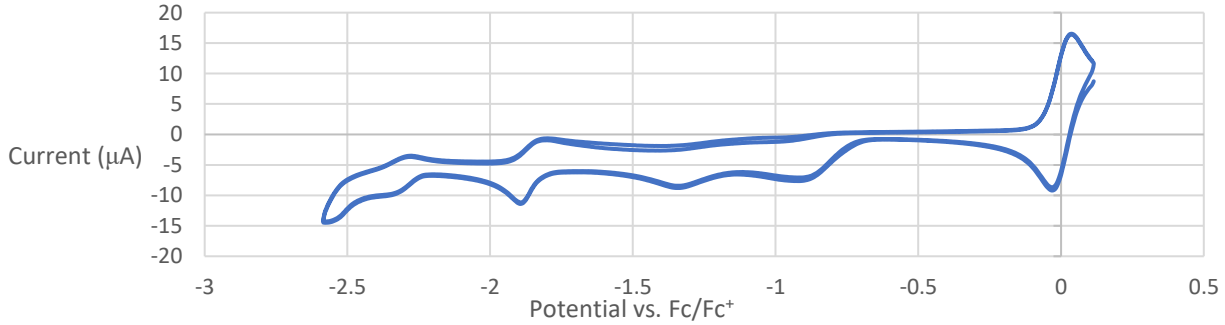

$E_{1/2}$ (vs. Fc/Fc^+) = –0.81 V, $E_{1/2}$ (vs. SCE) = –0.51 V

Figure 3-11. CV for *p*-toluenesulfonic acid monohydrate

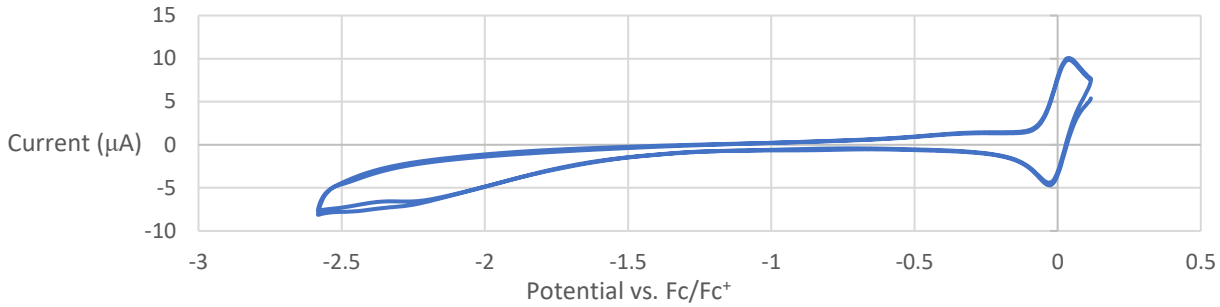

3.5.8 Fluorescence Quenching Data

Experimental Details: Stock solutions of $Ru(bpy)_3Cl_2•6H_2O$, cinnamoyl-1-methylimidazole (**3.12**), *p*-toluenesulfonic acid monohydrate (*p*-TsOH), and a 1:1 mixture of **3.12** and *p*-TsOH were prepared in HPLC-grade CH_3CN. These were combined by volume to give 2.0 mL samples which contained $5x10^{-5}$ M $Ru(bpy)_3Cl_2•6H_2O$, as well as the concentration of reagents indicated in each table below. Each sample was transferred to a 1 cm path cuvette, which was fitted with an appropriate septum, and sparged for 10 minutes prior to data acquisition. Samples were excited @ 450 nm, then emission data collected from 460-700 nm. Emission intensities at 610 nm were recorded, the repeated three-fold and averaged. All fluorescence data was acquired on an ISS PC1 photon counting spectrofluorimeter with a 300 W high-pressure xenon arc lamp.

Table 3-5. Sample Set 0 (blank), Contents: $5x10^{-5}$ M $Ru(bpy)_3Cl_2•6H_2O$

Entry	Concentration, M	Intensity	Average	F/F_0
0-1	N/A	10135	10195	1.000
0-2	N/A	10168		
0-3	N/A	10282		

Table 3-6. Sample Set 1, $5x10^{-5}$ M $Ru(bpy)_3Cl_2•6H_2O$ + **3.12**

Entry	Concentration, M	Intensity	Average	F/F_0
1A-1	0.005	9416	9470	1.077
1A-2	0.005	9475		
1A-3	0.005	9519		
1B-1	0.010	9108	9033	1.129
1B-2	0.010	8972		
1B-3	0.010	9018		
1C-1	0.015	8943	8932	1.141
1C-2	0.015	8893		
1C-3	0.015	8960		
1D-1	0.020	8550	8393	1.215
1D-2	0.020	8273		
1D-3	0.020	8356		
1E-1	0.025	7967	8062	1.265
1E-2	0.025	8139		
1E-3	0.025	8081		

Table 3-7. Sample Set 2, $5x10^{-5}$ M $Ru(bpy)_3Cl_2•6H_2$ + *p*-TsOH

Entry	Concentration, M	Intensity	Average	F/F_0
2A-1	0.005	9861	9697	1.051
2A-2	0.005	9591		
2A-3	0.005	9638		
2B-1	0.010	9968	9884	1.031
2B-2	0.010	9952		
2B-3	0.010	9732		
2C-1	0.015	9644	9467	1.077
2C-2	0.015	9343		
2C-3	0.015	9413		
2D-1	0.020	9673	9719	1.049
2D-2	0.020	9709		
2D-3	0.020	9770		
2E-1	0.025	10016	10006	1.019
2E-2	0.025	9779		
2E-3	0.025	10223		

Table 3-8. Sample Set 3, $5x10^{-5}$ M $Ru(bpy)_3Cl_2•6H_2$ + **3.12** + *p*-TsOH

Entry	Concentration, M	Intensity	Average	F/F_0
3A-1	0.005	7928	7979	1.278
3A-2	0.005	8133		
3A-3	0.005	7876		
3B-1	0.010	5228	5143	1.982
3B-2	0.010	5128		
3B-3	0.010	5072		
3C-1	0.015	4366	3941	2.480
3C-2	0.015	4024		
3C-3	0.015	3941		
3D-1	0.020	3317	3394	3.068
3D-2	0.020	3257		
3D-3	0.020	3394		
3E-1	0.025	2875	2902	3.575
3E-2	0.025	2779		
3E-3	0.025	2902		

5.8.9 Computational Data

General details: The calculations for the present Brønsted acid co-catalyzed photocyclization were carried out using density functional theory[58] (DFT) implemented in the Jaguar 9.1 suite program.[59] Geometry optimization were performed with B3LYP-D3[60–62] levels of theory and 6-31G** basis set.[63] For the Ru metal center, Los Alamos LACVP**[64–66] basis set which is including effective core potentials was applied. Once in the optimized geometries, the single point energies were re-evaluated using triple-ζ quality of basis set, cc-pVTZ(-f)[67], where Ru metal was evaluated with LACV3P** basis set. Vibrational frequencies were evaluated using the optimized structures at the same level as the geometry optimizations. Zero-point energies and entropy correction terms were derived from frequency calculations. Solvation correction energies were calculated from the self-consistent reaction field (SCRF) approximations,[68–70] which is the solution for the linearized Poisson-Boltzmann equations with the proper dielectric constants (ε=37.5 for acetonitrile). Transition states were found by using the quadratic synchronous transit search method (QST).[71] Finally, the solution phase Gibbs free energies were computed as follows:

$$G(Sol) = G(gas) + G^{solv} \quad (2)$$

$$G(gas) = H(gas) - TS(gas) \quad (3)$$

$$H(Gas) = E(SCF) + ZPE \quad (4)$$

$$\Delta G(Sol) = \Sigma G(Sol) \text{ for products} - \Sigma G(Sol) \text{ for reactants} \quad (5)$$

G(Sol) is the solvation corrected Gibbs free energy; G(gas) is the gas phase free energy; H(gas) is the enthalpy in the gas phase; T is the temperature (298.15 K); S(gas) is the entropy in the gas phase; E(SCF) is the electronic energy converged from the self-consistent field method; ZPE is

the vibrational zero-point energy; and S for the vibrational entropy correction. Note that here entropy refers specifically to the vibrational/rotational/translational entropy of the solute(s). The solvent entropies are implicitly included in the continuum model.

Evaluation of triplet energies, frontier orbital energies: To evaluate the triplet energies of substrates (**3.12** and **3.12-H**$^+$) and photocatalyst, we optimized both singlet ground state and the first triplet state geometries. Gibbs free energy of each state was assessed as mentioned previously, and triplet energies were computed through eqn. 6:

$$E_T = G(T_1) - G(S_0) \qquad (6)$$

Figure 3-12. Structure of ^{3}**3.12**

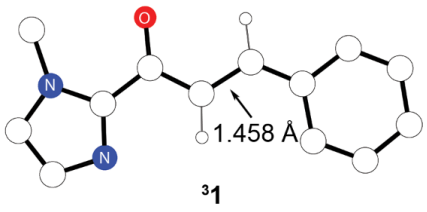

^{3}**1**

E_T = 48.07 kcal/mol

Frontier orbital energy levels were calculated with B3LYP-D3/cc-pVTZ(-f) level. For **3.12** and **3.12-H**$^+$, π and π* orbitals of the C=C bond were found and for $Ru(bpy)_3^{2+}$, two singly occupied molecular orbitals (SOMO) were found and their energies were used for comparison.

Evaluation of vertical reorganization energies: Vertical reorganization energy was evaluated by following Nelson's four-point model.[72] As described in Figure 3-13, the vertical reorganization energy for triplet donor can be assessed as λ_D(triplet), which is the structural reorganization cost required for ^{3}D to ^{1}D geometry change. Similarly, for triplet acceptor molecule, λ_A(singlet) should be assessed, as they changes their geometry from ^{1}A to ^{3}A.

Figure 3-13. Coordinates for triplet donor and acceptor in evaluating vertical reorganization energy.

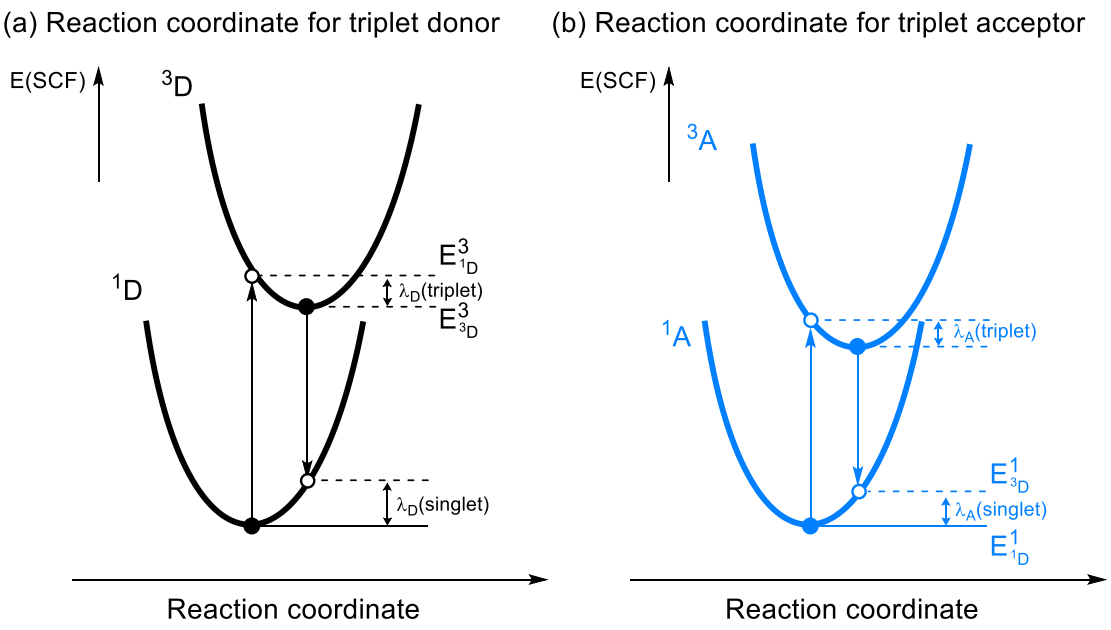

Hence, the reorganization energy of each was calculated using the four-point model with B3LYP-D3/cc-pVTZ(-f) level. Total reorganization energy for the Dexter energy transfer can be computed as below:

$$\lambda = \lambda_D(\text{triplet}) + \lambda_A(\text{singlet}) \quad (7)$$

$$\lambda_D(\text{triplet}) = E^3_{1_D} - E^3_{3_D} \quad (8)$$

$$\lambda_A(\text{singlet}) = E^1_{3_A} - E^1_{1_A} \quad (9)$$

Above, E^y_x is the SCF converged energy of the state y (y = 1 for singlet, 3 for triplet) in gas-phase optimized geometry of x. (x = ^{1}D/^{3}D for singlet/triplet donor, ^{1}A/^{3}A for singlet/triplet acceptor) The computed vertical reorganization energies of **^{1}3.12(≡^{1}I)**, **^{1}3.12H$^+$(≡^{1}IV)** and ^{3}Ru(bpy)$_3^{2+}$ are enumerated in Table 3-9.

Table 3-9. Computed vertical reorganization energies

	$E^3_{1_D}$ (eV)	$E^3_{3_D}$ (ev)	λ_D (kcal/mol)
^{3}Ru(bpy)$_3^{2+}$	-42998. 422	-42999.379	22.07

	$E^1_{3_A}$ (eV)	$E^1_{1_A}$ (ev)	λ_A (kcal/mol)
^{1}1	-18709.127	-18709.588	10.63
^{1}1H+	-18719.670	-18719.945	6.34

Energies, Coordinates, and Vibrational Frequencies of Optimized Structures

Table 3-10. Computed energies of the optimized geometries

	E(SCF)/(eV)	**ZPE/(kcal/mol)**	**S(gas)/(cal/mol·K)**	**G(solv)/(kcal/mol)**
	cc-pVTZ(-f)/ LACV3P**	6-31G**/ LACVP**	6-31G**/ LACVP**	6-31G**/ LACVP**
$^1Ru(bpy)_3^{2+}$	-43001.434	304.61	186.44	-126.09
$^3Ru(bpy)_3^{2+}$	-42999.379	303.16	197.92	-124.76
***p*-TsOH**	-24370.111	89.12	101.30	-14.86
***p*-TsO^-**	-24356.299	82.02	101.33	-68.14
^{1}I(^{1}3.12)	-18709.588	140.91	120.05	-11.29
^{3}I	-18707.348	138.57	124.88	-11.59
^{3}I-TS	-27136.678	223.92	158.71	-12.96
^{3}II	-27137.473	225.61	158.14	-12.01
^{1}II	-27137.520	225.50	155.67	-11.84
^{1}II-TS	-27137.293	225.30	151.35	-12.52
^{1}III	-27139.053	228.73	153.88	-11.75
^{1}IV(^{1}3.12H^+)	-18719.945	149.19	120.26	-55.46
^{3}IV	-18717.982	147.14	125.46	-52.69
^{3}IV-TS	-27147.439	232.45	159.34	-52.05
^{3}V	-27147.760	233.67	158.91	-56.12
^{1}V	-27147.790	233.57	149.28	-56.39
^{1}V-TS	-27147.605	233.68	150.26	-55.99
^{1}VI	-27149.598	236.83	152.79	-51.15

Table 3-11. Cartesian coordinates of the optimized geometries.

==========

$^{1}Ru(bpy)_3^{2+}$

==========

C	-1.657469869	4.599597454	-0.029567523
C	-0.707512379	4.232200623	-0.982709825
C	-0.221517518	2.930230379	-0.972596109
C	-1.560348511	2.357465744	0.857971132
C	-2.085834026	3.652616024	0.896282613
C	-1.948890448	1.282713532	1.796257257
C	-1.630765676	-0.951297641	2.412594795
C	-2.553867102	-0.847897649	3.446117163
C	-3.193097115	0.374445766	3.653684139
C	-2.885608196	1.446836114	2.821198463
C	-2.696708202	-0.660598397	-1.260902405
C	-3.589166880	-0.919300616	-2.293882370
C	-3.112140656	-0.928623378	-3.604739904
C	-1.761641979	-0.679989994	-3.833192825
C	-0.910181224	-0.427489042	-2.752832174
C	0.537198544	-0.154718295	-2.891168356
C	1.211892128	-0.133930489	-4.115607738
C	2.577458858	0.133084789	-4.148361206
C	3.248594522	0.373282224	-2.949468613
C	2.526077271	0.340640992	-1.762533188
C	0.189963460	-3.040341139	-0.245138884
C	1.972304702	1.521496773	1.865329385
C	3.009477854	1.656298876	2.779964685
C	3.674900055	0.509367347	3.214356899
C	3.278662682	-0.730301976	2.719995260
C	2.227575302	-0.802324712	1.800024509
C	1.734086394	-2.066658497	1.215160728
C	2.262300730	-3.325209856	1.521079779
C	1.727521896	-4.461018085	0.919066429
C	0.672083974	-4.316782951	0.018073989
H	-2.060475349	5.607342243	-0.006708314
H	-0.346834213	4.938145161	-1.723294258
H	0.514951646	2.595405579	-1.693727374
H	-2.824355602	3.924315214	1.641095281
H	-1.108811140	-1.878944993	2.209144115
H	-2.763265848	-1.708897829	4.071919918
H	-3.919588089	0.492877543	4.451559067
H	-3.373628855	2.402438402	2.971907377
H	-3.018784523	-0.639377892	-0.226466238
H	-4.634347439	-1.106322169	-2.071248055
H	-3.780687571	-1.124486923	-4.437300205
H	-1.377966046	-0.683115780	-4.846469879
H	0.680012345	-0.325120926	-5.039583683
H	3.107765675	0.151554659	-5.095314503
H	4.312479496	0.584081531	-2.928864241
H	3.000190496	0.522974312	-0.805132151
H	-0.628276050	-2.875339270	-0.936866283
H	1.425085545	2.381263733	1.496548891
H	3.285376787	2.640813351	3.142291784
H	4.489410400	0.578122556	3.928600550
H	3.785466194	-1.629846811	3.047951221
H	3.082859278	-3.422366381	2.221604824
H	2.129296780	-5.442708015	1.149688840
H	0.227009103	-5.174651623	-0.474681169
N	-0.631032586	2.010957003	-0.076884821
N	-1.333060026	0.082738906	1.601669431
N	-1.388154626	-0.421127886	-1.476819992
N	1.203511238	0.087599665	-1.726505280
N	1.586971045	0.325105071	1.380213141
N	0.699776292	-1.938606977	0.336593151
Ru	0.027806319	0.021382269	0.007655812

==========

$^{3}Ru(bpy)_3^{2+}$

==========

C	-1.936032534	4.536324024	-0.083726056
C	-1.022511244	4.133548737	-1.057990432
C	-0.486106068	2.854931116	-0.974950790
C	-1.680144668	2.382421494	0.981348574
C	-2.269612789	3.650905609	0.936772108
C	-1.988420248	1.398227453	2.051561832
C	-1.883083344	-0.822984099	2.725327015
C	-2.503953934	-0.544560313	3.939927816
C	-2.860834599	0.777016819	4.210267067
C	-2.596689224	1.761082888	3.259984255
C	-2.631384611	-0.485204607	-1.418367982
C	-3.545995951	-0.681468070	-2.445496559
C	-3.071179390	-0.745855570	-3.755595684
C	-1.704448223	-0.619855404	-3.986398697
C	-0.827830672	-0.444841743	-2.909581661
C	0.641766191	-0.313551694	-3.089470625
C	1.296464205	-0.673272669	-4.274263859
C	2.676984787	-0.510834873	-4.365389824
C	3.377115488	-0.002816677	-3.270505428
C	2.659378290	0.311935335	-2.119996786
C	0.562859774	-2.965176582	-0.618780255
C	1.612350941	1.395965338	2.274149179
C	2.533009529	1.497633219	3.308787584
C	3.274583340	0.367897630	3.657849550
C	3.070755005	-0.819100261	2.960519075
C	2.132570267	-0.862125635	1.925013900
C	1.840808272	-2.067367792	1.127825618
C	2.476513386	-3.298589945	1.312675357
C	2.133954048	-4.379717350	0.506018460
C	1.158924341	-4.211499214	-0.478297919
H	-2.390333652	5.521256447	-0.122052059
H	-0.734252930	4.789684296	-1.871832371
H	0.217179358	2.484410048	-1.712732315
H	-3.001040697	3.937813759	1.682331800
H	-1.569971800	-1.832082272	2.469912529
H	-2.696158648	-1.339835763	4.652056694
H	-3.332638025	1.041067481	5.151456356
H	-2.846350193	2.794270515	3.470432043
H	-2.944952726	-0.412948012	-0.382616043
H	-4.602656364	-0.772677660	-2.219505548
H	-3.754809618	-0.882425487	-4.587451935
H	-1.325336576	-0.637559772	-5.000833988
H	0.748359382	-1.089833260	-5.110314846
H	3.198665857	-0.783996761	-5.277188301
H	4.451693058	0.141798571	-3.303149939
H	3.155576229	0.696098804	-1.232495785

H	-0.195533767	-2.780819893	-1.370486856
H	1.008441925	2.241726398	1.967111588
H	2.662277222	2.441296101	3.827193737
H	4.001589298	0.409554541	4.462561607
H	3.639207363	-1.702673435	3.224002123
H	3.233846188	-3.416855097	2.078010082
H	2.622216940	-5.339121819	0.643684864
H	0.863925159	-5.028541088	-1.127465248
N	-0.798652947	1.998918891	0.018818231
N	-1.634715676	0.118075721	1.804263234
N	-1.305777311	-0.375605077	-1.637889147
N	1.330335140	0.165961593	-2.030925751
N	1.413313389	0.249156073	1.593813896
N	0.888842046	-1.915868402	0.162344456
Ru	0.033224087	0.004679526	0.019114867

==========

***p*-TsOH**

==========

C	-3.909461021	0.087634914	-1.301102161
C	-4.901912212	-0.642064273	-0.627754748
C	-2.919746161	0.731659710	-0.546642840
H	-5.665424824	-1.159643173	-1.202280402
H	-2.137423277	1.288829446	-1.054581523
C	-4.920924664	-0.718608797	0.761212170
C	-2.920313597	0.668601871	0.845548987
H	-5.677700520	-1.292166233	1.284584880
H	-2.153278112	1.159733891	1.434172273
C	-3.930353880	-0.049564689	1.482805014
C	-3.928541899	0.190889686	-2.806713820
H	-2.947540283	0.463469744	-3.205130577
H	-4.235987186	-0.752607465	-3.268326283
H	-4.641890049	0.958572924	-3.131108522
S	-3.943365812	-0.143426701	3.257040501
O	-4.679003716	-1.328527451	3.703764915
O	-2.610447407	0.132988691	3.787150383
O	-4.898898125	1.180127025	3.513310671
H	-5.241266727	1.085560203	4.586587429

==========

***p*-TsO$^-$**

==========

C	-3.935457230	-0.015764803	-1.332505584
C	-5.077348709	-0.411128342	-0.621300519
C	-2.816570997	0.403838187	-0.601749480
H	-5.960253239	-0.736025333	-1.171120048
H	-1.921185970	0.721104860	-1.135157347
C	-5.100435257	-0.388242513	0.773101926
C	-2.835266352	0.428690493	0.793777645
H	-5.988220692	-0.675339282	1.328014612
H	-1.978525519	0.773868024	1.363841772
C	-3.975940466	0.027650680	1.490480065
C	-3.931199789	-0.004220272	-2.845211983
H	-2.910915613	-0.007105505	-3.244049072
H	-4.454311848	-0.875275731	-3.257440805
H	-4.433000088	0.888126373	-3.244465351
S	-3.976434469	-0.003313641	3.315807819
O	-3.486042976	-1.367406487	3.651330948
O	-3.042726994	1.094311833	3.688036680
O	-5.400592327	0.240665719	3.673270226

==========

^{1}I(^{1}3.12)

==========

N	0.115229376	-0.118081972	-3.039816856
C	-0.023184463	1.028723717	-2.374508142
C	0.231319815	-1.083942652	-2.090475321
C	0.162775934	-0.524187982	-0.827671170
N	0.001965524	0.821029663	-1.012326360
H	0.217448115	-0.957290649	0.160076588
H	0.356701761	-2.127005100	-2.346743107
C	-0.119392820	1.816444755	0.050719399
H	-1.074213147	2.337256670	-0.027932940
H	-0.048572648	1.302303076	1.011327147
H	0.673216701	2.560254574	-0.036988609
C	-0.190237895	2.355970860	-2.990581751
O	-0.318542510	3.368569136	-2.293561459
C	-0.189184904	2.375805616	-4.465725422
H	-0.066802882	1.421971798	-4.965116024
C	-0.324595809	3.541696072	-5.127821922
H	-0.431062132	4.435194016	-4.513179779
C	-0.333467841	3.745752573	-6.574998856
C	-0.207099199	2.692103624	-7.502269268
C	-0.470412463	5.055099010	-7.072043419
C	-0.220259115	2.943450689	-8.869272232
C	-0.480493963	5.307366371	-8.442064285
C	-0.355957627	4.251730442	-9.346067429
H	-0.108552679	1.671137691	-7.148686409
H	-0.565566421	5.878720760	-6.369138718
H	-0.126597106	2.117754936	-9.568895340
H	-0.589084744	6.325577259	-8.804203987
H	-0.368382871	4.443560600	-10.415128708

==========

^{3}I

==========

N	0.115783721	-0.122301444	-3.070152760
C	-0.021965532	1.017331481	-2.392442703
C	0.228648886	-1.100982308	-2.129063368
C	0.159313485	-0.557447731	-0.862831593
N	-0.000152193	0.795110583	-1.034797788
H	0.210064217	-1.000289798	0.120486721
H	0.352791071	-2.141143799	-2.397757292
C	-0.121897861	1.779056311	0.037571844
H	-1.075008869	2.304068804	-0.035508748
H	-0.055927634	1.253856182	0.992666125
H	0.673189282	2.521570921	-0.037071031
C	-0.180459350	2.351775885	-2.998603344
O	-0.307620734	3.388387442	-2.294828415
C	-0.181026638	2.398250580	-4.426435471
H	-0.065579697	1.460458398	-4.956147671
C	-0.327135414	3.664039612	-5.135107040
H	-0.431255817	4.542419434	-4.505757809
C	-0.334969342	3.804393053	-6.516732693
C	-0.202408791	2.692720890	-7.432068825
C	-0.480864614	5.115364552	-7.106479168
C	-0.216887668	2.891204596	-8.796857834
C	-0.491354614	5.289877415	-8.469974518
C	-0.359793901	4.182434082	-9.337229729
H	-0.093635969	1.688718796	-7.038929462

H	-0.581860662	5.968582630	-6.441636086
H	-0.116755195	2.039309740	-9.463614464
H	-0.602577388	6.286951542	-8.886676788
H	-0.370182335	4.327147007	-10.412937164

==========

^{3}I-twisted

==========

N	0.582259417	-0.070431262	-3.074938774
C	0.072959624	1.032967091	-2.529695988
C	0.542016566	-1.016982794	-2.097745419
C	-0.000232956	-0.488276362	-0.942099631
N	-0.298800468	0.818843126	-1.221707463
H	-0.194345638	-0.917775333	0.029454475
H	0.898991466	-2.024484396	-2.261451721
C	-0.896523595	1.773368478	-0.290447533
H	-1.845582366	2.140473843	-0.682344496
H	-1.054389238	1.267664671	0.664162695
H	-0.237805232	2.631783724	-0.154862866
C	-0.100060716	2.325484276	-3.222489834
O	-0.603977144	3.307269096	-2.648343086
C	0.351860076	2.367248297	-4.598653316
H	0.816857338	1.464574456	-4.992835999
C	0.209743261	3.563113451	-5.422719479
H	1.012181640	4.300229073	-5.387488365
C	-0.915828526	3.840764284	-6.236068249
C	-2.027116776	2.951798439	-6.308786392
C	-0.967913508	5.028669357	-7.020025730
C	-3.115237236	3.239154577	-7.117838860
C	-2.062115908	5.304180622	-7.824771404
C	-3.144152403	4.414090633	-7.881836414
H	-2.011924982	2.040245056	-5.718274117
H	-0.132432312	5.722676754	-6.978756428
H	-3.951752186	2.546954632	-7.158593178
H	-2.080171347	6.216747761	-8.414194107
H	-3.999000788	4.633162975	-8.514685631

==========

^{3}I-TS

==========

N	1.185414791	0.122632220	-2.624961376
C	0.234657422	0.799266100	-1.977903962
C	1.660435319	-0.793473244	-1.731309772
C	0.993330359	-0.678587794	-0.529499412
N	0.080803528	0.333740890	-0.693680704
H	1.074236989	-1.221078992	0.400444895
H	2.447444916	-1.488572955	-1.990167975
C	-0.802496076	0.852197826	0.347273856
H	-1.822822332	0.922568500	-0.027251752
H	-0.760158956	0.171200141	1.200419664
H	-0.479945689	1.850519776	0.646991074
C	-0.494663060	1.966412306	-2.507730961
O	-1.228036880	2.658721924	-1.765677214
C	-0.248391643	2.310784578	-3.883170366
H	0.251445115	1.575900435	-4.502816200
C	-0.948781490	3.445044994	-4.471593380
H	-1.606455922	3.982853889	-3.795443773
C	-0.826441288	3.884927273	-5.799517632
C	0.035369396	3.260544062	-6.759778500
C	-1.581008315	5.018038750	-6.247432232
C	0.126480296	3.740188122	-8.055565834
C	-1.480955124	5.482960224	-7.544507027
C	-0.625875056	4.851721287	-8.465818405
H	0.623792291	2.396904469	-6.468286514
H	-2.244067907	5.509831905	-5.540318489
H	0.787677586	3.246953964	-8.763020515
H	-2.068283319	6.342892170	-7.854886055
H	-0.550113738	5.219393253	-9.484356880
C	1.919074297	3.337296009	-3.531961679
C	1.675404310	4.273303986	-2.564915657
H	1.915101886	3.632741213	-4.574775219
H	2.315229416	2.353185177	-3.307034016
H	1.334390044	5.255675316	-2.885859013
C	1.724451184	4.059790611	-1.129948616
C	1.247477174	5.073024273	-0.270035684
C	2.223880768	2.874654055	-0.543602645
C	1.253312707	4.908625126	1.110284328
C	2.230350971	2.714236736	0.837137759
C	1.743601203	3.725976229	1.672919273
H	0.855547667	5.989418983	-0.703473985
H	2.599791765	2.074055433	-1.170073986
H	0.872905552	5.699673176	1.750116110
H	2.614419460	1.792124271	1.263749003
H	1.750346780	3.595482111	2.751169443

==========

^{3}II

==========

N	1.729790449	0.308447003	-2.577512264
C	0.756077051	0.971654713	-1.953379273
C	2.096881151	-0.690013528	-1.729698896
C	1.343564391	-0.632833064	-0.570506454
N	0.489244282	0.422903627	-0.718506038
H	1.344010234	-1.239177465	0.322944641
H	2.872388840	-1.399858236	-1.982350111
C	-0.442118436	0.914278388	0.294143289
H	-1.454732895	0.944180250	-0.106289774
H	-0.394397020	0.244837090	1.154979825
H	-0.156934872	1.924290419	0.594099343
C	0.087400623	2.174661875	-2.467573166
O	-0.863194823	2.675349951	-1.876174331
C	0.699379325	2.797606468	-3.719506264
H	0.998339772	1.983576894	-4.390089035
C	-0.254703194	3.741353989	-4.377628803
H	-1.051169276	4.136999130	-3.755599022
C	-0.161908135	4.171892166	-5.720084667
C	0.839239717	3.706268549	-6.623189926
C	-1.101941228	5.118646145	-6.225131035
C	0.889947891	4.163403034	-7.931948185
C	-1.041529298	5.566822529	-7.534214020
C	-0.044690203	5.095556259	-8.400967598
H	1.571191311	2.979554176	-6.285181522
H	-1.877280116	5.486783981	-5.558037281
H	1.663246274	3.791712761	-8.598937035
H	-1.772010684	6.288122177	-7.890536308
H	0.001858802	5.449266911	-9.426482201
C	2.050710440	3.520467997	-3.301768303
C	1.846359849	4.570213795	-2.259165525
H	2.447469234	3.975313902	-4.215649605
H	2.755753040	2.747182846	-2.986899376

H	1.431139708	5.516632557	-2.597118378
C	1.994753480	4.389139175	-0.862433791
C	1.599624991	5.428590298	0.031102516
C	2.507333517	3.193264008	-0.275863707
C	1.687375784	5.274354458	1.404816270
C	2.588772774	3.049965858	1.102367401
C	2.177892208	4.081872463	1.956579328
H	1.207050920	6.351956844	-0.386817694
H	2.837378025	2.379291058	-0.910826743
H	1.369216561	6.082215786	2.058158159
H	2.980026245	2.125152826	1.518530726
H	2.243493319	3.962046385	3.033870935

==========

^{1}II

==========

N	1.676574230	0.416210771	-2.537428141
C	0.701372862	1.093351364	-1.930487037
C	2.077330589	-0.529079437	-1.645731807
C	1.344791889	-0.422807336	-0.476314098
N	0.465947866	0.605061352	-0.664975226
H	1.375182509	-0.978394508	0.449028611
H	2.860541344	-1.238143563	-1.875442743
C	-0.433937758	1.153006792	0.347420007
H	-1.456650615	1.170001268	-0.026516251
H	-0.365040421	0.528338611	1.239595056
H	-0.133273616	2.174401760	0.589357138
C	0.010214211	2.262593746	-2.489130974
O	-0.952634633	2.766874075	-1.921206594
C	0.628160357	2.862894297	-3.746148825
H	1.001653314	2.047294140	-4.374138832
C	-0.333698779	3.727793455	-4.472810268
H	-1.177000523	4.105746746	-3.902848005
C	-0.187957019	4.135391712	-5.819512367
C	0.895087183	3.719276667	-6.647865772
C	-1.151335716	5.011044502	-6.400673389
C	0.999821603	4.156424999	-7.960650921
C	-1.037600517	5.438881397	-7.713183403
C	0.039577320	5.017702103	-8.506226540
H	1.647269011	3.045211792	-6.250603676
H	-1.987508059	5.341995239	-5.789935112
H	1.835444331	3.823526382	-8.570454597
H	-1.788210273	6.105504036	-8.129167557
H	0.127758414	5.355086327	-9.534543037
C	1.959102631	3.651131153	-3.287065744
C	1.731520653	4.578115940	-2.151816368
H	2.294900656	4.196506977	-4.175143242
H	2.707252264	2.889676571	-3.057314396
H	1.194898009	5.497832775	-2.374049664
C	1.984425426	4.298314095	-0.784029782
C	1.545069575	5.217587471	0.213590518
C	2.641054630	3.116691589	-0.329314381
C	1.731571913	4.965634346	1.563561201
C	2.819550991	2.873727322	1.025382876
C	2.367175341	3.788958311	1.985183716
H	1.040394425	6.126608849	-0.103228994
H	2.997621298	2.385904312	-1.046234488
H	1.377699614	5.683632851	2.298526287
H	3.316868782	1.959916472	1.339684486
H	2.510380745	3.591616392	3.043441296

==========

^{1}II-TS

==========

N	1.796099901	-0.197537228	-2.653477430
C	0.895712972	0.482380360	-1.945598602
C	2.146234989	-1.260049582	-1.878902316
C	1.459399343	-1.225142479	-0.679137886
N	0.662012994	-0.115257077	-0.724867225
H	1.474413276	-1.875733852	0.182527900
H	2.868005276	-1.994722247	-2.207955837
C	-0.216319904	0.352816731	0.345603853
H	-1.258886576	0.309293389	0.028917693
H	-0.060040887	-0.282672614	1.219550133
H	0.017617121	1.390450120	0.590007007
C	0.225576684	1.719329238	-2.374472857
O	-0.728196740	2.165427208	-1.744393945
C	0.804689050	2.407873392	-3.608375549
H	0.822602630	1.652622581	-4.405954838
C	-0.013656041	3.629486084	-3.955610752
H	-0.731949151	3.953123808	-3.211041689
C	-0.000759275	4.284912586	-5.214732170
C	0.797261059	3.857023478	-6.311547756
C	-0.809049964	5.440430641	-5.409979343
C	0.786554992	4.546997070	-7.516714573
C	-0.811091781	6.123414040	-6.615871429
C	-0.012018047	5.684813976	-7.680812836
H	1.416766882	2.971747875	-6.211118221
H	-1.430121303	5.785028458	-4.587132454
H	1.403949142	4.196705818	-8.339615822
H	-1.438033342	7.002957344	-6.735390186
H	-0.014625521	6.220968246	-8.625109673
C	2.254929066	2.927416086	-3.349854708
C	2.113930225	4.305926323	-2.748157263
H	2.770520449	3.005437136	-4.310681343
H	2.839053869	2.232025385	-2.740423679
H	2.199851990	5.156056881	-3.416398048
C	1.952882648	4.572427750	-1.361397982
C	1.712256551	5.903797150	-0.918670952
C	2.016611814	3.559293509	-0.363466471
C	1.523973465	6.195679188	0.422903240
C	1.832100153	3.863064766	0.978910863
C	1.577791572	5.178112984	1.385555267
H	1.663957238	6.697837353	-1.659672618
H	2.228471279	2.535125017	-0.650609612
H	1.333338380	7.220824718	0.728963137
H	1.894842386	3.070571423	1.720536828
H	1.430478692	5.409273148	2.436281681

==========

^{1}III

==========

N	-0.369583756	0.091638878	-3.712664127
C	-0.111663640	1.013916850	-2.784065008
C	0.351086110	-1.003740788	-3.357180595
C	1.058986783	-0.753121436	-2.195469379
N	0.762059212	0.530233741	-1.833198667
H	1.729438901	-1.365582466	-1.611205220
H	0.331777900	-1.915092826	-3.938469172
C	1.304185510	1.235770345	-0.674270689

H	0.493964702	1.600270748	-0.042706914
H	1.934217095	0.541990578	-0.114393629
H	1.890188813	2.097457647	-0.997291803
C	-0.650468647	2.379629612	-2.777533531
O	-0.337795258	3.188007116	-1.903095841
C	-1.569316506	2.771062374	-3.905749798
H	-1.882744908	1.905789614	-4.490016460
C	-1.024263859	3.916953564	-4.814867496
H	-0.365684807	4.544239521	-4.200205803
C	-0.367015511	3.613070965	-6.132510185
C	0.125260741	2.340215206	-6.444048882
C	-0.228980616	4.641819954	-7.077349663
C	0.744640231	2.102634668	-7.673590183
C	0.387172103	4.402775288	-8.304087639
C	0.878037572	3.129973412	-8.607064247
H	0.019699354	1.527426958	-5.731693268
H	-0.613257229	5.631919384	-6.846544266
H	1.119535923	1.108201027	-7.901239395
H	0.483810842	5.209780216	-9.025591850
H	1.359941721	2.942893982	-9.562732697
C	-2.754115582	3.706125498	-3.540650129
C	-2.452099323	4.556076050	-4.805459499
H	-3.744803667	3.250790596	-3.469266415
H	-2.535938025	4.252777100	-2.620040178
H	-3.014060497	4.161733627	-5.659030914
C	-2.567109346	6.053541183	-4.770949841
C	-1.977890730	6.797751904	-3.737692595
C	-3.228125334	6.743897438	-5.795717716
C	-2.048555613	8.189463615	-3.731292725
C	-3.299911499	8.138091087	-5.793327332
C	-2.709128141	8.865649223	-4.760097980
H	-1.451959252	6.283051014	-2.937795639
H	-3.684355021	6.180412769	-6.606267452
H	-1.582962751	8.749039650	-2.924599886
H	-3.815686703	8.654090881	-6.598655224
H	-2.763345003	9.950592995	-4.754743099

==========

^{1}IV(^{1}3.12-H^{+})

==========

N	0.065397322	-0.213681832	-2.924163103
C	-0.033623263	1.011449695	-2.363708019
C	0.188838899	-1.177279234	-1.953268290
C	0.164855301	-0.513870776	-0.758227706
N	0.026651511	0.831116915	-1.028244019
H	0.235313281	-0.885510683	0.251935452
H	0.280296654	-2.227542400	-2.181257010
C	-0.042527683	1.876053214	0.014172458
H	-1.002206445	2.388513803	-0.049277715
H	0.071546622	1.385331631	0.981502473
H	0.753928006	2.602370262	-0.145828217
C	-0.194479302	2.335618496	-3.058727741
O	-0.341803253	3.317879677	-2.333297729
C	-0.163825095	2.341194153	-4.509630680
H	0.002419107	1.414693713	-5.053743362
C	-0.331593484	3.518486738	-5.176106930
H	-0.483286887	4.396724224	-4.547710896
C	-0.332678586	3.749715567	-6.603113651
C	-0.156447679	2.722652435	-7.557857990
C	-0.519927263	5.073919773	-7.057189465
C	-0.167910337	3.014893532	-8.913661003
C	-0.529780388	5.364602089	-8.416899681
C	-0.354012728	4.335696220	-9.346416473
H	-0.012389988	1.694577575	-7.238006115
H	-0.656366229	5.870738506	-6.330221176
H	-0.032474391	2.219874144	-9.640811920
H	-0.674106479	6.386634827	-8.752475739
H	-0.361930311	4.558391094	-10.408986092
H	0.038667522	-0.390057743	-3.920508146

==========

^{3}IV

==========

N	-0.318701804	-0.196710140	-2.849495173
C	-0.099451452	1.014316320	-2.270716667
C	-0.030307444	-1.214175701	-1.961655498
C	0.378163218	-0.611969769	-0.813138247
N	0.333794087	0.757288456	-1.011564493
H	0.697790980	-1.037601709	0.124393851
H	-0.131299421	-2.255741119	-2.219990969
C	0.701021552	1.750063896	0.012346744
H	-0.140576810	2.415626764	0.199996233
H	0.962355137	1.205687284	0.919565618
H	1.544557214	2.344378233	-0.334746271
C	-0.283568323	2.343427658	-2.850985289
O	0.114103913	3.360116243	-2.196408510
C	-0.919822931	2.490793705	-4.119139194
H	-1.314923406	1.616628885	-4.630048275
C	-1.068954825	3.771909237	-4.715794086
H	-0.655241251	4.603561878	-4.154542923
C	-1.721808791	4.034277916	-5.932885647
C	-2.347498894	3.021971941	-6.745142460
C	-1.776094198	5.392961502	-6.407001972
C	-2.964670658	3.351981640	-7.931175232
C	-2.395650625	5.706335068	-7.594590187
C	-2.995646477	4.691160679	-8.370883942
H	-2.342337370	1.987252116	-6.421007633
H	-1.311347961	6.169045448	-5.806658268
H	-3.433332443	2.579471111	-8.532305717
H	-2.425103903	6.735002995	-7.938545704
H	-3.483268023	4.941729069	-9.307363510
H	-0.621180415	-0.332069039	-3.802249908

==========

^{3}IV-TS

==========

N	1.123260498	-0.005723800	-2.632698774
C	0.368194431	0.931641877	-1.992878795
C	1.479524732	-1.015118718	-1.759648204
C	0.927237272	-0.692513049	-0.559485018
N	0.240092516	0.497856200	-0.711245596
H	0.956560552	-1.212343454	0.384490103
H	2.073335648	-1.862370014	-2.061636209
C	-0.461657286	1.191842198	0.378395140
H	-1.502205849	1.352253199	0.102509297
H	-0.392071158	0.562433064	1.266140342
H	0.006732326	2.158443928	0.558138490
C	-0.206315175	2.161064386	-2.529773474
O	-0.857750535	2.910696745	-1.765352488
C	0.093417451	2.544799089	-3.898055077

H	0.579778790	1.827890277	-4.556465626
C	-0.700766683	3.573484421	-4.502633095
H	-1.392877698	4.075794220	-3.833504438
C	-0.625922918	4.007843971	-5.849501610
C	0.300836295	3.485345125	-6.798303604
C	-1.514758945	5.031492710	-6.290242195
C	0.328514218	3.959298134	-8.099800110
C	-1.482839823	5.494170666	-7.594751835
C	-0.561429977	4.963638306	-8.509408951
H	0.999227762	2.707808495	-6.504835129
H	-2.228917360	5.443161488	-5.582625866
H	1.043058634	3.550406694	-8.807615280
H	-2.172764301	6.270858288	-7.909404278
H	-0.535447359	5.329008102	-9.530900955
C	1.984929919	3.644889593	-3.515850306
C	1.726388812	4.447240829	-2.411720514
H	1.955386043	4.083544731	-4.506363869
H	2.608470917	2.761702538	-3.418099642
H	1.221907020	5.393504620	-2.587451458
C	1.953420639	4.087674618	-1.040096402
C	1.428736210	4.915831089	-0.016494334
C	2.684348822	2.933616877	-0.658349454
C	1.620804429	4.604350090	1.322054863
C	2.878543854	2.629900694	0.681703806
C	2.349910975	3.462568521	1.677538753
H	0.859243035	5.798046112	-0.293187231
H	3.123349190	2.291916847	-1.414908051
H	1.209668875	5.248468876	2.092693806
H	3.454786062	1.752492785	0.959120274
H	2.511271954	3.225812674	2.724760294
H	1.348264217	0.017336167	-3.615360022

==========

^{3}V

==========

N	1.586710811	0.155257225	-2.614762306
C	0.756486654	1.001365542	-1.961938977
C	1.932089925	-0.897058487	-1.801060915
C	1.285237789	-0.687482476	-0.616184235
N	0.559746563	0.477500588	-0.732312083
H	1.280768752	-1.272108197	0.289997548
H	2.584186792	-1.693834901	-2.120974064
C	-0.216030970	1.089375734	0.360963255
H	-1.247514844	1.229950309	0.044940226
H	-0.160731375	0.419339955	1.218076587
H	0.225516483	2.056194067	0.605687797
C	0.155399278	2.258388042	-2.480464697
O	-0.677725017	2.822905779	-1.789146662
C	0.699773610	2.836484909	-3.763339758
H	0.951111436	2.032671452	-4.471497536
C	-0.263703376	3.794280529	-4.381237984
H	-1.043260336	4.181281090	-3.735187054
C	-0.180002049	4.263298035	-5.710292816
C	0.810795367	3.830899000	-6.640004635
C	-1.132679224	5.222711086	-6.164931297
C	0.843367755	4.334722996	-7.931432724
C	-1.092794418	5.714993954	-7.458013535
C	-0.104156643	5.277879238	-8.351203918
H	1.554818273	3.097204208	-6.343179226
H	-1.899968743	5.563457012	-5.475137234
H	1.608846545	3.994629383	-8.622490883
H	-1.830437899	6.443531513	-7.780344009
H	-0.072600827	5.667944908	-9.363432884
C	2.100255013	3.553481102	-3.400102377
C	1.960457683	4.568797112	-2.326298952
H	2.422348738	4.020824432	-4.334567070
H	2.833997250	2.779422522	-3.150444508
H	1.530949116	5.524883270	-2.610726595
C	2.191741943	4.330141068	-0.949953556
C	1.806371808	5.312528133	0.009330950
C	2.771691084	3.125858307	-0.451883554
C	1.967415810	5.094536781	1.367344856
C	2.934512377	2.920415163	0.912505031
C	2.529561043	3.895879507	1.832470536
H	1.364331484	6.240262508	-0.342699140
H	3.136253119	2.372507811	-1.142892122
H	1.658422470	5.857148647	2.075631618
H	3.399117231	2.004044294	1.266645551
H	2.663897514	3.732644320	2.897076368
H	1.896420717	0.288785577	-3.568006516

==========

^{1}V

==========

N	1.491951227	0.308413267	-2.575487137
C	0.685898304	1.191026211	-1.946312308
C	1.869234204	-0.690675080	-1.712410688
C	1.269201040	-0.404218763	-0.517677605
N	0.535305977	0.747744739	-0.681618869
H	1.304843903	-0.926886439	0.424837083
H	2.508458138	-1.507546425	-2.006901026
C	-0.183770761	1.440881610	0.403580189
H	-1.234652877	1.539154172	0.140029430
H	-0.062631682	0.847486734	1.308616996
H	0.253930986	2.430736780	0.540101230
C	0.079913683	2.432658911	-2.510348320
O	-0.774750113	2.992797613	-1.847436905
C	0.663544476	3.002469301	-3.777277708
H	1.026944757	2.203110456	-4.437835693
C	-0.322872430	3.851420641	-4.489876747
H	-1.151202917	4.235124111	-3.904236078
C	-0.206643209	4.236416340	-5.845791340
C	0.873250723	3.840278387	-6.686943054
C	-1.213498116	5.067805290	-6.417915821
C	0.933909357	4.252481461	-8.010052681
C	-1.144090176	5.470311642	-7.740951061
C	-0.070606396	5.067409515	-8.547699928
H	1.665727854	3.207780123	-6.296954155
H	-2.046595335	5.383040428	-5.795596600
H	1.766824841	3.940674305	-8.633157730
H	-1.925274134	6.101288795	-8.153809547
H	-0.017693125	5.385159492	-9.584052086
C	2.023782969	3.814867020	-3.336627007
C	1.851287961	4.635339737	-2.122048378
H	2.257000208	4.425041199	-4.212514400
H	2.820329189	3.073398352	-3.225216389
H	1.291518211	5.560469151	-2.227179050
C	2.184201002	4.216098309	-0.804718792
C	1.723403692	4.974246979	0.311030656
C	2.941998243	3.042649746	-0.520293951

C	1.986744046	4.577025890	1.613202929
C	3.204712629	2.655533075	0.788466215
C	2.726658344	3.411991358	1.865901589
H	1.146375775	5.875830173	0.126079038
H	3.357450247	2.455065489	-1.333014846
H	1.619982719	5.175599575	2.441546917
H	3.803471804	1.768116593	0.974843681
H	2.941556454	3.110347033	2.886002064
H	1.761303425	0.380321294	-3.547885180

==========

^{1}V-TS

==========

N	0.981047332	-0.115204491	-2.406836271
C	0.652573228	1.066904306	-1.837122679
C	1.153340816	-1.079565763	-1.441883326
C	0.924288034	-0.462881684	-0.245288253
N	0.613909543	0.855264783	-0.503903449
H	0.955836654	-0.853144944	0.759528399
H	1.414652228	-2.099272966	-1.675087929
C	0.355718106	1.874668717	0.529633522
H	-0.662944615	2.246200085	0.432432175
H	0.506091475	1.404627323	1.501083374
H	1.052228689	2.702485561	0.390270889
C	0.362215877	2.359533310	-2.518309116
O	-0.127719507	3.254514217	-1.847766399
C	0.689212859	2.470735312	-3.992470264
H	0.105233908	1.683936477	-4.501453400
C	0.340259850	3.850540638	-4.495512009
H	0.096466780	4.591082573	-3.743883371
C	0.171078160	4.185135841	-5.863446236
C	0.282121837	3.245023727	-6.924920559
C	-0.121685274	5.534950733	-6.207602501
C	0.121121071	3.639119387	-8.245612144
C	-0.279818177	5.918714046	-7.529359818
C	-0.156944647	4.975323677	-8.558324814
H	0.479067713	2.199087858	-6.708252430
H	-0.219110623	6.268393993	-5.411811829
H	0.206555650	2.904628992	-9.040842056
H	-0.503109336	6.954265594	-7.767192841
H	-0.281538099	5.277518272	-9.593242645
C	2.219110489	2.292795181	-4.299157143
C	2.843367100	3.630492926	-4.006410599
H	2.317637444	2.068225145	-5.363019943
H	2.685825586	1.462327957	-3.753931284
H	3.019309759	4.299828053	-4.840325832
C	3.238547087	4.038142204	-2.704507828
C	3.565509319	5.400387287	-2.453658104
C	3.316780090	3.134353876	-1.606760859
C	3.902448416	5.834142208	-1.182642460
C	3.666625500	3.578587055	-0.335843414
C	3.948617697	4.929464340	-0.111220255
H	3.526182890	6.107297421	-3.277710676
H	3.169075012	2.071816444	-1.771488190
H	4.135504723	6.881155491	-1.014960647
H	3.750019550	2.866501331	0.481160223
H	4.222363949	5.273131847	0.881170273
H	1.074732780	-0.256457508	-3.403736830

==========

^{1}VI

==========

N	-0.910197854	0.936228395	-4.094486237
C	-0.376114279	1.095040679	-2.866492748
C	-2.069754601	0.212534115	-4.013898849
C	-2.246312857	-0.087466046	-2.689943552
N	-1.196008563	0.468820244	-1.995384455
H	-3.025506020	-0.644920290	-2.194367409
H	-2.668846369	-0.022949046	-4.878977299
C	-1.018716335	0.383534521	-0.533246517
H	-1.053238153	1.383712888	-0.103884786
H	-1.823339105	-0.234643698	-0.136899456
H	-0.050727740	-0.062614828	-0.308238566
C	0.880257845	1.841676474	-2.521034718
O	1.131996870	2.031269073	-1.344530702
C	1.686305285	2.347386122	-3.674377441
H	1.879272580	1.532806516	-4.382271767
C	1.063213348	3.590486526	-4.427257061
H	0.543350160	4.215211391	-3.692872047
C	0.189157382	3.383833408	-5.629448414
C	0.543980300	2.475245476	-6.644402027
C	-1.023708582	4.080260754	-5.750133514
C	-0.296739608	2.266116619	-7.741121292
C	-1.858026028	3.879462719	-6.850100994
C	-1.500411034	2.967069626	-7.845266342
H	1.492106915	1.945368052	-6.591814518
H	-1.308925033	4.789754391	-4.977899551
H	-0.004606071	1.566691041	-8.518611908
H	-2.787880898	4.434492588	-6.929646015
H	-2.150577545	2.808647156	-8.700070381
C	2.946410418	3.194092751	-3.399208784
C	2.529091358	4.132106781	-4.569409847
H	3.910759449	2.690047741	-3.477330923
H	2.878152847	3.681566000	-2.424700737
H	2.947636127	3.749971628	-5.506997108
C	2.712429762	5.621363640	-4.496364117
C	2.388129950	6.335328579	-3.333960772
C	3.153822184	6.329885960	-5.620368958
C	2.505622387	7.723529339	-3.296659708
C	3.271375179	7.719671249	-5.586577415
C	2.947001219	8.419833183	-4.424336910
H	2.041964531	5.807664871	-2.448123693
H	3.404736519	5.789545536	-6.529930592
H	2.254421473	8.262856483	-2.388168573
H	3.615923882	8.253878593	-6.466935635
H	3.038208485	9.501325607	-4.395525455
H	-0.538288891	1.373692155	-4.94433736

Table 3-12. Vibrational frequencies of all optimized geometries

==========

$^1Ru(bpy)_3^{2+}$

==========

34.70 35.50 37.91 39.23 40.18 51.65
84.52 84.93 89.47 116.09 117.77 122.70
154.10 174.23 179.43 180.38 193.43 195.17
229.20 230.82 254.29 270.60 270.95 281.16
322.15 332.84 333.22 360.84 367.67 372.81
434.38 436.03 438.58 443.88 444.66 459.38
466.39 477.95 479.32 492.39 493.13 494.43
565.18 565.55 567.55 647.82 652.81 655.17
658.91 660.75 662.48 668.48 670.86 677.41
746.43 749.56 749.95 763.30 763.73 765.86
768.33 775.35 780.02 787.17 788.23 788.72
824.07 824.40 825.93 907.50 907.85 909.60
914.96 915.37 917.91 984.73 985.49 986.74
987.36 987.83 989.28 1026.66 1027.13 1027.55
1027.73 1031.35 1031.57 1031.90 1032.00 1033.94
1038.71 1040.73 1051.98 1056.93 1060.19 1061.88
1090.83 1093.49 1094.33 1100.05 1101.66 1102.30
1139.32 1139.58 1141.28 1157.10 1157.70 1158.38
1202.97 1203.51 1203.74 1214.67 1215.23 1215.86
1302.53 1303.37 1305.64 1306.01 1306.77 1308.20
1324.62 1325.15 1325.51 1338.97 1339.59 1340.14
1347.34 1347.63 1349.19 1465.76 1466.71 1466.91
1486.15 1486.43 1486.75 1505.67 1510.56 1511.47
1528.23 1528.52 1529.23 1611.10 1611.67 1612.18
1620.86 1621.30 1622.09 1647.81 1648.72 1649.03
1654.25 1656.01 1656.47 3211.47 3211.76 3211.80
3212.84 3212.94 3213.13 3221.76 3222.20 3222.76
3223.60 3223.91 3224.20 3229.11 3229.96 3230.25
3234.35 3235.98 3236.31 3236.76 3237.25 3237.80
3239.93 3241.44 3241.81

==========

$^3Ru(bpy)_3^{2+}$

==========

28.62 29.95 30.98 33.70 36.62 47.84
61.82 80.17 84.00 91.11 92.47 104.18
123.66 126.99 142.69 150.88 155.34 177.37
182.56 210.59 213.07 223.77 256.65 257.13
261.03 281.30 311.41 351.32 359.36 377.59
414.50 415.85 422.78 430.51 435.93 437.11
446.55 460.86 464.45 481.74 482.75 484.23
562.92 564.13 566.18 635.75 642.67 643.99
659.00 661.44 661.82 663.03 669.84 689.18
743.52 749.39 751.98 758.75 759.63 761.55
771.80 778.27 780.70 783.95 786.06 787.01
824.07 826.88 827.97 907.15 913.36 913.85
915.34 920.11 921.32 985.00 986.64 988.30
988.91 994.93 995.32 1017.79 1025.58 1028.22
1028.41 1030.08 1030.31 1031.40 1032.61 1033.06
1033.19 1034.17 1056.41 1057.62 1058.09 1059.98
1088.03 1088.72 1092.76 1100.54 1103.30 1103.71
1135.41 1137.74 1139.68 1151.94 1152.64 1158.02
1201.08 1201.23 1203.96 1212.96 1213.36 1214.79
1304.18 1305.29 1307.31 1309.32 1310.16 1312.38
1321.11 1321.97 1327.39 1338.80 1339.34 1342.42
1346.54 1347.09 1349.64 1463.77 1464.06 1466.39
1480.93 1481.34 1485.75 1507.63 1510.61 1511.42
1522.22 1522.88 1527.81 1609.56 1612.22 1612.78
1619.85 1625.88 1626.42 1640.27 1640.88 1649.71
1652.32 1653.48 1656.41 3187.63 3188.17 3212.44
3212.93 3213.81 3213.85 3214.61 3215.82 3219.83
3220.06 3225.50 3226.26 3226.71 3227.47 3231.06
3231.69 3231.92 3233.92 3234.91 3238.63 3239.54
3240.51 3242.29 3242.71

==========

***p*-TsOH**

==========

40.63 51.91 99.58 164.89 216.48 283.90
305.87 360.57 379.09 416.24 465.86 477.86
534.08 549.96 646.53 656.03 713.40 775.23
822.22 834.18 856.93 976.69 984.93 1020.31
1035.37 1064.95 1082.86 1102.95 1153.23 1160.30
1223.31 1235.86 1330.77 1341.10 1359.36 1427.84
1444.76 1448.23 1500.69 1505.58 1539.48 1631.60
1657.01 2045.45 3040.66 3102.49 3131.60 3185.83
3188.19 3223.65 3225.02

==========

***p*-TsO^-**

==========

29.77 53.60 89.25 164.61 206.55 272.72
317.94 352.37 390.28 417.02 480.47 529.40
555.10 568.30 651.24 660.73 717.30 811.33
831.01 854.63 964.01 974.74 992.82 1009.73
1042.05 1060.67 1121.00 1135.39 1206.60 1219.64
1220.74 1231.32 1325.74 1347.80 1420.72 1436.32
1500.54 1508.45 1535.75 1624.45 1655.85 3015.13
3069.91 3100.46 3142.28 3145.09 3206.02 3207.83

==========

$^1I(^1$3.12)

==========

25.75 41.03 60.03 97.73 115.54 149.20
185.25 204.39 215.86 238.30 285.71 310.18
407.57 412.60 454.07 500.28 546.57 587.66
629.80 632.41 667.46 701.63 711.10 751.59
766.34 791.37 798.50 853.64 865.84 907.33
911.83 935.81 937.53 975.91 1000.75 1013.91
1042.60 1047.86 1060.88 1084.99 1105.73 1116.18
1152.53 1197.34 1198.81 1217.86 1242.82 1256.89
1322.58 1335.37 1348.41 1371.53 1374.47 1407.06
1451.98 1463.15 1486.57 1492.15 1504.03 1527.58
1540.08 1551.56 1630.46 1655.83 1668.48 1732.41
3075.74 3159.10 3164.06 3164.93 3176.28 3182.98
3193.16 3203.76 3210.91 3227.82 3251.76 3278.94

==========

^3I

==========

18.20 42.09 59.63 69.79 123.91 132.52
183.06 189.36 214.46 229.74 291.41 301.49
400.11 403.44 450.69 466.31 533.35 544.86
571.14 610.96 636.38 653.40 708.10 708.88
747.14 749.21 777.53 793.74 804.88 836.34
858.95 870.50 877.92 933.83 969.01 976.13
985.65 1022.16 1055.29 1079.85 1105.62 1113.48
1152.47 1153.60 1180.19 1195.95 1221.14 1252.47
1265.76 1330.56 1354.11 1367.42 1379.80 1397.60
1430.77 1457.61 1463.51 1479.87 1487.20 1498.18
1517.68 1542.41 1559.18 1560.42 1586.88 1630.10
3074.66 3161.52 3163.33 3179.65 3185.77 3196.95
3203.96 3209.60 3219.23 3238.91 3250.20 3280.39

==========

^3I-twisted

==========

21.37 29.08 50.82 67.36 141.62 142.47
164.13 201.06 229.10 255.24 273.57 317.71
396.69 409.51 473.41 485.33 536.61 558.14
594.83 621.49 626.29 645.30 688.67 706.63
710.09 761.03 765.30 783.76 835.18 838.37
846.91 864.67 900.69 932.18 968.24 989.25
992.35 1023.40 1045.69 1077.49 1105.95 1113.22
1135.44 1152.50 1189.60 1193.88 1195.65 1231.59
1251.55 1327.50 1336.49 1362.82 1371.84 1403.67
1422.59 1456.67 1463.27 1487.72 1492.02 1501.86
1514.04 1524.54 1549.86 1595.37 1616.75 1623.60
3076.21 3136.59 3160.31 3164.15 3164.95 3173.31

3178.28 3188.90 3195.31 3206.76 3252.48 3279.74

==========

^{3}I-TS

==========

-231.06 14.40 36.00 42.20 52.58 57.12
67.38 81.03 100.14 106.44 136.36 159.54
188.61 189.55 208.83 219.30 250.84 267.28
299.05 311.25 335.86 403.50 413.60 417.93
454.48 458.57 482.75 486.06 546.35 569.79
577.17 620.80 622.30 629.57 653.62 676.24
687.89 709.09 725.92 739.46 743.77 749.12
782.30 787.88 799.23 803.03 809.72 828.35
853.92 855.01 886.25 892.65 931.10 937.21
966.86 969.99 980.19 982.01 984.90 989.59
1001.04 1009.04 1036.67 1048.40 1060.89 1068.72
1087.21 1106.21 1110.68 1125.51 1155.04 1160.92
1187.14 1192.84 1194.70 1208.99 1217.87 1241.08
1247.79 1260.40 1309.75 1326.39 1347.53 1351.90
1365.13 1370.38 1373.51 1394.07 1451.35 1453.85
1462.27 1477.92 1488.76 1494.18 1498.25 1502.50
1520.44 1532.06 1550.13 1551.79 1575.93 1587.91
1599.91 1616.64 1628.01 1646.78 3072.54 3156.82
3164.34 3173.11 3173.18 3175.36 3176.34 3179.39
3183.66 3190.76 3193.99 3199.32 3202.44 3205.73
3209.91 3221.46 3227.99 3248.61 3269.42 3278.83

==========

^{3}II

==========

12.74 28.97 41.18 49.49 58.60 72.43
76.32 107.05 126.37 148.60 155.46 185.13
192.49 199.22 234.27 248.21 287.31 309.04
334.03 402.69 408.90 415.90 427.20 454.17
484.56 489.38 512.97 559.03 563.02 577.04
625.11 626.01 633.66 668.09 682.36 691.68
701.97 707.92 719.37 750.41 768.52 770.39
771.03 783.33 813.43 834.54 841.44 865.31
876.30 897.88 899.66 903.15 929.56 967.27
969.11 971.67 987.46 988.19 992.41 993.70
1017.19 1044.49 1048.02 1072.39 1081.66 1098.65
1105.13 1122.00 1148.06 1154.61 1189.00 1190.45
1194.55 1197.14 1201.02 1208.62 1234.20 1249.75
1261.10 1267.42 1322.02 1338.77 1343.48 1344.47
1360.69 1365.09 1366.16 1407.78 1442.09 1448.40
1460.63 1464.62 1489.26 1492.70 1497.98 1507.12
1509.40 1522.75 1527.44 1529.74 1550.65 1593.79
1594.32 1618.05 1619.10 1751.03 3057.14 3064.37
3076.15 3120.29 3159.34 3170.93 3171.54 3174.22
3176.07 3177.62 3177.81 3189.01 3189.85 3198.74
3202.43 3203.61 3207.45 3219.21 3253.12 3280.10

==========

^{1}II

==========

15.26 29.03 42.35 54.20 57.87 69.59
77.84 105.91 125.05 136.96 154.76 186.75
193.05 201.68 235.59 250.56 273.47 308.75
327.92 404.12 408.60 415.27 428.31 455.77
485.89 491.09 504.74 557.09 561.91 577.28
626.43 626.75 631.94 659.23 681.26 693.02
696.35 709.49 723.08 743.58 769.94 771.98
772.59 780.37 814.26 835.52 842.59 851.70
866.51 896.98 899.60 904.47 930.38 965.51
968.07 972.76 987.81 988.54 993.83 994.48
1006.47 1033.85 1048.82 1052.50 1082.23 1100.45
1104.84 1119.10 1154.15 1155.26 1182.93 1189.33
1190.96 1197.17 1202.13 1208.66 1234.67 1250.54
1261.45 1271.20 1316.52 1335.11 1343.00 1343.40
1359.13 1365.45 1366.56 1408.96 1441.29 1449.24
1460.91 1465.76 1488.76 1491.71 1499.39 1506.76
1510.59 1523.61 1528.33 1532.71 1551.14 1595.20
1596.30 1619.85 1621.51 1752.90 3061.94 3074.77

3076.89 3128.56 3158.40 3168.08 3171.54 3172.52
3177.94 3178.47 3179.34 3188.97 3189.63 3196.86
3199.28 3203.03 3207.46 3217.52 3253.47 3280.23

==========

^{1}II-TS

==========

-244.77 25.40 36.59 43.52 51.85 57.93
63.37 91.19 112.81 130.82 177.96 181.75
195.30 198.32 226.43 234.99 244.80 303.04
331.20 392.62 408.98 416.43 419.73 440.68
490.75 498.23 526.69 553.85 575.27 585.17
599.68 627.56 628.91 637.61 673.05 693.95
696.00 699.82 734.37 746.20 763.39 766.38
770.99 790.67 802.36 837.92 841.63 865.96
873.02 900.09 902.17 920.97 941.93 968.54
970.10 982.75 988.27 988.59 996.43 998.52
1016.53 1048.25 1051.52 1068.56 1082.60 1091.29
1105.22 1127.79 1133.39 1155.36 1190.25 1191.63
1194.21 1199.67 1204.71 1209.79 1216.23 1246.34
1257.09 1260.41 1314.26 1335.87 1342.36 1345.11
1355.23 1366.40 1366.97 1406.57 1437.97 1441.22
1455.89 1463.55 1490.50 1494.77 1496.00 1509.02
1512.66 1525.43 1526.74 1528.56 1550.91 1600.02
1600.89 1624.98 1626.57 1742.71 3034.00 3072.88
3074.20 3117.16 3159.51 3164.04 3169.32 3171.58
3173.91 3177.81 3187.94 3189.16 3199.60 3201.17
3202.56 3207.44 3209.90 3216.37 3254.00 3280.40

==========

^{1}III

==========

10.98 25.32 38.23 44.60 47.77 58.93
86.31 133.53 144.16 149.91 157.14 195.73
213.53 234.99 237.02 254.23 298.26 343.34
371.70 414.67 416.78 418.30 444.46 459.77
513.56 534.57 555.59 626.17 631.79 632.96
636.59 654.89 681.29 710.61 716.70 717.97
747.19 767.96 772.13 781.73 792.39 823.61
863.43 869.15 869.64 871.52 926.50 928.17
938.30 943.99 975.67 980.19 985.05 993.92
1000.37 1003.35 1014.63 1015.32 1026.79 1050.89
1060.08 1062.71 1078.03 1092.69 1105.74 1109.70
1124.69 1141.78 1152.20 1195.82 1195.98 1198.04
1216.97 1223.43 1227.20 1240.23 1243.73 1252.41
1257.93 1272.29 1276.33 1330.86 1338.68 1343.79
1361.61 1368.53 1377.45 1383.00 1408.23 1418.53
1454.55 1463.52 1487.53 1489.77 1496.12 1504.69
1508.01 1528.19 1542.62 1546.08 1551.61 1638.60
1640.83 1664.18 1665.58 1735.91 3041.69 3065.84
3076.65 3080.05 3133.74 3147.15 3161.53 3168.29
3169.32 3169.77 3174.04 3178.34 3183.55 3188.85
3191.99 3197.44 3202.95 3203.61 3255.01 3280.82

==========

^{1}IV(^{1}3.12-H^{+})

==========

25.76 37.04 63.61 90.44 113.16 185.27
194.98 203.64 214.75 259.50 289.54 318.08
407.26 408.56 442.68 486.52 535.57 588.28
623.71 628.45 637.53 670.73 688.69 690.40
749.41 772.16 790.49 792.46 841.13 853.47
880.83 907.35 946.89 947.45 987.64 1012.42
1021.20 1038.84 1045.52 1054.89 1103.01 1122.44
1123.87 1147.46 1154.27 1204.91 1221.26 1236.77
1256.18 1295.47 1317.79 1344.68 1362.22 1377.01
1389.70 1424.26 1465.90 1485.29 1490.67 1495.28
1505.73 1536.46 1538.65 1614.66 1623.52 1638.18
1658.38 1730.25 3090.18 3158.96 3172.92 3184.89
3186.88 3188.62 3190.11 3200.03 3209.32 3219.54
3297.73 3314.24 3638.68

==========

^{3}IV

==========

13.01 39.77 61.15 75.80 131.64 157.13
180.56 207.12 216.24 234.59 280.56 316.89
389.46 403.36 449.66 460.73 510.06 539.92
567.04 575.25 598.52 619.12 647.53 687.93
692.12 747.77 774.89 787.34 799.78 823.99
861.84 874.07 876.65 921.46 940.34 986.09
986.83 1008.30 1023.66 1044.91 1105.58 1115.62
1129.84 1139.90 1150.82 1178.83 1205.04 1222.71
1245.03 1269.32 1298.28 1303.81 1348.64 1377.36
1384.87 1401.32 1419.38 1458.18 1462.48 1486.44
1497.53 1506.25 1526.82 1535.30 1556.98 1583.59
1621.13 1642.79 3096.20 3182.79 3190.31 3195.35
3199.73 3202.95 3212.65 3213.60 3219.43 3226.70
3301.26 3319.24 3675.21

==========

^{3}IV-TS

==========

-262.01 14.93 33.43 37.46 51.93 56.61
64.16 74.39 89.21 123.41 143.86 178.71
183.12 193.04 205.56 232.66 253.79 263.93
310.38 319.51 356.93 406.85 408.65 410.32
456.78 462.08 484.03 489.08 535.81 542.49
565.59 580.46 605.71 615.63 622.77 624.32
681.15 682.32 690.30 710.40 743.75 745.41
763.50 785.51 799.16 812.46 817.57 839.80
846.23 855.18 858.27 899.54 922.73 932.26
937.91 953.99 980.42 984.33 995.93 1005.04
1006.89 1011.57 1013.52 1042.68 1045.62 1048.65
1071.11 1100.28 1113.69 1124.75 1127.67 1136.09
1152.26 1187.57 1200.18 1200.89 1208.49 1217.59
1238.91 1242.32 1260.88 1288.64 1289.35 1301.65
1351.56 1355.09 1370.40 1374.13 1379.65 1398.56
1452.36 1456.98 1479.22 1484.71 1491.32 1500.77
1510.23 1513.32 1524.39 1526.74 1544.75 1565.41
1591.48 1594.00 1609.44 1621.84 1624.74 1636.21
3093.65 3154.67 3163.05 3186.50 3188.52 3189.25
3189.43 3190.94 3196.87 3197.17 3201.38 3202.80
3203.94 3208.63 3211.32 3219.56 3220.44 3259.09
3299.73 3318.11 3678.17

==========

^{3}V

==========

13.20 27.96 35.79 50.89 57.13 70.65
84.09 103.66 122.81 155.87 164.30 184.96
192.38 196.55 231.65 259.42 280.18 313.18
330.81 397.49 409.04 411.61 422.26 451.24
479.50 485.46 501.10 549.78 562.87 577.85
615.52 624.17 625.19 633.13 656.56 674.78
688.26 689.60 695.43 708.54 739.13 765.35
767.61 773.70 784.82 801.81 831.52 836.27
842.61 876.53 894.91 911.74 912.41 932.60
962.77 973.24 975.81 993.66 995.15 1002.36
1004.26 1012.21 1035.54 1048.04 1052.95 1081.74
1100.87 1117.77 1122.61 1136.79 1152.58 1154.78
1165.97 1195.04 1196.86 1205.07 1209.38 1232.48
1233.09 1258.91 1267.63 1295.95 1305.56 1327.76
1344.85 1346.48 1366.07 1367.16 1369.39 1416.70
1449.39 1457.96 1463.67 1486.50 1489.39 1490.64
1499.60 1506.09 1507.55 1522.89 1527.42 1536.63
1595.03 1595.74 1613.05 1618.93 1619.16 1742.89
3000.61 3056.30 3093.96 3116.97 3177.89 3178.19
3184.55 3185.99 3189.13 3195.62 3197.06 3197.79
3204.08 3204.45 3204.95 3216.41 3217.41 3218.54
3299.81 3317.00 3644.95

==========

^{1}V

==========

9.07 24.88 38.50 53.09 64.51 66.74
86.99 96.53 120.12 153.92 175.99 182.38
195.61 199.68 237.32 256.69 266.92 311.73
325.55 400.06 409.76 410.26 421.50 452.42
478.89 489.26 493.16 535.96 556.78 573.34
600.17 621.82 621.98 624.82 651.47 670.03
685.30 689.89 691.65 706.42 734.18 767.14
769.51 775.36 783.01 797.45 823.63 831.93
840.77 879.32 893.11 911.84 913.33 936.72
956.11 975.23 975.65 987.90 994.88 997.96
1002.77 1003.74 1027.52 1048.71 1050.08 1084.40
1103.57 1117.40 1121.00 1137.91 1153.36 1159.79
1165.08 1194.60 1197.21 1205.32 1211.03 1229.14
1237.73 1260.04 1266.64 1295.63 1305.26 1319.85
1342.67 1344.10 1365.27 1368.04 1369.20 1423.70
1444.02 1460.50 1466.21 1485.17 1487.97 1489.62
1500.26 1506.68 1508.31 1522.62 1528.40 1541.65
1595.40 1597.31 1620.08 1620.53 1620.68 1764.50
3014.29 3070.06 3095.19 3127.30 3177.05 3179.01
3184.24 3187.74 3187.86 3191.65 3196.60 3196.85
3203.71 3204.02 3206.69 3211.23 3216.51 3217.46
3300.27 3316.89 3641.17

==========

^{1}V-TS

==========

-217.42 27.87 38.54 49.25 54.44 58.20
73.79 91.86 122.60 130.39 181.82 192.85
197.53 208.29 232.51 246.98 259.57 307.63
335.56 393.63 408.23 414.02 421.44 434.47
484.41 494.49 509.81 548.68 567.00 580.13
592.42 618.12 626.27 627.21 645.72 666.93
681.78 691.98 697.66 717.41 741.62 755.36
770.36 771.71 795.02 798.83 836.50 838.49
870.81 876.81 909.81 914.42 919.32 941.58
971.92 974.51 977.26 998.10 999.94 1004.57
1005.00 1014.46 1048.26 1051.42 1065.66 1085.29
1097.80 1119.08 1127.73 1134.20 1143.90 1155.41
1182.32 1196.52 1198.52 1205.29 1211.53 1219.74
1229.34 1254.55 1258.17 1298.14 1301.81 1330.06
1343.49 1348.37 1359.43 1369.00 1370.21 1418.04
1439.37 1450.38 1462.45 1488.27 1492.60 1493.36
1497.91 1508.37 1510.42 1524.78 1526.59 1537.26
1599.68 1602.67 1618.34 1626.02 1627.40 1740.29
2966.77 3033.93 3090.30 3126.55 3174.62 3179.42
3183.32 3184.28 3187.70 3195.77 3197.14 3198.40
3203.34 3204.50 3216.42 3217.35 3220.81 3230.01
3300.11 3317.23 3647.01

==========

^{1}VI

==========

19.64 30.89 34.61 46.00 48.84 63.03
75.26 135.65 144.22 148.56 173.05 194.95
209.75 229.60 233.69 252.50 315.15 364.53
370.72 379.50 414.89 415.81 417.89 478.29
516.39 517.20 546.80 623.19 630.27 631.57
632.02 637.95 654.48 695.09 713.71 716.63
730.98 752.99 770.19 773.89 787.06 798.70
815.48 858.73 863.55 871.32 885.90 919.99
929.31 939.14 952.04 955.76 973.68 978.56
990.76 1009.28 1013.21 1014.52 1015.94 1020.32
1048.13 1059.68 1060.02 1074.36 1097.30 1114.12
1117.55 1128.96 1138.32 1151.27 1162.38 1198.44
1200.51 1202.58 1219.52 1222.11 1235.62 1238.23
1239.62 1243.94 1263.02 1272.69 1306.76 1320.58
1335.47 1346.82 1367.07 1367.54 1380.62 1396.90
1422.98 1431.58 1466.06 1486.57 1493.97 1495.25
1498.83 1505.37 1513.32 1537.35 1543.48 1544.43
1630.62 1634.24 1642.86 1655.27 1663.64 1781.89
3060.46 3065.97 3077.47 3098.14 3102.67 3161.10
3168.35 3174.76 3175.01 3184.49 3191.39 3193.73
3197.05 3198.63 3200.94 3205.53 3213.20 3216.79
3298.67 3315.81 3374.

3.6 References and Notes

[1] Fagnoni, M.; Dondi, D.; Ravelli, D.; Albini, A. Photocatalysis for the Formation of the C–C Bond. *Chem. Rev.* **2007**, *107*, 2725–2756.

[2] Hoffman, N. Photochemical Reactions as Key Steps in Organic Synthesis. *Chem Rev.* **2008**, *108*, 1051–1103.

[3] Narayanam, J. M. R.; Stephenson, C. J. R. Visible Light Photoredox Catalysis: Applications in Organic Synthesis. *Chem. Soc. Rev.* **2011**, *40*, 102–113.

[4] Tucker, J. W.; Stephenson, C. J. R. Shining Light on Photoredox Catalysis: Theory and Synthetic Applications. *J. Org. Chem.* **2012**, *77*, 1617–1622.

[5] Prier, C. K.; Rankic, D. A.; MacMillan, D. W. C. Visible Light Photoredox Catalysis with Transition Metal Complexes: Applications in Organic Synthesis. *Chem. Rev.* **2013**, *113*, 5322–5363.

[6] Reckenthäler, M.; Griesbeck, A. G. Photoredox Catalysis for Organic Synthesis. *Adv. Synth. Catal.* **2013**, *355*, 2727–2744.

[7] Koike, T; Akita, M. Visible Light Radical Reaction Designed by Ru- and Ir-Based Photoredox Catalysis. *Inorg. Chem. Front.* **2014**, *1*, 562–576.

[8] Kalyanasundaram, K. Photophysics, Photochemistry, and Solar Energy Conversion with Tris(bipyridyl)ruthenium(II) and Its Analogues. *Coord. Chem. Rev.* **1982**, *46*, 159–244.

[9] Juris, A.; Balzani, V.; Barigelletti, F.; Campagna, S.; Belser, P.; von Zelewsky, A. Ru(II) Polypyridine Complexes: Photophysics, Photochemistry, Electrochemistry, and Chemiluminescence. *Coord. Chem. Rev.* **1988**, *84*, 85–277.

[10] Balzani, V.; Bergamini, G.; Campagna, S.; Punteriero, F. Photochemistry and Photophysics of Coordination Compounds: Overview and General Concepts. *Top. Curr. Chem.* **2007**, *280*, 1–36.

[11] Wrighton, M.; Markham, J. Quenching The Luminescent State of Tris(2,2'-bipyridine)ruthenium by Electronic Energy Transfer. *J. Phys. Chem.* **1973**, *77*, 3042–3044.

[12] Turro, N. J. Triplet-triplet Excitation Transfer in Fluid Solution: Applications to Organic Photochemistry. *J. Chem. Educ.* **1966**, *43*, 13–16.

[13] Zhou, Q.-Q.; Zou, Y.-Q.; Lu, L.-Q.; Xiao, W.-J. Visible-Light-Induced Organic Photochemical Reactions through Energy Transfer Pathways. *Angew. Chem. Int. Ed.* **2019**, *58*, 1586–1604.

[14] Studer, A.; Curran, D. P. Catalysis of Radical Reactions: A Radical Chemistry Perspective. *Angew. Chem. Int. Ed.* **2016**, *55*, 58–102.

[15] Lewis, F.D.; Howard, D. K.; Oxman, J. D. Lewis Acid Catalysis of Coumarin Photodimerization. *J. Am. Chem. Soc.* **1983**, *105*, 3344–3345.

[16] Lewis, F. D.; Quillen, S. L.; Hale, P. D.; Oxman, J. D. Lewis Acid Catalysis of Photochemical Reactions. 7. Photodimerization and Cross-Cycloaddition of Cinnamic Esters. *J. Am. Chem. Soc.* **1988**, *110*, 1261–1267.

[17] Guo, H.; Herdtweck, E.; Bach, T. Enantioselective Lewis Acid Catalysis in Intramolecular [2+2] Photocycloaddition Reactions of Coumarins. *Angew. Chem. Int. Ed.* **2010**, *49*, 7782–7785.

[18] Brimoulle, R.; Guo, H.; Bach, T. Enantioselective Intramolecular [2+2] Photocycloaddition Reactions of 4-Substituted Coumarins Catalyzed by a Chiral Lewis Acid. *Chem. Eur. J.* **2012**, *18*, 7552–7560.

[19] Brimoulle, R.; Bach, T. Enantioselective Lewis Acid Catalysis of Intramolecular Enone [2+2] Photocycloaddition Reactions. *Science* **2013**, *342*, 840–843.

[20] Brimoulle, R.; Bach, T. [2+2] Photocycloaddition of 3-Alkenyloxy-2-cycloalkenones: Enantioselective Lewis Aicd Catalysis and Ring Expansion. *Angew. Chem. Int. Ed.* **2014**, *53*, 12921–12924.

[21] Stegbauer, S.; Jandl, C.; Bach, T. Enantioselective Lewis Acid Catalyzed *ortho* Photocycloaddition of Olefins to Phenanthrene-9-carboxyaldehydes. *Angew. Chem. Int. Ed.* **2018**, *57*, 14593–14596.

[22] Huang, X.; Quinn, T.R.; Harms, K.; Webster, R. D.; Zhang, L.; Wiest, O.; Meggers, E. Direct Visible-Light-Excited Asymmetric Lewis Acid Catalysis of Intermolecular [2+2] Photocycloadditions. *J. Am. Chem. Soc.* **2017**, *139*, 9120–9123.

[23] Hu, N.; Jung, H.; Zheng, Y.; Lee, J.; Zhang, L.; Ullah, Z.; Xie, X.; Harms, K.; Baik, M.-H.; Meggers, E. Catalytic Asymmetric Dearomatization by Visible-Light-Activated [2+2] Photocycloaddition. *Angew. Chem. Int. Ed.* **2018**, *57*, 6242–6246.

[24] Brenninger, C.; Jolliffe, J. D.; Bach, T. Chromophore Activation of α,β-Unsaturated Carbonyl Compounds and Its Application to Enantioselective Photochemical Reactions. *Angew. Chem. Int. Ed.* **2018**, *44*, 14338–14349.

[25] Blum, T.R.; Miller, Z. D.; Bates, D. M.; Guzei, I. A.; Yoon, T. P. Enantioselective Photochemistry through Lewis Acid-Catalyzed Triplet Energy Transfer. *Science* **2016**, *354*, 1391–1395.

[26] Miller, Z. D., Lee, B.J.; Yoon, T. P. Enantioselective Crossed Photocycloadditions of Styrenic Olefins by Lewis Acid Catalyzed Triplet Sensitization. *Angew. Chem. Int. Ed.* **2017**, *56*, 11891–11895.

[27] Daub, M. E.; Jung. H.; Lee, B. J.; Won, J.; Baik, M.-H.; Yoon, T. P. Enantioselective [2+2] Cycloadditions of Cinnamate Esters: Generalizing Lewis Acid Catalysis of Triplet Energy Transfer. *J. Am. Chem. Soc.* **2019**, *141*, 9543–9547.

[28] Skubi, K. L.; Blum, T.R.; Yoon, T. P. Dual Catalysis Strategies in Photochemical Synthesis. *Chem. Rev.* **2016**, *116*, 10035–10074.

[29] Childs, R. F. The Photochemistry of Protonated Unsaturated Carbonyl Compounds. *Res. Chem. Intermed.* **1980**, *3*, 285–314.

[30] Zalewski, R. I.; Dunn, G. E. Protonation of Conjugated Carbonyl Groups in Sulfuric Acid Solutions. I. Adaptation of the Amide Acidity Function H_A for Protonation of the Carbonyl Group in Non-Hammett Bases. *Can. J. Chem.* **1968**, *46*, 2469–2470.

[31] Zalewski, R. I.; Dunn, G. E. Protonation of Conjugated Carbonyl Groups in Sulfuric Acid Solutions. II. Protonation and Basicity of α,β-Unsaturated Alicyclic Ketones. *Can. J. Chem.* **1969**, *47*, 2263–2270.

[32] Childs, R. F.; Lund, E. F.; Marshall, A. G.; Morrisey, W. J.; Rogerson, C. V. Stereomutation of 1-Hydroxyallyl Cations. Thermal and Photochemical Isomerizations of Protonated Enones. *J. Am. Chem. Soc.* **1976**, *98*, 5924–5931.

[33] Childs, R. F.; Duffey, B.; Mika-Gibala, A. Use of Solid Acids to Catalyze the Cis/Trans Photoisomerization of α,β-Unsaturated Carbonyl Compounds. *J. Org. Chem.* **1984**, *49*, 4352–4358.

[34] Childs, R. F.; Mahendran, M.; Blackburn, C.; Antoniadis, G. The Importance of Ground State Conformation in the Photoisomerizations of Protonated Enones. *Can. J. Chem.* **1988**, *66*, 1355–1358.

[35] Cornell, D. G.; Filipescu, N. Photorearrangement of 10-Methyloctalone in Concentrated Acid Solution. *J. Org. Chem.* **1977**, *42*, 3331–3336.

[36] Vallavoju, N.; Selvakumar, S.; Jockusch, S.; Sibi, M. P.; Sivaguru, J. Enantioselective Organo-Photocatalysis Mediated by Atropisomeric Thiourea Derivatives. *Angew. Chem. Int. Ed.* **2014**, 53, 5604–5608.

[37] Vallavoju, N.; Selvakumar, S.; Jockusch, S.; Prabhakaran, M. T.; Sibi, M. P.; Sivaguru, J. Evaluating Thiourea Architecture for Intramolecular [2+2] Photocycloaddition of 4-Alkenylcoumarins. *Adv. Synth. Catal.* **2014**, *356*, 2763–2768.

[38] Telmesani, R; Park, S. H.; Lynch-Colameta, T.; Beeler, A. B. [2+2] Photocycloaddition of Cinnamates in Flow and Development of a Thiourea Catalyst. *Angew. Chem. Int. Ed.* **2015**, *54*, 11521–11525.

[39] Rusakowicz, R.; Byers, G. W.; Leermakers, P. A. Electronically Excited Aromatic Carbonyl Compounds in Hydrogen Bonding and Acidic Media. *J. Am. Chem. Soc.* **1971**, *93*, 3263–3266.

[40] Davies, D. H.; Haire, N. A.; Hall, J.; Smith E. H. Synthesis of γ-Lactones from Intermediate 2-(γ-Hydroxyacyl)-imidazoles by *N*-Methylation and Base-catalyzed C–C Bond Cleavage. Application to the Synthesis of (±)-Caveernosine. *Tetrahedron* **1992**, *48*, 7839–7856.

[41] Evans, D. A.; Song, H.-J.; Fandrink, K. R. Enantioselective Nitrone Cycloadditions of α,β-Unsaturated 2-Acyl Imidazoles Catalyzed by Bis(oxazolinyl)pyridine-Cerium(IV) Triflate Complexes. *Org. Lett.* **2006**, *8*, 3351–3354.

[42] Tyson, E. L.; Farney, E. P.; Yoon, T. P. Photocatalytic [2+2] Photocycloadditions of Enones with Cleavable Redox Auxiliaries. *Org. Lett.* **2012**, *14*, 1110–1113.

[43] Nelsen, S. F.; Blackstock, S. C.; Kim, Y. Estimation of Inner Shell Marcus Terms for Amino Nitrogen Compounds by Molecular Orbital Calucations. *J. Am. Chem. Soc.*, **1987**, *109*, 677–682.

[44] Anderson, G. M.; Cameron, I.; Murphy, J. A.; Tuttle T. Predicting the Reducing Power of Organic Super Electron Donors. *RSC Adv.* **2016**, *6*, 11335–11343.

[45] Smith, A. J.; Young, A.; Rohrbach, S.; O'Connor, E. F.; Allison, M.; Wang, H.-S.; Poole, D. L.; Tuttle, T.; Murphy, J. A. Electron-Transfer and Hydride-Transfer Pathways in the Stoltz-Grubbs Reducing System (KO*t*Bu/Et_3SiH). Angew. *Chem. Int. Ed.*, **2017**, *129*, 13935–13939.

[46] Barham, J. P.; Coulthard, G.; Emery, K. J.; Doni, E.; Cumine, F.; Nocera, G.; John, M. P.; Berlouis, L. E. A.; McGuire, T.; Tuttle, T.; Murphy, J. A. KO*t*Bu: A Privileged Reagent for Electron Transfer Reactions? *J. Am. Chem. Soc.* **2016**, *138*, 7402–7410.

[47] Singh, V. K.; Yu, C.; Badgujar, S.; Kim, Y.; Kwon, Y.; Kim, D.; Lee, J.; Akhter, T.; Thangavel, G.; Park, L. S.; Lee, J.; Nandajan, P. C.; Wannemacher, R.; Milián-Medina, B.; Lüer, L.; Kim, K. S.; Gierschner, J.; Kwon, M. S. Highly Efficient Organic Photocatalysts Discovered *via* a Computer-Aided-Design Strategy for Visible-Light-Driven Atom Transfer Radical Polymerization. *Nat. Catal.* **2018**, 1, 794–804.

[48] Fukui, N.; Li, X.-X.; Nam, W.; Fukuzumi, S.; Fujii, H. Small Reorganization Energy for Ligand-Centered Electron-Transfer Reduction of Compound I to Compound II in a Heme Model Study. *Inorg. Chem.* **2019**, *58*, 8263–8266.

[49] Zhu, M.; Zheng, C.; Zhang, X.; You, S.-L. Synthesis of Cyclobutane-Fused Angular Tetracyclic Spiroindolines *via* Visible-Light-Promoted Intramolecular Dearomatization of Indole Derivatives. *J. Am. Chem. Soc.* **2019**, *141*, 2636–2644.

[50] Pangborn, A. B.; Giardello, M. A.; Grubbs, R. H.; Rosen, R. K.; Timmers, F. J. Safe and Convenient Procedure for Solvent Purification. *Organometallics*, **1996**, *15*, 1518–1520.

[51] Hiyama, T.; Reddy, G. B.; Minami, T.; Hanamoto, T. Stereoselective Reduction of β,δ-Diketo Esters. A Novel Strategy for the Synthesis of Artificial HMG-CoA Reductase Inhibitors. *Bull. Chem. Soc. Jpn.* **1995**, *68*, 350–363.

[52] Ruan, J.; Li, X.; Saidi, O., Xiao, J. Oxygen and Base-Free Oxidative Heck Reactions of Arylboronic Acids with Olefins. *J. Am. Chem. Soc.* **2008**, *130*, 2424–2425.

[53] Kanazawa, Y.; Tsuchiya, Y.; Kobayashi, K.; Shiomi, T.; Itoh, J.-i.; Kikuchi, M.; Yamamoto, Y.; Nishiyama. H. Asymmetric Conjugate Reduction of α,β-Unsaturated Ketones and Esters with Chiral Rhodium (2,6-Bisoxazolinylphenyl) Catalysts. *Chem. Eur. J.* **2006**, *12*, 63–71.

[54] Davies, D. H.; Hall, J.; Smith, E. H. Non-Oxidative Conversion of Ketone Carbonyls into Carboxy Carbonyls. Comparison of 2-Acylthiazoles and 2-Acylimidazoles in the Aldol Condensation and Stereospecific Cleavage of an Example of the Latter to a β-Hydroxy Ester *via* the Azolium Salt. *J. Chem. Soc. Perkin Trans. 1* **1991**, 2691–2698.

[55] Evans, D. A.; Fandrick, K. R.; Song, H.-J. Enantioselective Friedel-Crafts Alkylations of α,β-Unsaturated 2-Acyl Imidazoles Catalyzed by Bis(oxazolinyl)pyridine-Scandium(III) Triflate Complexes. *J. Am. Chem. Soc.* **2005**, *127*, 8942–8943.

[56] Myers, M. C.; Bharadwaj, A. R.; Milgram, B. C.; Scheidt, K. A. Catalytic Conjugate Additions of Carbonyl Anions Under Neutral Aqueous Conditions. *J. Am. Chem. Soc.* **2005**, *127*, 14675–14680.

[57] The NMR data in ref. 6 do not match the proton and carbon shifts that we identify here. Instead the reported data for this 2-OMeAr substrate is *quite* consistent with our reported data for the corresponding 3-OMeAr substrate. To rule out error on our part, we established that the coupling patterns for the 2-OMeAr and 3-OMeAr substrates reported above are consistent with their structure. They are exceedingly consistent. We believe this substrate has been misidentified in ref. 6, but this mistake seems isolated.

[58] Parr, R. G.; Yang, W. *Density Functional Theory of Atoms and Molecules*; Oxford University Press: New York, NY, 1989.

[59] Bochevarov, A. D.; Harder, E.; Hughes, T. F.; Greenwood, J. R.; Braden, D. A.; Philipp, D. M.; Rinaldo, D.; Halls, M. D.; Zhang, J.; Friesner, R. A. Jaguar: A high-performance quantum chemistry software program with strengths in life and materials sciences. *Int. J. Quantum Chem*. **2013**, *113*, 2110–2142.

[60] Becke, A. D. Density-functional thermochemistry. III. The role of exact exchange. *J. Chem. Phys*. **1993**, *98*, 5648–5652.

[61] Lee, C.; Yang, W.; Parr, R. G. Development of the Colle-Salvetti correlation-energy formula into a functional of the electron density. *Phys. Rev. B* **1988**, *37*, 785–789.

[62] Grimme, S.; Antony, J.; Ehrlich, S.; Krieg, H. A. A consistent and accurate *ab initio* parametrization of density functional dispersion correction (DFT-D) for the 94 elements H-Pu. *J. Chem. Phys*. **2010**, *132*, 154104 (1-19).

[63] Ditchfield, R.; Hehre, W. J.; Pople, J. A. Self-Consistent Molecular-Orbital Methods. IX. An Extended Gaussian-Type Basis for Molecular-Orbital Studies of Organic Molecules. *J. Chem. Phys*. **1971**, *54*, 724–728.

[64] Hay, P. J; Wadt, W. R. *Ab initio* effective core potentials for molecular calculations. Potentials for the transition metal atoms Sc to Hg. *J. Chem. Phys.* **1985**, *82*, 270–283.

[65] Wadt, W. R.; Hay, P. J. *Ab initio* effective core potentials for molecular calculations. Potentials for main group elements Na to Bi. *J. Chem. Phys.* **1985**, *82*, 284–298.

[66] Hay, P. J; Wadt, W. R. *Ab initio* effective core potentials for molecular calculations. Potentials for K to Au including the outermost core orbitals. *J. Chem. Phys.* **1985**, *82*, 299–310.

[67] Dunning, T. H. Gaussian basis sets for use in correlated molecular calculations. I. The atoms boron through neon and hydrogen. *J. Chem. Phys.* **1989**, *90*, 1007–1023.

[68] Marten, B.; Kim, K.; Cortis, C.; Friesner, R. A.; Murphy, R. B.; Ringnalda, M. N.; Sitkoff, D. Honig, B. New Model for Calculation of Solvation Free Energies: Correction of Self-Consistent Reaction Field Continuum Dielectric Theory for Short-Range Hydrogen-Bonding Effects. *J. Phys. Chem.* **1996**, *100*, 11775–11788.

[69] Edinger, S. R.; Cortis, C.; Shenkin P. S.; Friesner, R. A. Solvation Free Energies of Peptides: Comparison of Approximate Continuum Solvation Models with Accurate Solution of the Poisson−Boltzmann Equation. *J. Phys. Chem. B* **1997**, *101*, 1190–1197.

[70] Friedrichs, M.; Zhou, R. H.; Edinger, S. R.; Friesner, R. A. Poisson−Boltzmann Analytical Gradients for Molecular Modeling Calculations. *J. Phys. Chem. B* **1999**, *103*, 3057–3061.

[71] Peng, C.; Schlegel, H. B. Combining Synchronous Transit and Quasi-Newton Methods to Find Transition States. *Isr. J. Chem.* **1993**, *33*, 449–454.

[72] Nelsen, S. F.; Blackstock, S. C.; Kim, Y. Estimation of inner shell Marcus terms for amino nitrogen compounds by molecular orbital calculations. *J. Am. Chem. Soc.*, **1987**, *109*, 677–682.

Chapter 4. The Development of Enantioselective Bronsted-Acid Catalyzed [2+2] Photocycloadditions

4.1: Introduction

4.1.1: Enantioselective Triplet-State Photoreactions

The development of organic photochemistry as a synthetic tool, especially for the preparation of drugs and drug-like molecules, requires that photochemical methods be capable of being conducted in a stereoselective fashion. This goal has been an integral part in the explosive development of synthetically relevant photoreactions that has occurred in the last few decades.[1,2] Notably, the majority of these newly developed enantioselective photoreactions occur through photoinduced electron transfer (*i.e.* photoredox catalysis).[3,4] In contrast, enantioselective photoreactions that occur through excited-state intermediates *via* energy transfer are far rarer.

Figure 4-1. Asymmetric catalysis in thermal reactions vs. photochemical reactions

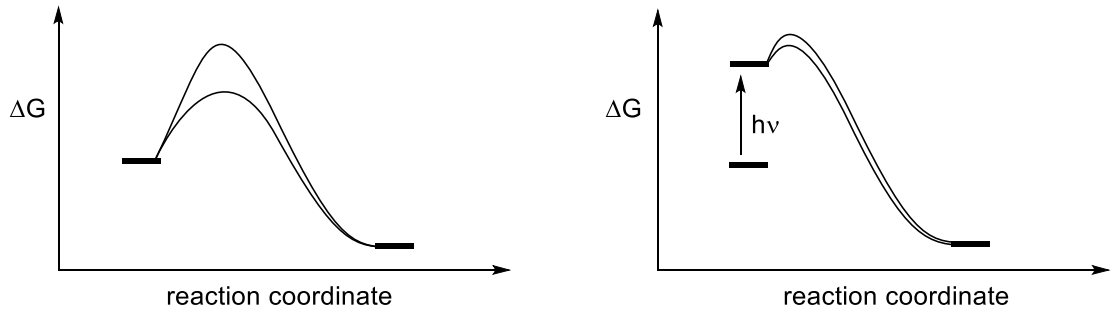

Stereochemical control is inherently quite challenging when excited states are involved. While radical and radical ion intermediates are relatively short-lived, the lifetimes excited states are typically many orders of magnitude shorter. The general hypothesis underlying the field of asymmetric catalysis is that a chiral catalyst can lower the transition state energy of one enantiomeric product such that its formation is slightly more favorable in the resulting asymmetric reaction (Figure 1-1).[5] In contrast, when a molecule reaches a photochemical excited state, if often has already achieved the energy it requires to undergo a reaction.[6] Therefore, the further

differentiation between two reaction surfaces of exceedingly similar energies is a significant challenge.

The observation that has been integral to recent developments in enantioselective excited-state photoreactions is that a substrate molecule must be present in an established chiral environment prior to excitation if synthetically useful stereoselectivities are to be obtained. Earlier work in asymmetric triplet-state reactions relied upon the use of chiral aryl ketones as photosensitizers.[7–9] Aside from extremely brief interactions in the exited state, these types of photocatalysts have no means of associating with the substrates of their respective reactions, and consequently, the enantioselectivities in these early reactions were extremely low.

In 1990, seminal work by Krische exploited hydrogen-bonding interactions between a chiral benzophenone photocatalyst and a quinolone substrate, leading to the first catalytic asymmetric excited-state photoreaction to approach 20% ee.[10] Subsequently, Bach has published extensively on the application of chiral hydrogen-bond donors and chiral Lewis acids to a variety of highly enantioselective intra- and intermolecular [2+2] photocycloaddition reactions.[11–16]

4.1.2: Acid Catalysis of Energy Transfer Reactions

Work by the Yoon group on asymmetric excited-state photoreactions began with a desire to resolve what appeared to be an outstanding problem with previous approaches to this type of reaction: the need to identify singular catalysts which have both desirable photochemical and enantioinductive properties. We hoped instead to use transition metal photosensitizers such as $Ru(bpy)_3^{2+}$, the photochemical properties of which are well understood,[17,18] in cooperation with the well-developed field asymmetric catalysis. There exists a plethora of well-studied asymmetric catalysts, the syntheses of which are often already well optimized.

Scheme 4-1. Enantioselective intermolecular [2+2] photocycloadditions *via* Lewis-acid catalyzed energy transfer

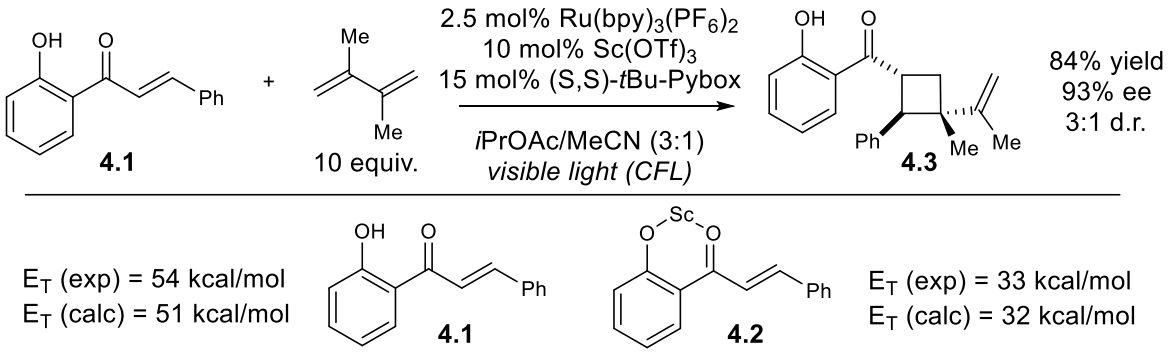

In 2016, our group reported a potentially general mechanism for this cooperativity between transition metal photocatalysts and specific class of chiral Lewis acid catalysts (Scheme 4-1).[19,20] The paper described the use of $Sc(OTf)_3$ in combination with a (*S*,*S*)-*t*Bu-Pybox ligand to enable enantioselective [2+2] cycloadditions between 2'-hydroxychalcone (**4.1**) and dienes. More specifically, we found that coordination of scandium to the hydroxychalcone lowers the substrate's triplet energy (E_T) such that visible-light triplet sensitization by a photocatalyst ($Ru(bpy)_3(PF_6)_2$ in this case) becomes possible. Notably, this coordination event to form **4.1a** lowers the E_T of the complex lowers *by more than 20 kcal/mol* vs. **4.1**. In turn, the use of a chiral ligands along with a scandium Lewis acid allows the corresponding cycloaddition to become highly enantioselective.

More recently, continued investigations of Lewis-acid catalyzed sensitization reactions led to development of an enantioselective [2+2] photocycloaddition of cinnamate esters and styrenes using a chiral oxazaboroldine-$NHTf_2$ salt and iridium photocatalyst.[21] In this case, a computational analysis of the system indicated that energy transfer is enabled by Lewis acids though two significant factors: (1) reduction of the substrate triplet energy and, (2) increase of the frontier molecular orbital overlap between the substrate and the transition metal photocatalyst.

As this unusual mechanism of substrate activation had not previously been invoked, we were curious if it could be more generally applied to the activation of substrates by photochemical energy transfer. We thought that if this general principle could be expanded to include activation by Brønsted acid catalysts, the types of substrates that would be available to enantioselective cycloaddition reactions could be significantly broadened.

Table 4-1. The development of Brønsted acid-catalyzed [2+2] photocycloadditions of cinnamoyl-1-methylimidazole and alkenes.

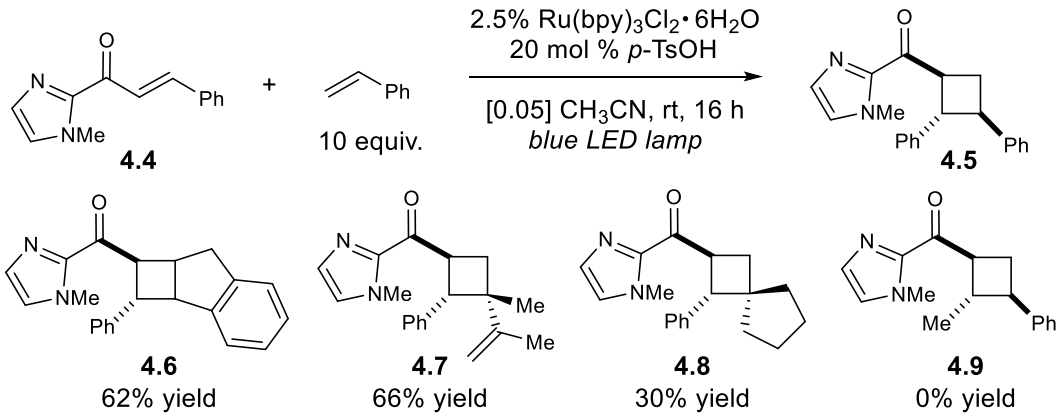

We were indeed able to develop a [2+2] photocycloaddition that occurs through a Brønsted acid-catalyzed triplet energy transfer process (Table 4-1).[22] This reaction employs *p*-toluenesulfonic acid as a simple achiral co-catalyst that accelerates the triplet sensitization of β-aryl enone **4.4** by $Ru(bpy)_3Cl_2$. This acceleration of energy transfer is the result of several factors, including a decreased energetic cost for reorganization upon excitation to the triplet state. In the course of this investigation, we found that this reaction allows for us to prepare not only diaryl cyclobutanes (**4.5**), but several different varieties of cyclobutane scaffolds (**4.6**-**4.8**). Notably, we were unable to generate products derived from β-alkyl enones (**4.9**). Conveniently, however, this acyl imidazole functionality can be cleaved to carboxylic acid derivatives *via* a known procedure.

4.2 Results and Discussion

4.2.1: Preliminary Reaction Design

Following the successful development of an unusual and unprecedented Brønsted acid-catalyzed [2+2] photocycloaddition (Chapter 3), we wondered if this type of catalysis could be made enantioselective. As discussed here and in Chapter 1, stereoselective photochemical reactions, especially those that do not occur through photoinduced electron transfer, are unusual. At the outset of these preliminary efforts, we began by screening a handful of established chiral Brønsted acid scaffolds under the previously optimized reaction conditions (Table 4-2). The substrates used for optimization in Chapter 3, cinnamoyl-1-methylimidazole (**4.10)** and styrene, with $Ru(bpy)_3Cl_2$ serving as the photocatalyst, were chosen as a starting point.

Table 4-2. Screening of chiral Brønsted acids in an enantioselective [2+2] photocycloaddition

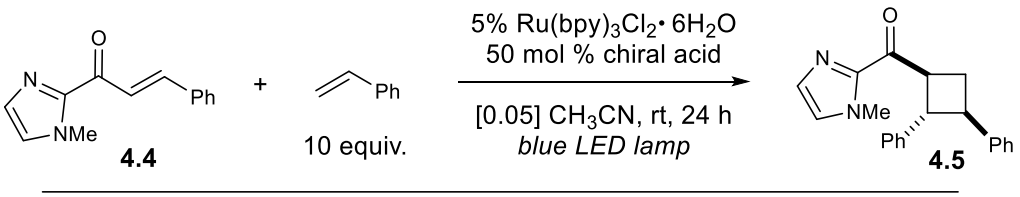

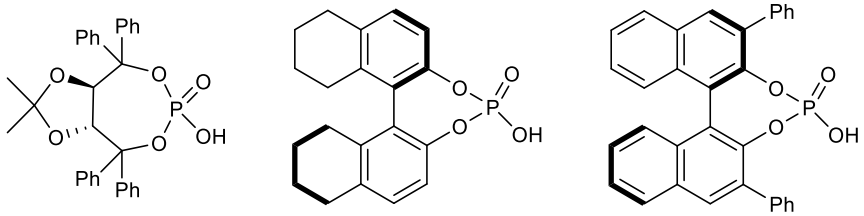

4.10	**4.11**	**4.12**
58% yield	58% yield	62% yield
1.4:1 d.r.	1.7:1 d.r.	1.7:1 d.r.
-11% ee	-5% ee	14% ee

Gratifyingly, we were able to achieve small but significant levels of enantioinduction almost immediately with a series of chiral phosphoric acids **4.10**–**4.12**. While both TADDOL and BINOL derived phosphoric acids both have fairly tunable structures, the unsaturated (*R*)-Ph_2-

BINOL phosphoric acid (**4.12**) gave the highest enantioselectivity for this preliminary test with 14% ee, and was therefore chosen as the central scaffold for additional optimization experiments.

4.2.2: Development and Optimization

Table 4-3. Screening of chiral Brønsted acids in an enantioselective [2+2] photocycloaddition

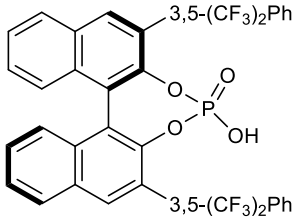

4.12
62% yield
1.5:1 d.r.
10% ee

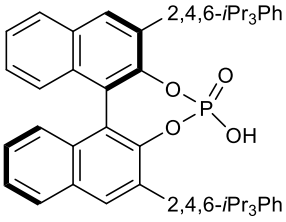

4.13
70% yield
1.8:1 d.r.
5% ee

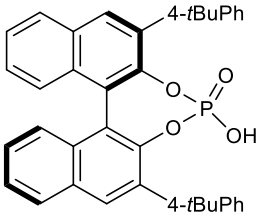

4.14
57% yield
1.5:1 d.r.
2% ee

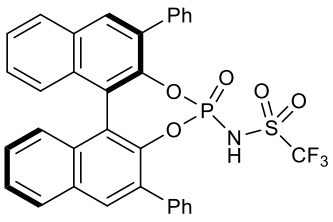

4.15
47% yield
1.6:1 d.r.
31% ee

With proof-of-principle experiments having demonstrated that an enantioselective Brønsted acid-catalyzed energy transfer reaction was indeed possible, we moved forward with reaction optimization aimed at improving both yield and selectivity. The tunable nature of the optimal BINOL phosphoric acid had not yet been fully explored, and therefore changes were made to both the pendant diaryl substituents and to the phosphoric acid itself (Table 4-3). Modification of the diaryl groups to several bulky electron-deficient (**4.12)** and electron-rich (**4.13**,**4.14)** arenes were met with largely negative results. Since all the enantioselectivites were extremely low, it was difficult to draw conclusions about these perturbations. Instead, catalyst analogue **4.15** was prepared, and while still low overall, this catalyst provided significantly higher selectivity than observed previously. Furthermore, this *N*-triflylphosphoramide (pka 6.4, MeCN) is nearly $8x10^6$ times more acidic than the analogous phosphoric acid (pka 13.3, MeCN). We suspect that the

increased acidity of this catalyst improves binding with the substrate, making sensitization within the catalyst's chiral environment more likely, leading to greater enantioenrichment.

Table 4-4. Solvent and temperature optimization

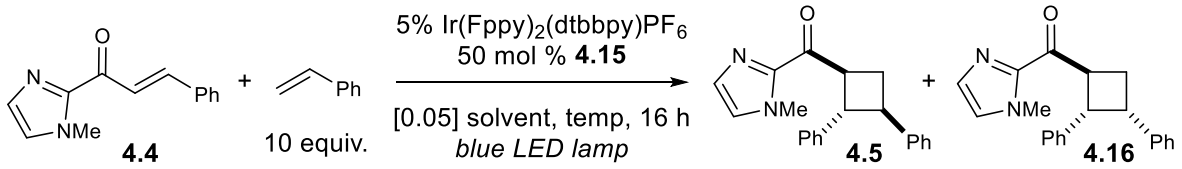

Entry	Solvent	Temp.	% Yield (d.r.)	% ee (4.10a)	% ee (4.18b)
1	MeCN	25 °C	62 (1.5:1)	39	42
2	MeOH	25 °C	78 (2.0:1)	8	8
3	CH_2Cl_2	25 °C	64 (1.7:1)	37	53
4	$PhCH_3$	25 °C	60 (1.6:1)	15	35
5	CH_2Cl_2	–78 °C	35 (1:2.0)	59	82
6[a]	$PhCH_3$	–78 °C	89 (1:5.0)	50	85

[a] Using Kessil lamp (very high-intensity blue LED lamp)

We suspected the enantioselectivity of this reaction would benefit from reduced temperature; however, using the previously optimized solvent, acetonitrile, the lowest achievable temperature would be limited to only –45 °C (**Entry 1**, Table 4-4**)**. A screen of alternate solvents with lower freezing points were explored, initially at room temperature (**Entries 2–4**). Of these, dichloromethane provided comparable selectivity to acetonitrile, although toluene provided modest ee's. We next explored the use of dichloromethane solvent at –78 °C (**Entry 5**), and as expected, this provided improved selectivities of the *trans-trans* diastereomeric product (**4.5**). However, cooling the reaction also unexpectedly resulted in a reversal of diastereoselectivity, such that the *trans-cis* product (**4.16**) was now the major diastereomer. This is beneficial, as the enantioselectivity of **4.16** is much higher than **4.5**, which appears more prevalent in non-polar solvents. Finally, repeating the reaction in toluene at –78 °C (**Entry 6**), while providing similar

selectivities of both **4.5** and **4.16**, further increased the diastereoselectivity in favor of **4.16**. This reaction was also performed with a more intense light source (Kessil lamp), allowing for recovery of the reduced yields observed in **Entry 5**.

Table 4-5. Controls and final catalyst optimizations

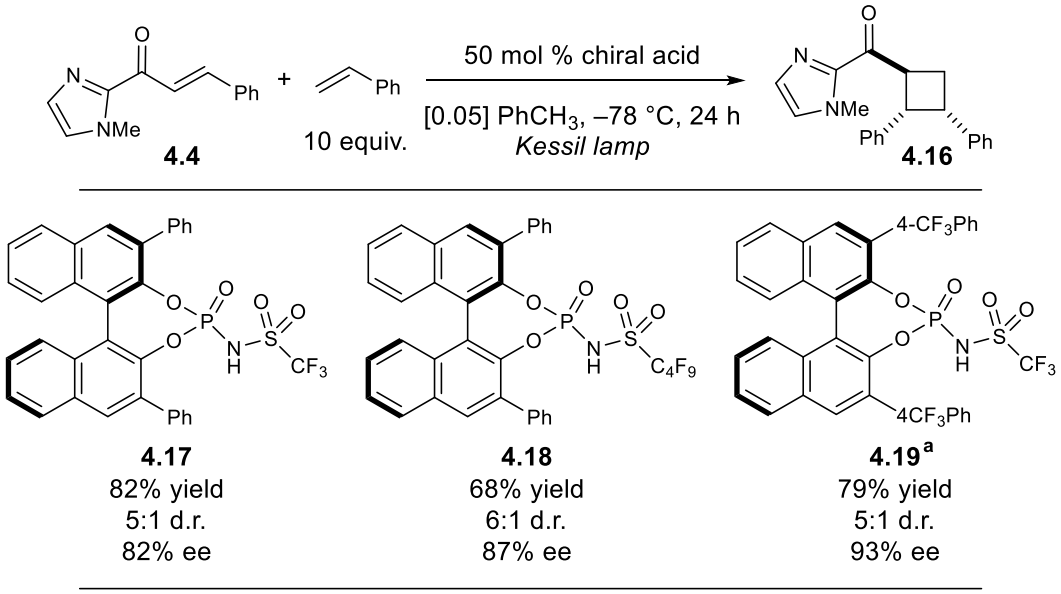

[a] Using only 20 mol% acid catalyst for 14 h

Having achieved excellent yields, and good diastereoselectivies and enantioselectivities, we carried out several final controls and additional optimizations to the Brønsted acid structure (Table 4-5). Unexpectedly, we observed that Ru- and Ir-photosensiters were entirely unnecessary for this reaction to work in high yield, and comparable selectivity. This observation indicated that the optimal BINOL-derived phosphoramidate was serving as both a photocatalyst and a source of chiral information. This type of catalysis is surprising but not entirely unprecedented;[23,24] the method by which these class of catalysts activate and control this enantioselective [2+2] photocycloaddition is explored in section 4.2.4. Additional structural modifications were made to the Brønsted acid and tested in the absence of transition-metal photosensitizers. While alteration of the sulfonamide side chain from trifluoromethyl (**4.17**) to perfluorobutyl (**4.18**) gave a small

increase in enantioselectivity, the optimal catalyst was identified as a *N*-triflylphosphoramide substituted 4-trifluoromethylphenyl-BINOL (**4.19**). Furthermore, this catalyst gave high diastereo- and enantioselectivity at only 20 mol% loading of the catalyst, with full conversion in just 14 h.

4.2.3: Reaction Scope

We investigated the substrate scope of this enantioselective [2+2] photocycloaddition reaction under the conditions optimized in Section 4.2.2. Although these scope investigations are still ongoing, we decided to first focus on the alkene coupling partner. This component reacts from its ground state, and therefore significant structural variation in the alkene is unlikely to affect the photosensitization step (Table 4-6). First, a large variety of styrenes were explored including potentially reactive aryl halides (**4.20**, **4.21**), as well as highly electron-deficient (**4.22**, **4.23**) and electron-rich (**4.24**) arenes, all of which gave good yields and excellent enantioselectivities. Several tethered functional groups such as azides (**4.25**) and protected primary alcohols (**4.26**, **4.27**) were also well tolerated. Bulkier styrenes such as 2-vinylnaphthelene (**4.28**) and 2-chlorostyrene (**4.29)** reacted efficiently and selectively, while α-methylstyrene (**4.30**) was sluggish and somewhat less selective. Gratifyingly, several other classes of alkenes gave reasonable yields and good selectivities overall, including phenyl vinyl sulfide (**4.31**), dienes (**4.32**, **4.33**), and 1,1-disubsituted aliphatic alkenes (**4.34**, **4.35**). Overall, our ability to selectively incorporate alkenes with large structural variations significantly broadens the types of cyclobutane cores that this methodology can access.

Table 4-6. Substrate scope studies for the alkene coupling partner

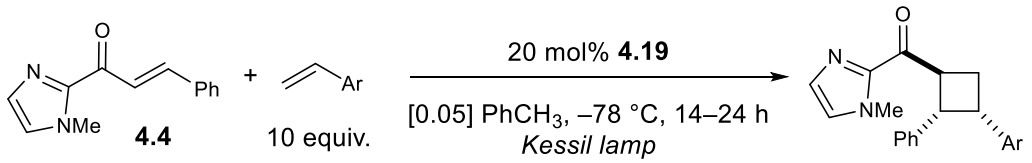

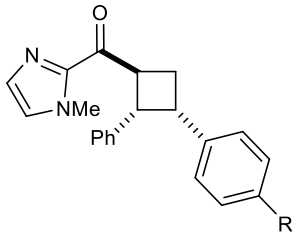

4.16 R = H, 78% yield, 95% ee, 7:1 d.r.
4.20 R = Cl, 77% yield, 98% ee, 6:1 d.r.
4.21 R = Br, 75% yield, 93% ee, 6:1 d.r.
4.22 R = CF_3, 83% yield, 96% ee, 5:1 d.r.
4.23 R = OAc, 56% yield, 97% ee, 11:1 d.r.
4.24 R = O*t*Bu, 76% yield, 99% ee, 6:1 d.r.

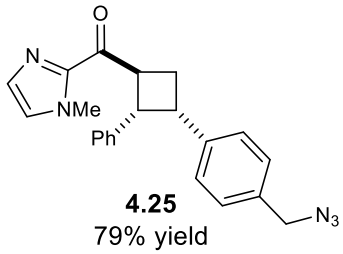

4.25
79% yield
94% ee, 3:1 d.r

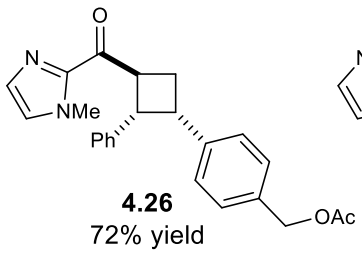

4.26
72% yield
97% ee, 3:1 d.r

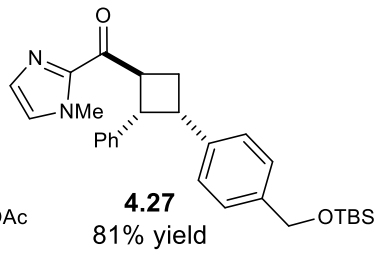

4.27
81% yield
95% ee, 3:1 d.r

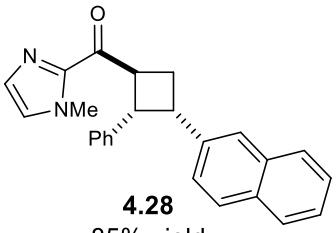

4.28
85% yield
90% ee, 2:1 d.r

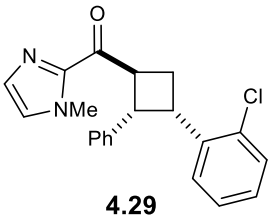

4.29
78% yield
94% ee, 10:1 d.r

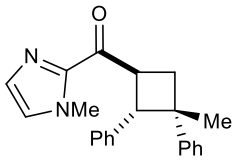

4.30
26% yield (NMR)
75% ee, 8:1 d.r

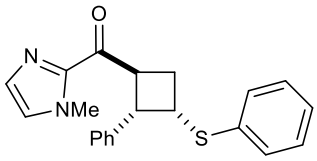

4.31[a]
57% yield
78% ee, 1:1 d.r

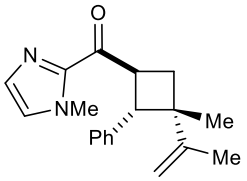

4.32
49% yield
62% ee, 10:1 d.r

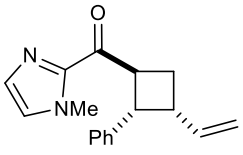

4.33
74% yield
87% ee, 3:1 d.r

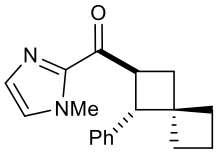

4.34[a]
37% yield
88% ee, >20:1 d.r

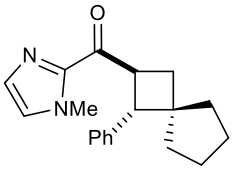

4.35[a]
42% yield
85% ee, 6:1 d.r

[a] Using 40 mol% acid catalyst

Preliminary investigations of the scope of the sensitized component, variations of **4.4**, have also been carried out (Table 4-7). So far, several electron-poor (**4.36**, **4.37**) and electron-rich (**4.38**) cinnamoyl-1-methylimidazoles have given good yields and good selectivities in the target cycloaddition with styrene. In addition, the combination of a complex electron-rich cinnamoyl imidazole and only 5 equivalents of an electron-rich styrene can selectively generate a new, unreported diastereomer (**4.39**) of a class of norlignin cyclobutanes that our group has prepared previously.

Table 4-7. Scope of cinnamoyl-1-methylimidazoles

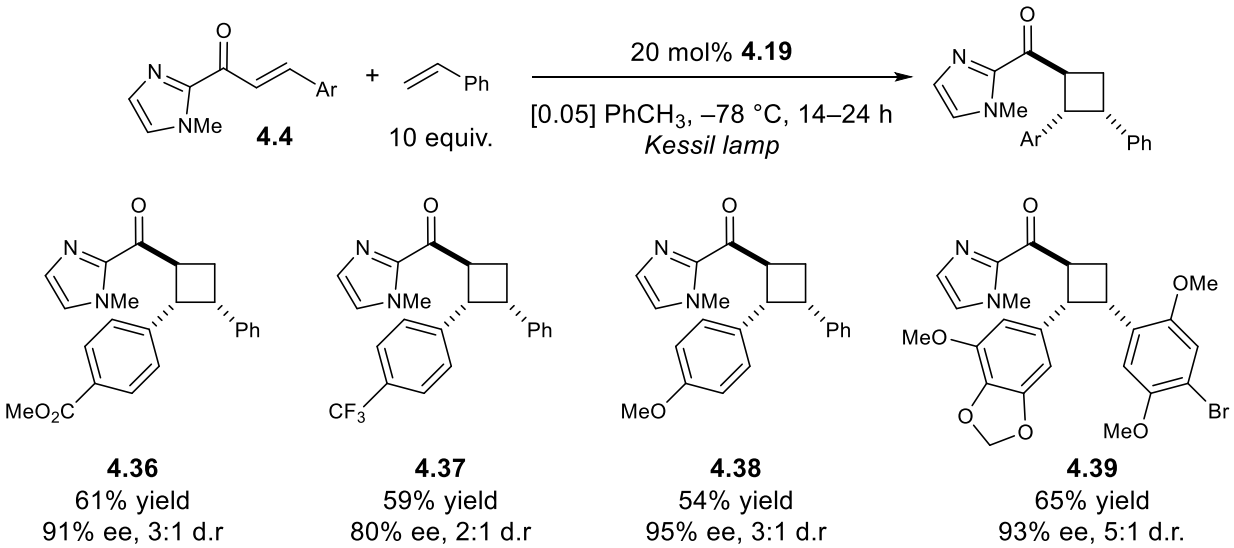

Furthermore, as in Chapter 3, we demonstrated that the imidazole moiety, which is instrumental to this mode of Brønsted acid activation, can be successfully cleaved to the corresponding methyl ester (**4.40**, Scheme 4-2). This occurs in good yield over a two-step *N*-alkylation/nucleophilic displacement sequence. In this case, we were able to accomplish this on a single diastereomer of **4.39** (*trans-cis*) with no loss of enantiopurity or epimerization. This cleavage approach can be used to generate a variety of carboxylic acid derivatives such as acids, esters, thioesters, and amides.[25,26]

Scheme 4-2. Representative Imidazole Cleavage to Cyclobutyl Methyl Ester **4.40**

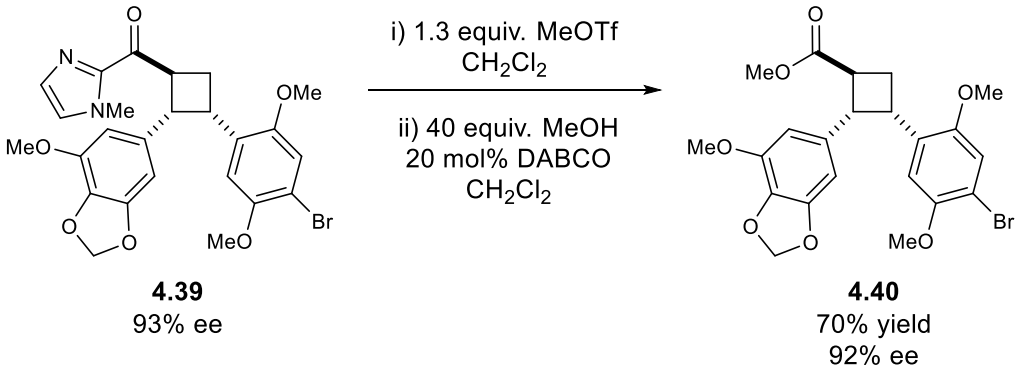

4.2.4: Mechanistic Experiments

Investigations into the mechanism of this reaction were primarily directed at understanding the unexpected observation that no transition-metal photocatalyst was required for this reaction (Table 4-4) to proceed efficiently. From this observation alone, it was concluded that the chiral BINOL phosphoramide catalyst **4.19** must be responsible for both sensitization of the substrate as well as induction of chirality in the resulting cycloaddition reaction. We established previously (Chapter 3) that direct sensitization this substrate with visible light in the presence of styrene did not produce identifiable quantities of product, nor did controls that included 20 mol% *p*-TsOH. Consequently, we set out to understand the interaction between **4.4** and **4.19**, and the means by which this leads to a highly stereoselective photocycloaddition.

4.2.4.1: Evidence for an Absorption Complex

One potential explanation for this unexpected reactivity is the formation of a charge-transfer absorption complex between the catalyst and substrate. An absorption complex is simply the unique species that is formed during the process of chromophore activation,[27] which is itself is

capable of absorbing lower energy light than either of the components of the complex. In this way selection of an appropriate light source can allow for selective activation of the absorption complex. The work of Bach[14,15,28] and Meggers[29,30] has recently established this method of activation toward asymmetric photochemical synthesis.

Figure 4-2. Absorption data for **4.4**, **4.19**, and **4.4** with 20 and 100 mol% loadings of **4.19**

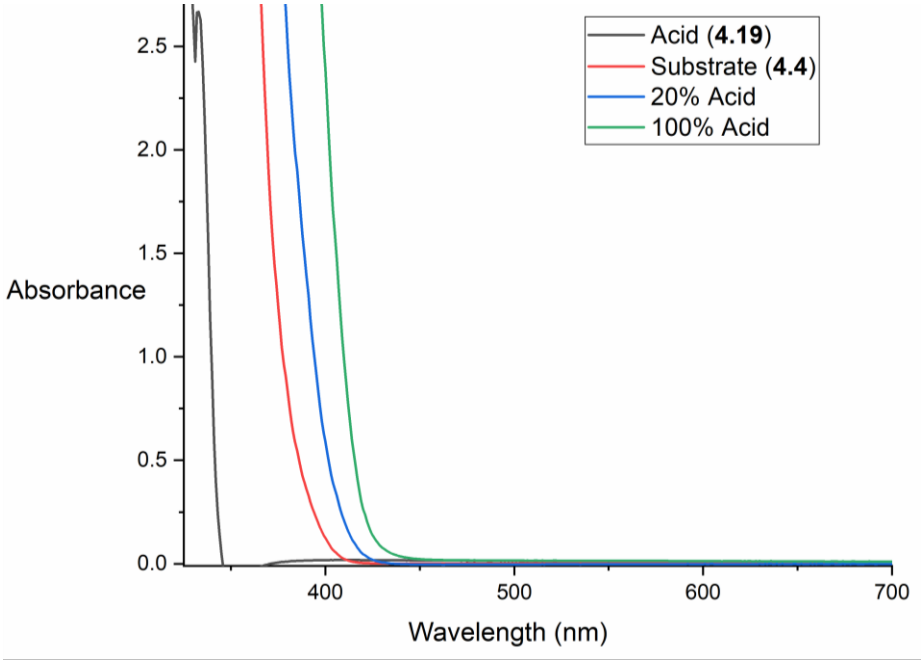

Testing this hypothesis was relatively straightforward: we analyzed the UV-vis absorption profiles of the catalyst, substrate, and mixtures of the two in solution. Upon performing these studies, we observe a modest bathochromic shift in the absorption of the substrate as increasing amounts of the chiral Brønsted acid are added (Figure 4-2). This shift amounts to approximately 30 nm in total from between the substrate and the 1:1 mixture of the substrate and the catalyst. Notably, the λ_{max} of the chosen light source is approximately 450 nm, and the intensity of light source below 400 nm is nearly zero. Importantly, the acid itself absorbs at a much shorter wavelength entirely outside of the visible range. Therefore, we propose that activation of this substrate is largely a result of increased absorbance when bound to **4.19**.

From these observations, the formation of an absorption complex appears not only likely, but crucial to the photochemical activation of **4.4**. Furthermore, we were interested in determining the stoichiometry of this complex. If the pKa of this class of *N*-triflyl phosphoramidate catalyst (6.4 in MeCN), and the pKa of the unsubstituted 1*H*-imidazole (15.0 in MeCN) are approximately representative of the acidities of **4.19** and **4.4**, we should expect essentially quantitative protonation of substrate by the available quantity of catalyst. Based on this interaction, a 1:1 complex is quite likely. Preliminary NMR titration experiments (see supporting information, Figure 4-9) indeed suggest that a 1:1 complex is formed, with a binding constant of ~7.5 x 10^6.

4.2.4.2: Singlet or Triplet Mechanism?

Having investigated the ground-state interactions that allow for the photochemical activation of **4.4**, we wondered if the photoexcited complex was reacting primarily from a singlet or triplet state. Consequently, we performed several experiments aimed at probing the predominant excited-state multiplicity involved in this transformation.

Scheme 4-3. Stereoconvergence study with *trans*- and *cis*-deuterostyrene

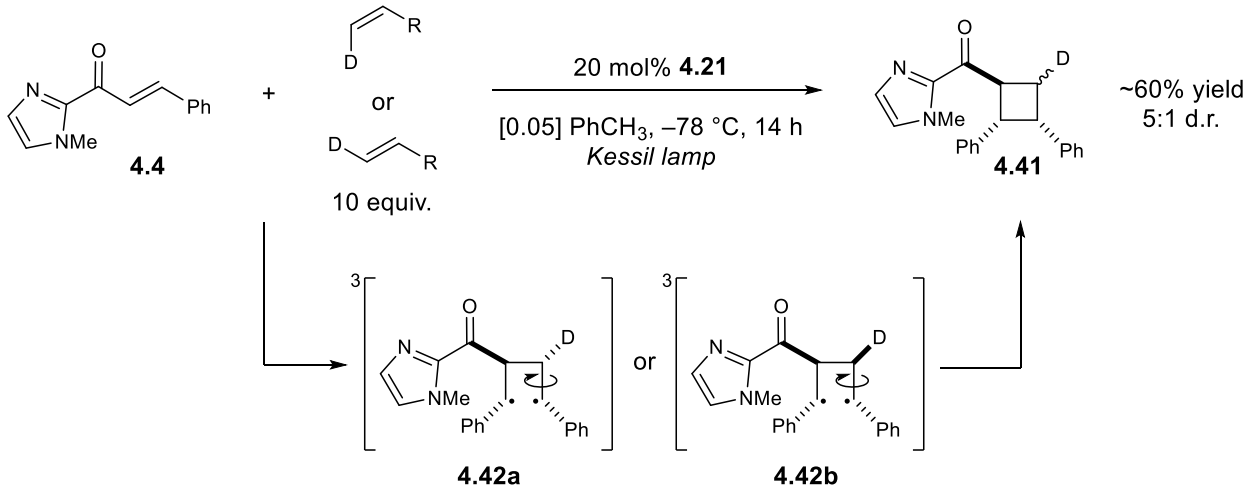

We began by carrying out a series of experiments using stereochemically-defined styrenes as acceptors. While *trans*- and *cis*-β-methylstyrene might serve as optimal acceptors for this test, reactivity with 1,2-disubstituted alkenes was demonstrated to be poor. Instead *trans*- and *cis*-deuterostyrene were independently synthesized and tested in the parent cycloaddition with **4.4**, using the optimal catalyst (Scheme 4-3). The ^{1}H- and ^{13}C-NMR data of the isolated product mixtures showed that an identical mixture of diastereomeric products are obtained regardless of the stereochemical relationship of the starting styrene. If this reaction occurred *via* a singlet excited state, we would expect to obtain distinct mixtures of diastereomeric products which retain the relationship set by the corresponding styrene acceptor.[31–36] Instead, the product mixtures appear nearly identical, consistent with a slower, stepwise triplet mechanism in which bond rotation occurs faster than radical recombination after formation of the 1,3-diradical intermediate **4.42**.

Figure 4-3. Fluorescence data for the optimal acid catalyst (**4.19**), the substrate (**4.4**), and a 1:1 mixture of catalyst and substrate.

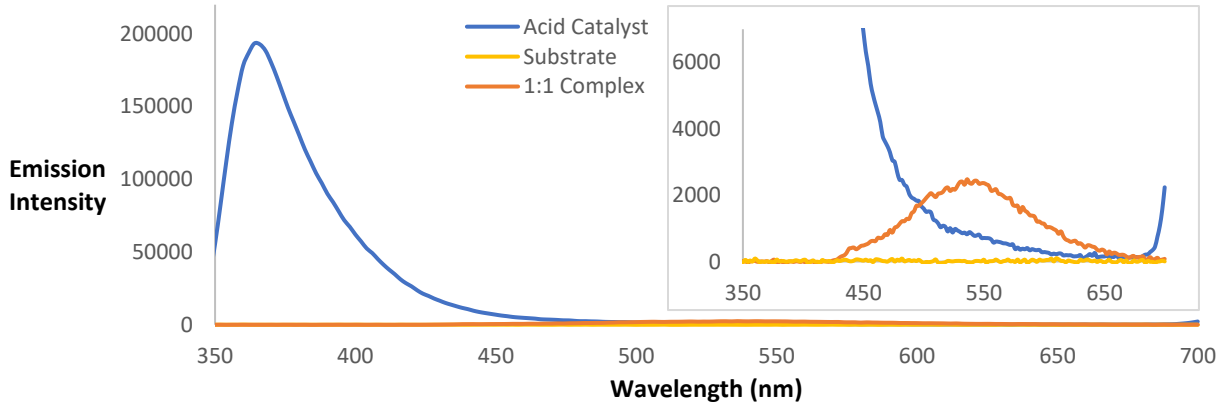

Fluorescence measurements of the optimal catalyst (**4.19**), the parent substrate (**4.4**), and catalyst/substrate mixtures were performed to determine if emission features corresponding to chemically relevant excited-state species could be visibly identified (Figure 4-3). When excited with 300 nm light, a solution of catalyst **4.19** returned an intense emission at 370 nm, appearing to

be its primary emission peak. While no emission is observed in this range for a solution containing only substrate, a new peak appears for a sample in which the catalyst and substrate have been combined in equal quantity. This significantly less intense feature has a λ_{max} of about 540 nm (see inlaid spectrum). This new emissive feature is clearly unique to the complex, and so additional fluorescence experiments were carried out to investigate its identity. This inlay also reveals an additional feature for **4.19** that appears to be present above 700 nm, and consequently, all additional fluorescence data was acquired from 330–800 nm to account for this low energy feature.

Figure 4-4. Fluorescence titration of Brønsted acid photocatalyst by **4.4**

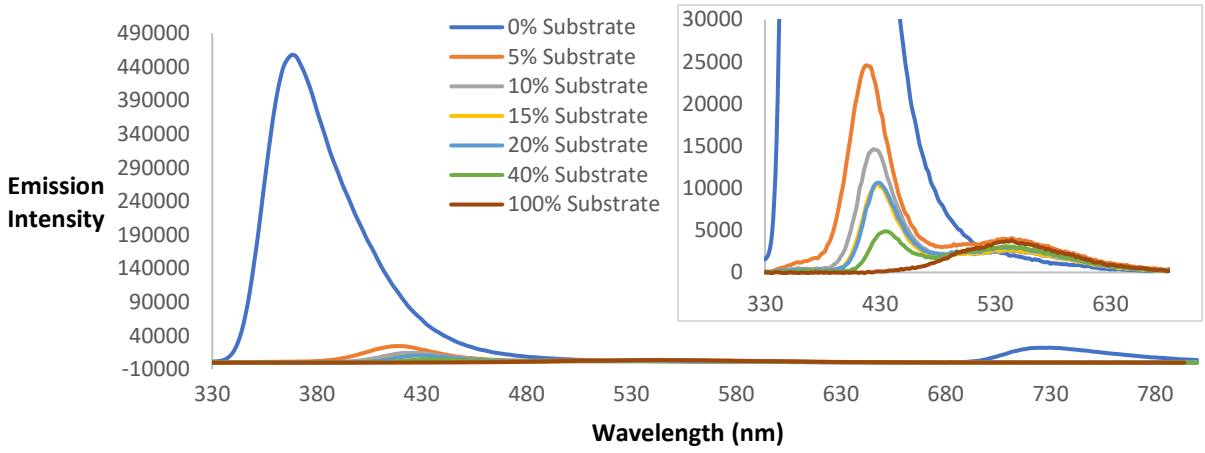

In addition, a fluorescence titration experiment was performed to understand the both the appearance of a new low-intensity emissive feature at 540 nm (Figure 4-4) and the complete disappearance of the catalyst emission at 370 nm. This was accomplished *via* sequential addition of increasing quantities of substrate to the acid catalyst and the observation of the changes therein.

First, the expansion of the overall emission window showed that there are two features that result from catalyst emission: a high-intensity emission at 370 nm and a low-intensity emission at 730 nm. These features likely correspond to the singlet emission (fluorescence) and triplet emission (phosphorescence) of the catalyst, respectively. Next, the addition of only 5 mol% of

substrate results in the complete disappearance of the emission at 730 nm, and a surprising >10-fold decrease in the intensity of emission at 370 nm, as well as a bathochromic shift of 50 nm (see inlaid spectrum). Not unexpectedly, continued additions of substrate results in further decreases in the intensity of this peak, which also continues to shift toward the red, though by diminishing degrees. Interestingly, the new emission feature that appears at 540 nm appears to be of a relatively constant intensity throughout this titration experiment.

Figure 4-5. Effects of oxygen addition on substrate-catalyst complex emission at 540 nm

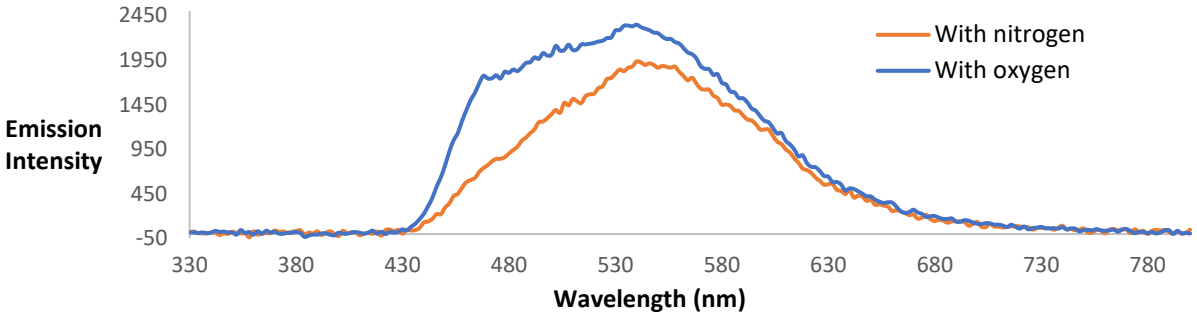

Figure 4-6. Effects of styrene addition on substrate-catalyst complex emission at 540 nm

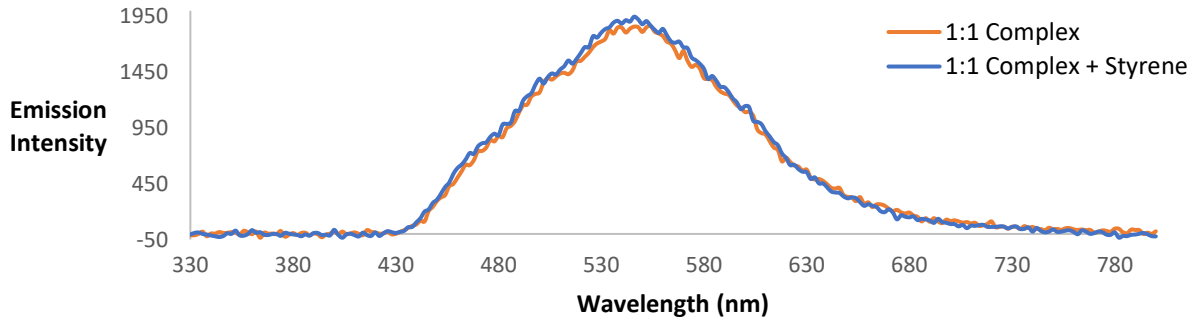

Additional fluorescence experiments focused on understanding this new emission feature at 540 nm. First, it was determined that this feature is not detectably quenched through the addition of a neat oxygen atmosphere to the sample (Figure 4-5). This indicates that this new feature is unlikely to be a triplet emission, which is expected to demonstrate significant quenching by O_2.

Secondly, we found that the addition of 10 equivalents of styrene also does not quench this emissive feature (Figure 4-6). Therefore, it is unlikely that the intermediate responsible for the peak at 540 nm is the one which productively and selectively leads to cycloadduct **4.5** or **4.16**.

At this point, we speculate that the high-intensity singlet and low-intensity triplet emissions of **4.19** both undergo a bathochromic shift in the presence of substrate. The peak at 540 nm results from the singlet emission of the complex, and empirically, is uninvolved in the productive cycloaddition reaction. A bathochromic shift of the peak at 730 nm would place the triplet emission peak of the complex in the near IR, outside the detection range for the fluorimeter. Future experiments require the observation and identification of a near IR triplet emission, which is expected to be quenched by both oxygen and styrene.

4.2.5: Future Work

Experiments remain to be performed toward a complete analysis of this transformation. First, the variation of the structure of the imidazoyl enone component of the reaction is one significant variable that has yet to be investigated. We anticipate that there will be certain limitations on this variable due to the molecule's role in the photoexcitation process, in contrast to the role of the acceptor alkene, which reacts from its ground state. Results obtained in Chapter 3 suggest that removal of the aryl component of this β-aryl enone will likely limit reactivity of the substrate in the target cycloaddition. It is also uncertain if heterocycles other than imidazole will retain high levels of selectivity on the corresponding products, as the acid catalyst **4.19** was optimized for this substrate.

Additional mechanistic experiments will focus on further verifying the predominance of a triplet state intermediate in this reaction. As discussed above, investigation of the near IR for a

triplet emission feature corresponding to this predicted intermediate may prove fruitful. Preliminary evaluation of the course of the reaction in the presence of a nitrogen and oxygen atmosphere has established that the reaction gives higher yields in the absence of oxygen (see supporting information, Figure 4-7). However, the effect is small, perhaps due to the limited solubility of oxygen in reaction solvent, toluene.

4.3 Conclusions

The use of Brønsted acids to control photochemical reactions has been underexplored, especially those involving the generation of excited-state intermediates. Following the development of a Brønsted acid-catalyzed cycloaddition *via* Dexter energy transfer in Chapter 3, we have now established that *chiral* Brønsted acids can, in fact, be used to control the selectivity of cycloaddition reactions involving the same class of imidazolyl enones. However, the mechanisms of these reactions are not comparable. Notably, we have found that BINOL-derived phosphoramidates are themselves competent chiral photocatalysts for the [2+2] photocycloaddition of **4.4** with a variety of electron rich alkenes. This unexpected and largely unprecedented behavior has since been attributed to the formation of an absorption complex, which allows for selective sensitization of the substrate within the chiral sphere of the BINOL acid catalyst *via* a triplet state intermediate. Although this investigation is not yet complete, we believe the insights acquired here and in Chapter 3 will allow for the continued development of Brønsted acid catalyzed excited-state photoreactions. Furthermore, the expansion of catalytic methods to include this class of catalysts should expand the types of substrate molecules which can be successfully activated and controlled using photocatalysis, continuing to expand the impact of robust photochemical methods in organic synthesis.

4.4 Contributions

Matt Genzink aided in the investigation of the substrate scope (Table 4-2) and will be responsible for continued investigations in the development of this work.

4.5 Supporting Information

4.5.1: General Information

MeCN, THF, CH_2Cl_2, and toluene were purified by elution through alumina as described by Grubbs.[37] Most styrenes, all dienes, phenyl vinyl sulfide, methylenecyclopentane, and methylenecyclobutane were purchased from Sigma Aldrich and distilled prior to use. Excluding those prepared below, all other starting materials, catalysts, or solvents were used as received from the supplier. Flash-column chromatography (FCC) was performed with Silicycle 40-63 Å (230-40 mesh) silica. Photochemical reactions were carried out with a 15 W EagleLight PAR38 blue LED flood light or a standard Kessil Lamp (model H150, $\lambda_{em.}$ (max) = ~450 nm)

Diastereomer ratios for reactions were determined by ^{1}H NMR analysis of crude reaction mixtures vs. a phenanthrene internal standard. ^{1}H and ^{13}C NMR data were obtained using a Bruker Avance-500 spectrometer with DCH cryoprobe and are referenced to tetramethylsilane (0.0 ppm) and $CDCl_3$ (77.0 ppm), respectively. This instrument and supporting facilities are funded by Paul J. Bender, Margaret M. Bender, and the University of Wisconsin. ^{1}H, ^{19}F, and ^{31}P NMR data were obtained using Bruker Avance-400 spectrometer. This instrument and supporting facilities are funded by the NSF (CHE-1048642) and the University of Wisconsin. NMR data are reported as follows: chemical shift, multiplicity (s = singlet, d = doublet, t = triplet, q = quartet, p = pentet, sext = sextet, sept = septet, m = multiplet), coupling constant(s) in Hz, integration. NMR spectra

were obtained at 298 K unless otherwise noted. FT-IR spectra were obtained using a Bruker Tensor 27 spectrometer and are reported in terms of frequency of absorption (cm^{-1}). Melting points (mp) were obtained using a Stanford Research Systems DigiMelt MPA160 melting point apparatus and are uncorrected. Mass spectrometry was performed with a Thermo Q Exactive™ Plus using ESI-TOF (electrospray ionization-time of flight). This instrument and supporting facilities are funded by the NIH (1S10 OD020022-1) and the University of Wisconsin. Enantiomeric excesses were determined by chiral HPLC of isolated materials using a Waters e2695 separations module with 2998 PDA detector and Diacel CHIRALPAK® columns and HPLC grade *i*-PrOH and hexanes. Traces were acquired using Empower 3® software. Optical rotations were measured using a Rudolf Research Autopol III polarimeter at room temperature in CH_2Cl_2.

4.5.2: Catalyst Synthesis

(R)-(+)-2,2'-Bis(methoxymethoxy)-1,1'-binaphthalene: Reaction performed in accordance with

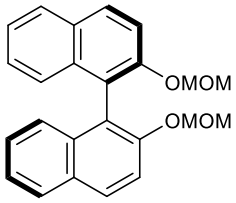

previously reported procedures. A 500 mL RBF was charged with 200 mL dry THF, followed by 3.00 g (75.0 mmol, 2.5 equiv.) of 60% NaH in mineral oil. This mixture was cooled to 0 °C and 8.59 g (30.0 mmol, 1.0 equiv.) (R)-BINOL added as a solution in 50 mL dry THF *via* cannula over approximately 20 minutes, controlling the resulting gas evolution. Then 5.70 mL (75.0 mmol, 2.5 equiv.) freshly distilled chloromethyl methyl ether (MOMCl) was added portionwise at 0 °C. The reaction was then warmed to room temperature and stirred overnight. The reaction was then slowly quenched with 20 mL sat. aq. NH_4Cl. This mixture was transferred to a separatory funnel with 100 mL CH_2Cl_2. After separating the organic layer, the aqueous layer was extracted additionally with 3 x 100 mL CH_2Cl_2. The combined organics were washed with 20 mL brine, dried over Na_2SO_4, and

concentrated. The resulting material was recrystallized from CH_2Cl_2/pentanes to give 9.06 g (24.0 mmol, 80% yield) of a crystalline white solid. Spectral data was consistent with that previously reported.[38] ^{1}H NMR (500 MHz, $CDCl_3$) δ 7.95 (d, *J* = 9.0 Hz, 2H), 7.85 (d, *J* = 8.3 Hz, 2H), 7.57 (d, *J* = 9.0 Hz, 2H), 7.34 (ddd, *J* = 8.0, 6.7, 1.2 Hz, 2H), 7.22 (ddd, *J* = 8.0, 6.7, 1.2 Hz, 2H), 7.15 (d, *J* = 8.3 Hz, 2H), 5.08 (d, *J* = 6.9 Hz, 2H), 4.97 (d, *J* = 6.9 Hz, 2H), 3.14 (s, 6H).

(±)-2,2'-Bis(methoxymethoxy)-1,1'-binaphthalene: Prepared and isolated through the above procedure for (R)-(+)-2,2'-Bis(methoxymethoxy)-1,1'-binaphthalene using 1.00 g (25.0 mmol) NaH in 100 mL THF, 2.86 g (10.0 mmol) (±)-BINOL in 25 mL THF, and 1.95 mL (25.0 mmol) MOMCl to give 2.84 g (7.6 mmol, 76% yield) of a white solid. Spectral data was consistent with that reported above.

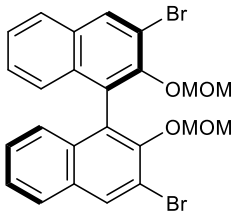

(R)-(+)-3,3'-Dibromo-2,2'-bis(methoxymethoxy)-1,1'-binaphthalene: In a flame dried 100 mL RBF 3.74 g (10.0 mmol, 1.0 equiv.) (R)-(+)-2,2'-bis(methoxymethoxy)-1,1'-binaphthalene was prepared in 50 mL dry THF and cooled to –78 °C. Then 12.5 mL (25.0 mmol, 2.5 equiv.) *n*BuLi (~2.0 M in hexanes) was added portionwise. This mixture was warmed to 0 °C for 1 hour before returning to –78 °C and adding a solution of 1.28 mL (25.0 mmol, 2.5 equiv.) Br_2 in 10 mL pentanes. The reaction was then warmed to room temperature and stirred overnight. Remaining Br_2 was quenched by stirring with 30 mL sat. aq. Na_2SO_3 for 30 min. The resulting heterogeneous mixture was transferred to a separatory funnel with 30 mL H_2O. After separating the organic layer, the aqueous layer was extracted additionally with 3 x 100 mL CH_2Cl_2. The combined organics were dried over Na_2SO_4, and concentrated. The resulting residue was dry loaded onto silica and purified

by flash column chromatography with a gradient of 2% → 5% → 10% EtOAc in hexanes to give 2.80 g (5.4 mmol, 54%) of a white solid. Spectroscopic data was consistent with that previously reported. [38] ^{1}H NMR (500 MHz, $CDCl_3$) δ 8.27 (s, 2H), 7.80 (d, *J* = 8.0 Hz, 2H), 7.44 (ddd, *J* = 8.0, 6.8, 1.2 Hz, 2H), 7.31 (ddd, *J* = 8.3, 6.8, 1.2 Hz, 2H) , 7.18 (d, *J* = 8.6 Hz, 2H), 4.83 (d, *J* = 5.9, 2H), 4.81(d, *J* = 5.9, 2H), 2.57 (s, 6H).

(±)-3,3'-Dibromo-2,2'-bis(methoxymethoxy)-1,1'-binaphthalene: Prepared and isolated through the above procedure for (R)-(+)-3,3'-Dibromo-2,2'-bis(methoxymethoxy)-1,1'-binaphthalene using 2.81 g (7.5 mmol) (±)-2,2'-Bis(methoxymethoxy)-1,1'-binaphthalene in 50 mL THF, 9.2 mL (18.25 mmol) *n*BuLi (~2.0 M in hexanes), and 0.93 mL (18.25 mmol) Br_2 in 10 mL pentanes to give 2.08 g (4.0 mmol, 53% yield) of a white solid. Spectral data was consistent with that reported above.

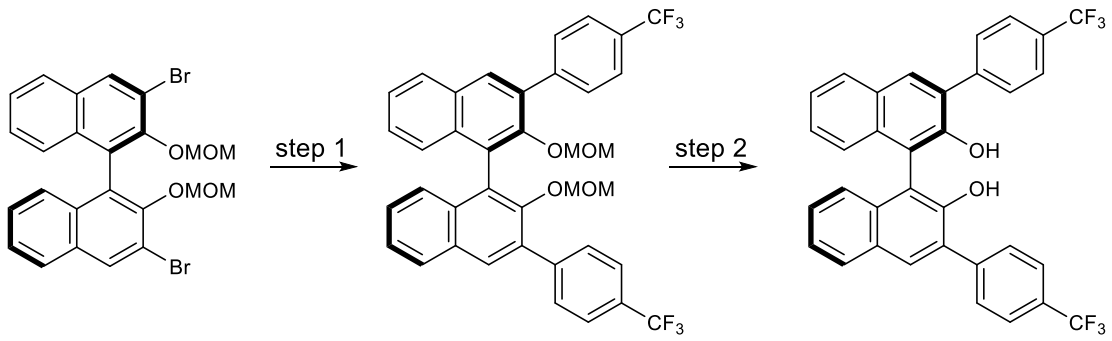

(R)-(+)-3,3'-Di-(4-trifluoromethyl)phenyl-[1,1'-binaphthalene]-2,2'-diol: *Step 1:* A 100 mL RBF was charged with 2.80 g (5.35 mmol 1.0 equiv.) (R)-(+)-3,3'-dibromo-2,2'-bis(methoxymethoxy)-1,1'-binaphthalene, 3.56 g (18.73 mmol, 3.5 equiv.) 4-trifluoromethylphenylboronic acid, 15 mL 2 M aq. Na_2CO_3, and 30 mL 1,2-dimethoxyethane (DME) and fitted with a reflux condenser. The apparatus was purged with N_2 for 15 min before

the addition of 340 mg (0.27 mmol, 0.05 equiv.) $Pd(PPh_3)_4$. The mixture was heated to 95 °C for 16 hours. After cooling to room temperature, the mixture was filtered over a pad of Celite, the pad washed with EtOAc, and the resulting solution concentrated. This residue was partitioned into 100 mL EtOAc and 25 mL H_2O. After separating the organic layer, the remaining aqueous was washed with 3 x 20 mL EtOAc. Combined organics were dried over Na_2SO_4 and concentrated. *Step 2:* The resulting yellow solid, primarily composed of MOM-protected cross-coupling product, was taken up in 30 mL THF, and 0.8 mL conc. HCl added. The mixture was heated to 65 °C for 3 hours. This mixture was concentrated, and the residue partitioned into 100 mL EtOAc and 25 mL H_2O. After separating the organic layer, the remaining aqueous was washed with 3 x 50 mL EtOAc. Combined organics were dried over Na_2SO_4, then concentrated directly on silica for purification by FCC with 2 → 5% EtOAc in hexanes to give 2.67 g (4.65 mmol, 87% yield) of a white solid. Spectroscopic data was consistent with that previously reported.[39] ^{1}H NMR (500 MHz, $CDCl_3$) δ 8.06 (s, 2H), 7.96 (d, *J* = 8.0 Hz, 2H), 7.87 (d, *J* = 8.1 Hz, 4H), 7.74 (d, *J* = 8.2 Hz, 4H), 7.44 (ddd, *J* = 8.0, 6.8, 1.1 Hz, 2H), 7.37 (ddd, *J* = 8.2, 6.8, 1.2 Hz, 2H), 7.23 (d, *J* = 8.2 Hz, 2H), 5.32 (s, 2H).

(±)-3,3'-Di-(4-trifluoromethyl)phenyl-[1,1'-binaphthalene]-2,2'-diol: Prepared and isolated through the above procedure for **(R)-(+)-3,3'-Di-(4-trifluoromethyl)phenyl-[1,1'-binaphthalene]-2,2'-diol.** *Step 1:* 2.08 g (4.0 mmol) (±)-3,3'-Dibromo-2,2'-bis(methoxymethoxy)-1,1'-binaphthalene, 2.65 (13.9 mmol) 4-trifluoromethylphenylboronic acid, 260 mg $Pd(PPh_3)_4$, 15 mL 2 M aq. Na_2CO_3, and 30 mL 1,2-DME were combined to give a yellow solid. *Step 2*: This yellow solid was combined with 20 mL THF and 0.6 mL conc. HCl to give 1.44 g (2.51 mmol, 63% yield) of a white solid. Spectral data was consistent with that reported above.

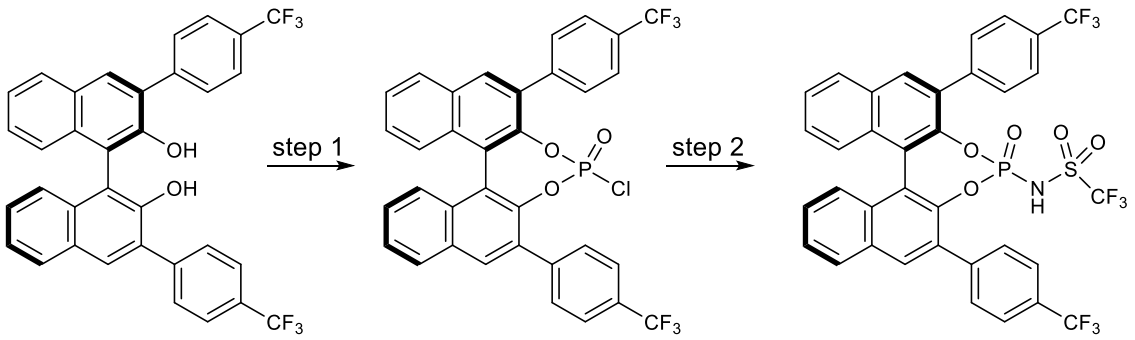

(R)-BINOL *N*-triflyl phosphoramide (4.19): *Step 1:* A 100 mL flame-dried RBF was charged with 2.48 g (4.3 mmol, 1.0 equiv.) (R)-(+)-3,3'-di-(4-trifluoromethyl)phenyl-[1,1'-binaphthalene]-2,2'-diol and 25 mL dry CH_2Cl_2, then cooled to 0 °C. To this solution was added 0.84 mL (9.0 mmol, 2.1 equiv.) freshly distilled $POCl_3$ and 1.90 mL (13.5 mmol, 3.1 equiv.) freshly distilled Et_3N. The reaction was warmed to room temperature and stirred under N_2 for 16 hours. The resulting mixture was washed once with 10 mL H_2O. This aqueous layer was extracted with 2 x 10 mL CH_2Cl_2. After drying over Na_2SO_4, the solution was concentrated to give a brown solid which was passed through a short plug of silica with 5% EtOAc in pentanes to give a quantitative yield of white solid. This was presumed to be the organic phosphoryl chloride and carried forward to the next step without additional purification. *Step 2:* A 100 mL flame-dried RBF was charged with 2.78 g (4.25 mmol, 1.0 equiv) of the organic phosphoryl chloride synthesized above, 634 mg (4.25 mmol, 1.0 equiv.) trifluromethanesulfonamide, 1.04 g (8.50 mmol, 2.0 equiv.) dimethylaminopyridine (DMAP), and 50 mL dry CH_2Cl_2. This mixture was stirred under N_2 at room temperature for 24 h. The crude reaction mixture was washed directly with 20 mL 6 M HCl and dried over Na_2SO_4. The resulting solution was concentrated directly onto silica and purified by FCC with 10% → 50% → 70% EtOAc in pentanes to give 1.64 g (2.14 mmol, 50% yield) of a fine white crystalline solid (dec. pt. = 250+ °C). $[\alpha]_D^{22}$ –234.0° (c0.970, CH_2Cl_2). ν_{max} (film) / cm^{-1} 2931, 1722, 1462, 1324, 1270, 1122, 1067, 973, 846, 775. ^1H NMR (500 MHz, $CDCl_3$) δ

8.13 (s, 1H), 8.05 (d, *J* = 8.0 Hz, 1H), 8.04 (s, 1H), 8.02 (d, *J* = 8.0 Hz, 1H), 7.76 (d, *J* = 8.1 Hz, 2H), 7.64–7.60 (m, 7H), 7.56 (ddd, *J* = 8.0, 6.3, 1.4 Hz, 1H), 7.48 (d, *J* = 8.3 Hz, 1H), 7.45–7.35 (m, 3H), 6.35 (br s, 1H). ^{13}C NMR (125 MHz, $CDCl_3$) δ 142.76, 142.66, 142.41, 142.33, 139.49, 139.20, 132.47, 132.45, 132.19, 132.18, 132.14, 132.02, 132.00, 131.95, 131.91, 131.82, 130.48, 130.22, 130.02, 129.96, 129.70, 128.85, 128.64, 127.49, 127.39, 127.33, 127.10, 127.02, 126.93, 126.85, 125.39, 125.36, 125.33, 125.30, 125.16, 124.96, 124.94, 124.91, 124.88, 124.85, 123.00, 122.78, 122.76, 122.68, 122.33, 121.95, 121.93, 120.84, 120.52, 119.78, 117.22, 114.67 (including signals due to unassigned C-F and C-P couplings, some signals are overlapped). ^{19}F NMR (377 MHz, $CDCl_3$) δ –62.92, –63.37, –78.32. ^{31}P NMR (162 MHz, $CDCl_3$) δ –5.05. HRMS (ESI) calculated for $[C_{35}H_{23}F_9N_2O_5PS]^+$ ($M+NH_4^+$) requires *m/z* 785.0916, found 785.0918.

(±)-BINOL *N*-triflyl phosphoramide (*rac*-4.19): Prepared and isolated through the above procedure for **4.19**. *Step 1:* 1.43 g (2.5 mmol) (±)-3,3'-Di-(4-trifluoromethyl)phenyl-[1,1'-binaphthalene]-2,2'-diol, 0.47 mL (5.0 mmol) $POCl_3$, and 1.03 mL (7.5 mmol) Et_3N were combined to give a white solid. *Step 2*: This white solid (1.47 g, 2.25 mmol) was combined with 335 mg (2.25 mmol) trifluoromethanesulfonamide, 550 mg (4.50 mmol) DMAP, and 25 mL CH_2Cl_2 to give 0.87 g (1.13 mmol, 50% yield. Spectral data was consistent with that reported above.

4.5.3: Substrate Synthesis

2-Acetyl-1-methylimidazole: A solution 0.84 mL (10.5 mmol, 1.05 equiv.) 1-methylimidazole in

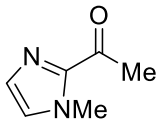

25 mL dry THF was prepared in a flame-dried 100 mL RBF. After cooling to –78 °C, 5.5 mL (10.5 mmol, 1.05 equiv.) nBuLi (1.91 M in hexanes) was added portionwise. The reaction was warmed to 0 °C for about 30 minutes before returning to –78 °C. A solution of 1.15 mL (10.0 mmol, 1.0 equiv.) 4-acetylmorpholine in 25 mL THF was prepared in a flame-dried 50 mL conical bottom flask and added to the solution of deprotonated 1-methylimidazole *via* cannula. The reaction was warmed to room temperature and stirred overnight. The resulting solution was stirred vigorously and 2 mL glacial acetic acid added dropwise. This solution was transferred to separatory funnel with 100 mL EtOAc, then washed with 30 mL sat. aq. $NaHCO_3$ and 30 mL sat. aq. NaCl. Each wash solution was back-extracted with 30 mL additional EtOAc. The combined organics were dried over Na_2SO_4 and concentrated. Products were purified by FCC with 2:3 EtOAc/pentanes to give 700 mg (5.6 mmol, 56% yield) of a colorless oil. The compound was consistent with reported spectroscopic data.[40] ^1H NMR (400 MHz, $CDCl_3$) δ 7.14 (s, 1H), 7.03 (s, 1H), 4.00 (s, 3H), 2.66 (s, 3H).

***N*-Methoxy-*N*-methylcinnamide:** A flame-dried 50 mL RBF was charged with 8.64 g (52.0

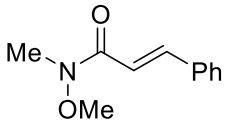

mmol, 1.0 equiv.) cinnamoyl chloride and 5.34 g (54.7 mmol, 1.05 mmol) *N,O*-dimethylhydroxylamine hydrochloride in 150 mL dry CH_2Cl_2. The mixture was cooled to 0 °C and 9.20 mL (114.4, 2.2 equiv.) pyridine added slowly. The reaction was then warmed to room temperature and stirred overnight. Then 1 M HCl was added, the organic layer separated, and the aqueous layer extracted with 3 x 25 mL additional EtOAc. The combined organics were washed with 25 mL sat. aq. $NaHCO_3$ and 25 mL sat. aq. NaCl. After drying over

Na_2SO_4, the crude material was concentrated. Products were purified by FCC with 1:1 Et_2O/pentanes to give 8.14 g (42.6 mmol, 82% yield) of a viscous oil which solidified after extended drying on *in vacuo*. The compound was consistent with reported spectroscopic data.[41] ^{1}H NMR (400 MHz, $CDCl_3$) δ 7.74 (d, *J* = 15.9 Hz, 1H), 7.59–7.56 (m, 2H), 7.41–7.36 (m, 3H), 7.04 (d, *J* = 15.9 Hz, 1H), 3.77(s, 3H), 3.32 (s, 3H).

2-cinnamoyl-1-methyl-1*H*-imidazole (4.4): A flame-dried 100 mL RBF was charged with 0.71

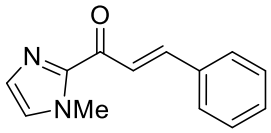

mL (8.93 mmol, 1.05 equiv.) *N*-methylimidazole and 30 mL dry THF, then cooled to –78 °C. A volume of 3.6 mL (8.93 mmol, 1.05 equiv.) nBuLi (2.50 M in hexanes) was added portionwise. The reaction was warmed to 0 °C for 30 minutes, then returned to –78 °C. A solution of 1.62 g (8.50 mmol, 1.0 equiv.) Weinreb amide in 10 mL THF was prepared in a flame-dried conical bottom flask and added to the solution of deprotonated 1-methylimidazole *via* cannula. The reaction was warmed to room temperature and stirred overnight. The resulting solution was stirred vigorously and 2 mL glacial acetic acid added dropwise. This solution was transferred to separatory funnel with 50 mL EtOAc and shaken with 20 mL water. The organic layer was separated and the aqueous extracted with 3 x 25 mL additional EtOAc. The combined organics were then washed with 30 mL sat. aq. $NaHCO_3$ and 30 mL sat. aq. NaCl, dried over Na_2SO_4, and concentrated. Products were purified by FCC with 1:1 Et_2O/pentanes. Yield: 1.32 g (6.2 mmol, 73% yield) of an off-white solid. The compound was consistent with reported spectroscopic data.[42] ^{1}H NMR (400 MHz, $CDCl_3$) δ 8.08 (d, *J* = 16.0 Hz, 1H), 7.83 (d, *J* = 16.0 Hz, 1H), 7.72–7.68 (m, 2H), 7.43–7.38 (m, 3H), 7.23 (s, 1H), 7.09 (s, 1H), 4.10 (s, 3H).

General Method for the Preparation of Substituted Cinnamoyl Methylimidazole Derivatives: A RBF was charged with 2-acetyl-1-methylimidazole (1.0 equiv.), and mixture of EtOH and H_2O. This solution was sparged briefly with N_2 (~5 minutes). Aromatic aldehyde (1.0-1.1 equiv., freshly distilled if possible) was then added to the solution, followed by a catalytic quantity of KOH. This was then stirred under N_2 for 12-16 h (overnight). *Work-up 1*: If the resulting solution was hetereogeneous, the product was filtered and washed with H_2O and cold EtOH to give the pure desired product. *Work-up 2*: If the resulting solution was homogeneous, the crude reaction mixture was diluted with CH_2Cl_2 and transferred to separatory funnel and shaken with H_2O. The organic layer was separated and the aqueous extracted with 3-fold with additional CH_2Cl_2. The combined organics were dried over Na_2SO_4, concentrated, then purified by FCC.

(*E*)-1-(1-methyl-1*H*-imidazol-2-yl)-3-(4-trifluoromethylphenyl)prop-2-en-1-one: Prepared

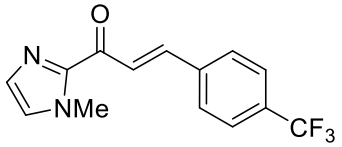

using the general method above using 328.0 mg (3.0 mmol, 1.0 equiv.) 2-acetyl-1-methylimidazole, 0.45 mL (3.3 mmol, 1.1 equiv.) 4-trifluoromethylbenzaldehyde, ~25 mg (1/2 pellet) KOH, 12 mL EtOH, and 6 mL H_2O. Work-up 2, then purified by FCC with 1:1 Et_2O/pentanes to give 442 mg (1.58 mmol, 53% yield) of an off-white solid. Spectroscopic data was consistent with that previously reported.[22] ^{1}H NMR (400 MHz, $CDCl_3$) δ 8.14 (d, *J* = 16.0 Hz, 1H), 7.81 (d, *J* = 16.0 Hz, 1H), 7.79 (d, *J* = 8.3 Hz, 2H), 7.65 (d, *J* = 8.3 Hz, 2H), 7.24 (s, 1H), 7.11 (s, 1H), 4.11 (s, 3H).

Methyl 4-[(1*E*)-3-(1-methyl-1*H*-imidazol-2-yl)-3-oxoprop-1-en-1-yl]benzoate (4.43):

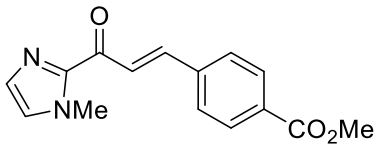

Prepared using the general method above using 416.0 mg (3.3 mmol, 1.0 equiv.) 2-acetyl-1-methylimidazole, 594 mg (3.6 mmol,

1.1 equiv.) methyl 4-formylbenzoate, ~25 mg (1/2 pellet) KOH, 6 mL MeOH[43], and 3 mL H_2O. Work-up 1 to give 428 mg (1.58 mmol, 48% yield) of an off-white solid (mp = 138–140 °C). ν_{max} (film) / cm^{-1} 1715, 1660, 1605, 1401, 1272, 1108, 1017, 919, 847, 774, 738, 694. ^1H NMR (400 MHz, $CDCl_3$) δ 8.15 (d, *J* = 16.0 Hz, 1H), 8.06 (d, *J* = 8.3 Hz, 2H), 7.82 (d, *J* = 16.0 Hz, 1H), 7.75 (d, *J* = 8.3 Hz), 7.24 (s, 1H), 7.11 (s, 1H), 4.11 (s, 3H), 3.94 (s, 3H). ^{13}C NMR (125 MHz, $CDCl_3$) δ. HRMS (ESI) calculated for $[C_{15}H_{15}N_2O_3]^+$ ($M+H^+$) requires *m/z* 271.1077, found 271.1080.

(*E*)-3-(4-methoxyphenyl)-1-(1-methyl-1*H*-imidazol-2-yl)prop-2-en-1-one: Prepared using

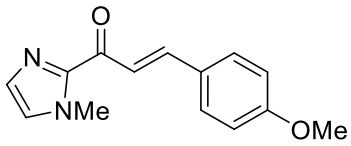

general method B using 2-acetyl-1-methylimidazole (372.7 mg, 3.0 mmol, 1.0 equiv.), 4-methoxybenzaldehyde (0.26 mL, 3.0 mmol, 1.0 equiv.), KOH (½ pellet, ~25 mg), 6 mL EtOH, and 3 mL H_2O. Work-up 2, then purified by FCC with 1:1 Et_2O/pentanes to give 382 mg (1.58 mmol, 53% yield) of an off-white solid. The compound was consistent with reported spectroscopic data.[44] ^1H NMR (400 MHz, $CDCl_3$) δ 7.96 (d, *J* = 15.9 Hz, 1H), 7.80 (d, *J* = 15.9 Hz, 1H), 7.66 (d, *J* = 8.7 Hz, 1H), 7.21 (s, 1H), 7.07 (s, 1H), 6.92 (d, *J* = 8.7 Hz, 1H), 4.10 (s, 3H), 3.85 (s, 3H).

(*E*)-3-(7-methoxy-2*H*-1,3-benzodioxol-5-yl)-1-(1-methyl-1*H*-imidazol-2-yl)prop-2-en-1-one

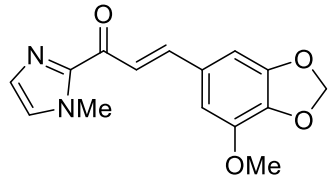

(4.44): Prepared using the general method above using 250.0.0 mg (2.0 mmol, 1.0 equiv.) 2-acetyl-1-methylimidazole, 360 mg (2.0 mmol, 1.0 equiv.) 5-methoxypiperonal, ~25 mg (1/2 pellet) KOH, 9 mL EtOH, and 1 mL H_2O. Work-up 1 to give 480 mg (1.68 mmol, 84% yield) of a yellow solid (mp = 210 – 212 °C). ν_{max} (film) / cm^{-1} 1656, 1625, 1588, 1439, 1409, 1330, 1274, 1140, 1098, 1026, 974, 918, 823, 789. ^1H NMR (400 MHz, $CDCl_3$) δ 7.91 (d, *J* = 15.8 Hz, 1H), 7.71 (d, *J* =

15.8 Hz, 1H), 7.21 (d, *J* = 0.8 Hz, 1H), 7.08 (d, *J* = 0.8 Hz, 1H), 6.92 (d, *J* = 1.4 Hz, 1H), 6.88 (d, *J* = 1.4 Hz, 1H), 6.03 (s, 2H), 4.10 (s, 3H), 3.95 (s, 3H). ^{13}C NMR (125 MHz, $CDCl_3$) δ 180.37, 149.29, 144.10, 143.77, 143.41, 137.70, 129.83, 129.25, 127.22, 121.30, 109.31, 102.46, 102.05, 56.67, 36.41. HRMS (ESI) calculated for $[C_{15}H_{15}N_2O_4]^+$ ($M+H^+$) requires *m/z* 287.1026, found 287.1027.

1-bromo-2,5-dimethoxy-4-vinylbenzene: A flame-dried 100 mL RBF was charged with 1.57 g

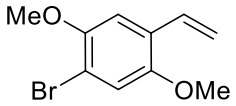

(4.4 mmol, 1.1 equiv.) methyltriphenylphosphonium bromide in 40 mL dry THF, the vessel cooled to 0 °C, and 500 mg of potassium *tert*-butoxide was added. The mixture was stirred for 30 minutes before cooling to –78 °C, at which point 0.98 g of 4-bromo-2,5-dimethoxybenzaldehyde in 5 mL THF was added portionwise. The mixture was warmed to room temperature and stirred for 18 hours. The reaction mixture was then diluted with 50 mL 1:1 Et_2O/pentanes and filtered over a plug of Celite. The eluent was concentrated directly onto silica, then purified by FCC with 10% Et_2O in pentanes to give 710 mg (2.90 mmol, 66% yield) of a white solid. Spectroscopic data was consistent with that previously reported.[45] ^{1}H NMR (500 MHz, $CDCl_3$) δ 7.90 (d, *J* = 15.9 Hz, 1H), 7.71 (d, *J* = 15.9 Hz, 1H), 7.26 (s, 1H), 7.08 (s, 1H), 6.92 (d, *J* = 1.3 Hz, 1H), 6.88 (d, *J* = 1.3 Hz, 1H), 6.03 (s, 2H), 4.10 (s, 3H), 3.95 (s, 3H).

1-(azidomethyl)-4-vinylbenzene: A flame-dried 250 mL RBF was charged with 0.65 g (10.0

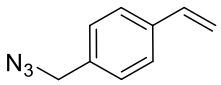

mmol, 2 equiv.) sodium azide and 0.76 g (5.0 mmol, 1.0 equiv.) 4-vinylbenzyl chloride dissolved in 50 mL DMF. The mixture was stirred for 24 hours at room temperature. The reaction was diluted with water (100 mL) and extracted with Et_2O (3 x 50 mL). The organic layers were combined and washed with water (2 x 50 mL) and brine (50 mL). The organic layer was

dried over Na_2SO_4, filtered, and concentrated. The crude product was purified by flash column chromatography eluting from 1:9 EtOAc:hexanes to give 0.75 g (4.7 mmol, 93%) of a light yellow oil. Spectroscopic data were consistent with that previously reported.[46] ^{1}H NMR (500 MHz, $CDCl_3$) δ 7.43 (AA'BB', *J* = 8.1 Hz, 2H), 7.28 (AA'BB', *J* = 8.1 Hz, 2H), 6.72 (dd, J = 17.7, 10.9 Hz, 1H), 5.77 (dd, *J* = 17.7, 0.7 Hz, 1H), 5.28 (dd, *J* = 10.9, 0.7 Hz, 1H), 4.33 (s, 2H).

1-(acetoxymethyl)-4-vinylbenzene: To a solution of pyridine (0.5 mL) and acetic anhydride (0.5 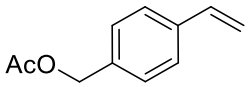

mL) a flame-dried 50 mL RBF was charged with 1.07 g (8.0 mmol, 1.0 equiv) (4-vinylphenyl) methanol and 98 mg (0.8 mmol, 0.1 equiv.) 4-dimethylaminopyrdine. The reaction was stirred at room temperature for 20 hours. The reaction was diluted with water (30 mL) and extracted with EtOAc (3 x 30 mL). The organic layers were combined and washed with 1M HCl (30 mL) and sat. aq. $NaHCO_3$ (30 mL). The organic layers were dried over Na_2SO4, filtered, and concentrated. The crude product was purified by flash column chromatography eluting from a gradient of 0% Et_2O in pentanes →10% Et_2O in pentanes to give 1.35 g (7.7 mmol, 96%) of a colorless oil. Spectroscopic data were consistent with that previously reported.[47] ^{1}H NMR (500 MHz, $CDCl_3$) δ 7.41 (d, *J* = 8.3 Hz, 2H), 7.32 (d, *J* = 8.3 Hz, 2H), 6.72 (dd, *J* = 17.8, 11.0 Hz, 1H), 5.77 (dd, *J* = 17.8, 0.8 Hz, 1H), 5.27 (dd, *J* = 11.0, 0.8 Hz 1H), 5.10 (s, 2H), 2.11 (s, 3H).

***tert*-butyldimethyl(4-vinylbenzyloxy) silane:** A vial was charged with DCM (6 mL) and 0.39 g 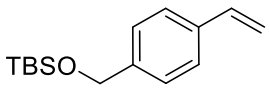

(2.87 mmol, 1.0 equiv.) (4-vinylphenyl) methanol followed by 0.25 g (3.73 mmol, 1.3 equiv.) imidazole. The reaction was stirred until everything dissolved then 0.52 g (3.44 mmol, 1.2 equiv.) tert-butyldimethylsilyl chloride was added and the reaction was stirred at room

temperature for 6 hours. The reactions was diluted in sat. aq. NH_4Cl and extracted with DCM (3 x 10 mL). The organic layers were combined, dried over Na_2SO_4, filtered, and concentrated. The crude product was purified with flash column chromatography eluting from a gradient of 0% Et_2O in pentanes → 2:1 pentanes:Et_2O. Spectroscopic data were consistent with that previously reported.[48] ^{1}H NMR (500 MHz, $CDCl_3$) δ 7.38 (AA'BB', *J* = 8.1 Hz, 2H), 7.28 (AA'BB', *J* = 8.1 Hz, 2H), 6.71 (dd, *J* = 17.6, 10.9 Hz, 1H), 5.72 (d, *J* = 17.6 Hz, 1H), 5.21 (d, *J* = 10.9 Hz, 1H), 4.73 (s, 2H), 0.94 (s, 9H), 0.10 (s, 6H).

4.5.4: Asymmetric [2+2] Photocycloaddition Reactions

General Procedure for Isolation-Scale Asymmetric [2+2] Cycloadditions: An oven dried Schlenk tube was charged with the 1-methylimidazoyl enone (0.4 mmol, 1.0 equiv), styrene (4.0 mmol, 10.0 equiv.), **4.19** (0.08 mmol, 0.2 equiv.), and 8 mL toluene. The Schlenk was sealed with a glass stopper and degassed *via* freeze-pump-thaw technique (3 x 5 min). This was then cooled to –78 °C and irradiated with a standard Kessil Lamp (H150) for 14 hours. The crude reaction mixture was then diluted 2-3x with CH_2Cl_2 before addition 2 mL sat. aq. $NaHCO_3$. The mixture was vigorously stirred for 60 seconds, the organic layer separated, and the aqueous layer extracted with CH_2Cl_2 (2 x 4 mL). The combined organics were dried over Na_2SO_4, concentrated, and analyzed by ^{1}H-NMR vs. internal standard (phenanthrene) to determine conversion and diastereomeric ratio. The crude mixture was then purified *via* flash column chromatography (FCC) using Et_2O/pentanes as the eluent, giving an isolated mixture of separable diastereomers. The major diastereomer of each mixture was characterized.

(2,3-diphenylcyclobutyl)(1-methyl-1H-imidazol-2-yl)methanone (4.16): Prepared according to

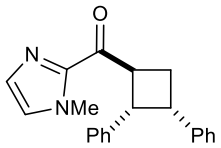

the general procedure for isolation-scale asymmetric experiments using 84.6 mg (0.40 mmol) 2-cinnamoyl-1-methylimidazole, 0.46 mL (4.0 mmol) styrene, 61.6 mg (0.08 mmol) **4.19**, and 8 mL toluene. The resulting material was purified by FCC using a gradient of 1:2 to 1:1 Et_2O/pentanes to give 98.0 mg (0.31 mmol, 78% yield) of two diastereomers (7:1 d.r.). Spectroscopic data for the major diastereomer were consistent with that previously reported.[22] Major diastereomer: 95% ee [Diacel CHIRALPAK OD-H, 5% to 50% iPrOH, 18 minutes, 1 mL/min, t_1=8.97 min, t_2=11.84 min]. ^{1}H NMR (500 MHz, $CDCl_3$) δ 7.18 (d, *J* = 0.8 Hz, 1H), 7.14–7.11 (m, 2H), 7.09–7.04 (m, 6H), 6.99–6.98 (m, 3H), 5.05 (q, *J* = 9.0 Hz, 1H), 4.47 (t, *J* = 9.2 Hz, 1H), 4.04 (s, 3H), 3.99 (td, *J* = 8.7, 6.0 Hz, 1H), 2.78–2.74 (m, 2H).

(3-(4-chlorophenyl)-2-phenylcyclobutyl)(1-methyl-1H-imidazol-2-yl)methanone (**4.20**):

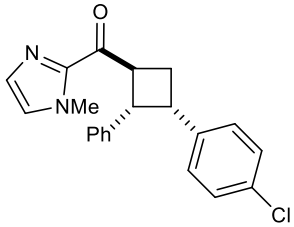

Prepared according to the general procedure for isolation-scale asymmetric experiments using 85.5 mg (0.40 mmol) 2-cinnamoyl-1-methylimidazole, 0.48 mL (4.0 mmol) 4-chlorostyrene, 63.0 mg (0.08 mmol) **4.19**, and 8 mL toluene. The resulting material was purified by FCC using 1:1 Et_2O/pentanes to give 109.5 mg (0.31 mmol, 77% yield) of three diastereomers (6:1 d.r.). Major diastereomer: 96% ee [Diacel CHIRALPAK AD, 5% to 50% iPrOH, 18 minutes, 1 mL/min, t_1=7.16 min, t_2=9.77 min]. White solid (mp = 121–124 °C). $[\alpha]_D^{22}$ –104.8° (c0.460, CH_2Cl_2). ν_{max} (film) / cm^{-1} 2930, 1723, 1667, 1493, 1407, 1272, 1122, 1072, 1014, 913, 769, 719. ^{1}H NMR (500 MHz, $CDCl_3$) δ 7.18 (s, 1H), 7.10–7.06 (m, 5H), 7.03–6.97 (m, 5H), 5.03 (q, *J* = 9.0 Hz, 1H), 4.46 (t, *J* = 9.3 Hz, 1H), 4.04 (s, 3H), 3.95 (td, *J* = 9.3, 4.6 Hz, 1H), 2.79–2.67 (m, 2H). ^{13}C NMR (125 MHz, $CDCl_3$) δ 192.81, 142.53, 139.40, 139.28, 131.53, 129.54, 129.48, 127.97, 127.86 (2C),

127.44, 126.03, 45.64, 43.50, 41.43, 36.25, 28.68. HRMS (ESI) calculated for $[C_{21}H_{20}ClN_2O]^+$ ($M+H^+$) requires *m/z* 351.1259, found 351.1261.

(3-(4-bromophenyl)-2-phenylcyclobutyl)(1-methyl-1H-imidazol-2-yl)methanone (**4.21**):

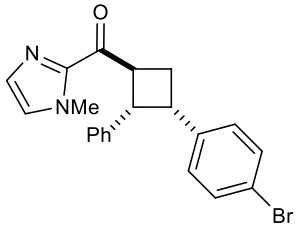

Prepared according to the general procedure for isolation-scale asymmetric experiments using 84.9 mg (0.40 mmol) 2-cinnamoyl-1-methylimidazole, 0.52 mL (4.0 mmol) 4-bromostyrene, 61.4 mg (0.08 mmol) **4.19**, and 8 mL toluene. The resulting material was purified by FCC eluting from a gradient of 1:2 Et_2O/pentanes → 1:1 Et_2O/pentanes to give 118.5 mg (0.30 mmol, 75% yield) of two diastereomers (6:1 d.r.). Major diastereomer: 92% ee [Diacel CHIRALPAK OD-H, 5% to 30% iPrOH, 20 minutes, 1 mL/min, t_1=11.18 min, t_2=12.23 min]. White solid (mp = 131-135 °C). $[\alpha]_D^{22}$ = -84.5° (c = 1.2, CH_2Cl_2). ν_{max} (film) 2959, 2929, 2859, 1724, 1669, 1409, 1274, 1073, 698 cm^{-1}. ^1H NMR (500 MHz, $CDCl_3$) δ 7.23 (d, *J* = 8.4 Hz, 2H), 7.18 (s, 1H), 7.10-7.06 (m, 3H), 7.03-6.93 (m, 5H), 5.02 (q, *J* = 8.9 Hz, 1H), 4.46 (t, *J* = 9.3 Hz, 1H), 4.04 (s, 3H), 3.94 (td, *J* = 9.2, 4.5 Hz, 1H), 2.77-2.69 (m, 2H). ^{13}C NMR (125 MHz, $CDCl_3$) δ 192.78, 142.51, 139.94, 139.26, 130.91, 129.94, 129.48, 127.88, 127.85, 127.44, 126.04, 119.66, 45.56, 43.51, 41.48, 36.24, 28.65. HRMS (ESI) calculated for $[C_{21}H_{19}BrN_2O]^+$ ($M+H^+$) requires *m/z* 395.0754, found 395.0757.

(1-methyl-1H-imidazol-2-yl)(2-phenyl-3-(4-(trifluoromethyl)phenyl)cyclobutyl)methanone

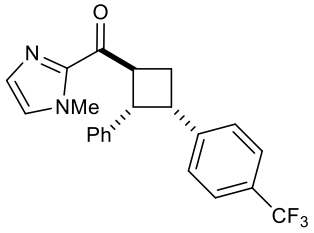

(4.22): Prepared according to the general procedure for isolation-scale asymmetric experiments using 84.3 mg (0.40 mmol) 2-cinnamoyl-1-methylimidazole, 0.59 mL (4.0 mmol) 4-(trifluoromethyl)styrene, 63.0 mg (0.08 mmol) **4.19**, and 8 mL toluene. The resulting material was purified by FCC eluting from

a gradient of 1:2 Et_2O/pentanes → 1:1 Et_2O/pentanes to give 126.6 mg (0.33 mmol, 83% yield) of two diastereomers (5:1 d.r.). Major diastereomer: 96% ee [Diacel CHIRALPAK OD-H, 5% to 50% iPrOH, 13 minutes, 1 mL/min, t_1=8.17 min, t_2=9.45 min]. Viscous oil/semisolid. $[\alpha]_D^{22}$ = -74.4° (c = 2.0, CH_2Cl_2). ν_{max} (film) 2960, 1724, 1670, 1462, 1325, 1118, 1069, 699 cm^{-1}. ^1H NMR (500 MHz, $CDCl_3$) δ 7.36 (d, *J* = 8.1 Hz, 2H), 7.19-7.16 (m, 3H), 7.08-7.05 (m, 3H), 6.98-6.96 (m, 3H), 5.06 (q, *J* = 8.9 Hz, 1H), 4.51 (t, *J* = 9.4 Hz, 1H), 4.07-4.02 (m, 4H), 2.82-2.73 (m, 2H). ^{13}C NMR (125 MHz, $CDCl_3$) δ 192.64, 145.09, 142.49, 139.03, 129.52, 128.47, 128.15, 127.90, 127.80, 127.49, 126.15, 124.76, 123.18, 45.71, 43.50, 41.85, 36.24, 28.47. HRMS (ESI) calculated for $[C_{22}H_{19}F_3N_2O]^+$ ($M+H^+$) requires *m/z* 385.1522, found 385.1526.

(3-(4-acetoxyphenyl)-2-phenylcyclobutyl)(1-methyl-1H-imidazol-2-yl)methanone (**4.23**):

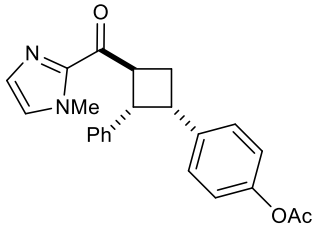

Prepared according to the general procedure for isolation-scale asymmetric experiments 84.9 mg (0.40 mmol) 2-cinnamoyl-1-methylimidazole, 0.61 mL (4.0 mmol) 4-acetoxystyrene, 62.7 mg (0.08 mmol) **4.19**, and 8 mL toluene, The resulting material was purified by FCC using 1:1 Et_2O/pentanes to give 84.4 mg (0.23 mmol, 56% yield) of three diastereomers (11:1 d.r.). Major diastereomer: 97% ee [Diacel CHIRALPAK AD, 5% to 50% iPrOH, 18 minutes, 1 mL/min, t_1=10.79 min, t_2=12.47 min]. White solid (mp = 81–83 °C). $[\alpha]_D^{22}$ –90.0° (c1.180, CH_2Cl_2). ν_{max} (film) / cm^{-1} 2932, 1760, 1723, 1666, 1508, 1407, 1289, 1195, 1167, 1017, 743, 698. ^1H NMR (500 MHz, $CDCl_3$) δ 7.17 (s, 1H), 7.08–7.04 (m, 5H), 7.01–6.98 (m, 3H), 6.85 (d, *J* = 8.6 Hz, 2H), 5.03 (q, *J* = 8.9 Hz, 1H), 4.45 (t, *J* = 9.2 Hz, 1H), 4.02 (s, 3H), 3.98 (td, *J* = 8.8, 5.5 Hz, 1H), 2.77–2.71 (m, 2H), 2.22 (s, 3H). ^{13}C NMR (125 MHz, $CDCl_3$) δ 192.90, 169.42, 148.69, 142.54, 139.39,

138.39, 129.44, 129.12, 127.93, 127.78, 127.39, 125.94, 120.85, 45.73, 43.58, 41.47, 36.22, 28.72, 21.11. HRMS (ESI) calculated for $[C_{23}H_{23}N_2O_3]^+$ ($M+H^+$) requires *m/z* 375.1703 found 375.1702.

(3-(4-*tert*-butoxyphenyl)-2-phenylcyclobutyl)(1-methyl-1H-imidazol-2-yl)methanone (**4.24**):

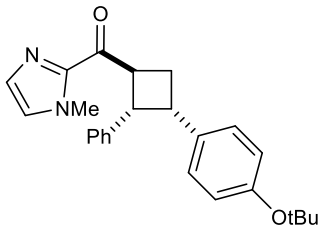

Prepared according to the general procedure for isolation-scale asymmetric experiments using 85.2 mg (0.40 mmol) 2-cinnamoyl-1-methylimidazole, 0.75 mL (4.0 mmol) 4-tert-butoxystyrene, 63.3 mg (0.08 mmol) **4.19**, and 8 mL toluene. The resulting material was purified by FCC using a 1:1 Et_2O/pentanes to give 117.9 mg (0.30 mmol, 76% yield) of three diastereomers (5:1 d.r.). Major diastereomer: 83% ee [Diacel CHIRALPAK AD-H, 5% to 30% iPrOH, 20 minutes, 1 mL/min, t_1=7.90 min, t_2=8.56 min]. Viscous semisolid. $[\alpha]_D^{22}$ –69.0° (c0.620, CH_2Cl_2). ν_{max} (film) / cm^{-1} 2931, 1726, 1668, 1506, 1409, 1274, 1162, 1123, 1073, 898, 744, 698. ^{1}H NMR (500 MHz, $CDCl_3$) δ 7.17 (s, 1H), 7.04 (s, 1H), 7.03–7.00 (m, 2H), 6.97–6.93 (m, 5H), 6.75 (d, *J* = 8.4 Hz, 1H), 5.03 (q, *J* = 9.0 Hz, 1H), 4.41 (t, *J* = 9.3 Hz, 1H), 4.03 (s, 3H), 3.94 (dt, *J* = 9.3, 6.6 Hz, 1H), 2.76–2.73 (m, 2H), 1.23 (s, 9H). ^{13}C NMR (125 MHz, $CDCl_3$) δ 193.09, 153.13, 142.63, 139.54, 135.68, 129.40, 128.51, 128.04, 127.55, 127.33, 125.75, 123.90, 45.97, 43.53, 41.55, 36.23, 28.72 (2C), 28.25. HRMS (ESI) calculated for $[C_{25}H_{29}N_2O_2]^+$ ($M+H^+$) requires *m/z* 389.2224, found 329.2225.

(3-(4-(azidomethyl)phenyl)-2-phenylcyclobutyl)(1-methyl-1H-imidazol-2-yl)methanone

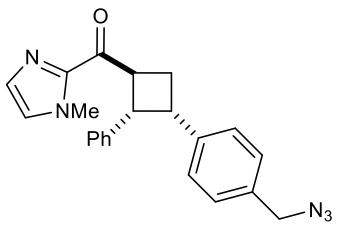

(**4.25**): Prepared according to the general procedure for isolation-scale asymmetric experiments using 82.7 mg (0.39 mmol) 2-cinnamoyl-1-methylimidazole, 0.64 g (4.0 mmol) 1-(azidomethyl)-4-vinylbenzene, 61.2 mg (0.08 mmol) **4.19**, and 8 mL toluene. The resulting material was purified by FCC eluting

from a gradient of 1:2 Et_2O/pentanes → 1:1 Et_2O/pentanes to give 114.6 mg (0.31 mmol, 79% yield) of three diastereomers (10:2:1 d.r.). Major diastereomer: 94% ee [Diacel CHIRALPAK AD, 5% to 50% iPrOH, 18 minutes, 1 mL/min, t_1=8.51 min, t_2=10.99 min]. Viscous oil/semisolid. $[\alpha]_D^{22}$ = -88.0° (c = 0.5, CH_2Cl_2). ν_{max} (film) 2958, 2931, 2095, 1724, 1668, 1408, 1271, 1072, 697 cm^{-1}. ^1H NMR (500 MHz, $CDCl_3$) δ 7.18 (d, *J* = 0.9 Hz, 1H), 7.11-7.04 (m, 7H), 7.00-6.96 (m, 3H), 5.05 (q, *J* = 9.1 Hz, 1H), 4.47 (t, *J* = 9.3 Hz, 1H), 4.19 (s, 2H), 4.04 (s, 3H), 4.00 (dt, *J* = 9.7, 6.8 Hz, 1H), 2.76 (dd, *J* = 8.9, 6.6 Hz, 2H). ^{13}C NMR (125 MHz, $CDCl_3$) δ 192.92, 142.57, 141.11, 139.40, 132.57, 129.46, 128.69, 127.95, 127.90, 127.76, 127.39, 125.92, 54.46, 45.78, 43.68, 41.76, 36.24, 28.51. HRMS (ESI) calculated for $[C_{22}H_{21}N_5O]^+$ ($M+H^+$) requires *m/z* 372.1819, found 372.1826.

(3-(4-(acetoxymethyl)phenyl)-2-phenylcyclobutyl)(1-methyl-1H-imidazol-2-yl)methanone

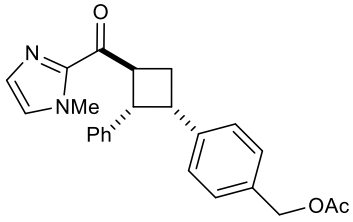

(**4.26**): Prepared according to the general procedure for isolation-scale asymmetric experiments using 83.9 mg (0.40 mmol) 2-cinnamoyl-1-methylimidazole, 0.71 g (4.0 mmol) 4-acetoxymethylstyrene, 61.4 mg (0.08 mmol) **4.19**, and 8 mL toluene. The resulting material was purified by FCC eluting from a gradient of 0% EtOAc in hexanes → 30% EtOAc in hexanes to give 110.0 mg (0.28 mmol, 72% yield) of three diastereomers (10:2:1 d.r.). Major diastereomer: 97% ee [Diacel CHIRALPAK OD-H, 5% to 50% iPrOH, 28 minutes, 1 mL/min, t_1=13.45 min, t_2=23.64 min]. Viscous oil/semisolid. $[\alpha]_D^{22}$ = -51.0° (c = 0.2, CH_2Cl_2). ν_{max} (film) 2959, 2931, 1725, 1260, 1120, 1071, 799, 698 cm^{-1}. ^1H NMR (500 MHz, $CDCl_3$) δ 7.18 (d, *J* = 0.9 Hz, 1H), 7.12-7.05 (m, 7H), 7.02-6.98 (m, 3H), 5.04 (q, *J* = 9.6 Hz, 1H), 4.98 (s, 2H) 4.47 (t, *J* = 9.6 Hz, 1H), 4.04 (s, 3H), 4.00 (td, *J* = 8.7, 6.1 Hz, 1H), 2.77-2.73 (m, 2H), 2.06 (s, 3H). ^{13}C NMR (125

MHz, $CDCl_3$) δ 192.98, 170.89, 142.57, 141.08, 139.56, 133.32, 129.45, 128.43, 127.91, 127.89, 127.75, 125.87, 66.13, 45.70, 43.73, 41.72, 36.25, 28.79, 21.05. HRMS (ESI) calculated for $[C_{24}H_{24}N_2O_3]^+$ ($M+H^+$) requires *m/z* 389.1860, found 339.1867.

3-(4-(((tert-butyldimethylsilyl)oxy)methyl)phenyl)-2-phenylcyclobutyl)(1-methyl-1H-imidazol-2-yl)methanone (**4.27**): Prepared according to the general procedure for isolation-scale asymmetric experiments using 81.8 mg (0.39 mmol) 2-cinnamoyl-1-methylimidazole, 1.00 g (4.0 mmol) O-(tert-butyl)dimethylsilyl(4-vinylphenyl)methanol, 60.9 mg (0.08 mmol) **4.19**, and 8 mL toluene. The resulting material was purified by FCC eluting from a gradient of 1:2 Et_2O/pentanes → 1:1 Et_2O/pentanes to give 144.3 mg (0.31 mmol, 81% yield) of three diastereomers (10:2:1 d.r.). Major diastereomer: 95% ee [Diacel CHIRALPAK OD-H, 5% to 50% iPrOH, 20 minutes, 1 mL/min, t_1=6.99 min, t_2=11.26 min]. Viscous oil/semisolid. $[\alpha]_D^{22}$ = -31.7° (c = 0.3, CH_2Cl_2). ν_{max} (film) 2959, 2932, 2860, 1727, 1273, 1122, 1072, 804 cm^{-1}. ^1H NMR (500 MHz, $CDCl_3$) δ 7.18 (s, 1H), 7.09-7.03 (m, 7H), 7.00-6.96 (m, 3H), 5.05 (q, *J* = 9.5 Hz, 1H), 4.62 (s, 2H) 4.45 (t, *J* = 9.3 Hz, 1H), 4.04 (s, 3H), 3.97 (dt, *J* = 9.5, 6.6 Hz, 1H), 2.74 (dd, *J* = 9.0, 6.7 Hz, 2H), 0.90 (s, 9H), 0.02 (d, *J* = 1.8 Hz, 6H). ^{13}C NMR (125 MHz, $CDCl_3$) δ 193.14, 142.62, 139.69, 139.43, 138.90, 129.43, 128.09, 127.93, 127.69, 127.33, 125.76, 125.76, 64.87, 45.72, 43.84, 41.73, 36.25, 28.85, 25.95, 18.39, -5.17. HRMS (ESI) calculated for $[C_{28}H_{36}SiN_2O_2]^+$ ($M+H^+$) requires *m/z* 461.2619, found 461.2626.

(1-methyl-1H-imidazol-2-yl)(3-(naphthalen-2-yl)-2-phenylcyclobutyl)methanone (**4.28**):

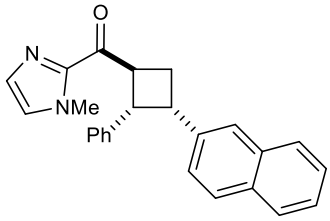

Prepared according to the general procedure for isolationn-scale asymmetric experiments using 82.1 mg (0.39 mmol) 2-cinnamoyl-1-methylimidazole, 0.61 g (4.0 mmol) 2-vinylnapthalene, 60.3 mg (0.08 mmol) **4.19**, and 8 mL toluene. The resulting material was purified by FCC eluting from a gradient of 1:2 Et_2O/pentanes → 1:1 Et_2O/pentanes to give 120.0 mg (0.33 mmol, 85% yield) of three diastereomers (5:1.5:1 d.r.). Major diastereomer: 90% ee [Diacel CHIRALPAK AD, 5% to 50% iPrOH, 13 minutes, 1 mL/min, t_1=7.61 min, t_2=9.76 min]. Viscous oil/semisolid. $[\alpha]_D^{22}$ = -97.7° (c = 0.4, CH_2Cl_2). ν_{max} (film) 2959, 2931, 2859, 1726, 1409, 1273, 1073, 698 cm^{-1}. ^1H NMR (500 MHz, $CDCl_3$) δ 7.75 (d, *J* = 6.9 Hz, 1H), 7.68 (d, *J* = 8.1 Hz, 1H), 7.65 (s, 1H), 7.52 (d, *J* = 8.5 Hz, 1H), 7.42-7.34 (m, 2H), 7.20 (d, *J* = 0.9 Hz, 1H), 7.07-7.05 (m, 2H), 7.03-6.98 (m, 4H), 6.94-6.91 (m, 1H), 5.12 (q, *J* = 9.5 Hz, 1H), 4.55 (t, *J* = 9.2 Hz, 1H), 4.16 (td, *J* = 9.1, 4.6 Hz, 1H), 4.05 (s, 3H), 2.90-2.82 (m, 2H). ^{13}C NMR (125 MHz, $CDCl_3$) δ 193.10, 142.61, 139.61, 138.56, 133.25, 131.90, 129.44, 127.94, 127.73, 127.67, 127.45, 127.39, 127.35, 127.25, 126.07, 125.86, 125.61, 125.11, 45.75, 43.95, 42.05, 36.27, 28.61.HRMS (ESI) calculated for $[C_{25}H_{22}N_2O]^+$ ($M+H^+$) - requires *m/z* 367.1805, found 367.1808.

(3-(2-chlorophenyl)-2-phenylcyclobutyl)(1-methyl-1H-imidazol-2-yl)methanone (**4.29**):

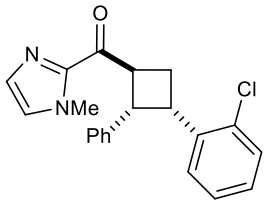

Prepared according to the general procedure for isolation-scale asymmetric experiments using 85.1 mg (0.40 mmol) 2-cinnamoyl-1-methylimidazole, 0.51 mL (4.0 mmol) 2-chlorostyrene, 62.4 mg (0.08 mmol) **4.19**, and 8 mL toluene The resulting material was purified by FCC using 1:1 Et_2O/pentanes to give 109.0 mg (0.31 mmol, 78% yield) of two diastereomers (10:1 d.r.). Major Diastereomer: 94% ee [Diacel

CHIRALPAK AD, 5% to 50% iPrOH, 18 minutes, 1 mL/min, t_1=6.72 min, t_2=8.55 min]. White solid (mp = 94–97 °C). $[\alpha]_D^{22}$ –7.9° (c1.750, CH_2Cl_2). ν_{max} (film) / cm^{-1} 2958, 1722, 1668, 1408, 1266, 1123, 1038, 912, 735, 698. ^{1}H NMR (500 MHz, $CDCl_3$) δ 7.39 (dd, *J* = 8.0, 1.2 Hz, 1H), 7.16–6.98 (m, 10 H), 4.87 (dt, *J* = 9.7, 7.2 Hz, 1H), 4.51 (dd, *J* = 9.4, 7.2 Hz, 1H), 4.44 (td, *J* = 9.2, 6.2 Hz, 1H), 4.06 (s, 3H), 2.92 (ddd, *J* = 12.0, 10.1, 6.0 Hz, 1H), 2.74–2.68 (m, 1H). ^{13}C NMR (125 MHz, $CDCl_3$) δ 192.85, 142.45, 139.38, 138.15, 134.61, 129.40, 129.05, 128.15, 128.05, 127.52, 127.29, 127.23, 126.30, 126.03, 45.80, 43.87, 39.15, 36.26, 27.14. HRMS (ESI) calculated for $[C_{21}H_{20}ClN_2O]^+$ ($M+H^+$) requires *m/z* 351.1259, found 351.1258. Minor diastereomer: unable to isolate cleanly from major diastereomer.

(1-methyl-1H-imidazol-2-yl)(2-phenyl-3-(phenylthio)cyclobutyl)methanone (**4.31**): Prepared

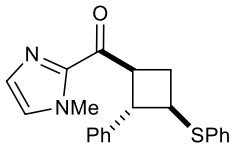

according to the general procedure for isolation-scale asymmetric experiments using 85.2 mg (0.41 mmol) 2-cinnamoyl-1-methylimidazole, 0.53 mL (4.0 mmol) of phenyl vinyl sulfide, 121.8 mg (0.16 mmol) **4.19**, and 8 mL toluene. The resulting material was purified by FCC using 1:1 Et_2O/pentanes to give 79.9 mg (0.23 mmol, 57% yield) of two diastereomers (1.2:1 d.r.). Spectroscopic data for both diastereomers were consistent with those previously reported.[22] Major Diastereomer: 78% ee [Diacel CHIRALPAK AD, 5% to 50% iPrOH, 18 minutes, 1 mL/min, t_1= 8.44 min, t_2= 12.46 min]. $[\alpha]_D^{22}$ –4.3° (c0.470, CH_2Cl_2). ^{1}H NMR (500 MHz, $CDCl_3$) δ 7.34 (d, *J* = 7.7 Hz, 2H), 7.30–7.28 (m, 4H), 7.25–7.18 (d, 4H), 7.12 (s, 1H), 7.02 (s, 1H), 4.48 (q, *J* = 9.1 Hz, 1H), 3.99 (s, 3H), 3.93 (t, *J* = 9.5 Hz, 1H), 3.85 (td, *J* = 9.4, 7.3 Hz, 1H), 2.93 (dt, *J* = 10.8, 8.2 Hz, 1H), 2.22 (q, *J* = 10.1 Hz, 1H). Minor Diastereomer: 75% ee [Diacel CHIRALPAK AD, 5% to 50% iPrOH, 18 minutes, 1 mL/min, t_1= 9.06 min, t_2= 10.22 min]. $[\alpha]_D^{22}$ –173.0° (c0.770, CH_2Cl_2). ^{1}H NMR (500 MHz, $CDCl_3$) δ 7.34 (d, *J* = Hz, 2H),

7.29 (t, *J* = 7.4 Hz, 1H), 7.24–7.15 (m, 4H), 7.12–7.07 (m, 3H), 7.04 (s, 1H), 5.14 (q, *J* = 8.9 Hz, 1H), 4.47 (t, *J* = 8.7 Hz, 1H), 4.35 (td, *J* = 7.8, 3.3 Hz, 1H), 4.01 (s, 3H), 2.76 (dt, *J* = 11.8 7.9 Hz, 1H), 2.47 (ddd, *J* = 12.1, 9.5, 3.0 Hz, 1H).

(1-methyl-1H-imidazol-2-yl)(3-methyl-2-phenyl-3-(prop-1-en-2-yl)cyclobutyl)methanone

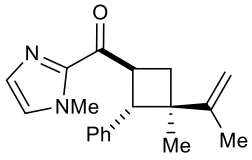

(**4.32**): Pre Prepared according to the general procedure isolation-scale asymmetric experiments using 86.1 mg (0.41 mmol) 2-cinnamoyl-1-methylimidazole, 0.45 mL (4.0 mmol) of 2,3-dimethylbutadiene, 61.0 mg (0.08 mmol) **4.19**, and 8 mL toluene. The resulting material was purified by FCC using a gradient of 1:2 to 1:1 Et_2O/pentanes to give 58.0 mg (0.20 mmol, 49% yield) of two diastereomers (10:1 d.r.). Spectroscopic data for the major diastereomer were consistent with that previously reported.[22] Major diastereomer: 63% ee [Diacel CHIRALPAK AD-H, 5% to 30% iPrOH, 20 minutes, 1 mL/min, t_1= 5.75 min, t_2= 8.43 min]. $[\alpha]_D^{22}$ –52.5° (c0.640, CH_2Cl_2). ^{1}H NMR (500 MHz, $CDCl_3$) δ 7.31–7.25 (m, 4H), 7.19–7.16 (m, 1H), 7.18 (s, 1H), 7.04 (s, 1H), 4.91 (br s, 1H), 4.84 (p, *J* = 1.4 Hz, 1H), 4.79 (q, *J* = 9.5 Hz, 1H), 4.13 (d, *J* = 10.0 Hz, 1H) 3.99 (s, 3H), 2.28 (t, *J* = 9.9 Hz, 1H), 2.19 (dd, *J* = 10.3, 9.1 Hz, 1H), 1.78 (s, 3H), 1.10 (s, 3H).

(3-ethenyl-2-phenylcyclobutyl)(1-methyl-1H-imidazol-2-yl)methanone (**4.33**): Prepared according to the general procedure for isolation-scale asymmetric experiments using 85.1 mg (0.40 mmol) 2-cinnamoyl-1-methylimidazole, 2.2 mL (4.0 mmol) of 1,3-butadiene (15% in toluene), 63.2 mg (0.08 mmol) **4.19**, and 6 mL toluene. The resulting material was purified by FCC using a gradient of 1:2 to 1:1 Et_2O/pentanes to give 78.8 mg (0.30 mmol, 74% yield) of two diastereomers (3:1 d.r.). Major Diastereomer: 87 % ee

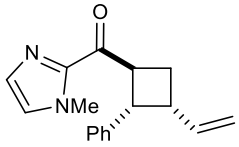

[Diacel CHIRALPAK AD, 5% to 50% iPrOH, 18 minutes, 1 mL/min, t_1=6.31 min, t_2=7.24 min]. Viscous oil. $[\alpha]_D^{22}$ –121.4° (c2.500, CH_2Cl_2). ν_{max} (film) / cm^{-1} 2934, 1723, 1664, 1406, 1289, 1154, 1074, 993, 913, 839, 758, 698. ^{1}H NMR (500 MHz, $CDCl_3$) δ 7.28–7.25 (m, 2H), 7.20 (d, *J* = 7.6 Hz, 2H), 7.18 (s, 1H), 7.15 (tt, *J* = 7.2, 1.4 Hz, 1H), 7.05 (s, 1H), 5.76 (ddd, *J* = 17.0, 10.2, 8.5 Hz, 1H), 5.03 (dq, *J* = 17.0, 1.0 Hz, 1H), 4.97–4.91(m, 2H), 4.23 (t, *J* = 9.3 Hz, 1H), 3.33–3.27 (m, 1H), 2.52 (dt, *J* = 11.2, 8.7 Hz, 1H), 2.30 (ddd, *J* = 11.8, 9.5, 2.6 Hz, 1H). ^{13}C NMR (125 MHz, $CDCl_3$) δ 192.96, 142.62, 140.02, 138.84, 129.39, 128.00, 127.75, 125.98, 115.28, 44.21, 43.27, 40.53, 36.22, 28.86. HRMS (ESI) calculated for $[C_{17}H_{19}N_2O]^+$ ($M+H^+$) requires *m/z* 267.1492, found 267.1491. Minor Diastereomer: 48% ee [Diacel CHIRALPAK AD, 5% to 50% iPrOH, 18 minutes, 1 mL/min, t_1=6.15 min, t_2=7.41 min]. Viscous oil. $[\alpha]_D^{22}$ –34.8° (c0.270, CH_2Cl_2). ν_{max} (film) / cm^{-1} 2930, 1726, 1667, 1462, 1409, 1275, 1123, 1072, 914, 873, 743, 699. ^{1}H NMR (500 MHz, $CDCl_3$) δ 7.29–7.27 (m, 4H), 7.20–7.16 (m, 1H), 7.14 (s, 1H), 7.03 (s, 1H), 6.00 (ddd, *J* = 17.0, 10.2, 7.0 Hz, 1H), 5.09 (dt, *J* = 17.1, 1.5 Hz, 1H), 5.03 (dt, *J* = 10.3, 1.3 Hz, 1H), 4.49 (td, *J* = 9.7, 8.7 Hz, 1H), 4.02 (s, 3H), 3.76 (t, *J* = 9.7 Hz, 1H), 3.02 (pent, *J* =8.5 Hz, 1H), 2.59 (dt, *J* = 10.2, 8.4 Hz, 1H), 2.04 (q, *J* = 10.1 Hz, 1H). ^{13}C NMR (125 MHz, $CDCl_3$) δ 192.49, 142.62, 142.55, 140.74, 129.37, 128.32, 127.22, 126.80, 126.33, 114.50, 46.96, 44.91, 42.60, 36.17, 30.54. HRMS (ESI) calculated for $[C_{17}H_{19}N_2O]^+$ ($M+H^+$) requires *m/z* 267.1492, found 267.1488.

(1-methyl-1H-imidazol-2-yl)(1-phenylspiro[3.3]heptan-2-yl)methanone (**4.34**): Prepared

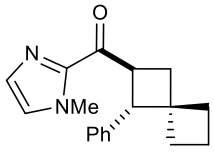

according to the general procedure for isolation-scale asymmetric experiments 85.0 mg (0.40 mmol) 2-cinnamoyl-1-methylimidazole, 0.37 mL (4.0 mmol) methylenecyclobutane, 121.0 mg (0.16 mmol) **4.19**, and 8 mL toluene, The resulting material was purified by FCC using 1:1 Et_2O/pentanes to give 65.2 mg (0.23 mmol, 58% yield) of a single

diastereomer (>20:1). 88% ee [Diacel CHIRALPAK AD, 5% to 50% iPrOH, 18 minutes, 1 mL/min, t_1=5.86 min, t_2=7.63 min]. White solid (mp = 80–82 °C). $[\alpha]_D^{22}$ –75.1° (c1.110, CH_2Cl_2). ν_{max} (film) / cm^{-1} 2926, 1725, 1666, 1408, 1289, 1154, 1072, 1032, 915, 765, 699. ^{1}H NMR (500 MHz, $CDCl_3$) δ 7.33–7.29 (m, 4H), 7.22–7.19 (m, 1H), 7.15 (s, 1H), 7.01 (s, 1H), 4.65 (q, *J* = 9.4 Hz, 1H), 3.97 (s, 3H), 3.67 (d, *J* = 9.8 Hz, 1H), 2.44 (dd, *J* = Hz, 1H), 2.20 (t, *J* = 10.3, 8.9 Hz, 1H), 2.11–2.06 (m, 1H), 2.00–1.94(m, 1H), 1.84–1.76 (m, 3H), 1.57–1.50 (m, 1H). ^{13}C NMR (125 MHz, $CDCl_3$) δ 192.75, 142.80, 140.01, 129.26, 128.16, 127.82, 127.21, 126.28, 50.21, 45.33, 40.57, 37.77, 36.18, 33.36, 29.38, 16.12. HRMS (ESI) calculated for $[C_{18}H_{21}N_2O]^+$ ($M+H^+$) - requires *m/z* 281.1648, found 281.1648.

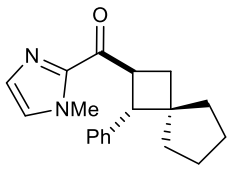

(1-methyl-1H-imidazol-2-yl)(1-phenylspiro[3.4]octan-2-yl)methanone (**4.35**): Prepared according to the general procedure for isolation-scale asymmetric experiments using 85.1 mg (0.40 mmol) 2-cinnamoyl-1-methylimidazole, 0.46 mL (4.0 mmol) methylenecyclopentane, 121.8 mg (0.16 mmol) **4.19**, and 8 mL toluene, The resulting material was purified by FCC using a gradient of 1:2 to 1:1 Et_2O/pentanes to give 49.0 mg (0.17 mmol, 42% yield) of two of diastereomers (6:1 d.r.). Spectroscopic data for the major diastereomer were consistent with that previously reported.[22] Major diastereomer: 85% ee [Diacel CHIRALPAK OD-H, 5% to 50% iPrOH, 18 minutes, 1 mL/min, t_1=6.07 min, t_2=6.65 min]. $[\alpha]_D^{22}$ –71.0° (c0.600, CH_2Cl_2). ^{1}H NMR (500 MHz, $CDCl_3$) δ 7.28–7.27 (m, 4H), 7.19–7.16 (m, 1H), 7.17 (s, 1H), 7.02 (s, 1H), 4.79 (q, *J* = 9.5 Hz, 1H), 3.98 (s, 3H), 3.91 (d, *J* = 10.1 Hz, 1H), 2.21 (t, *J* = 9.6 Hz, 1H), 2.06 (t, *J* = 9.9 Hz, 1H), 1.83–1.72 (m, 2H), 1.55–1.46 (m, 4H), 1.33–1.26 (m, 2H).

Methyl 4-(2-(1-methyl-1*H*-imidazole-2-carbonyl)-4-phenylcyclobutyl)benzoate (4.36):

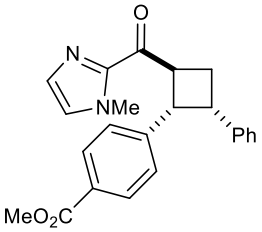

Prepared according to the general procedure for isolation-scale asymmetric experiments using 108.2 mg (0.40 mmol) methyl 4-[(1*E*)-3-(1-methyl-1*H*-imidazol-2-yl)-3-oxoprop-1-en-1-yl]benzoate, 0.46 mL (4.0 mmol) of styrene, 61.8 mg (0.08 mmol) **4.19**, and 8 mL toluene. The resulting material was purified by FCC using a gradient of 1:1 Et_2O/pentanes to 3:1 Et_2O/pentanes to give 90.0 mg (0.24 mmol, 60% yield) of three diastereomers (2:1 d.r.). Major Diastereomer: Viscous semisolid. 91% ee [Diacel CHIRALPAK IC, 5% to 50% iPrOH, 18 minutes, 1 mL/min, t_1=12.44 min, t_2=14.70 min]. $[\alpha]_D^{22}$ –97.4° (c1.590, CH_2Cl_2). ν_{max} (film) / cm^{-1} 2952, 1719, 1667, 1610, 1407, 1277, 1110, 1020, 913, 765, 700. ^{1}H NMR (500 MHz, $CDCl_3$) δ 7.72 (d, *J* = 8.1 Hz, 2H), 7.19 (s, 1H), 7.13–7.03 (m, 8H), 5.07 (q, *J* = 9.0 Hz, 1H), 4.50 (t, *J* = 9.2 Hz, 1H), 4.04 (s, 3H), 4.03–4.00 (m, 1H), 3.82 (s, 3H), 2.80–7.76 (m, 2H). ^{13}C NMR (125 MHz, $CDCl_3$) δ 192.59, 167.11, 145.27, 142.40, 140.29, 129.51, 129.03, 128.12, 128.04, 127.91, 127.59, 127.50, 126.11, 51.87, 45.63, 43.65, 42.04, 36.24, 28.64. HRMS (ESI) calculated for $[C_{23}H_{23}N_2O_3]^+$ ($M+H^+$) requires *m/z* 375.1703, found 375.1699.

(1-methyl-1H-imidazol-2-yl)(3-phenyl-2-(4-(trifluoromethyl)phenyl)cyclobutyl)methanone

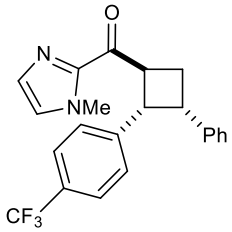

(4.37): Prepared according to the general procedure for isolation-scale asymmetric experiments using 113.5 mg (0.40 mmol) (*E*)-1-(1-methyl-1*H*-imidazol-2-yl)-3-(4-trifluoromethylphenyl)prop-2-en-1-one, 0.46 mL (4.0 mmol) of styrene, 62.6 mg (0.08 mmol) **4.19**, and 8 mL toluene. The resulting material was purified by FCC using a gradient of 1:3 to 1:1 Et_2O/pentanes to give 91.5 mg (0.24 mmol, 59% yield) of three diastereomers (2:1 d.r.). Spectroscopic data for the major diastereomer were consistent with those previously reported.[22] Major Diastereomer: 80% ee [Diacel CHIRALPAK OD-H, 5% to

50% iPrOH, 18 minutes, 1 mL/min, t_1= 8.44 min, t_2= 11.42 min]. $[\alpha]_D^{22}$ –48.3° (c0.360, CH_2Cl_2). ^{1}H NMR (500 MHz, $CDCl_3$) δ 7.30 (d, *J* = 8.1 Hz, 2H), 7.19 (d, *J* = 0.7 Hz, 1H), 7.16–7.13 (m, 2H), 7.10–7.05 (m, 6H), 5.04 (q, *J* = 9.0 Hz, 1H), 4.49 (t, *J* = 9.3 Hz, 1H), 4.05 (s, 3H), 4.01 (td, *J* = 9.1, 5.0 Hz, 1H), 2.81–2.75 (m, 2H).

(3-(4-bromo-2,5-dimethoxyphenyl)-2-(7-methoxy-2*H*-1,3-benzodioxol-5-yl)cyclobutyl)(1-methyl-1*H*-imidazol-2-yl)methanone (4.39) Prepared according to the general procedure for isolation-scale asymmetric experiments using 144.5 mg (0.50 mmol) (*E*)-3-(7-methoxybenzo[d][1,3]dioxol-5-yl)-1-(1-methyl-1*H*-imidazol-2-yl)prop-2-en-1-one, 582.1 mg (2.4 mmol) 4-bromo-2,5-methoxystyrene, 74.0 mg (0.10 mmol) **4.19**, and 10 mL CH_2Cl_2. The resulting material was purified by FCC with 50% → 100% EtOAc in pentanes to give 173.0 mg (0. 33 mmol, 65% yield) of two diastereomers (5:1 d.r.). Major Diastereomer: White solid (mp = 78–82 °C, liquid phase is a *very* viscous oil). 93% ee [Diacel CHIRALPAK AD, 5% to 50% iPrOH, 20 minutes, 1 mL/min, t_1=13.00 min, t_2=14.46 min]. $[\alpha]_D^{22}$ –57.1° (c0.280, CH_2Cl_2). ν_{max} (film) / cm^{-1} 2931, 1723, 1667, 1493, 1407, 1273, 1210, 1127, 1038, 858, 782, 742, 705. ^{1}H NMR (500 MHz, $CDCl_3$) δ 7.15 (s, 1H), 7.05 (s, 1H), 6.88 (s, 1H), 6.79 (s, 1H), 6.30 (d, *J* = 1.3 Hz, 1H), 6.20 (d, *J* = 1.3 Hz, 1H), 5.82 (dd, *J* = 4.5, 1.4 Hz, 2H), 4.75 (q, *J* = 8.1 Hz, 1H), 4.29 (dd, *J* = 9.6, 7.6 Hz, 1H), 4.21 (td, *J* = 9.2, 6.2 Hz, 1H), 4.05 (s, 3H), 3.83 (s, 3H), 3.69 (s, 3H), 3.54 (s, 3H), 2.77–2.66 (m, 2H). ^{13}C NMR (125 MHz, $CDCl_3$) δ 192.82, 151.98, 149.80, 148.08, 142.76, 142.44, 134.99, 133.24, 129.77, 129.38, 127.33, 115.06, 112.76, 109.01, 107.10, 102.10, 101.06, 57.41, 56.29, 55.62, 46.03, 44.62, 36.24, 36.16, 26.76. HRMS (ESI) calculated for $[C_{25}H_{26}BrN_2O_6]^+$ ($M+H^+$) requires *m/z* 529.0969, found 529.0968. Minor Diastereomer: White solid (mp = 138–141 °C). 68% ee

[Diacel CHIRALPAK AS-H, 5% to 30% EtOH, 35 minutes, 1 mL/min, t_1=17.84 min, t_2=18.80 min. $[\alpha]_D^{22}$ –17.8° (c0.540, CH_2Cl_2). ν_{max} (film) / cm^{-1} 2933, 1722, 1664, 1490, 1408, 1275, 1211, 1137, 1041, 833, 737, 697. ^1H NMR (500 MHz, $CDCl_3$) δ 7.15 (s, 1H), 7.05 (s, 1H), 7.00 (s, 1H), 6.98 (s, 1H), 6.51 (d, *J* = 1.3 Hz, 1H), 6.48 (d, *J* = 1.3 Hz, 1H), 5.90–5.89 (m, 2H), 4.44 (q, *J* = 9.2 Hz, 1H), 4.04 (s, 3H), 4.02 (q, 9.9 Hz, 1H), 3.88–3.83 (m, 1H), 3.87 (s, 3H), 3.84 (s, 3H), 3.70 (s, 3H), 2.83 (dt, *J* = 10.2, 8.6 Hz, 1H), 2.14 (q, *J* = 10.1 Hz, 1H). ^{13}C NMR (125 MHz, $CDCl_3$) δ 192.37, 151.86, 150.16, 148.77, 143.38, 142.59, 137.40, 133.69, 131.98, 129.46, 127.33, 115.87, 112.09, 109.18, 106.23, 101.23, 101.08, 57.12, 56.52, 56.14, 47.18, 46.32, 37.63, 36.18, 31.82. HRMS (ESI) calculated for $[C_{25}H_{26}BrN_2O_6]^+$ ($M+H^+$) requires *m/z* 529.0969, found 529.0967.

4.5.5: Racemic [2+2] Photocycloaddition Reactions

General Procedure for Racemic [2+2] Cycloadditions: An oven dried Schlenk tube was charged with the 1-methylimidazoyl enone (0.10 mmol, 1.0 equiv), styrene (1.0 mmol, 10.0 equiv.), *rac*-**4.19** (0.02 mmol, 0.2 equiv.), and 2 mL toluene. The Schlenk was sealed with a glass stopper and degassed *via* freeze-pump-thaw technique (3 x 5 min). This was then cooled to –78 °C and irradiated with a standard Kessil Lamp (H150) for 14 hours. The crude reaction mixture was then diluted 2-3x with CH_2Cl_2 before addition 2 mL sat. aq. $NaHCO_3$. The mixture was vigorously stirred for 60 seconds, the organic layer separated, and the aqueous layer extracted with CH_2Cl_2 (2 x 4 mL). The combined organics were dried over Na_2SO_4, concentrated, and analyzed by ^1H-NMR vs. internal standard (phenanthrene) to determine conversion and diastereomeric ratio. The crude mixture was then purified *via* flash column chromatography (FCC).

(2,3-diphenylcyclobutyl)(1-methyl-1H-imidazol-2-yl)methanone (*rac-4*.16): Prepared

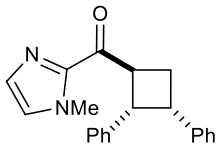

according to the general procedure for racemic experiments using 22.4 mg (0.11 mmol) 2-cinnamoyl-1-methylimidazole, 0.12 mL (1.0 mmol) styrene, 16.4 mg (0.02 mmol) BINOL-phosphoramide catalyst *rac*-**4.19**, and 2 mL toluene. The resulting material was purified by FCC using a gradient of 1:2 to 1:1 Et_2O/pentanes to give 23.5 mg (0.07 mmol, 70% yield) of two diastereomers (7:1 d.r.). Spectroscopic data for major diastereomer were consistent with that reported above.

(3-(4-chlorophenyl)-2-phenylcyclobutyl)(1-methyl-1H-imidazol-2-yl)methanone (***rac*-4.20**):

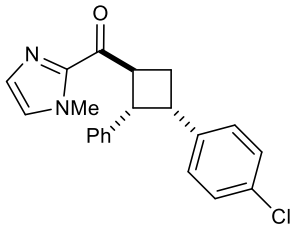

Prepared according to the general procedure for racemic experiments using 21.2 mg (0.10 mmol) 2-cinnamoyl-1-methylimidazole, 0.12 mL (1.0 mmol) 4-chlorostyrene, 15.3 mg (0.02 mmol) *rac*-**4.19**, and 2 mL toluene. The resulting material was purified by FCC using a 1:1 Et_2O/pentanes to give 26.7 mg (0.08 mmol, 76% yield) of three diastereomers (6:1 d.r.). Spectroscopic data for major diastereomer were consistent with that reported above.

(3-(4-bromophenyl)-2-phenylcyclobutyl)(1-methyl-1H-imidazol-2-yl)methanone (***rac*-4.21**):

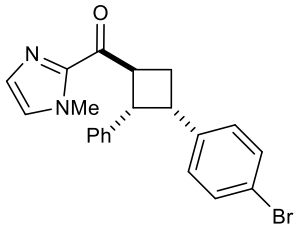

Prepared according to the general procedure for racemic experiments using 21.2 mg (0.10 mmol) 2-cinnamoyl-1-methylimidazole, 0.13 mL (1.0 mmol) 4-bromostyrene, 15.4 mg (0.02 mmol) ***rac*-4.19**, and 2 mL toluene. The resulting material was purified by FCC eluting from a gradient of 1:2 Et_2O/pentanes → 1:1 Et_2O/pentanes to give 3.4 mg (0.01 mmol, 9% yield) of two diastereomers (6:1 d.r.). Spectroscopic data was consistent with those reported above.

(1-methyl-1H-imidazol-2-yl)(2-phenyl-3-(4-(trifluoromethyl)phenyl)cyclobutyl)methanone

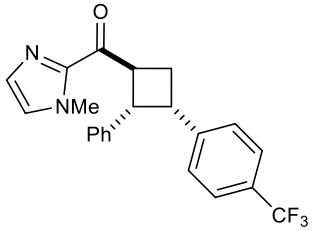

(*rac*-4.22): Prepared according to the general procedure for racemic experiments using 21.7 mg (0.10 mmol) 2-cinnamoyl-1-methylimidazole, 0.15 mL (1.0 mmol) 4-(trifluoromethyl)styrene, 16.1 mg (0.02 mmol) ***rac*-4.19**, and 2 mL toluene. The resulting material was purified by FCC eluting from a gradient of 1:2 Et_2O/pentanes → 1:1 Et_2O/pentanes to give 33.6 mg (0.09 mmol, 85% yield) of two diastereomers (5:1 d.r.). Spectroscopic data was consistent with those reported above.

(3-(4-acetoxyphenyl)-2-phenylcyclobutyl)(1-methyl-1H-imidazol-2-yl)methanone (***rac*-4.23**):

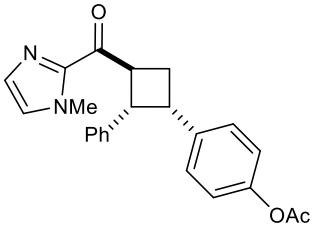

Prepared according to the general procedure for racemic experiments using 21.1 mg (0.10 mmol) 2-cinnamoyl-1-methylimidazole, 0.15 mL (1.0 mmol) 4-acetoxystyrene, 16.0 mg (0.02 mmol) *rac*-**4.19**, and 2 mL toluene. The resulting material was purified by FCC using a 1:1 Et_2O/pentanes to give 22.6 mg (0.06 mmol, 61% yield) of three diastereomers (8:1 d.r.). Spectroscopic data for major diastereomer were consistent with that reported above.

(3-(4-*tert*-butoxyphenyl)-2-phenylcyclobutyl)(1-methyl-1H-imidazol-2-yl)methanone (***rac*-4.24**):

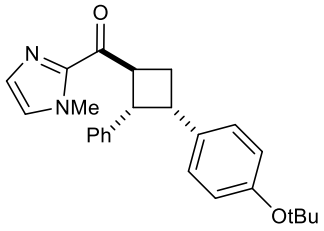

Prepared according to the general procedure for racemic experiments using 22.2 mg (0.10 mmol) 2-cinnamoyl-1-methylimidazole, 0.19 mL (1.0 mmol) 4-tert-butoxystyrene, 16.0 mg (0.02 mmol) *rac*-**4.19**, and 2 mL toluene. The resulting material was purified by FCC using a 1:1 Et_2O/pentanes to give 28.0 mg (0.07 mmol, 69% yield) of three diastereomers (4:1 d.r.). Spectroscopic data for major diastereomer were consistent with that reported above.

(3-(4-(azidomethyl)phenyl)-2-phenylcyclobutyl)(1-methyl-1H-imidazol-2-yl)methanone

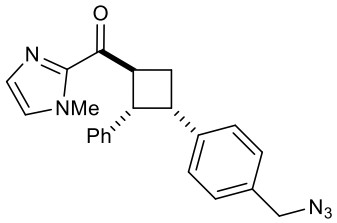

(***rac*-4.25**): Prepared according to the general procedure for racemic experiments using 20.5 mg (0.10 mmol) 2-cinnamoyl-1-methylimidazole, 158.0 mg (1.0 mmol) 1-(azidomethyl)-4-vinylbenzene, 15.3 mg (0.02 mmol) ***rac*-4.19**, and 2 mL toluene. The resulting material was purified using a gradient of 1:2 Et_2O/pentanes → 1:1 Et_2O/pentanes to give a 57% NMR yield of three diastereomers (3:1 d.r.). Spectroscopic data was consistent with those reported above.

(3-(4-(acetoxymethyl)phenyl)-2-phenylcyclobutyl)(1-methyl-1H-imidazol-2-yl)methanone

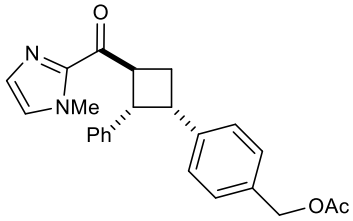

(***rac*-4.26**): Prepared according to the general procedure for racemic experiments using 21.3 mg (0.10 mmol) 2-cinnamoyl-1-methylimidazole, 180.0 mg (1.0 mmol) 1-(acetoxymethyl)-4-vinylbenzene, 16.0 mg (0.02 mmol) ***rac*-4.19**, and 2 mL toluene. The resulting material was purified by FCC eluting from a gradient of 1:2 Et_2O/pentanes → 1:1 Et_2O/pentanes to give a 70% NMR yield of three diastereomers (3:1 d.r.). Spectroscopic data was consistent with those reported above.

3-(4-(((tert-butyldimethylsilyl)oxy)methyl)phenyl)-2-phenylcyclobutyl)(1-methyl-1H-imidazol-2-yl)methanone (***rac*-4.27**): Prepared according to the general procedure for racemic experiments using 20.6 mg (0.10 mmol) 2-cinnamoyl-1-methylimidazole, 247.9 mg (1.0 mmol) *tert*-butyldimethyl(4-vinylbenzyloxy) silane, 15.4 mg (0.02 mmol) ***rac*-4.19**, and 2 mL toluene. The resulting material was purified by FCC eluting from a gradient of 1:2 Et_2O/pentanes → 1:1

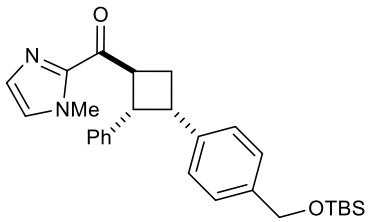

Et_2O/pentanes to give 40.0 mg (0.09 mmol, 89% yield) of three diastereomers (3:1 d.r.). Spectroscopic data was consistent with those reported above.

(1-methyl-1H-imidazol-2-yl)(3-(naphthalen-2-yl)-2-phenylcyclobutyl)methanone (***rac*-4.28**):

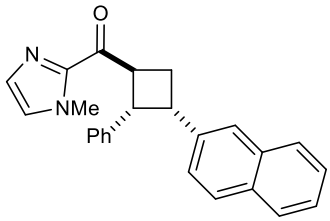

Prepared according to the general procedure for racemic experiments using 22.0 mg (0.10 mmol) 2-cinnamoyl-1-methylimidazole, 150.4 mg (1.0 mmol) 2-vinylnapthalene, 15.0 mg (0.02 mmol) ***rac*-4.19**, and 2 mL toluene. The resulting material was purified by FCC eluting from a gradient of 1:2 Et_2O/hexanes → 1:1 Et_2O/hexanes to give 33.1 mg (0.09 mmol, 87% yield) of three diastereomers (2:1 d.r.). Spectroscopic data was consistent with those reported above.

(3-(2-chlorophenyl)-2-phenylcyclobutyl)(1-methyl-1H-imidazol-2-yl)methanone (***rac*-4.29**):

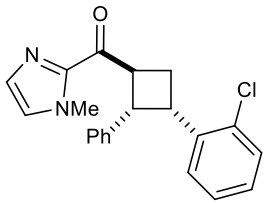

Prepared according to the general procedure for racemic experiments using 22.2 mg (0.10 mmol) 2-cinnamoyl-1-methylimidazole, 0.13 mL (1.0 mmol) 2-chlorostyrene, 16.5 mg (0.02 mmol) *rac*-**4.19**, and 2 mL toluene. The resulting material was purified by FCC using a 1:1 Et_2O/pentanes to give 19.7 mg (0.06 mmol, 54% yield) of two diastereomers (10:1 d.r.). Spectroscopic data for major diastereomer were consistent with that reported above.

(1-methyl-1H-imidazol-2-yl)(2-phenyl-3-(phenylthio)cyclobutyl)methanone (***rac*-4.31**):

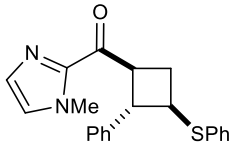

Prepared according to the general procedure for racemic experiments using 21.6 mg (0.10 mmol) 2-cinnamoyl-1-methylimidazole, 0.13 mL (1.0 mmol) phenyl vinyl sulfide, 30.1 mg (0.02 mmol) *rac*-**4.19**, and 2 mL toluene. The resulting material was

purified by FCC using a 1:1 Et_2O/pentanes to give 7.9 mg (0.03 mmol, 29% yield) of two diastereomers (1.3:1 d.r.). Spectroscopic data for both diastereomers were consistent with that reported above.

(1-methyl-1H-imidazol-2-yl)(3-methyl-2-phenyl-3-(prop-1-en-2-yl)cyclobutyl)methanone (***rac*-4.32**): Prepared according to the general procedure for racemic experiments using 22.0 mg (0.10 mmol) 2-cinnamoyl-1-methylimidazole, 0.11 mL (1.0 mmol) 2,3-dimethylbutadiene, 15.8 mg (0.02 mmol) *rac*-**4.19**, and 2 mL toluene. The resulting material was purified by FCC using a gradient of 1:2 to 1:1 Et_2O/pentanes to give 17.7 mg (0.06 mmol, 57% yield) of two diastereomers (10:1 d.r.). Spectroscopic data for major diastereomer were consistent with that reported above.

(3-ethenyl-2-phenylcyclobutyl)(1-methyl-1H-imidazol-2-yl)methanone (***rac*-4.33**): Prepared according to the general procedure for racemic experiments using 21.1 mg (0.10 mmol) 2-cinnamoyl-1-methylimidazole, 0.55 mL (1.0 mmol) 1,3-butadiene (15% in toluene), 15.8 mg (0.02 mmol) *rac*-**4.19**, and 2 mL toluene. The resulting material was purified by FCC using a gradient of 1:2 to 1:1 Et_2O/pentanes to give 17.0 mg (0.06 mmol, 64% yield) of two diastereomers (3:1 d.r.). Spectroscopic data for both diastereomers were consistent with that reported above.

(1-methyl-1H-imidazol-2-yl)(1-phenylspiro[3.3]heptan-2-yl)methanone (***rac*-4.34**): Prepared according to the general procedure for racemic experiments using 22.4 mg (0.11 mmol) 2-cinnamoyl-1-methylimidazole, 0.10 mL (1.0 mmol)

methylenecyclobutane, 34.0 mg (0.04 mmol) *rac*-**4.19**, and 2 mL toluene. The resulting material was purified by FCC using a 1:1 Et_2O/pentanes to give 11.0 mg (0.04 mmol, 37% yield) of a single diastereomer. Spectroscopic data were consistent with that reported above.

(1-methyl-1H-imidazol-2-yl)(1-phenylspiro[3.4]octan-2-yl)methanone (***rac*-4.35**): Prepared

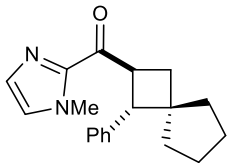

according to the general procedure for racemic experiments using 21.6 mg (0.10 mmol) 2-cinnamoyl-1-methylimidazole, 0.08 mL (1.0 mmol) methylenecyclopentane, 30.7 mg (0.04 mmol) *rac*-**4.19**, and 2 mL toluene. The resulting material was purified by FCC using a gradient of 1:2 to 1:1 Et_2O/pentanes to give 14.2 mg (0.05 mmol, 47% yield) of two diastereomers (8:1 d.r.). Spectroscopic data for major diastereomer were consistent with that reported above.

Methyl 4-(2-(1-methyl-1*H*-imidazole-2-carbonyl)-4-phenylcyclobutyl)benzoate (*rac*-4.36):

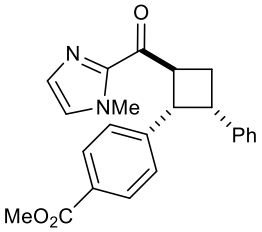

Prepared according to the general procedure for racemic experiments using 21.6 mg (0.10 mmol) 2-cinnamoyl-1-methylimidazole, 0.13 mL (1.0 mmol) phenyl vinyl sulfide, 30.1 mg (0.02 mmol) *rac*-**4.19**, and 2 mL toluene. The resulting material was purified by FCC using a 1:1 to 3:1 Et_2O/pentanes to give 7.9 mg (0.03 mmol, 29% yield) of three diastereomers (3:1 d.r.). Spectroscopic data for major diastereomer were consistent with that reported above.

(1-methyl-1H-imidazol-2-yl)(3-phenyl-2-(4-(trifluoromethyl)phenyl)cyclobutyl)methanone

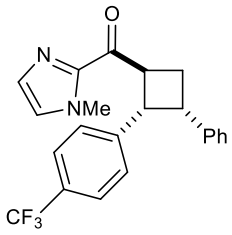

(*rac*-4.37): Prepared according to the general procedure for racemic experiments using 28.0 mg (0.10 mmol) (*E*)-1-(1-methyl-1*H*-imidazol-2-yl)-3-(4-trifluoromethylphenyl)prop-2-en-1-one, 0.12 mL (1.0 mmol) styrene, 15.9 mg (0.02 mmol) *rac*-**4.19**, and 2 mL toluene. The resulting material was purified by FCC using a gradient of 1:3 to 1:1 Et_2O/pentanes to give 23.5 mg (0.07 mmol, 70% yield) of three diastereomers (2:1 d.r.). Spectroscopic data for major diastereomer were consistent with that reported above.

(3-(4-bromo-2,5-dimethoxyphenyl)-2-(7-methoxy-2*H*-1,3-benzodioxol-5-yl)cyclobutyl)(1-

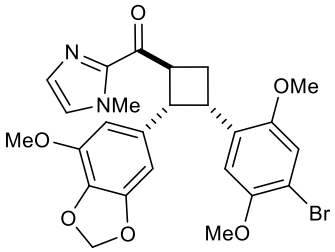

methyl-1*H*-imidazol-2-yl)methanone (*rac*-4.39) Prepared according to the general procedure for racemic experiments using 142.8 mg (0.50 mmol) (*E*)-3-(7-methoxybenzo[d][1,3]dioxol-5-yl)-1-(1-methyl-1*H*-imidazol-2-yl)prop-2-en-1-one, 244.1 mg (1.0 mmol) 4-bromo-2,5-methoxystyrene, 78.0 mg (0.10 mmol) *rac*-**4.19**, and 10 mL CH_2Cl_2. The resulting material was purified by FCC with 50% → 100% EtOAc in pentanes to give 137.0 mg (0.26 mmol, 52% yield) of two diastereomers (5:1 d.r.). Spectroscopic data for both diastereomers were consistent with that reported above.

4.5.6: Imidazole Cleavage of A Complex Cycloadduct

Methyl 3-(4-bromo-2,5-dimethoxyphenyl)-2-(7-methoxy-2*H*-1,3-benzodioxol-5-

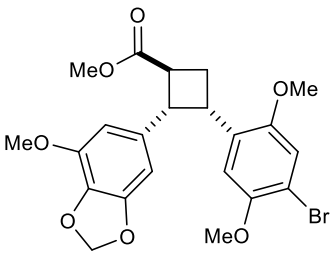

yl)cyclobutane-1-carboxylate (4.40) A flame-dried 6 mL vial with a stir bar was charged with 100.5 mg (0.19 mmol, 1.0 equiv.) of the major diastereomer of cycloadduct **4.39** and 1.5 mL dry CH_2Cl_2, and

the solution stirred under N_2 for about 10 minutes. To this was added 30 µL (0.25 mmol, 1.3 equiv.) freshly distilled MeOTf, and the reaction mixture stirred for 3 hours at room temperature. This was then concentrated *in vacuo* and dried under high-vac for 30 minutes to remove any remaining MeOTf. The resulting yellow foam was then taken up in 1.5 mL dry CH_2Cl_2 to which was added 0.32 mL (8.0 mmol, 40.0 equiv.) distilled MeOH and 4.5 mg (0.04 mmol, 0.2 equiv.) 1,4-diazabicyclo[2.2.2]octane (DABCO), and the reaction mixture stirred for 3 hours at room temperature. The crude mixture was directly concentrated and purified by FCC with 10% → 50% EtOAc/pentanes to give 63.4 mg (0.13 mmol, 70% yield) of a viscous semisolid. 92% ee [Diacel CHIRALPAK AD, 5% to 50% iPrOH, 20 minutes, 1 mL/min, t_1=9.30 min, t_2=10.73 min]. $[\alpha]_D^{22}$ –64.2° (c1.090, CH_2Cl_2). ν_{max} (film) / cm^{-1} 2930, 1727, 1633, 1495, 1382, 1275, 1209, 1091, 1041, 931, 780, 747. ^{1}H NMR (500 MHz, $CDCl_3$) δ 6.79 (s, 1H) , 6.76 (s, 1H), 6.19 (d, *J* = 1.1 Hz, 1H), 6.01 (d, *J* = 1.1 Hz, 1H), 5.86–5.85 (m, 2H), 4.19 (td, *J* = Hz, 1H), 4.13 (t, *J* = 8.8 Hz, 1H), 3.81 (s, 3H), 3.73 (s, 3H), 3.68 (s, 3H), 3.49 (s, 3H), 3.43 (q, *J* = 8.5 Hz, 1H), 2.72 (dt, *J* = 12.1, 8.5 Hz, 1H), 2.57–2.51 (m, 1H). ^{13}C NMR (125 MHz, $CDCl_3$) δ 174.98, 152.04, 149.83, 148.18, 142.79, 134.38, 133.47, 129.21, 115.26, 112.33, 109.26, 106.87, 101.75, 101.16, 57.33, 56.32, 55.59, 51.98, 47.51, 41.52, 36.76, 25.53. HRMS (ESI) calculated for $[C_{22}H_{27}BrNO_7]^+$ ($M+NH_4^+$) requires *m/z* 496.0965, found 496.0965.

Methyl 3-(4-bromo-2,5-dimethoxyphenyl)-2-(7-methoxy-2*H*-1,3-benzodioxol-5-yl)cyclobutane-1-carboxylate (*rac*-4.40) Racemic material prepared according to the procedure above for the analogous enriched product **XX** using 86.2 mg (0.16 mmol, 1.0 equiv.) (3-(4-bromo-2,5-dimethoxyphenyl)-2-(7-methoxy-2*H*-1,3-benzodioxol-5-

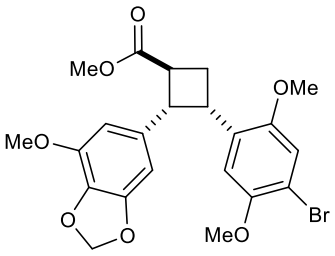

yl)cyclobutyl)(1-methyl-1*H*-imidazol-2-yl)methanone and 25 µL (0.20 mmol, 1.3 equiv.) MeOTf in 1 mL CH_2Cl_2, and then 0.25 mL (6.0 mmol, 40.0 equiv.) MeOH, and 3.5 mg (0.3 mmol, 0.2 equiv.) DABCO in 1 mL CH_2Cl_2. The resulting material was purified by FCC with 10% → 50% EtOAc in pentanes to give 12.0 mg (0.03 mmol, 15% yield) of a single product Spectroscopic data were consistent with that reported above.

4.5.7: Mechanistic Experiments

4.5.7.1: Absorbance Data

Experimental Details: Solutions of cinnamoyl-1-methylimidazole (**4.4**), Bronsted acid (**4.19**), and mixtures of **4.4** and **4.19** were prepared in HPLC-grade CH_2Cl_2. Each sample was acquired in a 1 cm path cuvette, and background performed vs. CH_2Cl_2. Absorbance data collected from 325-700 nm using a Varian Cary 50 UV-Vis spectrophotometer.

4.5.7.2: Fluorescence Data

Experimental Details: Solutions of cinnamoyl-1-methylimidazole (**4.4**), Bronsted acid (**4.19**), and mixtures of **4.4** and **4.19** were prepared in HPLC-grade CH_2Cl_2. Each sample was transferred to a 1 cm path cuvette, which was fitted with an appropriate septum, and sparged for 10 minutes prior to data acquisition. Samples were excited @ 300 nm, then emission data collected from 330-700/800 nm. All fluorescence data was acquired on an ISS PC1 photon counting spectrofluorimeter with a 300 W high-pressure xenon arc lamp.

4.5.7.3: Reaction Time Course vs. Atmosphere

Experimental Details: Reaction under nitrogen atmosphere prepared according to standard reaction setup described in Section 4.5.4. with degassing *via* Freeze-Pump-Thaw technique. Reaction under oxygen atmosphere prepared identically, except backfilled with an oxygen balloon. Yields were determined by GC vs internal standard.

Figure 4-7. Reaction progress with a nitrogen atmosphere vs an oxygen atmosphere

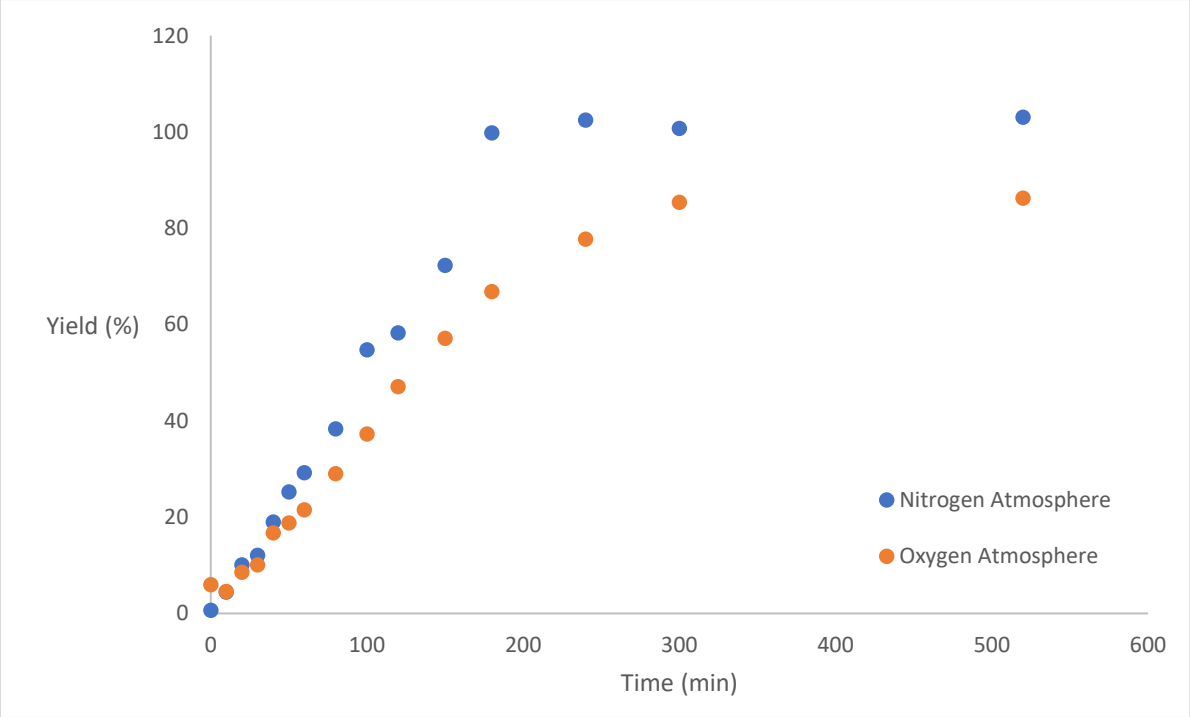

4.5.7.4: NMR Titration

Experimental Details: A stock solution of **4.19** (11.0 mg, 0.014 mmol) was prepared in *d*8-toluene (700 µL) and added to a solution of **4.4** (2.1 mg, 0.01 mmol) in *d*8-toluene (500 µL) in a 7" NMR tube in 50 µL increments. Then a more concentrated stock solution of **4.19** (94.6 mg, 0.12 mmol), prepared in *d*8-toluene (1.2 mL), was added to the same tube in 200 µL increments. Standard 1H-NMRs were acquired on a 600 mHz instrument with a DCI-F cryoprobe. The titration was quantified by monitoring the chemical shift of the imidazole methyl protons (~3.4 ppm in **4.4** only) in the substrate, which moved upfield with increasing **4.19**. When multiple peaks appeared, chemical shifts were averaged.

Figure 4-8. Stacked NMR spectra of titration of 0 to 11 equiv. catalyst **4.19** to **4.4**.

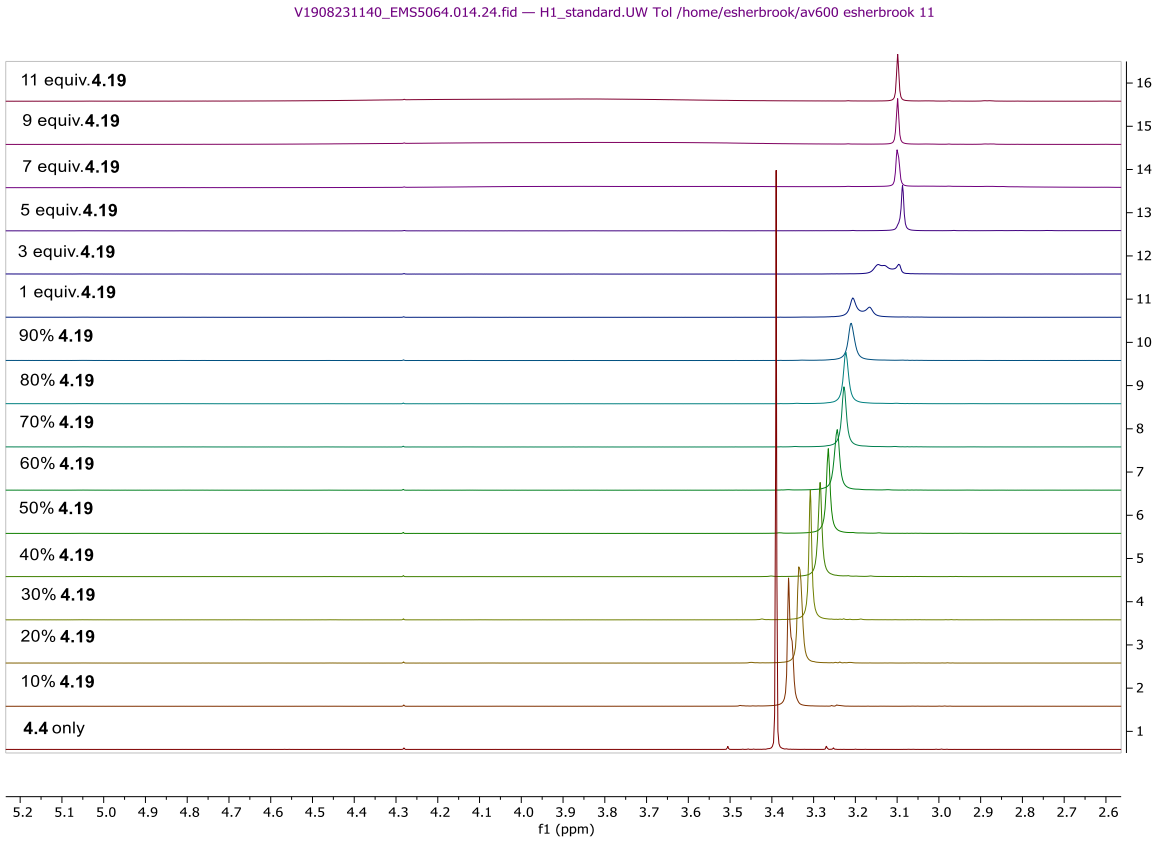

Figure 4-9. Preliminary binding isotherm, measured vs. calculated

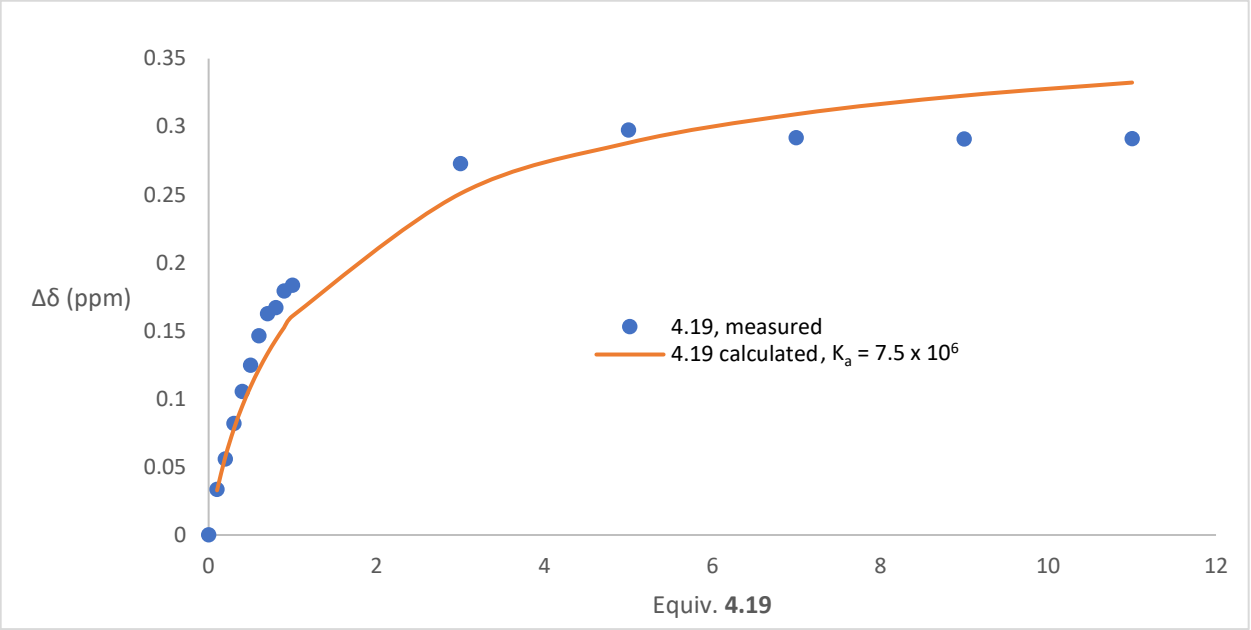

These data were fit to a 1:1 binding model following the method developed by Thordarson.[49] Microsoft excel used to estimate K_a by minimizing difference between experiment and predicted chemical shifts using nonlinear regression analysis.

4.5.8: Assignment of Diastereomers by 1D-NOE

Figure 4-10. Observed nOe enhancements

Major Diastereomer(**5**:1)
(in C_6D_6)

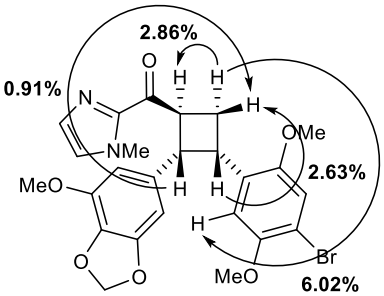

Major Diastereomer(5:**1**)
(in C_6D_6)

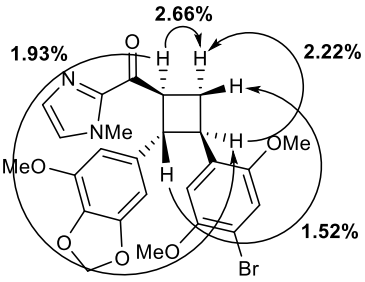

Major Diastereomer(**3**:1)
(in $CDCl_3$)

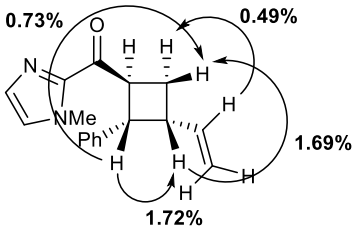

Major Diastereomer(3:**1**)
(in $CDCl_3$)

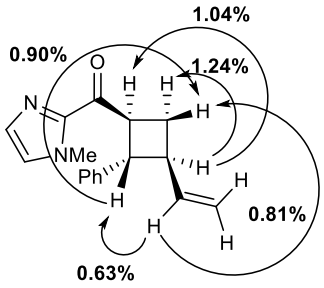

Major Diastereomer(**1.2**:1)
(in $CDCl_3$)

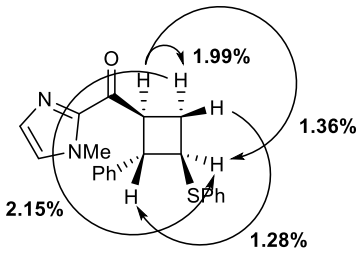

Major Diastereomer(1.2:**1**)
(in $CDCl_3$)

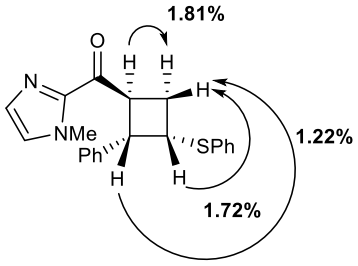

Major Diastereomer(**10**:1)
(in $CDCl_3$)

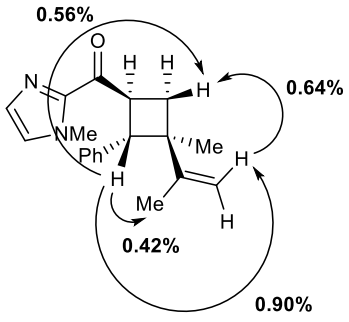

4.6 References and Notes

[1] Inoue, Y. Asymmetric Photochemical Reactions in Solution. *Chem. Rev.*, **1992**, *92*, 741–770.

[2] Inoue, Y.; Ramamurthy, V. *Molecular and Supramolecular Photochemistry, Vol. 11: Chiral Photochemistry*; Marcel Dekker, New York, NY, 2004.

[3] Hopkinson, M. N.; Sahoo, B.; Li, J.-L.; Glorius, F. Dual Catalysis Sees the Light: Combining Photoredox with Organo-, Acid, and Transition-Metal Catalysis. *Chem. Eur. J.* **2014**, *20*, 3874–3886.

[4] Brimioulle, R.; Lenhart, D.; Maturi, M. M.; Bach, T. Enantioselective Catalysis of Photochemical Reactions. *Angew. Chem. Int. Ed.*, **2015**, *54*, 3872–3890.

[5] A 1.4 kcal/mol difference in enantiomer $\Delta\Delta G^{\ddagger}$ is equivalent to ~80% ee at room temperature.

[6] A 400 nm photon corresponds to ~75 kcal/mol, a 300 nm photon to ~100kcal/mol.

[7] Ouannès, C.; Beugelmans, R.; Rossi, G. Asymmetric Induction During Triplet Energy Transfer. *J. Am. Chem. Soc.*, **1973**, *95*, 8472–8474.

[8] Hoshi, N.; Furukawa, Y.; Hagiwara, H.; Uda, H.; Sato, K. *Chem. Lett.*, **1980**, *9*, 47–50.

[9] Demuth, M.; Raghavan, P. R.; Carter, C.; Nakano, K. Schaffner, K. Photochemical High-yield Preparation of Tricyclo[3.3.0.0]octan-3-ones. Potential Synthons for Polycyclopentanoid Terpenes and Prostacyclin Analogues. Preliminary Communication. *Hel. Chim. Acta*, **1980**, *63*, 2434–2439.

[10] Cauble, D. F.; Lynch, V.; Krische, M. J. Studies on the Enantioselective Catalysis of Photochemically Promoted Transformations: "Sensitizing Receptors" as Chiral Catalysts. *J. Org. Chem.*, **2003**, *68*, 15–21.

[11] Müller, C.; Bauer, A.; Bach, T. Light-Driven Enantioselective Organocatalysis. *Angew. Chem. Int. Ed.*, **2009**, *48*, 6640–6642.

[12] Maturi, M. M.; Bach, T. Enantioselective Catalysis of the Intermolecular [2+2] Photocycloaddition between 2-Pyridones and Acetylenedicarboxylates. *Angew. Chem. Int. Ed.* **2014**, *53*, 7661–7664.

[13] Tröster, A.; Alonso, R.; Bauer, A.; Bach, T. Enantioselective Intermolecular [2 + 2] Photocycloaddition Reactions of 2(1*H*)-Quinolones Induced by Visible Light Irradiation. *J. Am. Chem. Soc.*, **2016**, 138, 7808–7811.

[14] Brimoulle, R.; Guo, H.; Bach, T. Enantioselective Intramolecular [2+2] Photocycloaddition Reactions of 4-Substituted Coumarins Catalyzed by a Chiral Lewis Acid. *Chem. Eur. J.* **2012**, *18*, 7552–7560.

[15] Brimoulle, R.; Bach, T. Enantioselective Lewis Acid Catalysis of Intramolecular Enone [2+2] Photocycloaddition Reactions. *Science* **2013**, *342*, 840–843.

[16] Poplata, S.; Bach, T. Enantioselective Intermolecular [2+2] Photocycloaddition Reaction of Cyclic Enones and Its Application in a Synthesis of (−)-Grandisol. *J. Am. Chem. Soc.*, **2018**, *140*, 3228–3231.

[17] Kalyanasundaram, K. Photophysics, Photochemistry, and Solar Energy Conversion with Tris(bipyridyl)ruthenium(II) and Its Analogues. *Coord. Chem. Rev.* **1982**, *46*, 159–244.

[18] Balzani, V.; Bergamini, G.; Campagna, S.; Punteriero, F. Photochemistry and Photophysics of Coordination Compounds: Overview and General Concepts. *Top. Curr. Chem.* **2007**, *280*, 1–36.

[19] Blum, T.R.; Miller, Z. D.; Bates, D. M.; Guzei, I. A.; Yoon, T. P. Enantioselective Photochemistry through Lewis Acid-Catalyzed Triplet Energy Transfer. *Science* **2016**, *354*, 1391–1395.

[20] Miller, Z. D., Lee, B.J.; Yoon, T. P. Enantioselective Crossed Photocycloadditions of Styrenic Olefins by Lewis Acid Catalyzed Triplet Sensitization. *Angew. Chem. Int. Ed.* **2017**, *56*, 11891–11895.

[21] Daub, M. E.; Jung. H.; Lee, B. J.; Won, J.; Baik, M.-H.; Yoon, T. P. Enantioselective [2+2] Cycloadditions of Cinnamate Esters: Generalizing Lewis Acid Catalysis of Triplet Energy Transfer. *J. Am. Chem. Soc.* **2019**, *141*, 9543–9547.

[22] This work has recently been submitted for publication (July 2019).

[23] Vallavoju, N.; Selvakumar, S.; Jockusch, S.; Sibi, M. P.; Sivaguru, J. Enantioselective Organo-Photocatalysis Mediated by Atropisomeric Thiourea Derivatives. *Angew. Chem. Int. Ed.* **2014**, 53, 5604–5608.

[24] Vallavoju, N.; Selvakumar, S.; Jockusch, S.; Prabhakaran, M. T.; Sibi, M. P.; Sivaguru, J. Evaluating Thiourea Architecture for Intramolecular [2+2] Photocycloaddition of 4-Alkenylcoumarins. *Adv. Synth. Catal.* **2014**, *356*, 2763–2768.

[25] Davies, D. H.; Haire, N. A.; Hall, J.; Smith E. H. Synthesis of γ-Lactones from Intermediate 2-(γ-Hydroxyacyl)-imidazoles by *N*-Methylation and Base-catalyzed C–C Bond Cleavage. Application to the Synthesis of (+)-Caveernosine. *Tetrahedron* **1992**, *48*, 7839–7856.

[26] Tyson, E. L.; Farney, E. P.; Yoon, T. P. Photocatalytic [2+2] Photocycloadditions of Enones with Cleavable Redox Auxiliaries. *Org. Lett.* **2012**, *14*, 1110–1113.

[27] Brenninger, C.; Jolliffe, J. D.; Bach, T. Chromophore Activation of α,β-Unsaturated Carbonyl Compounds and Its Application to Enantioselective Photochemical Reactions. *Angew. Chem. Int. Ed.* **2018**, *44*, 14338–14349.

[28] Stegbauer, S.; Jandl, C.; Bach, T. Enantioselective Lewis Acid Catalyzed *ortho* Photocycloaddition of Olefins to Phenanthrene-9-carboxyaldehydes. *Angew. Chem. Int. Ed.* **2018**, *57*, 14593–14596.

[29] Huang, X.; Quinn, T.R.; Harms, K.; Webster, R. D.; Zhang, L.; Wiest, O.; Meggers, E. Direct Visible-Light-Excited Asymmetric Lewis Acid Catalysis of Intermolecular [2+2] Photocycloadditions. *J. Am. Chem. Soc.* **2017**, *139*, 9120–9123.

[30] Hu, N.; Jung, H.; Zheng, Y.; Lee, J.; Zhang, L.; Ullah, Z.; Xie, X.; Harms, K.; Baik, M.-H.; Meggers, E. Catalytic Asymmetric Dearomatization by Visible-Light-Activated [2+2] Photocycloaddition. *Angew. Chem. Int. Ed.* **2018**, *57*, 6242–6246.

[31] Becker, D.; Nagler, M.; Hirsh, S.; Ramun, J. Intramolecular [2+2] Photocycloadditions of *E* and *Z* Olefins to Cyclohex-2-enone. *J. Chem. Soc. Chem. Commun.* **1983**, 371–373.

[32] Becker, D.; Nagler, M.; Sahali, Y.; Haddad, N. Regiochemistry and Stereochemistry of Intramolecular [2+2] Photocycloadditions of Carbon–Carbon Double Bonds to Cyclohexenones. *J. Org. Chem.* **1991**, *56*, 4537–4543

[33] Schuster, D. I.; Lem, G.; Kaprinidis, N. A. New Insights into an Old Mechanism: [2+2] Photocycloaddition of Enones to Alkenes. *Chem. Rev.* **1993**, *93*, 3–22.

[34] Maturi, M. M.; Wenninger, M.; Alonso, R.; Bauer, A.; Pöthig, A.; Riedle, E.; Bach, T. Intramolecular [2+2] Photocycloaddition of 3- and 4-(But-3-enyl)oxyquinolones: Influence of the Alkene Substitution Pattern, Photophysical Studies, and Enantioselective Catalysis by a Chiral Sensitizer. *Chem. - Eur. J.* **2013**, *19*, 7461−7472.

[35] Skubi, K. L.; Kidd, J. B.; Jung, H.; Guzei, I. A.; Baik, M.-H.; Yoon, T. P. Enantioselective Excited-State Photoreactions Controlled by a Hydrogen-Bonding Iridium Sensitizer. *J. Am. Chem. Soc.* **2017**, *139*, 17186–17192.

[36] Abe, M.; Adam, W.; Ino, Y.; Nojima, M. Stereochemical Deuterium Labeling as Mechanistic Probe for Differentiating the Singlet- and Triplet-Diradical Spin States in the Rearrangement of the 2-Spiroepoxy-1,3-cyclopentanediyl to Oxetanes. *J. Am. Chem. Soc.* **2000**, *122*, 6508–6509.

[37] Pangborn, A. B.; Giardello, M. A.; Grubbs, R. H.; Rosen, R. K.; Timmers, F. J. Safe and Convenient Procedure for Solvent Purification. *Organometallics*, **1996**, *15*, 1518–1520.

[38] Ooi, T.; Kameda, M.; Maruoka, K. Design of N-Spiro C2-Symmetric Chiral Quaternary Ammonium Bromides as Novel Chiral Phase-Transfer Catalysts: Synthesis and Application to Practical Asymmetric Synthesis of α-Amino Acids. *J. Am. Chem. Soc.* **2003**, *125*, 5139–5151.

[39] Ahmed, I.; Clark, D. A. Rapid Synthesis of 3,3′ Bis-Arylated BINOL Derivatives Using a C–H Borylation in Situ Suzuki–Miyaura Coupling Sequence. *Org. Lett.* **2014**, *16*, 4332–4335.

[40] Davies, D. H.; Hall, J.; Smith, E. H. Non-oxidative conversion of ketone carbonyls into carboxy carbonyls. Comparison of 2-acylthiazoles and 2-acylimidazoles in the aldol condensation and the stereospecific cleavage of an example of the latter to a β-hydroxy ester *via* the azolium salt. *J. Chem. Soc. Perkin Trans. 1* **1991**, 2691–2698.

[41] Hiyama, T.; Reddy, G. B.; Minami, T.; Hanamoto, T. Stereoselective Reduction of β,δ-Diketo Esters. A Novel Strategy for the Synthesis of Artificial HMG-CoA Reductase Inhibitors. *Bull. Chem. Soc. Jpn.* **1995**, *68*(1), 350–363.

[42] Evans, D. A.; Fandrick, K. R.; Song, H.-J. Enantioselective Friedel−Crafts Alkylations of α,β-Unsaturated 2-Acyl Imidazoles Catalyzed by Bis(oxazolinyl)pyridine−Scandium(III) Triflate Complexes. *J. Am. Chem. Soc.* **2005**, *127*, 8942–8943.

[43] Note that MeOH is used in this case to avoid transesterification to generate mixed ester products.

[44] Myers, M. C.; Bharadwaj, A. R.; Milgram, B. C.; Scheidt, K. A. Catalytic Conjugate Additions of Carbonyl Anions under Neutral Aqueous Conditions. *J. Am. Chem. Soc.* **2005**, *127*, 14675–14680.

[45] Texter, K. B.; Waymach, R.; Kavanagh, P. V.; O'Brien, J. E.; Talbot, B.; Brandt, S. D.; Gardner, E. A. Identification of pyrolysis products of the new psychoactive substance 2-amino-1-(4-bromo-2,5-dimethoxyphenyl)ethanone hydrochloride (bk-2C-B) and its iodo analogue bk-2C-I. *Drug Test. Analysis*, **2018**, *10*, 229–236.

[46] Williamson, K. S.; Yoon, T. P. Iron-Catalyzed Aminohydroxylation of Olefins. *J. Am. Chem. Soc.* **2010**, *132*, 4570-4571.

[47] Zhao, L. J.; Kwong, C. K. W.; Shi, M.; Toy, P. H. Optimization of Polystyrene-Supported Triphenylphosphine Catalysts for Aza-Morita–Baylis–Hillman Reactions. *Tetrahedron* **2005**, *61*, 12026-12032.

[48] Stals, P. J. M.; Phan, T. N. T.; Gigmes, D.; Paffen, T. F. E.; Meijer, E. W.; Palmans, A. R. A. Improving the Control of Styrene Polymerization at 60 °C Using a Dialkylated α-Hydrogenated Nitroxide. *J. Polym. Sci. Part A: Polym. Chem.* **2012**, *50*, 780–791.

[49] Thordarson, P. Determining association constants from titration experiments in supramolecular chemistry. *Chem. Soc. Rev.* **2011**, *40*, 1305–1323.

Appendix A. ^{1}H and ^{13}C Spectra for New Compounds

Figure A-1. List of New Compounds for Chapter 2

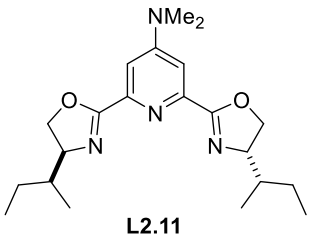

L2.11

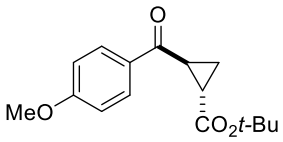

2.43

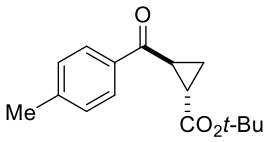

2.44

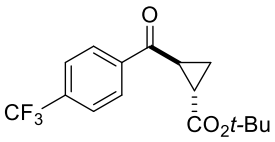

2.45

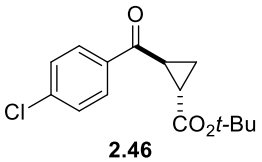

2.46

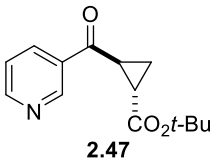

2.47

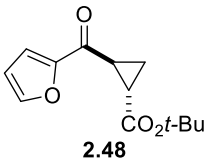

2.48

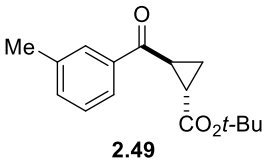

2.49

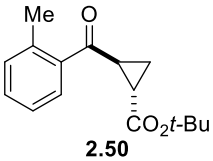

2.50

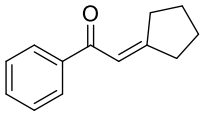

2.51

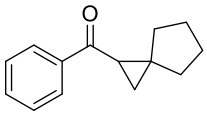

2.52

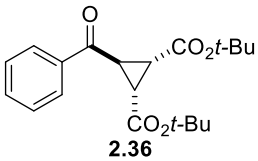

2.36

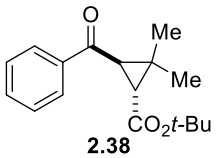

2.38

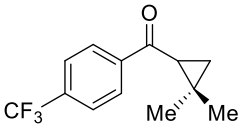

2.53

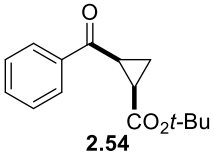

2.54

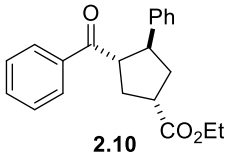

2.10

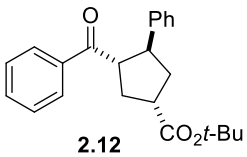

2.12

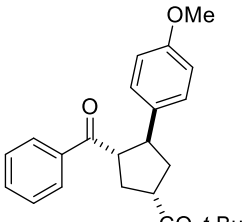

2.13

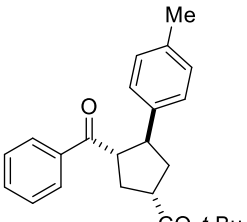

2.14

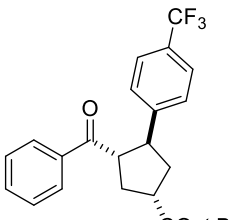

2.15

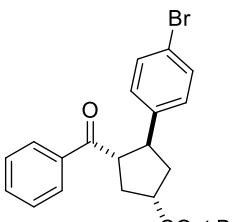

2.16

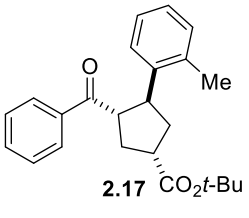

2.17

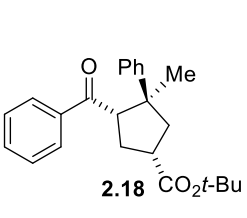

2.18

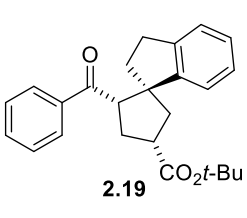

2.19

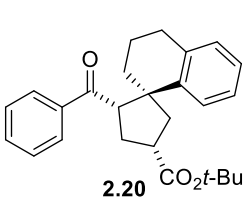

2.20

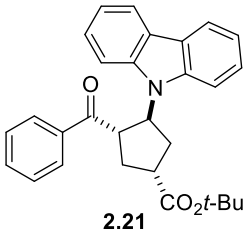

2.21

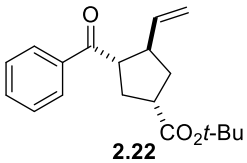

2.22

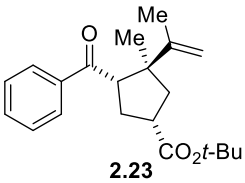

2.23

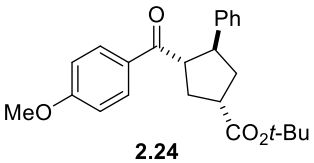

2.24

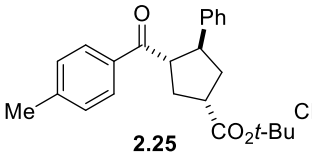

2.25

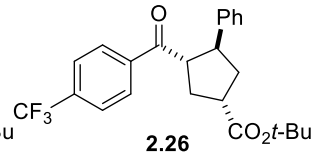

2.26

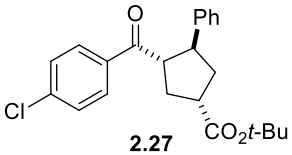

2.27

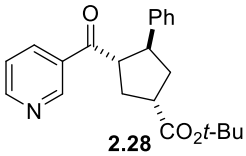

2.28

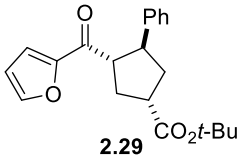

2.29

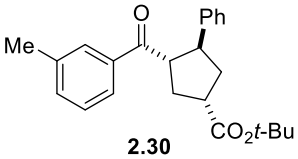

2.30

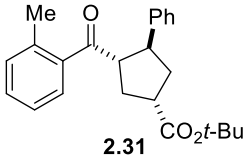

2.31

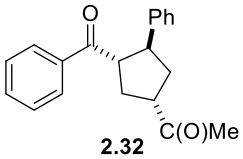

2.32

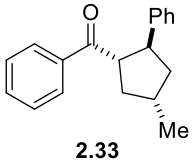

2.33

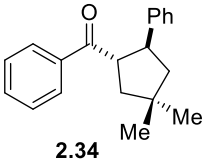

2.34

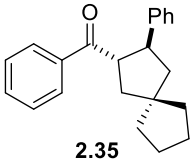

2.35

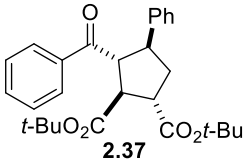

2.37

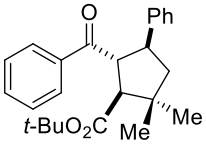

2.39

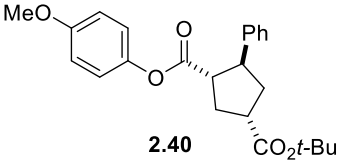

2.40

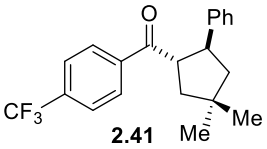

2.41

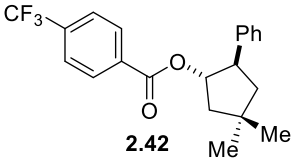

2.42

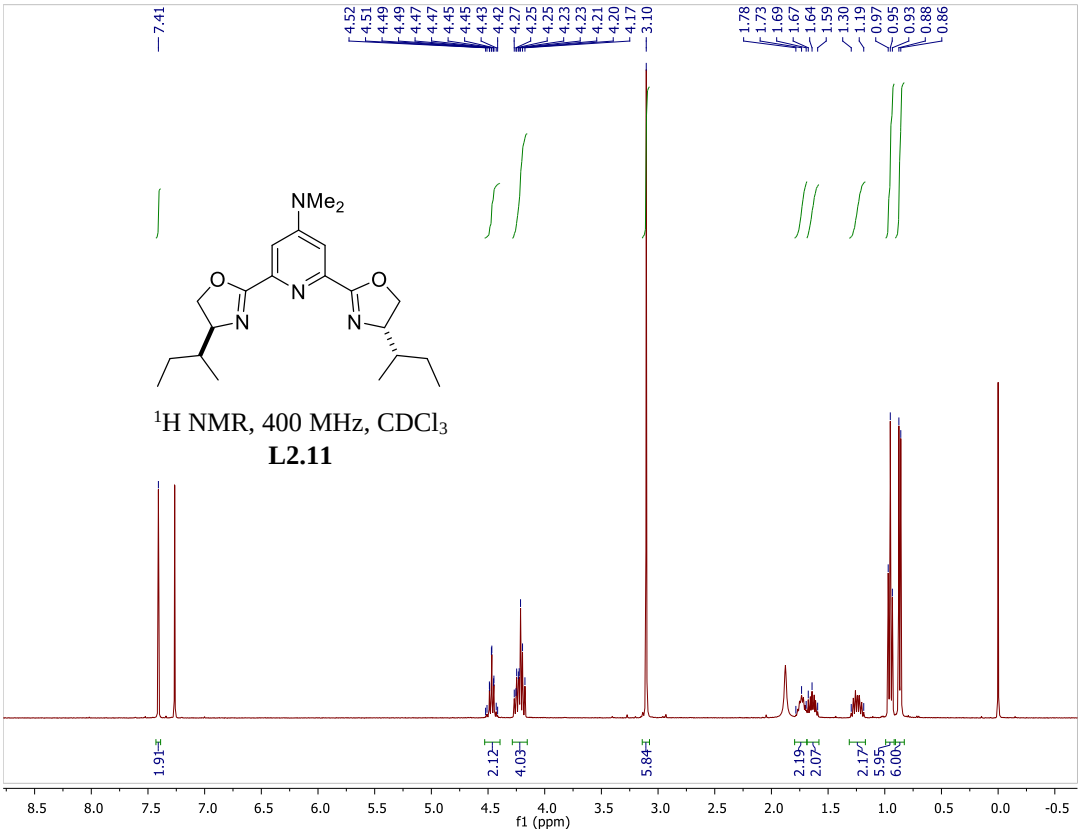

^{1}H NMR, 400 MHz, $CDCl_3$

L2.11

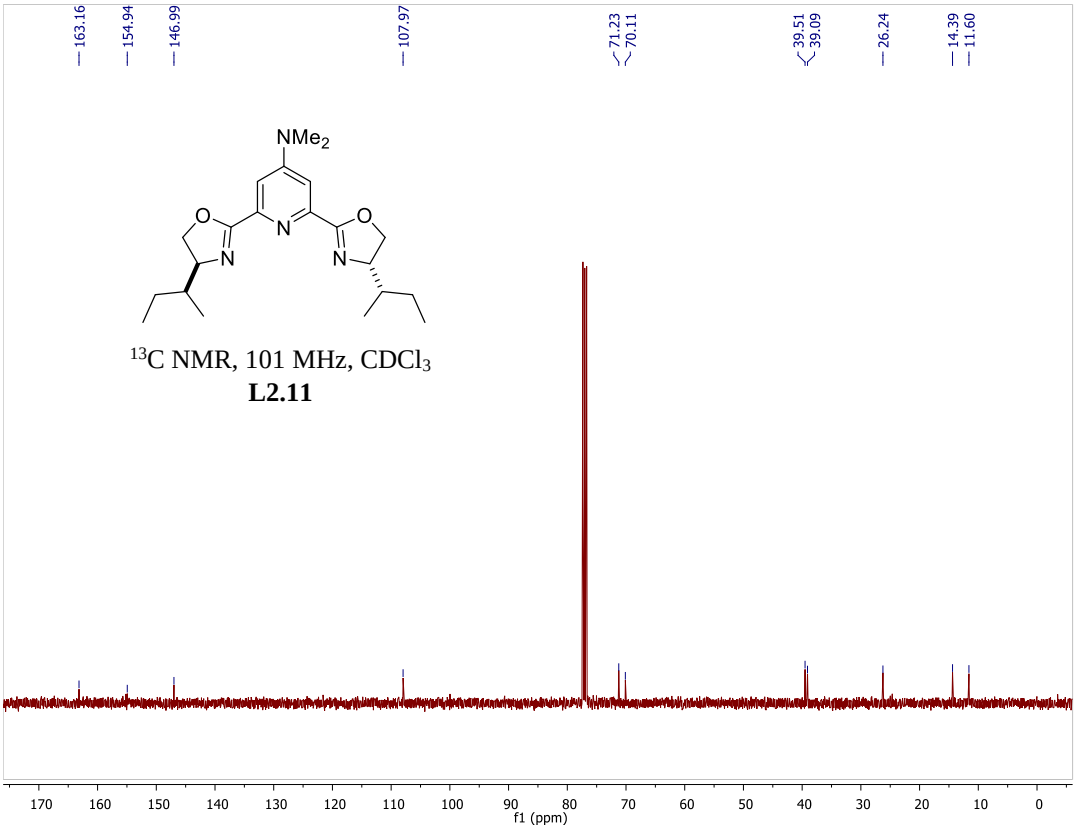

^{13}C NMR, 101 MHz, $CDCl_3$

L2.11

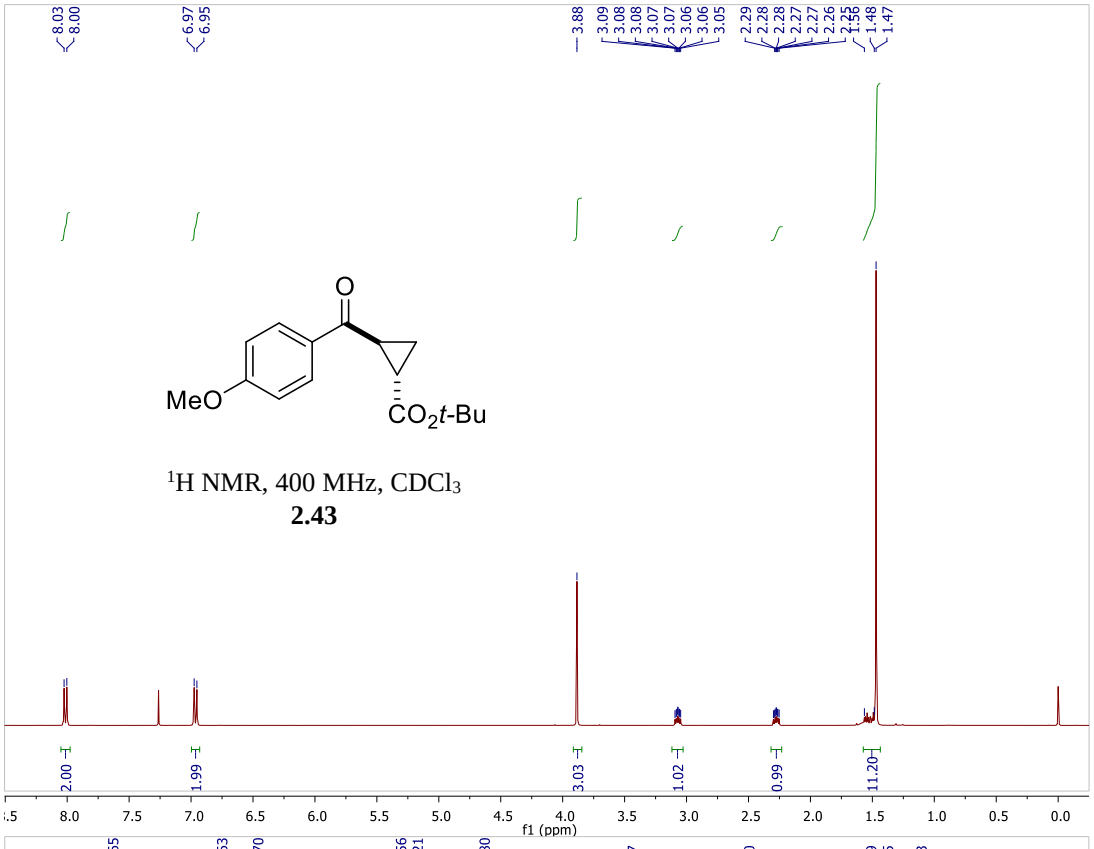

^{1}H NMR, 400 MHz, $CDCl_3$

2.43

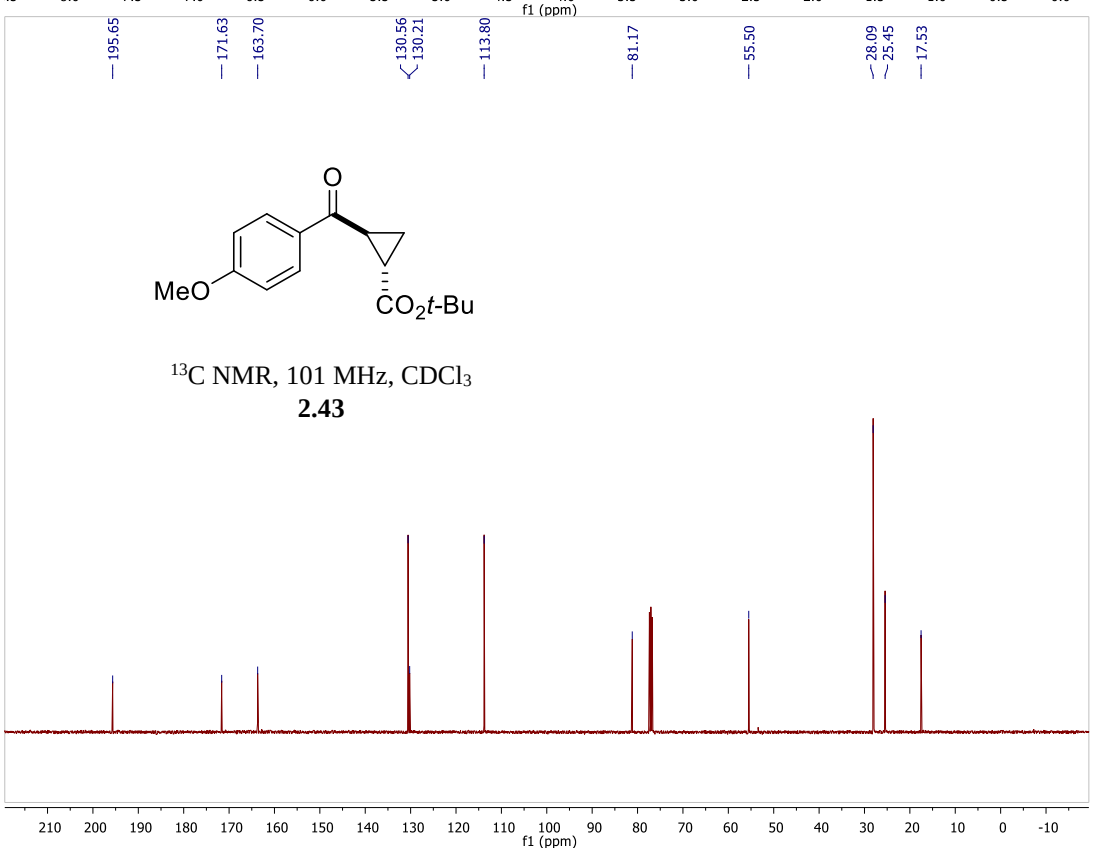

^{13}C NMR, 101 MHz, $CDCl_3$

2.43

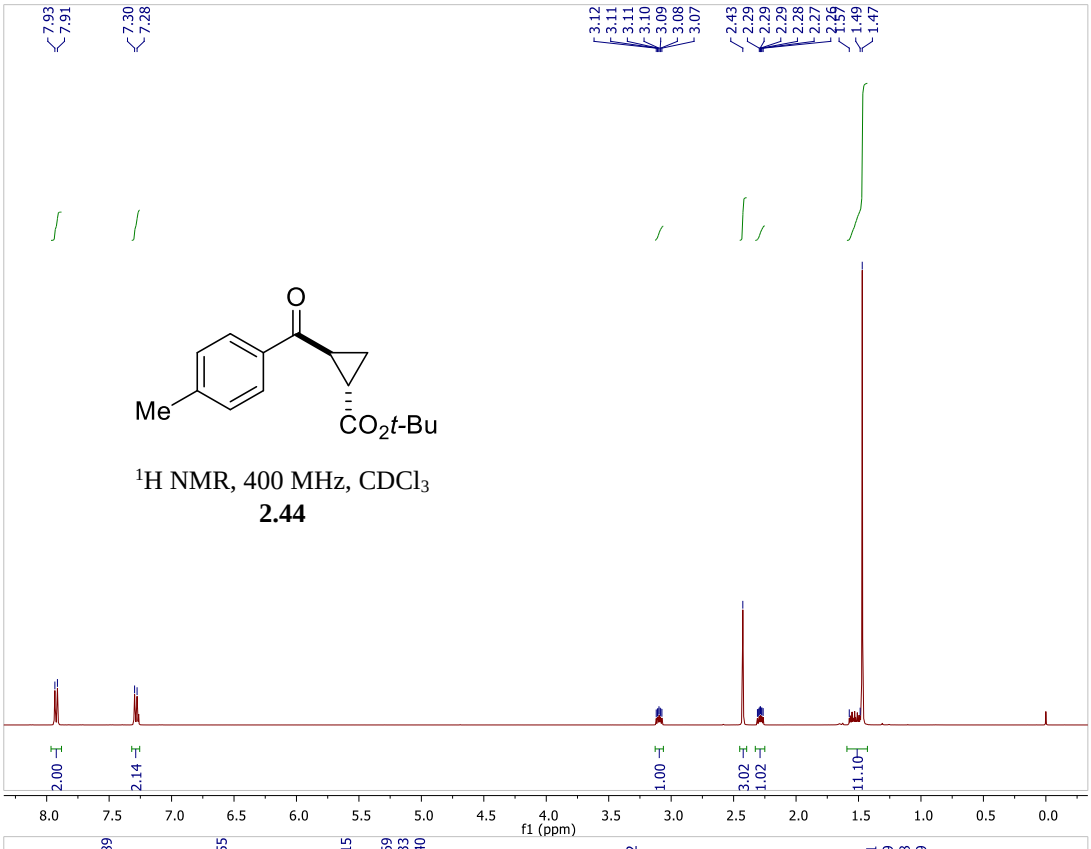

^{1}H NMR, 400 MHz, $CDCl_3$
2.44

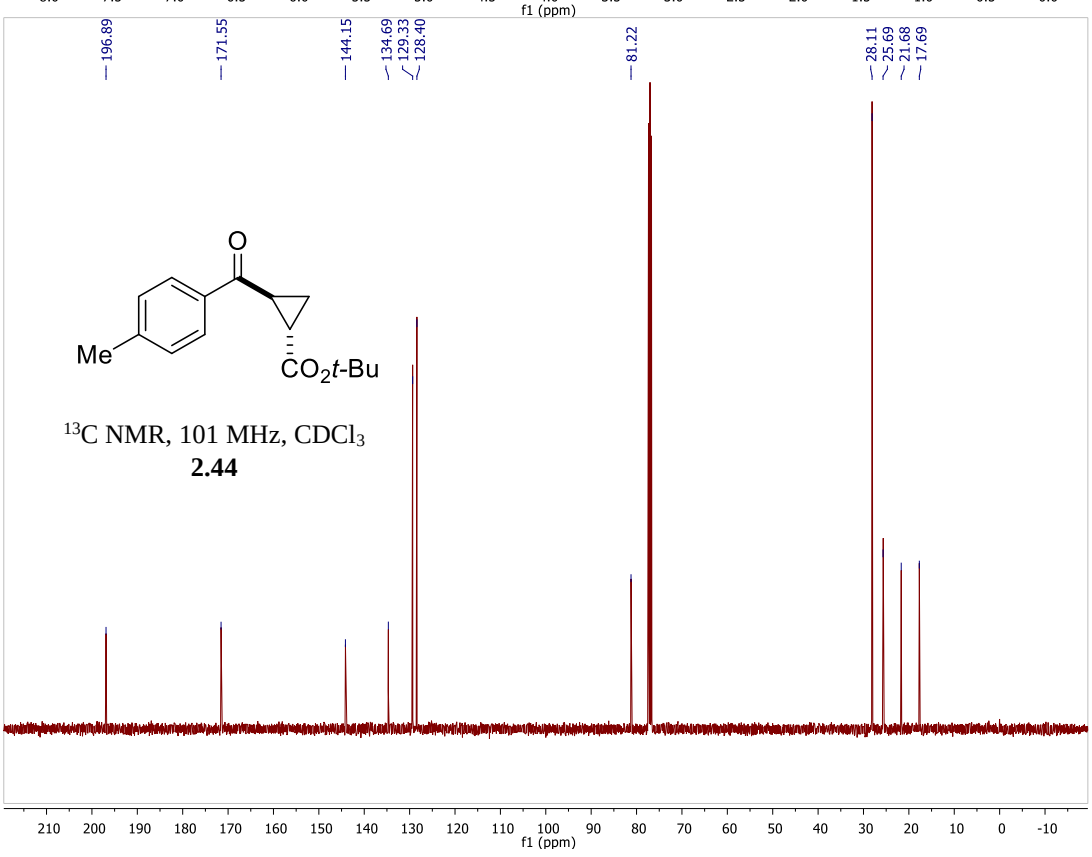

^{13}C NMR, 101 MHz, $CDCl_3$
2.44

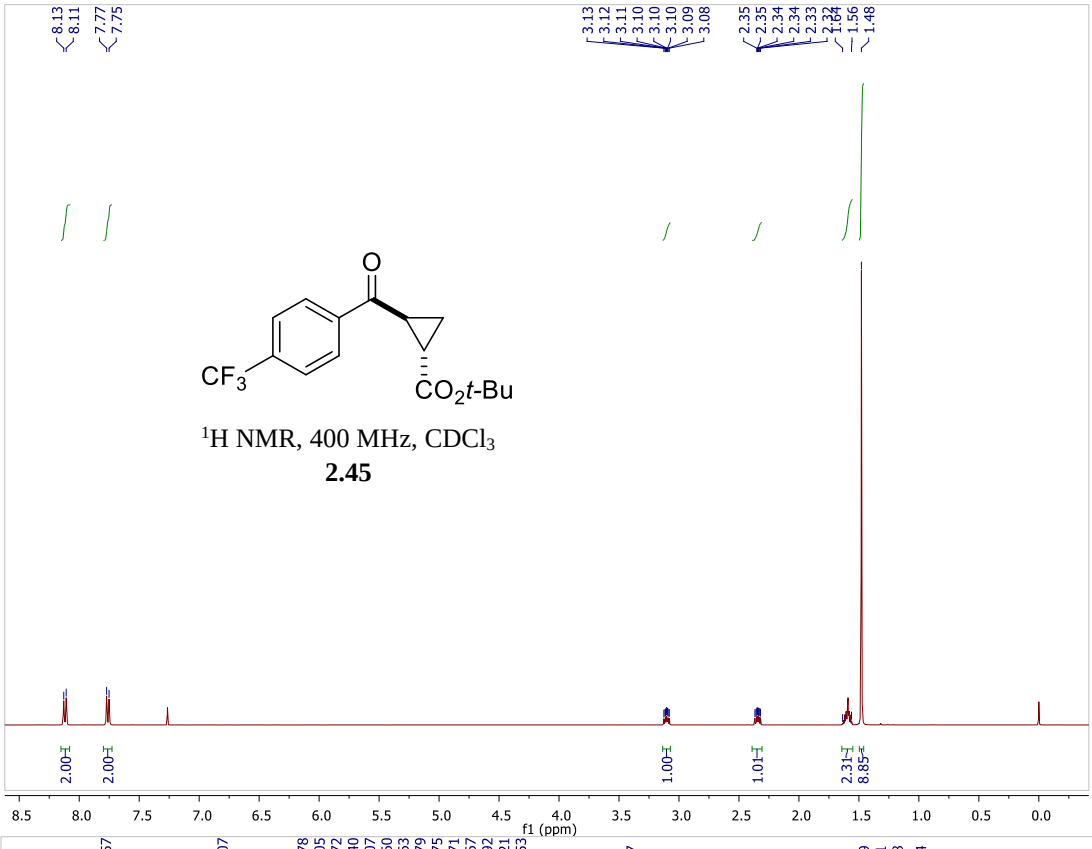

^{1}H NMR, 400 MHz, $CDCl_3$

2.45

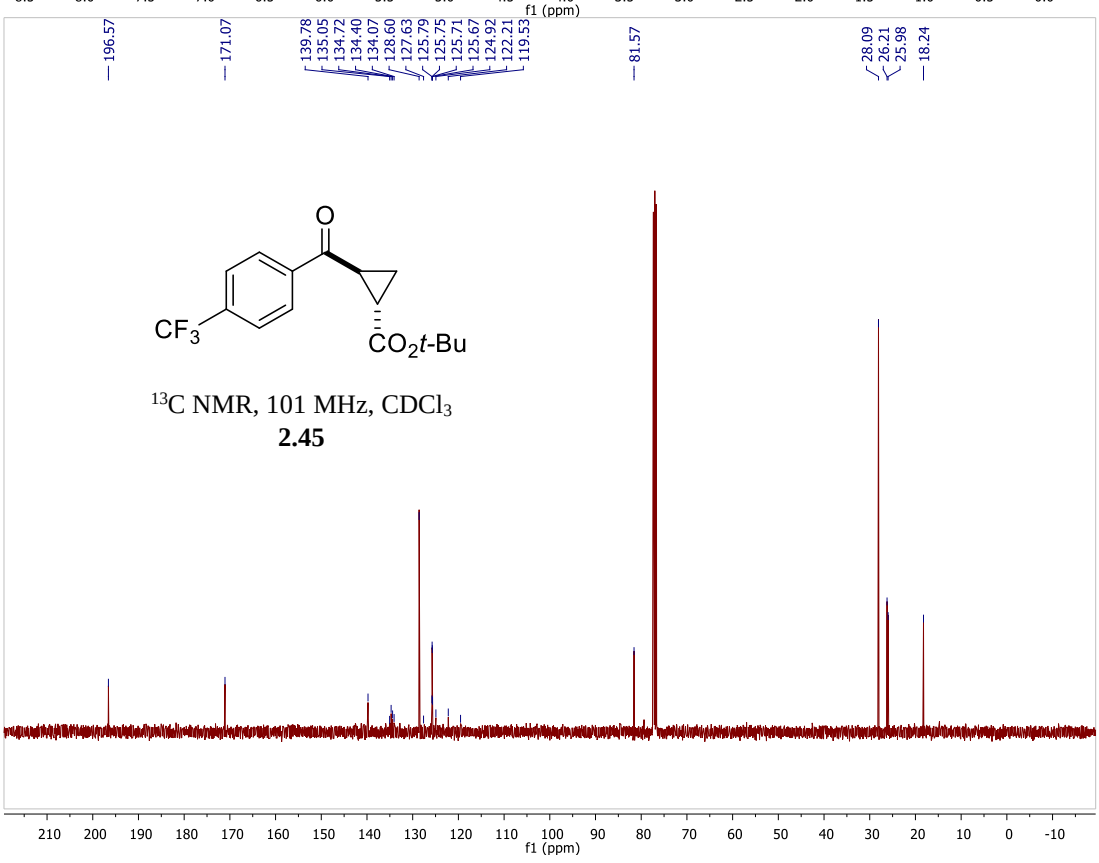

^{13}C NMR, 101 MHz, $CDCl_3$

2.45

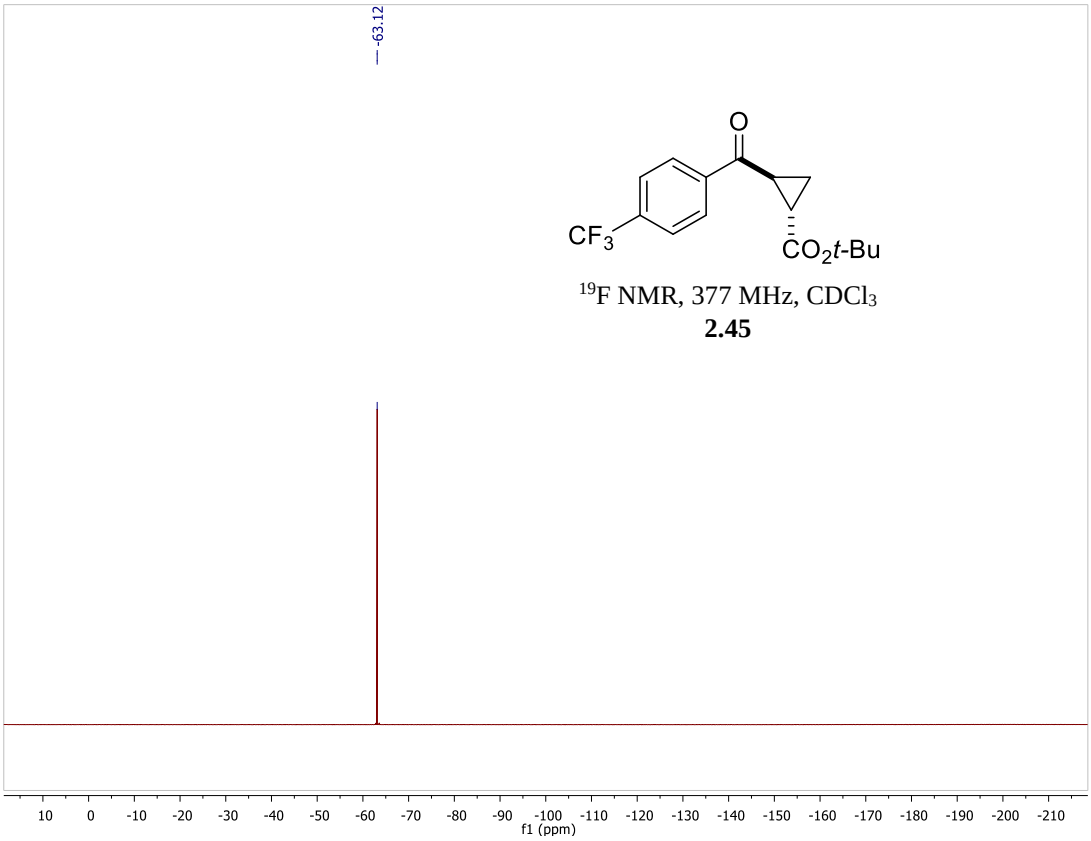

^{19}F NMR, 377 MHz, $CDCl_3$

2.45

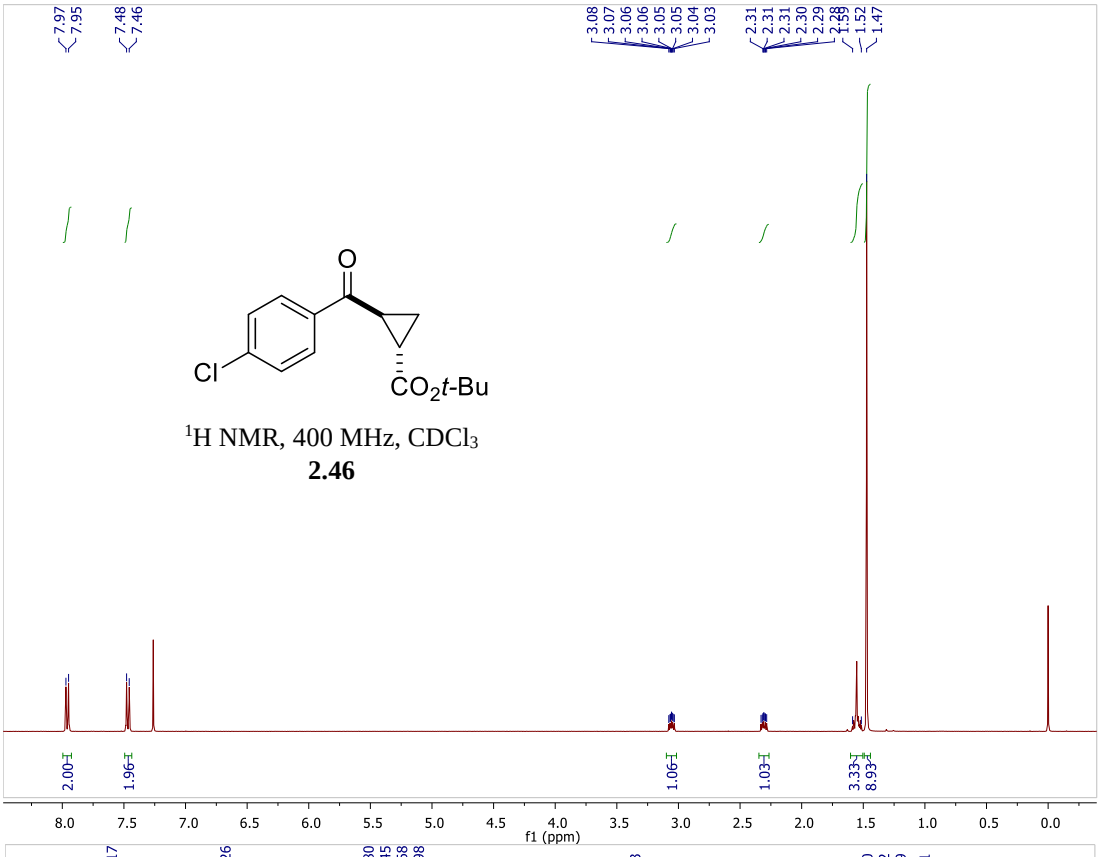

^{1}H NMR, 400 MHz, $CDCl_3$

2.46

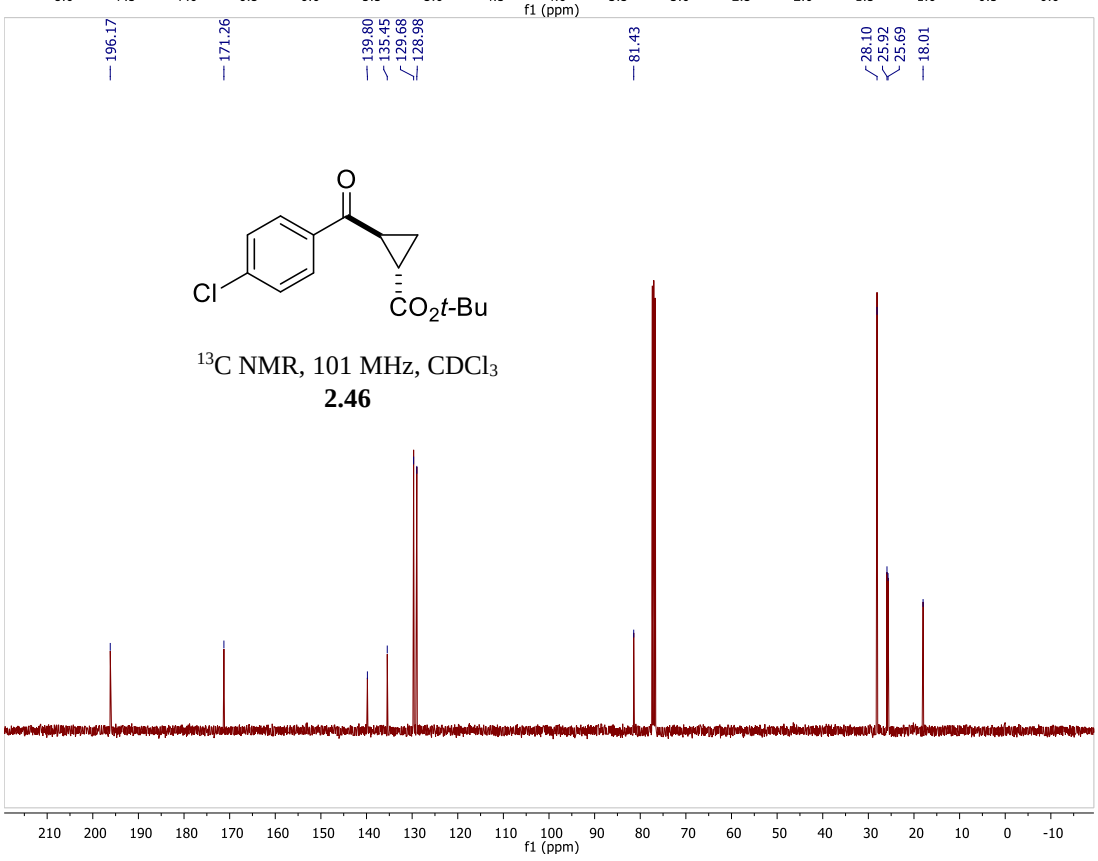

^{13}C NMR, 101 MHz, $CDCl_3$

2.46

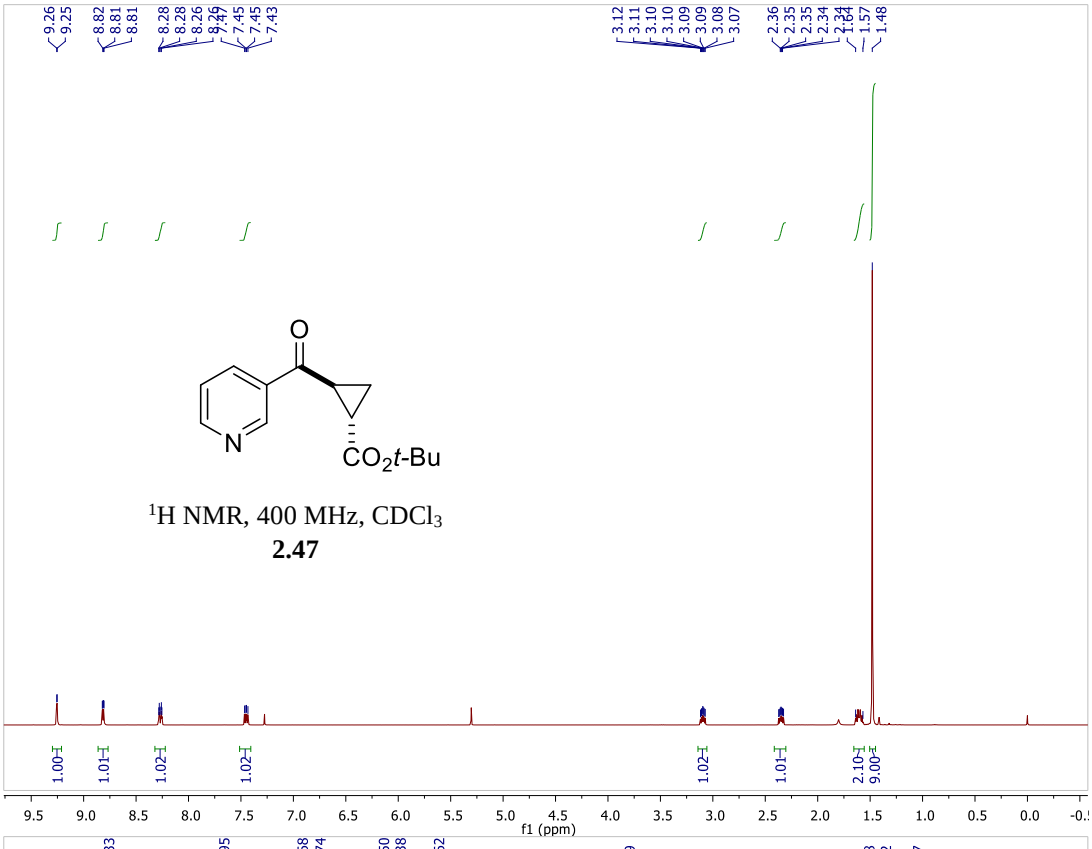

^{1}H NMR, 400 MHz, $CDCl_3$
2.47

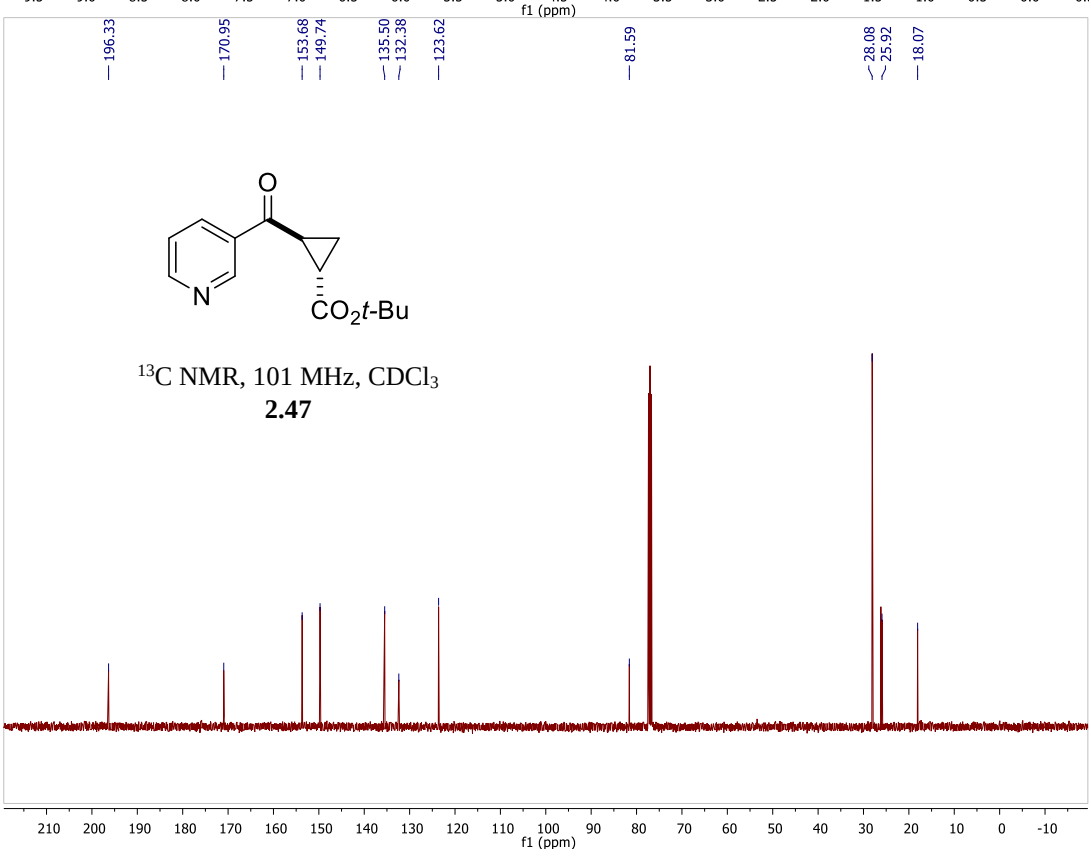

^{13}C NMR, 101 MHz, $CDCl_3$
2.47

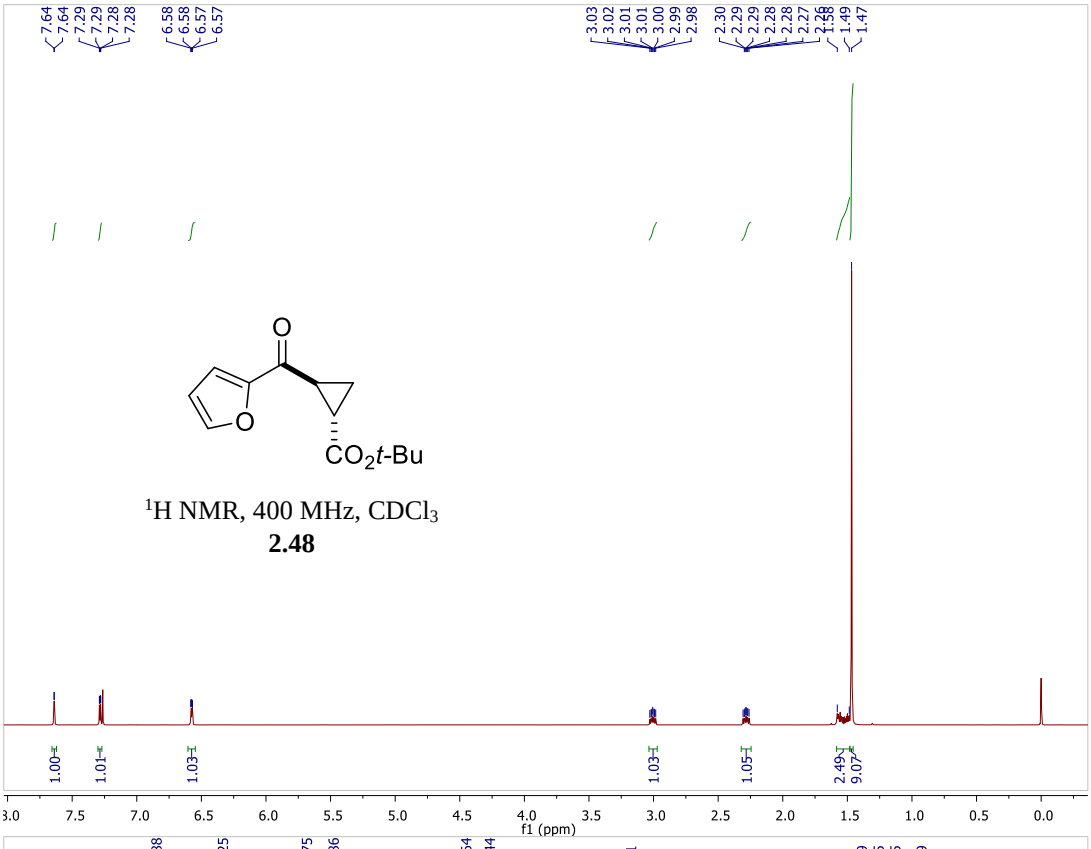

^{1}H NMR, 400 MHz, $CDCl_3$
2.48

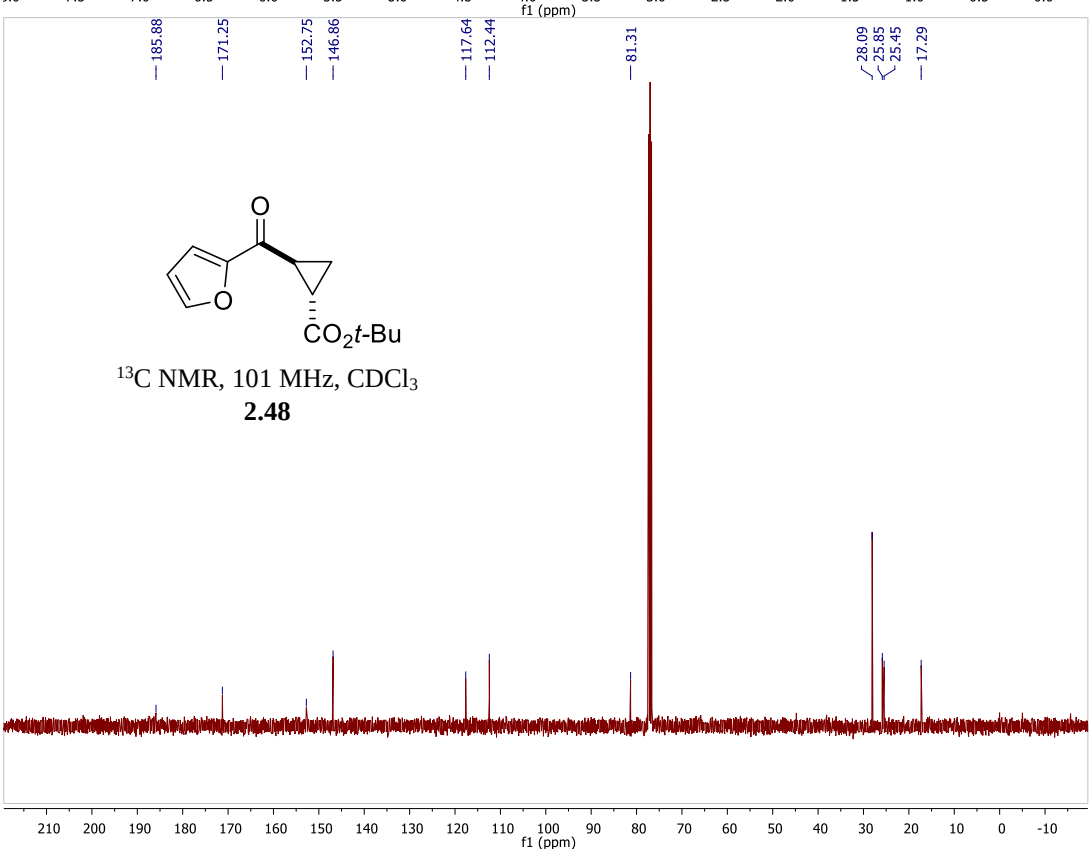

^{13}C NMR, 101 MHz, $CDCl_3$
2.48

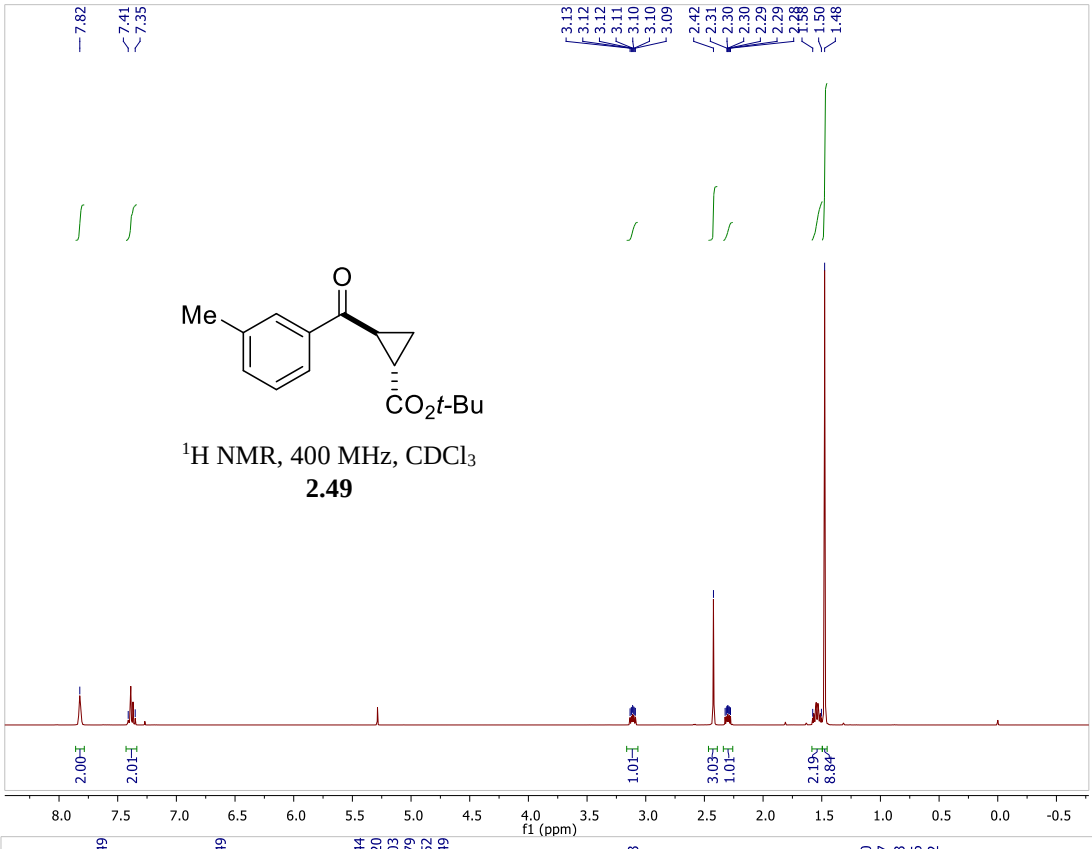

^{1}H NMR, 400 MHz, $CDCl_3$

2.49

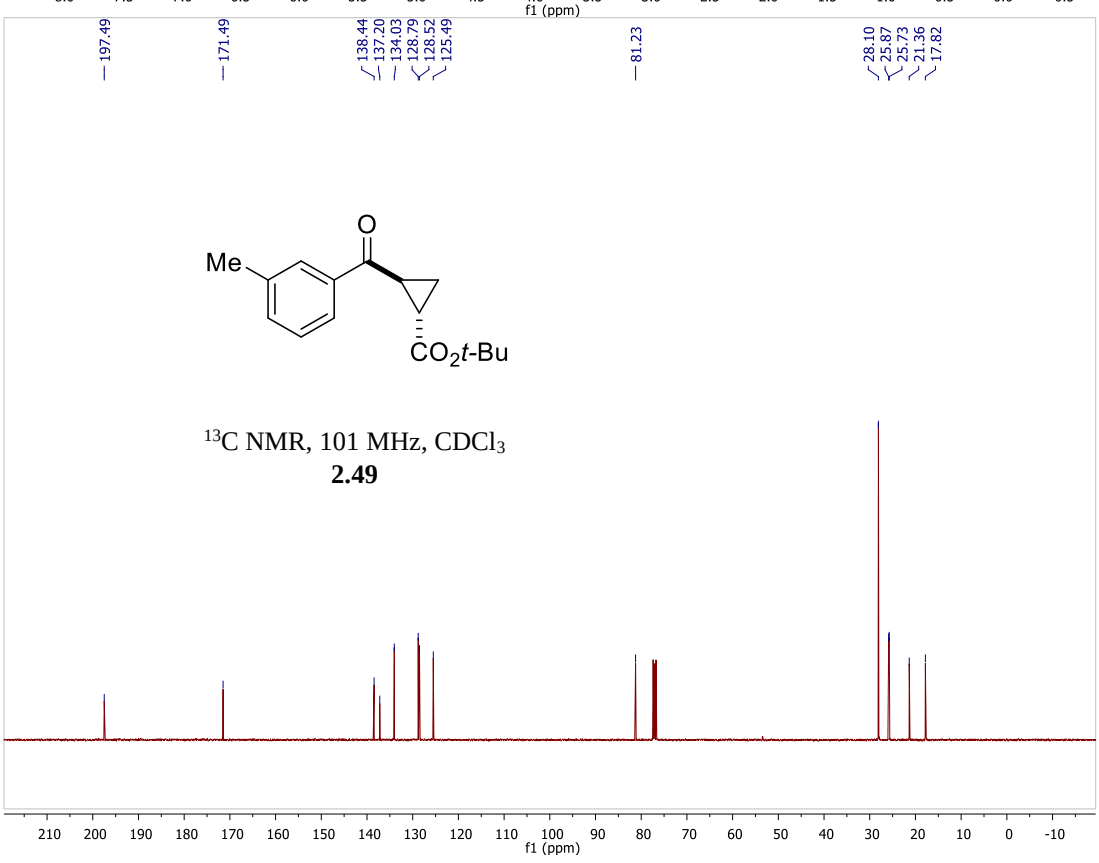

^{13}C NMR, 101 MHz, $CDCl_3$

2.49

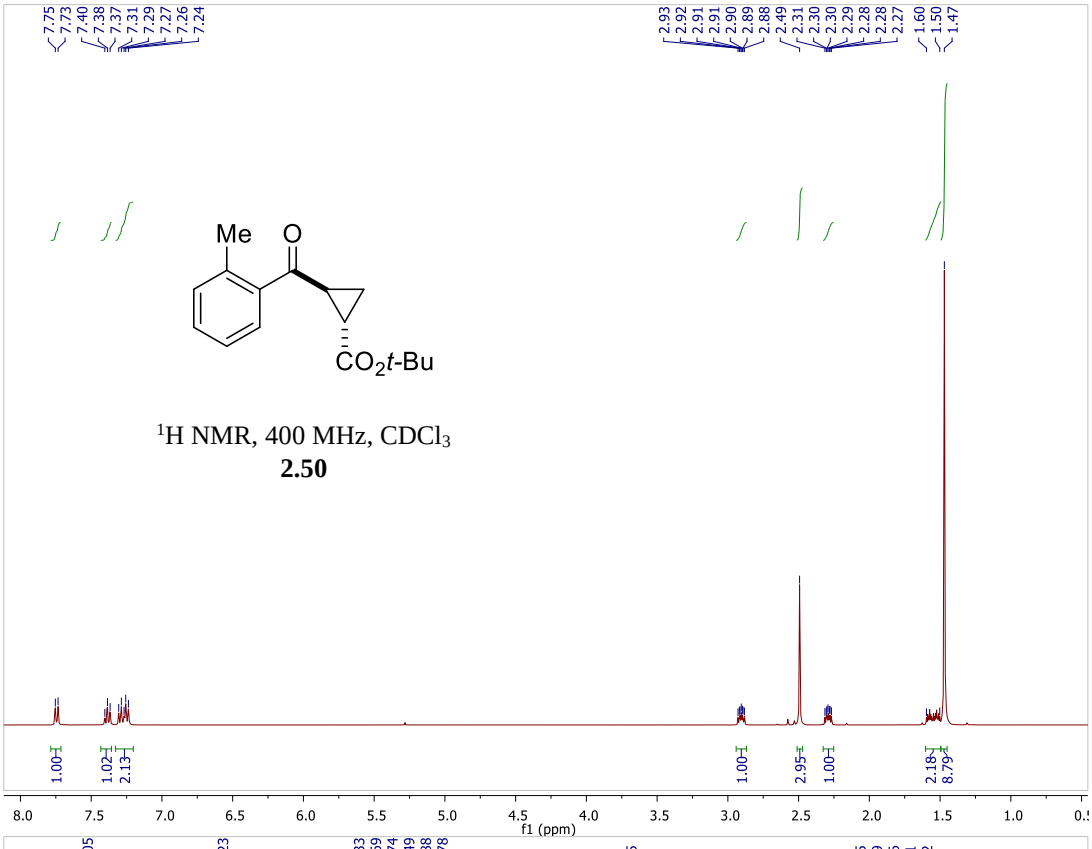

^{1}H NMR, 400 MHz, $CDCl_3$
2.50

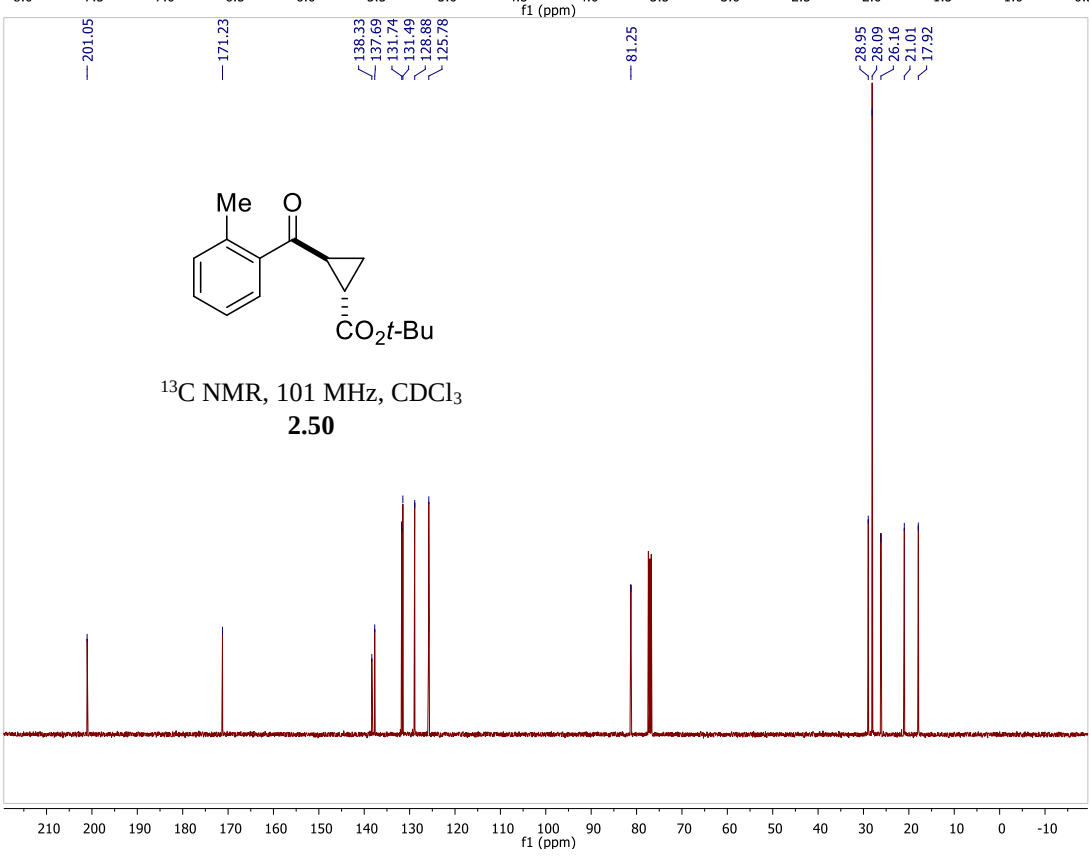

^{13}C NMR, 101 MHz, $CDCl_3$
2.50

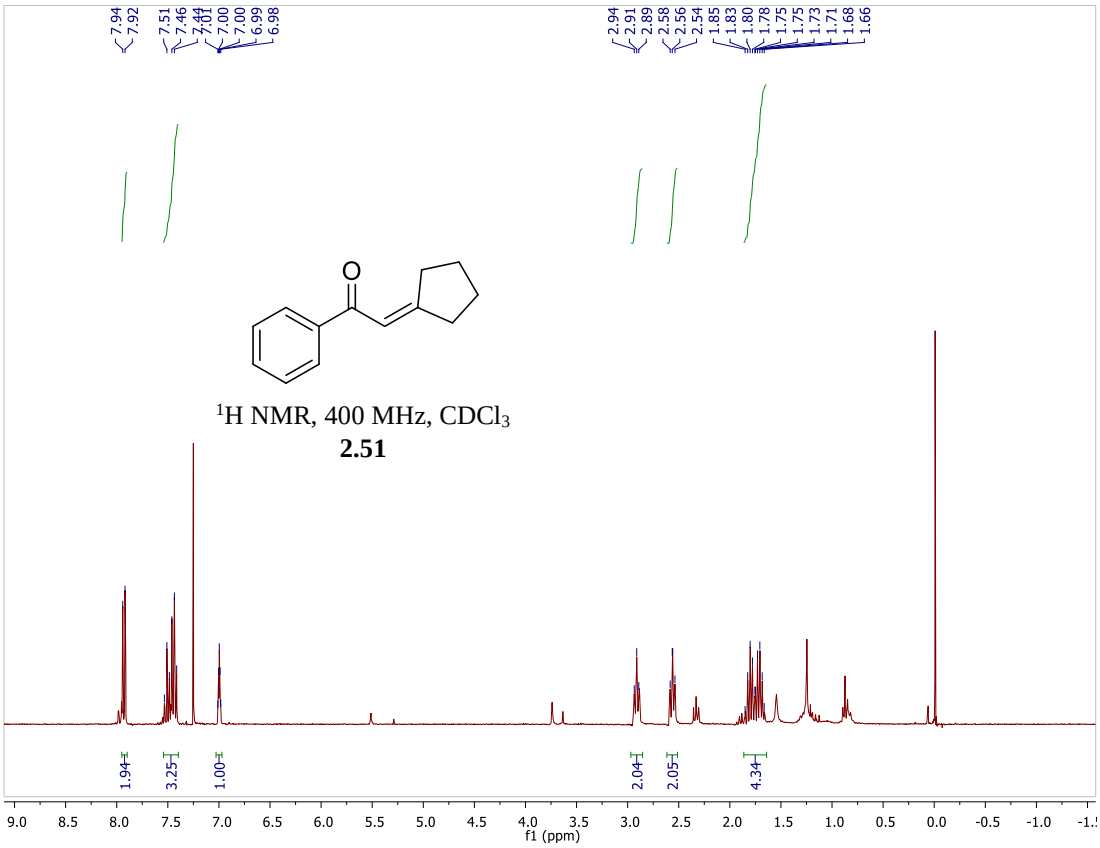

^{1}H NMR, 400 MHz, $CDCl_3$

2.51

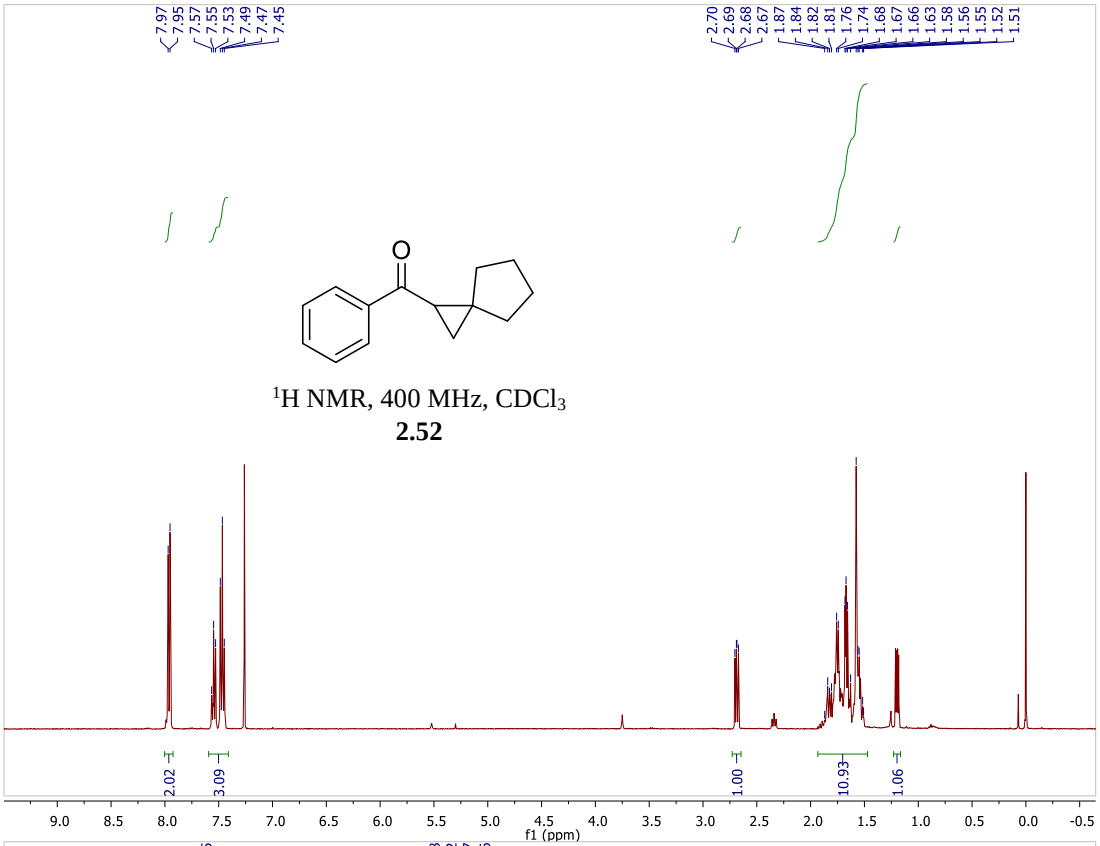

^{1}H NMR, 400 MHz, $CDCl_3$

2.52

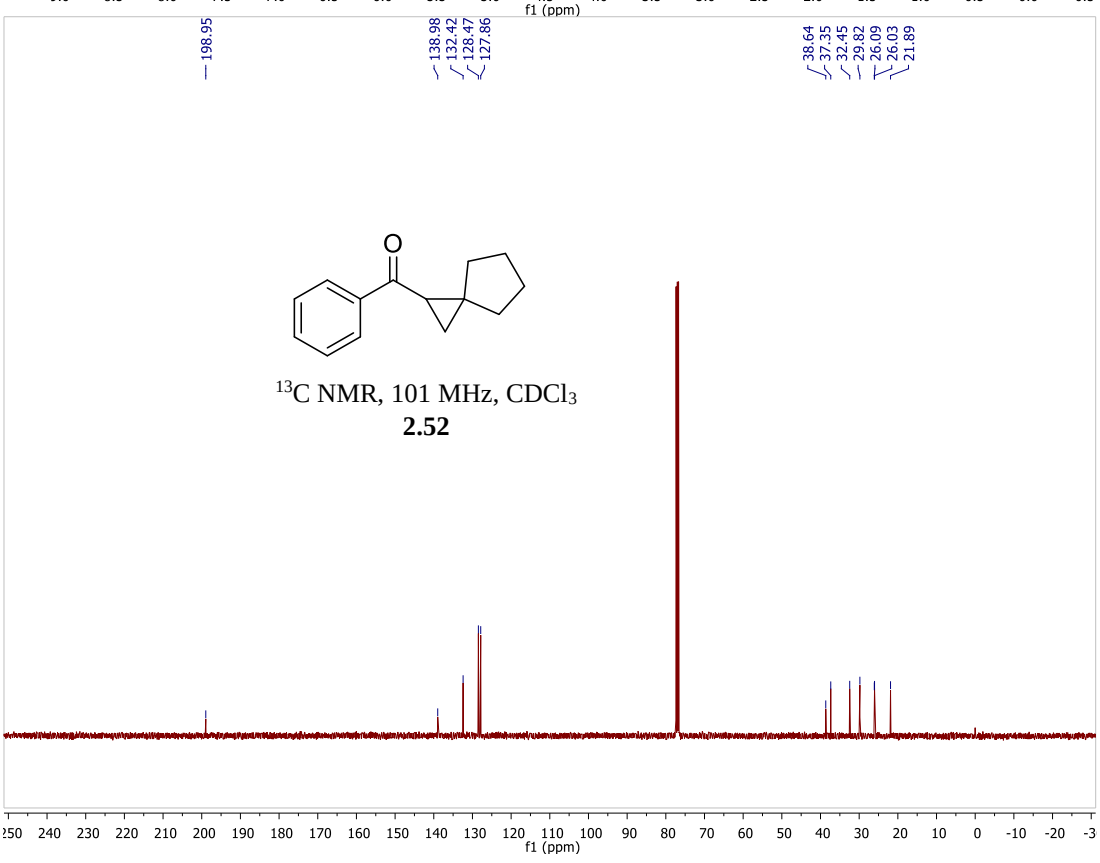

^{13}C NMR, 101 MHz, $CDCl_3$

2.52

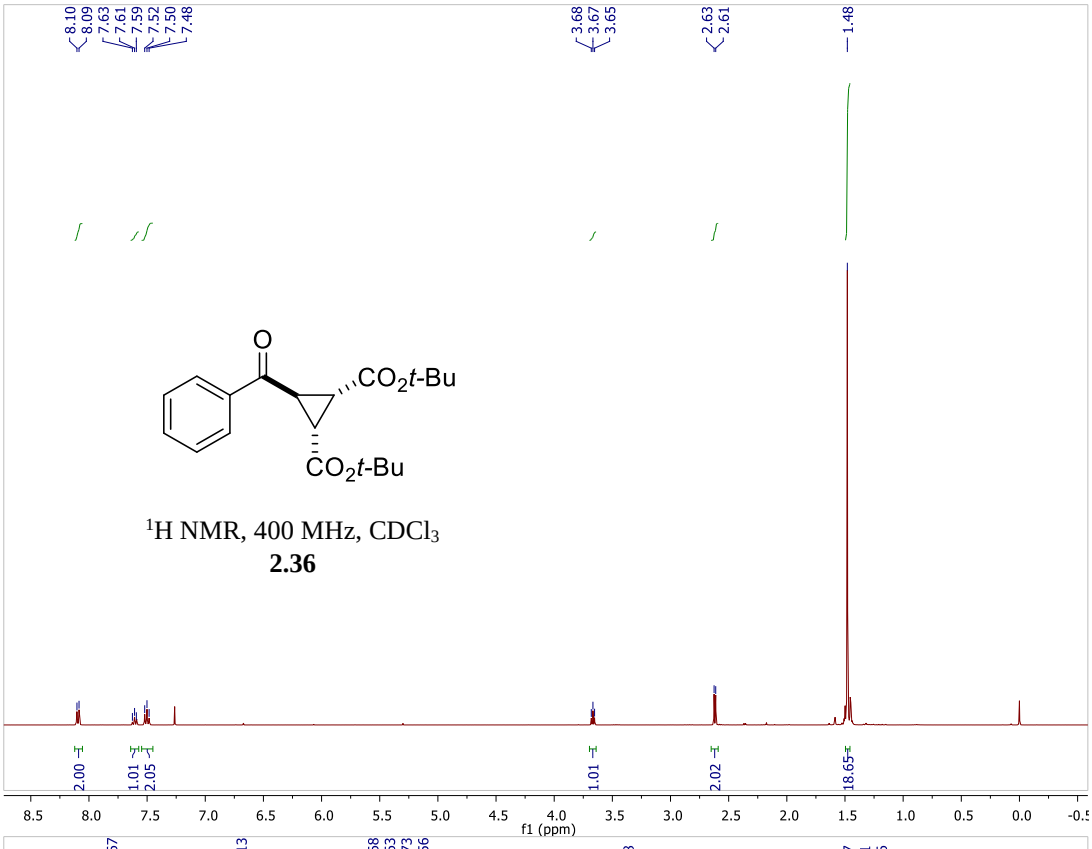

^{1}H NMR, 400 MHz, $CDCl_3$
2.36

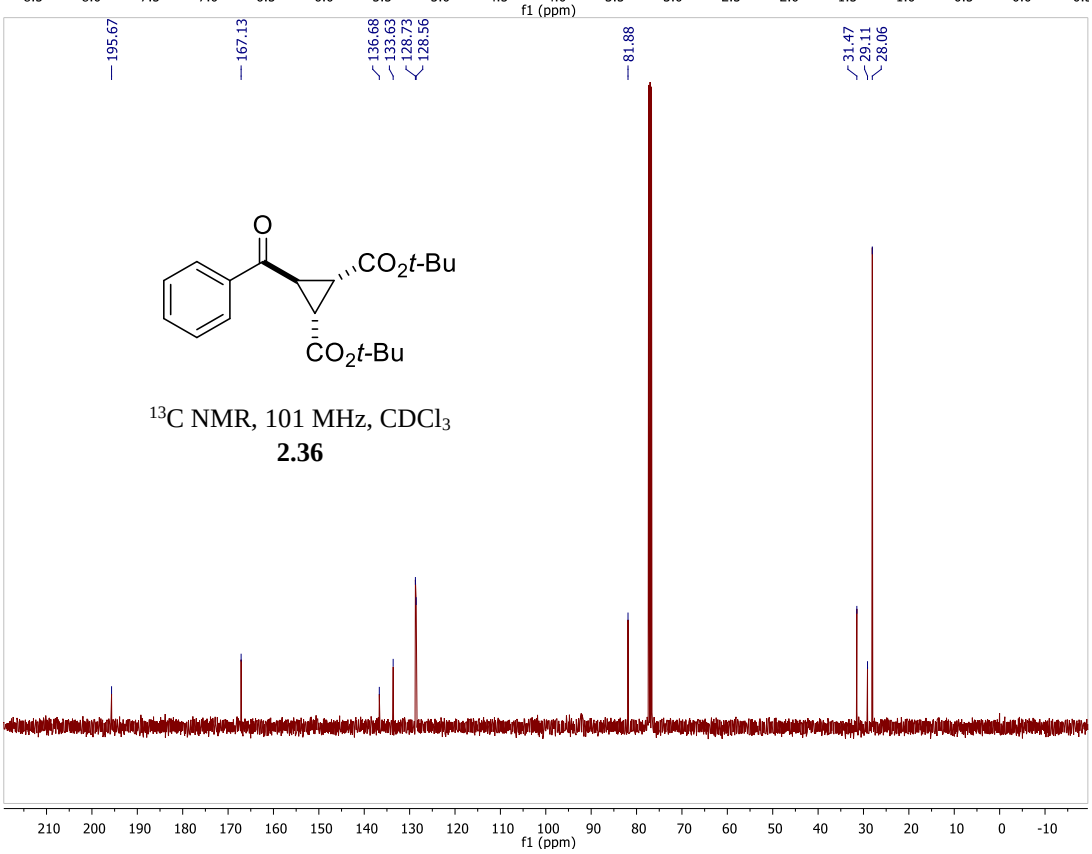

^{13}C NMR, 101 MHz, $CDCl_3$
2.36

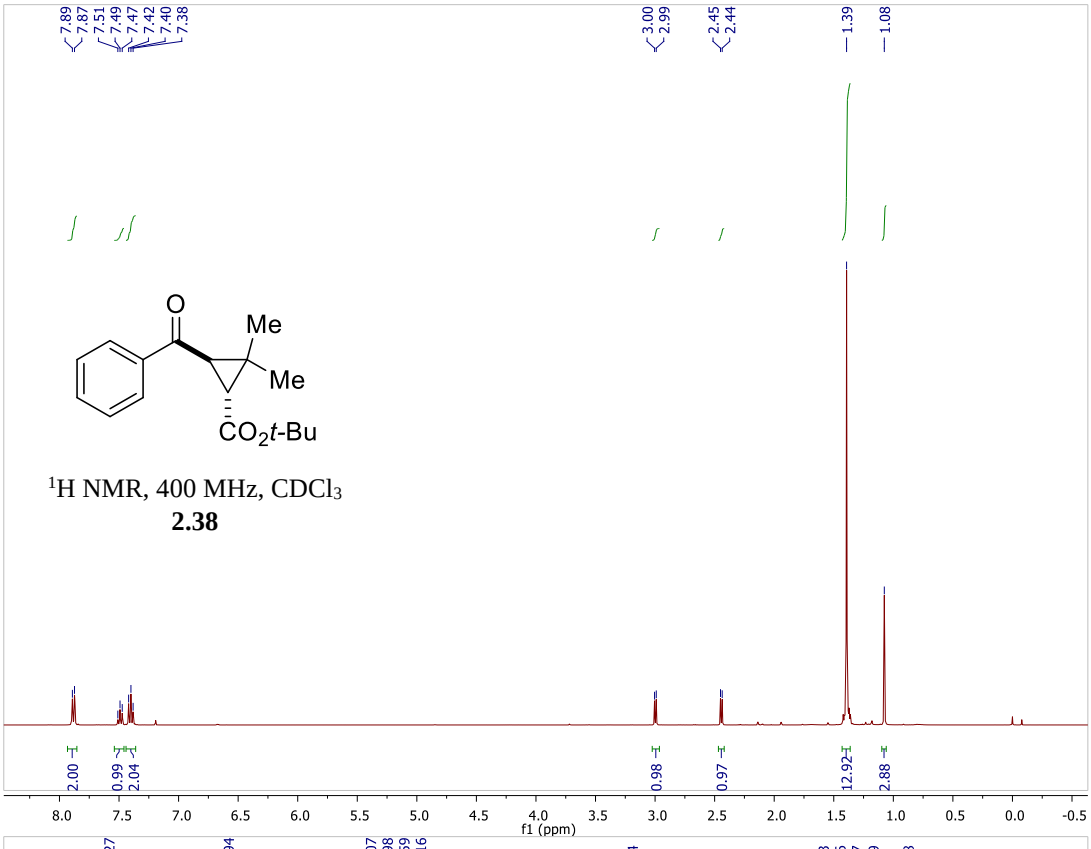

^{1}H NMR, 400 MHz, $CDCl_3$
2.38

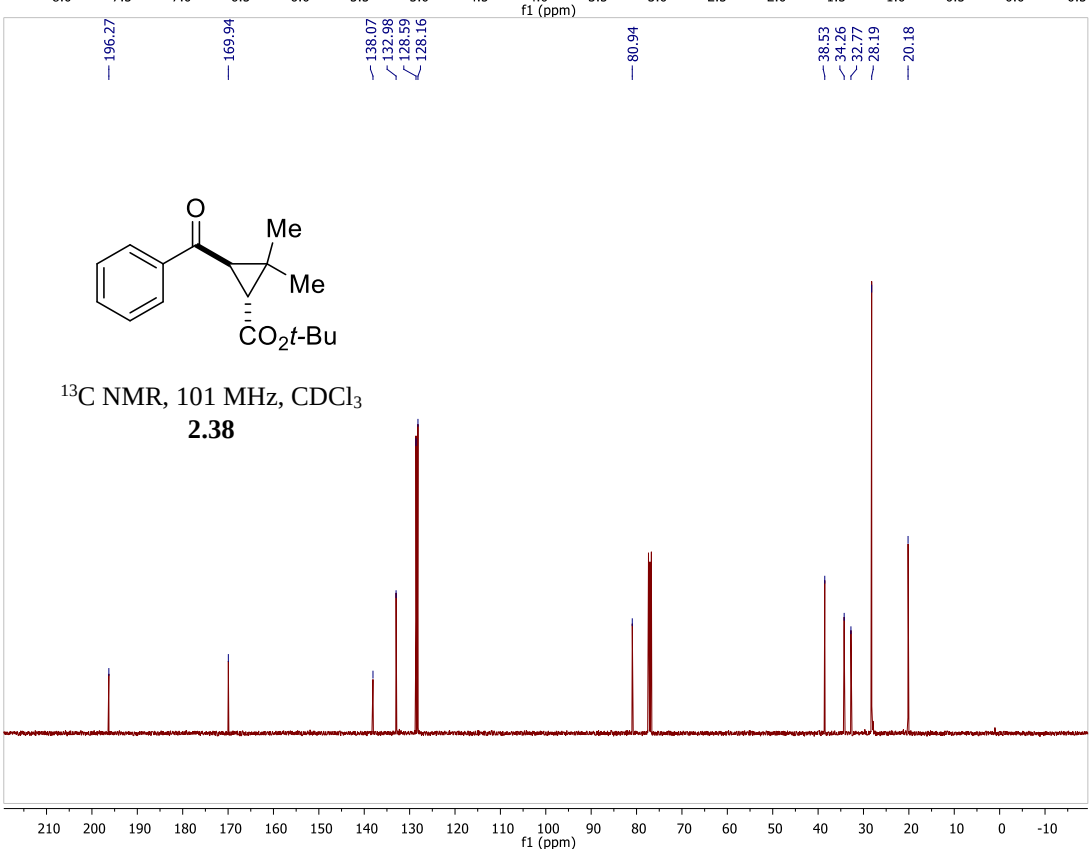

^{13}C NMR, 101 MHz, $CDCl_3$
2.38

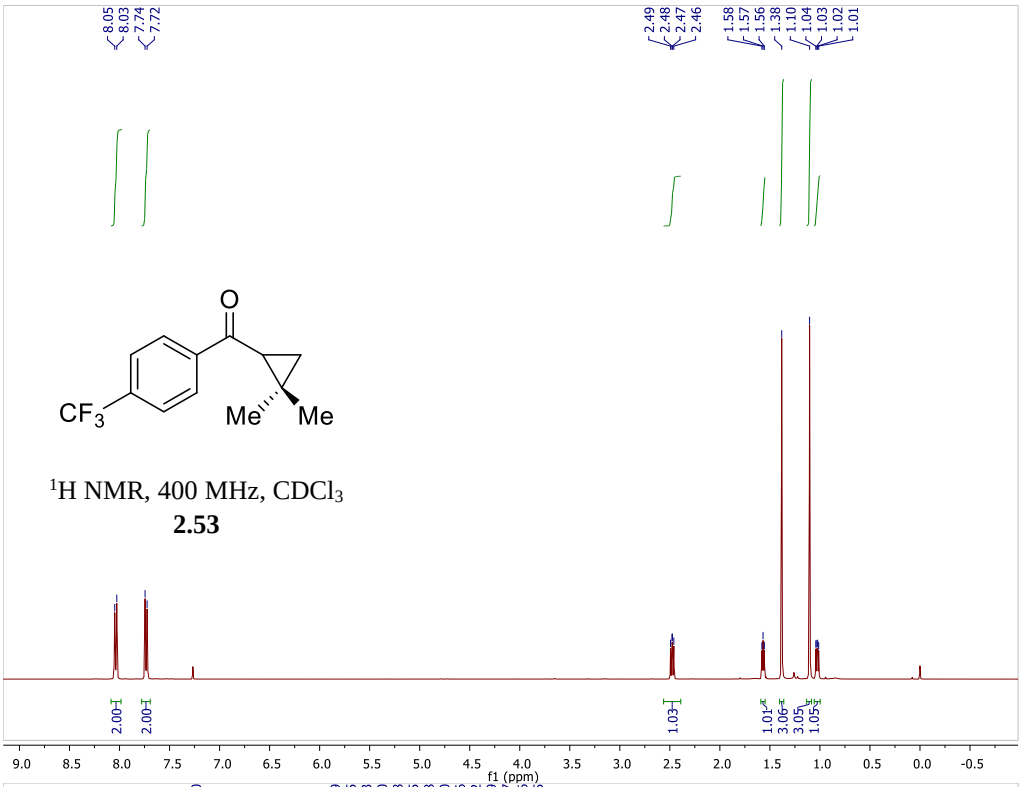

^{1}H NMR, 400 MHz, $CDCl_3$

2.53

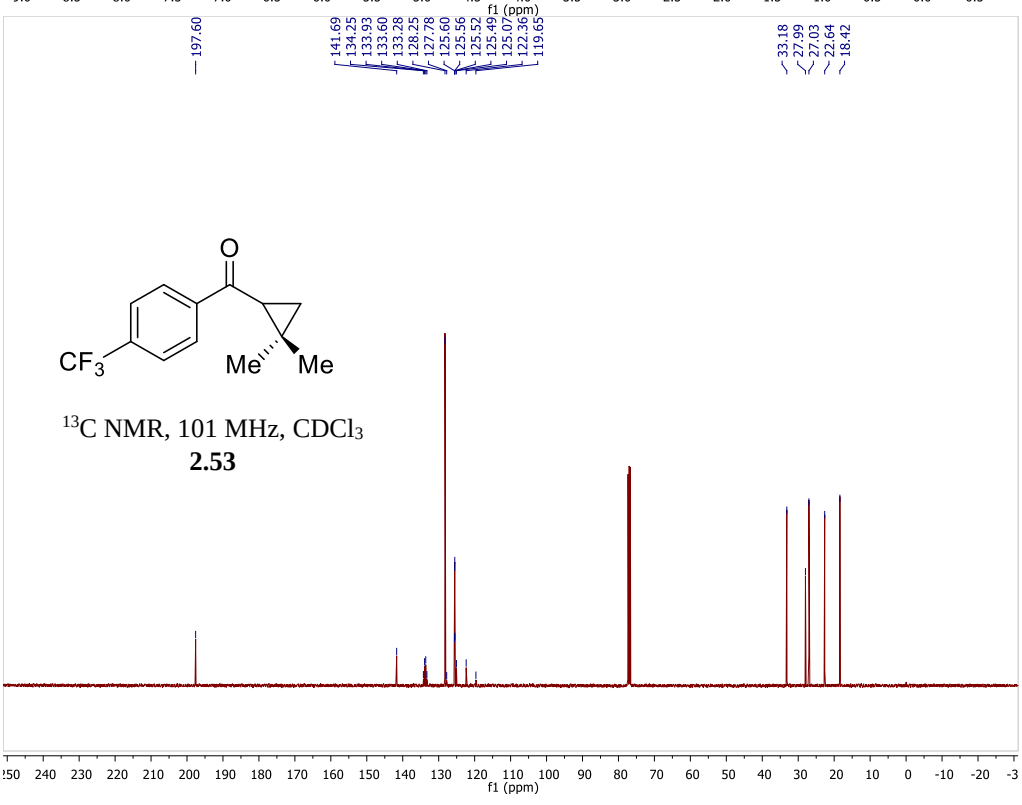

^{13}C NMR, 101 MHz, $CDCl_3$

2.53

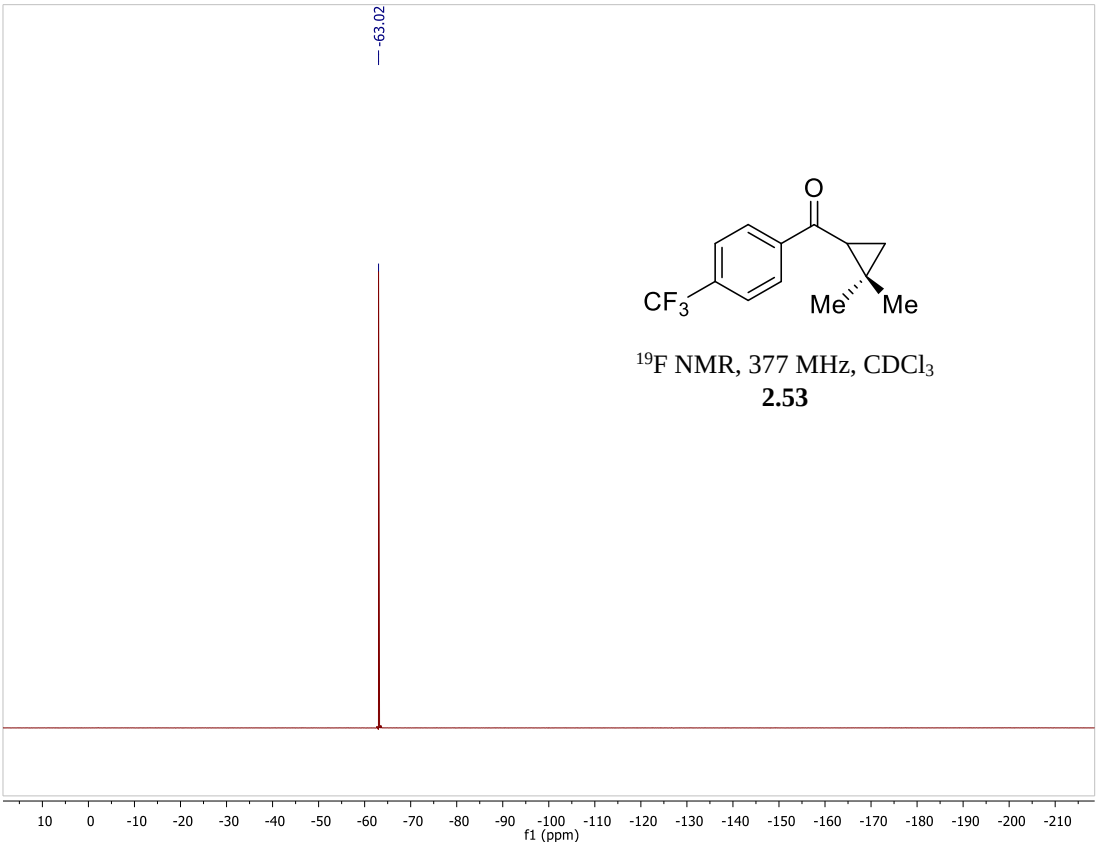

^{19}F NMR, 377 MHz, $CDCl_3$

2.53

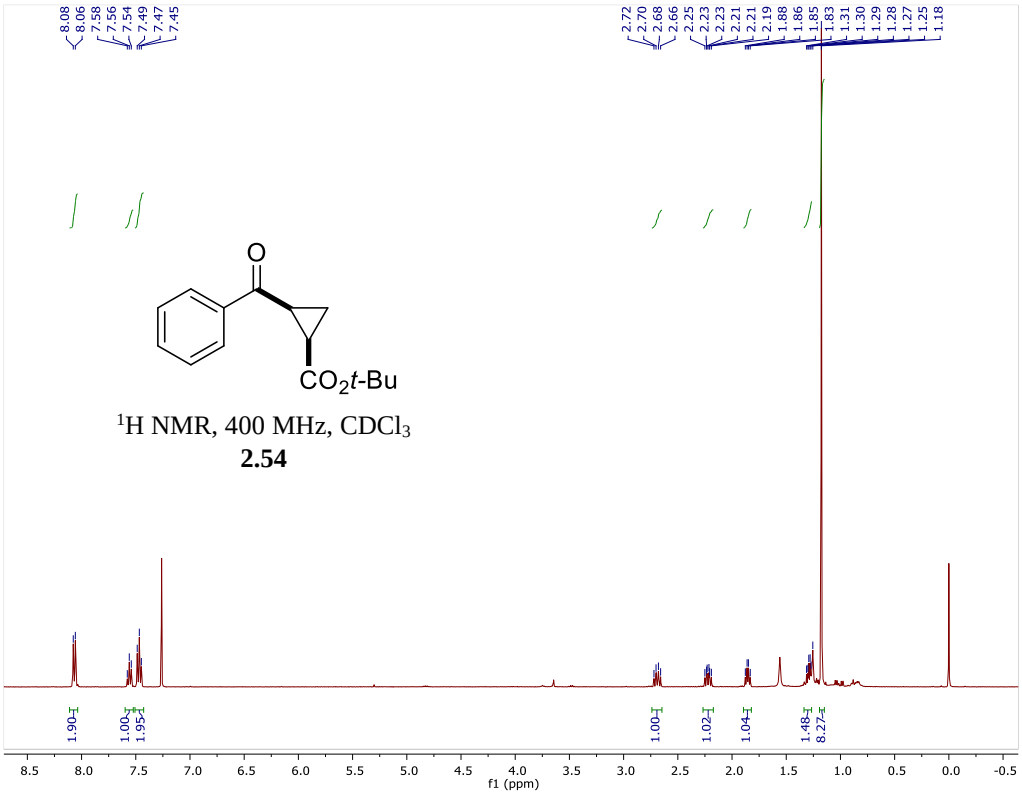

^{1}H NMR, 400 MHz, $CDCl_3$

2.54

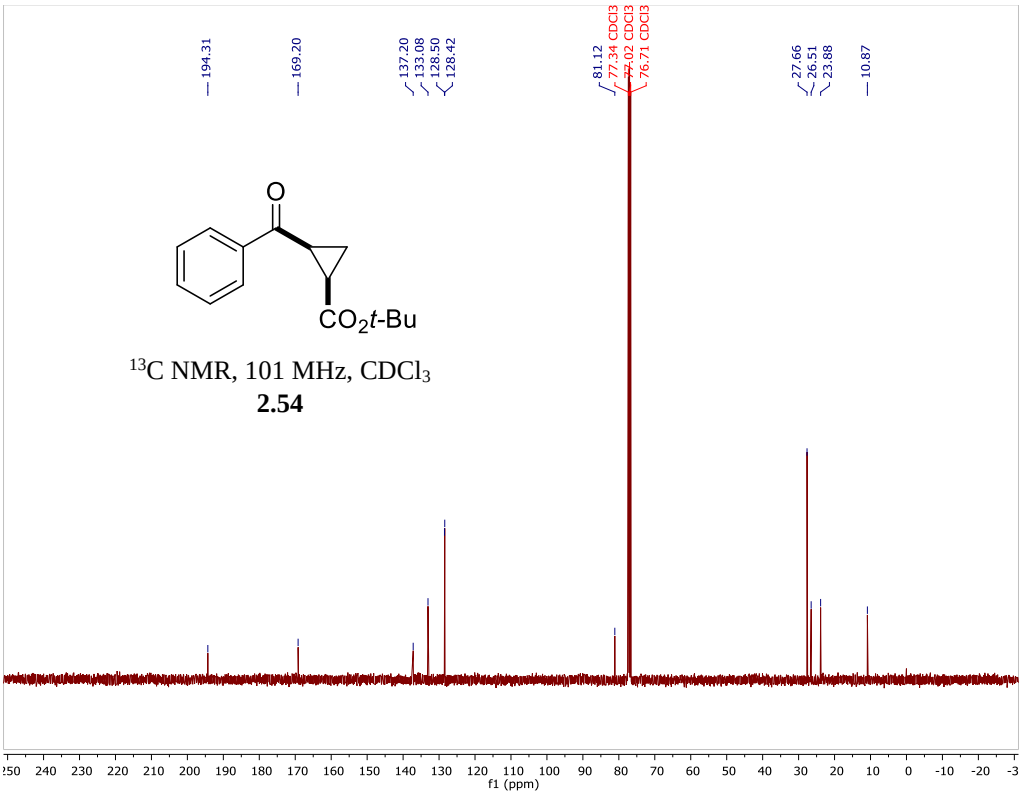

^{13}C NMR, 101 MHz, $CDCl_3$

2.54

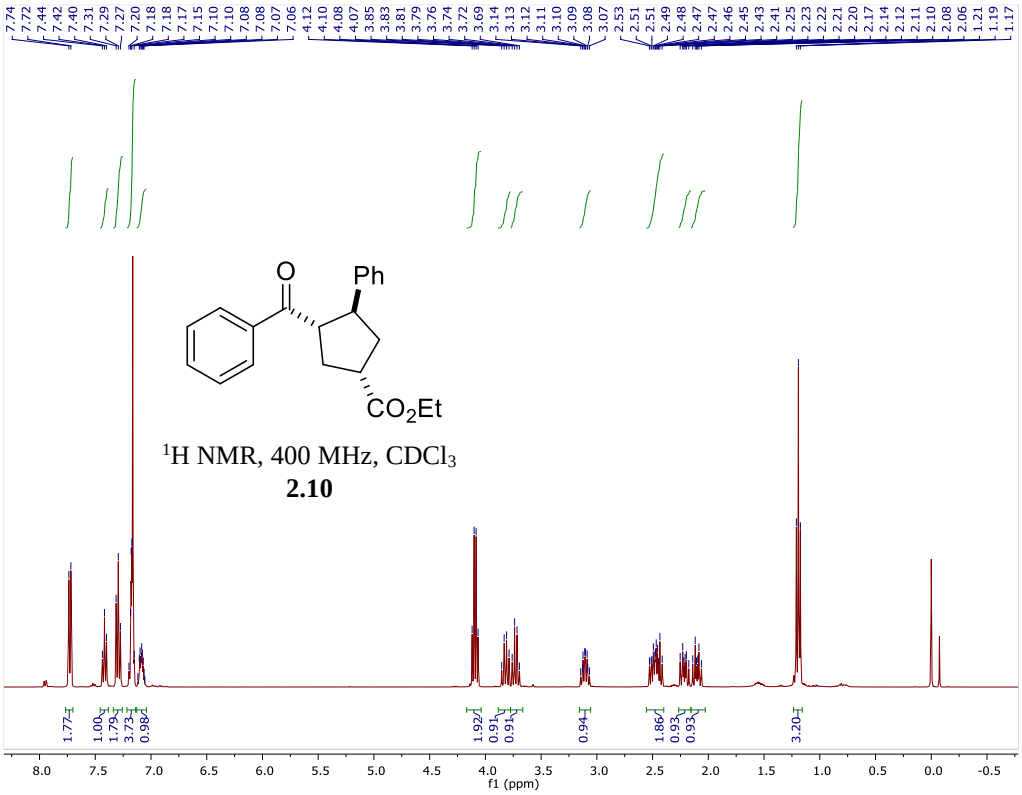

^{1}H NMR, 400 MHz, $CDCl_3$

2.10

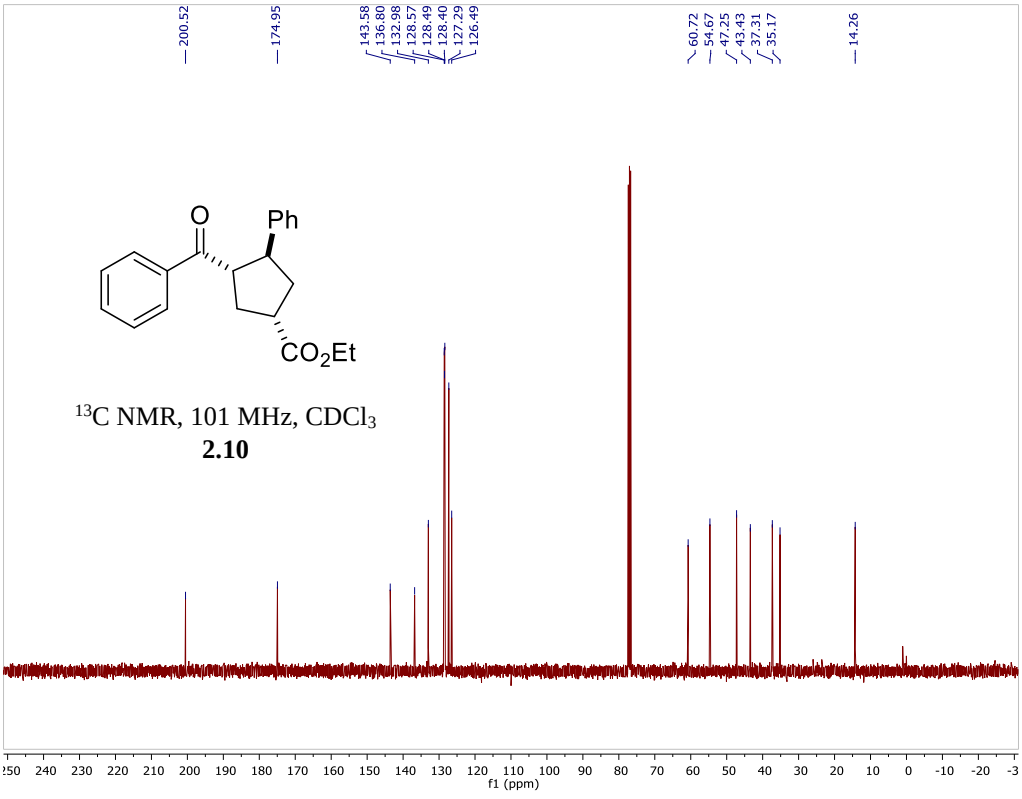

^{13}C NMR, 101 MHz, $CDCl_3$

2.10

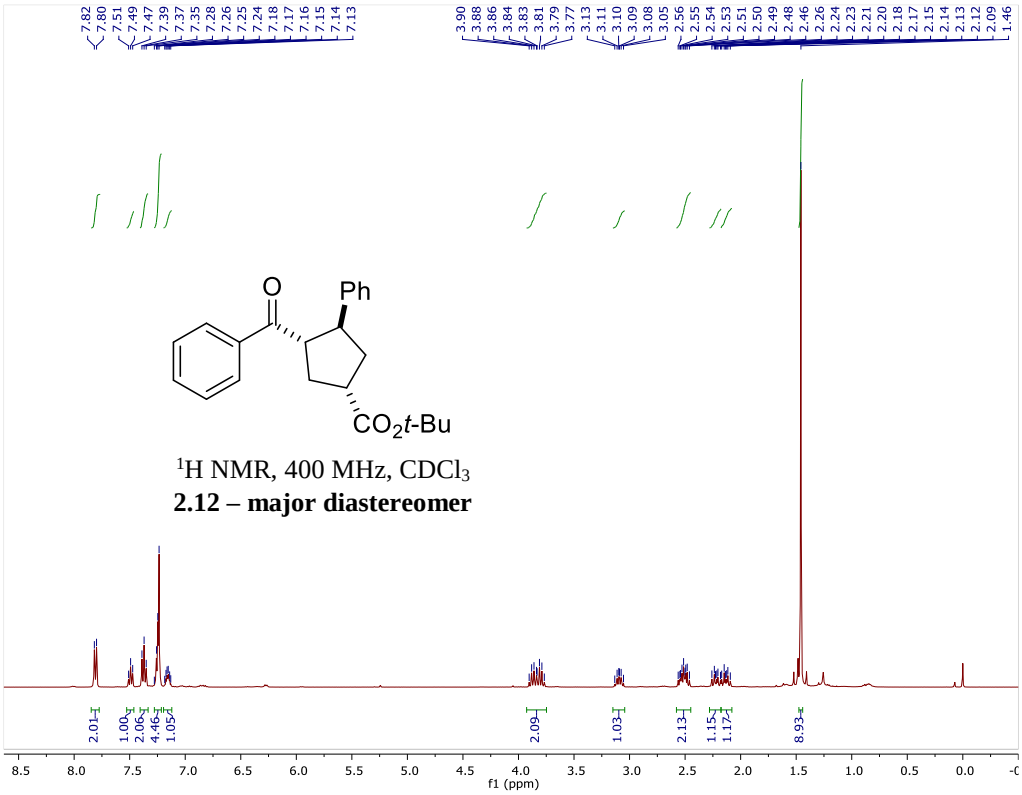

^{1}H NMR, 400 MHz, $CDCl_3$

2.12 – major diastereomer

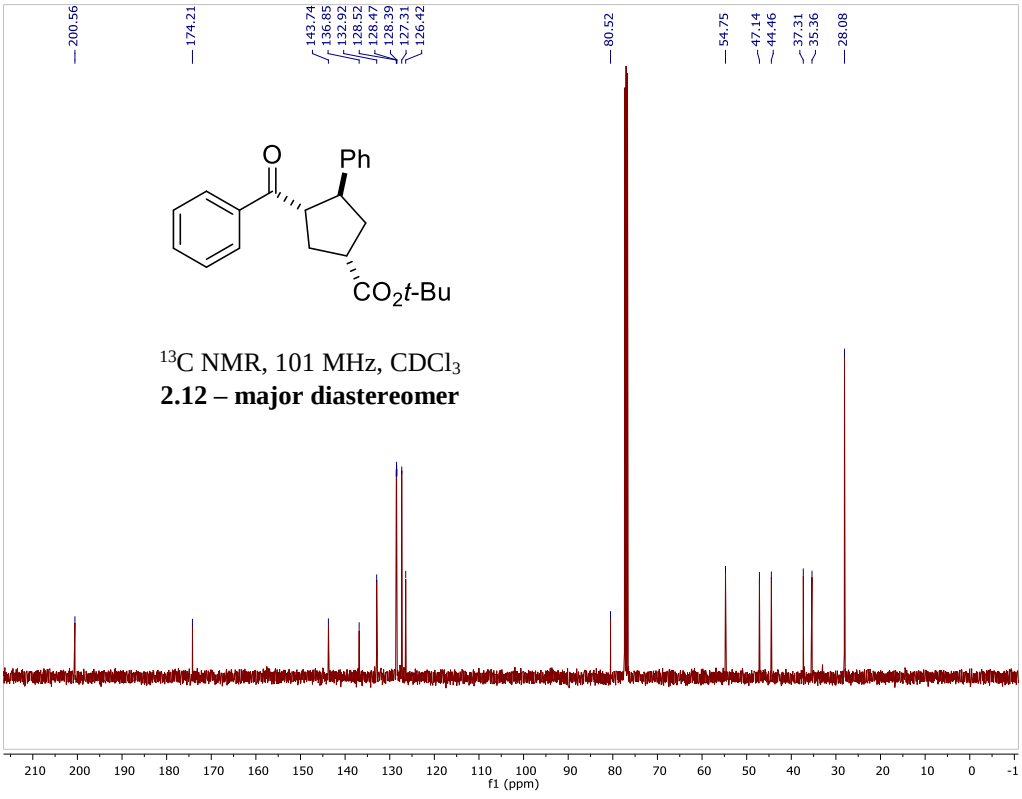

^{13}C NMR, 101 MHz, $CDCl_3$

2.12 – major diastereomer

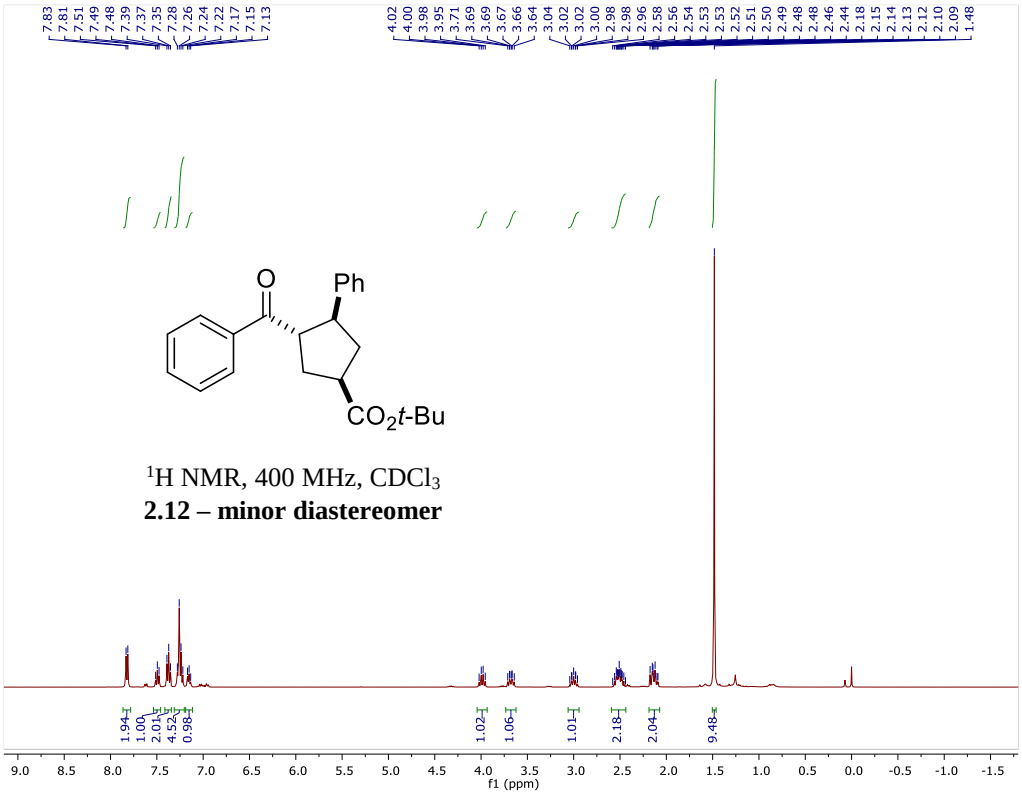

^{1}H NMR, 400 MHz, $CDCl_3$

2.12 – minor diastereomer

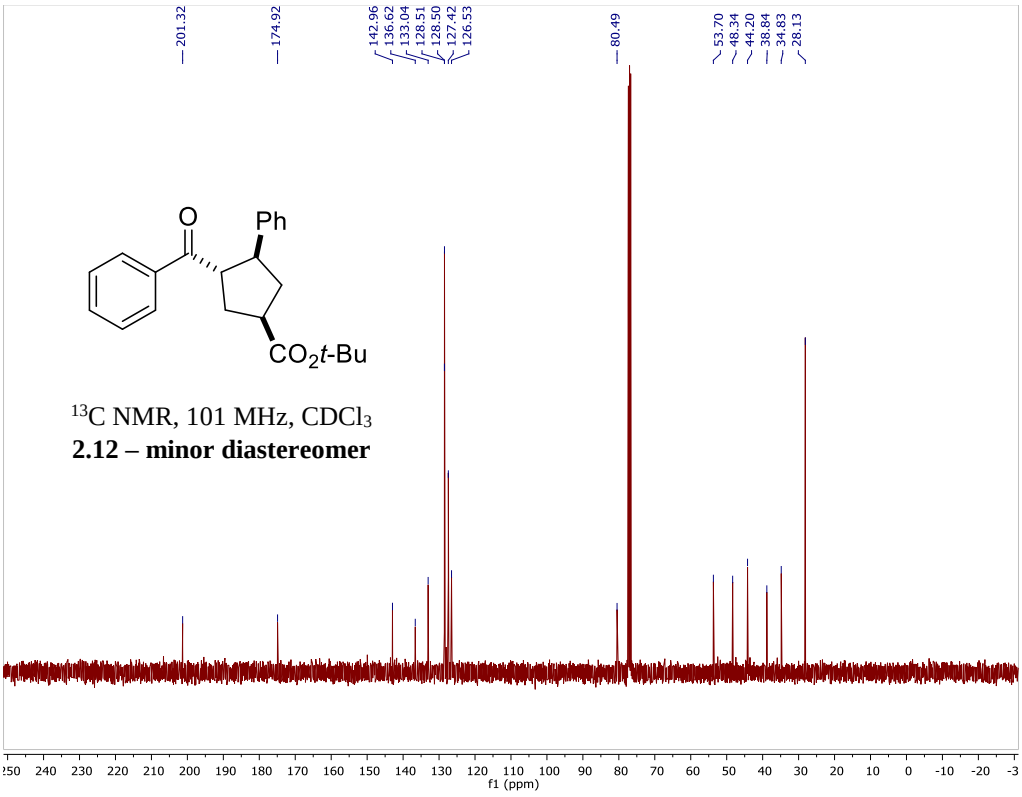

^{13}C NMR, 101 MHz, $CDCl_3$

2.12 – minor diastereomer

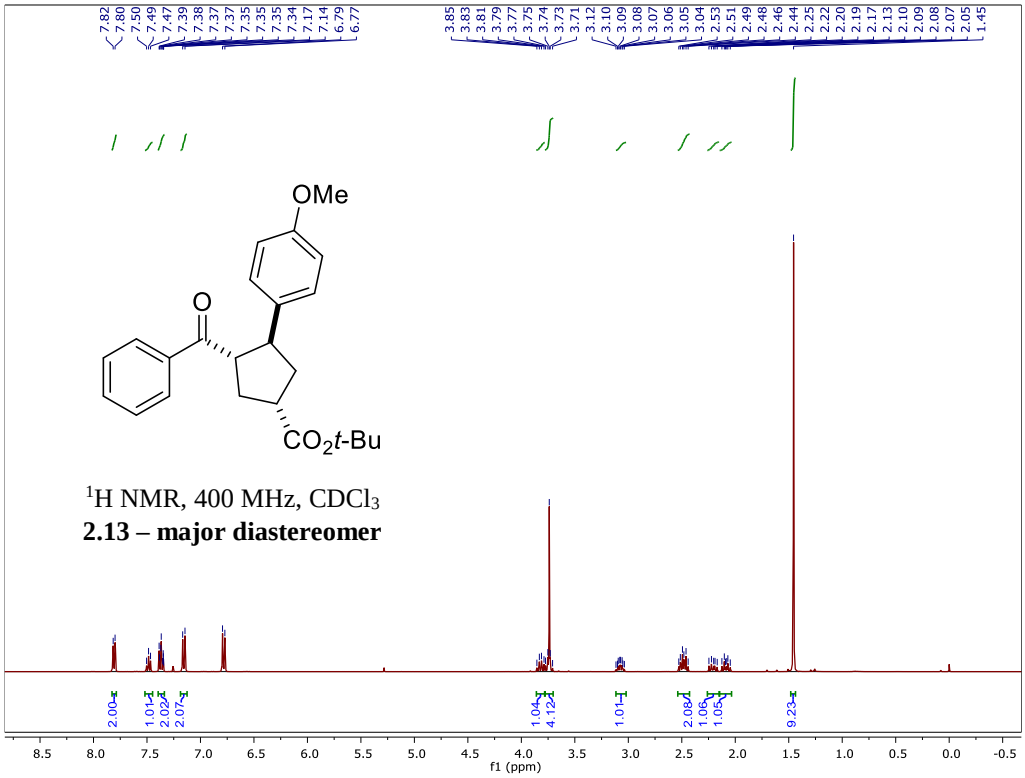
OMe
O
CO2t-Bu
1H NMR, 400 MHz, CDCl3
2.13 – major diastereomer
f1 (ppm)

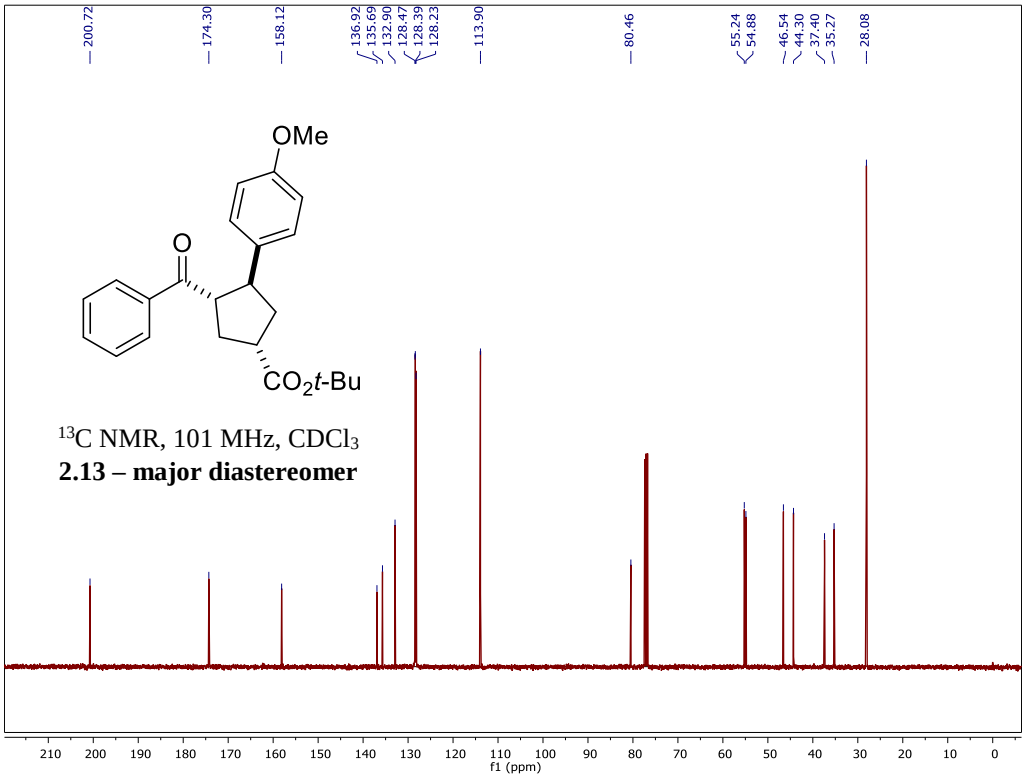
OMe
O
CO2t-Bu
13C NMR, 101 MHz, CDCl3
2.13 – major diastereomer
f1 (ppm)

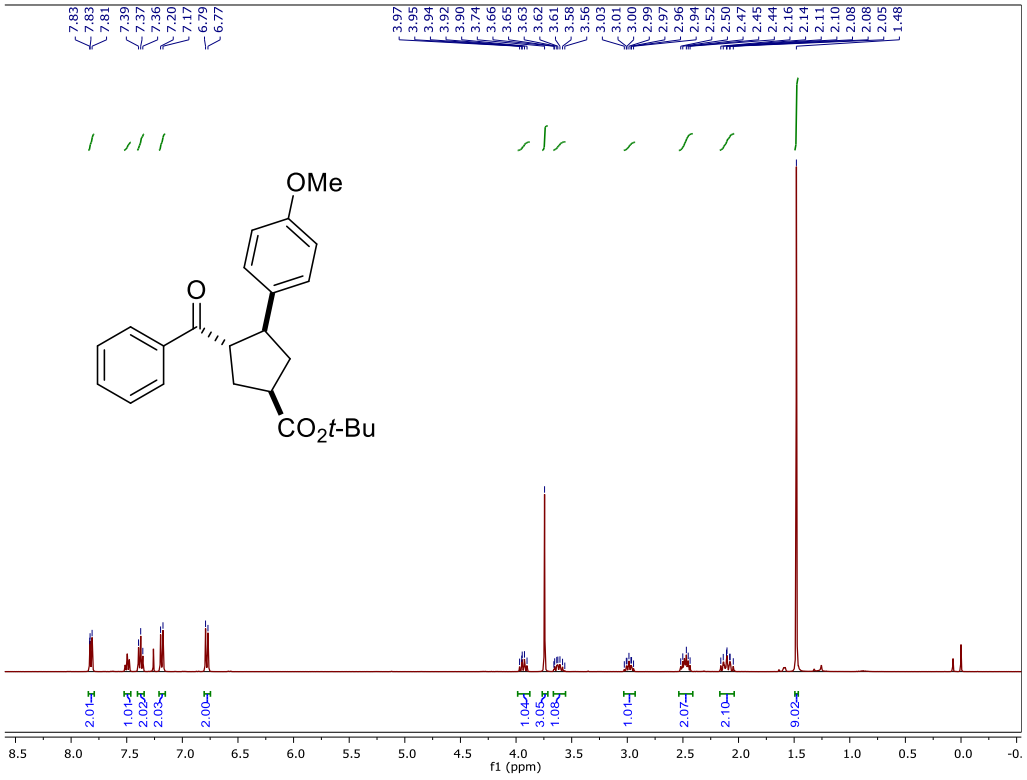
OMe
O
CO2t-Bu
f1 (ppm)

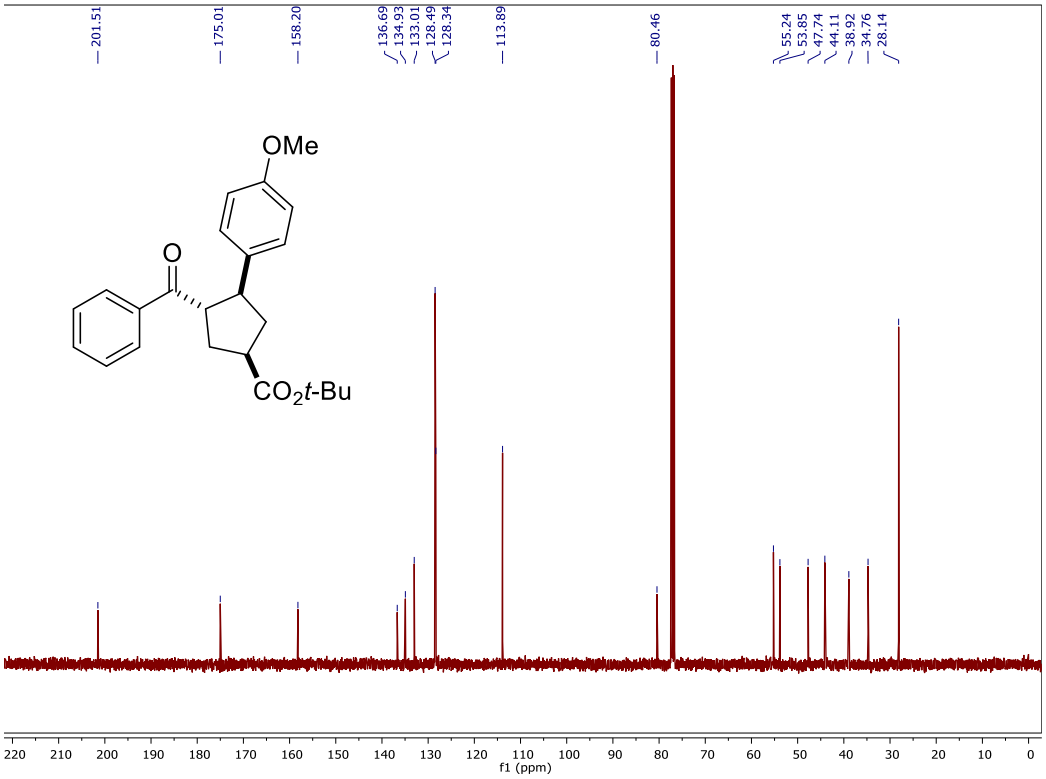
OMe
O
CO2t-Bu
f1 (ppm)

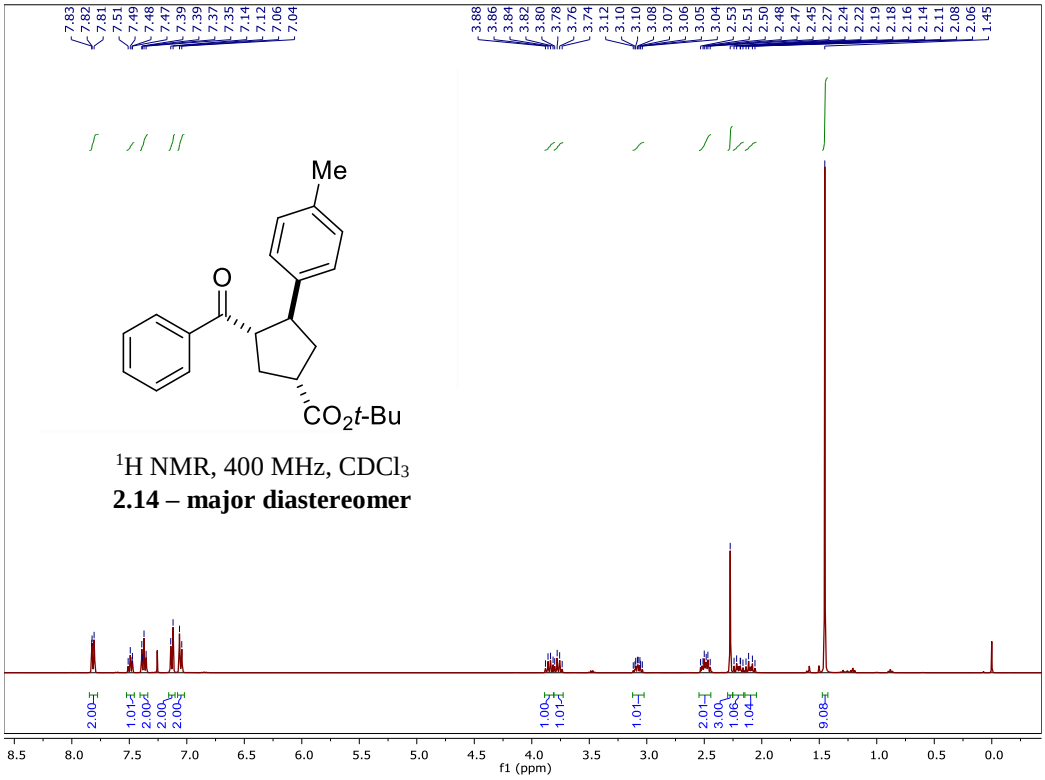

^{1}H NMR, 400 MHz, $CDCl_3$

2.14 – major diastereomer

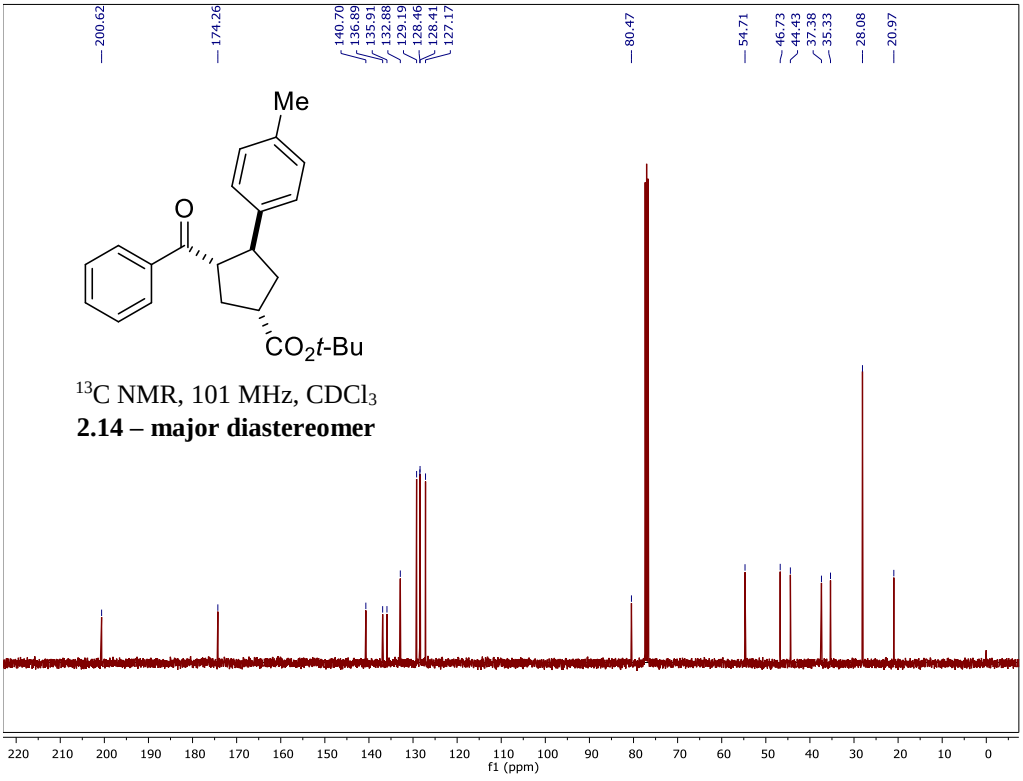

^{13}C NMR, 101 MHz, $CDCl_3$

2.14 – major diastereomer

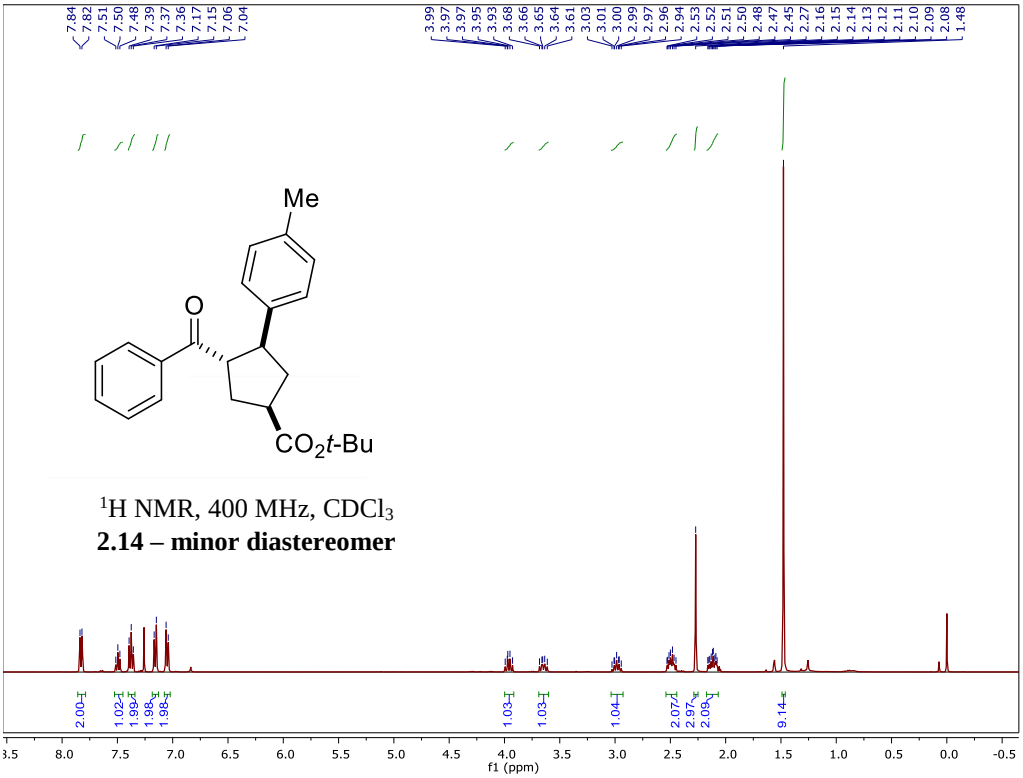
Me
O
CO2t-Bu
1H NMR, 400 MHz, CDCl3
2.14 – minor diastereomer
f1 (ppm)

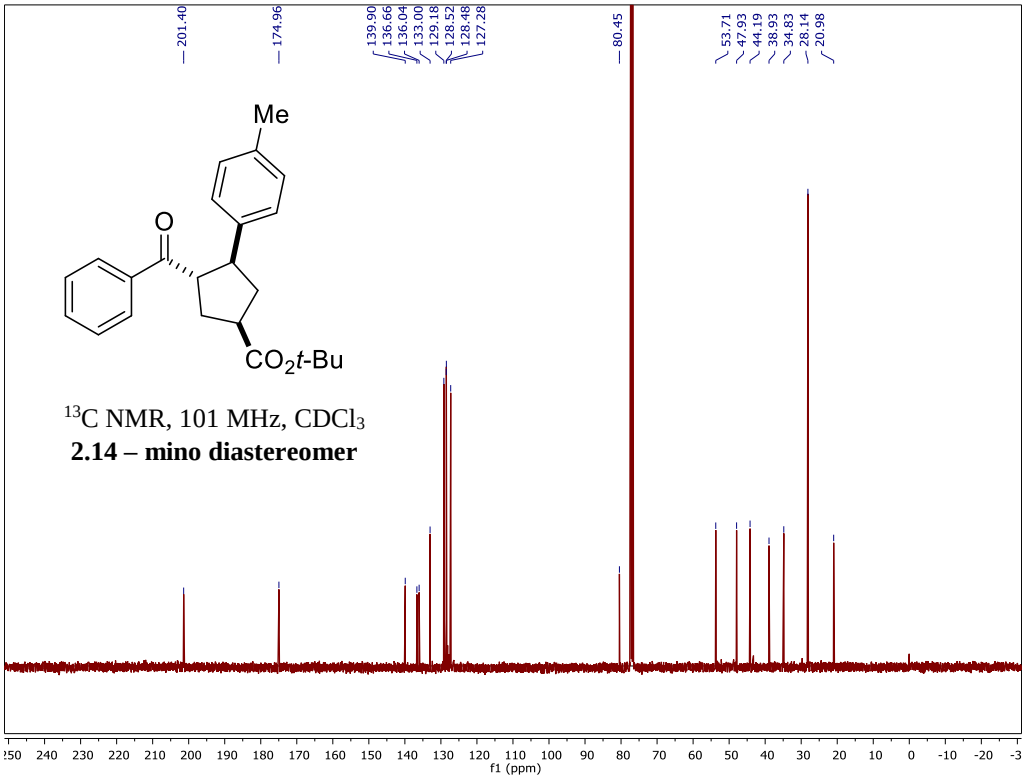
Me
O
CO2t-Bu
13C NMR, 101 MHz, CDCl3
2.14 – mino diastereomer
f1 (ppm)

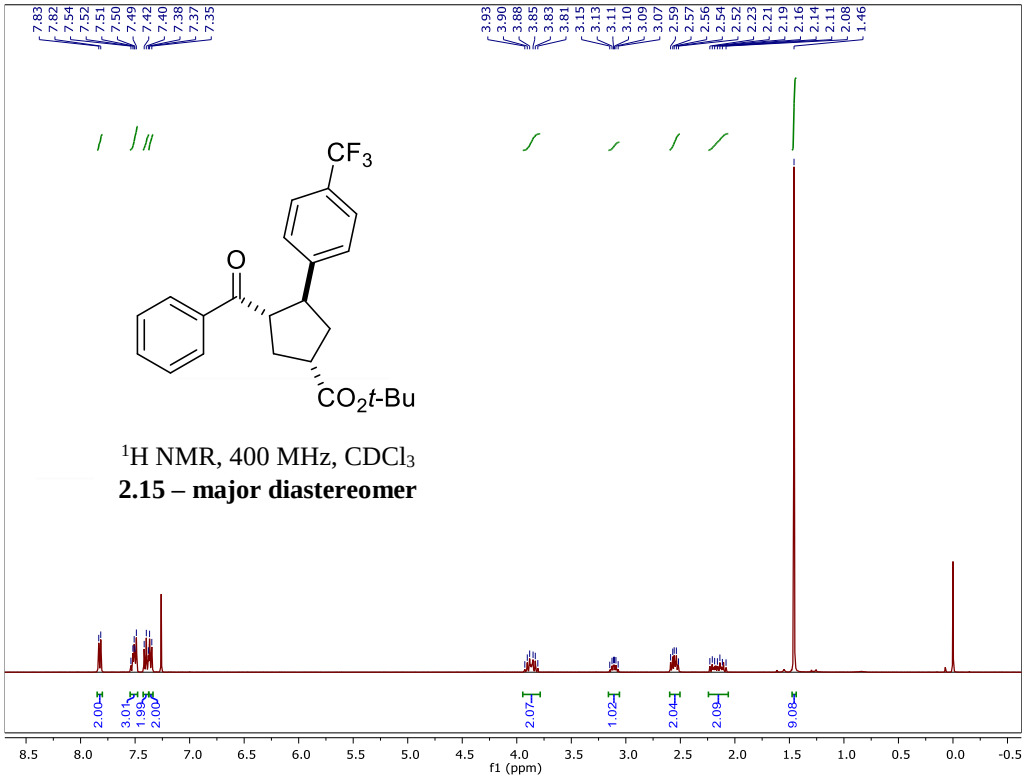

^{1}H NMR, 400 MHz, $CDCl_3$

2.15 – major diastereomer

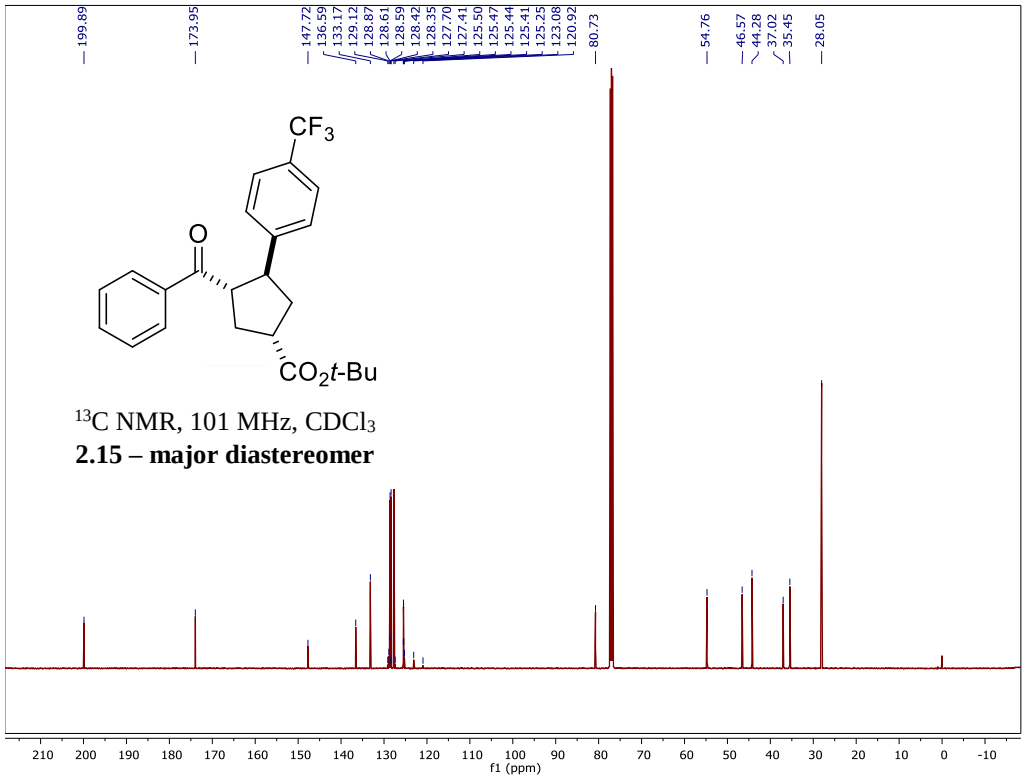

^{13}C NMR, 101 MHz, $CDCl_3$

2.15 – major diastereomer

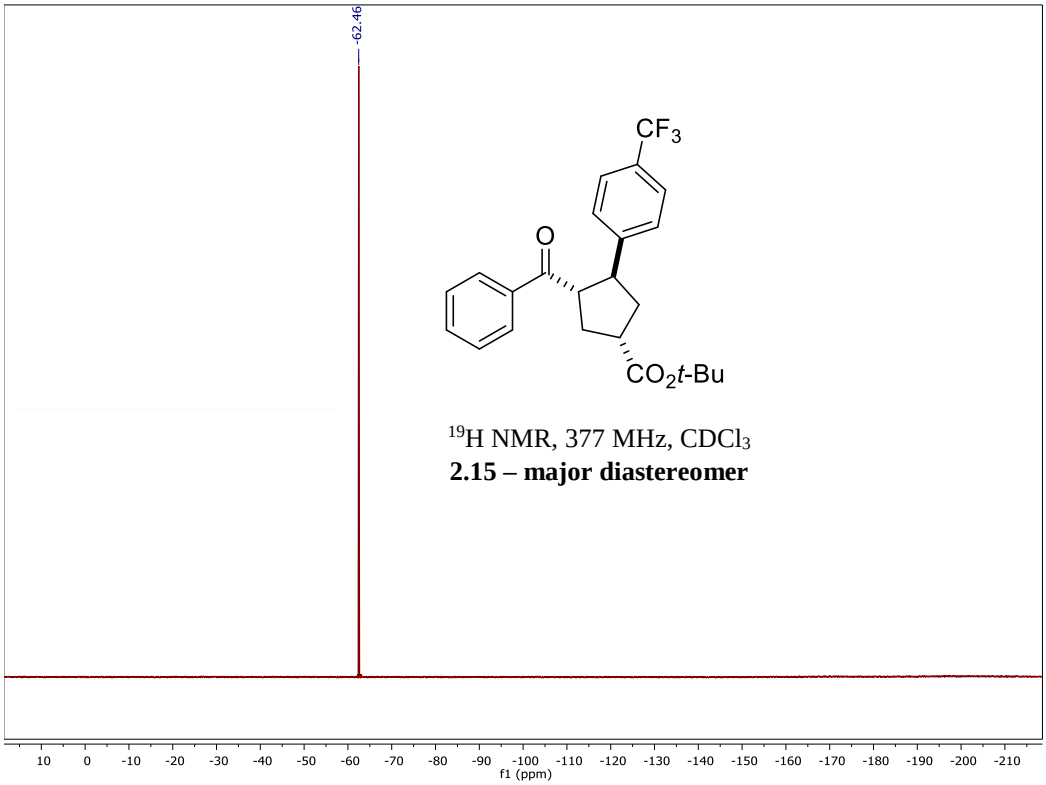

^{19}H NMR, 377 MHz, $CDCl_3$

2.15 – major diastereomer

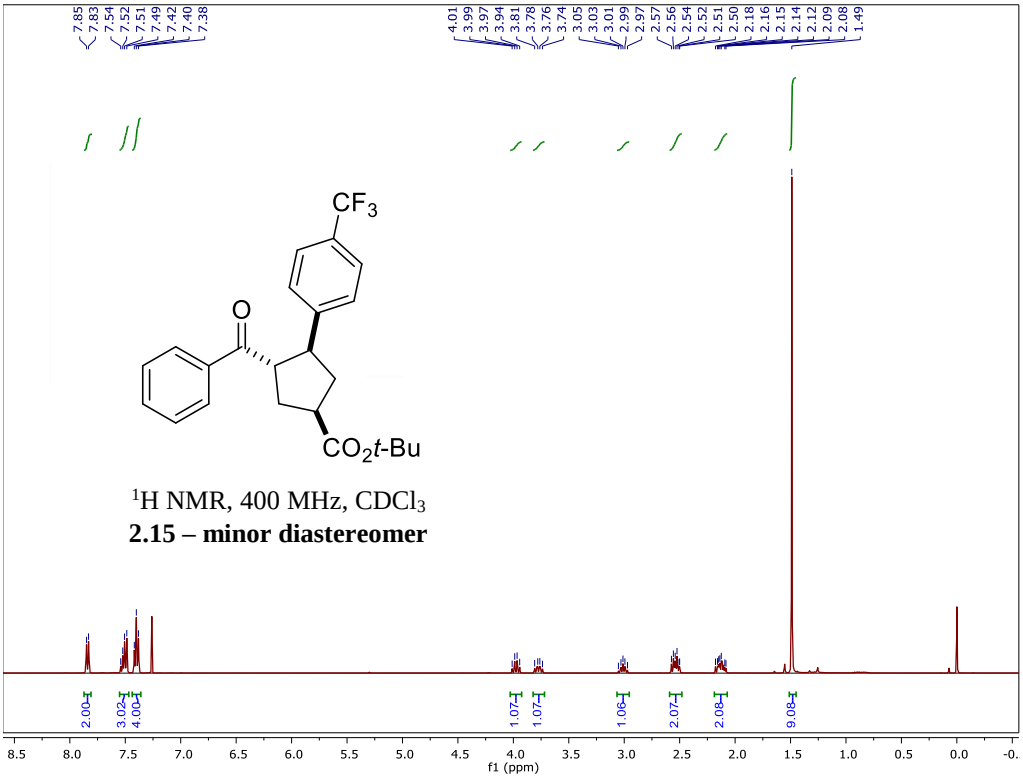

^{1}H NMR, 400 MHz, $CDCl_3$

2.15 – minor diastereomer

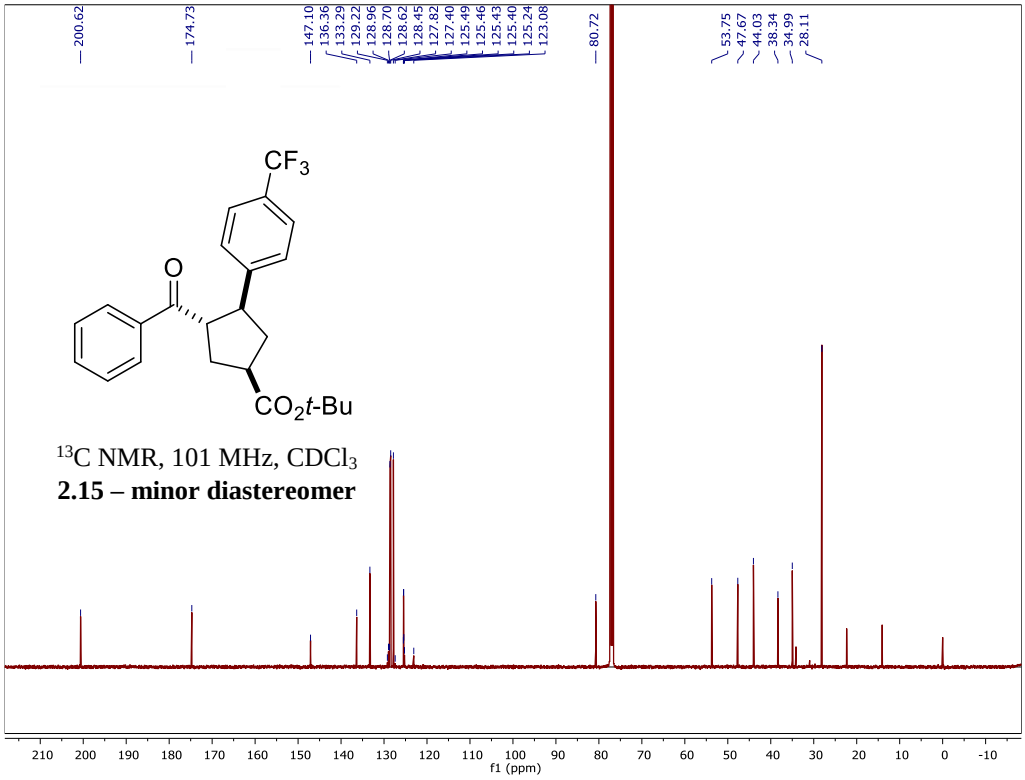

^{13}C NMR, 101 MHz, $CDCl_3$

2.15 – minor diastereomer

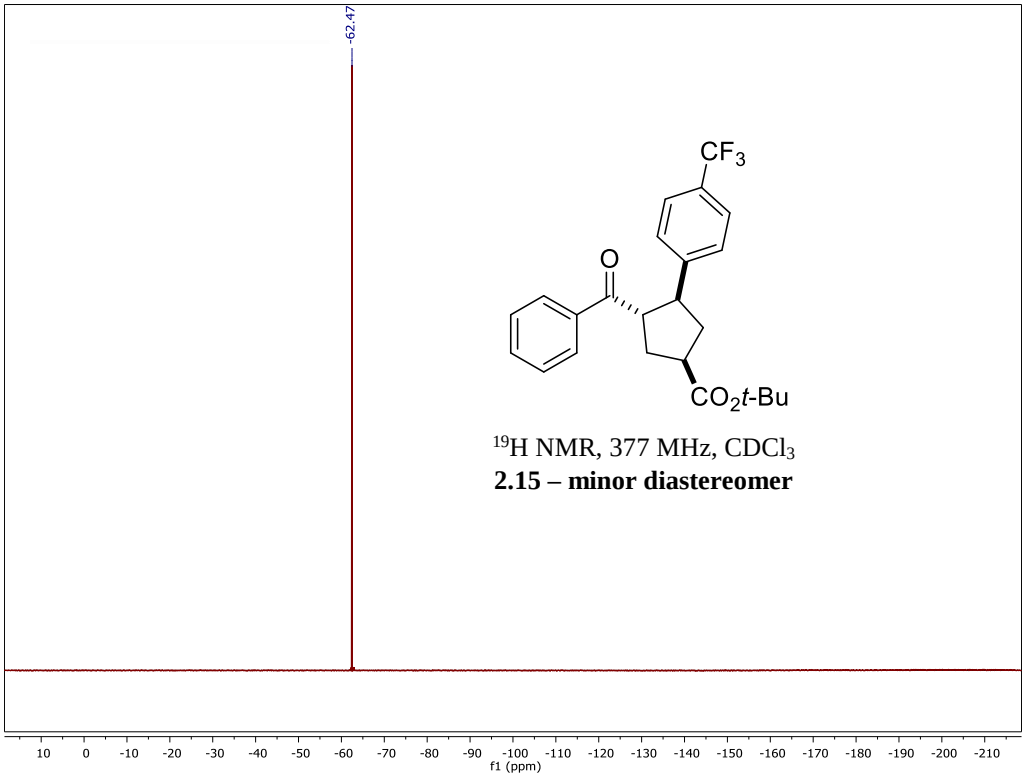

^{19}H NMR, 377 MHz, $CDCl_3$

2.15 – minor diastereomer

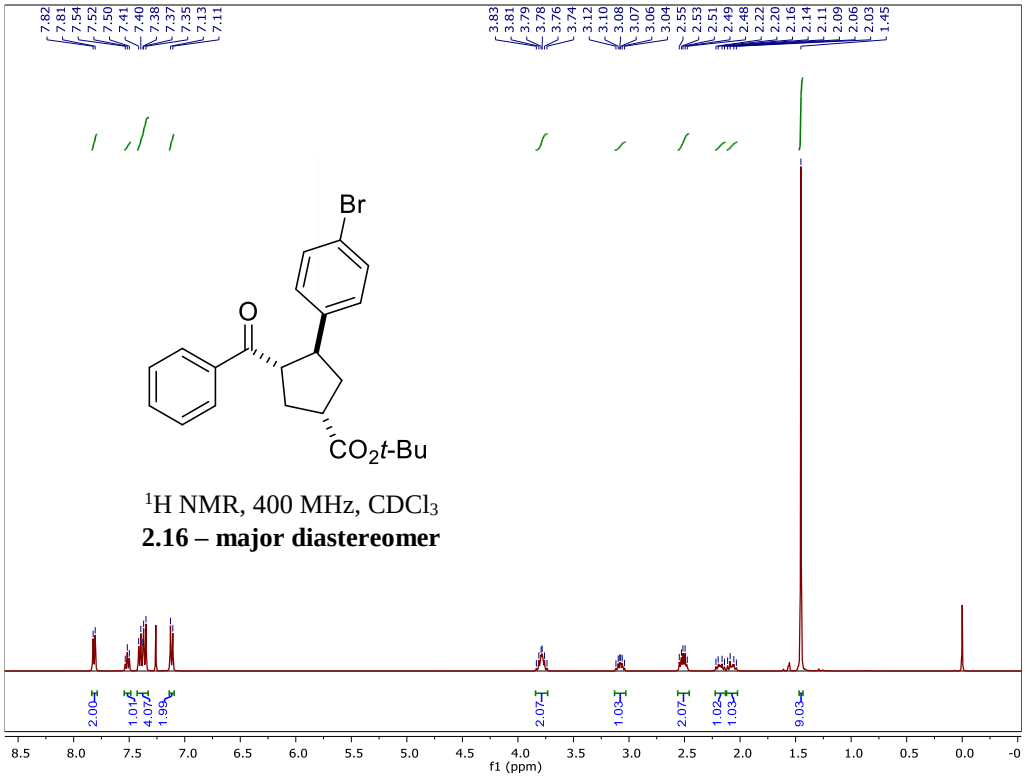

^{1}H NMR, 400 MHz, $CDCl_3$

2.16 – major diastereomer

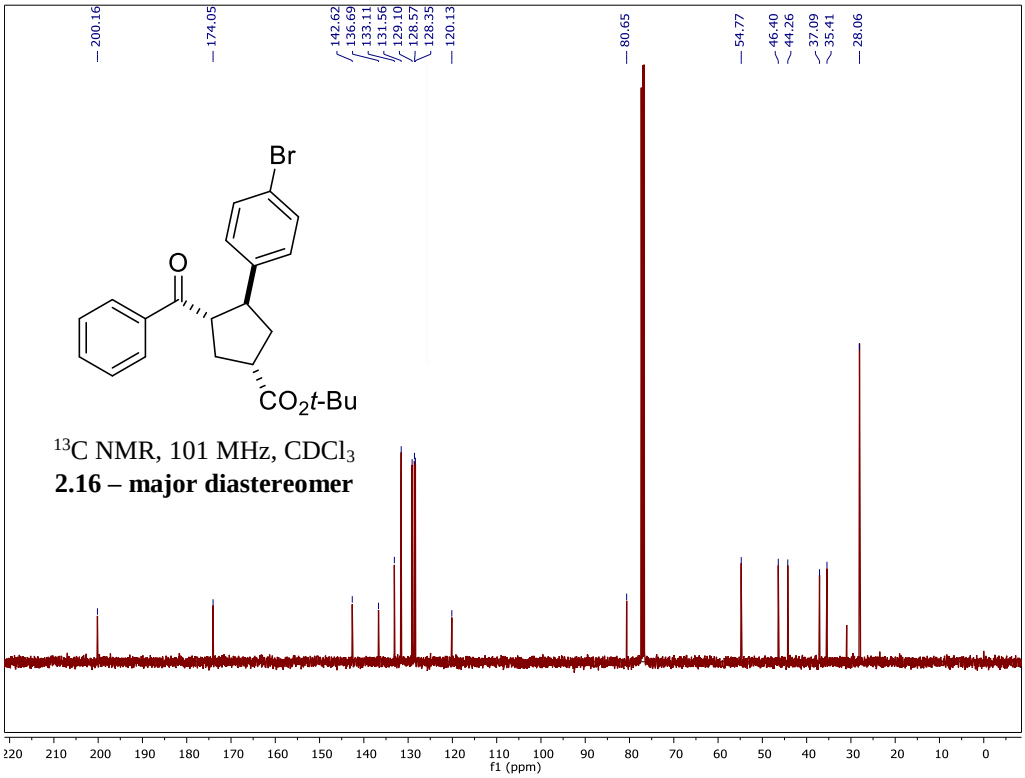

^{13}C NMR, 101 MHz, $CDCl_3$

2.16 – major diastereomer

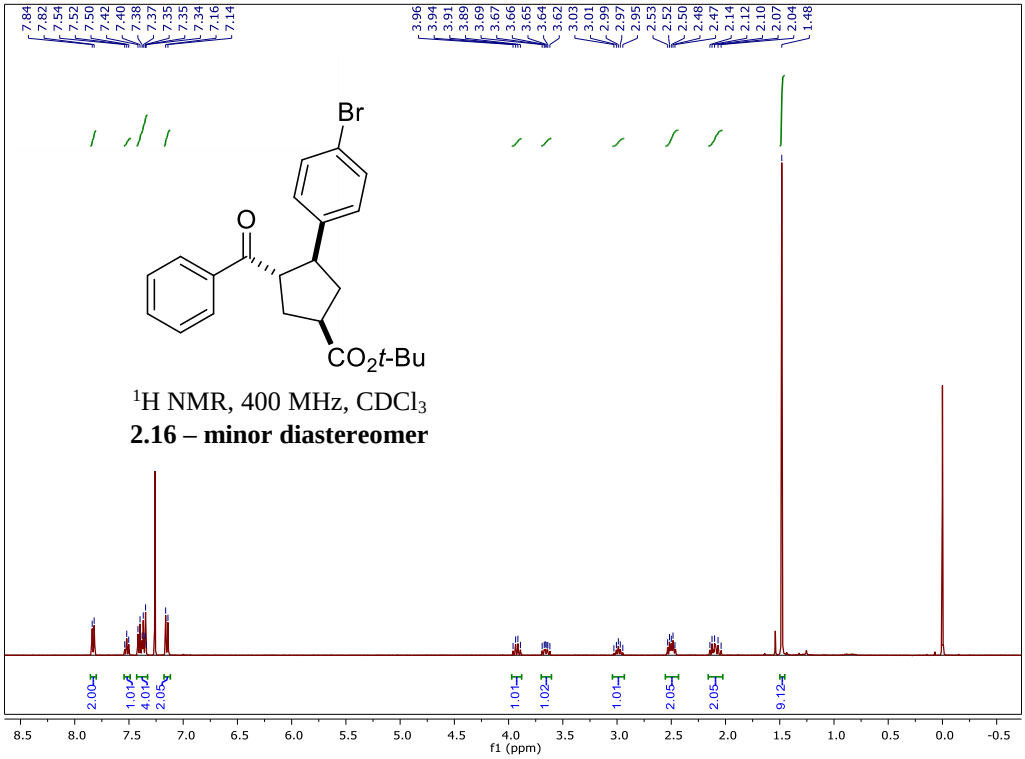

^{1}H NMR, 400 MHz, $CDCl_3$

2.16 – minor diastereomer

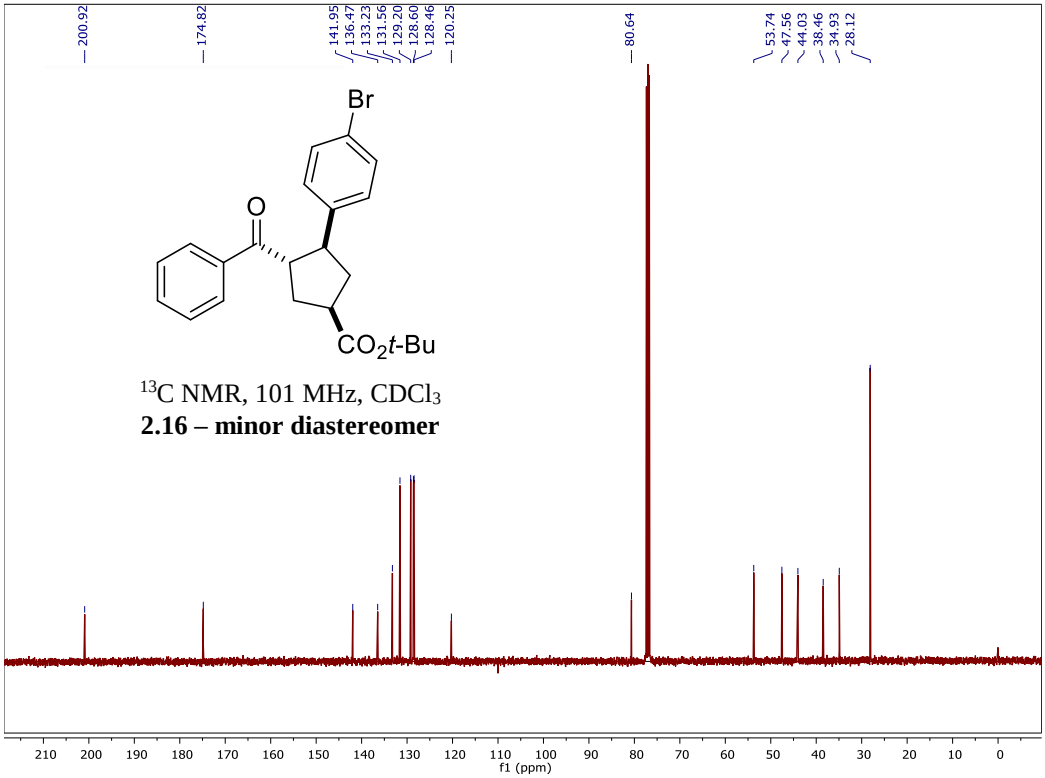

^{13}C NMR, 101 MHz, $CDCl_3$

2.16 – minor diastereomer

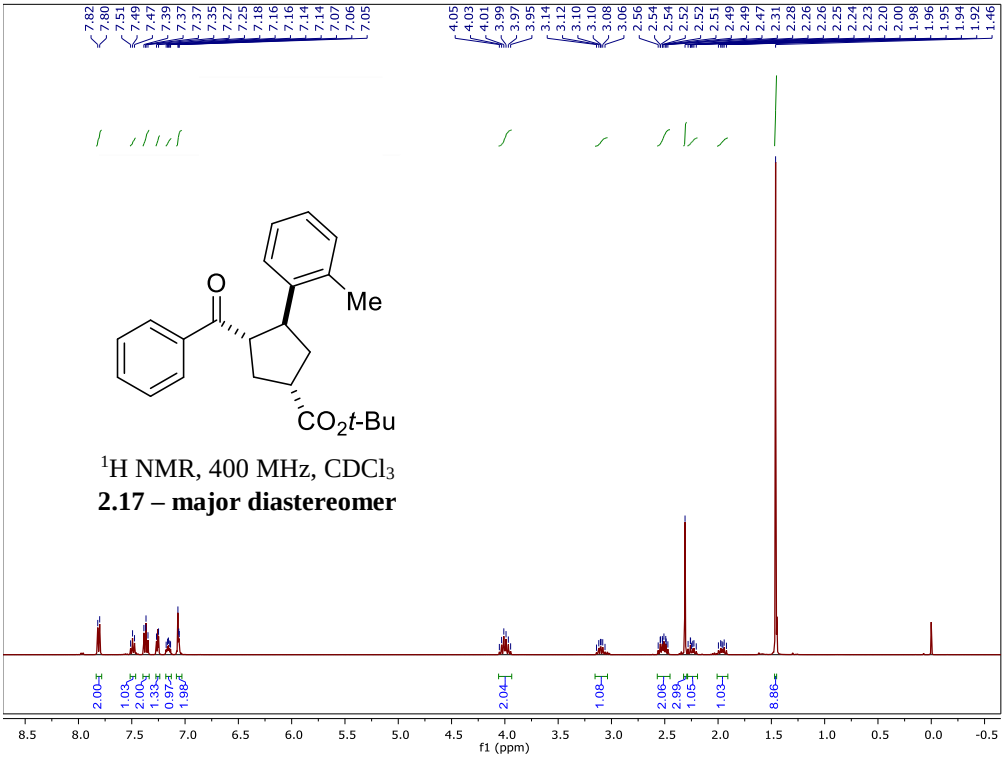

^{1}H NMR, 400 MHz, $CDCl_3$

2.17 – major diastereomer

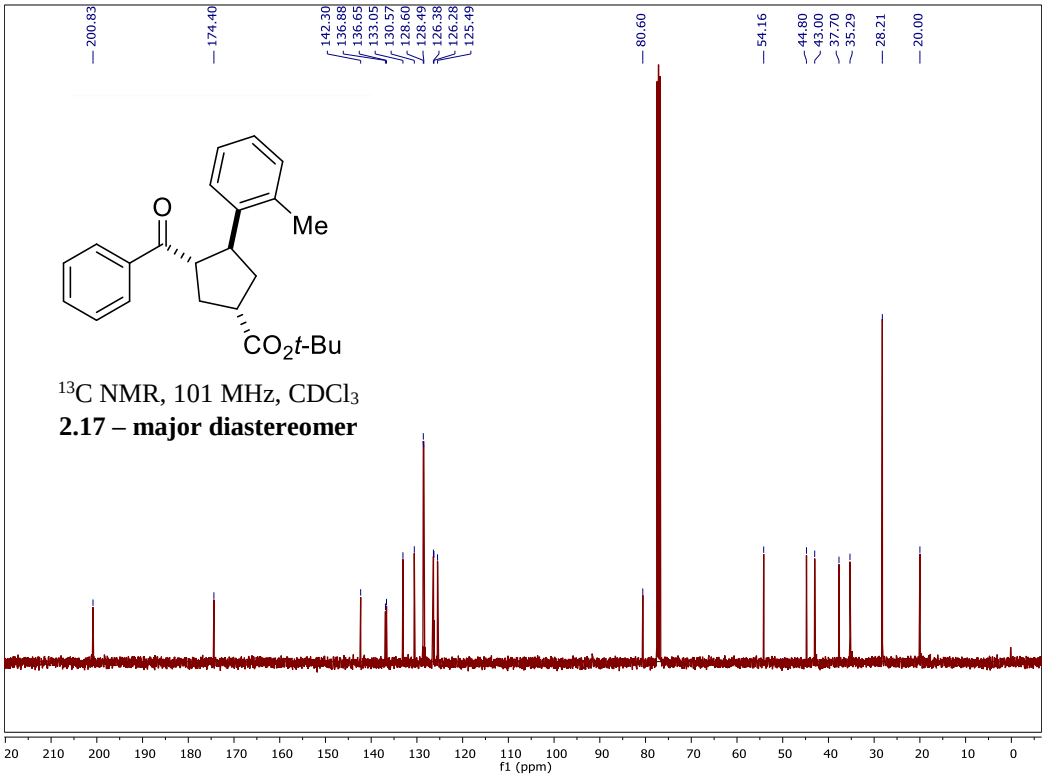

^{13}C NMR, 101 MHz, $CDCl_3$

2.17 – major diastereomer

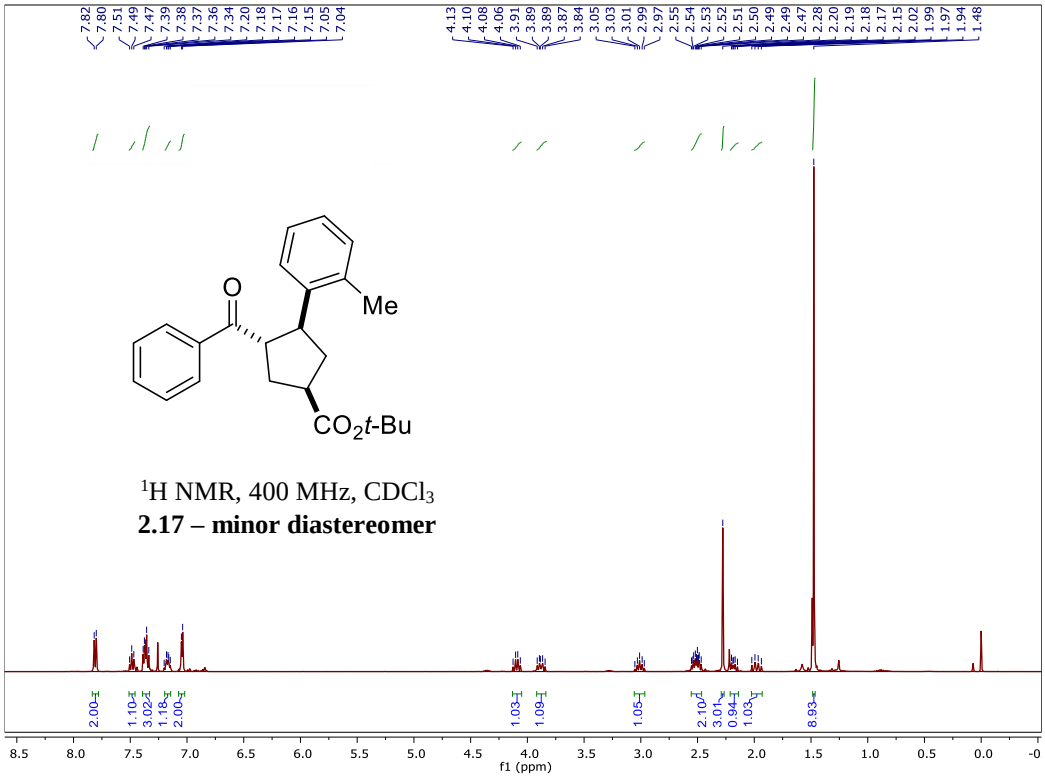

^{1}H NMR, 400 MHz, $CDCl_3$

2.17 – minor diastereomer

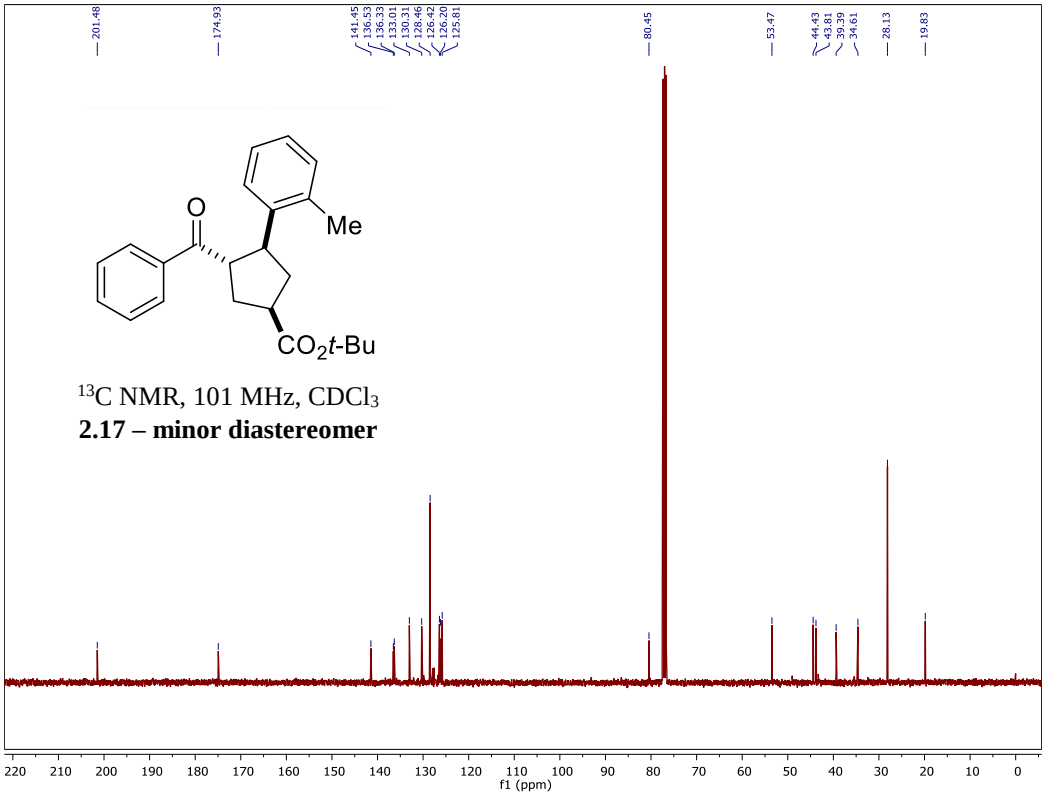

^{13}C NMR, 101 MHz, $CDCl_3$

2.17 – minor diastereomer

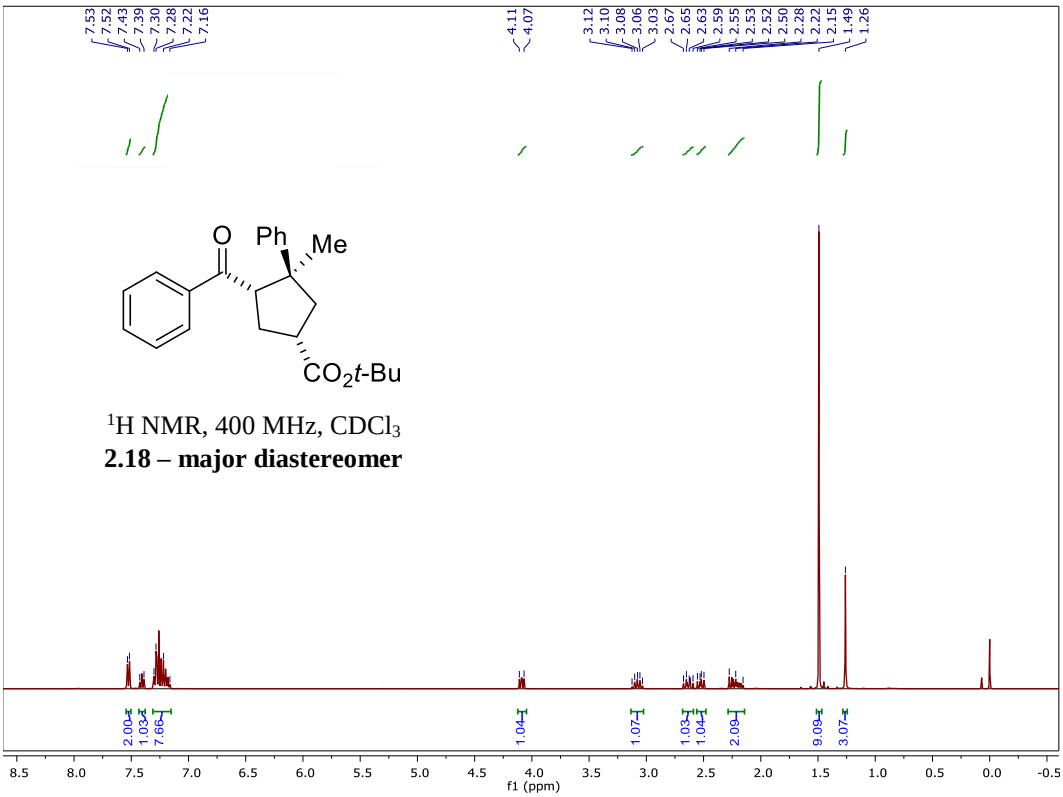

^{1}H NMR, 400 MHz, $CDCl_3$

2.18 – major diastereomer

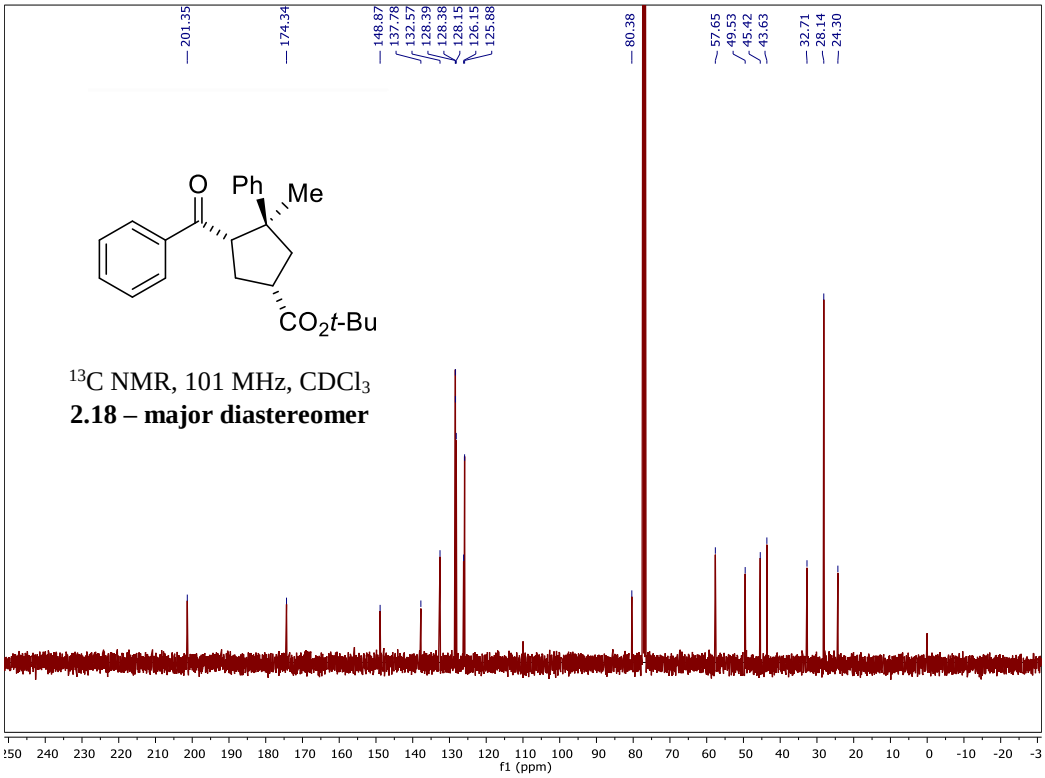

^{13}C NMR, 101 MHz, $CDCl_3$

2.18 – major diastereomer

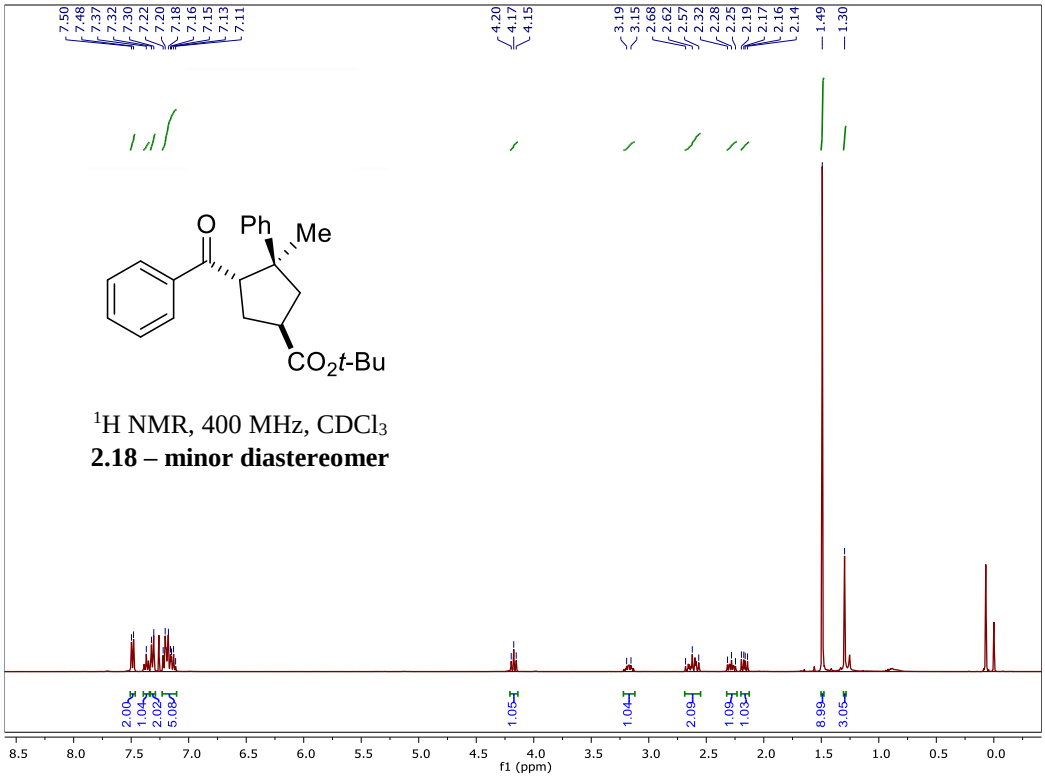

^{1}H NMR, 400 MHz, $CDCl_3$

2.18 – minor diastereomer

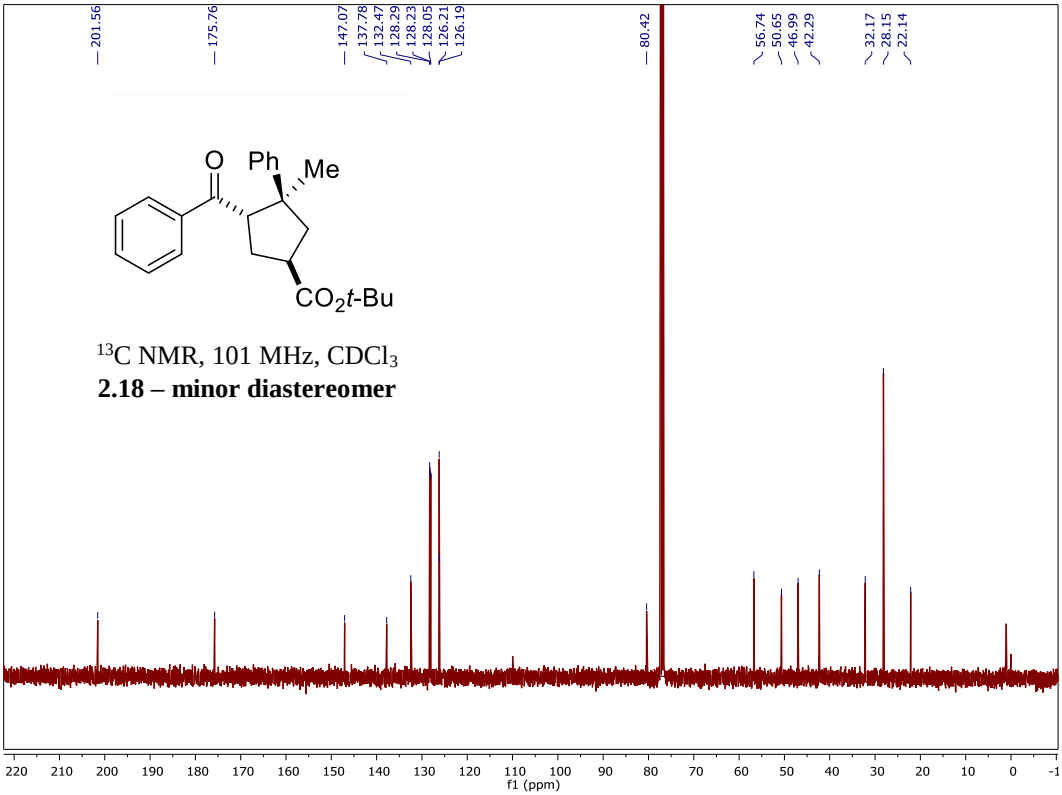

^{13}C NMR, 101 MHz, $CDCl_3$

2.18 – minor diastereomer

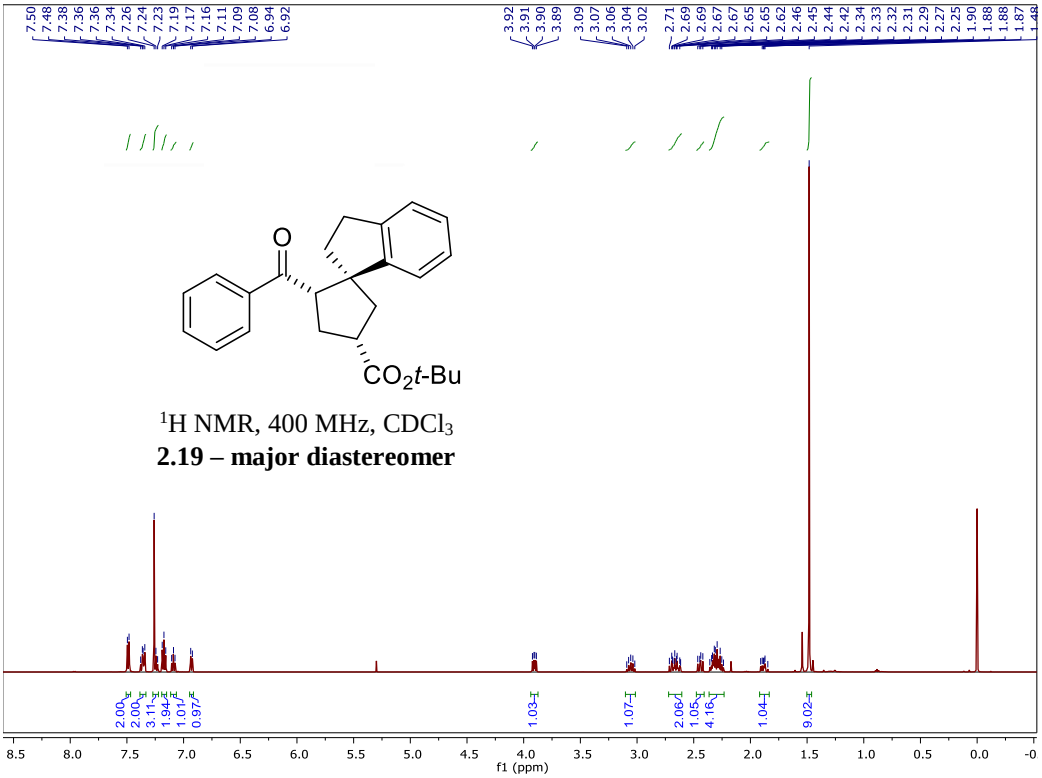

^{1}H NMR, 400 MHz, $CDCl_3$

2.19 – major diastereomer

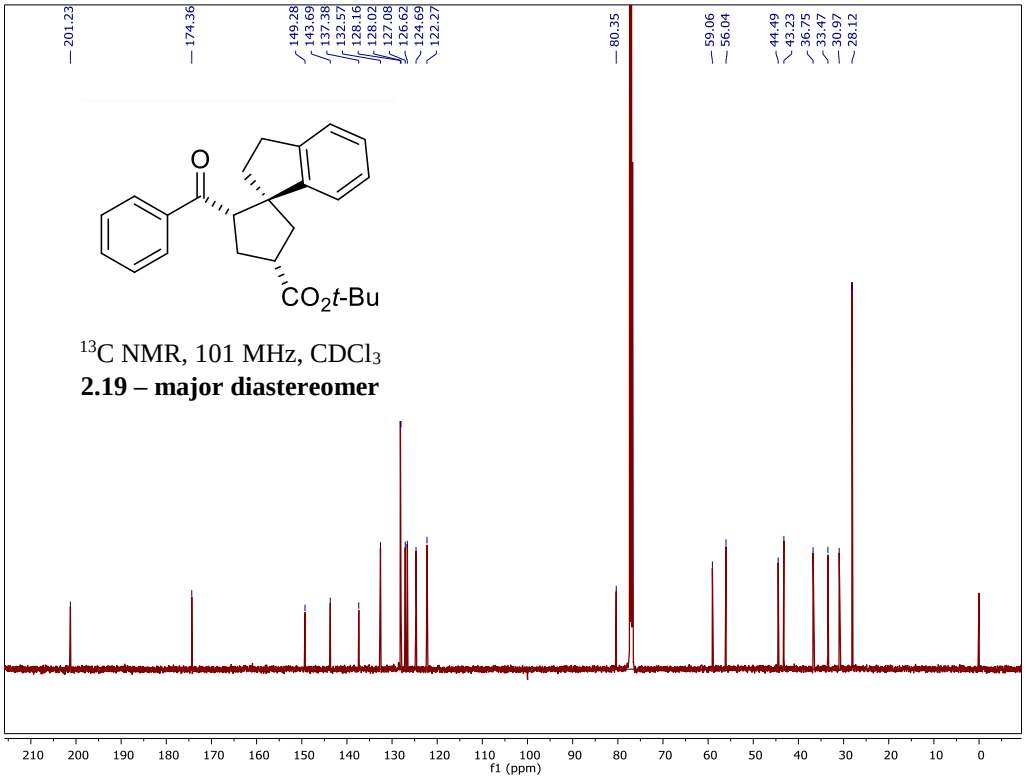

^{13}C NMR, 101 MHz, $CDCl_3$

2.19 – major diastereomer

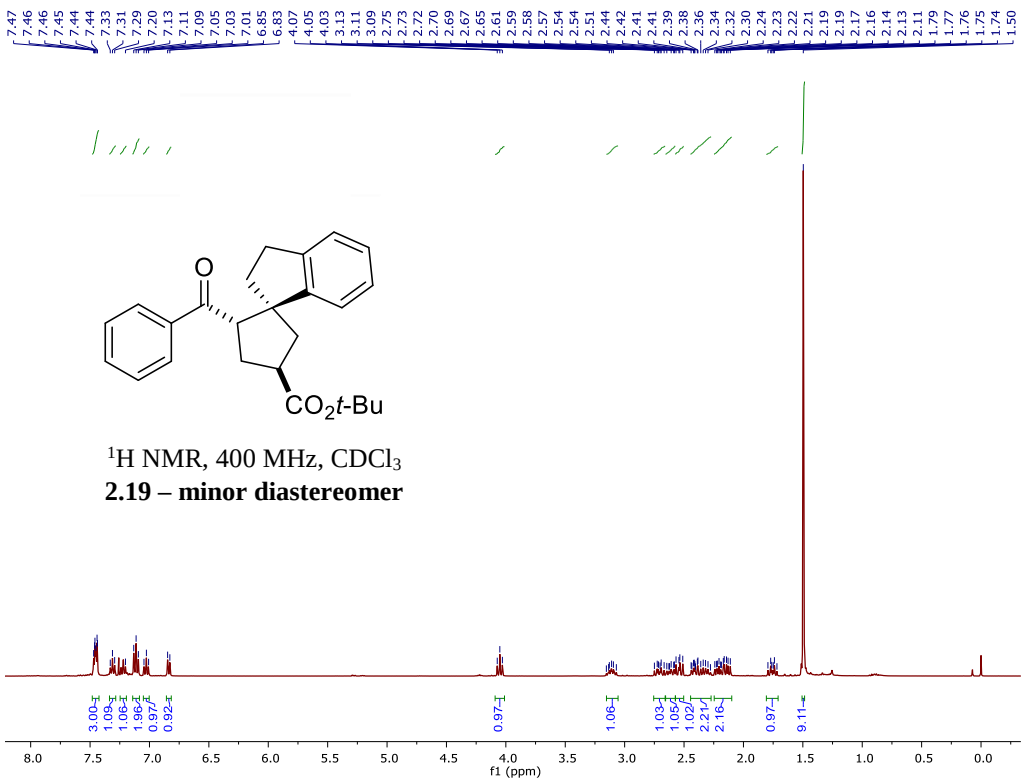

^{1}H NMR, 400 MHz, $CDCl_3$

2.19 – minor diastereomer

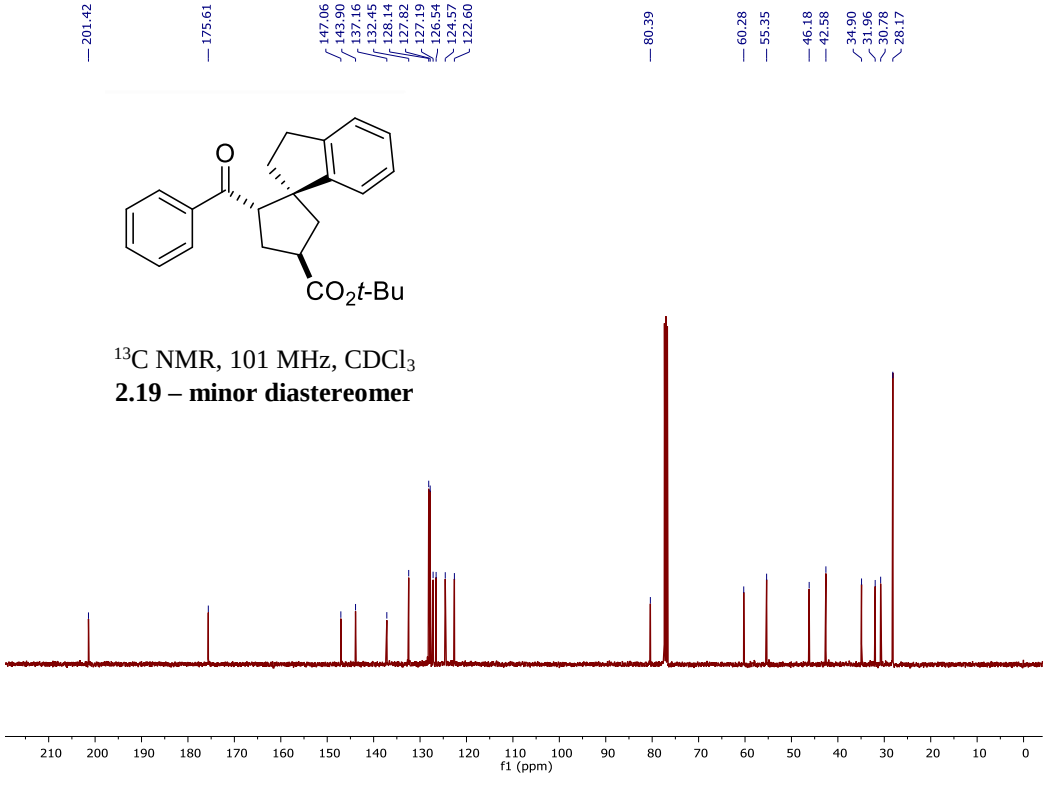

^{13}C NMR, 101 MHz, $CDCl_3$

2.19 – minor diastereomer

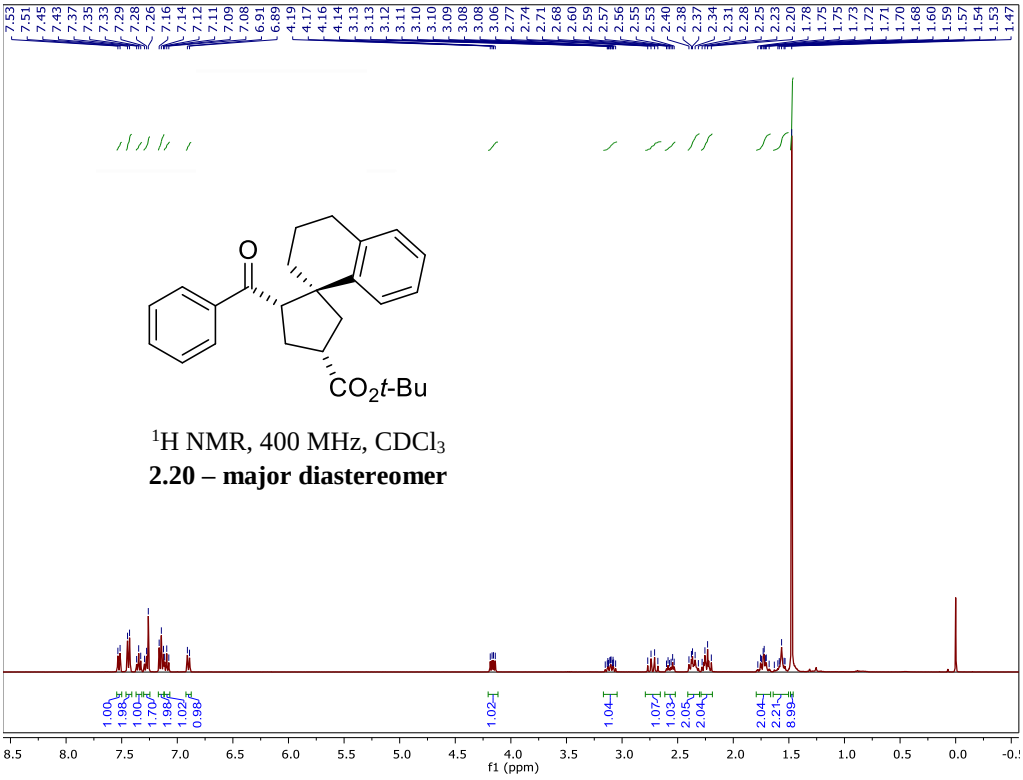

^{1}H NMR, 400 MHz, $CDCl_3$

2.20 – major diastereomer

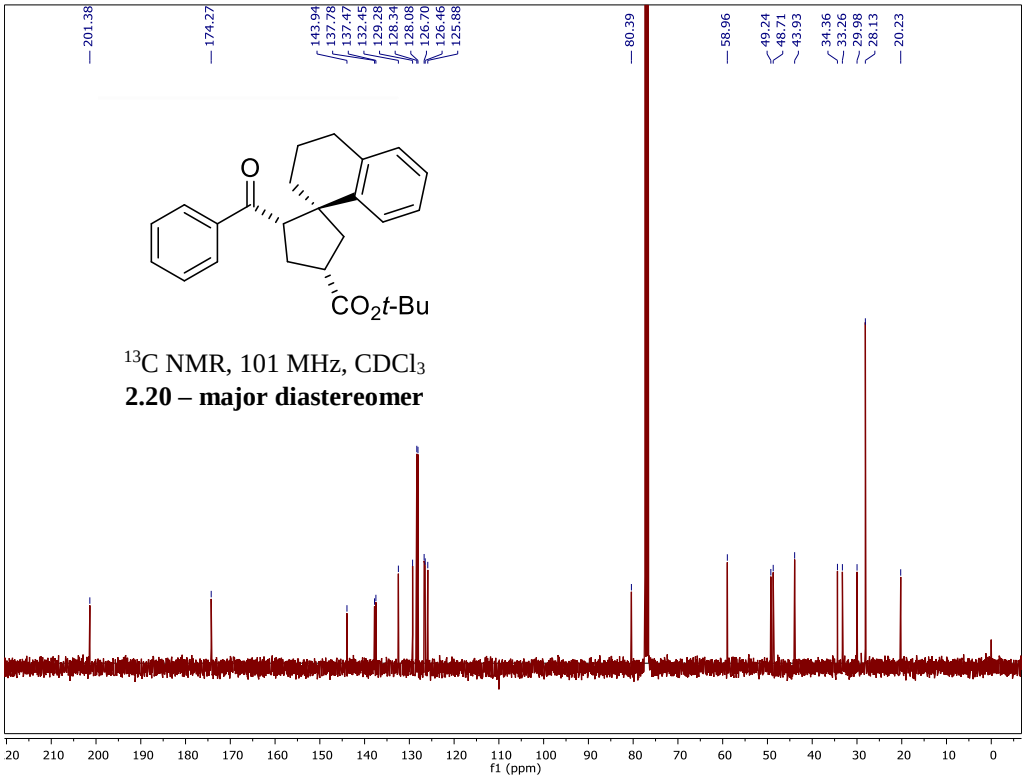

^{13}C NMR, 101 MHz, $CDCl_3$

2.20 – major diastereomer

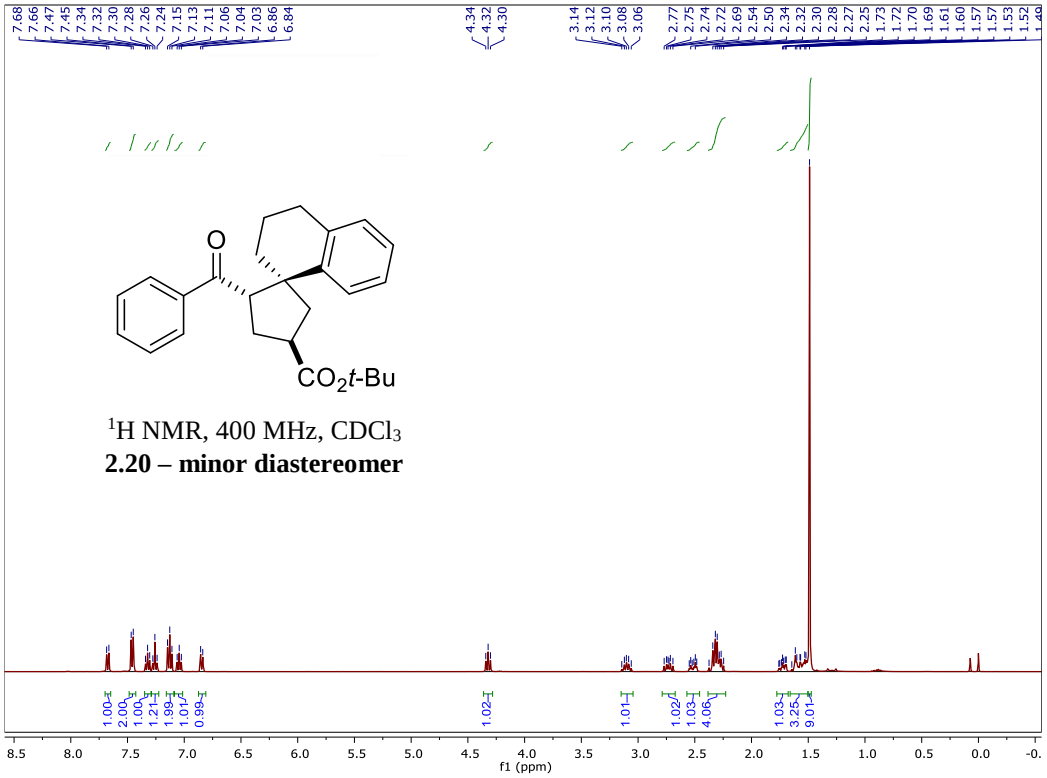

^{1}H NMR, 400 MHz, $CDCl_3$

2.20 – minor diastereomer

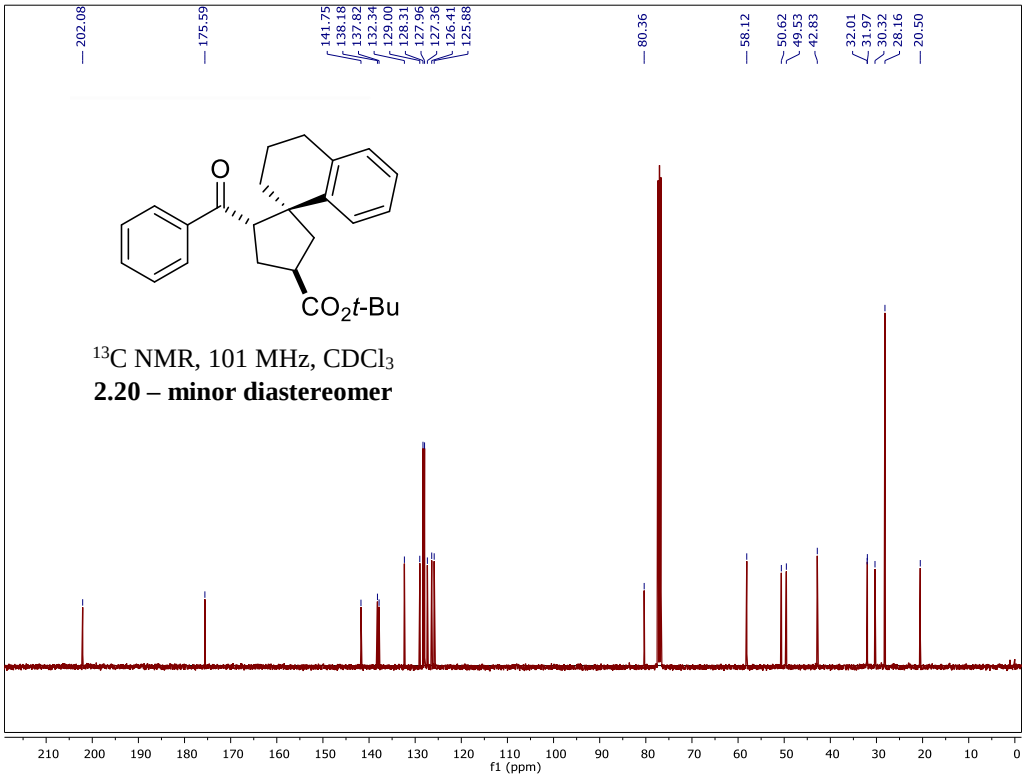

^{13}C NMR, 101 MHz, $CDCl_3$

2.20 – minor diastereomer

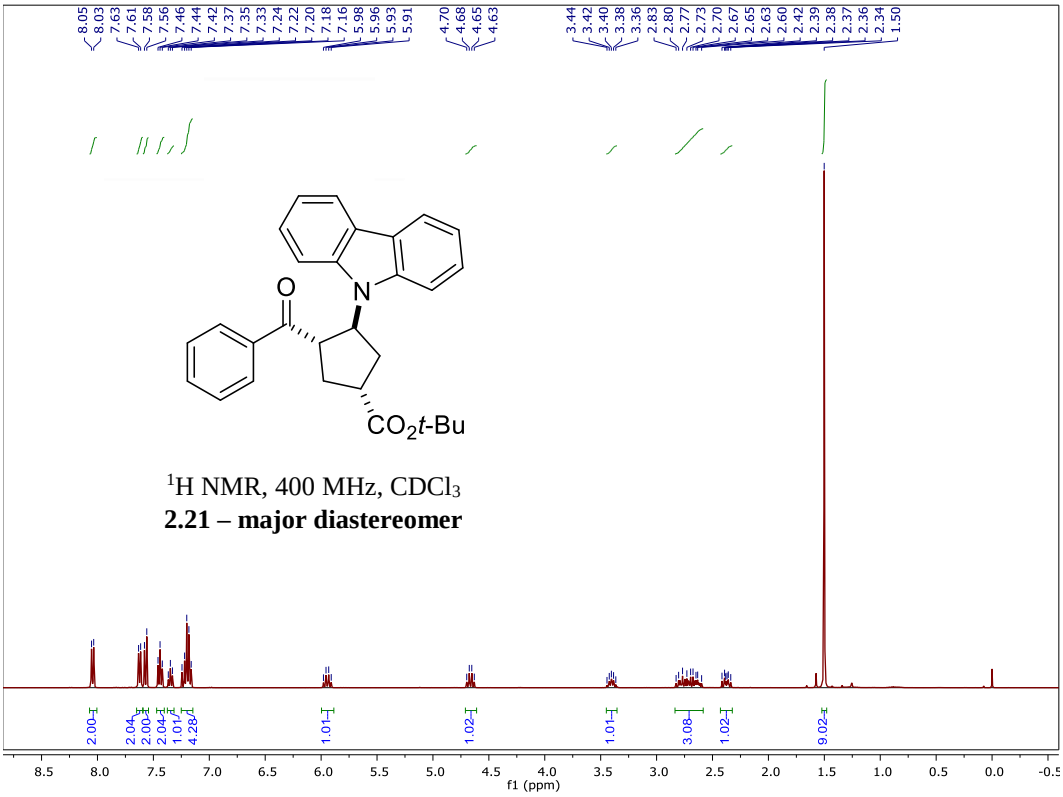

^{1}H NMR, 400 MHz, $CDCl_3$

2.21 – major diastereomer

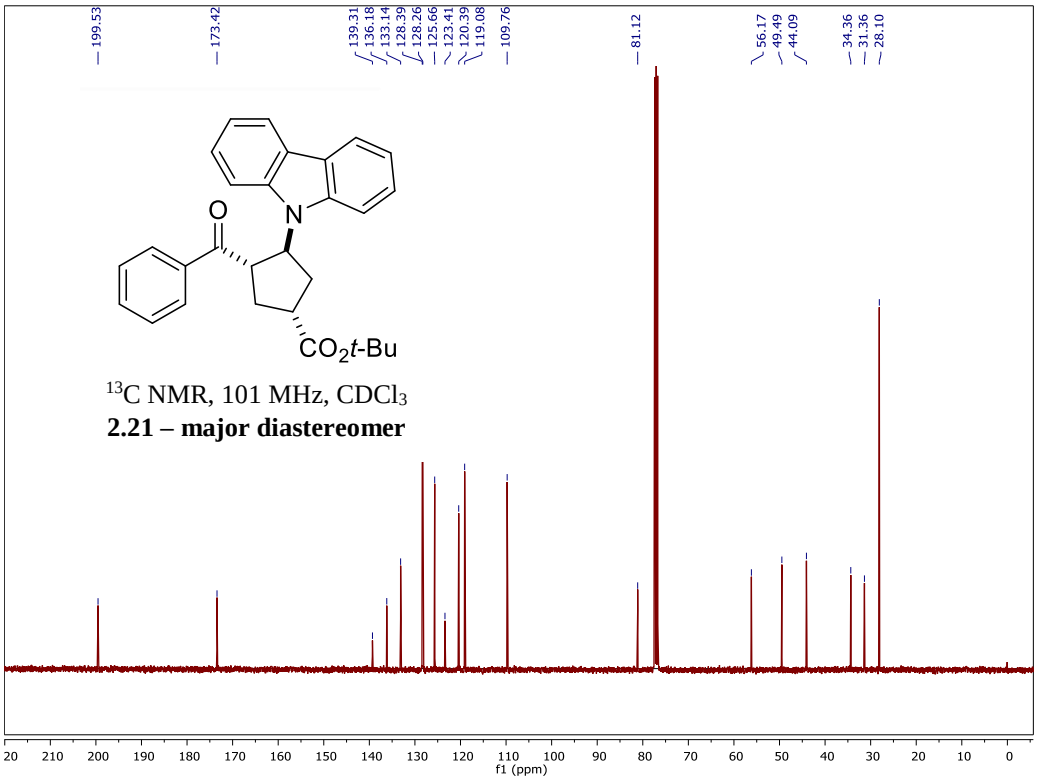

^{13}C NMR, 101 MHz, $CDCl_3$

2.21 – major diastereomer

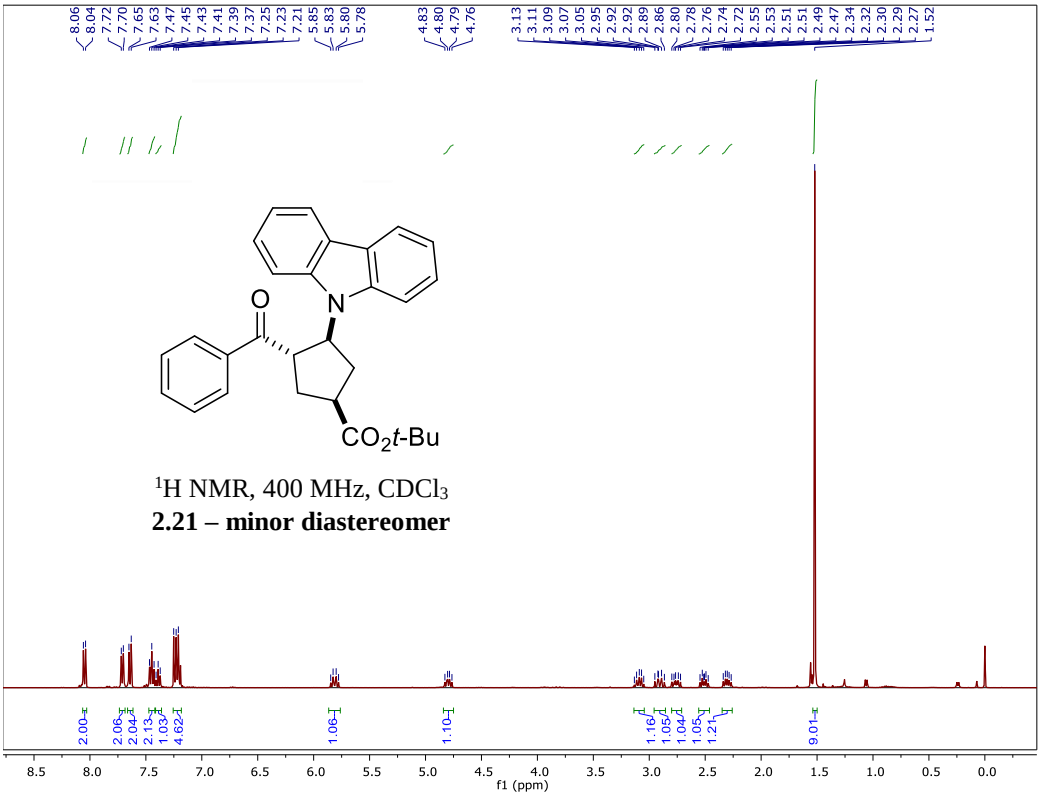

^{1}H NMR, 400 MHz, $CDCl_3$
2.21 – minor diastereomer

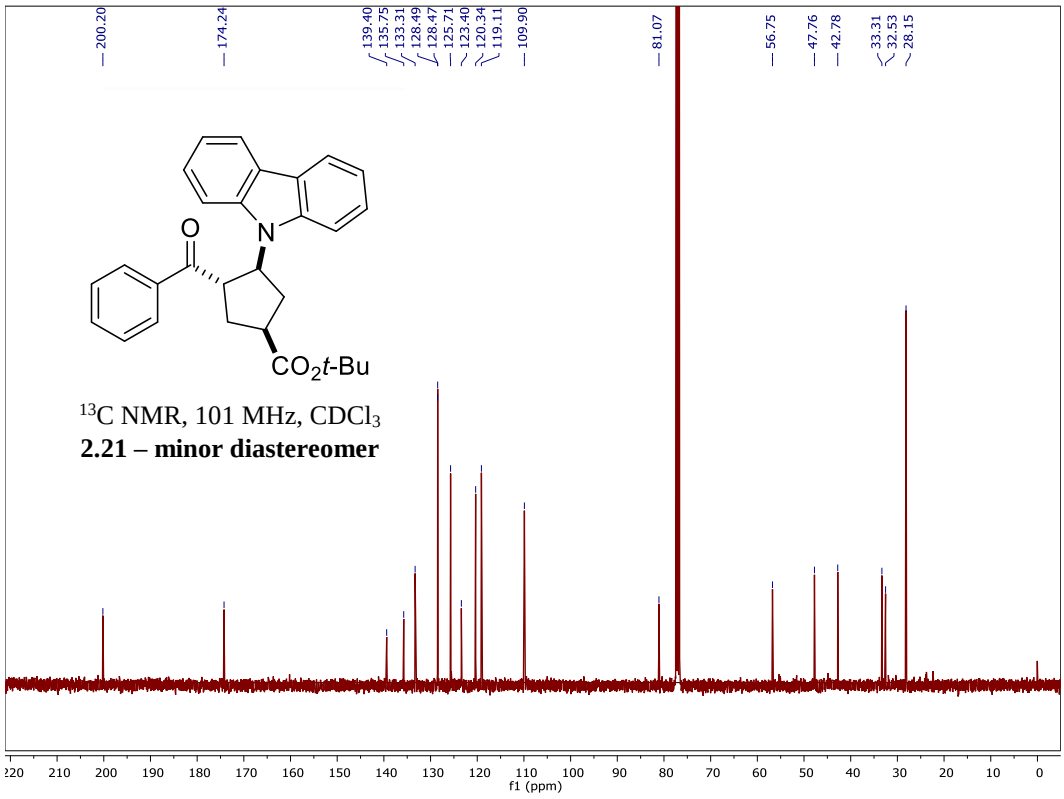

^{13}C NMR, 101 MHz, $CDCl_3$
2.21 – minor diastereomer

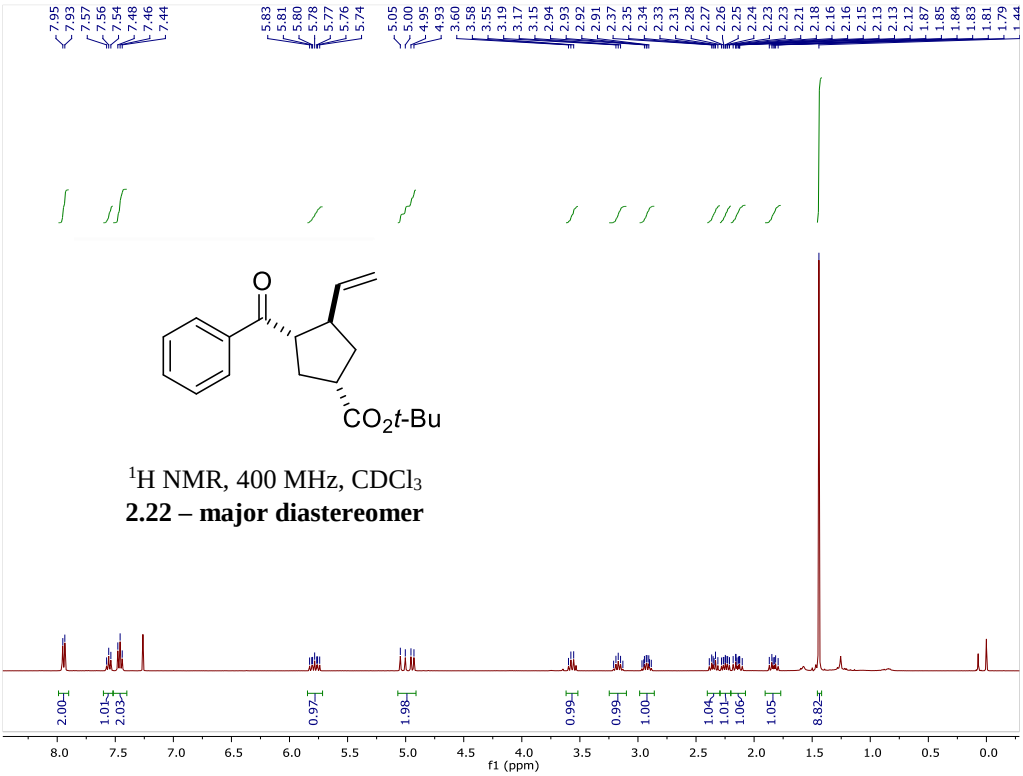

^{1}H NMR, 400 MHz, $CDCl_3$
2.22 – major diastereomer

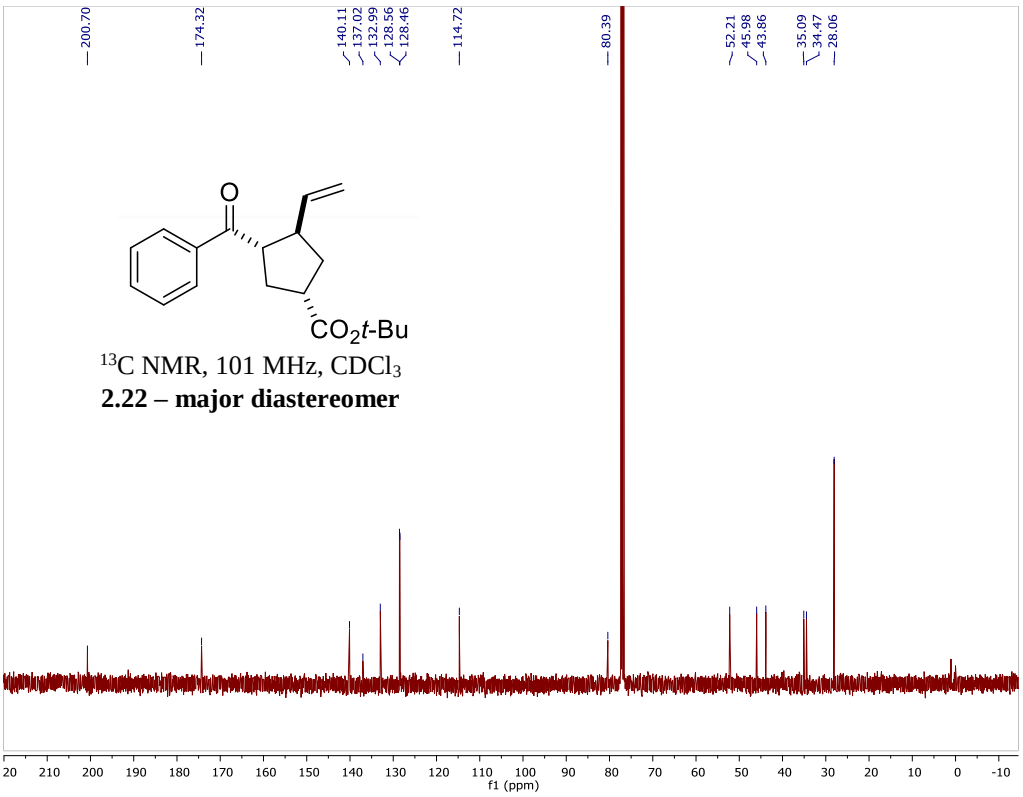

^{13}C NMR, 101 MHz, $CDCl_3$
2.22 – major diastereomer

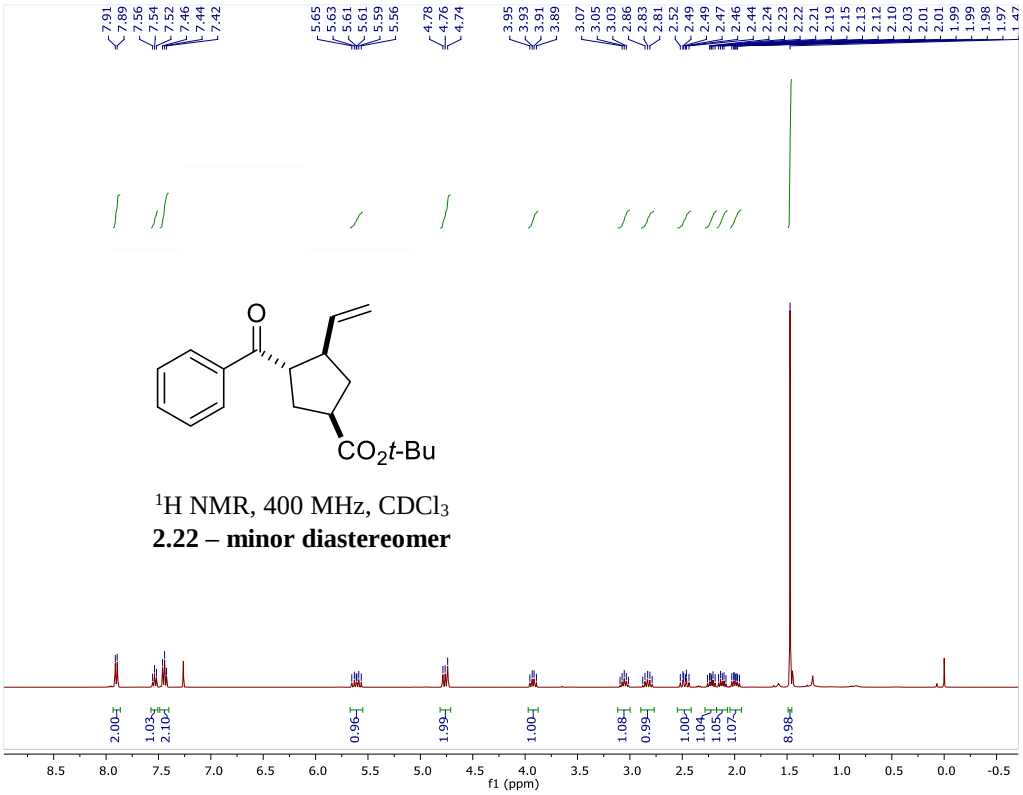

^{1}H NMR, 400 MHz, $CDCl_3$
2.22 – minor diastereomer

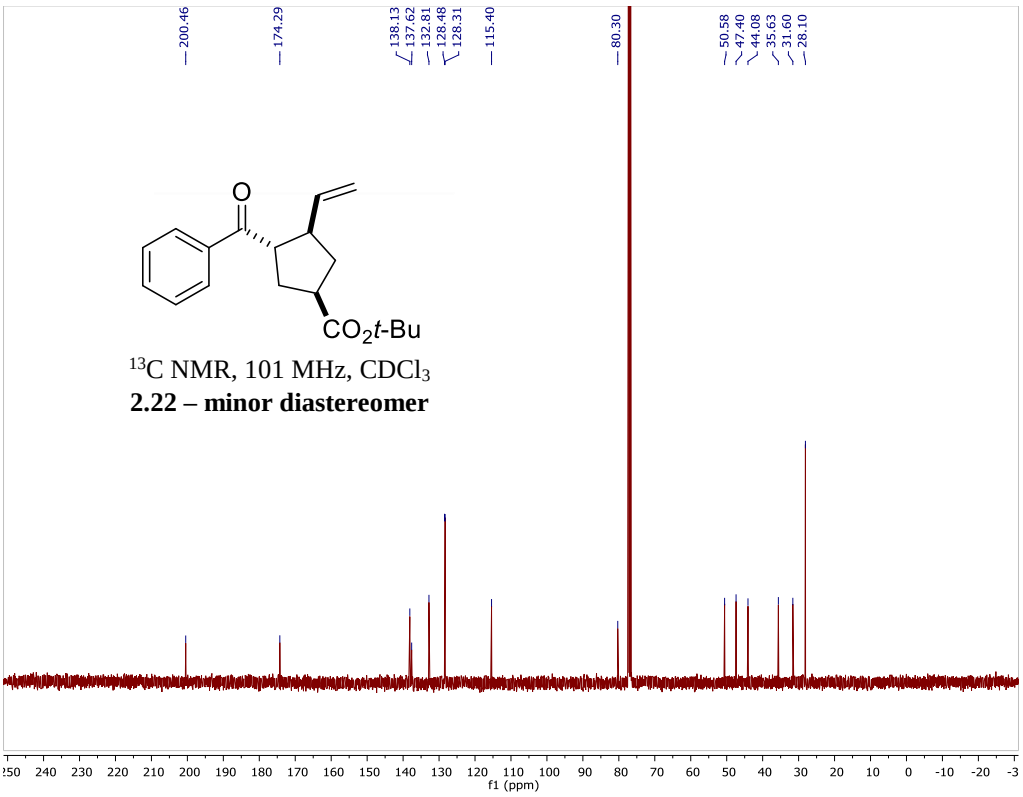

^{13}C NMR, 101 MHz, $CDCl_3$
2.22 – minor diastereomer

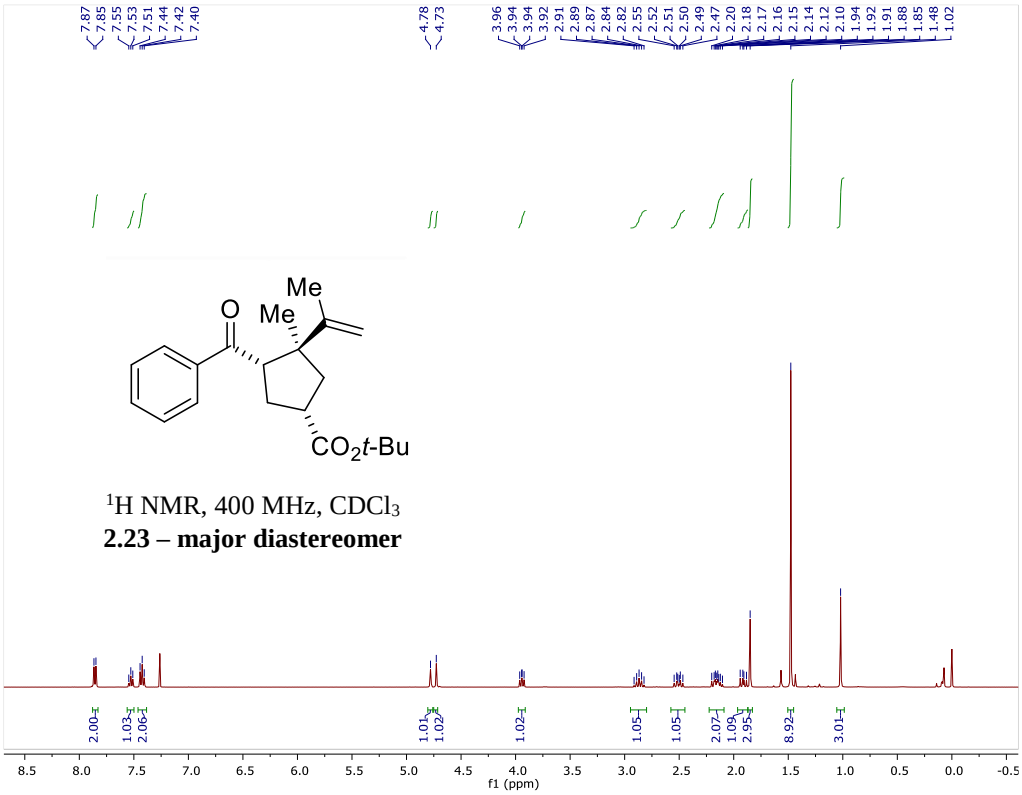

^{1}H NMR, 400 MHz, $CDCl_3$

2.23 – major diastereomer

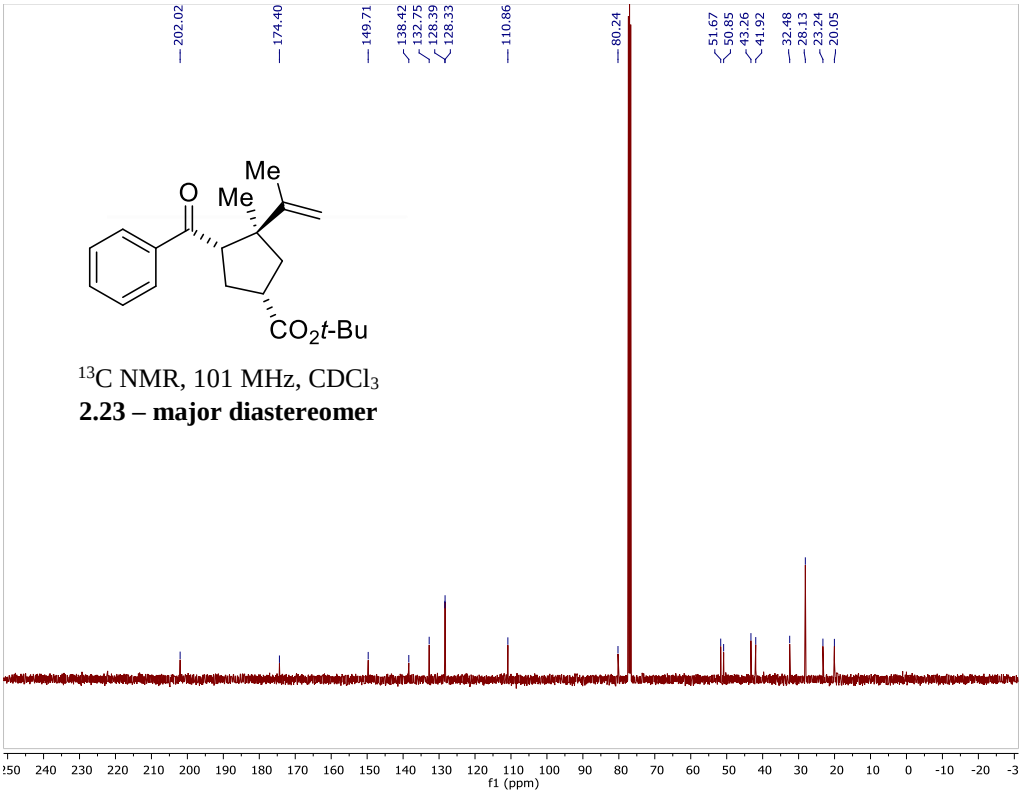

^{13}C NMR, 101 MHz, $CDCl_3$

2.23 – major diastereomer

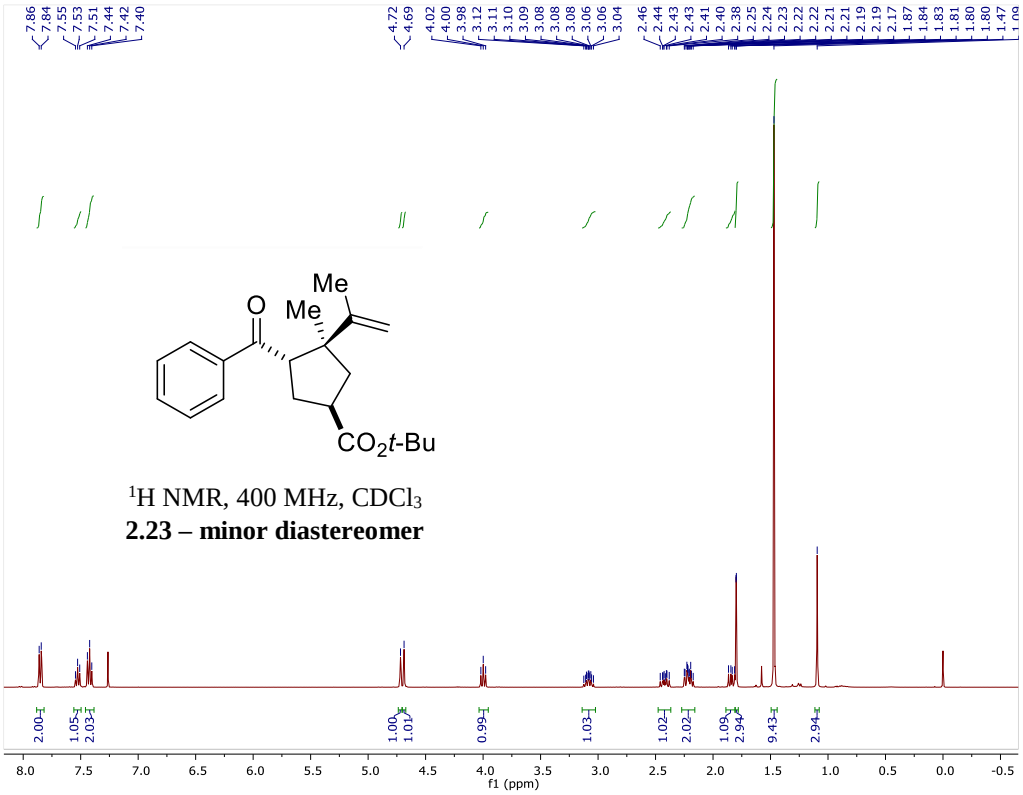

^{1}H NMR, 400 MHz, $CDCl_3$
2.23 – minor diastereomer

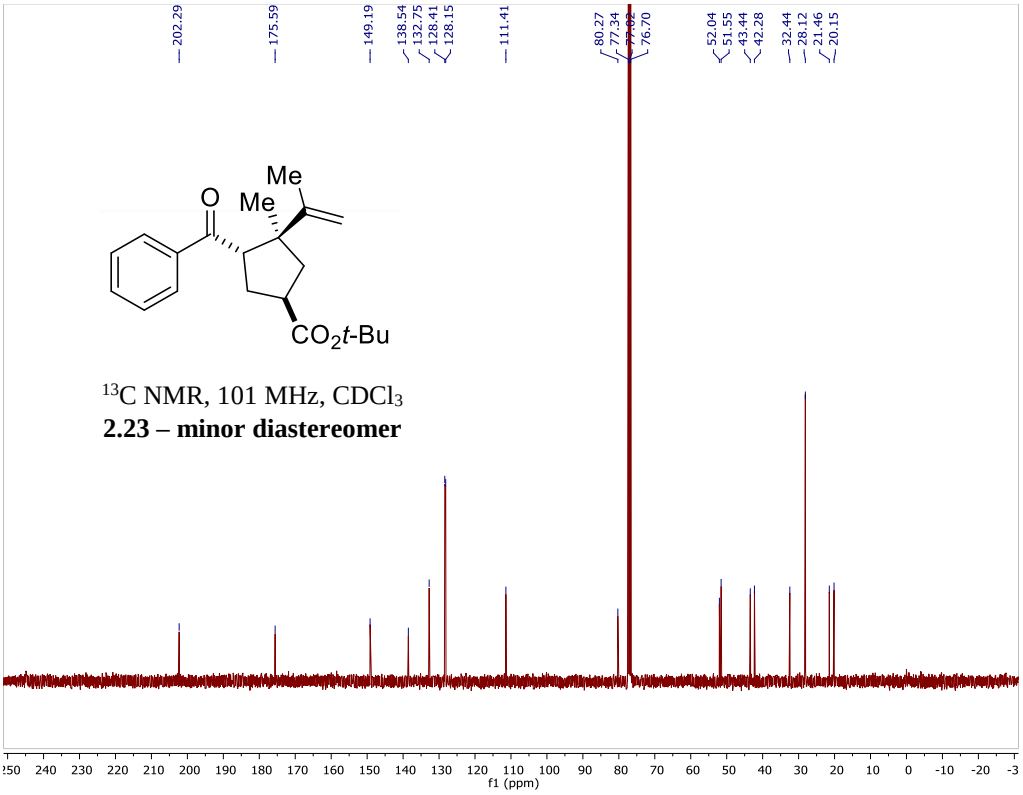

^{13}C NMR, 101 MHz, $CDCl_3$
2.23 – minor diastereomer

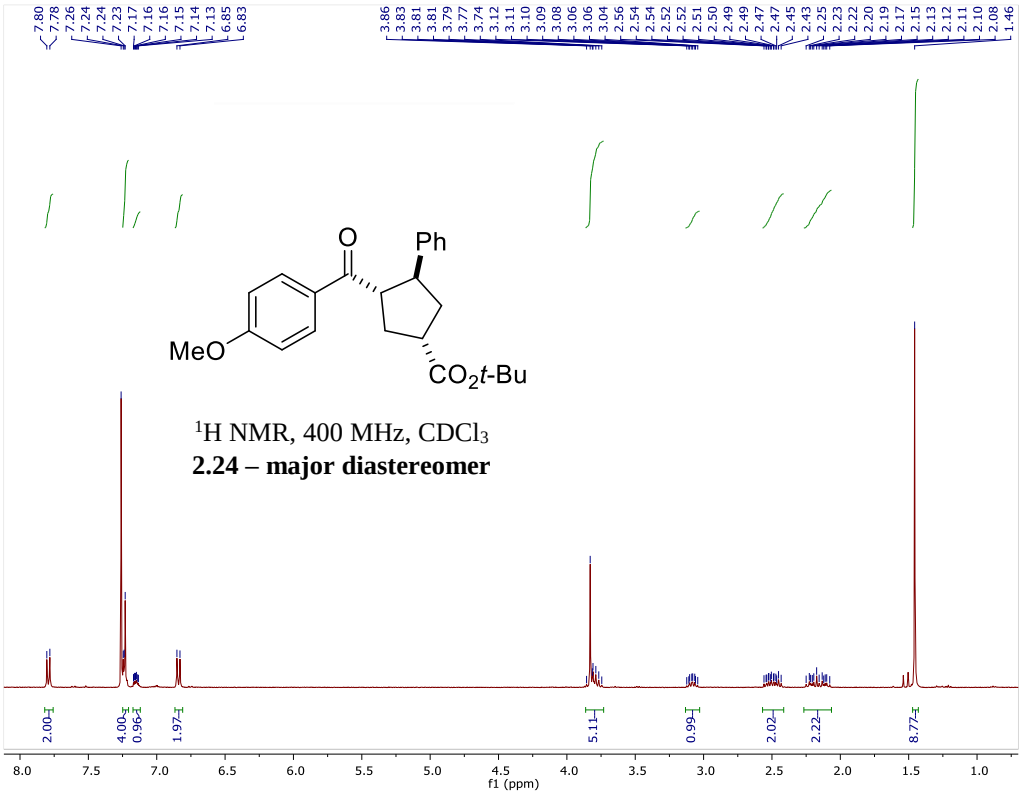

^{1}H NMR, 400 MHz, $CDCl_3$
2.24 – major diastereomer

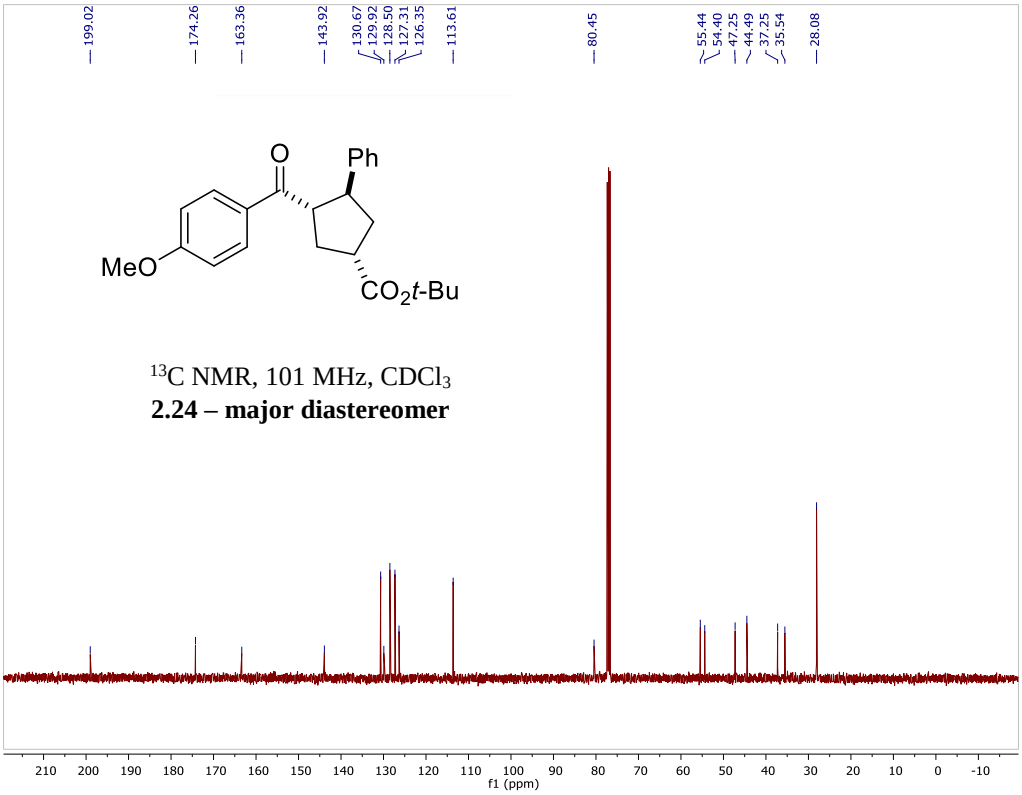

^{13}C NMR, 101 MHz, $CDCl_3$
2.24 – major diastereomer

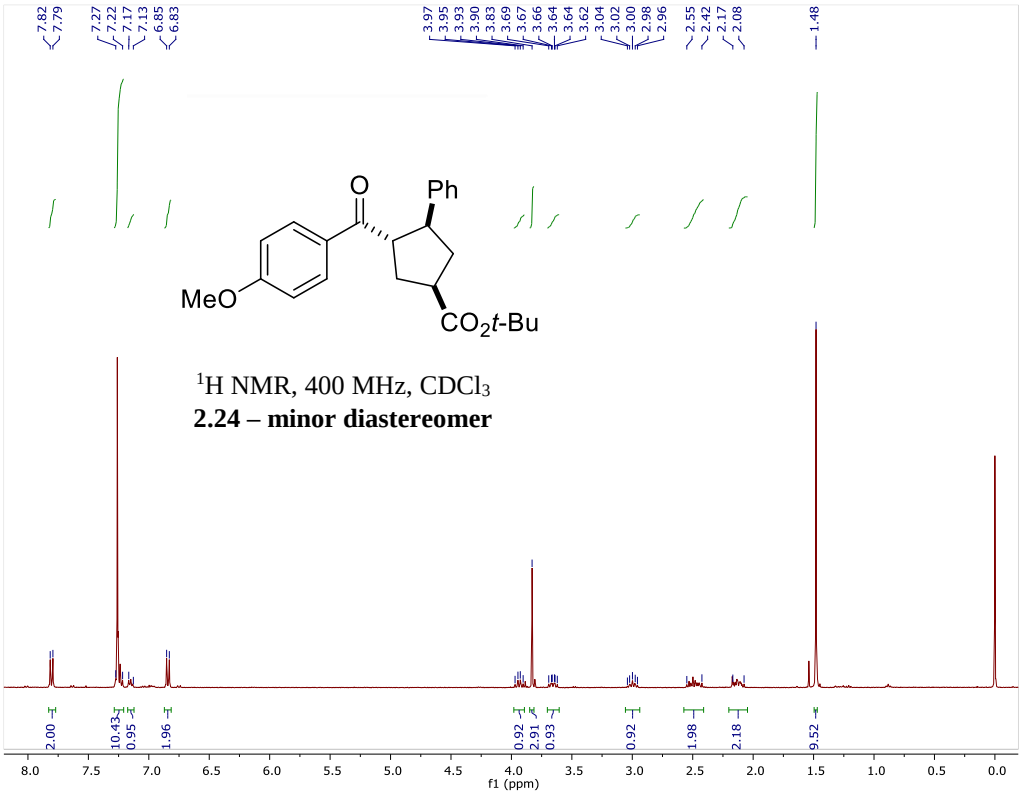

^{1}H NMR, 400 MHz, $CDCl_3$
2.24 – minor diastereomer

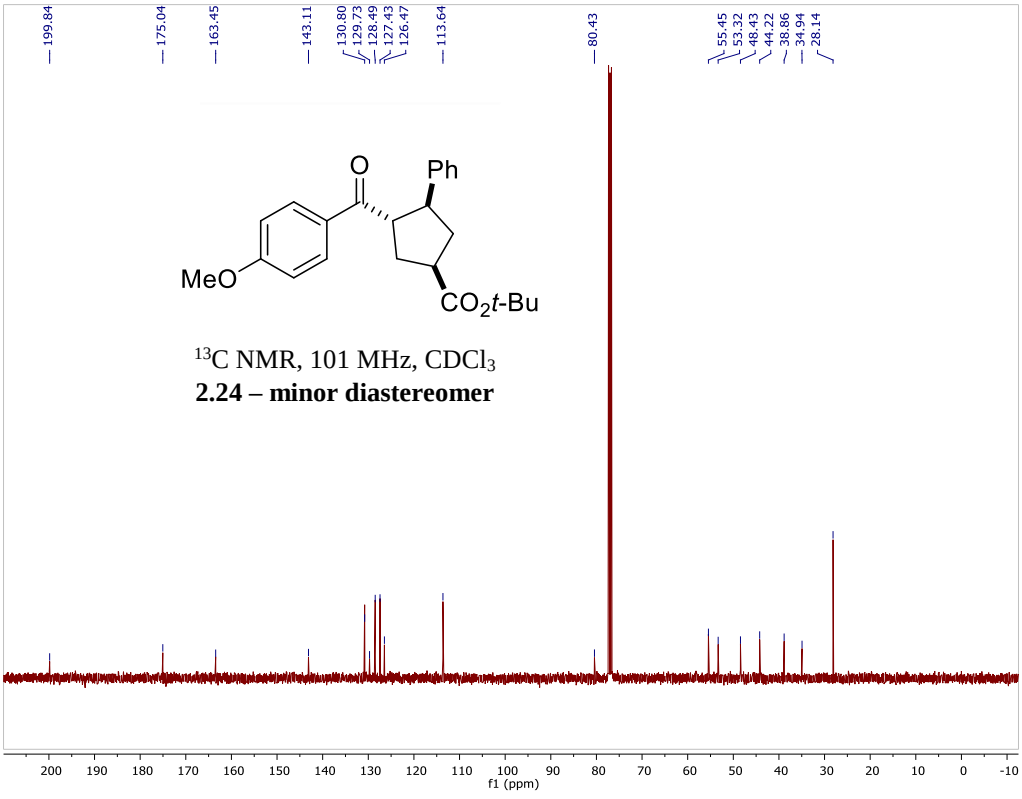

^{13}C NMR, 101 MHz, $CDCl_3$
2.24 – minor diastereomer

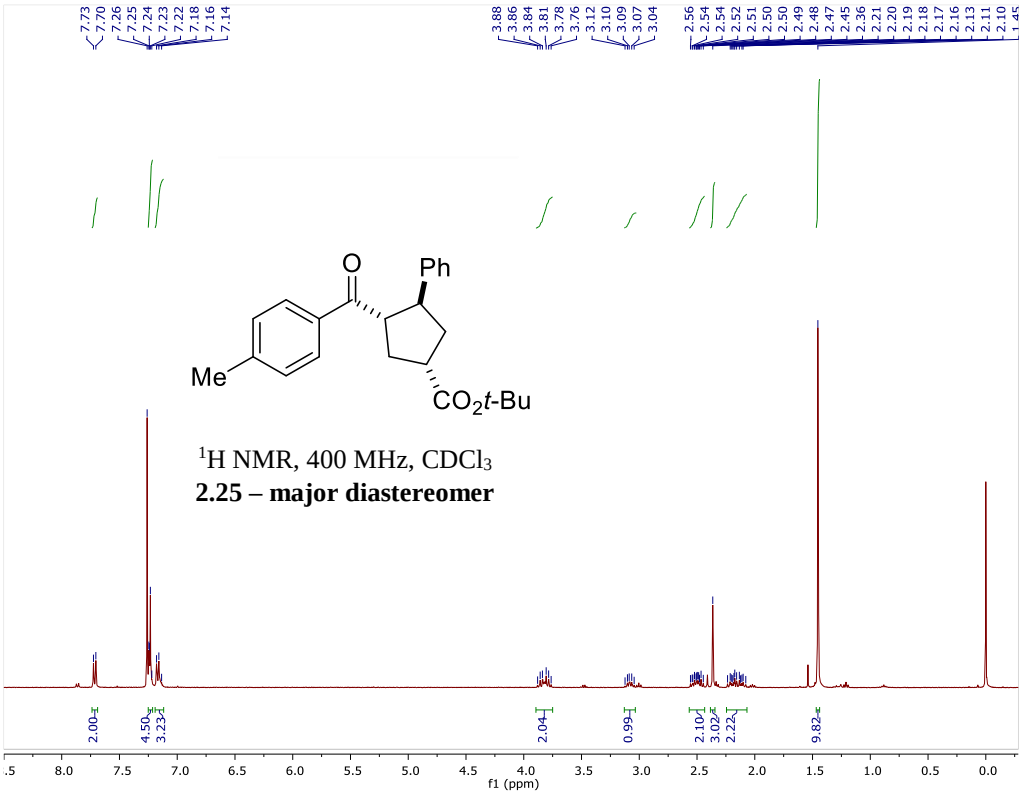

^{1}H NMR, 400 MHz, $CDCl_3$

2.25 – major diastereomer

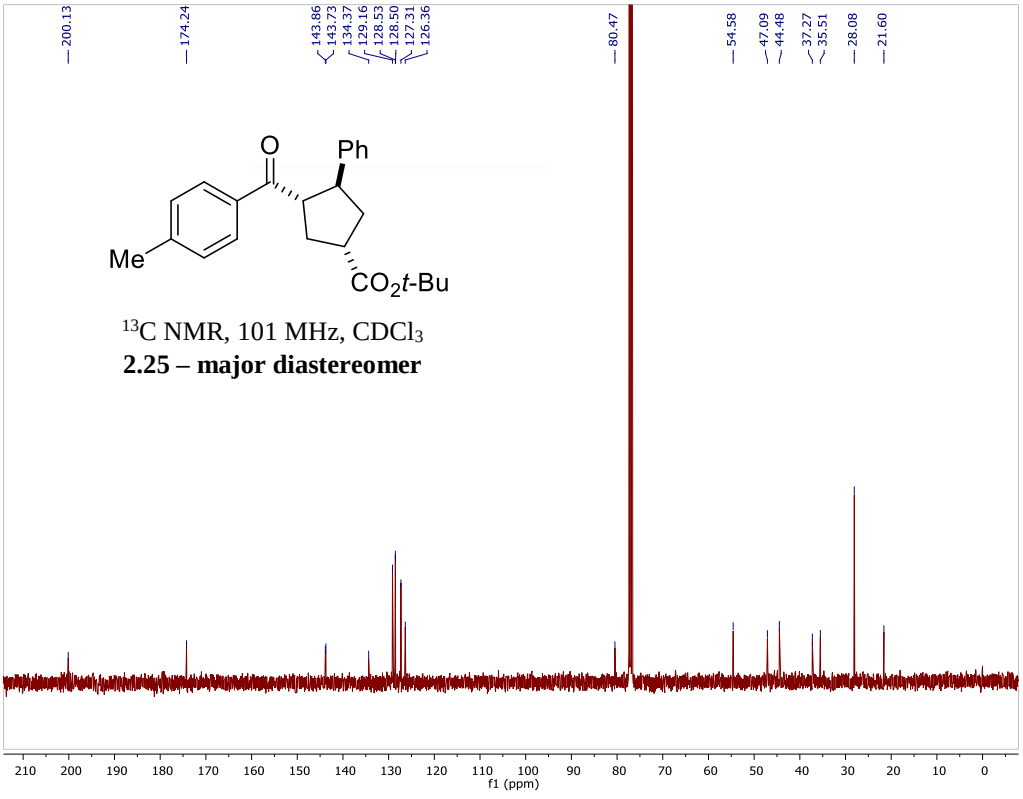

^{13}C NMR, 101 MHz, $CDCl_3$

2.25 – major diastereomer

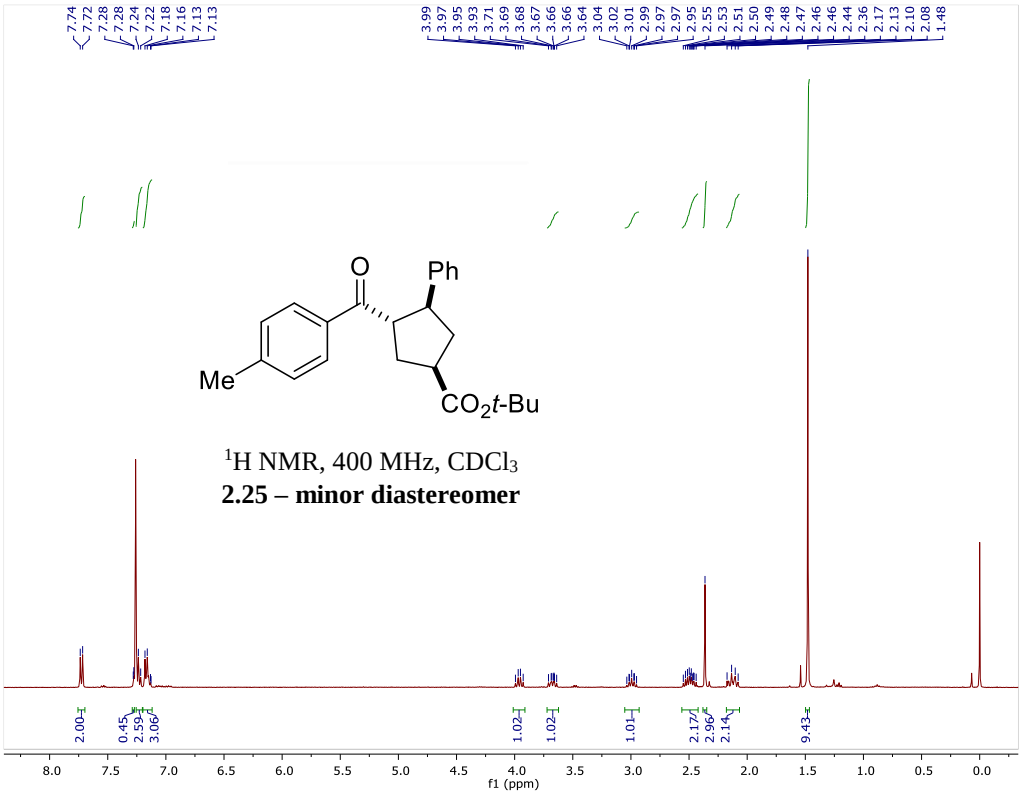

^{1}H NMR, 400 MHz, $CDCl_3$

2.25 – minor diastereomer

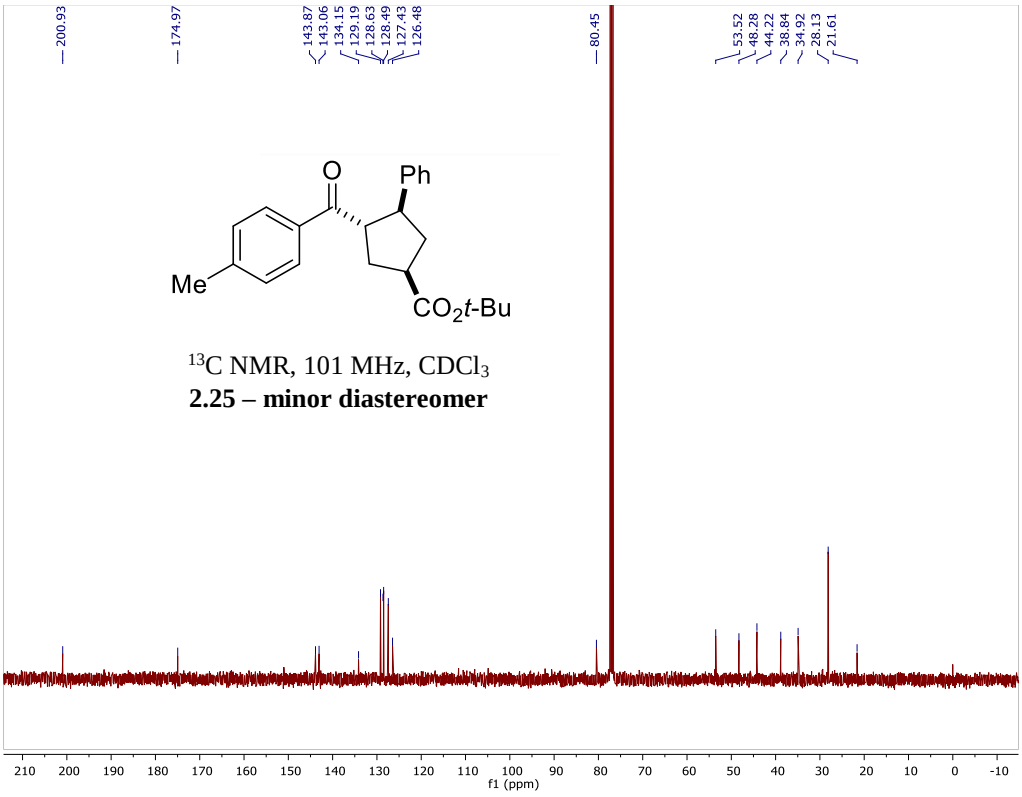

^{13}C NMR, 101 MHz, $CDCl_3$

2.25 – minor diastereomer

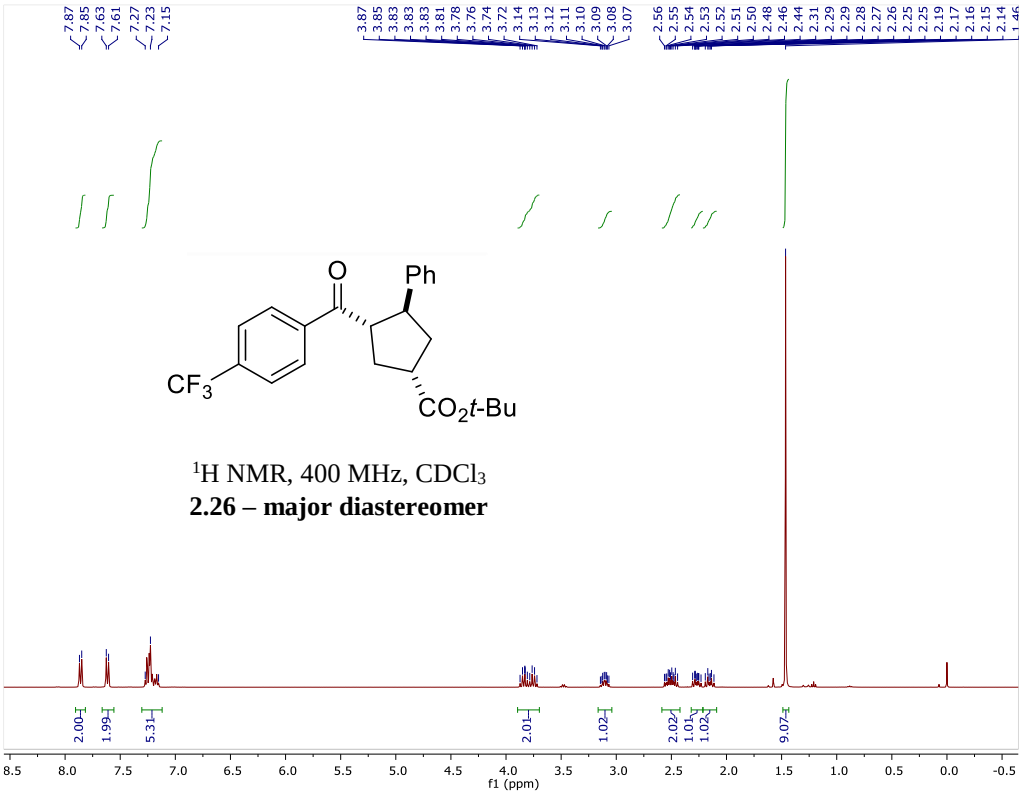

^{1}H NMR, 400 MHz, $CDCl_3$
2.26 – major diastereomer

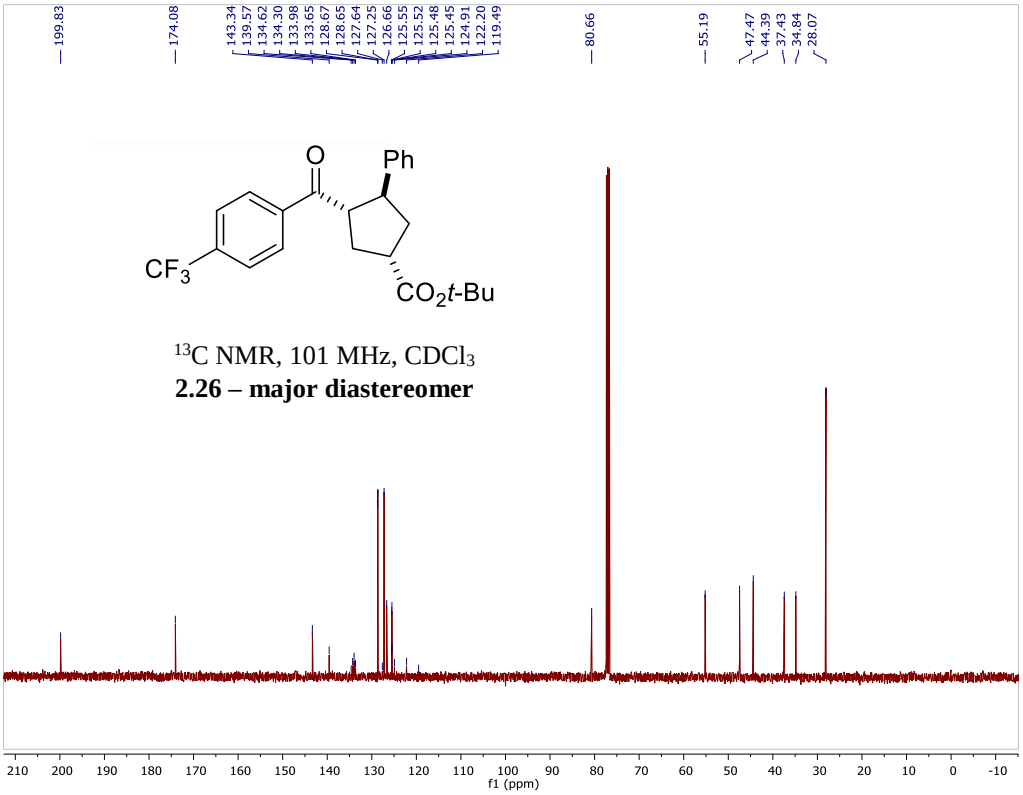

^{13}C NMR, 101 MHz, $CDCl_3$
2.26 – major diastereomer

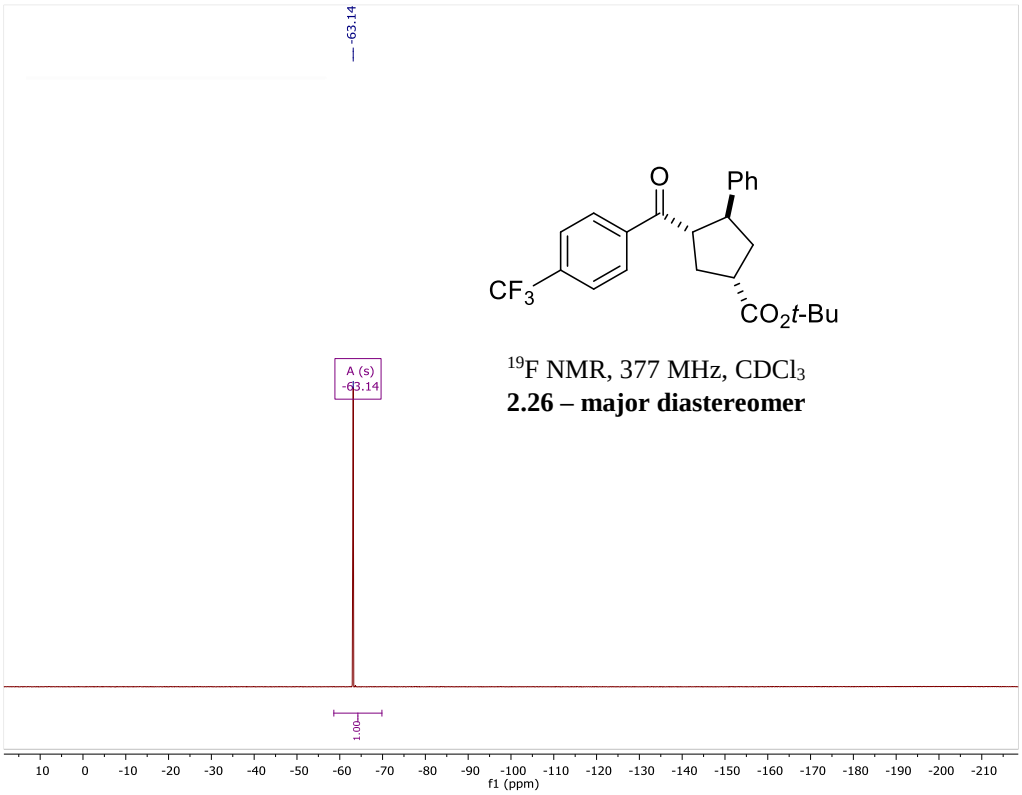

^{19}F NMR, 377 MHz, $CDCl_3$

2.26 – major diastereomer

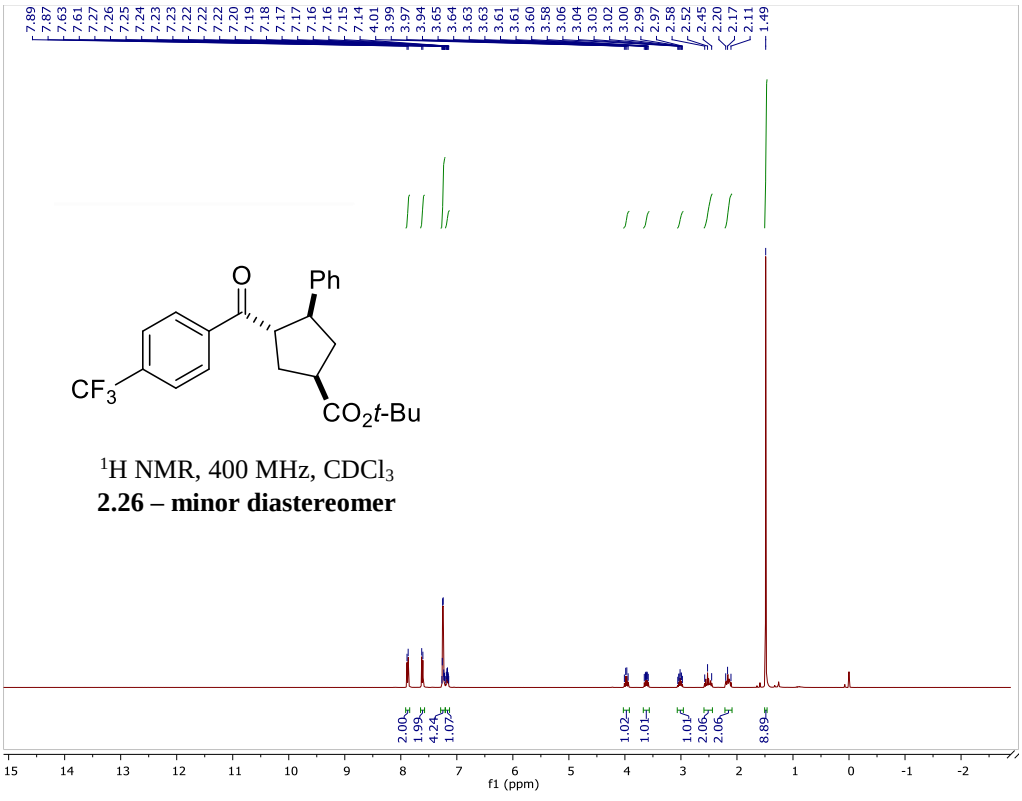

^{1}H NMR, 400 MHz, $CDCl_3$

2.26 – minor diastereomer

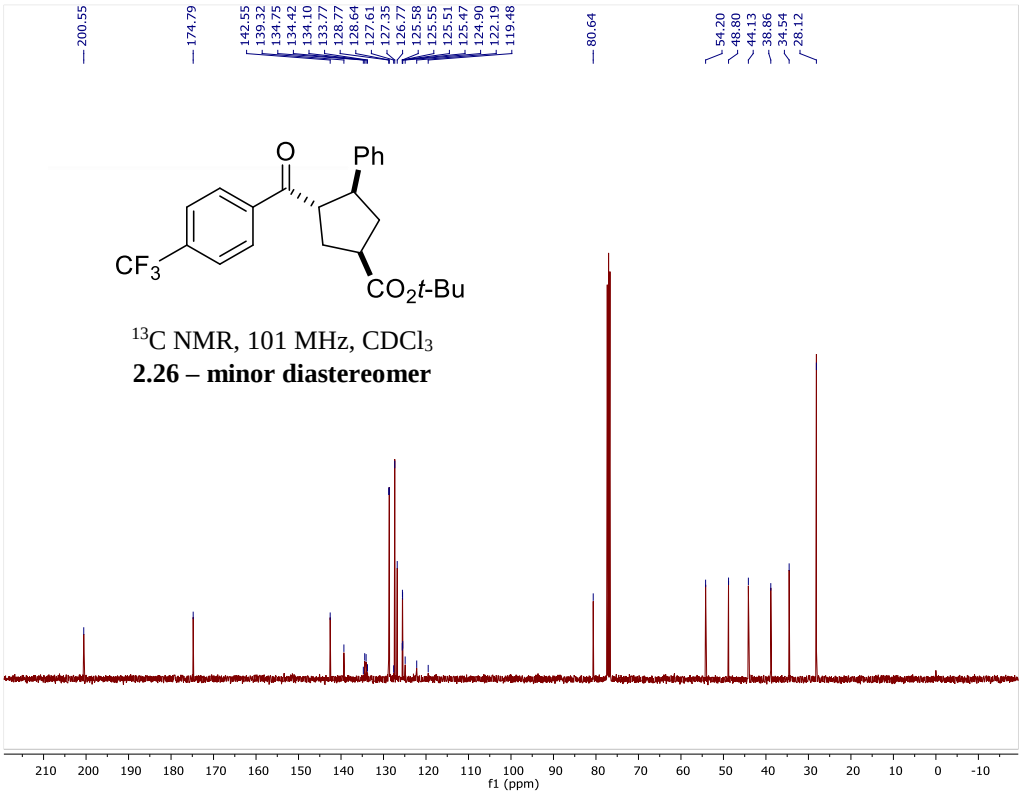

^{13}C NMR, 101 MHz, $CDCl_3$

2.26 – minor diastereomer

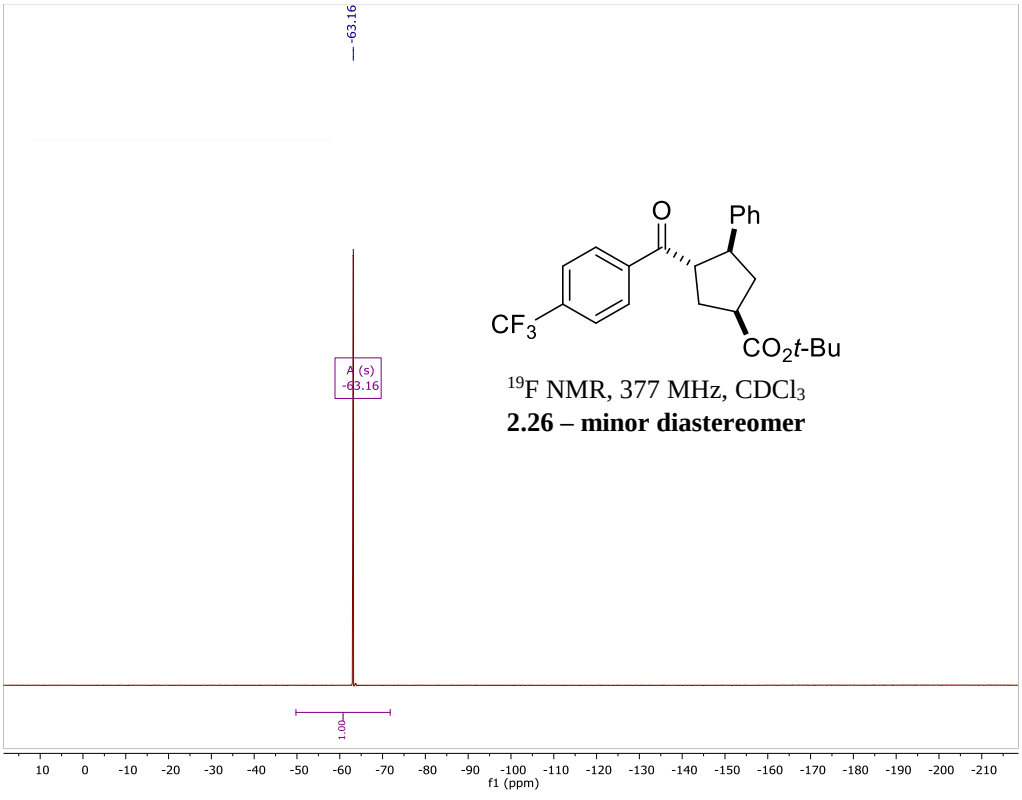

^{19}F NMR, 377 MHz, $CDCl_3$

2.26 – minor diastereomer

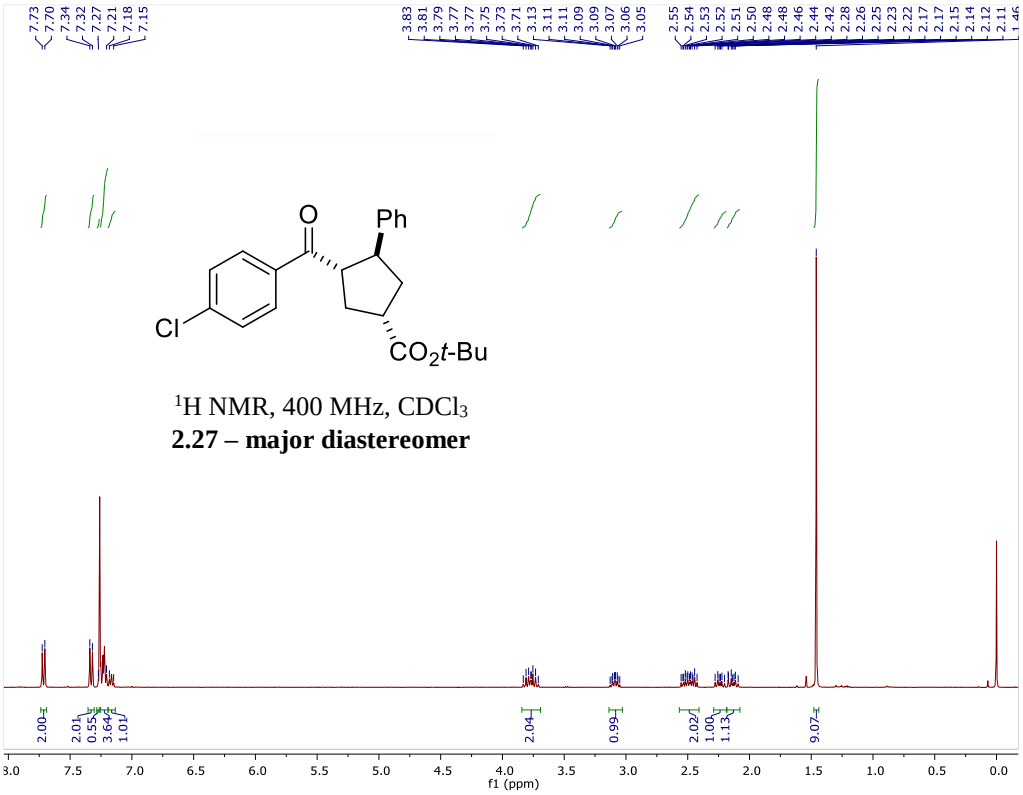

^{1}H NMR, 400 MHz, $CDCl_3$
2.27 – major diastereomer

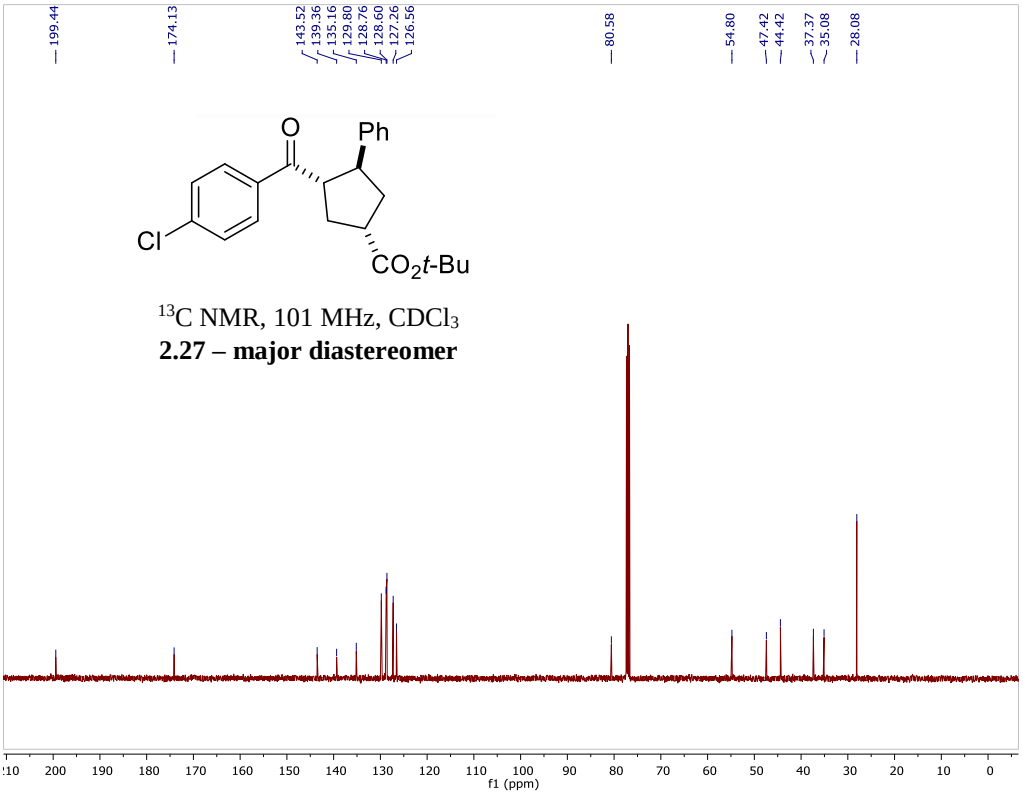

^{13}C NMR, 101 MHz, $CDCl_3$
2.27 – major diastereomer

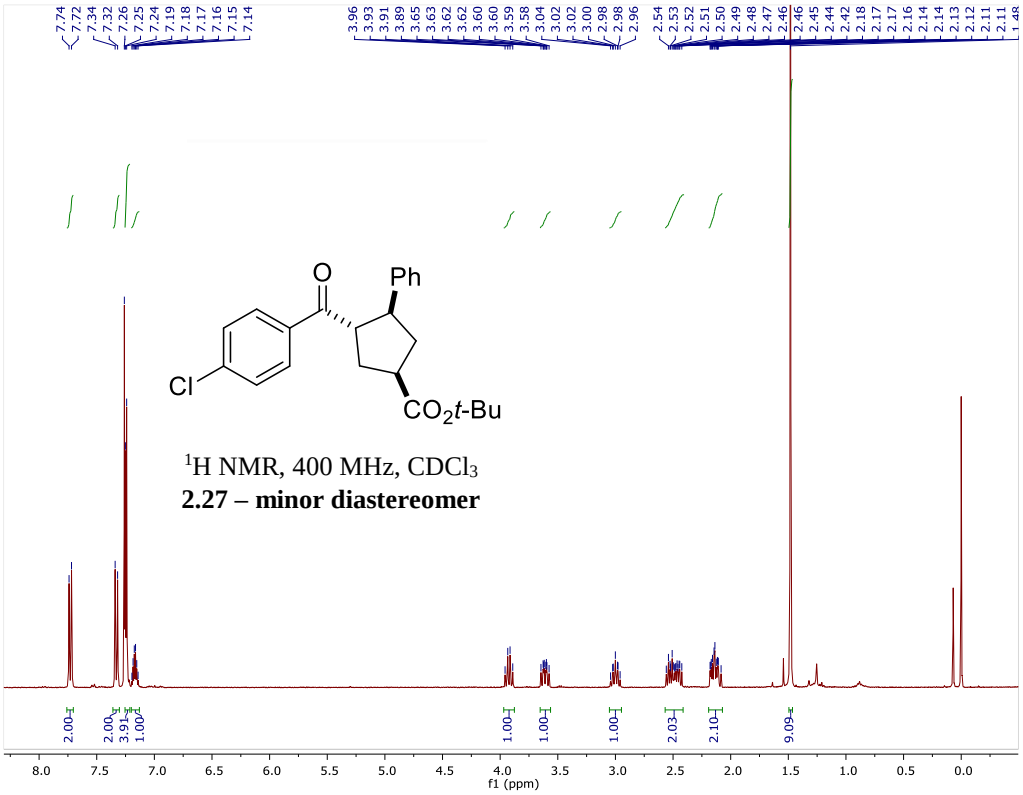
O
Ph
Cl
CO2t-Bu
1H NMR, 400 MHz, CDCl3
2.27 – minor diastereomer
f1 (ppm)

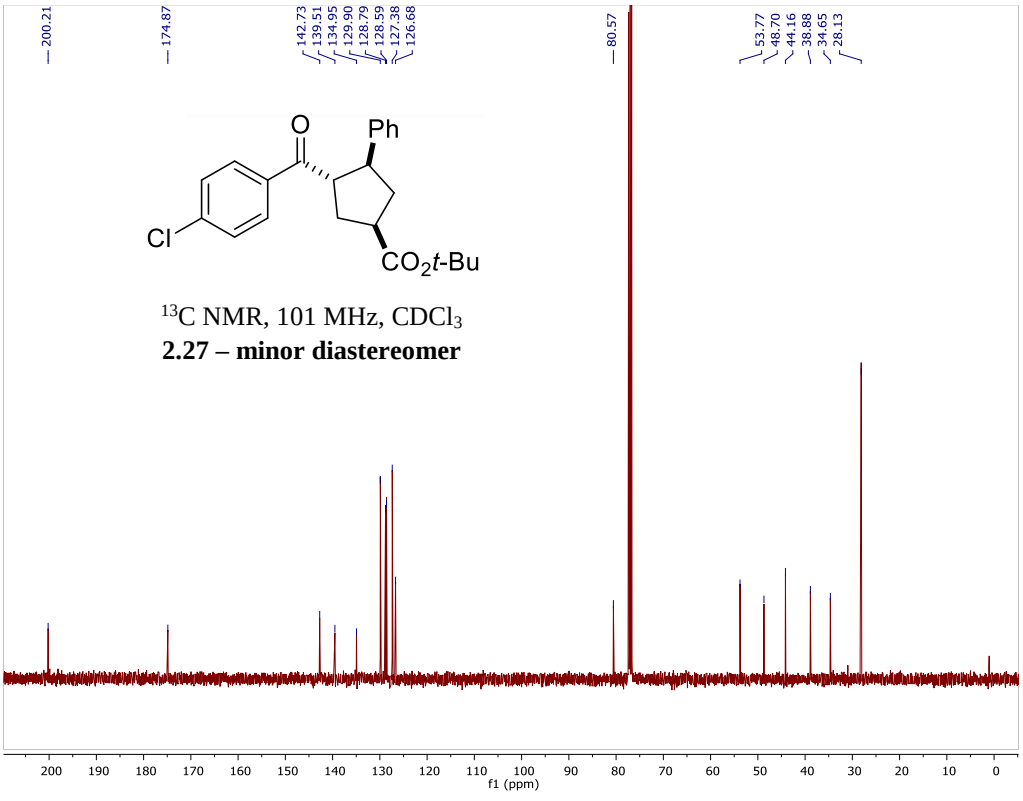
O
Ph
Cl
CO2t-Bu
13C NMR, 101 MHz, CDCl3
2.27 – minor diastereomer
f1 (ppm)

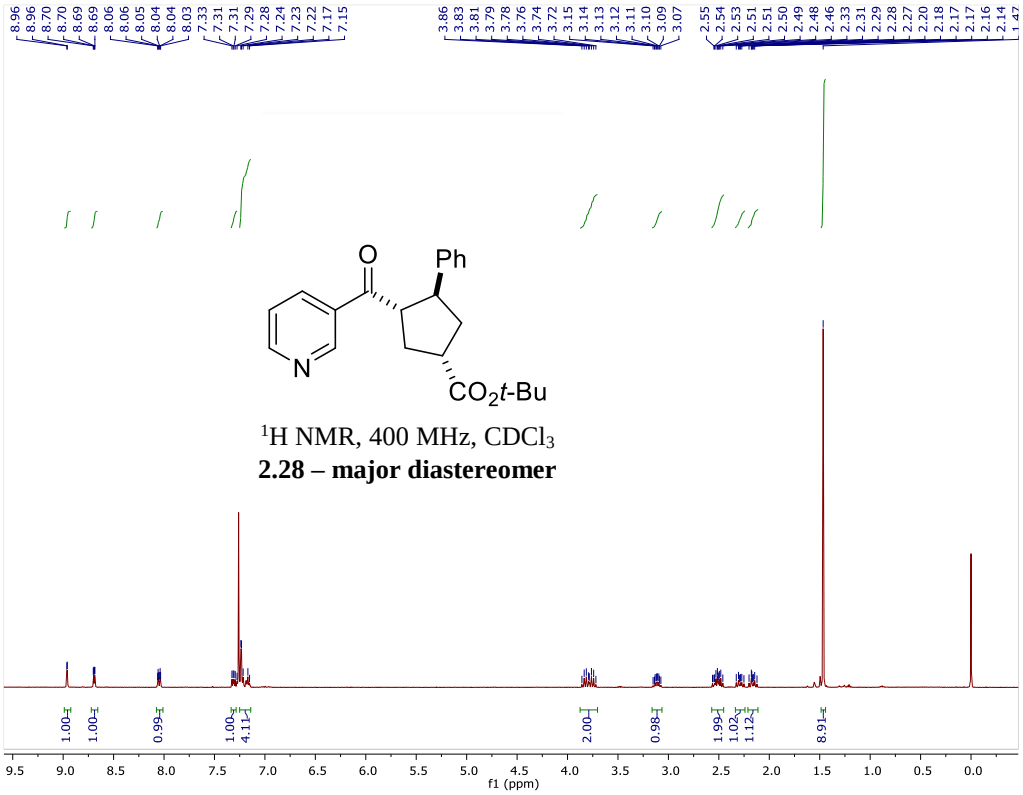

^{1}H NMR, 400 MHz, $CDCl_3$

2.28 – major diastereomer

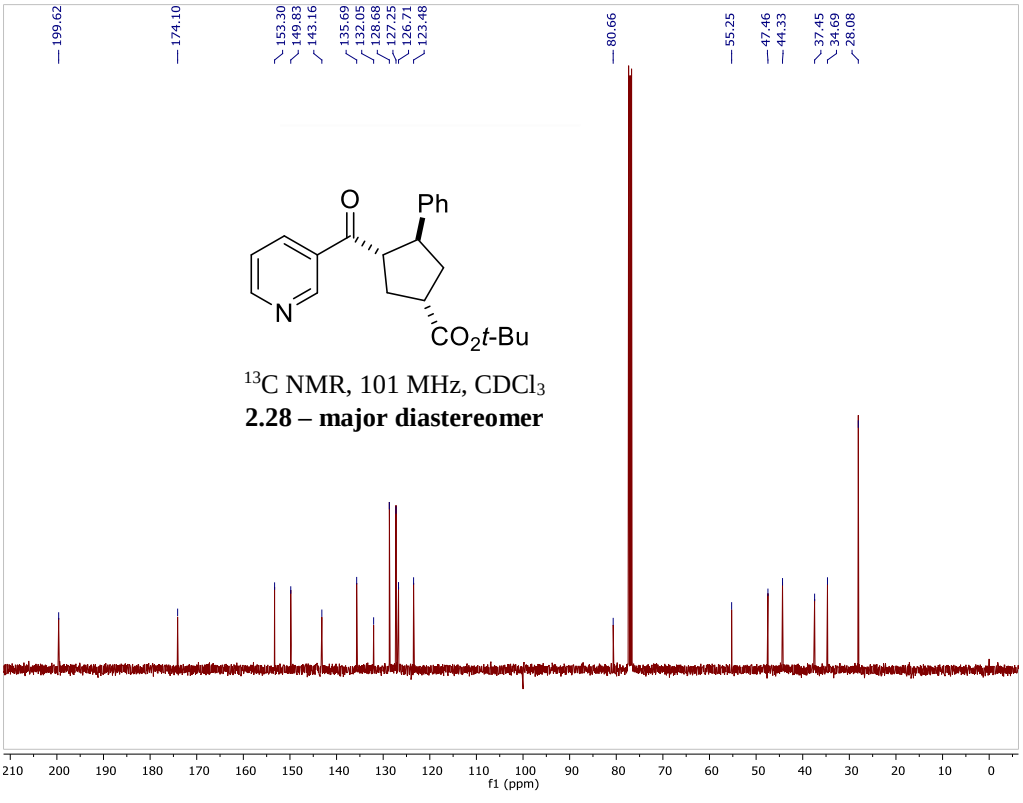

^{13}C NMR, 101 MHz, $CDCl_3$

2.28 – major diastereomer

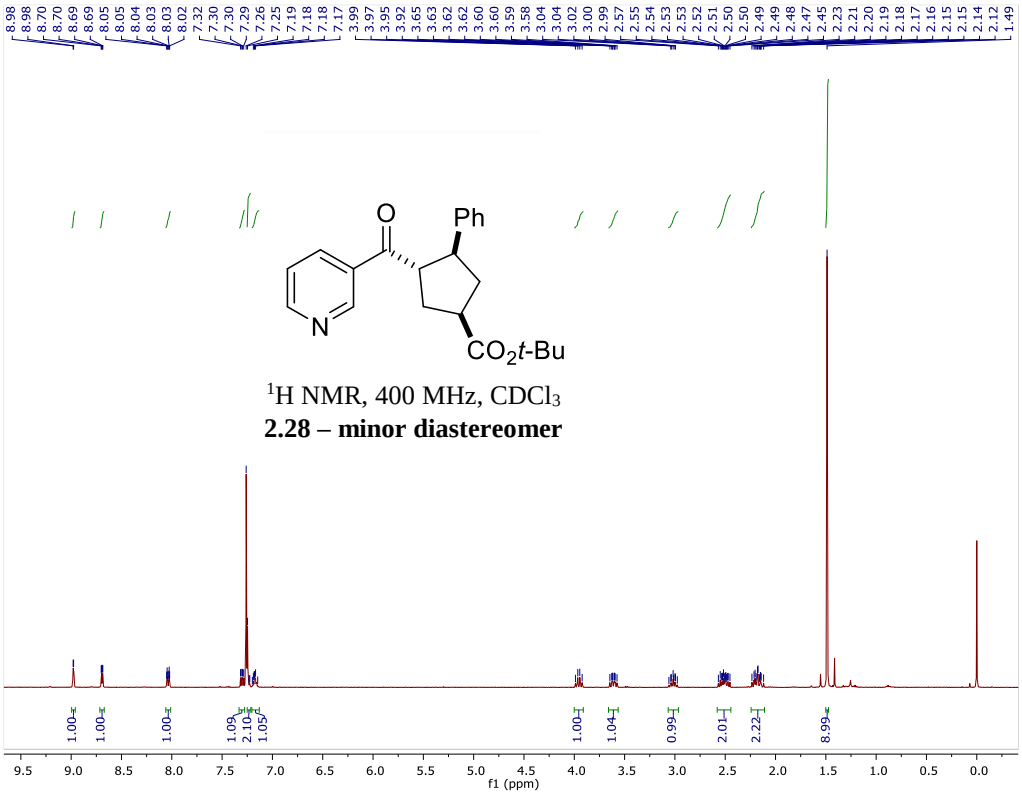

^{1}H NMR, 400 MHz, $CDCl_3$

2.28 – minor diastereomer

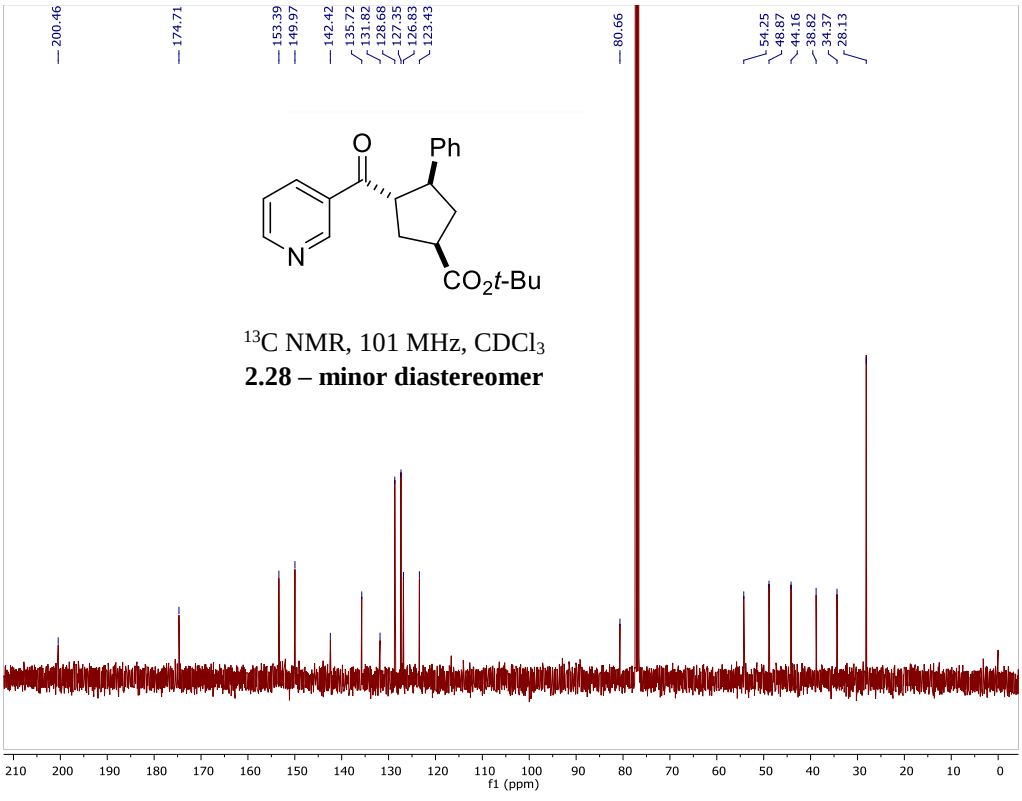

^{13}C NMR, 101 MHz, $CDCl_3$

2.28 – minor diastereomer

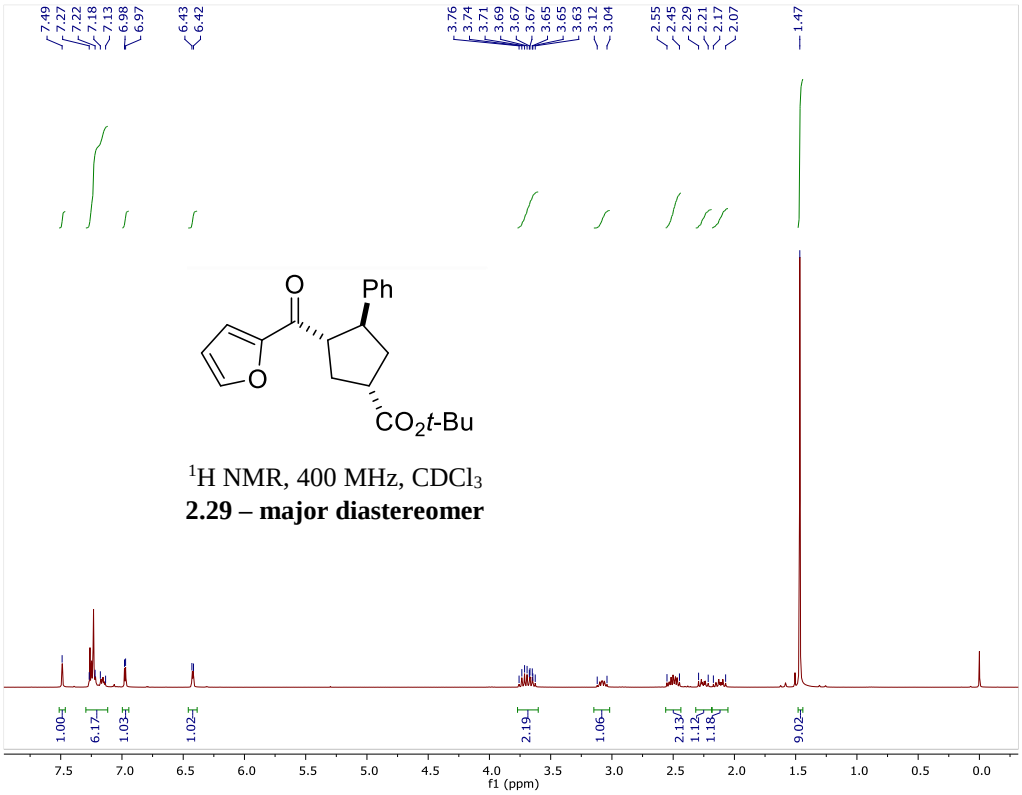

^{1}H NMR, 400 MHz, $CDCl_3$
2.29 – major diastereomer

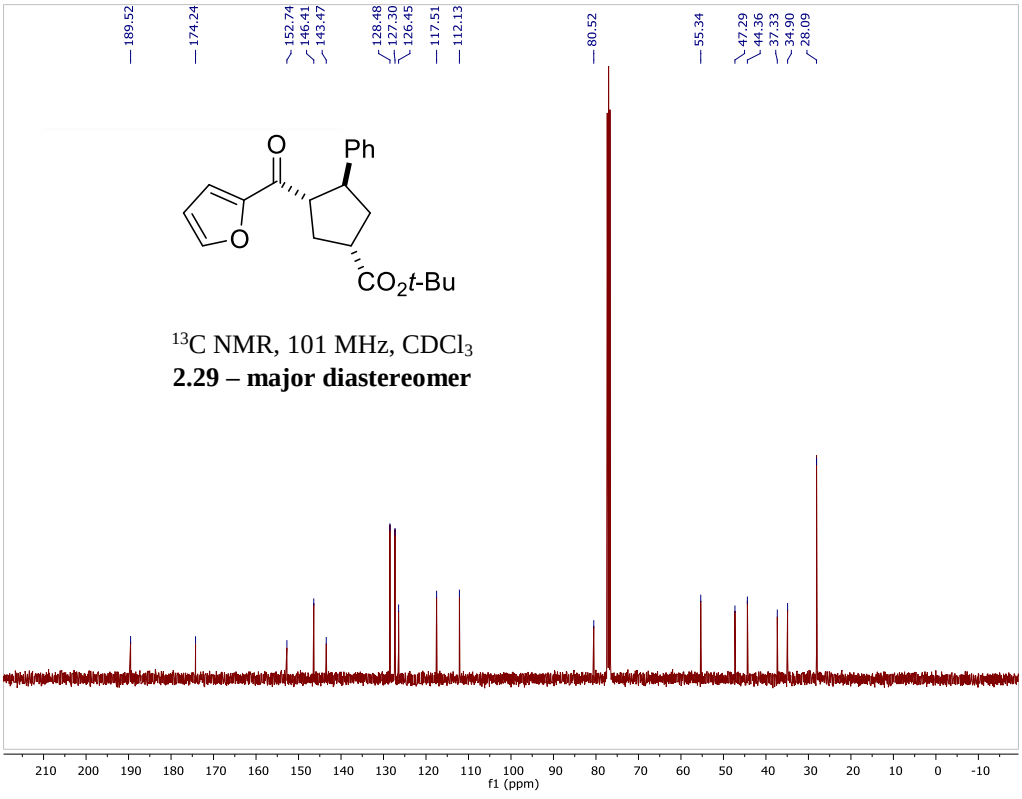

^{13}C NMR, 101 MHz, $CDCl_3$
2.29 – major diastereomer

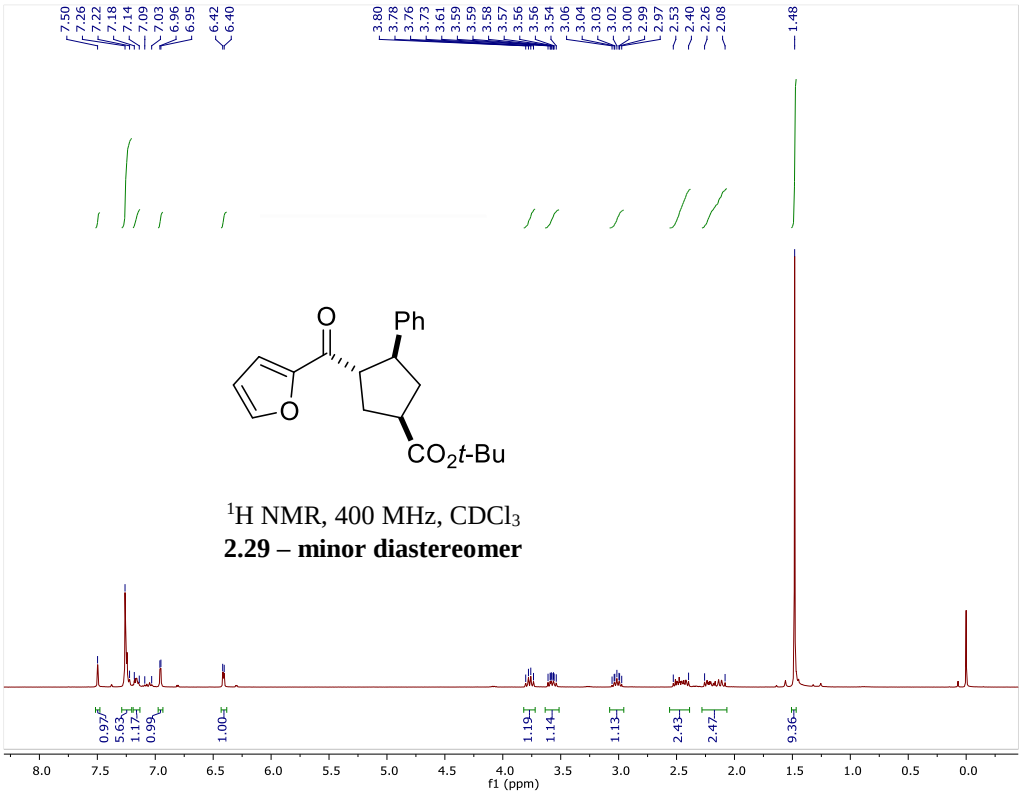

^{1}H NMR, 400 MHz, $CDCl_3$
2.29 – minor diastereomer

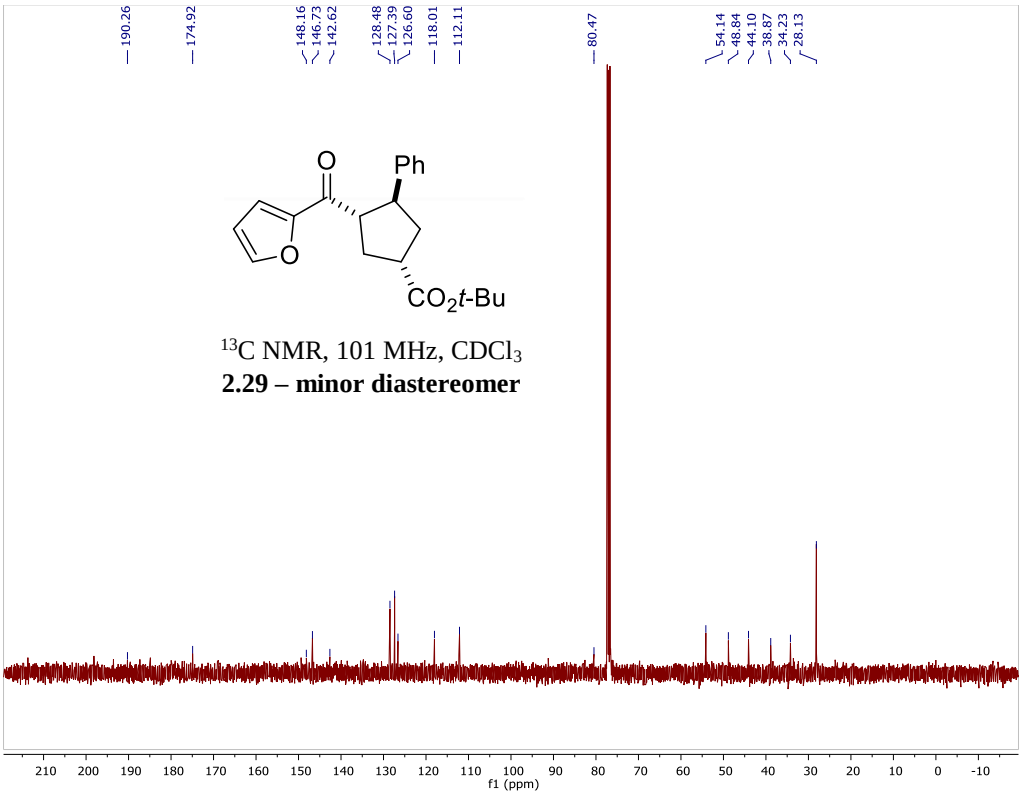

^{13}C NMR, 101 MHz, $CDCl_3$
2.29 – minor diastereomer

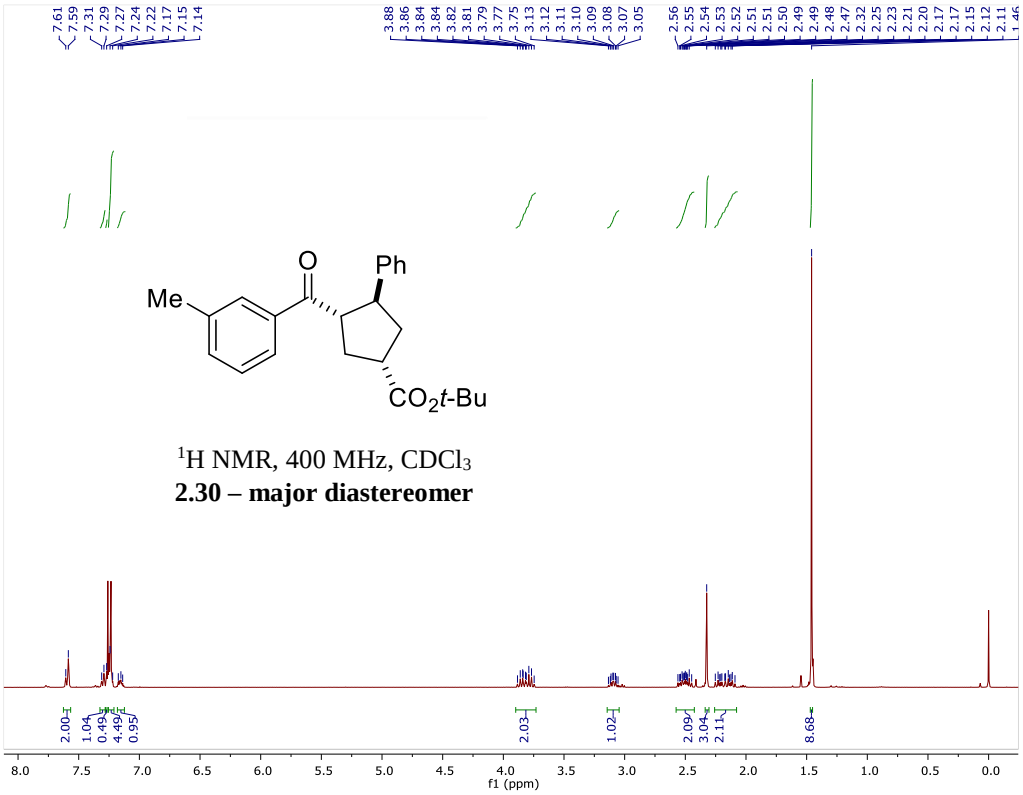

^{1}H NMR, 400 MHz, $CDCl_3$

2.30 – major diastereomer

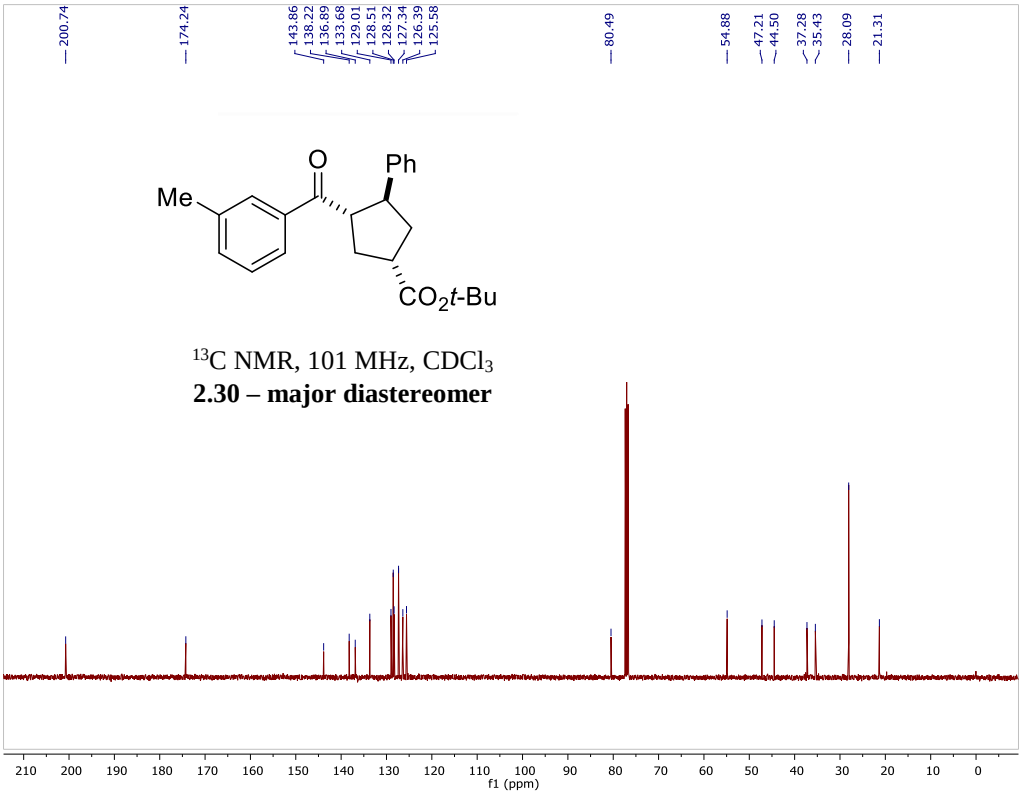

^{13}C NMR, 101 MHz, $CDCl_3$

2.30 – major diastereomer

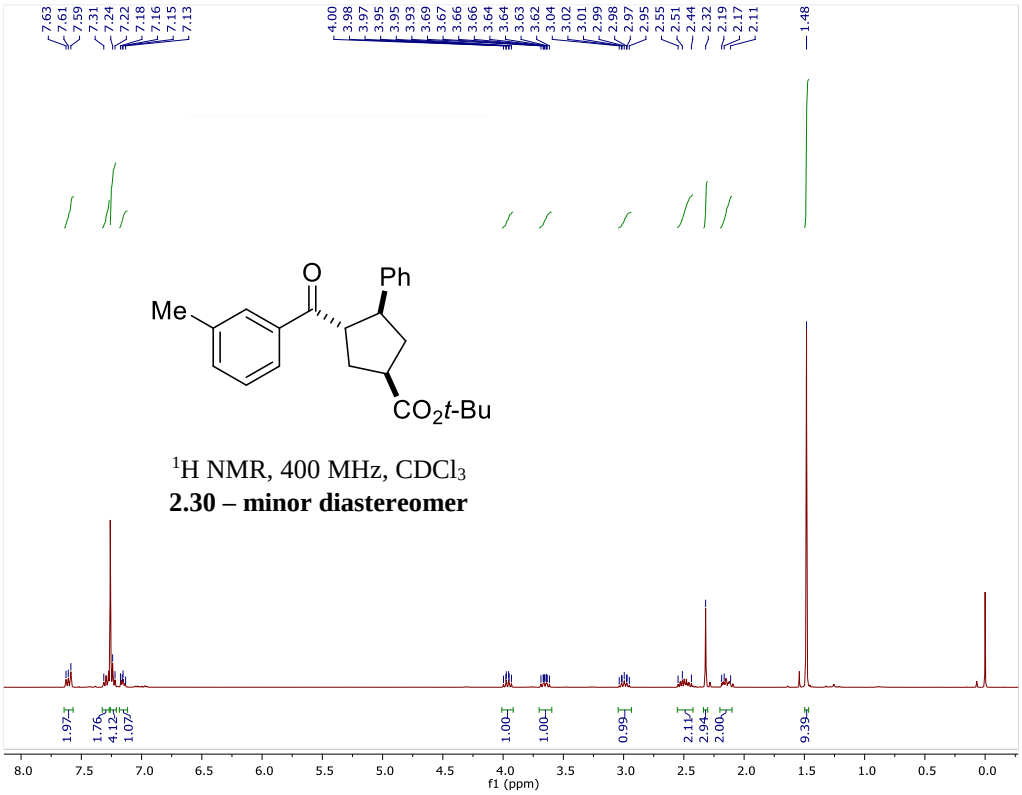

^{1}H NMR, 400 MHz, $CDCl_3$

2.30 – minor diastereomer

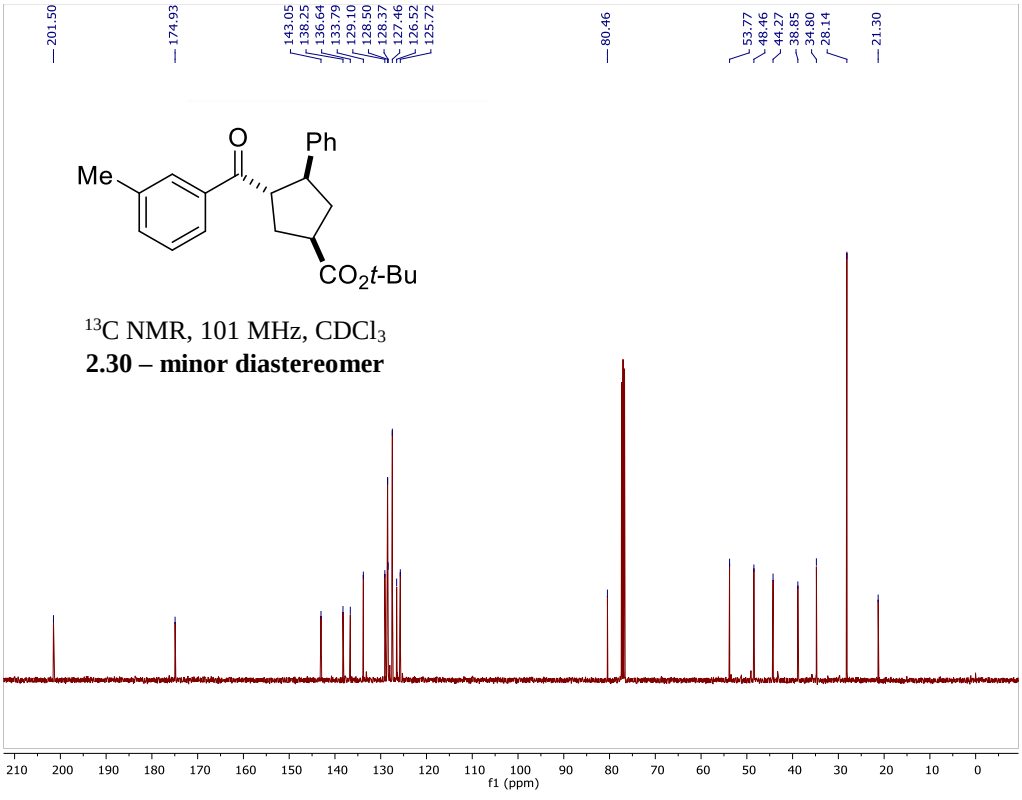

^{13}C NMR, 101 MHz, $CDCl_3$

2.30 – minor diastereomer

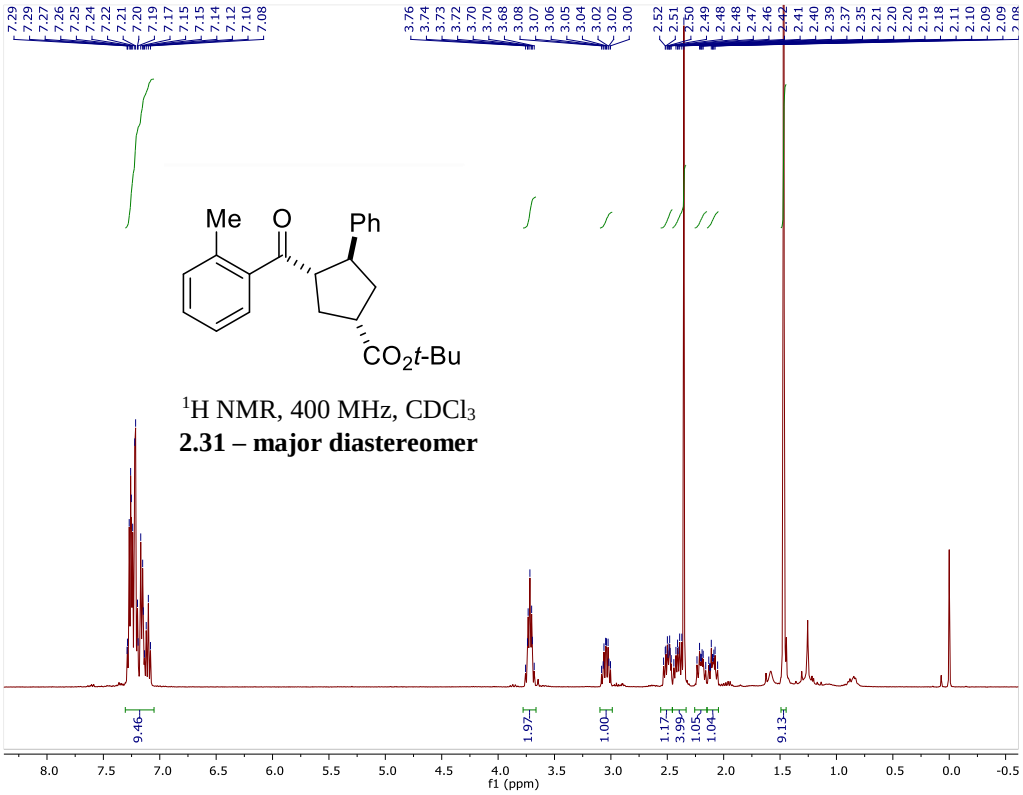

^{1}H NMR, 400 MHz, $CDCl_3$

2.31 – major diastereomer

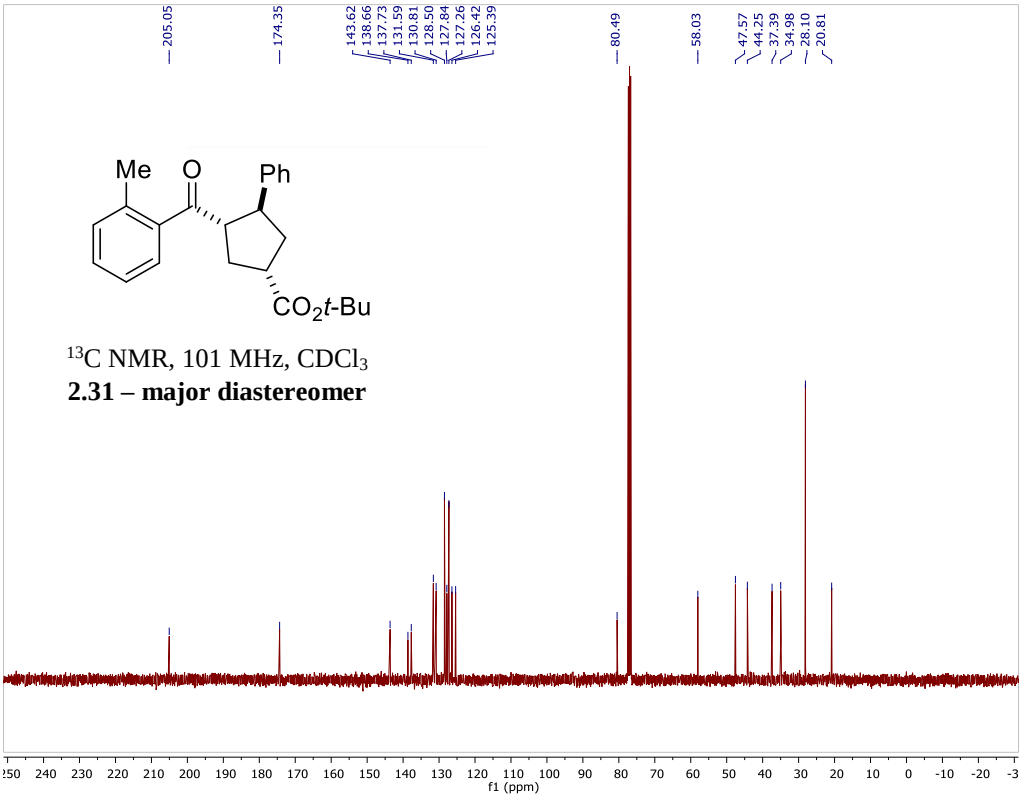

^{13}C NMR, 101 MHz, $CDCl_3$

2.31 – major diastereomer

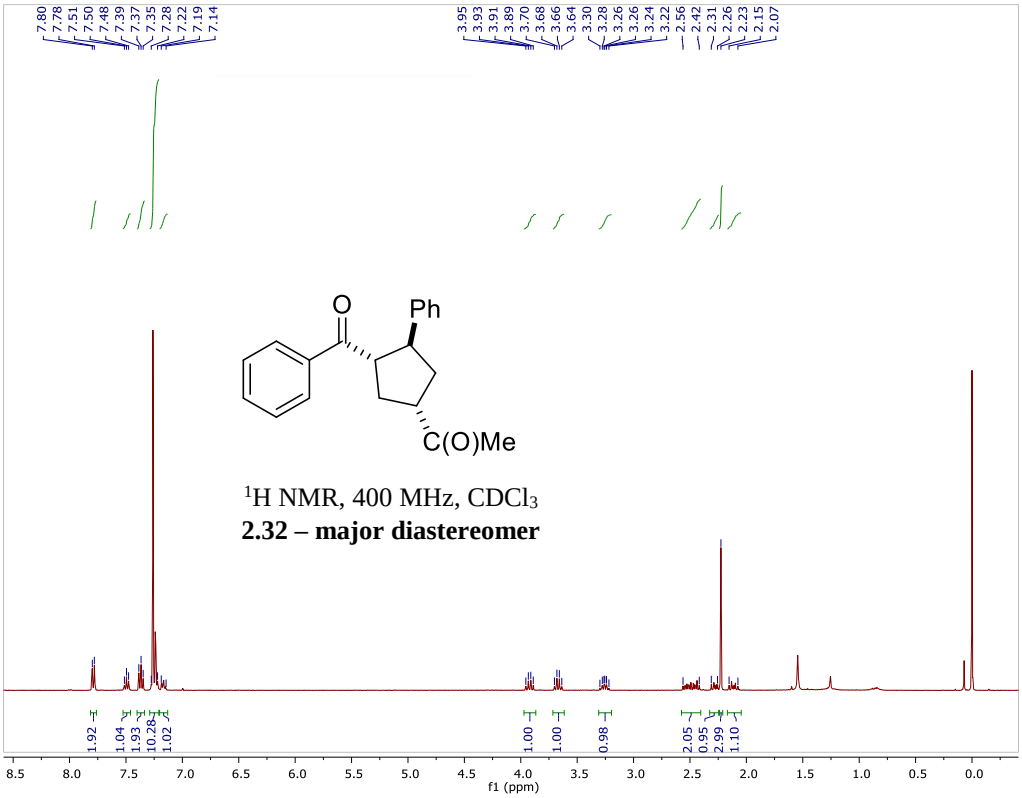

^{1}H NMR, 400 MHz, $CDCl_3$
2.32 – major diastereomer

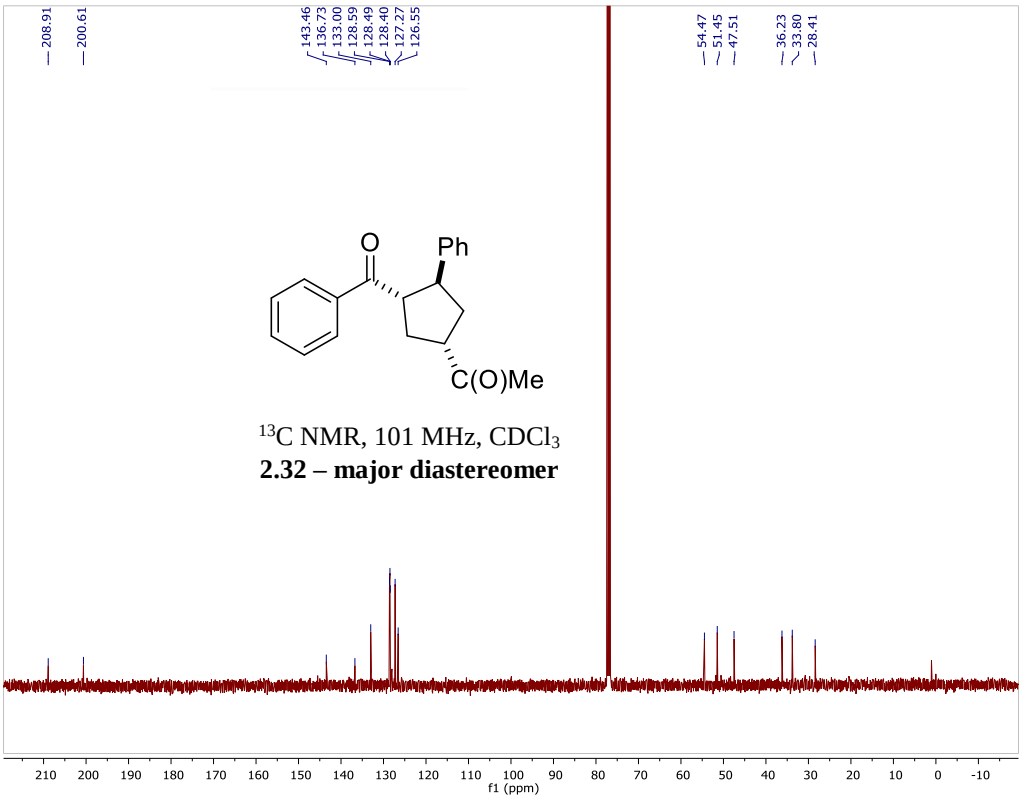

^{13}C NMR, 101 MHz, $CDCl_3$
2.32 – major diastereomer

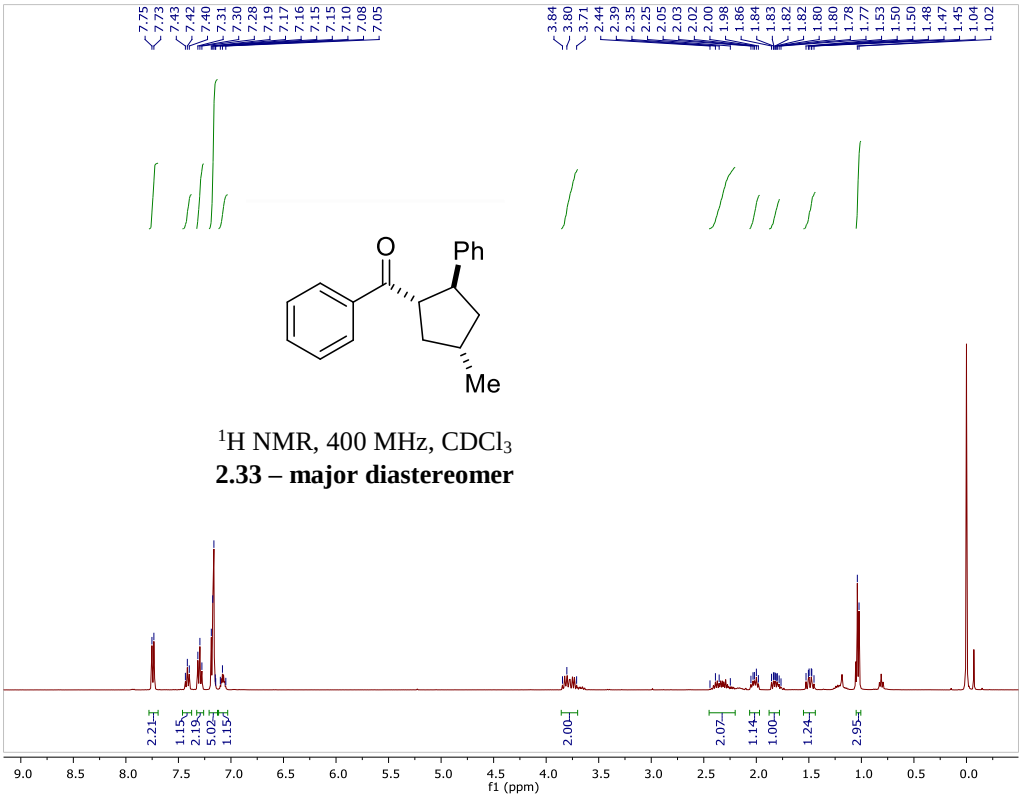

^{1}H NMR, 400 MHz, $CDCl_3$

2.33 – major diastereomer

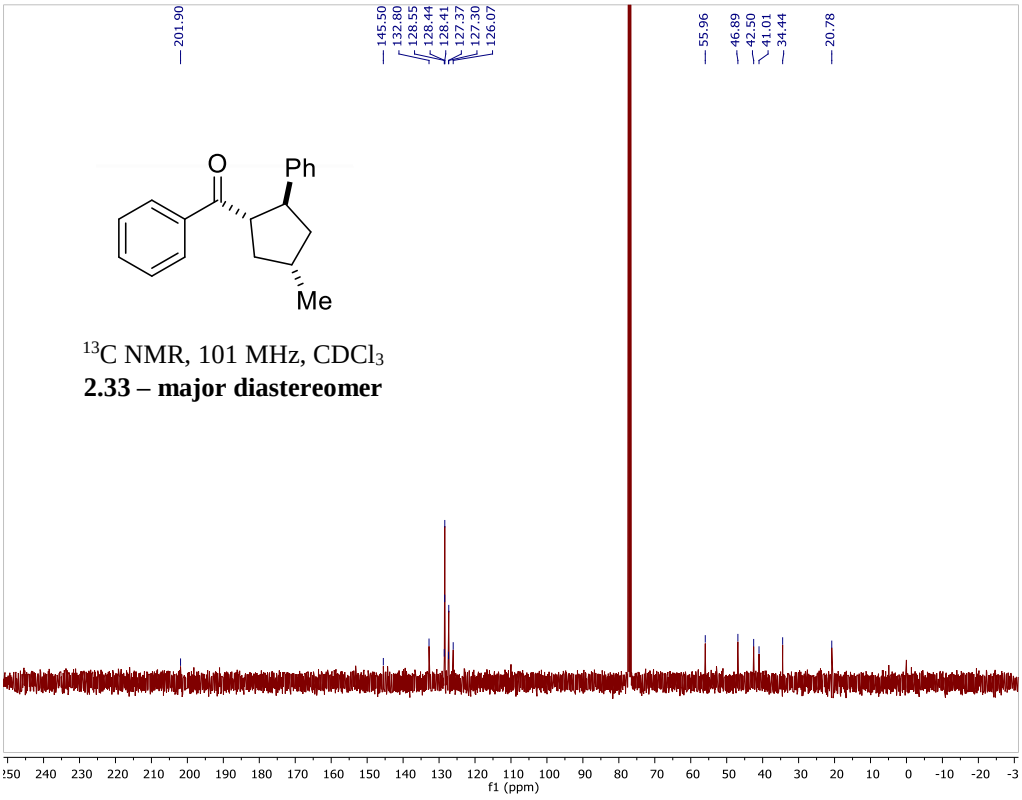

^{13}C NMR, 101 MHz, $CDCl_3$

2.33 – major diastereomer

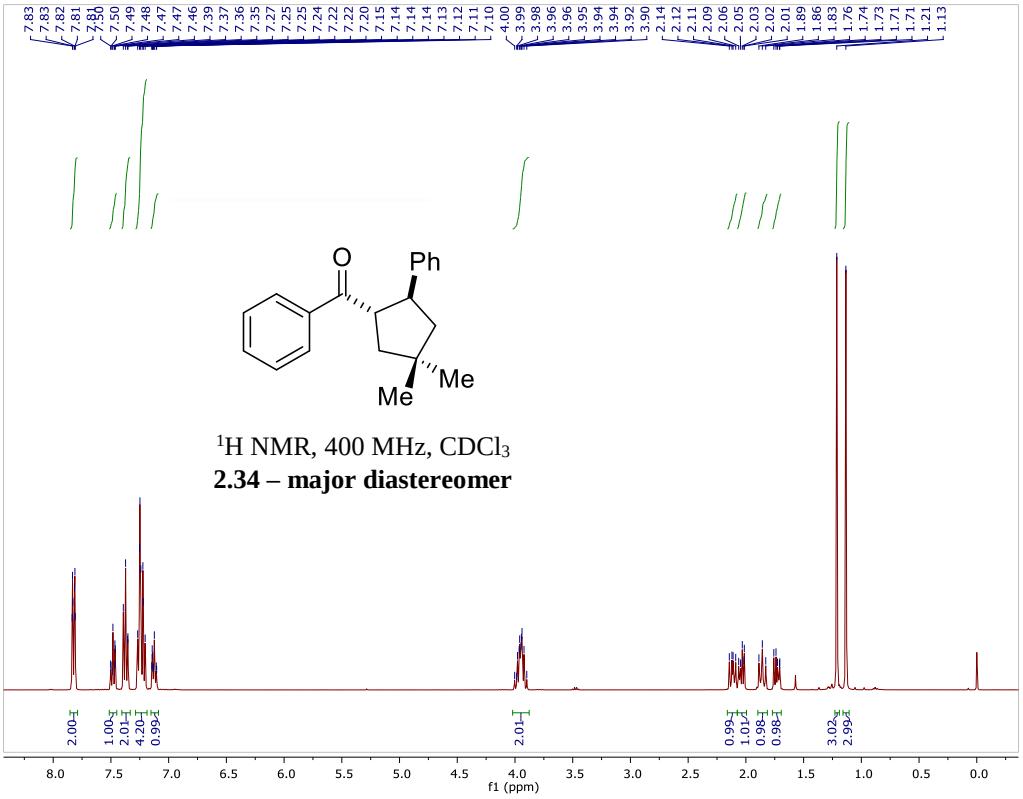

^{1}H NMR, 400 MHz, $CDCl_3$

2.34 – major diastereomer

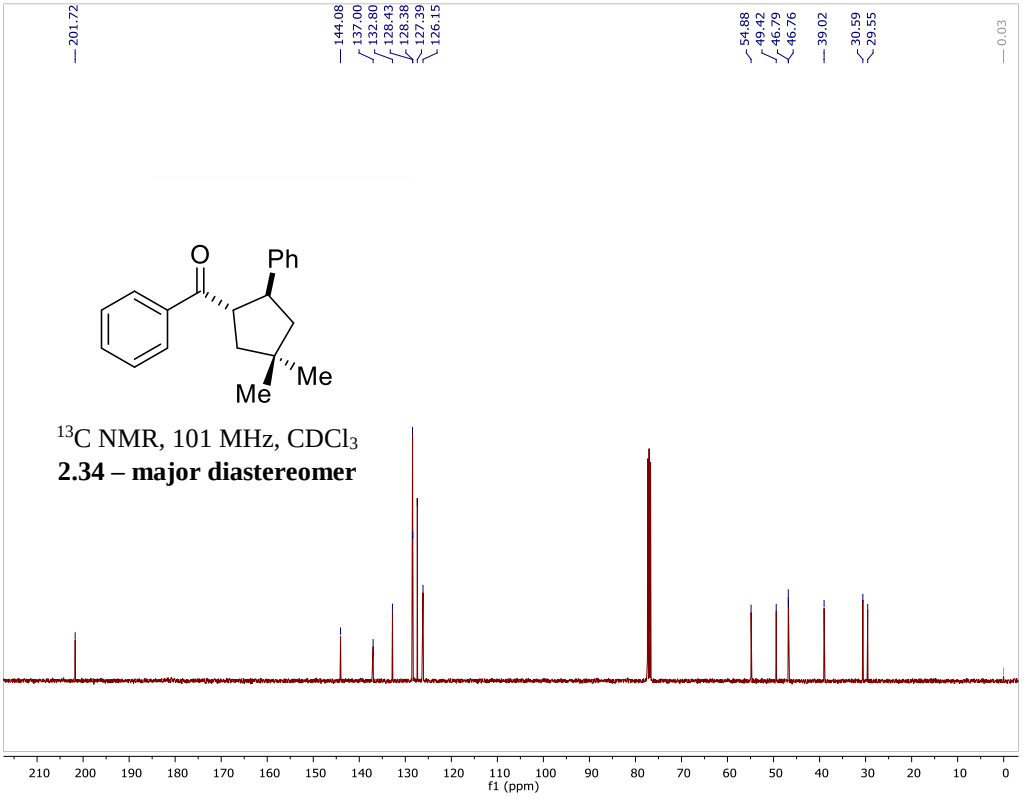

^{13}C NMR, 101 MHz, $CDCl_3$

2.34 – major diastereomer

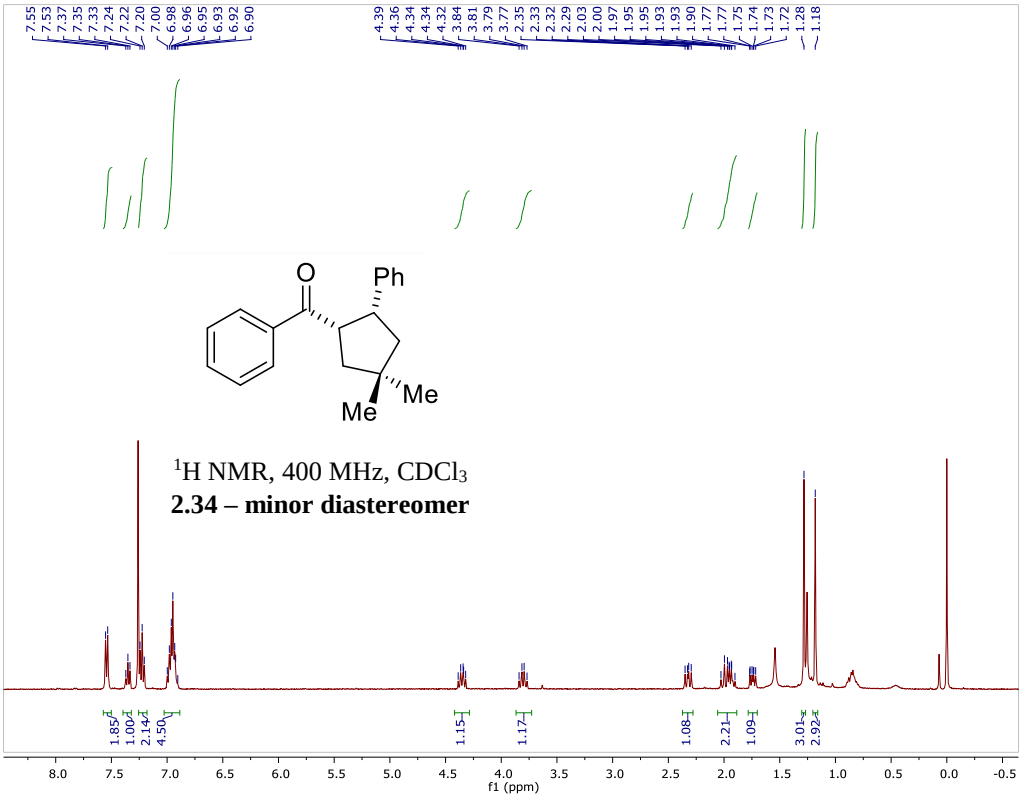

^{1}H NMR, 400 MHz, $CDCl_3$

2.34 – minor diastereomer

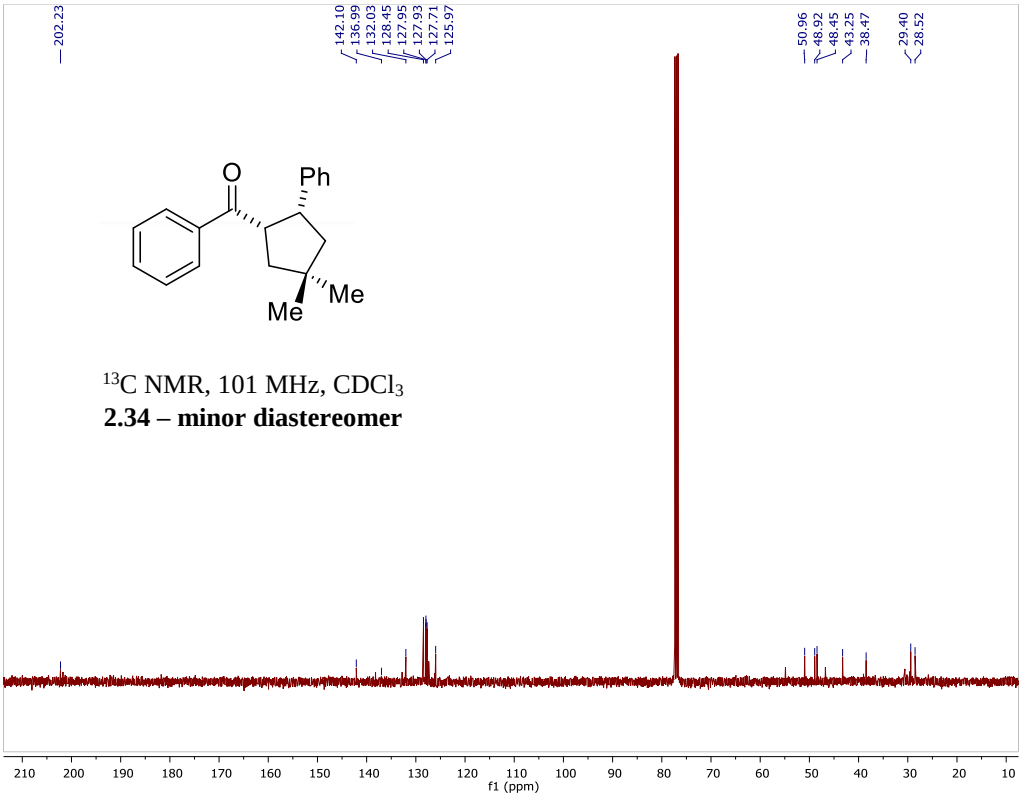

^{13}C NMR, 101 MHz, $CDCl_3$

2.34 – minor diastereomer

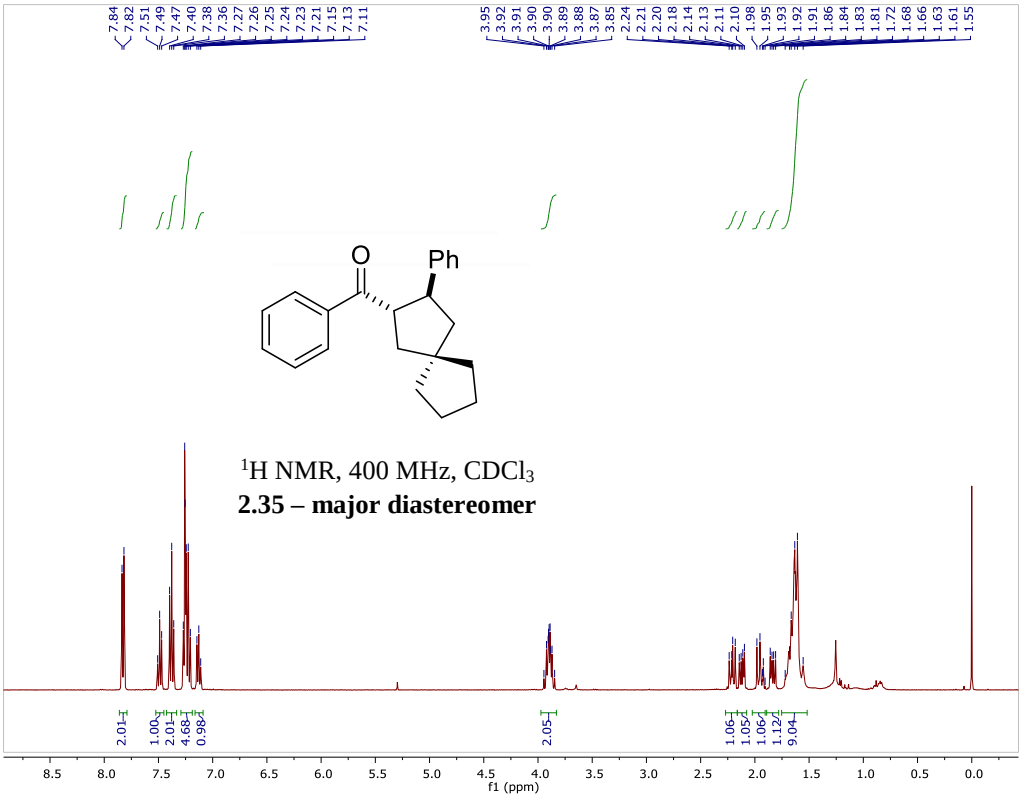
O
Ph
^{1}H NMR, 400 MHz, $CDCl_3$
2.35 – major diastereomer
f1 (ppm)

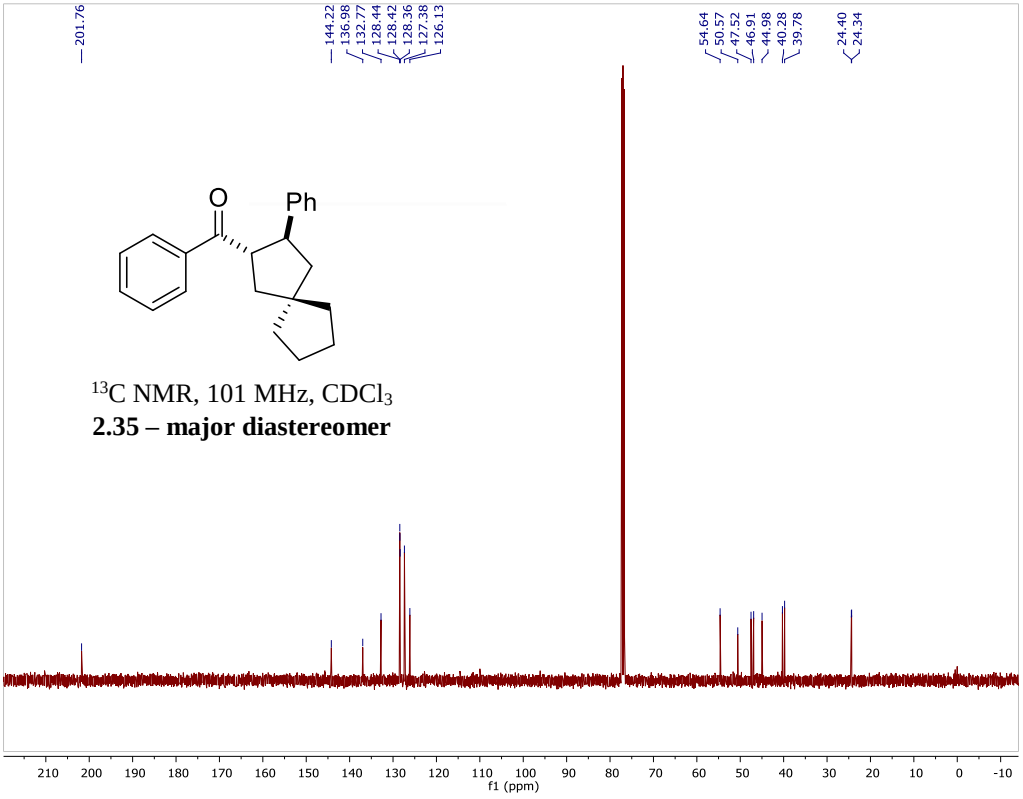
O
Ph
^{13}C NMR, 101 MHz, $CDCl_3$
2.35 – major diastereomer
f1 (ppm)

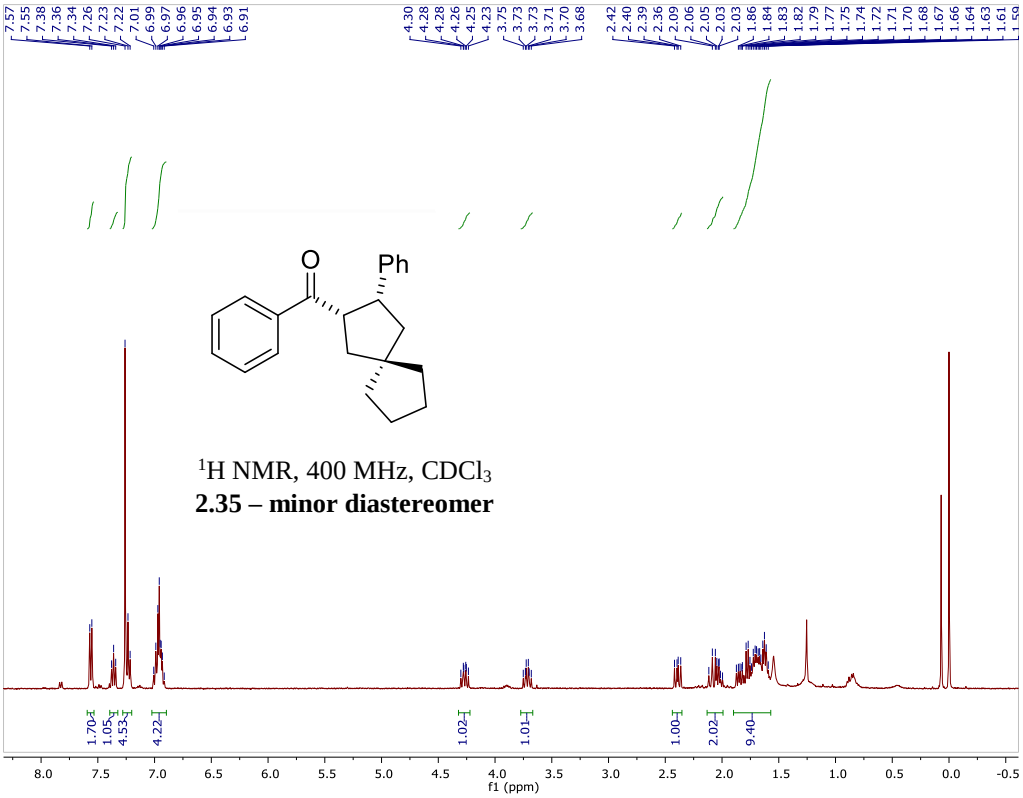
O
Ph
^{1}H NMR, 400 MHz, $CDCl_3$
2.35 – minor diastereomer
f1 (ppm)

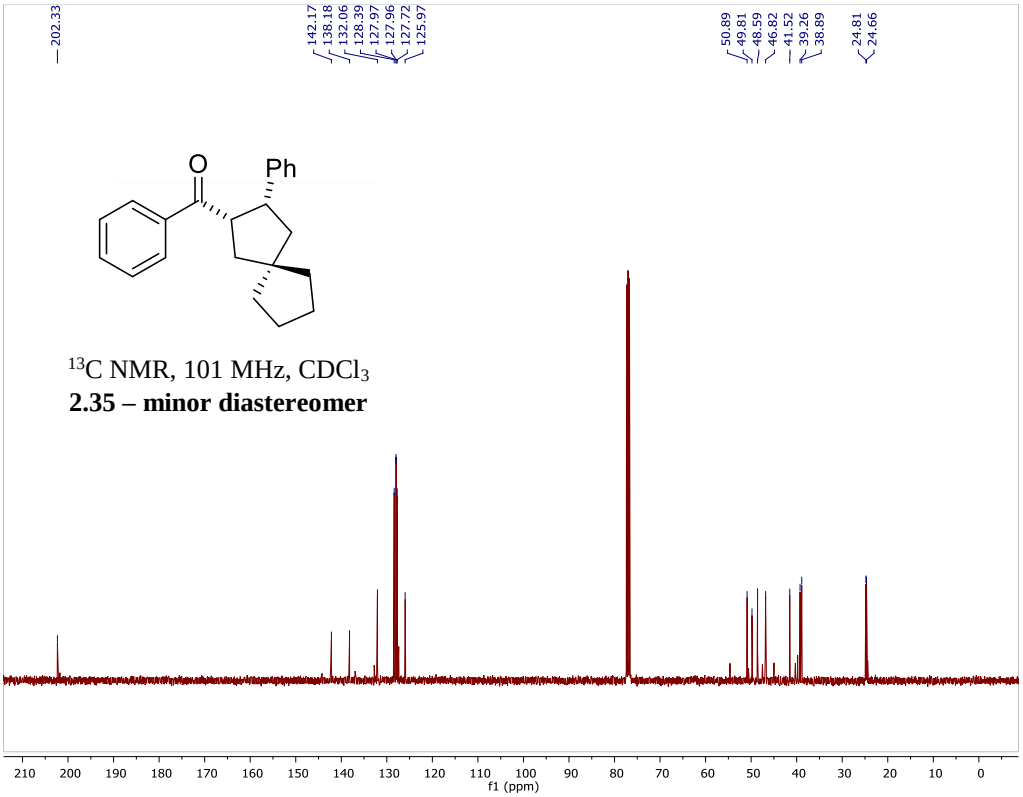
O
Ph
^{13}C NMR, 101 MHz, $CDCl_3$
2.35 – minor diastereomer
f1 (ppm)

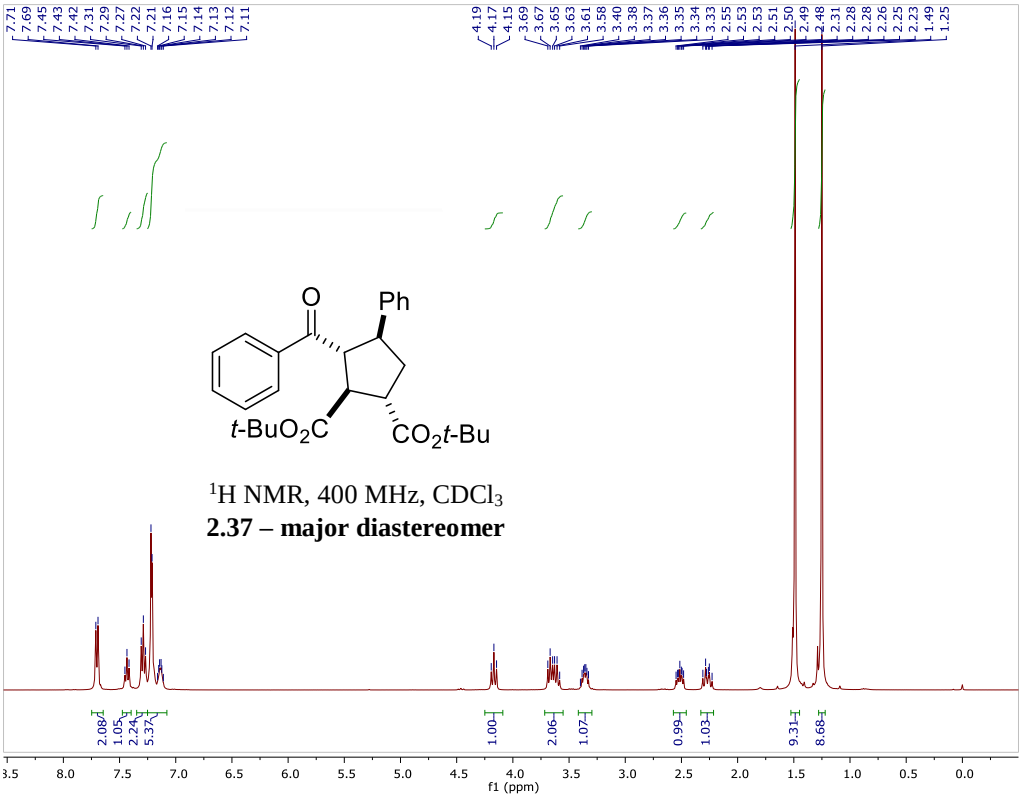

^{1}H NMR, 400 MHz, $CDCl_3$

2.37 – major diastereomer

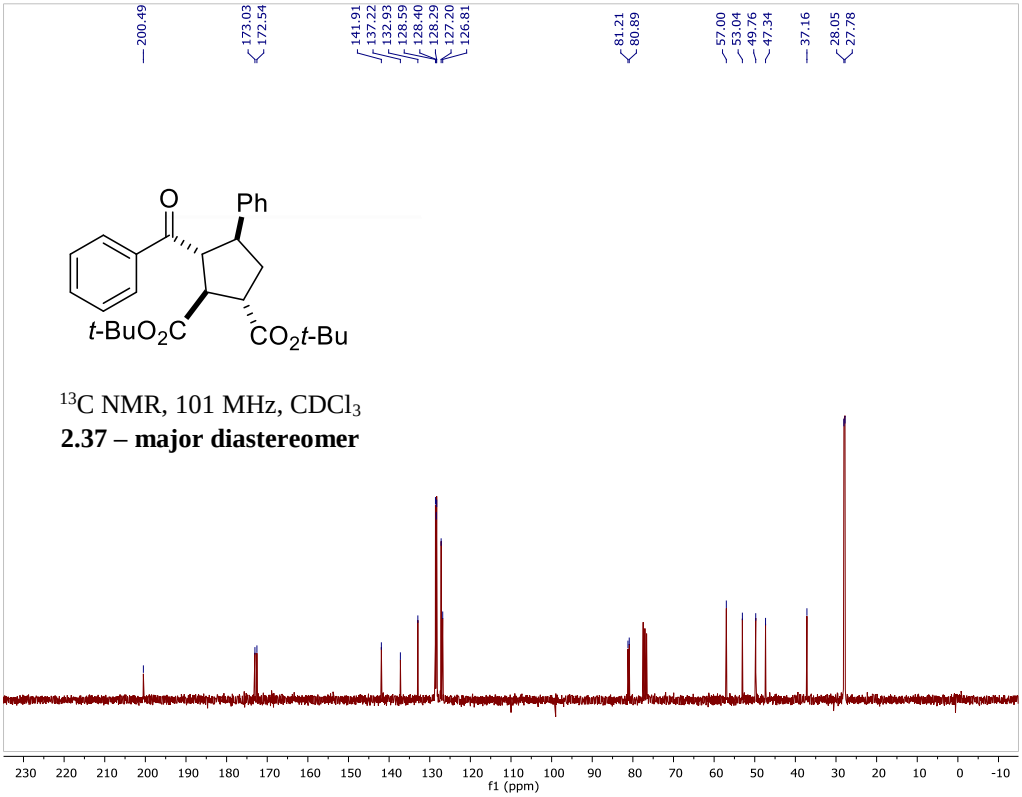

^{13}C NMR, 101 MHz, $CDCl_3$

2.37 – major diastereomer

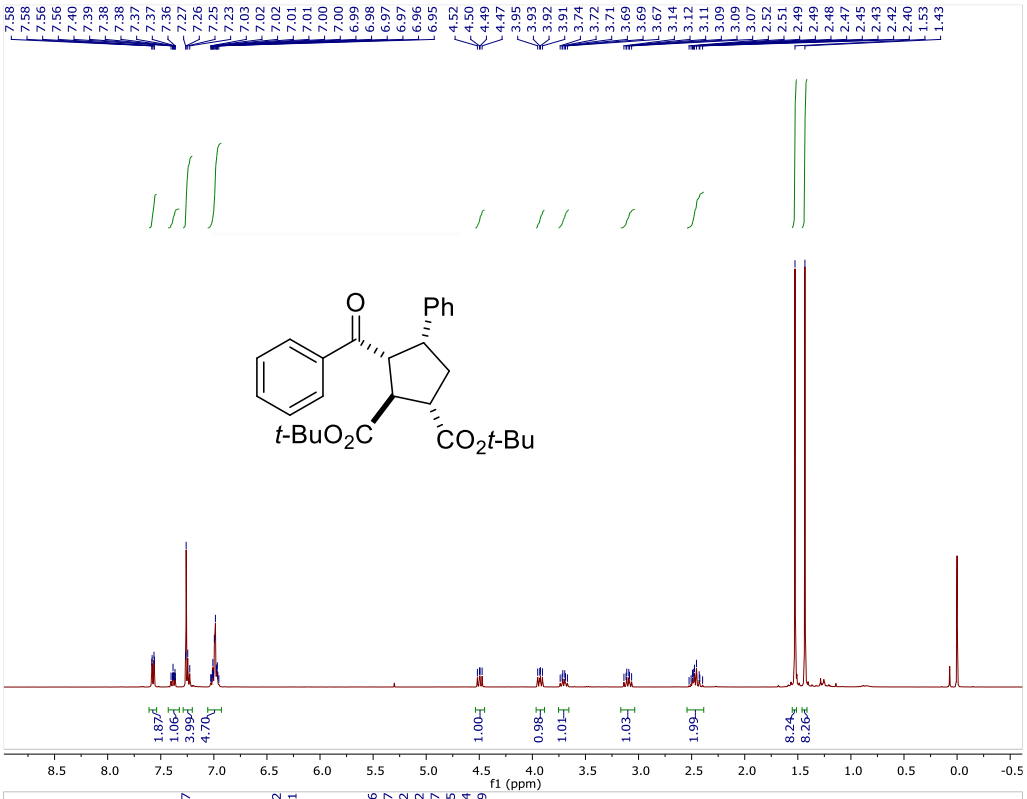

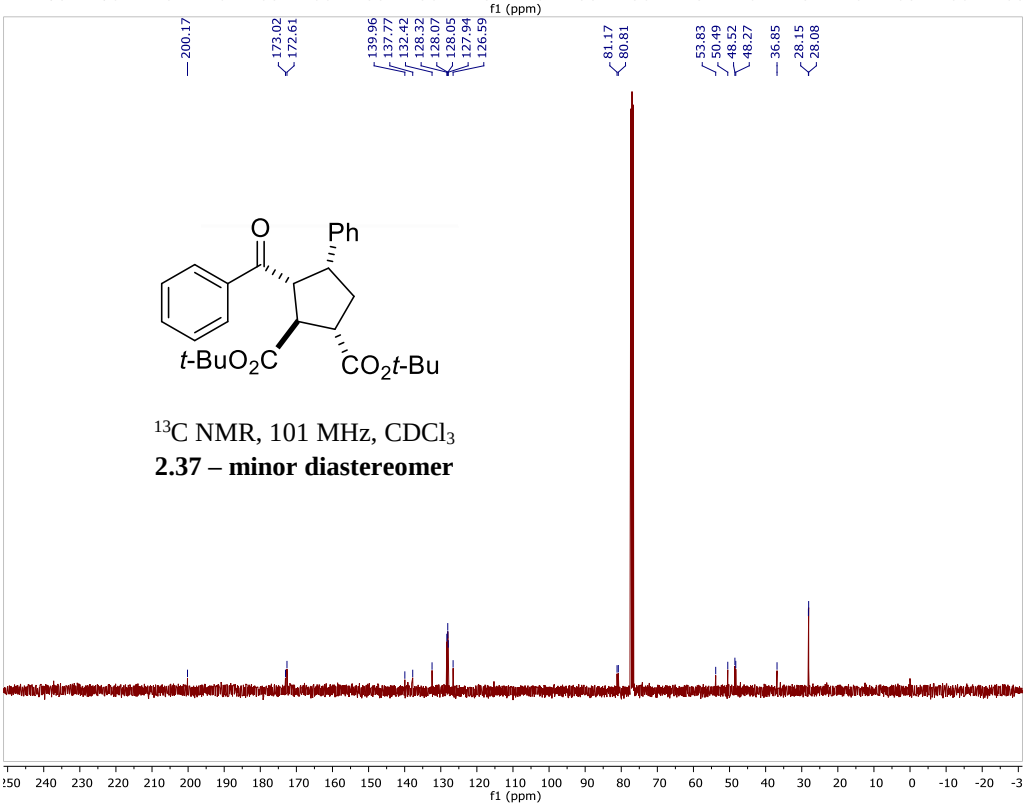

^{13}C NMR, 101 MHz, $CDCl_3$

2.37 – minor diastereomer

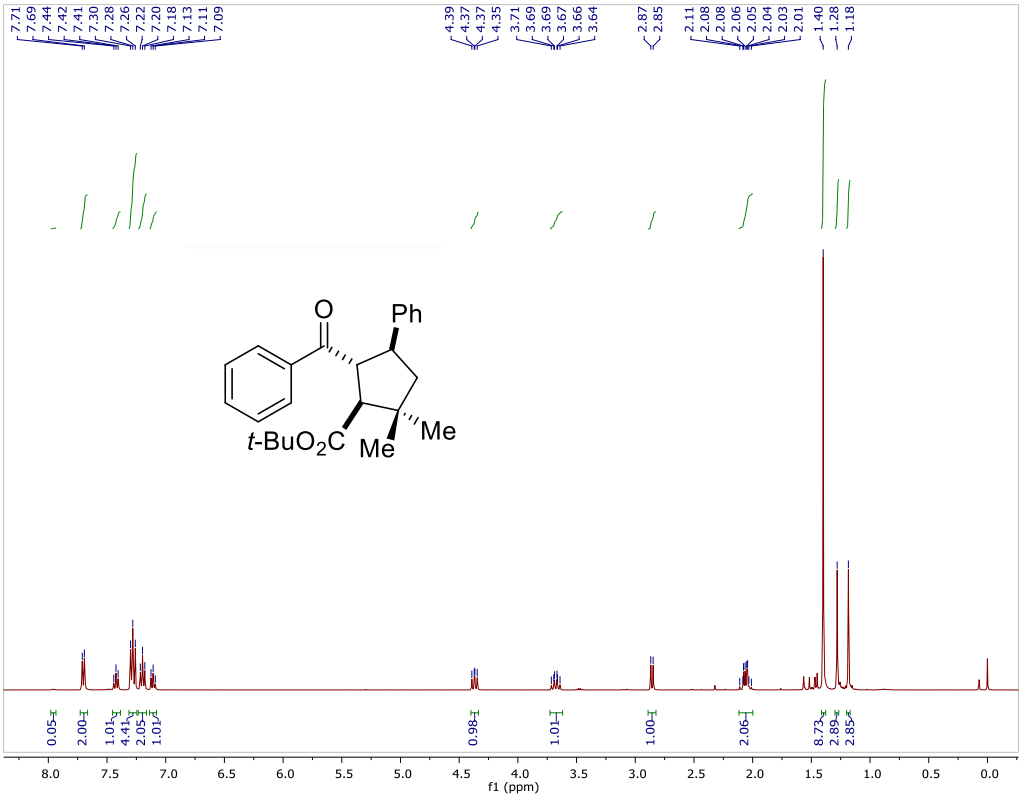

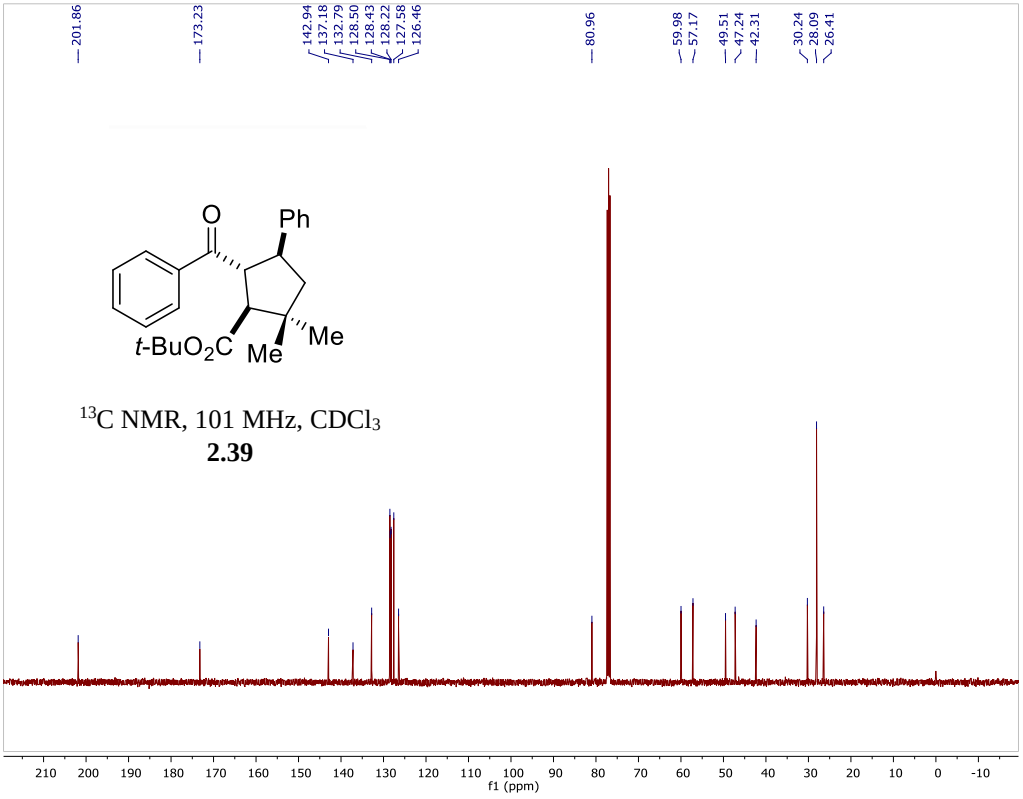

^{13}C NMR, 101 MHz, $CDCl_3$

2.39

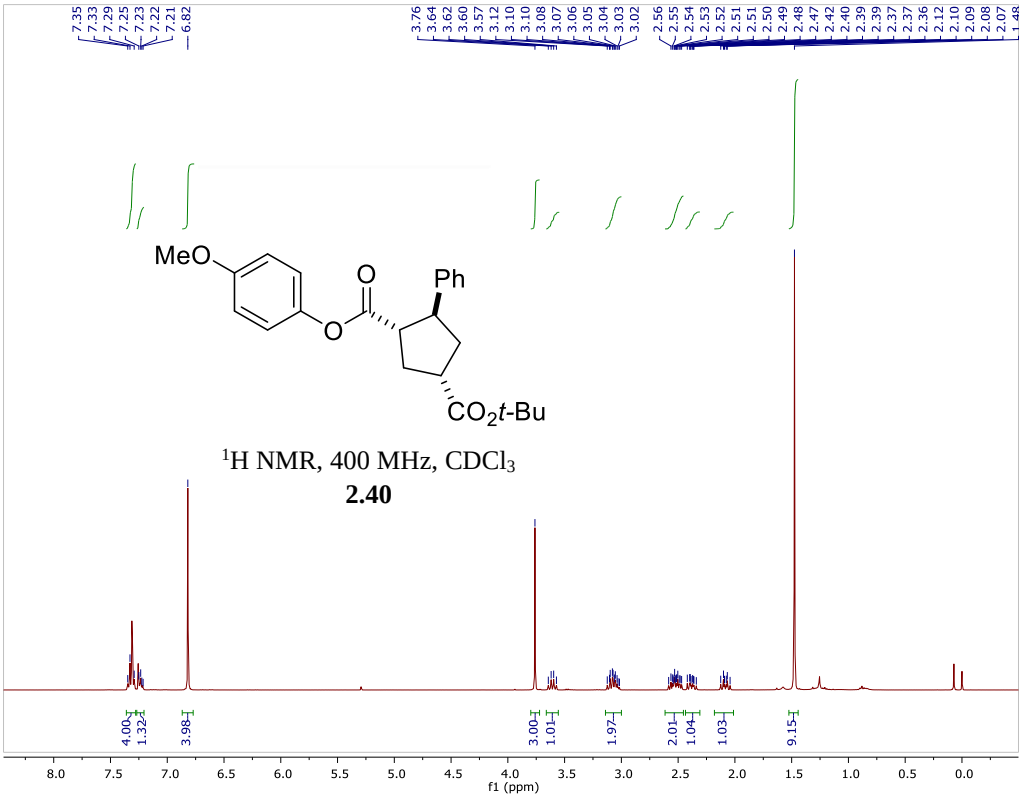

^{1}H NMR, 400 MHz, $CDCl_3$

2.40

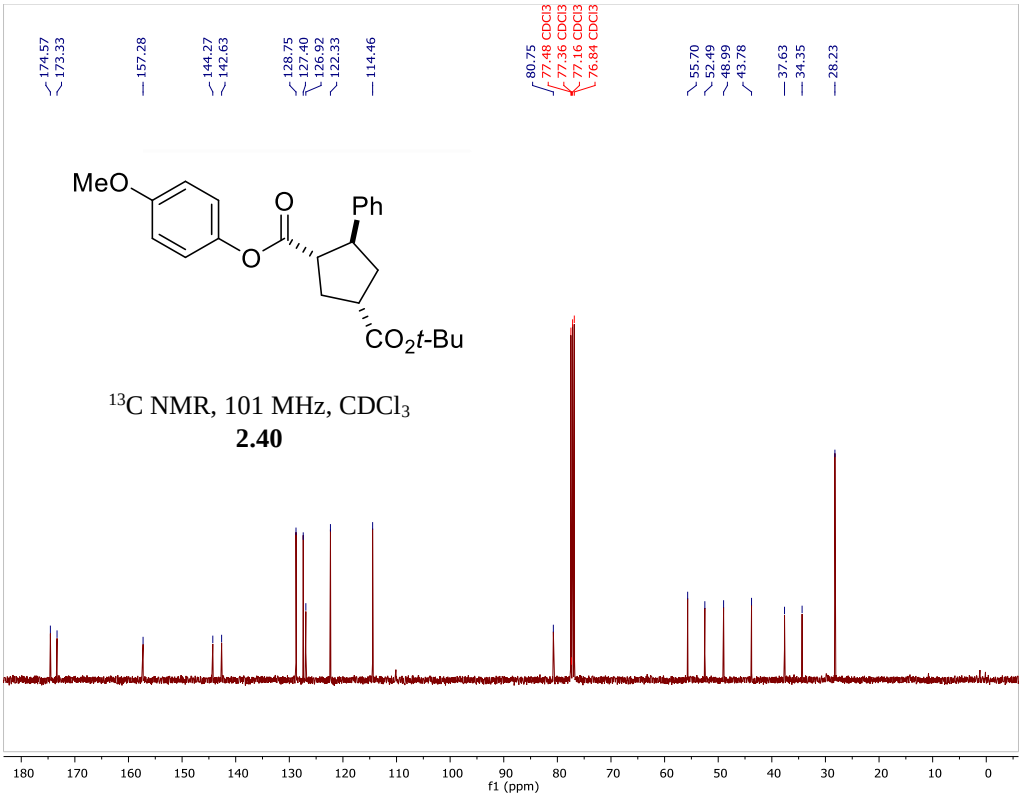

^{13}C NMR, 101 MHz, $CDCl_3$

2.40

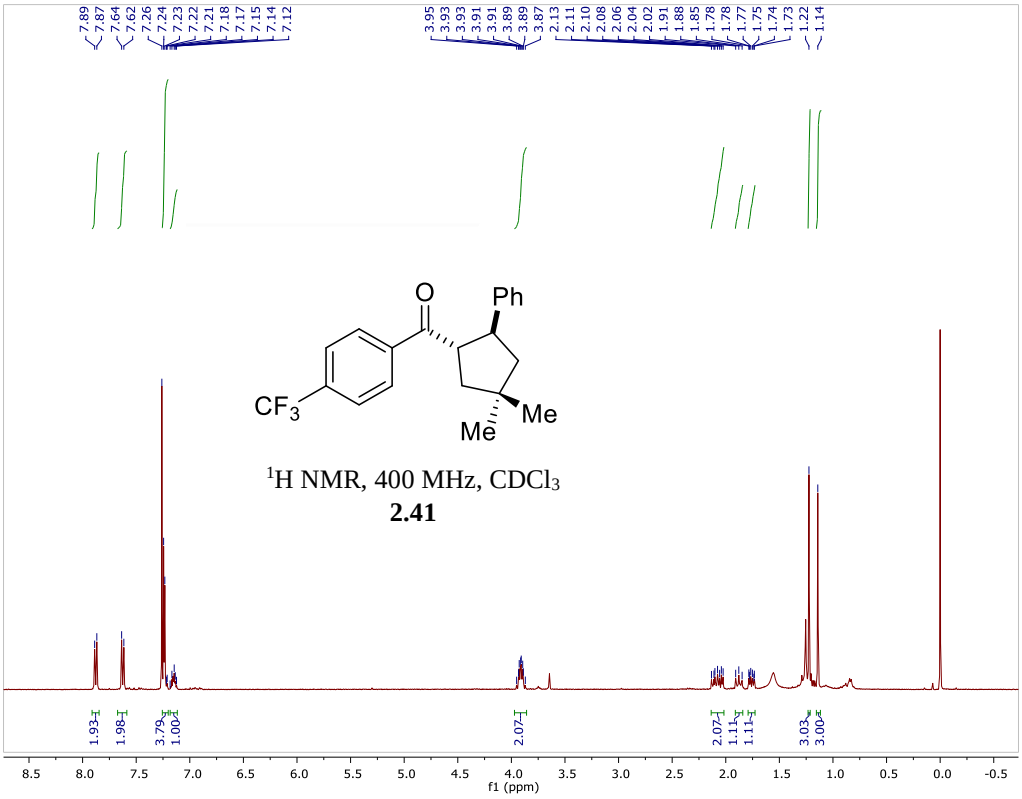

^{1}H NMR, 400 MHz, $CDCl_3$

2.41

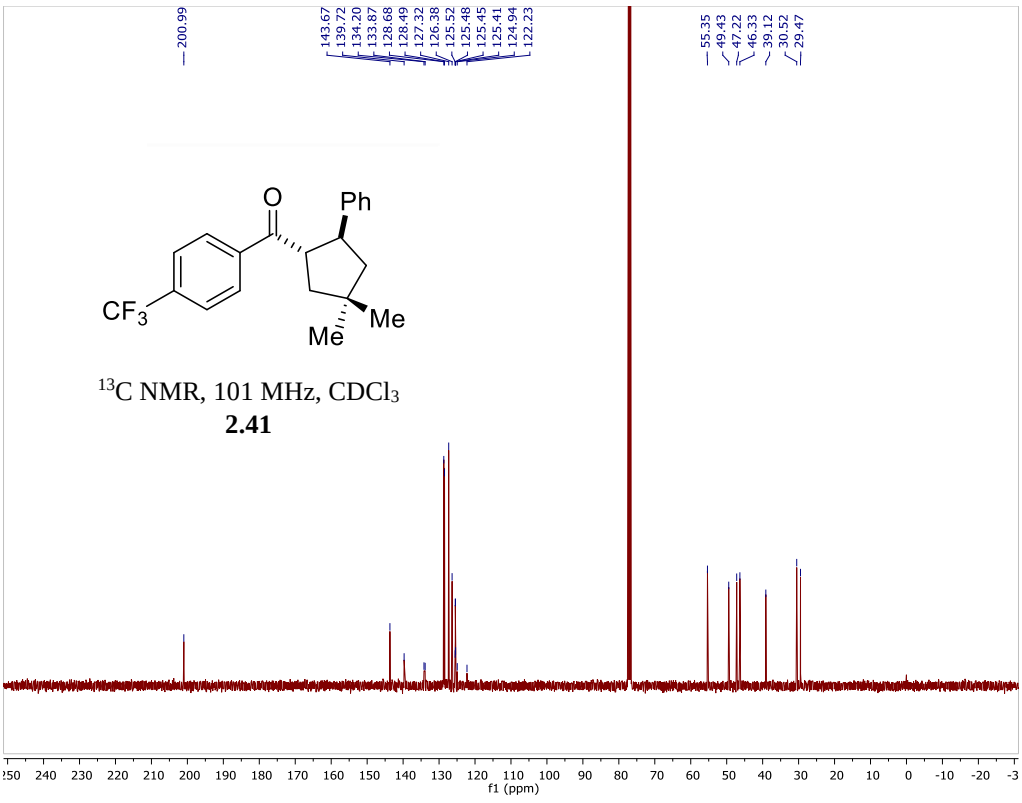

^{13}C NMR, 101 MHz, $CDCl_3$

2.41

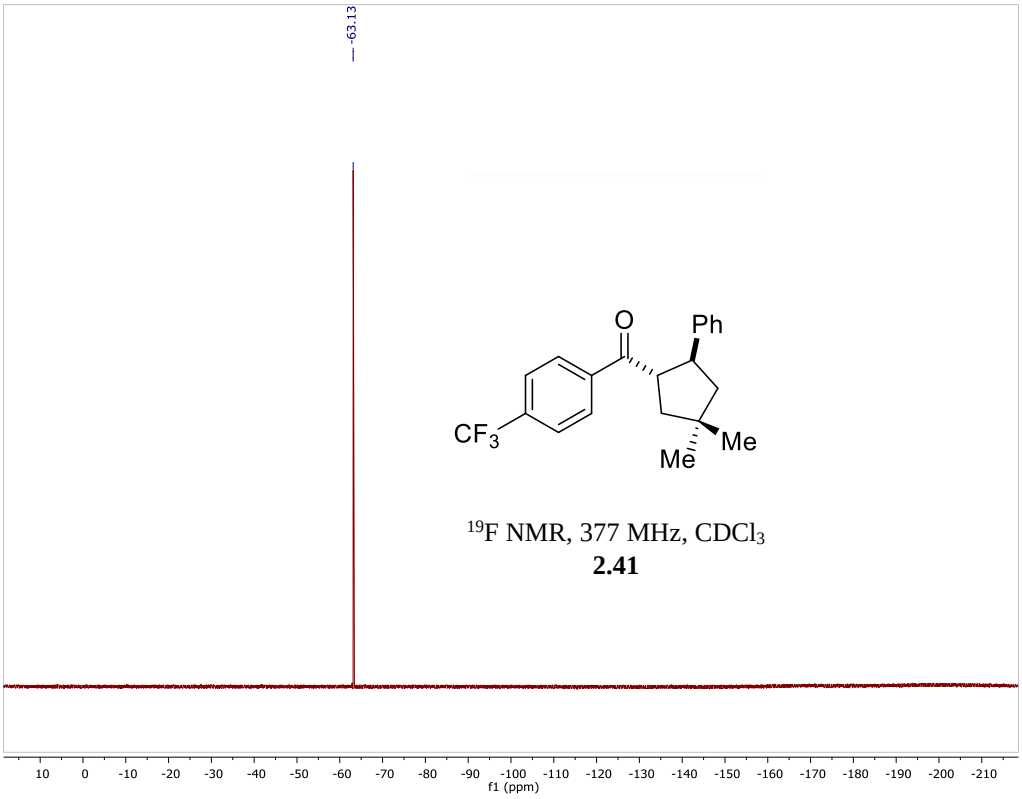

^{19}F NMR, 377 MHz, $CDCl_3$

2.41

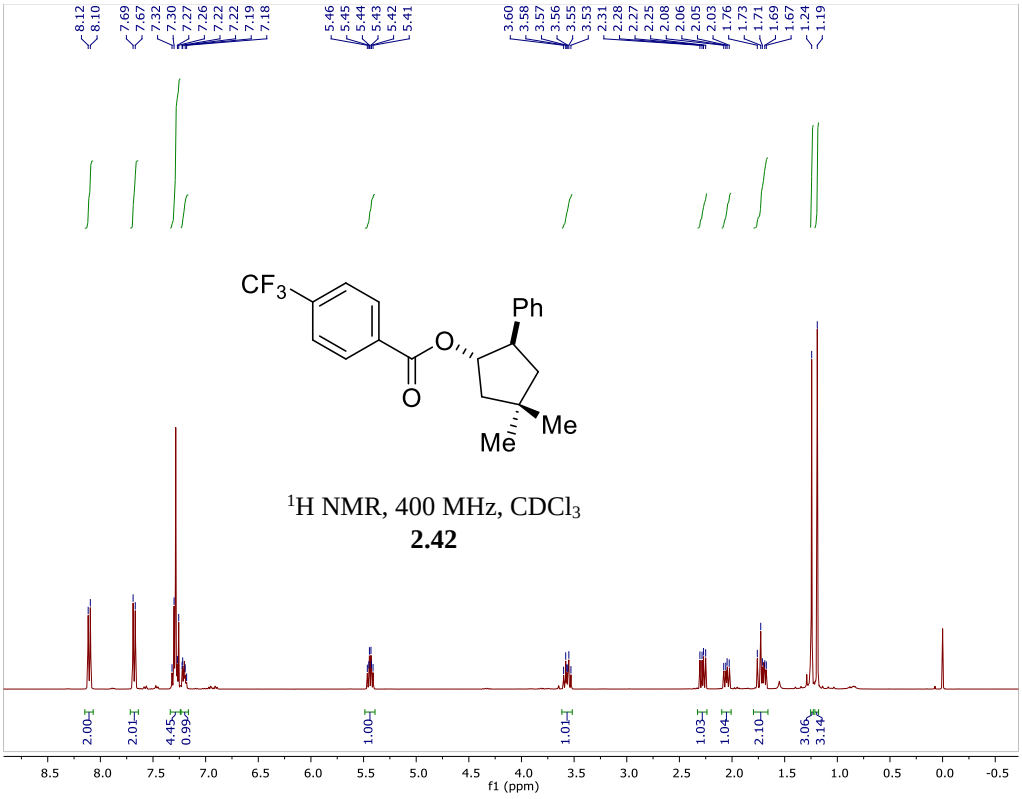

^{1}H NMR, 400 MHz, $CDCl_3$

2.42

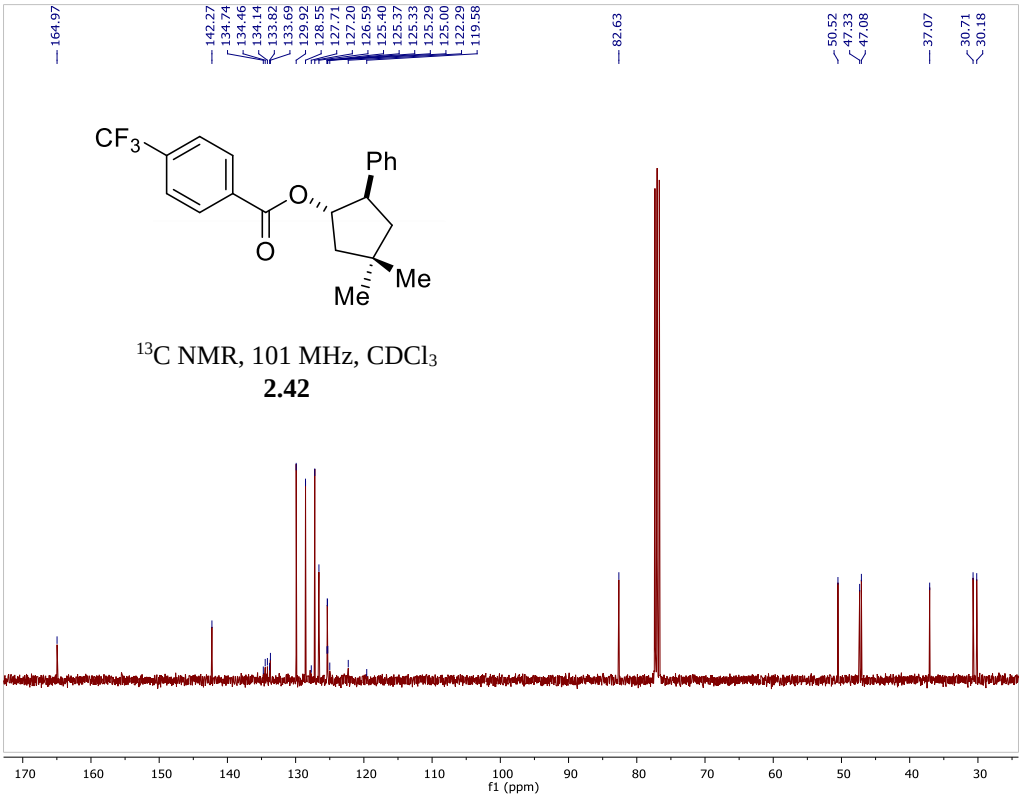

^{13}C NMR, 101 MHz, $CDCl_3$

2.42

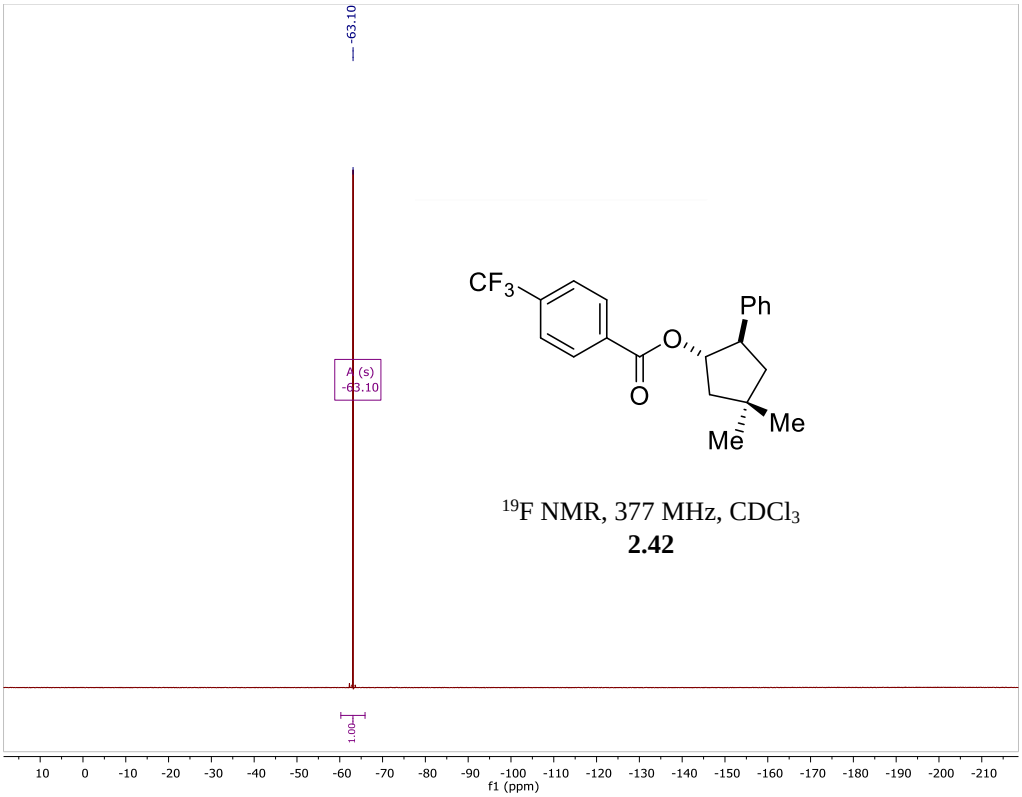

^{19}F NMR, 377 MHz, $CDCl_3$

2.42

Figure A-2. List of New Compounds for Chapter 3

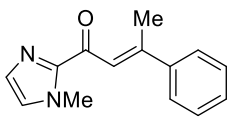

3.37

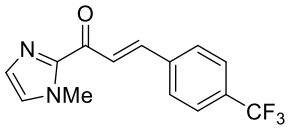

3.38

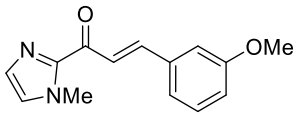

3.39

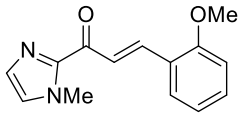

3.40

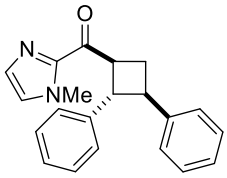

3.13

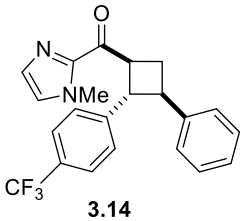

3.14

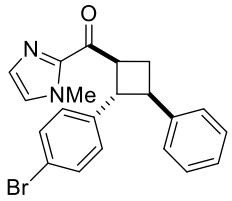

3.15

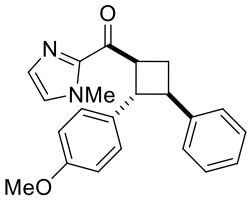

3.16

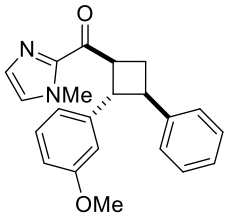

3.17

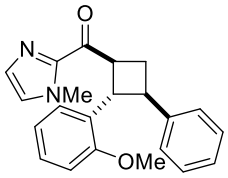

3.18

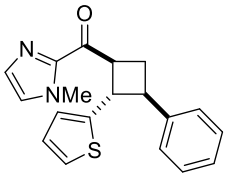

3.19

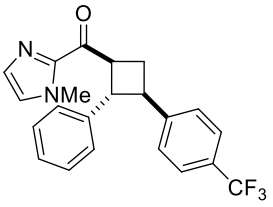

3.23

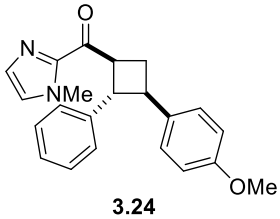

3.24

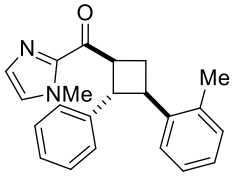

3.25

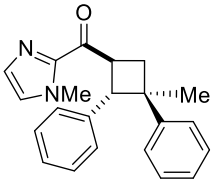

3.26

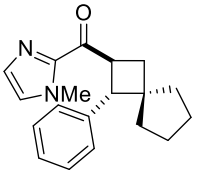

3.27

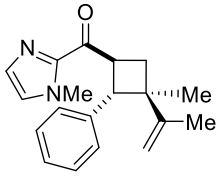

3.28

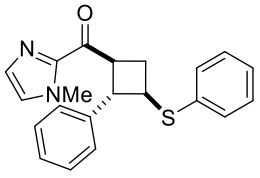

3.29

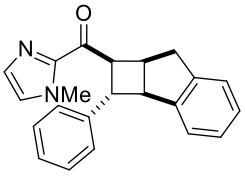

3.32

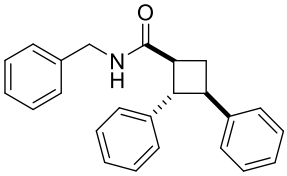

3.35

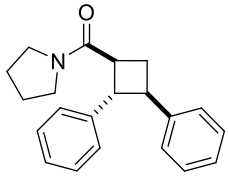

3.36

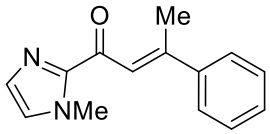

^{1}H NMR, 500 MHz, $CDCl_3$

3.37

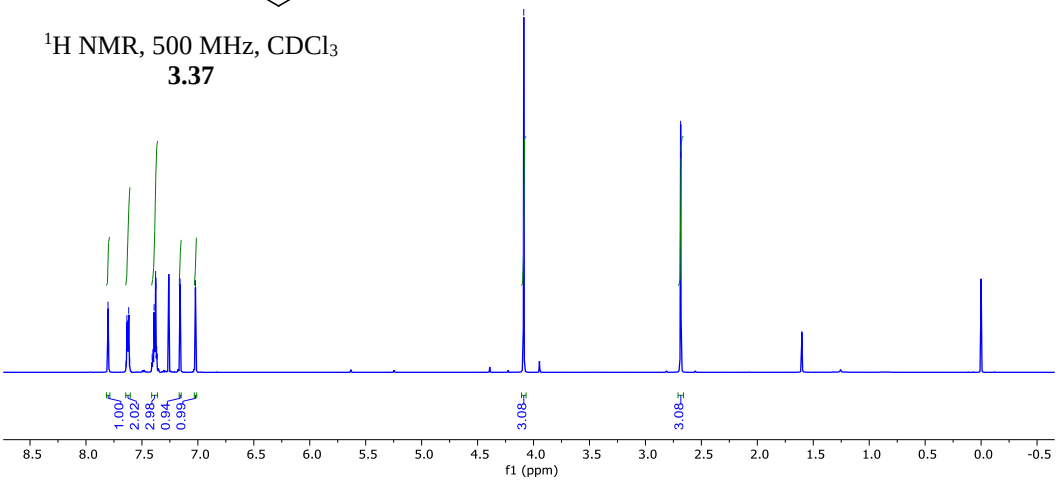

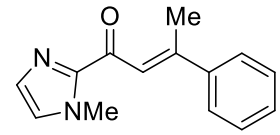

^{13}C NMR, 125 MHz, $CDCl_3$

3.37

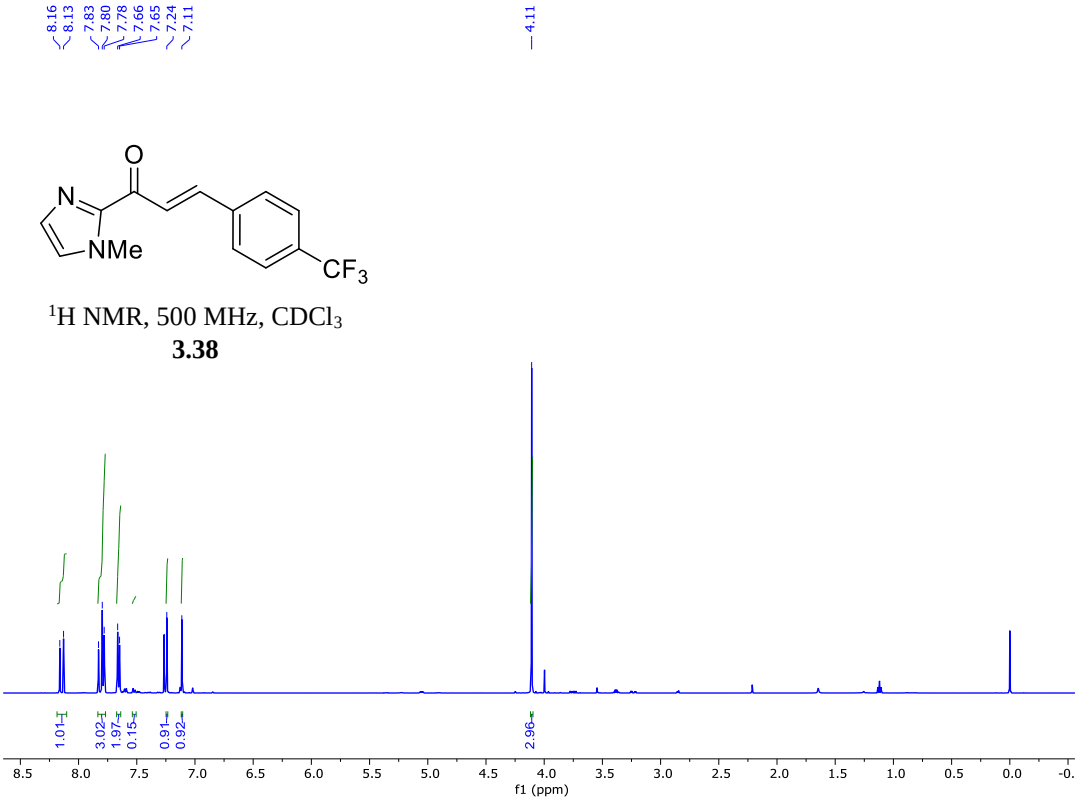

^{1}H NMR, 500 MHz, $CDCl_3$

3.38

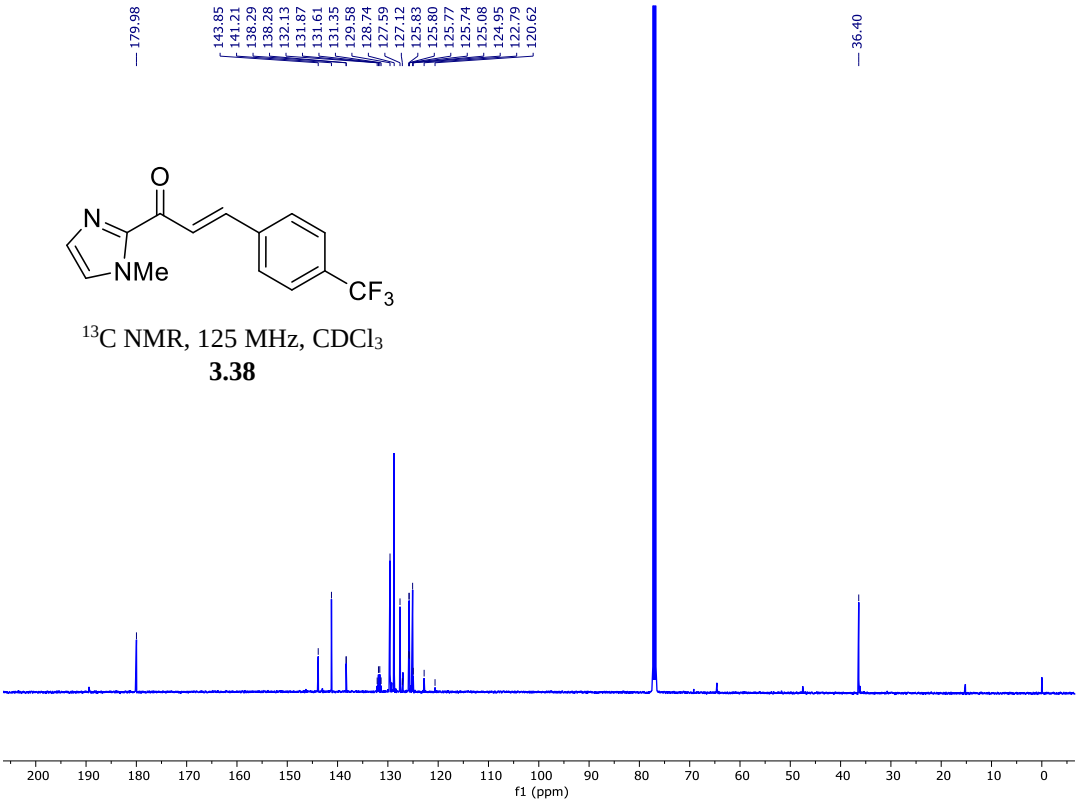

^{13}C NMR, 125 MHz, $CDCl_3$

3.38

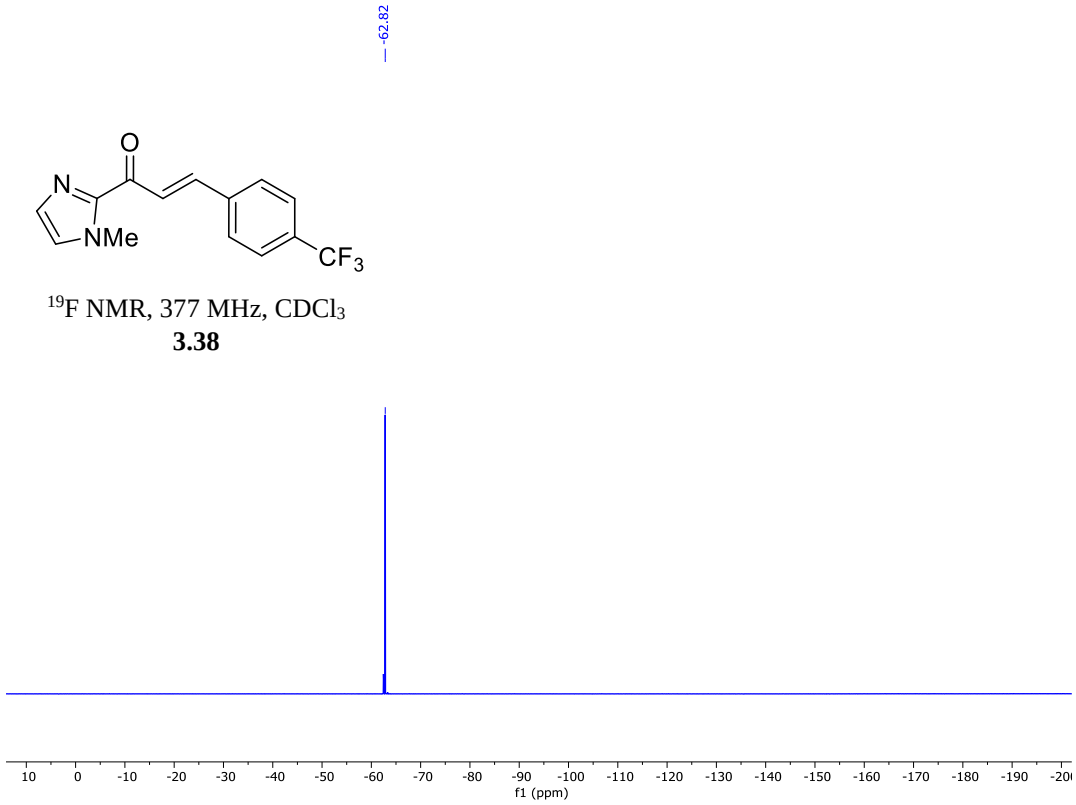

^{19}F NMR, 377 MHz, $CDCl_3$

3.38

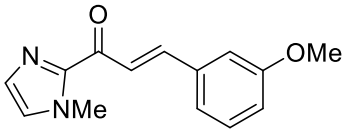

^{1}H NMR, 500 MHz, $CDCl_3$

3.39

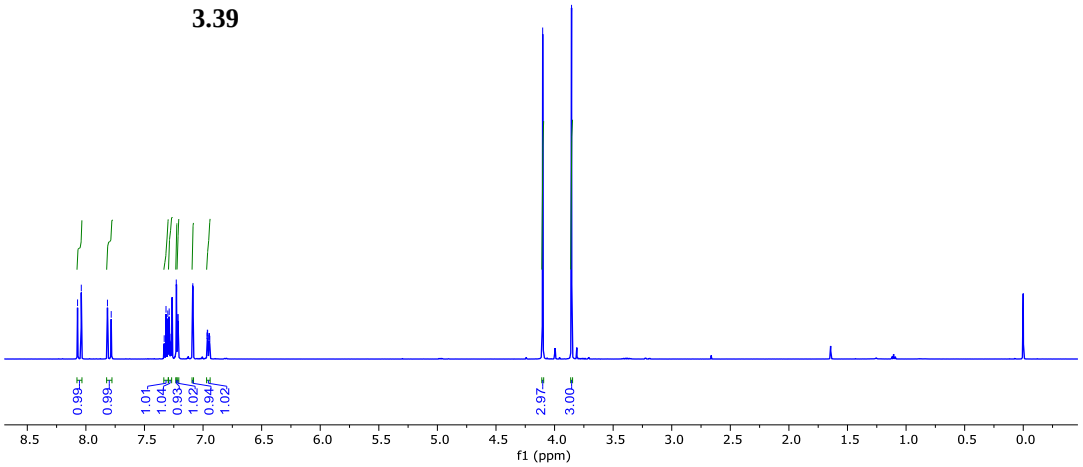

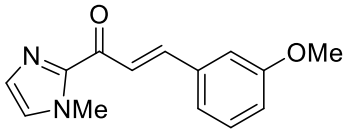

^{13}C NMR, 125 MHz, $CDCl_3$

3.39

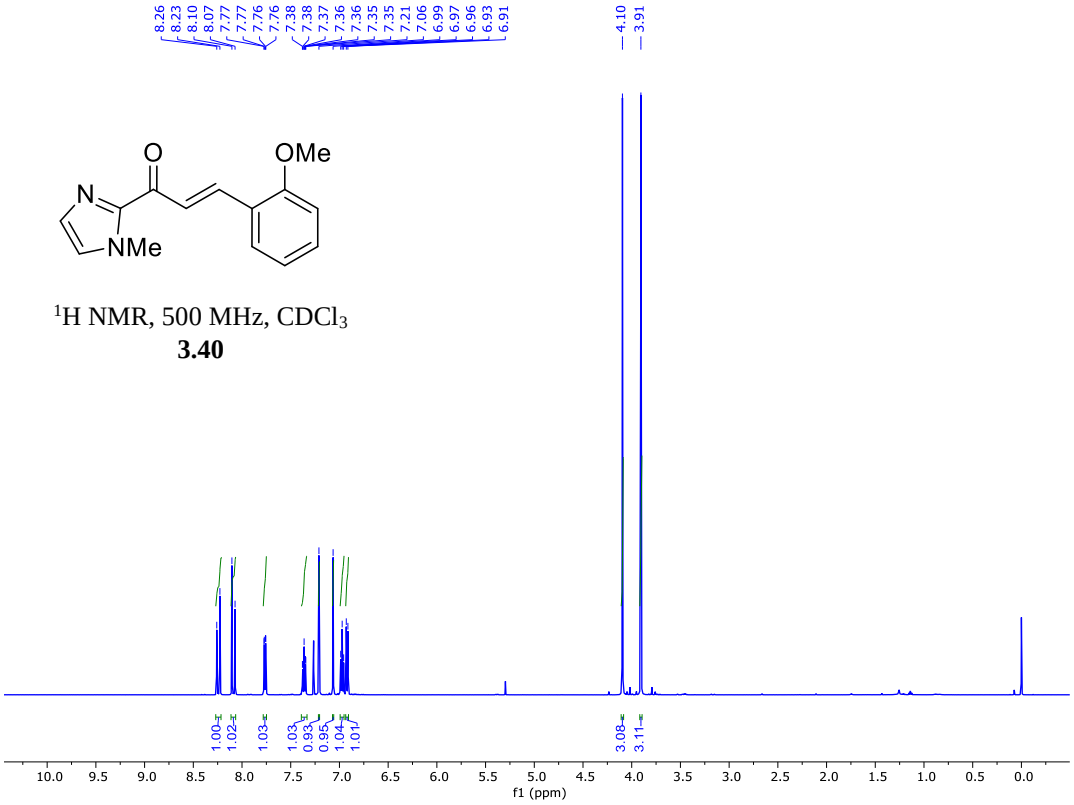

^{1}H NMR, 500 MHz, $CDCl_3$
3.40

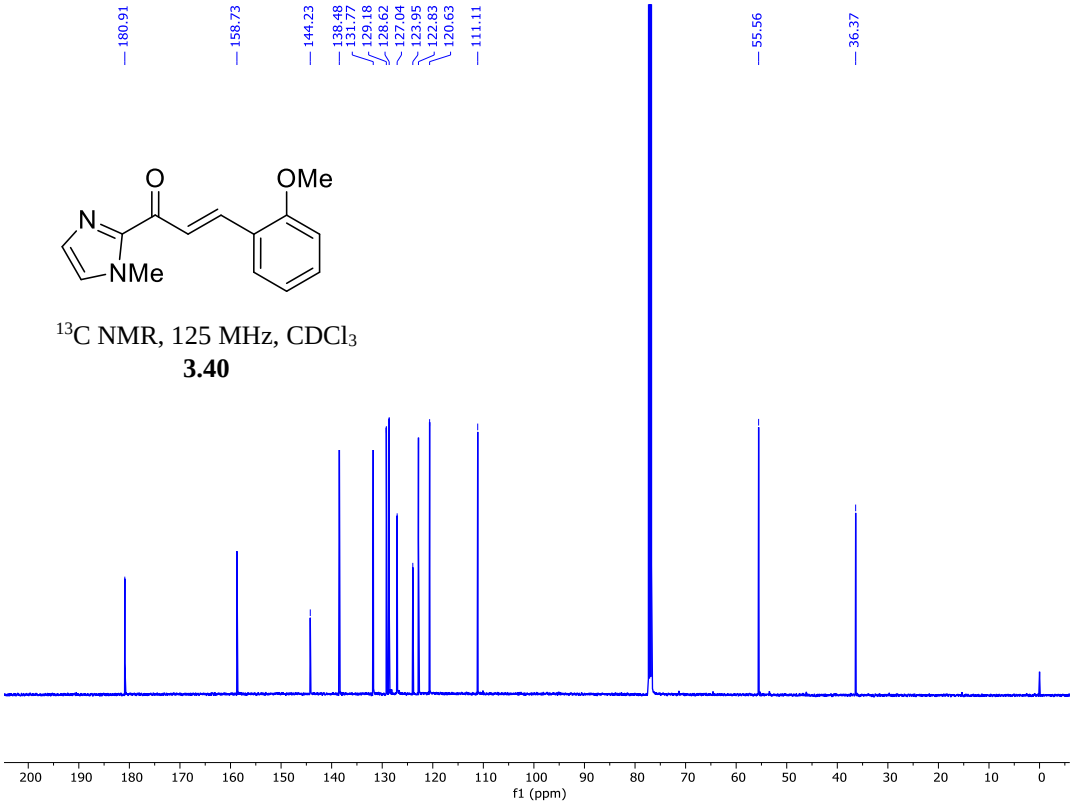

^{13}C NMR, 125 MHz, $CDCl_3$
3.40

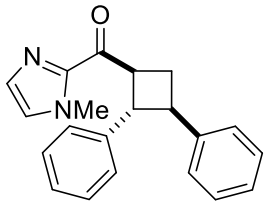

^{1}H NMR, 500 MHz, $CDCl_3$

3.13 – major diastereomer

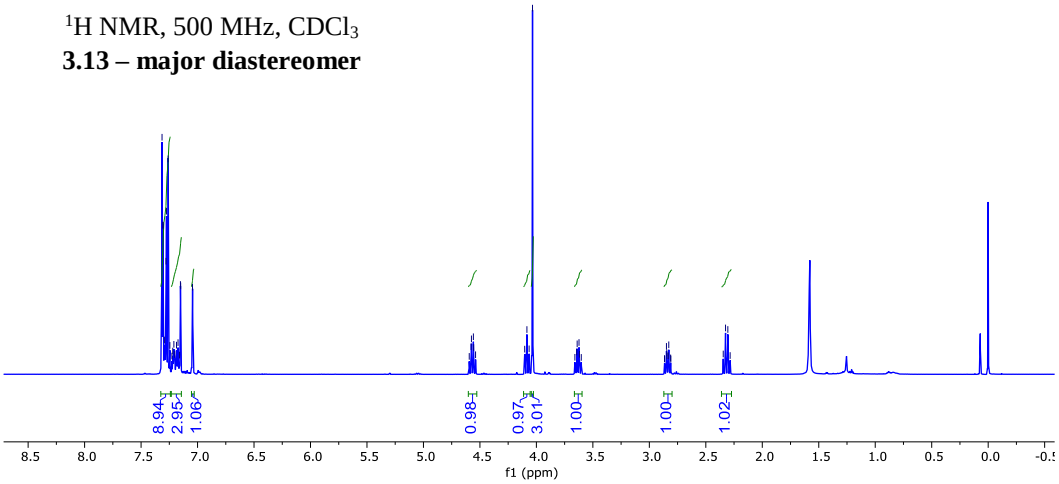

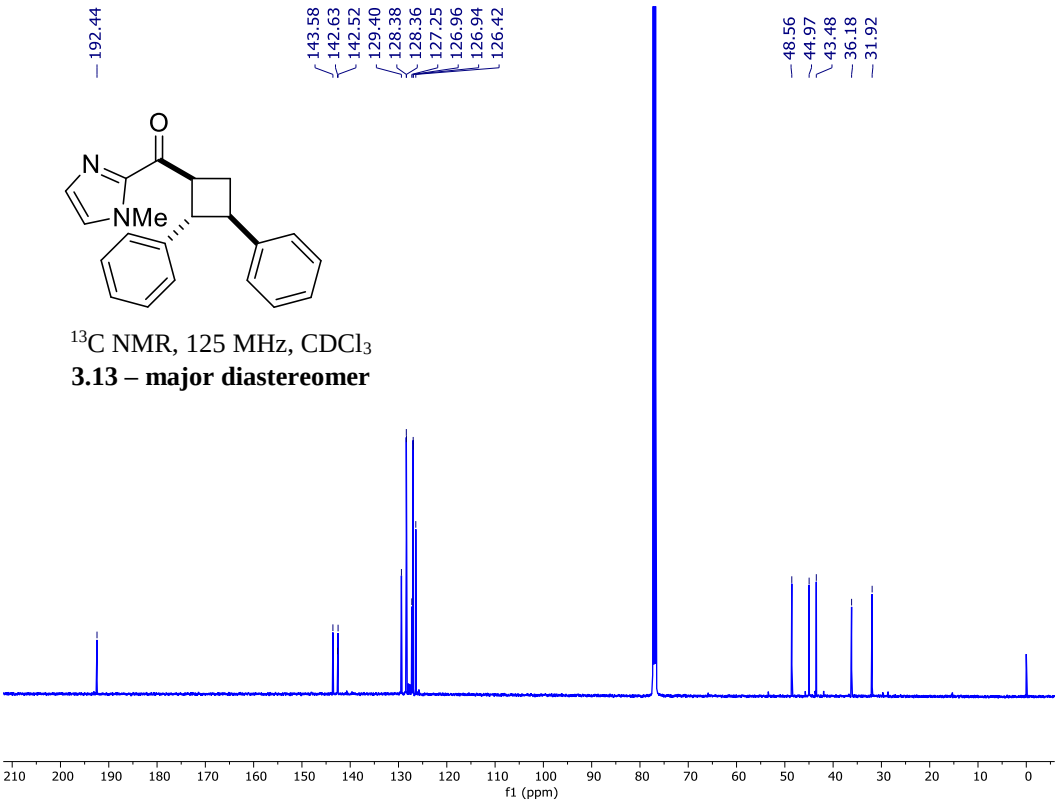

^{13}C NMR, 125 MHz, $CDCl_3$

3.13 – major diastereomer

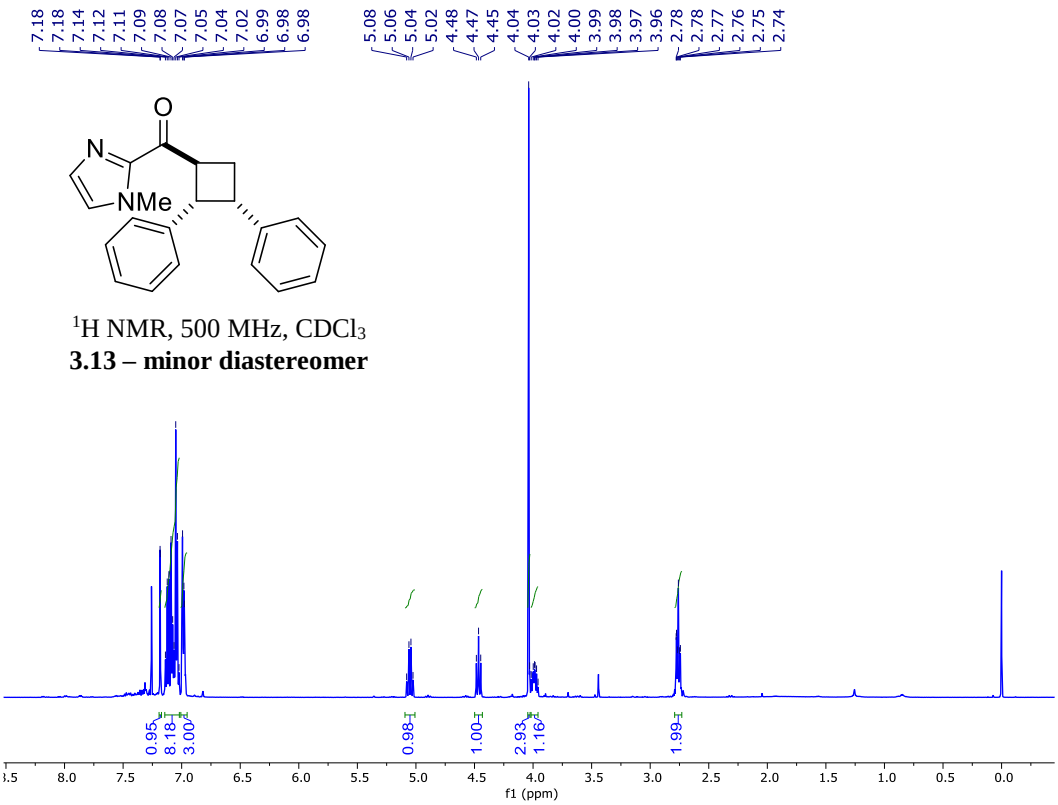

^{1}H NMR, 500 MHz, $CDCl_3$

3.13 – minor diastereomer

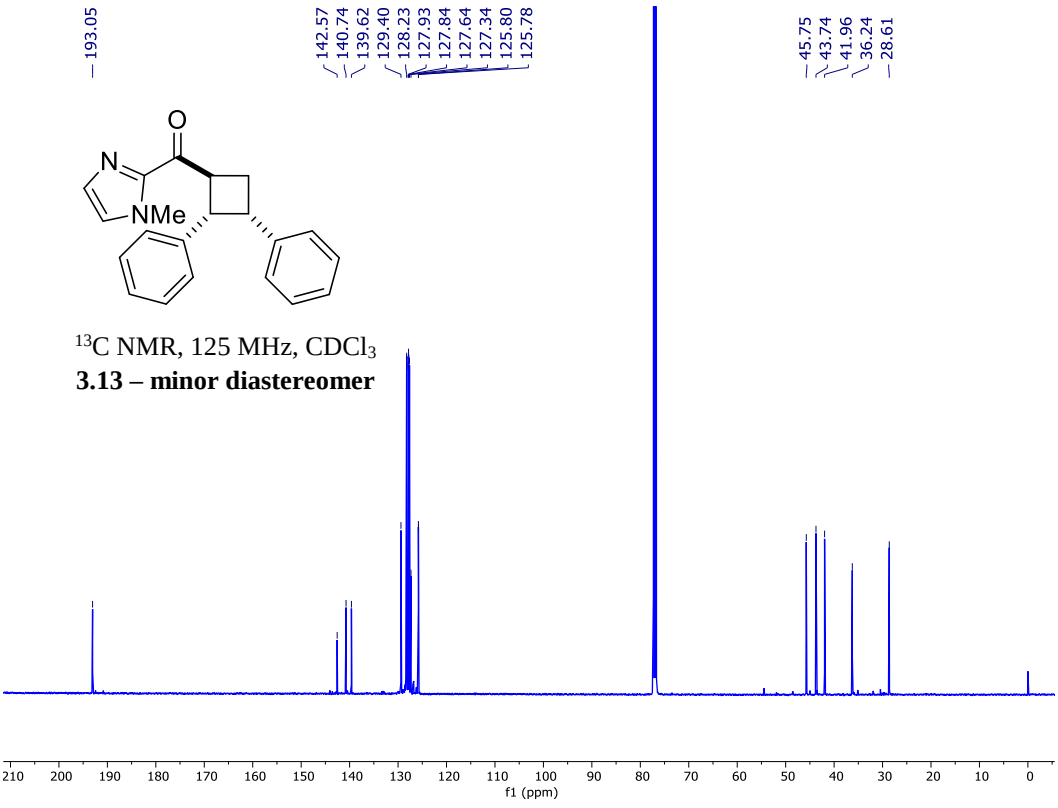

^{13}C NMR, 125 MHz, $CDCl_3$

3.13 – minor diastereomer

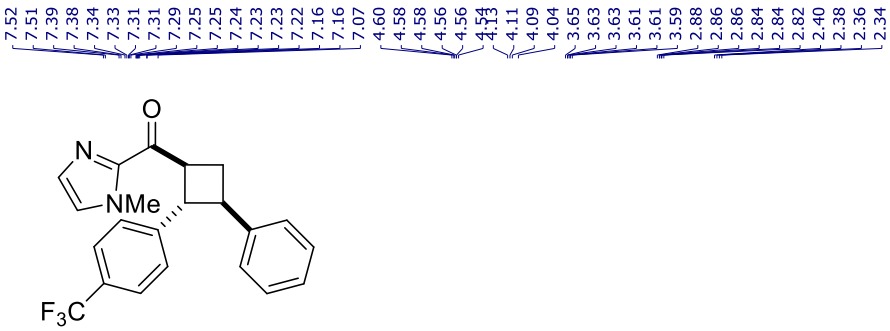

^{1}H NMR, 500 MHz, $CDCl_3$

3.14 – major diastereomer

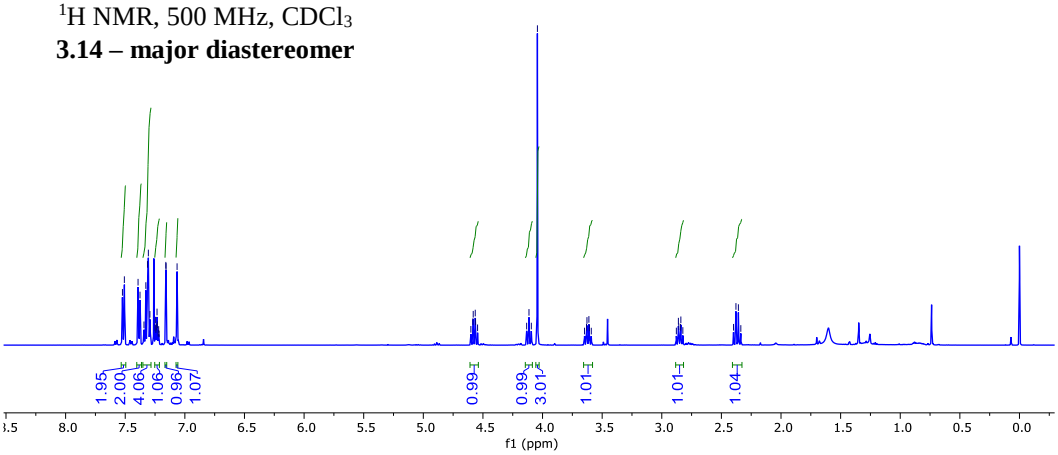

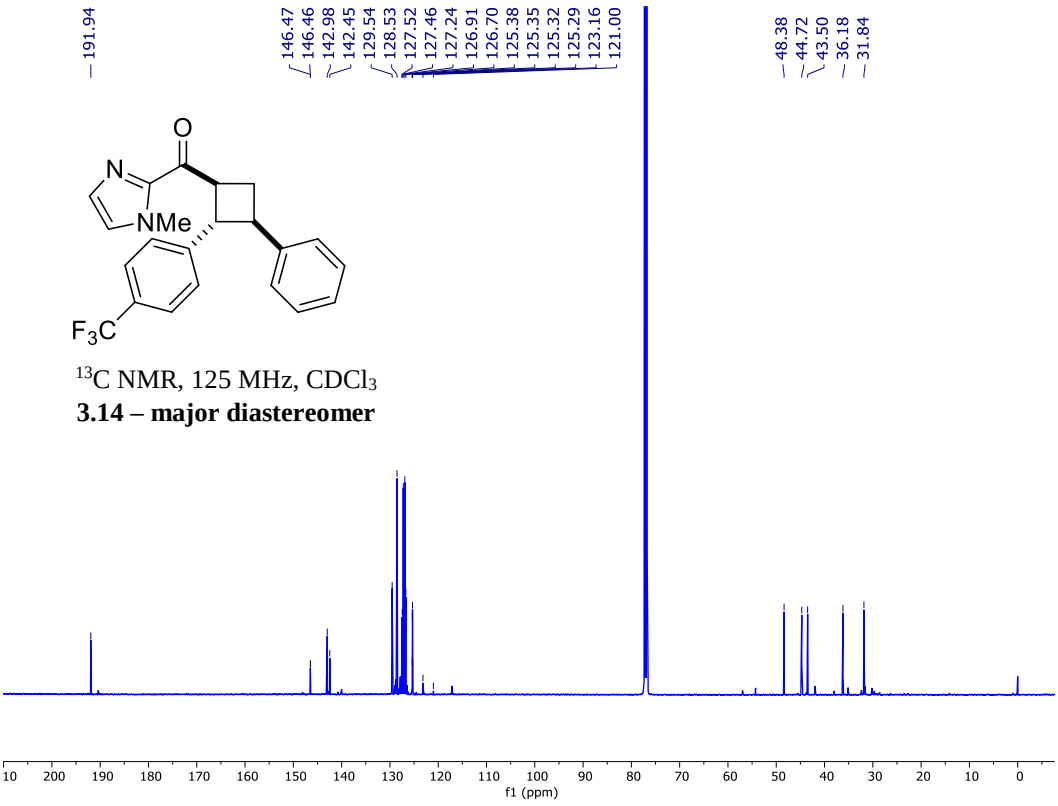

^{13}C NMR, 125 MHz, $CDCl_3$

3.14 – major diastereomer

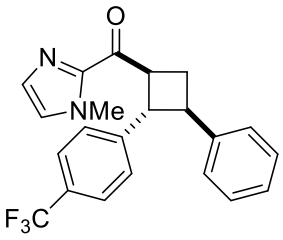

^{19}F NMR, 377 MHz, $CDCl_3$

3.14 – major diastereomer

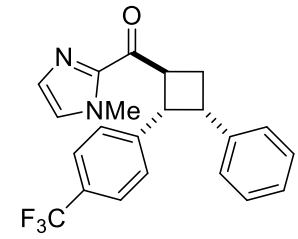

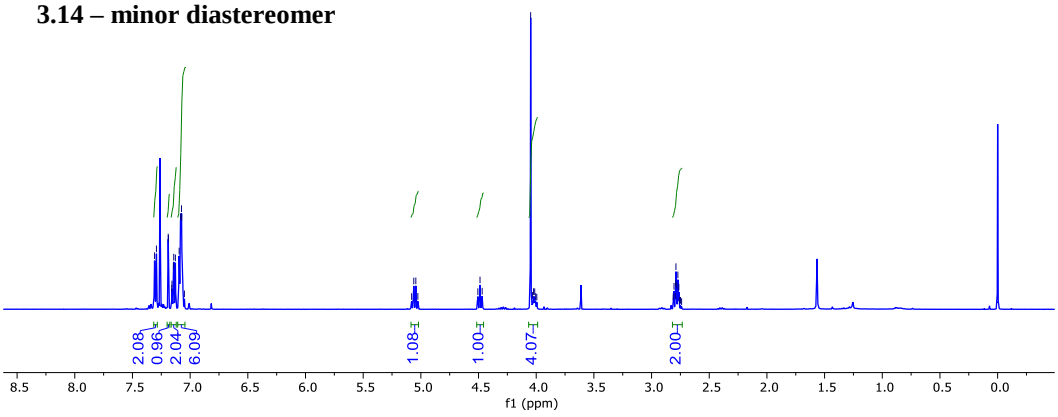

^{1}H NMR, 500 MHz, $CDCl_3$

3.14 – minor diastereomer

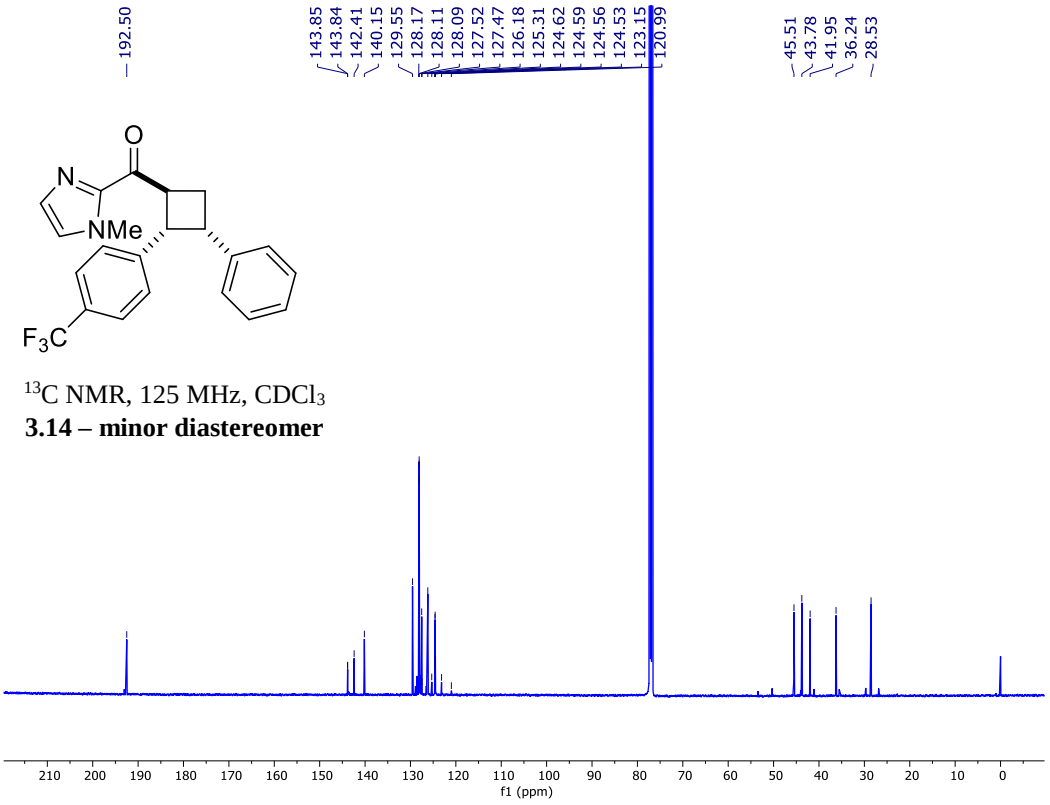

^{13}C NMR, 125 MHz, $CDCl_3$

3.14 – minor diastereomer

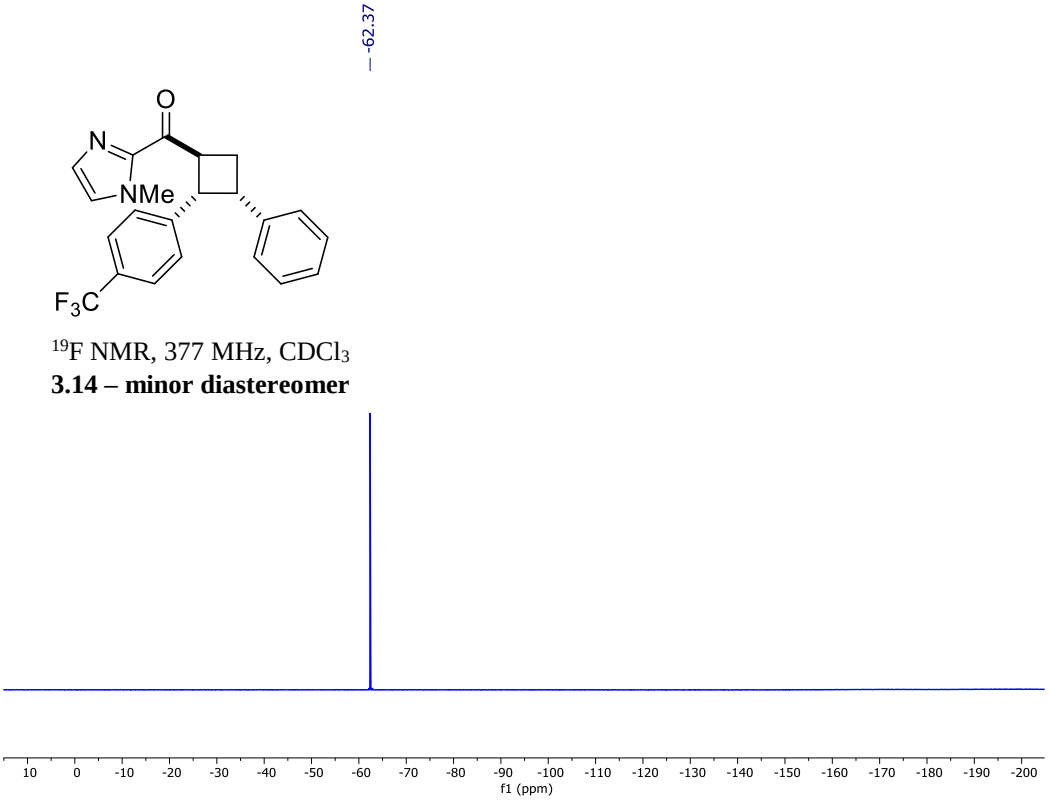

^{19}F NMR, 377 MHz, $CDCl_3$

3.14 – minor diastereomer

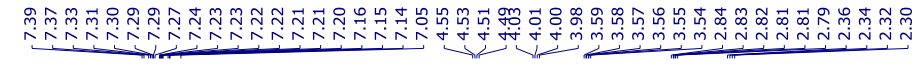

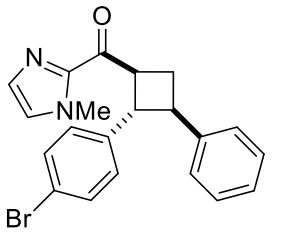

^{1}H NMR, 500 MHz, $CDCl_3$

3.15 – major diastereomer

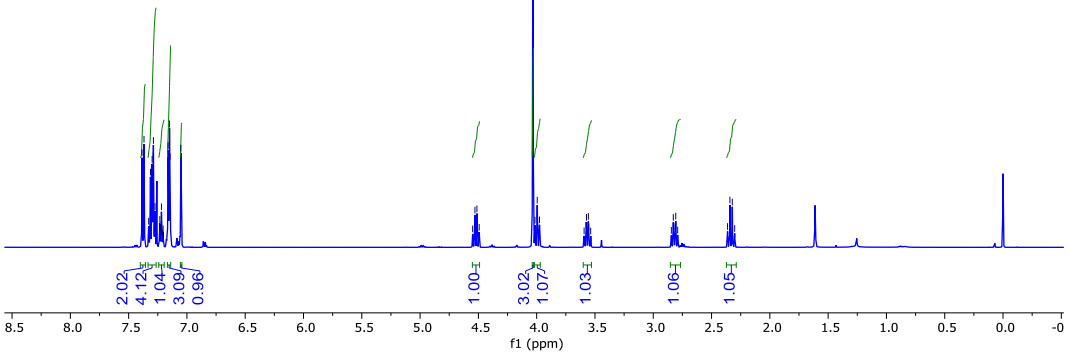

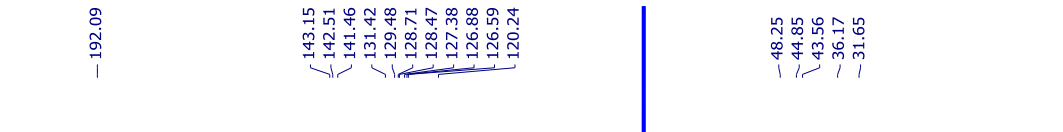

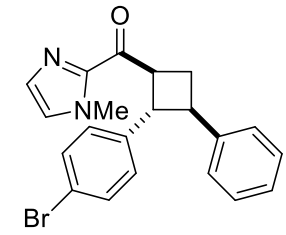

^{13}C NMR, 125 MHz, $CDCl_3$

3.15 – major diastereomer

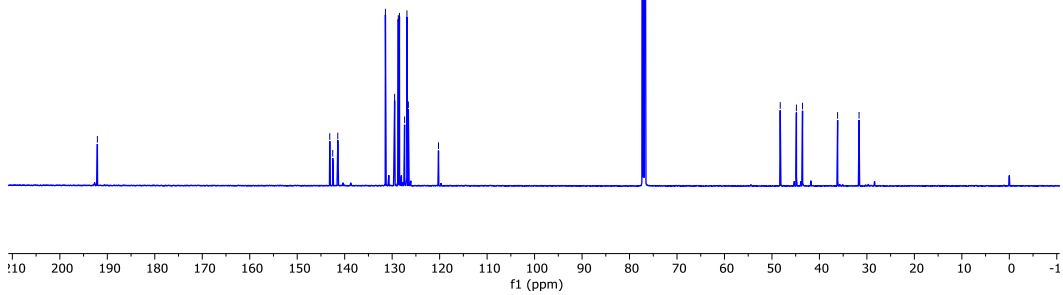

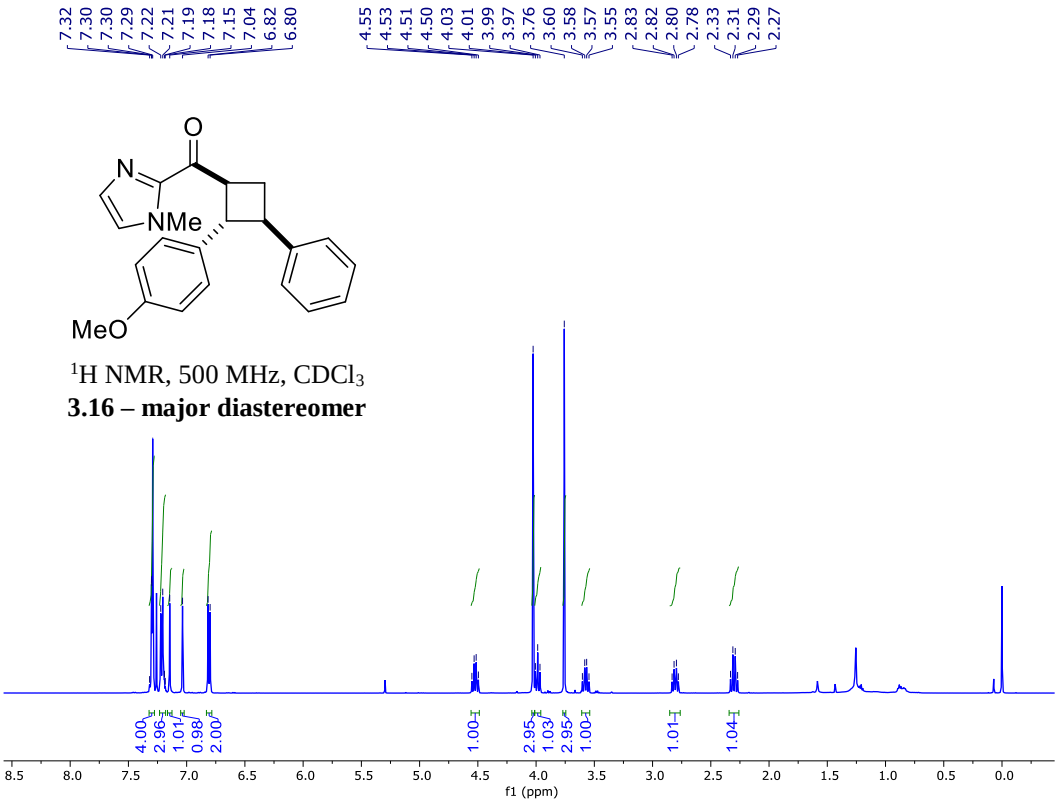

^{1}H NMR, 500 MHz, $CDCl_3$

3.16 – major diastereomer

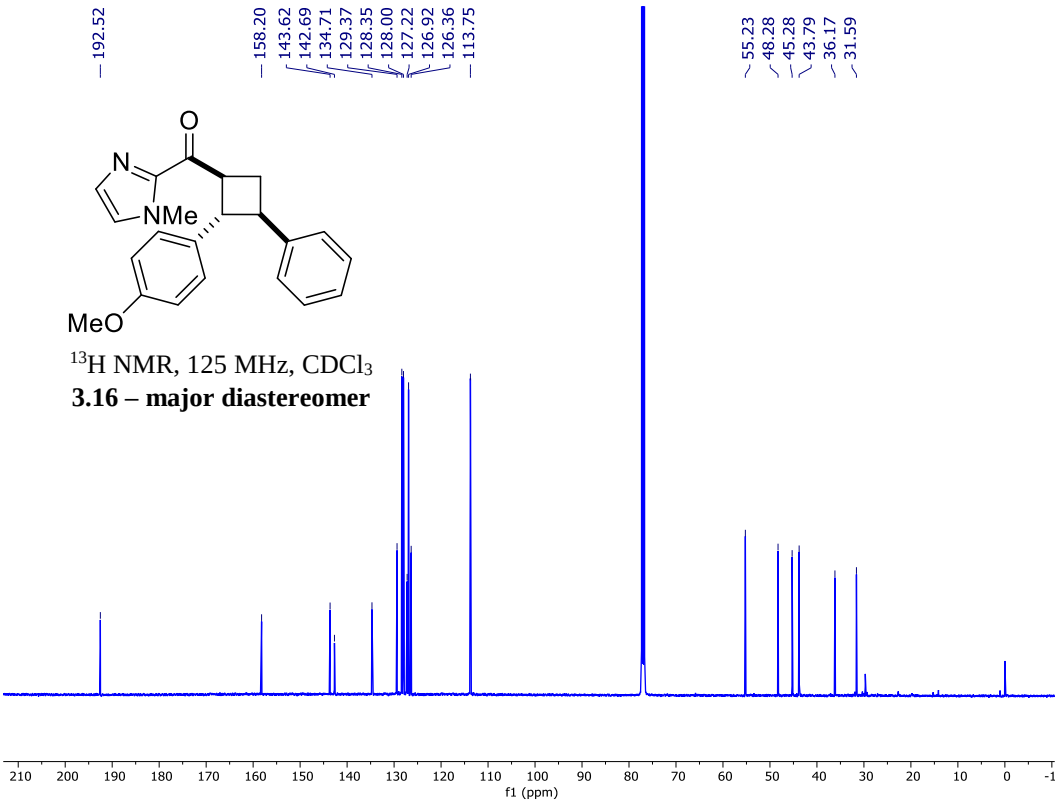

^{13}H NMR, 125 MHz, $CDCl_3$

3.16 – major diastereomer

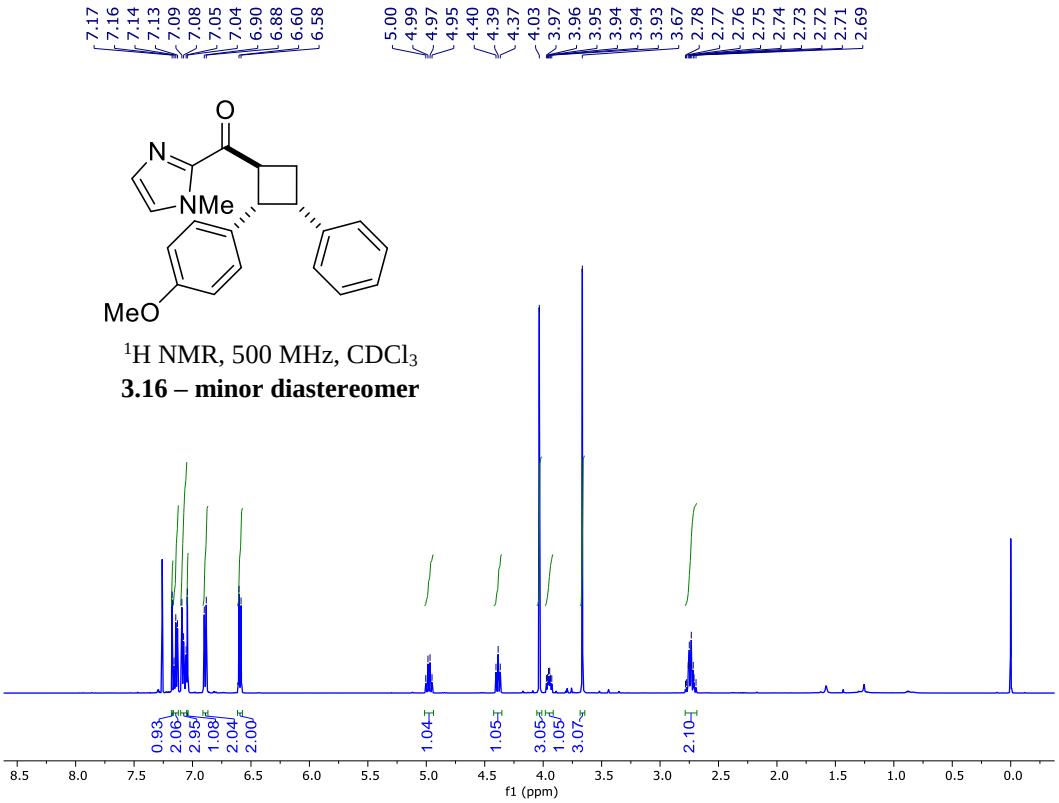

^{1}H NMR, 500 MHz, $CDCl_3$

3.16 – minor diastereomer

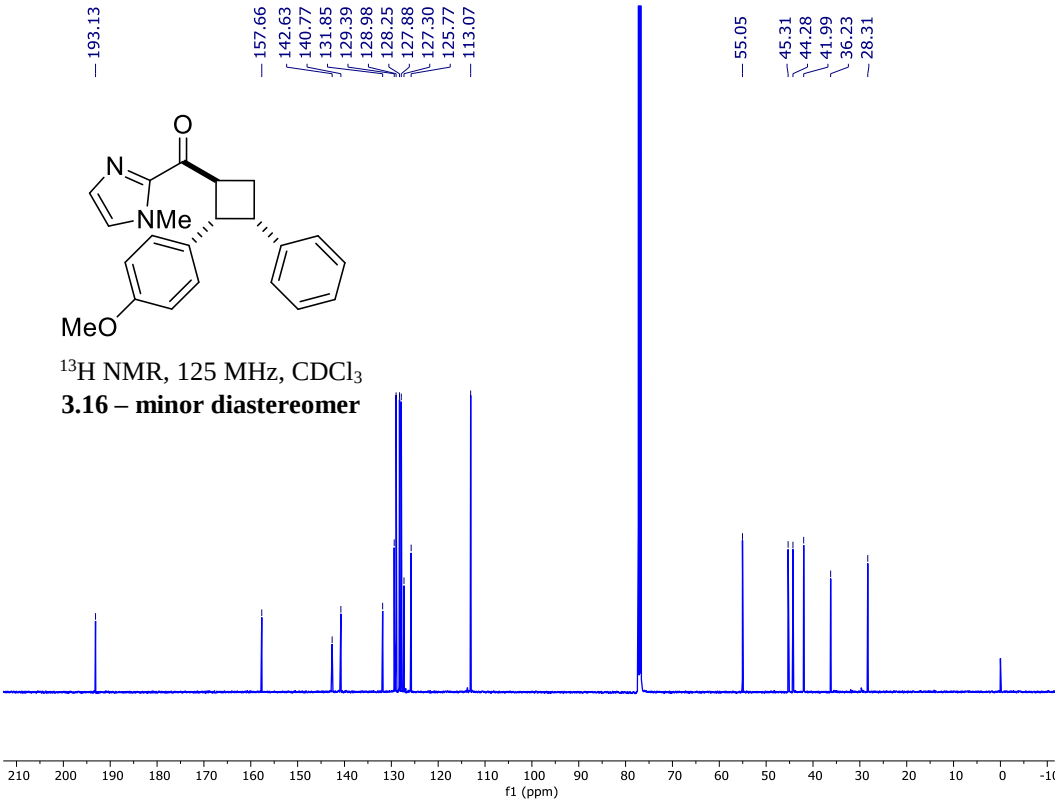

^{13}H NMR, 125 MHz, $CDCl_3$

3.16 – minor diastereomer

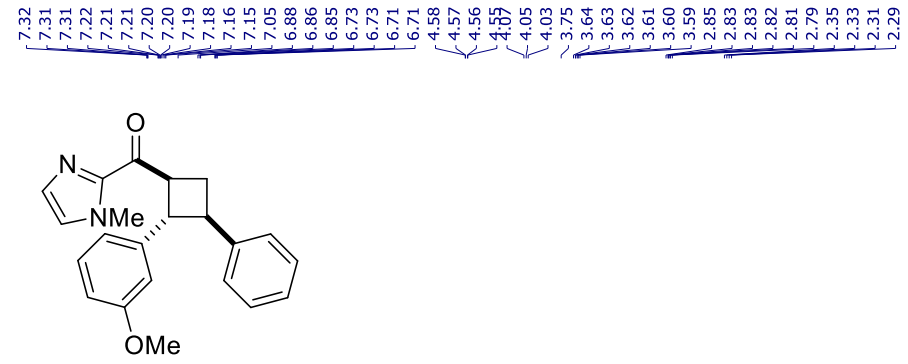

^{1}H NMR, 500 MHz, $CDCl_3$

3.17 – major diastereomer

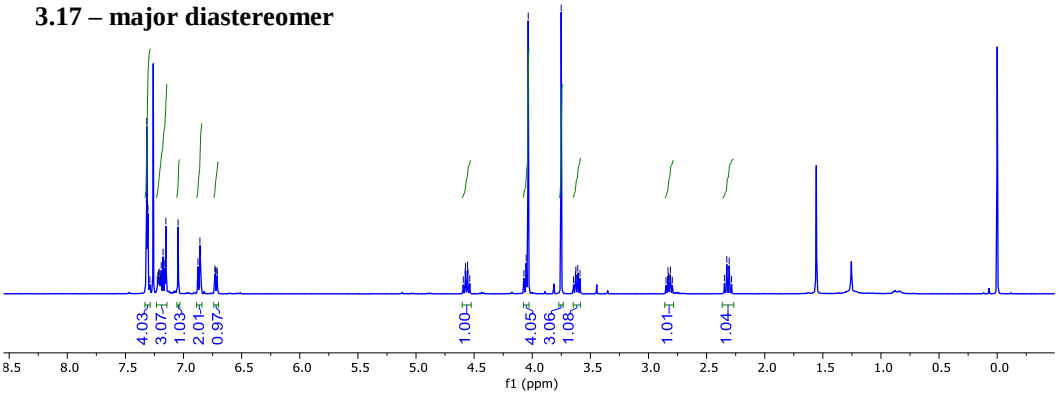

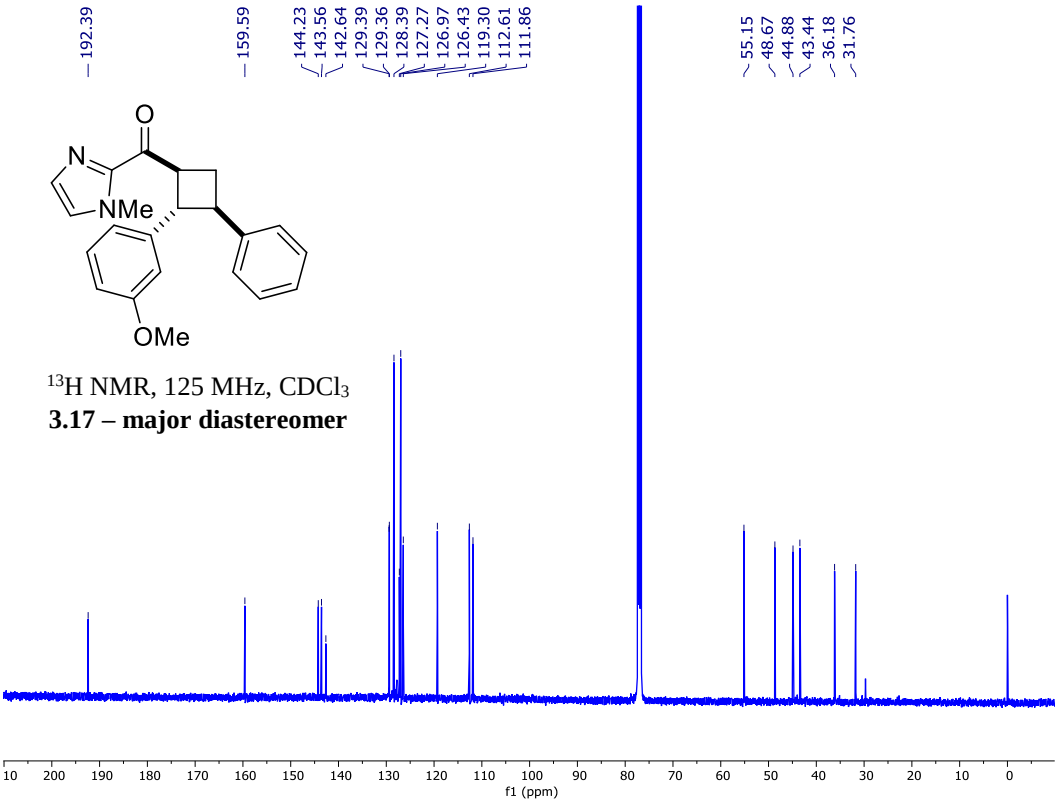

^{13}H NMR, 125 MHz, $CDCl_3$

3.17 – major diastereomer

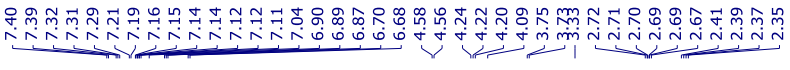

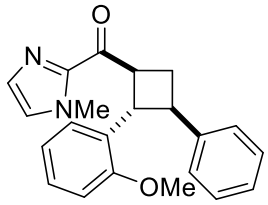

^{1}H NMR, 500 MHz, $CDCl_3$

3.18 – major diastereomer

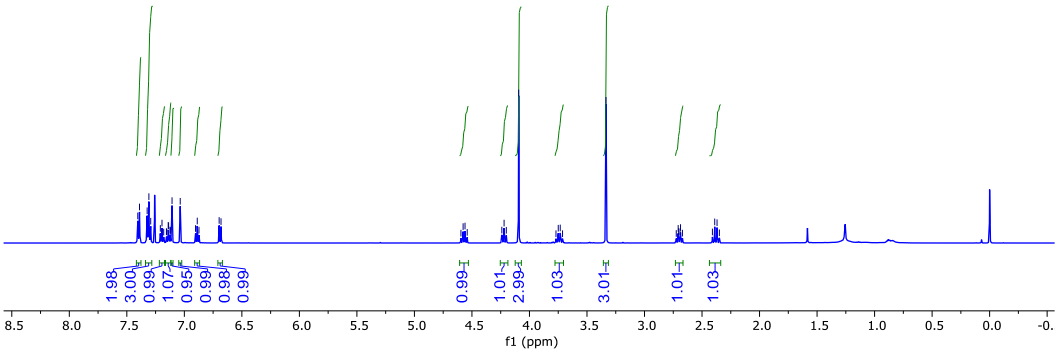

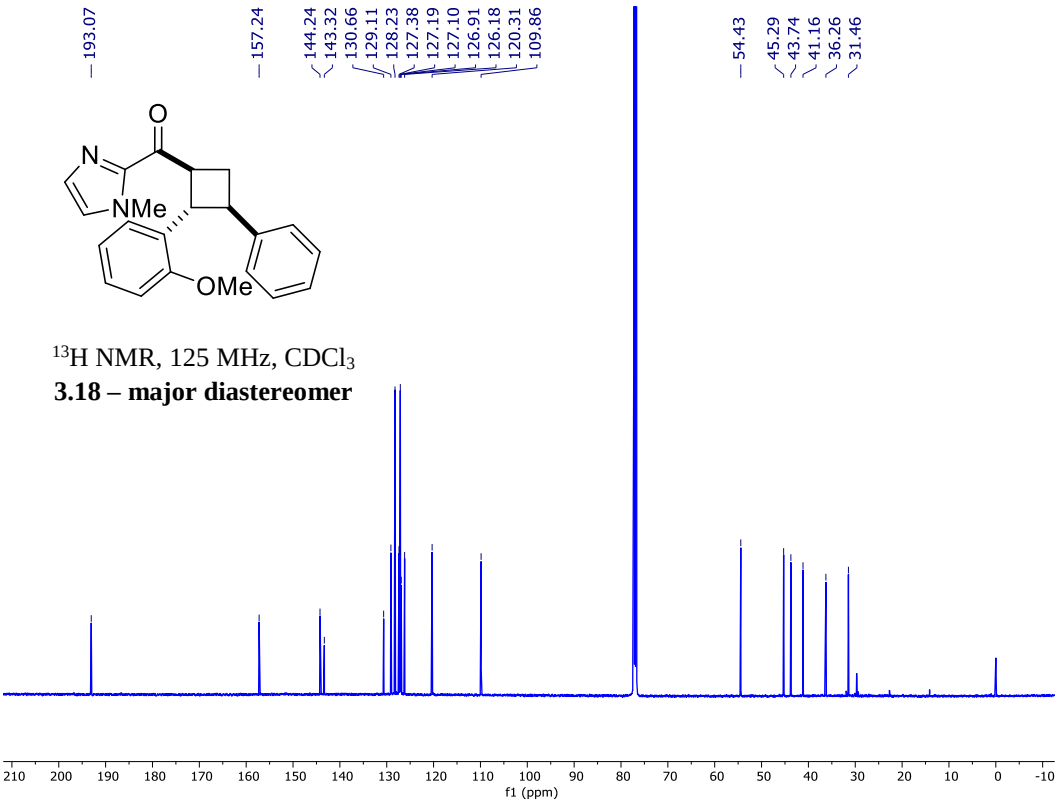

^{13}H NMR, 125 MHz, $CDCl_3$

3.18 – major diastereomer

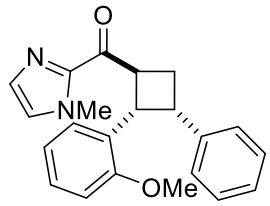

^{1}H NMR, 500 MHz, $CDCl_3$

3.18 – minor diastereomer

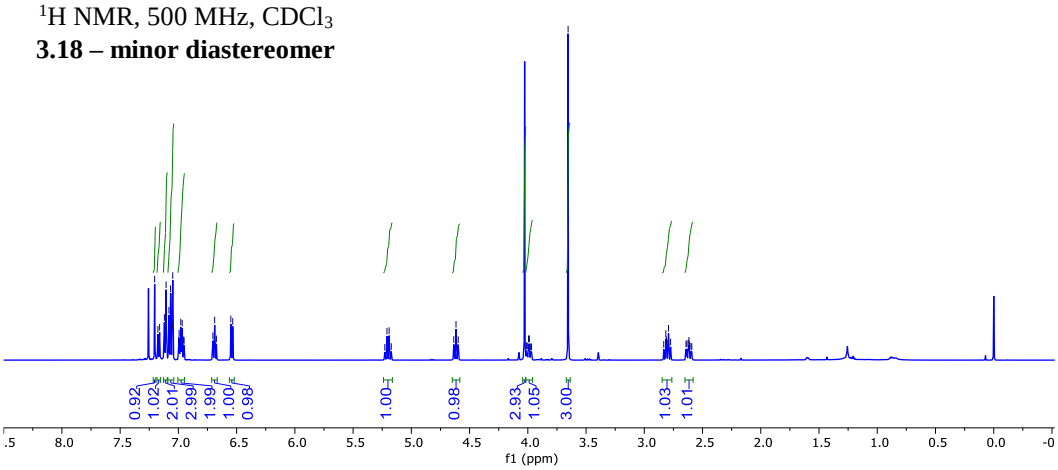

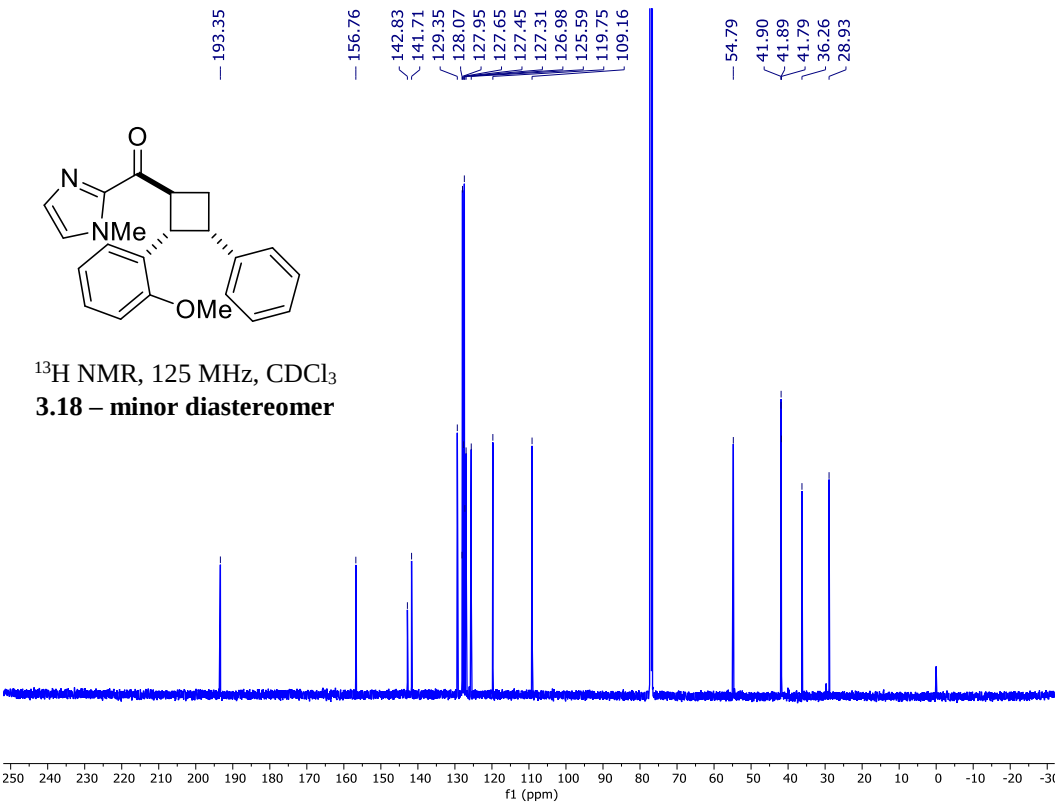

^{13}H NMR, 125 MHz, $CDCl_3$

3.18 – minor diastereomer

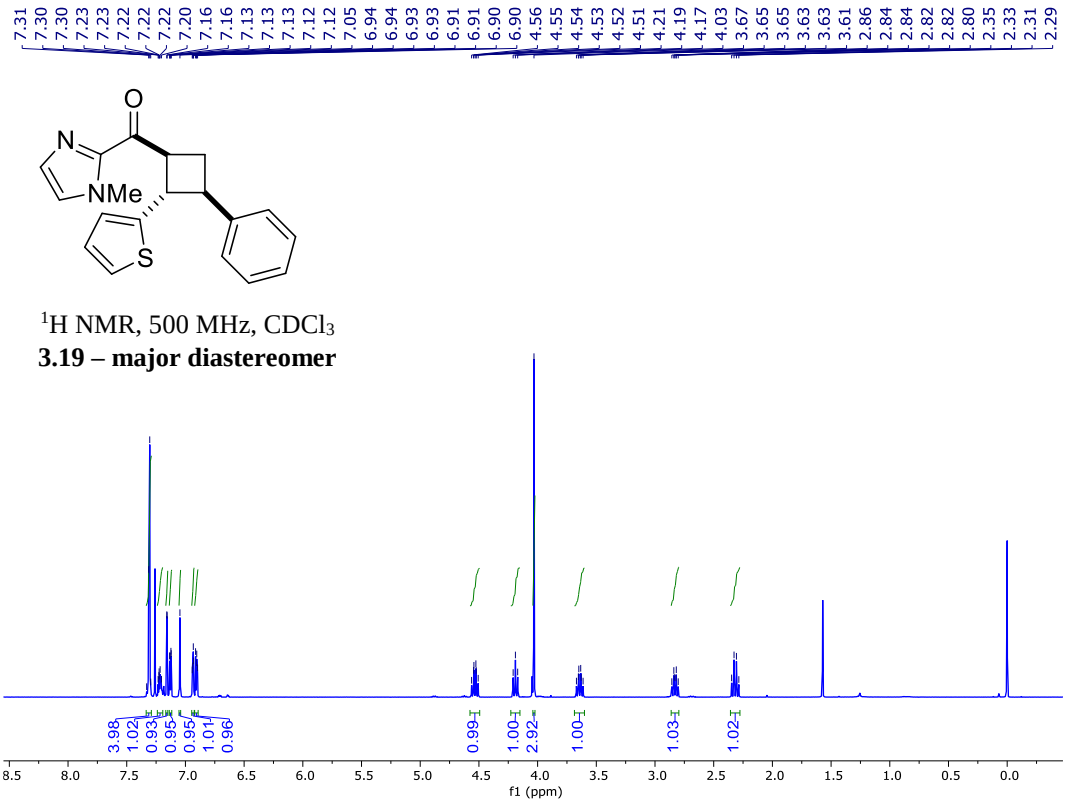

^{1}H NMR, 500 MHz, $CDCl_3$

3.19 – major diastereomer

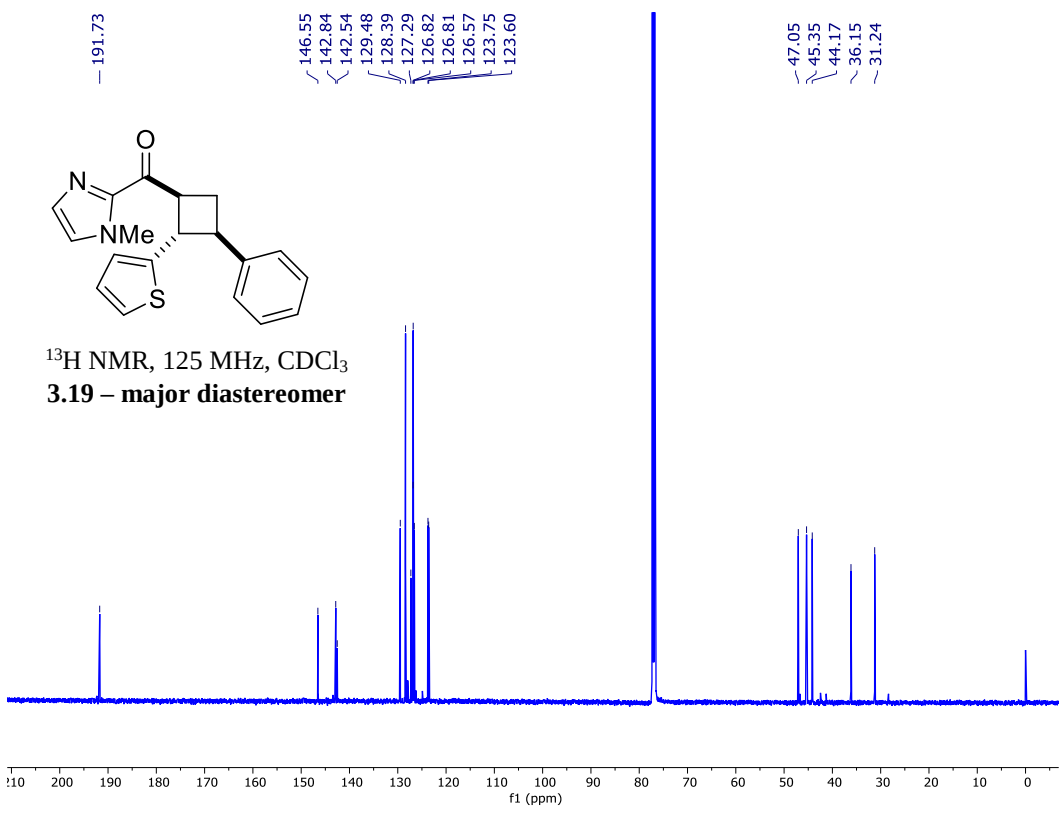

^{13}H NMR, 125 MHz, $CDCl_3$

3.19 – major diastereomer

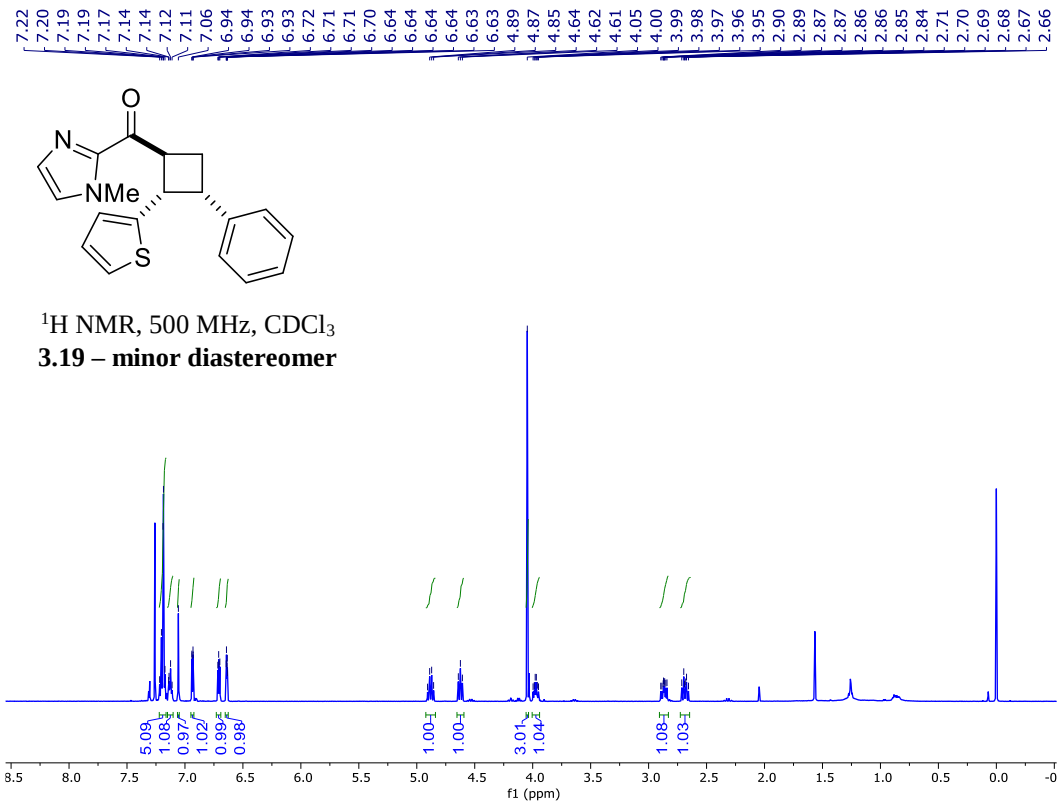

^{1}H NMR, 500 MHz, $CDCl_3$

3.19 – minor diastereomer

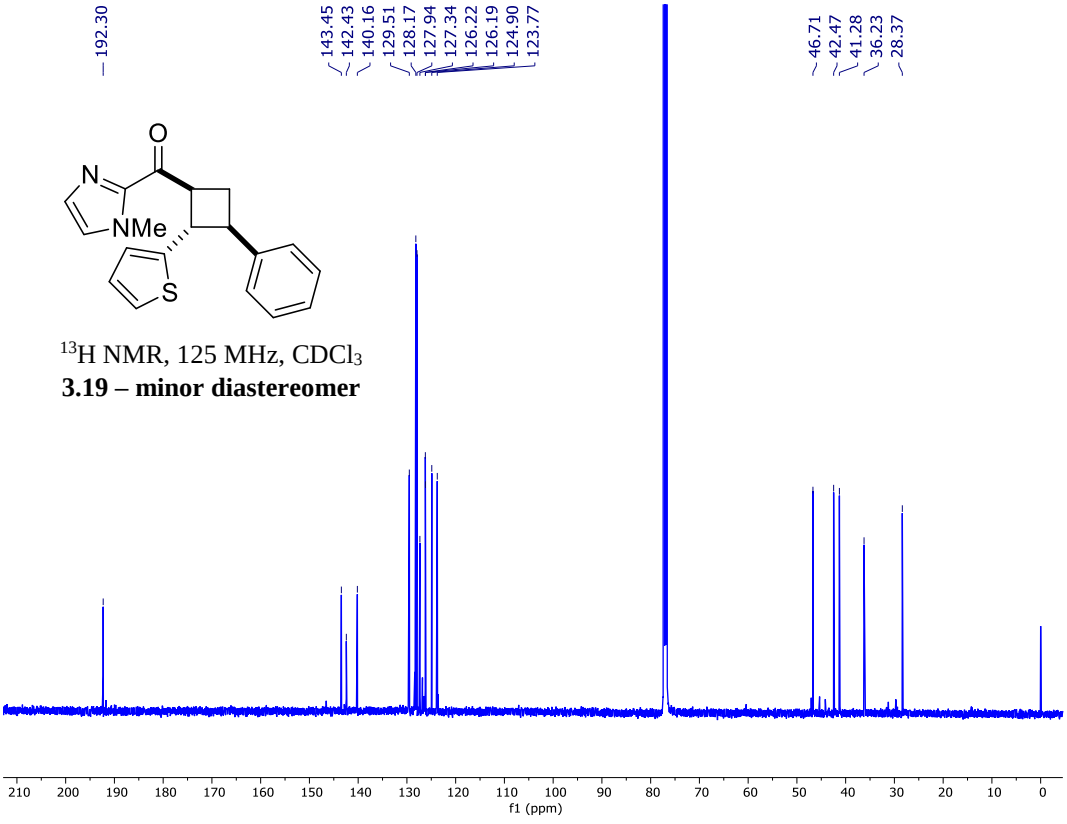

^{13}H NMR, 125 MHz, $CDCl_3$

3.19 – minor diastereomer

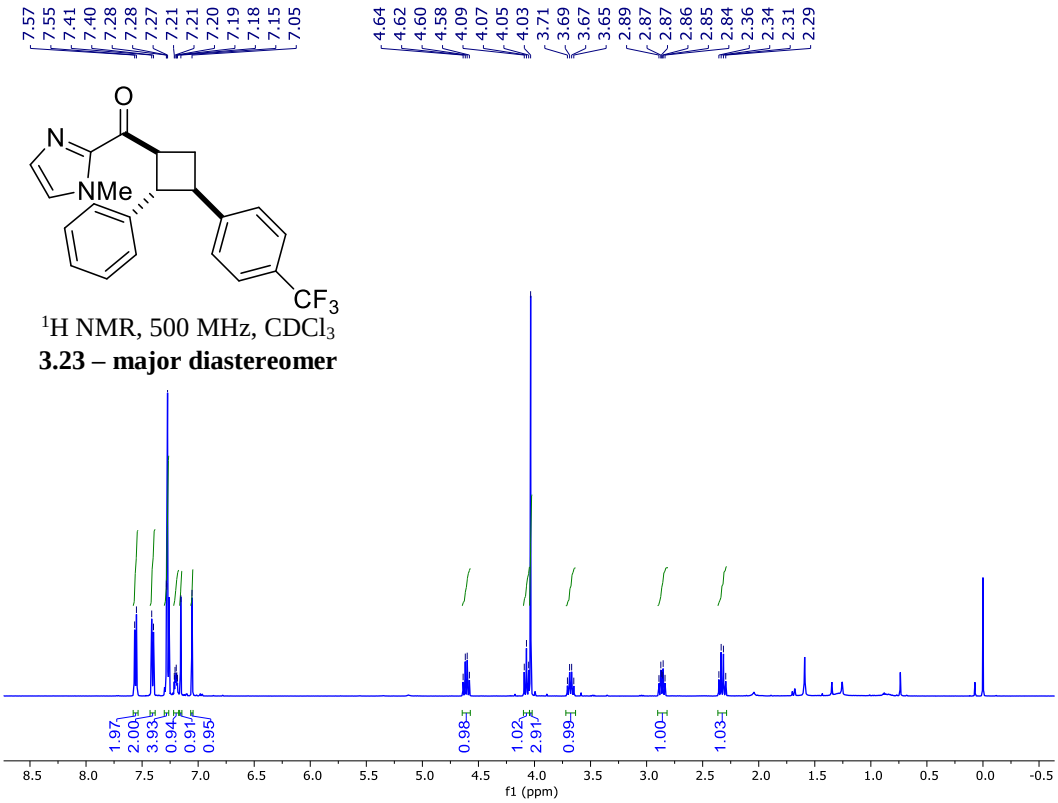

^{1}H NMR, 500 MHz, $CDCl_3$

3.23 – major diastereomer

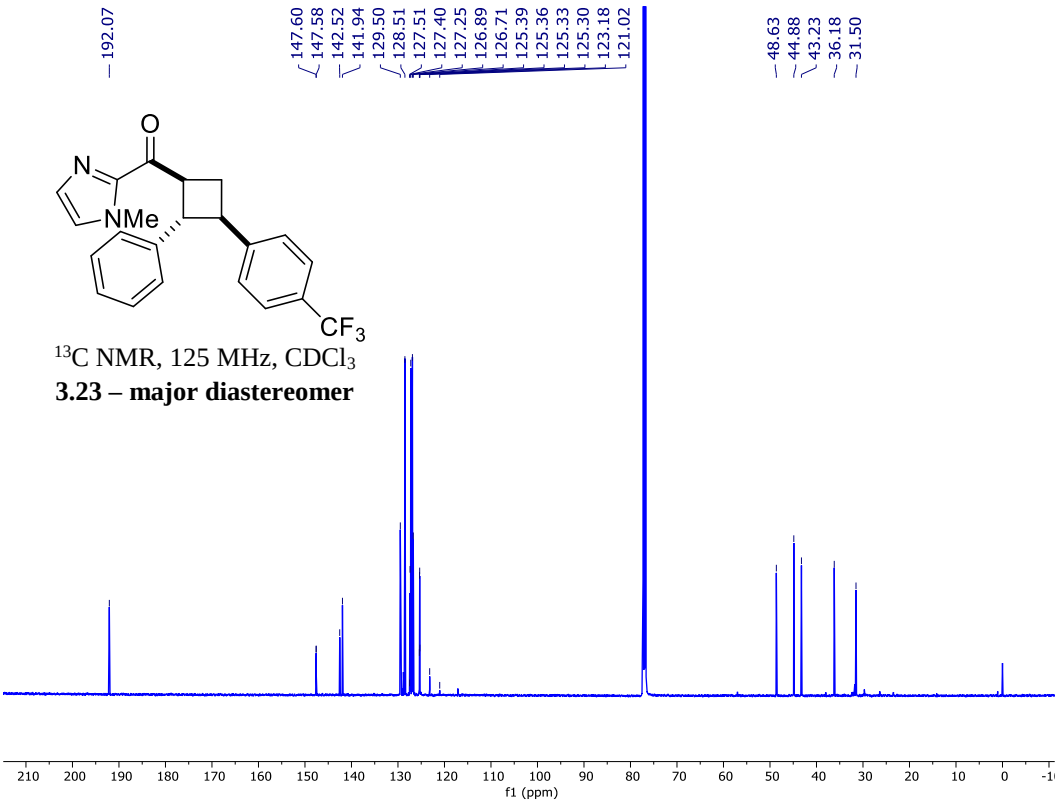

^{13}C NMR, 125 MHz, $CDCl_3$

3.23 – major diastereomer

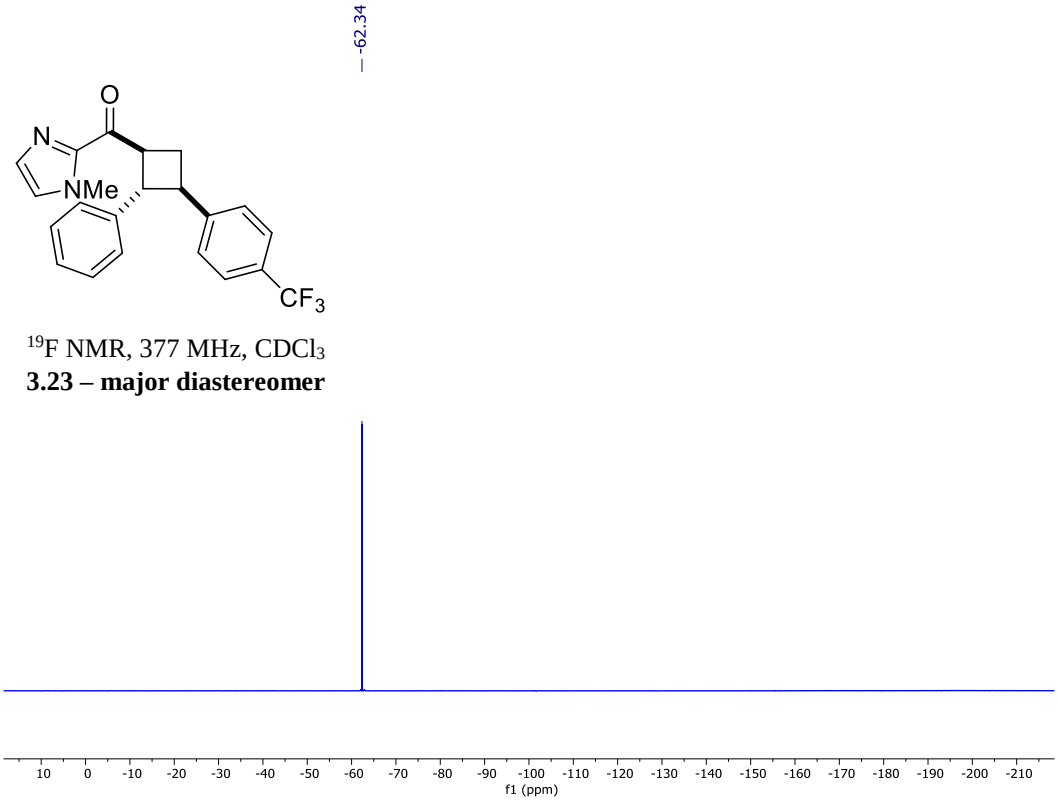

^{19}F NMR, 377 MHz, $CDCl_3$

3.23 – major diastereomer

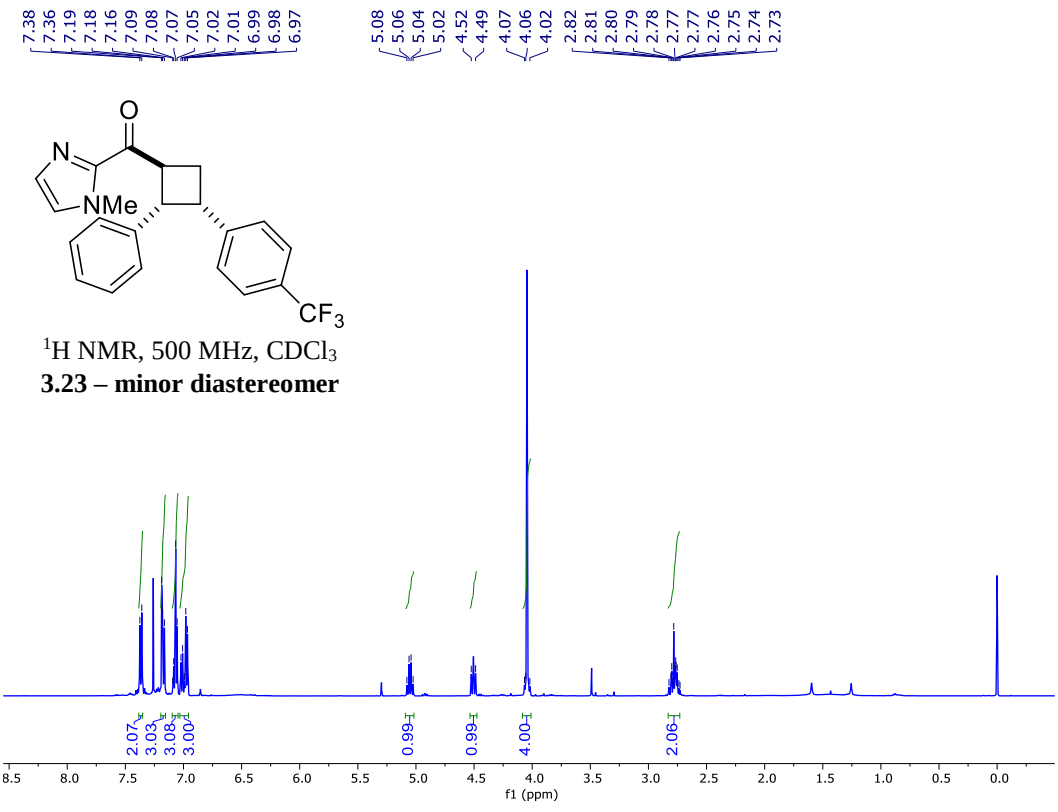

^{1}H NMR, 500 MHz, $CDCl_3$

3.23 – minor diastereomer

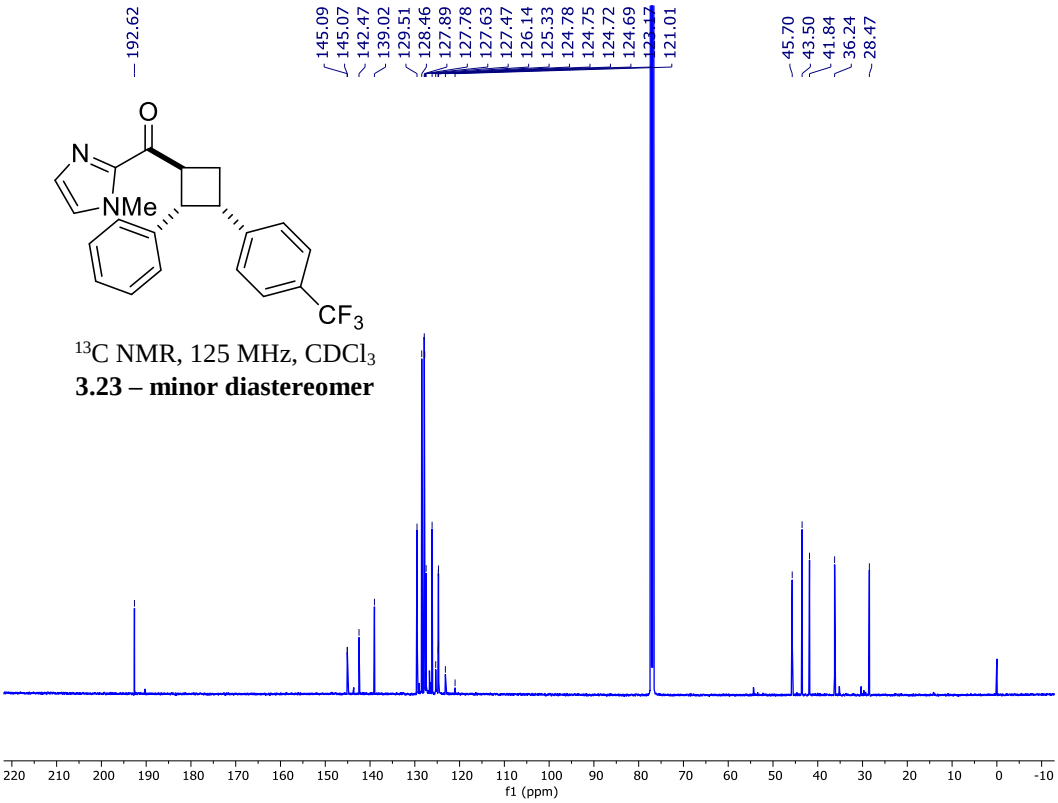

^{13}C NMR, 125 MHz, $CDCl_3$

3.23 – minor diastereomer

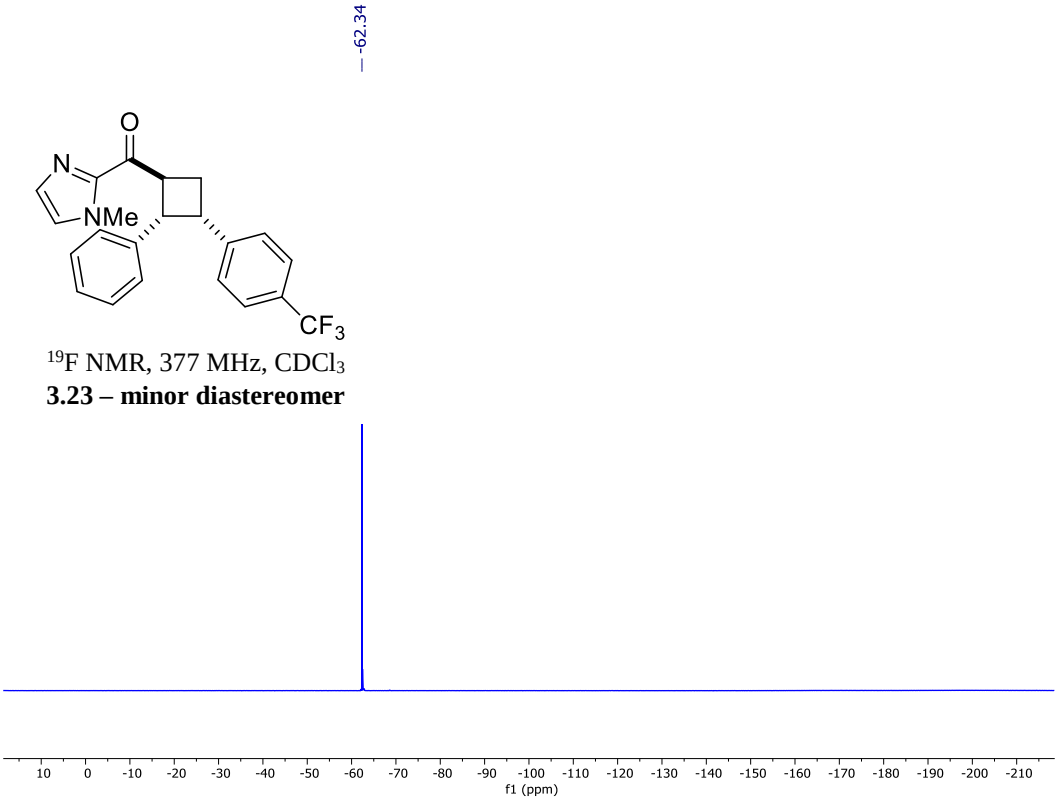

^{19}F NMR, 377 MHz, $CDCl_3$

3.23 – minor diastereomer

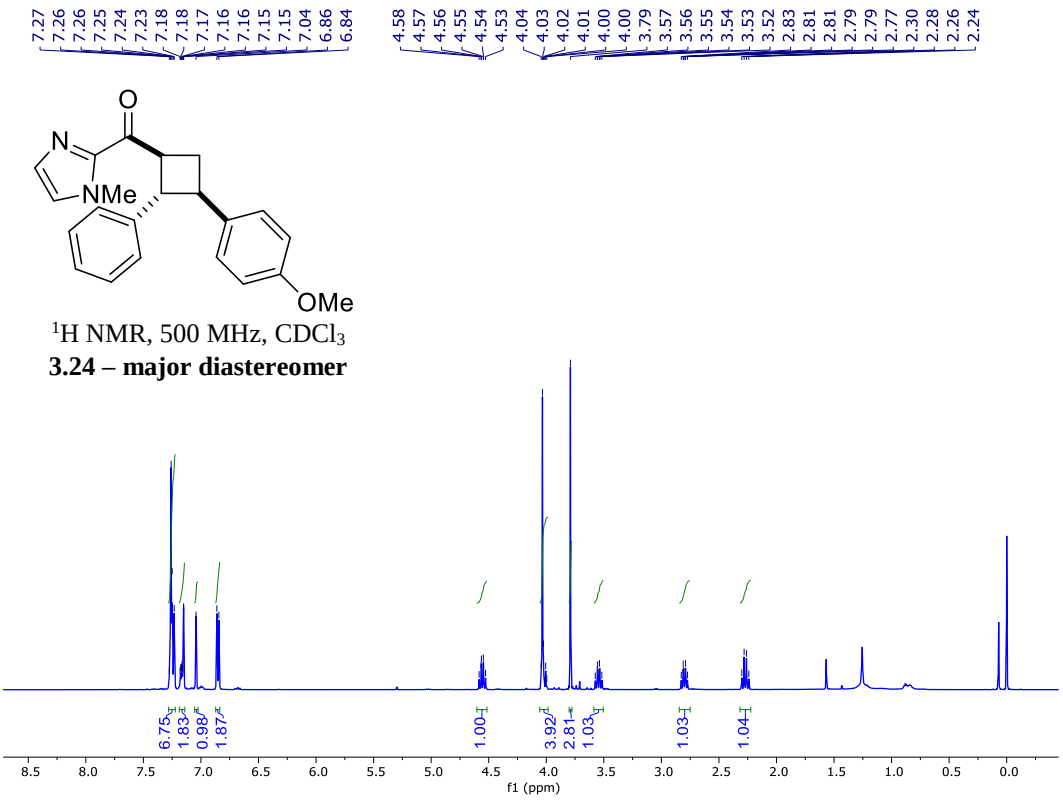

^{1}H NMR, 500 MHz, $CDCl_3$

3.24 – major diastereomer

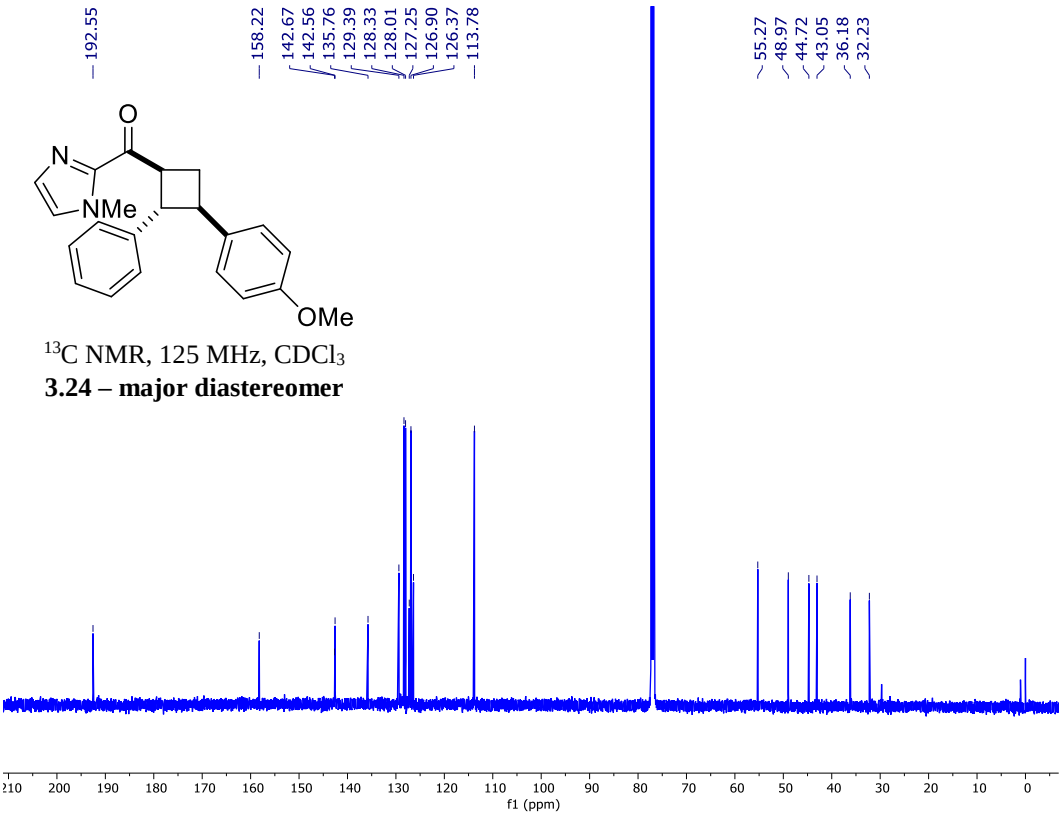

^{13}C NMR, 125 MHz, $CDCl_3$

3.24 – major diastereomer

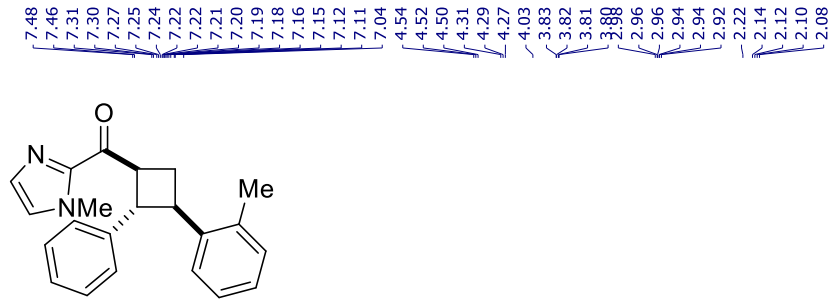

^{1}H NMR, 500 MHz, $CDCl_3$

3.25 – major diastereomer

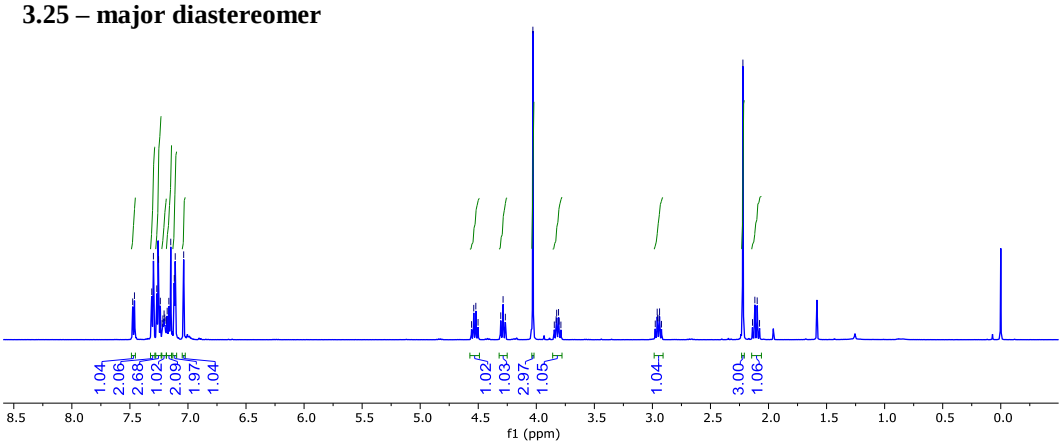

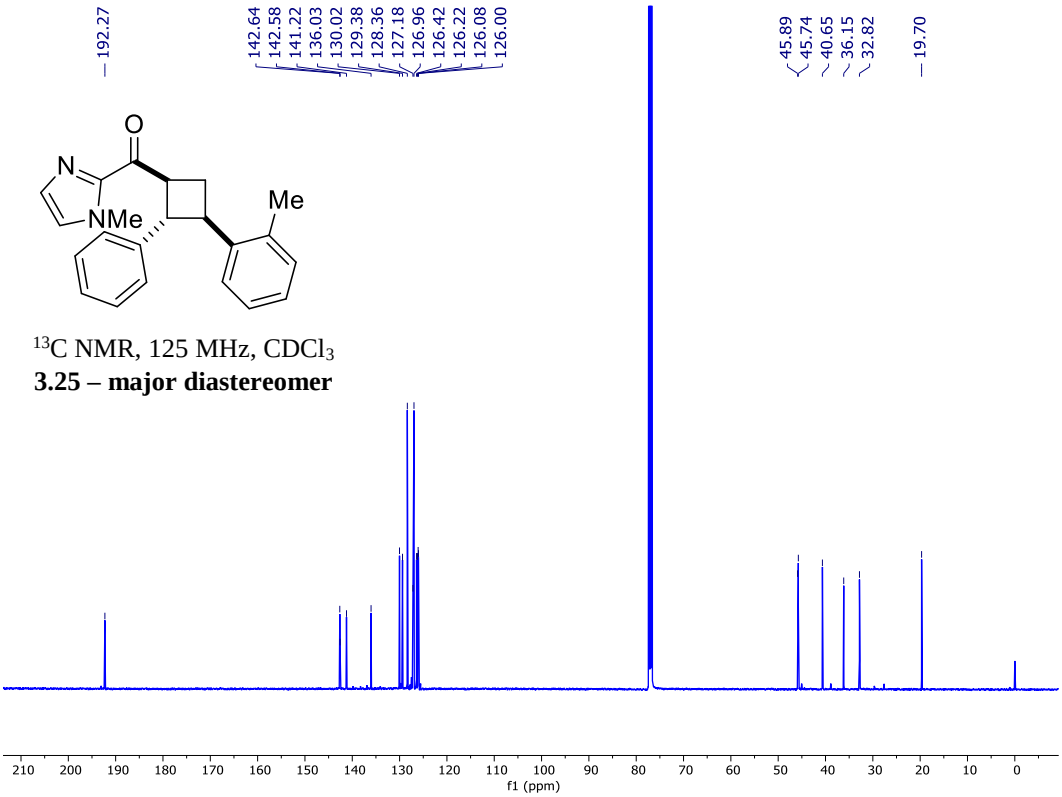

^{13}C NMR, 125 MHz, $CDCl_3$

3.25 – major diastereomer

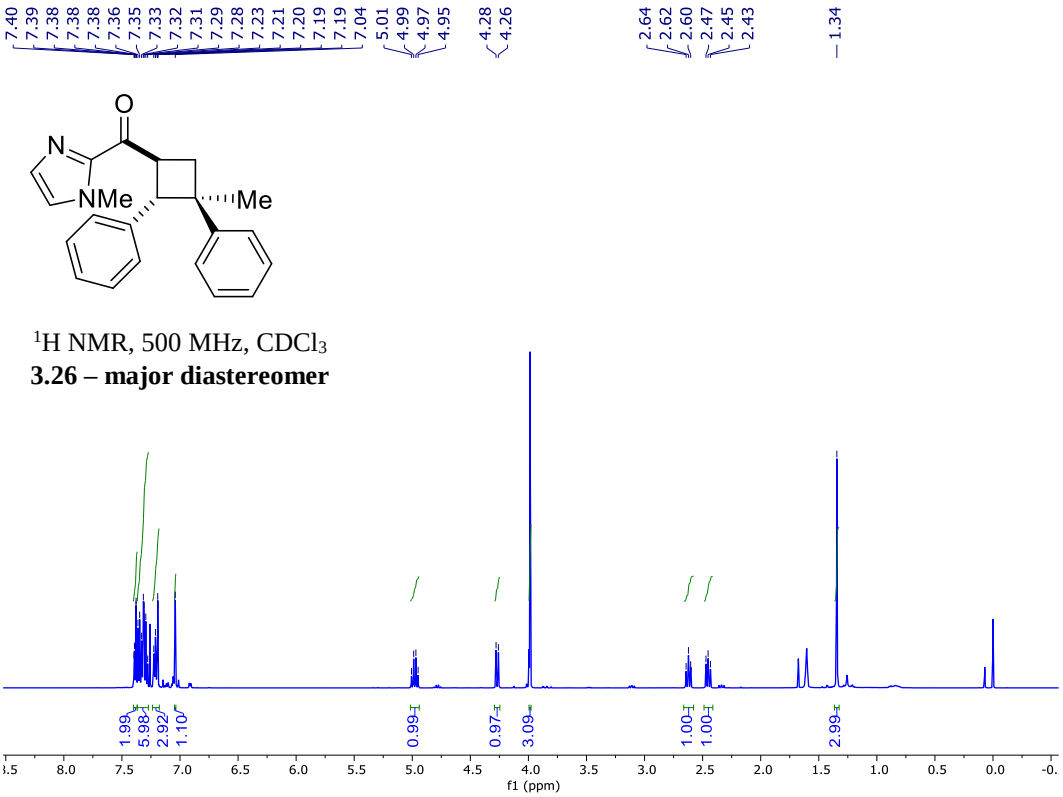

^{1}H NMR, 500 MHz, $CDCl_3$

3.26 – major diastereomer

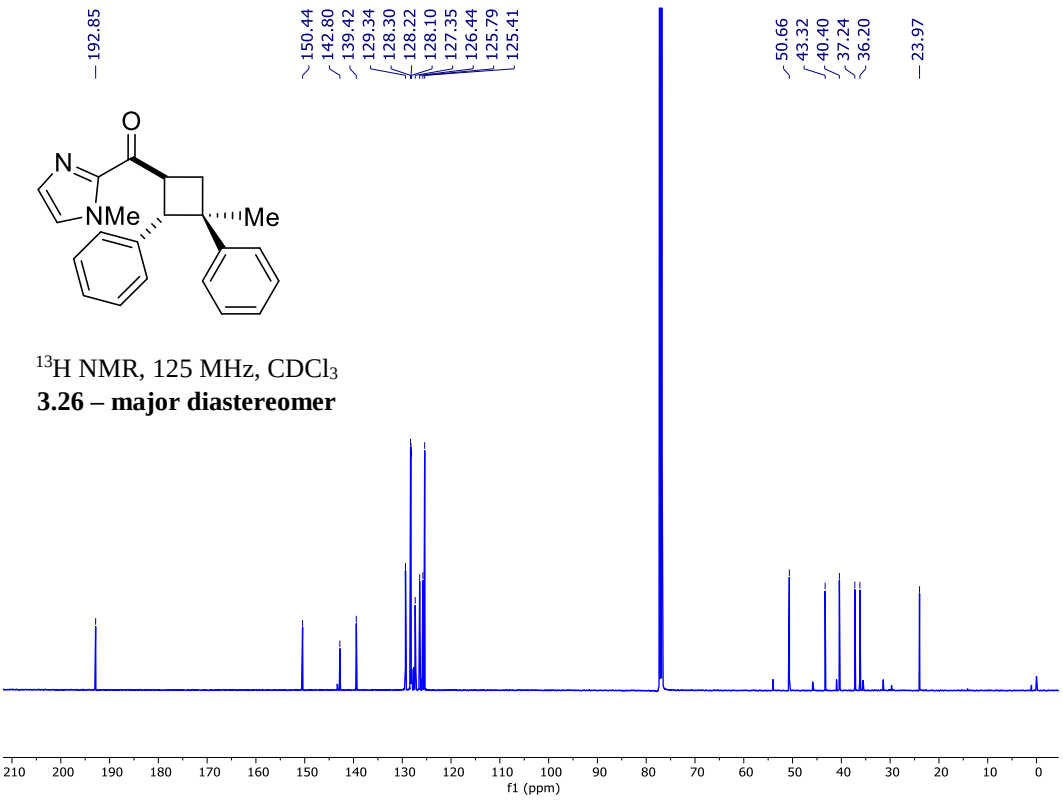

^{13}H NMR, 125 MHz, $CDCl_3$

3.26 – major diastereomer

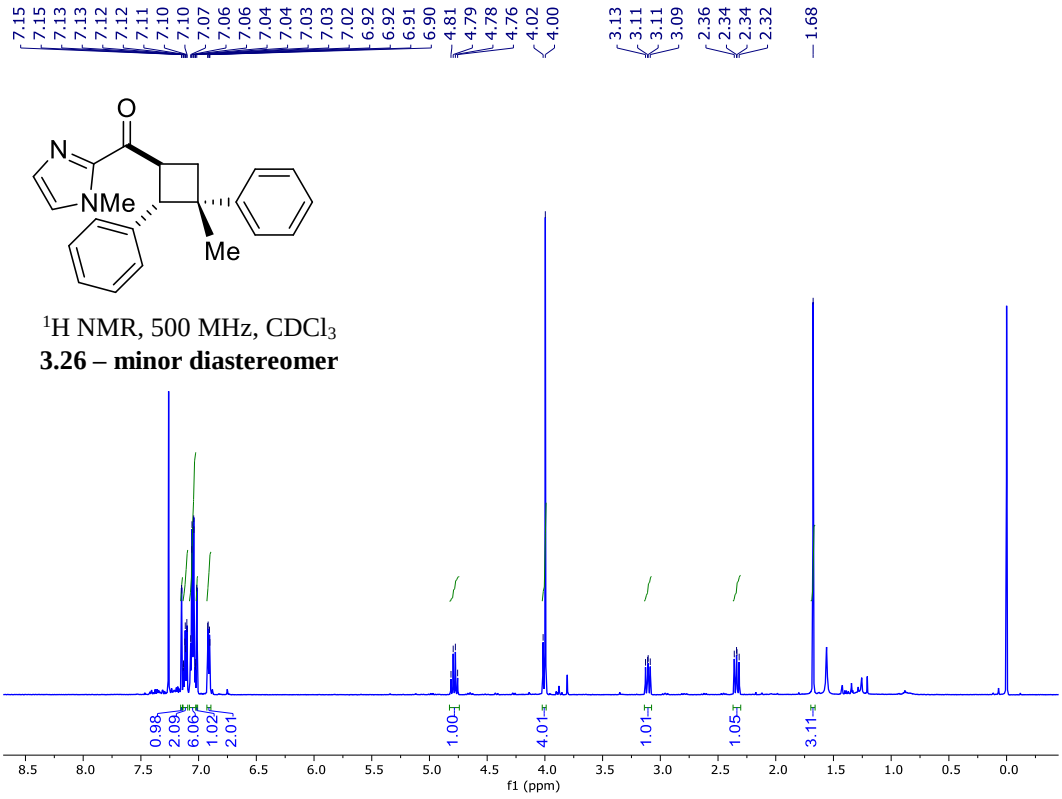

^{1}H NMR, 500 MHz, $CDCl_3$

3.26 – minor diastereomer

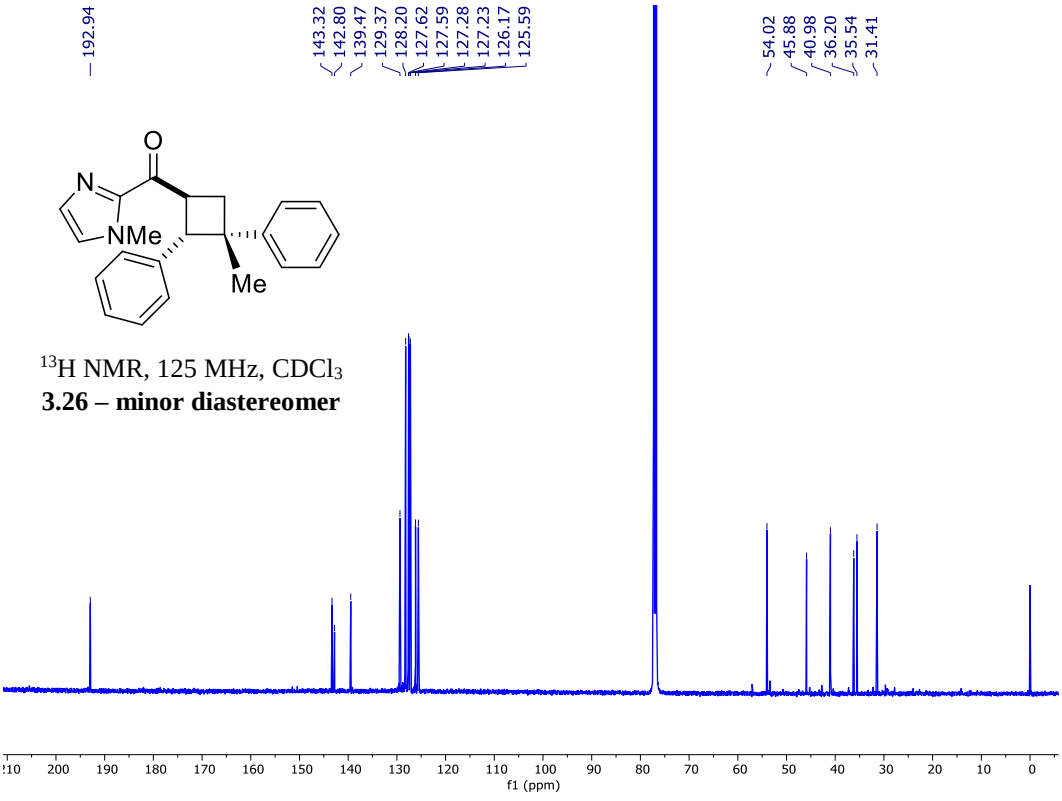

^{13}H NMR, 125 MHz, $CDCl_3$

3.26 – minor diastereomer

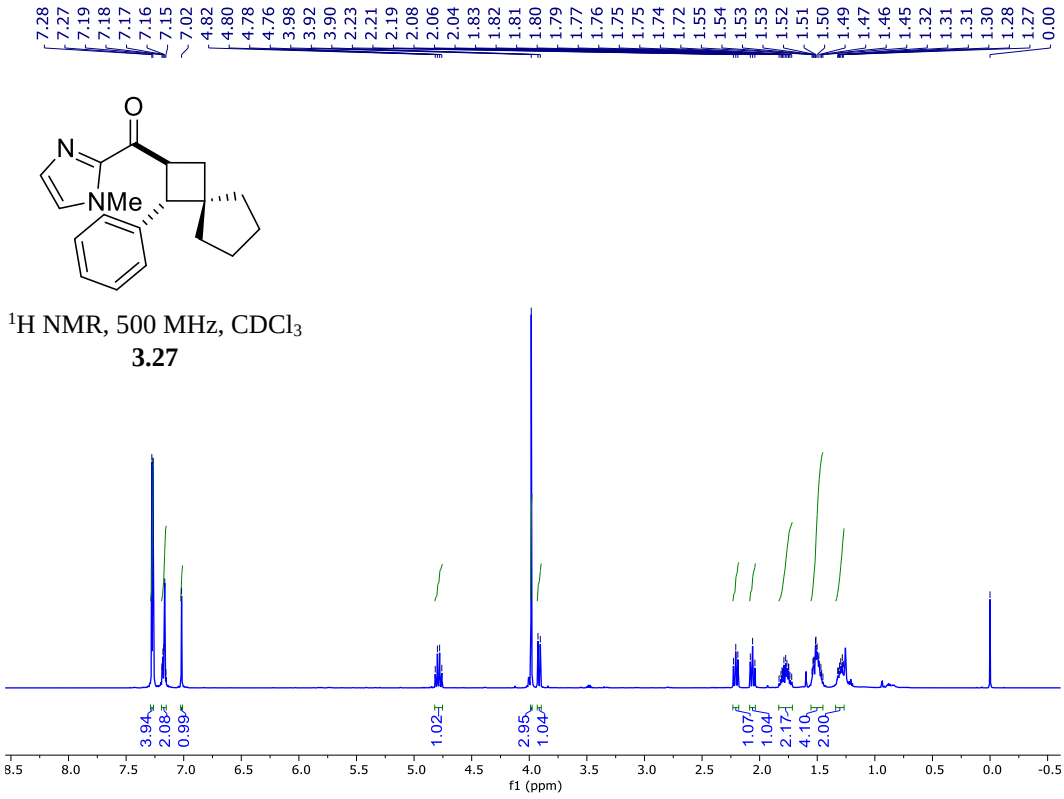

^{1}H NMR, 500 MHz, $CDCl_3$
3.27

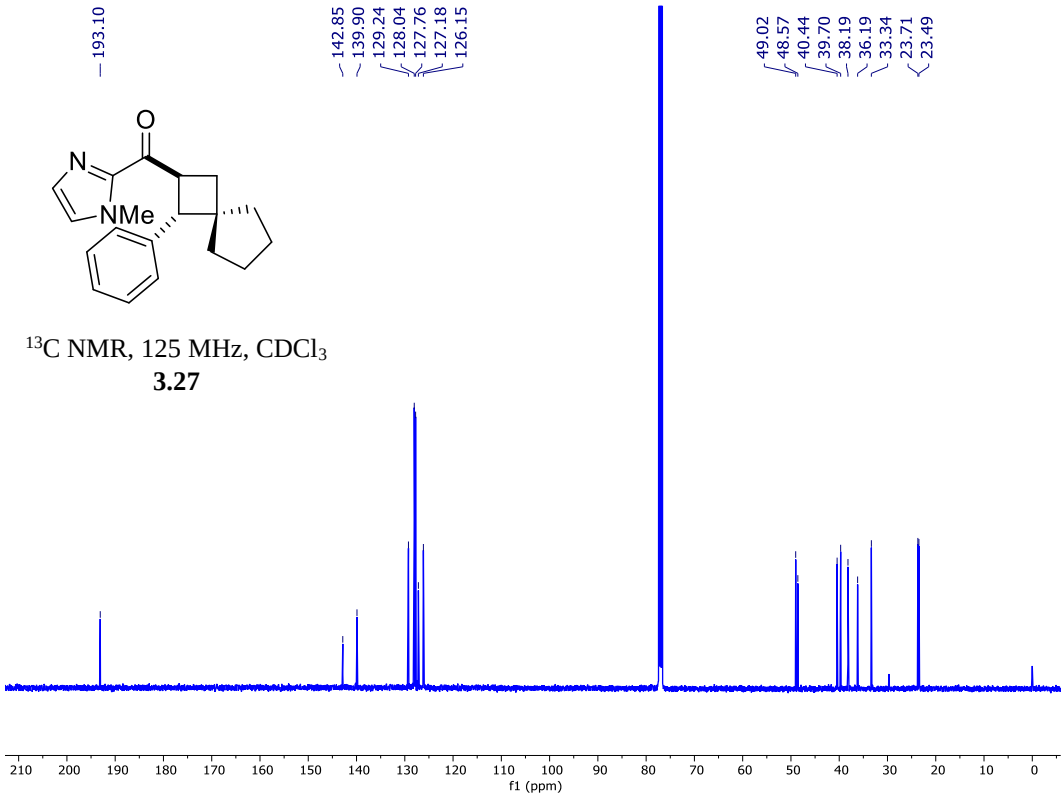

^{13}C NMR, 125 MHz, $CDCl_3$
3.27

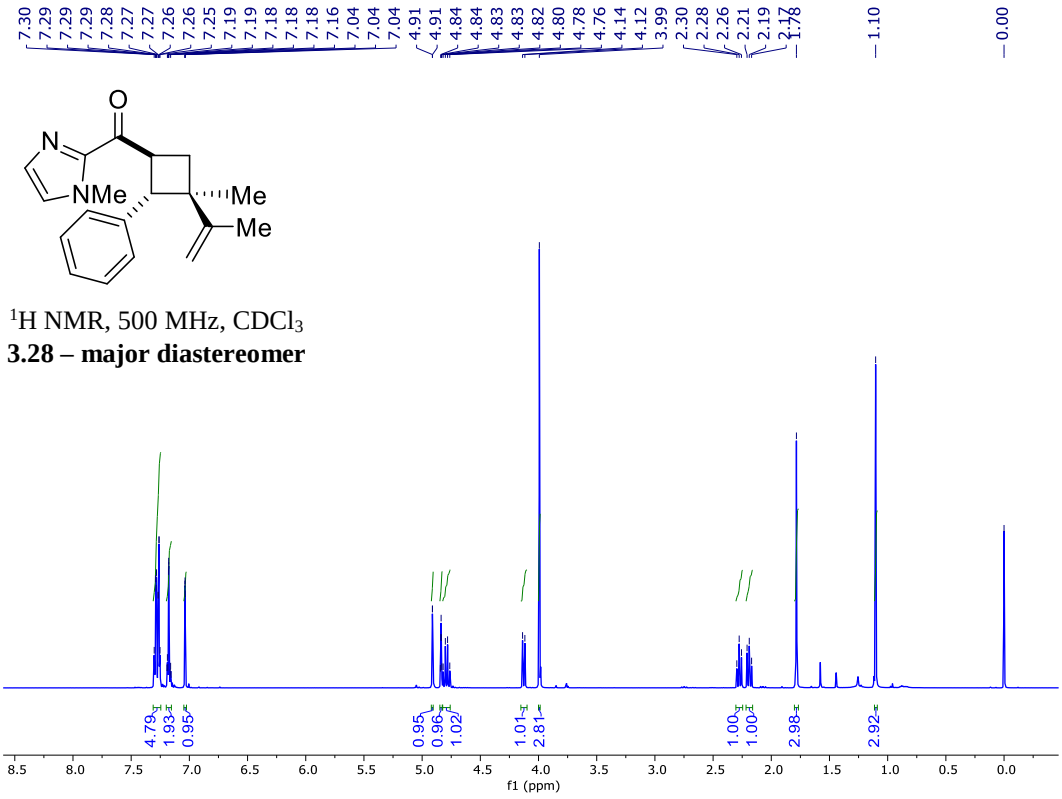

^{1}H NMR, 500 MHz, $CDCl_3$

3.28 – major diastereomer

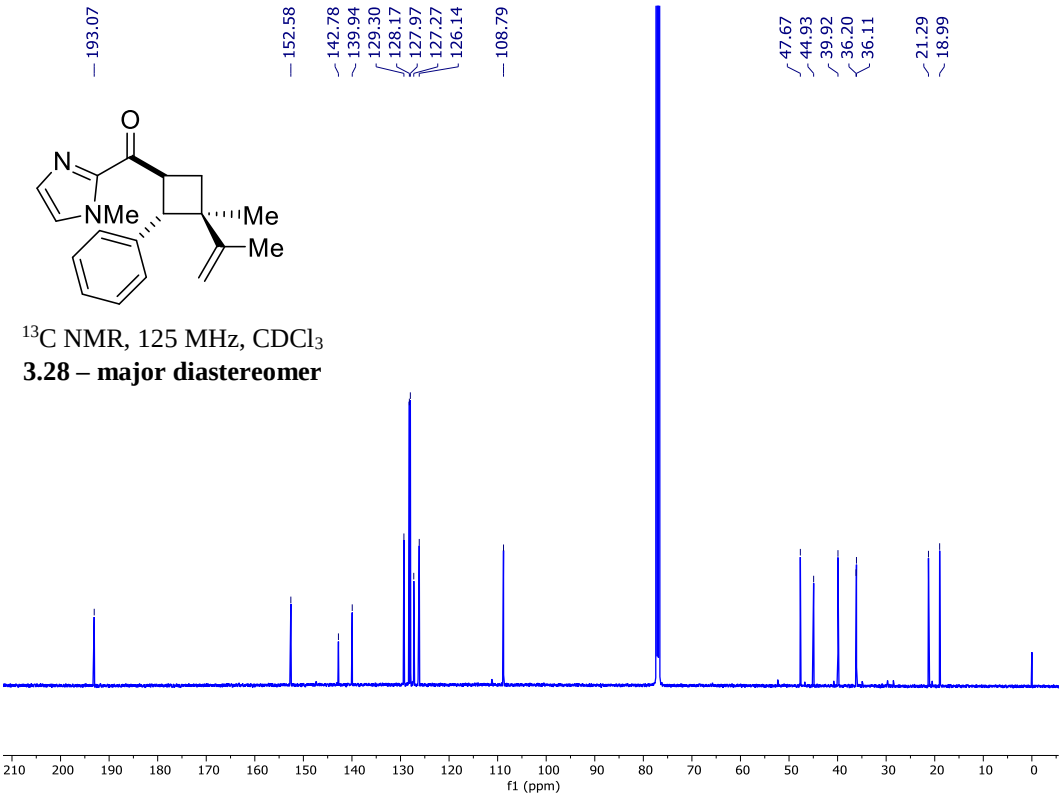

^{13}C NMR, 125 MHz, $CDCl_3$

3.28 – major diastereomer

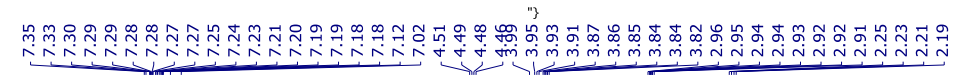

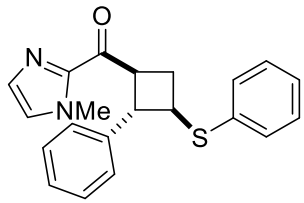

^{1}H NMR, 500 MHz, $CDCl_3$

3.29 – major diastereomer

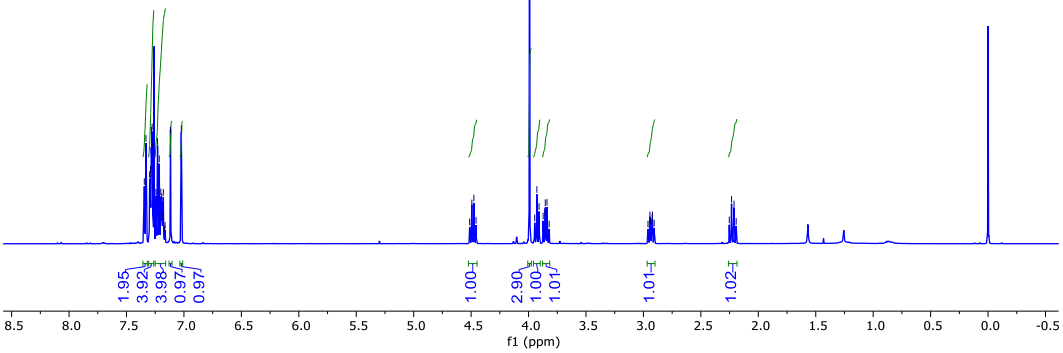

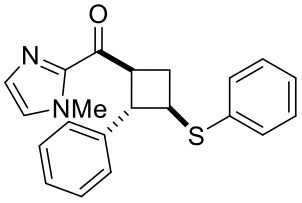

^{13}C NMR, 125 MHz, $CDCl_3$

3.29 – major diastereomer

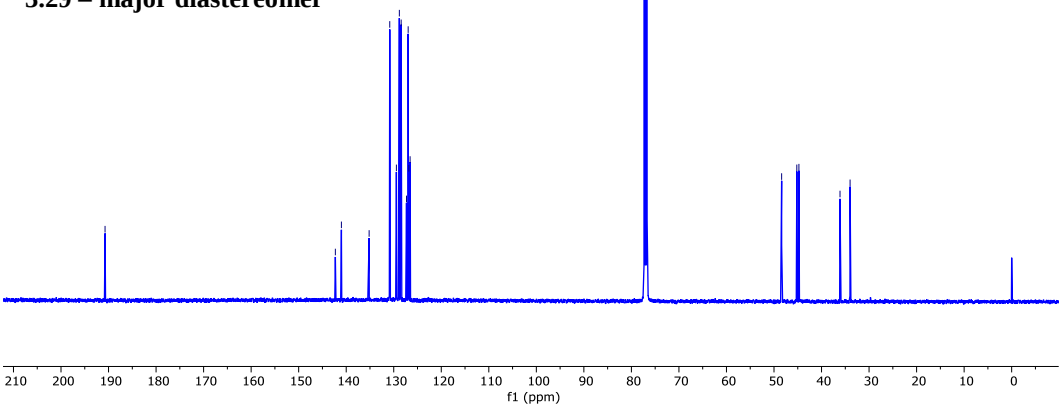

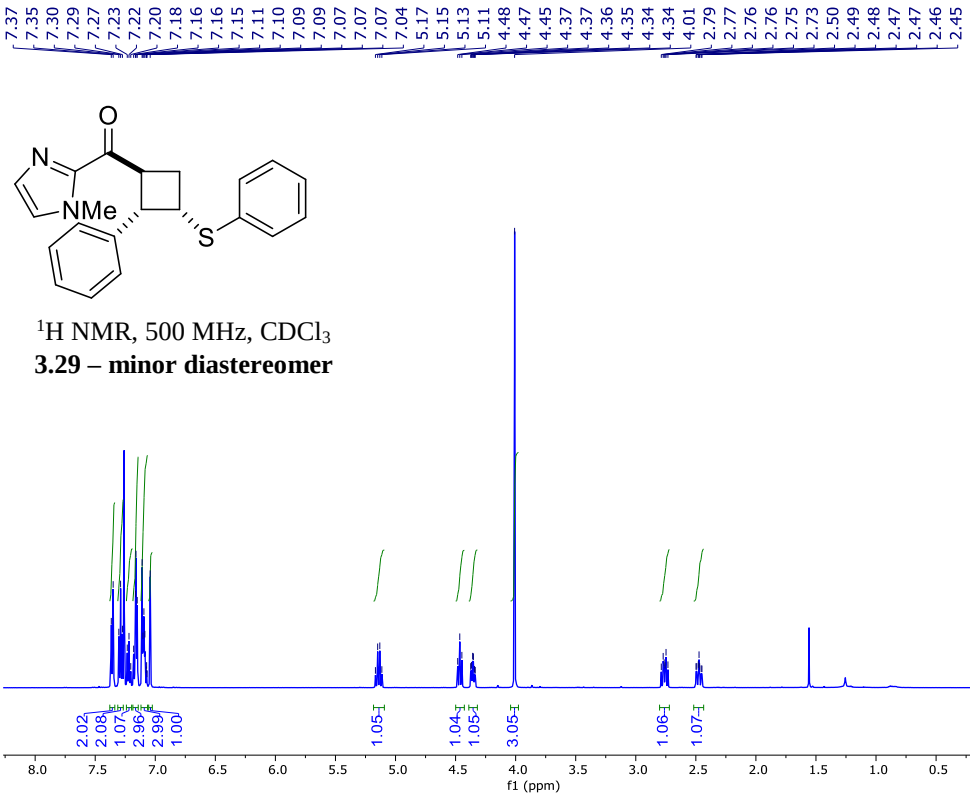

^{1}H NMR, 500 MHz, $CDCl_3$

3.29 – minor diastereomer

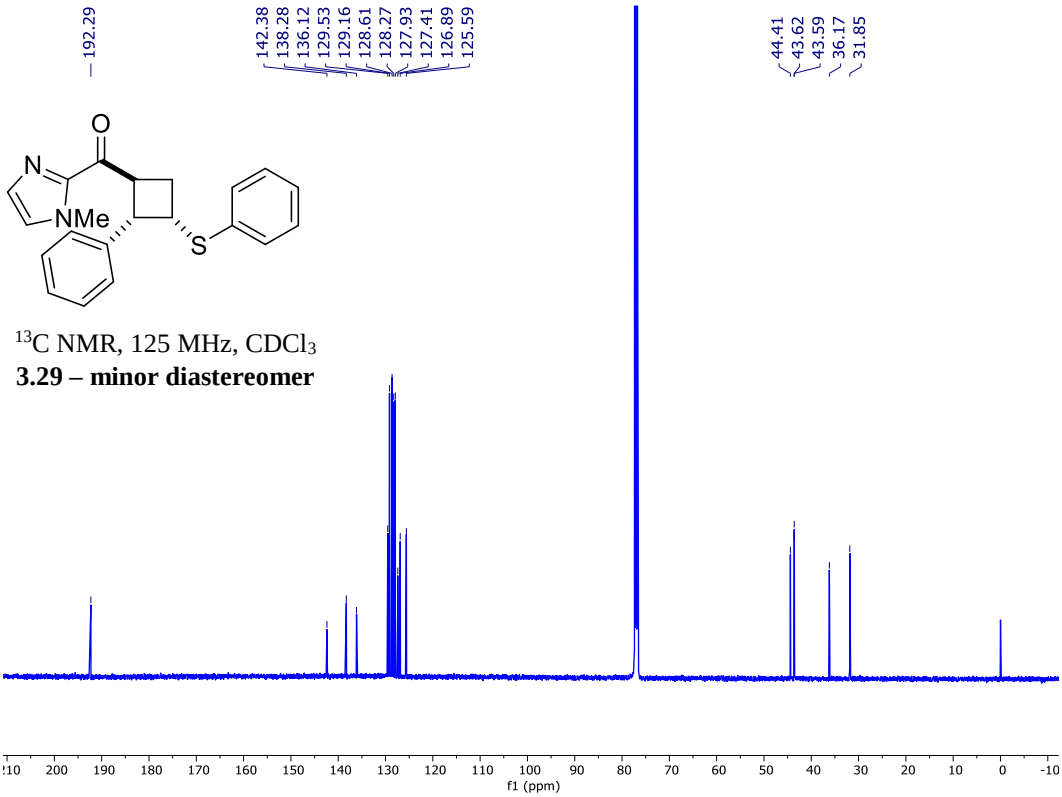

^{13}C NMR, 125 MHz, $CDCl_3$

3.29 – minor diastereomer

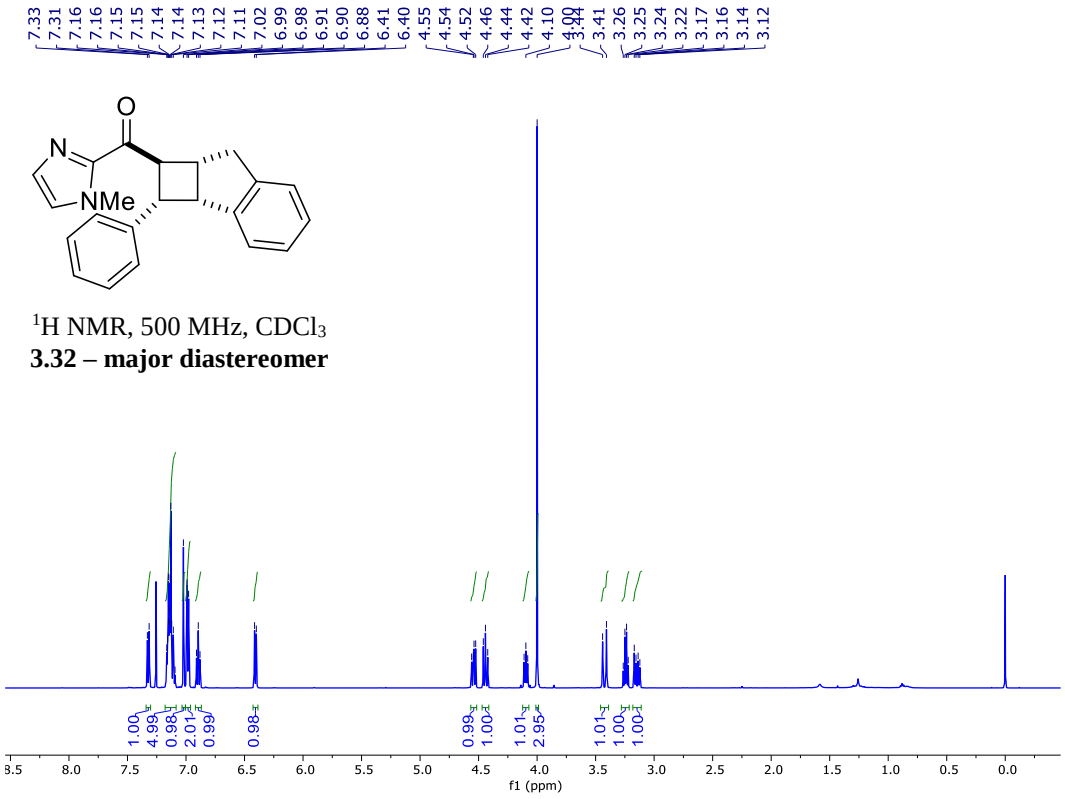

^{1}H NMR, 500 MHz, $CDCl_3$

3.32 – major diastereomer

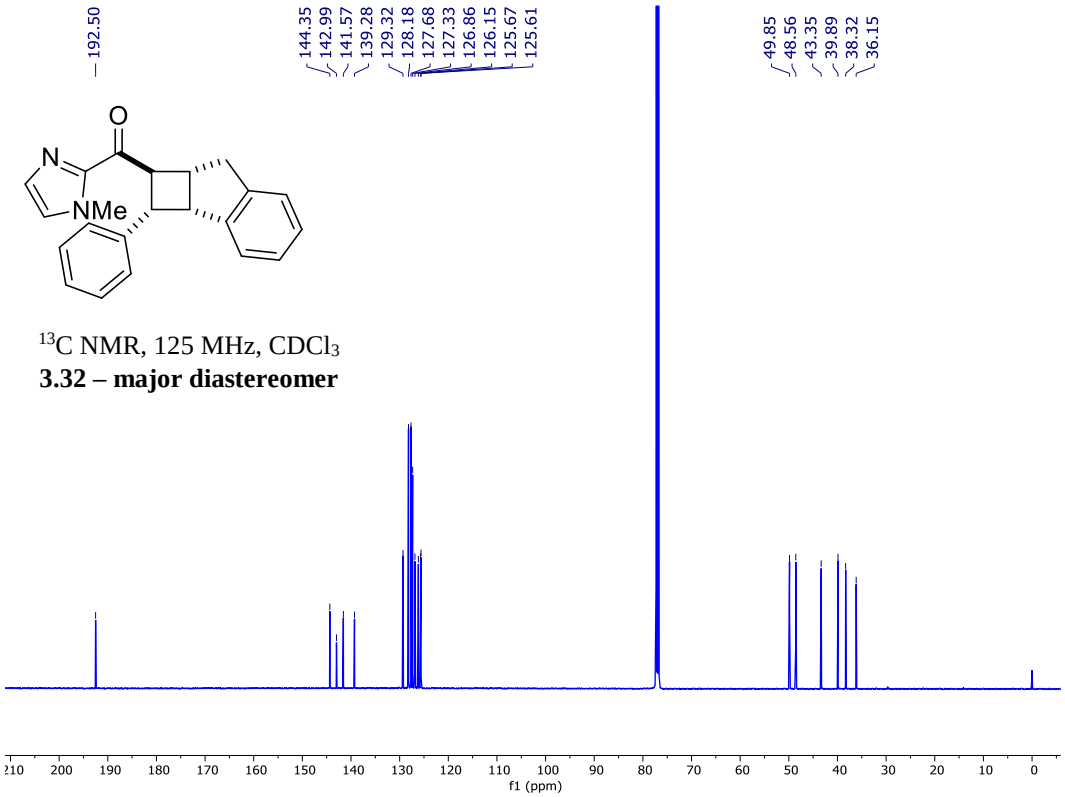

^{13}C NMR, 125 MHz, $CDCl_3$

3.32 – major diastereomer

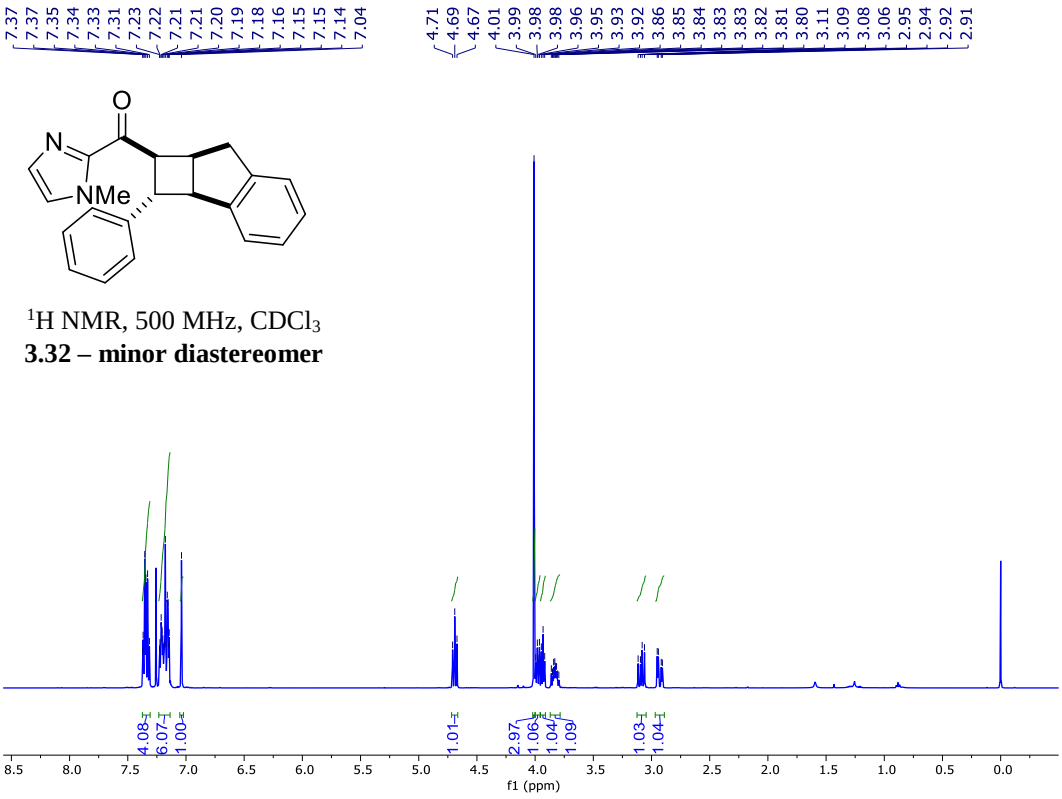

^{1}H NMR, 500 MHz, $CDCl_3$

3.32 – minor diastereomer

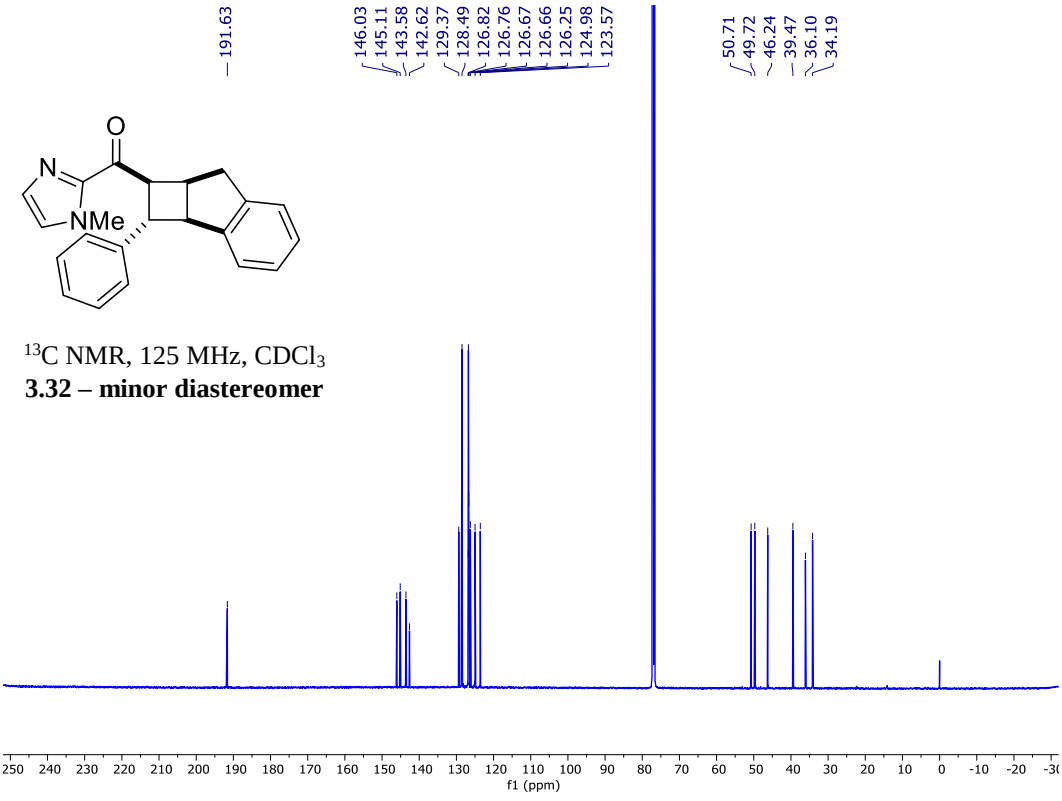

^{13}C NMR, 125 MHz, $CDCl_3$

3.32 – minor diastereomer

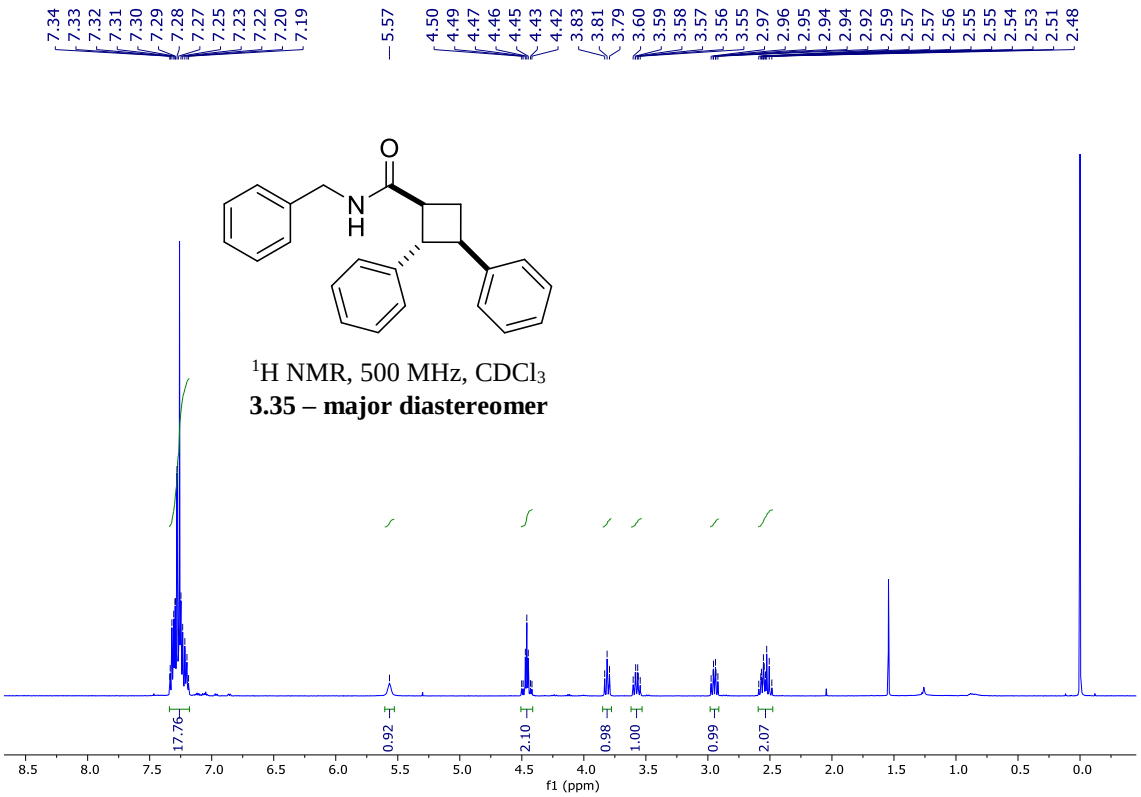

^{1}H NMR, 500 MHz, $CDCl_3$

3.35 – major diastereomer

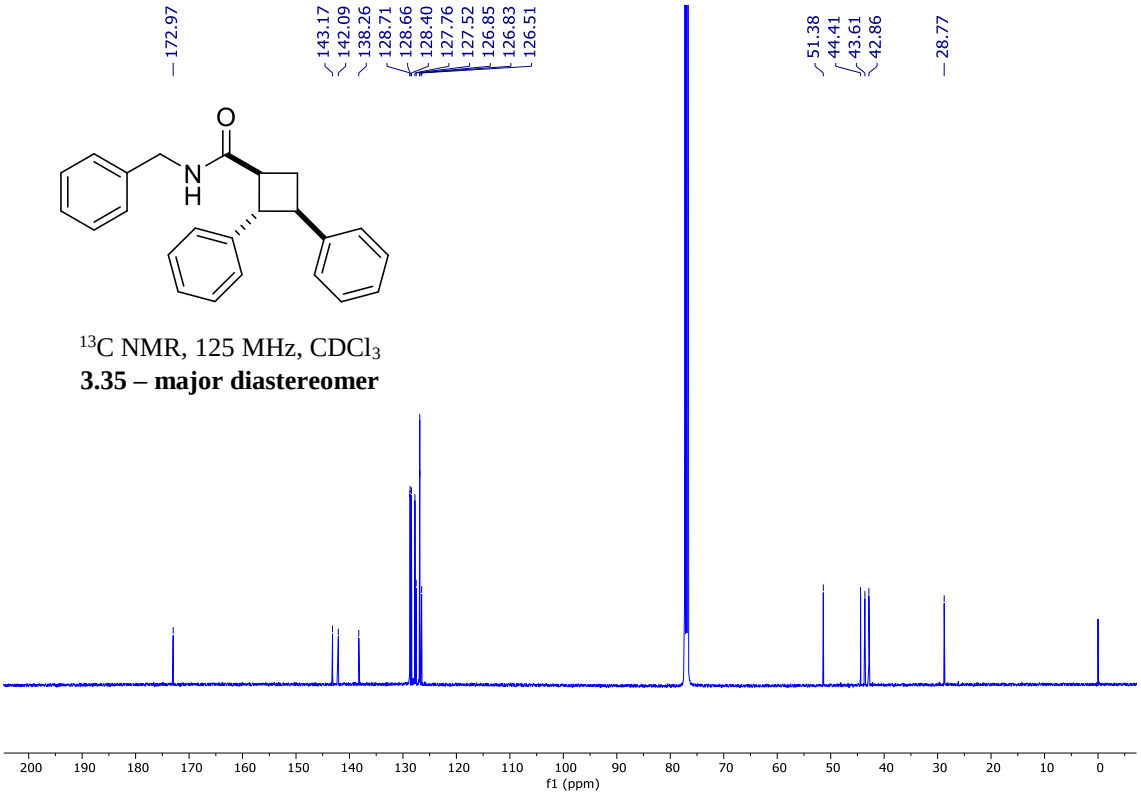

^{13}C NMR, 125 MHz, $CDCl_3$

3.35 – major diastereomer

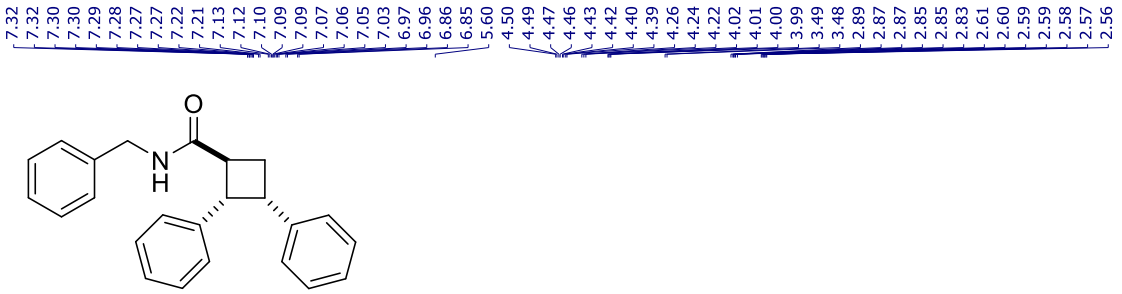

^{1}H NMR, 500 MHz, $CDCl_3$

3.35 – minor diastereomer

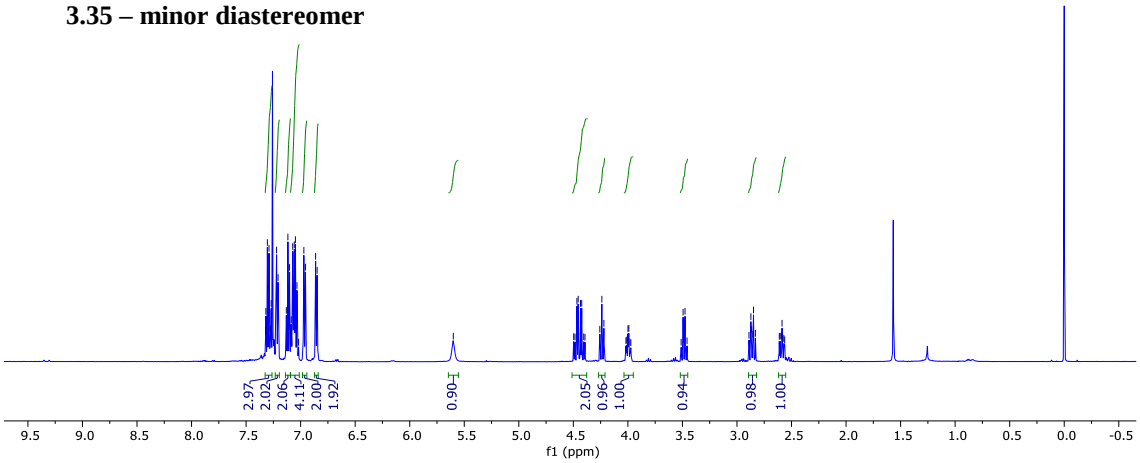

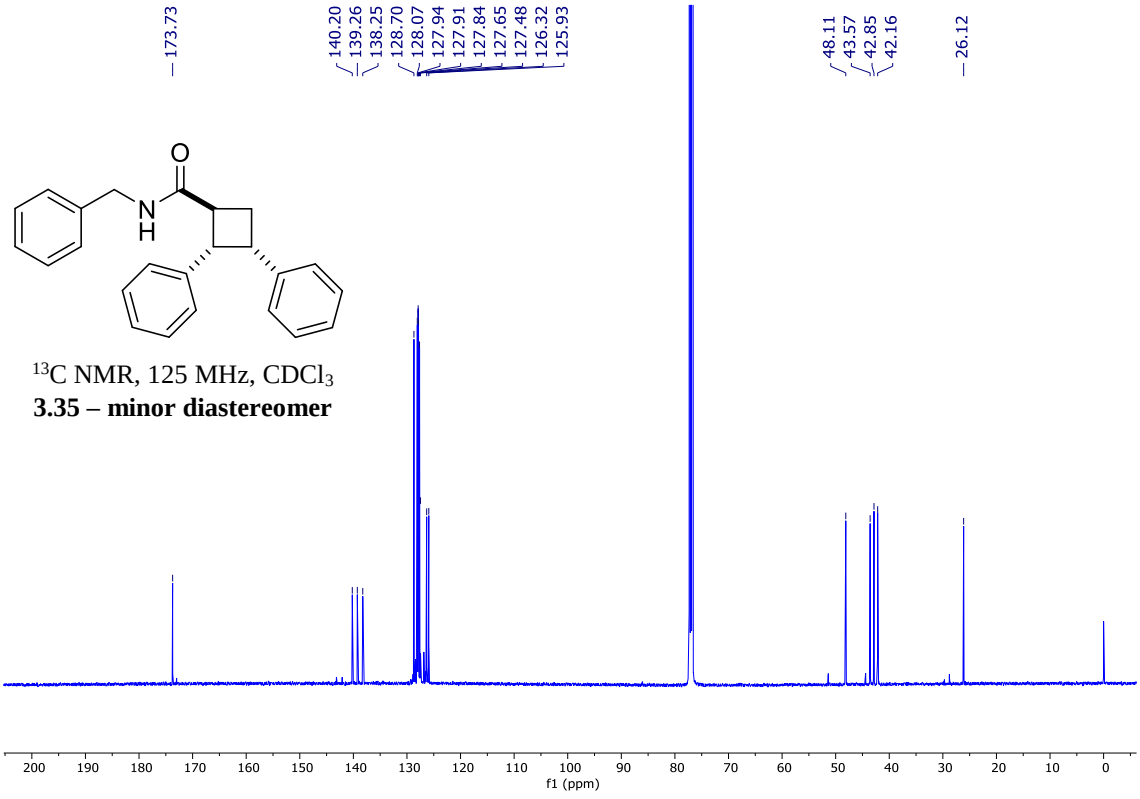

^{13}C NMR, 125 MHz, $CDCl_3$

3.35 – minor diastereomer

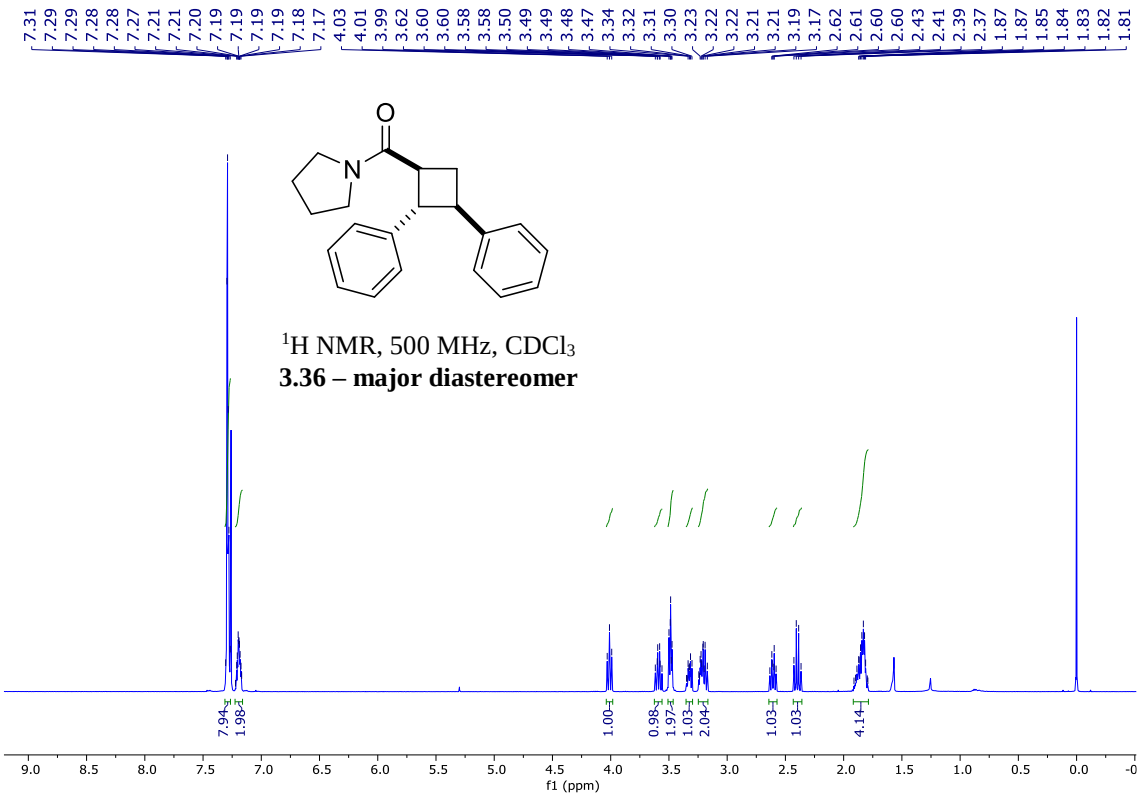

^{1}H NMR, 500 MHz, $CDCl_3$
3.36 – major diastereomer

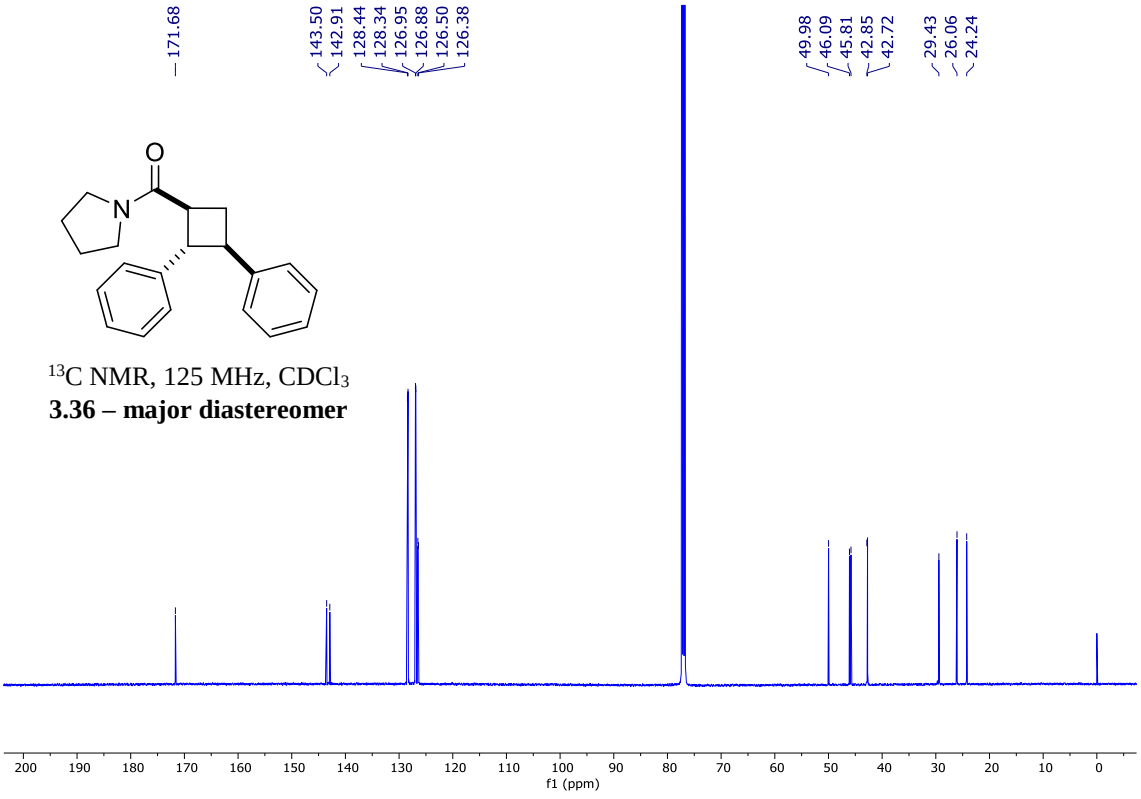

^{13}C NMR, 125 MHz, $CDCl_3$
3.36 – major diastereomer

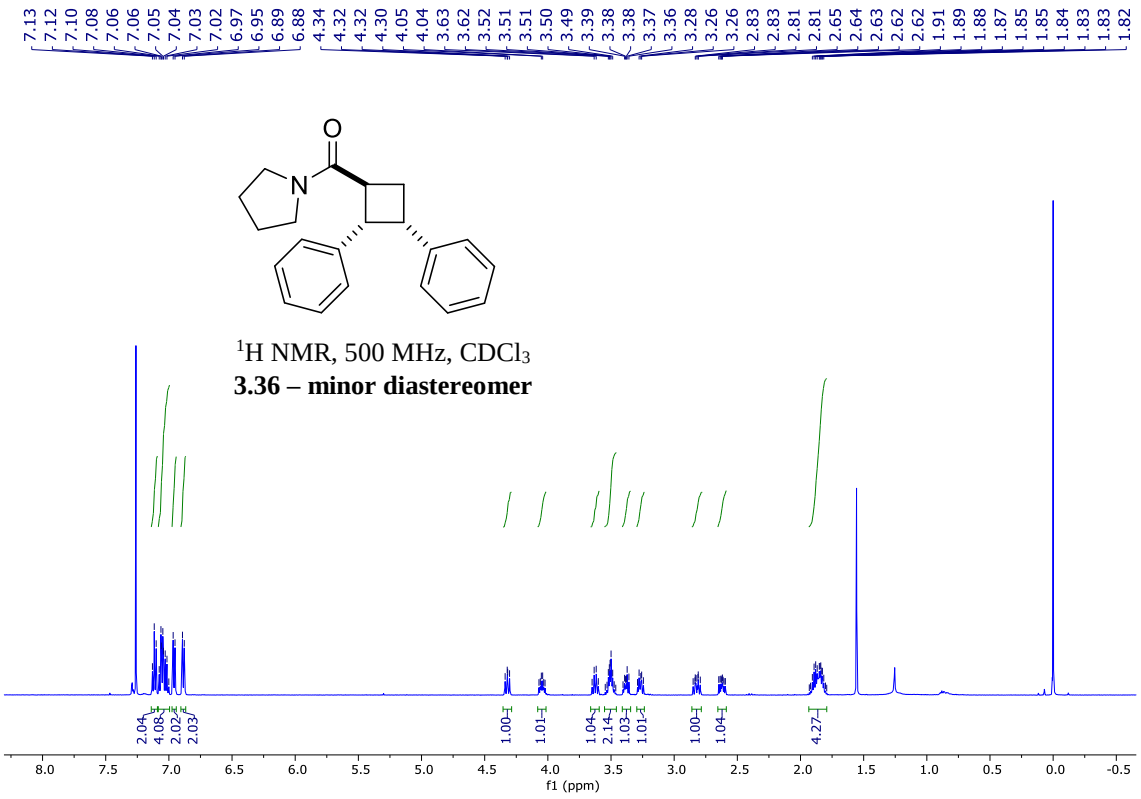

^{1}H NMR, 500 MHz, $CDCl_3$

3.36 – minor diastereomer

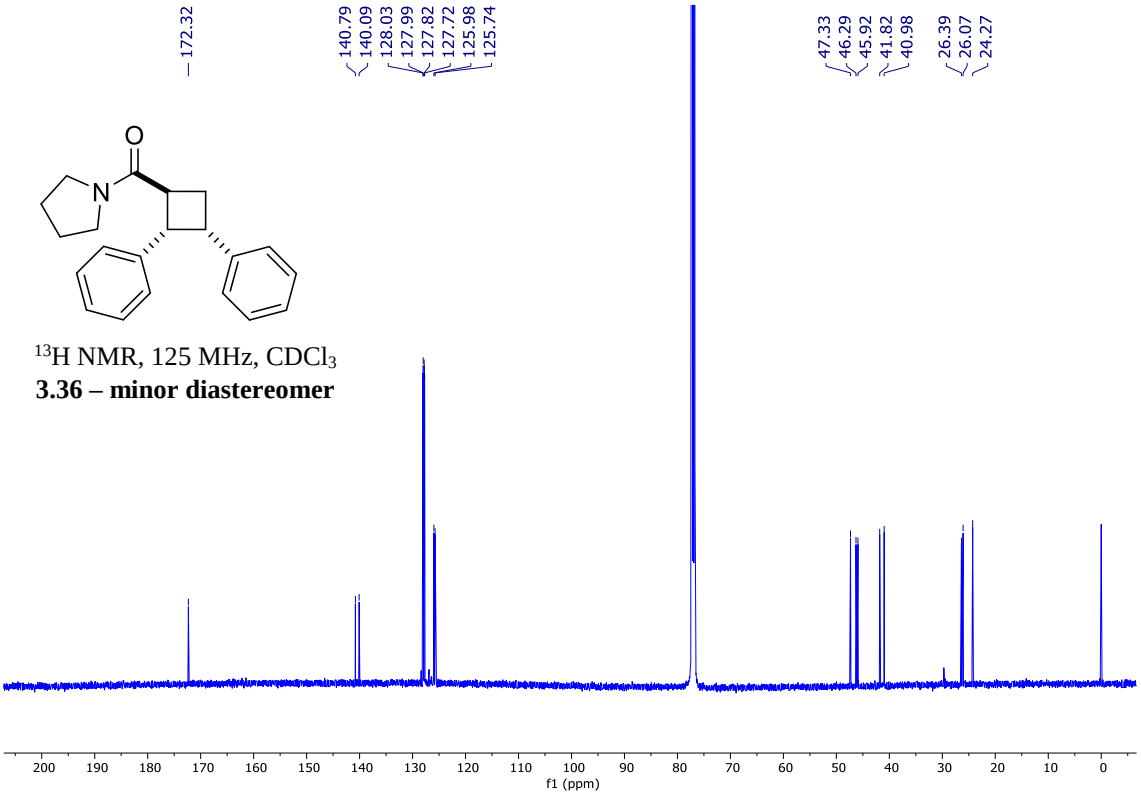

^{13}H NMR, 125 MHz, $CDCl_3$

3.36 – minor diastereomer

Figure A-3. List of New Compounds for Chapter 4

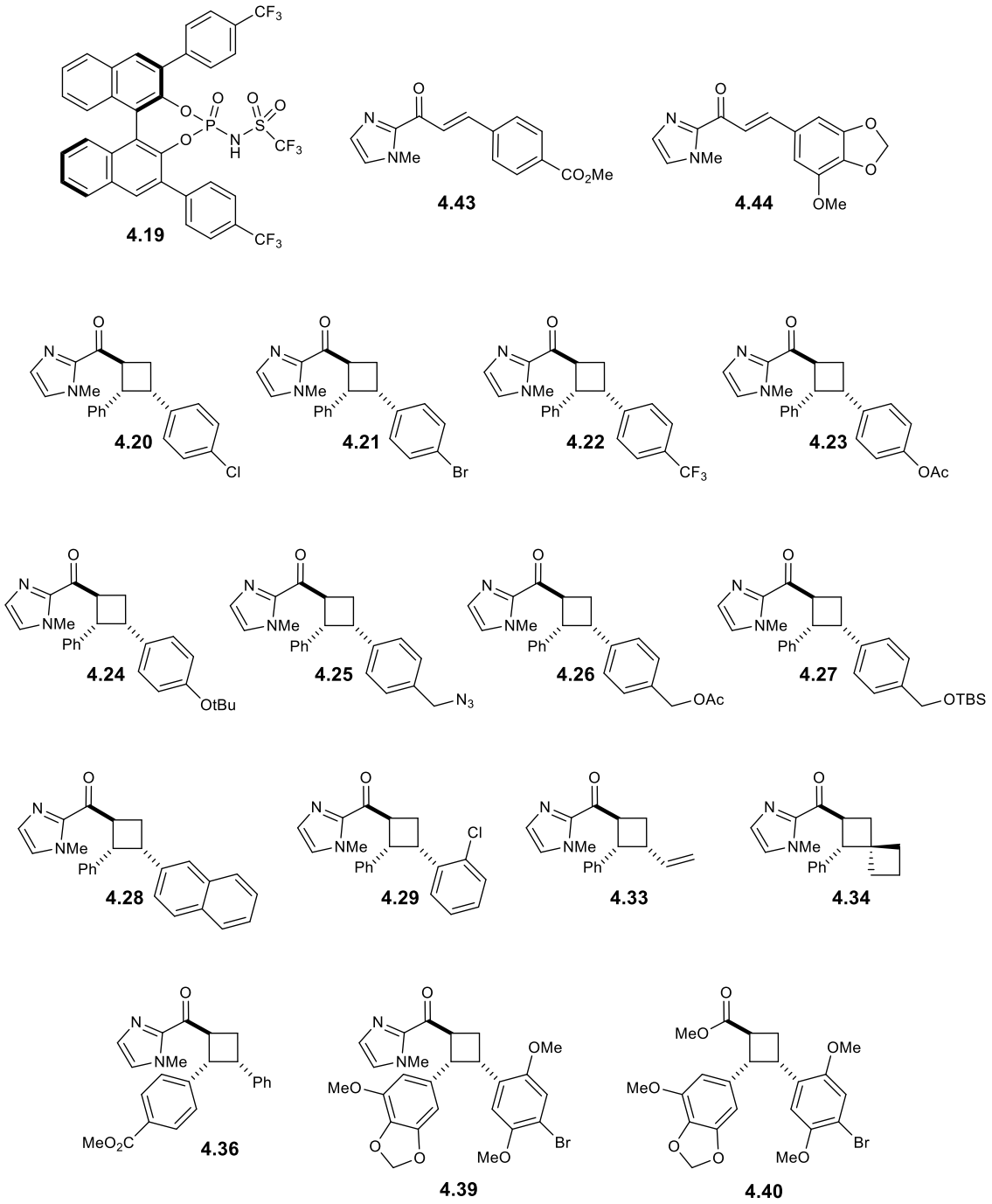

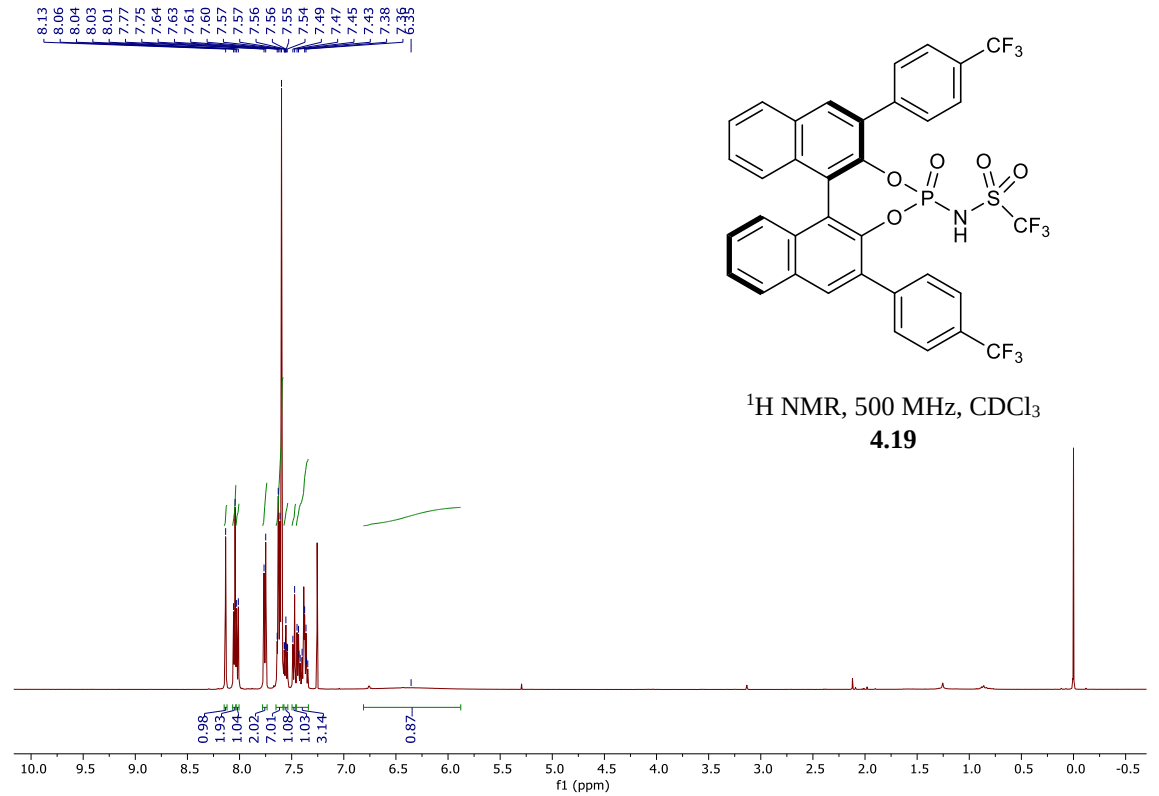

^{1}H NMR, 500 MHz, $CDCl_3$
4.19

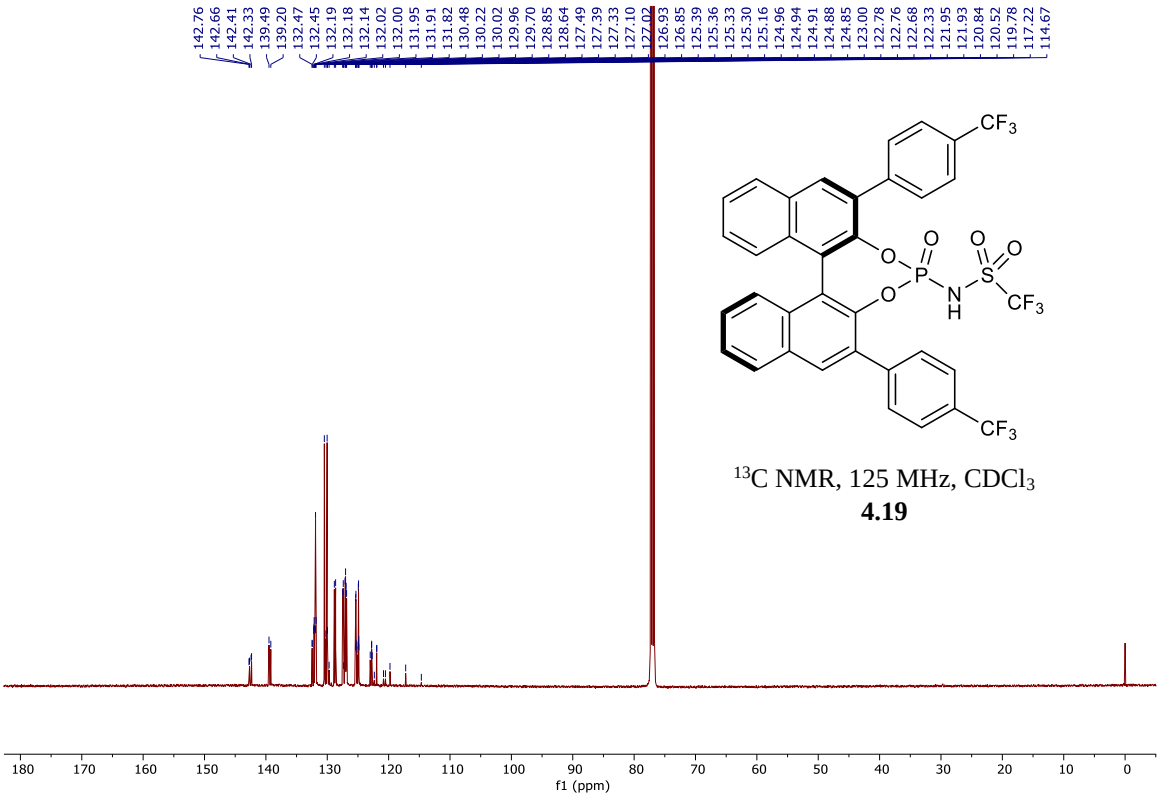

^{13}C NMR, 125 MHz, $CDCl_3$
4.19

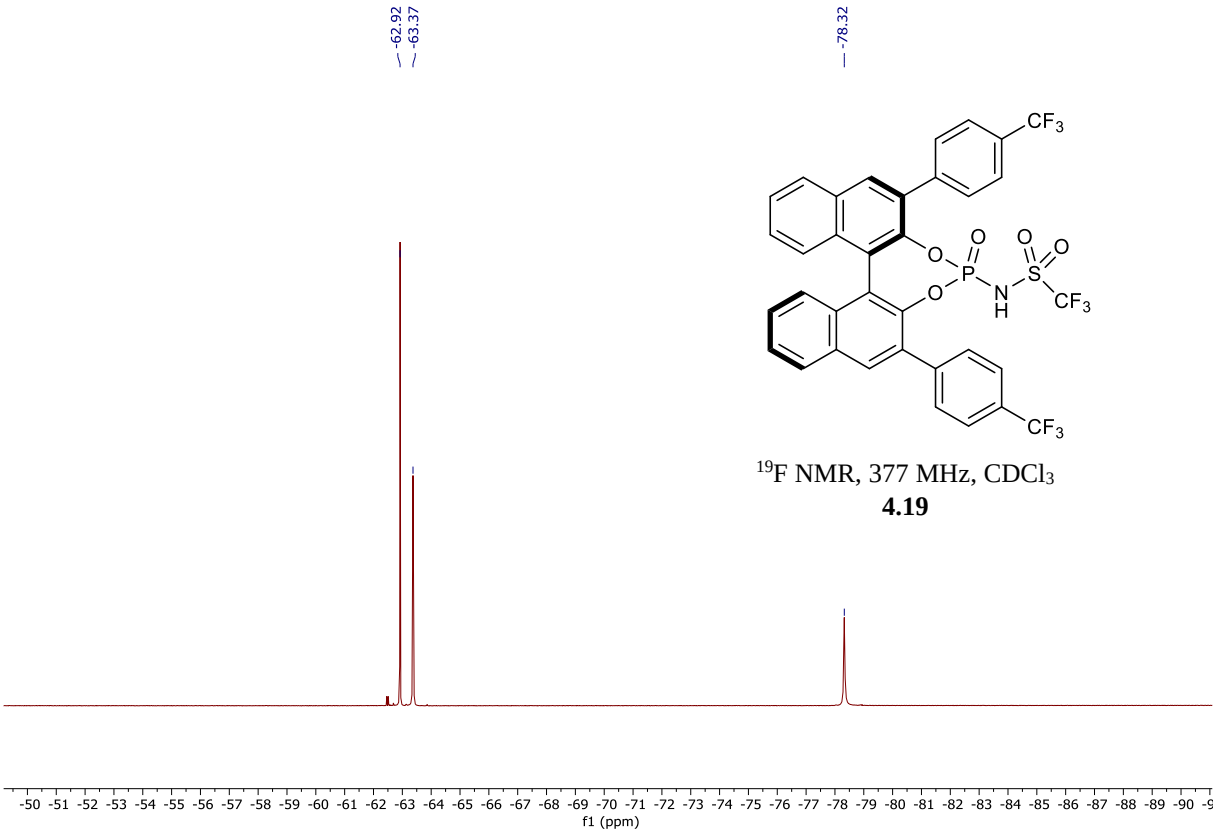

^{19}F NMR, 377 MHz, $CDCl_3$

4.19

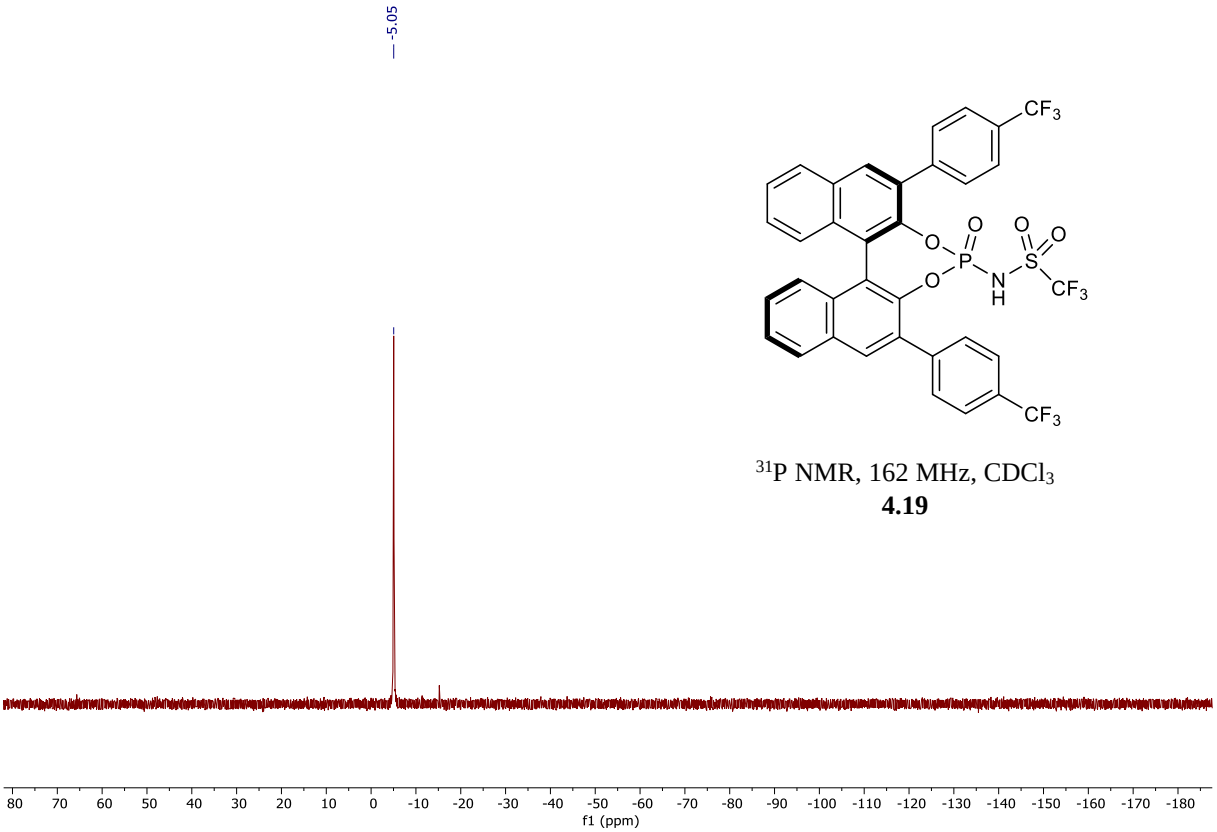

^{31}P NMR, 162 MHz, $CDCl_3$

4.19

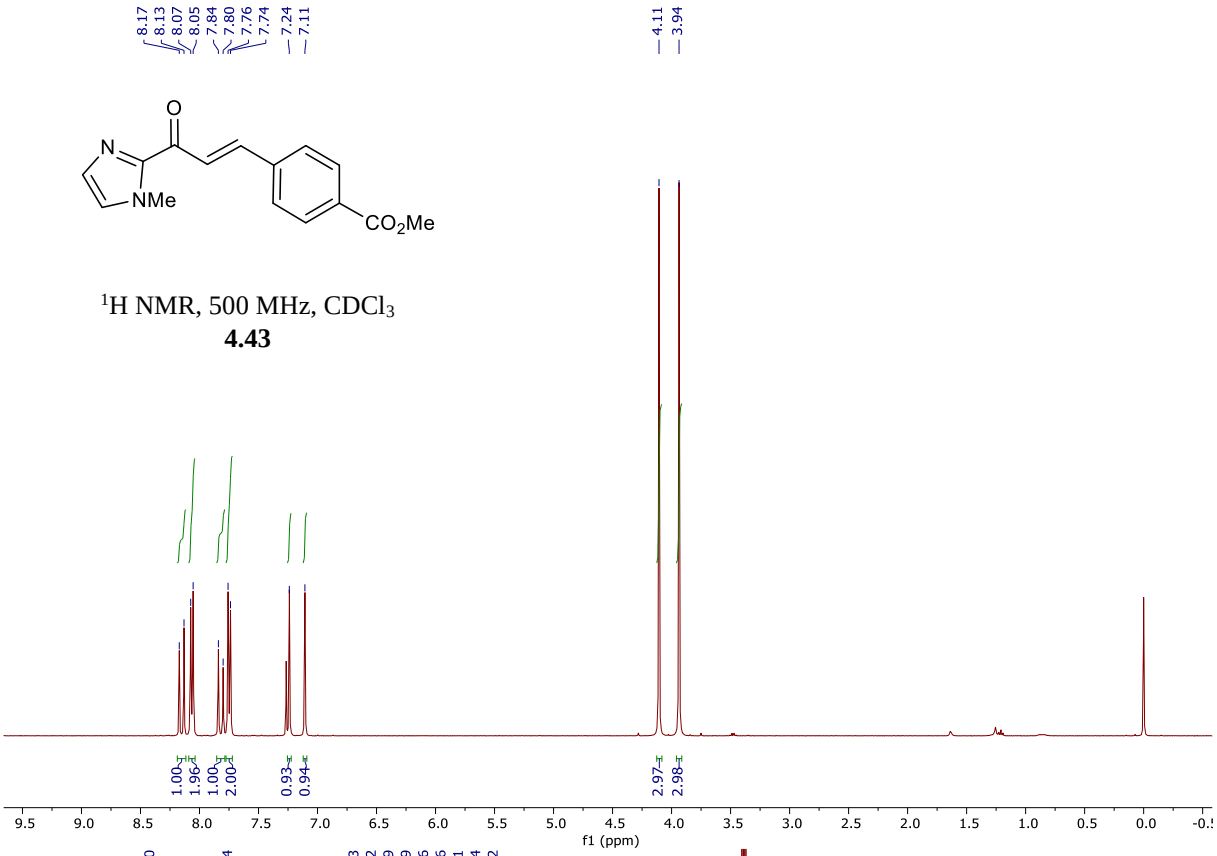

^{1}H NMR, 500 MHz, $CDCl_3$
4.43

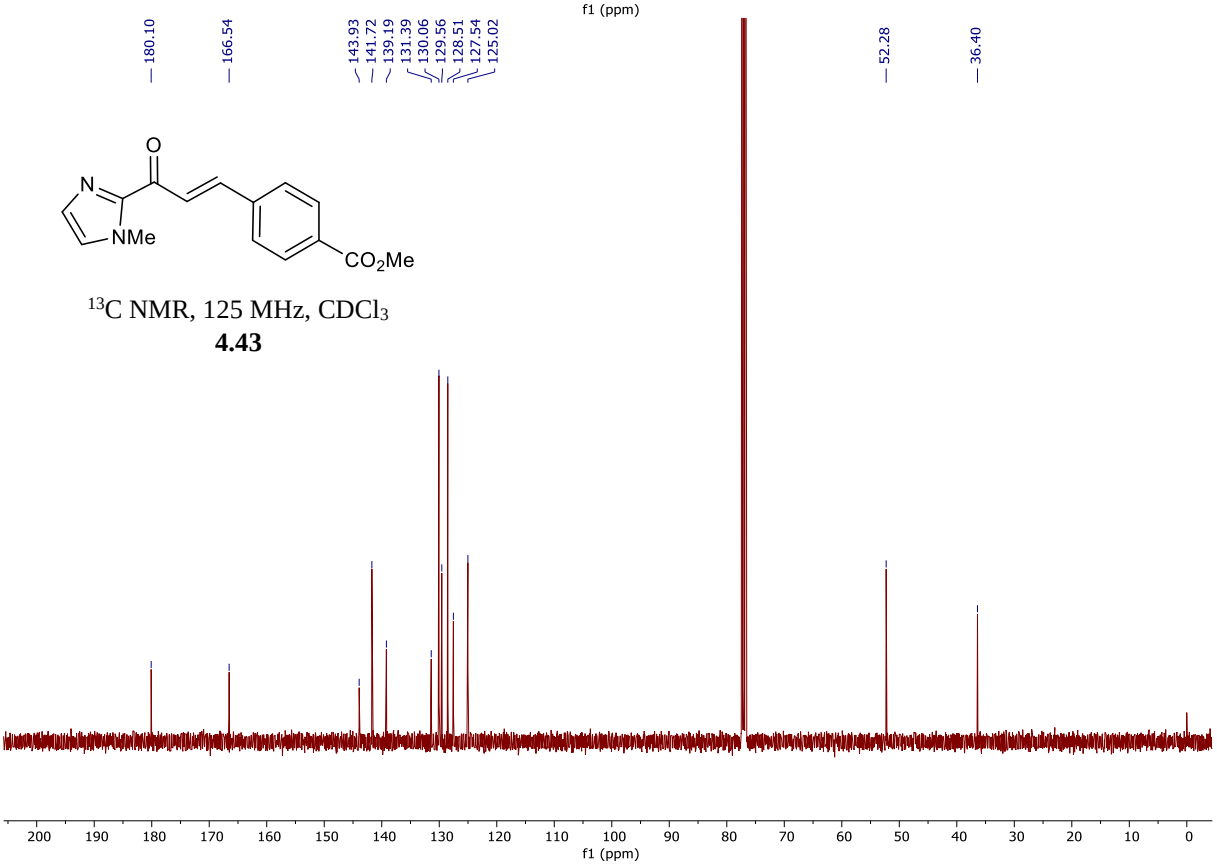

^{13}C NMR, 125 MHz, $CDCl_3$
4.43

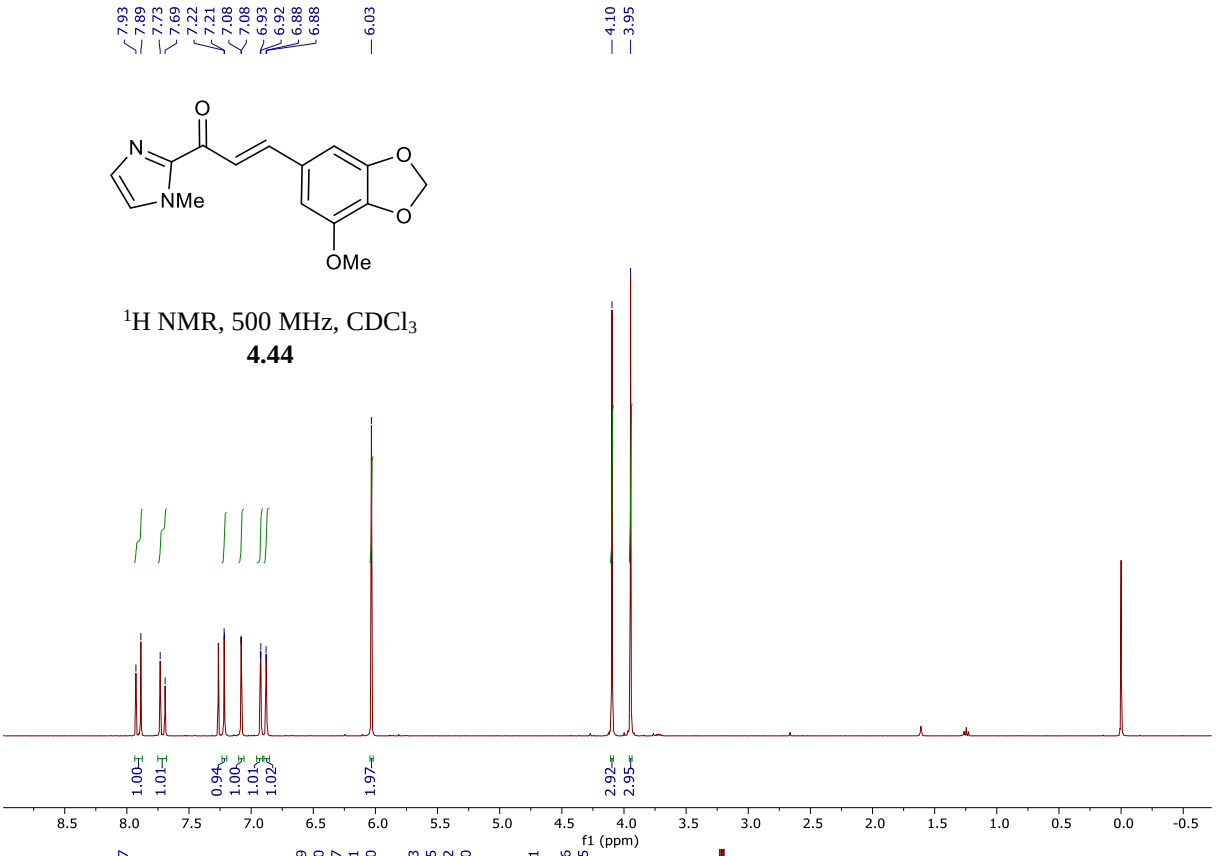

^{1}H NMR, 500 MHz, $CDCl_3$
4.44

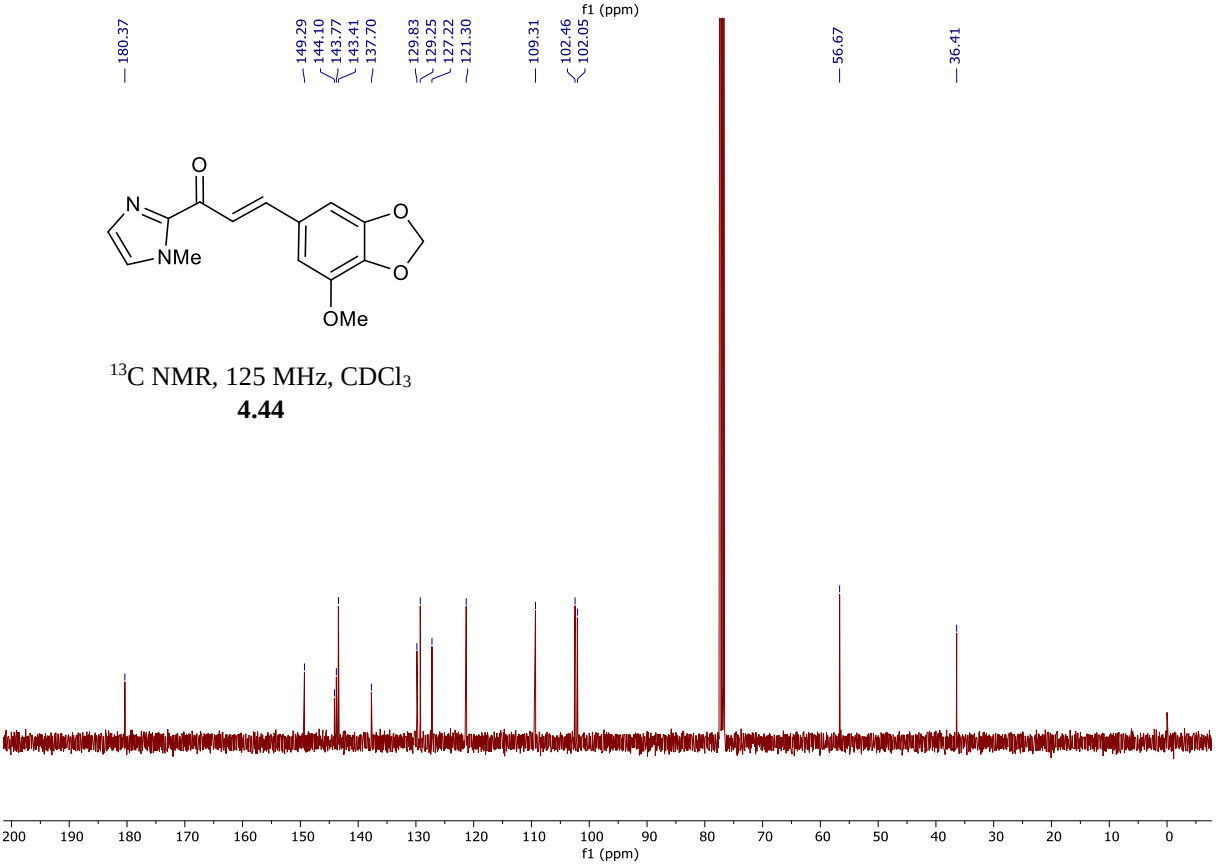

^{13}C NMR, 125 MHz, $CDCl_3$
4.44

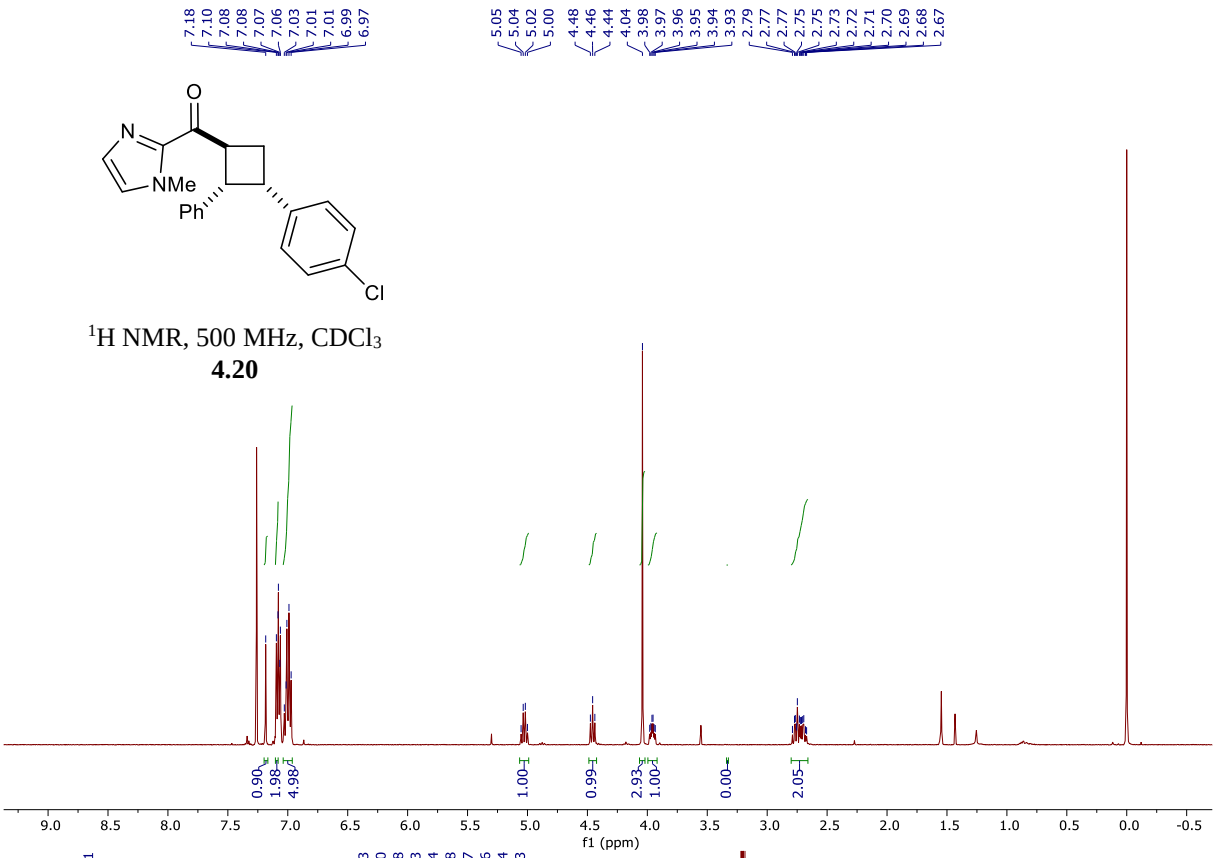

^{1}H NMR, 500 MHz, $CDCl_3$
4.20

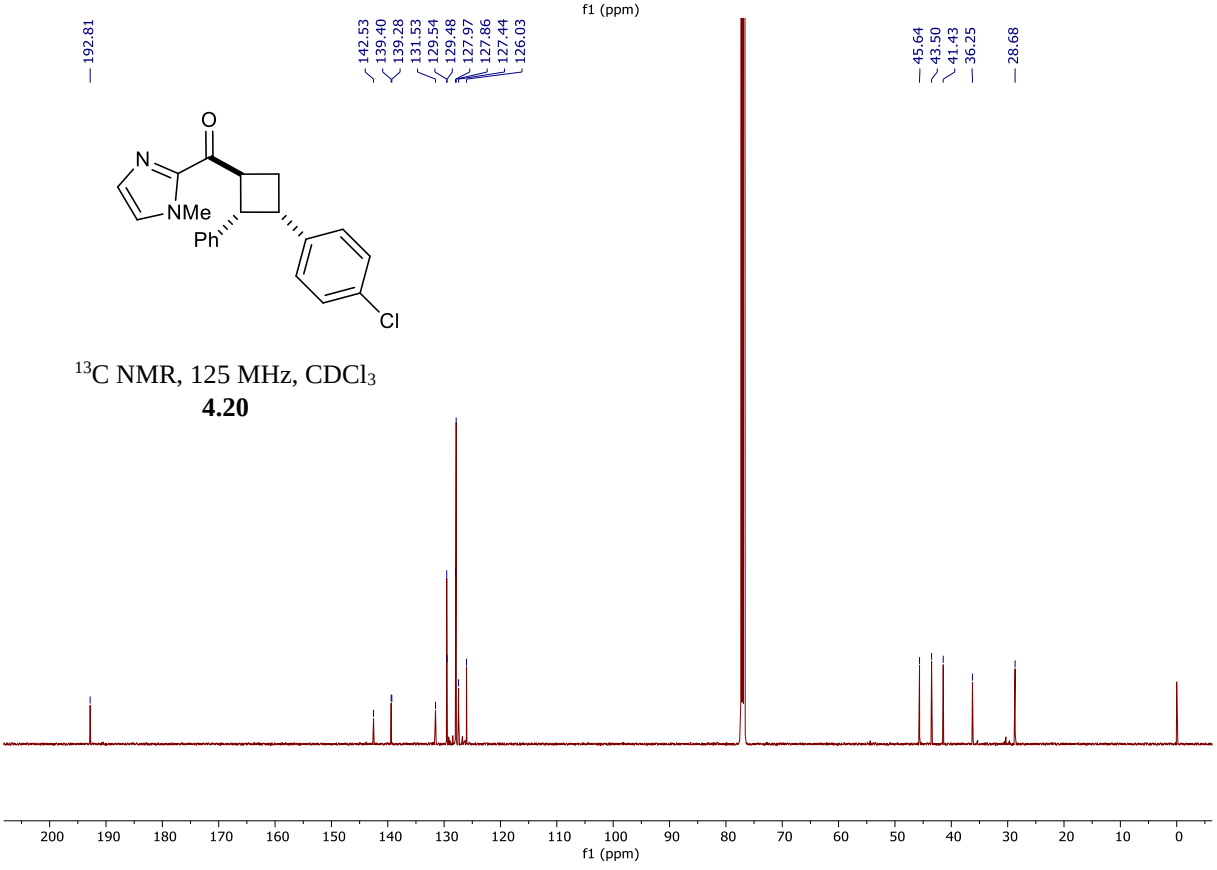

^{13}C NMR, 125 MHz, $CDCl_3$
4.20

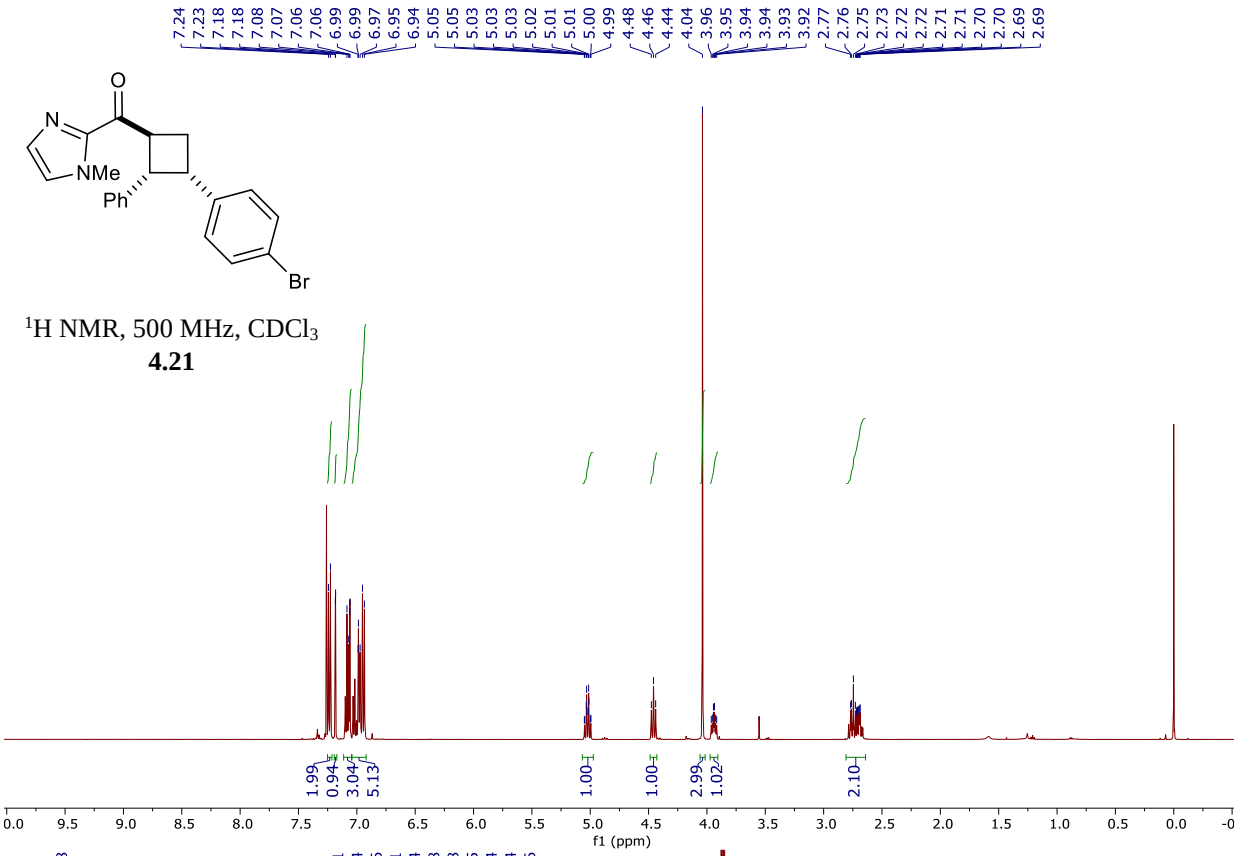

^{1}H NMR, 500 MHz, $CDCl_3$
4.21

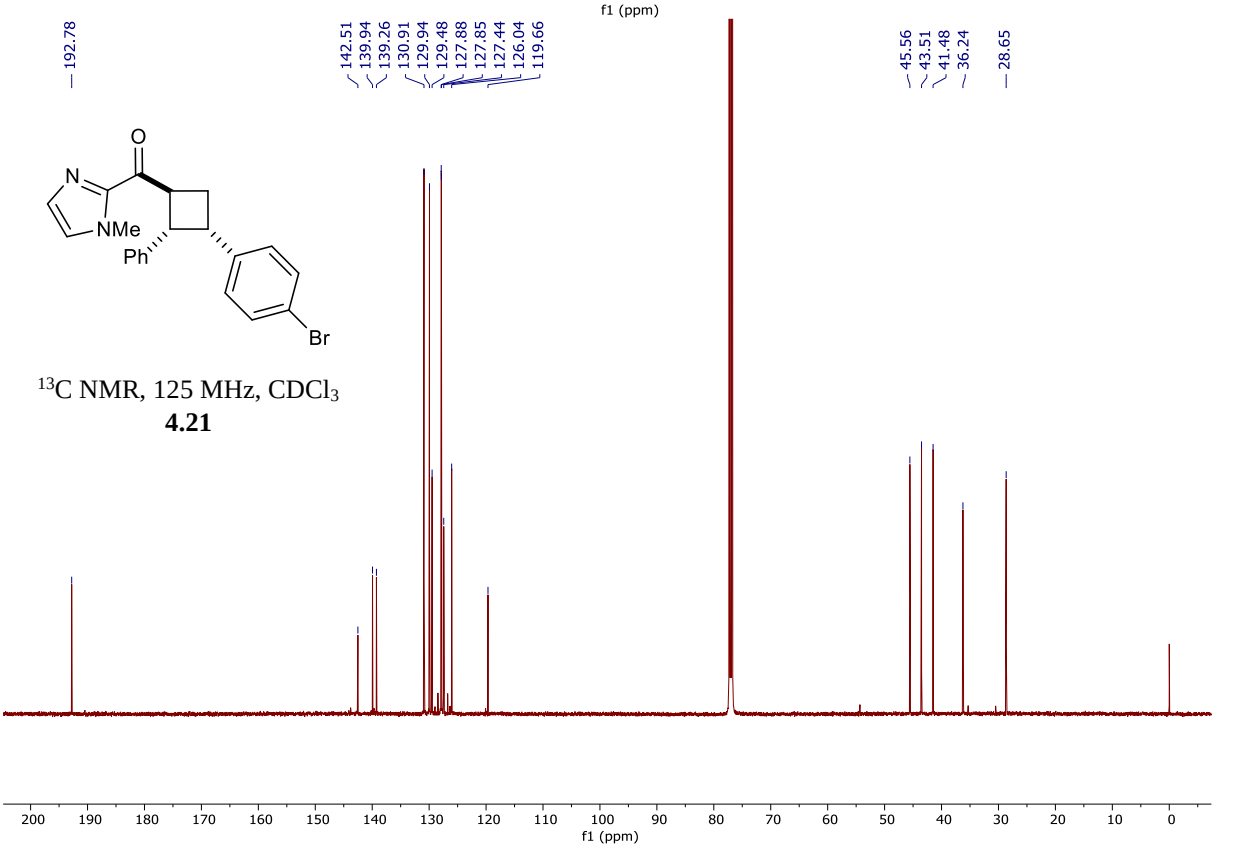

^{13}C NMR, 125 MHz, $CDCl_3$
4.21

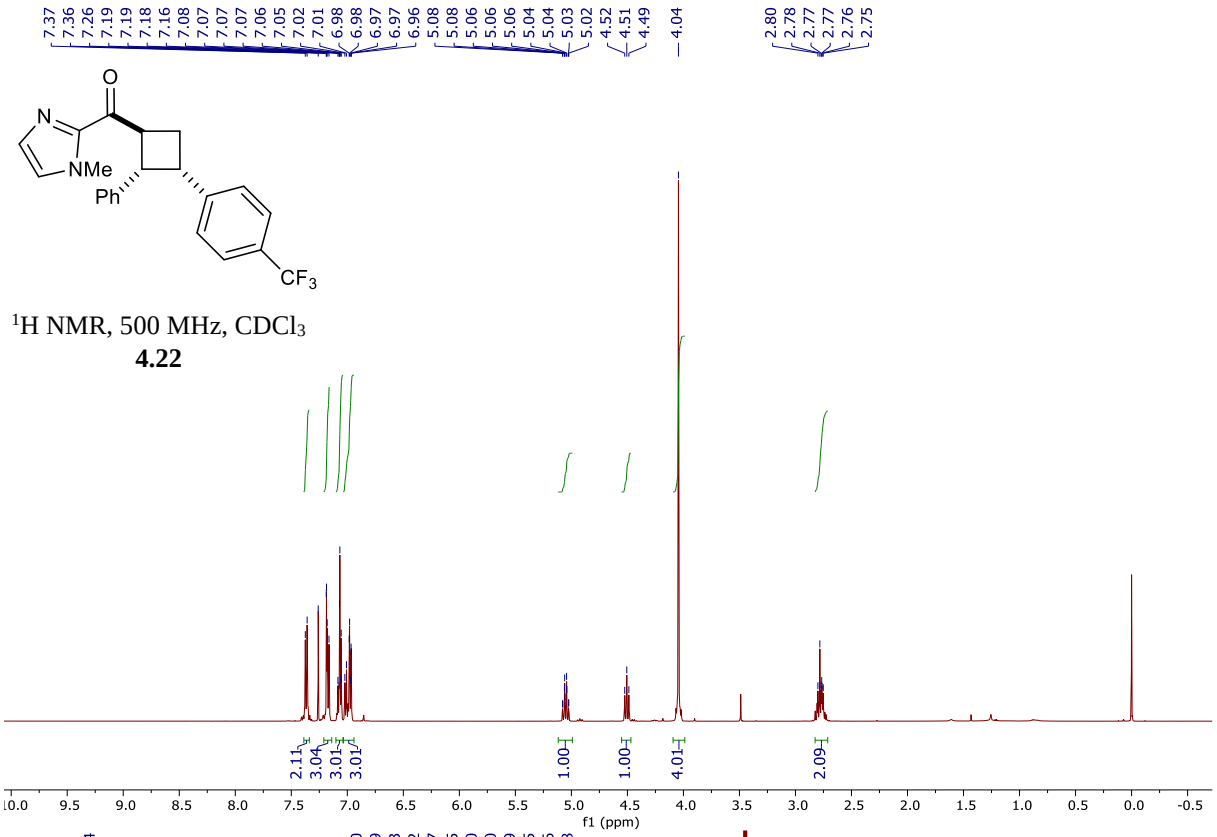

^{1}H NMR, 500 MHz, $CDCl_3$

4.22

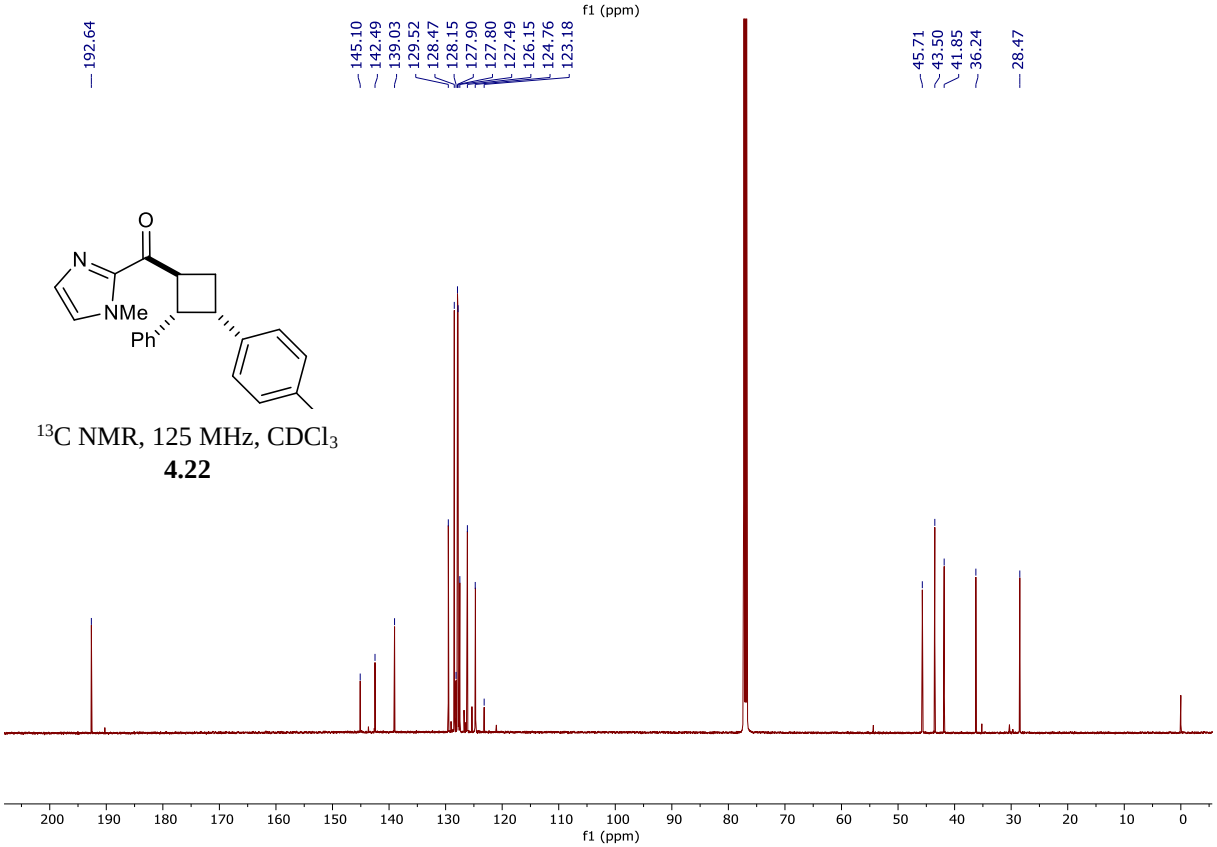

^{13}C NMR, 125 MHz, $CDCl_3$

4.22

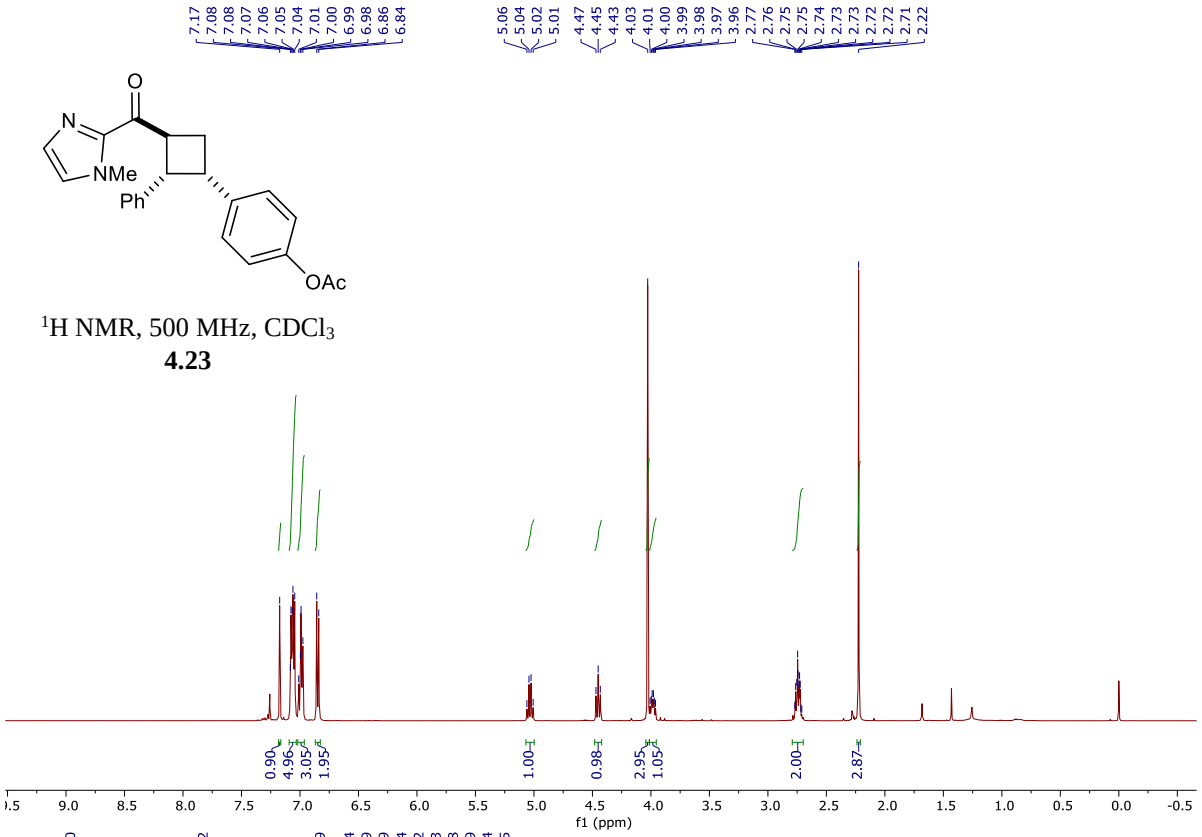

^{1}H NMR, 500 MHz, $CDCl_3$

4.23

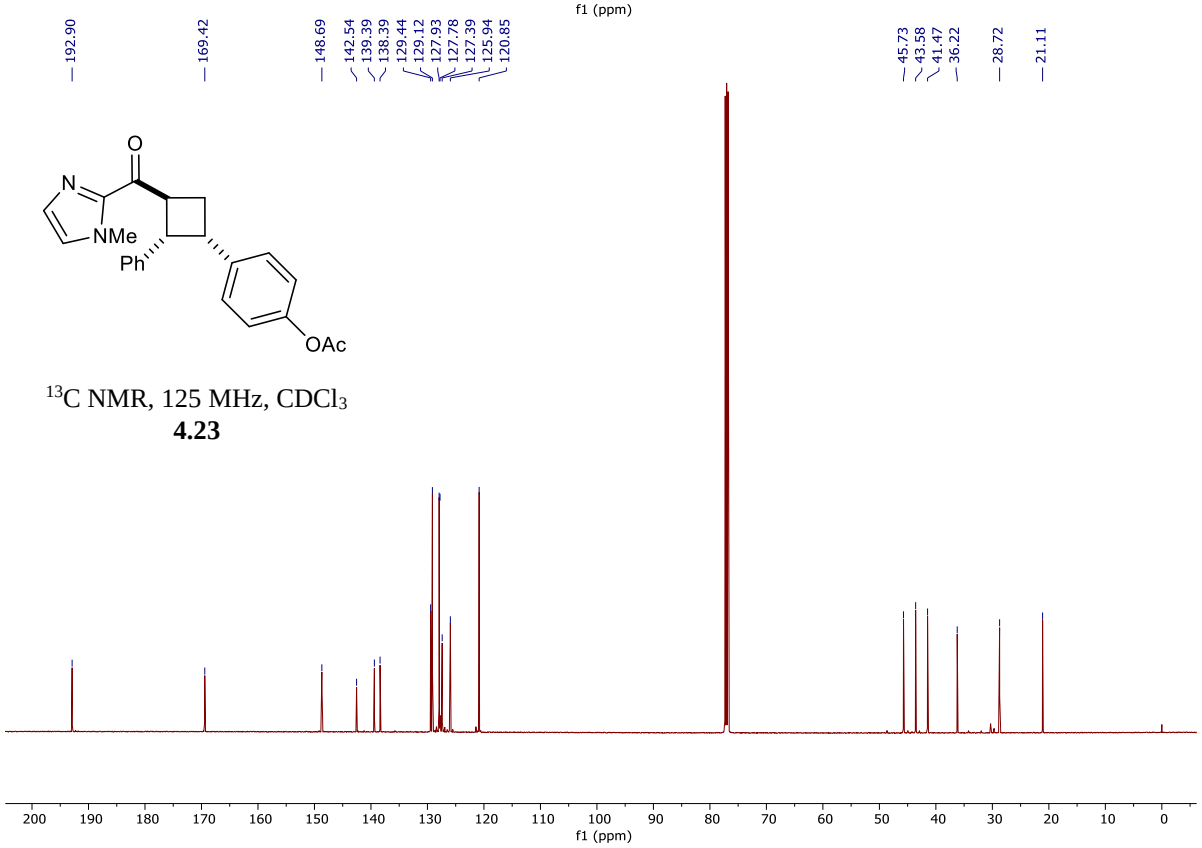

^{13}C NMR, 125 MHz, $CDCl_3$

4.23

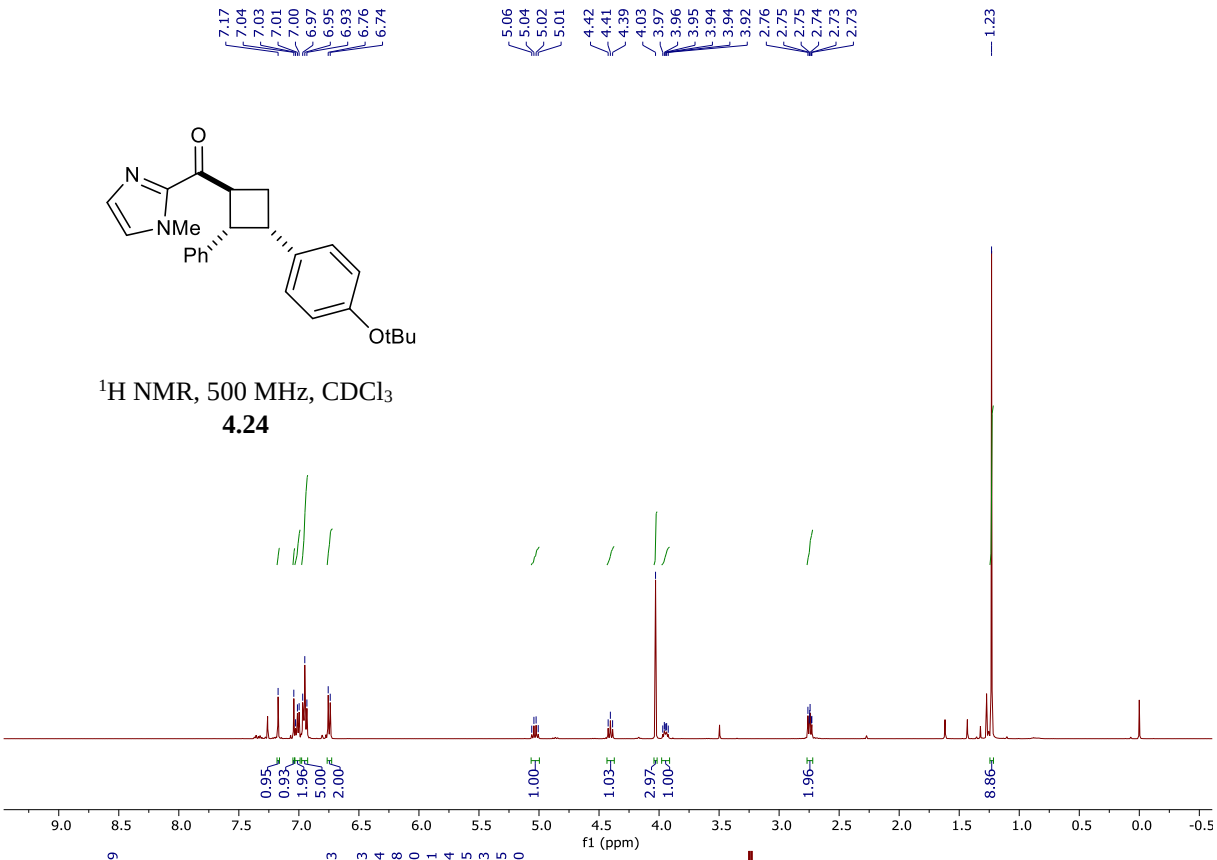

^{1}H NMR, 500 MHz, $CDCl_3$

4.24

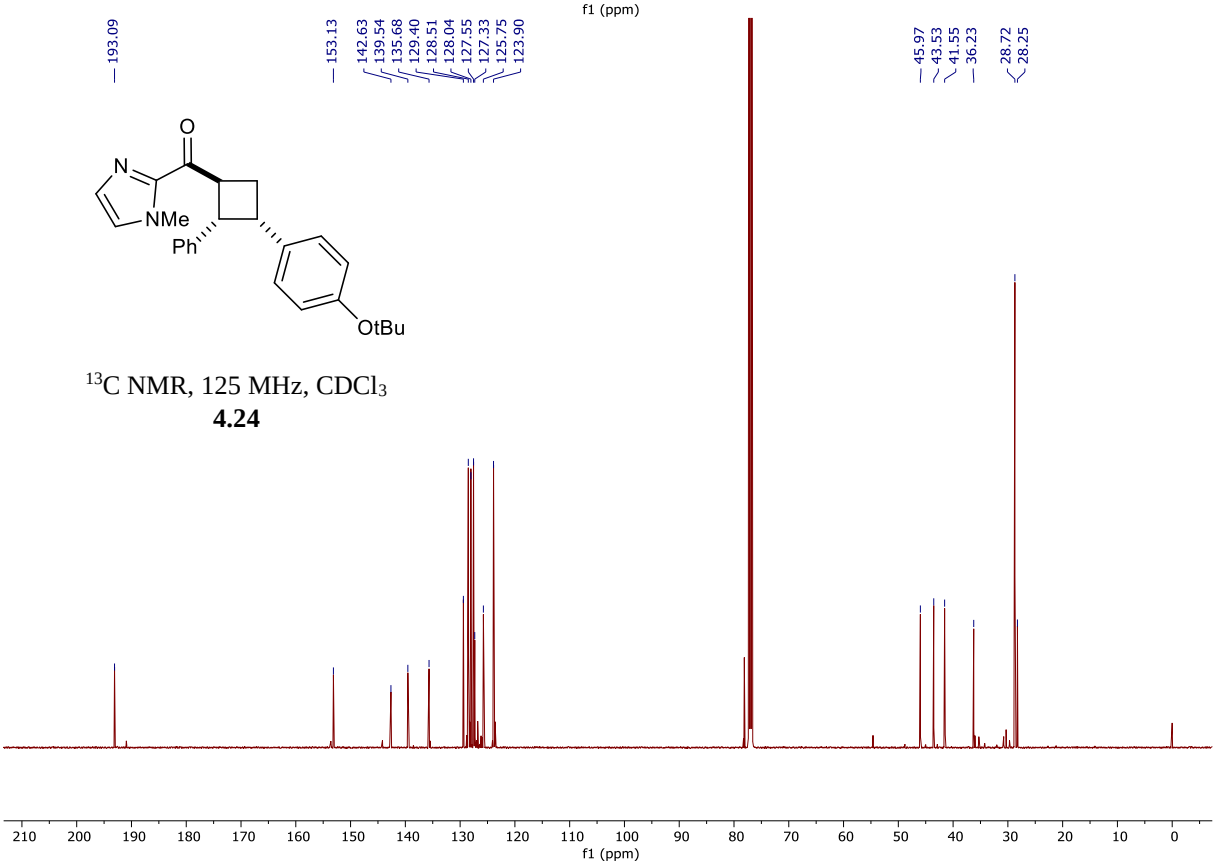

^{13}C NMR, 125 MHz, $CDCl_3$

4.24

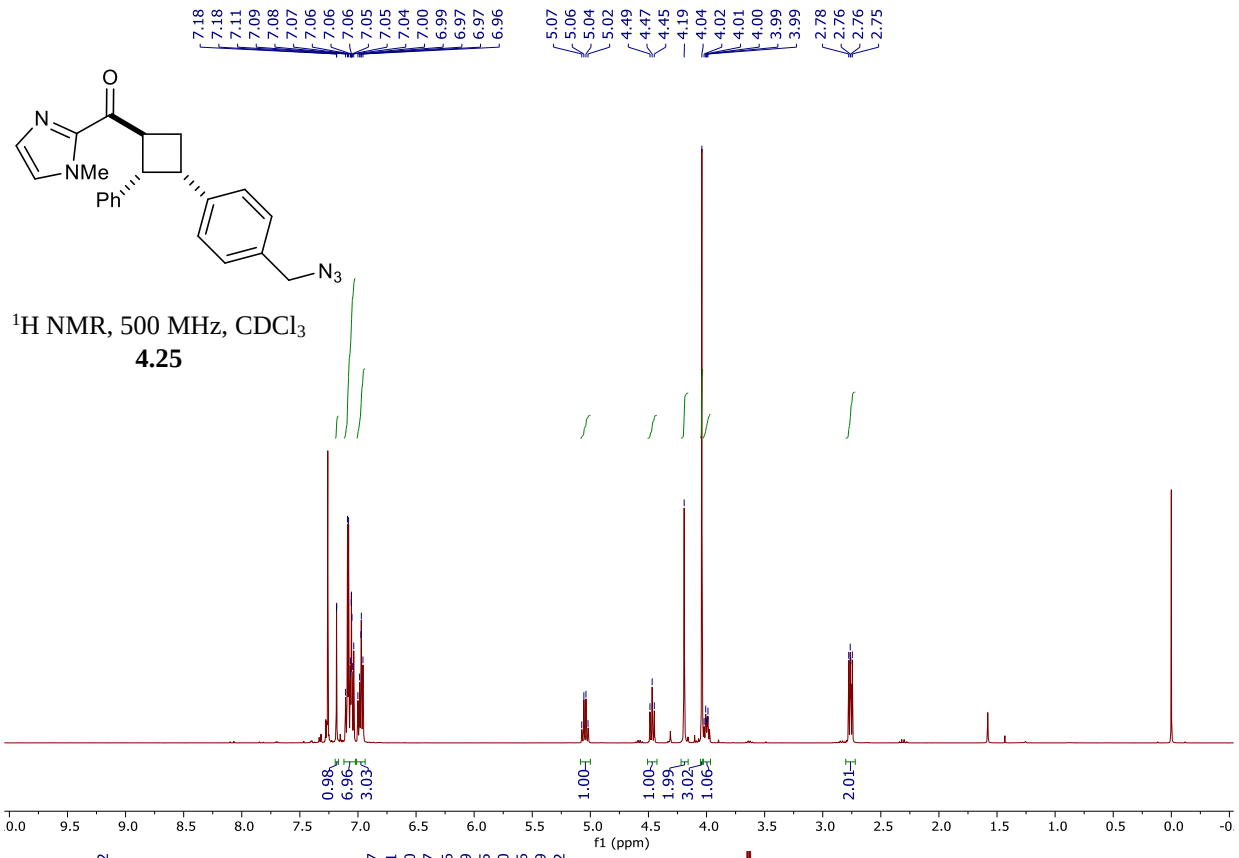

^{1}H NMR, 500 MHz, $CDCl_3$

4.25

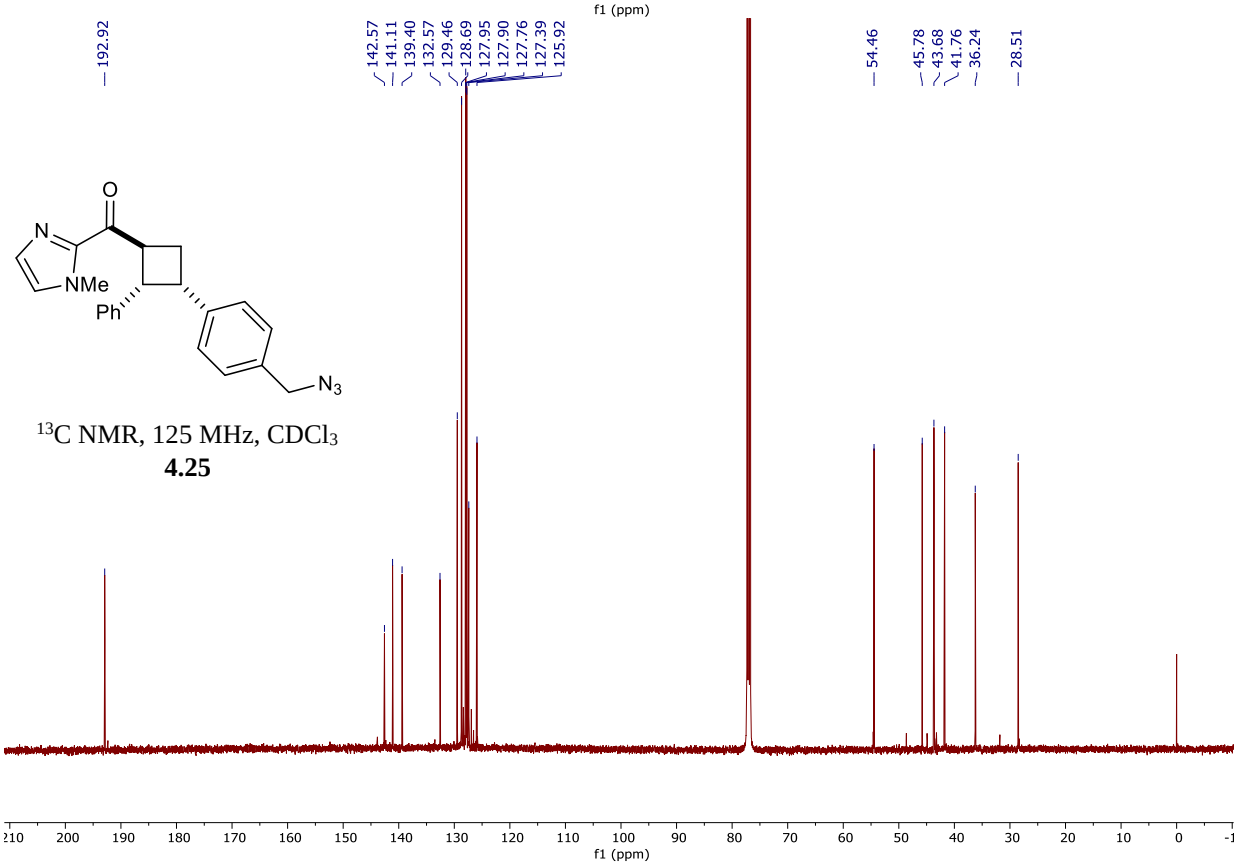

^{13}C NMR, 125 MHz, $CDCl_3$

4.25

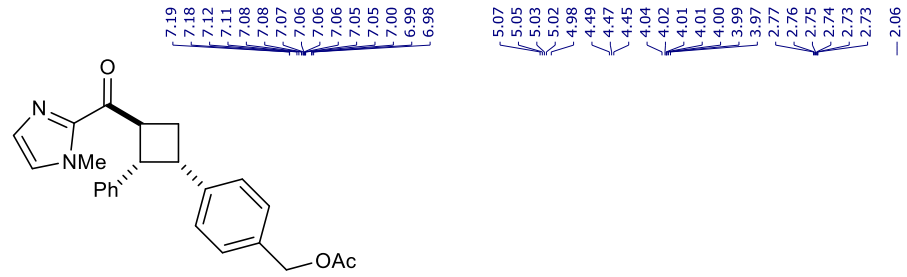

^{1}H NMR, 500 MHz, $CDCl_3$

4.26

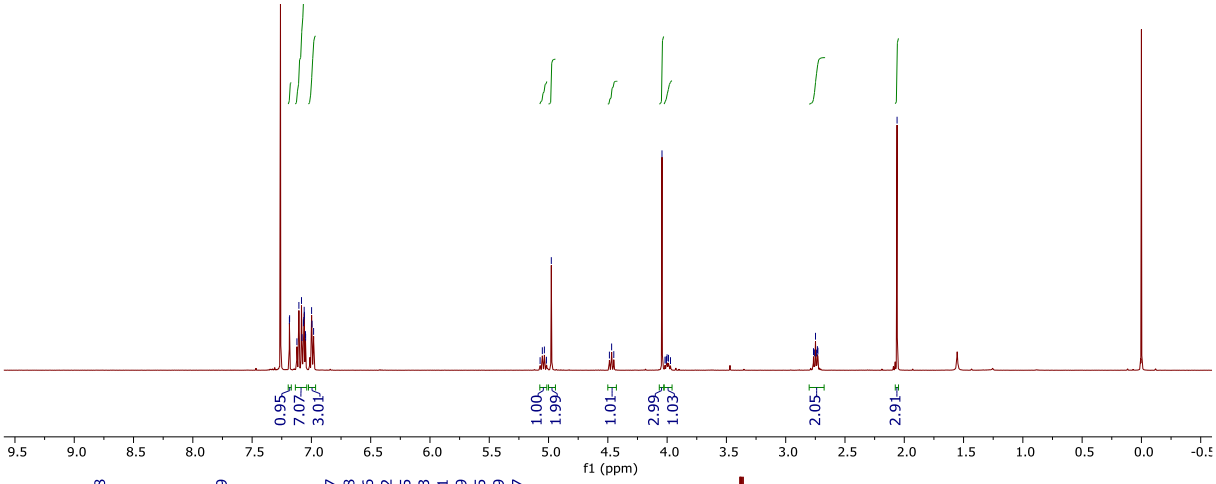

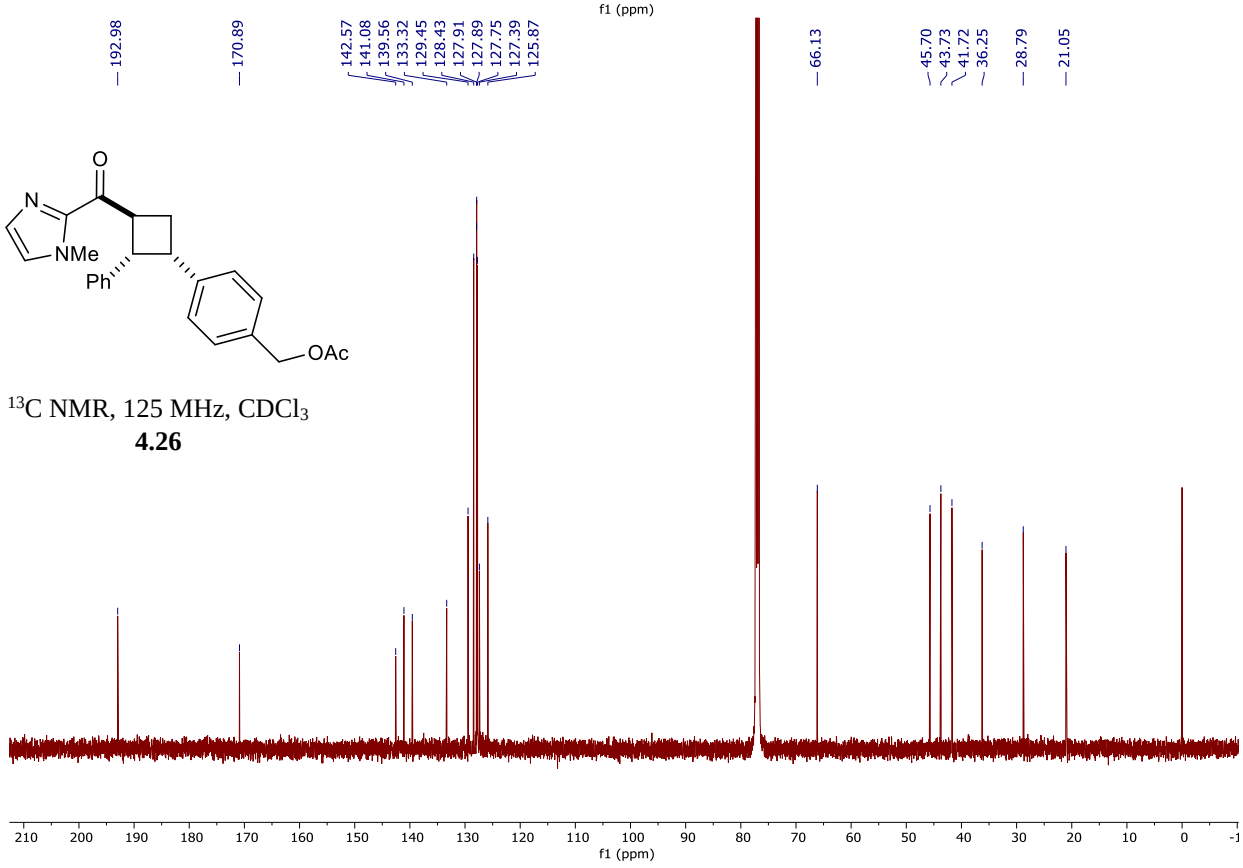

^{13}C NMR, 125 MHz, $CDCl_3$

4.26

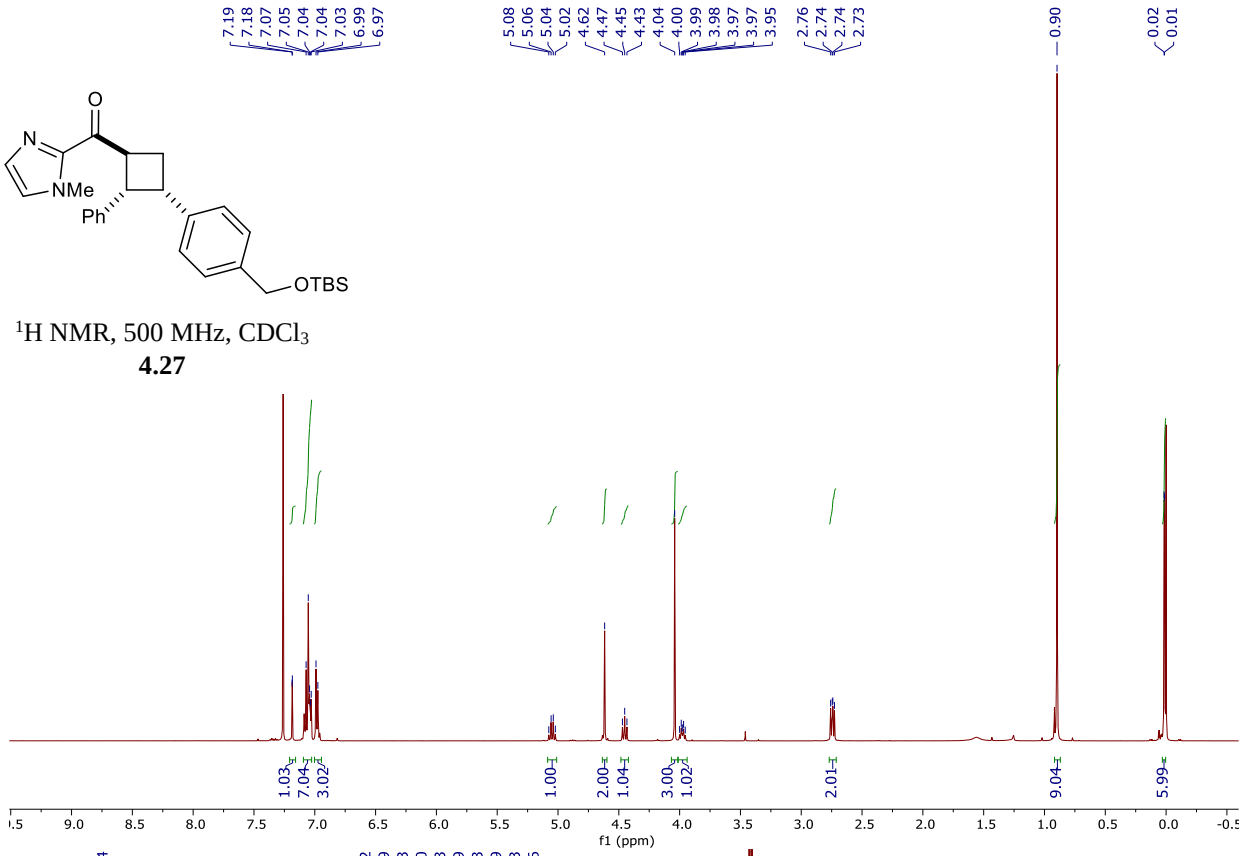

^{1}H NMR, 500 MHz, $CDCl_3$
4.27

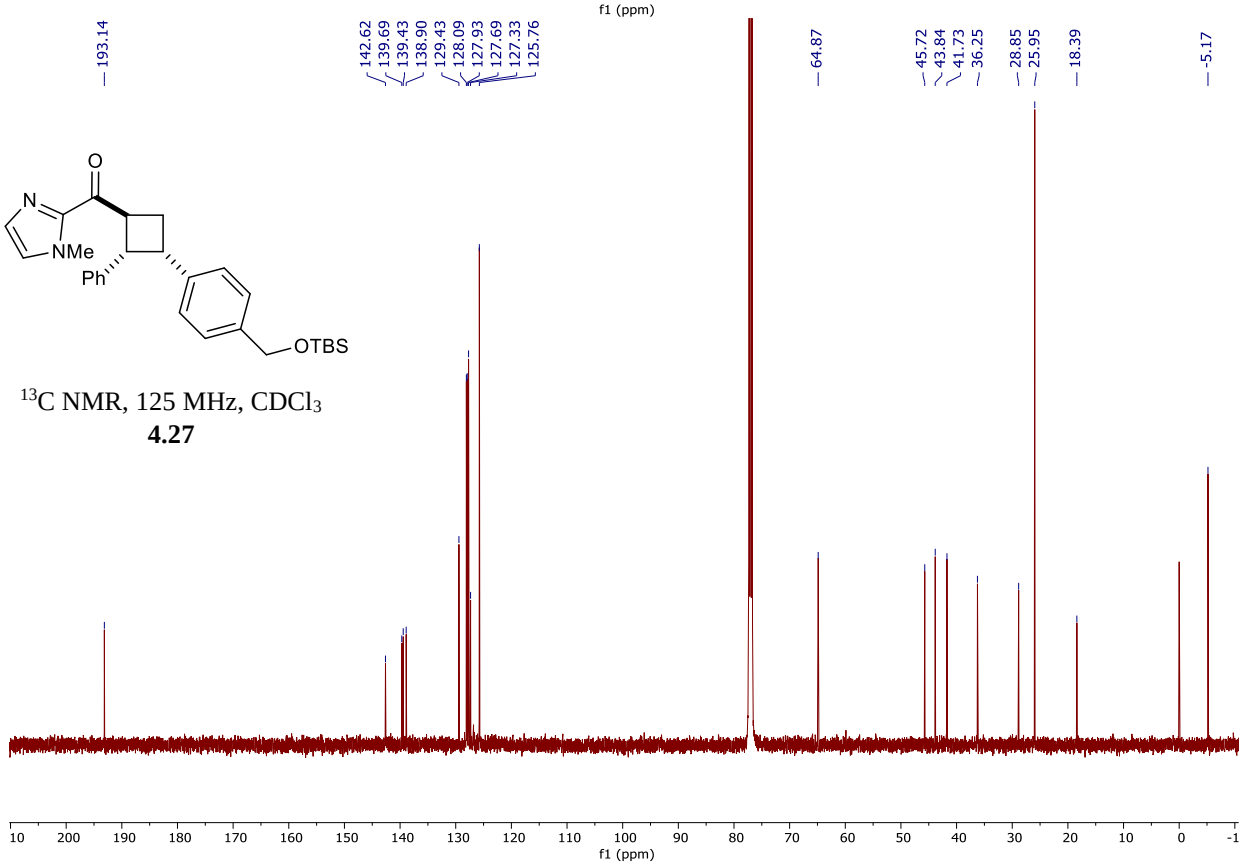

^{13}C NMR, 125 MHz, $CDCl_3$
4.27

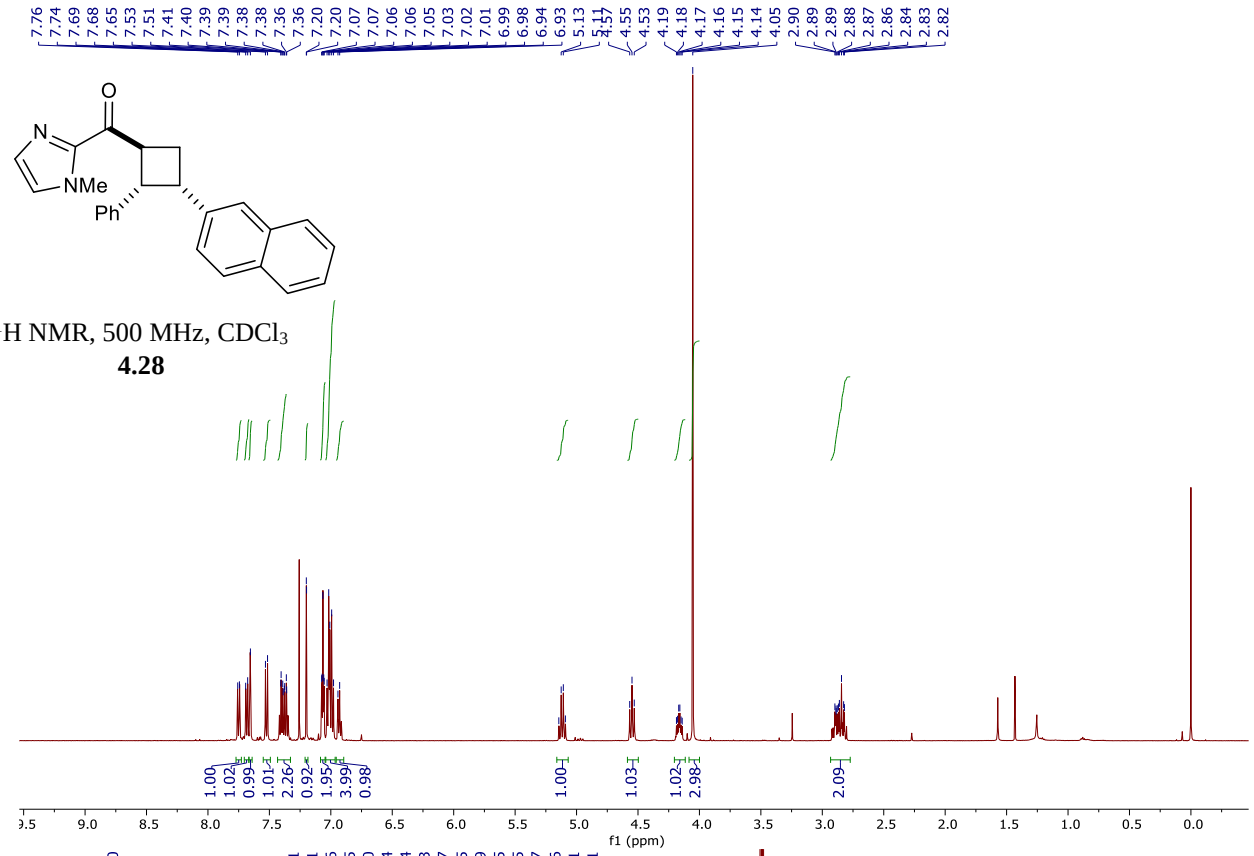

^{1}H NMR, 500 MHz, $CDCl_3$

4.28

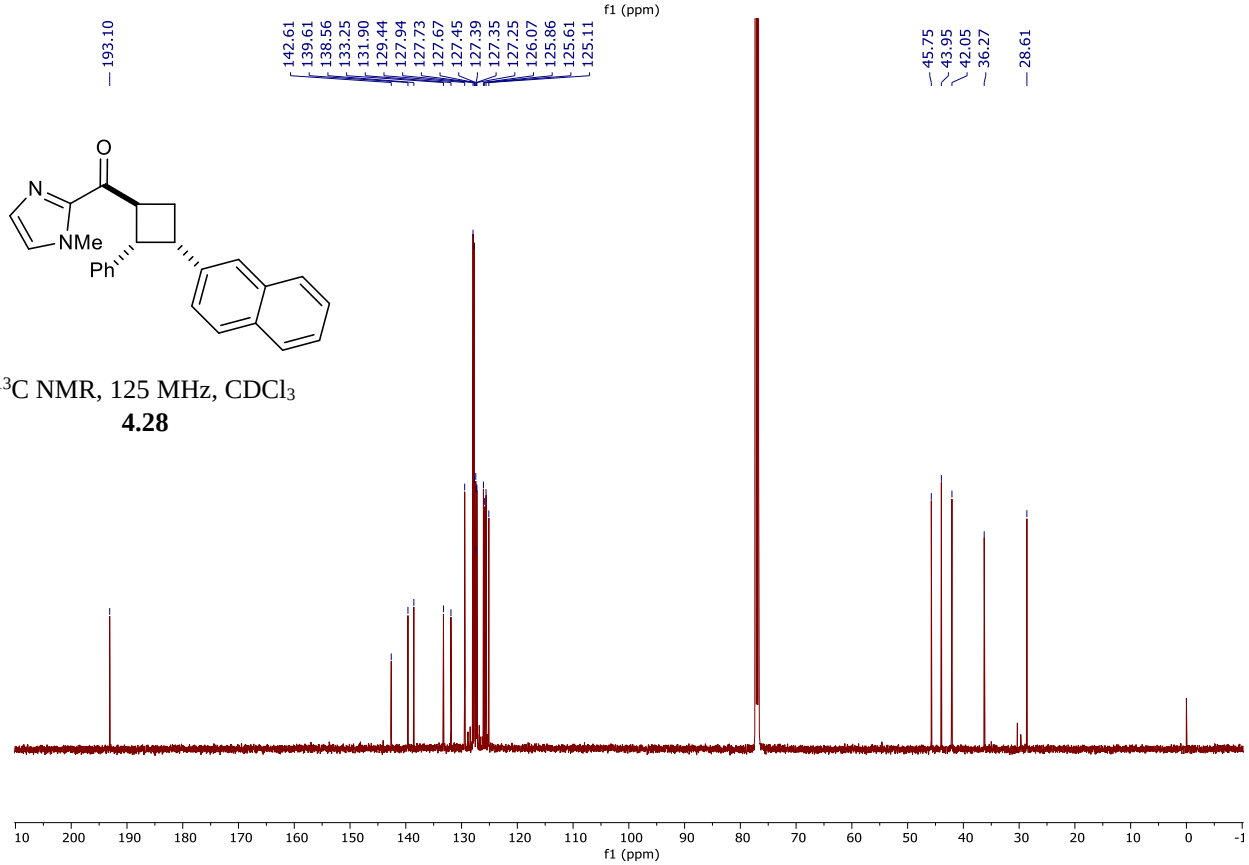

^{13}C NMR, 125 MHz, $CDCl_3$

4.28

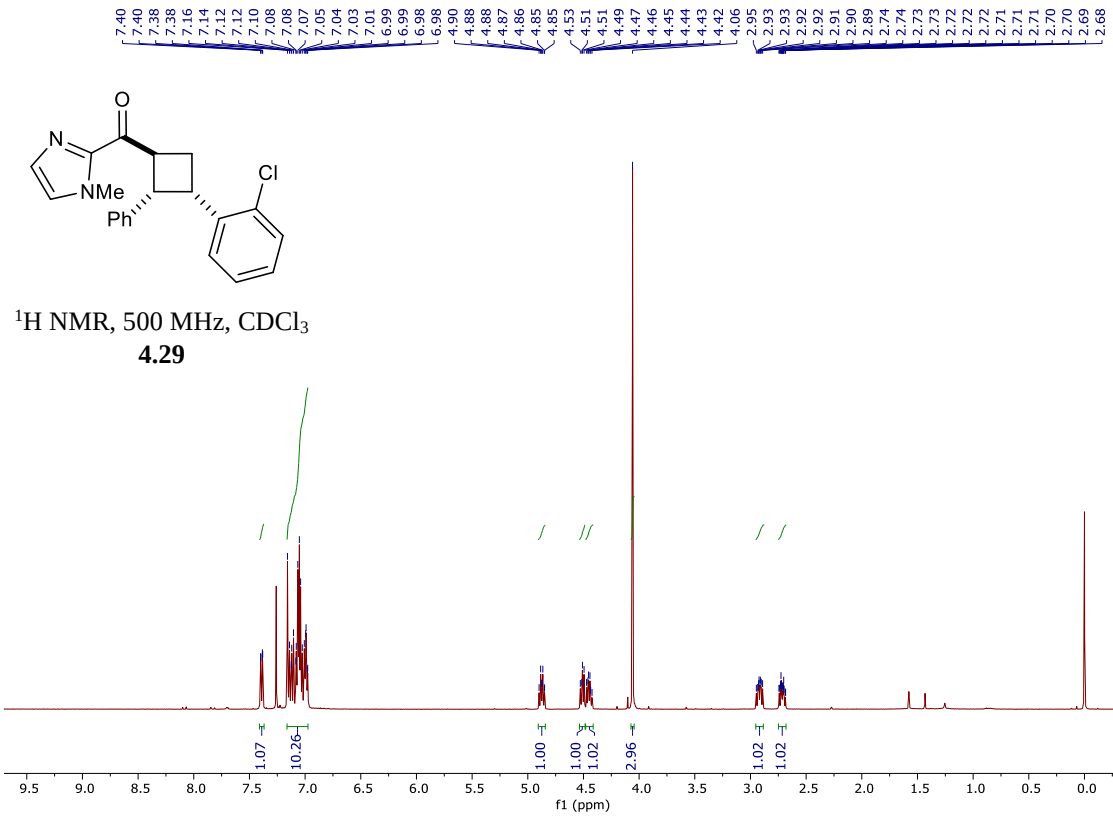

^{1}H NMR, 500 MHz, $CDCl_3$

4.29

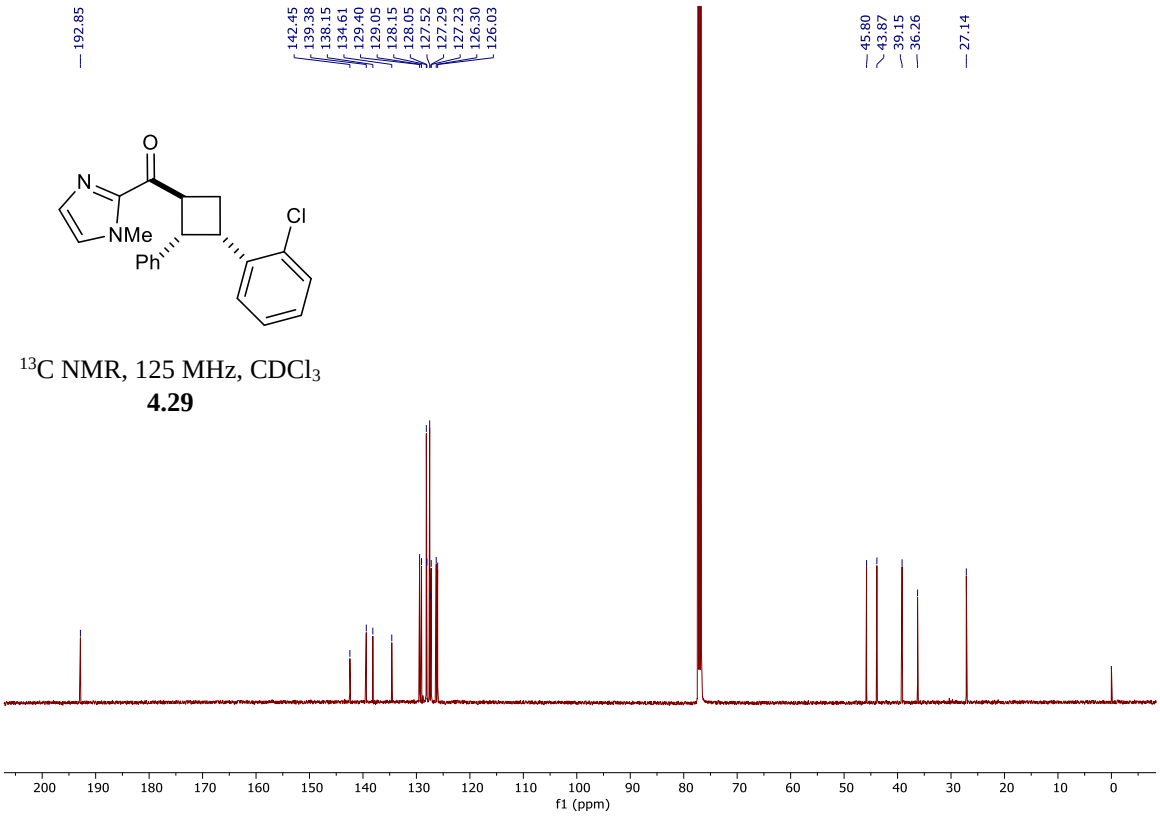

^{13}C NMR, 125 MHz, $CDCl_3$

4.29

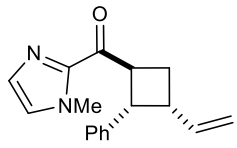

^{1}H NMR, 500 MHz, $CDCl_3$

4.33 – major diastereomer

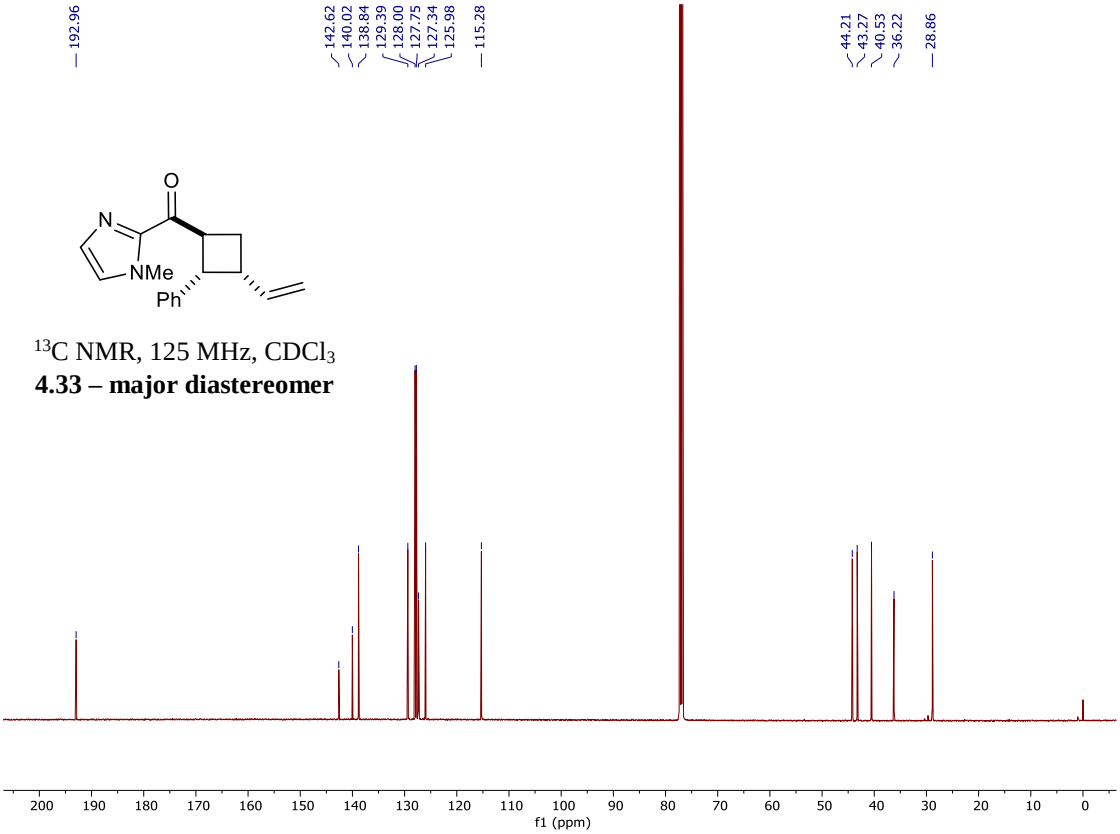

^{13}C NMR, 125 MHz, $CDCl_3$

4.33 – major diastereomer

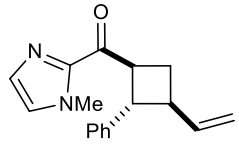

^{1}H NMR, 500 MHz, $CDCl_3$

4.33 – minor diastereomer

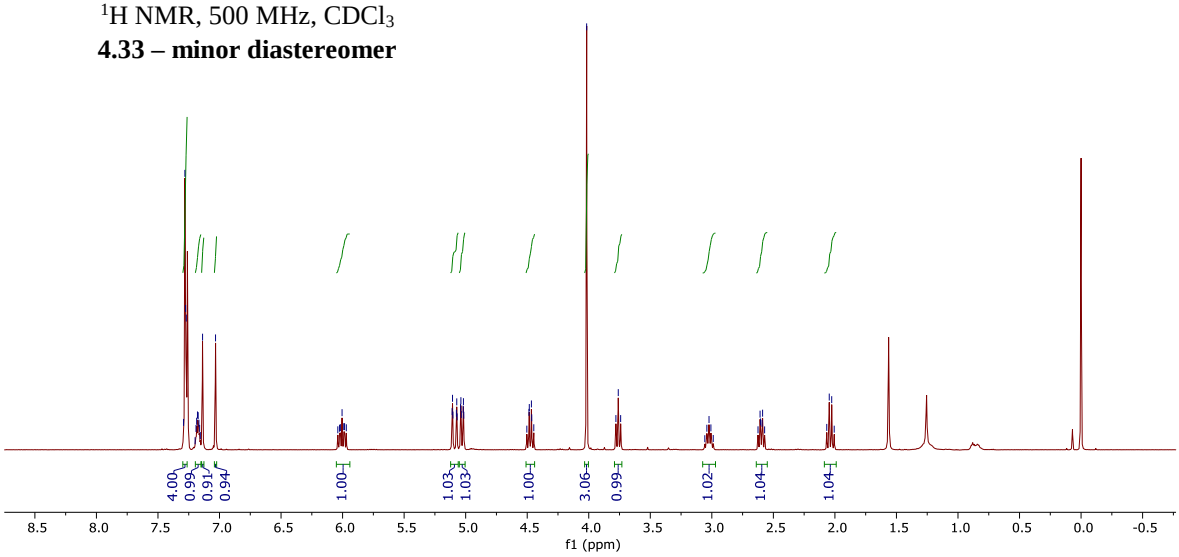

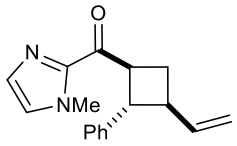

^{13}C NMR, 125 MHz, $CDCl_3$

4.33 – minor diastereomer

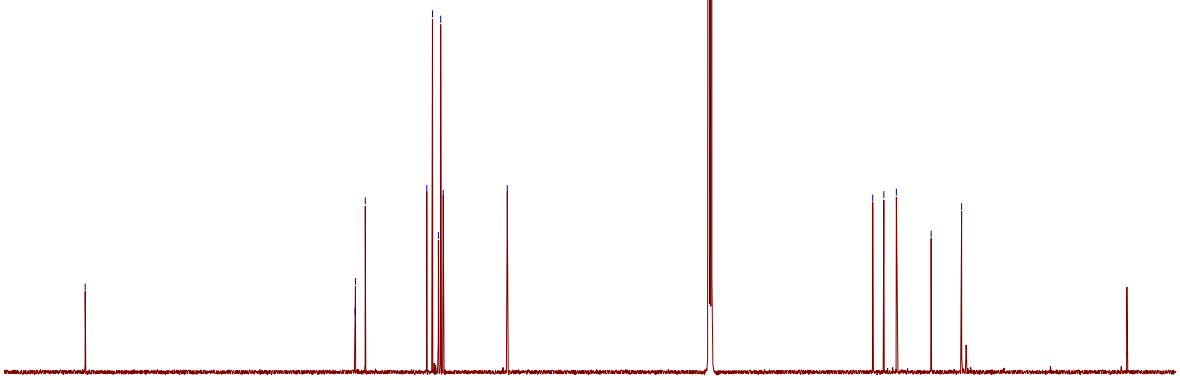

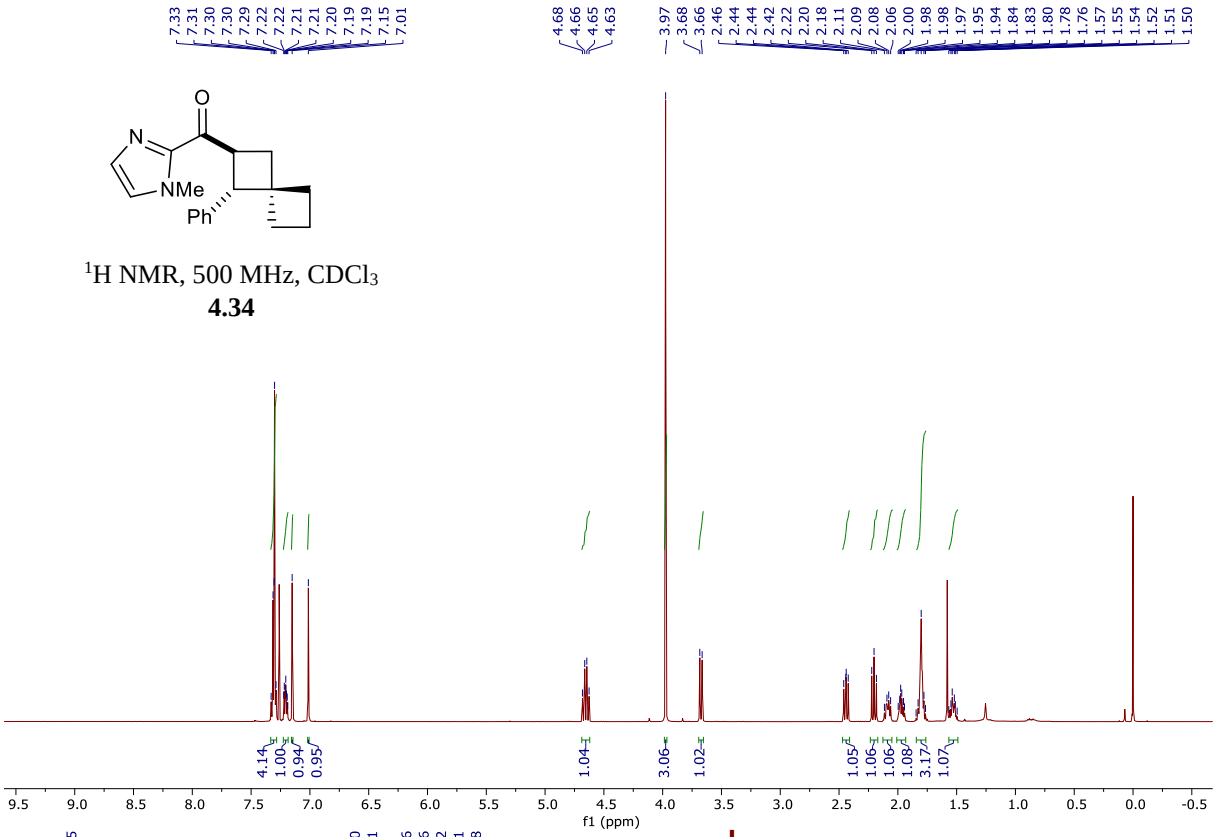

^{1}H NMR, 500 MHz, $CDCl_3$

4.34

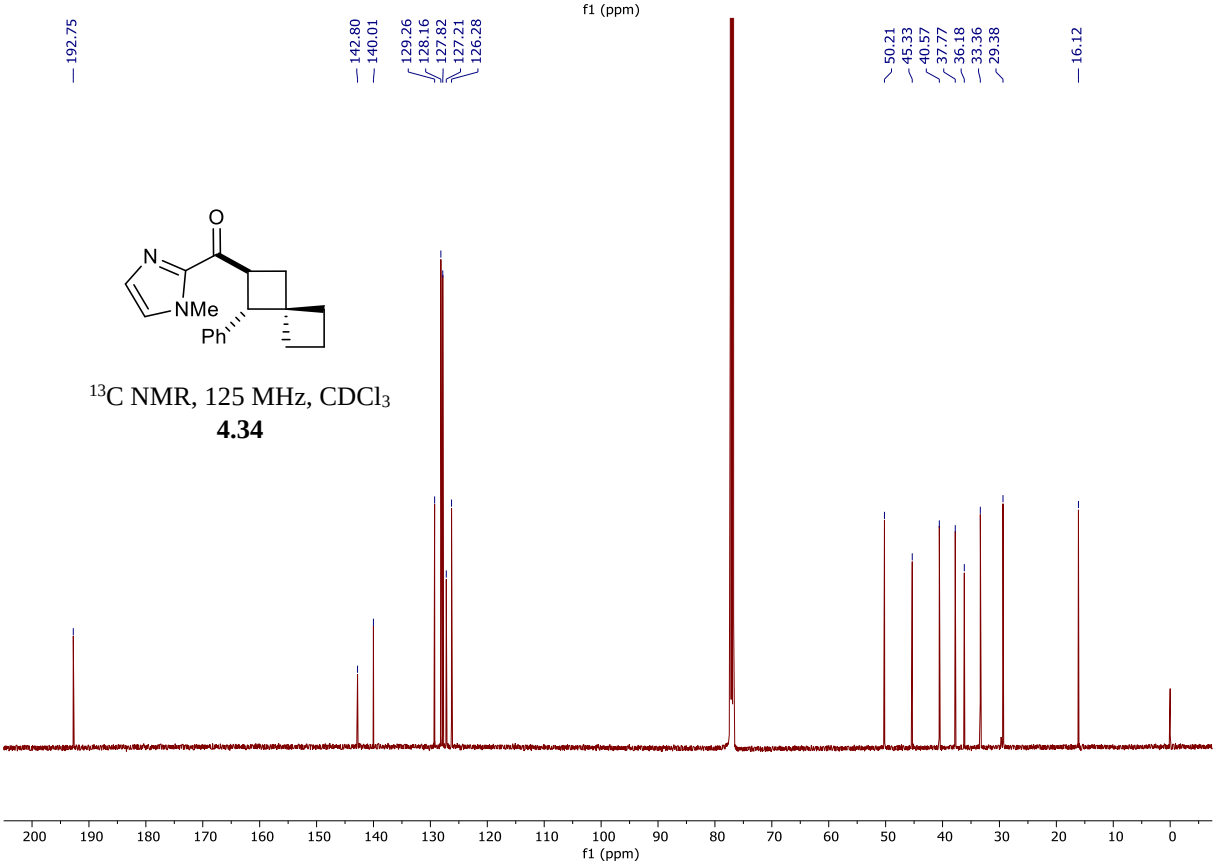

^{13}C NMR, 125 MHz, $CDCl_3$

4.34

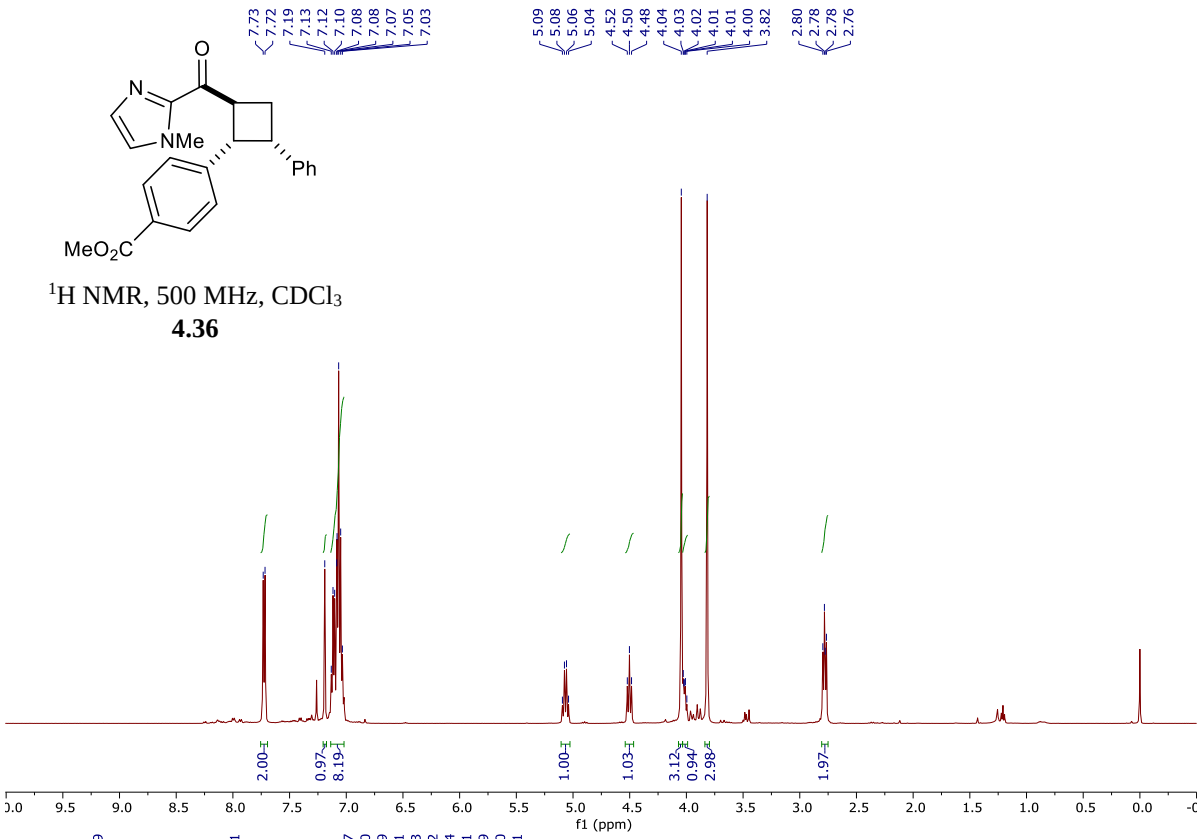

^{1}H NMR, 500 MHz, $CDCl_3$

4.36

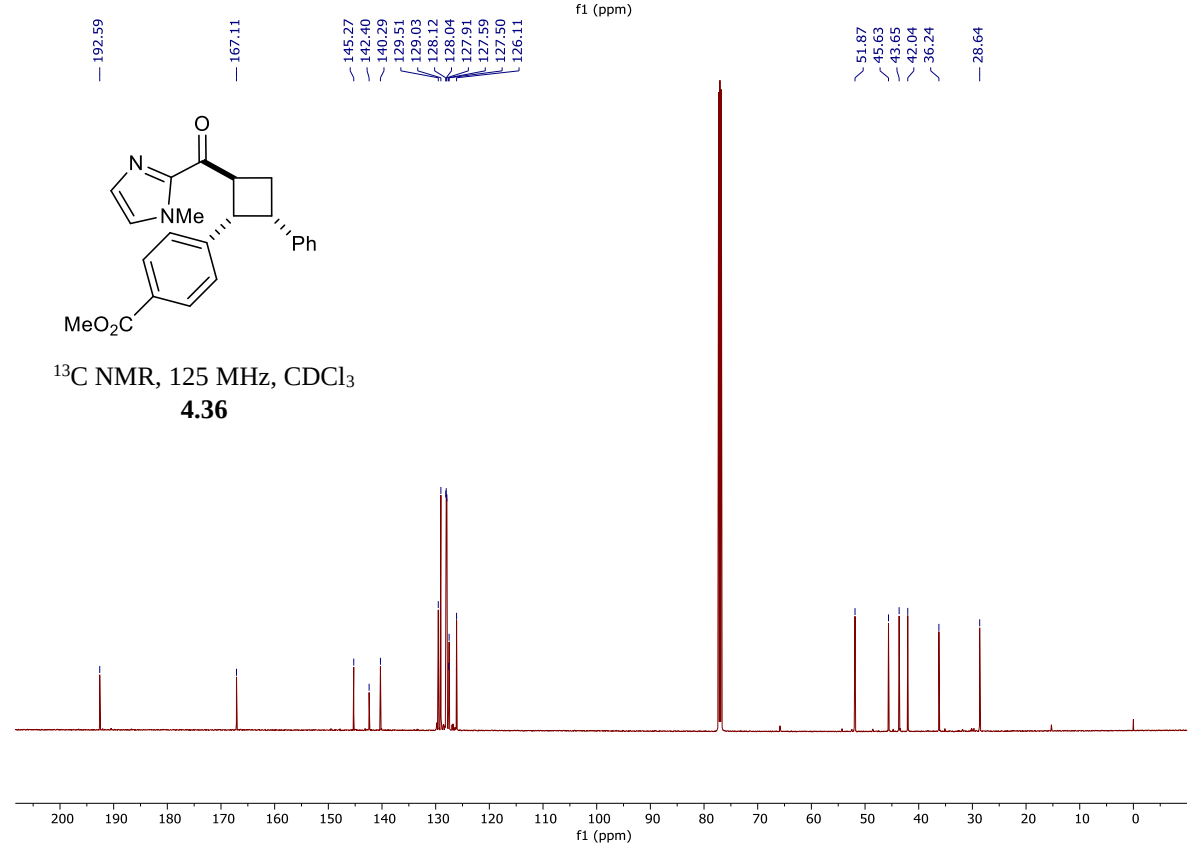

^{13}C NMR, 125 MHz, $CDCl_3$

4.36

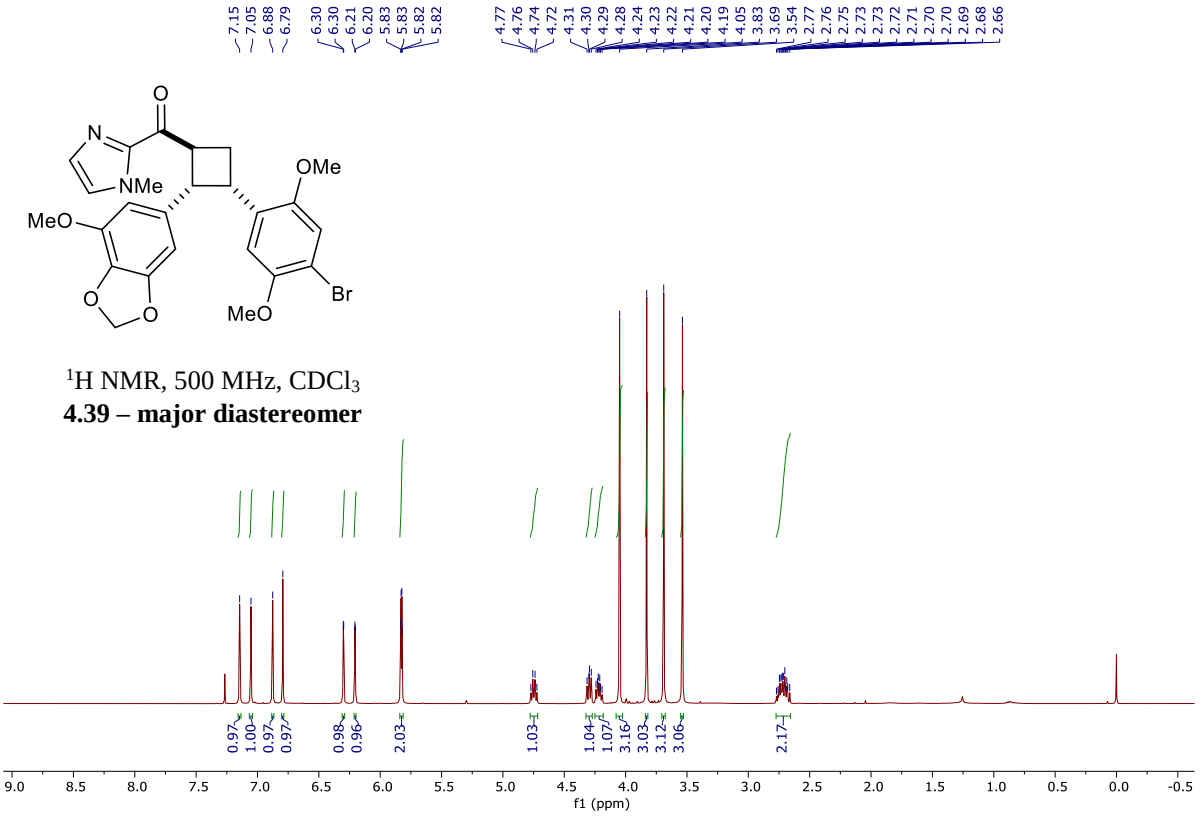

^{1}H NMR, 500 MHz, $CDCl_3$

4.39 – major diastereomer

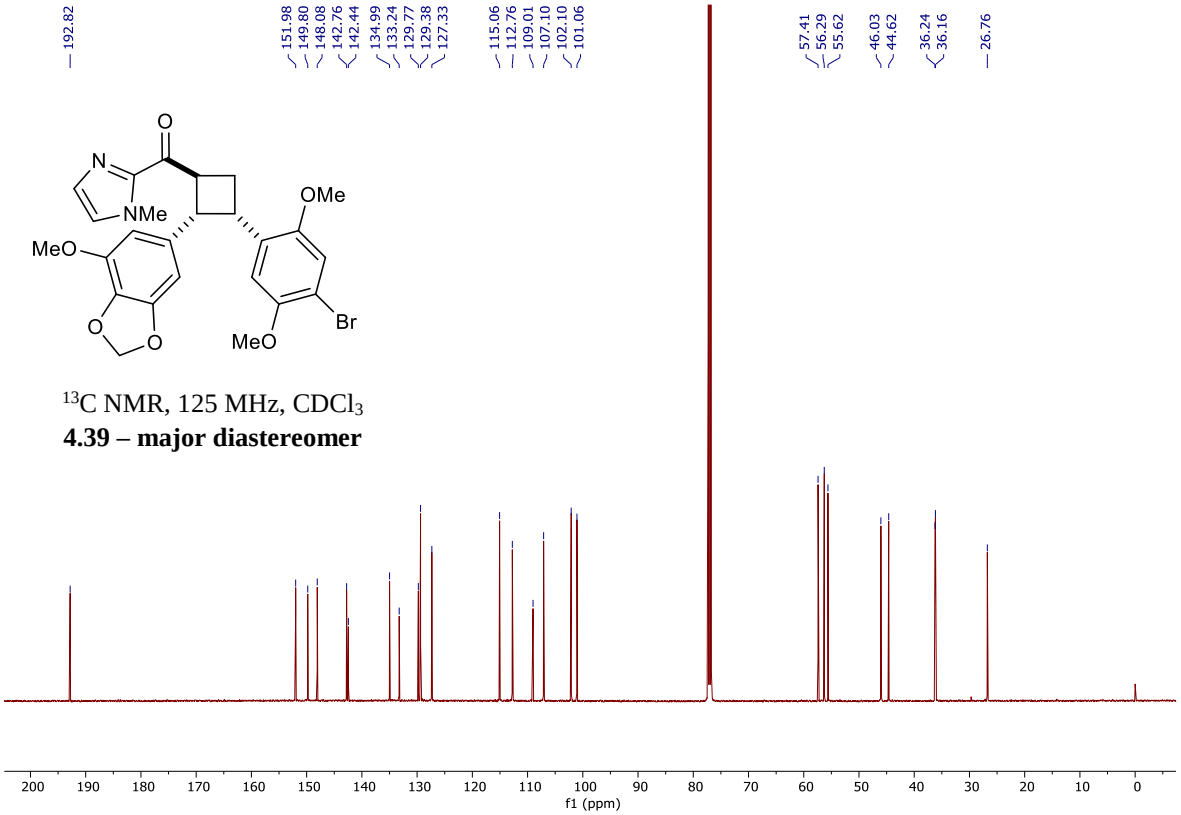

^{13}C NMR, 125 MHz, $CDCl_3$

4.39 – major diastereomer

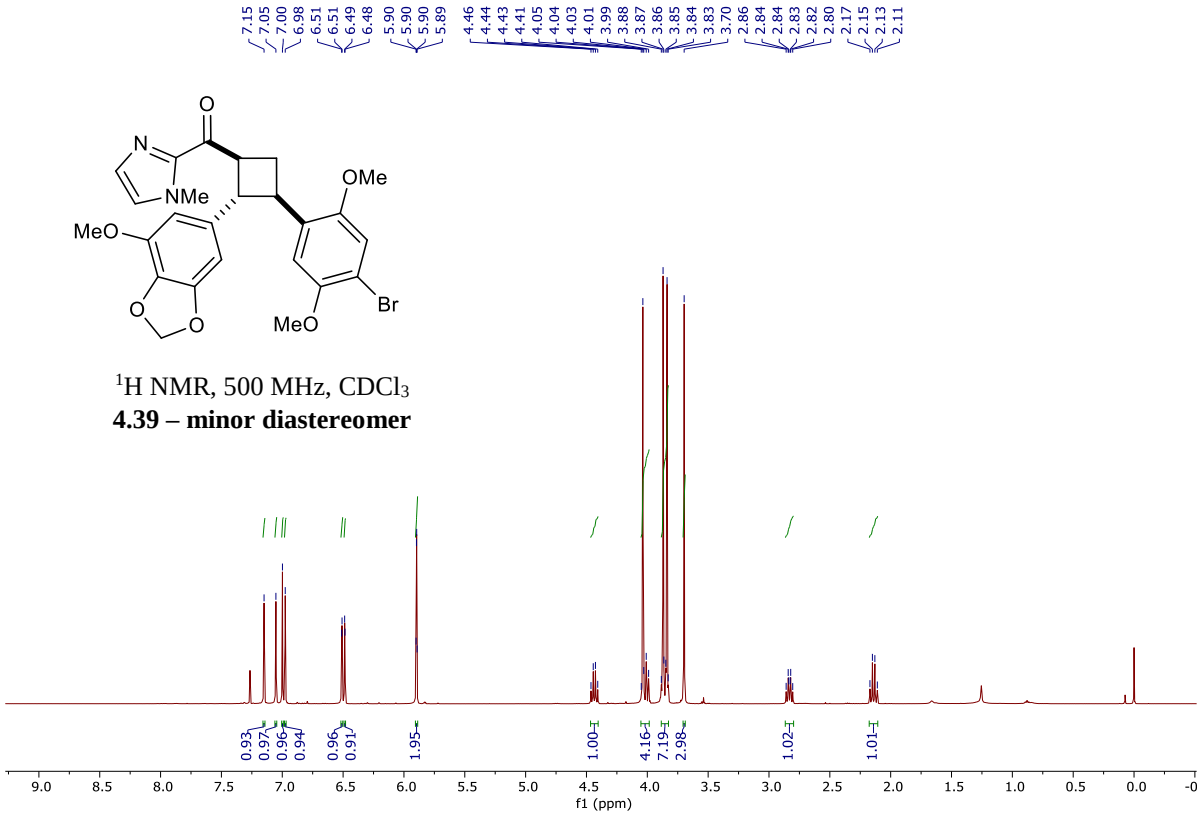

^{1}H NMR, 500 MHz, $CDCl_3$
4.39 – minor diastereomer

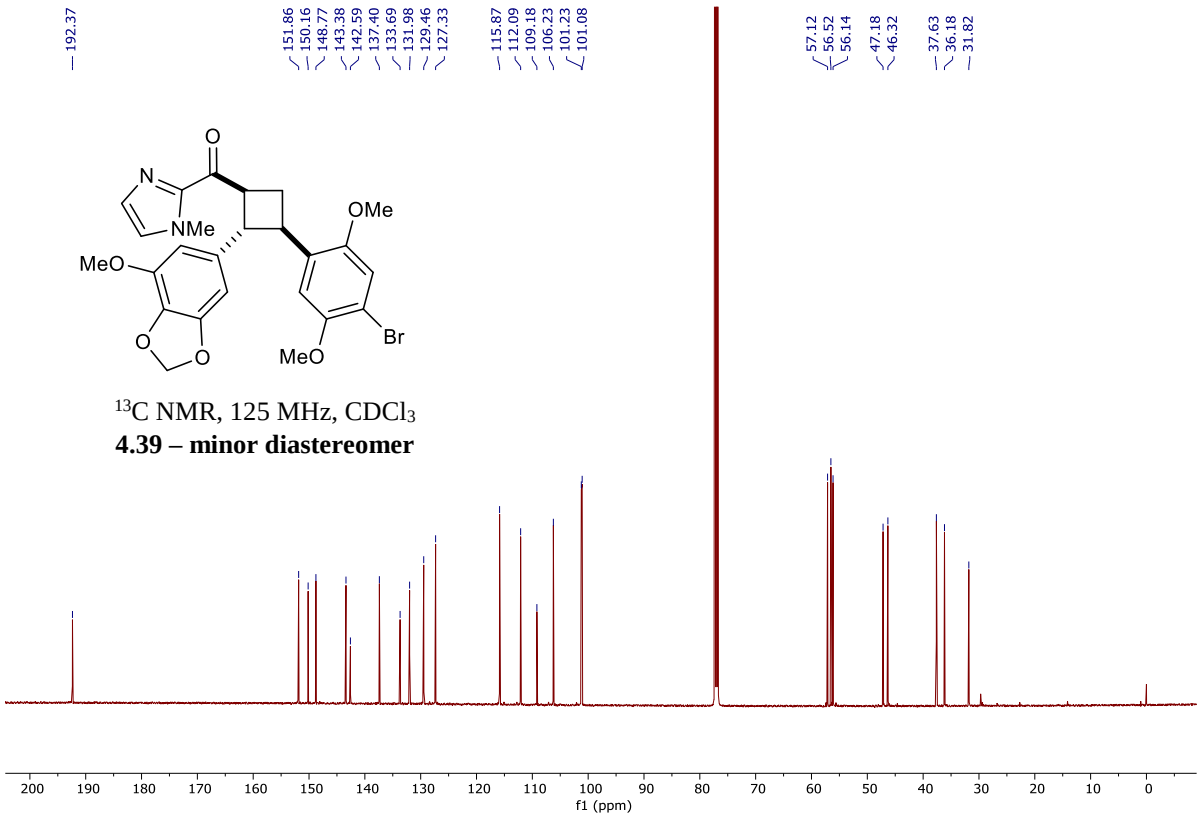

^{13}C NMR, 125 MHz, $CDCl_3$
4.39 – minor diastereomer

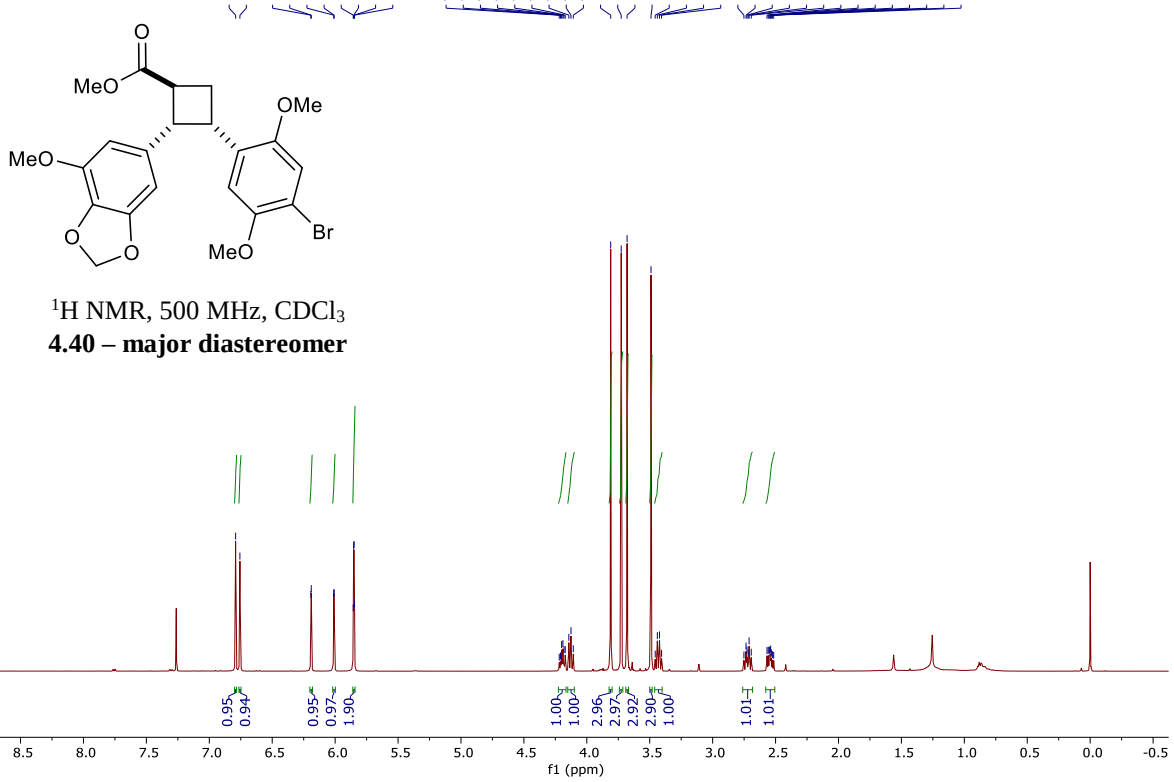

^{1}H NMR, 500 MHz, $CDCl_3$

4.40 – major diastereomer

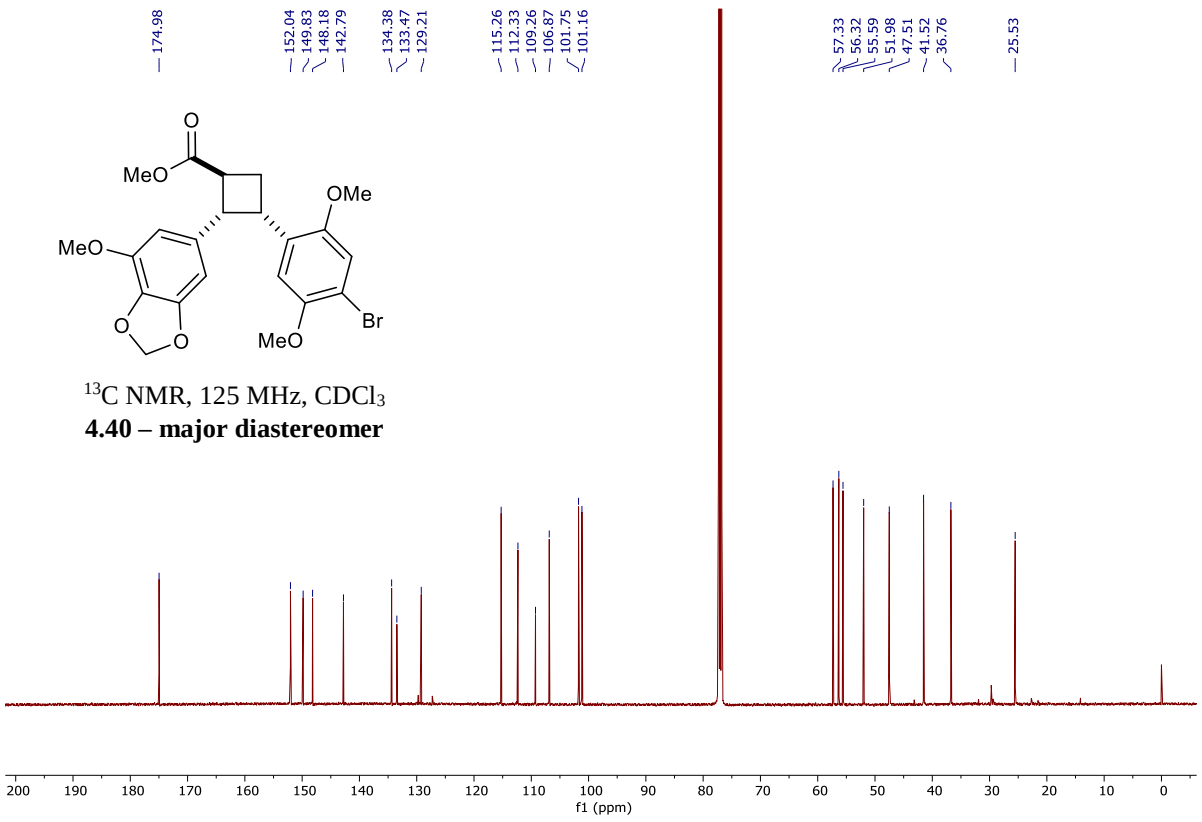

^{13}C NMR, 125 MHz, $CDCl_3$

4.40 – major diastereomer

Appendix B. SFC Traces for New Compounds (Chapter 2)

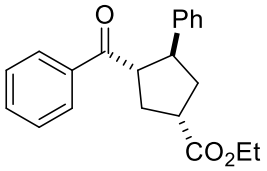

(1S,3S,4S)-ethyl 3-benzoyl-4-phenylcyclopentanecarboxylate (2.10)

Racemic: SFC, Chiracel AD-H, gradient 10% iPrOH/CO_2 to 40% iPrOH/CO_2, 3 mL/min, 263 nm

Peak	% area	area	RT(min)	height (mV)
1	50.0154	3947.7773	4.72	395.6174
2	49.9846	3945.353	6.04	344.3234
Total	100	7893.1302		

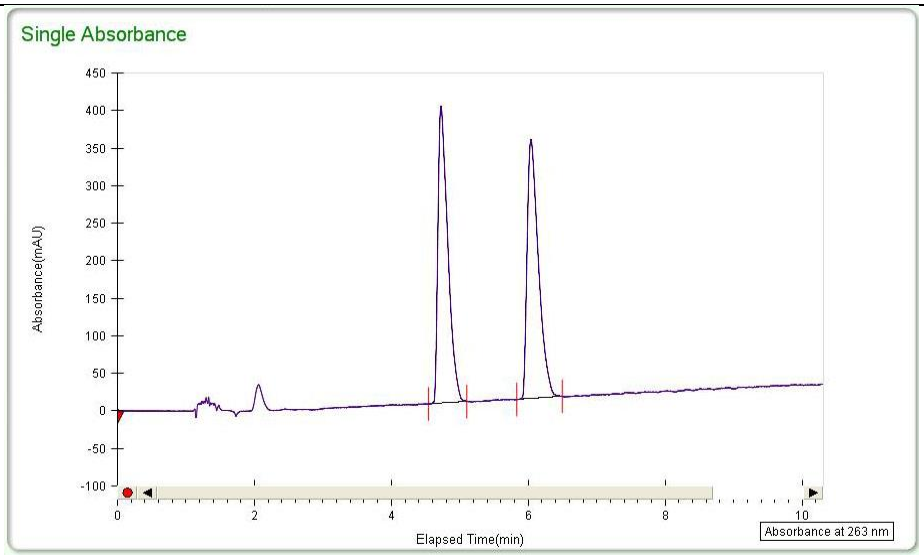

Scalemic: SFC, Chiracel AD-H, gradient 10% iPrOH/CO_2 to 40% iPrOH/CO_2, 3 mL/min, 263 nm

Peak	% area	area	RT(min)	height (mV)
1	89.634	18949.1538	4.71	1759.1921
2	10.366	2191.4435	6.04	197.1945
Total	100	21140.5973		

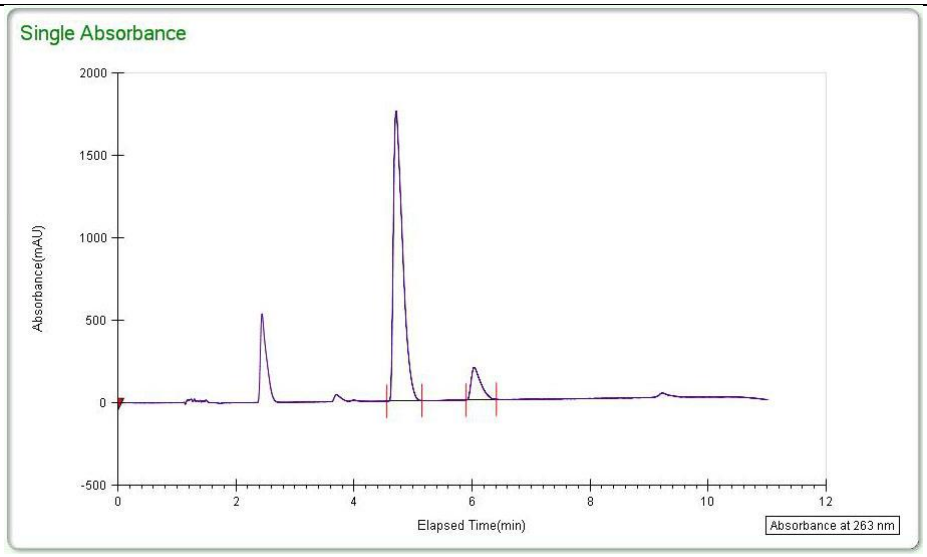

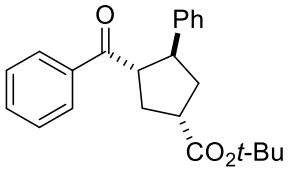

(1S,3S,4S)-tert-butyl 3-benzoyl-4-phenylcyclopentanecarboxylate (2.12)

Racemic: SFC, Chiracel AD-H, gradient 5% iPrOH/CO_2 to 50% iPrOH/CO_2, 3 mL/min, 263 nm

Peak	% area	area	RT(min)	height (mV)
1	49.8493	12332.9287	6.05	1634.0623
2	50.1507	12407.5172	6.94	1402.5703
Total	100	24740.4459		

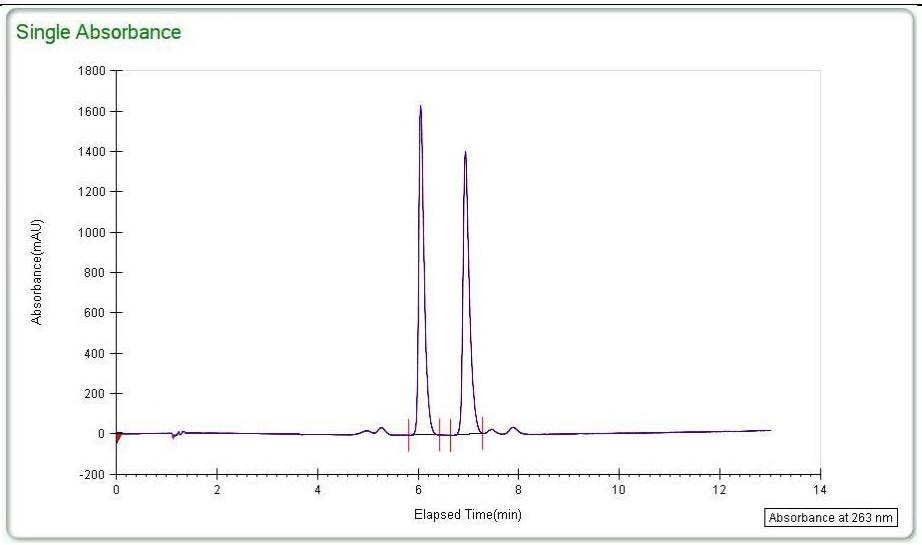

Scalemic: SFC, Chiracel AD-H, gradient 5% iPrOH/CO_2 to 50% iPrOH/CO_2, 3 mL/min, 263 nm

Peak	% area	area	RT(min)	height (mV)
1	96.5603	1974.8991	6.10	244.1414
2	3.4397	70.3497	7.08	10.9968
Total	100	2045.2488		

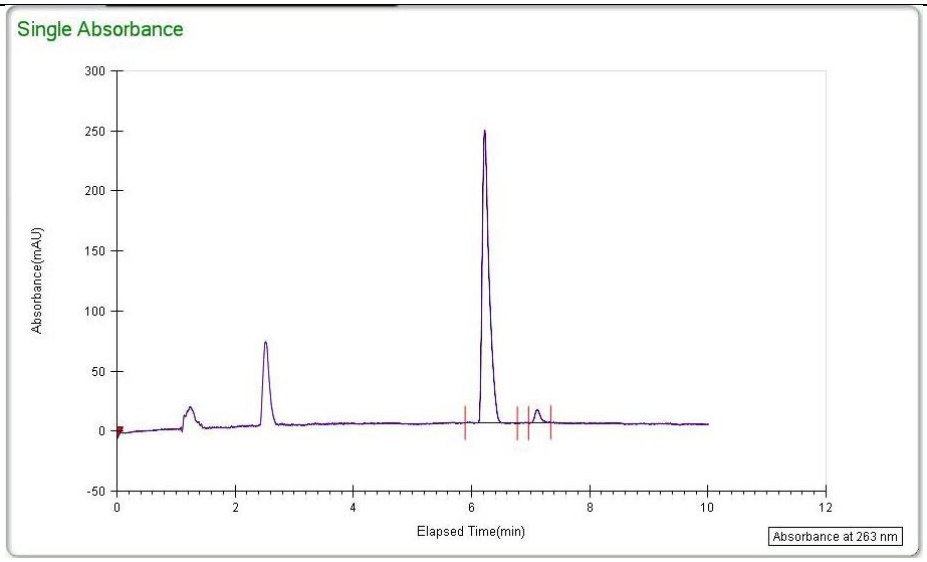

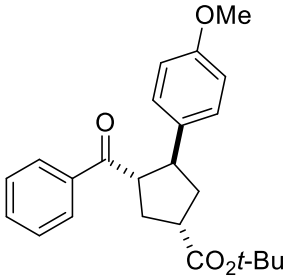

(1S,3S,4S)-tert-butyl 3-benzoyl-4-(4-methoxyphenyl)cyclopentanecarboxylate (2.13)

Racemic: SFC, Chiracel AD-H, gradient 10% iPrOH/CO_2 to 20% iPrOH/CO_2, 3 mL/min, 240 nm

Peak	% area	area	RT(min)	height (mV)
1	49.8613	1535.3365	6.31	118.4
2	50.1387	1543.8767	8.83	97.473
Total	100	3079.2132		

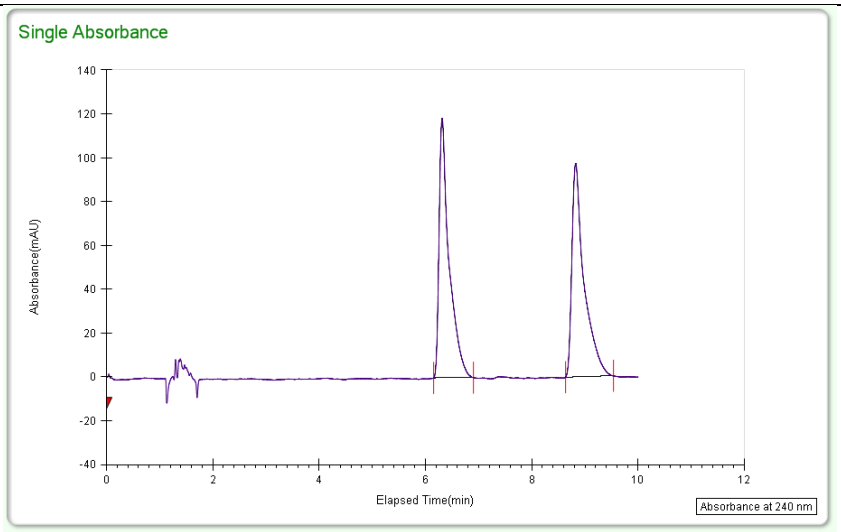

Scalemic: SFC, Chiracel AD-H, gradient 10% iPrOH/CO_2 to 20% iPrOH/CO_2, 3 mL/min, 240 nm

Peak	% area	area	RT(min)	height (mV)
1	95.3797	7181.3047	6.09	593.3232
2	4.6203	347.8706	8.71	27.2572
Total	100	7529.1753		

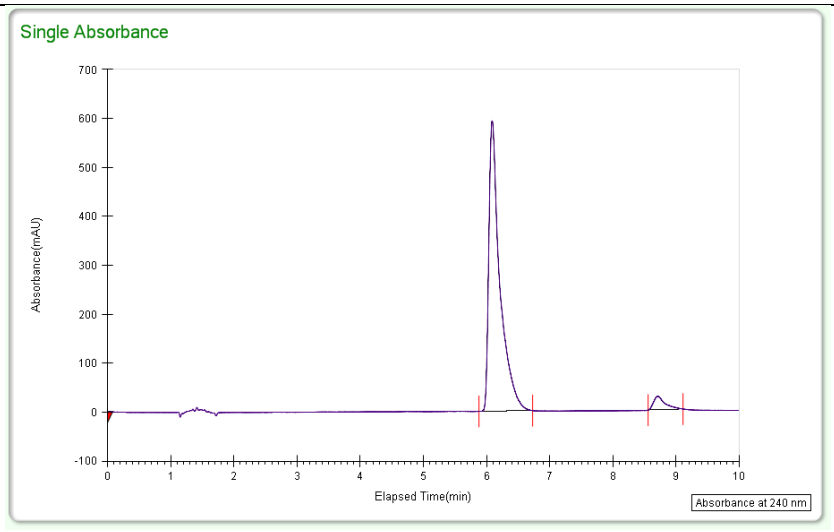

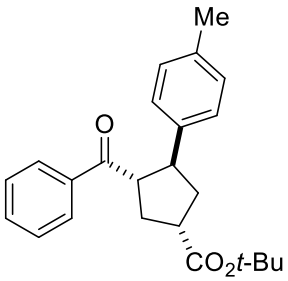

(1S,3S,4S)-tert-butyl 3-benzoyl-4-(4-methylphenyl)cyclopentanecarboxylate (2.14)

Racemic: SFC, Chiracel AD-H, gradient 10% iPrOH/CO_2 to 20% iPrOH/CO_2, 3 mL/min, 241 nm

Peak	% area	area	RT(min)	height (mV)
1	49.7681	3969.6702	6.06	229.3664
2	50.2319	4006.6698	7.41	202.5068
Total	100	7976.3400		

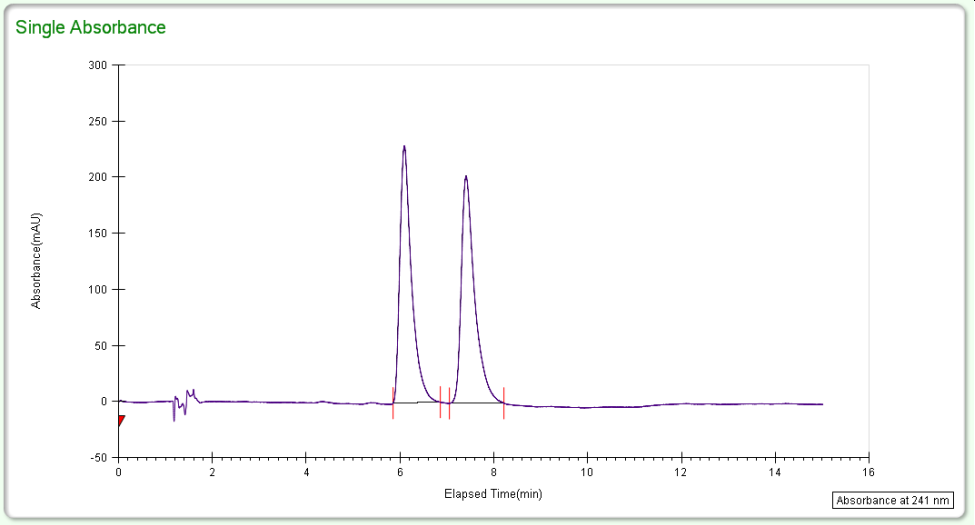

Scalemic: SFC, Chiracel AD-H, gradient 10% iPrOH/CO_2 to 20% iPrOH/CO_2, 3 mL/min, 241 nm

Peak	% area	area	RT(min)	height (mV)
1	94.3743	8492.9612	6.01	463.1925
2	5.6257	506.269	7.36	30.1824
Total	100	8999.2302		

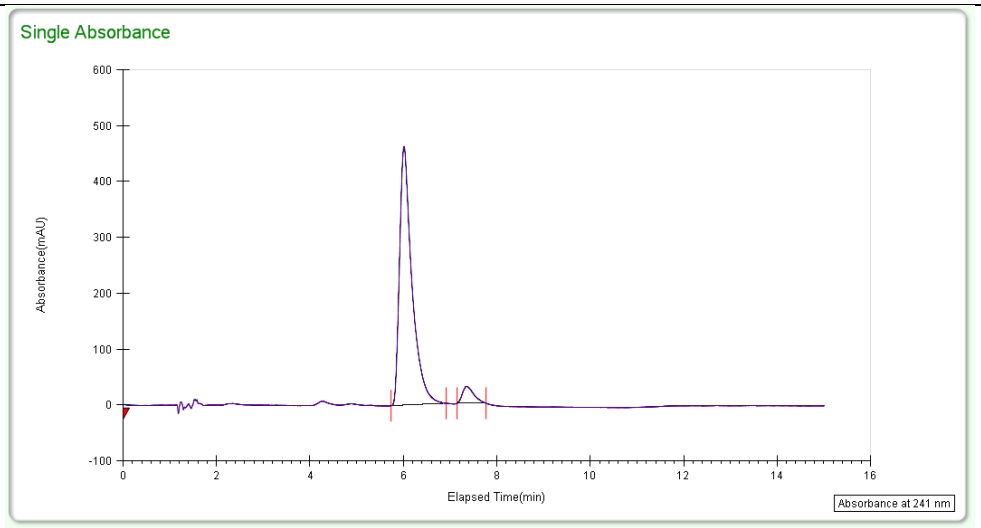

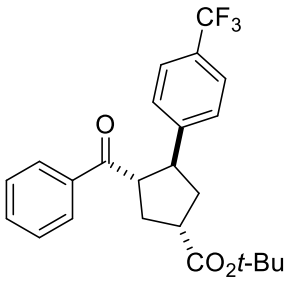

(1S,3S,4S)-tert-butyl 3-benzoyl-4-(4-(trifluoromethyl)phenyl)cyclopentanecarboxylate (2.15)

Racemic: SFC, Chiracel AD-H, gradient 10% iPrOH/CO_2 to 20% iPrOH/CO_2, 3 mL/min, 240 nm

Peak	% area	area	RT(min)	height (mV)
1	48.965	1431.0998	3.45	82.0461
2	51.035	1491.5985	4.63	92.2654
Total	100	2922.6983		

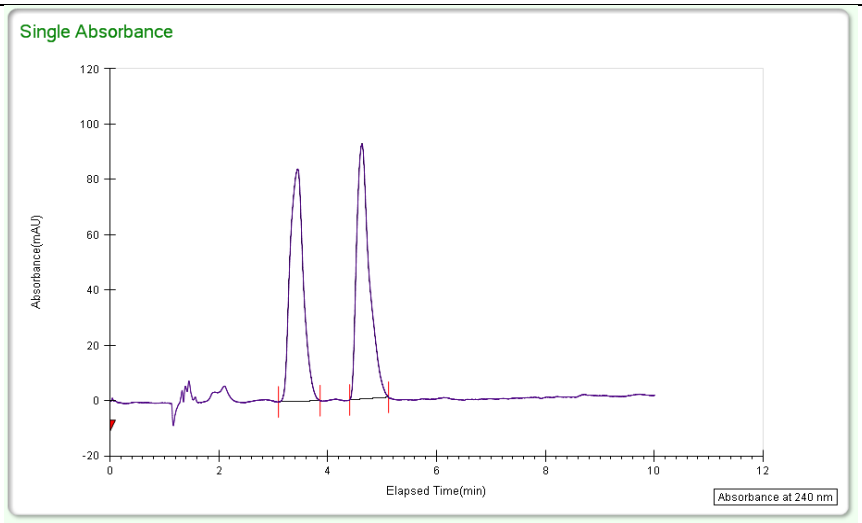

Scalemic: SFC, Chiracel AD-H, gradient 10% iPrOH/CO_2 to 20% iPrOH/CO_2, 3 mL/min, 240 nm

Peak	% area	area	RT(min)	height (mV)
1	94.7142	5582.4521	3.38	418.3291
2	5.2858	311.5478	4.67	31.4191
Total	100	5894.9999		

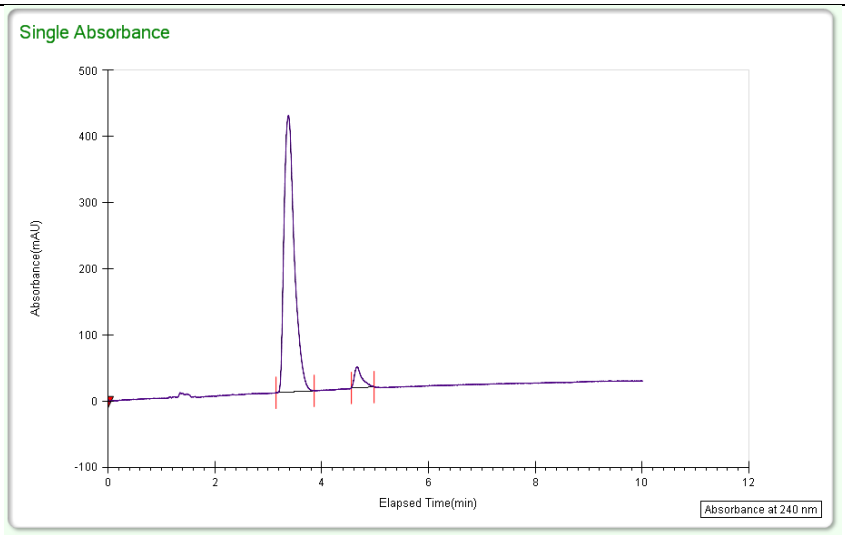

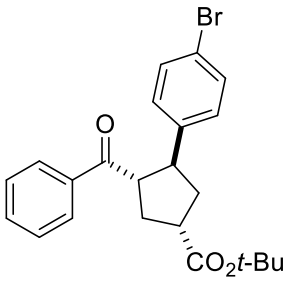

(1S,3S,4S)-tert-butyl 3-benzoyl-4-(4-bromophenyl)cyclopentanecarboxylate (2.16)

Racemic: SFC, Chiracel AD-H, gradient 10% iPrOH/CO_2 to 20% iPrOH/CO_2, 3 mL/min, 239 nm

Peak	% area	area	RT(min)	height (mV)
1	50.0808	4152.8595	7.99	159.582
2	49.9192	4139.4583	10.11	147.4783
Total	100	8292.3178		

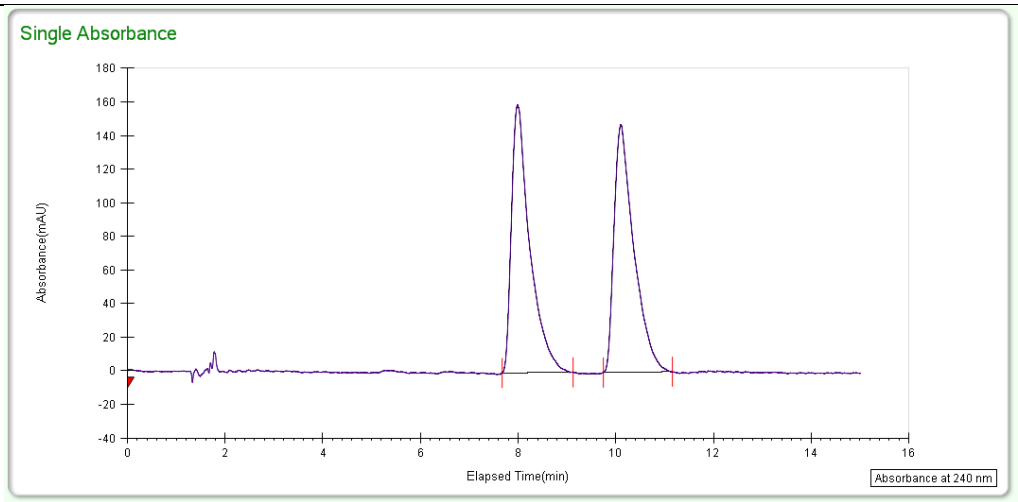

Scalemic: SFC, Chiracel AD-H, gradient 10% iPrOH/CO_2 to 20% iPrOH/CO_2, 3 mL/min, 239 nm

Peak	% area	area	RT(min)	height (mV)
1	94.8503	7412.6292	7.91	343.5924
2	5.1497	402.4546	10.09	20.5212
Total	100	7815.0838		

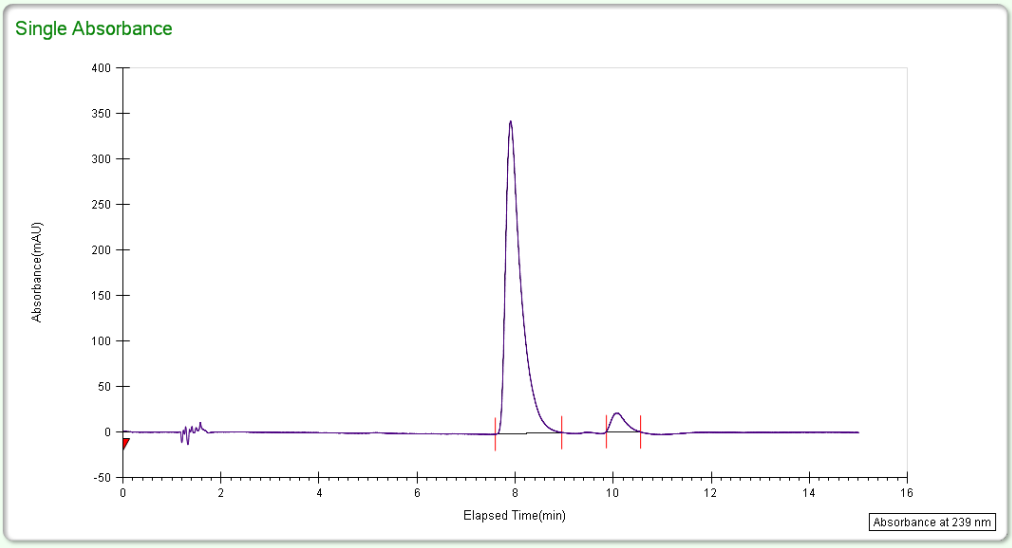

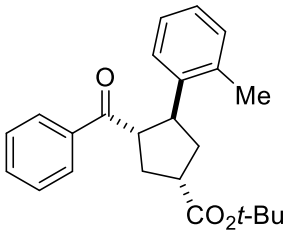

(1S,3S,4S)-tert-butyl 3-benzoyl-4-(o-tolyl)cyclopentanecarboxylate (2.17)

Racemic: SFC, Chiracel AD-H, gradient 10% iPrOH/CO_2 to 20% iPrOH/CO_2, 3 mL/min, 240 nm

Peak	% area	area	RT(min)	height (mV)
1	50.2217	3440.3314	4.34	232.2605
2	49.7783	3409.9550	5.49	141.8507
Total	100	6850.2864		

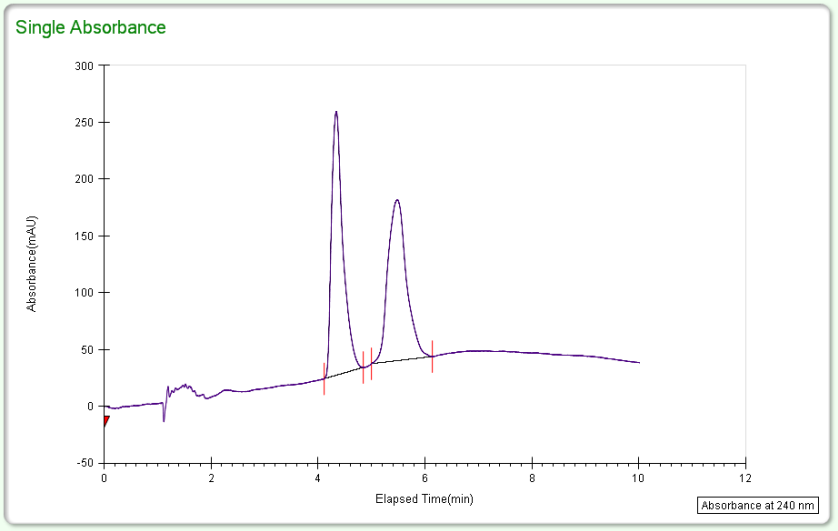

Scalemic: SFC, Chiracel AD-H, gradient 10% iPrOH/CO_2 to 20% iPrOH/CO_2, 3 mL/min, 240 nm

Peak	% area	area	RT(min)	height (mV)
1	93.4141	5276.7255	4.20	591.2448
2	6.5859	372.0188	5.47	30.3867
Total	100	5648.7443		

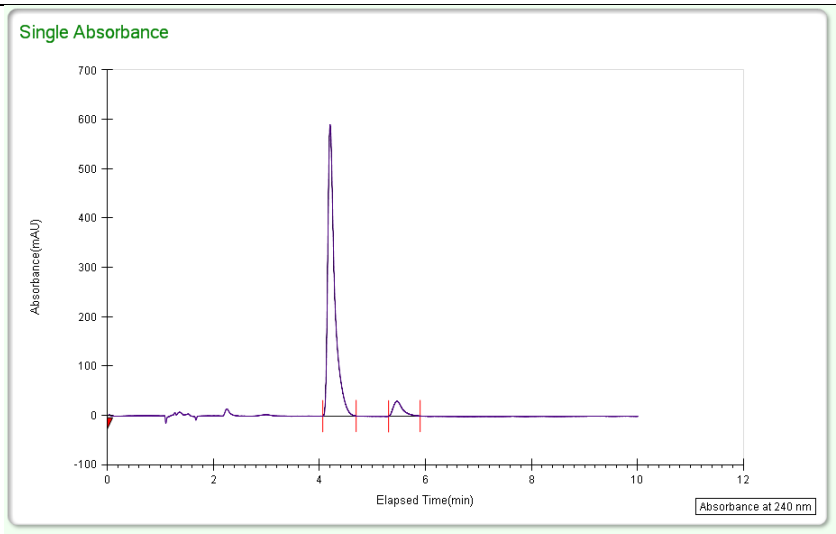

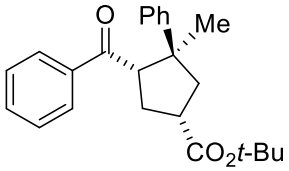

(1R,3S,4S)-tert-butyl 4-benzoyl-3-methyl-3-phenylcyclopentanecarboxylate (2.18)

Racemic: SFC, Chiracel AD-H, gradient 10% iPrOH/CO_2 to 20% iPrOH/CO_2, 3 mL/min, 240 nm

Peak	% area	area	RT(min)	height (mV)
1	50.1983	1300.4797	4.21	131.0374
2	49.8017	1290.2063	4.82	116.6899
Total	100	2560.6860		

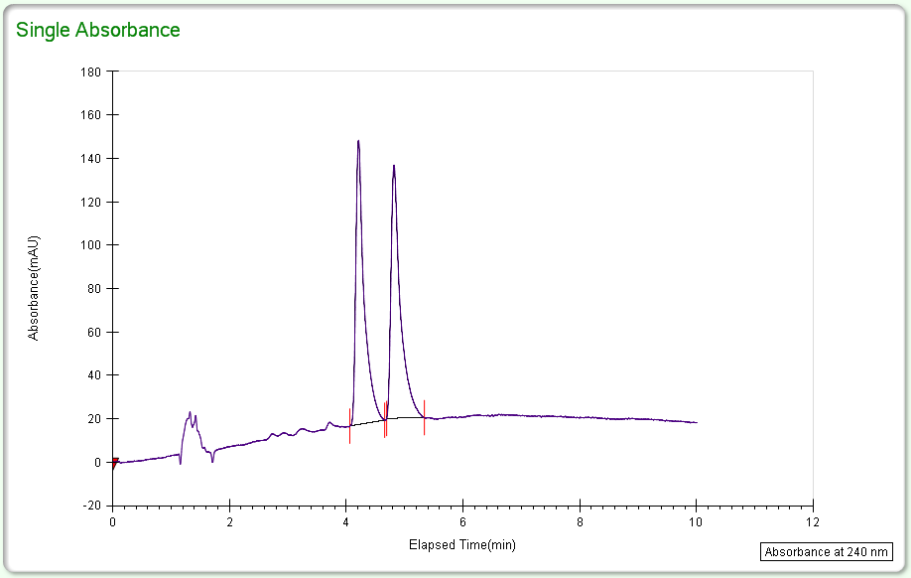

Scalemic: SFC, Chiracel AD-H, gradient 10% iPrOH/CO_2 to 20% iPrOH/CO_2, 3 mL/min, 240 nm

Peak	% area	area	RT(min)	height (mV)
1	94.7394	1739.5284	4.16	199.9115
2	5.2606	96.5903	4.78	10.8253
Total	100	1836.1187		

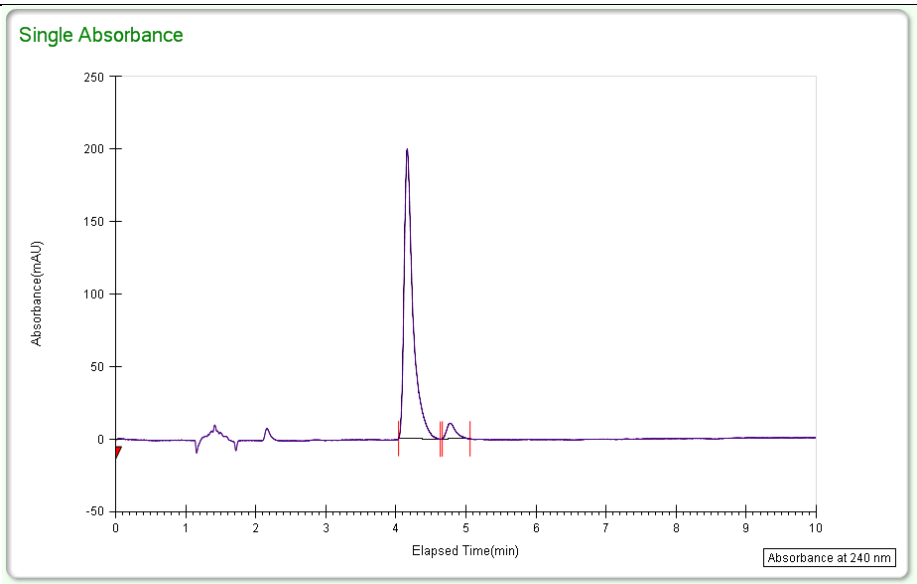

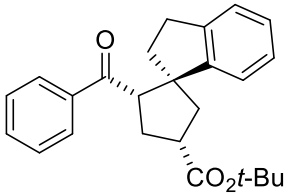

(1R,3S,4S)-tert-butyl 2-benzoyl-2',3'-dihydrospiro[cyclopentane-1,1'-indene]-4-carboxylate (2.19)

Racemic: SFC, Chiracel AD-H, 5% iPrOH/CO_2, 8 mL/min, 240 nm

Peak	% area	area	RT(min)	height (mV)
1	50.2199	1850.3655	3.66	89.066
2	49.7801	1834.1622	5.24	62.3639
Total	100	3684.5277		

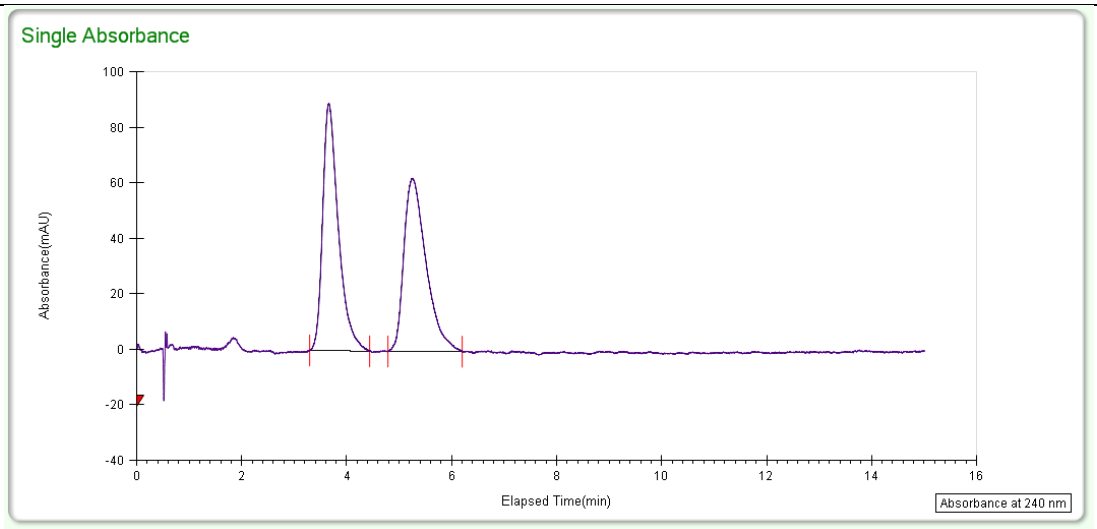

Scalemic: SFC, Chiracel AD-H, 5% iPrOH/CO_2, 8 mL/min, 240 nm

Peak	% area	area	RT(min)	height (mV)
1	1.4056	72.4063	3.57	5.6782
2	98.5944	5078.7299	5.09	1796159
Total	100	5151.1362		

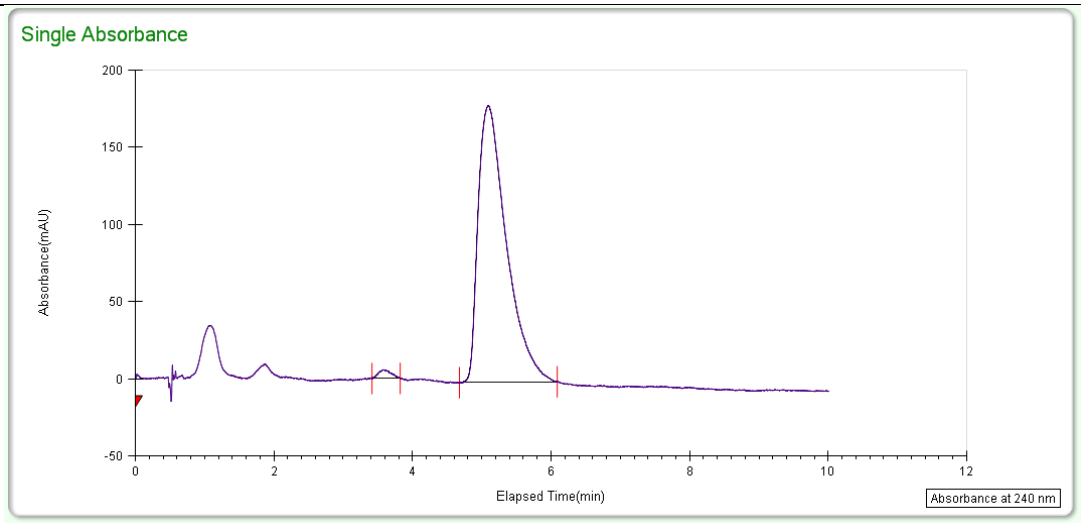

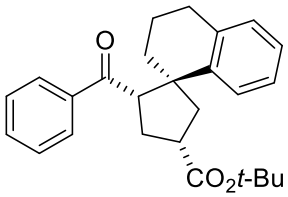

(1R,3S,4S)-tert-butyl 2-benzoyl-3',4'-dihydro-2'H-spiro[cyclopentane-1,1'-naphthalene]-4-carboxylate (2.20):

Racemic: SFC, Chiracel AD-H, 5% iPrOH/CO_2, 8 mL/min, 241 nm

Peak	% area	area	RT(min)	height (mV)
1	50.2772	18731.3836	4.12	432.3556
2	49.7228	18524.834	5.68	379.5763
Total	100	37256.2176		

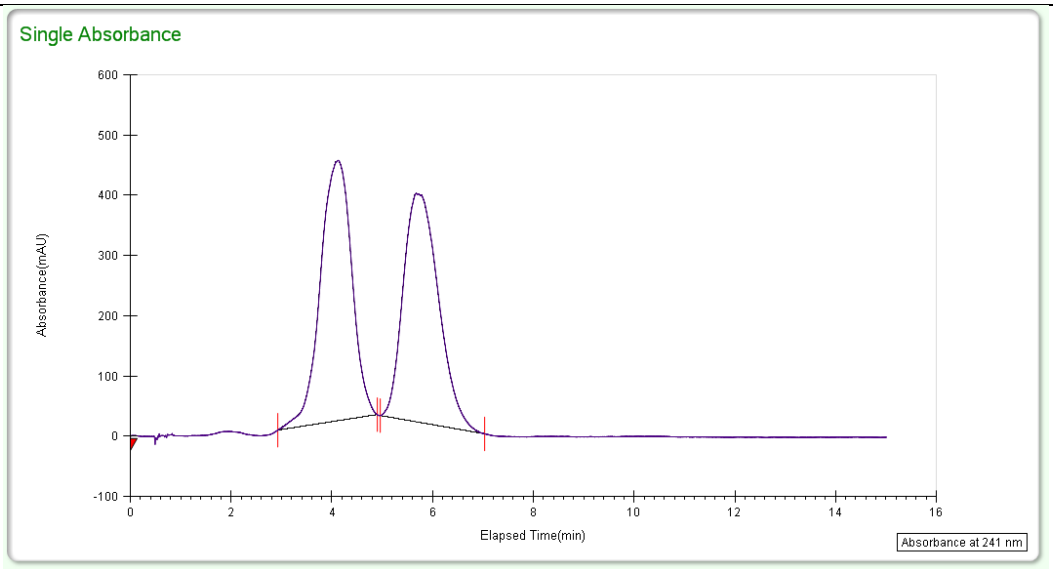

Scalemic: SFC, Chiracel AD-H, 5% iPrOH/CO_2, 8 mL/min, 241 nm

Peak	% area	area	RT(min)	height (mV)
1	99.7553	23569.4045	4.14	497.5829
2	0.2447	57.8048	5.94	379.5763
Total	100	37256.2176		

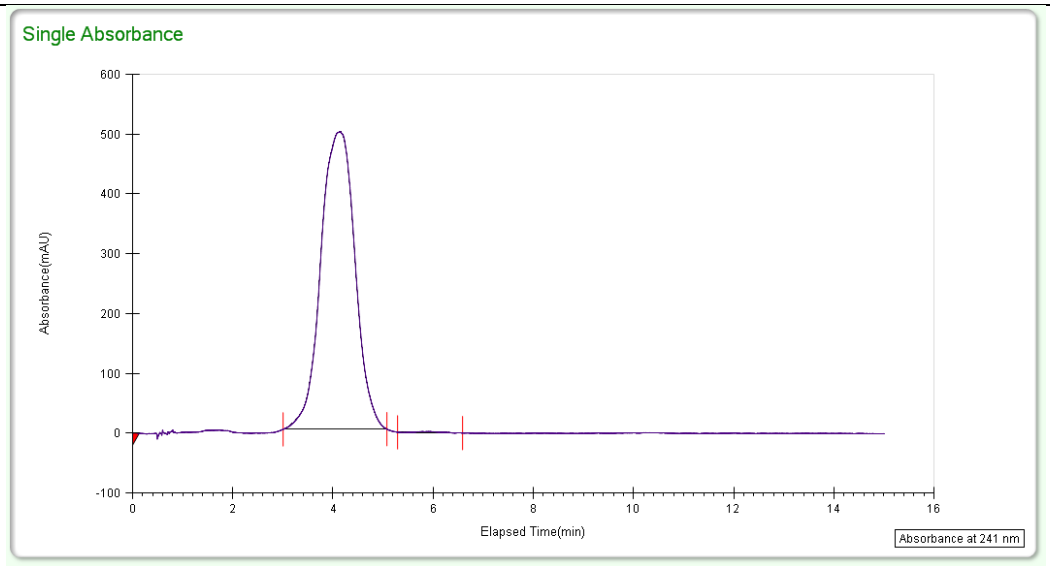

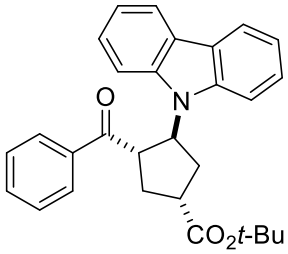

(1R,3S,4S)-tert-butyl 3-benzoyl-4-(9H-carbazol-9-yl)cyclopentanecarboxylate (2.21)

Racemic: SFC, Chiracel AD-H, 5% MeOH/CO_2, 5 mL/min, 241 nm

Peak	% area	area	RT(min)	height (mV)
1	50.0503	6587.3018	5.72	230.4808
2	49.9497	6574.0494	9.05	134.0597
Total	100	13161.3512		

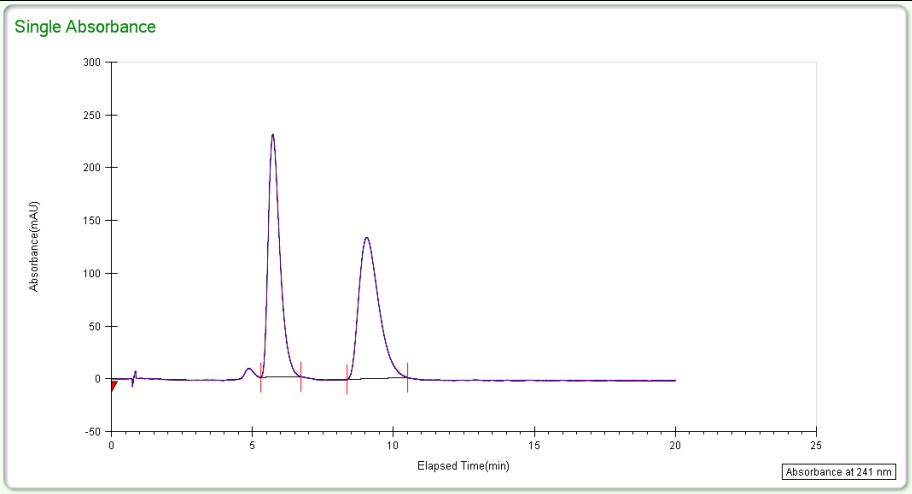

Scalemic: SFC, Chiracel AD-H, 5% MeOH/CO_2, 5 mL/min, 241 nm

Peak	% area	area	RT(min)	height (mV)
1	92.8928	2123.9728	5.76	70.7194
2	7.1072	162.5037	9.18	4.4185
Total	100	2286.4765		

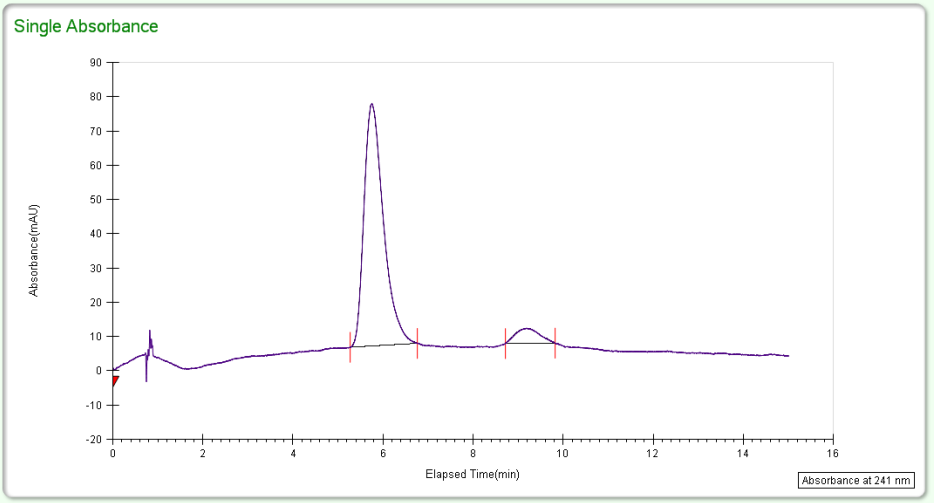

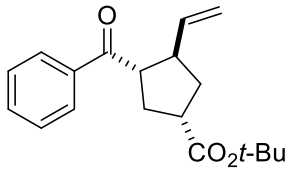

(1S,3S,4R)-tert-butyl 3-benzoyl-4-vinylcyclopentanecarboxylate (2.22)

Racemic: SFC, Chiracel AD-H, gradient 5% MeOH/CO_2 to 50% MeOH/CO_2, 3 mL/min, 240 nm

Peak	% area	area	RT(min)	height (mV)
1	49.6736	13545.4106	3.59	757.8009
2	50.3264	13723.4429	4.65	921.5475
Total	100	27268.8535		

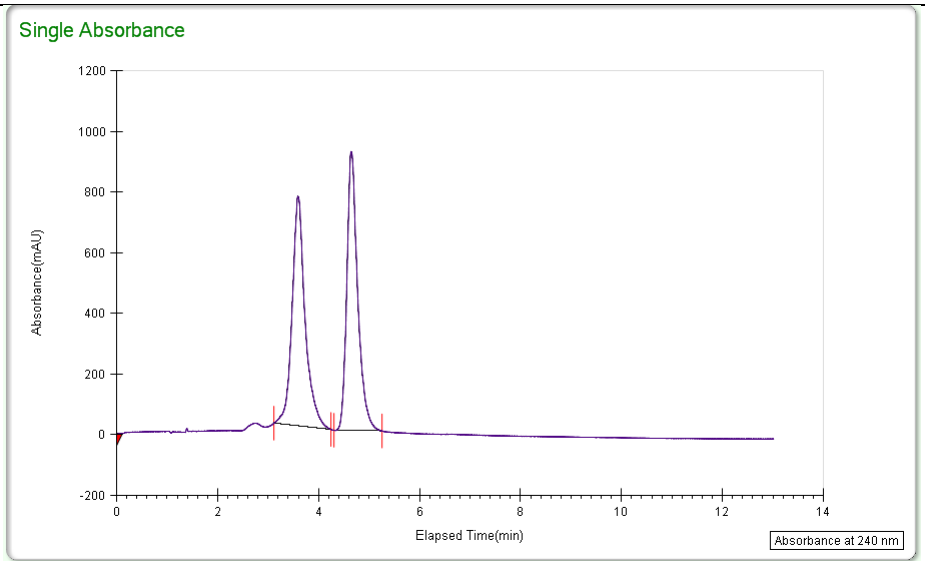

Scalemic: SFC, Chiracel AD-H, gradient 5% MeOH/CO_2 to 50% MeOH/CO_2, 3 mL/min, 240 nm

Peak	% area	area	RT(min)	height (mV)
1	93.5841	21958.5768	3.63	1171.4658
2	6.4159	1505.4166	4.68	112.4463
Total	100	23463.9934		

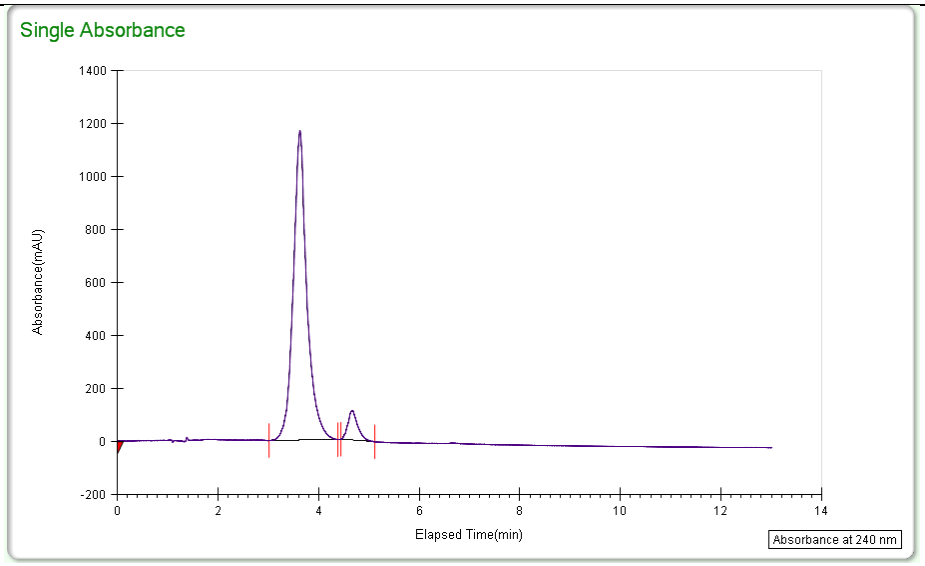

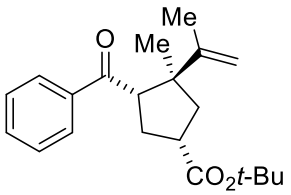

(1R,3S,4S)-tert-butyl 4-benzoyl-3-methyl-3-(prop-1-en-2-yl)cyclopentanecarboxylate (2.23)

Racemic: SFC, Chiracel AD-H, 5% MeOH/CO_2, 3 mL/min, 239 nm

Peak	% area	area	RT(min)	height (mV)
1	50.4774	10975.9081	3.38	518.6331
2	49.5226	10768.2770	5.39	366.5323
Total	100	21744.1851		

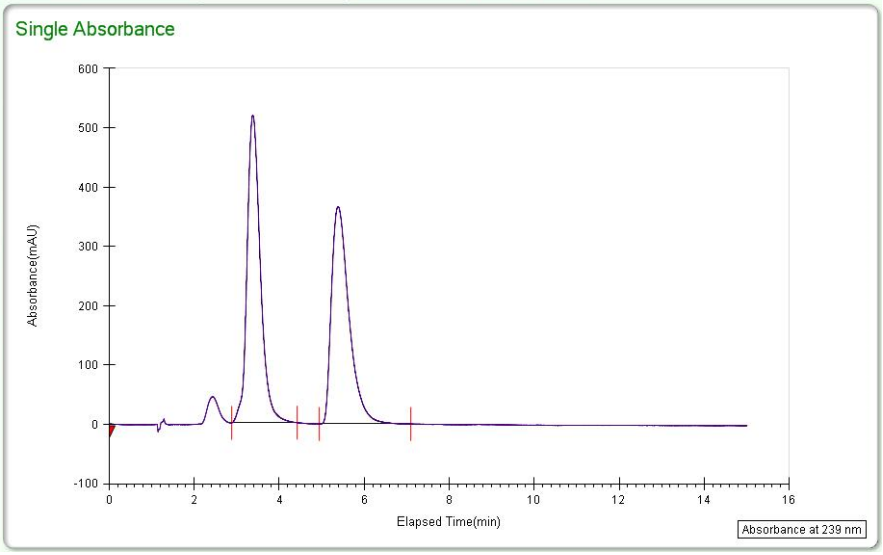

Scalemic: SFC, Chiracel AD-H, 5% MeOH/CO_2, 3 mL/min, 239 nm

Peak	% area	area	RT(min)	height (mV)
1	97.801	14687.9628	3.44	649.8146
2	2.199	330.2534	5.45	12.2647
Total	100	15018.2161		

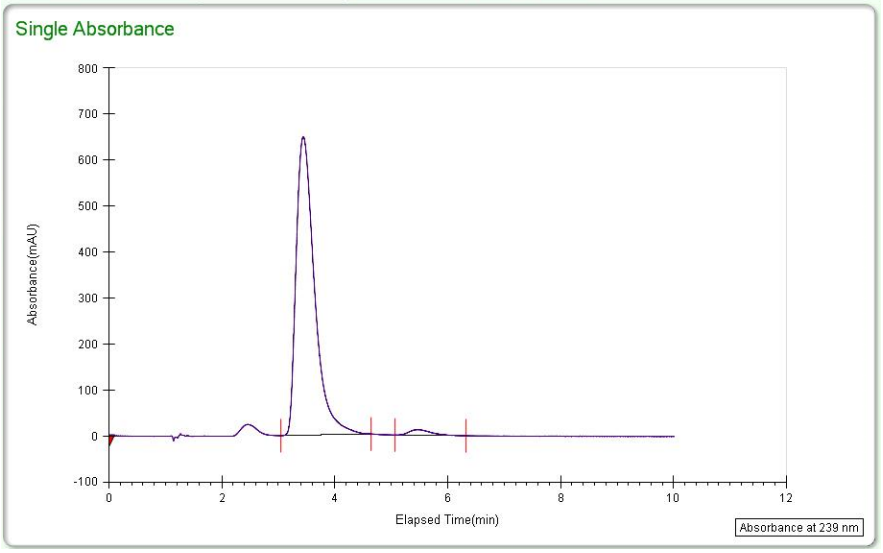

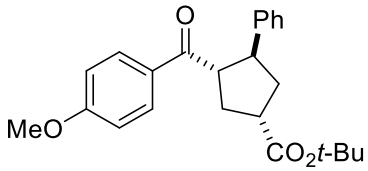

(1S,3S,4S)-tert-butyl 3-(4-methoxybenzoyl)-4-phenylcyclopentanecarboxylate (2.24)

Racemic: SFC, Chiracel AD-H, gradient 5% iPrOH/CO_2 to 50% iPrOH/CO_2, 3 mL/min, 238 nm

Peak	% area	area	RT(min)	height (mV)
1	50.9761	4885.3902	7.74	443.0142
2	49.0239	4669.4463	9.04	348.4219
Total	100	9524.8365		

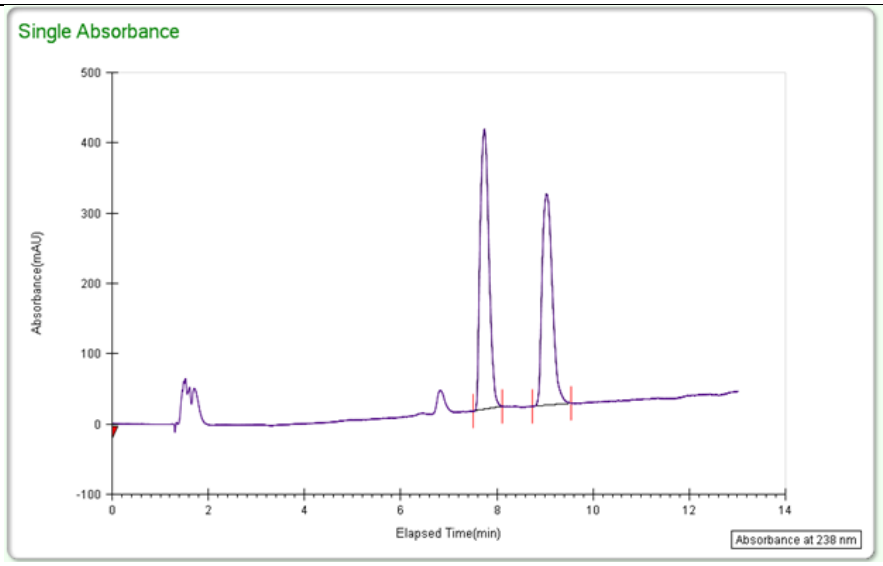

Scalemic: SFC, Chiracel AD-H, gradient 5% iPrOH/CO_2 to 50% iPrOH/CO_2, 3 mL/min, 238 nm

Peak	% area	area	RT(min)	height (mV)
1	95.5694	13807.2815	7.65	810.3921
2	4.4306	640.1019	8.98	20.1321
Total	100	14447.3834		

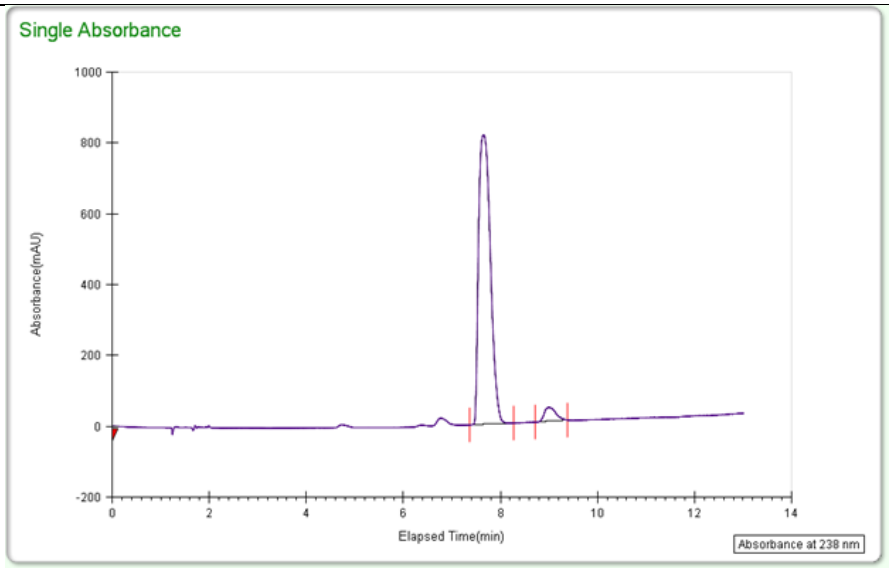

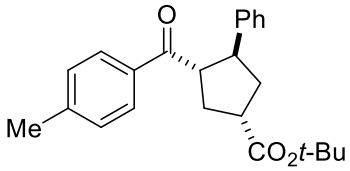

(1S,3S,4S)-tert-butyl 3-(4-methylbenzoyl)-4-phenylcyclopentanecarboxylate (2.25)

Racemic: SFC, Chiracel AD-H, gradient 10% iPrOH/CO_2 to 40% iPrOH/CO_2, 3 mL/min, 238 nm

Peak	% area	area	RT(min)	height (mV)
1	50.165	2676.8148	5.94	
2	49.835	2659.2028	8.12	
Total	100	5336.0176		

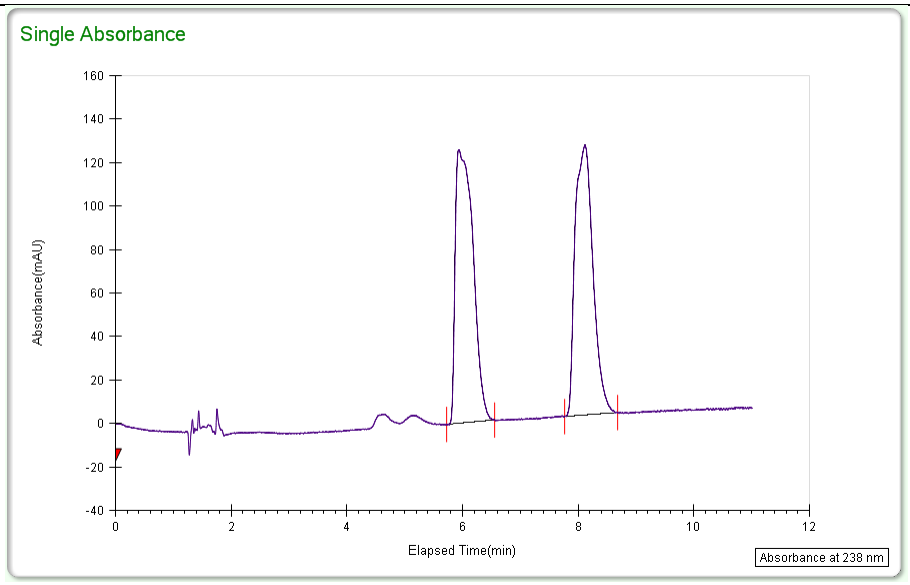

Scalemic: SFC, Chiracel AD-H, gradient 10% iPrOH/CO_2 to 40% iPrOH/CO_2, 3 mL/min, 238 nm

Peak	% area	area	RT(min)	height (mV)
1	98.4051	8582.6297	5.91	
2	1.5949	139.1014	8.09	
Total	100	8721.7311		

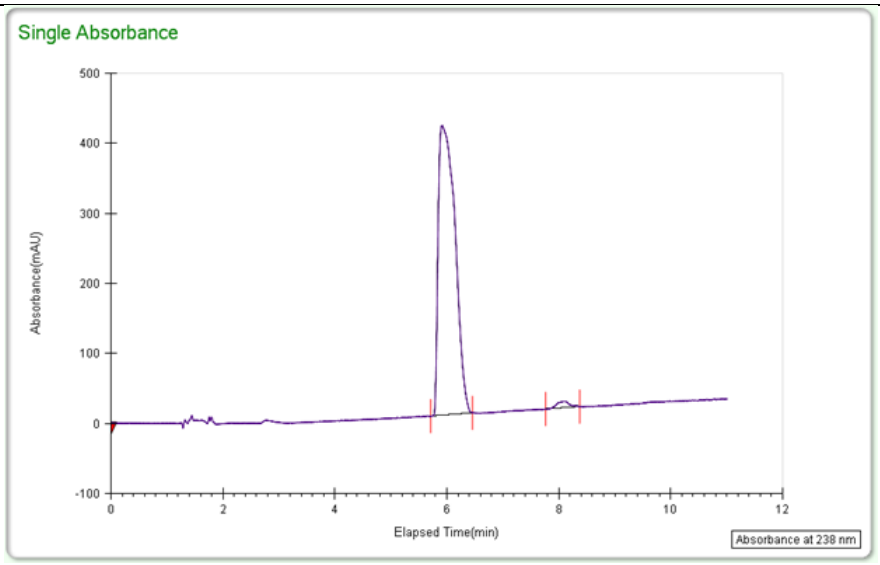

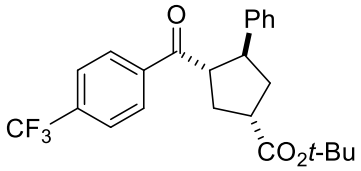

(1S,3S,4S)-tert-butyl 3-phenyl-4-(4-(trifluoromethyl)benzoyl)cyclopentanecarboxylate (2.26)

Racemic: SFC, Chiracel OD-H, gradient 1% iPrOH/CO_2 to 20% iPrOH/CO_2, 3 mL/min, 263 nm

Peak	% area	area	RT(min)	height (mV)
1	50.4908	1403.9646	5.95	
2	49.5092	1376.6717	6.33	
Total	100	2780.6363		

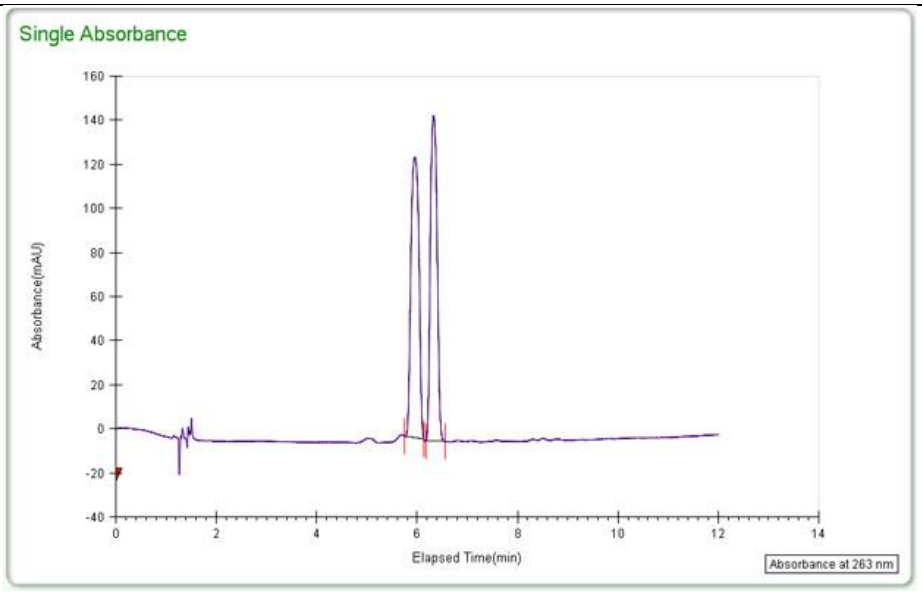

Scalemic: SFC, Chiracel OD-H, gradient 1% iPrOH/CO_2 to 20% iPrOH/CO_2, 3 mL/min, 263 nm

Peak	% area	area	RT(min)	height (mV)
1	5.2538	1025.1958	5.97	
2	94.7462	18488.2842	6.28	
Total	100	19513.48		

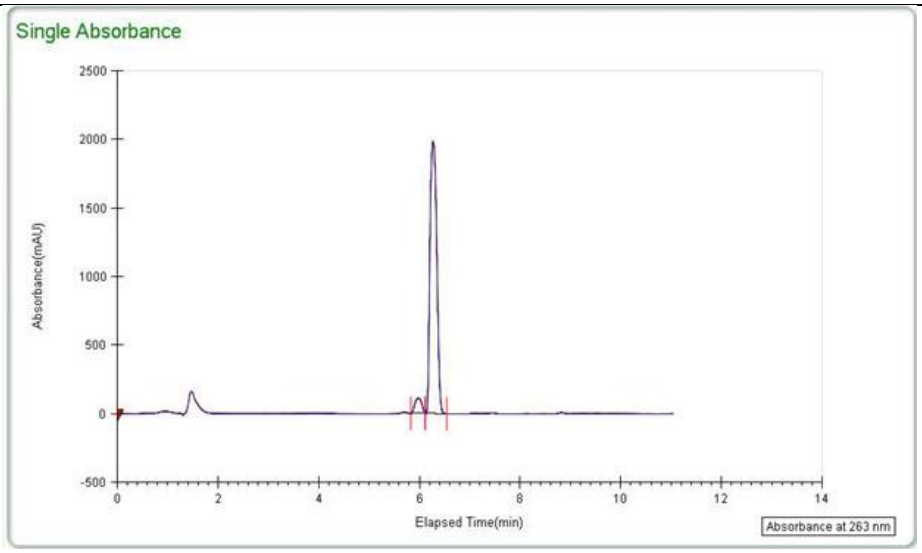

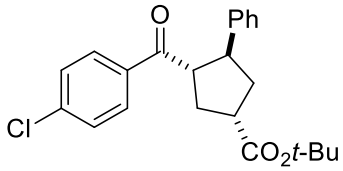

(1S,3S,4S)-tert-butyl 3-(4-chlorobenzoyl)-4-phenylcyclopentanecarboxylate (2.27)

Racemic: SFC, Chiracel AD-H, gradient 5% iPrOH/CO_2 to 50% iPrOH/CO_2, 3 mL/min, 263 nm

Peak	% area	area	RT(min)	height (mV)
1	49.8029	25505.2367	7.4	2737.1797
2	50.1971	25707.1071	7.78	2623.8135
Total	100	51212.3438		

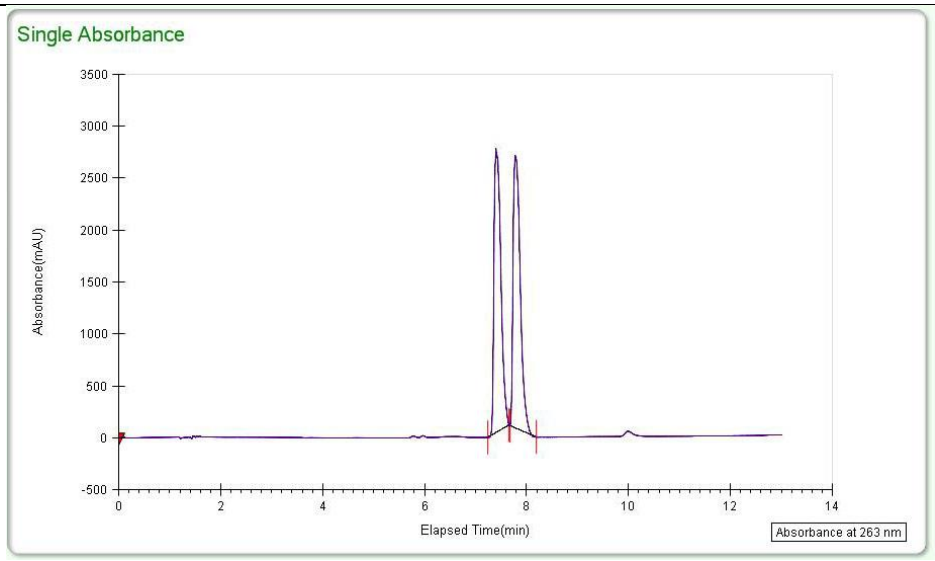

Scalemic: SFC, Chiracel AD-H, gradient 5% iPrOH/CO_2 to 50% iPrOH/CO_2, 3 mL/min, 263 nm

Peak	% area	area	RT(min)	height (mV)
1	96.1766	4487.9187	6.34	
2	3.8234	178.411	7.00	
Total	100	4666.3297		

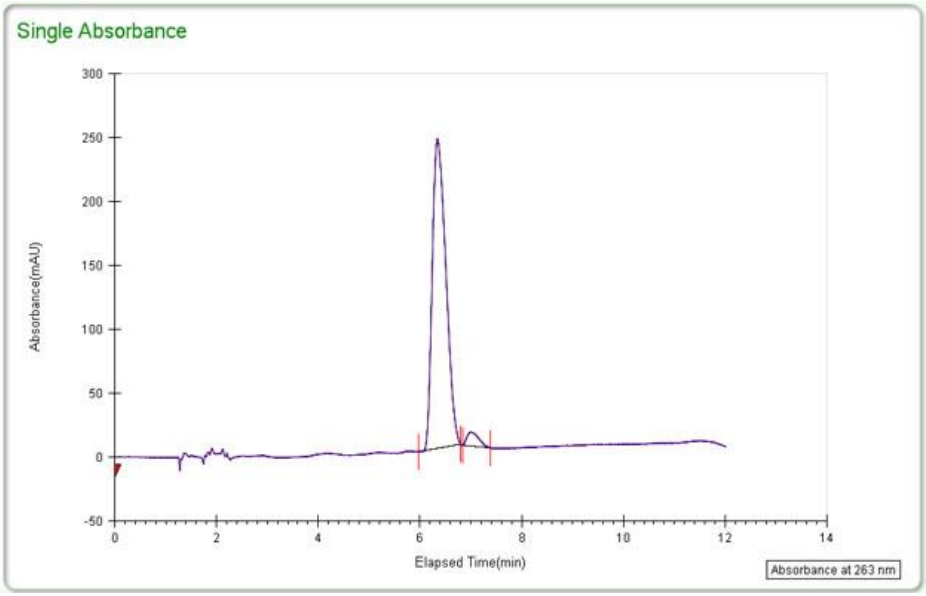

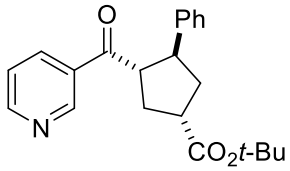

(1S,3S,4S)-tert-butyl 3-nicotinoyl-4-phenylcyclopentanecarboxylate (2.28)

Racemic: SFC, Chiracel AD-H, gradient 5% iPrOH/CO_2 to 50% iPrOH/CO_2, 3 mL/min, 238 nm

Peak	% area	area	RT(min)	height (mV)
1	50.0521	5567.4095	6.53	680.9274
2	49.9479	5555.829	6.95	660.2215
Total		11123.2385		

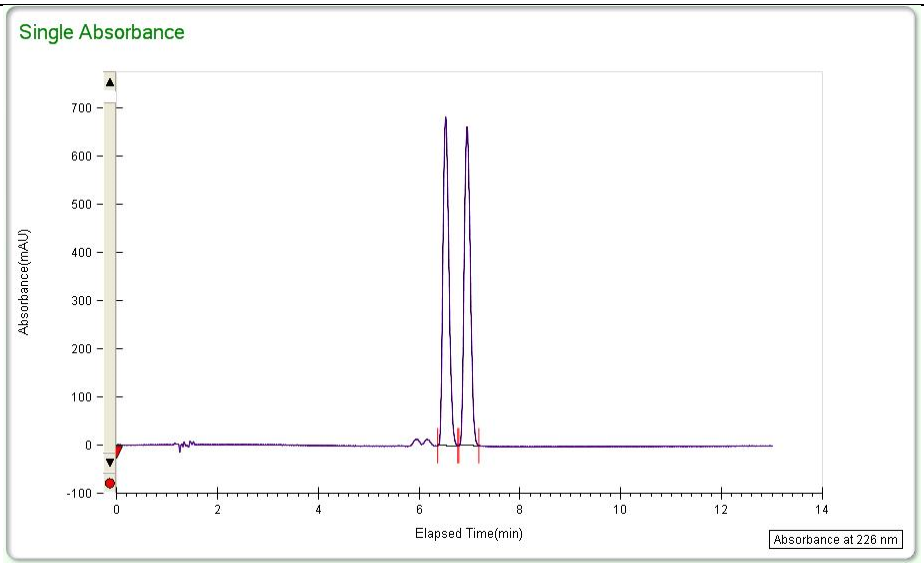

Scalemic: SFC, Chiracel AD-H, gradient 5% iPrOH/CO_2 to 50% iPrOH/CO_2, 3 mL/min, 238 nm

Peak	% area	area	RT(min)	height (mV)
1	94.2451	10092.6171	6.45	1089.0392
2	5.7549	616.2901	6.92	70.1372
Total	100	10708.9071		

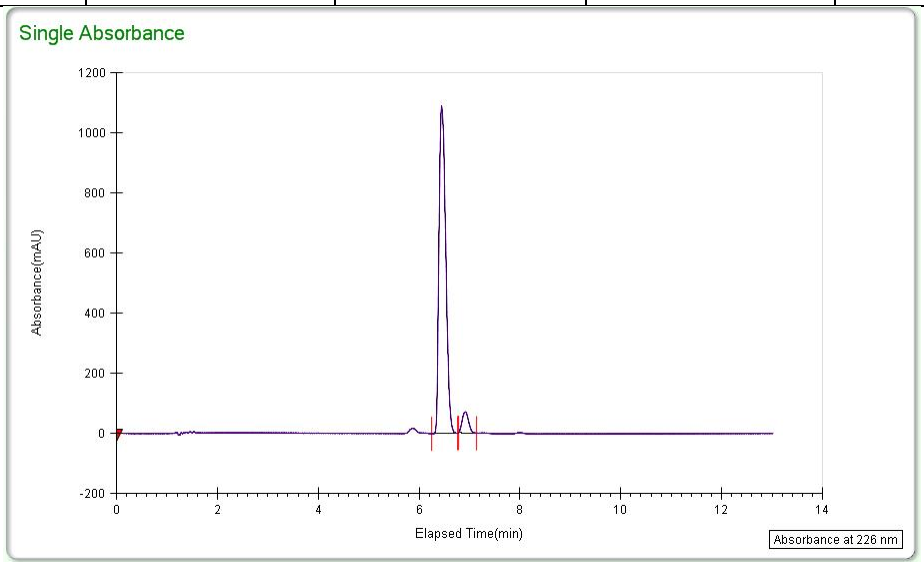

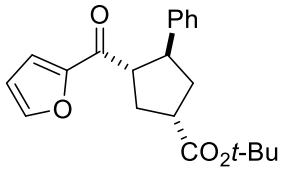

(1S,3S,4S)-tert-butyl 3-(furan-2-carbonyl)-4-phenylcyclopentanecarboxylate (2.29)

Racemic: SFC, Chiracel AD-H, gradient 10% iPrOH/CO_2, 6 mL/min, 263 nm

Peak	% area	area	RT(min)	height (mV)
1	49.83	2455.0862	1.9	244.5986
2	50.17	2471.8394	2.74	155.6862
Total	100	4926.9256		

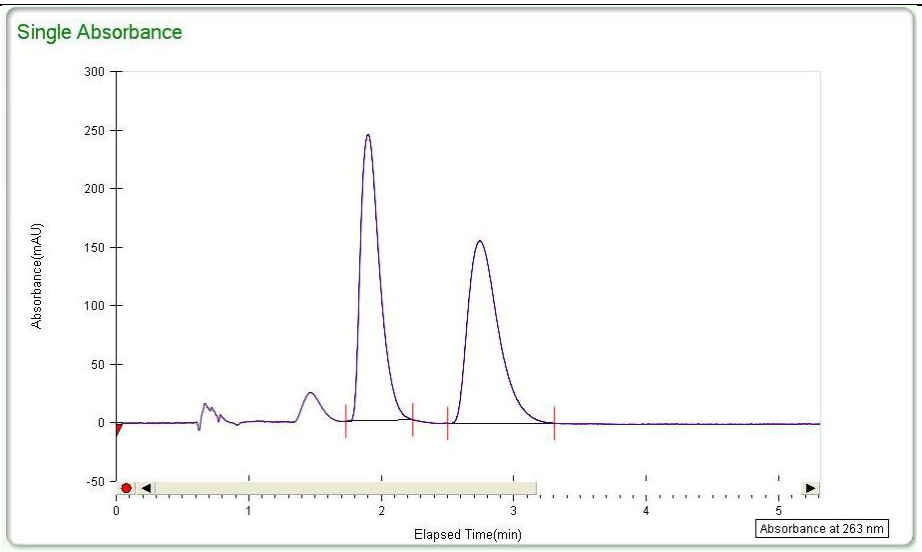

Scalemic: SFC, Chiracel AD-H, gradient 10% iPrOH/CO_2, 6 mL/min, 263 nm

Peak	% area	area	RT(min)	height (mV)
1	89.4167	26631.9992	1.89	2327.4631
2	10.5833	3152.1447	2.74	192.9336
Total	100	39784.144		

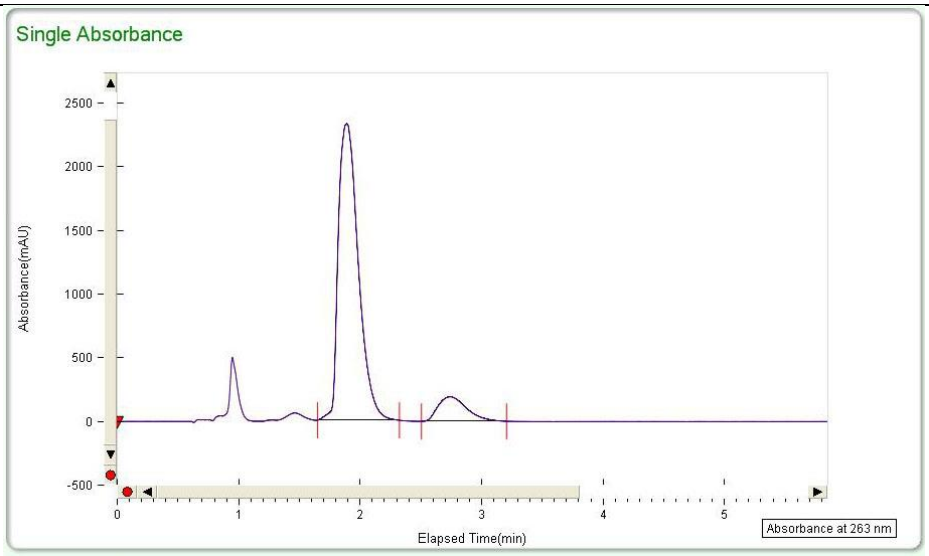

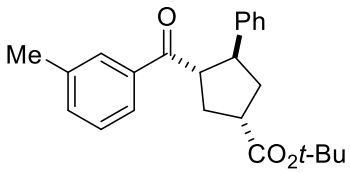

(1S,3S,4S)-tert-butyl 3-(3-methylbenzoyl)-4-phenylcyclopentanecarboxylate (3.30)

Racemic: SFC, Chiracel AD-H, gradient 5% iPrOH/CO_2 to 50% iPrOH/CO_2, 3 mL/min, 238 nm

Peak	% area	area	RT(min)	height (mV)
1	50.8315	2675.353	5.47	
2	49.1685	2587.8288	6.09	
Total	100	5263.1818		

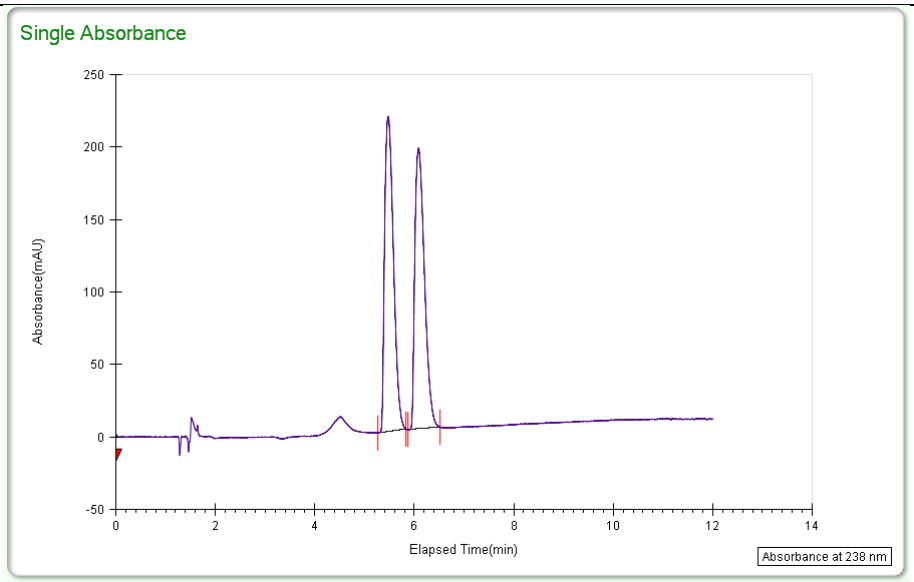

Scalemic: SFC, Chiracel AD-H, gradient 5% iPrOH/CO_2 to 50% iPrOH/CO_2, 3 mL/min, 238 nm

Peak	% area	area	RT(min)	height (mV)
1	94.6587	8541.643	5.37	
2	5.3413	481.9796	6.00	
Total	100	9023.6226		

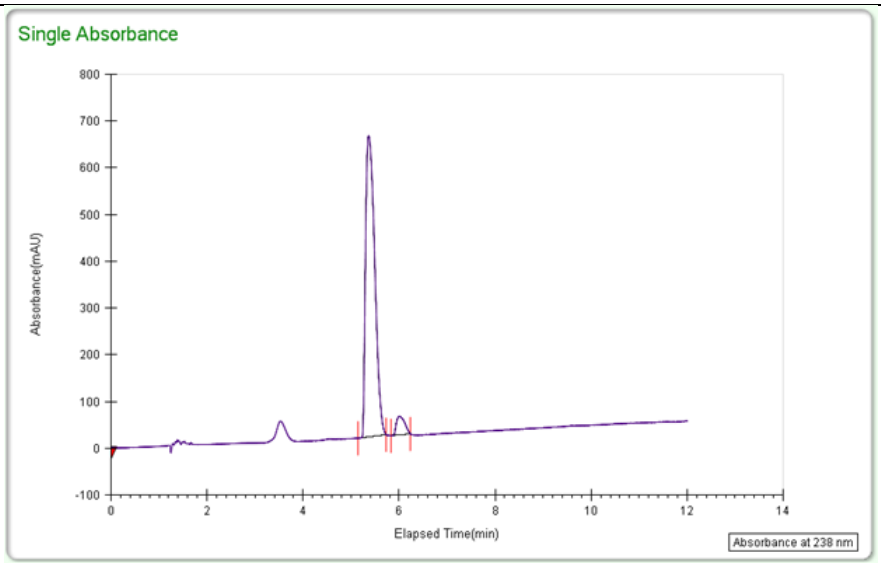

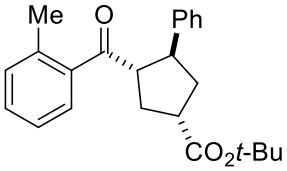

(1S,3S,4S)-tert-butyl 3-(2-methylbenzoyl)-4-phenylcyclopentanecarboxylate (2.31)

Racemic: SFC, Chiracel AD-H, 7% iPrOH/CO_2 iPrOH/CO_2, 6 mL/min, 263 nm

Peak	% area	area	RT(min)	height (mV)
1	50.0604	4391.855	2.47	305.0626
2	49.9396	4381.2509	4.63	165.3425
Total	100	8773.1059		

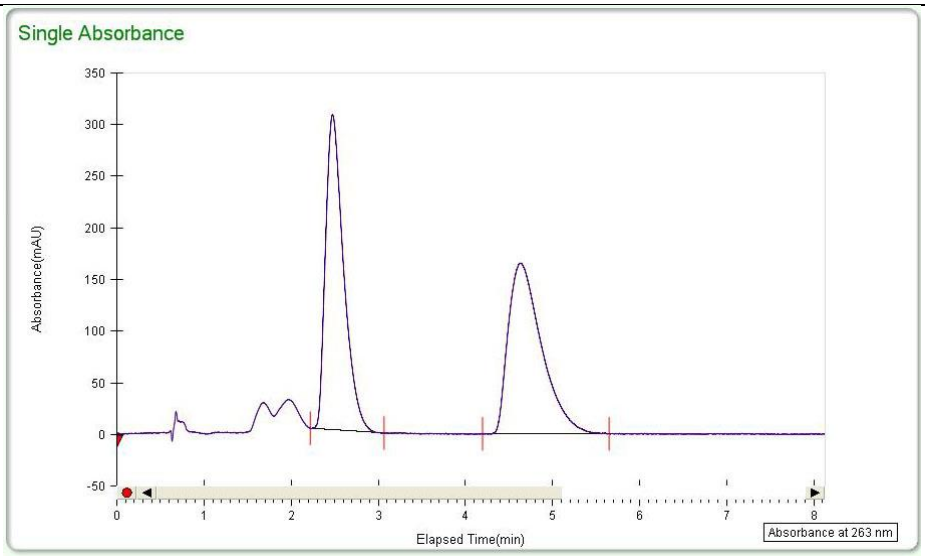

Scalemic: SFC, Chiracel AD-H, gradient 7% iPrOH/CO_2 iPrOH/CO_2, 6 mL/min, 263 nm

Peak	% area	area	RT(min)	height (mV)
1	85.6284	3103.9517	2.47	213.1387
2	14.3716	520.9562	4.65	20.933
Total	100	3624.9078		

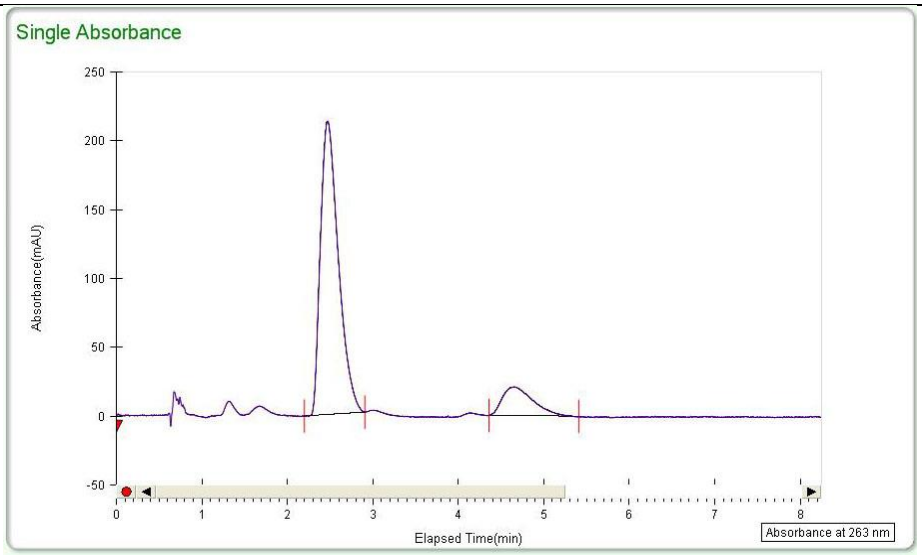

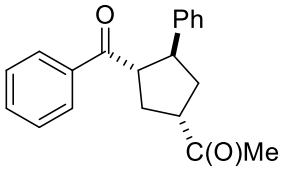

1-((1S,3S,4S)-3-benzoyl-4-phenylcyclopentyl)ethanone (3.32)

Racemic: SFC, Chiracel AD-H, 5% iPrOH/CO_2, 6 mL/min, 238 nm

Peak	% area	area	RT(min)	height (mV)
1	46.3168	1306.1541	3.05	92.1535
2	53.6832	1513.8883	3.87	71.7254
Total	100	2820.0424		

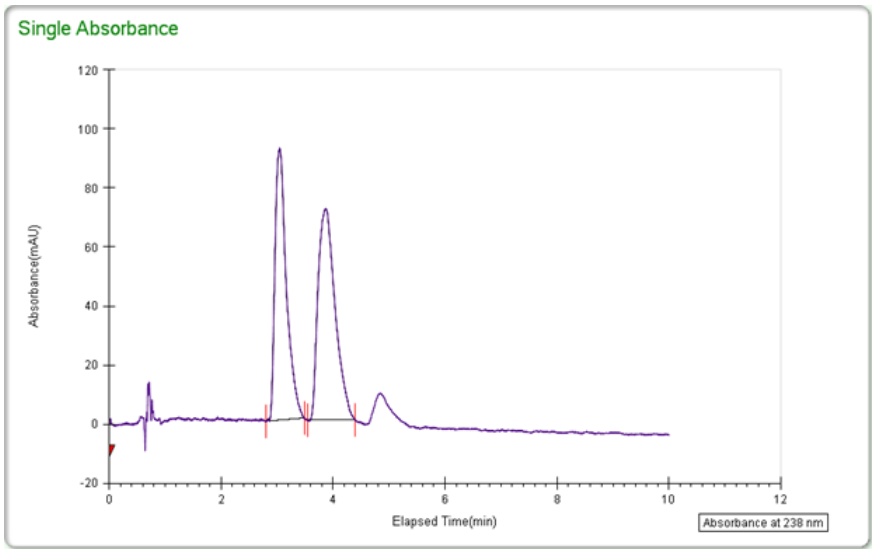

Scalemic: SFC, Chiracel AD-H, 5% iPrOH/CO_2, 6 mL/min, 238 nm

Peak	% area	area	RT(min)	height (mV)
1	6.0123	90.6390	3.02	8.1857
2	93.9877	1416.9201	3.78	70.6342
Total	100	1507.5591		

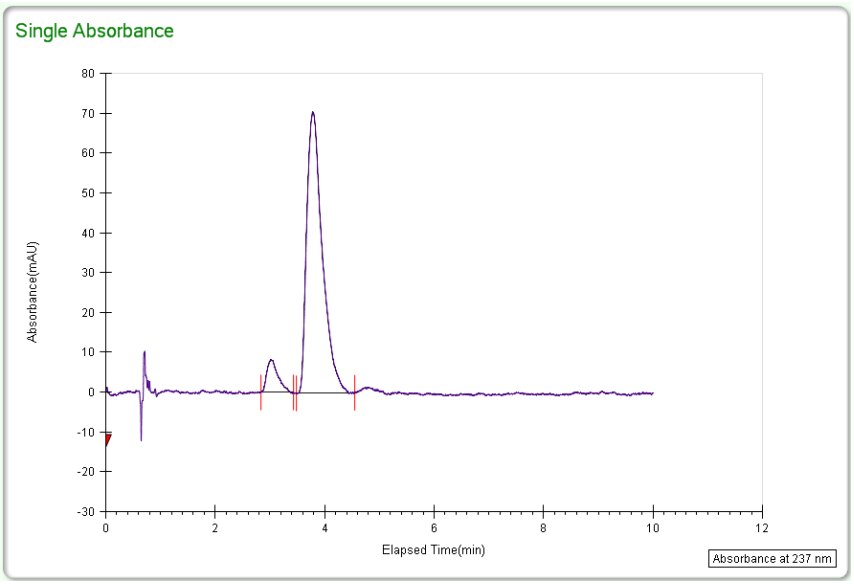

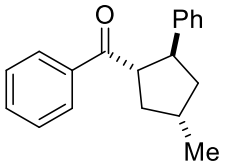

((1S,2S,4S)-4-methyl-2-phenylcyclopentyl)(phenyl)methanone (2.33)

Racemic: SFC, Chiracel AD-H, gradient 5% iPrOH/CO_2, 3 mL/min, 263 nm

Peak	% area	area	RT(min)	height (mV)
1	52.4608	6592.7457	3.85	368.6752
2	47.5392	5974.2576	6.23	199.1554
Total	100	12567.0034		

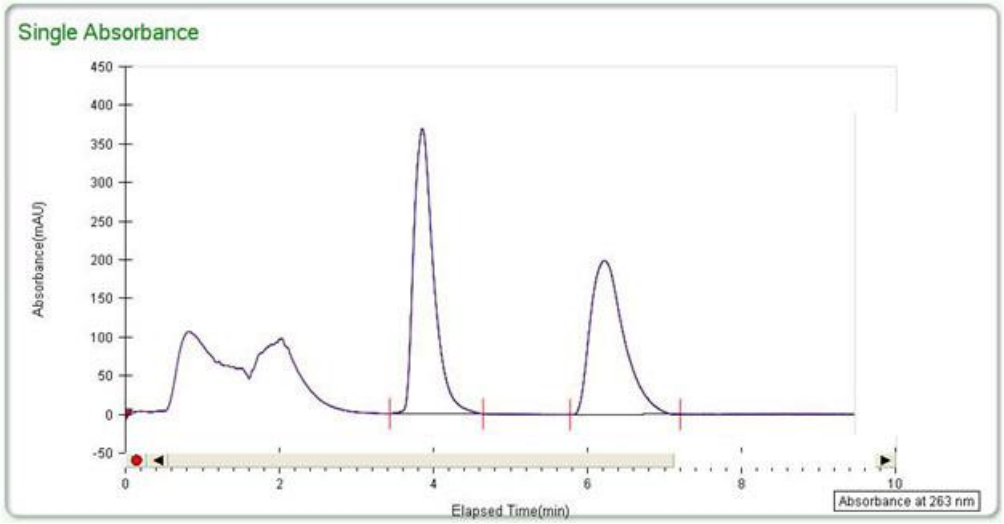

Scalemic: SFC, Chiracel AD-H, gradient 5% iPrOH/CO_2, 3 mL/min, 263 nm

Peak	% area	area	RT(min)	height (mV)
1	74.7414	22252.5356	3.78	1001.6165
2	25.2586	7520.1736	6.26	210.3868
Total	100	29772.7091		

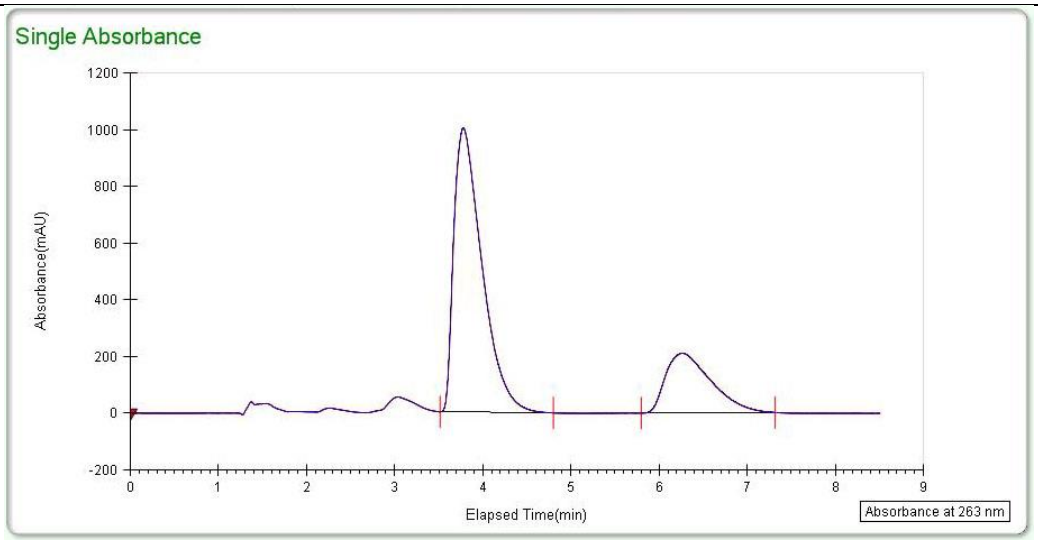

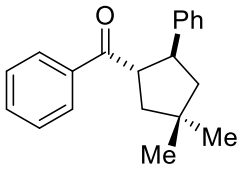

((1S,2S)-4,4-dimethyl-2-phenylcyclopentyl)(phenyl)methanone (2.34)

Racemic: SFC, Chiracel AD-H, gradient 5% iPrOH/CO_2 to 50% iPrOH/CO_2, 3 mL/min, 238 nm

Peak	% area	area	RT(min)	height (mV)
1	49.3999	8225.7657	5.18	472.1342
2	50.6001	8425.6056	6.7	548.1129
Total	100	16651.3712		

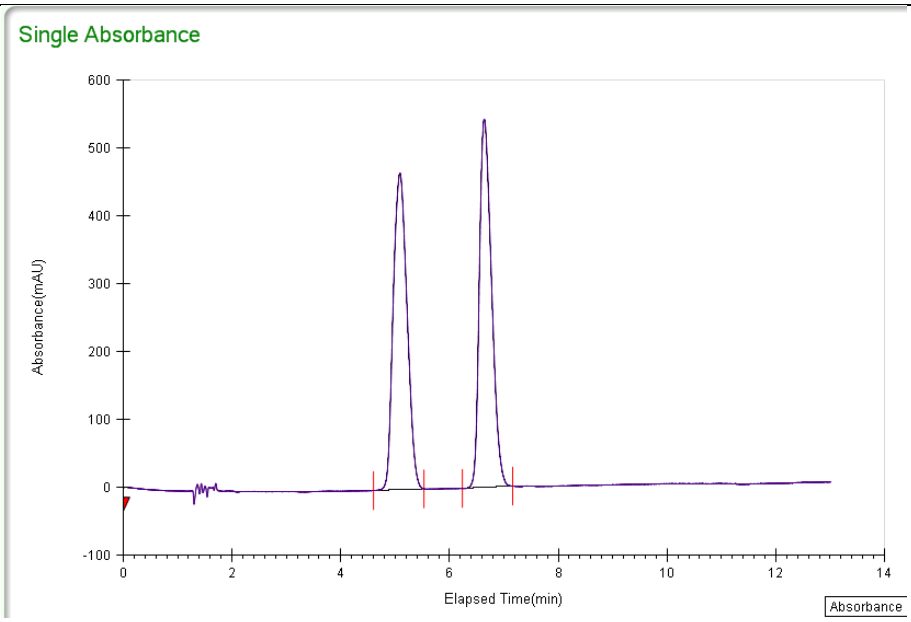

Scalemic: SFC, Chiracel AD-H, gradient 5% iPrOH/CO_2 to 50% iPrOH/CO_2, 3 mL/min, 238 nm

Peak	% area	area	RT(min)	height (mV)
1	94.3179	19058.3452	5.19	952.1298
2	5.6821	1148.1496	6.7	58.4213
Total	100	20206.4948		

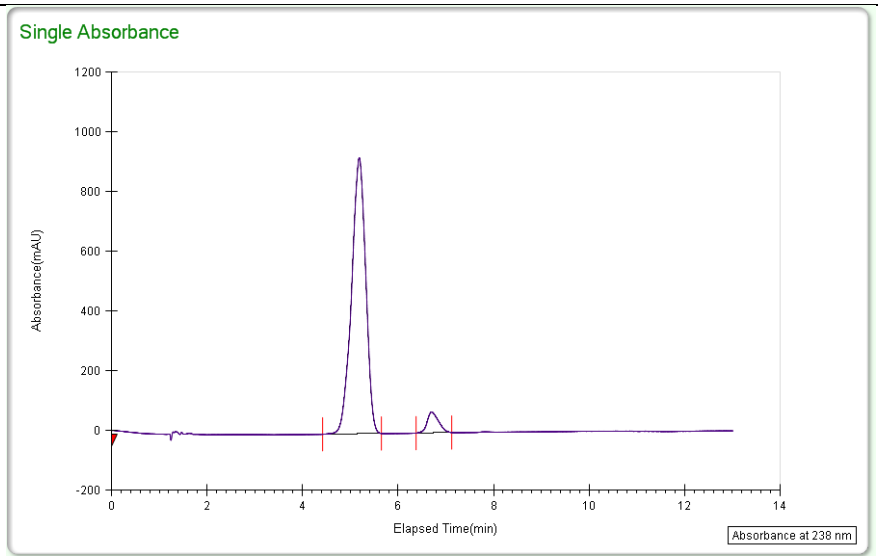

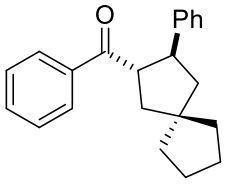

phenyl((2S,3S)-3-phenylspiro[4.4]nonan-2-yl)methanone (2.35)

Racemic: SFC, Chiracel AD-H, gradient 10% iPrOH/CO_2 to 50% iPrOH/CO_2, 3 mL/min, 263 nm

Peak	% area	area	RT(min)	height (mV)
1	50.2528	8530.2528	5.50	799.0081
2	49.7472	8444.3162	6.56	836.9197
Total	100	16974.4424		

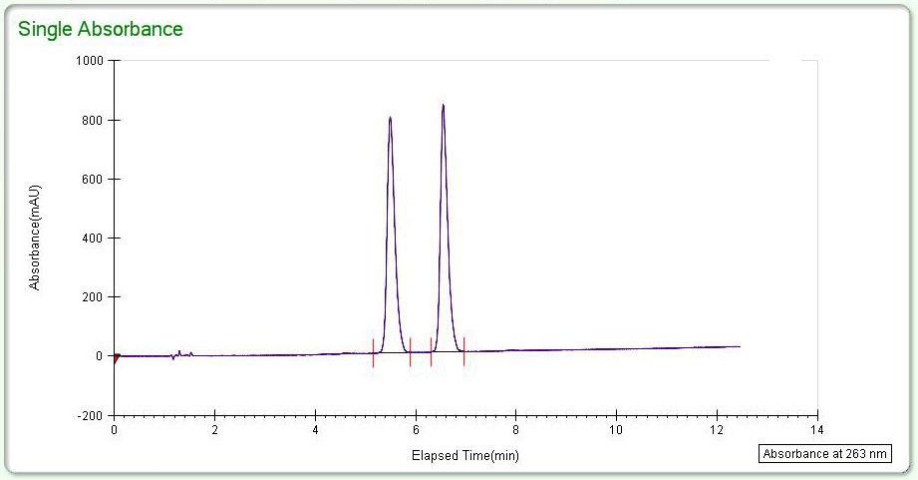

Scalemic: SFC, Chiracel AD-H, gradient 10% iPrOH/CO_2 to 50% iPrOH/CO_2, 3 mL/min, 263 nm

Peak	% area	area	RT(min)	height (mV)
1	97.0312	33733.6188	5.49	2186.4065
2	2.9688	1032.1149	6.60	99.95
Total	100	34765.7317		

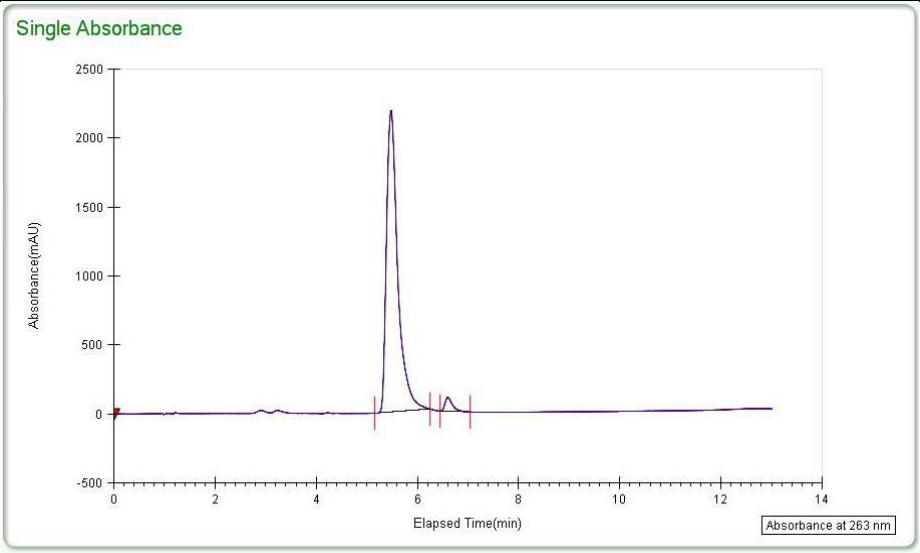

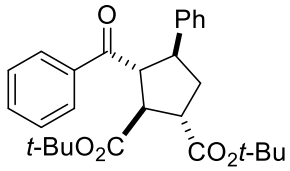

(1S,2S,3R,4S)-di-tert-butyl 3-benzoyl-4-phenylcyclopentane-1,2-dicarboxylate (2.37)

Racemic: SFC, Chiracel OD-H, gradient 5% iPrOH/CO_2 to 30% iPrOH/CO_2, 3 mL/min, 238 nm

Peak	% area	area	RT(min)	height (mV)
1	48.589	11704.4724	4.27	827.3701
2	51.411	12384.259	4.66	991.9261
Total	100	24088.259		

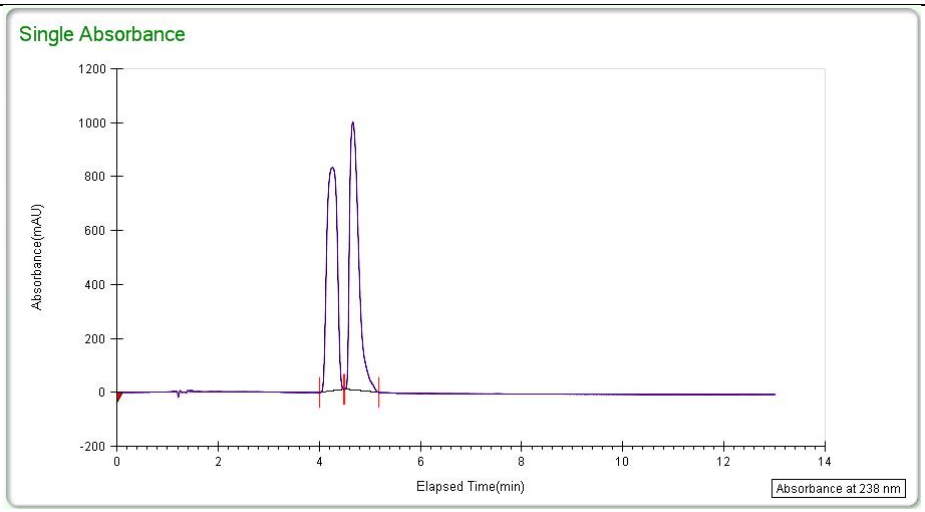

Scalemic: SFC, Chiracel OD-H, gradient 5% iPrOH/CO_2 to 30% iPrOH/CO_2, 3 mL/min, 238 nm

Peak	% area	area	RT(min)	height (mV)
1	0.6737	93.2733	4.26	6.8032
2	99.3263	13750.9824	4.67	1073.6484
Total	100	13844.2557		

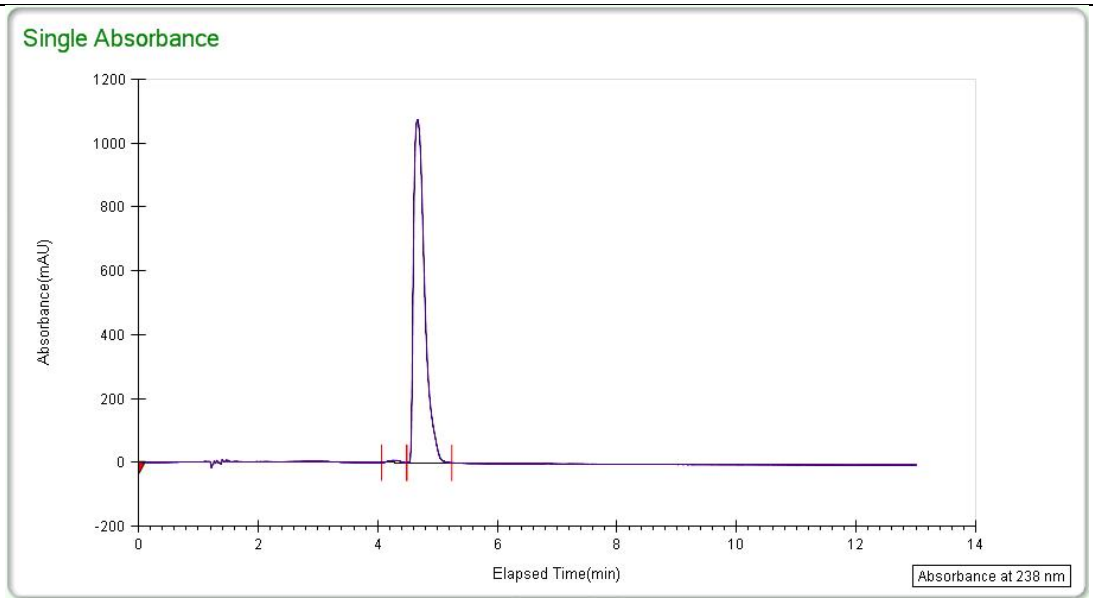

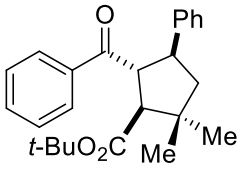

(1S,4S,5R)-tert-butyl 5-benzoyl-2,2-dimethyl-4-phenylcyclopentanecarboxylate (2.39)

Racemic: SFC, Chiracel OD-H, gradient 5% iPrOH/CO_2 to 30% iPrOH/CO_2, 3 mL/min, 238 nm

Peak	% area	area	RT(min)	height (mV)
1	50.0018	6620.3362	3.65	386.714
2	49.9982	6619.8586	4.66	506.2026
Total	100	13240.1948		

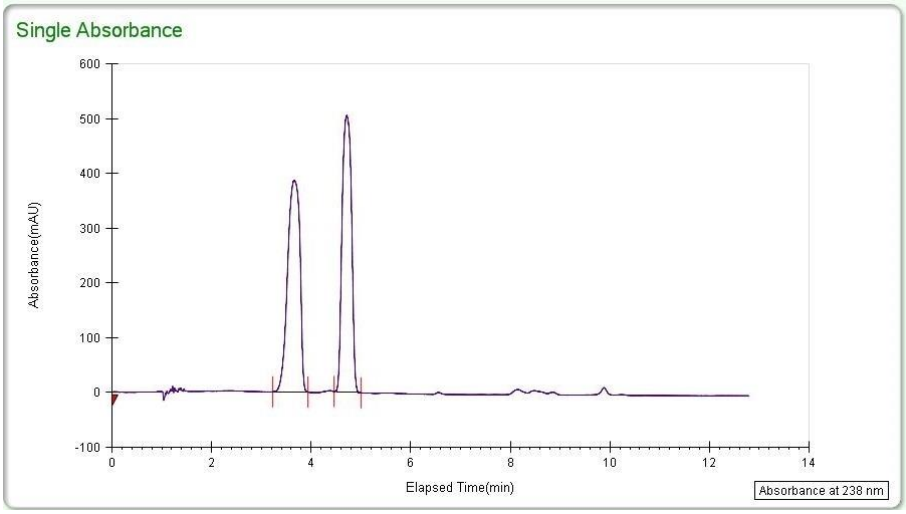

Scalemic: SFC, Chiracel OD-H, gradient 5% iPrOH/CO_2 to 30% iPrOH/CO_2, 3 mL/min, 238 nm

Peak	% area	area	RT(min)	height (mV)
1	1.7468	277.4604	3.64	17.5799
2	98.2532	15606.8709	4.69	1080.9641
Total	100	15884.3313		

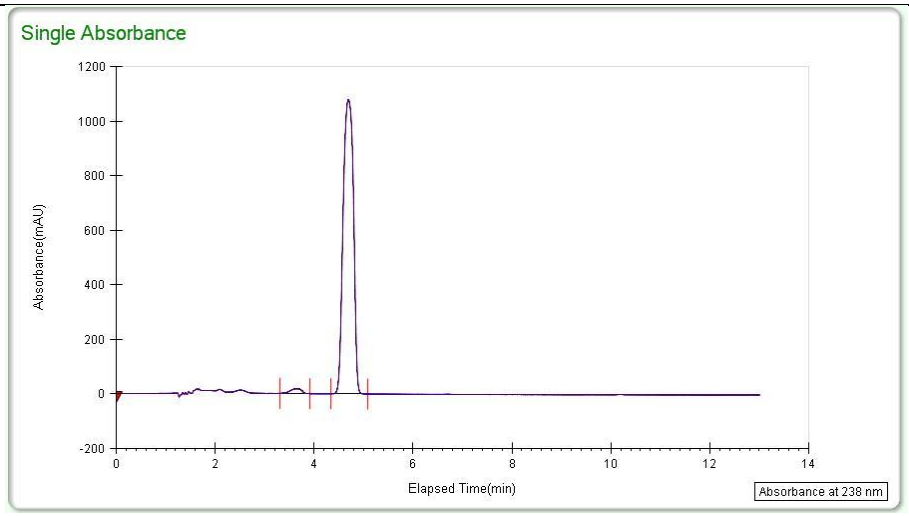

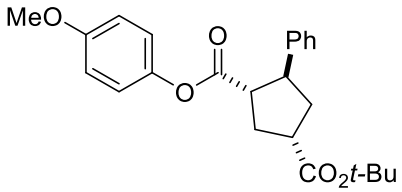

(1S,3S,4S)-1-tert-butyl 3-(4-methoxyphenyl) 4-phenylcyclopentane-1,3-dicarboxylate (2.40)

Racemic: SFC, Chiracel AD-H, gradient 15% iPrOH/CO_2, 3 mL/min, 263 nm

Peak	% area	area	RT(min)	height (mV)
1	50.2109	10299.0288	4.15	
2	49.7891	10212.4956	5.75	
Total	100	20511.5245		

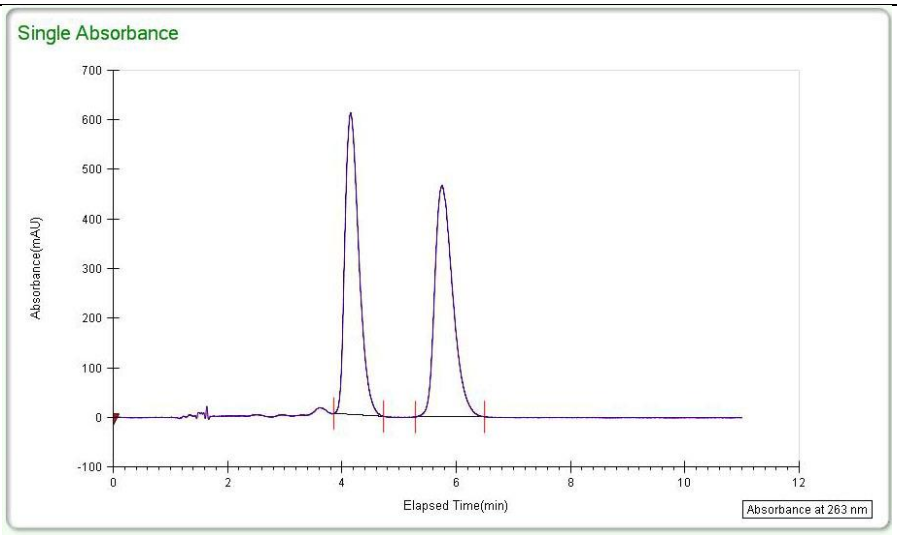

Scalemic: SFC, Chiracel AD-H, gradient 15% iPrOH/CO_2, 3 mL/min, 263 nm

Peak	% area	area	RT(min)	height (mV)
1	94.3301	12566.3858	4.08	
2	5.6699	755.324	5.7	
Total	100	13321.7098		

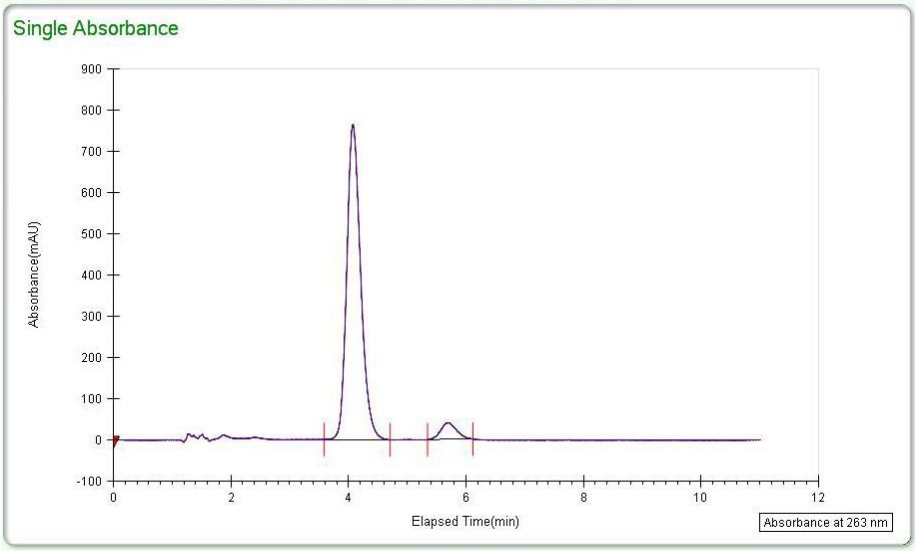

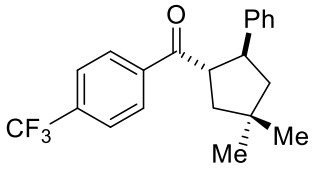

((1S,2S)-4,4-dimethyl-2-phenylcyclopentyl)(4-(trifluoromethyl)phenyl)methanone (2.41)

Racemic: SFC, Chiracel OD-H, gradient 5% (1:4 iPrOH/hexane)/CO_2 to 50% (1:4 iPrOH/hexane)/CO_2, 3 mL/min, 235 nm

Peak	% area	area	RT(min)	height (mV)
1	49.5291	7852.5027	2.85	606.6880
2	50.4709	8001.8218	3.79	830.5841
Total	100	15854.3245		

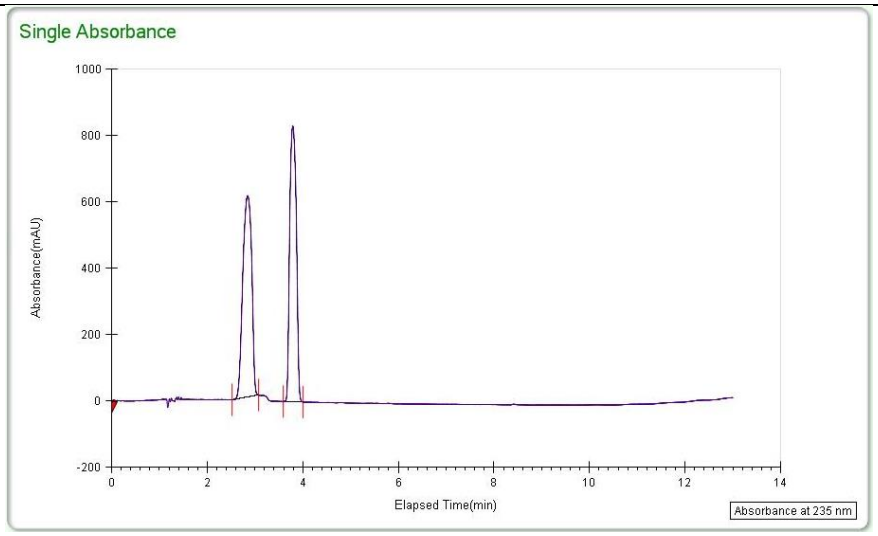

Scalemic: SFC, Chiracel OD-H, gradient 5% (1:4 iPrOH/hexane)/CO_2 to 50% (1:4 iPrOH/hexane)/CO_2, 3 mL/min, 235 nm

Peak	% area	area	RT(min)	height (mV)
1	8.5386	1631.0355	2.68	99.9694
2	91.4614	17470.7852	3.66	1833.1693
Total	100	19101.8206		

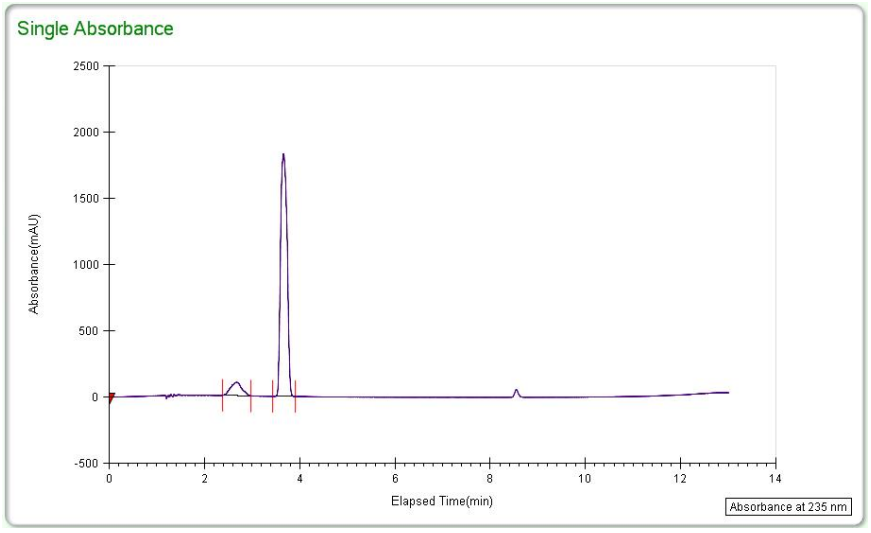

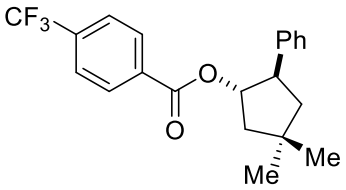

(1S,2R)-4,4-dimethyl-2-phenylcyclopentyl 4-(trifluoromethyl)benzoate (2.42)

Racemic: SFC, Chiracel OD-H, gradient 5% iPrOH/CO_2 to 30% iPrOH/CO_2, 3 mL/min, 235 nm

Peak	% area	area	RT(min)	height (mV)
1	49.4434	12968.7309	2.47	1112.3162
2	50.5566	13260.7238	3.72	1292.3761
Total	100	26229.4547		

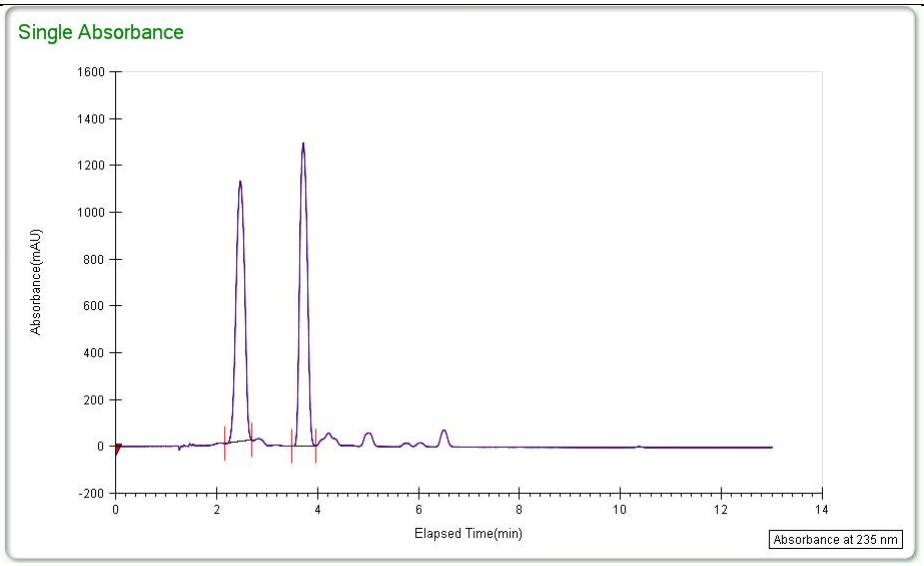

Scalemic: SFC, Chiracel OD-H, gradient 5% iPrOH/CO_2 to 30% iPrOH/CO_2, 3 mL/min, 235 nm

Peak	% area	area	RT(min)	height (mV)
1	8.4522	1809.6007	2.51	128.8436
2	91.5478	19600.2886	3.73	1833.1819
Total	100	21409.8893		

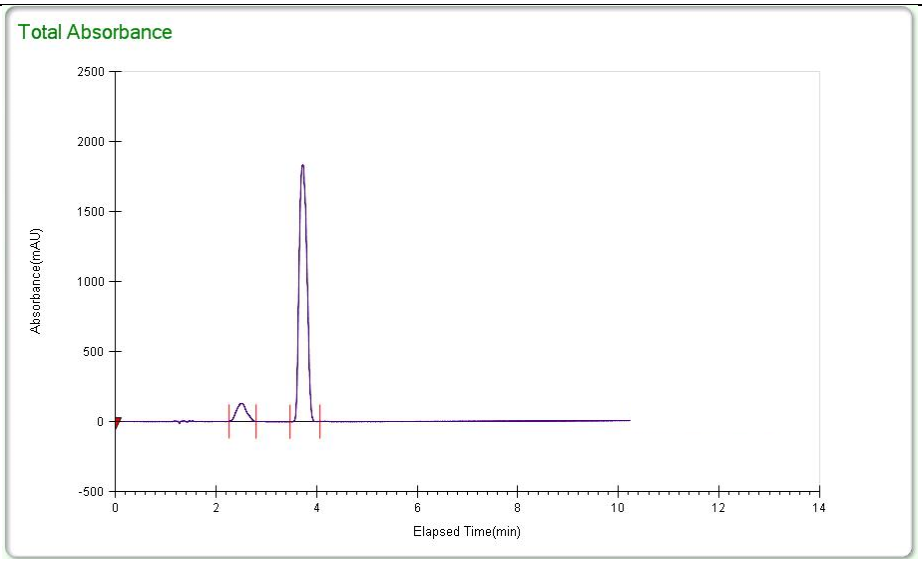

Appendix C. HPLC Traces for New Compounds (Chapter 4)

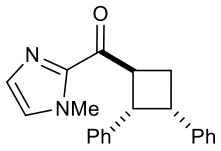

4.16 – Major Diastereomer
Run Details: HPLC, Diacel CHIRALPAK OD-H,
10.00 µL, gradient 5% to 50% iPrOH/hexanes,
18 minutes, 1 mL/min, 295.0 nm.

Racemic Chromatogram

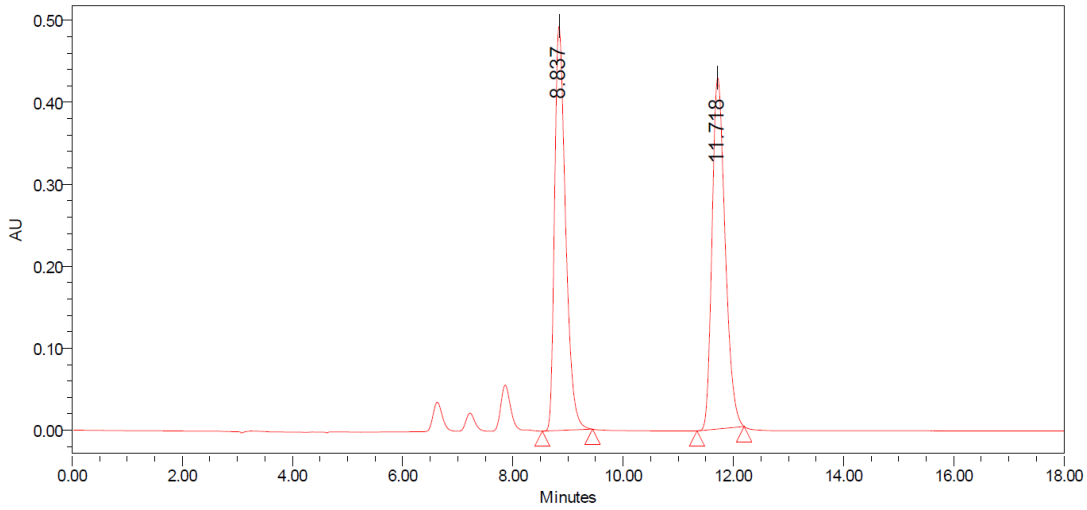

Peak	% Area	Retention Time	Area	Height
1	49.16	8.837	6844274	493024
2	50.84	11.718	7078999	428301
Total	100.00			

Scalemic Chromatogram

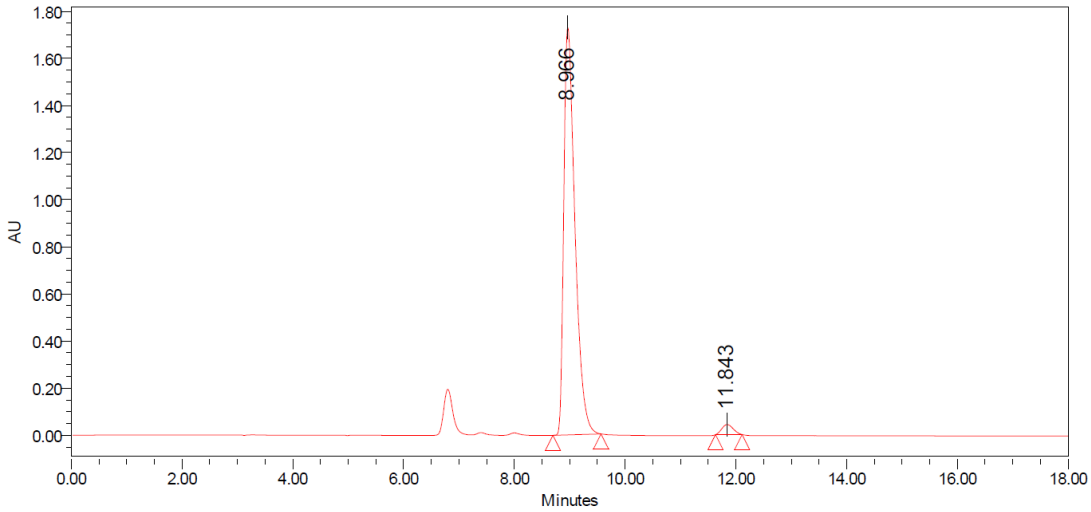

Peak	% Area	Retention Time	Area	Height
1	97.55	8.966	24201086	1729670
2	2.45	11.843	608085	42774
Total	100.00			

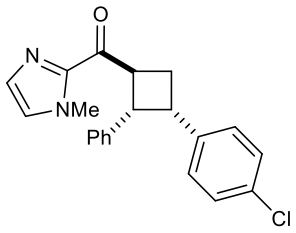

4.20 – Major Diastereomer
Run Details: HPLC, Diacel CHIRALPAK AD,
10.00 µL, gradient 5% to 50% iPrOH/hexanes,
18 minutes, 1 mL/min, 285.0 nm.

Racemic Chromatogram

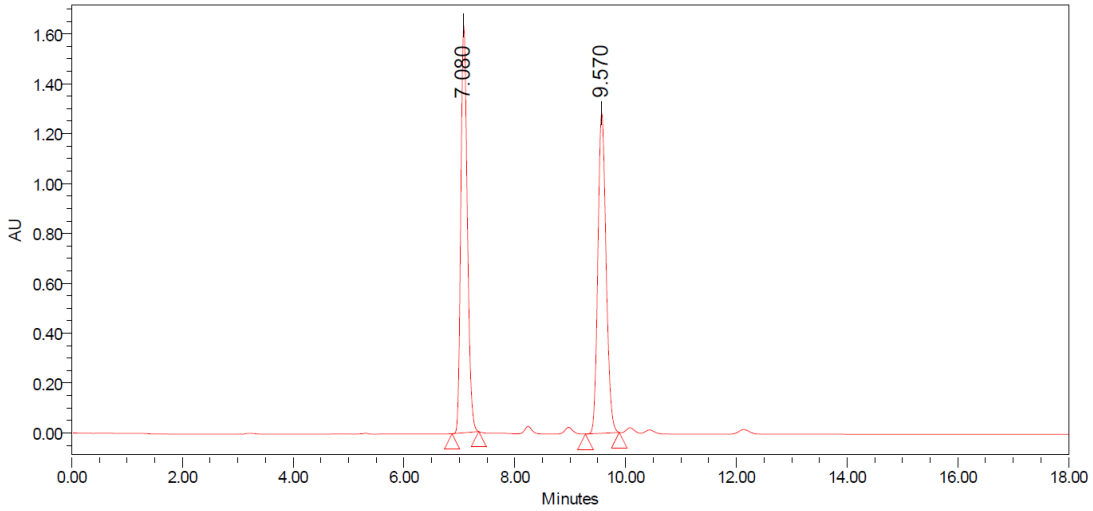

Peak	% Area	Retention Time	Area	Height
1	50.13	7.080	13336366	1633332
2	49.87	9.570	13269671	1283622
Total	100.00			

Scalemic Chromatogram

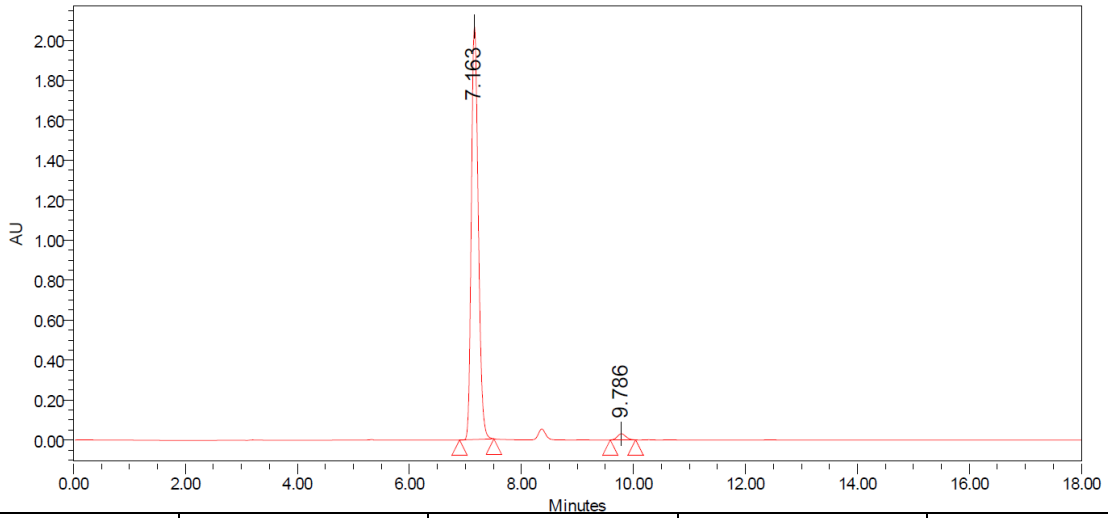

Peak	% Area	Retention Time	Area	Height
1	98.24	7.163	17804766	2064862
2	1.79	9.786	318815	30470
Total	100.00			

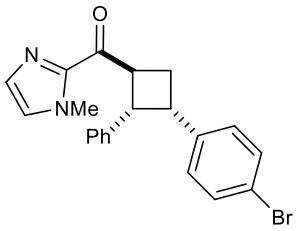

4.21 – Major Diastereomer
Run Details: HPLC, Diacel CHIRALPAK OD-H,
10.00 µL, gradient 5% to 30% iPrOH/hexanes,
20 minutes, 1 mL/min, 285.0 nm.

Racemic Chromatogram

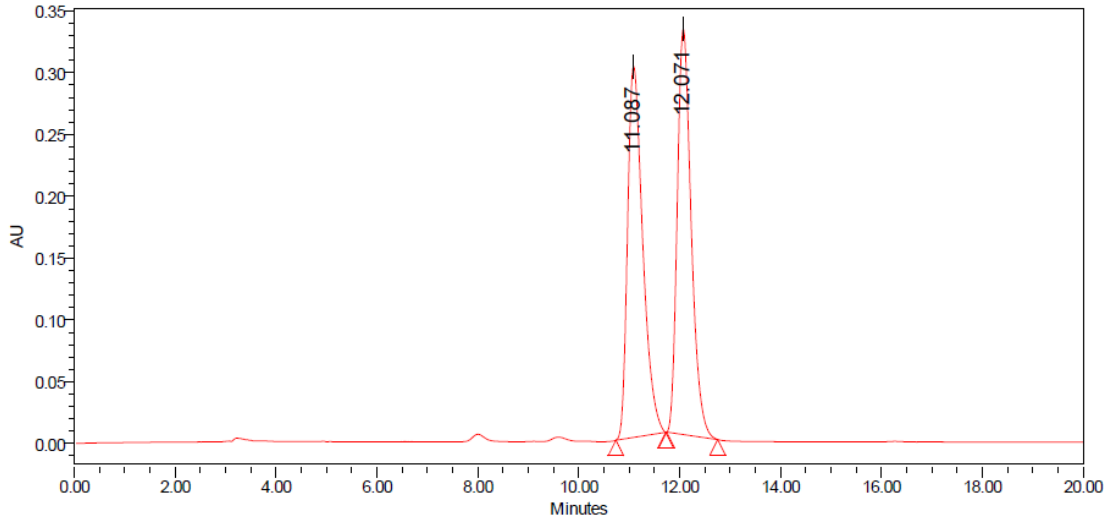

Peak	% Area	Retention Time	Area	Height
1	49.92	11.087	6271700	300296
2	50.08	12.071	6290694	328124
Total	100.00			

Scalemic Chromatogram

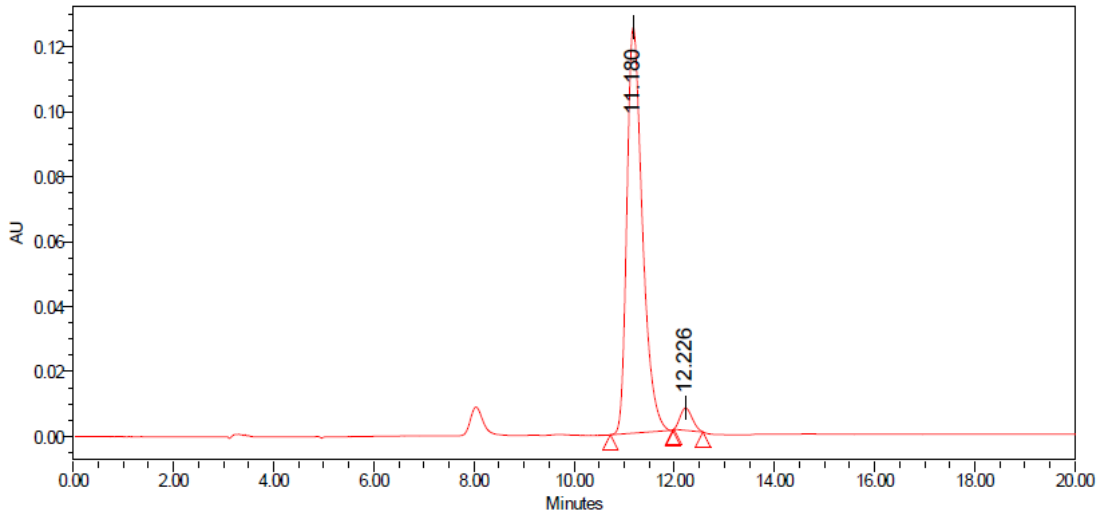

Peak	% Area	Retention Time	Area	Height
1	95.89	11.180	2684924	124948
2	4.11	12.226	115218	6870
Total	100.00			

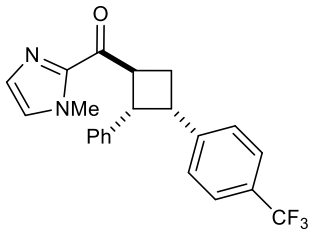

4.22 – Major Diastereomer
Run Details: HPLC, Diacel CHIRALPAK OD-H,
10.00 µL, gradient 5% to 50% iPrOH/hexanes,
13 minutes, 1 mL/min, 280.0 nm.

Racemic Chromatogram

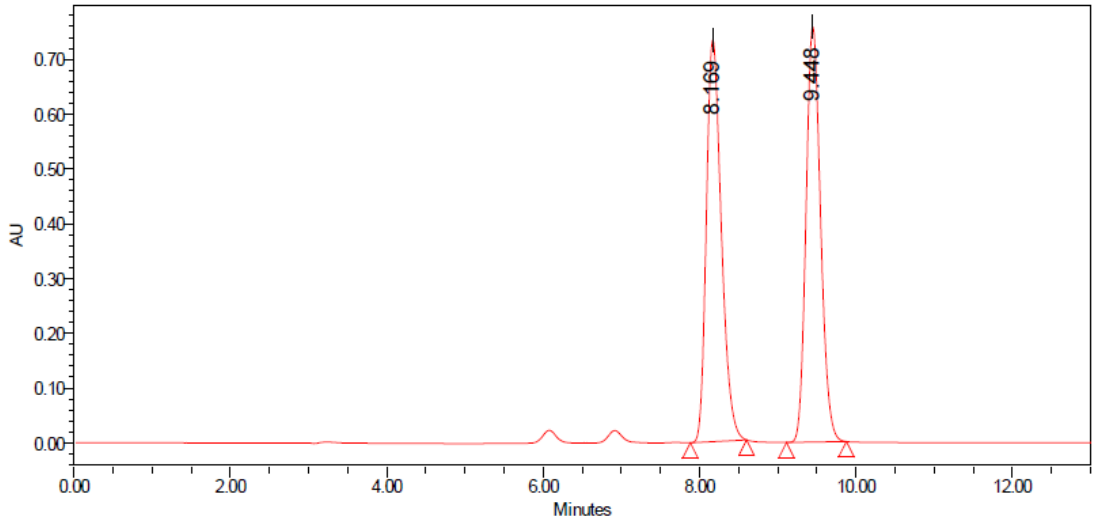

Peak	% Area	Retention Time	Area	Height
1	49.89	8.169	9741011	733077
2	50.11	9.448	9785893	757999
Total	100.00			

Scalemic Chromatogram

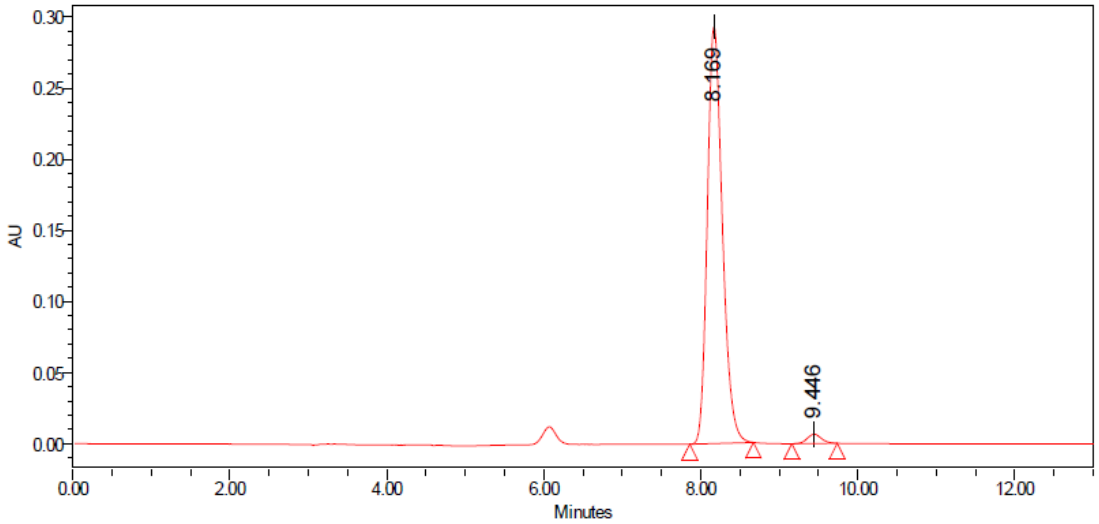

Peak	% Area	Retention Time	Area	Height
1	97.96	8.196	3904779	292916
2	2.04	9.446	81183	6513
Total	100.00			

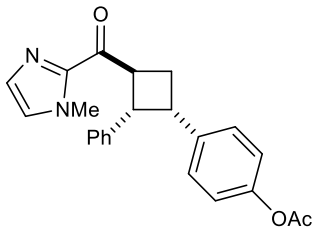

4.23 – Major Diastereomer
Run Details: HPLC, Diacel CHIRALPAK OD-H,
10.00 µL, gradient 5% to 50% iPrOH/hexanes,
18 minutes, 1 mL/min, 285.0 nm.

Racemic Chromatogram

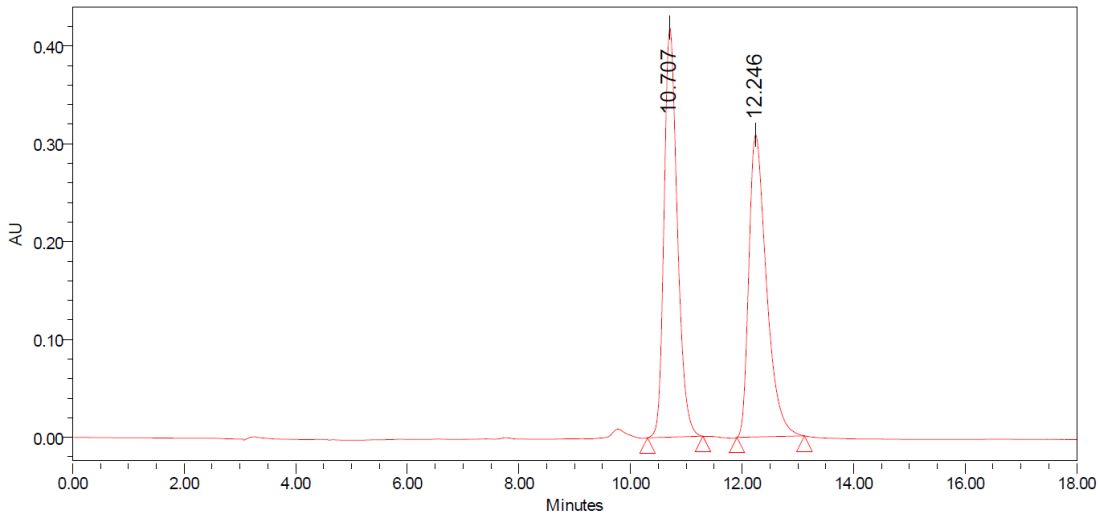

Peak	% Area	Retention Time	Area	Height
1	50.54	10.707	6903222	418287
2	49.46	12.246	6754542	308996
Total	100.00			

Scalemic Chromatogram

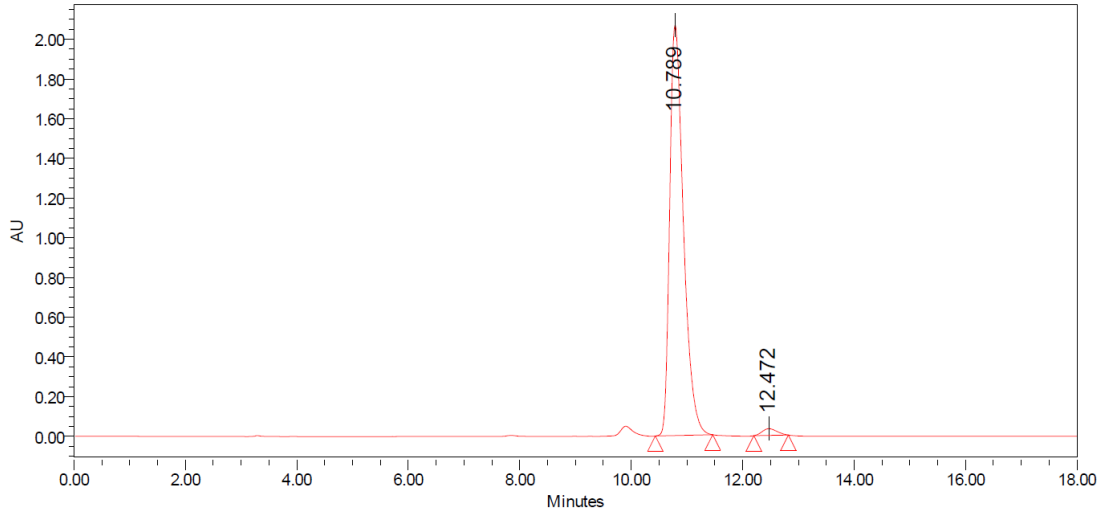

Peak	% Area	Retention Time	Area	Height
1	98.26	10.789	35347991	2066329
2	1.74	12.472	626226	33837
Total	100.00			

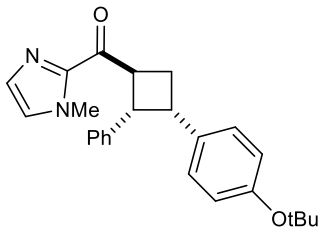

4.24 – Major Diastereomer
Run Details: HPLC, Diacel CHIRALPAK OD-H,
10.00 µL, gradient 5% to 50% iPrOH/hexanes,
18 minutes, 1 mL/min, 285.0 nm.

Racemic Chromatogram

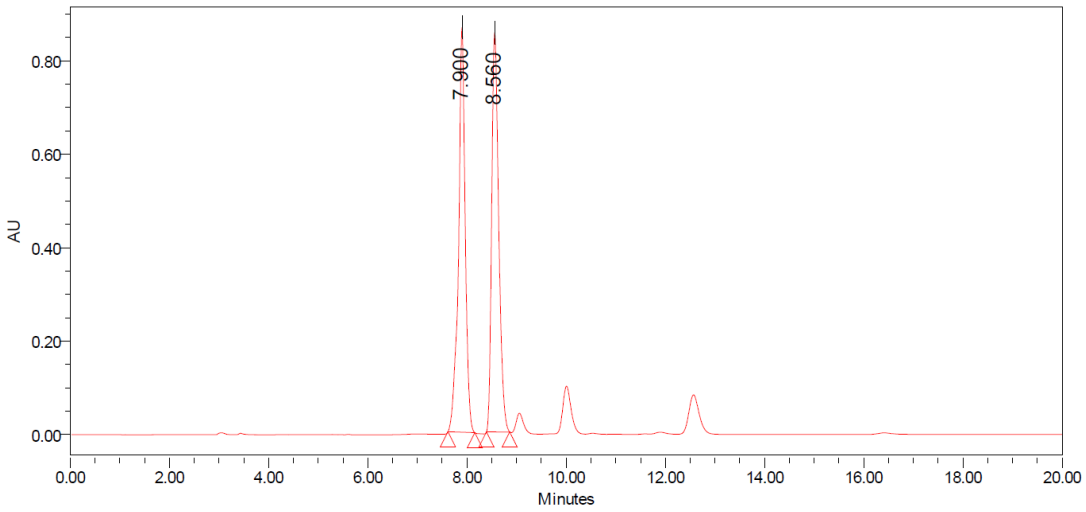

Peak	% Area	Retention Time	Area	Height
1	49.32	7.900	8150154	866166
2	50.68	8.560	8374564	854725
Total	100.00			

Scalemic Chromatogram

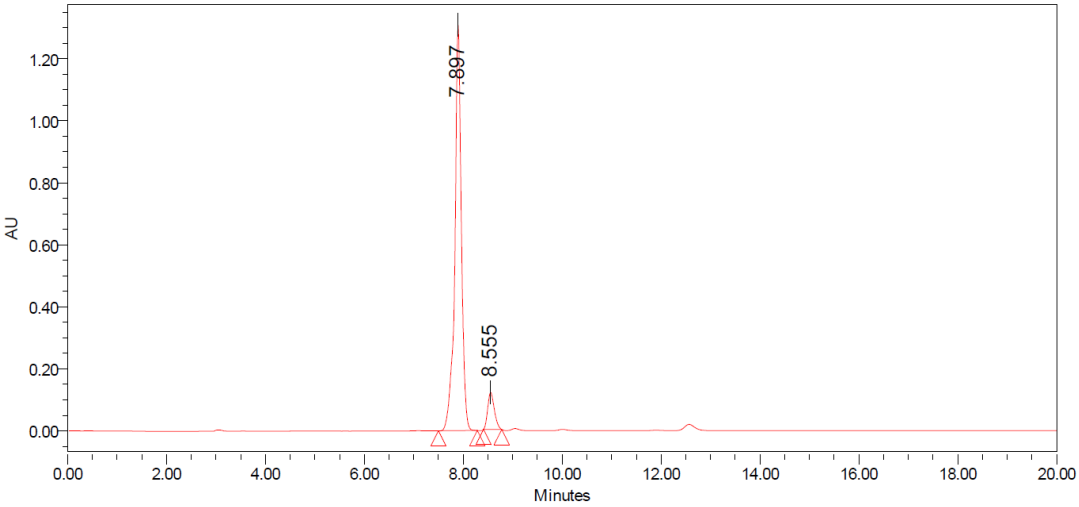

Peak	% Area	Retention Time	Area	Height
1	91.50	7.897	12010713	1308606
2	8.50	8.555	1115558	119100
Total	100.00			

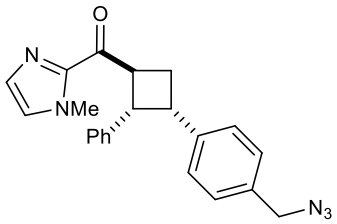

4.25 – Major Diastereomer
Run Details: HPLC, Diacel CHIRALPAK AD,
10.00 µL, gradient 5% to 50% iPrOH/hexanes,
18 minutes, 1 mL/min, 280.0 nm.

Racemic Chromatogram

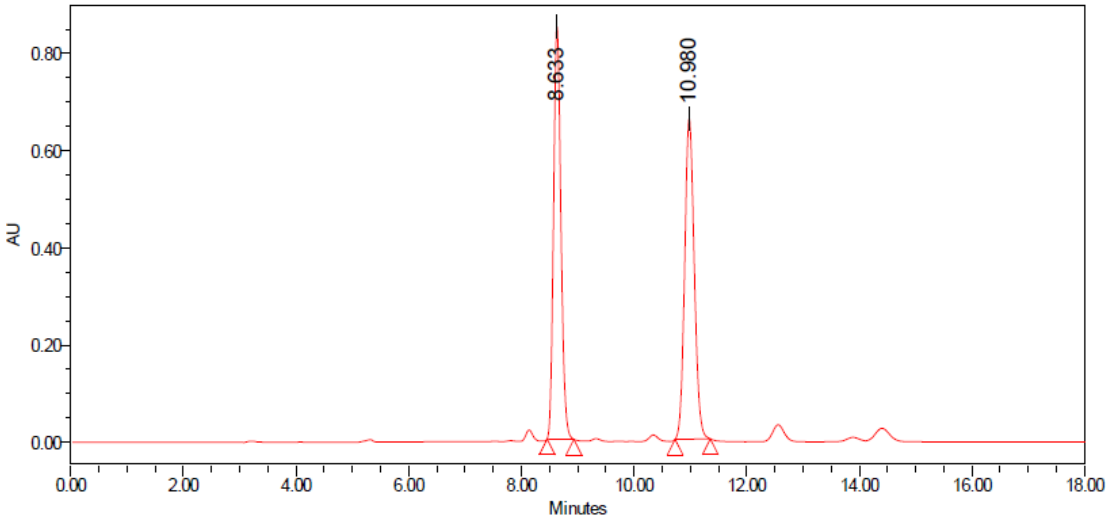

Peak	% Area	Retention Time	Area	Height
1	49.70	8.633	7691352	848642
2	50.30	10.980	7784586	659174
Total	100.00			

Scalemic Chromatogram

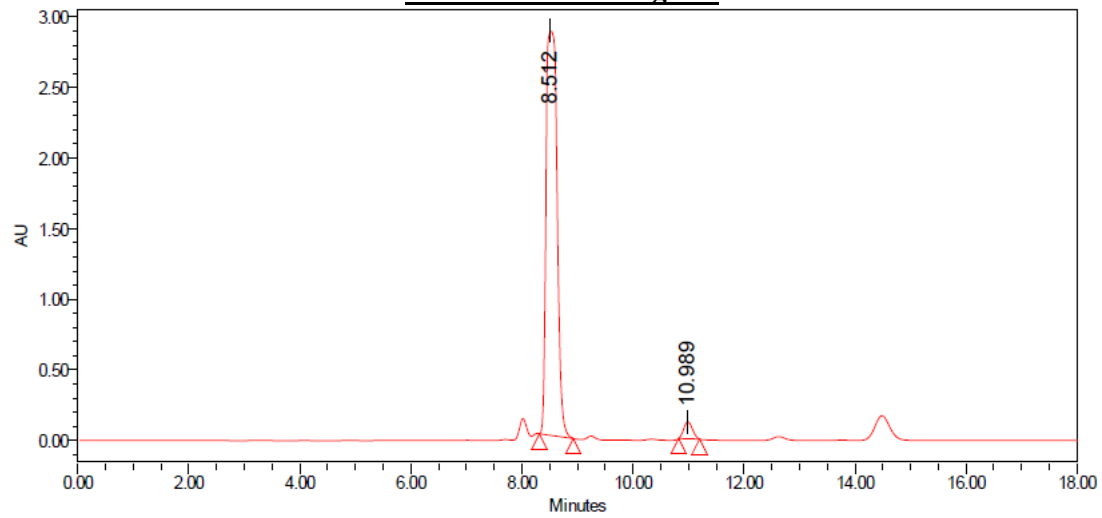

Peak	% Area	Retention Time	Area	Height
1	96.78	8.512	2865539	2865539
2	3.22	10.989	119972	119972
Total	100.00			

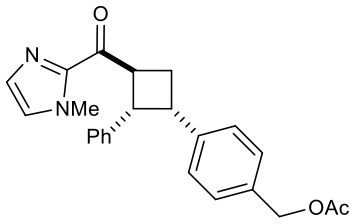

4.26 – Major Diastereomer
Run Details: HPLC, Diacel CHIRALPAK OD-H,
10.00 µL, gradient 5% to 50% iPrOH/hexanes,
28 minutes, 1 mL/min, 280.0 nm.

Racemic Chromatogram

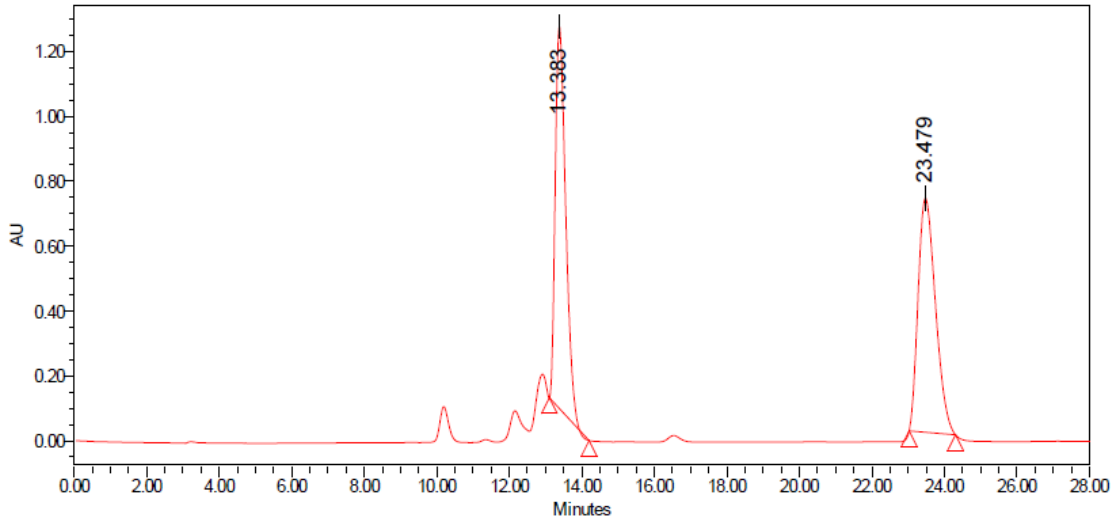

Peak	% Area	Retention Time	Area	Height
1	49.66	13.383	23641117	1176330
2	50.34	23.479	23961968	721251
Total	100.00			

Scalemic Chromatogram

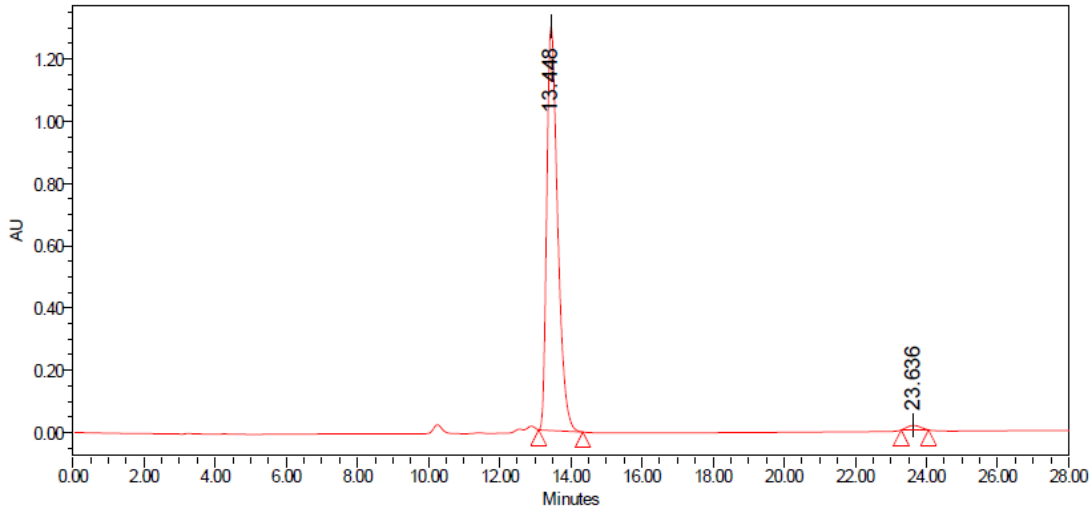

Peak	% Area	Retention Time	Area	Height
1	98.67	13.448	27623051	1298019
2	1.33	23.636	373592	14428
Total	100.00			

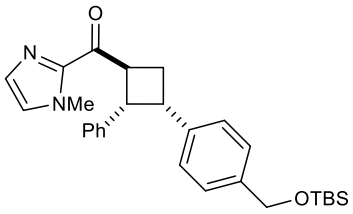

4.27 – Major Diastereomer
Run Details: HPLC, Diacel CHIRALPAK OD-H,
10.00 µL, gradient 5% to 50% iPrOH/hexanes,
18 minutes, 1 mL/min, 285.0 nm.

Racemic Chromatogram

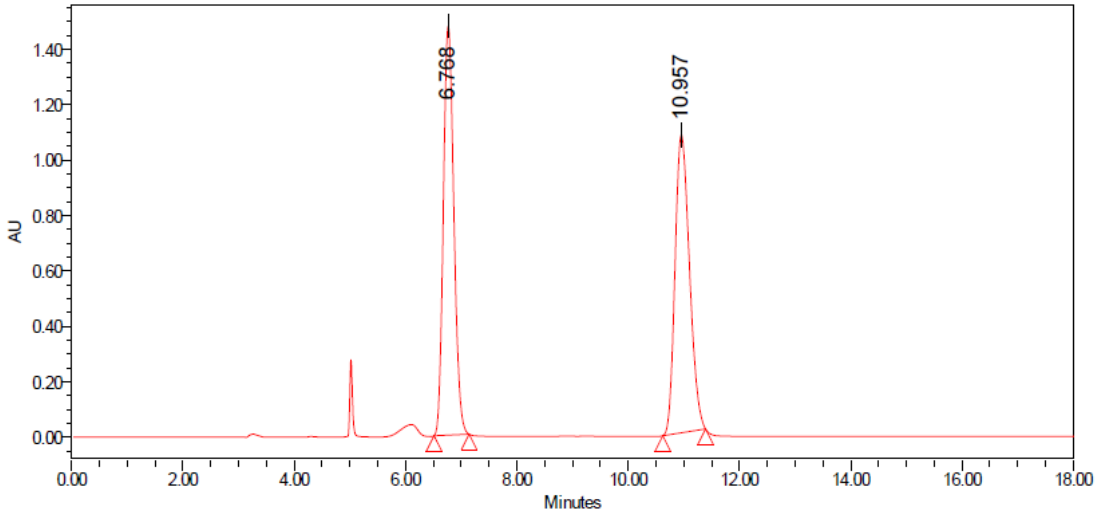

Peak	% Area	Retention Time	Area	Height
1	49.92	6.768	19293809	1476222
2	50.08	10.957	19357563	1074753
Total	100.00			

Scalemic Chromatogram

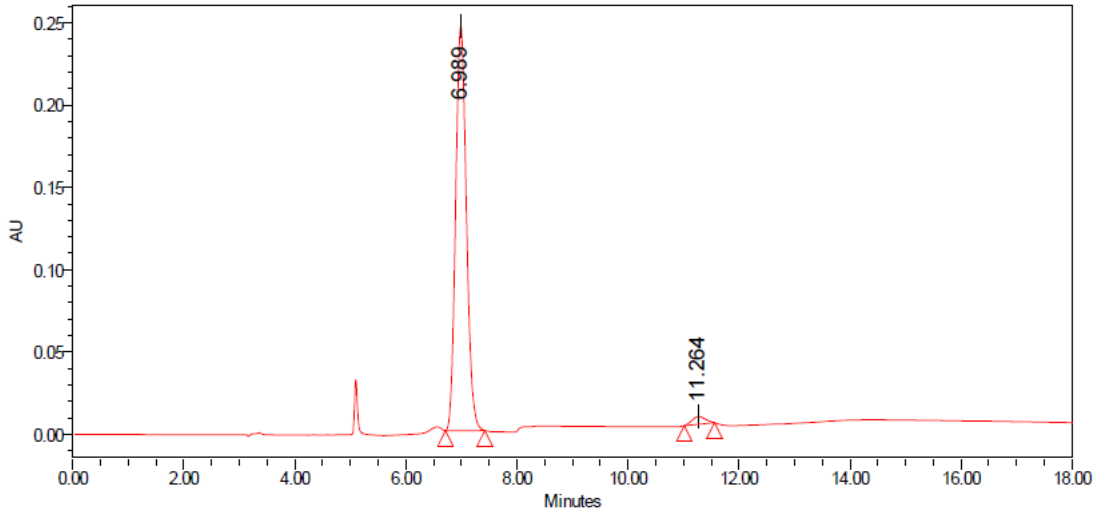

Peak	% Area	Retention Time	Area	Height
1	97.65	6.989	3307673	245547
2	2.35	11.264	79739	4704
Total	100.00			

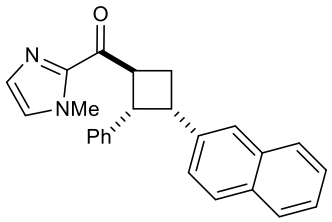

4.28 – Major Diastereomer
Run Details: HPLC, Diacel CHIRALPAK AD-H,
10.00 µL, gradient 5% to 50% iPrOH/hexanes,
13 minutes, 1 mL/min, 280.0 nm.

Racemic Chromatogram

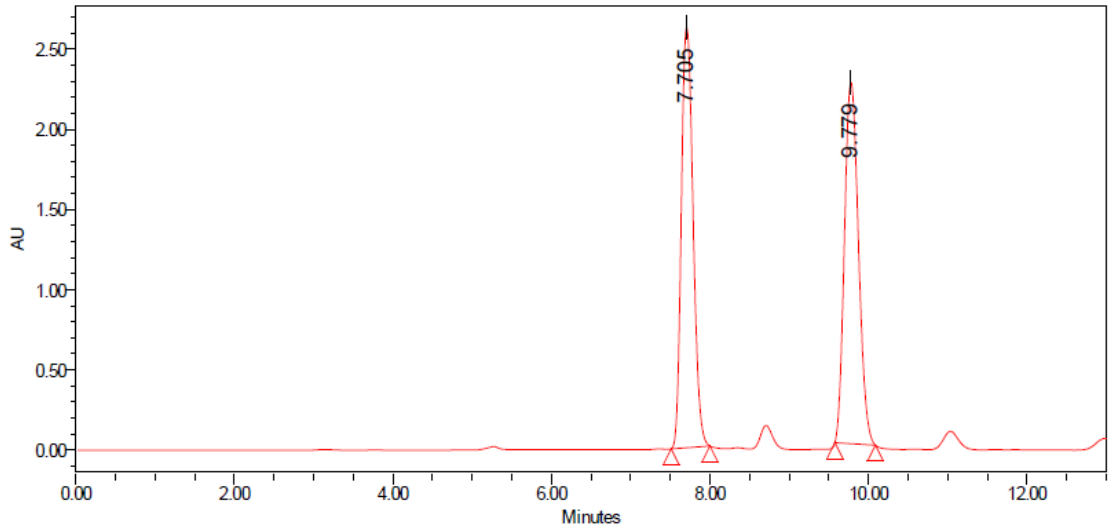

Peak	% Area	Retention Time	Area	Height
1	49.38	7.705	26951400	2618716
2	50.62	9.779	27633264	2251612
Total	100.00			

Scalemic Chromatogram

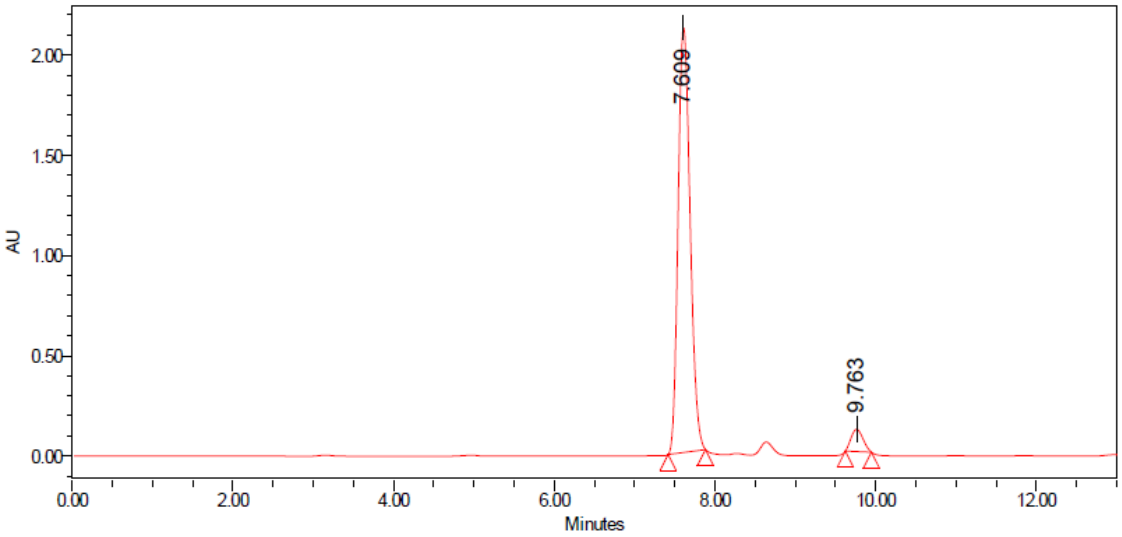

Peak	% Area	Retention Time	Area	Height
1	95.05	7.609	21961022	2117815
2	4.95	9.763	1143222	110920
Total	100.00			

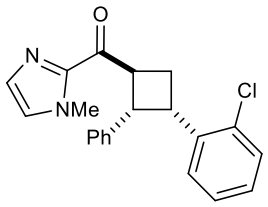

4.29 – Major Diastereomer
Run Details: HPLC, Diacel CHIRALPAK AD,
10.00 µL, gradient 5% to 50% iPrOH/hexanes,
18 minutes, 1 mL/min, 285.0 nm.

Racemic Chromatogram

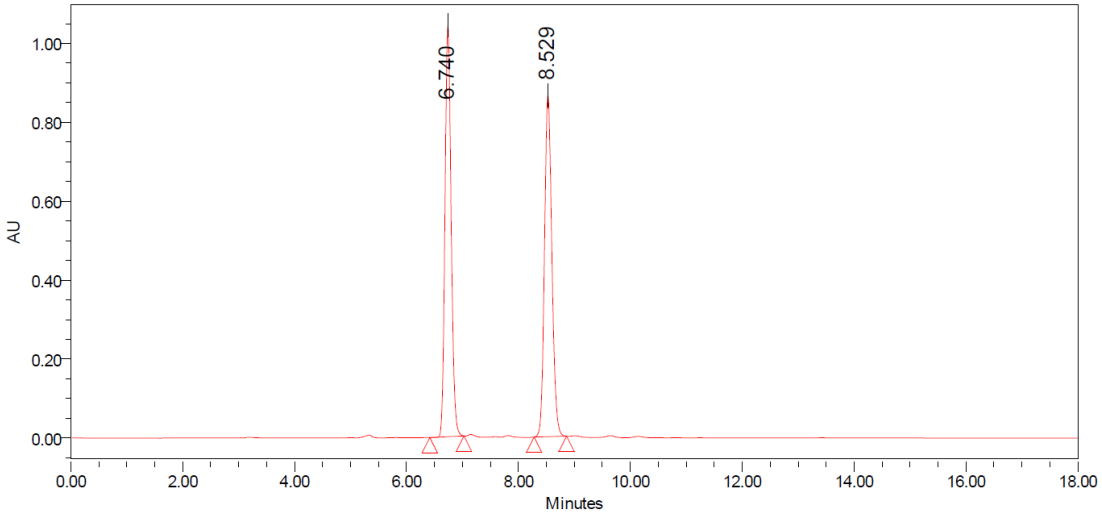

Peak	% Area	Retention Time	Area	Height
1	50.19	6.740	7983942	10419808
2	49.81	8.529	7923782	864460
Total	100.00			

Scalemic Chromatogram

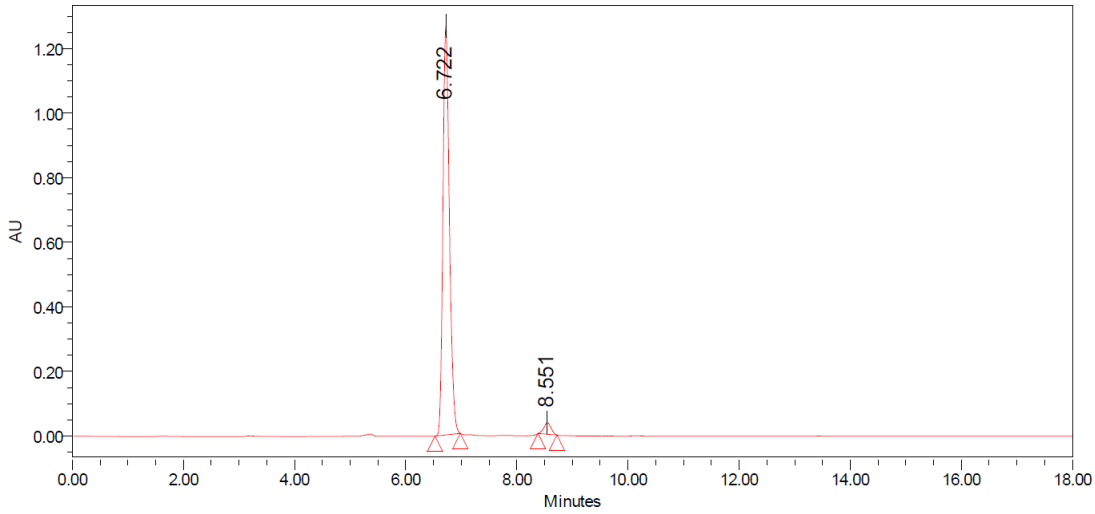

Peak	% Area	Retention Time	Area	Height
1	96.88	6.722	10250099	1265982
2	3.12	8.551	329693	36031
Total	100.00			

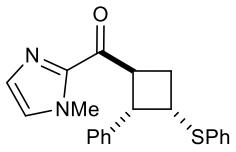

4.31 – Major Diastereomer
Run Details: HPLC, Diacel CHIRALPAK AD,
10.00 µL, gradient 5% to 50% iPrOH/hexanes,
18 minutes, 1 mL/min, 285.0 nm.

Racemic Chromatogram

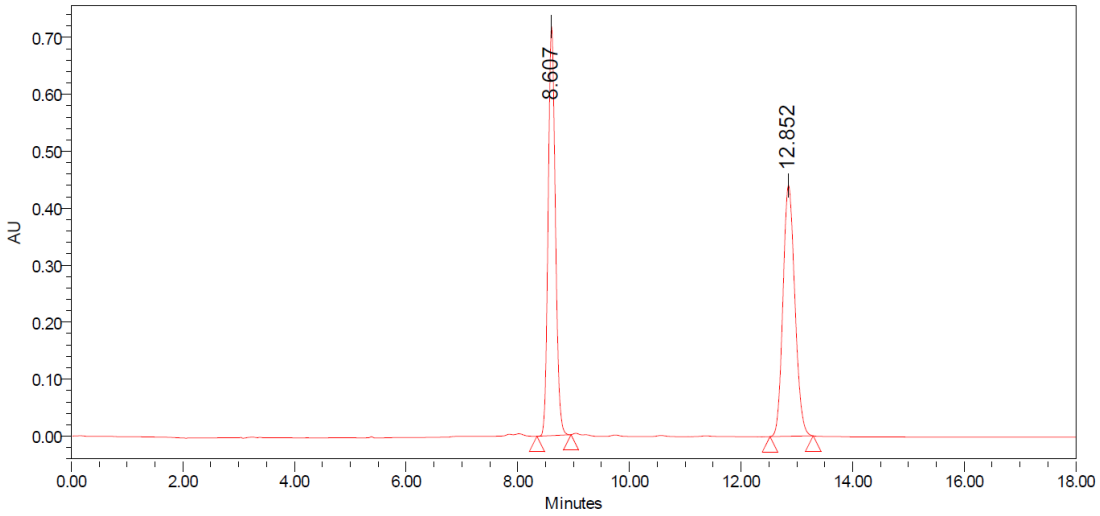

Peak	% Area	Retention Time	Area	Height
1	49.62	8.607	6435841	718229
2	50.38	12.852	6534797	440270
Total	100.00			

Scalemic Chromatogram

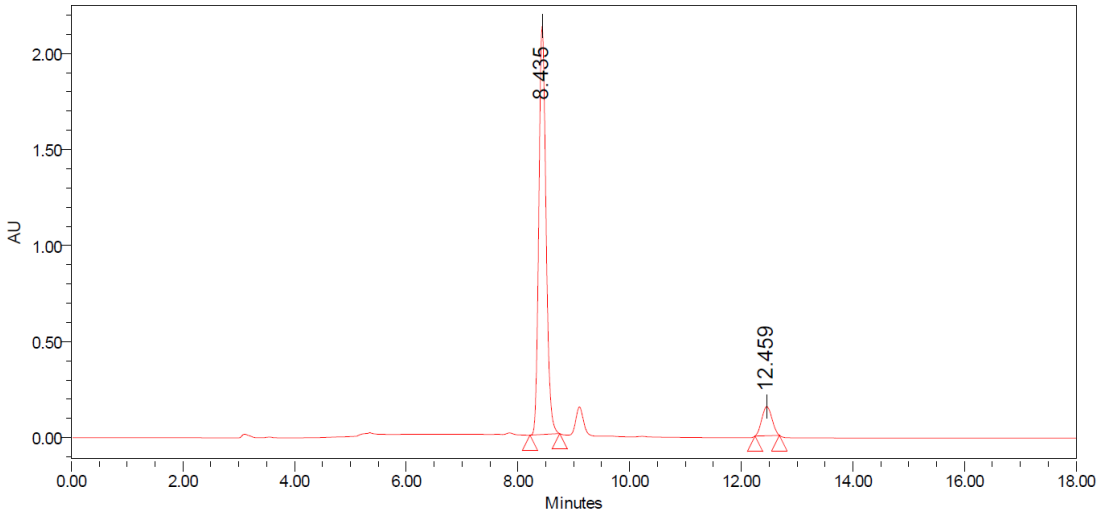

Peak	% Area	Retention Time	Area	Height
1	90.84	8.435	19057924	2126287
2	9.16	12.459	1921213	151508
Total	100.00			

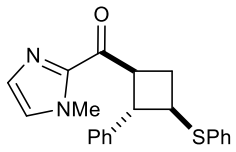

4.31 – Minor Diastereomer
Run Details: HPLC, Diacel CHIRALPAK OD-H,
10.00 µL, gradient 5% to 50% iPrOH/hexanes,
18 minutes, 1 mL/min, 285.0 nm.

Racemic Chromatogram

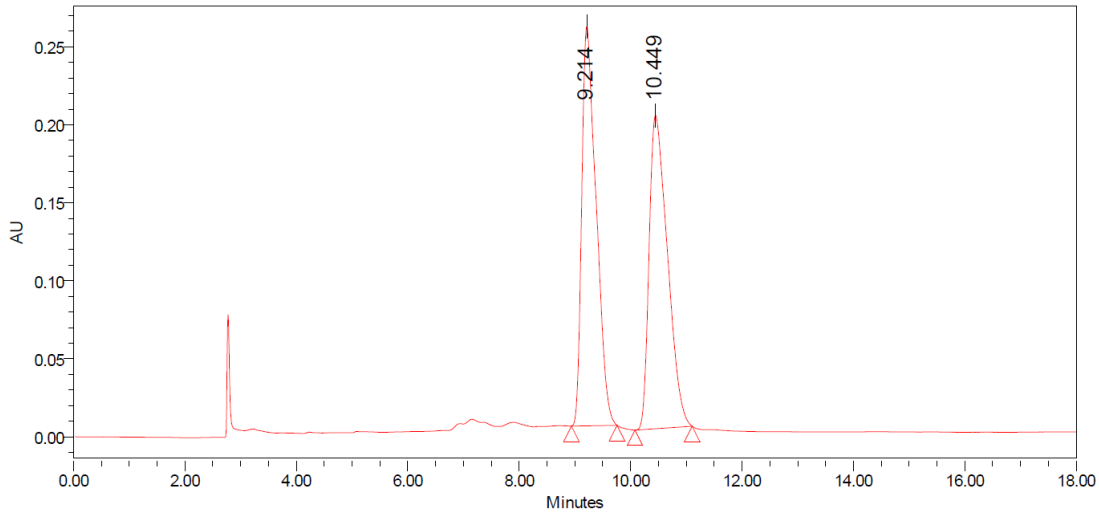

Peak	% Area	Retention Time	Area	Height
1	50.02	9.214	4597067	255909
2	49.98	10.449	4593163	200910
Total	100.00			

Scalemic Chromatogram

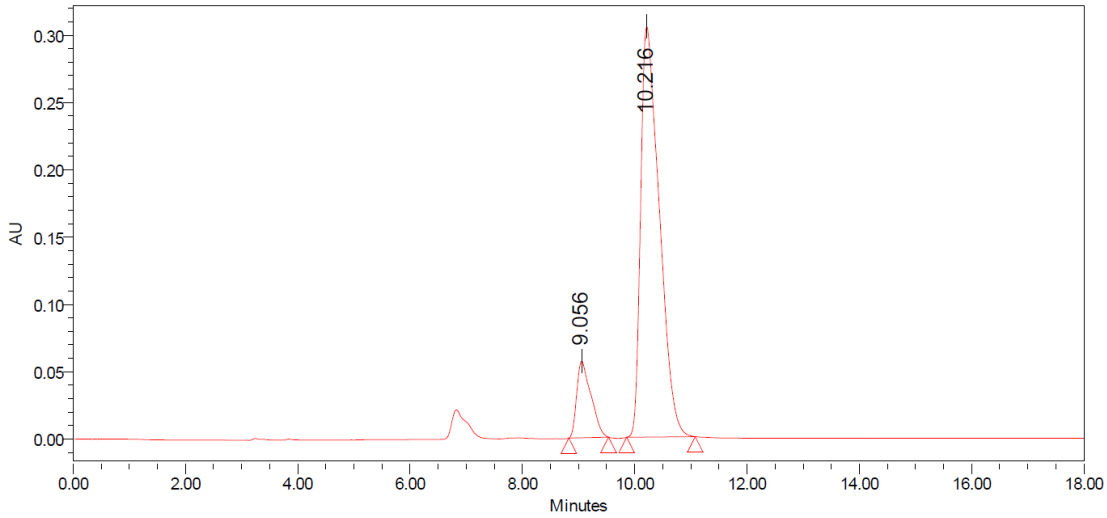

Peak	% Area	Retention Time	Area	Height
1	12.45	9.056	999244	56884
2	87.55	10.216	7025160	305015
Total	100.00			

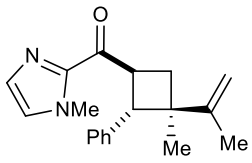

4.32 – Major Diastereomer
Run Details: HPLC, Diacel CHIRALPAK AD,
10.00 µL, gradient 5% to 50% iPrOH/hexanes,
18 minutes, 1 mL/min, 295.0 nm.

Racemic Chromatogram

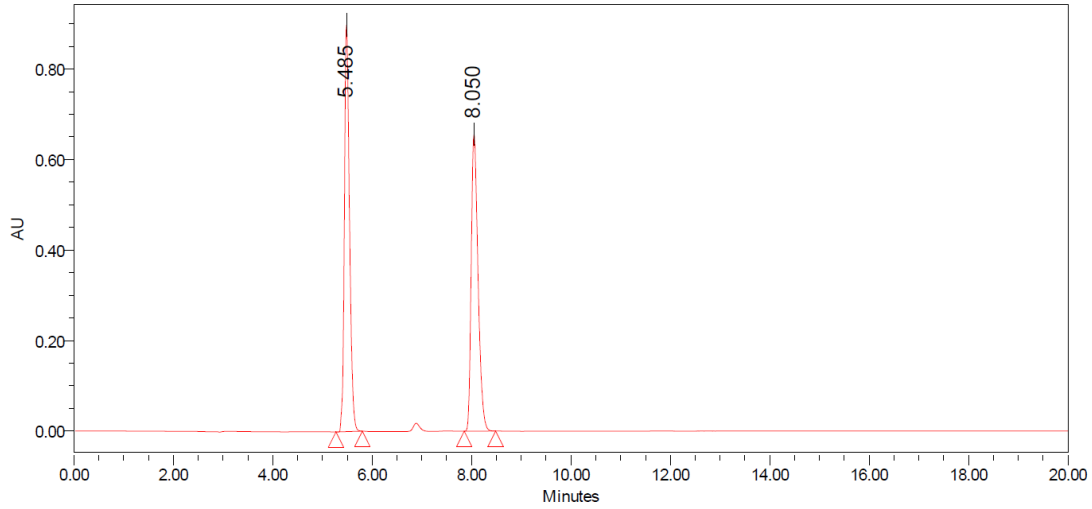

Peak	% Area	Retention Time	Area	Height
1	50.53	5.485	6398300	898523
2	49.47	8.050	6264920	656586
Total	100.00			

Scalemic Chromatogram

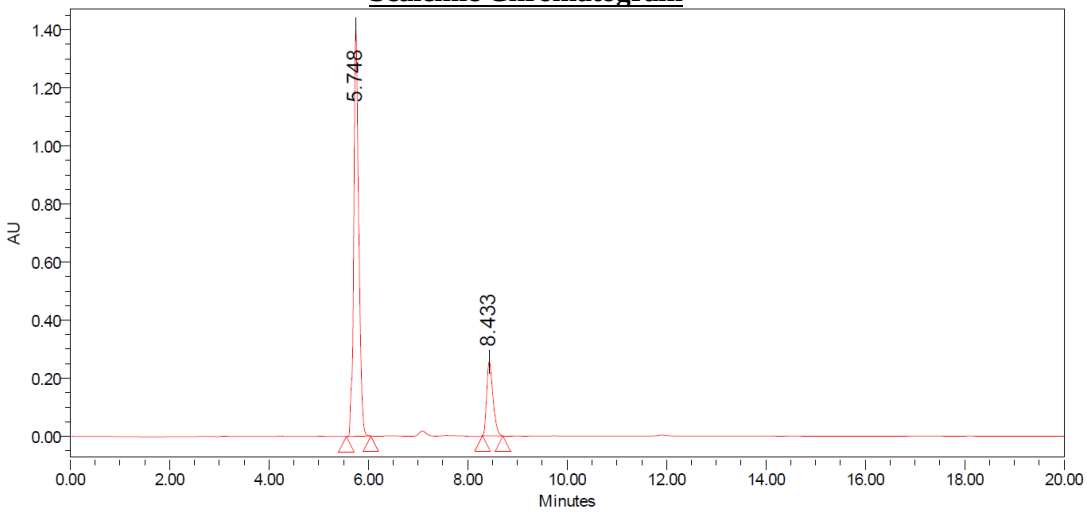

Peak	% Area	Retention Time	Area	Height
1	81.38	5.748	9802518	1401129
2	18.62	8.433	2243334	255768
Total	100.00			

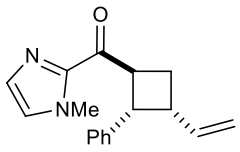

4.33 – Major Diastereomer
Run Details: HPLC, Diacel CHIRALPAK AD,
10.00 µL, gradient 5% to 50% iPrOH/hexanes,
18 minutes, 1 mL/min, 295.0 nm.

Racemic Chromatogram

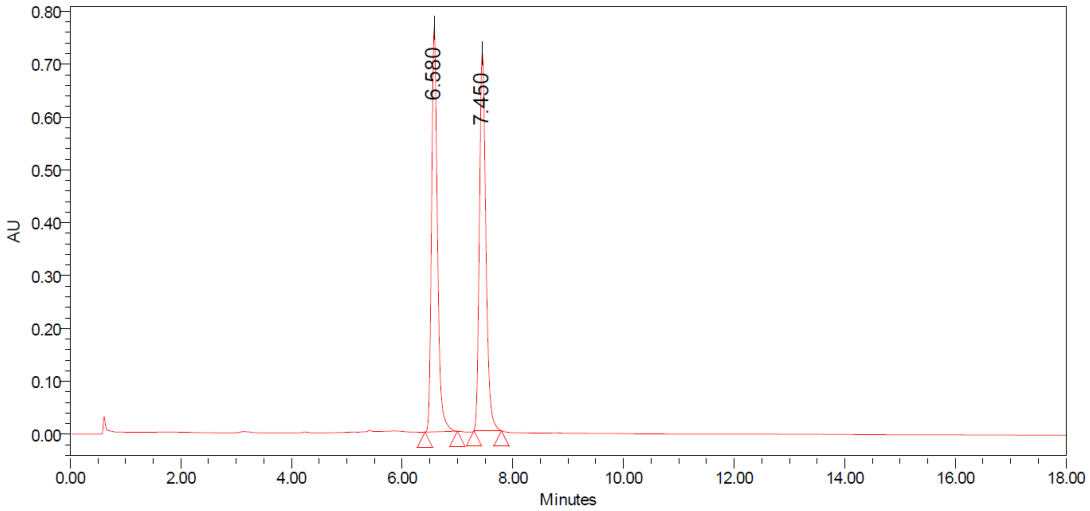

Peak	% Area	Retention Time	Area	Height
1	49.18	6.580	5619294	767670
2	50.82	7.450	5806639	714161
Total	100.00			

Scalemic Chromatogram

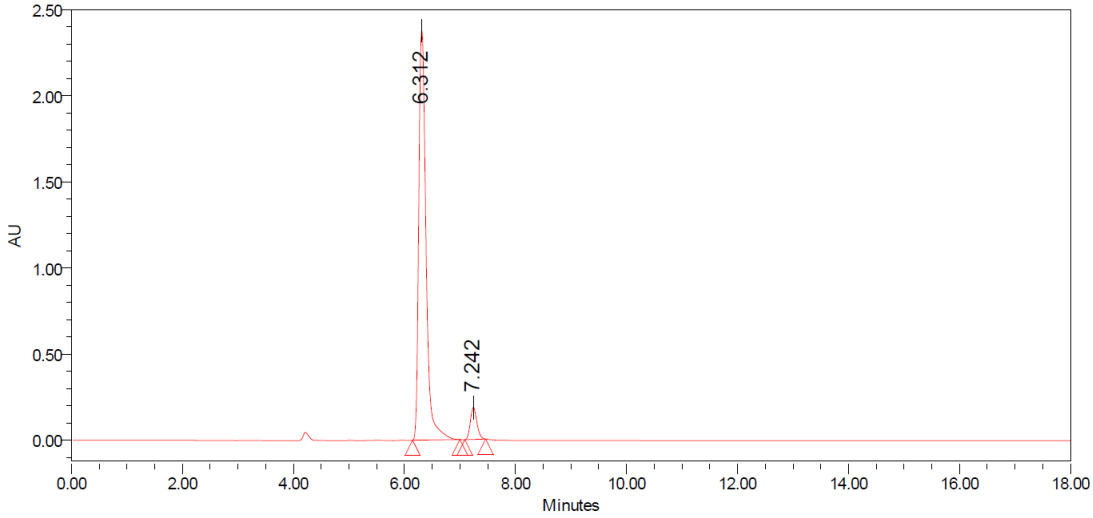

Peak	% Area	Retention Time	Area	Height
1	93.48	6.312	21698128	2379222
2	6.52	7.242	1513611	185695
Total	100.00			

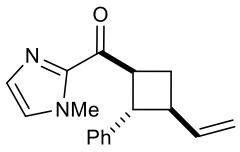

4.33 – Minor Diastereomer
Run Details: HPLC, Diacel CHIRALPAK AD,
10.00 µL, gradient 5% to 50% iPrOH/hexanes,
18 minutes, 1 mL/min, 295.0 nm.

Racemic Chromatogram

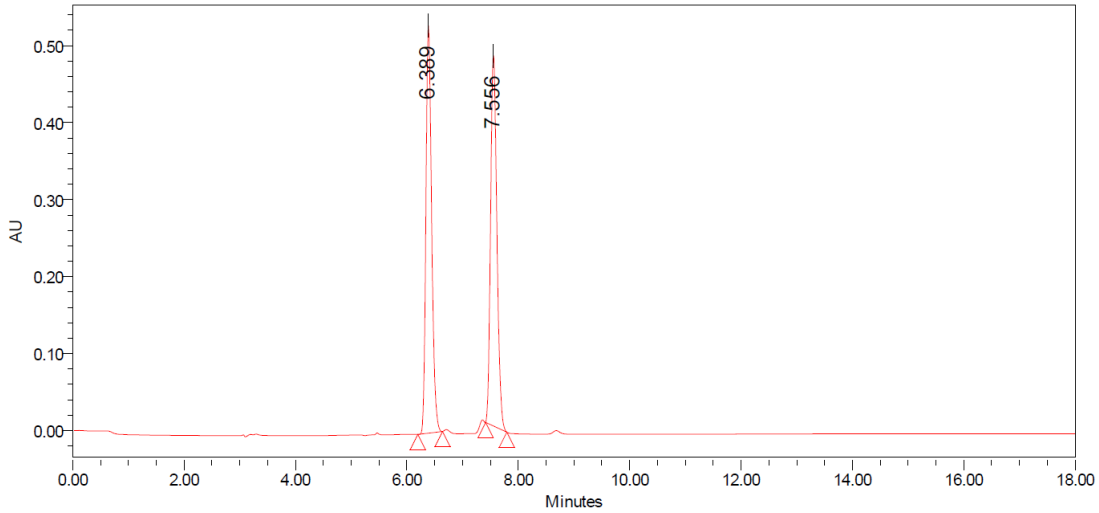

Peak	% Area	Retention Time	Area	Height
1	49.99	6.389	3780701	529097
2	50.01	7.556	3782575	481054
Total	100.00			

Scalemic Chromatogram

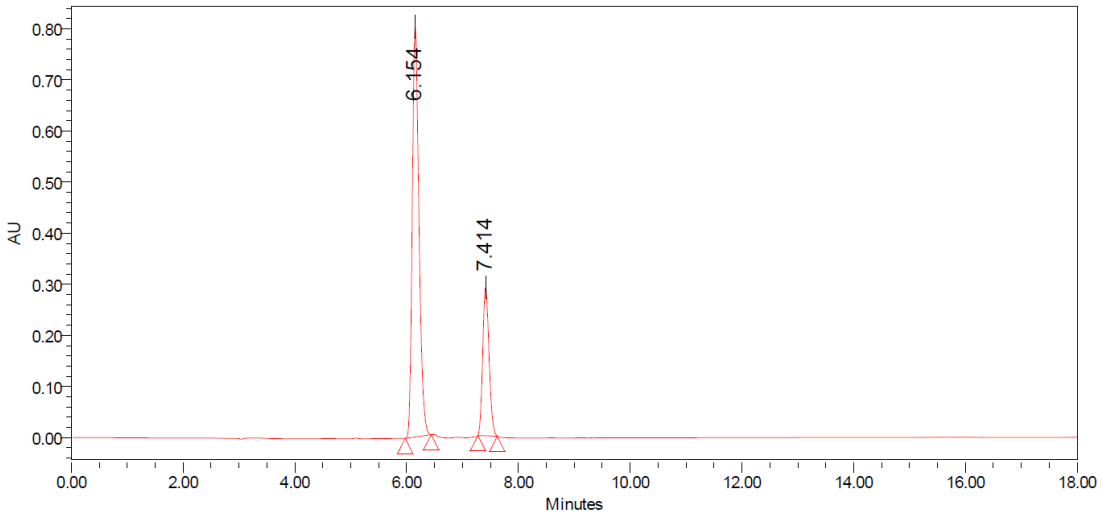

Peak	% Area	Retention Time	Area	Height
1	74.35	6.154	6640710	802202
2	26.65	7.414	2290774	290511
Total	100.00			

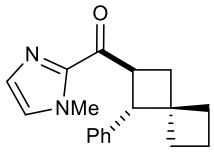

4.34

Run Details: HPLC, Diacel CHIRALPAK AD, 10.00 µL, gradient 5% to 50% iPrOH/hexanes, 18 minutes, 1 mL/min, 285.0 nm.

Racemic Chromatogram

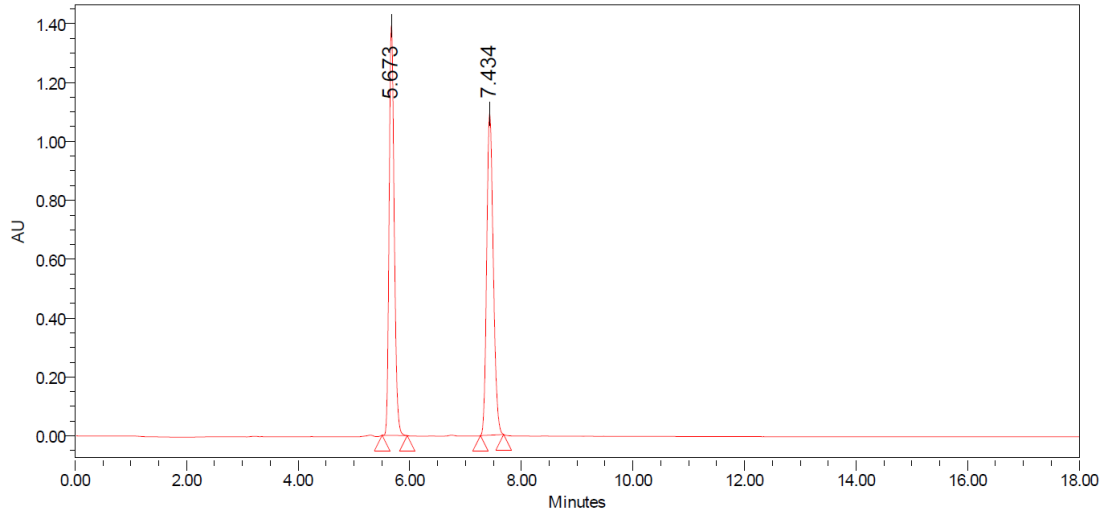

Peak	% Area	Retention Time	Area	Height
1	49.53	5.673	8797392	1391958
2	50.47	7.434	8962578	1091598
Total	100.00			

Scalemic Chromatogram

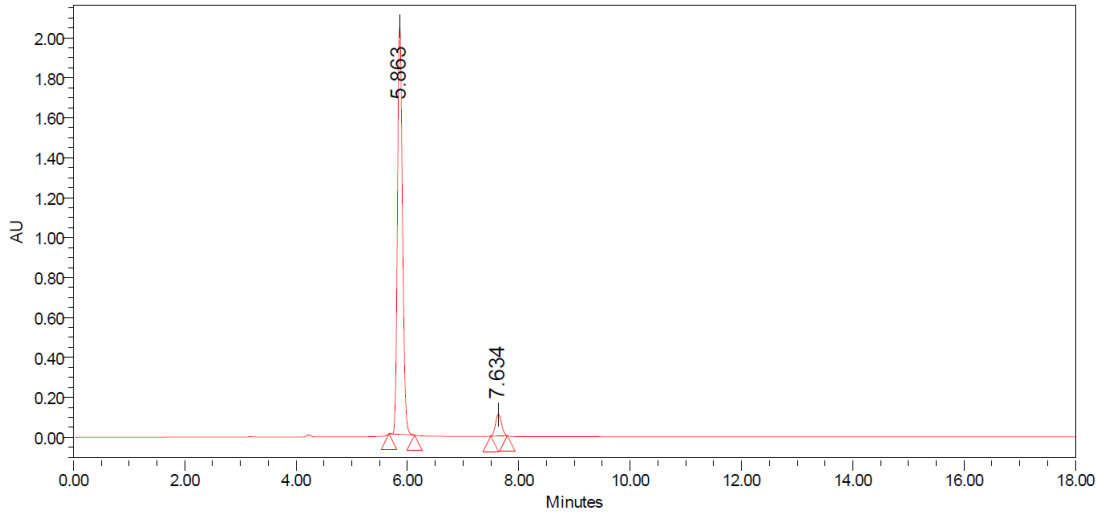

Peak	% Area	Retention Time	Area	Height
1	93.99	5.863	12847379	2044953
2	6.01	7.634	820925	108421
Total	100.00			

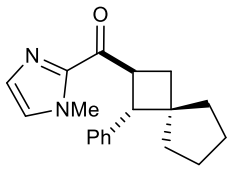

4.35 – Major Diastereomer
Run Details: HPLC, Diacel CHIRALPAK OD-H,
10.00 µL, gradient 5% to 50% iPrOH/hexanes,
18 minutes, 1 mL/min, 295.0 nm.

Racemic Chromatogram

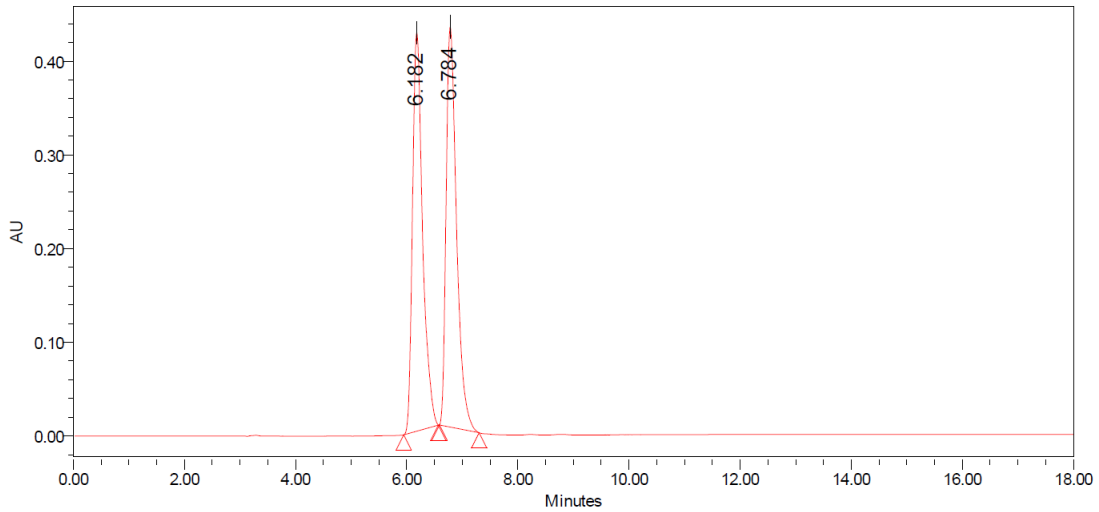

Peak	% Area	Retention Time	Area	Height
1	49.10	6.182	5361808	425302
2	50.90	6.784	5559201	427104
Total	100.00			

Scalemic Chromatogram

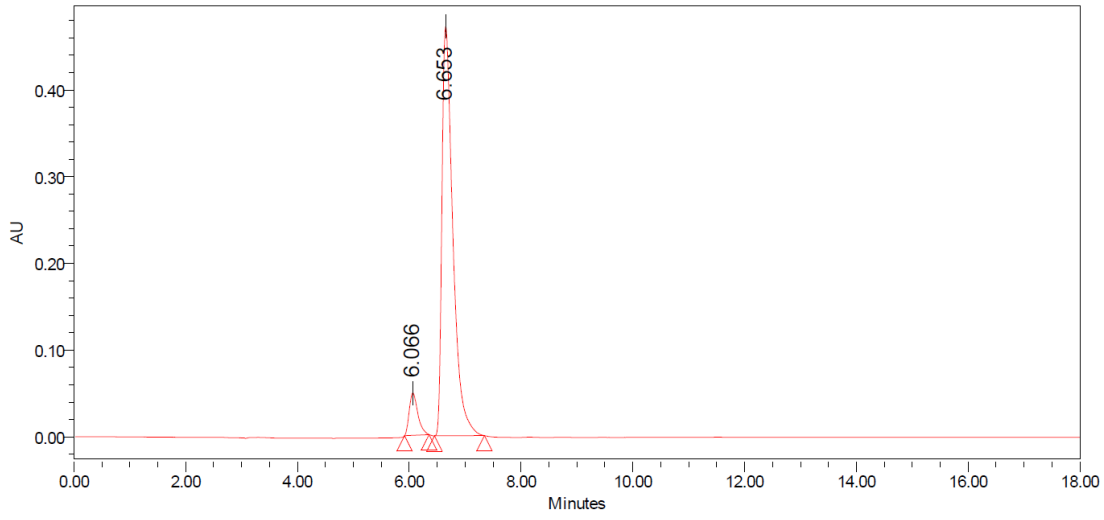

Peak	% Area	Retention Time	Area	Height
1	7.52	6.066	519995	48805
2	92.48	6.653	6395904	471931
Total	100.00			

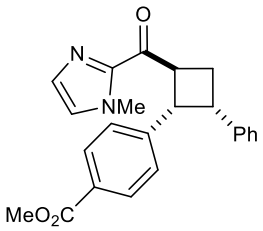

4.36 – Major Diastereomer
Run Details: HPLC, Diacel CHIRALPAK IC,
10.00 µL, gradient 5% to 50% iPrOH/hexanes,
18 minutes, 1 mL/min, 285.0 nm.

Racemic Chromatogram

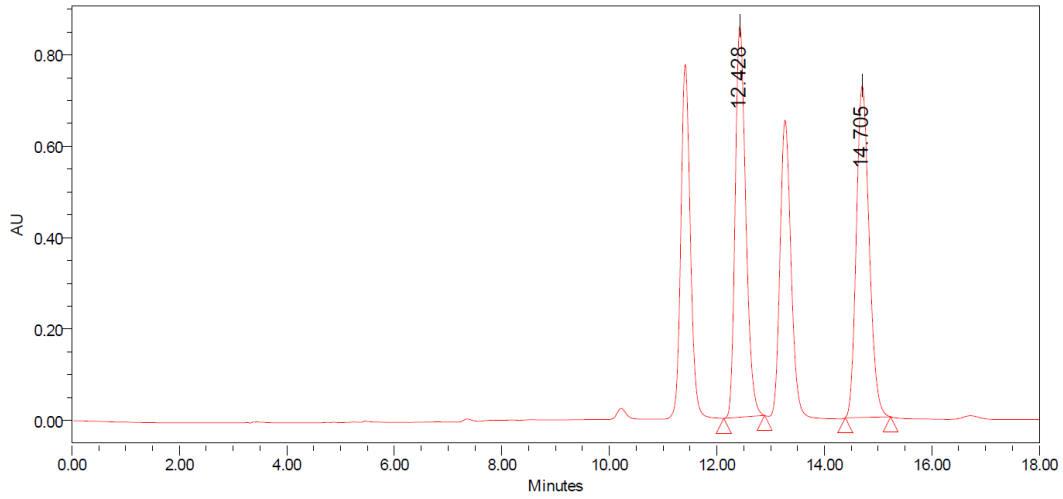

Peak	% Area	Retention Time	Area	Height
1	49.30	12.428	11713056	856183
2	50.70	14.705	12046092	726276
Total	100.00			

Scalemic Chromatogram

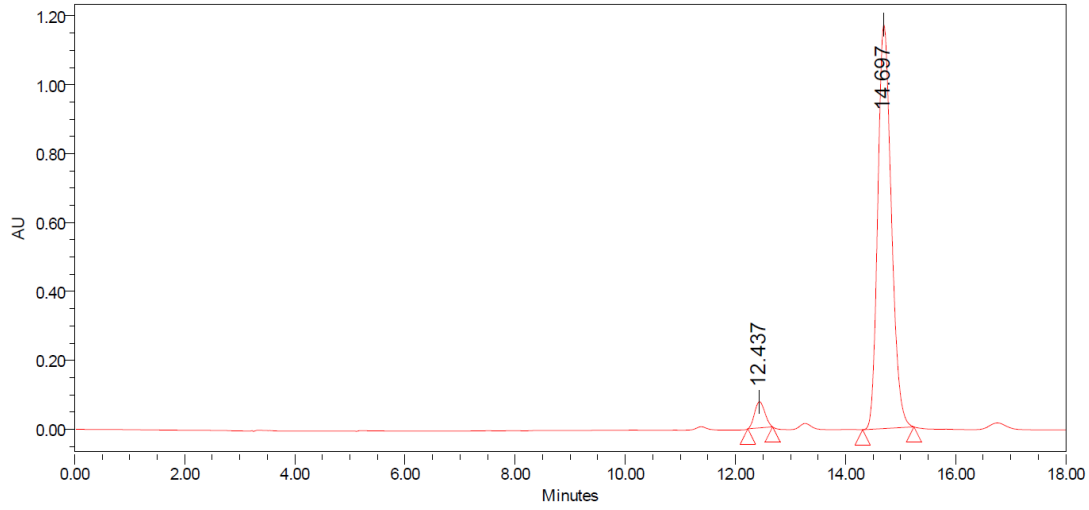

Peak	% Area	Retention Time	Area	Height
1	4.69	12.437	984839	76126
2	95.31	14.697	20027600	1171914
Total	100.00			

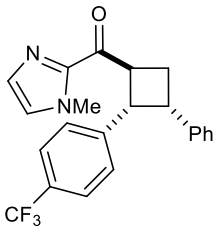

4.37 – Major Diastereomer
Run Details: HPLC, Diacel CHIRALPAK OD-H,
10.00 µL, gradient 5% to 50% iPrOH/hexanes,
18 minutes, 1 mL/min, 285.0 nm.

Racemic Chromatogram

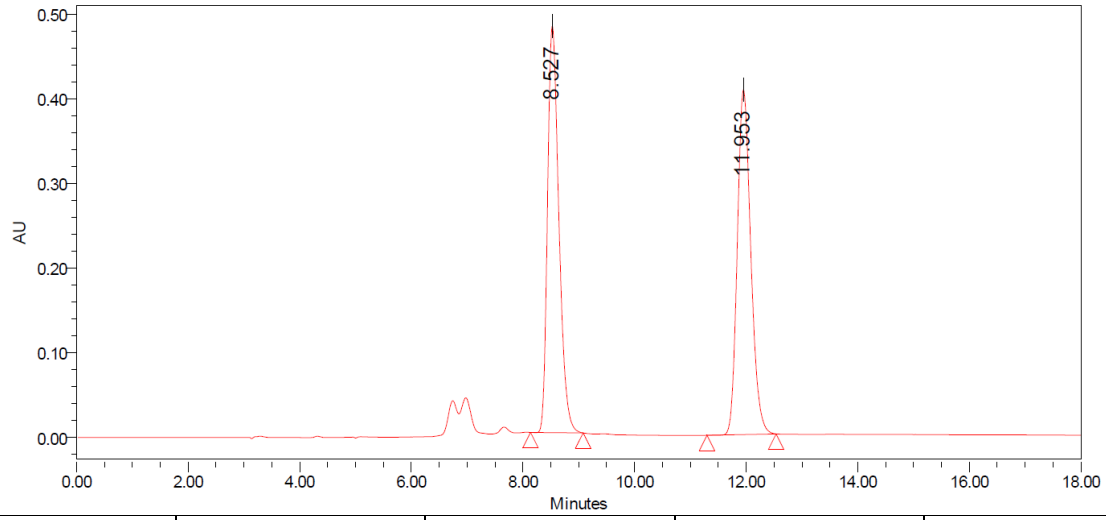

Peak	% Area	Retention Time	Area	Height
1	49.80	8.527	6786719	480179
2	50.20	11.953	6842091	407223
Total	100.00			

Scalemic Chromatogram

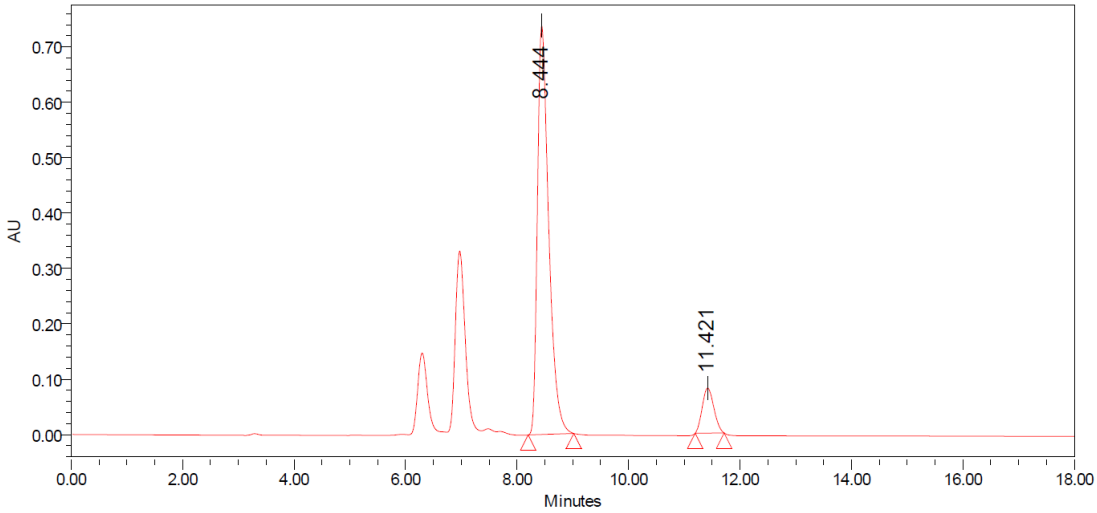

Peak	% Area	Retention Time	Area	Height
1	89.84	8.444	103377818	738048
2	10.16	11.421	1173611	81243
Total	100.00			

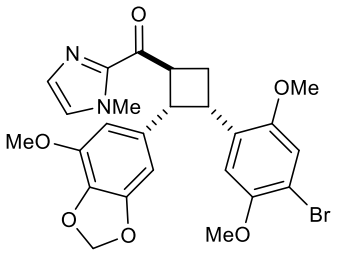

4.39 – Major Diastereomer
Run Details: HPLC, Diacel CHIRALPAK AD, 10.00 µL, gradient 5% to 50% iPrOH/hexanes, 20 minutes, 1 mL/min, 285.0 nm.

Racemic Chromatogram

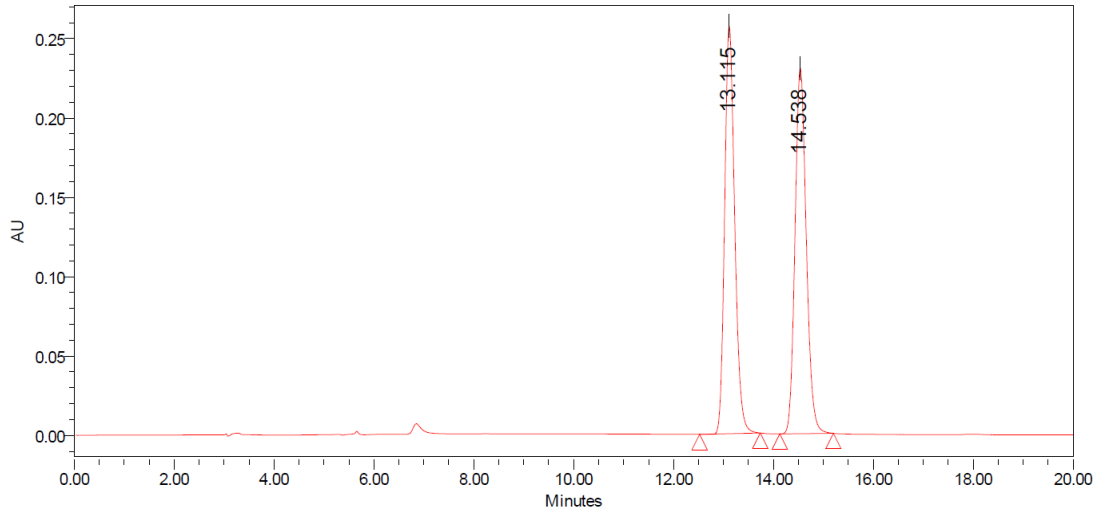

Peak	% Area	Retention Time	Area	Height
1	49.98	13.115	3596281	256807
2	50.02	14.538	3599837	230267
Total	100.00			

Scalemic Chromatogram

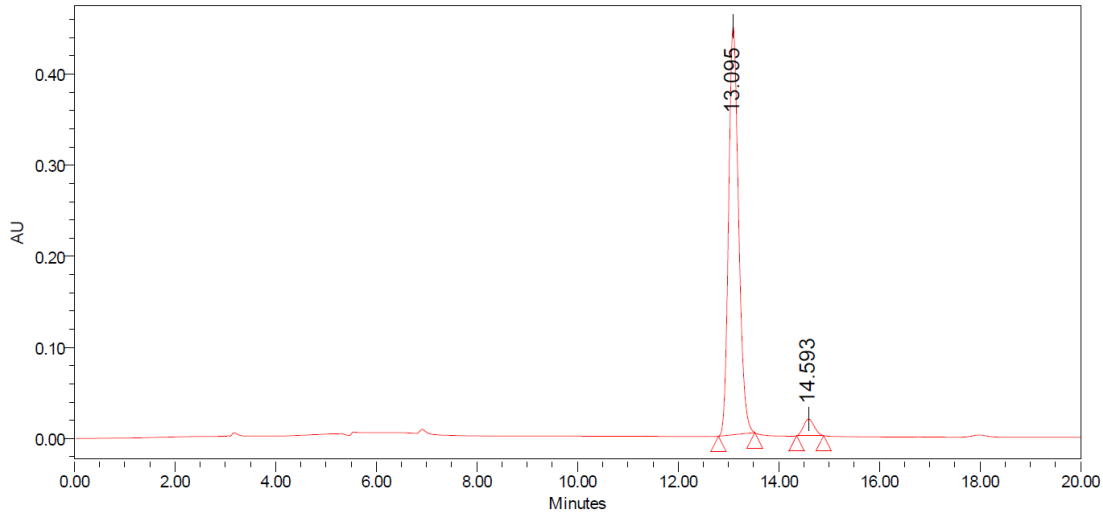

Peak	% Area	Retention Time	Area	Height
1	95.88	13.095	6183232	448302
2	4.12	14.593	265927	18169
Total	100.00			

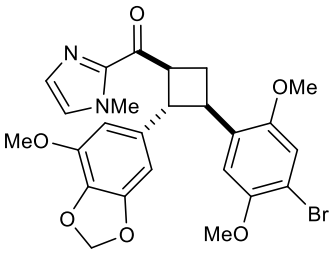

4.39 – Minor Diastereomer
Run Details: HPLC, Diacel CHIRALPAK AS-H,
10.00 µL, gradient 5% to 30% EtOH/hexanes,
35 minutes, 1 mL/min, 285.0 nm.

Racemic Chromatogram

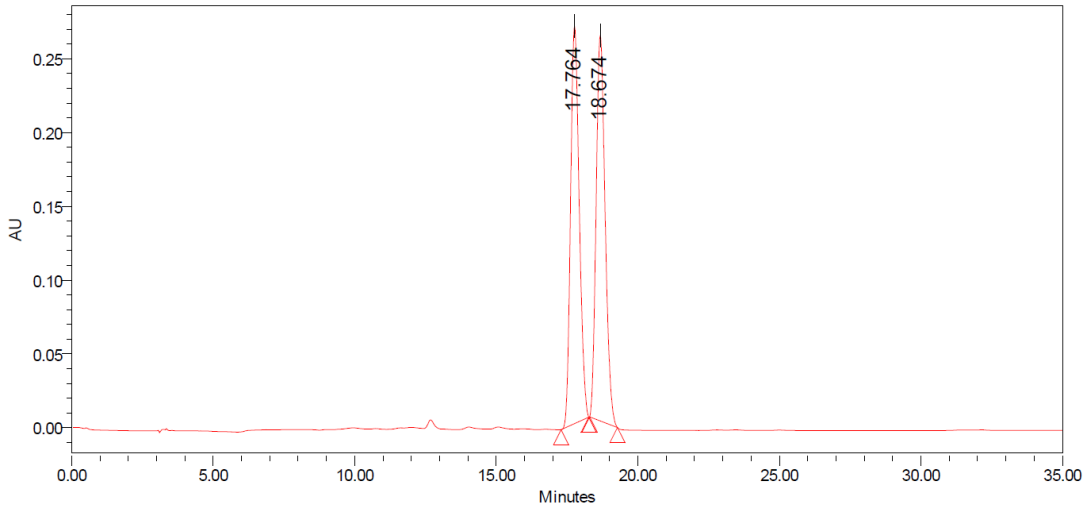

Peak	% Area	Retention Time	Area	Height
1	49.86	17.764	5725848	269376
2	50.14	18.674	5758071	261335
Total	100.00			

Scalemic Chromatogram

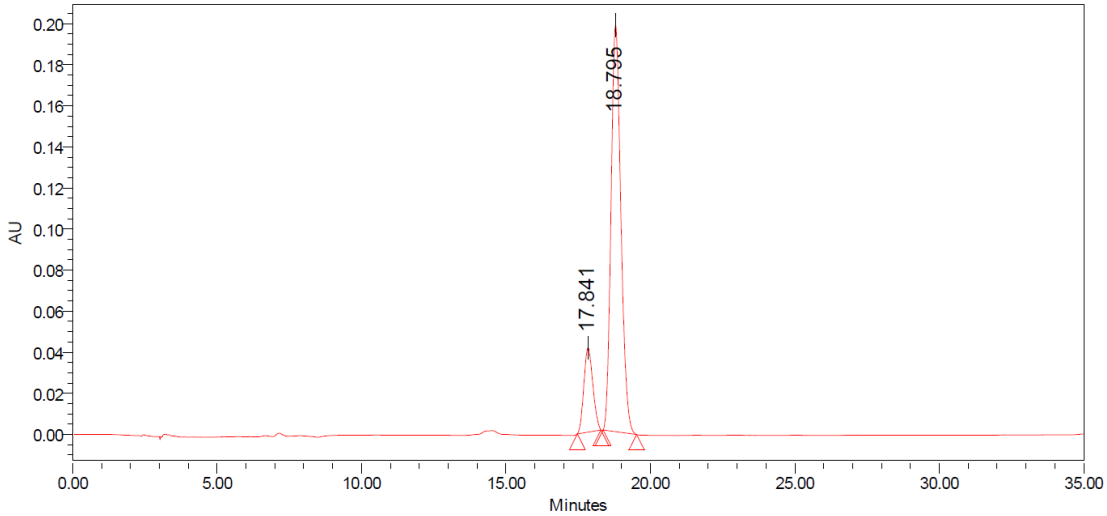

Peak	% Area	Retention Time	Area	Height
1	15.92	17.841	885618	41061
2	84.08	18.795	4678118	197836
Total	100.00			

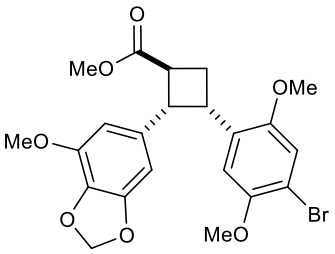

4.40

Run Details: HPLC, Diacel CHIRALPAK AD, 10.00 µL, gradient 5% to 50% iPrOH/hexanes, 20 minutes, 1 mL/min, 285.0 nm.

Racemic Chromatogram

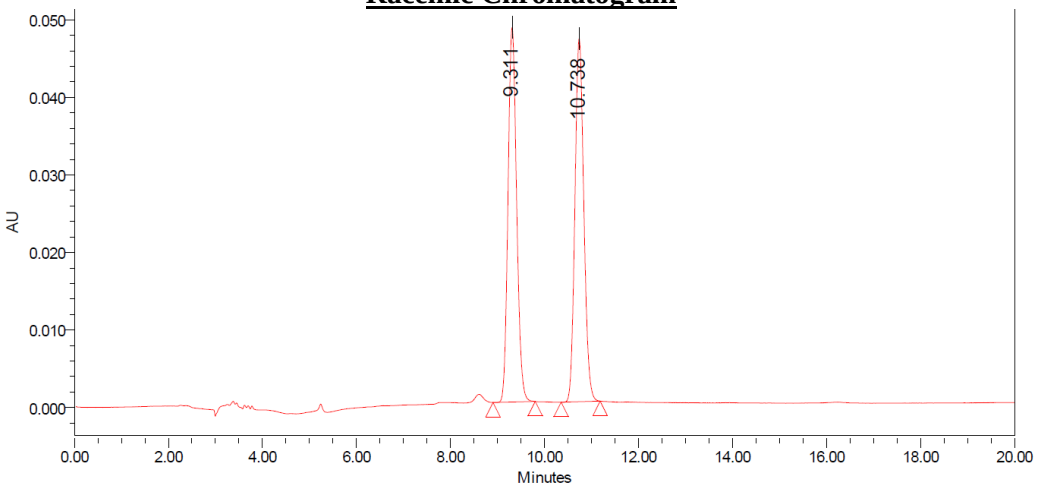

Peak	% Area	Retention Time	Area	Height
1	49.86	9.311	611954	48313
2	50.14	10.738	615302	46848
Total	100.00			

Scalemic Chromatogram

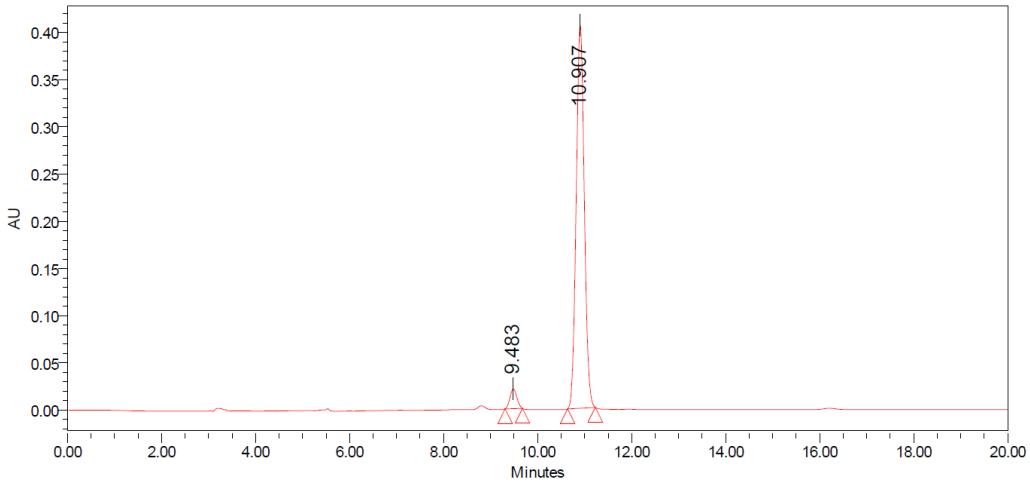

Peak	% Area	Retention Time	Area	Height
1	4.20	9.483	212731	20891
2	95.80	10.907	4848368	405365
Total	100.00			